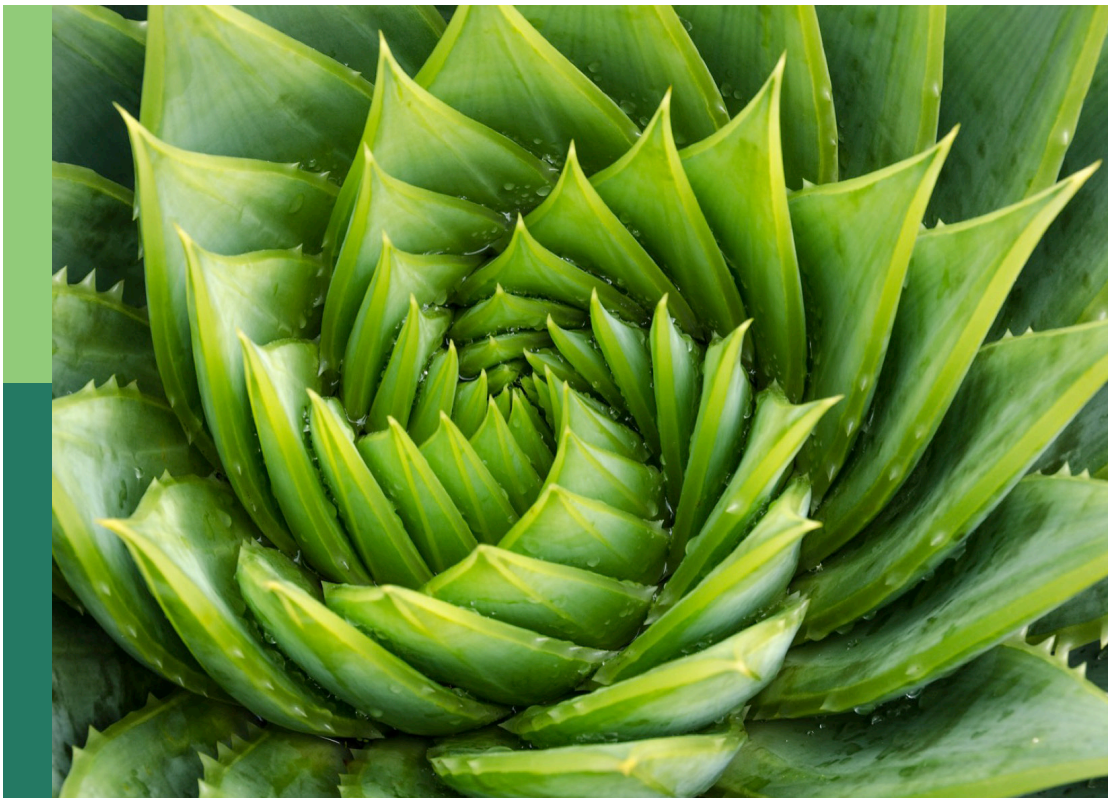
frontiers | Research Topics

Physiological, biochemical and molecular approaches in response to abiotic stresses in plants

Edited by
Giselle Camargo Mendes, Caroline Müller and Andrea Miyasaka Almeida

Published in
Frontiers in Plant Science



FRONTIERS EBOOK COPYRIGHT STATEMENT

The copyright in the text of individual articles in this ebook is the property of their respective authors or their respective institutions or funders. The copyright in graphics and images within each article may be subject to copyright of other parties. In both cases this is subject to a license granted to Frontiers.

The compilation of articles constituting this ebook is the property of Frontiers.

Each article within this ebook, and the ebook itself, are published under the most recent version of the Creative Commons CC-BY licence. The version current at the date of publication of this ebook is CC-BY 4.0. If the CC-BY licence is updated, the licence granted by Frontiers is automatically updated to the new version.

When exercising any right under the CC-BY licence, Frontiers must be attributed as the original publisher of the article or ebook, as applicable.

Authors have the responsibility of ensuring that any graphics or other materials which are the property of others may be included in the CC-BY licence, but this should be checked before relying on the CC-BY licence to reproduce those materials. Any copyright notices relating to those materials must be complied with.

Copyright and source acknowledgement notices may not be removed and must be displayed in any copy, derivative work or partial copy which includes the elements in question.

All copyright, and all rights therein, are protected by national and international copyright laws. The above represents a summary only. For further information please read Frontiers' Conditions for Website Use and Copyright Statement, and the applicable CC-BY licence.

ISSN 1664-8714
ISBN 978-2-8325-2361-2
DOI 10.3389/978-2-8325-2361-2

About Frontiers

Frontiers is more than just an open access publisher of scholarly articles: it is a pioneering approach to the world of academia, radically improving the way scholarly research is managed. The grand vision of Frontiers is a world where all people have an equal opportunity to seek, share and generate knowledge. Frontiers provides immediate and permanent online open access to all its publications, but this alone is not enough to realize our grand goals.

Frontiers journal series

The Frontiers journal series is a multi-tier and interdisciplinary set of open-access, online journals, promising a paradigm shift from the current review, selection and dissemination processes in academic publishing. All Frontiers journals are driven by researchers for researchers; therefore, they constitute a service to the scholarly community. At the same time, the *Frontiers journal series* operates on a revolutionary invention, the tiered publishing system, initially addressing specific communities of scholars, and gradually climbing up to broader public understanding, thus serving the interests of the lay society, too.

Dedication to quality

Each Frontiers article is a landmark of the highest quality, thanks to genuinely collaborative interactions between authors and review editors, who include some of the world's best academicians. Research must be certified by peers before entering a stream of knowledge that may eventually reach the public - and shape society; therefore, Frontiers only applies the most rigorous and unbiased reviews. Frontiers revolutionizes research publishing by freely delivering the most outstanding research, evaluated with no bias from both the academic and social point of view. By applying the most advanced information technologies, Frontiers is catapulting scholarly publishing into a new generation.

What are Frontiers Research Topics?

Frontiers Research Topics are very popular trademarks of the *Frontiers journals series*: they are collections of at least ten articles, all centered on a particular subject. With their unique mix of varied contributions from Original Research to Review Articles, Frontiers Research Topics unify the most influential researchers, the latest key findings and historical advances in a hot research area.

Find out more on how to host your own Frontiers Research Topic or contribute to one as an author by contacting the Frontiers editorial office: frontiersin.org/about/contact

Physiological, biochemical and molecular approaches in response to abiotic stresses in plants

Topic editors

Giselle Camargo Mendes — Instituto Federal de Santa Catarina (IFSC), Brazil
Caroline Müller — Universidade Federal da Fronteira Sul, Brazil
Andrea Miyasaka Almeida — Universidad Mayor, Chile

Citation

Mendes, G. C., Müller, C., Almeida, A. M., eds. (2023). *Physiological, biochemical and molecular approaches in response to abiotic stresses in plants*. Lausanne: Frontiers Media SA. doi: 10.3389/978-2-8325-2361-2

Table of contents

05 Editorial: Physiological, biochemical and molecular approaches in response to abiotic stresses in plants
Giselle Camargo Mendes, Caroline Müller and Andréa Miyasaka Almeida

09 *GhHAI2*, *GhAHG3*, and *GhABI2* Negatively Regulate Osmotic Stress Tolerance *via* ABA-Dependent Pathway in Cotton (*Gossypium hirsutum* L.)
Hamna Shazadee, Nadeem Khan, Lu Wang and Xinyu Wang

23 RNA-Seq Analysis of Developing Grains of Wheat to Intrigue Into the Complex Molecular Mechanism of the Heat Stress Response
Surinder Paul, Joginder Singh Duhan, Sarika Jaiswal, Ulavappa B. Angadi, Ruchika Sharma, Nishu Raghav, Om Prakash Gupta, Sonia Sheoran, Pradeep Sharma, Rajender Singh, Anil Rai, Gyanendra Pratap Singh, Dinesh Kumar, Mir Asif Iquebal and Ratan Tiwari

39 Characteristics and Regulating Roles of Wheat TaHsfA2-13 in Abiotic Stresses
Xiangzhao Meng, Baihui Zhao, Mingyue Li, Ran Liu, Qianqian Ren, Guoliang Li and Xiulin Guo

51 Trehalose alleviates salt tolerance by improving photosynthetic performance and maintaining mineral ion homeostasis in tomato plants
Yan Yang, Jianming Xie, Jing Li, Jing Zhang, Xiaodan Zhang, Yandong Yao, Cheng Wang, Tianhang Niu and Emily Patience Bakpa

73 Characterization of the gene expression profile response to drought stress in *Haloxylon* using PacBio single-molecule real-time and Illumina sequencing
Fang Yang and Guanghui Lv

91 Genome-wide identification of wheat ABC1K gene family and functional dissection of *TaABC1K3* and *TaABC1K6* involved in drought tolerance
Xiaoran Gao, Rong Zou, Haocheng Sun, Junxian Liu, Wenjing Duan, Yingkao Hu and Yueming Yan

111 Excess nitrogen responsive HvMADS27 transcription factor controls barley root architecture by regulating abscisic acid level
Aleksandra Smoczynska, Andrzej Pacak, Aleksandra Grabowska, Dawid Bielewicz, Marcin Zadworny, Kashmir Singh, Jakub Dolata, Mateusz Bajczyk, Przemyslaw Nuc, Jacek Kesy, Magdalena Wozniak, Izabela Ratajczak, Wendy Harwood, Wojciech M. Karlowski, Artur Jarmolowski and Zofia Szweykowska-Kulinska

130 Tomato salt tolerance mechanisms and their potential applications for fighting salinity: A review
Meng Guo, Xin-Sheng Wang, Hui-Dan Guo, Sheng-Yi Bai, Abid Khan, Xiao-Min Wang, Yan-Ming Gao and Jian-She Li

156 Current perspectives of ubiquitination and SUMOylation in abiotic stress tolerance in plants
Madhavi Singh, Ananya Singh, Neelam Yadav and Dinesh Kumar Yadav

183 Root system architecture for abiotic stress tolerance in potato: Lessons from plants
Rasna Zinta, Jagesh Kumar Tiwari, Tanuja Buckseth, Kanika Thakur, Umesh Goutam, Devendra Kumar, Clarissa Challam, Nisha Bhatia, Anuj K. Poonia, Sharmistha Naik, Rajesh K. Singh, Ajay K. Thakur, Dalamu Dalamu, Satish K. Luthra, Vinod Kumar and Manoj Kumar

192 Melatonin enhanced low-temperature combined with low-light tolerance of pepper (*Capsicum annuum* L.) seedlings by regulating root growth, antioxidant defense system, and osmotic adjustment
Jing Li, Jianming Xie, Jihua Yu, Jian Lyv, Junfeng Zhang, Dongxia Ding, Nenghui Li, Jing Zhang, Emily Patience Bakpa, Yan Yang, Tianhang Niu and Feng Gao

207 Systematic analysis of the pectin methylesterase gene family in *Nicotiana tabacum* and reveal their multiple roles in plant development and abiotic stresses
Jinhao Sun, Zhen Tian, Xiaoxu Li, Shaopeng Li, Zhiyuan Li, Jinling Wang, Zongyu Hu, Haiqing Chen, Cun Guo, Minmin Xie and Ruyan Xu

221 ZmNAC074, a maize stress-responsive NAC transcription factor, confers heat stress tolerance in transgenic *Arabidopsis*
Yan Xi, Qiqi Ling, Yue Zhou, Xiang Liu and Yexiong Qian

239 Combined analysis of transcriptome and metabolome reveals the molecular mechanism and candidate genes of *Haloxylon* drought tolerance
Fang Yang and Guanghui Lv

263 Comprehensive physiological, transcriptomic, and metabolomic analyses reveal the synergistic mechanism of *Bacillus pumilus* G5 combined with silicon alleviate oxidative stress in drought-stressed *Glycyrrhiza uralensis* Fisch.
Xin Ma, Zhanchao Xu, Duoyong Lang, Li Zhou, Wenjin Zhang and Xinhui Zhang

287 Sucrose non-fermenting1-related protein kinase VcSnRK2.3 promotes anthocyanin biosynthesis in association with VcMYB1 in blueberry
Xuan Wang, Qi Tang, Fumei Chi, Hongdi Liu, Hongjun Zhang and Yang Song

frontiers | Frontiers in Plant Science

TYPE Editorial
PUBLISHED 21 April 2023
DOI 10.3389/fpls.2023.1194937

Check for updates

OPEN ACCESS

EDITED AND REVIEWED BY
Pavel Kerchev,
Mendel University in Brno, Czechia

*CORRESPONDENCE
Giselle Camargo Mendes
giselle.mendes@ifsc.edu.br
Caroline Müller
carolinemulleram@gmail.com

†These authors have contributed equally to this work

SPECIALTY SECTION
This article was submitted to Plant Abiotic Stress, a section of the journal Frontiers in Plant Science

RECEIVED 27 March 2023
ACCEPTED 10 April 2023
PUBLISHED 21 April 2023

CITATION
Mendes GC, Müller C and Almeida AM (2023) Editorial: Physiological, biochemical and molecular approaches in response to abiotic stresses in plants.
Front. Plant Sci. 14:1194937.
doi: 10.3389/fpls.2023.1194937

COPYRIGHT
© 2023 Mendes, Müller and Almeida. This is an open-access article distributed under the terms of the Creative Commons Attribution License (CC BY). The use, distribution or reproduction in other forums is permitted, provided the original author(s) and the copyright owner(s) are credited and that the original publication in this journal is cited, in accordance with accepted academic practice. No use, distribution or reproduction is permitted which does not comply with these terms.

Editorial: Physiological, biochemical and molecular approaches in response to abiotic stresses in plants

Giselle Camargo Mendes[1*†], Caroline Müller[2†] and Andréa Miyasaka Almeida[3†]

[1]Departamento de Biotecnologia, Instituto Federal de Santa Catarina, Lages, Brazil, [2]Programa de Pós-Graduação em Ciência e Tecnologia Ambiental, Universidade Federal da Fronteira Sul, Erechim, Brazil, [3]Centro de Genómica y Bioinformática, Universidad Mayor, Santiago, Chile

KEYWORDS

drought, high temperature, salinity, transcriptome, metabolome, signaling response, ubiquitination, plant growth promoting bacteria

Editorial on the Research Topic
Physiological, biochemical and molecular approaches in response to abiotic stresses in plants

As sessile organisms, plants are constantly exposed to abiotic stresses such as drought, extreme temperatures, and high salinity which negatively affect their growth and development. The response to abiotic stress is multigenic with complex signaling pathways involving hormones, specific transcription factors, and second messengers such as Ca^{2+}. There are signaling pathways that are common to different abiotic stresses and plant species, and those that occur only in response to specific stresses. Morphological and physiological responses are triggered at the end of these signaling pathways. Endemic and cultivated plants differ in their response to stress. There are several endemic species that are extremely tolerant to various abiotic stresses and exhibit characteristics that could be transferred to cultivated plants. Knowledge of the molecular and physiological responses to various abiotic stresses could provide the basis for potential applications to improve tolerance through genetic engineering, marker-assisted breeding, grafting and other sustainable approaches. Many responses to the abiotic stressors discussed in this topic are summarized in Figure 1.

Drought, exacerbated by climate change in recent decades, is one of the major stresses affecting the growth and productivity of various plant species. Abscisic acid (ABA) plays a central role in the response of plants to drought and other abiotic stresses. Analysis of full-length transcripts from two xerophytic desert trees showed that three genes for zeaxanthin epoxidase (ZEP) and one gene for NINE-CIS-EPOXYCAROTENOID DIOXYGENASE (NCED), gene, a rate-limiting enzyme in the ABA biosynthetic pathway, were up-regulated, which could explain the increase in synthesis of ABA during stress (Yang and Lv). In addition, the authors reported that signaling pathways involving *CaM*, *CIPK*, and *MAPKK* genes were upregulated in these species. In a later work, Yang and Lv observed 217 differentially expressed genes (DEGs)

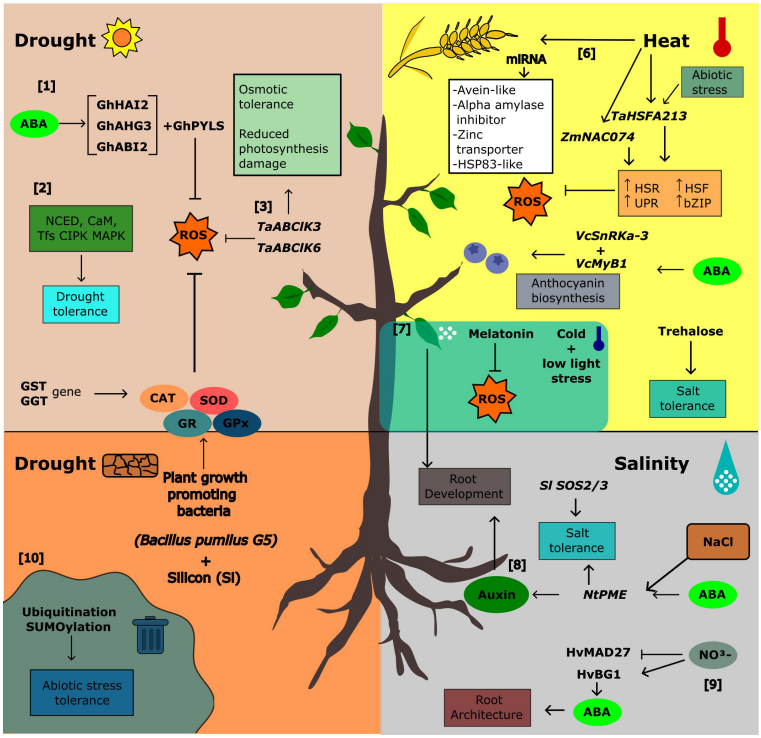


FIGURE 1
Integration of signals in abiotic stress and adaptive responses in plants. [1] The sensitivity and synthesis of ABA were regulated by the GhHAI2, GhAHG3, and GhABI2 genes in cotton (Shazadee et al.), and [2] NINE-CIS-EPOXYCAROTENOID DIOXYGENASE (NCED) and zeaxanthin epoxidase (ZEP) in two xerophytic desert trees (Yang and Lv). In these trees, signaling pathways under drought stress also involves CaM, CIPK, and MAPKK genes (Yang and Lv), and [3] overexpression of TaABC1K3 and TaABC1K6 in Arabidopsis and wheat improved drought tolerance (Gao et al.) by inducing osmotic tolerance and reduced photosynthetic damage. In addition, drought stress tolerance is also promoted by [4] application of plant growth-promoting bacteria (PGPB) and silicon (Si) which increase antioxidant enzymes such as catalase (CAT), superoxide dismutase (SOD), GR, and GPx and regulate GST and GGT genes in Glycyrrhiza uralensis (Ma et al.). [5] Low light and low-temperature stress could be mitigated by melatonin foliar application in pepper by controlling root development and ROS production (Li et al.). [6] In heat stress, ZmNAC074 from maize (Xi et al.) and TaHsfA2-13 from wheat (Meng et al.) were important genes related to heat shock response (HSR), unfolded protein response (UPR), basic leucine zipper (bZIP), heat shock proteins (HSP), and reactive oxygen species removal, conferring tolerance to these plants. Heat stress tolerance has also been observed through the upregulation of avenin-like cysteine-rich storage proteins, amylase inhibitors, zinc transporters, and HSP83-like proteins expressed by miRNA in the early stages of wheat seed development (Paul et al.). [7] In blueberry fruit, ABA is also involved in anthocyanin biosynthesis (VcMYB1 and VcSnRK2.3) (Wang et al.). [8] Modulation of root system architecture is also mediated by abscisic acid (ABA) in tomato (Zinta et al.) and barley (HvMADS27 x ABA) (Smoczynska et al.). NtPME genes in tobacco roots were also induced by ABA and auxin pathways, mediating root development under salinity (Sun et al.). [9] Release of ABA from conjugates can also inhibit root development under conditions of nitrogen excess in barley (Smoczynska et al.). [10] Other post-transcriptional processes such as ubiquitination and SUMOylation play an important role in tolerance to various abiotic stresses (Singh et al.).

belonging to the WRKY, Maf, ER, MYB, and FAR1 transcription factor (TF) families in these xerophytic desert plants under drought stress. TFs are important for regulating gene expression networks of target genes and the expression of different families reveals their central role in the complex regulatory network of drought tolerance.

In cultivated cotton, members of the ABA pathway, such as 2C-type protein phosphatases (PP2Cs), were shown to act as negative regulators in the osmotic stress response through ABA-mediated signaling (Shazadee et al.). According to the authors, *GhHAI2*, *GhAHG3*, and *GhABI2* showed altered phenotypes in response to osmotic stress (induced by polyethylene glycol) through changes in leaf physiology and root morphology and regulation of reactive oxygen species (ROS) degradation in the genetic VIGS (virus-induced gene silencing) studies.

Silencing of *PP2C* genes in this species significantly increased the expression of ABA-dependent stress marker genes and resulted in altered phenotypes in response to osmotic stress (Shazadee et al.). Twenty-nine and 41 *PP2C* genes were also detected in *Haloxylon ammodendron* and *Haloxylon persicum*, two species of xerophytic trees, in addition to one *PYL9* and one *PYL8* and one and four *SnRK2* genes, that were upregulated, indicating their role in the ABA-signaling regulatory system, which plays an important role in the drought tolerance process (Yang and Lv).

Gao et al. performed a comprehensive genome-wide analysis of the BC1 complex kinase (ABC1K) activity gene family of wheat using the newly released published wheat genome database (IWGSC RefSeq v2.1). The genome-wide analysis identified 44 wheat ABC1K family genes that contained the typical ABC1K kinase domain and three (I–III) clades. Overexpression of *TaABC1K3* and *TaABC1K6* in yeast and *Arabidopsis* significantly improved drought tolerance. Moreover, *TaABC1K3* and *TaABC1K6* were shown to play essential roles in scavenging ROS and mitigating

photosynthetic damage caused by drought stress. In addition, wheat ABC1K genes such as *TaABC1K3 and TaABC1K6* have numerous cis-elements associated with environmental stress, including ABRE, MBS, and G-box, which may play important roles in defending against various abiotic stresses.

Despite the activation of various cellular signaling pathways for plant resistance to drought stress, this may lead to excessive accumulation of ROS as secondary stress that causes oxidative damage in plants. Under stress conditions, plants tend to increase the production of antioxidant enzymes and non-enzymatic components such as ROS and the AsA-GSH cycle, which may contribute to plant tolerance to drought. Assessment of the antioxidant system was important to determine the role of synergistic application of plant growth-promoting bacteria (PGPB) and silicon (Si) in alleviating drought stress in *Glycyrrhiza uralensis*, a perennial herb widely distributed in arid and semiarid desert steppes and commonly used in Chinese folk medicine (Ma et al.). Using physiological, transcriptomic, and metabolomic techniques, the authors demonstrated that PGPB in combination with Si significantly increased the activities of SOD and CAT. The combination of *Bacillus pumilus* (G5) and Si further enhanced GSH formation by increasing the activities of GR and GPX and upregulating the *GST* and *GGT* genes, which contributed to a reduction in oxidative stress (Ma et al.).

Like drought stress, tolerance to heat stress (HS) is a highly complex process involving multiple cell signaling pathways. There are several types of TFs that act as master regulators and coordinate the expression of genes involved in the response to heat stress, such as the NAC proteins (NAM, ATAF1/2, and CUC2). In particular, the transcription factor *ZmNAC074* isolated from maize was upregulated after 8-h exposure to heat stress (42°C) (Xi et al.). The authors also confirmed the increase in tolerance to heat stress by overexpression of *ZmNAC074* in *A. thaliana* and discovered genes related to heat shock response (HSR), unfolded protein response (UPR), and removal of ROS, as well as the interaction proteins between different transcription factors such as bZIP (basic leucine zipper) and HSF (heat shock factor) TFs in response to heat treatment. Also using wheat plants, Meng et al. analyzed the heat shock transcription factor *TaHsfA2-13* cloned from wheat and found that its expression, as well as overexpression of *TaHsfA2-13* in the Col-o or *athsfa2* mutant of *A. thaliana* was up-regulated by heat stress, H_2O_2, mannitol, and salinity, suggesting that this gene may increase tolerance to various abiotic stresses in wheat plants.

Paul et al. used the transcriptome to analyze wheat plants exposed to thermal stress during the grain filling stage and identified 309 DEGs from 115,656 conserved genes involved in processes such as signal transduction, starch synthesis, the antioxidant system, and conserved and uncharacterized putative genes that respond to heat stress. Among the major proteins, the authors detected upregulation of avenin-like cysteine-rich storage proteins expressed in the early stages of seed development; amylase inhibitors responsible for protecting seed starch reserves from degradation into simpler oligosaccharides; aspartic proteinase, which plays an important role in protein processing in response to various stresses; elongation factor 1-alpha, a multifunctional protein that transcribes elongation factors, which play an essential role in mediating critical cellular processes related to cell growth, proliferation, and differentiation by interacting with other cellular proteins; and α-gliadin, heat shock protein, and zinc transporter, which have been described to confer heat stress tolerance in plants.

Salinity has steadily increased in irrigated areas, significantly affecting crop yields. Guo et al. conducted a comprehensive review on the morphological, physiological, and biochemical effects of salt and discussed in detail the mechanisms of salt tolerance in tomato, the most widely grown fruit crop in the world. In particular, the exogenous application of trehalose (Ter), a non-reducing sugar known to be an osmoprotective molecule, was able to reverse the negative effects on photosynthetic rate and Calvin cycle enzymes in tomato plants (Yang et al.). In addition, the authors reported that Ter increased transport selectivity and ion levels and affected the expression of genes related to ion homeostasis under salt stress conditions. Tobacco plants overexpressing the gene *NtPME043*, which is related to the enzyme pectin methylesterase (PME), an important cell wall component, showed greater root growth after three weeks of salt treatment, indicating greater tolerance to this abiotic stress (Sun et al.).

In countries with subtropical climates and very cold winters, the cultivation of vegetables such as peppers, can suffer from the effects of low light and low temperatures, even in protected facilities (Li et al.). These authors showed that the application of melatonin, an important hormone that acts as a secondary metabolite, mitigate low light and low temperature stresses by modulating of root growth and improving antioxidant defense systems in this species.

Abiotic stress also affects the availability and uptake of nutrients by plants. Nitrogen (N) is the macroelement that plants require in greater amounts. In a comprehensive review of root system architecture for tolerance to various abiotic stresses in potato, Zinta et al. highlight that the efficiency of N uptake and utilization depends on plant root development. Therefore, knowledge of genes involved in N metabolism is essential for plant breeding studies to increase plant tolerance to abiotic stress. Several studies are available on the response to nitrogen deficiency stress, but responses to N excess, common in agricultural systems with fertilizers, are limited. Smoczynska et al. had shown that the HvMADS transcription factor is down-regulated under N excess in barley roots, resulting in increased *HvBG1* expression and ABA release of ABA-glucose conjugates and consequent inhibition of root growth. ABA-induced tobacco roots, the expression of *NtPME029* was high (Sun et al.), which has ABA response elements (ABRE) and auxin-responsive region (AuxRR-core) in the promoter regions, indicating the involvement of this gene in the ABA and auxin pathways in mediating root development.

ABA is also involved in the ripening process of non-climacteric fruits such as blueberries. In the work of Wang et al., SUCROSE NON-FERMENTING1-RELATED PROTEIN KINASE-2 (SnRK2), an important component of the ABA signaling pathway, was shown to interact interacts with a positive anthocyanin regulator VcMYB1 and promotes the synthesis of this pigment in blueberries. Heterologous expression of *VcSnRK2.3* in *Arabidopsis* also induced anthocyanin pigmentation in seeds and seedlings.

Finally, post-transcriptional events such as ubiquitination and SUMOylation were shown to play important roles in regulating gene transcription, the quality of DNA replication and repair, and

the abundance of short-lived regulatory proteins that are important for tolerance to various abiotic stresses and have been studied in detail by Singh et al.. The authors described the functions of ubiquitination and SUMOylation under drought stress, salinity, extreme temperatures, UV radiation, nutrient deprivation, ABA-mediated, flooding, and epigenetic regulation of stress responses and elucidated the molecular and enzymatic mechanisms of covalent protein modifications in plant immunity to abiotic stress.

Author contributions

All authors listed have made a substantial, direct, and intellectual contribution to the work and approved it for publication.

Funding

This work was supported by grants from the Chilean ANID/ACT210007 (AA); and Universidad Mayor (grant no. I-2022006; AA).

Acknowledgments

CM is grateful to the Coordenação de Aperfeiçoamento de Pessoal de Nivel Superior - Brazil (CAPES/PNPD 88887.352933/2019-00) for fellowship. The authors also thank Dr. Claudio Urra for elaboration of the figure.

Conflict of interest

The authors declare that the research was conducted in the absence of any commercial or financial relationships that could be construed as a potential conflict of interest.

Publisher's note

All claims expressed in this article are solely those of the authors and do not necessarily represent those of their affiliated organizations, or those of the publisher, the editors and the reviewers. Any product that may be evaluated in this article, or claim that may be made by its manufacturer, is not guaranteed or endorsed by the publisher.

frontiers | Frontiers in Plant Science

ORIGINAL RESEARCH
published: 19 May 2022
doi: 10.3389/fpls.2022.905181

GhHAI2, *GhAHG3,* and *GhABI2* Negatively Regulate Osmotic Stress Tolerance *via* ABA-Dependent Pathway in Cotton (*Gossypium hirsutum* L.)

*Hamna Shazadee[1,2,3], Nadeem Khan[2,3], Lu Wang[1] and Xinyu Wang[1]**

[1]College of Life Sciences, Nanjing Agricultural University, Nanjing, China, [2]Agriculture and Agri-Food Canada, Ottawa Research and Development Centre, Ottawa, ON, Canada, [3]Department of Biology, University of Ottawa, Ottawa, ON, Canada

OPEN ACCESS

Edited by:
Caroline Müller, Universidade Federal da Fronteira Sul, Brazil

Reviewed by:
Danilo M. Daloso, Federal University of Ceara, Brazil
Agata Daszkowska-Golec, University of Silesia in Katowice, Poland
Kazuo Nakashima, Japan International Research Center for Agricultural Sciences (JIRCAS), Japan

***Correspondence:**
Xinyu Wang
xywang@njau.edu.cn

Specialty section:
This article was submitted to Plant Abiotic Stress, a section of the journal Frontiers in Plant Science

Received: *26 March 2022*
Accepted: *26 April 2022*
Published: *19 May 2022*

Citation:
Shazadee H, Khan N, Wang L and Wang X (2022) GhHAI2, GhAHG3, and GhABI2 Negatively Regulate Osmotic Stress Tolerance via ABA-Dependent Pathway in Cotton (Gossypium hirsutum L.). Front. Plant Sci. 13:905181. doi: 10.3389/fpls.2022.905181

The type 2C protein phosphatases (PP2Cs) are well known for their vital roles in plant drought stress responses, but their molecular mechanisms in cotton (*Gossypium hirsutum* L.) remain largely unknown. Here, we investigated the role of three clade A *PP2C* genes, namely, *GhHAI2*, *GhAHG3,* and *GhABI2*, in regulating the osmotic stress tolerance in cotton. The transcript levels of *GhHAI2*, *GhAHG3,* and *GhABI2* were rapidly induced by exogenous abscisic acid (ABA) and polyethylene glycol (PEG) treatment. Silencing of *GhHAI2*, *GhAHG3,* and *GhABI2 via* virus-induced gene silencing (VIGS) improved osmotic tolerance in cotton due to decreased water loss, increase in both relative water content (RWC) and photosynthetic gas exchange, higher antioxidant enzyme activity, and lower malondialdehyde (MDA) content. The root analysis further showed that *GhHAI2*, *GhAHG3,* and *GhABI2*-silenced plants were more responsive to osmotic stress. Yeast two-hybrid (Y2H) and luciferase complementation imaging (LCI) assays further substantiated that GhHAI2, GhAHG3, and GhABI2 interact with the core receptors of ABA signaling, GhPYLs. The expression of several ABA-dependent stress-responsive genes was significantly upregulated in *GhHAI2*-, *GhAHG3-,* and *GhABI2*-silenced plants. Our findings suggest that *GhHAI2*, *GhAHG3*, and *GhABI2* act as negative regulators in the osmotic stress response in cotton through ABA-mediated signaling.

Keywords: PP2Cs, osmotic tolerance, cotton, VIGS, abscisic acid

INTRODUCTION

Plants are constantly exposed to diverse environmental conditions, such as water deficit, high salinity, flooding, and extreme temperatures, which adversely affect their growth and productivity (Claeys and Inzé, 2013). These abiotic stresses greatly impact plant morphology and cause damage to plant cells. For instance, excessive accumulation of reactive oxygen species (ROS) affects cell membrane stability, reduces photosynthetic efficiency, accelerates protein deformation, and causes leaf wilting (Hanin et al., 2011; Choudhury et al., 2013, 2017). As plants are sessile

in nature, various complex mechanisms have been developed to respond appropriately to such harmful conditions. One of these mechanisms is the induction of diverse number of stress-responsive genes (Nakashima and Yamaguchi-Shinozaki, 2006). Previous studies have reported many stress-induced proteins, such as enzymes involved in the ABA signaling pathway, protein phosphatases, numerous protein kinases, osmotic adaptive proteins, cellular protective enzymes, and transcription factors (Zhu, 2002, 2016).

The type 2C protein phosphatases (PP2Cs) belong to a major group of gene families known to mediate abiotic stress signaling pathways and signal transduction processes. PP2Cs have been identified as the first key component of the ABA signaling pathway (Koornneef et al., 1984). The phytohormone ABA plays a vital role in regulation of plant drought stress responses (Yoshida et al., 2014; Zhu, 2016). Genetic studies have reported a canonical mechanism underlying ABA signal transduction in *Arabidopsis thaliana*. Under water deficit conditions, plants exhibit an elevated level of ABA which is perceived by the pyrabactin resistance 1 (PYR1)/PYR1-like (PYL)/regulatory component of the ABA receptor (RCAR) protein family (Ma et al., 2009; Park et al., 2009). In the absence of ABA, clade A PP2Cs interact with sucrose nonfermenting 1-related protein kinase 2 (SnRK2), thereby preventing their activity by dephosphorylation. ABA perception leads to the binding of PYL receptors to PP2Cs, which release SnRK2 for subsequent phosphorylation of ABA-Responsive Element (ABRE) Binding Factors (ABFs) which regulate transcription of ABA-responsive genes (Cutler et al., 2010; Nakashima and Yamaguchi-Shinozaki, 2013).

In recent years, several studies have functionally characterized PP2C family members, for example, in *Arabidopsis*, nine PP2C group A members have been identified as component of ABA signaling pathway; *ABI1* (ABA insensitive1), *ABI2*, *HAB1* (hypersensitive to ABA1), *HAB2*, *AHG1* (ABA-hypersensitive germination1), *AHG3/AtPP2CA*, *HAI1* (highly ABA-induced) *HAI2,* and *HAI3* (Saez et al., 2004; Schweighofer et al., 2004; Rubio et al., 2009; Antoni et al., 2012; Kim et al., 2013; Rodrigues et al., 2013; Née et al., 2017; Yoshida et al., 2019). Double mutant plants of *abi1* and *abi2* were responsive to ABA, suggesting that *ABI1* and *ABI2* function negatively in ABA signaling pathway (Merlot et al., 2001). Under ABA treatment, *ahg1* and *ahg3* double mutants displayed stronger phenotypes than single parental mutant, implying that *AHG1* and *AHG3* function together in regulating ABA signaling pathway (Nishimura et al., 2007). Similarly, all members of *PP2C-A* were upregulated when subjected to exogenous ABA; however, *HAI1*, *HAI2,* and *HAI3* expressions were strongly induced in vegetative phase (Fujita et al., 2009). Likewise, transgenic *Arabidopsis* overexpressing rice clade A *OsPP108* showed enhanced tolerance under salt, mannitol, and drought stress, but reduction in ABA sensitivity (Singh et al., 2015). The overexpression of *OsABIL2,* which encodes another rice clade A of *PP2C*, exhibits ABA insensitivity and significantly altered phenotypes, such as stomatal density and root architecture, leading to the drought hypersensitivity (Li et al., 2015). Similarly, maize *ZmPP2C-As* were recently characterized and their role in drought tolerance were elucidated. For instance, *Arabidopsis* plants overexpressing *ZmPP2C-2A* and *ZmPP2C-6A* were sensitive to drought stress, suggesting their negative role in drought stress response (He et al., 2019). Also, transgenic studies in maize and *Arabidopsis* verified that *ZmPP2C-A10* function as negative regulator of drought tolerance (Xiang et al., 2017). So far, using bioinformatics analysis, the *PP2C* gene family has been identified in several species, including *Arabidopsis* (Schweighofer et al., 2004), rice (Xue et al., 2008), cotton (Shazadee et al., 2019), wheat (Yu et al., 2019), soybean (Chen et al., 2018), and Chinese cabbage (Khan et al., 2019). However, the functional characterization of *PP2C* genes in cotton remains largely obscure.

Cotton (*Gossypium hirsutum* L.) is one of the most important fiber and oil crops, commercially grown worldwide. Various abiotic stresses particularly drought stress greatly affect cotton growth and limit fiber yield and lint quality, resulting in a significant production losses (Pettigrew, 2004). Moreover, 57% of global cotton is grown in regions with high water stress (WRI, 2013). Thus, development of drought resistant cotton cultivars and improving water use efficiency are crucial to sustain the cotton industry. In a previous study, we identified 18 Clade A PP2Cs in cotton (*G. hirsutum*; Shazadee et al., 2019) but their functional role was unexplored. It has been recently reported (Lu et al., 2019) and observed that the expression of clade A *PP2Cs* is highly induced under osmotic and ABA treatment in cotton. These observations suggest a role of cotton clade A PP2Cs in abiotic stress; however, no stress-related phenotype has been associated with group A PP2Cs in cotton yet. Hence, it is important to further investigate the molecular mechanism of clade A PP2Cs in response to drought stress in cotton.

In this study, we characterized three members of clade A *PP2Cs*; *GhHAI2, GhAHG3,* and *GhABI2* in cotton in order to investigate their roles in drought tolerance. The *GhHAI2, GhAHG3,* and *GhABI2* were highly induced by ABA and PEG treatment. Silencing of *GhHAI2*, *GhAHG3,* and *GhABI2* improved osmotic tolerance of cotton plants. Yeast two-hybrid (Y2H) and luciferase complementation imaging (LCI) assays revealed that GhHAI2, GhAHG3, and GhABI2 interact with GhPYLs and regulate ABA signaling pathway. Furthermore, we demonstrated that *GhHAI2-*, *GhAHG3-,* and *GhABI2*-silenced plants increased the expression of ABA-dependent stress-responsive genes. In brief, our results suggest that *GhHAI2*, *GhAHG3,* and *GhABI2* function as crucial negative regulators in osmotic stress response by an ABA-dependent pathway indicating their potential roles in drought tolerance.

MATERIALS AND METHODS

Plant Material and Stress Treatment

For expression analysis of *GhHAI2*, *GhAHG3,* and *GhABI2* in cotton, seedlings were planted in Hoagland nutrient solution with a 16 h/8 h light/dark cycle at 25°C. Then, three-week-old

seedlings were subjected to 15% PEG 6000 for osmotic treatment. For ABA treatment, the plants were sprayed with 200 μm ABA. Leaves were collected after stress treatment at the designated time (0, 6, 12, 24, and 48 h).

For evaluation of osmotic stress tolerance, *G. hirsutum*, cultivar Xinluzao, plants were used to perform the experiments. Cotton plants were grown in a growth chamber under a 16 h/8 h light/dark cycle at 25°C. Pot-grown cotton seedlings at two true leaves stage were treated with 15% PEG for osmotic stress, and in parallel, water treatment was used as mock control. After PEG stress, plant leaves were collected at different time points, immediately frozen in liquid nitrogen and stored at −80°C until further use. Root assay was performed after 7 days of osmotic stress. Each of the experiments was performed in triplicate.

Cloning and Sequence Analysis of GhHAI2, GhAHG3, and GhABI2

We obtained the full-length ORFs of *GhHAI2*, *GhAHG3,* and *GhABI2 via* PCR; the primers were designed using the coding sequence of *GhHAI2*, *GhAHG3,* and *GhABI2* (**Supplementary Table S1**). Alignment of cotton GhHAI2, GhAHG3, and GhABI2 and *Arabidopsis* HAI2, AHG3, and ABI2 was performed with ClustalW (Thompson et al., 1994). The MEGA program (version 7.0) was used to construct the phylogenetic tree *via* the Neighbor-Joining (NJ) method and 1,000 bootstrap replications.

Subcellular Localization

The coding regions of *GhHAI2*, *GhAHG3,* and *GhABI2* were amplified by PCR and inserted into the pBin-GFP4 (green fluorescent protein) expression vector. The three vectors were separately introduced into *Agrobacterium tumefaciens* strain GV3101 cells and transiently expressed in *Nicotiana benthamiana* leaf cells *via A. tumefaciens* infiltration method. After 3 days of infiltration, fluorescence signals were detected using a confocal laser-scanning microscope (Zeiss, LSM710).

Agrobacterium tumefaciens-Mediated VIGS

Inserts to generate TRV2:*GhHAI2*, TRV2:*GhAHG3*, TRV2:*GhABI2,* and positive control TRV2:*GhCLA1* were amplified from *G. hirsutum* cultivar Xinluzao cDNA with primers containing the restriction sites *Eco*RI and *Xho*I. The primers for cloning are listed in **Supplementary Table S1**. Vectors constructed in binary tobacco rattle virus (TRV) vector, including pTRV1 and pTRV2 (*GhHAI2*, *GhAHG3,* and *GhABI2* and *GhCLA1*), were introduced into *A. tumefaciens* strain GV3101 by electroporation. The Agrobacteria culture carrying the above pTRV1 and pTRV2 constructs was infiltrated into two fully expanded cotyledons of seven-day-old cotton plants using a needle-less syringe as previously described (Gao et al., 2011, 2013). The *GhCLA1* construct was used as a visual marker to determine VIGS efficiency. After 14 days of Agrobacteria inoculation, the silenced plants were subjected to 15% PEG treatment for the indicated times. VIGS experiments were repeated three times with more than 30 plants for each construct per replicate.

Measurement of Water Loss and RWC

For relative water content (RWC) measurement, six leaves were detached from individual cotton plants and the fresh weight (FW) was recorded. To record turgid weight (TW), the leaves were soaked in distilled water for 4 h at room temperature with constant light. The leaves were then dried at 65°C for 24 h to obtain the dry weight (DW). RWC was calculated using the formula: $RWC\ (\%) = [(FW-DW)/(TW-DW)] \times 100$. To measure water loss, aerial parts of six cotton seedlings were detached and placed on clean filter paper on a laboratory bench. At various time intervals, the total FW was recorded. Water loss was calculated as the decrease in fresh weight as a percentage of the initial fresh weight of the detached seedlings parts. Both assays were performed in three biological repeats.

Gas Exchange

Gas exchange measurements were taken from three-week-old cotton plants under normal and PEG conditions. The photosynthetic rate (A, μmol CO_2 m^{-2} s^{-1}), stomatal conductance (gs, mol H_2O m^{-2} s^{-1}), intercellular CO_2 concentration (Ci, μmol CO_2 mol^{-1}), and transpiration rate (E, mmol H_2O m^{-2} s^{-1}) were measured with a portable photosynthesis system Li-6400XT (Li-COR Inc., United States) under 1,500 μmol m^{-2} s^{-2} light intensity, 23°C ± 2°C temperature, and 300 μmol mol^{-1} CO_2 concentration. For each gene, at least seven biological replicates per treatment were measured.

Measurement of Antioxidant Enzymes and MDA Content

Fresh leaves of cotton plants under normal and PEG conditions were used for the measurement of antioxidant enzymes activity and Malondialdehyde (MDA) content. The peroxidase (POD; U mg^{-1} protein), superoxide dismutase (SOD; U mg^{-1} protein), catalase (CAT; U mg^{-1} protein) activities, and MDA (nmol g^{-1}) content were determined using analytical kits (Nanjing Jiancheng Bioengineering Institute, Nanjing, China) following the manufacturer's protocol as described (Kumar et al., 2020). Three biological replicates were used to investigate each physiological index.

RNA Extraction, First-Strand cDNA Synthesis, and qPCR

Total RNA was extracted from various organs of cotton plants using Biospin plant Total RNA Extraction Kit (Bioer technology, Hangzhou, China) according to the manufacturer's protocol. gDNase-treated RNA was reverse transcribed to generate first-strand cDNA using Prime Script™ RT Reagent Kit (TaKaRa, United States). Gene expression levels were determined using qPCR assay, which was conducted with SYBR® Premix Ex Taq™ (TaKaRa, United States) and an ABI 7300 qPCR System (Applied Biosystems, CA, United States). The real-time PCR amplification reactions are briefly described in our previously reported study (Shazadee et al., 2019). The $2^{-\Delta\Delta Ct}$ method was

used to determine relative expression level (Livak and Schmittgen, 2001). Cotton histone3 (*AF024716*) gene was used as an internal control. All the primers were designed using Primer Blast in NCBI (**Supplementary Table S1**). Three biological replicates, each containing three technical replicates, were used for each sample.

Y2H Assay

The Y2H assay was based on the Matchmaker GAL4 two-hybrid system (Clontech, United States). The *GhHAI2, GhAHG3,* and *GhABI2* and *GhPYLs* coding regions were independently cloned into the pGBKT7 (BD) and pGADT7 (AD) vectors, respectively. The construct pairs were co-transformed into AH109 yeast strain cells and grown on SD/−Trp/−Leu/-His/−Ade (SD/-QDO) medium containing 5-bromo-4-chloro-3-indolyl-alpha- D-galactopyranoside (X-α-gal). Photographs of resulting yeast growth were taken 3 days after incubation.

LCI Assay

For luciferase complementation imaging (LCI) assay, the open reading frames of *GhHAI2, GhAHG3,* and *GhABI2* and *GhPYLs* without stop codons were cloned into pCAMBIA1300-CLuc or pCAMBIA1300-NLuc vectors using *Kpn*I and *Bam*HI or *Bam*HI and *Sal*I restriction sites, respectively. The fusion constructs were then transformed to *A. tumefaciens* GV3101. The suspensions were prepared by mixing the three *Agrobacterium* strains carrying the CLuc, and NLuc fusion and the gene silencing inhibitor p19 at a 1:1:1 ratio. For transient expression, the bacterial mixture was infiltrated into different locations on the same *N. benthamiana* leaves using a needle-less syringe. To measure LUC activity, 1 mM luciferin was sprayed into the leaves and kept in the dark for 5 min to quench the fluorescence. A low-light cooled CCD imaging apparatus was used to capture the LUC image at 3 min intervals.

Statistical Analyses

All data are represented herein as the means ± standard deviations. The significant levels were determined by using Student's *t*-test: $^{*}p < 0.05$; $^{**}p < 0.01$.

RESULTS

Induction of *GhHAI2*, *GhAHG3,* and *GhABI2* After Exposure to PEG and ABA

In an RNA-seq assay and our previously reported study (Zhang et al., 2015; Shazadee et al., 2019), several *PP2C* genes were identified that were induced in response to osmotic stress. Of these candidate genes, we selected three strongly induced genes for their functional characterization in order to confirm their potential role in osmotic tolerance. Phylogenetic analysis revealed that these PP2Cs belong to clade A and share a close relationships with *Arabidopsis* HAI2, AHG3, and ABI2 (**Figure 1A**). Based on their similarity with *Arabidopsis*, we renamed them as GhHAI2, GhAHG3, and GhABI2, respectively. The deduced amino acid sequence of GhHAI2, GhAHG3, and GhABI2 encodes a protein of 417, 409, and 471 amino acids, and shares 56, 59, and 54% sequence similarity with *Arabidopsis* HAI2, AHG3, and ABI2, respectively (**Figure 1B**). The *Arabidopsis* clade A PP2Cs, HAI2, AHG3, and ABI2 have been known to function as negative regulators in ABA signaling pathway (Merlot et al., 2001; Leonhardt et al., 2004; Nishimura et al., 2007; Xue et al., 2008; Bhaskara et al., 2012). Therefore, we predicted that *GhHAI2*, *GhAHG3,* and *GhABI2* might show a similar expression pattern to *Arabidopsis HAI2*, *AHG3,* and *ABI2* and function in osmotic stress response in cotton.

qPCR analysis revealed that *GhHAI2*, *GhAHG3,* and *GhABI2* genes are constitutively expressed in root, stem, and leaf tissues; however, the expression level of *GhHAI2* was relatively lower (**Figure 1C**). To verify that *GhHAI2*, *GhAHG3,* and *GhABI2* respond to osmotic stress, we monitored their expression levels in cotton leaves after exposure to PEG and ABA using qPCR. Before treatment, the *GhHAI2*, *GhAHG3,* and *GhABI2* expressions were weakly induced. However, PEG and ABA triggered a significant accumulation of *GhHAI2*, *GhAHG3,* and *GhABI2* transcripts within 6–48 h (**Figures 1D–I**). These results suggested that *GhHAI2*, *GhAHG3,* and *GhABI2* expressions are strongly induced after PEG and ABA treatment indicating that these genes could function in response to dehydration in cotton.

Subcellular Localization of GhHAI2, GhAHG3, and GhABI2

To investigate the subcellular localization of GhHAI2, GhAHG3, and GhABI2, we fused their coding regions to the green fluorescent protein (GFP) reporter gene under the control of the 35S promoter. We found that the transient expression of the 35S:GhHAI2-GFP, 35S:GhAHG3-GFP, and 35S:GhABI2-GFP fusion proteins in *N. benthamiana* leaves generated GFP signals in the nucleus. Using the 4′,6-diamidino-2-phenylindole (DAPI) staining, we observed that the blue signal localized to the nucleus overlapped with the GFP signals (**Figure 2**). These results indicate that GhHAI2, GhAHG3, and GhABI2 have a functional role in the nucleus.

Silencing of *GhHAI2*, *GhAHG3,* and *GhABI2* Confers Osmotic Stress Tolerance in Cotton

To investigate the biological function of *GhHAI2, GhAHG3,* and *GhABI2* in responding to osmotic stress, we performed TRV-based virus-induced gene silencing (VIGS). Seven-day-old plants were hand-infiltrated using *Agrobacterium* cultures carrying VIGS vectors into cotton cotyledons. At 14 days post-infiltration (dpi), plants inoculated with TRV2:*GhCLA1*, a chlorophyll biosynthesis gene, exhibited obvious albino phenotype, which was uniformly distributed on entire true leaves (**Supplementary Figure S1A**). The expression levels of *GhHAI2*, *GhAHG3,* and *GhABI2* were significantly reduced in the silenced plants (TRV2:*GhHAI2*, TRV2:*GhAHG3,* and TRV2:*GhABI2*) than in control plants (TRV2:00; **Supplementary Figures S1B–D**). Subsequently, the VIGS plants were subjected to 15% PEG for 18 days and then re-watering for two days. Under well-watered

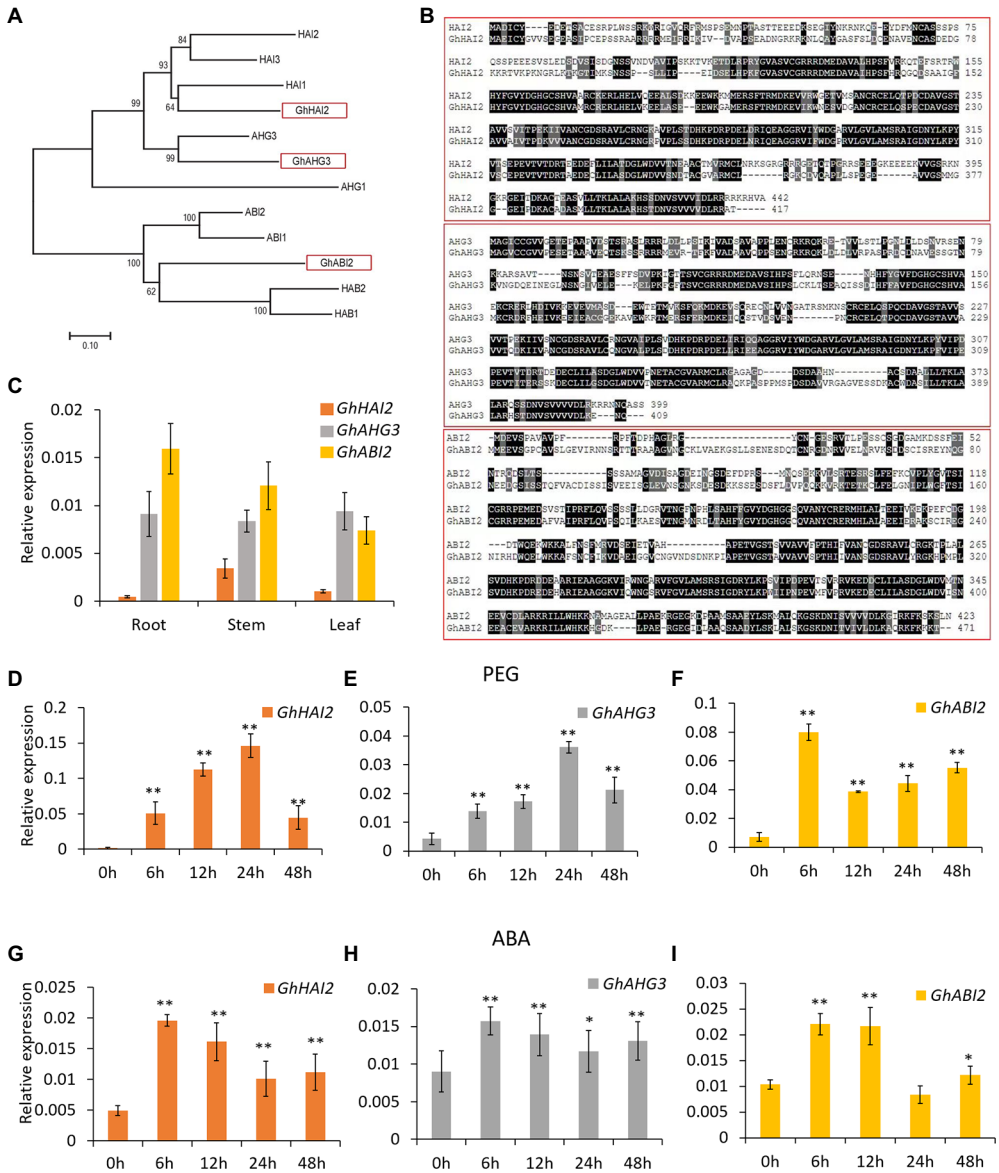


FIGURE 1 | Sequence analysis and expression pattern of *GhHAI2*, *GhAHG3,* and *GhABI2* in different tissues and after exposure to PEG and ABA. **(A)** Phylogenetic analysis of GhHAI2, GhAHG3, and GhABI2 and *Arabidopsis* group A PP2Cs. The neighbor-joining tree was constructed using MEGA software (version 7.0) based on multiple alignments of GhHAI2, GhAHG3, and GhABI2 protein sequence and their homologous proteins in *Arabidopsis*. **(B)** Comparisons of deduced amino acid sequence of GhHAI2, GhAHG3, and GhABI2 with those of *Arabidopsis*. Identical amino acid residues are highlighted in black. **(C)** qPCR analysis of *GhHAI2*, *GhAHG3,* and *GhABI2* genes expression levels in three different tissues. **(D–F)** PEG- and **(G–I)** ABA-induced expression pattern of *GhHAI2*, *GhAHG3,* and *GhABI2* genes. Bars represent means ± standard deviation of three biological replicates. Asterisks represent statistically significant differences compared with untreated control (0 h; Student's *t*-test; $^{*}p < 0.05$; $^{**}p < 0.01$).

conditions, no obvious difference was observed between TRV2:00 and TRV2:*GhHAI2*, TRV2:*GhAHG3,* and TRV2:*GhABI2* plants. However, after 10 days of PEG stress, TRV2:00 plants displayed serious wilting sooner than TRV2:*GhHAI2*, TRV2:*GhAHG3,* and TRV2:*GhABI2* plants. After further 8 days of water deficit condition and re-watering, *GhHAI2*-, *GhAHG3*-, and *GhABI2*-silenced plants displayed a stronger osmotic-tolerant phenotype in comparison with control plants (**Figure 3A**). At two days after re-watering, the survival rates of TRV2:*GhHAI2*, TRV2:*GhAHG3,* and TRV2:*GhABI2* plants were 53, 72, and 68%, respectively, whereas only 27% of TRV2:00 plants survived (**Figure 3B**). To determine whether the resistant phenotype to PEG stress exhibited by *GhHAI2*-, *GhAHG3*-, and *GhABI2*-silenced plants was caused by more water retention capacity, the water loss rate and RWC of detached cotton seedlings and leaves were measured. Consistently, the water loss was significantly lower in TRV2:*GhHAI2*, TRV2:*GhAHG3,* and TRV2:*GhABI2* plants compared with TRV2:00 plants (**Figure 3C**). In addition,

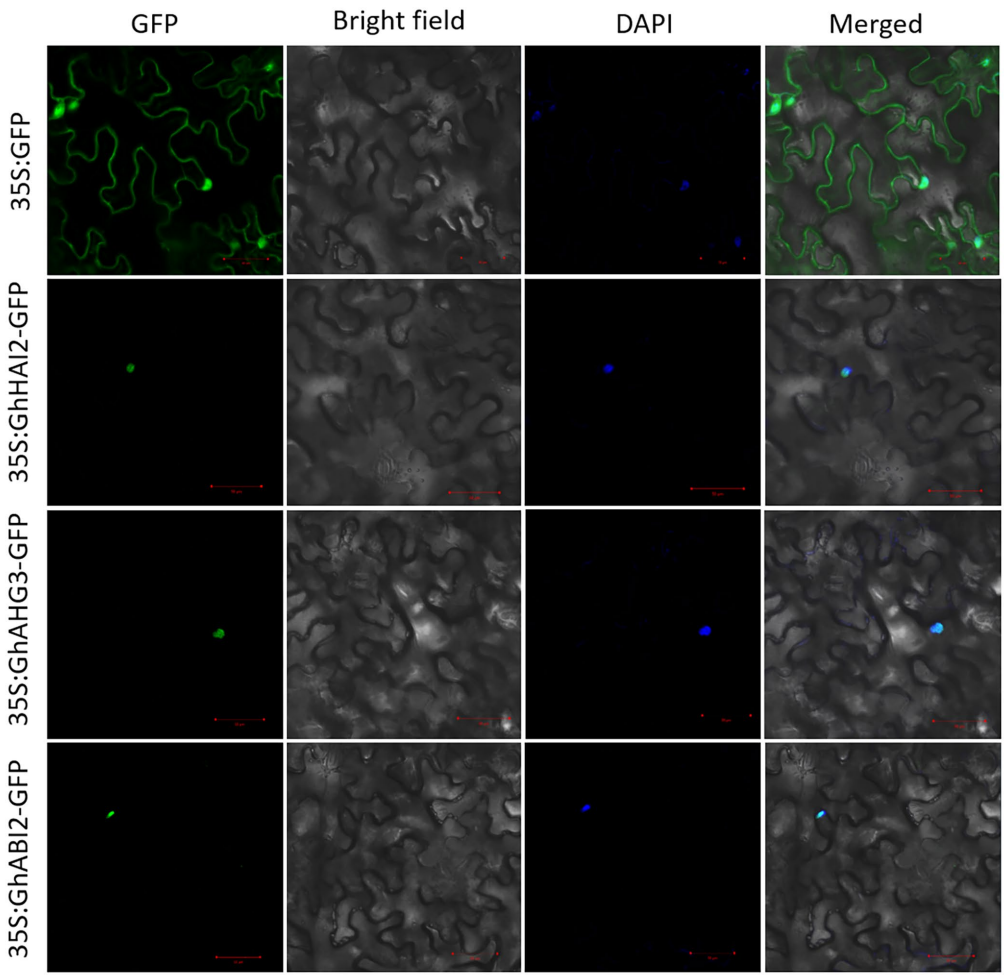


FIGURE 2 | Subcellular localization of GhHAI2, GhAHG3, and GhABI2 based on the transient expression of green fluorescent (GFP) fusion protein in the epidermal cells of *N. benthamiana*. The 35S:GhHAI2-GFP, 35S:GhAHG3-GFP, and 35S:GhABI2-GFP constructs were expressed in the leaves of *N. benthamiana* using agroinfiltration method. The GFP signal was observed using a confocal laser-scanning microscope. The DAPI staining was used as nucleus marker.

silencing of *GhHAI2*, *GhAHG3,* and *GhABI2* under PEG conditions caused more RWC (93, 94, and 94%, respectively) than TRV2:00 plants (72%) and well-watered conditions (**Figure 3D**).

Furthermore, to determine whether the osmotic tolerance in *GhHAI2*-, *GhAHG3*-, and *GhABI2*-silenced plants is associated with the alterations in leaf physiology, we compared photosynthetic gas exchange between TRV2:*GhHAI2*, TRV2:*GhAHG3,* and TRV2:*GhABI2* plants and TRV2:00 plants. Compared with normal watering conditions and TRV2:00 plants after PEG, all three genes silenced plants showed significantly increased photosynthetic rates that were approximately double than that of control plants (**Figure 3E**). Similarly, significant inductions in stomatal conductance, intracellular CO_2, and transpiration rate were also observed, indicating that *GhHAI2*-, *GhAHG3*-, and *GhABI2*-silenced plants were more tolerant to osmotic stress than control plants (**Figures 3F–H**). Taken together, these results indicate that silencing of *GhHAI2*, *GhAHG3,* and *GhABI2* in cotton plants significantly improved osmotic stress response.

Silencing of *GhHAI2*, *GhAHG3,* and *GhABI2* Probably Promotes ROS Scavenging and Increases Root Biomass

In order to determine whether antioxidative mechanism is involved in *GhHAI2*, *GhAHG3,* and *GhABI2* osmotic stress response, we detected the activity of three significant antioxidant enzymes in TRV2:00 and TRV2:*GhHAI2*, TRV2:*GhAHG3,* and TRV2:*GhABI2* plants. Under both normal and PEG conditions, peroxidase (POD) superoxide dismutase (SOD) and catalase (CAT) activity increased much more in *GhHAI2*-, *GhAHG3*-, and *GhABI2*-silenced plants compared with the control plants (**Figures 4A–C**). Further, the MDA, which is a byproduct of lipid peroxidation under oxidative stress, was measured and compared between normal and PEG stressed plants. The MDA content was significantly lower in *GhHAI2*-, *GhAHG3*-, and *GhABI2*-silenced plants under PEG conditions compared to the control plants, indicating that silenced plants were more tolerant to osmotic stress (**Figure 4D**). These results showed that TRV2:00 plants were more severely damaged by

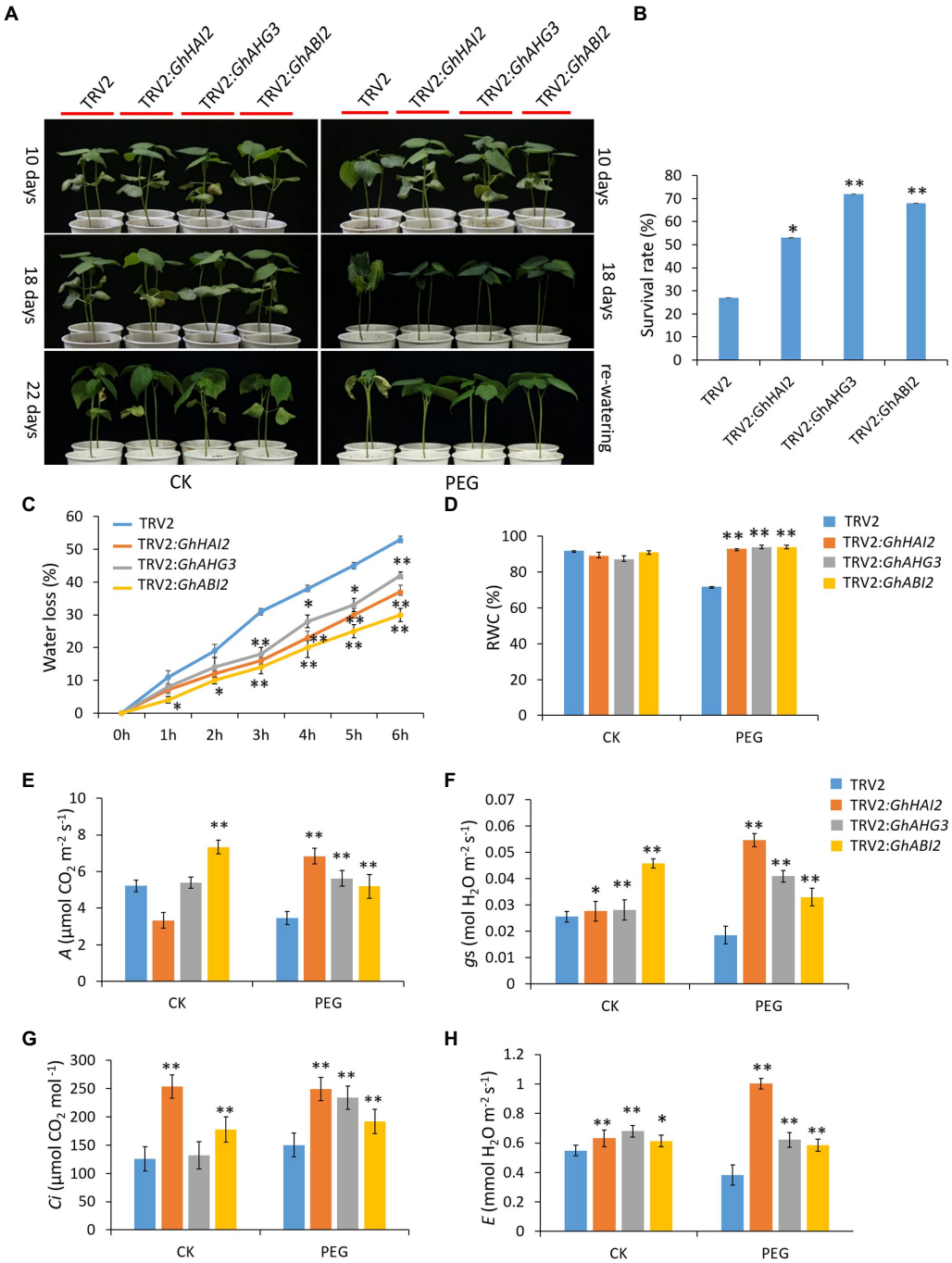


FIGURE 3 | *GhHAI2*, *GhAHG3,* and *GhABI2* genes negatively regulate cotton osmotic response. **(A)** Phenotypic observations on the *GhHAI2*-, *GhAHG3*-, and *GhABI2*-silenced and control plants under normal (left panel) and PEG conditions (right panel). Three-week old plants were subjected to PEG treatment for 18 days and re-watered for 2 days. **(B)** Percentage of surviving plants after re-watering for 2 days. **(C)** Water loss from TRV2:*GhHAI2*, TRV2:*GhAHG3,* and TRV2:*GhABI2* and TRV2:00 seedlings under PEG conditions. **(D)** Relative water content (RWC) in the leaves of TRV2:*GhHAI2*, TRV2:*GhAHG3,* and TRV2:*GhABI2* and TRV2:00 plants under normal and PEG conditions. **(E–H)** Analyses of gas exchange parameters including, photosynthetic rate (*A*), stomatal conductance (*gs*), intracellular CO_2 concentration (*Ci*), and transpiration rate (*E*) in TRV2:*GhHAI2*, TRV2:*GhAHG3,* and TRV2:*GhABI2* and TRV2:00 plants under normal and PEG conditions. Bars represent means ± standard deviation of three biological replicates. At least 30 plants were used for each biological replicate. Asterisks represent statistically significant difference between TRV2:*GhHAI2*, TRV2:*GhAHG3,* and TRV2:*GhABI2* and TRV2:00 plants (Student's *t*-test; $*p < 0.05$; $**p < 0.01$).

ROS, while silencing of *GhHAI2*, *GhAHG3,* and *GhABI2* protected the plants from damage. Hence, *GhHAI2*, *GhAHG3,* and *GhABI2* negatively participated in the ROS scavenging pathway by increasing the activity of POD, SOD, and CAT and decreasing the MDA level in the antioxidant system under osmotic stress.

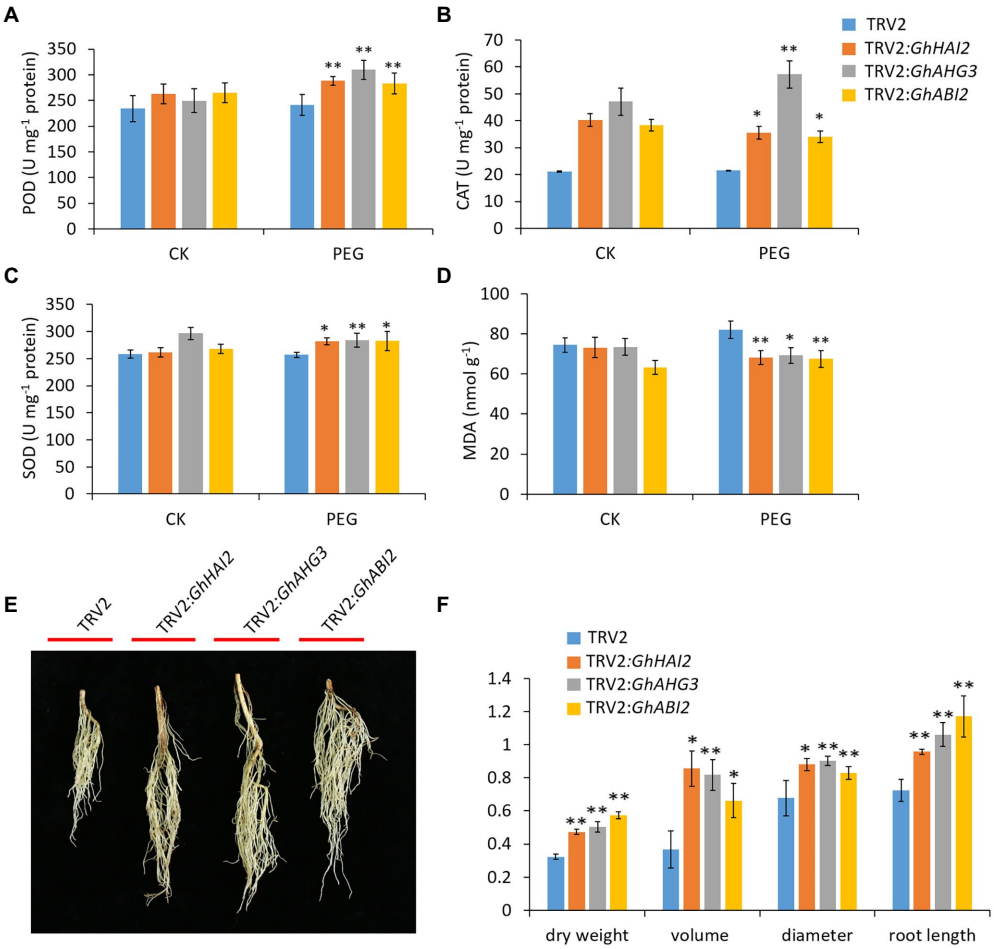


FIGURE 4 | Silencing of *GhHAI2*, *GhAHG3,* and *GhABI2* promotes ROS scavenging and increases root biomass. **(A–D)** Analyses of three antioxidant enzymes; SOD, POD, and CAT activities and MDA content in TRV2:*GhHAI2*, TRV2:*GhAHG3,* and TRV2:*GhABI2* and TRV2:00 plants under normal and PEG conditions. **(E)** Root phenotype and **(F)** the root dry weight, volume, diameter, and length of TRV2:*GhHAI2*, TRV2:*GhAHG3,* and TRV2:*GhABI2* and TRV2:00 plants under PEG conditions. Bars represent means ± standard deviation of three biological replicates. Asterisks represent statistically significant difference between TRV2:*GhHAI2*, TRV2:*GhAHG3,* and TRV2:*GhABI2* and TRV2:00 plants (Student's *t*-test; $*p<0.05$; $**p<0.01$).

Furthermore, VIGS cotton plants exhibited significant variation in root length and biomass accumulation. We measured the root volume, dry weight, length, and diameter of *GhHAI2*-, *GhAHG3*-, and *GhABI2*-silenced and control plants under PEG conditions. The roots of *GhHAI2*-, *GhAHG3*-, and *GhABI2*-silenced plants were denser and the volume, length, and dry weight increased relative to that of control plants. Thus, under PEG conditions, the silenced plants had more vigorous root phenotypes than the control plants, which is consistent with enhanced osmotic tolerance (**Figures 4E,F**).

GhHAI2, GhAHG3, and GhABI2 Interact With Cotton ABA Receptors GhPYLs

In *Arabidopsis*, physical protein–protein interaction between clade A PP2Cs and ABA receptors PYL/PYR/RCARs is one of the principal regulatory mechanisms of ABA signaling (Santiago et al., 2012). Hence, we hypothesized that GhHAI2, GhAHG3, and GhABI2 might interact with cotton ABA receptors and therefore performed a Y2H assay. Cotton possesses 40 PYL proteins, of which we selected GhPYL4, GhPYL6, GhPYL9-4D, and GhPYL9-6A (Zhang et al., 2017) (hereafter referred to as GhPYLs). GhHAI2, GhAHG3, and GhABI2 were fused to the binding domain of GaL4 and used as bait, while GhPYLs fused to the activation domain of GaL4 and were used as prey proteins. To ensure that GhHAI2, GhAHG3, and GhABI2 alone were not able to activate the yeast reporter genes, the bait constructs were first evaluated for self-activation. The preliminary experiment revealed that there was no auto-activation of reporter genes (**Figure 5A**); therefore, full-length sequences of GhHAI2, GhAHG3, and GhABI2 were used to perform Y2H. The GhHAI2, GhAHG3, and GhABI2 and GhPYLs were co-transformed in a pairwise fashion into yeast. Co-transformants expressing bait and prey were able to grow on SD/−Trp/−Leu/-His/−Ade

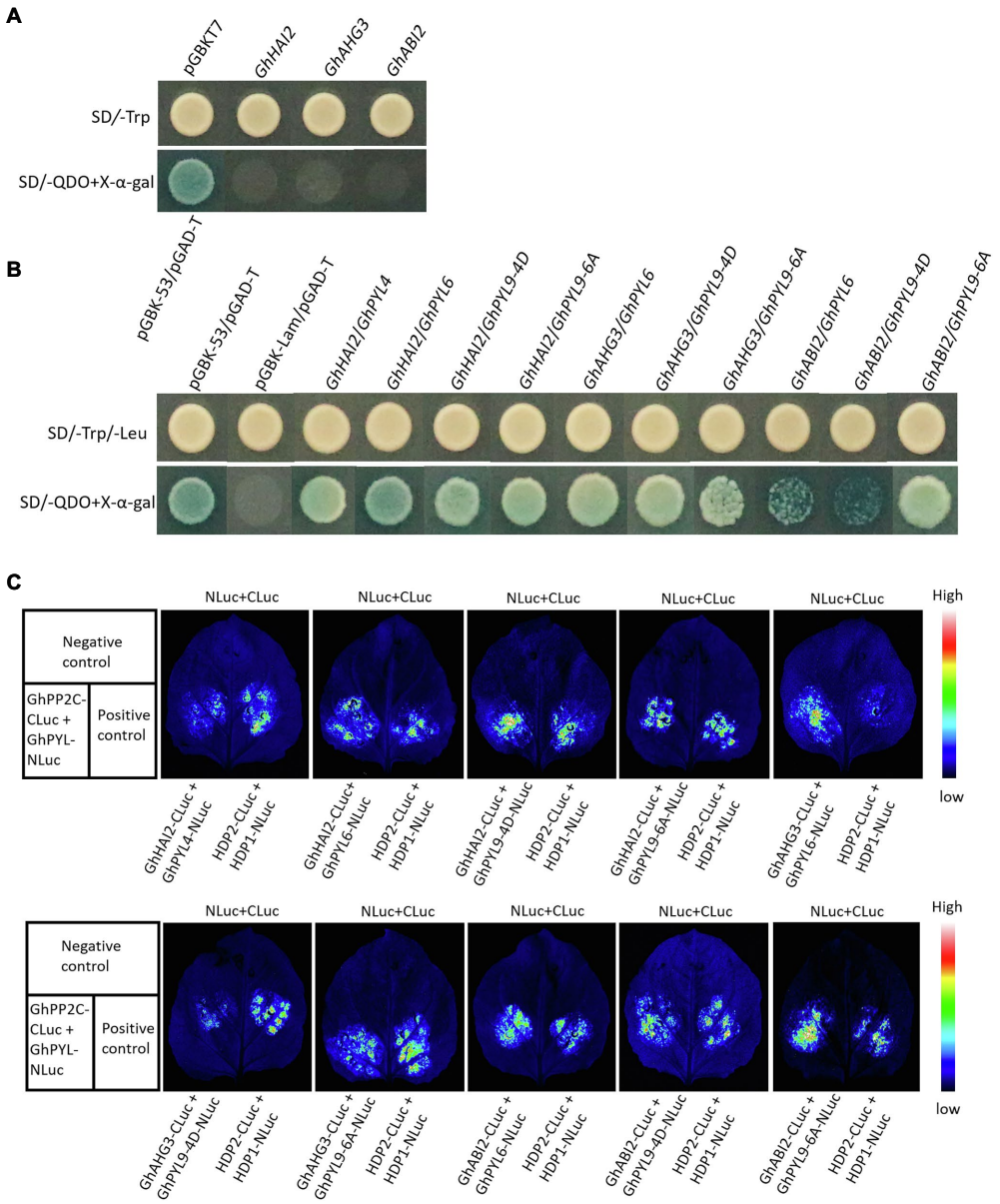


FIGURE 5 | Interaction between GhHAI2, GhAHG3, and GhABI2 and ABA receptors GhPYLs. **(A)** Determination of self-activation of GhHAI2, GhAHG3, and GhABI2 in the absence of prey. **(B)** Interaction of GhHAI2, GhAHG3, and GhABI2 and GhPYLs in yeast two-hybrid assay (Y2H). The yeast strain AH109 harboring the construct pairs were plated on synthetic dropout medium either without Trp and Leu (upper panel) or without Trp, Leu, His, and Ade (SD/-QDO) containing X-α-gal (lower panel). The vectors pGBKT7-53/pGADT7-T and pGBKT7-Lam/pGADT7-T were used as positive and negative controls, respectively. **(C)** Luciferase (LUC) complementation imaging assay for analyzing the protein–protein interaction between GhHAI2, GhAHG3, and GhABI2 and GhPYLs. The specific combinations used for each interaction are indicated. The fluorescence signals represent their interaction activities.

(SD/-QDO) selection medium containing X-α-galactosidase (X-α-gal), indicating the direct interaction of GhHAI2, GhAHG3, and GhABI2 and GhPYLS. Of the all co-transformants, GhAHG3/GhPYL4 and GhABI2/GhPYL4 did not grow on the selection medium, suggesting that GhAHG3 and GhABI2 do not directly interact with GhPYL4 (**Figure 5B**).

The binary protein–protein interactions were further examined *in planta* using LCI assays. Co-expression of GhHAI2-CLuc, GhAHG3-CLuc, and GhABI2-CLuc and GhPYLs-NLuc in *N. benthamiana* strongly complemented the LUC activity similar to the positive control HDP2-CLuc/HDP1-NLuc, confirming the interaction between GhHAI2, GhAHG3, and GhABI2 and GhPYLs (**Figure 5C**). The negative control (NLuc/CLuc) showed no visible fluorescence in tobacco leaves. Collectively, these results suggest that GhHAI2, GhAHG3, and GhABI2 interact with cotton GhPYLs and are involved in ABA signaling pathway.

GhHAI2, GhAHG3, and *GhABI2* Regulate ABA-Dependent Stress-Responsive Gene Expression

Previous studies have revealed that the phytohormone ABA is essential for plant drought response (Xiong et al., 2006). Since clade A *PP2C* family genes have been reported to regulate plant drought stress in an ABA-dependent manner (Schweighofer et al., 2004; Antoni et al., 2012; Rodrigues et al., 2013); thus, in order to further confirm the role of *GhHAI2*, *GhAHG3,* and *GhABI2* in ABA pathway, we detected the expression level of ABA-dependent genes in *GhHAI2*-, *GhAHG3*-, and *GhABI2*-silenced cotton leaves *via* qPCR. Notably, silencing of *GhHAI2*, *GhAHG3,* and *GhABI2* exerted dramatically upregulated expression in *GhABF1, GhABF2,* and *GhABF3* (*GhABFs*) in response to osmotic stress (**Figures 6A–C**). However, silencing of *GhHAI2, GhAHG3,* and *GhABI2* had less effect on the induction of cotton dehydration-responsive element-binding protein 2 (*GhDREB2*) after osmotic stress (**Figure 6D**). ABFs and DREBs are the two major groups of transcription factors that are involved in the ABA-dependent and ABA-independent drought responses, respectively (Yoshida et al., 2014). Apparently, *GhHAI2, GhAHG3,* and *GhABI2* exerted a stronger effect on osmotic-induced expression of *GhABFs* than that of *GhDREB2*, suggesting that *GhHAI2, GhAHG3,* and *GhABI2* regulate cotton osmotic response in ABA-dependent manner. Based on this, we next examined the expression levels of ABA biosynthesis genes in *GhHAI2*-, *GhAHG3*-, and *GhABI2*-silenced cotton leaves under osmotic conditions. *GhNCED3a* and *GhNCED3c* are the orthologues of *Arabidopsis* key ABA biosynthetic gene *AtNCED3* in cotton (Jensen et al., 2013; Shang et al., 2020). Consistently, the transcripts of *GhNCED3a* and *GhNCED3c* were found to be significantly upregulated in *GhHAI2*-, *GhAHG3*-, and *GhABI2*-silenced plants after osmotic stress, compared to the control plants (**Figures 6E,F**). According to these observations, *GhHAI2*, *GhAHG3,* and *GhABI2* modulate osmotic stress by regulating

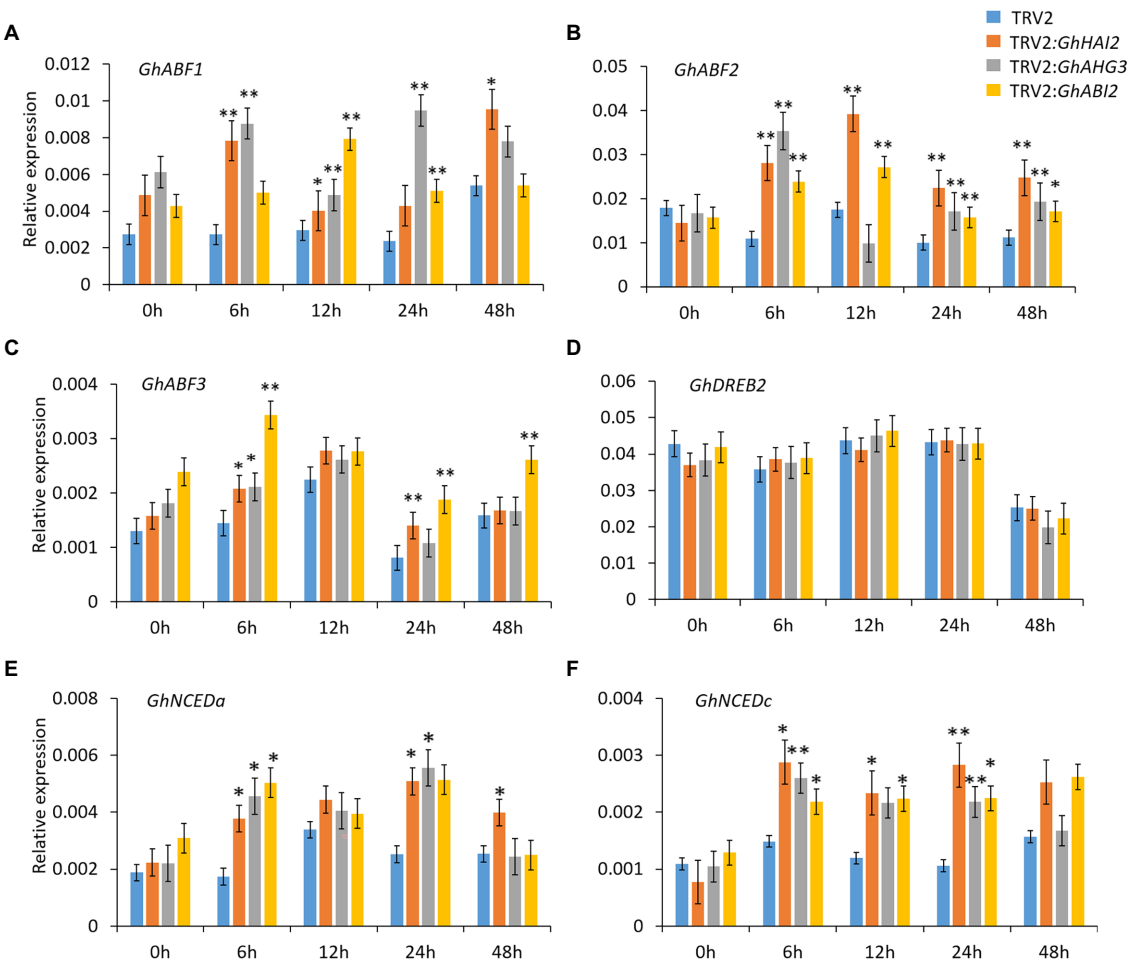


FIGURE 6 | *GhHAI2*, *GhAHG3,* and *GhABI2* regulate ABA-dependent gene expression. **(A–C)** qPCR expression analysis of ABA-dependent and **(D)** ABA-independent stress-responsive genes in TRV2:*GhHAI2*, TRV2:*GhAHG3,* and TRV2:*GhABI2* and TRV2:00 plants under PEG conditions. **(E,F)** Expression levels of ABA biosynthesis genes in TRV2:*GhHAI2*, TRV2:*GhAHG3,* and TRV2:*GhABI2* and TRV2:00 plants under PEG conditions. The transcript levels were normalized by *GhHistone*. Bars represent means ± standard deviation of three biological replicates. Asterisks represent statistically significant difference between TRV2:*GhHAI2*, TRV2:*GhAHG3,* and TRV2:*GhABI2* and TRV2:00 plants (Student's *t*-test; $*p < 0.05$; $**p < 0.01$).

ABA signaling pathway, probably by targeting ABA-dependent stress-responsive and ABA biosynthesis genes.

DISCUSSION

With rising water scarcity and global climate change, drought is emerging as a significant factor for limiting crop production (Zhu, 2002). Particularly, cotton production is challenged by drought stress, the reason for this may be due to more than half of the world's cotton is produced in high water-stressed regions. Thus, there is an imperative need of understanding the molecular and genetic basis underlying cotton drought response for the development of cultivars with improved tolerance.

The plant hormone ABA plays a crucial role in many plant cellular processes, such as growth, development, and adaptation to abiotic stress (Osakabe et al., 2014). Under water deficit conditions, ABA regulates abiotic stress responses by inducing a large number of stress-related genes (Kilian et al., 2007). Previous studies have investigated the ABA signaling pathway from perception of ABA to response to stimulus (Lee and Luan, 2012). The RCAR-PP2C-SnRK2 cascade is the most well-studied ABA signaling pathway (Cutler et al., 2010). The perception of ABA by receptors and other signaling components including PP2Cs and SnRKs is critical for abiotic stress adaptation (Santiago et al., 2009; Vlad et al., 2009; Gonzalez-Guzman et al., 2012; Lim et al., 2013; Ding et al., 2015). The *Arabidopsis* group A PP2Cs have been known to function as negative regulators in ABA pathway (Saez et al., 2004; Schweighofer et al., 2004). Similarly, cotton plants presumably possess a number of drought and ABA-induced PP2Cs (Lu et al., 2019). To comprehend the importance of *PP2C* gene family in drought tolerance, we characterized three cotton clade A *PP2Cs*; *GhHAI2*, *GhAHG3,* and *GhABI2*, all of which have high sequence similarity to the *Arabidopsis* homologs *HAI2*, *AHG3,* and *ABI2*, respectively. We showed that GhHAI2, GhAHG3, and GhABI2 are nuclear-localized proteins which are responsive to PEG and ABA treatment in cotton plants. The reason for this may be due to similar functions to *Arabidopsis* group A *PP2Cs* for inducing altered phenotypes in response to ABA and drought stress, as well as their interactions with ABA signaling components.

To elucidate the role of *GhHAI2*, *GhAHG3,* and *GhABI2*, we conducted VIGS genetic analysis in cotton plants. In our phenotypic assays, *GhHAI2-*, *GhAHG3-,* and *GhABI2*-silenced plants displayed a pronounced osmotic-tolerant phenotype, which was accompanied by high RWC and increased photosynthetic gas exchange. Hence, these parameters collectively suggest that reduced expression of *GhHAI2*, *GhAHG3,* and *GhABI2* enhance the cotton plants resistance to osmotic stress.

Abiotic stresses led to oxidative damage and accumulation of MDA in plants (Alexieva et al., 2001; Hu et al., 2012). In cotton, drought stress caused the production of ROS. While, the antioxidant enzyme activity increased and regulated the ROS scavenging mechanism until the plants recovered from the stress (Ratnayaka et al., 2003). *CsATAF1-OE* plants promoted drought tolerance by enhancing the activity of antioxidant enzymes and decreasing MDA content in cucumber (Wang et al., 2018). Consistently, in our study, silencing of *GhHAI2*, *GhAHG3,* and *GhABI2* protected the plants against oxidative damage by increasing the activity of SOD, POD, and CAT and less MDA accumulation under osmotic stress.

Furthermore, we analyzed the root phenotype of VIGS plants after osmotic stress. Drought tolerance was found to be improved by root thickness, since roots can increase water absorption by encouraging root length density and growing larger root branches (Jeong et al., 2010). Under osmotic stress conditions, *GhHAI2-*, *GhAHG3-,* and *GhABI2*-silenced plants maintained their root growth, in terms of root length, volume, and root density. Additionally, the dry weight of *GhHAI2-*, *GhAHG3-,* and *GhABI2*-silenced plants was also higher than that of control plants. Hence, we propose that *GhHAI2-*, *GhAHG3-,* and *GhABI2*-mediated root modification enhance water uptake by increasing the total root surface area. Overexpression of *AtEDT1/HDG11* and *HYR* in rice has previously been shown to improve drought tolerance through such root-mediated system (Yu et al., 2013; Ambavaram et al., 2014). Collectively, these results suggest that silencing of *GhHAI2*, *GhAHG3,* and *GhABI2* enhances the cotton response to osmotic stress.

The interaction between PP2C and the ABA receptor PYL is the key step that triggers the downstream signaling genes to evoke ABA signaling (Fujii et al., 2009). This signaling network has been reported in different plants species such as *Arabidopsis* (Ma et al., 2009), rice (Kim et al., 2011), tomato (González-Guzmán et al., 2014), and cucumber (Wang et al., 2012). Several studies have shown the interaction between ABI1, ABI2, HABI, and AHG3 and RCAR/PYR/PYL family of ABA receptors (Ma et al., 2009; Park et al., 2009; Vlad et al., 2009). For instance, AHG3 interacts with PYL12 in response to ABA and functions specifically in seed germination and early seedling growth (Kuhn et al., 2006; Yoshida et al., 2006; Kim et al., 2011). *ABI2* has been reported to transduce ABA signals to downstream targets through selectively interplaying with PYL9/RCAR1 (Ma et al., 2009). The HAI PP2Cs interacted with PYL5 and PYL7-10 in *Arabidopsis* (Bhaskara et al., 2012). Similarly, the cotton GhPYLs are thought to interact with and inhibit GhHAI2, GhAHG3, and GhABI2, thereby activating ABA signaling pathway. Consistent with the previously reported studies, the physical interaction between GhHAI2, GhAHG3, and GhABI2 and GhPYLs was confirmed by Y2H and LCI assays. The results show that GhPYLs act as potent inhibitors of GhHAI2, GhAHG3, and GhABI2 phosphatase activity. Hence, the interaction between ABA receptors and GhHAI2, GhAHG3, and GhABI2 is necessary for the activation of downstream targets in regulating osmotic stress response.

Under water deficit conditions, plants evoke defense mechanisms *via* induction of elevated levels of ABA to moderate water consumption and enhance stress tolerance (Urano et al., 2009). The expression of drought stress-responsive genes is regulated by both ABA-dependent as well as ABA-independent pathways (Yamaguchi-Shinozaki and Shinozaki, 2006). ABFs are the bZIP family transcription factors that play pivotal role in ABA-dependent gene expression and are known as positive regulators of ABA pathway (Uno et al., 2000; Yoshida et al., 2010, 2014). Further, DREBs are large family of transcription

factors that mediate drought stress through an ABA-independent pathway (Yoshida et al., 2014). Our results reveal that silencing of *GhHAI2*, *GhAHG3*, and *GhABI2* significantly increased the expression of ABA-dependent stress marker genes *GhABFs* than the ABA-independent *GhDREB2* marker gene. The expression of ABA biosynthesis genes *NCED* positively regulates the endogenous ABA levels and the transcription of both ABA- and drought-inducible genes (Iuchi et al., 2001). We found that the expression levels of the ABA biosynthesis genes *GhNCEDa* and *GhNCEDc* vary significantly between control and *GhHAI2*-, *GhAHG3*-, and *GhABI2*-silenced plants, which was consistent with the enhanced induction of *NCED3* expression in the *HAI* double and triple mutants (Bhaskara et al., 2012). These results showed that *GhHAI2*, *GhAHG3*, and *GhABI2* involved in the ABA signaling pathway by upregulating ABA-responsive genes.

CONCLUSION

In conclusion, we have demonstrated that *GhHAI2*, *GhAHG3,* and *GhABI2* negatively regulate the plant adaptive response to osmotic stress *via* ABA-mediated signaling. In our VIGS genetic studies, *GhHAI2*, *GhAHG3,* and *GhABI2* displayed altered phenotypes in response to osmotic stress *via* changes in leaf physiology and root morphology and regulating ROS scavenging. Further, we have demonstrated that GhHAI2, GhAHG3, and GhABI2 act as core components of ABA signaling *via* interaction with ABA receptors. Hence, our findings provide valuable insights into the defense mechanism that occurs during osmotic stress and therefore may facilitate that these genes might be essential for drought tolerance in cotton; however, it needs further evaluation under drought stress. Furthermore, the utilization of *GhHAI2*, *GhAHG3,* and *GhABI2* mutations through genome editing techniques might also be effective.

DATA AVAILABILITY STATEMENT

The original contributions presented in the study are included in the article/**Supplementary Material**; further inquiries can be directed to the corresponding author.

AUTHOR CONTRIBUTIONS

HS conceived the study, designed the experiments, performed the experiments, interpreted the data, made figures, and wrote the manuscript. NK reviewed and edited the manuscript. LW provided assistance in qPCR analysis. XW supervised the project. All authors contributed to the article and approved the submitted version.

FUNDING

This work was supported by the funding of Xinjiang Uygur Autonomous Region Major Science and Technology Project (2021A02001-3).

SUPPLEMENTARY MATERIAL

The Supplementary Material for this article can be found online at: https://www.frontiersin.org/articles/10.3389/fpls.2022.905181/full#supplementary-material

Supplementary Table S1 | List of primer sequences used in this study.

Supplementary Figure S1 | (A) Albino appearance on the leaves of TRV2:*GhCLA1* plants. **(B–D)** Verification of *GhHAI2*, *GhAHG3*, and *GhABI2* silencing in VIGS plants by qPCR.

REFERENCES

Alexieva, V., Sergiev, I., Mapelli, S., and Karanov, E. (2001). The effect of drought and ultraviolet radiation on growth and stress markers in pea and wheat. *Plant Cell Environ.* 24, 1337–1344. doi: 10.1046/j.1365-3040.2001.00778.x

Ambavaram, M. M., Basu, S., Krishnan, A., Ramegowda, V., Batlang, U., Rahman, L., et al. (2014). Coordinated regulation of photosynthesis in Rice increases yield and tolerance to environmental stress. *Nat. Commun.* 5:5302. doi: 10.1038/ncomms6302

Antoni, R., Gonzalez-Guzman, M., Rodriguez, L., Rodrigues, A., Pizzio, G. A., and Rodriguez, P. L. (2012). Selective inhibition of clade A phosphatases type 2C by PYR/PYL/RCAR abscisic acid receptors. *Plant Physiol.* 158, 970–980. doi: 10.1104/pp.111.188623

Bhaskara, G. B., Nguyen, T. T., and Verslues, P. E. (2012). Unique drought resistance functions of the highly ABA-induced clade A protein phosphatase 2Cs. *Plant Physiol.* 160, 379–395. doi: 10.1104/pp.112.202408

Chen, C., Yu, Y., Ding, X., Liu, B., Duanmu, H., Zhu, D., et al. (2018). Genome-wide analysis and expression profiling of PP2C clade D under saline and alkali stresses in wild soybean and *Arabidopsis*. *Protoplasma* 255, 643–654. doi: 10.1007/s00709-017-1172-2

Choudhury, S., Panda, P., Sahoo, L., and Panda, S. K. (2013). Reactive oxygen species signaling in plants under abiotic stress. *Plant Signal. Behav.* 8:e23681. doi: 10.4161/psb.23681

Choudhury, F. K., Rivero, R. M., Blumwald, E., and Mittler, R. (2017). Reactive oxygen species, abiotic stress and stress combination. *Plant J.* 90, 856–867. doi: 10.1111/tpj.13299

Claeys, H., and Inzé, D. (2013). The agony of choice: how plants balance growth and survival under water-limiting conditions. *Plant Physiol.* 162, 1768–1779. doi: 10.1104/pp.113.220921

Cutler, S. R., Rodriguez, P. L., Finkelstein, R. R., and Abrams, S. R. (2010). Abscisic acid: emergence of a core signaling network. *Annu. Rev. Plant Biol.* 61, 651–679. doi: 10.1146/annurev-arplant-042809-112122

Ding, Y., Li, H., Zhang, X., Xie, Q., Gong, Z., and Yang, S. (2015). *OST1* kinase modulates freezing tolerance by enhancing ICE1 stability in *Arabidopsis*. *Dev. Cell* 32, 278–289. doi: 10.1016/j.devcel.2014.12.023

Fujii, H., Chinnusamy, V., Rodrigues, A., Rubio, S., Antoni, R., Park, S. Y., et al. (2009). *In vitro* reconstitution of an abscisic acid signalling pathway. *Nature* 462, 660–664. doi: 10.1038/nature08599

Fujita, Y., Nakashima, K., Yoshida, T., Katagiri, T., Kidokoro, S., Kanamori, N., et al. (2009). Three SnRK2 protein kinases are the main positive regulators of abscisic acid signaling in response to water stress in *Arabidopsis*. *Plant Cell Physiol.* 50, 2123–2132. doi: 10.1093/pcp/pcp147

Gao, X., Li, F., Li, M., Kianinejad, A. S., Dever, J. K., Wheeler, T. A., et al. (2013). Cotton *GhBAK1* mediates *Verticillium* wilt resistance and cell death. *J. Integr. Plant Biol.* 55, 586–596. doi: 10.1111/jipb.12064

Gao, X., Wheeler, T., Li, Z., Kenerley, C. M., He, P., and Shan, L. (2011). Silencing *GhNDR1* and *GhMKK2* compromises cotton resistance to *Verticillium* wilt. *Plant J.* 66, 293–305. doi: 10.1111/j.1365-313X.2011.04491.x

Gonzalez-Guzman, M., Pizzio, G. A., Antoni, R., Vera-Sirera, F., Merilo, E., Bassel, G. W., et al. (2012). *Arabidopsis* PYR/PYL/RCAR receptors play a major role in quantitative regulation of stomatal aperture and transcriptional response to abscisic acid. *Plant Cell* 24, 2483–2496. doi: 10.1105/tpc.112.098574

González-Guzmán, M., Rodríguez, L., Lorenzo-Orts, L., Pons, C., Sarrión-Perdigones, A., Fernández, M. A., et al. (2014). Tomato PYR/PYL/RCAR abscisic acid receptors show high expression in root, differential sensitivity to the abscisic acid agonist quinabactin, and the capability to enhance plant drought resistance. *J. Exp. Bot.* 65, 4451–4464. doi: 10.1093/jxb/eru219

Hanin, M., Brini, F., Ebel, C., Toda, Y., Takeda, S., and Masmoudi, K. (2011). Plant dehydrins and stress tolerance: versatile proteins for complex mechanisms. *Plant Signal. Behav.* 6, 1503–1509. doi: 10.4161/psb.6.10.17088

He, Z., Wu, J., Sun, X., and Dai, M. (2019). The maize clade A PP2C phosphatases play critical roles in multiple abiotic stress responses. *Int. J. Mol. Sci.* 20:3573. doi: 10.3390/ijms20143573

Hu, L., Li, H., Pang, H., and Fu, J. (2012). Responses of antioxidant gene, protein and enzymes to salinity stress in two genotypes of perennial ryegrass (*Lolium perenne*) differing in salt tolerance. *J. Plant Physiol.* 169, 146–156. doi: 10.1016/j.jplph.2011.08.020

Iuchi, S., Kobayashi, M., Taji, T., Naramoto, M., Seki, M., Kato, T., et al. (2001). Regulation of drought tolerance by gene manipulation of 9-cis-epoxycarotenoid dioxygenase, a key enzyme in abscisic acid biosynthesis in *Arabidopsis*. *Plant J.* 27, 325–333. doi: 10.1046/j.1365-313x.2001.01096.x

Jensen, M. K., Lindemose, S., De Masi, F., Reimer, J. J., Nielsen, M., Perera, V., et al. (2013). *ATAF1* transcription factor directly regulates abscisic acid biosynthetic gene *NCED3* in *Arabidopsis thaliana*. *FEBS Open Bio.* 3, 321–327. doi: 10.1016/j.fob.2013.07.006

Jeong, J. S., Kim, Y. S., Baek, K. H., Jung, H., Ha, S. H., Do Choi, Y., et al. (2010). Root-specific expression of *OsNAC10* improves drought tolerance and grain yield in rice under field drought conditions. *Plant Physiol.* 153, 185–197. doi: 10.1104/pp.110.154773

Khan, N., Ke, H., Hu, C. M., Naseri, E., Haider, M. S., Ayaz, A., et al. (2019). Genome-wide identification, evolution, and transcriptional profiling of *PP2C* gene family in *Brassica rapa*. *Biomed. Res. Int.* 2019, 1–15. doi: 10.1155/2019/2965035

Kilian, J., Whitehead, D., Horak, J., Wanke, D., Weinl, S., Batistic, O., et al. (2007). The AtGenExpress global stress expression data set: protocols, evaluation and model data analysis of UV-B light, drought and cold stress responses. *Plant J.* 50, 347–363. doi: 10.1111/j.1365-313X.2007.03052.x

Kim, H., Hwang, H., Hong, J.-W., Lee, Y.-N., Ahn, I. P., Yoon, I. S., et al. (2011). A rice orthologue of the ABA receptor, *OsPYL/RCAR5*, is a positive regulator of the ABA signal transduction pathway in seed germination and early seedling growth. *J. Exp. Bot.* 63, 1013–1024. doi: 10.1093/jxb/err338

Kim, W., Lee, Y., Park, J., Lee, N., and Choi, G. (2013). HONSU, a protein phosphatase 2C, regulates seed dormancy by inhibiting ABA signaling in *Arabidopsis*. *Plant Cell Physiol.* 54, 555–572. doi: 10.1093/pcp/pct017

Koornneef, M., Reuling, G., and Karssen, C. M. (1984). The isolation and characterization of abscisic acid-insensitive mutants of *Arabidopsis thaliana*. *Physiol. Plant.* 61, 377–383. doi: 10.1111/j.1399-3054.1984.tb06343.x

Kuhn, J. M., Boisson-Dernier, A., Dizon, M. B., Maktabi, M. H., and Schroeder, J. I. (2006). The protein phosphatase *AtPP2CA* negatively regulates abscisic acid signal transduction in *Arabidopsis*, and effects of *abh1* on *AtPP2CA* mRNA. *Plant Physiol.* 140, 127–139. doi: 10.1104/pp.105.070318

Kumar, S., Li, G., Yang, J., Huang, X., Ji, Q., Zhou, K., et al. (2020). Investigation of an antioxidative system for salinity tolerance in *Oenanthe javanica*. *Antioxidants* 9:940. doi: 10.3390/antiox9100940

Lee, S. C., and Luan, S. (2012). ABA signal transduction at the crossroad of biotic and abiotic stress responses. *Plant Cell Environ.* 35, 53–60. doi: 10.1111/j.1365-3040.2011.02426.x

Leonhardt, N., Kwak, J. M., Robert, N., Waner, D., Leonhardt, G., and Schroeder, J. I. (2004). Microarray expression analyses of *Arabidopsis* guard cells and isolation of a recessive abscisic acid hypersensitive protein phosphatase 2C mutant. *Plant Cell* 16, 596–615. doi: 10.1105/tpc.019000

Li, C., Shen, H., Wang, T., and Wang, X. (2015). ABA regulates subcellular redistribution of *OsABI-LIKE2*, a negative regulator in ABA signaling, to control root architecture and drought resistance in *Oryza sativa*. *Plant Cell Physiol.* 56, 2396–2408. doi: 10.1093/pcp/pcv154

Lim, C. W., Baek, W., Han, S. W., and Lee, S. C. (2013). *Arabidopsis* PYL8 plays an important role for ABA signaling and drought stress responses. *Plant Pathol. J.* 29, 471–476. doi: 10.5423/PPJ.NT.07.2013.0071

Livak, K. J., and Schmittgen, T. D. (2001). Analysis of relative gene expression data using real-time quantitative pcr and the $2^{-\Delta\Delta CT}$ method. *Methods* 25, 402–408. doi: 10.1006/meth.2001.1262

Lu, T., Zhang, G., Wang, Y., He, S., Sun, L., and Hao, F. (2019). Genome-wide characterization and expression analysis of PP2CA family members in response to ABA and osmotic stress in *Gossypium*. *PeerJ* 7:e7105. doi: 10.7717/peerj.7105

Ma, Y., Szostkiewicz, I., Korte, A., Moes, D., Yang, Y., Christmann, A., et al. (2009). Regulators of PP2C phosphatase activity function as abscisic acid sensors. *Science* 324, 1064–1068. doi: 10.1126/science.1172408

Merlot, S., Gosti, F., Guerrier, D., Vavasseur, A., and Giraudat, J. (2001). The ABI1 and ABI2 protein phosphatases 2C act in a negative feedback regulatory loop of the abscisic acid signalling pathway. *Plant J.* 25, 295–303. doi: 10.1046/j.1365-313x.2001.00965.x

Nakashima, K., and Yamaguchi-Shinozaki, K. (2006). Regulons involved in osmotic stress-responsive and cold stress-responsive gene expression in plants. *Physiol. Plant.* 126, 62–71. doi: 10.1111/j.1399-3054.2005.00592.x

Nakashima, K., and Yamaguchi-Shinozaki, K. (2013). ABA signaling in stress-response and seed development. *Plant Cell Rep.* 32, 959–970. doi: 10.1007/s00299-013-1418-1

Née, G., Kramer, K., Nakabayashi, K., Yuan, B., Xiang, Y., Miatton, E., et al. (2017). Delay of germination1 requires PP2C phosphatases of the ABA signalling pathway to control seed dormancy. *Nat. Commun.* 8:72. doi: 10.1038/s41467-017-00113-6

Nishimura, N., Yoshida, T., Kitahata, N., Asami, T., Shinozaki, K., and Hirayama, T. (2007). ABA-hypersensitive germination1 encodes a protein phosphatase 2C, an essential component of abscisic acid signaling in *Arabidopsis* seed. *Plant J.* 50, 935–949. doi: 10.1111/j.1365-313X.2007.03107.x

Osakabe, Y., Osakabe, K., Shinozaki, K., and Tran, L. S. (2014). Response of plants to water stress. *Front. Plant Sci.* 5:86. doi: 10.3389/fpls.2014.00086

Park, S. Y., Fung, P., Nishimura, N., Jensen, D. R., Fujii, H., Zhao, Y., et al. (2009). Abscisic acid inhibits type 2C protein phosphatases via the PYR/PYL family of START proteins. *Science* 324, 1068–1071. doi: 10.1126/science.1173041

Pettigrew, W. T. (2004). Physiological consequences of moisture deficit stress in cotton. *Crop Sci.* 44, 1265–1272. doi: 10.2135/cropsci2004.1265

Ratnayaka, H. H., Molin, W. T., and Sterling, T. M. (2003). Physiological and antioxidant responses of cotton and spurred anoda under interference and mild drought. *J. Exp. Bot.* 54, 2293–2305. doi: 10.1093/jxb/erg251

Rodrigues, A., Adamo, M., Crozet, P., Margalha, L., Confraria, A., Martinho, C., et al. (2013). ABI1 and PP2CA phosphatases are negative regulators of Snf1-related protein kinase1 signaling in *Arabidopsis*. *Plant Cell* 25, 3871–3884. doi: 10.1105/tpc.113.114066

Rubio, S., Rodrigues, A., Saez, A., Dizon, M. B., Galle, A., Kim, T.-H., et al. (2009). Triple loss of function of protein phosphatases type 2C leads to partial constitutive response to endogenous abscisic acid. *Plant Physiol.* 150, 1345–1355. doi: 10.1104/pp.109.137174

Saez, A., Apostolova, N., Gonzalez-Guzman, M., Gonzalez-Garcia, M. P., Nicolas, C., Lorenzo, O., et al. (2004). Gain-of-function and loss-of-function phenotypes of the protein phosphatase 2C HAB1 reveal its role as a negative regulator of abscisic acid signalling. *Plant J.* 37, 354–369. doi: 10.1046/j.1365-313X.2003.01966.x

Santiago, J., Dupeux, F., Betz, K., Antoni, R., Gonzalez-Guzman, M., Rodriguez, L., et al. (2012). Structural insights into PYR/PYL/RCAR ABA receptors and PP2Cs. *Plant Sci.* 182, 3–11. doi: 10.1016/j.plantsci.2010.11.014

Santiago, J., Rodrigues, A., Saez, A., Rubio, S., Antoni, R., Dupeux, F., et al. (2009). Modulation of drought resistance by the abscisic acid receptor PYL5 through inhibition of clade A PP2Cs. *Plant J.* 60, 575–588. doi: 10.1111/j.1365-313X.2009.03981.x

Schweighofer, A., Hirt, H., and Meskiene, I. (2004). Plant PP2C phosphatases: emerging functions in stress signaling. *Trends Plant Sci.* 9, 236–243. doi: 10.1016/j.tplants.2004.03.007

Shang, X., Yu, Y., Zhu, L., Liu, H., Chai, Q., and Guo, W. (2020). A cotton NAC transcription factor *GhirNAC2* plays positive roles in drought tolerance via regulating ABA biosynthesis. *Plant Sci.* 296:110498. doi: 10.1016/j.plantsci.2020.110498

Shazadee, H., Khan, N., Wang, J., Wang, C., Zeng, J., Huang, Z., et al. (2019). Identification and expression profiling of protein phosphatases (*PP2C*) gene family in *Gossypium hirsutum* L. *Int. J. Mol. Sci.* 20:1395. doi: 10.3390/ijms20061395

Singh, A., Jha, S. K., Bagri, J., and Pandey, G. K. (2015). ABA inducible rice protein phosphatase 2C confers ABA insensitivity and abiotic stress

tolerance in *Arabidopsis*. *PLoS One* 10:e0125168. doi: 10.1371/journal.pone.0125168

Thompson, J. D., Higgins, D. G., and Gibson, T. J. (1994). CLUSTAL W: improving the sensitivity of progressive multiple sequence alignment through sequence weighting, position-specific gap penalties and weight matrix choice. *Nucleic Acids Res.* 22, 4673–4680. doi: 10.1093/nar/22.22.4673

Uno, Y., Furihata, T., Abe, H., Yoshida, R., Shinozaki, K., and Yamaguchi-Shinozaki, K. (2000). *Arabidopsis* basic leucine zipper transcription factors involved in an abscisic acid-dependent signal transduction pathway under drought and high-salinity conditions. *Proc. Natl. Acad. Sci. U. S. A.* 97, 11632–11637. doi: 10.1073/pnas.190309197

Urano, K., Maruyama, K., Ogata, Y., Morishita, Y., Takeda, M., Sakurai, N., et al. (2009). Characterization of the ABA-regulated global responses to dehydration in *Arabidopsis* by metabolomics. *Plant J.* 57, 1065–1078. doi: 10.1111/j.1365-313X.2008.03748.x

Vlad, F., Rubio, S., Rodrigues, A., Sirichandra, C., Belin, C., Robert, N., et al. (2009). Protein phosphatases 2C regulate the activation of the Snf1-related kinase OST1 by abscisic acid in *Arabidopsis*. *Plant Cell* 21, 3170–3184. doi: 10.1105/tpc.109.069179

Wang, Y., Wu, Y., Duan, C., Chen, P., Li, Q., Dai, S., et al. (2012). The expression profiling of the *CsPYL*, *CsPP2C* and *CsSnRK2* gene families during fruit development and drought stress in cucumber. *J. Plant Physiol.* 169, 1874–1882. doi: 10.1016/j.jplph.2012.07.017

Wang, J., Zhang, L., Cao, Y., Qi, C., Li, S., Liu, L., et al. (2018). *CsATAF1* positively regulates drought stress tolerance by an ABA-dependent pathway and by promoting ROS scavenging in cucumber. *Plant Cell Physiol.* 59, 930–945. doi: 10.1093/pcp/pcy030

WRI (2013). One-quarter of world's agriculture grows in highly water-stressed areas. Available at: https://www.wri.org/insights/one-quarter-worlds-agriculture-grows-highly-water-stressed-areas.

Xiang, Y., Sun, X., Gao, S., Qin, F., and Dai, M. (2017). Deletion of an endoplasmic reticulum stress response element in a *ZmPP2C-A* gene facilitates drought tolerance of maize seedlings. *Mol. Plant* 10, 456–469. doi: 10.1016/j.molp.2016.10.003

Xiong, L., Wang, R. G., Mao, G., and Koczan, J. M. (2006). Identification of drought tolerance determinants by genetic analysis of root response to drought stress and abscisic acid. *Plant Physiol.* 142, 1065–1074. doi: 10.1104/pp.106.084632

Xue, T., Wang, D., Zhang, S., Ehlting, J., Ni, F., Jakab, S., et al. (2008). Genome-wide and expression analysis of protein phosphatase 2C in rice and *Arabidopsis*. *BMC Genomics* 9:550. doi: 10.1186/1471-2164-9-550

Yamaguchi-Shinozaki, K., and Shinozaki, K. (2006). Transcriptional regulatory networks in cellular responses and tolerance to dehydration and cold stresses. *Annu. Rev. Plant Biol.* 57, 781–803. doi: 10.1146/annurev.arplant.57.032905.105444

Yoshida, T., Christmann, A., Yamaguchi-Shinozaki, K., Grill, E., and Fernie, A. R. (2019). Revisiting the basal role of ABA – roles outside of stress. *Trends Plant Sci.* 24, 625–635. doi: 10.1016/j.tplants.2019.04.008

Yoshida, T., Fujita, Y., Sayama, H., Kidokoro, S., Maruyama, K., Mizoi, J., et al. (2010). AREB1, AREB2, and ABF3 are master transcription factors that cooperatively regulate ABRE-dependent ABA signaling involved in drought stress tolerance and require ABA for full activation. *Plant J.* 61, 672–685. doi: 10.1111/j.1365-313X.2009.04092.x

Yoshida, T., Mogami, J., and Yamaguchi-Shinozaki, K. (2014). ABA-dependent and ABA-independent signaling in response to osmotic stress in plants. *Curr. Opin. Plant Biol.* 21, 133–139. doi: 10.1016/j.pbi.2014.07.009

Yoshida, T., Nishimura, N., Kitahata, N., Kuromori, T., Ito, T., Asami, T., et al. (2006). ABA-hypersensitive germination3 encodes a protein phosphatase 2C (*AtPP2CA*) that strongly regulates abscisic acid signaling during germination among *Arabidopsis* protein phosphatase 2Cs. *Plant Physiol.* 140, 115–126. doi: 10.1104/pp.105.070128

Yu, L., Chen, X., Wang, Z., Wang, S., Wang, Y., Zhu, Q., et al. (2013). *Arabidopsis* enhanced drought tolerance1/homeodomain glabrous11 confers drought tolerance in transgenic rice without yield penalty. *Plant Physiol.* 162, 1378–1391. doi: 10.1104/pp.113.217596

Yu, X., Han, J., Wang, E., Xiao, J., Hu, R., Yang, G., et al. (2019). Genome-wide identification and homoeologous expression analysis of *PP2C* genes in wheat (*Triticum aestivum* L.). *Front. Genet.* 10:561. doi: 10.3389/fgene.2019.00561

Zhang, T., Hu, Y., Jiang, W., Fang, L., Guan, X., and Chen, J. (2015). Sequencing of allotetraploid cotton (*Gossypium hirsutum* L. acc. TM-1) provides a resource for fiber improvement. *Nat. Biotechnol.* 33, 531–537. doi: 10.1038/nbt.3207

Zhang, G., Lu, T., Miao, W., Sun, L., Tian, M., Wang, J., et al. (2017). Genome-wide identification of ABA receptor PYL family and expression analysis of PYLs in response to ABA and osmotic stress in *Gossypium*. *PeerJ* 5:e4126. doi: 10.7717/peerj.4126

Zhu, J. K. (2002). Salt and drought stress signal transduction in plants. *Annu. Rev. Plant Biol.* 53, 247–273. doi: 10.1146/annurev.arplant.53.091401.143329

Zhu, J. K. (2016). Abiotic stress signaling and responses in plants. *Cell* 167, 313–324. doi: 10.1016/j.cell.2016.08.029

Conflict of Interest: The authors declare that the research was conducted in the absence of any commercial or financial relationships that could be construed as a potential conflict of interest.

Publisher's Note: All claims expressed in this article are solely those of the authors and do not necessarily represent those of their affiliated organizations, or those of the publisher, the editors and the reviewers. Any product that may be evaluated in this article, or claim that may be made by its manufacturer, is not guaranteed or endorsed by the publisher.

Copyright © 2022 Shazadee, Khan, Wang and Wang. This is an open-access article distributed under the terms of the Creative Commons Attribution License (CC BY). The use, distribution or reproduction in other forums is permitted, provided the original author(s) and the copyright owner(s) are credited and that the original publication in this journal is cited, in accordance with accepted academic practice. No use, distribution or reproduction is permitted which does not comply with these terms.

frontiers | Frontiers in Plant Science

ORIGINAL RESEARCH
published: 02 June 2022
doi: 10.3389/fpls.2022.904392

RNA-Seq Analysis of Developing Grains of Wheat to Intrigue Into the Complex Molecular Mechanism of the Heat Stress Response

Surinder Paul[1,2,3], Joginder Singh Duhan[1], Sarika Jaiswal[4], Ulavappa B. Angadi[4], Ruchika Sharma[2], Nishu Raghav[2], Om Prakash Gupta[2], Sonia Sheoran[2], Pradeep Sharma[2], Rajender Singh[2], Anil Rai[4], Gyanendra Pratap Singh[2], Dinesh Kumar[4,5], Mir Asif Iquebal[4] and Ratan Tiwari[2]**

[1]Department of Biotechnology, Chaudhary Devi Lal University, Sirsa, India, [2]Indian Council of Agricultural Research, Indian Institute of Wheat and Barley Research, Karnal, India, [3]ICAR, National Bureau of Agriculturally Important Microorganisms, Kushmaur, Maunath Bhanjan, India, [4]Indian Council of Agricultural Research, Indian Agricultural Statistics Research Institute, New Delhi, India, [5]Department of Biotechnology, Central University of Haryana, Gurgaon, India

Heat stress is one of the significant constraints affecting wheat production worldwide. To ensure food security for ever-increasing world population, improving wheat for heat stress tolerance is needed in the presently drifting climatic conditions. At the molecular level, heat stress tolerance in wheat is governed by a complex interplay of various heat stress-associated genes. We used a comparative transcriptome sequencing approach to study the effect of heat stress (5°C above ambient threshold temperature of 20°C) during grain filling stages in wheat genotype K7903 (Halna). At 7 DPA (days post-anthesis), heat stress treatment was given at four stages: 0, 24, 48, and 120 h. In total, 115,656 wheat genes were identified, including 309 differentially expressed genes (DEGs) involved in many critical processes, such as signal transduction, starch synthetic pathway, antioxidant pathway, and heat stress-responsive conserved and uncharacterized putative genes that play an essential role in maintaining the grain filling rate at the high temperature. A total of 98,412 Simple Sequences Repeats (SSR) were identified from *de novo* transcriptome assembly of wheat and validated. The miRNA target prediction from differential expressed genes was performed by psRNATarget server against 119 mature miRNA. Further, 107,107 variants including 80,936 Single nucleotide polymorphism (SNPs) and 26,171 insertion/deletion (Indels) were also identified in *de novo* transcriptome assembly of wheat and wheat genome Ensembl version 31. The present study enriches our understanding of known heat response mechanisms during the grain filling stage supported by discovery of novel transcripts, microsatellite markers, putative miRNA targets, and genetic variant. This enhances gene functions and regulators, paving the way for improved heat tolerance in wheat varieties, making them more suitable for production in the current climate change scenario.

Keywords: heat stress, grain filling, transcriptomics, gene expression, molecular markers, miRNA targets

OPEN ACCESS

Edited by:
Giselle Camargo Mendes, Instituto Federal de Santa Catarina (IFSC), Brazil

Reviewed by:
Humberto Carvalho, Federal University of Ceara, Brazil
Gursharn Singh Randhawa, Sardar Bhagwan Singh Post Graduate Institute of Biomedical Science and Research, India
Eduardo Gorayeb, Santa Catarina State University, Brazil

***Correspondence:**
Mir Asif Iquebal
ma.iquebal@icar.gov.in
Ratan Tiwari
ratan.tiwari@icar.gov.in

Specialty section:
This article was submitted to Plant Abiotic Stress, a section of the journal Frontiers in Plant Science

Received: *25 March 2022*
Accepted: *13 May 2022*
Published: *02 June 2022*

Citation:
Paul S, Duhan JS, Jaiswal S, Angadi UB, Sharma R, Raghav N, Gupta OP, Sheoran S, Sharma P, Singh R, Rai A, Singh GP, Kumar D, Iquebal MA and Tiwari R (2022) RNA-Seq Analysis of Developing Grains of Wheat to Intrigue Into the Complex Molecular Mechanism of the Heat Stress Response. Front. Plant Sci. 13:904392. doi: 10.3389/fpls.2022.904392

INTRODUCTION

Wheat (*Triticum aestivum* L.) is the most widely grown cereal crop, accounting for roughly 220 million hectares of agricultural land. Sixty percent of calorie requirement is met by wheat, maize, and rice while wheat alone meets about 25% of protein requirement of the world's population (Sheoran et al., 2019; Singh et al., 2019). Several abiotic factors affect wheat production, including heat, drought, and salinity. In the present climate scenario, heat stress (HS) is a main constraint affecting the normal growth and productivity of crops, including wheat (Siebert and Ewert, 2014; Fahad et al., 2017), thereby posing a major threat to the global food and nutritional security. Elevated temperature above a threshold level negatively affects all the growth stages. The extent of yield loss depends on the sensitivity of the plant and the phenological/growth stage at which it is exposed to heat stress (Akter and Islam, 2017).

Among all the phenological stages in wheat, the reproductive stage (anthesis and seed development) is considered to be the most sensitive stage for HS (Kumar et al., 2018). It is estimated that during the grain filling stage, per degree temperature rise over and above 18–22°C, decreases grain filling rate and grain yield by 5% and 3–4%, respectively (Gupta et al., 2012). Based on this it was speculated that exposure of 32–38°C temperature during the grain filling stage may cause about 50% yield potential reduction in wheat (Awlachew et al., 2016).

HS tolerance is a very complex process that involves cellular pathway cross-talk. In the early stages of grain filling, HS affects the starch biosynthesis and assimilates translocation leading to poor yield and quality of wheat produce (Farooq et al., 2011; Kumar et al., 2013; Shamloo et al., 2017). Plants modulate their molecular machinery at the transcriptional, post-transcriptional, and epigenetic levels in order to regulate the differential expression of HS-related genes, photosynthetic machinery, cell membrane thermostability, induction of heat shock proteins (HSPs), stress hormones (ABA, ethylene), reactive oxygen species (ROS), compatible solutes (proline, glycine betaine, and sugars) accumulation, and non-coding RNAs synthesis (Farooq et al., 2011; Grover et al., 2013; Goswami et al., 2014; Lal et al., 2021; Zhao et al., 2021).

Many transcriptome studies exist for elucidating molecular mechanisms involving overlapping and distinct regulatory transcriptional mechanism of abiotic stresses response in model plants, as well as in some crops at a specific plant development stage (Coolen et al., 2016; Kang and Yeom, 2018; Cohen and Leach, 2019; Iquebal et al., 2019; Li et al., 2019; Kang et al., 2020; Rangan et al., 2020).

Wheat being a hexaploid with large and complex genome requires modern NGS-based approaches to elucidate tissue and growth stage-specific heat-responsive gene expressions. Wheat transcriptome profiling can reveal the differential gene expression, genome annotations, regulatory factors, molecular markers and expression quantitative trait loci (eQTLs) as well as their sequence variants, controlling the traits of importance (Morozova and Marra, 2008; Berkman et al., 2012; Lal et al., 2021). In wheat, RNA-seq has been adopted mainly to identify new and conserved transcripts associated with abiotic, biotic stress, and nutrient responsive genes (Kumar et al., 2015; Iquebal et al., 2019; Rangan et al., 2020). It is accurate, rapid, and comparatively cheaper and can be applied to non-model plant systems to extract novel genetic information (Unamba et al., 2015). *De novo* transcriptome assembly may be utilized to study the temporal and spatial gene expression of non-model organisms, which is an otherwise difficult task in the absence of complete genome sequence information (Grabherr et al., 2011).

The expression of genes in developing wheat grain is key in determining the ultimate composition of nutritional properties and yield (Henry et al., 2016). Moreover, response to HS is very complex and governed by numerous genes and their regulated expression (Mwadzingeni et al., 2016). Thus, it is of great importance to study the expression of various crucial genes contributing in grain filling and their regulation under HS. Transcriptomics-based expression analysis utilizing RNA-seq is a rapid, sensitive, and accurate way to identify crucial genes, their transcript level variations along with the regulating factors in wheat (Chu et al., 2021). In the present study, we have utilized NGS-based *de novo* assembly approach of RNA-seq to unearth the novel and conserved heat-responsive genes transcripts, transcription factors, gene regulatory network, and their complex interactions in response to heat stress during the initial phases of grain filling stage in heat-tolerant wheat variety K7903 (Halna). Further, the study revealed the discovery of putative molecular markers (SSRs, SNPs, and Indel markers), prediction of transcription factors (TFs), and microRNA and their putative targets. The findings of the study will enrich knowledge-based utilization of heat-tolerant varieties in the crossing block for genetic advancement of wheat.

MATERIALS AND METHODS

Plant Material, Heat Treatment, and Sample Collection

Healthy seeds of a heat stress-tolerant late sown wheat variety, K7903 (Halna), were procured from the germplasm unit of ICAR-Indian Institute of Wheat and Barley Research (IIWBR) Karnal, India. The seeds were surface sterilized with 0.1% $HgCl_2$, followed by three subsequent washing with sterile distilled water. Four wheat seeds were sown in 10-cm pots in the soil in the net house (15 h light, 9 h dark; 40% RH). A total of 18 such pots were sown and labeled. At seven days post-anthesis (DPA), *that is*, approximately 3-month-old wheat plants, 9 out of 18 pots were shifted carefully to Temperature Controlled Phenotyping Facility (TCPF), equipped with automatic sensing of the outside environmental temperature and maintained inside temperature up by +5°C (Sharma et al., 2019). Other environmental factors including humidity, light intensity etc. were maintained similar to outside. The remaining nine pots in the net house served as control. The main tiller spike of each wheat plant in both, control (normal temperature) and TCPF (under HS) conditions was tagged, and the spikelets (wheat grains) were harvested from the middle of the spike at 0-, 24-, 48-, and 120-h intervals after starting from 7 DPA from three main tiller spike and pooled. At each sampling

point, four spikelets from the middle of spikes from all the plants were harvested and frozen immediately in liquid nitrogen in a 50 ml sterile plastic tube. The samples taken from controlled or normal conditions were labeled as C1, C2, C5, and C7, while samples from heat stress conditions were labeled as R1, R2, R5, and R7 with two biological replicates.

RNA Isolation, Library Construction, and Sequencing

The developing wheat grain samples were carefully taken out of the liquid nitrogen without thawing and grounded to a very fine powder using sterile pestle and mortar in liquid nitrogen. Thereafter, total RNA was extracted using RNeasy RNA isolation kit (Qiagen, Germany) according to the manufacturer's instructions. DNA was removed by digestion with RNase-free DNase (Qiagen, Germany), and RNA was purified and concentrated using RNeasy column (Qiagen, Germany). RNA quality was evaluated by 1% agarose gel electrophoresis for 28 S/18 S rRNA band intensity (2:1) and Agilent 2,100 Bioanalyser and quantified by using NanoDrop Spectrophotometer (Thermo Fisher Scientific, United States). RNA samples were immediately stored in −80°C and subsequently sent for further processing, library construction, and sequencing to AgriGenome Labs Pvt. Ltd., Hyderabad, Telangana, India.

Pre-processing, *de novo* Assembly, and Expression Analysis

Paired-end (100 bp × 2) read of control and treated samples were generated using Illumina Hiseq 2,500. The quality assessment of reads was performed using FastQC tool.[1] Cutadapt version 1.8.1 (Martin, 2011) and Sickle version 1.33[2] were used for removal of adaptors and low-quality reads. Reads having average quality score ≤ 30 were removed. Further, rRNA data from samples were removed with the SILVA database (Quast et al., 2012).[3] Transcriptome assembly of wheat was performed using *trinity* (at default k-mer length of 25), which uses de Bruijn graphs and dynamic programming algorithm (Haas et al., 2013). Finally, the CD-HIT-EST package was employed to remove redundant sequences from *trinity* assembly (Fu et al., 2012). For the expression analysis, Bowtie 2 (Langmead et al., 2009) was used for alignment of reads, followed by RSEM (RNA-Seq by Expectation–Maximization; Li and Dewey, 2011) for calculation of expression values in the form of FPKM (Fragments per kilobase million reads). RSEM implements improved quantification method having superior accuracy than other methods. Differential gene expression analysis between two biological replicates of each pair was performed using DESeq 1.16.0 program (Anders and Huber, 2010) with parameters, such as $Log_2FC \pm 2$ and adjusted value of p <0.05.

Homology Search, Functional Characterization, and Gene Ontology

Blastx[4] program was used for sequence similarity search against NCBI non-redundant protein database with expected threshold e-value 10^{-5} and identity cutoff 40% (Camacho et al., 2009). Contig Annotator Pipeline (CANoPI) was used for gene ontology, pathways analysis of differential expressed genes, and *de novo* transcriptome assembly transcripts whose length was ≥200 bp and FPKM ≥1.0. We also identified transcription factors from the sets of differentially expressed genes using PlantTFDB 4.0 (Jin et al., 2016). The miRNA target prediction from differential expressed genes was performed by psRNATarget server (Dai and Zhao, 2011).

Identification and Validation of Simple Sequences Repeat Markers

Simple Sequences Repeats were identified from *de novo* transcriptome assembly of wheat using perl script of MISA (MIcroSAtellite identification tool) with default parameters, such as ten repeating units for mononucleotides, six repeating units for dinucleotide, and five for tri, tetra, penta, and hexanucleotides (Thiel et al., 2003). Also, the Primer3 tool was used for generating three sets of primers of identified markers (Untergasser et al., 2012).

From the mined SSRs markers, fifteen were randomly selected for validation in 20 different wheat genotypes panel. Genomic DNA was extracted from seedlings by CTAB method. PCR amplification was carried out in BioRad S1000 Thermocycler in 25 µl reaction mixture containing 2.5 µl 10 × buffer,0.5 µl of 10 mM dNTPs, 0.5 µl of 10 µM each reverse and forward primer, 0.5 µl of Taq polymerase (5 U/µl), 60 ng template DNA and nuclease-free water. PCR amplification was performed using the program: 94°C for 5 min for initial denaturation, 30 cycles of 1 min at 94°C, 50 s at 55–63°C, 72°C for 1 min, and a final amplification of 5 min at 72°C. PCR products were analyzed using 3% agarose gel electrophoresis.

Identification of Single Nucleotide Polymorphism and Indels

Single Nucleotide Polymorphism (SNP) and Indels (insertion/deletions) were identified from a sample of prior treatment, *that is,* C1 and R1 using two references, *viz.*, *de novo* transcriptome assembly and wheat genome release-31.[5] Burrows-Wheeler Aligner (BWA; Li and Durbin, 2009) and SAM tools (Li et al., 2009) was used for alignment and calling of variants. Filters, such as read depth coverage >10, quality score > 30, and at least 2 SNPs in 50 bps, were applied to identify significant SNPs and Indels.

Validation of RNA-seq Analysis by q-PCR

RNA-seq results were confirmed by performing q-PCR of 10 randomly selected differentially expressed transcripts (DETs).

[1]http://www.bioinformatics.babraham.ac.uk/projects/fastqc/
[2]https://github.com/najoshi/sickle
[3]https://www.arb-silva.de/
[4]https://blast.ncbi.nlm.nih.gov/Blast.cgi
[5]ftp://ftp.ensemblgenomes.org/pub/plants/release-31/fasta/triticum_aestivum/dna/

cDNA preparation was performed using Superscript® III First-Strand Synthesis System (Invitrogen, UK) following manufacturer's instructions. Prior to q-PCR, the PCR conditions were optimized by performing successful routine PCR. qPCR mixture contained 1 µl of cDNA (10 ng/µl), 6.0 µl of 2 × SYBR Green Master Mix (Thermo Scientific), and 1 µl (10 µM) each of forward and reverse primer of the selected DET and nuclease-free water to a final 12.0 µl total reaction volume. The quantitative reaction was done on Bio-Rad CFX96™ Real-Time PCR System (Bio-Rad, United States). The qPCR program consisted of 95°C for 5 min, then 40 cycles of 94°C for 15 s, 58°C for 30 s, and 72°C for 30 s and a final melt curve step from 65°C to 95°C with a rise of 0.5°C for 5 s. The relative expression level study of target transcripts was done by comparative $2^{-\Delta\Delta Ct}$ method (Livak and Schmittgen, 2001) using GAPDH as endogenous control.

RESULTS

Pre-processing and *de novo* Assembly

In this study, a total of 16 samples of control and treated data were generated at four different developmental crop stages *viz.*, 7 days post-anthesis, 0, 24, 48, and 120 h after treatment. Sample names C1, C2, C5, and C7 belonged to the control condition, whereas R1, R2, R5, and R7 represented treated samples. Both control and treated samples had biological replicates. The generated transcriptome data at different developmental crop stages were pre-processed for quality assessment. After trimming and removal of rRNA reads, 253,046,594 (20.5%) poor quality reads were dropped and finally, 979,825,192 (79.47%) high-quality reads were retained (from overall generated data) for *de novo* transcriptome assembly and further downstream analysis. Trinity generated 2,302,239 transcripts with a minimum read length of 200 and GC content of 50.24%. Finally, 1,696,570 transcripts were obtained after removal of redundant sequences with N50 value ≥473 bp, GC content 50.48%, and transcript lengths ranging between 200 to 18,870 bp (**Figure 1**).

Functional Characterization and Gene Ontology

For homology search and functional annotation, we filtered transcripts having sequence length ≥ 200 bp and FPKM ≥1.0 to finally arrive to a total of 319,879 transcripts for further analyses. The criteria of e-value 10^{-5} and % identity cutoff 40% were employed for searching known sequences against NCBI non-redundant protein database. Out of 319,879 transcripts, 152,842 had similarities with other known proteins in the database. Blastx results showed top hits with *Aegilops tauschii* (49204), *Triticum urartu* (42504), and *Hordeum vulgare* (**Figure 2**). The identified proteins were further annotated using UniProt database, pathways database, PROSITE, InterProscan, TIGRFAMS, Pfam, PANTHER, and OrthoDB. Finally, a total of 105,127 transcripts were found to have significant Blastx hit and UniProt information (**Supplementary File 1**).

The complete annotations were categorized into Biological Processes (BP), Molecular Functions (MF), and Cellular Components (CC), having 4,345, 3,873, and 2,516 GO terms, respectively. In BP, we found full transcripts represented in DNA integration (5,688 transcripts), while nucleic acid binding (8379) an integral component of membrane (7433) in MF and CC, respectively (**Figure 3**; **Supplementary File 2**).

Abundance Estimation and Differential Expression Analysis

Reads of all the sixteen samples were mapped separately on the *de novo* transcriptome assembly, containing 1,696,570 transcripts and ~ 62.48–95.39% (average ~ 83.79%) of reads mapped. Also, expression values of each sample were calculated in the form of FPKM, to identify differentially expressed genes (**Figure 4**).

Differential expression analysis was performed and categorized into 3 sets. Set 1 contained the DEGs sets of control samples, such as C1 vs. C2, C2 vs. C5, and C5 vs. C7, whereas set 2 contained treated samples, such as R1 vs. R2, R2 vs. R5, and R5 vs. R7. In the 3rd set, DEGs were of control and treated samples, such as C1 vs. R1, C2 vs. R2, C5 vs. R5, and C7 vs. R7. The DEGs were identified from all the paired sets. In total, 109,455 DEGs were obtained, out of which 95,966 were upregulated and 13,489 were downregulated (**Table 1**).

In control samples, *that is,* set 1, no common DEGs were found in all the three comparisons, such as C1 vs. C2, C2 vs. C5, and C5 vs. C7. But, several common DEGs were obtained in the comparison set C1 vs. C2 and C2 vs. C5, *that is,* 12,332, while 1 and 10 DEGs were common in comparison "C1 vs. C2 and C5 vs. C7" and "C2 vs. C5 and C5 vs. C7," respectively. A total of 806, 34,670, and 86 DEGs were found unique in C1 vs. C2, C2 vs. C5, and C5 vs. C7, respectively. Similarly, in Set 2 (treated samples), no common DEGs were obtained. In Set 3, which contains the DEGs of control vs. treated samples, 23 DEGs were found common in between C2 vs. R2 and C5 vs. R5 while 48,904, 23, and 158 DEGs were unique in C2 vs. R2, C5 vs. R5, and C7 vs. R7, respectively (**Figure 5**).

Functional Characterization of DEGs

Functional characterization of DEGs was performed using Blastx against NCBI nr database. For identification of transcriptional factors, PlantTFDB v4.0 was used. Transcripts to the tune of 43,861, had hits with other known proteins in the databases (**Table 2**).

MicroRNA Target Prediction

The miRNA target prediction was made by psRNATarget server for DEGs sets against 119 mature miRNAs of *T. aestivum*. Out of 10 sets, only differential expressed genes of three sets were involved in miRNA target prediction, *that is*, C1 vs. C2, C2 vs. C5, and C2 vs. R2. In set C1 vs. C2, we found 24 miRNAs that targeted 65 transcripts. Maximum 12 transcripts were targeted by "tae-miR1117," followed by 5 transcripts each in "tae-miR1130b-3p" and "tae-miR1134." In set C2 vs. C5,

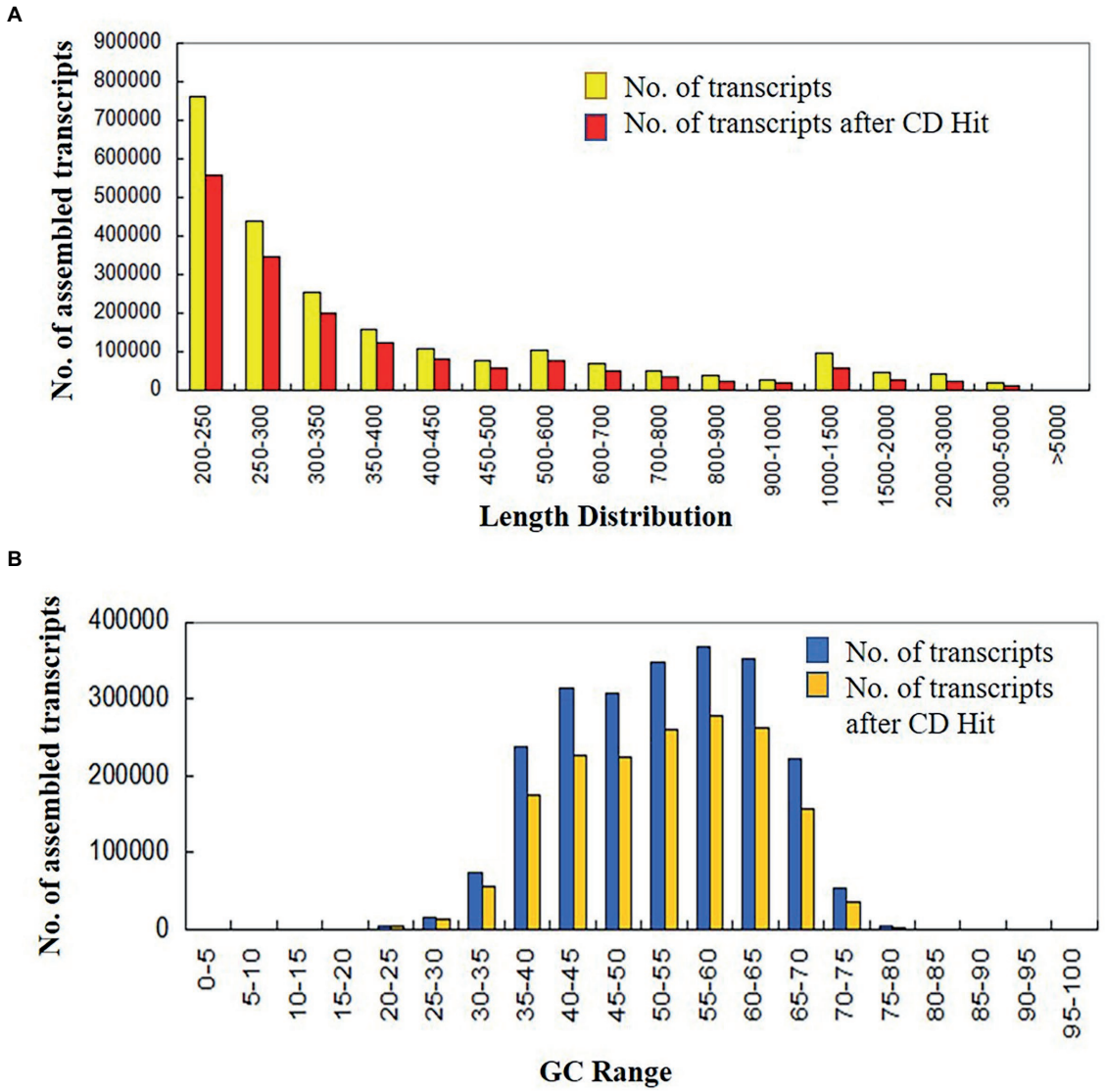


FIGURE 1 | (A) Length distribution, **(B)** GC content of assembled transcript in control and treated wheat sample at four different developmental stages (at 0, 24. 48 and 120 h of heat stress treatment).

29 miRNAs were found targeting 125 transcripts with a maximum number of transcripts targeted by "tae-miR1117," *that is,* 51, followed by 9 and 6 transcripts in "tae-miR1128" and "tae-miR1130b-3p," respectively. Lastly, in DEG set C2 vs. R2, 31 miRNAs were found targeting 154 transcripts and maximum hits were targeted by "tae-miR1117," *that is,* 55, followed by 9 transcripts each in "tae-miR1130b-3p"and "tae-miR1131" (**Supplementary File 5**). Twenty miRNAs were found common in C1 vs. C2, C2 vs. C5, and C2 vs. R2, whereas 5 and 3 miRNAs were found unique in C2 vs. C5 and C2 vs. R2, respectively (**Figure 6**).

In silico Identification of SSR Markers

A total of 98,412 simple sequences repeats (SSRs) were identified from 1,696,570 transcripts of wheat *de novo* transcriptome assembly, while 4,261 repeats were present in compound formation. Out of 98,412 markers, there was abundance of mononucleotides, *that is,* 37,716, followed by di- (27697), tri- (29659), tetra- (2773), penta- (381), and hexa (186)nucleotide repeats (**Supplementary File 6**). In dinucleotide repeats, we found the maximum number of repeats was GA, *that is,* 4,601, followed by AG (3247) and CT (3101). In the case of trinucleotides, the maximum was GGC repeats, *that is*, 1799, followed by GCG (1487) and GAG (1393; **Table 3**).

Validation of SSR Markers

Twenty highly diverse randomly selected wheat genotypes were used for validation of SSR. PCR primers were designed for randomly selected 20 SSR loci (**Table 4**), and PCR was amplified using genomic DNA as a template (**Figure 7**). Such SSR markers

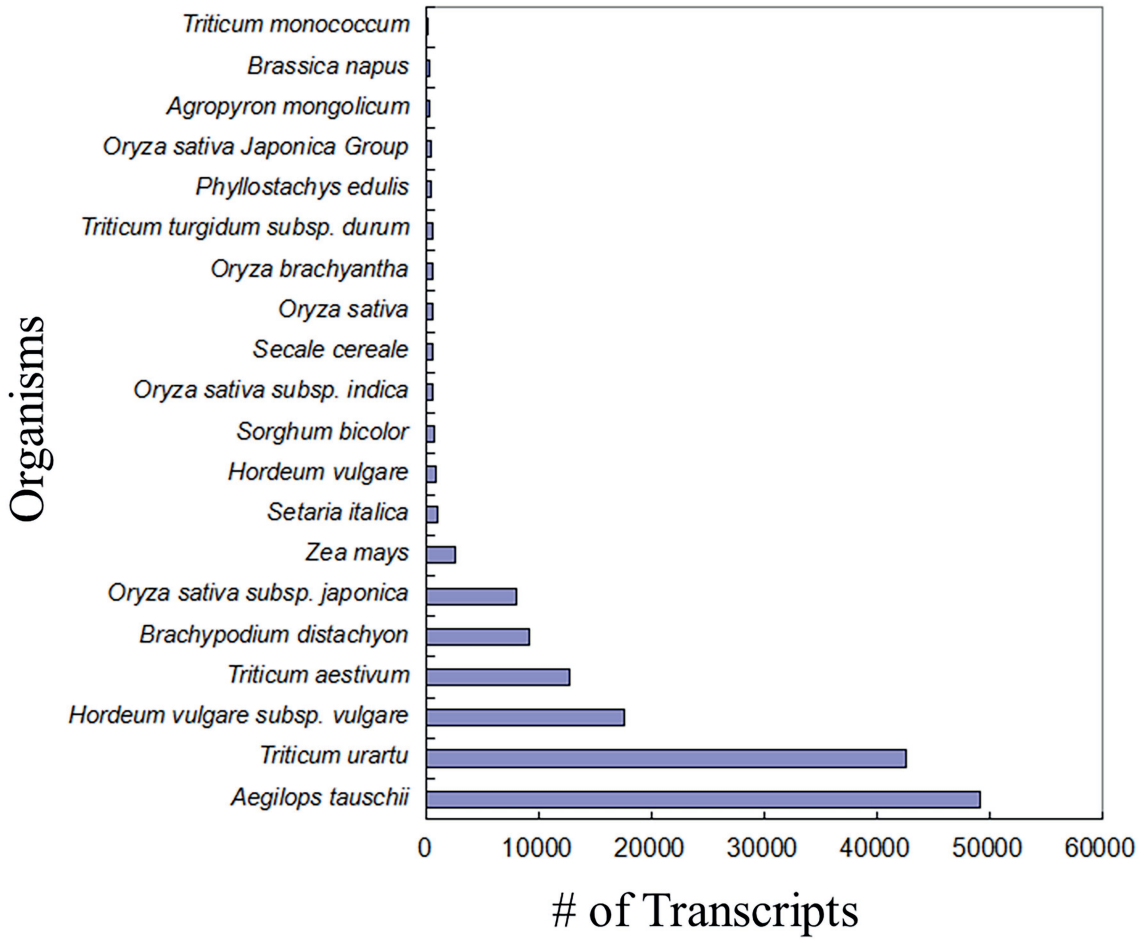


FIGURE 2 | Bar graph representing the species distribution of annotated DEGs. Maximum number of annotated DEGs was represented by *Aegilops tauschii* (49204) followed by *T. uratu* (42504). *Triticum aestivum* falling at the fourth place had approximately 10,000 annotated DEGs.

are extremely important in crop improvement programs for heat tolerance and wheat breeding not an exception.

Identification of Single Nucleotide Polymorphism and Indels

Single Nucleotide Polymorphism (SNPs) and insertion/deletion (Indels) were identified from pooled reads of C1 and R1 against *de novo* transcriptome assembly of wheat and wheat genome Ensembl version 31. We found a total of 107,107 variants against the *de novo* transcriptome assembly of wheat, containing 80,936 SNPs and 26,171 Indels. Maximum number of variants (38) were found in transcript ID "TRINITY_DN523265_c0_g1_i3 (WD repeat and FYVE domain-containing protein 3)" and interesting all 38 were SNPs (**Supplementary File 7**). Similarly, we obtained 110,787 variants against the wheat genome, which contains 99,791 SNPs and 10,996 Indels. Top variants identified from chromosome number 3B, *that is*, 12,977 (11,589 SNPs and 1,388 Indels), followed by 5,788 and 5,771 variants in chromosome 2B and 2A, respectively (**Supplementary File 7**).

Validation of RNA-seq Analysis by q-PCR

The RNA-seq results were verified by performing q-PCR of ten randomly selected differentially expressed transcripts (DETs; **Table 5**). The qPCR expression pattern results of these DETs were found to follow the same trend as the RNA-seq expression pattern results, confirming the accuracy of the RNA-seq data obtained in this investigation (**Figure 8**).

DISCUSSION

Global wheat production is highly vulnerable to climate change and environmental factors, such as heat stress and water deficit, which have severe adverse impact on the wheat crop productivity and quality (Pareek et al., 2020; Rangan et al., 2020). About

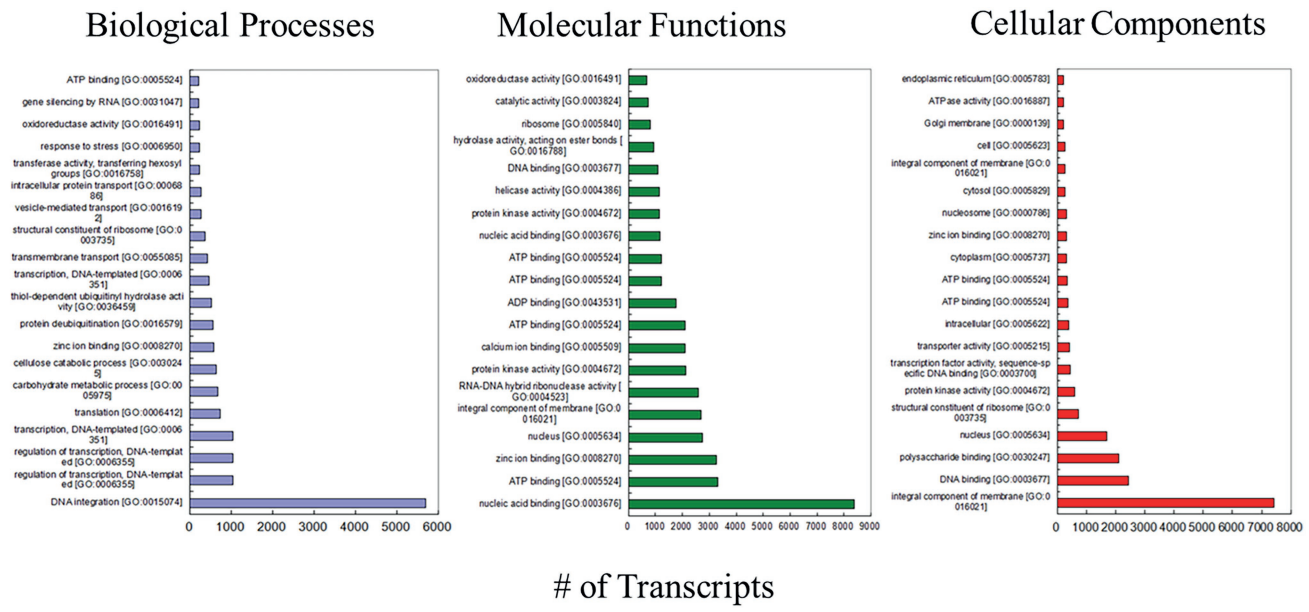


FIGURE 3 | Bar graph depicting gene ontology (GO) classification and enrichment of top 20 GO terms represented under biological (DNA integration: 5688 transcripts), molecular (nucleic acid binding: 8379 transcripts), and cellular components (an integral component of membrane: 7433).

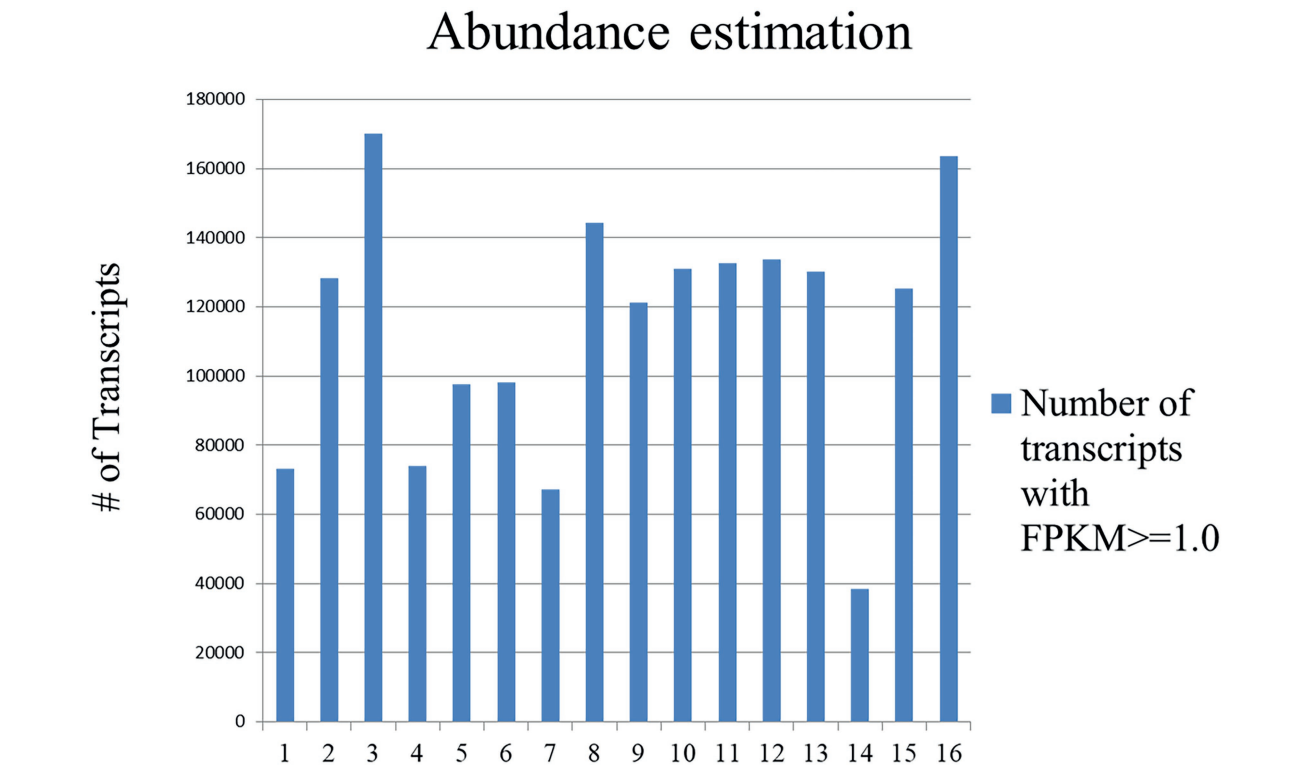


FIGURE 4 | Graphical representations of DEGs with FPKM value ≥1 of 16 libraries prepared in control and treated sample at four different developmental stages. Samples contained 1,696,570 transcripts and ~ 62.48–95.39% (average ~ 83.79%) of reads mapped.

57% wheat cultivated area in developing nations is affected by heat stress, thus it can be considered as primary abiotic factor threatening world wheat production and food security (Kosina et al., 2007). Wheat is more sensitive to the heat stress during reproductive (anthesis and post-anthesis) stages and grain filling period which is very crucial for sustaining

overall crop yield and quality (Rangan et al., 2020). Heat stress response is very complex mechanism that involves interplay and modulation of numerous biochemical and molecular machinery for sustaining yield and quality (Mwadzingeni et al., 2016). It is of great importance to study the expression of various crucial genes and their regulation in wheat, expressed during grain filling stage under the heat stress. RNA-seq-based next-generation sequencing (NGS) technology provides comparatively economic and efficient way of identifying crucial genes, their transcript level variations along with the regulating factors with high accuracy (Chu et al., 2021).

In the present work, we identified a total of 115,656 genes in heat stress-tolerant wheat genotype, that is, Halna (K7903), exposed to heat stress. Result indicated differential expression of 109,455 DEGs in different sets, out of which 95,966 were upregulated and 13,489 were downregulated (**Table 1**). The detailed information of DEGs with log2 fold change, adjusted value of p, and their functional characterization is presented in **Supplementary File 3**. **Supplementary File 4** provides the information of transcriptional factors which were obtained in each set. A total of 43,861 transcripts had hits with other known proteins in the databases (**Table 2**). These DEGs narrowed down to 309 which were involved in many critical processes *viz.*, signal transduction, starch synthetic pathway, antioxidant pathway, and heat stress-responsive conserved and uncharacterized putative genes that play an essential role in maintaining the grain filling rate at high temperature. Categorization of the annotations found their place into Biological Processes (BP), Molecular Functions (MF) and Cellular Components (CC), corresponding to 4,345, 3,873, and 2,516 GO terms, respectively. DNA integration (5,688 transcripts), nucleic acid binding (8379), and integral membrane components (7433) were observed in BP, MF, and CC, respectively (**Figure 3**; **Supplementary File 2**). Differential gene expression of transcripts functionally involved in diverse cellular functions is an indicator that the heat stress response in wheat is very complex and it simultaneously regulates different biochemical and molecular pathway sustaining the survival and developmental processes in wheat. Among differentially expressed transcripts, TRINITY_DN521405_c2_g2_i1 (Avenin-like a4) which is cysteine-rich storage proteins expressed during early stages of seed development (3–22 DPA) exclusively in developing endosperm of wheat and its related plant species. Expression of this gene during early grain development plays very significant role in ensuring wheat processing quality (Ma et al., 2013; Chen et al., 2016; Zhang et al., 2018). Jiang et al. (2012) conducted a proteomics-based study and reported that the avenin-like proteins expression is highly upregulated under drought stress and may have an

TABLE 1 | Detailed list of differentially expressed genes obtained in all the three sets.

Sets	Samples name	Upregulated	Downregulated	Total
Set 1	C1 vs. C2	704	12,435	13,139
	C2 vs. C5	46,543	469	47,012
	C5 vs. C7	70	27	97
Set 2	R1 vs. R2	0	0	0
	R2 vs. R5	29	43	72
	R5 vs. R7	4	0	4
Set 3	C1 vs. R1	0	0	0
	C2 vs. R2	48,444	483	48,927
	C5 vs. R5	14	32	46
	C7 vs. R7	158	0	158
	Total	95,966	13,489	109,455

In total, 109,455 DEGs were obtained, out of which 95,966 were upregulated and 13,489 were downregulated.

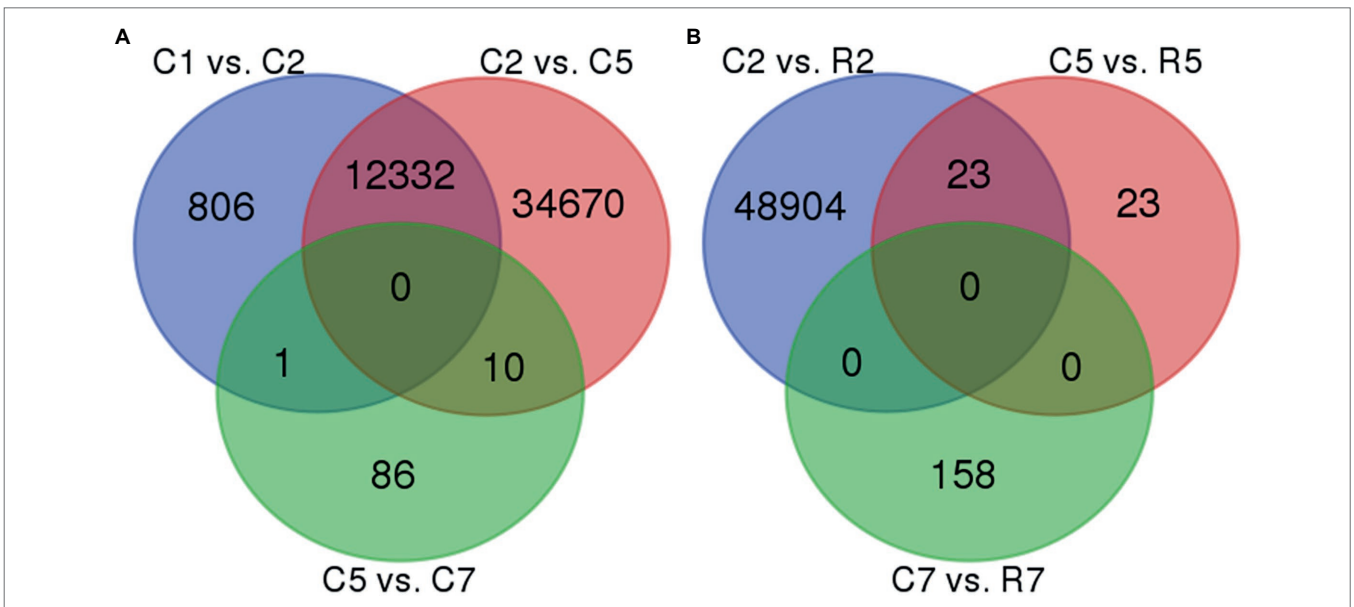


FIGURE 5 | Venn diagram representing two maximum common DEGs in set 1**(A)**-{(C_2 vs. C_5) vs. (C_5 vs. C_7)} and set 3**(B)**-{(C_2 vs. R_2) vs. (C_5 vs. R_5)}. 10 DEGs were common in set 1**(A)** and 23 DEGs were common in set 3**(B)**.

TABLE 2 | Number of DEGs in each set that showed similarity with other known proteins in the various databases.

S. No	DEGs	Blast results against NR database	Transcriptional factors (Blast against PlantTFDB v4.0)
1	13,139	5,620 (42.8%)	2064 (15.7%)
2	47,012	17,770 (37.8%)	6,820 (14.5%)
3	97	75 (77.3%)	27 (27.8%)
4	–	–	–
5	72	44 (61.1%)	14 (19.4%)
6	4	3 (75%)	3 (75%)
7	–	–	–
8	48,927	20,272 (41.4)	8,306 (16.9%)
9	46	36 (78.2%)	13 (28.2%)
10	158	41 (25.9%)	47 (29.7%)

A total of 43,861 transcripts had hits with other known proteins in the databases.

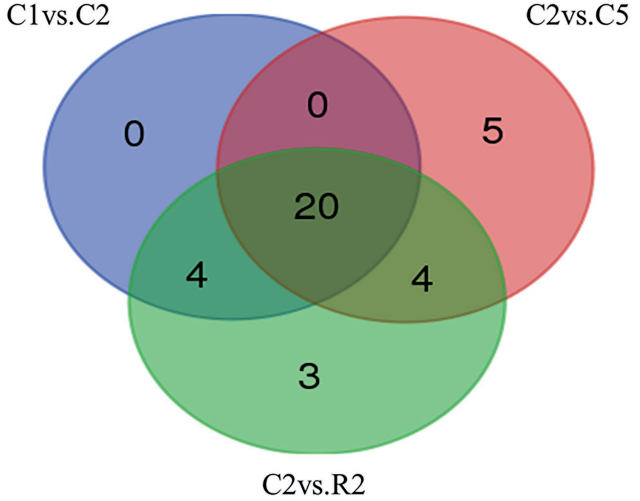


FIGURE 6 | Venn diagram of miRNAs found in DEG sets C_1 vs. C_2, C_2 vs. C_5, and C_2 vs. R_2. Among all the comparison sets, 20 miRNAs were found to be common.

essential role in seed quality. Similarly, Zhang et al. (2020) suggested that avenin-like proteins are multifunctional including role during disease resistance. In our study, we found very high expression of avenin-like proteins which suggests their important role during seed development/grain filling under heat stress. To the best of our knowledge, this is the first report of expression study of avenin-like protein under heat stress in wheat.

TRINITY_DN483169_c0_g1_i6 (Alpha-amylase inhibitor 0.19) are amylase inhibitors, found in cereal grains, including wheat and some legume seeds, which inhibit the target α-amylase enzymes thus protect the starchy seed reserves from degradation into simpler oligosaccharides (Petrucci et al., 1976; Franco et al., 2000; Dombrowski, 2003). Their role in protecting plant amylase inhibitors in biotic stress, particularly insect pests, is well established (Feng et al., 1996; Franco et al., 2000; Rane et al., 2020). Alpha-amylase inhibitors inhibit grain starch degradation and protect the plant against oxidative stress (Hajheidari et al., 2007). Reports suggest that the differential expression of amylase inhibitor at protein level in different cultivars during different grain filling stages play an essential role during grain filling under abiotic stress (Jiang et al., 2012; Zhang et al., 2014). The upregulation of α-amylase inhibitors transcripts under heat stress in our study also confirms their role in heat stress tolerance in wheat during grain filling.

TRINITY_DN518599_c1_g1_i2 (Aspartic proteinase oryzasin-1) are proteolytic enzymes with two highly conserved aspartate residues and play a crucial role in stress responses in plants (Alam et al., 2014). *APs* has been reported to play an important role in protein processing in response to pathogen attack, programmed cell death, water stress, drought, and other environmental stimuli in many plant species at different developmental stages in various plant organs (Runeberg-Roos et al., 1994; De Carvalho et al., 2001; Guevara et al., 2005; Mendieta et al., 2006; Simões et al., 2007; Muñoz et al., 2010; Yao et al., 2012; Rawlings and Salvesen, 2013). Asakura et al. (1995) reported that a rice aspartic proteinase, oryzasin 1 transcripts level was much more abundant from just after flowering stage up to final seed formation suggesting its active role in seed storage protein processing. Yao et al. (2012) reported overexpression of APs under water-deficient conditions in *Zea mays* and their role in drought avoidance through ABA-dependent signaling pathway. They also reported that transgenic *Arabidopsis* overexpressing gene VlAP17, encoding a Group C aspartic protease, enhanced tolerance to salt and drought stress during seed germination, seedling, and maturation. The transgenic Arabidopsis VlAP17 overexpression also increased ABA levels, a reduction in average stomatal aperture size, and elevated expression levels of stress response genes involved in the ABA-dependent pathway well as higher activities of several antioxidases: superoxide dismutase, catalase, and peroxidase. Recently, Sebastián et al. (2020) reported that APA1 encoding AP in known to be highly expressed under water stress in response to salinity, cold, and drought stress. Our study also found that AP expression increases in response to heat stress in plant seed tissue, suggesting their crucial role in response to heat stress.

TRINITY_DN326896_c0_g1_i1 (Elongation factor 1-alpha) Elongation factor 1α- is a multifunctional protein Transcript elongation factors (EFs) play essential role in mediating critical cellular processes related to cellular growth, proliferation, and cell differentiation by interacting with other cellular proteins (Bukovnik et al., 2009; Zheng et al., 2014). Its high expression during heat stress conditions in animals and plants has been reported and thus suggested its essential role in survival under stress conditions (Buckley, 2006; Shamovsky et al., 2006; Bukovnik et al., 2009). They further mentioned its role in heat stress in wheat as accumulation was high in cultivars with better heat tolerance. Zheng et al. (2014) characterized a transcript elongation factor gene in wheat through expression based association analysis, comparing near-isogenic lines and by overexpression in *Arabidopsis* and reported its role in regulating yield-related traits involved in vegetative growth and reproductive development. In our study, the upregulated expression of the

TABLE 3 | Details of SSR markers obtained from *de novo* transcriptome assembly as well as unique differential expressed genes of all the stages.

	De novo assembly	DEGs (unique DEGs of all sets)
Total number of sequences examined	1,696,570	60,051
Total number of identified SSRs	98,412	2,730
Number of SSR containing sequences	89,321	2,379
Number of sequences containing more than 1 SSR	7,986	292
Number of SSRs present in compound formation	4,261	243
Mono	37,716	668
Di	27,697	832
Tri	29,659	1,154
Tetra	2,773	59
Penta	381	3

A total of 98,412 simple sequences repeats (SSRs) were identified from 1,696,570 transcripts of wheat de novo transcriptome assembly, while 4,261 repeats were present in compound formation. Out of 98,412 markers, there was abundance of mononucleotides- (37716), followed by di- (27697), tri- (29659), tetra- (2773), penta- (381), and hexa (186) nucleotide repeats.

EF also suggests its role during the grain filling stage in wheat. Metabolic proteins of wheat, mainly involved in glycolysis, carbohydrate metabolism, and the stress response, show differential expression profiles in response to elevated temperature conditions (Laino et al., 2010).

TRINITY_DN490415_c0_g1_i8 (α-gliadin) was found to be upregulated in the present study. Yang et al. (2011) has reported that the expression of many storage proteins is under heat or water deficit, *viz.*, α-gliadin, γ-gliadin, low molecular weight glutenin, and globulins in the seeds altered. Further, the abundance of glidins was found to increase under heat stress from anthesis up to 10 DPA. Du Pont et al. (2006) also studied that amount of α-gliadins increases in response to elevated temperature conditions during endosperm development in wheat. Our results are in agreement of the above studies.

TRINITY_DN425597_c0_g2_i2 (heat shock protein 83-like) belongs to the heat shock protein group, which are well known for their protective role in response to elevated temperatures in almost all organisms, including plants. These proteins perform multiple functions, such as protein folding, translocation across membranes, facilitation of protein–protein interaction, and preventing protein aggregation and regulation of synthesis of other stress-related genes during heat stress conditions (Åkerfelt et al., 2010; Roy et al., 2019). Conner et al. (1990) reported the heat-inducible expression of AtHS83 in *Arabidopsis thaliana*. Felsheim and Das (1992) reported the differential expression of HSP83 member genes in response to heat stress and photoperiod duration in cotyledons. Disruption of genes encoding HSP83 has been shown to have detrimental effects on the growth and survival in yeast at high temperature (Borkovich et al., 1989). Our results also agree with the above study and we can conclude that heat shock proteins also have an essential role in wheat during heat stress.

TRINITY_DN385005_c2_g1_i2 (Zinc transporter), a transmembrane zinc transporter is reported to confer heat tolerance during grain filling stage by maintaining optimum cellular zinc concentration required for the proper working of an enzyme related to stress tolerance carbohydrate metabolism and normal seed filling process under heat stress (Kobayashi et al., 1998). They also reported zinc transporter's role in normal flowering and fruit development. Moreover, the Zn is crucial for plant growth and development as it is required by various enzymes involved in carbohydrate metabolism, cell membrane stability and integrity, protein synthesis, auxin synthesis regulation, ribosomal stabilization, and cytochrome synthesis (Marschner, 1995). Zn also plays role in the stress tolerance mechanism of plants by regulating gene expression of various stress-related genes (Cakmak, 2000). Homeostasis in cellular zinc concentration improves the plant tolerance to heat and salt stress in various plant species by improving the water uptake and transport (Peck and McDonald, 2010; Tavallali et al., 2010; Disante et al., 2011). Sarwar et al. (2019) reported the role of exogenously applied zinc and other micronutrients in heat stress alleviation in cotton. Specific Zn transporters maintain the optimum cellular concentration through influx, efflux, and compartmentalization. Thus, we can also suggest that upregulation in gene expression of zinc transporter 6 in our study contribute to heat tolerance in wheat.

Therefore, the transcripts validated randomly using q-PCR in the present study are multifunctional. Most of them are reported to be overexpressed in response to multiple stress conditions including heat, drought, pathogen, or insect attack. Some genes are very crucial for maintaining seed quality parameter *viz.,* number of different seed-specific protein content and carbohydrate metabolism specifically under heat stress. Some transcripts also play protective role during heat stress ensuring proper protein folding, protein translocation, and enzyme functioning. Other transcripts play significant role in regulating seed developmental processes under heat stress by regulating molecular processes including gene expression, protein synthesis etc. Further, these transcripts help in better understanding of complex molecular and biochemical mechanism of heat stress response in wheat.

In addition, we also identified SSRs from wheat *de novo* transcriptome assembly and characterized them. The repeat pattern of identified SSRs indicated an abundance of mononucleotides followed by di, tri, tetra, penta, and hexanucleotide repeats (**Supplementary File 6**). In dinucleotide repeats, we found the maximum number of repeats as GA followed by AG and CT. In the case of trinucleotides, GGC repeats were most abundant followed by GCG and GAG (**Table 3**). Additionally, we found a total of about one hundred thousand variants against the *de novo* transcriptome assembly of wheat, containing SNPs and Indels. Thirty-eight variants were reported in transcript ID "TRINITY_DN523265_c0_g1_i3 representing WD repeat and FYVE domain-containing protein 3" incidentally all of them being SNPs (**Supplementary File 7**). Similarly, we obtained one

TABLE 4 | Details of randomly selected SSR markers (thirteen dinucleotide and two trinucleotide repeats) along with their primer sequence and melting temperature ranging from 57.17°C to 60.99°C.

ID	SSR type	Unit	SSR	Primer Pairs (5′-3′)	Tm (°C)
TRINITY_DN252967_c0_g2_i1	Tri	10	(TGT)10	SP-SSR-F1-TGTTGTTGTTGCTTGTGTTGT SP-SSR-R1-TCATTTTATTTGCACATAAACTGCTT	57.62 57.17
TRINITY_DN510811_c3_g6_i3	Di	10	(TC)10	SP-SSR-F2-GACACGCACAAACACCCATT SP-SSR-R2-TGACAGAAAAACAGAAAACAGAACA	59.61 58.02
TRINITY_DN473094_c8_g3_i1	Di	19	(GA)19	SP-SSR-F3-GTCGTCCTCCTATGCACTCG SP-SSR-R3-CCGCGTGCTGGATTAATTGG	59.97 59.97
TRINITY_DN513544_c0_g11_i2	Di	10	(TC)10	SP-SSR-F4-CTGATGATGTTGCGGGCATG SP-SSR-R4-CTCACTGTTGAGCTGCACAA	59.97 58.69
TRINITY_DN503444_c13_g12_i1	Di	17	(AG)17	SP-SSR-F5-GGAGAGAGATTGGGCGAGTG SP-SSR-R5-AGGTATTCCCTCCTTCCCCC	59.89 60.02
TRINITY_DN438564_c3_g5_i2	Di	12	(TC)12	SP-SSR-F6-GGTATGTACCAGTAGCTATGTGT SP-SSR-R6-CCCATTGTCACCACGGGTAT	57.21 59.74
TRINITY_DN456622_c3_g1_i1	Di	10	(GT)10	SP-SSR-F7-TAGTCAGAGACGGGCATCCA SP-SSR-R7-ACACACTTCCACATGTTTATCTGC	60.03 59.78
TRINITY_DN523626_c2_g1_i3	Di	17	(TC)17	SP-SSR-F8-TGTCGTGATGCCCAAGTTGT SP-SSR-R8-TGGGTGCCATCCATTGACTC	60.17 60.03
TRINITY_DN511017_c1_g2_i7	Di	10	(AG)10	SP-SSR-F9-TGTCAGACTTGCTAGGCGAC SP-SSR-R9-TCAAGACCCACATGACACCT	59.75 58.56
TRINITY_DN431119_c0_g4_i2	Di	10	(AG)10	SP-SSR-F10-GTGTTGGGGAACGTAGCAGA SP-SSR-R10-GCGCTTGGATCGGAATCAAC	59.96 59.97
TRINITY_DN408106_c2_g1_i1	Di	10	(AG)10	SP-SSR-F11-TCGAAATCGAAAAACATGTCCACA SP-SSR-R11-TGTGCTTTATACTTCGATGTTGTGA	59.72 59.07
TRINITY_DN500214_c8_g1_i2	Di	10	(TC)10	SP-SSR-F12-ACGAACTGCTTGGGTGAGTT SP-SSR-R12-TTTGTCCCGGCCTTGTTCTT	59.82 60.10
TRINITY_DN459549_c1_g2_i1	Di	11	(TG)11	SP-SSR-F13- GTTGCGTGCGTGTGTGTG SP-SSR-R13-ACGCCTTCTCTTCCCTCTCT	60.64 59.96
TRINITY_DN517244_c1_g1_i2	Di	19	(AG)19	SP-SSR-F14-GTTGCATACGAGGAGGGGAC SP-SSR-R14-TCTCCCTCTCCCTCTCCCTC	60.17 60.99
TRINITY_DN17441_c0_g1_i1	Tri	13	(CAA)13	SP-SSR-F15-GCCATGTGATGCAGCAACAA SP-SSR-R15-GCTGAGCTTGGATGATACTCT	60.03 57.25

hundred and ten thousand variants against the wheat genome, containing SNPs and Indels. Maximum variants were identified from chromosome number 3B followed by chromosomes 2B and 2A (**Supplementary File 7**). Being high throughput and high density in nature coupled with widespread distribution throughout the genome, SNP markers are popular and important for their utilization in population genetic diversity studies, gene mapping, and high-density linkage map construction (Unterseer et al., 2014; Carrillo-Perdomo et al., 2020). Therefore, the genic-SSR markers and SNP markers reported in this study along with previously developed markers from other laboratories will be a powerful resource for molecular taxonomic studies and construction of a reference molecular map of the wheat genome. Since such genic-SSR and SNP markers represent the gene-rich regions of the genome, many of these can be utilized in marker-assisted breeding (Dutta et al., 2011). Also because of conservation of genic sequences, these markers have a greater chance of transferability across species, compared to genomic SSR markers which show high polymorphism but are less conserved between species (Wang et al., 2021).

The miRNAs are known as key players in regulating plant gene expression *via* targeting important genes involved in growth and developmental during heat stress (Xin et al., 2010; Kumar et al., 2015). DEGs sets using 119 mature miRNAs were subjected to miRNA target prediction for *T. aestivum*. Out of total ten sets, only differential expressed genes of three sets were involved in miRNA target prediction. miRNAs were found with a maximum number of transcripts targeted by "tae-miR1117." Also in DEG set C2 vs. R2, 31 miRNAs were found with maximum hits were targeted by "tae-miR1117" (**Supplementary File 5**). Common miRNAs in C1 vs.C2, C2 vs. C5, and C2 vs. R2 were 20 in number while there were only 5 and 3 miRNAs that were found unique in C2 vs. C5 and C2 vs. R2, respectively (**Figure 6**). These tiny miRNAs are very crucial to modulate the physiological, biochemical, and molecular responses by targeting key genes during heat stress.

Taking together, the present study enriches our current understanding of known heat response mechanisms during the grain filling stage in wheat supported by discovery of novel transcripts, microsatellite markers, putative miRNA targets, and genetic variant. Further work on functional validation of these genes, miRNAs, SSRs, and SNPs could pave the way for developing improved heat tolerance in wheat varieties, making them more suitable for production in the current climate change scenario.

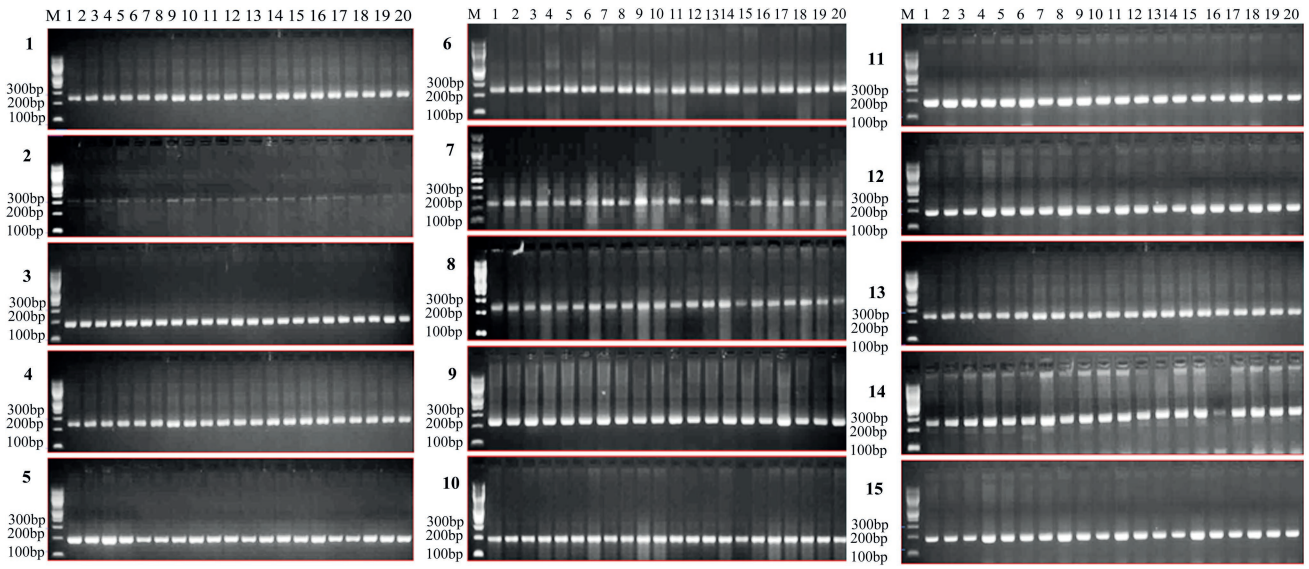


FIGURE 7 | Gel pictures depicting the expression of identified genic SSRs in highly diverse wheat genotypes (1-UP2425, 2-WR544, 3-SONARA64, 4-K7903 (HALNA), 5-WH730, 6-DBW14, 7-RAJ4014, 8-DBW71, 9-AKAW1071, 10-RAJ3765, 11-NIAW34, 12-NW1014, 13-K9465, 14-K9644, 15-HD2733, 16-K9107, 17-PBW502, 18-DBW17, 19-RAJ4083, and 20-WH542) for heat stress.

TABLE 5 | Differentially Expressed Transcripts (DETs) and primers used for qPCR.

Sr. No.	Transcript ID	Primer Pair	Primer Sequence	Tm (°C)	GC %	Amplicon Size (bp)
1	TRINITY_DN521405_c2_g2_i1 (Avenin-like a4)	SP-QF33 SP-QR33	TGCCCTTGCTGCTGTCGCATGA ACAGATGTGGCAGGCAAGCGGT	55.44 57.08	59.09 58.33	137
2	TRINITY_DN483169_c0_g1_i6 (Alpha-amylase inhibitor 0.19)	SP-QF24 SP-QR24	AGCCGAGTACGACGCATGGAGCGTT TGCCATTGCACTGGAGCCTCAGCA	58.21 57.21	60.00 58.33	119
3	TRINITY_DN518599_c1_g1_i2 (Aspartic proteinase oryzasin-1)	SP-QF31 SP-QR31	TTAAGCTAGCCCGCTTGTGCCA ACGGCAAACTAGCGAATCCTGCGT	52.72 55.07	54.55 54.17	114
4	TRINITY_DN326896_c0_g1_i1 (Elongation factor 1-alpha)	SP-QF10 SP-QR10	TGAAGGAGCCCTTTCCCATCTCAGCA ACACGTAGATTCGGGCAAGTCCACCA	55.92 56.02	53.85 53.85	122
5	TRINITY_DN385005_c2_g1_i2 (Zinc transporter 6)	SP-QF12 SP-QR12	GTCCCTGCTGTCAGGTGGAGGAATAA ACGACCGACATGCATCTGAAGTGGA	54.07 54.23	53.85 52.00	125
6	TRINITY_DN425597_c0_g2_i2 (heat shock protein 83-like)	SP-QF15 SP-QR15	AAGCCAGAAGACAGGAGCGCAGTT ACATGGCAGCAAAGAAACACCTGGAG	54.72 54.01	54.17 50.00	148
7	TRINITY_DN490415_c0_g1_i8 (Alpha-gliadin)	SP-QF25 SP-QR25	ATTTCCGCGAACTGGGGCAGTTGT TCCTTCCAACAGCCTCAGCAGCAA	55.47 54.81	54.17 54.17	119
8	TRINITY_DN365152_c1_g1_i1 (Curcuminoid synthase)	SP-QF11 SP-QR11	ACGCATTCCGTAGCGCCATTGT TATATTGTCCAGGATCGGACGCCCT	53.39 53.19	54.55 52.00	143
9	TRINITY_DN472370_c0_g2_i1 (Uncharacterized protein)	SP-QF21 SP-QR21	AGAGGCCTTGGGGTTGAAACAACCTT TTCATCCCGCATCGCCAGTTCTGCTT	55.02 56.99	50.00 53.85	146
10	TRINITY_DN441674_c0_g2_i1 (Putative uncharacterized protein)	SP-QF17 SP-QR17	GTTTGTTTTACGGCGTAGCCTCCCGA ACTCAAGCCTCGCTTGGTATTGGGCA	55.24 56.65	53.85 53.85	143

GC content of the primers was ranged from 50.00 to 60.00% and the size of amplicon was observed to be ranged from 114 to 148.

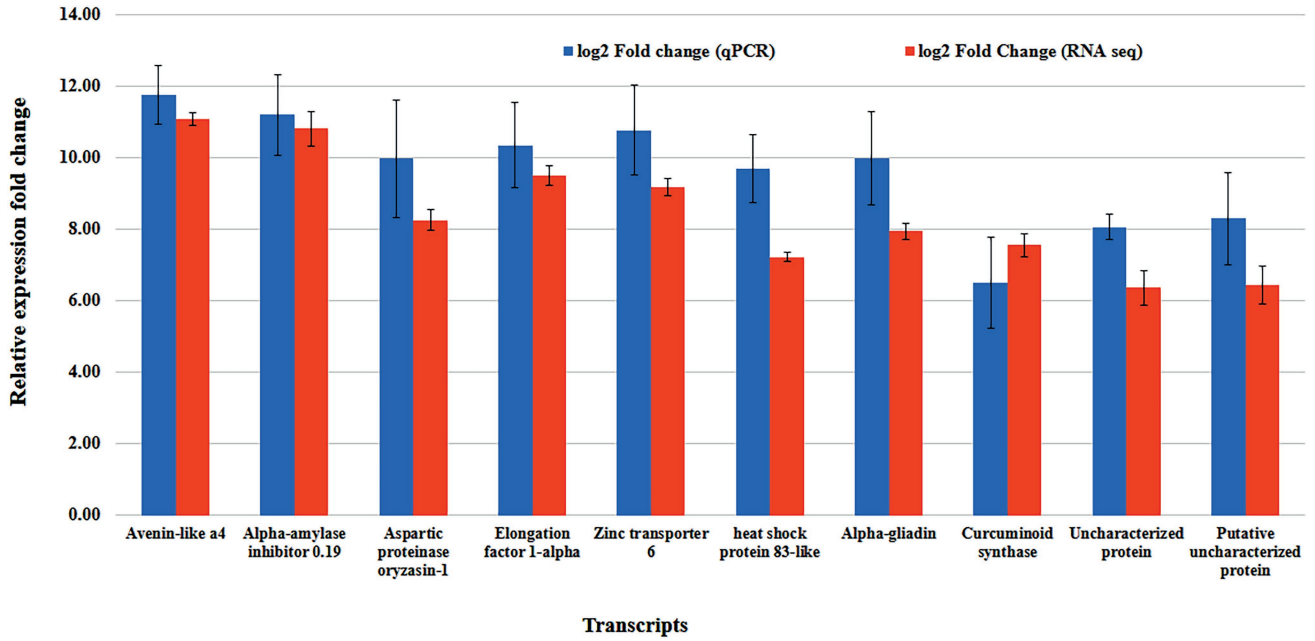


FIGURE 8 | Comparative expression analysis of selected DEGs using RNA-seq and qPCR. Data are means of two independent biological replicates ($p \leq 0.05$, $n = 2$). Error bars represent the means ± SD ($n = 2$). Accuracy of the RNA-seq data getting confirmation with the qPCR expression pattern results.

CONCLUSION

Climatic change has affected the quantity and quality of major food crops and thus poses a significant threat to global food security. Initial few days of grain filling are crucial for the net yield of the crop. Heat stress during this period drastically reduces the overall yield. Our *de novo* transcriptomics-based study of the heat stress-tolerant wheat genotype K7903 (Halna) reveals that the upregulation of key genes during initial grain filling stages might be playing crucial role in heat tolerance mechanism. K7903 (Halna) might have genetic and epigenetic (miRNA expression) control mechanism which might be contributing toward avoidance of the detrimental effect of heat stress and thereby maintaining yield and grain quality. The significant findings could further be functionally validated using reverse genetic tools either in wheat or any other model plants which might assist molecular breeders to design suitable strategies to develop heat-tolerant wheat genotypes. In this study, we identified heat stress-responsive miRNA and their target genes, which have critical role in gene regulation during grain filling under heat stress conditions. This valuable information will enrich our knowledge about involvement of different key genes and their expression pattern regulating the grain filling process when exposed to high temperature conditions. This knowledge can be further utilized in identification, characterization, and breeding strategies to develop heat stress-tolerant wheat varieties.

DATA AVAILABILITY STATEMENT

The datasets presented in this study can be found in online repositories. The names of the repository/repositories and accession number(s) can be found at: https://www.ncbi.nlm.nih.gov/, PRJNA813970, SAMN26531246, SAMN26531247, SAMN26531249, SAMN26531250, SAMN26531251, SAMN 26531252, SAMN26531253, SRR18273340, SRR18273339, SRR 18273338, SRR18273337, SRR18273336, SRR18273335, SRR 18273334, SRR18273333.

AUTHOR CONTRIBUTIONS

RT and JD conceived the theme of study. SP, SJ, UA, MI, and RS analyzed the data. SP, JD, MI, PS, RS, and RT drafted the manuscript. SP, NR, and SS conducted the field work. OG and DK were instrumental in formatting the tables and graphs. RT, JD, AR, GS, DK, and MI provided overall guidance and edited the manuscript. All authors read and approved the final version of the manuscript.

FUNDING

This work was supported by CABin grant (F. No. Agril. Edn.4–1/2013-A&P) of ICAR-IASRI, New Delhi in alignment with in-house project of ICAR-IIWBR, Karnal.

ACKNOWLEDGMENTS

The authors are thankful to the Director, ICAR-Indian Institute of Wheat and Barley Research, Karnal for providing research facility. Authors are thankful to Indian Council of Agricultural Research, Ministry of Agriculture and Farmers' Welfare, Govt. of India for providing financial assistance in the form of CABin grant (F. no.

Agril. Edn.4-1/2013-AandP) as well as Advanced Super Computing Hub for Omics Knowledge in Agriculture (ASHOKA) facility at ICAR-IASRI, New Delhi, India. The authors are also grateful for the support and guidance received from the department of Biotechnology, Chaudhary Devi Lal University, Sirsa, Haryana, India.

SUPPLEMENTARY MATERIAL

The Supplementary Material for this article can be found online at: https://www.frontiersin.org/articles/10.3389/fpls.2022.904392/full#supplementary-material

REFERENCES

Åkerfelt, M., Morimoto, R. I., and Sistonen, L. (2010). Heat shock factors: integrators of cell stress, development and lifespan. *Nat. Rev. Mol. Cell Biol.* 11, 545–555. doi: 10.1038/nrm2938

Akter, N., and Islam, M. R. (2017). Heat stress effects and management in wheat. A review. *Agron. Sustain. Dev.* 37, 1–17. doi: 10.1007/s13593-017-0443-9

Alam, M. M., Nakamura, H., Ichikawa, H., Miyao, A., Hirochika, H., Kobayashi, K., et al. (2014). Response of an aspartic protease gene OsAP77 to fungal, bacterial and viral infections in rice *Rice.* 7:9. doi: 10.1186/s12284-014-0009-2

Anders, S., and Huber, W. (2010). Differential expression analysis for sequence count data. *Genome Biol.* 11:R106. doi: 10.1186/gb-2010-11-10-r106

Asakura, T., Watanabe, H., Abe, K., and Arai, S. (1995). Rice aspartic proteinase, oryzasin, expressed during seed ripening and germination, has a gene organization distinct from those of animal and microbial aspartic proteinases. *Eur. J. Biochem.* 232, 77–83. doi: 10.1111/j.1432-1033.1995.tb20783.x

Awlachew, Z. T., Singh, R., Kaur, S., Bains, N. S., and Chhuneja, P. (2016). Transfer and mapping of the heat tolerance component traits of *Aegilops speltoides* in tetraploid wheat *Triticum durum*. *Mol. Breed.* 36, 1–15. doi: 10.1007/s11032-016-0499-2

Berkman, P. J., Lai, K., Lorenc, M. T., and Edwards, D. (2012). Next generation sequencing applications for wheat crop improvement. *American J. Bot.* 99, 365–371. doi: 10.3732/ajb.1100309

Borkovich, K. A., Farrelly, F. W., Finkelstein, D. B., Taulien, J., and Lindquist, S. (1989). hsp82 is an essential protein that is required in higher concentrations for growth of cells at higher temperatures. *Mol. Cell. Biol.* 9, 3919–3930.

Buckley, B. A. (2006). The cellular response to heat stress in the goby *Gillichthys mirabilis*: a cDNA microarray and protein-level analysis. *J. Exp. Biol.* 209, 2660–2677. doi: 10.1242/jeb.02292

Bukovnik, U., Fu, J., Bennett, M., Prasad, P. V., and Ristic, Z. (2009). Heat tolerance and expression of protein synthesis elongation factors, EF-Tu and EF-1α, in spring wheat. *Funct. Plant Biol.* 36, 234–241. doi: 10.1071/FP08266

Cakmak, I. (2000). Role of zinc in protecting plant cells from reactive oxygen species. *New Phytol.* 146, 185–205. doi: 10.1046/j.1469-8137.2000.00630.x

Camacho, C., Coulouris, G., Avagyan, V., Ma, N., Papadopoulos, J., Bealer, K., et al. (2009). BLAST+: architecture and applications. *BMC Bioinform.* 10:421. doi: 10.1186/1471-2105-10-421

Carrillo-Perdomo, E., Vidal, A., Kreplak, J., Duborjal, H., Leveugle, M., Duarte, J., et al. (2020). Development of new genetic resources for faba bean (*Vicia faba* L.) breeding through the discovery of gene-based SNP markers and the construction of a high-density consensus map. *Sci. Rep.* 10:6790. doi: 10.1038/s41598-020-63664-7

Chen, X. Y., Cao, X. Y., Zhang, Y. J., Islam, S., Zhang, J. J., Yang, R. C., et al. (2016). Genetic characterization of cysteine-rich type-b avenin-like protein coding genes in common wheat. *Sci. Rep.* 6, 1–12. doi: 10.1038/srep30692

Chu, C., Wang, S., Paetzold, L., Wang, Z., Hui, K., Rudd, J. C., et al. (2021). RNA-seq analysis reveals different drought tolerance mechanisms in two broadly adapted wheat cultivars 'TAM 111′ and 'TAM 112′. *Sci. Rep.* 11:4301. doi: 10.1038/s41598-021-83372-0

Cohen, S. P., and Leach, J. E. (2019). Abiotic and biotic stresses induce a core transcriptome response in rice. *Sci. Rep.* 9:6273. doi: 10.1038/s41598-019-42731-8

Conner, T. W., La Fayette, P. R., Nagao, R. T., and Key, J. L. (1990). Sequence and expression of a HSP83 from *Arabidopsis thaliana*. *Plant Physiol.* 94, 1689–1695. doi: 10.1104/pp.94.4.1689

Coolen, S., Proietti, S., Hickman, R., Davila Olivas, N. H., Huang, P. P., Van Verk, M. C., et al. (2016). Transcriptome dynamics of Arabidopsis during sequential biotic and abiotic stresses. *Plant J.* 86, 249–267. doi: 10.1111/tpj.13167

Dai, X., and Zhao, P. X. (2011). psRNATarget: a plant small RNA target analysis server. *Nucl. acids res.* 39, W155–W159. doi: 10.1093/nar/gkr319

De Carvalho, M. H. C., d'Arcy-Lameta, A., Roy-Macauley, H., Gareil, M., El Maarouf, H., Pham-Thi, A. T., et al. (2001). Aspartic protease in leaves of common bean (*Phaseolus vulgaris* L.) and cowpea (*Vigna unguiculata* L. Walp): enzymatic activity, gene expression and relation to drought susceptibility. *FEBS Lett.* 492, 242–246. doi: 10.1016/S0014-5793(01)02259-1

Disante, K. B., Fuentes, D., and Cortina, J. (2011). Response to drought of Zn-stressed *Quercus suber* L. seedlings. *Env. Exp. Bot.* 70, 96–103. doi: 10.1016/j.envexpbot.2010.08.008

Dombrowski, J. E. (2003). Salt stress activation of wound-related genes in tomato plants. *Plant Physiol.* 132, 2098–2107. doi: 10.1104/pp.102.019927

Du Pont, F. M., Hurkman, W. J., Vensel, W. H., Chan, R., Lopez, R., Tanaka, C. K., et al. (2006). Differential accumulation of sulfur-rich and sulfur-poor wheat flour proteins is affected by temperature and mineral nutrition during grain development. *J. Cereal Sci.* 44, 101–112. doi: 10.1016/j.jcs.2006.04.003

Dutta, S., Kumawat, G., Singh, B. P., Gupta, D. K., Singh, S., Dogra, V., et al. (2011). Development of genic-SSR markers by deep transcriptome sequencing in pigeon pea [*Cajanus cajan* (L.) Millspaugh]. *BMC Plant Biol.* 11:17. doi: 10.1186/1471-2229-11-17

Fahad, S., Bajwa, A. A., Nazir, U., Anjum, S. A., Farooq, A., Zohaib, A., et al. (2017). Crop production under drought and heat stress: plant responses and management options. *Front. Plant Sci.* 8:1147. doi: 10.3389/fpls.2017.01147

Farooq, M., Bramley, H., Palta, J. A., and Siddique, K. H. (2011). Heat stress in wheat during reproductive and grain-filling phases. *Crit. Rev. Plant Sci.* 30, 491–507. doi: 10.1080/07352689.2011.615687

Felsheim, R. F., and Das, A. (1992). Structure and expression of a heat-shock protein 83 gene of *Pharbitis nil*. *Plant Physiol.* 100, 1764–1771. doi: 10.1104/pp.100.4.1764

Feng, G. H., Richardson, M., Chen, M. S., Kramer, K. J., Morgan, T. D., and Reeck, G. R. (1996). α-Amylase inhibitors from wheat: amino acid sequences and patterns of inhibition of insect and human α-amylases. *Insect Biochem. Mol. Biol.* 26, 419–426. doi: 10.1016/0965-1748(95)00087-9

Franco, O. L., Rigden, D. J., Melo, R., Bloch, C. Jr., Silva, C. P., and Grossi de Sá, M. F. (2000). Activity of wheat αamylase inhibitors towards bruchid αamylases and structural explanation of observed specificities. *Eur. J. Biochem.* 267, 2166–2173. doi: 10.1046/j.1432-1327.2000.01199.x

Fu, L., Niu, B., Zhu, Z., Wu, S., and Li, W. (2012). CD-HIT: accelerated for clustering the next-generation sequencing data. *Bioinformatics* 28, 3150–3152. doi: 10.1093/bioinformatics/bts565

Goswami, S., Kumar, R. R., and Rai, R. D. (2014). Heat-responsive microRNAs regulate the transcription factors and heat shock proteins in modulating thermo stability of starch biosynthesis enzymes in wheat (*Triticum aestivum* L.) under the heat stress. *Aust. J. Crop. Sci.* 8:697

Grabherr, M. G., Haas, B. J., Yassour, M., Levin, J. Z., Thompson, D. A., Amit, I., et al. (2011). Full-length transcriptome assembly from RNA-Seq data without a reference genome. *Nat. Biotechnol.* 29, 644–652. doi: 10.1038/nbt.1883

Grover, A., Mittal, D., Negi, M., and Lavania, D. (2013). Generating high temperature tolerant transgenic plants: achievements and challenges. *Plant Sci.* 206, 38–47. doi: 10.1016/j.plantsci.2013.01.005

Guevara, M. G., Almeida, C., Mendieta, J. R., Faro, C. J., Veríssimo, P., Pires, E. V., et al. (2005). Molecular cloning of a potato leaf cDNA encoding an aspartic protease (StAsp) and its expression after *P. infestans* infection. *Plant Physiol. Biochem.* 43, 882–889. doi: 10.1016/j.plaphy.2005.07.004

Gupta, P. K., Balyan, H. S., Gahlaut, V., and Kulwal, P. L. (2012). Phenotyping, genetic dissection, and breeding for drought and heat tolerance in common

wheat: status and prospectus. *Plant Breed.* 6, 5–168. doi: 10.1002/9781118358566.ch2

Haas, B. J., Papanicolaou, A., Yassour, M., Grabherr, M., Blood, P. D., Bowden, J., et al. (2013). De novo transcript sequence reconstruction from RNA-seq using the trinity platform for reference generation and analysis. *Nat. Protoc.* 8, 1494–1512. doi: 10.1038/nprot.2013.084

Hajheidari, M., Eivazi, A., Buchanan, B. B., Wong, J. H., Majidi, I., and Salekdeh, G. H. (2007). Proteomics uncovers a role for redox in drought tolerance in wheat. *J. Proteome Res.* 6, 1451–1460. doi: 10.1021/pr060570j

Henry, R. J., Rangan, P., and Furtado, A. (2016). Functional cereals for production in new and variable climates. *Curr. Opin. Plant Biol.* 30, 11–18. doi: 10.1016/j.pbi.2015.12.008

Iquebal, M. A., Sharma, P., Jasrotia, R. S., Jaiswal, S., Kaur, A., Saroha, M., et al. (2019). RNAseq analysis reveals drought-responsive molecular pathways with candidate genes and putative molecular markers in root tissue of wheat. *Sci. Rep.* 9, 13917–13918. doi: 10.1038/s41598-019-49915-2

Jiang, S. S., Liang, X. N., Li, X., Wang, S. L., Lv, D. W., Ma, C. Y., et al. (2012). Wheat drought-responsive grain proteome analysis by linear and nonlinear 2-DE and MALDI-TOmass spectrometry. *Int. J. Mol. Sci.* 13, 16065–16083. doi: 10.3390/ijms131216065

Jin, J., Tian, F., Yang, D. C., Meng, Y. Q., Kong, L., Luo, J., et al. (2016). PlantTFDB 4.0: toward a central hub for transcription factors and regulatory interactions in plants. *Nucleic Acids Res.* 45, D1040–D1045. doi: 10.1093/nar/gkw982

Kang, W. H., Sim, Y. M., Koo, N., Nam, J. Y., Lee, J., Kim, N., et al. (2020). Transcriptome profiling of abiotic responses to heat, cold, salt, and osmotic stress of *Capsicum annuum* L. *Sci. Data.* 7:17. doi: 10.1038/s41597-020-0352-7

Kang, W. H., and Yeom, S. I. (2018). Genome-wide identification, classification, and expression analysis of the receptor-like protein family in tomato. *Plant Pathol. J.* 34, 435–444. doi: 10.5423/PPJ.OA.02.2018.0032

Kobayashi, A., Sakamoto, A., Kubo, K., Rybka, Z., Kanno, Y., and Takatsuji, H. (1998). Seven zincfinger transcription factors are expressed sequentially during the development of anthers in petunia. *Plant J.* 13, 571–576. doi: 10.1046/j.1365-313X.1998.00043.x

Kosina, P., Reynolds, M., Dixon, J., and Joshi, A. (2007). Stakeholder perception of wheat production constraints, capacity building needs, and research partnerships in developing countries. *Euphytica* 157, 475–483. doi: 10.1007/s10681-007-9529-9

Kumar, R. R., Goswami, S., Sharma, S. K., Kala, Y. K., Rai, G. K., Mishra, D. C., et al. (2015). Harnessing next generation sequencing in climate change: RNA-Seq analysis of heat stress-responsive genes in wheat (*Triticum aestivum* L.). *J. Int. Biol.* 19, 632–647. doi: 10.1089/omi.2015.0097

Kumar, R. R., Goswami, S., Singh, K., Dubey, K., Rai, G. K., Singh, B., et al. (2018). Characterization of novel heat-responsive transcription factor (TaHSFA6e) gene involved in regulation of heat shock proteins (HSPs)—A key member of heat stress-tolerance network of wheat. *J. Biotechnol.* 279, 1–12. doi: 10.1016/j.jbiotec.2018.05.008

Kumar, R. R., Sharma, S. K., and Goswami, S. (2013). Characterization of differentially expressed stress associated proteins in starch granule development under heat stress in wheat (*Triticum aestivum* L.). *Ind. J. Biochem. Biophys.* 50, 126–138.

Laino, P., Shelton, D., Finnie, C., De Leonardis, A. M., Mastrangelo, A. M., Svensson, B., et al. (2010). Comparative proteome analysis of metabolic proteins from seeds of durum wheat (cv. Svevo) subjected to heat stress. *Proteomics* 10, 2359–2368. doi: 10.1002/pmic.200900803

Lal, M. K., Tiwari, R. K., Gahlaut, V., Mangal, V., and Kumar, A. (2021). Physiological and molecular insights on wheat responses to heat stress. *Plant Cell Rep.* 41, 1–18. doi: 10.1007/s00299-021-02784-4

Langmead, B., Trapnell, C., Pop, M., and Salzberg, S. L. (2009). Ultrafast and memory-efficient alignment of short DNA sequences to the human genome. *Genome Biol.* 10:R25. doi: 10.1186/gb-2009-10-3-r25

Li, B., and Dewey, C. N. (2011). RSEM: accurate transcript quantification from RNA-Seq data with or without a reference genome. *BMC Bioinform.* 12, 1–16. doi: 10.1186/1471-2105-12-323

Li, H., and Durbin, R. (2009). Fast and accurate short read alignment with burrows-wheeler transform. *Bioinformatics* 25, 1754–1760. doi: 10.1093/bioinformatics/btp324

Li, H., Handsaker, B., Wysoker, A., Fennell, T., Ruan, J., Homer, N., et al. (2009). The sequence alignment/map format and SAM tools. *Bioinformatics* 25, 2078–2079. doi: 10.1093/bioinformatics/btp352

Li, M., Sui, N., Lin, L., Yang, Z., and Zhang, Y. (2019). Transcriptomic profiling revealed genes involved in response to cold stress in maize. *Funct. Plant Biol.* 46, 830–844. doi: 10.1071/FP19065

Livak, K. J., and Schmittgen, T. D. (2001). Analysis of relative gene expression data using real-time quantitative PCR and the $2^{-\Delta\Delta CT}$ method. *Methods* 25, 402–408. doi: 10.1006/meth.2001.1262

Ma, F., Li, M., Li, T., Liu, W., Liu, Y., Li, Y., et al. (2013). Overexpression of avenin-like b proteins in bread wheat (*Triticum aestivum* L.) improves dough mixing properties by their incorporation into glutenin polymers. *PLoS One* 8:e66758. doi: 10.1371/journal.pone.0066758

Marschner, H. (1995). *Mineral Nutrition of Higher Plants. 2nd Edn*. London: Academic Press.

Martin, M. (2011). Cutadapt removes adapter sequences from high-throughput sequencing reads. *EMBnet. J.* 17, 10–12. doi: 10.14806/ej.17.1.200

Mendieta, J. R., Pagano, M. R., Munoz, F. F., Daleo, G. R., and Guevara, M. G. (2006). Antimicrobial activity of potato aspartic proteases (StAPs) involves membrane permeabilization. *Microbiol.* 152, 2039–2047. doi: 10.1099/mic.0.28816-0

Morozova, O., and Marra, M. A. (2008). Applications of next-generation sequencing technologies in functional genomics. *Genomics* 92, 255–264. doi: 10.1016/j.ygeno.2008.07.001

Muñoz, F. F., Mendieta, J. R., Pagano, M. R., Paggi, R. A., Daleo, G. R., and Guevara, M. G. (2010). The swaposin-like domain of potato aspartic protease (StAsp-PSI) exerts antimicrobial activity on plant and human pathogens. *Peptides* 31, 777–785. doi: 10.1016/j.fitote.2009.10.004

Mwadzingeni, L., Shimelis, H., Dube, E., Laing, M. D., and Tsilo, T. J. (2016). Breeding wheat for drought tolerance: progress and technologies. *J. Integr. Agric.* 15, 935–943. doi: 10.1016/S2095-3119(15)61102-9

Pareek, A., Dhankher, O. P., and Foyer, C. H. (2020). Mitigating the impact of climate change on plant productivity and ecosystem sustainability. *J. Exp. Bot.* 71, 451–456. doi: 10.1093/jxb/erz518

Peck, A. W., and McDonald, G. K. (2010). Adequate zinc nutrition alleviates the adverse effects of heat stress in bread wheat. *Plant Soil* 337, 355–374. doi: 10.1007/s11104-010-0532-x

Petrucci, T., Rab, A., Tomasi, M., and Silano, V. (1976). Further characterization studies of the α-amylase protein inhibitor of gel electrophoretic mobility 0.19 from the wheat kernel. *Biochim. Biophys. Acta. Proteins Struc.* 420, 288–297. doi: 10.1016/0005-2795(76)90320-2

Quast, C., Pruesse, E., Yilmaz, P., Gerken, J., Schweer, T., Yarza, P., et al. (2012). The SILVA ribosomal RNA gene database project: improved data processing and web-based tools. *Nucleic Acids Res.* 41, D590–D596. doi: 10.1093/nar/gks1219

Rane, A. S., Joshi, R. S., and Giri, A. P. (2020). Molecular determinant for specificity: differential interaction of α-amylases with their proteinaceous inhibitors. *BBA Gen. Sub.* 1864:129703. doi: 10.1016/j.bbagen.2020.129703

Rangan, P., Furtado, A., and Henry, R. (2020). Transcriptome profiling of wheat genotypes under heat stress during grain-filling. *J. Cereal Sci.* 91:102895. doi: 10.1016/j.jcs.2019.102895

Rawlings, N. D., and Salvesen, G. (2013). *Handbook of Proteolytic Enzymes. Vol. 1*. United States: Academic Press.

Roy, S., Mishra, M., Dhankher, O. P., Singla-Pareek, S. L., and Pareek, A. (2019). "Molecular chaperones: key players of abiotic stress response in plants" in *Genetic Enhancement of Crops for Tolerance to Abiotic Stress: Mechanisms and Approaches. Vol. 1*. eds. N. Singh, S. Mittal and N. Thirunavukkarasu (Cham: Springer), 125–165.

Runeberg-Roos, P., Kervinen, J., Kovaleva, V., Raikhel, N. V., and Gal, S. (1994). The aspartic proteinase of barley is a vacuolar enzyme that processes probarleylectin in vitro. *Plant Physiol.* 105, 321–329. doi: 10.1104/pp.105.1.321

Sarwar, M., Saleem, M. F., Ullah, N., Ali, S., Rizwan, M., Shahid, M. R., et al. (2019). Role of mineral nutrition in alleviation of heat stress in cotton plants grown in glasshouse and field conditions. *Sci. Rep.* 9, 1–7. doi: 10.1038/s41598-019-49404-6

Sebastián, D., Fernando, F. D., Raúl, D. G., and Gabriela, G. M. (2020). Overexpression of Arabidopsis aspartic protease APA1 gene confers drought tolerance. *Plant Sci.* 292:110406. doi: 10.1016/j.plantsci.2020.110406

Shamloo, M., Babawale, E. A., Furtado, A., Henry, R. J., Eck, P. K., and Jones, P. J. (2017). Effects of genotype and temperature on accumulation of plant secondary

metabolites in Canadian and Australian wheat grown under controlled environments. *Sci. Rep.* 7, 1–13. doi: 10.1038/s41598-017-09681-5

Shamovsky, I., Ivannikov, M., Kandel, E. S., Gershon, D., and Nudler, E. (2006). RNA-mediated response to heat shock in mammalian cells. *Nature* 440, 556–560. doi: 10.1038/nature04518

Sharma, D., Chandra Pandey, G., Mamrutha, H. M., Singh, R., Singh, N. K., Singh, G. P., et al. (2019). Genotype–phenotype relationships for high-temperature tolerance: An integrated method for minimizing Phenotyping constraints in wheat. *Crop Sci.* 59, 1973–1982. doi: 10.2135/cropsci2019.01.0055

Sheoran, S., Jaiswal, S., Kumar, D., Raghav, N., Sharma, R., Pawar, S., et al. (2019). Uncovering genomic regions associated with 36 agro-morphological traits in Indian spring wheat using GWAS. *Front. Plant Sci.* 10:527. doi: 10.3389/fpls.2019.00527

Siebert, S., and Ewert, F. (2014). Future crop production threatened by extreme heat. *Environ. Res. Lett.* 9:041001. doi: 10.1088/1748-9326/9/4/041001

Simões, R., Faro, D., and Bur, F. C. (2007). Characterization of recombinant CDR1, an Arabidopsis aspartic proteinase involved in disease resistance. *J. Biol. Chem.* 282, 31358–31365. doi: 10.1074/jbc.M702477200

Singh, R., Iquebal, M. A., Mishra, C. N., Jaiswal, S., Kumar, D., Raghav, N., et al. (2019). Development of model web-server for crop variety identification using throughput SNP genotyping data. *Sci. Rep.* 9, 5122–5129. doi: 10.1038/s41598-019-41204-2

Tavallali, V., Rahemi, M., Eshghi, S., Kholdebarin, B., and Ramezanian, A. (2010). Zinc alleviates salt stress and increases antioxidant enzyme activity in the leaves of pistachio (Pistaciavera L.'Badami') seedlings. *Turk. J. Agr. Forest.* 34, 349–359. doi: 10.3906/tar-0905-10

Thiel, T., Michalek, W., Varshney, R., and Graner, A. (2003). Exploiting EST databases for the development and characterization of gene-derived SSR-markers in barley (*Hordeum vulgare* L.). *Theor. Appl. Genet.* 106, 411–422. doi: 10.1007/s00122-002-1031-0

Unamba, C. I. N., Nag, A., and Sharma, R. K. (2015). Next generation sequencing technologies: The doorway to the unexplored genomics of non-model plants. *Front. Plant Sci.* 6:1074. doi: 10.3389/fpls.2015.01074

Untergasser, I., Cutcutache, T., Koressaar, J., Ye, B. C., Faircloth, R. M., and Rozen, S. G. (2012). Primer3enew capabilities and interfaces. *Nucleic Acids Res.* 40:e115. doi: 10.1093/nar/gks596

Unterseer, S., Bauer, E., Haberer, G., Seidel, M., Knaak, C., Ouzunova, M., et al. (2014). A powerful tool for genome analysis in maize: development and evaluation of the high density 600 k SNP genotyping array. *BMC Genomics* 15:823. doi: 10.1186/1471-2164-15-823

Wang, C., Liu, R., Liu, Y., Hou, W., Wang, X., Miao, Y., et al. (2021). Development and application of the Faba_bean_130K targeted next-generation sequencing SNP genotyping platform based on transcriptome sequencing. *Theor. Appl. Genet.* 134, 3195–3207. doi: 10.1007/s00122-021-03885-0

Xin, M., Wang, Y., Yao, Y., Xie, C., Peng, H., Ni, Z., et al. (2010). Diverse set of microRNAs are responsive to powdery mildew infection and heat stress in wheat (*Triticum aestivum* L.). *BMC Plant Biol.* 10:123. doi: 10.1186/1471-2229-10-123

Yang, F., Jørgensen, A. D., Li, H., Søndergaard, I., Finnie, C., Svensson, B., et al. (2011). Implications of high-temperature events and water deficits on protein profiles in wheat (*Triticum aestivum* L. cv. Vinjett) grain. *Proteomics* 11, 1684–1695. doi: 10.1002/pmic.201000654

Yao, X., Xiong, W., Ye, T., and Wu, Y. (2012). Overexpression of the aspartic protease ASPG1 gene confers drought avoidance in Arabidopsis. *J. Exp. Bot.* 63, 2579–2593. doi: 10.1093/jxb/err433

Zhang, Y., Hu, X., Islam, S., She, M., Peng, Y., Yu, Z., et al. (2018). New insights into the evolution of wheat avenin-like proteins in wild emmer wheat (*Triticum dicoccoides*). *Proc. Natl. Acad. Sci.* 115, 13312–13317. doi: 10.1073/pnas.1812855115

Zhang, Y., Hu, X., Juhasz, A., Islam, S., Yu, Z., Zhao, Y., et al. (2020). Characterising avenin-like proteins (ALPs) from albumin/globulin fraction of wheat grains by RP-HPLC, SDS-PAGE, and MS/MS peptides sequencing. *BMC Plant Biol.* 20, 19–45. doi: 10.1186/s12870-020-2259-z

Zhang, X. M., Zhao, X. Q., Feng, C. X., Liu, N., Feng, H., Wang, X. J., et al. (2014). The cloning and characterization of a DEAD-box RNA helicase from stress-responsive wheat. *Physiol. Mol. Plant Pathol.* 88, 36–42. doi: 10.1016/j.pmpp.2014.07.004

Zhao, J., Lu, Z., Wang, L., and Jin, B. (2021). Plant responses to heat stress: physiology, transcription, noncoding RNAs, and epigenetics. *Int. J. Mol. Sci.* 22:117. doi: 10.3390/ijms22010117

Zheng, J., Liu, H., Wang, Y., Wang, L., Chang, X., Jing, R., et al. (2014). TEF-7A, a transcript elongation factor gene, influences yield-related traits in bread wheat (*Triticum aestivum* L.). *J. Exp. Bot.* 65, 5351–5365. doi: 10.1093/jxb/eru306

Conflict of Interest: The authors declare that the research was conducted in the absence of any commercial or financial relationships that could be construed as a potential conflict of interest.

Publisher's Note: All claims expressed in this article are solely those of the authors and do not necessarily represent those of their affiliated organizations, or those of the publisher, the editors and the reviewers. Any product that may be evaluated in this article, or claim that may be made by its manufacturer, is not guaranteed or endorsed by the publisher.

Copyright © 2022 Paul, Duhan, Jaiswal, Angadi, Sharma, Raghav, Gupta, Sheoran, Sharma, Singh, Rai, Singh, Kumar, Iquebal and Tiwari. This is an open-access article distributed under the terms of the Creative Commons Attribution License (CC BY). The use, distribution or reproduction in other forums is permitted, provided the original author(s) and the copyright owner(s) are credited and that the original publication in this journal is cited, in accordance with accepted academic practice. No use, distribution or reproduction is permitted which does not comply with these terms.

frontiers | Frontiers in Plant Science

ORIGINAL RESEARCH
published: 27 June 2022
doi: 10.3389/fpls.2022.922561

Characteristics and Regulating Roles of Wheat TaHsfA2-13 in Abiotic Stresses

Xiangzhao Meng[1], Baihui Zhao[1,2], Mingyue Li[1,2], Ran Liu[1,2], Qianqian Ren[1,3], Guoliang Li[1] and Xiulin Guo[1]**

[1]Institute of Biotechnology and Food Science, Hebei Academy of Agriculture and Forestry Sciences/Plant Genetic Engineering Center of Hebei Province, Shijiazhuang, China, [2]College of Life Sciences, Hebei Normal University, Shijiazhuang, China, [3]College of Landscape and Ecological Engineering, Hebei University of Engineering, Handan, China

OPEN ACCESS

Edited by:
Caroline Müller, Universidade Federal da Fronteira Sul, Brazil

Reviewed by:
Shabir Hussain Wani, Sher-e-Kashmir University of Agricultural Sciences and Technology, India
Harsh Chauhan, Indian Institute of Technology Roorkee, India
Xiaoxu Li, Chinese Academy of Agricultural Sciences, China

***Correspondence:**
Xiulin Guo
myhf2002@163.com
Guoliang Li
guolianglili@haafs.org

Specialty section:
This article was submitted to Plant Abiotic Stress, a section of the journal Frontiers in Plant Science

Received: 18 April 2022
Accepted: 10 June 2022
Published: 27 June 2022

Citation:
Meng X, Zhao B, Li M, Liu R, Ren Q, Li G and Guo X (2022) Characteristics and Regulating Roles of Wheat TaHsfA2-13 in Abiotic Stresses. Front. Plant Sci. 13:922561. doi: 10.3389/fpls.2022.922561

Heat shock transcription factor (Hsf) exists widely in eukaryotes and responds to various abiotic stresses by regulating the expression of downstream transcription factors, functional enzymes, and molecular chaperones. In this study, *TaHsfA2-13*, a heat shock transcription factor belonging to A2 subclass, was cloned from wheat (*Triticum aestivum*) and its function was analyzed. *TaHsfA2-13* encodes a protein containing 368 amino acids and has the basic characteristics of Hsfs. Multiple sequence alignment analysis showed that TaHsfA2-13 protein had the highest similarity with TdHsfA2c-like protein from *Triticum dicoccoides*, which reached 100%. The analysis of tissue expression characteristics revealed that *TaHsfA2-13* was highly expressed in root, shoot, and leaf during the seedling stage of wheat. The expression of *TaHsfA2-13* could be upregulated by heat stress, low temperature, H_2O_2, mannitol, salinity and multiple phytohormones. The TaHsfA2-13 protein was located in the nucleus under the normal growth conditions and showed a transcriptional activation activity in yeast. Further studies found that overexpression of *TaHsfA2-13* in *Arabidopsis thaliana* Col-0 or *athsfa2* mutant results in improved tolerance to heat stress, H_2O_2, SA and mannitol by regulating the expression of multiple heat shock protein (*Hsp*) genes. In summary, our study identified *TaHsfA2-13* from wheat, revealed its regulatory function in varieties of abiotic stresses, and will provide a new target gene to improve stress tolerance for wheat breeding.

Keywords: wheat, Hsf, *TaHsfA2-13*, abiotic stresses, transgenic, *Arabidopsis*

INTRODUCTION

Abiotic stresses such as drought, high salt, and high temperature can affect the survival, productivity, and geographical distribution of many important crops worldwidely (Gong et al., 2020). There seem to be significant differences among the various stresses, while they also show overlapping responses. For example, osmotic stress caused by drought and salinity is an important environmental threat, limiting plant growth and agricultural productivity (Chen et al., 2020). Oxidative stress is an integral component of various stress conditions, including excessive light, cold, heat, drought, and this fact largely determines the substantial overlap in plant physiological and molecular responses to various environmental challenges (Savchenko and Tikhonov, 2021). In the process

of fighting against these adverse environmental factors, plants have evolved a complex and elaborate regulatory network (Guo et al., 2016). With the development of molecular techniques such as large-scale transcriptome analysis, a large number of abiotic stress associated genes have been discovered in plants (Nakashima et al., 2009; Duan et al., 2019). Genes encoding transcription factors are downstream components of signal transduction and play indispensable roles in the regulation of multiple abiotic stresses. About 7% of the coding sequences in plant genomes are transcription factors, many of which typically belong to large gene families, such as the Hsf family (Baniwal et al., 2004; Udvardi et al., 2007). They are excellent candidates for crop improvement (Baillo et al., 2019). In contrast to the few Hsfs in yeast and mammals, the plant Hsf families contain a large number of Hsf members, forming a complex plant-specific superfamily that is widespread in many species (Guo et al., 2016). There are 21 *Hsfs* in *Arabidopsis*, 24 in tomato, 25 in pepper, 41 in bamboo, 52 in soybean, and 82 in wheat (Scharf et al., 2012; Fragkostefanakis et al., 2015; Guo et al., 2015; Duan et al., 2019; Huang et al., 2021). Compared to other plant species, the large number of *Hsfs* in wheat makes the corresponding research more complicated.

In general, plant Hsf proteins have conserved modular structures, including N-terminal DNA binding domain (DBD) characterized by a central helix-turn-helix motif, an oligomerization domain (OD) with a bipartite heptad pattern of hydrophobic amino acid residues (HR-A/B region), the C-terminal nuclear localization signal (NLS) and nuclear export signal (NES) for regulating Hsf proteins subcellular localization (Baniwal et al., 2004). Plant Hsf were classified into A, B, and C based on the sequence length between DBD and HR-A/B regions and the number of amino acid residues inserted into HR-A/B region (Guo et al., 2016; Liu et al., 2020). Among these three types of Hsf proteins, HsfA class members usually contain an activation domain at the C-terminal, characterized by aromatic, hydrophobic, and acidic amino acid residues (AHA), whereas HsfB and C lack the AHA motif and in many cases do not function as activator (Kotak et al., 2004). The different protein structures of HsfA, HsfB, and HsfC determine the different functions they perform. In *Arabidopsis*, HsfA1 and HsfA2 have been reported as positive regulators of plant responses to heat stress (HS), whereas two members of Class B Hsf, HsfB1, and HsfB2b, are active repressors of Hsfs and Hsps (Nishizawa et al., 2006; Charng et al., 2007; Ikeda et al., 2011; Liu et al., 2011; Nishizawa-Yokoi et al., 2011).

Current understanding about the individual functions for A2 subclass of Hsf in plant mainly comes from model species such as *Arabidopsis* and tomato (Heerklotz et al., 2001; Charng et al., 2007; Ogawa et al., 2007; Chan-Schaminet et al., 2009; Fragkostefanakis et al., 2016; Liu et al., 2019). The expression of *HsfA2* was not detected in control cell cultures, but was strongly upregulated after HS treatment, indicating an important regulatory role of *HsfA2* during HS in *Arabidopsis* (Nover et al., 2001). *HsfA2* transcript level was also strongly induced by HS in tomato (Scharf et al., 1998). In addition, the expression of *HsfA2* in tomato anther is higher than that in other flower tissues, and can be further induced under both short and prolonged HS conditions, similar to its expression in leaves (Giorno et al., 2010). Recent studies have found that HsfA2, as a central regulatory factor, is involved in the transgenerational memory to high temperature in plants through complex epigenetic regulation such as histone demethylation (Liu et al., 2019). In addition to heat stress, many other abiotic stresses such as cold, salt, and drought, as well as phytohormones such as abscisic acid (ABA), salicylic acid (SA), jasmonic acid (JA), and ethylene have also been shown to induce the expression of *HsfA2* in plants (Nishizawa et al., 2006; Zhang et al., 2015; Duan et al., 2019). As an important regulatory factor of HS, the *Arabidopsis* HsfA2 is involved in other abiotic stress, such as salt stress, osmotic stress and anoxia stress (Charng et al., 2007; Banti et al., 2010). Coincidentally, overexpression of *OsHsfA2e* in *Arabidopsis* also increased tolerance to high-salinity stress (Yokotani et al., 2008). Additionally, transgenic *Arabidopsis* plants overexpressing *TaHsfA2d* showed considerable tolerance to salinity and drought stresses (Chauhan et al., 2013). More recently, *TaHsfA2e-5D* has been shown to positively regulate heat and drought stress, at least in part by promoting the expression of stress-responsive genes (Bi et al., 2022). It seems that plant Hsfs may act as the intersection of multiple signaling pathways, on the one hand participating in the regulation of abiotic signaling pathways and on the other hand mediating phytohormone signaling (Guo et al., 2016). Indeed, our previous studies have shown that many Hsfs, such as the A2 subclass of Hsfs, are responsive to many abiotic stresses and phytohormones (Duan et al., 2019).

Although basic biological information about *Hsfs* in wheat is well known, fewer *Hsfs* have been cloned and identified from wheat than other crops, and the function of most Hsfs are unclear. Our previous studies have demonstrated the expression of *TaHsfA2-13* was induced by various abiotic stresses (Duan et al., 2019). In this study, the biological functions and potential mechanisms of wheat TaHsfA2-13 in plant tolerance to multiple abiotic stresses will be further revealed.

MATERIALS AND METHODS

Plant Materials and Growth Conditions

Cang6005, a semi-winter heat-tolerant wheat variety, was used for gene cloning and expression analysis. After surface disinfection with 0.1% $HgCl_2$, wheat seeds were cleaned with sterile water and soaked at room temperature for 12 h. When the germ grew to 1–2 cm, seedlings were transplanted and cultivated in Hoagland nutrient solution under day/night conditions of 16 h/8 h (70–100 $\mu mol\, m^{-2}\ S^{-1}$), 25°C, and 50–60% relative humidity. The stress treatments were performed as described by previous studies (Duan et al., 2019; Liu et al., 2020; Bi et al., 2022). Seedlings at the two-leaf and one-heart stage were treated with high temperature (37°C), low temperature (4°C), H_2O_2 (10 $mmol\, L^{-1}$), mannitol (15% W/V), NaCl (0.2 $mol\, L^{-1}$), MeJA (0.1 $mmol\, L^{-1}$), ABA (0.2 $mmol\, L^{-1}$) and SA (0.8 $mmol\, L^{-1}$) for different time, respectively. The second leaves

Abbreviations: Hsf, Heat shock transcription factor; HS, Heat shock; SA, Salicylic acid; WT, Wild type; Hsp, Heat shock protein; HSE, HS responsive element; DBD, DNA-binding domain; OD, Oligomerization domain; NLS, Nuclear localization signal; NES, Nuclear export signal; AHA, Activator peptide motif.

were collected in each treatment, and then immediately frozen in liquid nitrogen for RNA extraction.

Isolation of Total RNA and Gene Cloning

Total RNA of plants was extracted using the RNArose Reagent Systems Kit (Huashun Bioengineering Co., LTD., Shanghai, China), according to the manufacturer's instructions. RNA was further purified through the PrimeScript™ RT Reagent Kit with gDNA Eraser (TaKaRa, Dalian) to remove genomic DNA contamination. Then, 2 μg of purified RNA was used as template to synthesize first-strand cDNA. The specific primers were designed using DNAMAN 8.0[1] software to amplify the *TaHsfA2-13* sequence. The PCR amplified products were constructed to pEasy-Blunt cloning vectors (pEasy-Blunt Simple Cloning Kit, TransGen Biotech) and sequenced by Shanghai Shenggong Bioengineering Technology Co., LTD. Primer sequence information is presented in **Supplementary Table S1**.

Multiple Sequence Alignment Analysis

The protein sequences used for multiple sequence alignment analysis were downloaded from NCBI website.[2] GenBank accession numbers of the proteins are as follows: TaHsfA2-13 (*T. aestivum*, MT 680017), TdHsfA2c-like (*T. dicoccoides*, XP_037425119), AetHsfA2c (*Aegilops tauschii*, XP_020147337), BdHsfA2c (*Brachypodium distachyon*, XP_010234740), ZmHsf30 (*Zea mays*, NP_001147128), AtHsfA2 (*A. thaliana*, NP_001324815; Charng et al., 2007). Multiple sequence alignment analysis was carried out by the DNAMAN 8.0 software.[3]

Expression Analysis Using Quantitative RT-PCR

Real-time PCR was performed with SYBR Green PCR master mix (TaKaRa, Dalian) on a Bio-Rad CFX96 realtime PCR detector. According to the methods of Liu et al. (2020), *TaRP15* and *Atactin8* were selected as internal reference genes in wheat and *Arabidopsis*, respectively, to calculate the relative transcription levels of the interest genes. The primers used are listed in **Supplemental Table S1**. Three replicates were performed for each qRT-PCR reaction, and the results were reported as means and standard deviation. SPSS 19.0 software was used to analyze the significance.

Subcellular Localization

The coding sequence of *TaHsfA2-13* without a stop codon was inserted into the pJIT1-hGFP vector through LR recombination reaction to generate TaHsfA2-13-GFP fusion protein. The vectors was transformed into *Agrobacterium* strain GV3101 and injected into *N. benthamiana* leaves with a needleless 1 ml syringe. The nucleus was stained with 4′,6-diamidino-2-phenylindole (DAPI, 1 mg ml^{-1}) dye before imaging, fluorescence observation was performed under a fluorescence microscope (Zeiss META510).

[1]www.lynnon.com
[2]https://www.ncbi.nlm.nih.gov/
[3]www.lynnon.com

Transactivation Analysis

The full-length and truncated *TaHsfA2-13* were cloned into pGBKT7 and then introduced into yeast strain AH109, respectively. The transformants were grown on the SD/-Trp and SD/Trp-/His-/Ade-media for 3 days before observation. The transcriptional activation activities was evaluated according to their growth status and the activity of α-galactosidase.

Yeast One-Hybrid Assay

For the construction of prey, the coding sequence of *TaHsfA2-13* was amplified from wheat cDNA and then cloned into pGADT7 vector. For bait construction, the promoters of five *AtHsps* were amplified from *Arabidopsis* genomic DNA and then cloned into pHIS2.1 vector according to the methods described by Liu et al. (2020). The bait and prey constructs were co-transformed into yeast strain Y187, and grown on the selective medium with 10 mM 3-aminotriazole (3-AT) or not.

Genetic Transformation

To obtain the plants overexpressing *TaHsfA2-13* in *Arabidopsis*, the coding region of *TaHsfA2-13* was amplified by PCR and cloned into pCAMBIA1300. The recombinant plasmid was transformed into *Agrobacterium* strain GV3101. At the stage of flower-budding, *Arabidopsis* wild type (Col-0) and *athsfa2* mutants were transformed by classical floral dip method (Liu et al., 2020). The T-DNA insertion transgenic seeds were selected on MS-agar plates supplemented with 50 μg·μL^{-1} of hygromycin and confirmed by semi-quantitative RT-PCR. *Atactin8* gene was used for normalizing the gene expression in *Arabidopsis*.

Stress Treatments

For heat stress treatment, sterilized seeds of wild-type (or *athsfa2*) and *Arabidopsis* homozygous transgenic lines were planted on MS agar plates. Seedlings of 5 days old were subjected to basal thermotolerance (45°C for 50 min, placed at 22°C for 8 days) and acquired thermotolerance treatment (37°C for 1 h, incubated at 22°C for 2 days, 46°C for 50 min, placed at 22°C for 8 days) according to the previous methods (Larkindale et al., 2005; Li et al., 2019). After 8 days, photography was taken and the rosette leaves of different lines were collected to determine chlorophyll content. For oxidative stress, osmotic stress and phytohormone treatments, sterilized wild-type and transgenic seeds were planted on MS agar plates supplemented with H_2O_2 (10 mmol l^{-1}), mannitol (15% W/V), and SA (0.8 mmol l^{-1}), respectively. After 2 weeks, photography was taken and the rosette leaves of different lines were collected to determine chlorophyll content. The chlorophyll contents were measured as described by Liu et al. (2020). In each experiment, 30 seedlings of each line were treated at least, and three independent experiments were conducted.

Measurements of Physiological Indexes

The rosette leaves of *Arabidopsis* seedlings were harvested to measure the physiological indexes after seedlings of 5 days old were subjected to basal thermotolerance (45°C for 50 min, placed at 22°C for 8 days). The activities of superoxide dismutase (SOD)

and peroxidase (POD) were analyzed using the nitrotetrazolium blue chloride reduction and guaiacol colorimetric method, respectively (Li et al., 2015). Osmotic potential was determined with a VIESCOR 5100C vapour pressure osmometer (Wesor Inc., Logan, UT, United States of America) as described by Liu et al. (2002).

RESULTS

cDNA Sequence Amplification and Analysis of TaHsfA2-13 in Wheat

Our previous RNA-Seq data showed that *TaHsfA2-13*, a Hsf of subclass A2, was strongly upregulated by heat stress, H_2O_2 and ABA, suggesting that this gene may be an important node in abiotic stress and phytohormones (Duan et al., 2019). To further clarify the biological function of TaHsfA2-13, we obtained the coding sequence of it from heat-treated wheat leaves, which encoding 369 amino acids. Analysis of amino acid sequence showed that TaHsfA2-13 had the basic characteristics similar to other Hsfs of class A, including DNA binding domain (DBD), oligomerization domain (OD), nuclear localization signal (NLS), nuclear export signal (NES) and activator peptide motif (AHA). Moreover, multiple sequence alignment analysis revealed that TaHsfA2-13 shared the highest similarity with TdHsfA2c-like from *T. dicoccoides* (**Figure 1**).

Expression of *TaHsfA2-13* Was Induced by Various Abiotic Stresses and Phytohormones

In order to explore the expression patterns of *TaHsfA2-13* in wheat, qRT-PCR was used to detect the expression of *TaHsfA2-13* in different tissues at seedling and reproductive stages. Compared with the reproductive stage of wheat, *TaHsfA2-13* was more greatly expressed in seedling stage, and the expression level in young

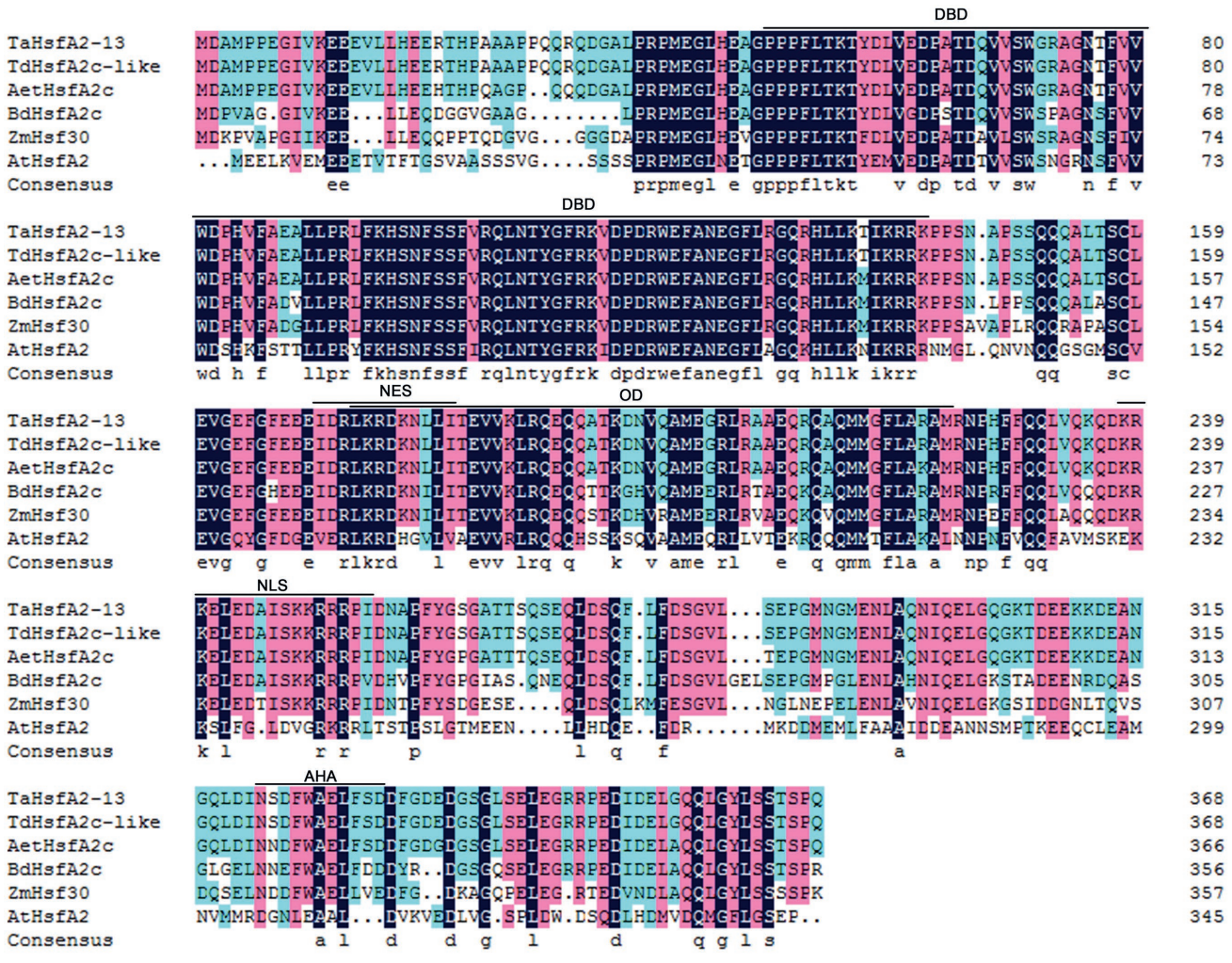


FIGURE 1 | Sequence alignment of TaHsfA2-13 and other plant HsfA2 proteins. Multiple sequence alignment of amino acid sequences from *Aegilops tauschii* (AetHsfA2c), *Arabidopsis thaliana* (AtHsfA2), *Brachypodium distachyon* (BdHsfA2c), *Triticum aestivum* (TaHsfA2-13), *Triticum dicoccoides* (TdHsfA2c-like), and *Zea mays* (ZmHsf30). Conservative domains such as: DNA-binding domain (DBD), Oligomerization domain (OD), Nuclear localization signal (NLS), Nuclear export signal (NES) and Activator peptide motif (AHA) are marked with line segments.

shoot or leaf was 2.5 fold higher than that in root under normal growth conditions. Specifically, the expression level of *TaHsfA2-13* in embryos was almost undetectable, suggesting that *TaHsfA2-13* may not be involved in embryonic development (**Figure 2A**).

Next, to confirm the induction of *TaHsfA2-13* gene expression under various abiotic stresses and phytohormones, we detected the transcript levels of *TaHsfA2-13* in wheat leaves which were treated with 37°C HS treatment, 4°C cold treatment, H_2O_2, mannitol, NaCl, MeJA, ABA and SA, respectively. It was found that the *TaHsfA2-13* gene was substantially induced by HS and its highest level was about 700 fold greater than the untreated control (**Figure 2B**). Under H_2O_2 treatment, the expression level of *TaHsfA2-13* was greatly increased and reached the peak at 60 min (**Figure 2C**). Following NaCl stress, *TaHsfA2-13* expression was induced at 2 h, peaked at 6 h, and then decreased slowly (**Figure 2I**). However, for mannitol and cold treatments, the responses of *TaHsfA2-13* were relatively weak, and its transcript levels slightly increased at 2 h (**Figures 2E,G**). Strikingly, the responses of *TaHsfA2-13* to phytohormones were extremely differently. SA treatment could rapidly induce expression of *TaHsfA2-13* to the peak within 30 min (**Figure 2D**). Compared with the SA treatment, the peak time of *TaHsfA2-13* transcription level reached under the MeJA and ABA treatments was delayed, which was 120 min and 2 h, respectively (**Figures 2F,H**).

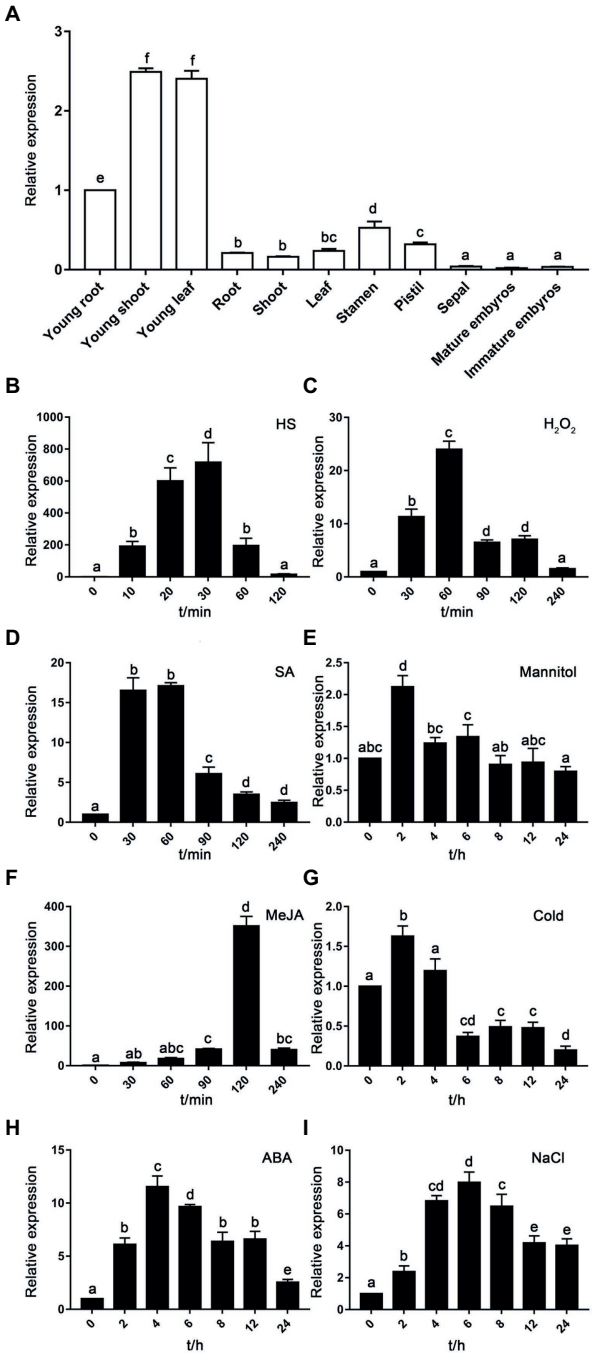


FIGURE 2 | Expression analysis of *TaHsfA2-13*. **(A)** Tissue-specific expression patterns of *TaHsfA2-13*. The expression level in young root was set as 1. **(B–I)** Expression levels of *TaHsfA2-13* in response to abiotic stresses and phytohormones. The expression of untreated samples was set as 1. The wheat *TaRP15* gene was used as an internal control. All data represent means ± standard deviation (SD) of three biological replicates. Different lowercase letters above the bars denote significant differences at the $p < 0.05$ level.

TaHsfA2-13 Is a Transcriptional Activator Localized to the Nucleus

As shown in **Figure 1**, TaHsfA2-13 has an AHA domain at the C-terminal of its protein, suggesting that TaHsfA2-13 may be a transcriptional activator. To verify this, we analyzed the transcriptional activation activity of TaHsfA2-13 in yeast with the GAL4 yeast system. The yeast harboring pGBKT7-TaHsfA2-13 and pGBKT7-TaHsfA2-13$^{301\text{-}368}$ grew well like positive controls, which carrying pGBKT7-P53 on the yeast medium (SD/Trp-/His−/Ade−/X-α-gal), while the yeast harboring pGBKT7-TaHsfA2-13$^{1\text{-}300}$ and negative controls barely grew at all (**Figure 3A**). These results indicate that TaHsfA2-13 has a transcriptional activation activity in yeast.

Analysis of amino acid sequence revealed that TaHsfA2-13 possesses both NLS and NES (**Figure 1**), so the true localization of its protein is worth considering. The transient expression vector pJIT1-TaHsfA2-13-hGFP was constructed and transformed into tobacco leaf epidermal cells. The subcellular localization of the target protein was revealed by fluorescence microscope. Under normal circumstances, compared to the whole cell distribution of free GFP, the green fluorescence of the target protein is only distributed in the nucleus, which completely overlaps with the fluorescence of the nuclear specific dye DAPI. This indicates that TaHsfA2-13 is a nuclear localization transcription factor (**Figure 3B**).

The Overexpression of *TaHsfA2-13* Enhanced the Tolerance of Transgenic *Arabidopsis* to Various Abiotic Stresses

To further explore the biological functions of TaHsfA2-13 in plants, transgenic plants overexpressing *TaHsfA2-13* in Col-0 (*7–28*, *8–29* and *18–30*) or *athsfa2* mutant (*6–11*, *10–16* and *11–12*) were obtained (**Supplementary Figure S1**). Firstly, the role of TaHsfA2-13 in thermotolerance was analyzed. As shown in **Figure 4A**; **Supplementary Figure S2**, under normal growth

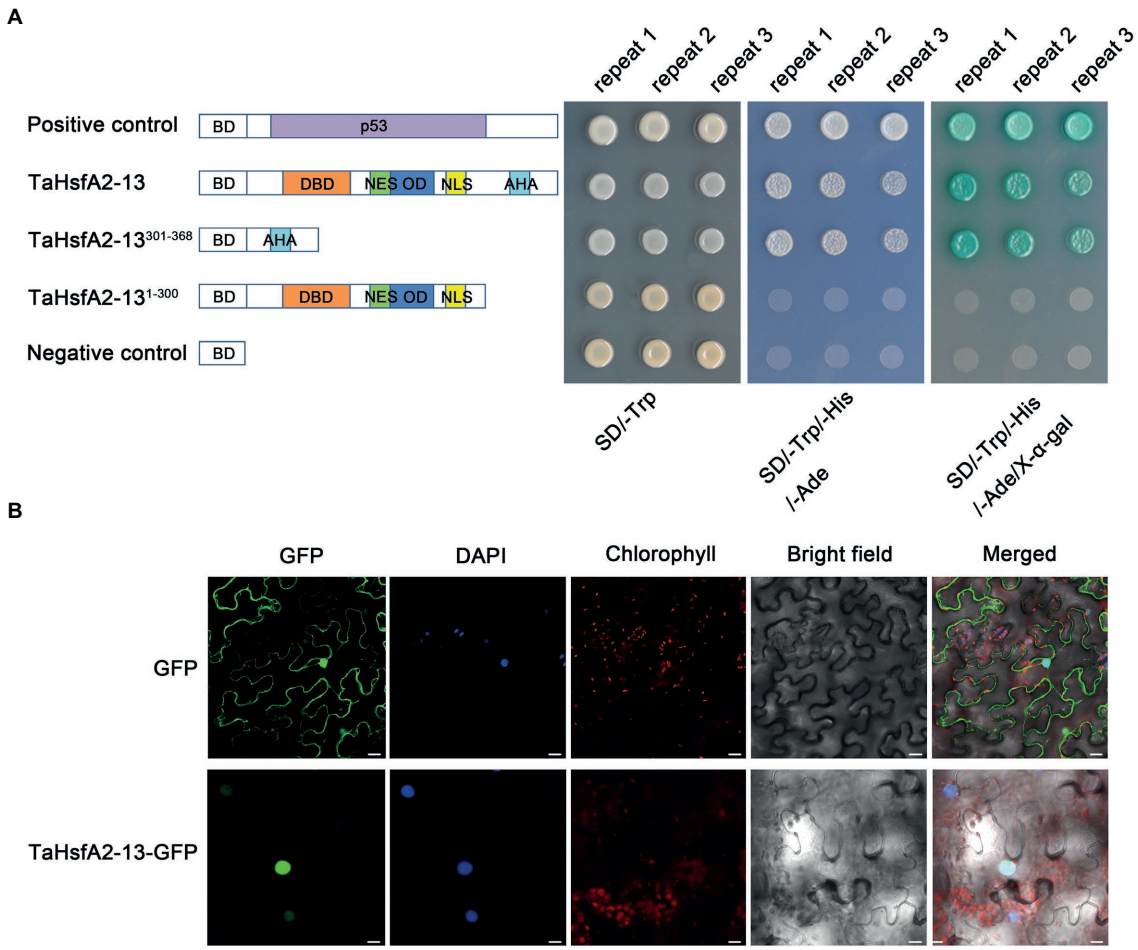


FIGURE 3 | Transcriptional activity and subcellular localization analyses of TaHsfA2-13. **(A)** Transcriptional activation of TaHsfA2-13 in yeast. Schematic representation of the full-length TaHsfA2-13 and truncated protein constructs in the pGBKT7 vector. Fusion proteins of the GAL4 DNA-binding domain (BD) and full-length TaHsfA2-13 or truncated TaHsfA2-13 with (301–368 aa) or without (1–300 aa) AHA domain were expressed in the yeast strain AH109. Transformants were spotted onto SD/-Trp and SD/Trp-/His-/Ade-media. The plates were incubated at 30°C for 3 days. The pGBKT7 and pGBKT7-P53 vectors were used as negative and positive controls, respectively. **(B)** Subcellular localization of TaHsfA2-13 in tobacco leaf epidermal cells. Bars = 20 μm.

conditions, there was no significant growth difference between transgenic lines and WT (or *athsfa2*). However, under heat stress conditions, transgenic plants had fewer withered leaves and better growth than WT (or *athsfa2*). Consistent with this, the content of chlorophyll in transgenic plants was also significantly higher than that in WT (or *athsfa2*), indicating a less degree of injury in transgenic lines after HS treatment (**Figure 4B**). Meanwhile, we also detected the activities of POD, SOD and osmotic potential in transgenic lines and WT under HS treatment or not. The results showed that under normal growth conditions, there was no difference between the transgenic lines and WT. But, when subjected to HS treatment, the activities of POD and SOD were significantly higher in transgenic lines, and osmotic potential of the transgenic lines was significantly lower (**Figures 4C–E**).

Next, we also explore the role of *TaHsfA2-13* in oxidative stress, osmotic stress and response to phytohormone. As expected, following the H_2O_2, SA and mannitol treatments, the growth of transgenic seedlings was better than that of WT (or *athsfa2*), and the chlorophyll content of transgenic seedlings was higher, suggesting that TaHsfA2-13 could also enhance the resistance to oxidative stress, osmotic stress and toxicity of excess phytohormone other than improve the basic and acquired thermotolerance of transgenic plants (**Figures 5A,B**; **Supplementary Figure S2**).

Expression Analysis of *Hsps* in the *TaHsfA2-13* Overexpressing Lines

To determine the regulatory role of TaHsfA2-13 on *Hsps* in *Arabidopsis*, five *Hsp* genes, including *Hsp21*, *Hsp70b*, *Hsp70T*, *Hsp90*, *Hsp101*, which can be positively regulated by AtHsfA2 were selected in this study (Nishizawa et al., 2006; Ogawa et al., 2007). After mannitol and SA treatments, the expression levels of these *Hsp* genes were higher in the *TaHsfA2-13* overexpressing lines than those in WT. However, not all the

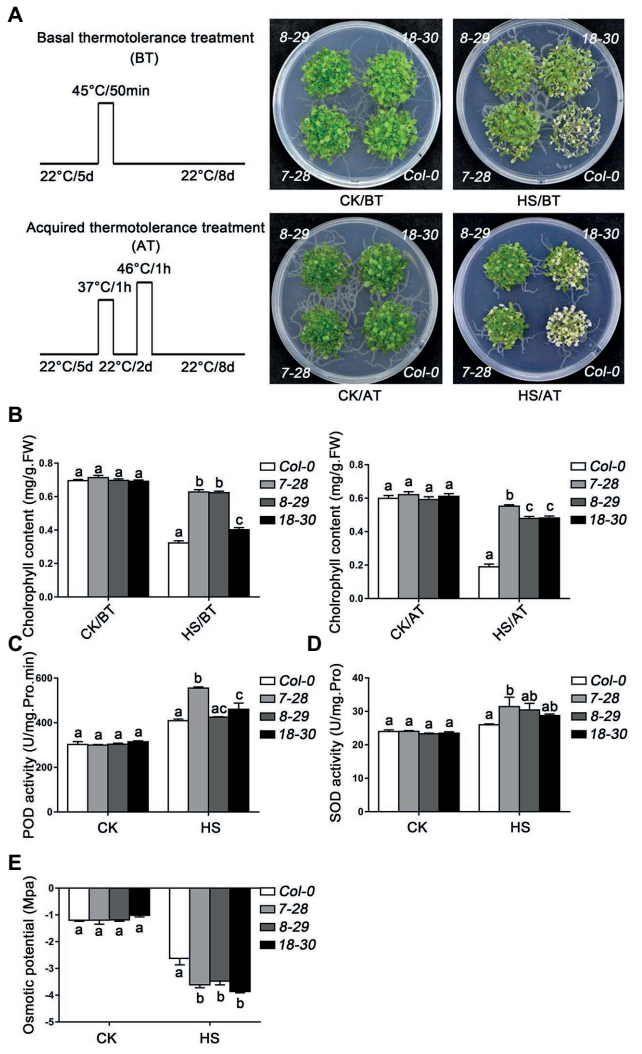


FIGURE 4 | Thermotolerance assays of *TaHsfA2-13* overexpressing transgenic *Arabidopsis* lines. **(A)** The phenotypes of WT and transgenic seedlings after basal thermotolerance (BT, 45°C for 50 min, placed at 22°C for 8 days) and acquired thermotolerance (AT, 37°C for 1 h, incubated at 22°C for 2 days, 46°C for 1 h, placed at 22°C for 8 days) treatment. The plants were photographed 8 d after different HS. **(B)** Chlorophyll content of WT and transgenic seedlings treated with different HS. **(C–E)** Peroxidase (POD), superoxide dismutase (SOD) activities, and osmotic potential of WT and transgenic seedlings under HS treatment or not. For each experiment, at least 30 plants per line were used. Values are means ± SD from three independent measurements. Different lowercase letters above the bars denote significant differences at the $p < 0.05$ level.

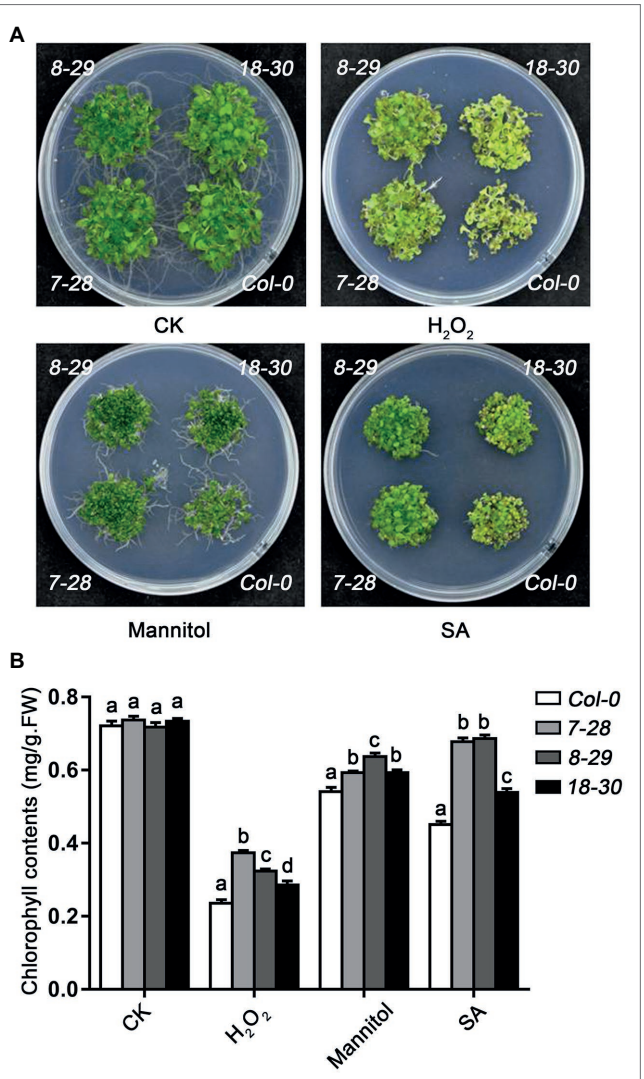


FIGURE 5 | Effect of H_2O_2, salicylic acid (SA) and mannitol on WT, and transgenic plants. **(A)** Morphology and **(B)** Chlorophyll content of WT and transgenic seedlings after H_2O_2 (10 mmol L^{-1}), mannitol (15% W/V), and SA (0.8 mmol L^{-1}) treatment. The data was recorded after 2 weeks of germination on MS agar plates. For each experiment, at least 30 plants per line were used. Values are means ± SD from three independent measurements. Different lowercase letters above the bars denote significant differences at the $p < 0.05$ level.

expression levels of these *Hsp* genes were higher in the *TaHsfA2-13* overexpressing lines, especially after heat treatment and H_2O_2 treatment. During basic thermotolerance, the expression level of *Hsp90* in transgenic lines was significantly lower than that in WT. The transcript levels of *Hsp70T* and *Hsp90* in transgenic lines were not changed during acquired thermotolerance or H_2O_2 treatment compared with WT (**Figure 6**). Further experiments showed that TaHsfA2-13 could interact with promoter sequences of these *Hsps*, which containing HSE motifs (**Figure 7**). These results suggest that TaHsfA2-13 enhances the tolerance of transgenic lines to various abiotic stresses, probably mediates by activation of *Hsps*. Of course, more experiments are needed to explore the specific molecular mechanisms involved in regulating plant responses to various abiotic stresses.

DISCUSSION

Wheat is one of the important staple food crops, providing 21% of calories and 20% of protein globally (Lobell and Gourdji,

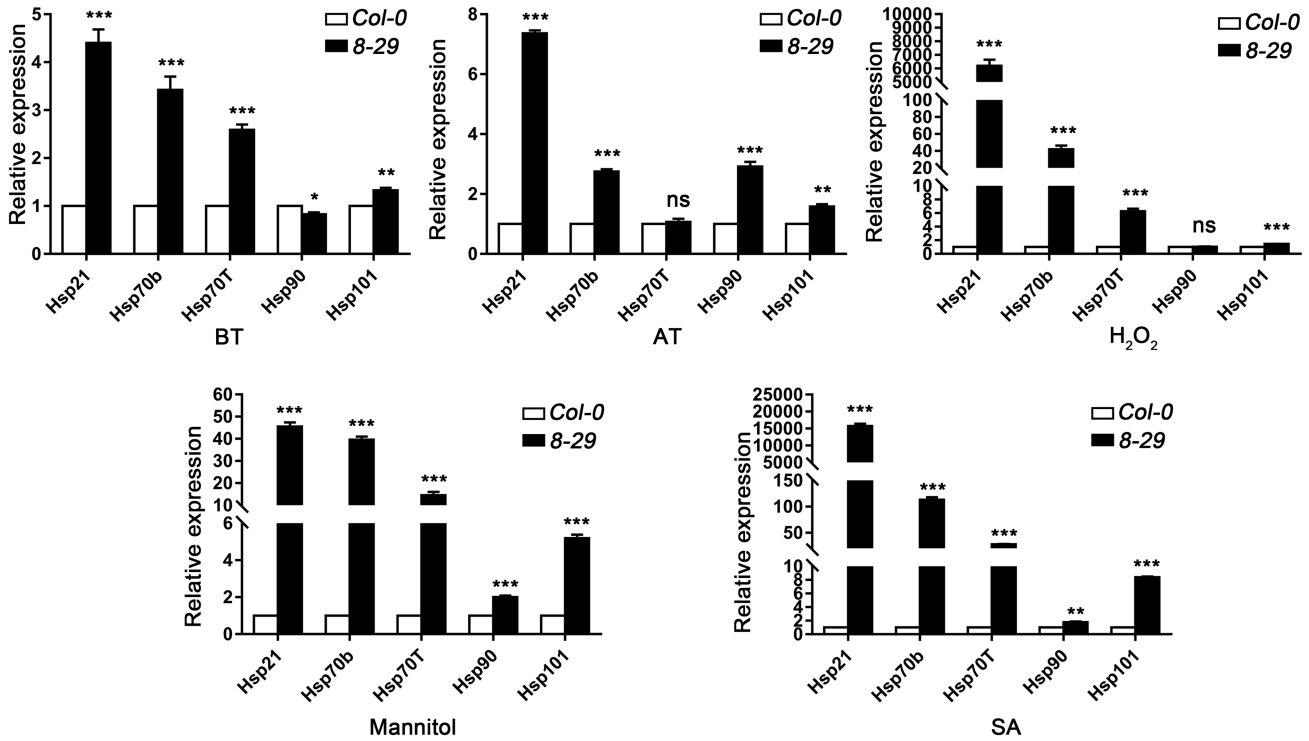


FIGURE 6 | Expression analysis of *Hsp* genes in WT and transgenic lines after various stresses and phytohormones treatments. For analysis of *Hsp* genes transcription levels under heat stress, total RNAs were extracted from five-old day seedlings after treatment with slightly modified BT (45°C for 50 min) or AT (37°C for 1 h, incubated at 22°C for 2 days, 46°C for 1 h). For analysis of *Hsp* genes transcription levels under H_2O_2, SA and mannitol treatments, total RNAs were extracted from 2-week-old seedlings grown on MS plates with H_2O_2 (10 mmol L^{-1}), mannitol (15% W/V), and SA (0.8 mmol L^{-1}). The relative expression of *Hsp* genes were normalized to that of *Atactin8*, which was used as an internal control gene. All values are presented as the mean ± standard error of values from three independent experiments. Asterisks indicate significant differences compared to WT, and ns means no significant difference (*$p < 0.05$, **$p < 0.01$, ***$p < 0.005$, Student's *t*-test).

2012; Shiferaw et al., 2013). It is estimated that the demand for wheat will increase by 60% by 2050, but yields might go down by 29% because of environmental stresses (Manickavelu et al., 2012; Kulkarni et al., 2017). The main objective of agronomic research remains to improve crop productivity under various abiotic stresses (Puranik et al., 2012). Therefore, understanding the molecular mechanisms of plant responses to abiotic stresses is a prerequisite for improving plant stress tolerance and productivity (Guo et al., 2016). Hsfs are downstream components of signal transduction and play important roles in regulating the expression of many genes responding to various environmental stresses (Hrmova and Hussain, 2021). Despite there are large number of Hsfs in wheat, few Hsfs have been cloned and identified due to the complexity of the wheat genome. In this study, we cloned *TaHsfA2-13*, a member of the A2 subclass, from wheat. Analysis of amino acid sequence showed that TaHsfA2-13 possessed the basic properties of HsfAs (**Figure 1**). Unlike HsfBs and HsfCs, HsfAs tend to have the AHA domain, which also determines their transcriptional activation activity (Kotak et al., 2004). Indeed, TaHsfA2-13 was found to exhibit transcriptional activation activity in this study (**Figure 3A**). Similarly, in a recent study, the AHA motif was found to be important for the transcriptional activity of TaHsfA2e-5D (Bi et al., 2022). Although NLS and NES coexist, TaHsfA2-13 is normally located in the nucleus (**Figures 1**, **3B**), which differs its orthologue from *Arabidopsis* (Evrard et al., 2013). Furthermore, the sequence of TaHsfA2-13 is highly similar to TdHsfA2c-like from diploid *T. dicoccoides*, indicating that TaHsfA2-13 is highly conserved during the polyploidization (**Figure 1**). In the A, B and D subgenomes of common bread wheat, approximately 60.1–61.3% of the genes have orthologues in diploid species (International Wheat Genome Sequencing, 2014). It seems that polyploidization has been shown to enhance abiotic stress tolerance in plants by aggregating stress resistance genes (Chao et al., 2013; Yang et al., 2014).

Although there is high sequence similarities among members of the A2 subclass, the expression pattern of each gene is quite different (Duan et al., 2019). In this study, gene expression profiles showed that *TaHsfA2-13* transcripts were differentially accumulated in all tested tissues, and the highest expression level was found in young roots, stems, and leaves, suggesting that TaHsfA2-13 might be involved in the growth of wheat seedlings (**Figure 2A**). However, previous study showed that subclass A2 members including A2b, A2c, and A2e were predominantly expressed in endosperm (Xue et al., 2014).

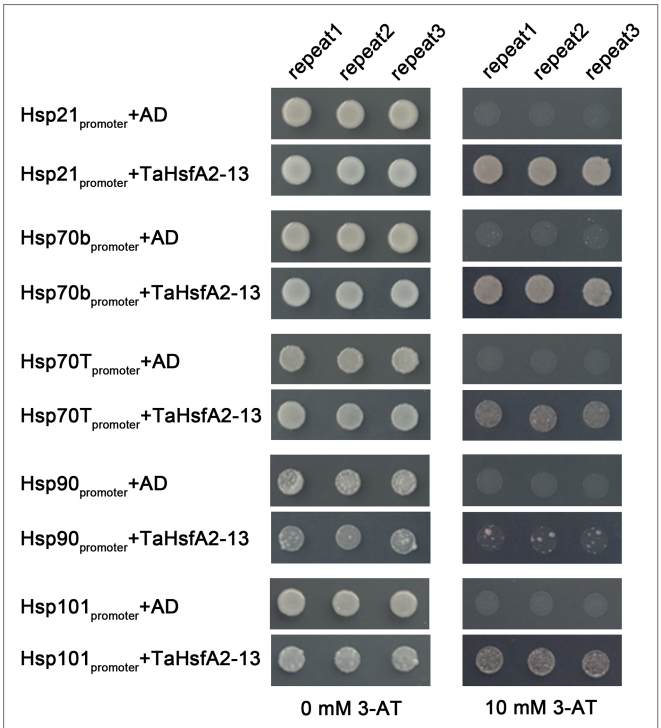


FIGURE 7 | Growth of yeast cells transformed with the bait and prey constructs on SD-Trp-Leu-His supplemented with or without 10 mM 3-AT. The transformation with the empty vector pGADT7 was taken as a negative control. The experiments were repeated three times with the same results.

TaHsfA2-1, also belonging to A2 subclass, was mainly expressed in mature leaves (Liu et al., 2020). These results indicate the functional diversity of A2 subclass members in wheat.

In recent years, there have been many reports about Hsfs regulating plant responses to various abiotic stresses and these transcription factors are not only involved in individual stress. For example, overexpression of *AtHsfA2* in *Arabidopsis* increases tolerance to heat, osmosis, and salt stress (Nishizawa et al., 2006). TaHsfA6f can enhance the tolerance of transgenic plants to high temperature, drought and salt stress in wheat (Xue et al., 2015; Bi et al., 2020). Like many Hsfs, TaHsfA2-13 not only improves the basic and acquired thermotolerance of transgenic plants, but also involve in response and tolerance to phytohormones, osmotic, and oxidative stresses (**Figures 2**, **4, 5**; **Supplementary Figure S2**). Firstly, *TaHsfA2-13* was dramatically induced by heat stress (**Figure 2B**) and transgenic plants overexpressing *TaHsfA2-13* in Col-0 or *athsfa2* mutant showed improved thermotolerance (**Figure 4**). These results imply that the improvement of heat tolerance by *TaHsfA2-13* is conserved between monocot and dicot plant species. Next, we found that *TaHsfA2-13* was upregulated by other abiotic stresses besides heat stress, such as osmotic and oxidative stresses (**Figure 2**). Indeed, transgenic *Arabidopsis* lines clearly exhibited better growth status under H_2O_2 and mannitol treatments, with fewer withered leaves and higher chlorophyll content (**Figure 5**). Finally, we also found that *TaHsfA2-13* responds to SA, ABA and MeJA treatments (**Figure 2**). A large number of studies have shown that phytohormones play critical roles in helping plants to adapt to various environmental stresses (Verma et al., 2016). For instance, SA alleviates the adverse effects of heat stress on photosynthesis by altering proline production and ethylene formation (Khan et al., 2013). In general, ABA is responsible for plant defense against abiotic stresses such as drought and salinity (Zhang et al., 2006). MeJA operate in parallel, presumably synergistically, to ABA, and are indispensable for osmotic stress tolerance in rice (Tang et al., 2020). Therefore, our future research will focus on the potential molecular mechanism of TaHsfA2-13 regulated by phytohormones in response to various abiotic stresses.

Plant Hsps, as chaperone proteins, play key roles in biotic and abiotic stress tolerance of plants by maintaining the functional conformation of plant proteins and preventing the aggregation of non-native proteins (Ul Haq et al., 2019). Numerous studies have shown that the regulation of *hsps* by hsfs plays an important role in plant response to various environmental stresses (Guo et al., 2008; Xue et al., 2014; Driedonks et al., 2015). For example, the overexpression of *GmHsfA1* improved the thermotolerance of transgenic soybeans, possibly due to the activation of downstream genes *GmHsp70*, *GmHsp22* and other *GmHsps* (Zhu et al., 2009). In *Arabidopsis*, *Hsp90* is regulated by HsfA2 and enhances tolerance to oxidative stress (Nishizawa-Yokoi et al., 2010). During seedling stage of wheat, TaHsfA6e was reported to regulate the expression of *TaHsps* genes, such as *Hsp17*, *Hsp70* and *Hsp90* in response to high temperature and drought (Kumar et al., 2018). Additionally, *TaHsfA6f* could improve thermotolerance in wheat, which depended on the function of downstream target genes, including *TaHsps* (*TaHSP16.8*, *TaHSP17*, *TaHSP17.3* and *TaHSP90.1-A1*), *TaRof1*, *galactinol synthase*, and *glutathione-S-transferase* (Xue et al., 2015). In this study, with a few exceptions, almost all tested *Hsps* were strongly upregulated in *TaHsfA2-13* overexpressing transgenic lines after various stresses and phytohormones treatments (**Figure 6**). Previous studies have found that *HSPs* genes (*sHsp., Hsp70*, *Hsp90* and *DnaJ*) and Hsfs may be closely related to the structural integrity and function of chloroplast (Wu et al., 2018). Here, due to the protection of high level of Hsps, *TaHsfA2-13* overexpressing transgenic lines grew better and had higher chlorophyll content than WT (or *athsfa2*; **Figures 4B, 5B**; **Supplementary Figure S2**). Taken together, our results suggest that TaHsfA2-13 is a positive regulator of abiotic stresses, including heat, osmotic and oxidative stress, and involved in response to phytohormones treatments, possibly by upregulation of stress-related response genes, such as Hsps.

CONCLUION

In summary, we clarified important roles of wheat *TaHsfA2-13* gene in response to HS, H_2O_2, mannitol, and SA in *Arabidopsis*. TaHsfA2-13 exerts stress tolerance functions by regulating the expression of downstream genes such as *Hsps*. It indicates that

different signal pathways share the same signal molecules under stress conditions. Our study elevates the mechanistic understanding of individual gene involved in various stress and cross-talk tolerance in plant and provides genetic materials for crop stress tolerance breeding.

DATA AVAILABILITY STATEMENT

The datasets presented in this study can be found in online repositories. The names of the repository/repositories and accession number(s) can be found in the article/**Supplementary Material**.

AUTHOR CONTRIBUTIONS

XM, XG, and GL designed this study. XM performed bioinformatics analysis, generated and analyzed data, and wrote the manuscript. BZ, ML, RL, and QR performed the experiments. XG and GL edited this manuscript and contributed with valuable discussions. All authors contributed to the article and approved the submitted version.

FUNDING

This work was supported by the Natural Science Foundation of Hebei Province (no. C2021301024); HAAFs Science and Technology Innovation Special Project (no. 2022KJCXZX-SSS-2); Talents Construction Project of Science and Technology Innovation of HAAFs (no. C22R1301); Basic Research Fund of Hebei Academy of Agriculture and Forestry Sciences (no. 2021110204).

ACKNOWLEDGMENTS

We thank Yee-Yung Charng (Agricultural Biotechnology Research Center, Academia Sinica, Taipei) for providing *athsfa2* mutant seeds.

SUPPLEMENTARY MATERIAL

The Supplementary Material for this article can be found online at: https://www.frontiersin.org/articles/10.3389/fpls.2022.922561/full#supplementary-material

Supplementary Figure S1 | Identification of transgenic plants. The mRNA levels of *TaHsfA2-13* overexpressing lines and WT (or *athsfa2*) were examined by semi-quantitative RT-PCR analysis, and the expression of *Atactin8* was analyzed as a loading control.

Supplementary Figure S2 | Comparison of wild type (WT), *athsfa2* and *TaHsfA2-13* overexpressing transgenic plants in response to various abiotic stresses and phytohormones. **(A)** Morphology and **(B)** Chlorophyll content of WT, *athsfa2* and transgenic seedlings after various abiotic stresses and phytohormones. For each experiment, at least 30 plants per line were used. Values are means ± SD from three independent measurements. Different lowercase letters above the bars denote significant differences ($p < 0.05$).

REFERENCES

Baillo, E. H., Kimotho, R. N., Zhang, Z., and Xu, P. (2019). Transcription factors associated with abiotic and biotic stress tolerance and their potential for crops improvement. *Genes (Basel)* 10:771. doi: 10.3390/genes10100771

Baniwal, S. K., Bharti, K., Chan, K. Y., Fauth, M., Ganguli, A., Kotak, S., et al. (2004). Heat stress response in plants: a complex game with chaperones and more than twenty heat stress transcription factors. *J. Biosci.* 29, 471–487. doi: 10.1007/BF02712120

Banti, V., Mafessoni, F., Loreti, E., Alpi, A., and Perata, P. (2010). The heat-inducible transcription factor HsfA2 enhances anoxia tolerance in Arabidopsis. *Plant Physiol.* 152, 1471–1483. doi: 10.1104/pp.109.149815

Bi, H., Miao, J., He, J., Chen, Q., Qian, J., Li, H., et al. (2022). Characterization of the wheat heat shock factor TaHsfA2e-5D conferring heat and drought tolerance in *Arabidopsis*. *Int. J. Mol. Sci.* 23, 2784. doi: 10.3390/ijms23052784

Bi, H., Zhao, Y., Li, H., and Liu, W. (2020). Wheat heat shock factor TaHsfA6f increases ABA levels and enhances tolerance to multiple abiotic stresses in transgenic plants. *Int. J. Mol. Sci.* 21, 3121. doi: 10.3390/ijms21093121

Chan-Schaminet, K. Y., Baniwal, S. K., Bublak, D., Nover, L., and Scharf, K. D. (2009). Specific interaction between tomato HsfA1 and HsfA2 creates hetero-oligomeric superactivator complexes for synergistic activation of heat stress gene expression. *J. Biol. Chem.* 284, 20848–20857. doi: 10.1074/jbc.M109.007336

Chao, D. Y., Dilkes, B., Luo, H., Douglas, A., Yakubova, E., Lahner, B., et al. (2013). Polyploids exhibit higher potassium uptake and salinity tolerance in Arabidopsis. *Science* 341, 658–659. doi: 10.1126/science.1240561

Charng, Y. Y., Liu, H. C., Liu, N. Y., Chi, W. T., Wang, C. N., Chang, S. H., et al. (2007). A heat-inducible transcription factor, HsfA2, is required for extension of acquired thermotolerance in *Arabidopsis*. *Plant Physiol.* 143, 251–262. doi: 10.1104/pp.106.091322

Chauhan, H., Khurana, N., Agarwal, P., Khurana, J. P., and Khurana, P. (2013). A seed preferential heat shock transcription factor from wheat provides abiotic stress tolerance and yield enhancement in transgenic *Arabidopsis* under heat stress environment. *PLoS One* 8:e79577. doi: 10.1371/journal.pone.0079577

Chen, K., Gao, J. H., Sun, S. J., Zhang, Z. J., Yu, B., Li, J., et al. (2020). BONZAI proteins control global osmotic stress responses in plants. *Curr. Biol.* 30, 4815–4825.e4. doi: 10.1016/j.cub.2020.09.016

Driedonks, N., Xu, J., Peters, J. L., Park, S., and Rieu, I. (2015). Multi-level interactions between heat shock factors, heat shock proteins, and the rRedox system regulate acclimation to heat. *Front. Plant Sci.* 6:999. doi: 10.3389/fpls.2015.00999

Duan, S., Liu, B., Zhang, Y., Li, G., and Guo, X. (2019). Genome-wide identification and abiotic stress-responsive pattern of heat shock transcription factor family in *Triticum aestivum* L. *BMC Genomics* 20:257. doi: 10.1186/s12864-019-5617-1

Evrard, A., Kumar, M., Lecourieux, D., Lucks, J., von Koskull-Doring, P., and Hirt, H. (2013). Regulation of the heat stress response in *Arabidopsis* by MPK6-targeted phosphorylation of the heat stress factor HsfA2. *PeerJ.* 1:e59. doi: 10.7717/peerj.59

Fragkostefanakis, S., Mesihovic, A., Simm, S., Paupiere, M. J., Hu, Y., Paul, P., et al. (2016). HsfA2 controls the activity of developmentally and stress-regulated heat stress protection mechanisms in yomato male reproductive tissues. *Plant Physiol.* 170, 2461–2477. doi: 10.1104/pp.15.01913

Fragkostefanakis, S., Roth, S., Schleiff, E., and Scharf, K. D. (2015). Prospects of engineering thermotolerance in crops through modulation of heat stress transcription factor and heat shock protein networks. *Plant Cell Environ.* 38, 1881–1895. doi: 10.1111/pce.12396

Giorno, F., Wolters-Arts, M., Grillo, S., Scharf, K. D., Vriezen, W. H., and Mariani, C. (2010). Developmental and heat stress-regulated expression of HsfA2 and small heat shock proteins in tomato anthers. *J. Exp. Bot.* 61, 453–462. doi: 10.1093/jxb/erp316

Gong, Z., Xiong, L., Shi, H., Yang, S., Herrera-Estrella, L. R., Xu, G., et al. (2020). Plant abiotic stress response and nutrient use efficiency. *Sci. China Life Sci.* 63, 635–674. doi: 10.1007/s11427-020-1683-x

Guo, M., Liu, J. H., Ma, X., Luo, D. X., Gong, Z. H., and Lu, M. H. (2016). The plant heat stress transcription factors (HSFs): structure, regulation, and function in response to abiotic stresses. *Front. Plant Sci.* 7:114. doi: 10.3389/fpls.2016.00114

Guo, M., Lu, J. P., Zhai, Y. F., Chai, W. G., Gong, Z. H., and Lu, M. H. (2015). Genome-wide analysis, expression profile of heat shock factor gene family (CaHsfs) and characterisation of CaHsfA2 in pepper (*Capsicum annuum L.*). *BMC Plant Biol.* 15:151. doi: 10.1186/s12870-015-0512-7

Guo, J., Wu, J., Ji, Q., Wang, C., Luo, L., Yuan, Y., et al. (2008). Genome-wide analysis of heat shock transcription factor families in rice and *Arabidopsis*. *J. Genet. Genomics* 35, 105–118. doi: 10.1016/S1673-8527(08)60016-8

Heerklotz, D., Doring, P., Bonzelius, F., Winkelhaus, S., and Nover, L. (2001). The balance of nuclear import and export determines the intracellular distribution and function of tomato heat stress transcription factor HsfA2. *Mol. Cell. Biol.* 21, 1759–1768. doi: 10.1128/MCB.21.5.1759-1768.2001

Hrmova, M., and Hussain, S. S. (2021). Plant transcription factors involved in drought and associated stresses. *Int. J. Mol. Sci.* 22:5662. doi: 10.3390/ijms22115662

Huang, B., Huang, Z., Ma, R., Chen, J., Zhang, Z., and Yrjala, K. (2021). Genome-wide identification and analysis of the heat shock transcription factor family in moso bamboo (*Phyllostachys edulis*). *Sci. Rep.* 11:16492. doi: 10.1038/s41598-021-95899-3

Ikeda, M., Mitsuda, N., and Ohme-Takagi, M. (2011). *Arabidopsis* HsfB1 and HsfB2b act as repressors of the expression of heat-inducible Hsfs but positively regulate the acquired thermotolerance. *Plant Physiol.* 157, 1243–1254. doi: 10.1104/pp.111.179036

International Wheat Genome Sequencing, C. (2014). A chromosome-based draft sequence of the hexaploid bread wheat (*Triticum aestivum*) genome. *Science* 345, 1251788. doi: 10.1126/science.1251788

Khan, M. I. R., Iqbal, N., Masood, A., Per, T. S., and Khan, N. A. (2013). Salicylic acid alleviates adverse effects of heat stress on photosynthesis through changes in proline production and ethylene formation. *Plant Signal. Behav.* 8:e26374. doi: 10.4161/psb.26374

Kotak, S., Port, M., Ganguli, A., Bicker, F., and von Koskull-Doring, P. (2004). Characterization of C-terminal domains of *Arabidopsis* heat stress transcription factors (Hsfs) and identification of a new signature combination of plant class A Hsfs with AHA and NES motifs essential for activator function and intracellular localization. *Plant J.* 39, 98–112. doi: 10.1111/j.1365-313X.2004.02111.x

Kulkarni, M., Soolanayakanahally, R., Ogawa, S., Uga, Y. G., Selvaraj, M., and Kagale, S. (2017). Drought response in wheat: key genes and regulatory mechanisms controlling root system architecture and transpiration efficiency. *Front. Chem.* 5:106. doi: 10.3389/fchem.2017.00106

Kumar, R. R., Goswami, S., Singh, K., Dubey, K., Rai, G. K., Singh, B., et al. (2018). Characterization of novel heat-responsive transcription factor (TaHSFA6e) gene involved in regulation of heat shock proteins (HSPs)—a key member of heat stress-tolerance network of wheat. *J. Biotechnol.* 279, 1–12. doi: 10.1016/j.jbiotec.2018.05.008

Larkindale, J., Hall, J. D., Knight, M. R., and Vierling, E. (2005). Heat stress phenotypes of *Arabidopsis* mutants implicate multiple signaling pathways in the acquisition of thermotolerance. *Plant Physiol.* 138, 882–897. doi: 10.1104/pp.105.062257

Li, H. C., Zhang, H. N., Li, G. L., Liu, Z. H., Zhang, Y. M., Zhang, H. M., et al. (2015). Expression of maize heat shock transcription factor gene ZmHsf06 enhances the thermotolerance and drought-stress tolerance of transgenic *Arabidopsis*. *Funct. Plant Biol.* 42, 1080–1091. doi: 10.1071/FP15080

Li, G. L., Zhang, H. N., Shao, H., Wang, G. Y., Zhang, Y. Y., Zhang, Y. J., et al. (2019). ZmHsf05, a new heat shock transcription factor from *Zea mays L.* improves thermotolerance in *Arabidopsis thaliana* and rescues thermotolerance defects of the *athsfa2* mutant. *Plant Sci.* 283, 375–384. doi: 10.1016/j.plantsci.2019.03.002

Liu, G. R., Chen, X. Z., and Duan, W. Q. (2002). The relationship between wheat leaf osmotic adjustment ability and varietal drought resistance under water stress [in Chinese]. *J. Agric. Univ. Hebei* 25, 1–3. doi: 10.3969/j.issn.1000-1573.2002.02.001

Liu, J., Feng, L., Gu, X., Deng, X., Qiu, Q., Li, Q., et al. (2019). An H3K27me3 demethylase-HSFA2 regulatory loop orchestrates transgenerational thermomemory in *Arabidopsis*. *Cell Res.* 29, 379–390. doi: 10.1038/s41422-019-0145-8

Liu, Z., Li, G., Zhang, H., Zhang, Y., Zhang, Y., Duan, S., et al. (2020). TaHsfA2-1, a new gene for thermotolerance in wheat seedlings: characterization and functional roles. *J. Plant Physiol.* 246-247:153135. doi: 10.1016/j.jplph.2020.153135

Liu, H. C., Liao, H. T., and Charng, Y. Y. (2011). The role of class A1 heat shock factors (HSFA1s) in response to heat and other stresses in *Arabidopsis*. *Plant Cell Environ.* 34, 738–751. doi: 10.1111/j.1365-3040.2011.02278.x

Lobell, D. B., and Gourdji, S. M. (2012). The influence of climate change on global crop productivity. *Plant Physiol.* 160, 1686–1697. doi: 10.1104/pp.112.208298

Manickavelu, A., Kawaura, K., Oishi, K., Shin-I, T., Kohara, Y., Yahiaoui, N., et al. (2012). Comprehensive functional analyses of expressed sequence tags in common wheat (*Triticum aestivum*). *DNA Res.* 19, 165–177. doi: 10.1093/dnares/dss001

Nakashima, K., Ito, Y., and Yamaguchi-Shinozaki, K. (2009). Transcriptional regulatory networks in response to abiotic stresses in *Arabidopsis* and grasses. *Plant Physiol.* 149, 88–95. doi: 10.1104/pp.108.129791

Nishizawa, A., Yabuta, Y., Yoshida, E., Maruta, T., Yoshimura, K., and Shigeoka, S. (2006). *Arabidopsis* heat shock transcription factor A2 as a key regulator in response to several types of environmental stress. *Plant J.* 48, 535–547. doi: 10.1111/j.1365-313X.2006.02889.x

Nishizawa-Yokoi, A., Nosaka, R., Hayashi, H., Tainaka, H., Maruta, T., Tamoi, M., et al. (2011). HsfA1d and HsfA1e involved in the transcriptional regulation of HsfA2 function as key regulators for the Hsf signaling network in response to environmental stress. *Plant Cell Physiol.* 52, 933–945. doi: 10.1093/pcp/pcr045

Nishizawa-Yokoi, A., Tainaka, H., Yoshida, E., Tamoi, M., Yabuta, Y., and Shigeoka, S. (2010). The 26S proteasome function and Hsp90 activity involved in the regulation of HsfA2 expression in response to oxidative stress. *Plant Cell Physiol.* 51, 486–496. doi: 10.1093/pcp/pcq015

Nover, L., Bharti, K., Döring, P., Mishra, S. K., Ganguli, A., and Scharf, K. D. (2001). *Arabidopsis* and the heat stress transcription factor world: how many heat stress transcription factors do we need? *Cell Stress Chaperones* 6, 177–189. doi: 10.1379/1466-1268(2001)006<0177:aathst>2.0.co;2

Ogawa, D., Yamaguchi, K., and Nishiuchi, T. (2007). High-level overexpression of the *Arabidopsis* HsfA2 gene confers not only increased themotolerance but also salt/osmotic stress tolerance and enhanced callus growth. *J. Exp. Bot.* 58, 3373–3383. doi: 10.1093/jxb/erm184

Puranik, S., Sahu, P. P., Srivastava, P. S., and Prasad, M. (2012). NAC proteins: regulation and role in stress tolerance. *Trends Plant Sci.* 17, 369–381. doi: 10.1016/j.tplants.2016.08.015

Savchenko, T., and Tikhonov, K. (2021). Oxidative stress-induced alteration of plant central metabolism. *Life (Basel).* 11:304. doi: 10.3390/life11040304

Scharf, K. D., Berberich, T., Ebersberger, I., and Nover, L. (2012). The plant heat stress transcription factor (Hsf) family: structure, function and evolution. *Biochim. Biophys. Acta* 1819, 104–119. doi: 10.1016/j.bbagrm.2011.10.002

Scharf, K. D., Heider, H., Hohfeld, I., Lyck, R., Schmidt, E., and Nover, L. (1998). The tomato Hsf system: HsfA2 needs interaction with HsfA1 for efficient nuclear import and may be localized in cytoplasmic heat stress granules. *Mol. Cell. Biol.* 18, 2240–2251. doi: 10.1128/MCB.18.4.2240

Shiferaw, B., Smale, M., Braun, H. J., Duveiller, E., Reynolds, M., and Muricho, G. (2013). Crops that feed the world 10. Past successes and future challenges to the role played by wheat in global food security. *Food Secur.* 5, 291–317. doi: 10.1007/s12571-013-0263-y

Tang, G. L., Ma, J. N., Hause, B., Nick, P., and Riemann, M. (2020). Jasmonate is required for the response to osmotic stress in rice. *Environ. Exp. Bot.* 175:104047. doi: 10.1016/j.envexpbot.2020.104047

Udvardi, M. K., Kakar, K., Wandrey, M., Montanari, O., Murray, J., Andriankaja, A., et al. (2007). Legume transcription factors: global regulators of plant development and response to the environment. *Plant Physiol.* 144, 538–549. doi: 10.1104/pp.107.098061

Ul Haq, S., Khan, A., Ali, M., Khattak, A. M., Gai, W. X., Zhang, H. X., et al. (2019). Heat shock proteins: dynamic biomolecules to counter plant biotic and abiotic stresses. *Int. J. Mol. Sci.* 20:5321. doi: 10.3390/ijms20215321

Verma, V., Ravindran, P., and Kumar, P. P. (2016). Plant hormone-mediated regulation of stress responses. *BMC Plant Biol.* 16:86. doi: 10.1186/s12870-016-0771-y

Wu, H., Shi, N., An, X., Liu, C., Fu, H., Cao, L., et al. (2018). Candidate genes for yellow leaf color in common wheat (*Triticum aestivum* L.) and major related metabolic pathways according to transcriptome profiling. *Int. J. Mol. Sci.* 19:1594. doi: 10.3390/ijms19061594

Xue, G. P., Drenth, J., and McIntyre, C. L. (2015). TaHsfA6f is a transcriptional activator that regulates a suite of heat stress protection genes in wheat (*Triticum aestivum L.*) including previously unknown Hsf targets. *J. Exp. Bot.* 66, 1025–1039. doi: 10.1093/jxb/eru462

Xue, G. P., Sadat, S., Drenth, J., and McIntyre, C. L. (2014). The heat shock factor family from *Triticum aestivum* in response to heat and other major abiotic stresses and their role in regulation of heat shock protein genes. *J. Exp. Bot.* 65, 539–557. doi: 10.1093/jxb/ert399

Yang, C., Zhao, L., Zhang, H., Yang, Z., Wang, H., Wen, S., et al. (2014). Evolution of physiological responses to salt stress in hexaploid wheat. *Proc. Natl. Acad. Sci. U. S. A.* 111, 11882–11887. doi: 10.1073/pnas.1412839111

Yokotani, N., Ichikawa, T., Kondou, Y., Matsui, M., Hirochika, H., Iwabuchi, M., et al. (2008). Expression of rice heat stress transcription factor OsHsfA2e enhances tolerance to environmental stresses in transgenic Arabidopsis. *Planta* 227, 957–967. doi: 10.1007/s00425-007-0670-4

Zhang, J. H., Jia, W. S., Yang, J. C., and Ismail, A. M. (2006). Role of ABA in integrating plant responses to drought and salt stresses. *Field Crops Res.* 97, 111–119. doi: 10.1016/j.fcr.2005.08.018

Zhang, J., Li, Y., Jia, H. X., Li, J. B., Huang, J., Lu, M. Z., et al. (2015). The heat shock factor gene family in *Salix suchowensis*: a genome-wide survey and expression profiling during development and abiotic stresses. *Front. Plant Sci.* 6:748. doi: 10.3389/fpls.2015.00748

Zhu, Y., Wang, Z., Jing, Y., Wang, L., Liu, X., Liu, Y., et al. (2009). Ectopic over-expression of BhHsf1, a heat shock factor from the resurrection plant *Boea hygrometrica*, leads to increased thermotolerance and retarded growth in transgenic *Arabidopsis* and tobacco. *Plant Mol. Biol.* 71, 451–467. doi: 10.1007/s11103-009-9538-2

Conflict of Interest: The authors declare that the research was conducted in the absence of any commercial or financial relationships that could be construed as a potential conflict of interest.

Publisher's Note: All claims expressed in this article are solely those of the authors and do not necessarily represent those of their affiliated organizations, or those of the publisher, the editors and the reviewers. Any product that may be evaluated in this article, or claim that may be made by its manufacturer, is not guaranteed or endorsed by the publisher.

Copyright © 2022 Meng, Zhao, Li, Liu, Ren, Li and Guo. This is an open-access article distributed under the terms of the Creative Commons Attribution License (CC BY). The use, distribution or reproduction in other forums is permitted, provided the original author(s) and the copyright owner(s) are credited and that the original publication in this journal is cited, in accordance with accepted academic practice. No use, distribution or reproduction is permitted which does not comply with these terms.

frontiers | Frontiers in Plant Science

TYPE Original Research
PUBLISHED 12 August 2022
DOI 10.3389/fpls.2022.974507

Check for updates

OPEN ACCESS

EDITED BY
Caroline Müller,
Universidade Federal da Fronteira Sul, Brazil

REVIEWED BY
Anup Kumar Sarkar,
Dukhulal Nibaran Chandra College, India
Piyada Theerakulpisut,
Khon Kaen University, Thailand
Neveen Talaat,
Cairo University, Egypt

*CORRESPONDENCE
Jianming Xie
xiejianming@gsau.edu.cn

SPECIALTY SECTION
This article was submitted to Plant Abiotic Stress, a section of the journal Frontiers in Plant Science

RECEIVED 21 June 2022
ACCEPTED 27 July 2022
PUBLISHED 12 August 2022

CITATION
Yang Y, Xie J, Li J, Zhang J, Zhang X, Yao Y, Wang C, Niu T and Bakpa EP (2022) Trehalose alleviates salt tolerance by improving photosynthetic performance and maintaining mineral ion homeostasis in tomato plants. *Front. Plant Sci.* 13:974507. doi: 10.3389/fpls.2022.974507

COPYRIGHT
© 2022 Yang, Xie, Li, Zhang, Zhang, Yao, Wang, Niu and Bakpa. This is an open-access article distributed under the terms of the Creative Commons Attribution License (CC BY). The use, distribution or reproduction in other forums is permitted, provided the original author(s) and the copyright owner(s) are credited and that the original publication in this journal is cited, in accordance with accepted academic practice. No use, distribution or reproduction is permitted which does not comply with these terms.

Trehalose alleviates salt tolerance by improving photosynthetic performance and maintaining mineral ion homeostasis in tomato plants

Yan Yang, Jianming Xie*, Jing Li, Jing Zhang, Xiaodan Zhang, Yandong Yao, Cheng Wang, Tianhang Niu and Emily Patience Bakpa

College of Horticulture, Gansu Agricultural University, Lanzhou, China

Trehalose (Tre), which was an osmoprotective or stabilizing molecule, played a protective role against different abiotic stresses in plants and showed remarkable perspectives in salt stress. In this study, the potential role of Tre in improving the resistance to salt stress in tomato plants was investigated. Tomato plants (Micro Tom) were treated with Hoagland nutrient solution (CK), 10 mM Tre (T), 150 mM sodium chloride (NaCl, S), and 10 mM Tre+150 mM NaCl (S+T) for 5 days. Our results showed that foliar application of Tre alleviated the inhibition of tomato plant growth under salt stress. In addition, salt stress decreased the values of net photosynthetic rate (Pn, 85.99%), stomata conductance (gs, 57.3%), and transpiration rate (Tr, 47.97%), but increased that of intercellular carbon dioxide concentration (Ci, 26.25%). However, exogenous application of Tre significantly increased photosynthetic efficiency, increased the activity of Calvin cycle enzymes [ribulose diphosphate carboxylase/oxygenase (Rubisco), fructose-1,6-bisphosphate aldolase (FBA), fructose-1, 6-bisphosphatase (FBPase), glyceraldehyde-3-phosphate dehydrogenase (GAPDH), and transketolase (TK)], up-regulated the expression of genes encoding enzymes, induced stomatal opening, and alleviated salt-induced damage to the chloroplast membrane and structure. In the saline environment, photosynthetic electron transport was restricted, resulting the J-I-P phase to decrease. At the same time, the absorption, capture, and transport energies per excited cross-section and per active reaction center decreased, and the dissipation energy increased. Conversely, Tre reversed these values and enhanced the photosystem response to salt stress by protecting the photosynthetic electron transport system. In addition, foliage application with Tre significantly increased the potassium to sodium transport selectivity ratio (S_{K-Na}) by 16.08%, and increased the levels of other ions to varying degrees. Principal component analysis (PCA) analysis showed that exogenous Tre could change the distribution of elements in different organs and affect the expressions of *SlSOS1*, *SlNHX*, *SlHKT1.1*, *SlVHA*, and

SlHA-A at the transcriptional level under salt stress, thereby maintaining ion homeostasis. This study demonstrated that Tre was involved in the process of mitigating salt stress toxicity in tomato plants and provided specific insights into the effectiveness of Tre in mediating salt tolerance.

KEYWORDS

trehalose, salt stress, photosystem fluorescence, OJIP transient, ionic homeostasis, tomato

Introduction

Recently, nearly 7% of agricultural land has been affected by salinization because of the anthropogenic activities, including irrigation practices, fertilizer application methods, industrial pollution, and climate change (Hashem et al., 2018; Yin et al., 2021). As a result, soil salinization has become a global ecological problem threatening the environment. It affects the sustainable development of agriculture and hinders and constraints agricultural development (Zamani et al., 2019; Guo et al., 2020). The high salt concentration absorbed by plant roots resulted in high osmotic potential, which caused the increase in sodium ions (Na^+) and chloride ions (Cl^-), exceeding the threshold level, impaired the structure of plant cell membrane, inhibited photosynthesis, produced toxic metabolites, and reduced nutrient absorption, thus hindering plant growth and productivity and causing death in serious cases (Wu et al., 2018a; Zamani et al., 2019; Bhattarai et al., 2021). Tanveer et al. (2020) found that salinity not only delayed the germination stage of tomato, but also reduced the plant growth, such as root and stem length, plant dry weight and fresh weight, leaf area, etc. Reportedly, the growth and development of plants under salt stress were related to photosynthetic performance and the carbon cycle (Asrar et al., 2017). Moreover, Goussi et al. (2018) found that high concentration of salt stress led to thylakoid expansion and starch accumulation, which affected the donor side of PSII and reduced the quantum yield of PSI. Sodium chloride (NaCl) treatment diminished the stomatal aperture of tomato leaves, decreased net photosynthetic rate (Pn) and stomata conductance (gs), and inhibited chlorophyll synthesis (Faizan et al., 2021; Hu et al., 2021). In addition, long-term salinity reduced the activity of ribulose diphosphate carboxylase/oxygenase (Rubisco) and ribulose-1,5-bisphosphate (RuBP), thereby altering the biochemical reactions that regulate stomatal exchange (Loudari et al., 2020). Subsequently, the ability of several parts of the photosynthetic electron transport process in tomato seedlings was obstructed by the salt environment. Plants adapt to salt stress and mitigate its adverse effects through various methods and physiological mechanisms. For example, excess Na^+ is compartmentalized into vacuoles and/or transported by apoplast pathways (Hashem et al., 2018). Loudari et al. (2020) showed that sodium (Na) was significantly enriched in the roots and copper (Cu) was greatly enriched in the aboveground of tomato plants, which affected the imbalance of ion homeostasis under salt stress. Salinity increased potassium ions (K^+) efflux and decreased hydrogen ions (H^+) efflux from tomato plants, resulting in a lower K^+/Na^+ ratio (Meng et al., 2020). Furthermore, salt stress significantly increased the transcriptional regulation of tonoplast Na^+/H^+ antiporter genes (Abdelaziz et al., 2019). In addition, plants exposed to salt stress synthesize and accumulate large amounts of compatible osmolytes, such as free amino acids, glycine betaine, and soluble sugars, to maintain their normal growth (Hashem et al., 2015; Farooq et al., 2017). However, not all sugars are considered involved in plant

Abbreviations: Na^+, sodium ions; Cl^-, chloride ions; Tre, trehalose; T6P, trehalose 6-phosphate; TPS, trehalose-6-phosphate synthase; G6P, glucose 6-phosphate; UDPG, uridine diphosphate glucose; TPP, trehalose-6-phosphate phosphatase; SEM, scanning electron microscope; TEM, transmission electron microscope; Ci, intercellular carbon dioxide concentration; Tr, transpiration rate; gs, stomata conductance; Pn, net photosynthetic rate; Rubisco, ribulose diphosphate carboxylase/oxygenase; FBPase, fructose-1, 6-bisphosphatase; TK, transketolase; GAPDH, glyceraldehyde-3-phosphate dehydrogenase; FBA, fructose-1,6-bisphosphate aldolase; V_j, relative variable fluorescence intensity at the J-step; V_j, relative variable fluorescence intensity at the I-step; M_o, approximated initial slope of the fluorescence transient; S_m, normalized total complementary area above the O-J-I-P; $S_{m/t(Fm)}$, the average redox state of Q_A; φP_o, maximum quantum yield for primary photochemistry (at t = 0); φE_o, quantum yield for electron transport (at t = 0); φR_o, the quantum yield of PSI final electron acceptor reduction per photon absorption; ψ_o, probability that a trapped exciton moves an electron into the electron transport chain beyond Q_A^- (at t = 0); δR_o, the efficiency of electron transfer from Q_B to PSI receptor; PI_{abs}, performance index on absorption basis; ABS/CS_m, absorption flux per cross section; TRo/CS_m, trapped energy flux per PSII cross section; ETo/CS_m, electron transport in PSII cross section; DIo/CS_m, dissipated energy flux per PSII cross section; ABS/RC, absorption flux per RC; TR_o/RC, trapped energy flux per RC; ET_o/RC, electron transport flux per RC; DI_o/RC, dissipated energy flux per RC; RCs, active reaction centers; Na, sodium; K, potassium; Ca, calcium; Mg, magnesium; Fe, iron; Mn, manganese; Zn, zinc; Cu, copper; S_{K-Na}, K-Na transport selectivity ratio; NaCl, sodium chloride; N, nitrogen; P, phosphorus; Cl, chlorine; H^+, hydrogen ions; K^+, potassium ions; RuBP, ribulose-1,5-bisphosphate; SOD, superoxide dismutase; POD, peroxidase; PBS, phosphate buffer saline; OsO_4, osmic acid; CO_2, carbon dioxide; OJIP curve, the chlorophyll fluorescence kinetics; PC1, the first principal component; PC2, the second principal component; SnRK1, sucrose non-fermenting-1-related protein kinase1; ROS, reactive oxygen species; PCA, principal component analysis.

stress response. Glucose, fructose, sucrose, and trehalose (Tre) have been involved in the regulation of plant growth and development of the environmental response process (Lastdrager et al., 2014; Sehar et al., 2019).

Tre is an important and non-reducing disaccharide widely existing in organisms, and it can be used as an effective cytoprotective agent under extreme environments. In plants, the Tre synthesis pathway is the trehalose 6-phosphate (T6P) by trehalose-6-phosphate synthase (TPS) catalyzed the glucose 6-phosphate (G6P) and uridine diphosphate glucose (UDPG), and T6P was converted to Tre by trehalose-6-phosphate phosphatase (TPP) (Nunes et al., 2013). Ambastha and Tiwari (2015) observed that the desert plant accumulated high levels of Tre, suggesting that Tre played an essential role in response to abiotic stress. This special function of Tre may be related to its physical and chemical properties. Reportedly, Tre can prevent the deformation of protein and membrane structures by replacing polar hydrogen-bonding groups of water molecules (Avonce et al., 2006). Therefore, Tre has been used as a tool to interfere with plant processes to better address plant growth and development mechanisms with the advantages of being available, absorbable, cheap, and non-toxic (Lin et al., 2017). Hossain et al. (2019) suggested that the improvement of Tre mediated abiotic stress may be related to the activation of stress responsive genes and transcription factors, rather than as an osmoprotective molecule. Overexpression of *OsTPS8* enhanced salt tolerance without any yield reduction, indicating its improvement in rice genetics (Sarkar and Sadhukhan, 2022). Similarly, a number of studies have confirmed this. Krasensky et al. (2014) found that *AtTPPD*-overexpressing plants were more tolerant of salt stress than wild-type Arabidopsis thaliana plants. Depletion mutations in TPPF, a member of the TPP gene family in Arabidopsis thaliana, lead to a drought-sensitive phenotype, while *AtTPPF* seedlings upregulated the gene expression of drought-related electron transport activity and cell wall modification and downregulated stress-related transcription factors associated with water deficit (Lin et al., 2019). *AtTPPE* and *AtTPPI* were regulated by ABA response element binding factors, which directly bind to their promoters to enhance the gene expression, leading to increased Tre levels and a rapid response to stress (Lin et al., 2020; Wang et al., 2020). The overexpression of *ClTPS3* in Arabidopsis thaliana significantly improved salt tolerance by increasing the Tre content, enhancing the activities of superoxide dismutase (SOD) and peroxidase (POD) (Yang et al., 2022). In addition, transgenic plants overexpressing certain TPS/TPP genes from bacterial, fungal, or plants can improve the tolerance to abiotic stresses. Occasionally, these processes are accompanied by elevated Tre levels (Lyu et al., 2013; Henry et al., 2015; Lin et al., 2020; Wang et al., 2020). Tre reduced the effects of NaCl on growth parameters, Na, K, K/Na ratio, phenolics, and the expression of AOX, NHX1, and SOS1, thereby alleviating the adverse effects of NaCl in wheat (Samadi et al., 2019). Interestingly, T6P is considered a signaling metabolite that regulates sucrose levels (Figueroa and Lunn, 2016). Yadav et al. (2014) considered the T6P: sucrose ratio to be a key parameter in plants, which forms a homeostatic mechanism that maintains sucrose levels within a range appropriate to cell types and developmental stages. The sucrose-T6P model proposes that high levels of sucrose are accompanied by high levels of T6P, but that high levels of T6P may have positive or negative consequences for growth, depending on the metabolic environment and sucrose levels (Figueroa and Lunn, 2016; Fichtner et al., 2021). The sucrose-T6P relationship also modulates with low temperature (Figueroa et al., 2016). Kretzschmar et al. (2015) confirmed that *OsTPP7* promoted the transcription of MYBS1 and CIPK15 genes by regulating T6P: sucrose in germination tissues, thereby promoting anaerobic germination tolerance. There, research has shown that T6P promoted starch synthesis through the thioredoxin-mediated triggering of AGPase. T6P controlled starch hydrolysis in plastids and it could be transformed to Tre (Sadak, 2019). Exogenous Tre or Tre derivatives increased the maximum electron rate, maximum light use efficiency and minimum saturating irradiance of maize inhibited by water deficit stress (de Novais Portugal et al., 2021). In another study, application of Tre alleviated the negative effects of drought by partially restoring chlorophyll levels and photosynthetic activity in Sweet Basil (Zulfiqar et al., 2021). In addition, the application of Tre not only alleviated the heat-induced chlorophyll content and gas exchange parameters of *Emmenopterys henryi* Oliv., but also promoted the recovery of photosynthesis after heat treatment (Feng et al., 2022). Alternatively, Tre decreased the Na^+/K^+ ratio of rice seedlings under salt stress (Nounjan et al., 2012). In Arabidopsis thaliana, Tre also has the ability to retain K and K/Na, thus improving salt tolerance of plants (Yang et al., 2014). Altogether, these data strongly suggest that Tre plays a central role in stress.

Tomato (*Solanum lycopersicum*), which belongs to *Solanaceae*, is one of the important economic crops globally and has worldwide distribution (Zhong et al., 2019). To date, although the effects of Tre on salt stress have attracted extensive attention, most studies have concentrated on gas exchange parameters and K^+ and Na^+ content. However, a limited number of researches focused on the photosynthetic electron transport chain, distribution of different mineral elements, and the interaction between photosynthesis and ion transport under salt stress. The purpose of this study was to verify the hypothesis that exogenous Tre could affect the absorption and distribution of mineral elements in tomato plants, and alter the photosynthetic electron transport chain to improve plant salt tolerance. The positive effects of Tre were investigated by measuring the growth parameters, stomatal morphology, chloroplast ultrastructure, gas exchange parameters, Calvin cycle, photosynthetic electron transport chain, mineral element content, and ion transport related genes of tomato plants under salt stress. Therefore, a primary objective of this study

is to determine whether Tre has a protective function on the photosynthetic mechanism and whether it can coordinate the beneficial distribution of different mineral elements in salt stress.

Materials and methods

Plant growth conditions

The experiment was carried out in plant growth chambers (RDN, Nibo) with a humidity of 70%, an ambient temperature of 26 ± 1°C during the day/20 ± 1°C at night, and photoperiod of 16 h/day. Germinated seeds of tomato (Micro-tom; **Supplementary Figure 1**) were sown in a tray with vermiculite and perlite. At the one-leaf stage, soilless-tray seedlings of similar size were transferred to plastic containers containing half-concentrated Hoagland's nutrient solution. After 5 days of adaptation to hydroponics, tomato seedlings were grown with whole Hoagland's nutrient solution, which was replaced every 5 days.

Experimental design and treatment

When the fourth real-leaf of the seedlings fully expanded (25–30 days after sowing), the experimental treatment was started. The experiment adopted a completely randomized design with four treatments. Three biological replicates of 40 plants each were set for each treatment, with a total of 120 seedlings per treatment.

The treatment combinations were as follows: normal conditions (CK, Hoagland nutrient solution); normal conditions + Tre (T, Hoagland nutrient solution, 10 mM Tre); salt conditions (S, 150 mM NaCl); salt conditions + Tre (S+T, 150 mM NaCl, 10 mM Tre). The formulation of the Hogeland nutrient solution was shown in **Supplementary Table 1**. Tre solution was sprayed on the leaf surface of tomato plants under T and S+T treatments until the water drops were about to drip, continuously for 2 days. Similarly, CK and S treatments were sprayed with the same volume of pure water (2 mL/plant/spray; between 8:00 and 9:00 a.m.). Then, the seedlings were exposed to either a normal or excess NaCl condition. After 5 days of salt treatment, the tomato seedlings were randomly sampled for physiological and genetic data analyses. Functional leaves (fully expanding the functional leaves from the bottom to the fourth or fifth branches) were collected to measure stomatal characteristics, chloroplast ultrastructure, photosynthetic gas exchange parameters, Calvin cycle key enzymes and genes, rapid fluorescence determination of chlorophyll, and JIP-test. Roots, stems and leaves of tomato plants were isolated to measure mineral element content and relative expression levels of ion transport genes. The concentrations of NaCl and exogenous Tre used in this study were referred to our previous studies (Yang et al., 2022).

Plant height and stem diameter

Plant height: the distance from the base of the stem to the growing point was measured using a scale (three tomato plants per treatment, n = 3). Stem thickness: the diameter of the hypocotyl at the base of the cotyledons was measured using vernier calipers (three tomato plants per treatment, n = 3).

Fresh weight and dry weight

The shoot and root of the tomato plants (three tomato plants per treatment, n = 3) were separated with a sterile scalpel and weighed separately for fresh weight using an analytical balance. Then, the samples were placed in an oven at 80°C to be dried to constant weight, and their dry weight was recorded.

Leaf area

Leaf images (three tomato plants per treatment, n = 3) were scanned with the Epson Expression 11000XL. The total leaf area of tomato plants was calculated using WinRHIZO software (WinRHIZO Pro LA2400, Canada).

Scanning electron microscopy

The fresh leaves (three tomato plants per treatment, n = 3) were immediately fixed by electron microscopy fixative for 2 h at room temperature and then transferred to 4°C for preservation. The samples were washed with 0.1 M phosphate buffer saline (PBS, pH = 6.8) for four times with each wash lasting for 10 min. Then, the leaf samples were dehydrated with different concentrations of ethanol (30, 40, 50, 60, 65, 70, 75, 80, 85, 90, 95%), for 20 min each dehydration. Afterward, the samples were rinsed thrice with absolute ethanol, for 30 min each session. Finally, the samples were transferred to different concentrations of tert-butanol (30, 50, 70, 80, 85, 90, 95, 100, 100, 100%), with each transfer lasting for 30 min. Dry specimens were attached to metallic stubs using carbon stickers and sputter-coated with gold. The images were observed and captured using scanning electron microscope (SEM, S-3400N, Hitachi, Tokyo, Japan) (Min et al., 2019).

Ultrastructure observation

The fresh leaves (three tomato plants per treatment, n = 3) were immediately fixed by electron microscopy fixative

for 2 h at room temperature and transferred to 4°C for preservation. Then, the tissues were washed thrice using 0.1 M PBS (pH = 7.4), and each wash lasted for 15 min. Tissues that avoided the light were post-fixed with 1% osmic acid (OsO_4) in 0.1 M PBS (pH = 7.4) for 7 h at room temperature. After removing OsO_4, the tissues were rinsed thrice with 0.1 M PBS (pH = 7.4), with each rinse lasting for 15 min. Then, the plant tissues were gradient dehydrated by ethanol, permeated by acetone, embedded by 812 embedding agent, and polymerized in an oven. The resin blocks were cut to 60–80 nm thickness on an ultra-microtome (Leica UC7, Germany), and the tissues were fished out onto the 150 meshes cuprum grids with a formvar film. Then, they were stained with 2% uranium acetate and 2.6% lead citrate solution and observed by transmission electron microscope (TEM, HT7800, Hitachi, Japan) for image analysis. Samples preparation was completed by Wuhan Servicebio Biological Information Technology Co., Ltd.

Gas exchange parameters

Intercellular carbon dioxide concentration (Ci), transpiration rate (Tr), gs, and Pn of tomato leaves were measured from 9:00 to 10:30 a.m. by a portable photosynthetic system (CIRAS-2, United Kingdom). The fourth or fifth fresh leaves of tomato plant were collected for measurement (three tomato plants per treatment, n = 3). The conditions set during measurement were as follows: leaf area, 1.7 cm^2; chamber flow rate, 200 ml min^{-1}; photosynthetically active irradiation, 1,000 μmol m^{-2} s^{-1}; carbon dioxide (CO_2) concentration, 400 μmol mol^{-1}; air temperature, 25°C; and relative humidity, 60% (Wu et al., 2018b).

Calvin cycle key enzymes

The activities of key enzymes of the Calvin cycle [Rubisco, fructose-1, 6-bisphosphatase (FBPase), transketolase (TK), glyceraldehyde-3-phosphate dehydrogenase (GAPDH), and fructose-1,6-bisphosphate aldolase (FBA)] were measured (three tomato plants per treatment, n = 3) using ELISA kits (Yaji Biotech, Shanghai, China). Leaf samples were thoroughly ground with extraction buffer (0.05 mM Tris-HCl, and 0.1 M phosphate buffer; pH 7.4) and then centrifuged at 3,000 g for 15 min at 4°C. The supernatant was used for enzyme activity assay. Added testing sample, standard and horseradish peroxidase-conjugate reagent to microplate wells. The antibody to Rubisco was pre-existing in the microplate wells. Then incubated for 60 min at 37°C and washed. The substrate 3,3',5,5'-tetramethylbenzidine was converted to blue under the catalysis of peroxidase and to the final yellow under the function of acid. The intensity of the color was measured at 450 nm using a Spectra Absorbance Reader (ABS, United States). Draw a standard curve of optical density versus Rubisco activity from the measured values of the standards. The activity of Rubisco in the samples was then determined by comparing the O.D. of samples to the standard curve. Similarly, the activities of other enzymes were also determined. Under optimal conditions, the amount of enzyme required to convert 1 μmol of substrate in 1 min is called an enzyme activity (U). U/L is the international unit of enzyme activity (U/L represents the enzyme activity per liter of enzyme preparation; U/mL represents the enzyme activity per milliliter of enzyme preparation).

Rapid fluorescence determination of chlorophyll and kinetics analysis

Referring to Tang et al. (2021) and Yang et al. (2021a). The chlorophyll fluorescence kinetics (OJIP curve) in the tomato plants (three tomato plants per treatment, n = 3) was measured with a multifunctional plant efficiency analyzer (Handy PEA, Hansatech, United Kingdom). Before determination, the leaves were darkened for 30 min and then exposed to continuous illumination (3,000 μmol $m^{-2}s^{-1}$). The OJIP curve was plotted with the logarithm of the measurement time as the abscissa and instantaneous fluorescence of 10 μs to 2 s as the ordinate. The parameters of the JIP-test and their calculation formulas were shown in **Supplementary Table 2**. Each treatment measurement was replicated 12 times from randomly selected plants.

Mineral ion content

In accordance with Li et al. (2020), the samples (three tomato plants per treatment, n = 3) were digested in concentrated hydrogen peroxide and sulfuric acid solution. The ion contents [Na, potassium (K), calcium (Ca), magnesium (Mg), iron (Fe), manganese (Mn), zinc (Zn), and Cu] in leaves, stems, and roots were measured using an atomic absorption spectrometer (ZEEnit 700P, Analytik Jena, Germany). Referring to the method of Wang et al. (2010), the K-Na transport selectivity ratio was calculated (S_{K-Na}):

$$S_{K-Na} = \{[K^+]_{\text{stem and leaf}}/[Na^+]\text{stem and leaf}\} /\{[K^+]_{root}/[Na^+]_{root}\} \quad (1)$$

Quantitative real-time PCR (qRT-pCR)

After 5 days of NaCl treatment, fresh samples from each treatment (three tomato plants per treatment, n = 3)

were washed with sterile water and placed in liquid nitrogen immediately. The tomato plant total RNA was extracted using the *SteadyPure* plant RNA extraction kit AG21019 (Accurate Biotechnology Co., Ltd, Hunan, China). The total amount, purity and integrity of the total RNA of the sample were shown in **Supplementary Table 4** and **Supplementary Figure 2**. The cDNA was synthesized using the *Evo M-MLV* RT Kit with gDNA Clean for qPCRII kit AG11711 (Accurate Biotechnology Co., Ltd, Hunan, China). Real-time PCR was performed using a Light Cycler® 96 Real-Time PCR System (Roche, Switzerland), following the methods in the SYBR® Green Premix *Pro Taq* HS qPCR Kit AG11701 (Accurate Biotechnology Co., Ltd, Hunan, China). Tomato actin was used as a reference gene to normalize the data. Shanghai Shenggong Bioengineering Co., Ltd synthesized all gene primer sequences as listed in **Supplementary Table 3**. The $2^{-\Delta\Delta Ct}$ method was used to calculate the relative expression data of mRNA (Livak and Schmittgen, 2001). Three biological replicates were set for each treatment.

Statistical analysis

Microsoft Excel 2010 and SPSS 22.0 (SPSS Institute Inc., United States) were used for collation and counting, respectively. Duncan's multiple range test ($p < 0.05$) was used to compare differences among various treatments. Principal component analysis (PCA) and other diagrams were compiled by OriginPro 2021 (OriginLab Institute Inc., United States). All experiments were performed in triplicate. The results were represented by mean values ± standard error.

Results

Effect of trehalose on growth attributes and growth parameters under salt stress

The phenotypes of tomato plants in each treatment at 5 d were observed and photographed (**Figures 1A,B**). The exogenous application of Tre had no evident effect on the plants cultivated in the normal nutrient solution. However, the leaves of the tomato plants treated with S and S+T, which inhibited the growth and development of tomato plants, were remarkably curled, and the color was dull. However, the wilting degree of leaves under S treatment was higher than that in S+T treatment. As shown in **Table 1**, S treatment significantly inhibited plant height, stem diameter, shoot fresh weight, shoot dry weight, root fresh weight, and leaf area compared to CK. There was no significant difference in stem diameter, root dry weight and fresh weight among CK, T and S+T treatments. Meanwhile, compared with S treatment, S+T treatment increased plant height, shoot fresh weight, shoot dry weight and leaf area by 13.73, 36.38, 35.22, and 17.89%, respectively. Thus, Tre might play promotive roles on growth in tomato seedlings under salt stress.

Effect of trehalose on growth attributes, photosynthetic gas exchange parameters, calvin cycle key enzymes, and genes under salt stress

Salt stress was associated with significantly lower Pn, gs, and Tr values than those of the control tomato plants at 5 days, whereas the reduction of these variables indicated that the exogenous Tre-pretreated plants were smaller than those under salt treatment (**Figures 1B–D**). However, the Ci of the tomato seedlings increased under NaCl treatment compared with the non-stressed control. The S+T treatment caused a significant decline (**Figure 1E**). As shown in **Figure 2**, NaCl treatment led to a significant decrease in Rubisco, FBA, FBPase, GAPDH, and TK activity and a downregulation in Calvin cycle-related genes. By contrast, exogenous Tre increased the activity of these enzymes. The genes involved in the Calvin cycle in the salt-stress tomato plants pretreated with Tre were primarily up-regulated.

Effect of trehalose on stomatal characteristics and chloroplast ultrastructure under salt stress

Scanning electron microscope was used to observe the stomatal morphology of tomato leaves under different treatments. As shown in **Figure 3**, salt stress changed the stomatal opening. However, no significant structural differences were observed between Tre and no Tre treatments under normal conditions. After 5 days of salt stress, the closure degree of S treatment was higher than that of the S+T treatment. In addition, the stomata number of tomato leaves under the S treatment was lesser than that in the S+T treatment.

The chloroplast ultrastructure of leaves observed by TEM was shown in **Figure 4**. In the control plants, the chloroplasts possessed clear membrane structures and were ellipsoidal, the stromal thylakoids were tightly arranged, starch grains were packed, and osmiophilic granules were low in number. When subjected to salt stress, several prominent changes were observed in the chloroplast: (a) most cell membranes and chloroplast membranes were dissolved; (b) the chloroplast shape was swollen severely, (c) the thylakoid structure became vague with faults; (d) starch grains were reduced, and osmiophilic granules were increased. Compared with those under salt stress treatment, the number of osmiophilic granules

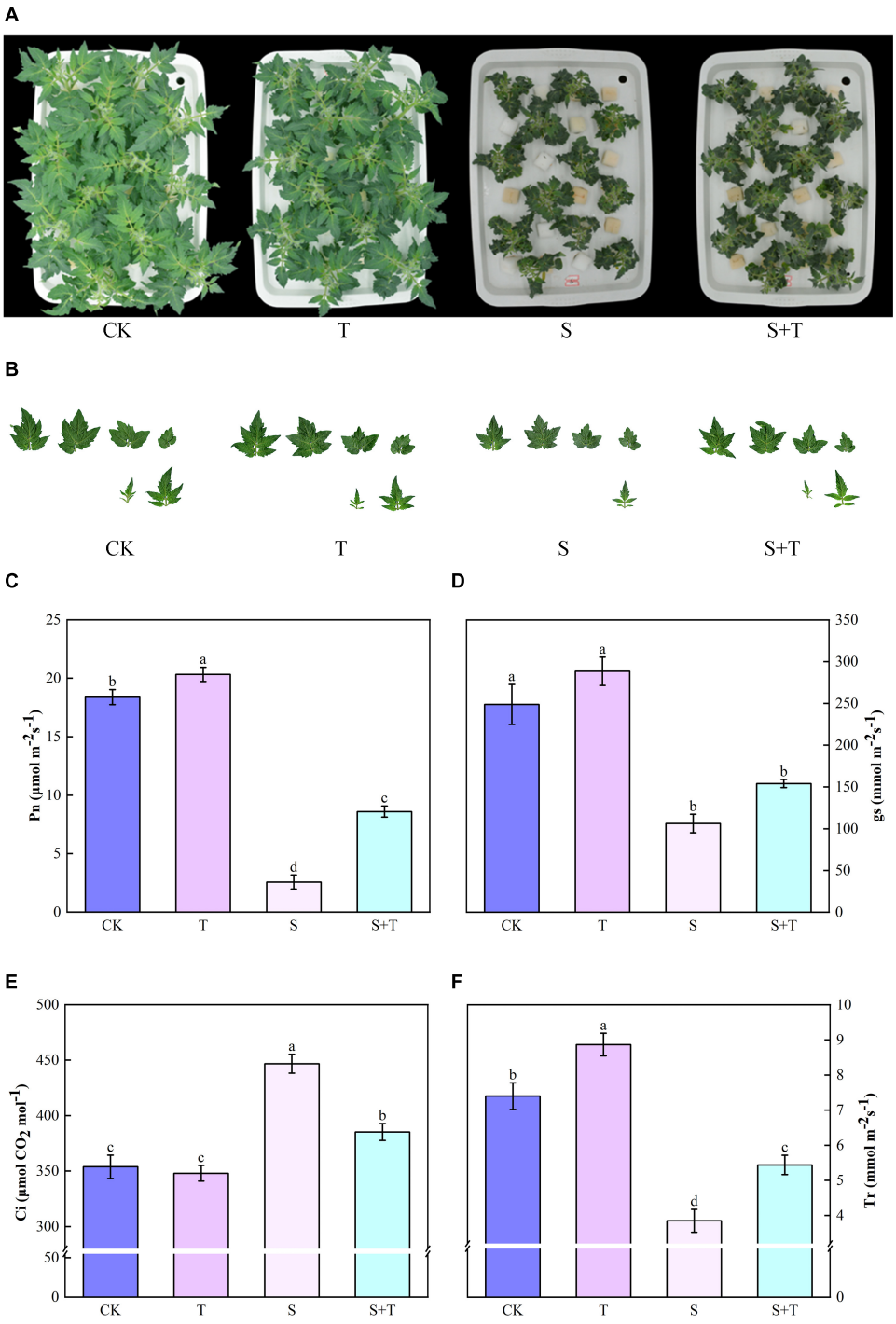


FIGURE 1
Effects of Tre treatment on growth attributes and photosynthetic gas exchange parameters of tomato seedlings exposed to salt stress for 5d. **(A)** Growth attributes. **(B)** Leaf area. **(C)** Net photosynthetic rate (Pn). **(D)** Stomata conductance (gs). **(E)** Intercellular carbon dioxide concentration (Ci). **(F)** Transpiration rate (Tr). The results showed the mean ± SE of three replicates, and the different letters denote the significant difference among treatments ($P < 0.05$), according to Duncan's multiple tests. CK, control; T, 10 mM Tre; S, 150 mM NaCl; S+T, 150 mM NaCl + 10 mM Tre.

decreased significantly with Tre addition, the status of the thylakoid membrane was optimized, and the number of grana and stroma lamellae increased. Interestingly, plasmolysis occurred in tomato leaves after the addition of Tre alone. In addition, the grana lamellae were loose, and the stroma lamellae were fuzzy.

TABLE 1 Effects of Tre treatment on the growth parameters in tomato seedlings under salt stress for 5 days.

Treatment	Plant height (mm)	Stem diameter (mm)	Shoot fresh weight (g)	Shoot dry weight (g)	Root fresh weight (g)	Root dry weight (g)	Leaf area (cm^2)
CK	88.358 ± 2.894a	3.286 ± 0.123a	4.233 ± 0.301a	0.44 ± 0.031a	1.187 ± 0.067a	0.068 ± 0.003a	54.508 ± 1.629a
T	76.304 ± 2.16b	3.253 ± 0.038a	3.583 ± 0.055b	0.365 ± 0.01b	1.093 ± 0.068ab	0.063 ± 0.004a	54.357 ± 1.338a
S	58.214 ± 1.139d	3.001 ± 0.02b	1.537 ± 0.051d	0.195 ± 0.006d	0.942 ± 0.045b	0.06 ± 0.002a	36.382 ± 1.485c
S+T	67.48 ± 0.168c	3.165 ± 0.065ab	2.416 ± 0.041c	0.301 ± 0.007c	1.046 ± 0.093ab	0.07 ± 0.006a	44.307 ± 1.068b

Data of tomato plants under saline condition were obtained after 5 days. The results showed the mean ± SE of three replicates, and the different letters denote the significant difference among treatments ($P < 0.05$), according to Duncan's multiple tests. CK, control; T, 10 mM Tre; S, 150 mM NaCl; S+T, 150 mM NaCl + 10 mM Tre.

Effect of trehalose on the electron transfer of photosystem II under salt stress (OJIP and JIP-test analysis)

To understand how Tre alleviated PSII photoinhibition induced by salt stress, we measured the OJIP curve of each treatment (Figure 5A). Experimental results showed no significant difference was found in the OJIP curve between the CK and T treatment. The J-I-P stage of the curve was significantly reduced by 5 days salt stress, compared with the normal control. However, the reduction in the J-I-P stage was more pronounced in S than in S+T treatment. In the radar representing various fluorescence parameters and performance indices, pronounced changes were observed in the tomato leaves when subjected to salt stress compared with the control seedlings (Figure 5B). In addition, Tre could effectively reverse the reduction of normalized total complementary area above the O-J-I-P (S_m), maximum quantum yield for primary photochemistry (φP_o), quantum yield for electron transport (φE_o), the quantum yield of PSI final electron acceptor reduction per photon absorption $(\varphi R)_o$, probability that a trapped exciton moves an electron into the electron transport chain beyond Q_A^- (ψ_o), the efficiency of electron transfer from Q_B to PSI receptor (δR_o), and performance index on absorption basis (PI_{abs}), and promote the enhancement of relative variable fluorescence intensity at the J-step (V_j), relative variable fluorescence intensity at the I-step (V_i), and approximated initial slope of the fluorescence transient (M_o) under salt stress, whereas no significant difference was observed in the average redox state of Q_A [$S_{m/t(Fm)}$].

Based on the structural and functional parameters obtained by the JIP-test experiment, changes in the energy distribution per cross section and per active reaction center under different treatments were compared and analyzed to understand further the photosynthetic behavior of tomato leaves under different treatments (Figures 6, 7). The results showed that exogenous Tre had no effect on the energy distribution per cross section and per active reaction center of tomato plants growing under normal conditions. Under salt stress, the absorption flux per cross section (ABS/CS_m), trapped energy flux per PSII cross section (TR_o/CS_m), and energy used for electron transport in PSII cross section (ET_o/CS_m) decreased significantly, whereas dissipated energy flux per PSII cross section (DI_o/CS_m) increased significantly. However, the application of exogenous Tre promoted the distribution trend of the above energy (ABS/CS_m, TR_o/CS_m, and ET_o/CS_m) and reduced the heat dissipation under salt stress. In addition, the number of active reaction centers (RCs) per unit leaf area decreased. The light energy absorption flux per RC (ABS/RC) and dissipative energy flux per RC (DI_o/RC) increased significantly after salt stress treatment, whereas, Tre application significantly inhibited these energy increases. In addition, salt stress reduced the trap energy flux per RC (TR_o/RC) and excitation energies for the electron transport flux per RC (ET_o/RC) in tomato leaves, while exogenous Tre reversed this trend. The membrane model visually showed the specific energy flux variation per cross section and per active reaction center (Figures 6B–E, 7B–E).

Effect of trehalose on mineral ion content under salt stress

The contents of six elements in the root, stem, and leaves of tomato under different treatments were demonstrated in Figure 8. Compared with the control group, the contents of Fe and Ca in the S-treated tomatoes were significantly reduced. Tomato roots contained more Fe, Mn, and Cu than stems and leaves for all treatments. Similarly, the leaves contained more Ca than stems and roots. The tomato plants treated with Tre exhibited unique ways of promoting the accumulation of mineral elements to varying degrees under salt stress. Compared with the S treatment, the S+T treatment promoted the accumulation of Mn and Fe in stems and leaves, Zn and Cu in stems, Mg in leaves, and Ca in roots.

Variable interaction through principal component analysis revealed the effect of trehalose on ionomers under salt stress

To thoroughly manifest the effect of Tre on mineral ions in different organs of tomato seedlings under salinity, we carried out PCA on previously measured mineral ions (Figure 9). PCA

10.3389/fpls.2022.974507

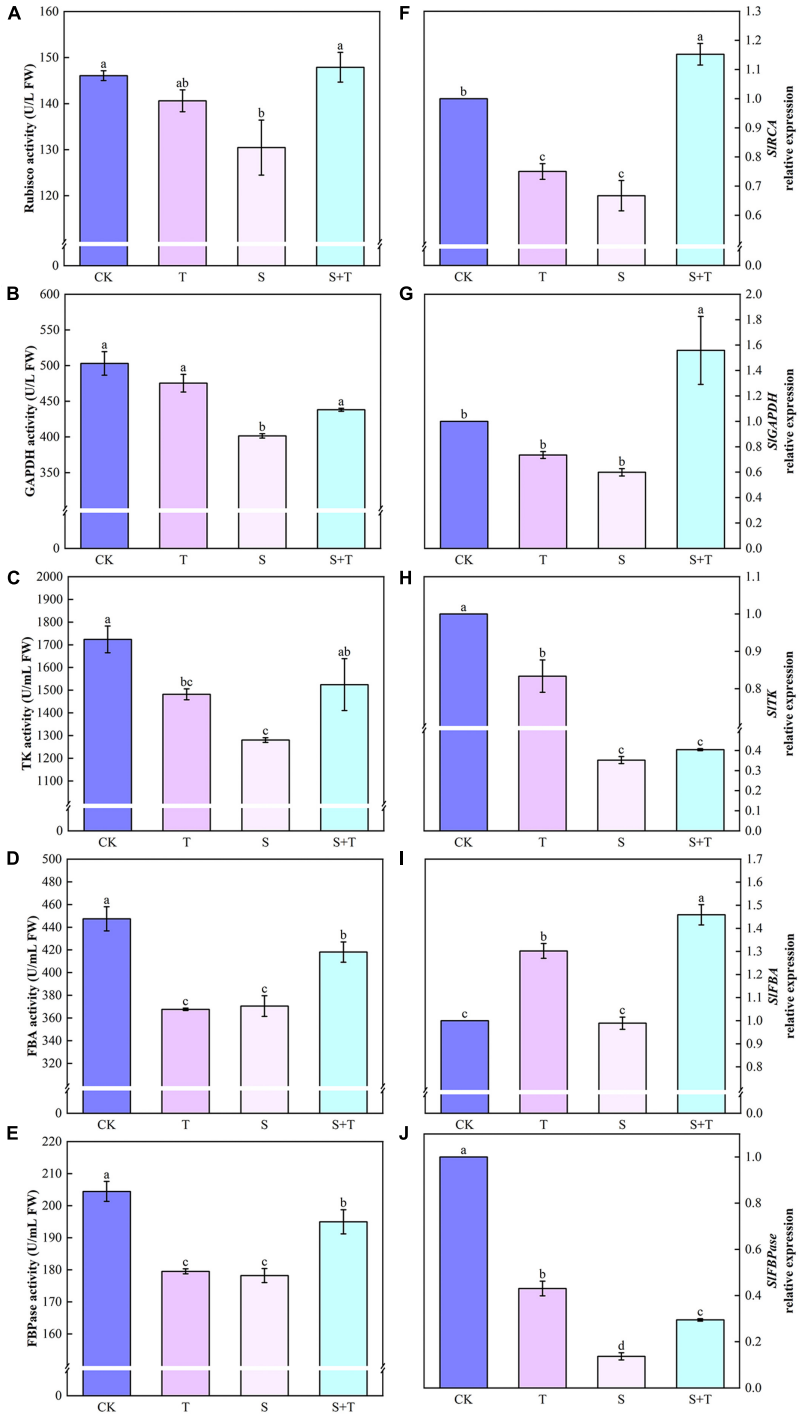


FIGURE 2
Effects of Tre treatment on Calvin cycle key enzymes and genes of tomato seedlings exposed to salt stress for 5 days. Panels **(A–E)** represent the activity of Rubisco, GAPDH, TK, FBA and FBPase, respectively. Panels **(F–J)** represent the expression levels of *SlRCA*, *SlGAPDH*, *SlTK*, *SlFBA*, and *SlFBPase*, respectively. The results showed the mean ± SE of three replicates, and the different letters denote the significant difference among treatments ($P < 0.05$), according to Duncan's multiple tests. CK, control; T, 10 mM Tre; S, 150 mM NaCl; S+T, 150 mM NaCl + 10mM Tre.

showed that the different treatments and organs of tomato plants could be distinguished. The first principal component (PC1) could be used to distinguish between S and S+T treatments, and represented 62.4, 55.9, and 44.7% of the total coefficient of variation in roots, stems, and leaves, respectively. In addition, the main contributing elements of PC1 were Ca

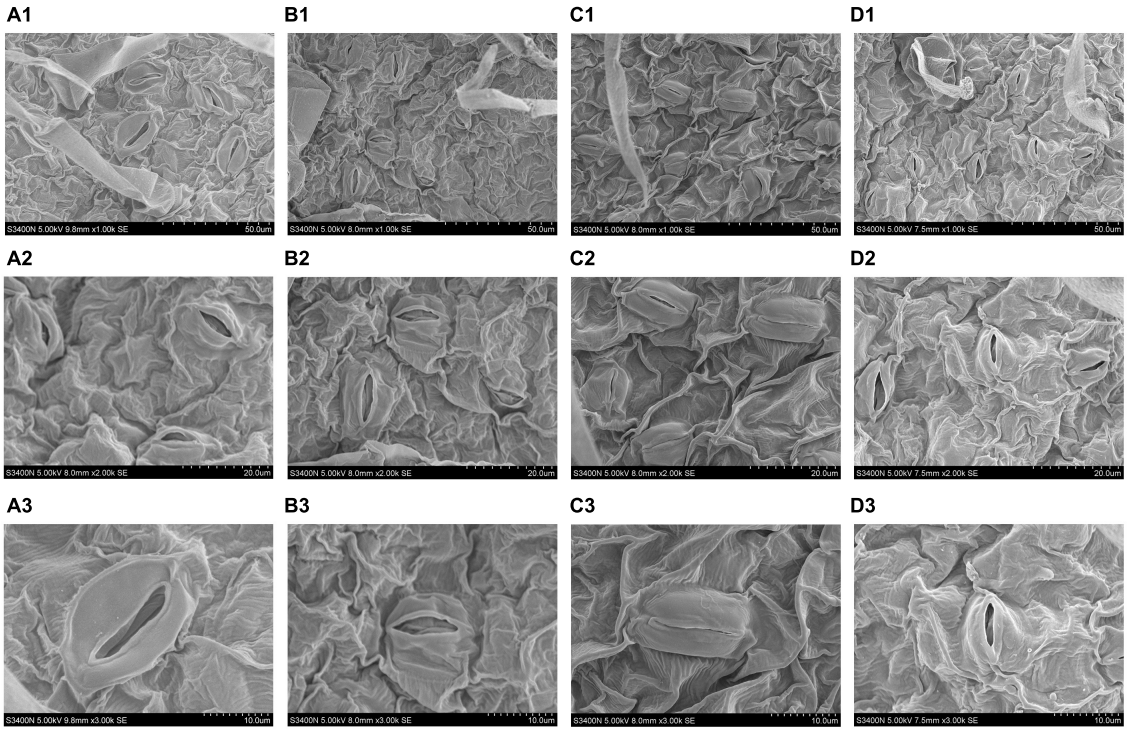


FIGURE 3
Effects of Tre treatment on stomatal characteristics of tomato seedlings exposed to salt stress for 5 days. Panels **(A1–D1)** represent stomatal distribution of tomato leaves in CK, T, S and S+T, respectively, 1,000×, scale bars = 50 μm; Panels **(A2–D2)** represent stomatal characteristics in CK-S+T, 2,000×, scale bars = 20 μm. Panels **(A3–D3)** represent stomatal characteristics in CK-S+T, 3,000×, scale bars = 10 μm.

and Fe in roots, Cu, Ca, and Na in stems, and K and Mg in leaves. The second principal component (PC2) could be used to distinguish between the salting and non-salting treatments, and accounted for 24.9, 22.2, and 30.5% of the total variance in roots, stems, and leaves, respectively. Subsequently, Na in roots, Zn in stems, and Mn and Cu in leaves had strong loading with the PC2, and they could be used as key elements for salt tolerance to reflect the difference in mineral elements in various organs of tomato plants.

Trehalose regulated S_{K-Na} parameters and the expression of ion transport-related genes under salt stress

As shown in **Figure 10A**, at the salinity treatment level, the S_{K-Na} value of tomato plants increased by 20.96% compared with the control treatment. After the exogenous addition of Tre, the selectivity coefficients of K and Na transport from tomato plant roots to shoots significantly improved. The lowest S_{K-Na} was observed when Tre was sprayed alone under normal conditions. Then, we checked the expression levels of genes associated with Na^+ and/or K^+ transport (**Figures 10B–F**). Compared with control, the relative expression levels of *SlSOS1* in roots, *SlHKT1.1* in leaves, and *SlNHX1* in roots and leaves were significantly up-regulated at moderate salinity level. In addition, *SlSOS1* and *SlNHX1* genes were abundantly expressed in roots, whereas, *SlHKT1.1* was mostly transcribed in leaves. By contrast, *SlVHA* and *SlHA-A* were significantly downregulated in plants. Compared with salt-stressed tomato seedlings, the transcripts of all genes were significantly higher when Tre was applied with NaCl, except for *SlVHA* and *SlHA-A* in stems and leaves.

Discussion

Salt stress obstructs plant growth and development, resulting in a loss of plant productivity. Previous studies demonstrated that Tre was critical in maintaining the growth development and osmotic equilibrium in plants exposed to salt stress (Sarkar and Sadhukhan, 2022; Yang et al., 2022). Tre treatment at 30 mM alleviated the inhibitory effects of NaCl on strawberry shoot growth (Samadi et al., 2019). Furthermore, Tre foliar treatments (10 and 50 mM) proved to be effective in increasing the value of the growth parameters (plant height, leaves number, fresh weight, and dry weight)

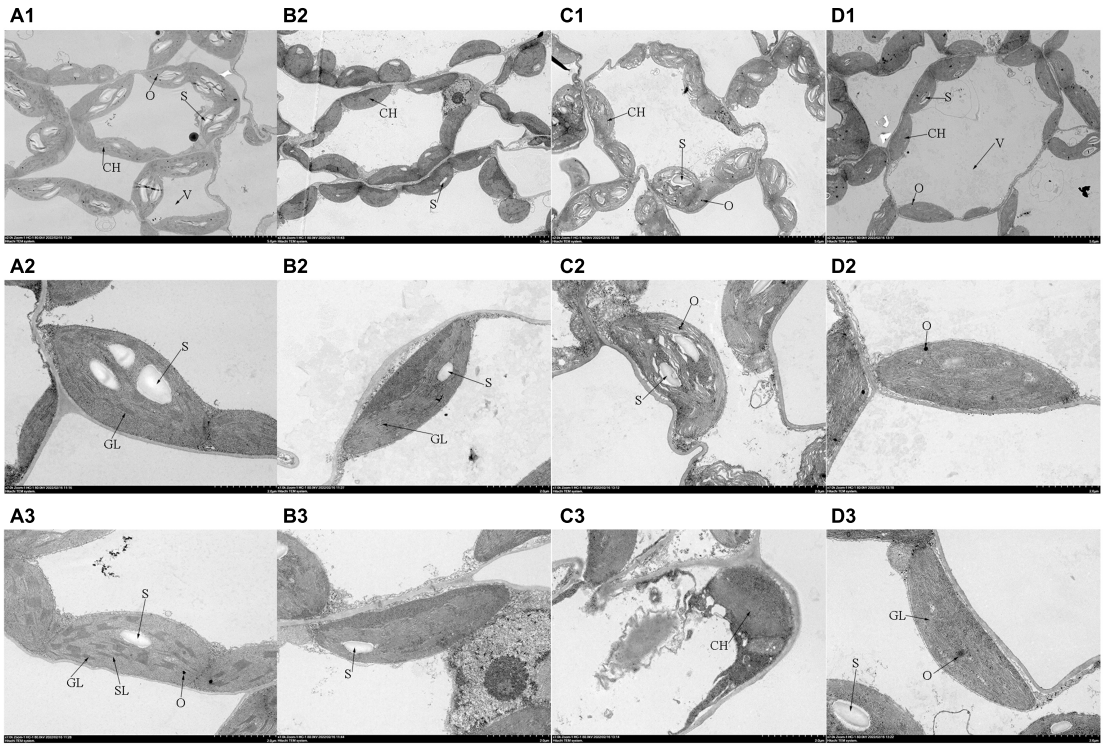


FIGURE 4
Effects of Tre treatment on the chloroplast ultrastructure of tomato seedlings exposed to salt stress for 5 days. Panels **(A–D)** represent the chloroplast ultrastructure of tomato leaves in CK, T, S, and S+T, respectively. **(A1–D1)** ×2,000, scale bars = 5 μm; **(A2–D3)** ×7,000, scale bars = 2 μm. CH, chloroplast; V, vacuole; GL, grana lamellae; SL, stroma lamellae; S, starch grains; O, osmiophilic granules.

and more accumulation of organic solutes of leaves (glucose, sucrose, Tre, and the soluble sugar) of salinity-stressed plants (Sadak, 2019). Tre ameliorated the responses of maize seedlings to salinity and alleviated the suppression of NaCl on shoot length, root length, and root volume (Rohman et al., 2019). In this work, NaCl treatment significantly inhibited tomato plants growth parameters (plant height, stem diameter, shoot fresh weight and dry weight, root fresh weight, and leaf area), whereas the application of Tre reversed this trend, thus increasing salinity tolerance (**Table 1**). Our result was in agreement with the findings of Abdallah et al. (2016) for rice, who indicated that Tre pretreatment resulted in the improvement of growth in plants exposed to salt stress. However, although Tre effectively enhanced the salt tolerance of tomato seedlings by increasing growth parameters, due to its complexity, the possible mechanisms need to be further studied.

Photosynthesis is a process sensitive to environmental stresses; for this, seeking a balance between the light energy absorbed by the photosystem and the energy consumed by metabolism is important for plant growth and development (Zhu et al., 2018). Numerous researchers have reported that salt stress could inhibit Pn, gs, and Tr parameters in plants (Tang et al., 2018; Castillejo-Morales et al., 2021; Yin et al., 2021). Our results showed that Pn, gs, and Tr decreased, and Ci increased under salt stress, which proved that the main factor of photosynthetic confinement was the non-stomatal limitation. Notably, the addition of exogenous Tre not only promoted the significant increase in Tr and Pn in tomato plants under normal growth conditions but also increased Pn and Tr and decreased Ci under salt stress (**Figure 1**). This was consistent with Feng et al. (2022). Under high temperature stress, Tre treatment increased Pn and Ci, but decreased gs and Tr, this differs from part of our results and may be that a Tre film was formed on the surface of leaves to reduce excessive evaporation of water and maintain water balance, thus inhibiting damage caused by high temperature (Zhao et al., 2019). In addition to the increased resistance of mesophyll cells to stomatal diffusion, decrease in CO_2 solubility, and stability of photosynthetic machinery, affinity of Rubisco enzymes for CO_2, and capability of RuBP to regenerate are important factors that led to the occurrence of non-stomatal factors (Castillejo-Morales et al., 2021; Pan et al., 2021). The Calvin cycle, as the final step of photosynthesis, is one of the non-stomata limiting factors, and it is the main pathway for plants to fix carbon (Ding et al., 2017; Sharma et al., 2020). Among them, Rubisco, GAPDH, and FBPase play important roles in carbon fixation, reduction, and RuBP regeneration stages, respectively (Niu and Ma, 2018; El Sayed et al., 2019; Wu et al., 2020). The enhancement of

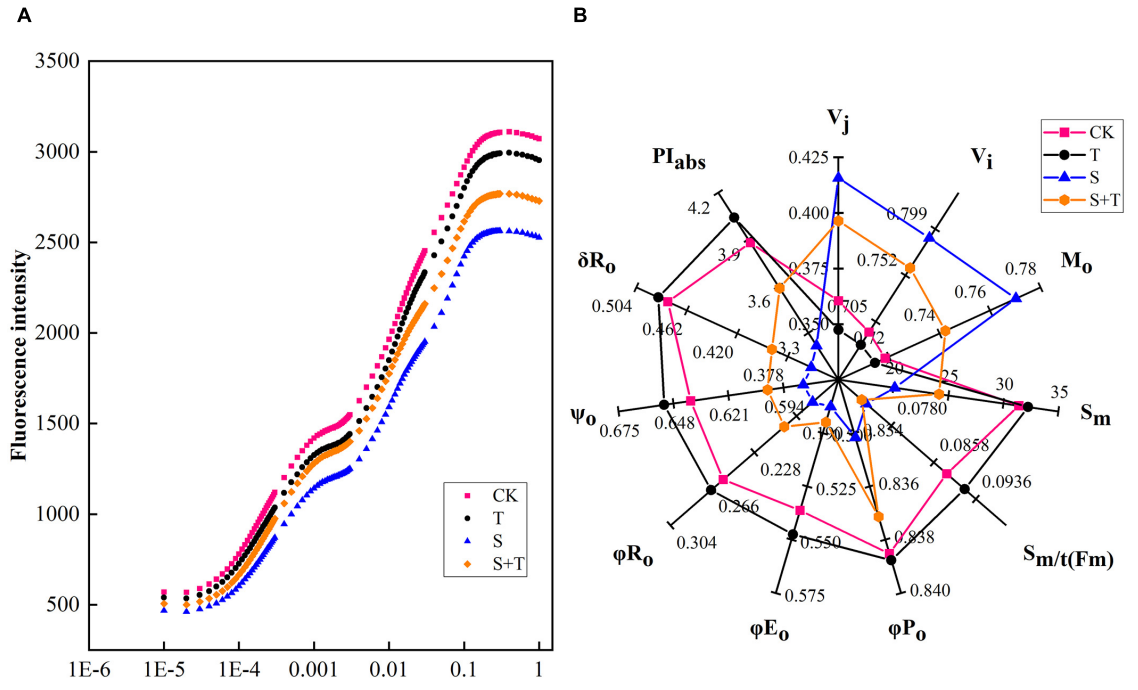


FIGURE 5
Effects of Tre treatment on chlorophyll fluorescence kinetics (OJIP curves) and JIP-text parameters of tomato seedlings exposed to salt stress for 5 days. **(A)** OJIP curves. **(B)** JIP-text parameters. The results showed the mean ± SE of three replicates. CK, control; T, 10 mM Tre; S, 150 mM NaCl; S+T, 150 mM NaCl + 10mM Tre.

FBA and TK activity can promote the assimilation of CO_2 in plant leaf tissues and the flow of carbon in the Calvin cycle, respectively (Lv et al., 2017). El Sayed et al. (2019) found that application of exogenous spermidine upregulated of Calvin Cycle related gene transcription levels in sweet sorghum seedlings under salt stress, which was similar to our results. We displayed that Tre promoted the increase in Rubisco, FBPase, FBA, GAPDH, and TK activities under salt stress and the up-regulation of related genes (**Figure 2**). This phenomenon might be explained by the adaptation to adversity, indicating that Tre pretreatment could alleviate the inhibitory effect of salt stress on the Calvin cycle by regulating the salinity-mediated accumulation of transcript of genes related to the Calvin cycle. In addition, an important response of plants to salt stress is to close the stomata, accompanied by a reduction in gs, which resulted to stomatal limitation of photosynthesis (Li et al., 2017). Niron et al. (2020) found that K^+ was the main osmoregulatory substance of stomatal guard cells, coordinating gs, and Tr. In this study, the addition of exogenous Tre significantly alleviated the inhibition of photosynthesis by maintaining the stomatal aperture (**Figure 3**). Sucrose is a key product of photosynthesis in the majority of plants and excessive sucrose accumulation can diminish photosynthesis by inhibiting the expression levels of photosynthetic genes (Lunn et al., 2014; Sarkar and Sadhukhan, 2022). Fichtner and Lunn (2021) concluded that there was a high correlation between T6P (an intermediate of alginate) and sucrose levels, but the effect of T6P on sucrose was attributed to its inhibitory effect on the sucrose non-fermenting-1-related protein kinase1 (SnRK1). Degradation of SnRK1 is mediated by sumoylation and ubiquitination as well as intracellular oxidative regulation mediated by redox. More, SnRK1 is also a positive regulator of stomatal development (Han et al., 2020). bZIP11, another transcription factor that affects carbohydrate metabolism regulation, is also regulated by T6P. bZIPs play a regulatory role in developmental transition, carbohydrate and amino acid metabolism (Tsai and Gazzarrini, 2014). In summary, the application of a particular concentration of Tre improved photosynthesis, we hypothesized that the intermediate T6P, rather than Tre itself, may play a key regulatory signaling role in gas exchange parameters and carbon metabolism. In addition, *AtTPPI* and *AtTPPF* may be important mechanisms for coping with abiotic stresses by triggering ABA-mediated stomatal regulation (Lin et al., 2020; Wang et al., 2020).

Alternatively, chlorophyll fluorescence is a non-destructive, direct, and efficient method that has been widely used to evaluate the effects of abiotic stress on photosynthetic electron transport (Bednaøíková et al., 2020). Electron transport occurs primarily on the thylakoids of chloroplasts (Ma et al., 2018). At this point, salt stress caused separation of cytoplasmic wall and destruction of chloroplast structure, which was consistent with the results of Hameed et al. (2021) and Wu et al. (2021). Tre pretreatment

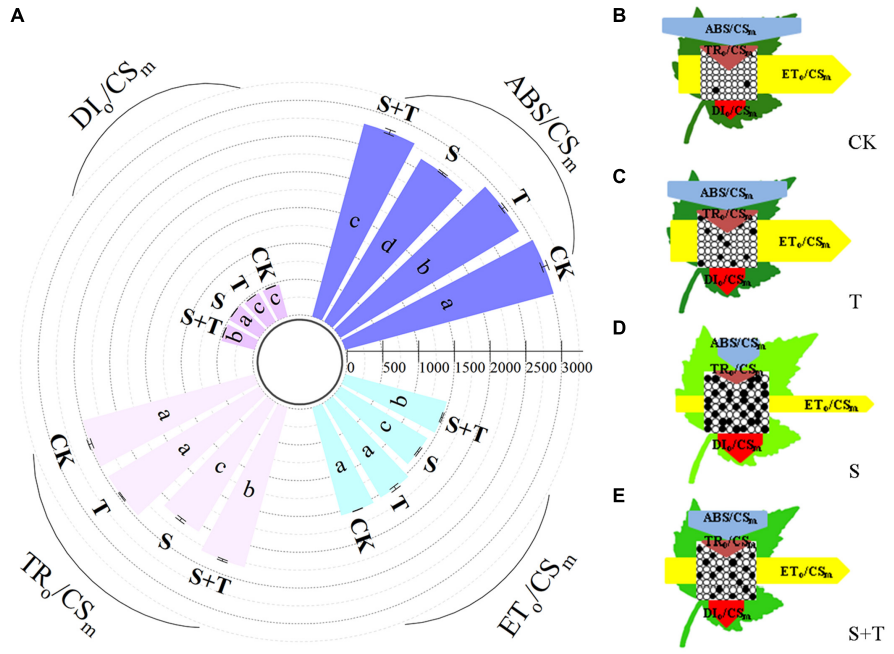


FIGURE 6
Effects of Tre treatment on phenomenological fluxes (per cross-section, CS_m) of tomato seedlings exposed to salt stress for 5 d. **(A)** Electron absorption, capture, transport and dissipation flux per cross-section. The results showed the mean ± SE of three replicates, and the different letters denote the significant difference among treatments ($P < 0.05$), according to Duncan's multiple tests. **(B–E)** Energy pipeline leaf model of phenomenological fluxes (per cross section, CS_m) in CK, T, S, and S+T, respectively. Changes in each energy flux were indicated by resizing the corresponding arrows. Empty and full black circles showed the percentages of active and non-active reaction centers of photosystem II (PSII), respectively. CK, control; T, 10 mM Tre; S, 150 mM NaCl; S+T, 150 mM NaCl + 10 mM Tre.

could improve chloroplast damage of tomato plants under salt stress (**Figure 4**). Zushi and Matsuzoe (2017) assumed that salt stress may destroy the excited chlorophyll molecules in light-harvesting complex II, resulting in a low O-step value. Wang et al. (2021) indicated that the shape of the OJIP curve changed during NaCl stress, decreasing the I-P phase and increasing the J-I phase. In this research, the photochemical stage (O-J) and thermal phases (J-I and I-P) were affected by salt stress compared with the control, in which the J-I and I-P stages of the OJIP curve decreased under salt stress (**Figure 5A**). The possible reasons were as follows: on the one hand, salt stress reduced the reduction rate of the rapidly reducing PQ pool during the electron transfer, resulting in the decrease in I value. On the other hand, salt stress destroyed the chlorophyll proteins on the PSI acceptor side and/or reduced the number of RCs in PSII, thereby reducing the *P*-value (Oukarroum et al., 2018). By contrast, Goussi et al. (2018) displayed that moderate saline conditions had no significant effect on the rate of O-J phase and J-I phase in *Thellungiella salsuginea*. This finding contradicted our research results, and we believed that it could be attributed to the various salt tolerances of plants themselves. In addition, Tre inhibited the OJIP phases of tomato plants under salt stress. We speculated that Tre might play an active role in preventing the reduction of the QA pool size or the transfer of electrons from the PSII donor side. JIP-test can be used to identify energy absorption, trapping, and electron transport parameters in PSII and PSI and has been used in plant response to stress conditions (Zushi and Matsuzoe, 2017; Sameena and Puthur, 2021). Under salt stress, φE_o and φR_o decreased drastically, showing that salt stress damaged the primary photochemical reaction of tomato leaves and inhibited electron transfer on the PSII receptor side. Similar results have been found in other plant studies (Zhang et al., 2018; Çiçek et al., 2018; Lotfi et al., 2020). In addition, higher values of PI_{abs}, φP_o, φE_o, ψE_o, δR_o, and φR_o were noted with S+T treatment than with S treatment, indicating that Tre treatment improved the photochemical efficiency (**Figure 5B**), electron transport flux ratio, and quantum efficiency of PSII to PSI under salt stress. PSII is one of the most sensitive components of photosynthesis, and abiotic stress can especially lead to the excessive reduction of electron transport chain (Lotfi et al., 2018). Our study showed that ABS/RC and DI_o/RC values increased mainly, and TR_o/RC and ET_o/RC values markedly decreased under salt stress compared with the control. Such result was observed because salt stress caused the inactivation of most RCs, which decreased the energy trapping efficiency and electron transport efficiency from PSII (Zushi and Matsuzoe, 2017; Kiran and Mohan, 2021). Similarly, the analysis of energy allocation per

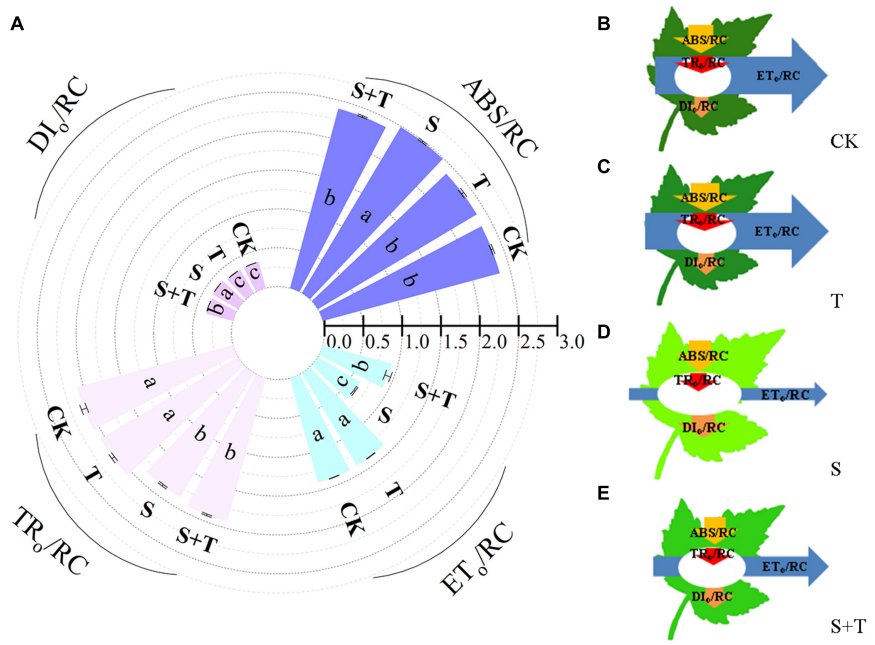


FIGURE 7
Effects of Tre treatment on phenomenological fluxes (per active reaction center, RC) of tomato seedlings exposed to salt stress for 5 d. **(A)** Electron absorption, capture, transport and dissipation flux per RC. The results showed the mean ± SE of three replicates, and the different letters denote the significant difference among treatments ($P < 0.05$), according to Duncan's multiple tests. **(B–E)** Energy pipeline leaf model of phenomenological fluxes (per active reaction center, RC) in CK, T, S, and S+T, respectively. Changes in each energy flux were indicated by resizing the corresponding arrows. CK, control; T, 10 mM Tre; S, 150 mM NaCl; S+T, 150 mM NaCl + 10 mM Tre.

unit cross-sectional area of tomato leaves under salt stress found a unique increase in DI$_o$/CS$_m$, whereas considerable decreases in ABS/CS$_m$, TR$_o$/CS$_m$, and ET$_o$/CS$_m$ were observed in S treatment compared with the CK. In addition, Zuo et al. (2017) reported that nano-ZnO stress resulted in a decrease in TR$_o$/CS$_m$ and ET$_o$/CS$_m$ of wheat plants. Interestingly, we showed that Tre improved the energy absorption efficiency of PSII by suppressing the dissipation (DI$_o$/CS$_m$, DI$_o$/RC) and increasing the trapped energy (TR$_o$/CS$_m$, TR$_o$/RC), and electron transport flux (ET$_o$/CS$_m$, ET$_o$/RC) per cross-section and per reaction center (**Figures 6**, **7**). Both reducing subunits in Tre are used to form glycosidic bonds that can displace water and stabilize membranes in stress situations (MacIntyre et al., 2020). This suggestive of the fact that the unique structure of Tre at salinity may be the main reason for the protection of chloroplast structure. In contrast, the protection of Tre to the structure of thylakoid membrane can directly prevent the shedding of attached proteins, thus stabilizing the electron transfer function. Furthermore, protein complexes play an important role in linear electron transfer (Zhang et al., 2019). For example, the central role of CP43 and CP47 proteins is to receive excitation energy from the pigment complex of CP24, CP26, and CP29, and transfer the excitation energy to the pigment protein complex in the reaction center (Casazza et al., 2010; Zhang et al., 2010). However, excessive excitation energy limited production of reactive oxygen species (ROS), which leads to oxidative damage of the photosynthetic mechanism. Several studies have shown that Tre can enhance the activity of antioxidant enzymes in plants under abiotic stress, and regulate the expression of osmoprotectant biosynthetic genes such as proline (de Novais Portugal et al., 2021; Kosar et al., 2021; Zulfiqar et al., 2021; Feng et al., 2022). Therefore, the enhancement of ROS scavenging system induced by Tre may be one of the important reasons for the increase of photosynthetic oxygenation capacity and electron transfer rate of tomato seedlings under NaCl stress. In conclusion, Tre alleviated the photoinhibition of tomato leaves under salt stress.

The absorption of mineral elements by plants is conducive to growth and resistance to environmental stress (Ju et al., 2017; Liang et al., 2018). Ionic stress causes competition among ions for absorption, which will substantially affect the uptake and transport of mineral elements and ultimately cause mineral nutrient stress and imbalance of plant ion homeostasis (Guo et al., 2020). Previous studies have proven that salt stress reduces the content of mineral elements in rape (Naeem et al., 2010), cotton (Guo et al., 2019), wheat, and maize (El-Fouly et al., 2011; Iqbal et al., 2018). This could explain their lower growth rates leading to a reduction in biomass accumulation due to the negative effects of salt stress on assimilation capacity (**Table 1**). Moreover, salt stress prevented the uptake of nitrogen

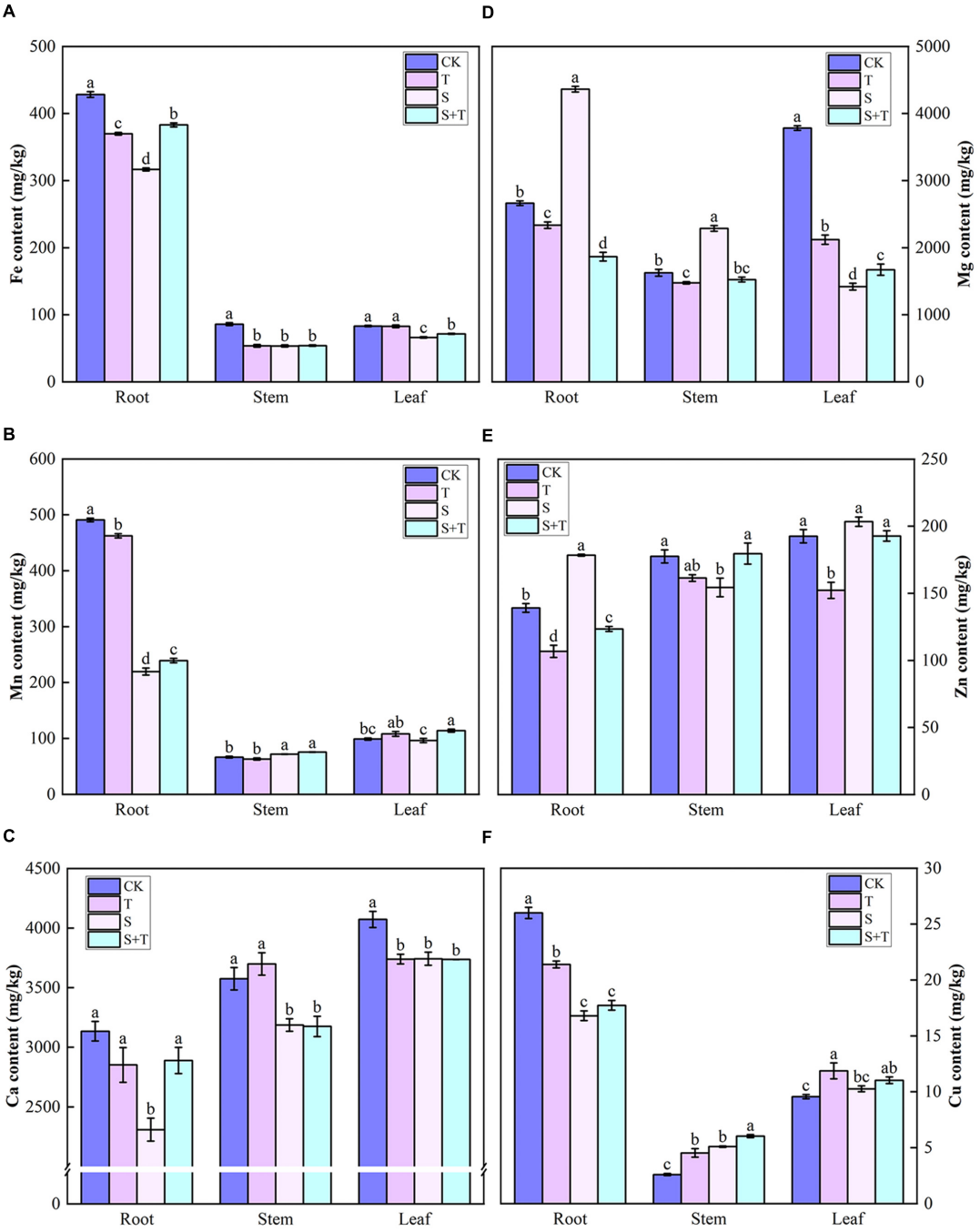


FIGURE 8
Effects of Tre treatment on mineral ion content in tomato seedlings under salt stress for 5 days. **(A)** Fe content. **(B)** Mn content. **(C)** Ca content. **(D)** Mg content. **(E)** Zn content. **(F)** Cu content. The results showed the mean ± SE of three replicates, and the different letters denote the significant difference among treatments ($P < 0.05$), according to Duncan's multiple tests. CK, control; T, 10 mM Tre; S, 150 mM NaCl; S+T, 150 mM NaCl + 10 mM Tre.

(N), phosphorus (P), Fe, Mn, Zn and other ions by plants, leading to symptoms of mineral deficiency (Ramireddy et al., 2018; Loudari et al., 2020). Zamani et al. (2019) found that micronutrient foliar sprays (Fe, Mn, Zn, and so on) can improve the salt tolerance of wheat; thus, changes in the mineral element contents are vital in the operation of resistance mechanism. Fe, Mg, and Mn are cofactors for multiple enzymes and have a pivotal position in chlorophyll biosynthesis (Ju et al., 2017; Zhang et al., 2017; Guo et al., 2020; Yang et al., 2021b). Mg concentration affects stomatal opening and can regulate the

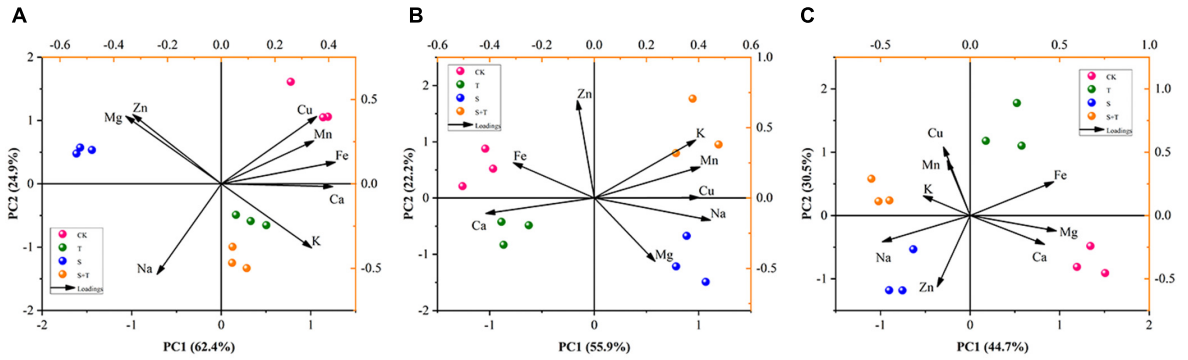


FIGURE 9
Principal component analysis (PCA) of tissue ionome variation in tomato under salt stress by Tre treatment, with the loadings of mineral elements to the PC1 and PC2. **(A)** Root ionome variation among treatments and the loadings of elements to the PC1 and PC2. **(B)** Stem ionome variation among treatments and the loadings of elements to the PC1 and PC2. **(C)** Leaf ionome variation among treatments and the loadings of elements to the PC1 and PC2. CK, control; T, 10 mM Tre; S, 150 mM NaCl; S+T, 150 mM NaCl + 10 mM Tre.

ionic currents across the chloroplast and vacuolar membrane (Misra et al., 2019). Recently, Yang et al. (2021b) discovered that Mn can reinforce plant cell walls, and such result was primarily attributed to the controlled formation of polysaccharides. In this experiment, salt stress suppressed the accumulation of Fe in the whole plant, Mg in leaves, and Mn in roots. By contrast, Guo et al. (2020) found that salt stress significantly increased the concentration of Mg in the roots and decreased in the leaves, while the concentrations of Fe and Mn in the leaves markedly increased, which was not completely consistent with our results. In our results, the content of Mg and Mn in leaves decreased, which may be caused by the damage of chlorophyll biosynthesis pathway under salt stress. Exogenous Tre facilitated the transport of Fe, Mg, and Mn from roots to their collection in leaves (**Figure 8**). This result may be one of the effective measures for Tre to maintain growth by chlorophyll synthesis, thereby enhancing photosynthesis to cope with salt stress (**Figure 1**). Zn is involved in stomatal opening and biotin synthesis. Meanwhile, it is also an essential element for the structural integrity of cell membranes (Tekdal and Cetiner, 2018; Misra et al., 2019; Guo et al., 2020). Zn was concentrated in the roots and decreased in the stems (**Figure 8**). This finding indicated that the reduction of Zn may inhibit stomatal opening, thereby affecting the photosynthesis of tomato leaves (**Figures 2**, **3**). Foliar-applied Tre promoted the upward transport of Zn and increased its content in the stem. In addition, Mn and Zn have similar functions in antioxidant stress defense and protection of plant cells from reactive oxygen species (Misra et al., 2019; Yang et al., 2021b); Zhang et al. (2017) and Hashem et al. (2018) stated that Ca not only serves as a cell messenger of plant growth signals but also provides intermolecular linkages, thus maintaining the stability of cell walls and membranes. The salinity caused the Ca content to decrease, and this result was similar to research reports by Zhang et al. (2014) and Guo et al. (2020) that salt stress significantly reduces Ca concentration in plants. But it was significantly increased by the addition of Tre (**Figure 8**), thereby maintaining the stability of the cell membrane structure, which was consistent with the chloroplast ultrastructure results (**Figure 4**). As well, Chang et al. (2014) and Shahbaz et al. (2017) reported that supplying Tre reduced the adverse effects of salinity by increasing Ca uptake in rice plants. Cu is a component of certain proteins in plants and an effective electron donor and acceptor. In particular, this element also has an influence on the activation of enzymes with oxidative functions. This study revealed that salt stress decreased the Cu content in roots but increased its levels in stems and leaves. Remarkably, the application of Tre prompted the further increase in the Cu content in the stems (**Figure 8**). PCA further confirmed that exogenous Tre could change the distribution of mineral elements and play a positive role in maintaining ion homeostasis (**Figure 9**).

Na and chlorine (Cl) in high concentrations are usually the most harmful and dominant elements (Zamani et al., 2019). Plants can resist salt stress in three ways: rejection, secretion, and diluter. Tang et al. (2019) and Li et al. (2020) indicated that salinity increased the concentration of Na and decreased the concentration of K in plants. In our study, salt stress increased SK-Na in tomato plants, and this parameter was further increased by the exogenous supply of Tre (**Figure 10A**). These results were consistent with Shahbaz et al. (2017) and Samadi et al. (2019). One possibility is that Tre can protect the pump with specific needs by maintaining the integrity of the protein and lipid bilayers to exclude excess NaCl from the cells. The accumulation and transport of Na and K are closely related to ion channel protein activity and related gene expressions. Plants have a complex system to maintain ion homeostasis in response to ion disturbance. For example, Javaid et al. (2019), Guo et al. (2020), and Li et al. (2020) found that SOS was a Na^+/H^+ anti-transporter, whereas, HKT is a high-affinity

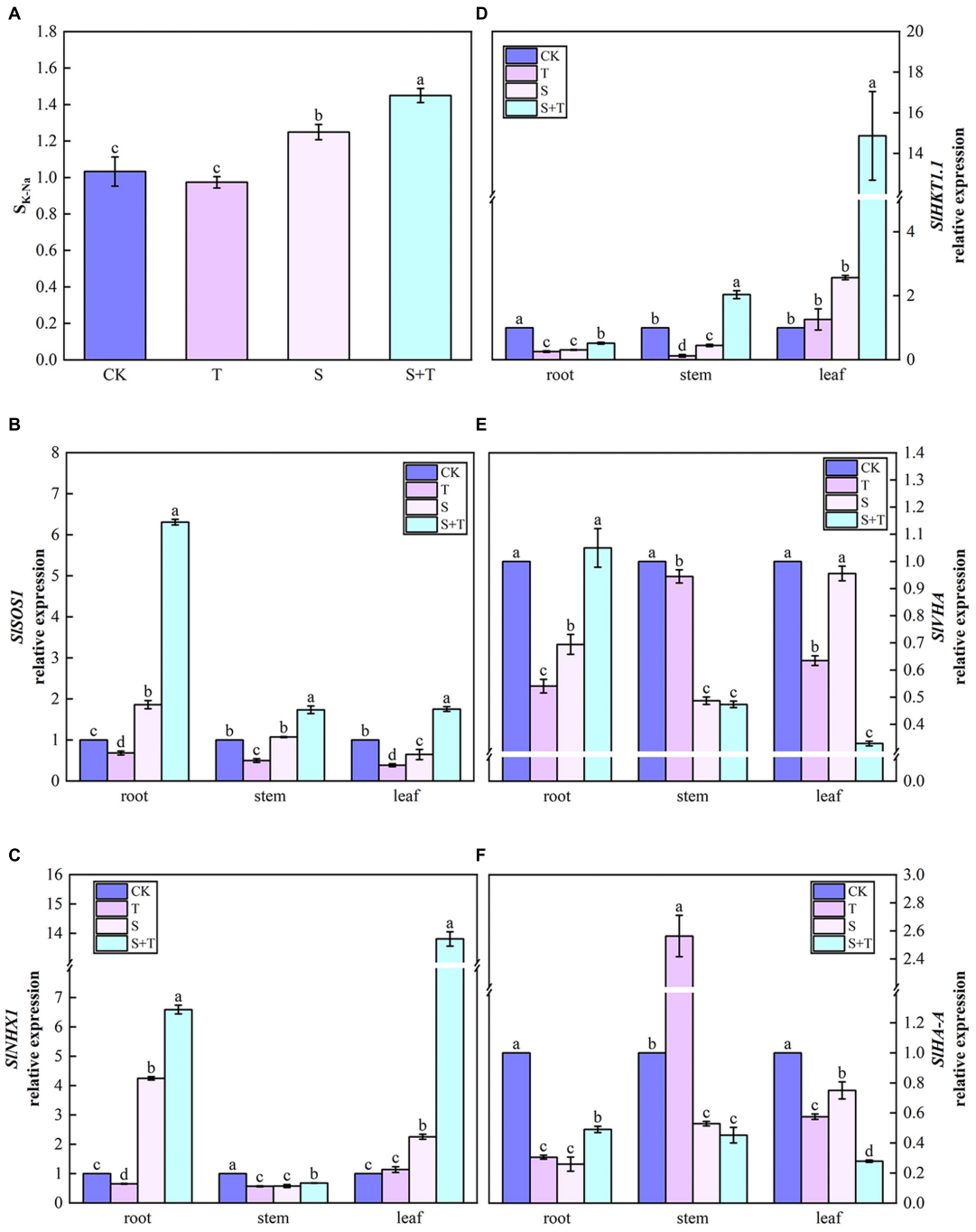


FIGURE 10
Effects of Tre treatment on the K-Na transport selectivity ratio and the relative expression of ion transport genes in tomato seedlings under salt stress for 5 days. Panel **(A)** represents the K-Na transport selectivity ratio (S_{K-Na}); Panels **(B–F)** represent the expression levels of *SlSOS1*, *SlNHX1*, *SlHKT1.1*, *SlVHA*, and *SlHA-A*, respectively. The results showed the mean ± SE of three replicates, and the different letters denote the significant difference among treatments ($P < 0.05$), according to Duncan's multiple tests. CK, control; T, 10 mM Tre; S, 150 mM NaCl; S+T, 150 mM NaCl + 10 mM Tre.

K^+ transporter. In addition, Wu (2018) displayed that NHX1 is a Na^+, and K^+/H^+ exchanger in the plasma membrane and intima, and it plays an important role in regulating pH and K^+ homeostasis and regulating the whole process from vesicle transport and cell expansion to plant development. However, ion transporters depend on the transmembrane H^+ concentration gradient (Wu et al., 2021). Plasma membrane H^+-ATPase is the main driving force for the secondary active

transport of mineral elements in plant cells, and the H^+ electrochemical potential gradient produced by its hydrolysis can transport Na^+ out of cells (Allakhverdiev et al., 1999). In addition, He et al. (2014) indicated that the overexpression of the V-type proton pump subunit can improve the salt tolerance of transgenic wheat. By investigating the transcription levels of K/Na transport-related genes under salt stress, we found that the expressions of *SlSOS1*, *SlNHX1*, and *SlHKT1.1* were significantly up-regulated under S+T treatment compared with S treatment in plants. Likewise, *SlHA-A* and *SlVHA* in roots showed the same trend (**Figure 10**). This result explained the different ionic changes in tomato plants under salt stress and was consistent with the results for S_{K-Na}. The results showed that Na^+ efflux by exogenous Tre could be mediated by HKT and SOS1 in roots. In previous studies, overexpression of SOS1 or NHX1 in transgenic plants improved salt tolerance (Banjara et al., 2012; Ma et al., 2014). However, Na^+ outflow is an energy-consuming process. Tre generated electrochemical H^+ gradient mainly by stimulating the activities of H^+-ATPase and V-type H^+-ATPase in the root plasma membrane and became the driving force of Na^+/H^+ antiporter operation, thus transporting Na^+ out of cells and preventing it from moving upward sequentially. In addition, Wu (2018) suggested that Na^+ backflow from stems to roots through the phloem sap may be the main mechanism of Na^+ transport from tissues to leaf cells in plants. We found that the expression of *SlHKT1.1* was significantly induced in stems and leaves (**Figure 10**), and this event was possibly involved in the recirculation of Na^+ from the aboveground to underground parts. Shi et al. (2019) demonstrated that when Tre was combined with other forms of stress, the transcriptome was significantly different from the absence of Tre. Tre was able to trigger elongation factor thermo unstable and chitin elicitor receptor kinase receptors in a time-specific manner and these receptors lead to changes in ion flux. There are also studies that ABA signal was involved in Tre induced resistance (Yu et al., 2019; Sarkar and Sadhukhan, 2022). *AtTPS5* negatively regulated ABA signaling in Arabidopsis thaliana, which activated MYB-like transcription factors and thereby triggered the expression of HKT genes to regulate ion transport (Wang et al., 2015; Qin and Huang, 2020; Nawaz et al., 2022). These may be one of the reasons why Tre responds tightly to salinity by controlling mineral ion homeostasis. However, the molecular mechanism by which Tre regulates the influx and outflow cells of different mineral elements remains unclear.

In this study, the mechanism of salt tolerance in tomato was explored by using a hydroponic experiment and various analytical methods to clarify the effect of Tre on photosynthetic electron energy transport and mineral element distribution in tomato plants under salt stress. The regulation of mineral elements by Tre under salt stress is a key factor affecting photosynthesis. However, the enhancement may be indirect. Nevertheless, this study fills the gap in the understanding of Tre on the photosynthetic electron transport chain and ion homeostasis under salt stress, and provides specific insights and new ideas for the effectiveness of Tre in mediating salt tolerance. At the same time, it is of great significance for basic and applied plant biology and agricultural production applications.

Conclusion

The protective functions of Tre on growth, photosynthetic performance and ion homeostasis in tomato seedlings exposed to salt stress were investigated. Our results showed that Tre could promote the growth of tomato seedlings, alleviate the degree of photoinhibition and improve photosynthetic performance under salt stress. On the one hand, Tre acts by altering stomatal opening, reducing the damage of chloroplast structure, maintaining the normal process of the Calvin cycle, and balancing the distribution of electrons. On the other hand, Tre contributes by regulating the absorption and distribution of mineral ions in different organs of tomato plants and maintaining the homeostasis of nutrient ions. Additionally, Tre can regulate key salt tolerance genes in different organs, improve the value of S_{K-Na}, reduce excess Na^+ toxicity in tomato plants, and improve salt tolerance. In conclusion, these results provide information on the theoretical basis for the study of the physiological functions of Tre in the context of salt stress. However, molecular biology and genomics were still needed to explore the specific role of genes in Tre biosynthesis pathway and a complex mechanism for the interaction of Tre with other signaling pathways in soil salinization.

Data availability statement

The original contributions presented in this study are included in the article/**Supplementary material**, further inquiries can be directed to the corresponding author/s.

Author contributions

YY and JX conceived and designed the research. YY, YDY, and JZ conducted the experiments. XZ, CW, and TN analyzed the data and prepared the figures and illustrations. YY wrote the manuscript. EB and JL read the manuscript and made valuable inputs. All authors read and approved the submission of the manuscript.

Funding

This research was supported by National Natural Science Foundation of China (32072657), China, the Special

Fund for Technical System of Melon and Vegetable Industry of Gansu Province (GARS-GC-1), China, the Outstanding Graduate Student "Innovation Star" Project of Gansu Province (2021CXZX-376), China, and Natural Science Foundation of Gansu Province (20JR10RA515).

Conflict of interest

The authors declare that the research was conducted in the absence of any commercial or financial relationships that could be construed as a potential conflict of interest.

Publisher's note

All claims expressed in this article are solely those of the authors and do not necessarily represent those of their affiliated organizations, or those of the publisher, the editors and the reviewers. Any product that may be evaluated in this article, or claim that may be made by its manufacturer, is not guaranteed or endorsed by the publisher.

Supplementary material

The Supplementary Material for this article can be found online at: https://www.frontiersin.org/articles/10.3389/fpls.2022.974507/full#supplementary-material

SUPPLEMENTARY FIGURE 1
Comparison of the Micro-Tom variety and the common variety. **(A)** Tomato plants. **(B)** Tomato fruits.

SUPPLEMENTARY FIGURE 2
Agarose gel electrophoresis of total RNA isolated from tomato roots, stems, and leaves. M: DNA Marker 2000; 1-12 bands were CK-root, CK-stem, CK-leaf, T-root, T-stem, T-leaf, S-root, S-stem, S-leaf, S+T-root, S+T-stem, and S+T-leaf, respectively. CK, control; T, 10 mM Tre; S, 150 mM NaCl; S+T, 150 mM NaCl + 10 mM Tre.

References

Abdallah, M., Abdelgawad, Z., and El-Bassiouny, H. (2016). Alleviation of the adverse effects of salinity stress using trehalose in two rice varieties. *S. Afr. J. Bot.* 103, 275–282. doi: 10.1016/j.sajb.2015.09.019

Abdelaziz, M. E., Abdelsattar, M., Abdeldaym, E. A., Atia, M. A., Mahmoud, A. W. M., Saad, M. M., et al. (2019). Piriformospora indica alters Na+/K+ homeostasis, antioxidant enzymes and LeNHX1 expression of greenhouse tomato grown under salt stress. *Sci. Hortic.* 256:108532. doi: 10.1016/j.scienta.2019.05.059

Allakhverdiev, S. I., Nishiyama, Y., Suzuki, I., Tasaka, Y., and Murata, N. (1999). Genetic engineering of the unsaturation of fatty acids in membrane lipids alters the tolerance of *Synechocystis* to salt stress. *Proc. Natl. Acad. Sci. U.S.A.* 96, 5862–5867. doi: 10.1073/pnas.96.10.5862

Ambastha, V., and Tiwari, B. S. (2015). Cellular water and anhydrobiosis in plants. *J. Plant Growth Regul.* 34, 665–671. doi: 10.1007/s00344-015-9497-6

Asrar, H., Hussain, T., Hadi, S. M. S., Gul, B., Nielsen, B. L., and Khan, M. A. (2017). Salinity induced changes in light harvesting and carbon assimilating complexes of *Desmostachya bipinnata* (L.) Staph. *Environ. Exp. Bot.* 135, 86–95. doi: 10.1016/j.envexpbot.2016.12.008

Avonce, N., Mendoza-Vargas, A., Morett, E., and Iturriaga, G. (2006). Insights on the evolution of trehalose biosynthesis. *BMC Evol. Biol.* 6:109. doi: 10.1186/1471-2148-6-109

Banjara, M., Zhu, L., Shen, G., Payton, P., and Zhang, H. (2012). Expression of an *Arabidopsis* sodium/proton antiporter gene (AtNHX1) in peanut to improve salt tolerance. *Plant Biotechnol. Rep.* 6, 59–67. doi: 10.1007/s11816-011-0200-5

Bednaoíková, M., Folgar-Cameán, Y., Kuèerová, Z., Lazár, D., Špundová, M., Hájek, J., et al. (2020). Analysis of K-and L-band appearance in OJIPs in Antarctic lichens in low and high temperature. *Photosynthetica* 58, 646–656. doi: 10.32615/ps.2019.180

Bhattarai, S., Liu, N., Karunakaran, C., Tanino, K. K., Fu, Y. B., Coulman, B., et al. (2021). Tissue specific changes in elements and organic compounds of alfalfa (*Medicago sativa* L.) cultivars differing in salt tolerance under salt stress. *J. Plant Physiol.* 264:153485. doi: 10.1016/j.jplph.2021.153485

Casazza, A. P., Szczepaniak, M., Müller, M. G., Zucchelli, G., and Holzwarth, A. R. (2010). Energy transfer processes in the isolated core antenna complexes CP43 and CP47 of photosystem II. *Biochim. Biophys. Acta Biomembr.* 1797, 1606–1616. doi: 10.1016/j.bbabio.2010.05.008

Castillejo-Morales, A., Jarma-Orozco, A., and Pompelli, M. F. (2021). Physiological and morphological features denote that salt stress in *Stevia rebaudiana* is based on nonstomatic instead of stomatic limitation. *Rev. Colomb. Cien. Hortíc.* 15:e12928. doi: 10.17584/rcch.2021v15i3.12928

Chang, B., Yang, L., Cong, W., Zu, Y., and Tang, Z. (2014). The improved resistance to high salinity induced by trehalose is associated with ionic regulation and osmotic adjustment in *Catharanthus roseus*. *Plant Physiol. Biochem.* 77, 140–148. doi: 10.1016/j.plaphy.2014.02.001

Çiçek, N., Oukarroum, A., Strasser, R. J., and Schansker, G. (2018). Salt stress effects on the photosynthetic electron transport chain in two chickpea lines differing in their salt stress tolerance. *Photosynth. Res.* 136, 291–301. doi: 10.1007/s11120-017-0463-y

de Novais Portugal, J. A., Ambrósio, A.d.S, de Souza, K. R. D., Dias, D. F., dos Santos Filho, P. R., de Souza, T. B., et al. (2021). A mixture of trehalose derivatives stimulates the antioxidant system and improves photosynthetic efficiency in maize under water deficit. *Acta Physiol. Plant.* 43:83. doi: 10.1007/s11738-021-03255-9

Ding, F., Wang, M., and Zhang, S. (2017). Overexpression of a Calvin cycle enzyme SBPase improves tolerance to chilling-induced oxidative stress in tomato plants. *Sci. Hortic.* 214, 27–33. doi: 10.1016/j.scienta.2016.11.010

El Sayed, A., El-Hamahmy, M., Rafudeen, M., and Ebrahim, M. (2019). Exogenous spermidine enhances expression of Calvin cycle genes and photosynthetic efficiency in sweet sorghum seedlings under salt stress. *Biol. Plant.* 63, 511–518. doi: 10.32615/bp.2019.046

El-Fouly, M. M., Mobarak, Z. M., and Salama, Z. A. (2011). Micronutrients (Fe, Mn, Zn) foliar spray for increasing salinity tolerance in wheat *Triticum aestivum* L. *Afr. J. Plant Sci.* 5, 314–322. doi: 10.5897/AJPS.9000165

Faizan, M., Bhat, J. A., Chen, C., Alyemeni, M. N., and Yu, F. (2021). Zinc oxide nanoparticles (ZnO-NPs) Induce salt tolerance by improving the antioxidant system and photosynthetic machinery in tomato. *Plant Physiol. Biochem.* 161, 122–130. doi: 10.1016/j.plaphy.2021.02.002

Farooq, M., Hussain, M., Nawaz, A., Lee, D. J., Alghamdi, S. S., and Siddique, K. H. (2017). Seed priming improves chilling tolerance in chickpea by modulating germination metabolism, trehalose accumulation and carbon assimilation. *Plant Physiol. Bioch.* 111, 274–283. doi: 10.1016/j.plaphy.2016.12.012

Feng, Y., Hao, Y., Cai, L., Wu, Q., Hou, M., and Song, L. (2022). Influence of trehalose on photosynthesis in the rare and endangered *Emmenopterys henryi* Oliv. during heat stress and recovery process. *Acta Physiol. Plant.* 44, 1–9. doi: 10.1007/s11738-021-03343-w

Fichtner, F., and Lunn, J. E. (2021). The role of trehalose 6-phosphate (Tre6P) in plant metabolism and development. *Annu. Rev. Plant Biol.* 72, 737–760. doi: 10.1146/annurev-arplant-050718-095929

Fichtner, F., Barbier, F. F., Annunziata, M. G., Feil, R., Olas, J. J., Mueller-Roeber, B., et al. (2021). Regulation of shoot branching in Arabidopsis by trehalose 6-phosphate. *New Phytol* 229, 2135–2151. doi: 10.1111/nph.17006

Figueroa, C. M., and Lunn, J. E. (2016). A tale of two sugars: Trehalose 6-phosphate and sucrose. *Plant Physiol.* 172, 7–27. doi: 10.1104/pp.16.00417

Figueroa, C. M., Feil, R., Ishihara, H., Watanabe, M., Kölling, K., Krause, U., et al. (2016). Trehalose 6–phosphate coordinates organic and amino acid metabolism with carbon availability. *Plant J.* 85, 410–423. doi: 10.1111/tpj.13114

Goussi, R., Manaa, A., Derbali, W., Cantamessa, S., Abdelly, C., and Barbato, R. (2018). Comparative analysis of salt stress, duration and intensity, on the chloroplast ultrastructure and photosynthetic apparatus in *Thellungiella salsuginea*. *J. Photoch. Photobio. B.* 183, 275–287. doi: 10.1016/j.jphotobiol.2018.04.047

Guo, H., Huang, Z., Li, M., and Hou, Z. (2020). Growth, ionic homeostasis, and physiological responses of cotton under different salt and alkali stresses. *Sci. Rep.* 10, 1–20. doi: 10.1038/s41598-020-79045-z

Guo, H., Li, S., Min, W., Ye, J., and Hou, Z. (2019). Ionomic and transcriptomic analyses of two cotton cultivars (*Gossypium hirsutum* L.) provide insights into the ion balance mechanism of cotton under salt stress. *PLoS One* 14:e0226776. doi: 10.1371/journal.pone.0226776

Hameed, A., Ahmed, M. Z., Hussain, T., Aziz, I., Ahmad, N., Gul, B., et al. (2021). Effects of salinity stress on chloroplast structure and function. *Cells* 10:2023. doi: 10.3390/cells10082023

Han, C., Liu, Y., Shi, W., Qiao, Y., Wang, L., Tian, Y., et al. (2020). KIN10 promotes stomatal development through stabilization of the SPEECHLESS transcription factor. *Nat. Commun.* 11, 1–10. doi: 10.1038/s41467-020-18048-w

Hashem, A., Abd_Allah, E. F., Alqarawi, A. A., Aldubise, A., and Egamberdieva, D. (2015). Arbuscular mycorrhizal fungi enhances salinity tolerance of *Panicum turgidum* Forssk by altering photosynthetic and antioxidant pathways. *J. Plant Interact.* 10, 230–242. doi: 10.1080/17429145.2015.1052025

Hashem, A., Alqarawi, A. A., Radhakrishnan, R., Al-Arjani, A. B. F., Aldehaish, H. A., Egamberdieva, D., et al. (2018). Arbuscular mycorrhizal fungi regulate the oxidative system, hormones and ionic equilibrium to trigger salt stress tolerance in *Cucumis sativus* L. *Saudi J. Biol. Sci.* 25, 1102–1114. doi: 10.1016/j.sjbs.2018.03.009

He, X., Huang, X., Shen, Y., and Huang, Z. (2014). Wheat V-H+-ATPase subunit genes significantly affect salt tolerance in *Arabidopsis thaliana*. *PLoS One* 9:e86982. doi: 10.1371/journal.pone.0086982

Henry, C., Bledsoe, S. W., Griffiths, C. A., Kollman, A., Paul, M. J., Sakr, S., et al. (2015). Differential role for trehalose metabolism in salt-stressed maize. *Plant Physiol.* 169, 1072–1089. doi: 10.1104/pp.15.00729

Hossain, M. A., Kumar, V., Burritt, D. J., Fujita, M., and Mäkelä, P. (2019). *Osmoprotectant-Mediated Abiotic Stress Tolerance in Plants. Proline Metabolism and Its Functions in Development and Stress Tolerance*. Cham: Springer, 41–72. doi: 10.1007/978-3-030-27423-8

Hu, E., Liu, M., Zhou, R., Jiang, F., Sun, M., Wen, J., et al. (2021). Relationship between melatonin and abscisic acid in response to salt stress of tomato. *Sci. Hortic.* 285:110176. doi: 10.1016/j.scienta.2021.110176

Iqbal, M. N., Rasheed, R., Ashraf, M. Y., Ashraf, M. A., and Hussain, I. (2018). Exogenously applied zinc and copper mitigate salinity effect in maize (*Zea mays* L.) by improving key physiological and biochemical attributes. *Environ. Sci. Pollut. R.* 25, 23883–23896. doi: 10.1007/s11356-018-2383-6

Javaid, T., Farooq, M. A., Akhtar, J., Saqib, Z. A., and Anwar-ul-Haq, M. (2019). Silicon nutrition improves growth of salt-stressed wheat by modulating flows and partitioning of Na+, Cl- and mineral ions. *Plant Physiol. Bioch.* 141, 291–299. doi: 10.1016/j.plaphy.2019.06.010

Ju, S., Wang, L., Yin, N., Li, D., Wang, Y., and Zhang, C. (2017). Silicon alleviates simulated acid rain stress of *Oryza sativa* L. seedlings by adjusting physiology activity and mineral nutrients. *Protoplasma* 254, 2071–2081. doi: 10.1007/s00709-017-1099-7

Kiran, B. R., and Mohan, S. V. (2021). Photosynthetic transients in Chlorella sorokiniana during phycoremediation of dairy wastewater under distinct light intensities. *Bioresour. Technol.* 340:125593. doi: 10.1016/j.biortech.2021.125593

Kosar, F., Akram, N. A., Ashraf, M., Ahmad, A., Alyemeni, M. N., and Ahmad, P. (2021). Impact of exogenously applied trehalose on leaf biochemistry, achene yield and oil composition of sunflower under drought stress. *Physiol. Plant.* 172, 317–333. doi: 10.1111/ppl.13155

Krasensky, J., Broyart, C., Rabanal, F. A., and Jonak, C. (2014). The redox-sensitive chloroplast trehalose-6-phosphate phosphatase AtTPPD regulates salt stress tolerance. *Antioxid. Redox Sign.* 21, 1289–1304. doi: 10.1089/ars.2013.5693

Kretzschmar, T., Pelayo, M. A. F., Trijatmiko, K. R., Gabunada, L. F. M., Alam, R., Jimenez, R., et al. (2015). A trehalose-6-phosphate phosphatase enhances anaerobic germination tolerance in rice. *Nat. Plants* 1, 1–5. doi: 10.1038/nplants.2015.124

Lastdrager, J., Hanson, J., and Smeekens, S. (2014). Sugar signals and the control of plant growth and development. *J. Exp. Bot.* 65, 799–807. doi: 10.1093/jxb/ert474

Li, H., Chang, J., Chen, H., Wang, Z., Gu, X., Wei, C., et al. (2017). Exogenous melatonin confers salt stress tolerance to watermelon by improving photosynthesis and redox homeostasis. *Front. Plant Sci.* 8:295. doi: 10.3389/fpls.2017.00295

Li, H., Shi, J., Wang, Z., Zhang, W., and Yang, H. (2020). H2S pretreatment mitigates the alkaline salt stress on *Malus hupehensis* roots by regulating Na+/K+ homeostasis and oxidative stress. *Plant Physiol. Bioch.* 156, 233–241. doi: 10.1016/j.plaphy.2020.09.009

Liang, B., Gao, T., Zhao, Q., Ma, C., Chen, Q., Wei, Z., et al. (2018). Effects of exogenous dopamine on the uptake, transport, and resorption of apple ionome under moderate drought. *Front. Plant Sci.* 9:755. doi: 10.3389/fpls.2018.00755

Lin, Q., Wang, S., Dao, Y., Wang, J., and Wang, K. (2020). Arabidopsis thaliana trehalose-6-phosphate phosphatase gene TPPI enhances drought tolerance by regulating stomatal apertures. *J. Exp. Bot.* 71, 4285–4297. doi: 10.1093/jxb/eraa173

Lin, Q., Yang, J., Wang, Q., Zhu, H., Chen, Z., Dao, Y., et al. (2019). Overexpression of the trehalose-6-phosphate phosphatase family gene AtTPPF improves the drought tolerance of *Arabidopsis thaliana*. *BMC Plant Biol.* 19:381. doi: 10.1186/s12870-019-1986-5

Lin, Y., Zhang, J., Gao, W., Chen, Y., Li, H., Lawlor, D. W., et al. (2017). Exogenous trehalose improves growth under limiting nitrogen through upregulation of nitrogen metabolism. *BMC Plant Biol.* 17:247. doi: 10.1186/s12870-017-1207-z

Livak, K. J., and Schmittgen, T. D. (2001). Analysis of relative gene expression data using real-time quantitative PCR and the $2-\Delta\Delta CT$ method. *Methods* 25, 402–408. doi: 10.1006/meth.2001.1262

Lotfi, R., Ghassemi-Golezani, K., and Pessarakli, M. (2020). Salicylic acid regulates photosynthetic electron transfer and stomatal conductance of mung bean (*Vigna radiata* L.) under salinity stress. *Biocatal. Agric. Biotechnol.* 26:101635. doi: 10.1016/j.bcab.2020.101635

Lotfi, R., Kalaji, H., Valizadeh, G., Behrozyar, E. K., Hemati, A., Gharavi-Kochebagh, P., et al. (2018). Effects of humic acid on photosynthetic efficiency of rapeseed plants growing under different watering conditions. *Photosynthetica* 56, 962–970. doi: 10.1007/s11099-017-0745-9

Loudari, A., Benadis, C., Naciri, R., Soulaimani, A., Zeroual, Y., Gharous, M. E., et al. (2020). Salt stress affects mineral nutrition in shoots and roots and chlorophyll a fluorescence of tomato plants grown in hydroponic culture. *J. Plant Interact.* 15, 398–405. doi: 10.1080/17429145.2020.1841842

Lunn, J. E., Delorge, I., Figueroa, C. M., Van Dijck, P., and Stitt, M. (2014). Trehalose metabolism in plants. *Plant J.* 79, 544–567. doi: 10.1111/tpj.12509

Lv, G. Y., Guo, X. G., Xie, L. P., Xie, C. G., Zhang, X. H., Yang, Y., et al. (2017). Molecular characterization, gene evolution, and expression analysis of the fructose-1, 6-bisphosphate aldolase (FBA) gene family in wheat (*Triticum aestivum* L.). *Front. Plant Sci.* 8:1030. doi: 10.3389/fpls.2017.01030

Lyu, J. I., Min, S. R., Lee, J. H., Lim, Y. H., Kim, J. K., Bae, C. H., et al. (2013). Overexpression of a trehalose-6-phosphate synthase/phosphatase fusion gene enhances tolerance and photosynthesis during drought and salt stress without growth aberrations in tomato. *Plant Cell Tiss. Org.* 112, 257–262. doi: 10.1007/s11240-012-0225-7

Ma, Q., Li, Y. X., Yuan, H. J., Hu, J., Wei, L., Bao, A. K., et al. (2014). ZxSOS1 is essential for long-distance transport and spatial distribution of Na+ and K+ in the xerophyte *Zygophyllum xanthoxylum*. *Plant Soil* 374, 661–676. doi: 10.1007/s11104-013-1891-x

Ma, X., Chen, C., Yang, M., Dong, X., Lv, W., and Meng, Q. (2018). Cold-regulated protein (SlCOR413IM1) confers chilling stress tolerance in tomato plants. *Plant Physiol. Bioch.* 124, 29–39. doi: 10.1016/j.plaphy.2018.01.003

MacIntyre, A. M., Barth, J. X., Pellitteri Hahn, M. C., Scarlett, C. O., Genin, S., and Allen, C. (2020). Trehalose synthesis contributes to osmotic stress tolerance and virulence of the bacterial wilt pathogen *Ralstonia solanacearum*. *Mol. Plant-Microbe Interact.* 33, 462–473. doi: 10.1094/MPMI-08-19-0218-R

Meng, X., Cai, J., Deng, L., Li, G., Sun, J., Han, Y., et al. (2020). SlSTE1 promotes abscisic acid-dependent salt stress-responsive pathways via improving ion homeostasis and reactive oxygen species scavenging in tomato. *J Integr Plant Biol* 62, 1942–1966. doi: 10.1111/jipb.12987

Min, Z., Li, R., Chen, L., Zhang, Y., Li, Z., Liu, M., et al. (2019). Alleviation of drought stress in grapevine by foliar-applied strigolactones. *Plant Physiol. Bioch.* 135, 99–110. doi: 10.1016/j.plaphy.2018.11.037

Misra, B. B., Reichman, S. M., and Chen, S. (2019). The guard cell ionome: Understanding the role of ions in guard cell functions. *Prog. Biophys. Mol. Biol.* 146, 50–62. doi: 10.1016/j.pbiomolbio.2018.11.007

Naeem, M., Jin, Z., Wan, G., Liu, D., Liu, H., Yoneyama, K., et al. (2010). 5-Aminolevulinic acid improves photosynthetic gas exchange capacity and ion

uptake under salinity stress in oilseed rape (*Brassica napus* L.). *Plant Soil* 332, 405–415. doi: 10.1007/s11104-010-0306-5

Nawaz, M., Hassan, M. U., Chattha, M. U., Mahmood, A., Shah, A. N., Hashem, M., et al. (2022). Trehalose: A promising osmo-protectant against salinity stress—physiological and molecular mechanisms and future prospective. *Mol. Biol. Rep.* 1–17. doi: 10.1007/s11033-022-07681-x

Niron, H., Barlas, N., Salih, B., and Türet, M. (2020). Comparative transcriptome, metabolome, and ionome analysis of two contrasting common bean genotypes in saline conditions. *Front. Plant Sci.* 11:2007. doi: 10.3389/fpls.2020.599501

Niu, K., and Ma, H. (2018). The positive effects of exogenous 5-aminolevulinic acid on the chlorophyll biosynthesis, photosystem and Calvin cycle of Kentucky bluegrass seedlings in response to osmotic stress. *Environ. Exp. Bot.* 155, 260–271. doi: 10.1016/j.envexpbot.2018.07.006

Nounjan, N., Nghia, P. T., and Theerakulpisut, P. (2012). Exogenous proline and trehalose promote recovery of rice seedlings from salt-stress and differentially modulate antioxidant enzymes and expression of related genes. *J. Plant Physiol.* 169, 596–604. doi: 10.1016/j.jplph.2012.01.004

Nunes, C., O'Hara, L. E., Primavesi, L. F., Delatte, T. L., Schluepmann, H., Somsen, G. W., et al. (2013). The trehalose 6-phosphate/SnRK1 signaling pathway primes growth recovery following relief of sink limitation. *Plant physiol.* 162, 1720–1732. doi: 10.1104/pp.113.220657

Oukarroum, A., Lebrihi, A., El Gharous, M., Goltsev, V., and Strasser, R. J. (2018). Desiccation-induced changes of photosynthetic transport in *Parmelina tiliacea* (Hoffm.) Ach. analysed by simultaneous measurements of the kinetics of prompt fluorescence, delayed fluorescence and modulated 820 nm reflection. *J. Lumin.* 198, 302–308. doi: 10.1016/j.jlumin.2018.02.040

Pan, T., Liu, M., Kreslavski, V. D., Zharmukhamedov, S. K., Nie, C., Yu, M., et al. (2021). Non-stomatal limitation of photosynthesis by soil salinity. *Crit. Rev. Env. Sci. Tec.* 51, 791–825. doi: 10.1080/10643389.2020.1735231

Qin, H., and Huang, R. (2020). The phytohormonal regulation of Na+/K+ and reactive oxygen species homeostasis in rice salt response. *Mol. Breed.* 40, 1–13. doi: 10.1007/s11032-020-1100-6

Ramireddy, E., Hosseini, S. A., Eggert, K., Gillandt, S., Gnad, H., von Wirén, N., et al. (2018). Root engineering in barley: Increasing cytokinin degradation produces a larger root system, mineral enrichment in the shoot and improved drought tolerance. *Plant Physiol.* 177, 1078–1095. doi: 10.1104/pp.18.00199

Rohman, M. M., Islam, M. R., Monsur, M. B., Amiruzzaman, M., Fujita, M., and Hasanuzzaman, M. (2019). Trehalose protects maize plants from salt stress and phosphorus deficiency. *Plants* 8:568. doi: 10.3390/plants8120568

Sadak, M. S. (2019). Physiological role of trehalose on enhancing salinity tolerance of wheat plant. *Bull. Natl. Res. Cent.* 43, 1–10. doi: 10.1186/s42269-019-0098-6

Samadi, S., Habibi, G., and Vaziri, A. (2019). Exogenous trehalose alleviates the inhibitory effects of salt stress in strawberry plants. *Acta Physiol. Plant.* 41, 1–11. doi: 10.1007/s11738-019-2905-y

Sameena, P., and Puthur, J. T. (2021). Differential modulation of photosynthesis and defense strategies towards copper toxicity in primary and cotyledonary leaves of *Ricinus communis* L. *J. Photochem. Photobiol.* 8:100059. doi: 10.1016/j.jpap.2021.100059

Sarkar, A. K., and Sadhukhan, S. (2022). Imperative role of trehalose metabolism and trehalose-6-phosphate signaling on salt stress responses in plants. *Physiol. Plant.* 174:e13647. doi: 10.1111/ppl.13647

Sehar, Z., Masood, A., and Khan, N. A. (2019). Nitric oxide reverses glucose-mediated photosynthetic repression in wheat (*Triticum aestivum* L.) under salt stress. *Environ. Exp. Bot.* 161, 277–289. doi: 10.1016/j.envexpbot.2019.01.010

Shahbaz, M., Abid, A., Masood, A., and Waraich, E. A. (2017). Foliar-applied trehalose modulates growth, mineral nutrition, photosynthetic ability, and oxidative defense system of rice (*Oryza sativa* L.) under saline stress. *J. Plant Nutr.* 40, 584–599. doi: 10.1080/01904167.2016.1263319

Sharma, S., Joshi, J., Kataria, S., Verma, S.K., Chatterjee, S., Jain, M., et al. (2020). "Regulation of the calvin cycle under abiotic stresses: An overview," in *Plant life under changing environment*, eds D. K. Tripathi, V. P. Singh, D. K. Chauhan, S. Sharma, S. M. Prasad, N. K. Dubey, et al. (London: Academic Press), 681–717. doi: 10.1016/B978-0-12-818204-8.00030-8

Shi, Y., Sun, H., Wang, X., Jin, W., Chen, Q., Yuan, Z., et al. (2019). Physiological and transcriptomic analyses reveal the molecular networks of responses induced by exogenous trehalose in plant. *PLoS One* 14:e0217204. doi: 10.1371/journal.pone.0217204

Tang, C., Xie, J., Lv, J., Li, J., Zhang, J., Wang, C., et al. (2021). Alleviating damage of photosystem and oxidative stress from chilling stress with exogenous zeaxanthin in pepper (*Capsicum annuum* L.) seedlings. *Plant Physiol. Bioch.* 162, 395–409. doi: 10.1016/j.plaphy.2021.03.010

Tang, H., Niu, L., Wei, J., Chen, X., and Chen, Y. (2019). Phosphorus limitation improved salt tolerance in maize through tissue mass density increase, osmolytes accumulation, and Na+ uptake inhibition. *Front. Plant Sci.* 10:856. doi: 10.3389/fpls.2019.00856

Tang, Y. Y., Yuan, Y. H., Shu, S., and Guo, S. R. (2018). Regulatory mechanism of NaCl stress on photosynthesis and antioxidant capacity mediated by transglutaminase in cucumber (*Cucumis sativus* L.) seedlings. *Sci. Hortic.* 235, 294–306. doi: 10.1016/j.scienta.2018.02.045

Tanveer, K., Gilani, S., Hussain, Z., Ishaq, R., Adeel, M., and Ilyas, N. (2020). Effect of salt stress on tomato plant and the role of calcium. *J. Plant Nutr.* 43, 28–35. doi: 10.1080/01904167.2019.1659324

Tekdal, D., and Cetiner, S. (2018). Investigation of the effects of salt (NaCl) stress and cadmium (cd) toxicity on growth and mineral acquisition of *Vuralia turcica*. *S. Afr. J. Bot.* 118, 274–279. doi: 10.1016/j.sajb.2018.07.029

Tsai, A. Y. L., and Gazzarrini, S. (2014). Trehalose-6-phosphate and SnRK1 kinases in plant development and signaling: The emerging picture. *Front. Plant Sci.* 5:119. doi: 10.3389/fpls.2014.00119

Wang, R., Jing, W., Xiao, L., Jin, Y., Shen, L., and Zhang, W. (2015). The rice high-affinity potassium transporter1; 1 is involved in salt tolerance and regulated by an MYB-type transcription factor. *Plant Physiol.* 168, 1076–1090. doi: 10.1104/pp.15.00298

Wang, W., Chen, Q., Xu, S., Liu, W. C., Zhu, X., and Song, C. P. (2020). Trehalose-6-phosphate phosphatase E modulates ABA-controlled root growth and stomatal movement in *Arabidopsis*. *J. Integr Plant Biol.* 62, 1518–1534. doi: 10.1111/jipb.12925

Wang, X., Dingxuan, Q., and Shi, M. (2021). Calcium amendment for improved germination, plant growth, and leaf photosynthetic electron transport in oat (*Avena sativa*) under NaCl stress. *PLoS One* 16:e0256529. doi: 10.1371/journal.pone.0256529

Wang, X., Li, Q., and Wu, F. (2010). Study on the characteristics of absorption, distribution and selective transport of Na+ and K+ in tomato plants under salt stress. *Sci. Agric. Sin.* 43, 1423–1432. doi: 10.4028/www.scientific.net/AMM.37-38.1549

Wu, H. (2018). Plant salt tolerance and Na+ sensing and transport. *Crop J.* 6, 215–225.

Wu, H., Zhang, X., Giraldo, J. P., and Shabala, S. (2018a). It is not all about sodium: Revealing tissue specificity and signalling roles of potassium in plant responses to salt stress. *Plant Soil* 431, 1–17. doi: 10.1007/s11104-018-3770-y

Wu, Y., Jin, X., Liao, W., Hu, L., Dawuda, M. M., Zhao, X., et al. (2018b). 5-Aminolevulinic acid (ALA) alleviated salinity stress in cucumber seedlings by enhancing chlorophyll synthesis pathway. *Front. Plant Sci.* 9:635. doi: 10.3389/fpls.2018.00635

Wu, P., Xiao, C., Cui, J., Hao, B., Zhang, W., Yang, Z., et al. (2020). Nitric oxide and its interaction with hydrogen peroxide enhance plant tolerance to low temperatures by improving the efficiency of the calvin cycle and the ascorbate–glutathione cycle in cucumber seedlings. *J. Plant Growth Regul.* 40, 2390–2408. doi: 10.1007/s00344-020-10242-w

Wu, Y., Liu, N., Hu, L., Liao, W., Tang, Z., Xiao, X., et al. (2021). 5-Aminolevulinic acid improves morphogenesis and Na+ subcellular distribution in the apical cells of *Cucumis sativus* L. under salinity stress. *Front. Plant Sci.* 12:404. doi: 10.3389/fpls.2021.636121

Yadav, U. P., Ivakov, A., Feil, R., Duan, G. Y., Walther, D., Giavalisco, P., et al. (2014). The sucrose–trehalose 6-phosphate (Tre6P) nexus: Specificity and mechanisms of sucrose signalling by Tre6P. *J. Exp. Bot.* 65, 1051–1068. doi: 10.1093/jxb/ert457

Yang, H., Zhang, J., Zhang, H., Xu, Y., An, Y., and Wang, L. (2021a). Effect of 5-aminolevulinic acid (5-ALA) on leaf chlorophyll fast fluorescence characteristics and mineral element content of buxus megistophylla grown along urban roadsides. *Horticulturae* 7:95. doi: 10.3390/horticulturae7050095

Yang, N., Jiang, W., Jiang, B., Liu, J., Liu, Y., Wang, H., et al. (2021b). Cotyledon loss of *Astragalus membranaceus* hindered seedling establishment through mineral element reallocation and carbohydrate depletion. *Plant Physiol. Bioch.* 167, 481–491. doi: 10.1016/j.plaphy.2021.08.027

Yang, L., Zhao, X., Zhu, H., Paul, M., Zu, Y., and Tang, Z. (2014). Exogenous trehalose largely alleviates ionic unbalance, ROS burst, and PCD occurrence

induced by high salinity in *Arabidopsis* seedlings. *Front. Plant Sci.* 5:570. doi: 10.3389/fpls.2014.00570

Yang, Y., Yao, Y., Li, J., Zhang, J., Zhang, X., Hu, L., et al. (2022). Trehalose alleviated salt stress in tomato by regulating ROS metabolism, photosynthesis, osmolyte synthesis, and trehalose metabolic pathways. *Front. Plant Sci.* 13:623. doi: 10.3389/fpls.2022.772948

Yin, F., Zhang, S., Cao, B., and Xu, K. (2021). Low pH alleviated salinity stress of ginger seedlings by enhancing photosynthesis, fluorescence, and mineral element contents. *PeerJ* 9:e10832. doi: 10.7717/peerj.10832

Yu, W., Zhao, R., Wang, L., Zhang, S., Li, R., Sheng, J., et al. (2019). ABA signaling rather than ABA metabolism is involved in trehalose-induced drought tolerance in tomato plants. *Planta* 250, 643–655. doi: 10.1007/s00425-019-03195-2

Zamani, H., Arvin, M. J., Jahromi, A. A., Abdossi, V., and Torkashvand, A. M. (2019). The effect of methyl jasmonate and sodium silicate on the mineral composition of *Solanum lycopersicum* L. grown under salinity stress. *Acta Agrobot.* 72:1782. doi: 10.5586/aa.1782

Zhang, C. M., Zou, Z. R., Huang, Z., and Zhang, Z. X. (2010). Effects of exogenous spermidine on photosynthesis of tomato seedlings under drought stress. *Agric. Res. Arid Areas* 28, 182–187. doi: 10.1016/S1002-0160(10)60014-8

Zhang, H. H., Shi, G. L., Shao, J. Y., Xin, L., Li, M. B., Liang, M., et al. (2019). Photochemistry and proteomics of mulberry (*Morus alba* L.) seedlings under NaCl and NaHCO3 stress. *Ecotoxicol. Environ. Saf.* 184:109624. doi: 10.1016/j.ecoenv.2019.109624

Zhang, H., Xu, N., Wu, X., Wang, J., Ma, S., Li, X., et al. (2018). Effects of four types of sodium salt stress on plant growth and photosynthetic apparatus in sorghum leaves. *J. Plant Interact.* 13, 506–513. doi: 10.1080/17429145.2018.1526978

Zhang, L., Ma, H., Chen, T., Pen, J., Yu, S., and Zhao, X. (2014). Morphological and physiological responses of cotton (*Gossypium hirsutum* L.) plants to salinity. *PLoS One* 9:e112807. doi: 10.1371/journal.pone.0112807

Zhang, R., Sun, Y., Liu, Z., Jin, W., and Sun, Y. (2017). Effects of melatonin on seedling growth, mineral nutrition, and nitrogen metabolism in cucumber under nitrate stress. *J. Pineal Res.* 62:e12403. doi: 10.1111/jpi.12403

Zhao, D. Q., Li, T. T., Hao, Z. J., Cheng, M. L., and Tao, J. (2019). Exogenous trehalose confers high temperature stress tolerance to herbaceous peony by enhancing antioxidant systems, activating photosynthesis, and protecting cell structure. *Cell Stress Chaperon.* 24, 247–257. doi: 10.1007/s12192-018-00961-1

Zhong, M., Wang, Y., Hou, K., Shu, S., Sun, J., and Guo, S. (2019). TGase positively regulates photosynthesis via activation of Calvin cycle enzymes in tomato. *Hortic. Res Engl.* 6, 1–11. doi: 10.1038/s41438-019-0173-z

Zhu, X., Liu, S., Sun, L., Song, F., Liu, F., and Li, X. (2018). Cold tolerance of photosynthetic electron transport system is enhanced in wheat plants grown under elevated CO2. *Front. Plant Sci.* 9:933. doi: 10.3389/fpls.2018.00933

Zulfiqar, F., Chen, J., Finnegan, P. M., Younis, A., Nafees, M., Zorrig, W., et al. (2021). Application of trehalose and salicylic acid mitigates drought stress in sweet basil and improves plant growth. *Plants* 10:1078. doi: 10.3390/plants10061078

Zuo, Z., Sun, L., Wang, T., Miao, P., Zhu, X., Liu, S., et al. (2017). Melatonin improves the photosynthetic carbon assimilation and antioxidant capacity in wheat exposed to nano-ZnO stress. *Molecules* 22:1727. doi: 10.3390/molecules22101727

Zushi, K., and Matsuzoe, N. (2017). Using of chlorophyll a fluorescence OJIP transients for sensing salt stress in the leaves and fruits of tomato. *Sci. Hortic.* 219, 216–221. doi: 10.1016/j.scienta.2017.03.01621

frontiers | Frontiers in Plant Science

TYPE Original Research
PUBLISHED 16 August 2022
DOI 10.3389/fpls.2022.981029

Check for updates

OPEN ACCESS

EDITED BY
Giselle Camargo Mendes,
Instituto Federal de Santa Catarina (IFSC), Brazil

REVIEWED BY
Aihua Sha,
Yangtze University, China
Xiao Ma,
Sichuan Agricultural University, China

*CORRESPONDENCE
Guanghui Lv
guanghui_xju@sina.com

SPECIALTY SECTION
This article was submitted to Plant Abiotic Stress, a section of the journal Frontiers in Plant Science

RECEIVED 29 June 2022
ACCEPTED 22 July 2022
PUBLISHED 16 August 2022

CITATION
Yang F and Lv G (2022) Characterization of the gene expression profile response to drought stress in *Haloxylon* using PacBio single-molecule real-time and Illumina sequencing.
Front. Plant Sci. 13:981029.
doi: 10.3389/fpls.2022.981029

COPYRIGHT
© 2022 Yang and Lv. This is an open-access article distributed under the terms of the Creative Commons Attribution License (CC BY). The use, distribution or reproduction in other forums is permitted, provided the original author(s) and the copyright owner(s) are credited and that the original publication in this journal is cited, in accordance with accepted academic practice. No use, distribution or reproduction is permitted which does not comply with these terms.

Characterization of the gene expression profile response to drought stress in *Haloxylon* using PacBio single-molecule real-time and Illumina sequencing

Fang Yang[1,2,3] and Guanghui Lv[1,2,3]*

[1]School of Ecology and Environment, Xinjiang University, Ürümqi, China, [2]Key Laboratory of Oasis Ecology, Ministry of Education, Ürümqi, China, [3]Xinjiang Jinghe Observation and Research Station of Temperate Desert Ecosystem, Ministry of Education, Ürümqi, China

Haloxylon ammodendron and *Haloxylon persicum* are important drought-tolerant plants in northwest China. The whole-genome sequencing of *H. ammodendron* and *H. persicum* grown in their natural environment is incomplete, and their transcriptional regulatory network in response to drought environment remains unclear. To reveal the transcriptional responses of *H. ammodendron* and *H. persicum* to an arid environment, we performed single-molecule real-time (SMRT) and Illumina RNA sequencing. In total, 20,246,576 and 908,053 subreads and 435,938 and 210,334 circular consensus sequencing (CCS) reads were identified by SMRT sequencing of *H. ammodendron* and *H. persicum*, and 15,238 and 10,135 unigenes, respectively, were successfully obtained. In addition, 9,794 and 7,330 simple sequence repeats (SSRs) and 838 and 71 long non-coding RNAs were identified. In an arid environment, the growth of *H. ammodendron* was restricted; plant height decreased significantly; basal and branch diameters became thinner and hydrogen peroxide (H_2O_2) content and peroxidase (POD) activity were increased. Under dry and wet conditions, 11,803 and 15,217 differentially expressed genes (DEGs) were identified in *H. ammodendron* and *H. persicum*, respectively. There were 319 and 415 DEGs in the signal transduction pathways related to drought stress signal perception and transmission, including the Ca^{2+} signal pathway, the ABA signal pathway, and the MAPK signal cascade. In addition, 217 transcription factors (TFs) and 398 TFs of *H. ammodendron* and *H. persicum* were differentially expressed, including FAR1, MYB, and AP2/ERF. Bioinformatic analysis showed that under drought stress, the expression patterns of genes related to active oxygen [reactive oxygen species (ROS)] scavenging, functional proteins, lignin biosynthesis, and glucose metabolism pathways were altered. Thisis

the first full-length transcriptome report concerning the responses of *H. ammodendron* and *H. persicum* to drought stress. The results provide a foundation for further study of the adaptation to drought stress. The full-length transcriptome can be used in genetic engineering research.

KEYWORDS

drought stress, *Haloxylon ammodendron*, *Haloxylon persicum*, RNA sequencing, single-molecule real-time sequencing

Introduction

Drought is one of the main environmental factors that restrict the survival, secondary metabolism, and productivity of plant species (Li et al., 2021). Under drought stress, plants undergo several changes, which eventually lead to the reduction in gas exchange and photosynthesis and a decrease in cell division and cell expansion due to reduced enzyme activities and energy deficiency (Thayale Purayil et al., 2020). To adapt to these conditions, plants employ a series of morphological, physiological, biochemical and molecular mechanisms, such as growth restriction (Gupta et al., 2020), reactive oxygen species (ROS) scavenging (Zhang et al., 2022) and transcriptional activation (Zhu, 2016). Functional proteins and regulatory proteins are two major categories of stress-inducible proteins that play an important role in plant adaptation to stress (Thayale Purayil et al., 2020). Regulatory proteins are involved in the regulation of downstream genes in stress response pathways. This includes different types of protein kinases and transcription factors (TFs) (Golldack et al., 2014).

In plants, abscisic acid-mediated signaling plays a central role in plant responses to stress (Kumar et al., 2019). Under drought stress, increased levels of abscisic acid (ABA) lead to binding to PYR/PYL, which changes the conformation of PYR/PYL protein, allowing PYR/PYL to interact with the negative regulator type 2 protein C phosphatase (PP2C) to form a temporary complex (ABA-PYR/PYL-PP2C), which can inhibit the activity of PP2C. The low expression of PP2C will slow down the inhibition of SNF1-related kinases (SnRKs), and the expression of SnRKs will induce stomatal closure and activate downstream drought stress related genes and adapt plants to water-deficient environments (Sah et al., 2016; Zhu, 2016). Under drought conditions, the regulation of drought-responsive genes is regulated by various TFs, such as the bZIP family, the AP2/ERF superfamily, and the NAC family. These TFs play important roles in plant defense through ABA-dependent and ABA-independent stress tolerance mechanisms (Yu et al., 2019). The mitogen-activated protein kinase (MAPK) cascade is one of the major abiotic stress response pathways involved in transduction of external stimuli to the nucleus to appropriately tune the cell's response under stress (Zhang et al., 2022). The role of MAPK signaling cascades in abiotic stresses such as drought, salt stress, high temperature and low temperature stress has been elucidated in different plants (Bigeard and Hirt, 2018). Under drought conditions, the phosphorylation of target genes is regulated by MAPK, which controls the activities of different structural proteins and various TFs involved in abiotic stress tolerance (Thayale Purayil et al., 2020). Together with TFs, MAPK signaling cascades play important roles in ABA-dependent and ABA-independent plant abiotic stress responses (Mahmood et al., 2019). In conclusion, multiple metabolic pathways and signaling molecules are involved in plant defense against drought stress.

One of the major challenges facing plant science today is to discover mechanisms that enable plants to maintain productivity under adverse environmental conditions and to use this knowledge to produce crops that are better adapted to climate change (Li et al., 2021). Molecular mechanisms to drought stress have been extensively studied in broad-leaved species such as *Populus nigra* (Yildirim and Kaya, 2017), *Betula platyphylla* (Li H. Y. et al., 2020), and *Morus* spp. (Sun et al., 2020), but only a few studies have focused on *Haloxylon ammodendron* (Long et al., 2014; Fan et al., 2018) and *Haloxylon persicum* (Thayale Purayil et al., 2020). Therefore, it is important to understand the drought tolerance of *H. ammodendron* and *H. persicum*.

H. ammodendron and *H. persicum* are plants of the genus *Haloxylon* in the family Lyceae. They often form large-area pure stands in desert regions and have the function of fixing dunes. As xerophytic desert trees, these species have the characteristics of resistance to drought, high temperatures, saline alkali soils, wind erosion, and cold (Long et al., 2014; Thayale Purayil et al., 2020). The genus is widely distributed in desert and semi-desert areas, and the plants have ecological benefits. Therefore, they play an important role in maintaining the structure and function of the ecosystem, and thus revealing the drought-tolerance mechanism of *Haloxylon* is of great significance for drought-tolerant breeding. *Haloxylon* has a complex genetic background and a large genome that limit the study on the molecular mechanisms of drought tolerance (Lai et al., 2014). However, the development of next-generation sequencing (NGS, Illumina RNA sequencing) technology can overcome this difficulty

(Thudi et al., 2012). Although the full-length transcript obtained by Illumina HiSeq has been completed, the length of the reads is insufficient, and this short-read sequencing hampers transcript reconstruction and annotation.

Single-molecule real-time sequencing (SMRT-seq) technology introduces powerful new tools (Rhoads and Au, 2015; Ardui et al., 2018). By virtue of its super long reading length advantage, SMRT-seq can directly obtain high-quality full-length transcript information without interruption and assembly (the average reading length of PacBio SMRT-seq is > 10 KB, and the actual length can reach 60 KB) (Van Dijk et al., 2018). However, according to current research, SMRT-seq often provides inaccurate gene information, and low gene coverage leads to a high error rate (Li et al., 2021). The incompleteness of Illumina HiSeq can be supplemented by more complete reading of SMRT-seq, while the inaccurate reading of SMRT-seq can be corrected by more accurate data of Illumina Hiseq (Li et al., 2021). Full-length transcripts that do not require assembly can be used to detect alternative splicing (AS) events, APA events, long non-coding RNAs (LncRNAs), and fusion transcripts. SMRT-seq has been successfully used to decipher the transcriptome of many plants, including *Larix kaempferi* (Li et al., 2021), *Crocus sativus* (Qian et al., 2019), *Dendranthema grandiflorum* (Zhao et al., 2018), and *C. obtusifolia* (Deng et al., 2018). Recently, a method combining SMRT-seq and Illumina HiSeq has been developed (Zhao et al., 2018; Zhang et al., 2019).

A previous study that screened candidate genes for *Haloxylon* drought stress mechanisms by the SMRT-seq technique obtained unclear results. In this study, SMRT and Illumina RNA-seq were used to study *H. ammodendron* (wet: soil water content 9.70–15.00%; drought: soil water content 2.41–4.00%) and *H. persicum* (wet: soil water content 3.38–5.12%; drought: Soil water content 1.05–3.11%) in both wet and dry ecological environments (Gong and Lü, 2017). First, the full-length transcriptome sequences from *H. ammodendron* and *H. persicum* obtained by Pacbio SMRT technology were described. These were then compared with Illumina RNA sequencing to generate a complete transcriptome. This study aimed to identify relevant genes and their molecular mechanisms in response to drought stress. In addition, this study also obtained the gene sequences of *H. ammodendron* and *H. persicum*, thereby providing a reference for further study of their transcriptomics.

Materials and methods

Sample plot setting

Plants were sampled during the vigorous plant growth season from June to July 2021 at the field scientific observation station of the Ministry of Education of the temperate desert ecosystem in Jinghe County, Xinjiang University, starting from the East Bridge Management Station of Ebinur Lake Wetland Nature Reserve. Transects (width 0.1 km × 2.0 km) were set up perpendicular to the Aqiksu River in the areas with *H. ammodendron* and *H. persicum* and labeled as transect 1 (in the distribution area of *H. ammodendron*) and transect 2 (in the distribution area of *H. persicum*). According to the research results of previous studies (by this research group) (Gong and Lü, 2017), two soil water environments, humid and arid, were selected. A quadrat size of 50 m × 50 m was used in each of the two soil moisture environments [*H. ammodendron*: A: humid and low salinity (HS), and B: drought and low salinity (LS); *H. persicum*: C: humid and low salinity (HB), and D: arid and low salinity (LB)] (**Figure 1**). We investigated the number and abundance of woody plant species in the plots and selected five individuals of *H. ammodendron* and *H. persicum* with similar individual sizes regarding plant height, crown width, and base diameter for sampling and determination.

Determination of phenotypic and physiological indexes under drought stress

Use a meter ruler (accuracy: 0.1 cm) to measure the plant height, and use a vernier caliper (accuracy: 0.1 mm) to measure the base diameter, branch length and branch diameter.

Approximately 0.1 g of plant tissue (assimilative branches) was weighed, and 1 ml of acetone was added followed by homogenization in an ice bath. The sample was transferred to an EP tube, diluted to 1 ml with acetone, centrifuged at 4°C at

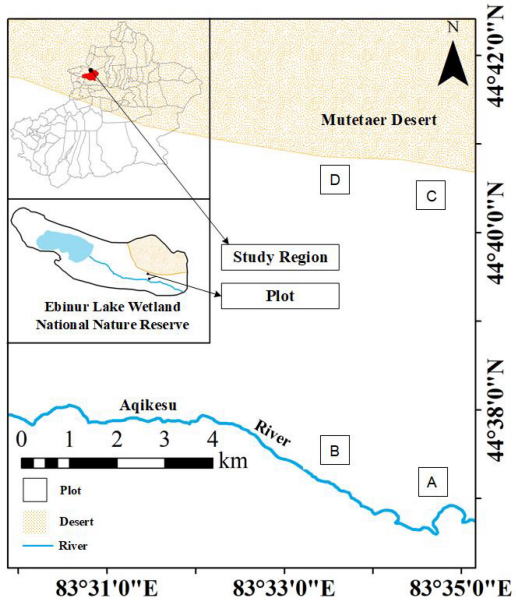


FIGURE 1
Study area and plot layout. The distribution area of *H. ammodendron*. **(A)** Humid and low salinity, and **(B)** arid and low salt; the distribution area of *H. persicum*, **(C)** humid and low salinity, and **(D)** arid and low-salinity.

10,000 rpm for 10 min, and the supernatant was collected and kept on ice to be tested. Take the supernatant; put it on ice for testing; use enzyme labeling method to determine H_2O_2 content at a wavelength of 415 nm; and determine the catalase (CAT) activity at a wavelength of 240 nm (Satterfield and Bonnell, 1955; Johansson and Borg, 1988). Approximately 0.1 g of plant tissue (assimilative branches) was added to 1 ml of extract, ground into a homogenate using an automatic frozen ball mill, and then centrifuged at 12,000 rpm, 4°C for 10 min. Take the supernatant, put it on ice for testing, and measure the peroxidase (POD) activity by enzyme labeling method at a wavelength of 470 nm (Doerge et al., 1997). The data were averaged from three replicates.

Full-length cDNA library, RNA-seq, PacBio single-molecule real-time-seq and error correction

Total RNA isolation was done according to the protocol outlined by Jaakola et al. (2001), and total RNA was quantified and assessed using an Agilent Bioanalyzer 2100 (*Haloxylon ammodendron*: 25 s:18 s $\geq$ 1.6, RIN $\geq$ 6; *Haloxylon persicum*: 25 s:18 s $\geq$ 2.0, RIN $\geq$ 7). Total RNA from three biological replicates (*Haloxylon ammodendron*: HS1, HS2, HS3, LS1, LS2, LS3; *Haloxylon persicum*: HB1, HB2, HB3, LB1, LB2, LB3) was pooled in equal amounts, and 1 μg of the pooled RNA was used for cDNA synthesis and SMRT bell library construction. The purified RNA was reverse transcribed into cDNA using a SMARTer PCR cDNA Synthesis Kit (Clontech, Mountain View, CA, United States). The cDNA was amplified using a Kapa HiFi PCR kit (Kapa Biosystems, Wilmington, MA, United States). Size selection was carried out on a BluePippin (Sage Science, Beverly, MA, United States) system, and 1–2 kb, 2–3 kb, 3–6 kb, and 5–10 kb fractions were collected. After size selection, the collected cDNA fractions were treated with DNA damage repair mix followed by end repair and ligation of SMRT adapters using the PacBio SMRTbell Template Prep Kit (Pacific Biosciences, Menlo Park, CA, United States) to construct PacBio libraries. The library construction and sequencing were performed by Beijing Novogene Technology Co., Ltd. (China).

Illumina data were used to validate and quantify the PacBio-based transcripts. A total amount of 2 μg RNA per sample was used as an input material for the RNA sample preparations. RNA purity was checked using a kaiao K5500® Spectrophotometer (Kaiao, Beijing, China). RNA integrity and concentration were assessed using the RNA Nano 6000 Assay Kit of the Bioanalyzer 2100 system (Agilent Technologies, Santa Clara, CA, United States). Sequencing libraries were generated using NEBNext® Ultra™ RNA Library Prep Kit for Illumina® (#E7530L, NEB, Ipswich, MA, United States) following the manufacturer's recommendations. Each biological replicate was individually barcoded. Libraries were sequenced in 150-bp paired-end mode using an Illumina HiSeq X Ten.

The software SMRTlink v8.0 was used to filter and process the output. The parameters were as follows: minlength 50 (minimum length: 50 bp), MaxLength 15,000 (maximum length: 15,000 bp), and minpasses 1 (minimum number of full passes: The final data were considered as the valid data). The subreads in offline data subreads.bam file passed through the circular consensus sequencing (CCS) algorithm, i.e., self-correction of single-molecule multiple sequencing results to obtain a CCS. The CCS data were classified by detecting whether the CCS contained 5′-primer, 3′-primer, or poly-A and by identifying FLNC (full-length non-chimera) sequences and nFL (non-full length non-chimera) sequences. The FLNC sequences of the same transcript were clustered by hierarchical n * log (n) algorithm to obtain the consensus sequence. Finally, the full-length sequence was polished to obtain a consensus sequence for subsequent analysis. RNA-seq data were corrected by LoRDEC (Salmela and Rivals, 2014) software to further improve the sequencing accuracy, resulting in an accuracy of $\geq$ 99%.

Transcript de redundancy and gene function annotation

CD-HIT (Fu et al., 2012) software was used to cluster and compare protein or nucleic acid sequences through sequence alignment clustering and to remove redundant and similar sequences. We clustered the corrected transcripts according to the 95% similarity between sequences to remove redundancy.

To obtain comprehensive gene function information, gene function annotation was performed on the sequences after using the cd-hit software to remove redundancy. The databases used included NCBI non-redundant protein sequences (Nr), NCBI nucleotide sequences (Nt), Protein family (Pfam), and EuKaryotic Ortholog Groups/Clusters of Orthologous Groups of proteins (KOG/COG), a manually annotated and reviewed protein sequence database (Swissprot), the Gene Ontology (GO) database, and the Kyoto Encyclopedia of Genes and Genomes (KEGG) database (*E-value* $< 1e^{-5}$).

CDS prediction, simple sequence repeat analysis, and prediction of long non-coding RNAs

We used ANGEL software for CDS prediction analysis (Shimizu et al., 2006). The program includes error-free and fault-tolerant modes (fault-tolerant mode is adopted by default). Genes were detected by SSR with MISA software. We used CNCI (Sun et al., 2013), PLEK (Li et al., 2014), and CPC2 (Kang et al., 2017) software and the Pfam (Finn et al., 2016) database to predict the coding potential of PacBio sequencing data, and subsequently analyzed the final LncRNAs.

Analysis of differentially expressed transcripts

To investigate the gene expression patterns of *H. ammodendron* and *H. Persicum* under drought stress (The experimental plots are located in arid areas, and are

limited by water conditions all year round, resulting in lower soil water content the farther away from the river bank, and the long-term arid environment is affected by drought stress), we mapped all Illumina clean reads to the SMRT full-length transcriptome. The fragments per kilobase of exon per million fragments mapped (FPKM) values were then used to normalize the reads from the RNA-seq. To obtain the full-length transcripts that were differentially expressed between the comparison groups, the full-length transcripts were used as a reference; the second-generation data were used for quantitative comparison; and the differences between the groups were compared based on the quantitative read count. Using the model based on a negative binomial distribution, three biological repeats of DESeq2 were analyzed for differentially expressed genes (DEGs) between plants in the arid environment and plants in a humid environment. A *P*-value was assigned to each gene and adjusted by the Benjamini and Hochberg approach for controlling the false discovery rate. Genes with padj < 0.05 and $|\log_2(\text{FoldChange})| > 1$ were identified as DEGs.

Gene Ontology and Kyoto Encyclopedia of Genes and Genomes enrichment analysis of differentially expressed transcripts

The Goseq R package was used for GO enrichment analysis of up-regulated and down-regulated DEGs between arid and humid samples (Young et al., 2010). We obtained the GO distribution of DEGs from three levels: Biological process (BP), molecular function (MF), and cell composition. Finally, KOBAS (3.0) software was used for KEGG pathway enrichment analysis to determine the pathways significantly enriched in DEGs (Wu et al., 2006).

Quantification and verification of gene expression levels

Ten DEGs were randomly selected for reverse transcription-quantitative PCR (qRT-PCR) assays to validate the reliability of the RNA-seq analysis. Reverse transcription was performed using a PrimeScript RT First Strand cDNA Synthesis Kit (Toyobo, Osaka, Japan). The first-strand cDNA synthesized from 1 μg of purified RNA was reverse transcribed using a Reverse Transcriptase kit (EP0442, Thermo Fisher Scientific). The qRT-PCR was carried out using an AceQ Universal SYBR qPCR Master Mix (Vazyme, Nanjing, China) system with PCR conditions following the manufacturer's instructions. Quantitative RT-PCR reactions were conducted in 96-well plates with a real-time PCR System (Stepone plus, ABI) using the AceQ Universal SYBR qPCR Master Mix (Vazyme, Nanjing, China). Ha18SrRNA was used as an internal control. The $2^{-\Delta\Delta CT}$ method was used to determine the relative abundance of transcripts. For accuracy, the whole experiment was conducted thrice. All primers used in this study are listed in **Supplementary Table 1**.

Statistical analysis of data

All statistical analyses were performed using statistical package for the social sciences (SPSS) software version 20 (IBM, Chicago, IL, United States), and significant differences were evaluated by using analysis of variance. Different letters indicate significant differences at $P < 0.05$.

Results

Phenotypic and physiological changes of *Haloxylon ammodendron* and *Haloxylon persicum* under drought stress

H. ammodendron and *H. persicum* were used as experimental materials to study the effects of drought stress on growth and development as well as the regulatory mechanisms in response to drought stress. The growth of *H. ammodendron* and *H. persicum* was observed by measuring the difference in soil water content under wet and dry conditions. The soil water content of *H. ammodendron* decreased rapidly from 12.88 to 3.80%. The lower the soil water content, the greater the inhibition of growth by drought stress; this was manifested as clear decreases in plant height, the thinning of basal and branch diameters, and the shortening of branch length. The soil water content of *H. persicum* decreased from 3.46 to 2.16%, primarily through increases in plant height, basal diameter, and branch length and the thinning of branch diameter (**Figures 2A–E**). Physiological response measurements showed that the H_2O_2 contents of *H. ammodendron* (4.75–5.73 μmol/g) and *H. persicum* (7.42–7.68 μmol/g) accumulated under an arid environment (**Figure 2F**). Normally, the plants remove ROS through their own enzyme and non-enzyme antioxidant protection systems. The results showed that drought stress significantly decreased catalase (CAT) activity and increased POD activity (0.64–0.75 μmol/min/mg prot) in *H. ammodendron* (**Figures 2G,H**). *H. persicum* showed no significant changes.

Haloxylon ammodendron and *Haloxylon persicum* transcriptome sequencing using PacBio single-molecule real-time-seq and RNA-seq

Short-read sequencing using the Illumina platform, the most widely used approach for RNA-seq, is a powerful technique for quantifying gene expression. The Pacific Biosciences SMRT-seq platform, which provides long reads up to transcript length, makes it possible to accurately reconstruct full-length splice

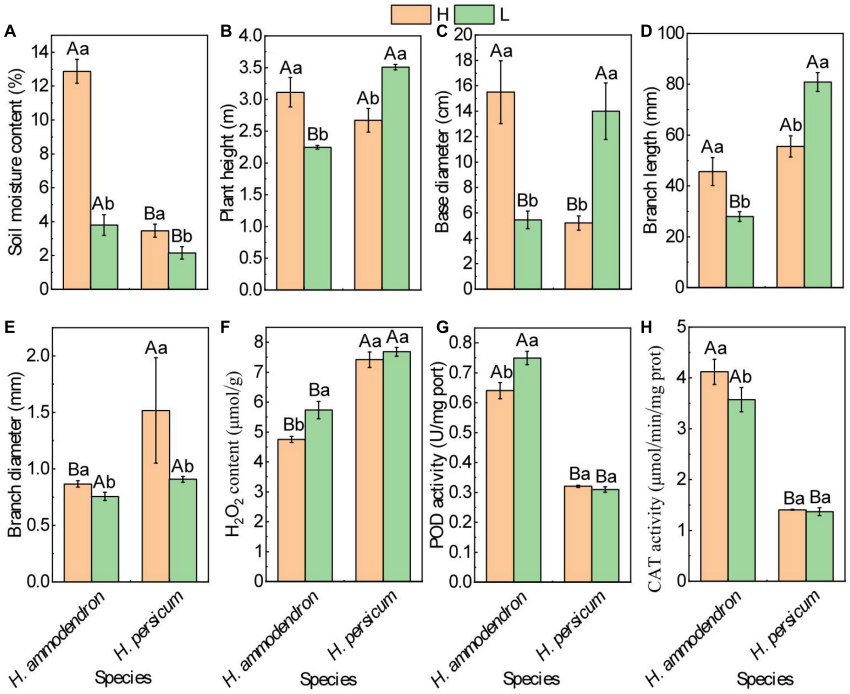


FIGURE 2
Effects of drought stress on phenotypic and biochemical parameters of *H. ammodendron* and *H. persicum*. **(A)** Soil moisture content; **(B)** plant height; **(C)** base diameter; **(D)** branch length; **(E)** branch diameter; **(F)** H_2O_2 content; **(G)** activities of POD; and **(H)** activities of CAT. H represents humid and low salinity.

variants. In total, 82 Gb of clean reads were produced by the Illumina HiSeq X Ten. The Q30 levels of *H. ammodendron* and *H. persicum* were greater than 93%, and the rate of clean reads was greater than 98% (Table 1). SMRT-seq showed that 20,246,576 and 8,908,053 subreads and 435,938 and 210,334 CCS reads were obtained from *H. ammodendron* and *H. persicum*, respectively. LoRDEC (Salmela and Rivals, 2014) software uses the second-generation data with high accuracy to correct the third-generation PacBio data. After multiple corrections, 35,096 and 20,621 consensus reads were obtained for *H. ammodendron* and *H. persicum* transcripts, respectively. According to the 95% similarity between sequences, the corrected transcripts were clustered to remove redundancy, and the numbers of transcripts remaining were 15,238 and 10,135 (Table 2).

Gene annotation and functional classification

To predict and analyze the functions of the unigenes, all full-length transcripts from SMRT were aligned to public databases: Nt, Nr, Pfam, SwissProt, KOG, GO, and KEGG (*E-value* $< 1e^{-5}$). Respective totals of 14,187 and 10,037 transcripts of *H. ammodendron* and *H. persicum* were annotated using each database. The resulting values were 12,025 (84.76%) and 9,000 (89.67%) for Nt; 13,956 (98.37%) and 9,983 (99.46%) for Nr; 10,186 (71.80%) and 7,885 (78.56%) for Pfam; 11,843 (83.48%) and 8,912 (88.79%) for SwissProt; 8,692 (61.27%) and 6,721 (66.96%) for KOG; 10,186 (71.80%) and 7,885 (78.56%) for GO; and 13,667 (96.33%) and 9,902 (98.65%) for KEGG (Figures 3A,C). In addition, 6,555 and 5,292 transcripts of the two species were jointly annotated into five databases (Figures 3A,C). For unknown genes, the KOG (euKaryotic Ortholog Groups) method was used for functional annotation. For *H. ammodendron* and *H. persicum*, 9,736 and 7,570 genes, respectively, were annotated into the KOG database, and the number of KOGs under each category was counted (Figures 3B,D). There were 42,320 and 31,942 single genes annotated successfully in *H. ammodendron* and *H. persicum*, respectively. These were divided into 51 functional groups in three categories of GO: BP (19,259, 14,305), cellular component (CC) (10,453, 7,499), and MF (12,608, 10,138) (Figures 3E,F).

Simple sequence repeat analysis and long non-coding RNA prediction

SSRs are also known as short tandem repeats or microsatellite markers. SSR mining was carried out with

TABLE 1 Illumina HiSeq of *H. ammodendron* and *H. persicum*, including three repetitions under humid (HS1, HS2, HS3 and HB1, HB2, HB3) and arid (LS1, LS2, LS3 and LB1, LB2, LB3) environments.

Sample	Raw reads (Mb)	Clean reads (Mb)	Clean bases(Gb)	Clean reads Q30 (%)	Clean reads rate (%)
HS1	43.08	42.37	6.35	93.29	98.35%
HS2	48.60	48.10	7.21	93.34	98.96%
HS3	48.96	48.32	7.25	93.1	98.69%
LS1	46.38	45.82	6.87	93.48	98.79%
LS2	48.06	47.37	7.11	93.52	98.57%
LS3	45.14	44.54	6.68	93.46	98.66%
HB1	47.10	46.45	6.97	93.54	98.63%
HB2	46.91	46.30	6.95	93.89	98.70%
HB3	48.05	47.44	7.12	93.07	98.72%
LB1	42.23	41.59	6.24	93.47	98.49%
LB2	41.78	41.19	6.18	93.06	98.59%
LB3	47.88	47.10	7.07	93.48	98.37%

LS1, LS2, LS3 and LB1, LB2, LB3, respectively, represent three repetitions of H. ammodendron and H. persicum in an arid environment; HS1, HS2, HS3 and HB1, HB2, HB3 denote three repetitions of H. ammodendron and H. persicum, respectively, under a humid environment.

TABLE 2 Overview of the single-molecule real-time sequencing in *H. ammodendron* and *H. persicum*.

Name		Subreads	Polymerases	CCS reads	Consensus reads	High-quality isoforms reads
Total number	SAB	20,246,576	491,508	435,938	35,096	15,238
	BAB	8,908,053	238,745	210,334	20,621	10,135
Mean length (bp)	SAB	1,286	56,104	1,868	1,860	1,982
	BAB	2,474	95,071	2,780	2,658	2,627

SAB and BAB are the names of mixed samples of H. ammodendron and H. persicum under two soil moisture conditions.

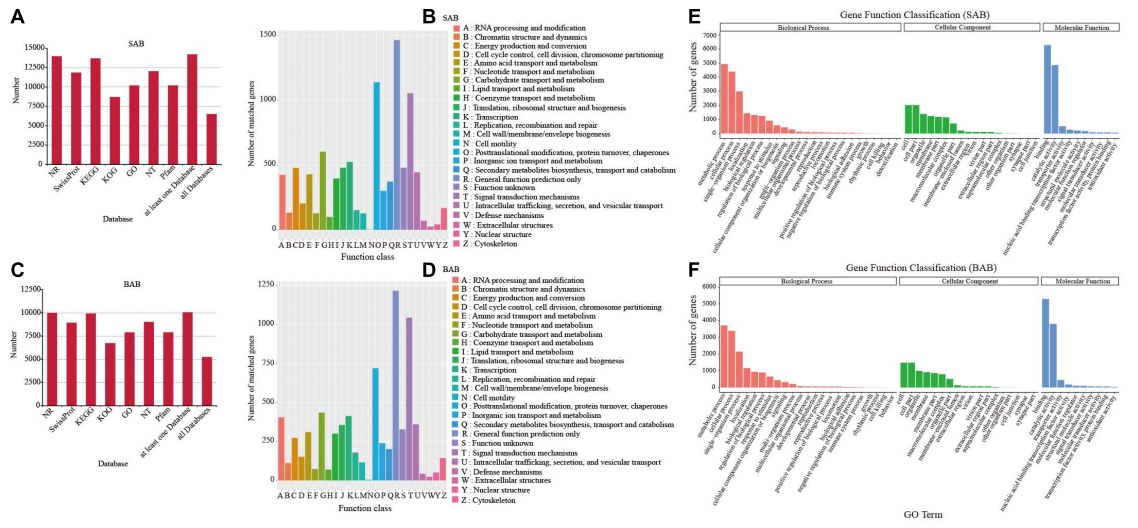


FIGURE 3
Gene annotation and functional classification. **(A)** Statistical chart of *H. ammodendron* transcripts annotated in 7 databases; **(B)** annotation results of *H. ammodendron* KOG distribution; **(C)** statistical chart of the results of annotation of the transcripts of *H. persicum* in 7 databases; **(D)** KOG distribution annotation results of *H. persicum*; **(E)** *H. ammodendron* GO annotation function diagram; **(F)** *H. persicum* GO annotation function diagram. SAB and BAB are the names of mixed samples of *H. ammodendron* and *H. persicum* under two soil moisture conditions.

MISA software. Totals of 9,794 and 7,330 SSR repeats were identified in *H. ammodendron* and *H. persicum* samples, respectively. From the whole samples of the two species, a large number of mono repeats were found followed by tri and di repeats (Figures 4A,B). LncRNAs (long-chain non-coding RNAs) are a type of RNA molecule with transcripts

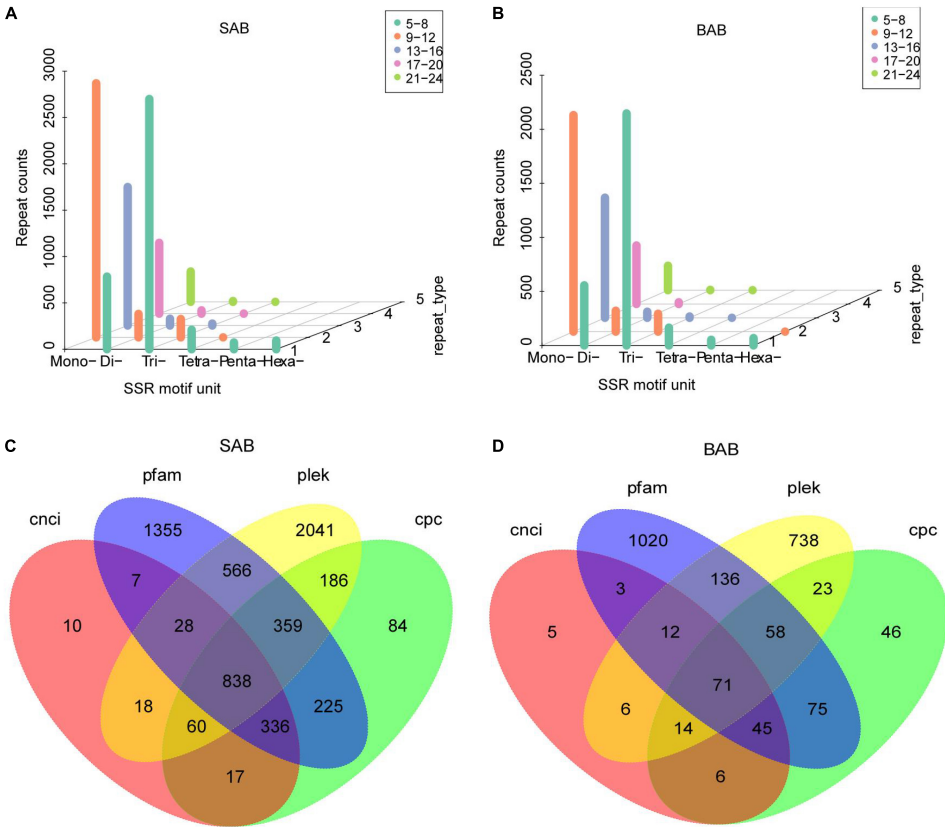


FIGURE 4
SSR analysis and forecasting for LncRNA. **(A)** SSR analysis of *H. ammodendron*; **(B)** SSR analysis of *H. persicum*; **(C)** Venn diagram of prediction results of LncRNA of *H. ammodendron*; and **(D)** Venn diagram of prediction results of LncRNA of *H. persicum*. SAB and BAB are the names of mixed samples of *H. ammodendron* and *H. persicum* under two soil moisture conditions; LS and LB, respectively, represent *H. ammodendron* and *H. persicum* in an arid environment; HS and HB denote *H. ammodendron* and *H. persicum*, respectively, under a humid environment.

longer than 200 nt, and they do not encode proteins. Four different software (PLEK, CNCI, CPC, and Pfam) were used to predict the coding potential of SMRT-seq data to maximize accuracy. The numbers of predicted non-coding transcripts in *H. ammodendron* and *H. persicum* were: PLEK (4,096, 1,058), CNCI (1,314, 162), CPC (2,105, 338), and Pfam (3,714, 1,420) (Figures 4C,D). Venn diagrams were generated to show the specificity and complementarity of the results predicted by each software. The following figure visually shows the common and unique numbers of non-coding transcripts predicted by each method. To ensure the accuracy of prediction results, the common prediction results of each software were selected for subsequent analysis.

Identification and analysis of differentially expressed genes

The FPKM density distribution map as a whole reflects the gene expression pattern of each sample. The graph shows a non-standard normal distribution. The area of each region is 1, and the sum of the representative probabilities is 1. The peak value of the density distribution curve represents the largest number of genes at this expression level. *H. ammodendron* and *H. persicum* had abundant gene expression, and drought stress affected the gene expression levels (Figure 5D). Using read counts as input, DESeq2 was used for DEG analysis, and the model based on a negative binomial distribution was used to compare plants in arid and humid environments. LS vs. HS and LB vs. HB had 11,803 (5,866 up-regulated and 5,937 down-regulated) and 15,217 (383 up-regulated and 6,834 down-regulated) DEGs [adjusted $P < 0.05$, $|\log_2(\text{FoldChange})| > 1$], respectively (Figures 5A,B). There were 16,303 DEGs between the two species (Figure 4C). A hierarchical cluster heat map was generated to view the expression patterns of the two species under different water conditions (Figure 5E). It can be seen from the figure that the gene expression of *H. ammodendron* and *H. persicum* could be divided into four groups, with significant differences among the groups. To further classify the expression patterns of all DEGs in each sample, K-means cluster analysis was performed (Figure 5F), and four subclasses with different average expression levels were identified. Cluster 2 and Cluster

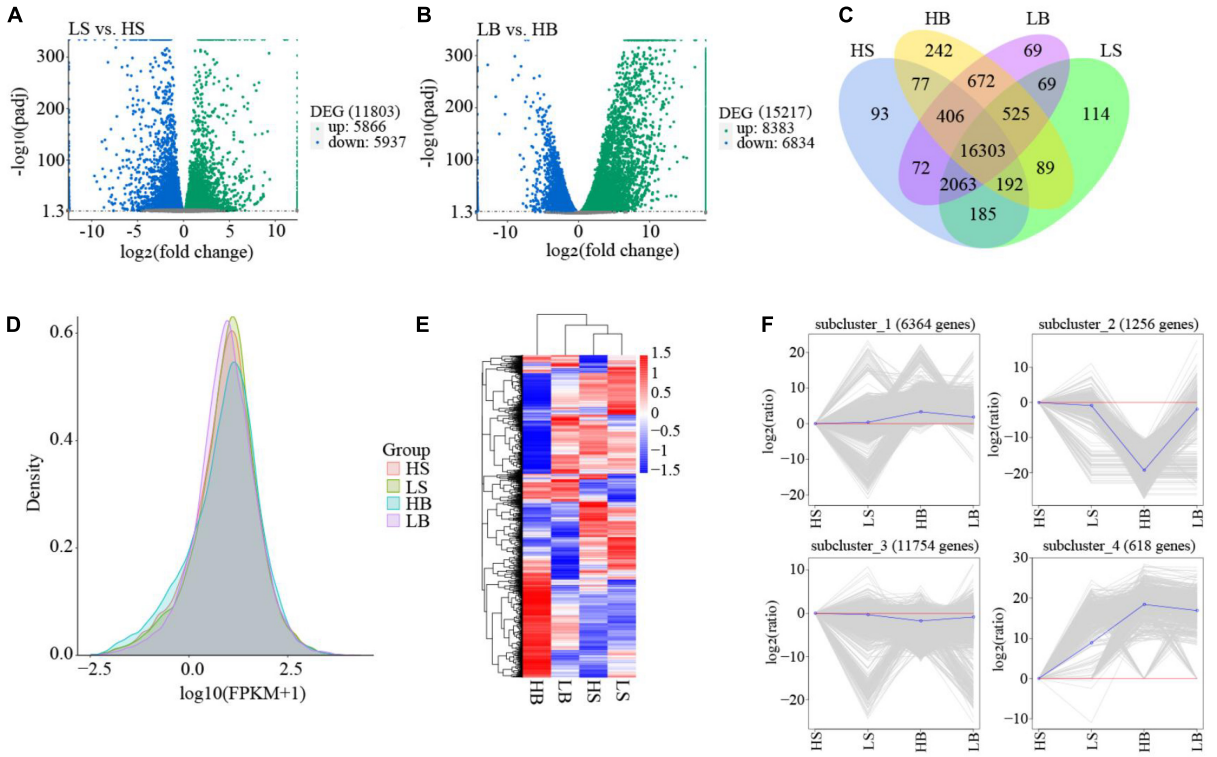


FIGURE 5
Overview of the RNA-seq data analysis. **(A)** The Volcano Plot of *H. ammodendron*. The *x*-axis represents the fold change of gene expression in different samples; the *y*-axis represents the statistical significance of the difference in gene expression; and the genes with significant differential expression are represented by green dots (up-regulated) and blue dots (down-regulated). **(B)** The Volcano Plot of *H. persicum*. The *x*-axis represents the fold change of gene expression in different samples; the *y*-axis represents the statistical significance of the difference in gene expression; and the genes with significant differential expression are represented by green dots (up-regulated) and blue dots (down-regulated). **(C)** Venn diagram of all samples of *H. ammodendron* and *H. persicum*; **(D)** FPKM density distribution; **(E)** DEG hierarchical clustering diagram of all samples; and **(F)** K-means clustering of gene expression trends. The gray line in each subgraph represents the relative expression of genes in a cluster under different experimental conditions (based on the expression of the first sample, i.e., shown by the red line), and the blue line represents the average relative expression of all genes in the cluster under different experimental conditions. LS and LB, respectively, represent *H. ammodendron* and *H. persicum* in an arid environment; HS and HB denote *H. ammodendron* and *H. persicum*, respectively, under a humid environment.

4 contained genes that were expressed throughout the drought period. In addition, in the process of hierarchical clustering and K-means clustering, the expression levels of most genes showed significant changes between LS vs. HS and LB vs. HB, indicating that DEGs at the level of LS vs. HS and LB vs. HB transcripts could determine the drought-tolerance specificity of *H. ammodendron* and *H. persicum*.

To determine the relative difference between DEGs and their products under drought stress, we performed the GO enrichment analysis for 46 functional groups of the BP category, the CC category, and the MF category. The first three GO terms of *H. ammodendron* were divided into two GO categories: "oxidation-reduction process" and "metabolic process" of the BP category; "binding," "oxidoreductase activity" and "catalytic activity" for the MF category (Figure 6A and Supplementary Table 2). The first three GO terms of *H. persicum* were "kinase activity," "cofactor binding," and "phosphotransferase activity" of the MF category (Figure 6C and Supplementary Table 3). In the KEGG database, a total of 4,618 DEGs of *H. ammodendron* were enriched in 115 pathways, and 20 pathways were significantly enriched. The significant pathways included endocytosis, plant-pathogen interaction, carbon fixation in photosynthetic organisms, and glycerophospholipid metabolism (Figure 6B and Supplementary Table 2). For *H. persicum*, 5,916 DEGs were enriched in 115 pathways, of which 20 were significantly enriched, including carbon fixation in photosynthetic organisms, plant-pathogen interaction, glycerophospholipid metabolism, glyoxylate and dicarboxylate metabolism, peroxisome, pyruvate metabolism, flavonoid biosynthesis, plant hormone signal transduction, and amino sugar and nucleotide sugar metabolism (Figure 6D and Supplementary Table 3).

Glycerophospholipid metabolism, ether lipid metabolism, glycine, serine and threonine metabolism, sesquiterpenoid and triterpenoid biosynthesis, carbon fixation in photosynthetic organisms, plant-pathogen interaction and stilbenoid,

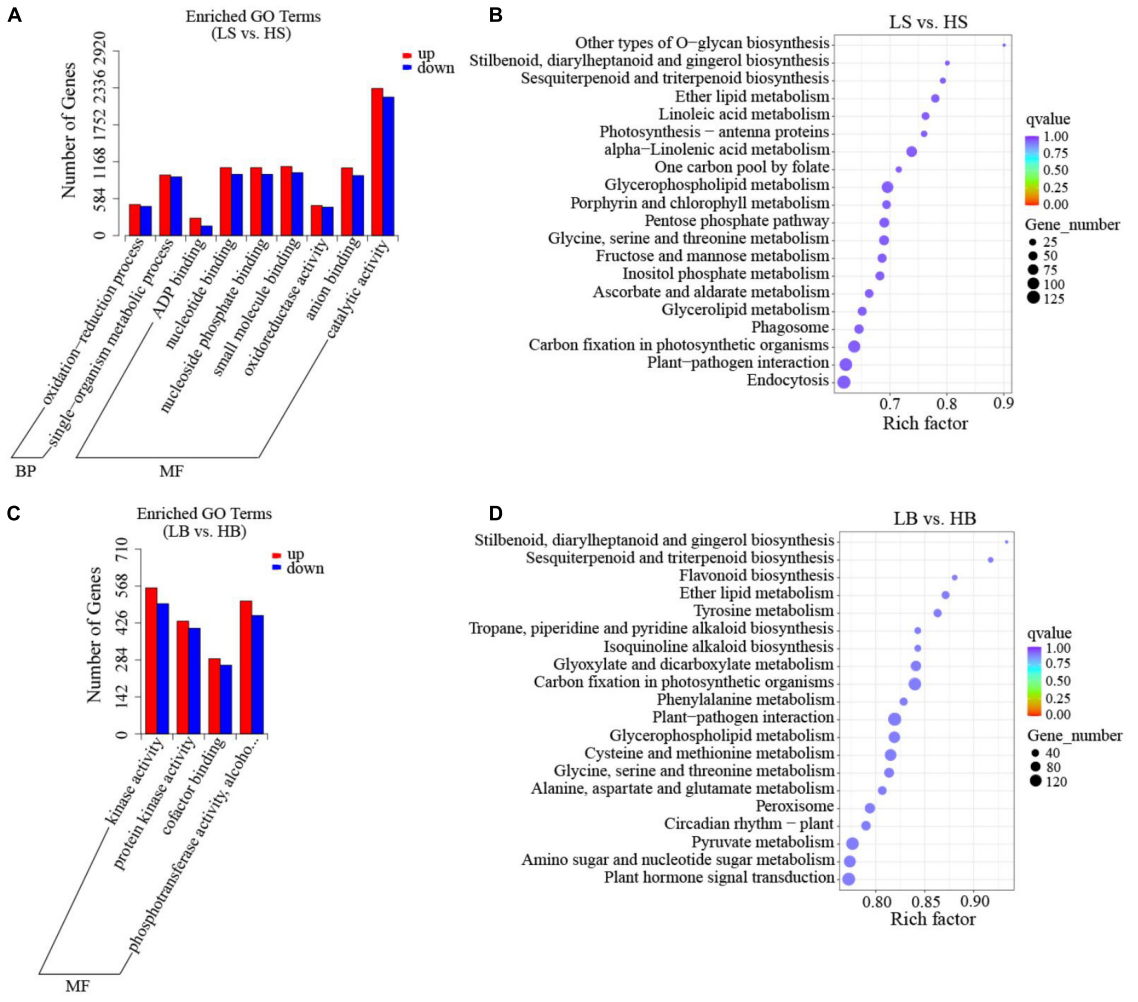


FIGURE 6
GO classification and KEGG enrichment analysis of DEGs. **(A)** GO classification of *H. ammodendron*; **(B)** KEGG enrichment analysis of *H. ammodendron*; **(C)** GO classification of *H. persicum*; and **(D)** KEGG enrichment analysis of *H. persicum*. LS and LB, respectively, represent *H. ammodendron* and *H. persicum* in an arid environment; HS and HB denote *H. ammodendron* and *H. persicum*, respectively, under a humid environment.

diarylheptanoid and gingerol biosynthesis pathways were significantly enriched in both *H. ammodendron* and *H. persicum*, indicating that secondary metabolism and amino acid metabolism were the main metabolic mechanisms of *H. ammodendron* and *H. persicum* in response to drought stress.

Differentially expressed genes related to drought stress signals in *Haloxylon ammodendron* and *Haloxylon persicum*

The perception and transmission of signals are crucial for plants under drought stress. A total of 319 (149 up-regulated and 170 down-regulated) and 415 (233 up-regulated and 182 down-regulated) DEGs involved in drought stress signal perception and transmission were found in *H. ammodendron* and *H. persicum*, respectively (Supplementary Table 4). Among these, 101 (55 up-regulated and 46 down-regulated) and 140 (76 up-regulated and 64 down-regulated) DEGs were involved in the synthesis and binding of ABA. For *H. ammodendron*, two genes encoding abscisic acid 8′- hydroxylase, one gene encoding abscisic acid receptor (PYL), two genes encoding 9-*cis*-epoxycarotenoid dioxygenase (NCED), 28 genes encoding protein phosphatase type-2C (PP2C), 16 genes encoding E3 ubiquitin-protein ligase (XERICO), and three genes encoding zeaxanthin epoxidase (ZEP) were significantly up-regulated under drought conditions. For *H. persicum*, one PYL (FC = 4.41), one NCED (FC = 41.44), four PP2C (FC = infinity), three SNF1-related protein kinase 2 (SnRK2) (FC = 2.03; FC = 7.84; FC = 6.80), three XERICO (FC = infinity), and

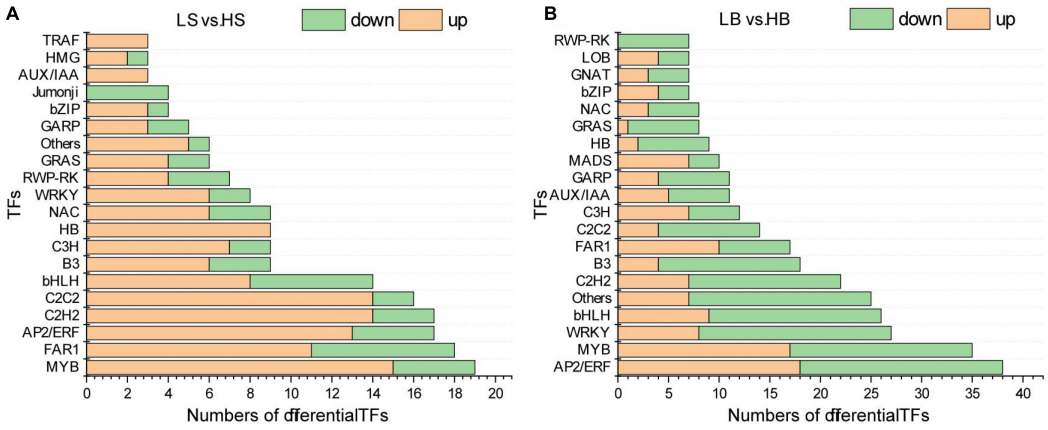


FIGURE 7
Differential transcription factors involved in drought stress (the top 20 differentially expressed were selected). **(A)** Different transcription factors of *H. ammodendron* involved in drought stress; **(B)** different transcription factors of *H. persicum* involved in drought stress. LS and LB, respectively, represent *H. ammodendron* and *H. persicum* in an arid environment; HS and HB denote *H. ammodendron* and *H. persicum*, respectively, under a humid environment.

one ZEP (FC = 20.37) genes were highly up-regulated. There were 182 and 237 DEGs in *H. ammodendron* and *H. persicum* that were identified as Ca^{2+} receptors, including calcium-transporting ATPase, calmodulin-binding protein (CaMBP), calcium-binding protein (CaBP), calcium-dependent protein kinase (CPK/CDPK), calmodulin (CAM), calmodulin-like protein (CML), calcineurin B-like protein (CBL), and CBL-interacting protein kinase (CIPK). In addition, most of the DEGs of MAPK and MAPKK components involved in the MAPK cascade in *H. ammodendron* and *H. persicum* were up-regulated. This indicated that the MAPK cascade played an important role in the response to drought stress.

Transcription factors in response to drought stress in *Haloxylon ammodendron* and *Haloxylon persicum*

Transcription factors are important regulatory genes in response to drought stress signals. In arid and humid environments, a total of 41 families of TFs of *H. ammodendron* were included in the DEGs (161 up-regulated and 56 down-regulated) (**Supplementary Table 5**). The largest group of TFs was the MYB followed by the FAR1, whereas other TFs belonged to the AP2/ERF, C2H2, C2C2, and basic helix-loop-helix (bHLH), and B3 families ($q \leq 0.05$) (**Figure 7A**). For *H. persicum*, there were 398 (165 up-regulated and 233 down-regulated) differentially expressed TFs belonging to 50 families ($q \leq 0.05$) (**Figure 7B** and **Supplementary Table 5**). The largest TF family was AP2/ERF followed by MYB, while other TFs belonged to WRKY, the bHLH family, others, and the C2H2 and B3 families. In addition to the common TFs, BBR-BPC (1), CSD (2), and HMG (3) were unique to *H. ammodendron*. TFs belonging to the ARID (1), CAMTA (1), CPP (1), mTERF (6), PHD (3), Rcd1-like (1), S1Fa-like (1), SWI/SNF-SWI3 (1), SWI/SNF-BAF60b (1), TAZ (1), Tify (2), and Whirly (1) families were unique to *H. persicum*. It is worth noting that FAR1 genes (Cluster-6558.3436, Cluster-6558.3407, Cluster-6558.1612, Cluster-363.0; Cluster-3181.2239, Cluster-3181.38499, Cluster-3181.261, Cluster-2360.1, Cluster-3181.43770, Cluster-629.0), AP2/ERF genes (Cluster-6558.1467, Cluster-6558.8862, Cluster-6558.23345; Cluster-3181.42435, Cluster-3181.42591, Cluster-3181.4445, Cluster-3181.12518; Cluster-3181.33858, Cluster-3181.4440, Cluster-3181.9216, Cluster-3181.18026, Cluster-3181.5615), MYB genes (Cluster-1167.0; Cluster-3181.1164, Cluster-3181.19228), C2H2 genes (Cluster-6558.3514; Cluster-1097.0, Cluster-11236.0), and bZIP genes (Cluster-1716.0; Cluster-3181.181, Cluster-3181.42470) of *H. ammodendron* and *H. persicum* were highly expressed under drought stress.

Differentially expressed genes of *Haloxylon ammodendron* and *Haloxylon persicum* in response to drought stress

In this study, a total of 94 DEGs (46 up-regulated and 48 down-regulated) related to ROS scavenging were identified in *H. ammodendron* and 93 (56 up-regulated and 37 down-regulated) in *H. persicum.* These included superoxide dismutase (SOD), POD, catalase (CAT), glutathione peroxidase (GPX), ascorbic acid peroxidase (APX), glutathione S-transferase (GST), and glutathione reductase (GR) (**Supplementary Table 6**). Nine APX, four CAT, and seven

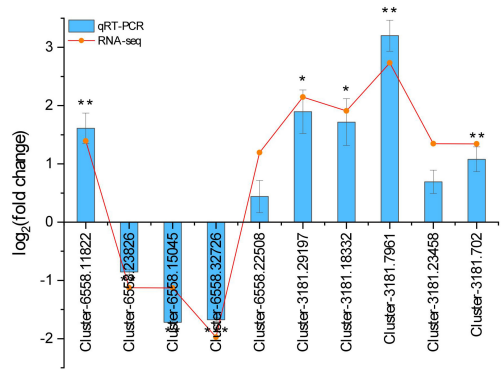


FIGURE 8
The relative expression levels of 10 DEGs between RNA-seq and qRT-PCR. The gene relative expression levels were determined by the $2^{-\Delta\Delta CT}$ method. RNA-seq, RNA sequencing; qRT-PCR, quantitative real-time polymerase chain reaction. All statistical analyses of data were performed using SPSS software (version 26, IBM, Chicago, IL, United States) to assess significant differences ($n = 3$). Significance was defined as *($P < 0.05$), **($P < 0.01$), and ***($P < 0.001$).

SOD genes in *H. ammodendron* were up-regulated after drought stress, while 18 POD, 21 GST, and 3 GPX genes in *H. persicum* were significantly up-regulated.

Lignin is a component of plant cell walls, and the content and composition of lignin may be altered under drought stress. As shown in **Supplementary Table 5**, 79 (49 up-regulated and 30 down-regulated) and 103 (50 up-regulated and 53 down-regulated) DEGs in *H. ammodendron* and *H. persicum* were related to lignin biosynthesis. These DEGs included those encoding 4-coumarate-CoA ligase (4CL), Beta-glucosidase, caffeoyl-CoA *O*-methyltransferase (CCOMT), caffeic acid 3-*O*-methyltransferase (COMT), cinnamoyl-CoA reductase (CCR), cinnamyl alcohol dehydrogenase (CADH), Laccase, Caffeoylshikimate esterase (CSE), ferulate-5-hydroxylase(F5H) and phenylalanine ammonia-lyase (PAL) (**Supplementary Table 7**).

In addition, other types of DEGs may be related to the drought stress responses of *H. ammodendron* and *H. persicum* (**Supplementary Table 8**). Totals of 80 (42 up-regulated and 38 down-regulated) and 114 (73 up-regulated and 41 down-regulated) DEGs were identified in *H. ammodendron* and *H. persicum*, belonging to heat shock protein (HSP), late embryogenesis-abundant (LEA) protein, abscisic stress-ripening (ASR) and aquaporin (AQP). It is noteworthy that most of these DEGs were highly expressed under drought stress, for example, Hsp90 (transcript_HQ_SAB_transcript8389/f2p0/2478, FC = Infinity) gene in *H. ammodendron* and HSP90 (transcript_HQ_SAB_transcript29992/f3p0/870, FC = 136.84) gene in *H. persicum*.

Sugar metabolism in plants becomes complex due to changes under drought stress (Du et al., 2020). In this study, 349 DEGs (197 up-regulated and 150 down-regulated) in *H. ammodendron* and 435 (250 up-regulated and 185 down-regulated) in *H. persicum*, were identified as being related to glucose metabolism (**Supplementary Table 9**). These DEGs were involved in starch/sucrose, fructose/mannose, amino sugar/nucleoside sugar, pentose/glucuronate, galactose, pentose phosphate, and glycolysis/gluconeogenesis metabolism.

Quantification and verification of gene expression level

To verify the reliability of RNA-seq data of *H. ammodendron* and *H. persicum* under drought stress, 10 DEGs were randomly selected for qRT-PCR. There was a strong similarity between the qRT-PCR results and RNA-seq data (**Figure 8**), indicating that the RNA-seq data were reliable.

Discussion

Characteristics of PacBio single-molecule real-time-seq and analysis of long non-coding RNA

H. ammodendron and *H. persicum* are extremely important wind- and sand-fixing plants, and as such, they are known as the guardians of the desert. However, they have been affected by drought stress for a long time. It is important to understand the drought-tolerance mechanism of these tree species. In this study, samples of *H. ammodendron* and *H. persicum* were collected under two soil environments (wet and dry), and SMRT-seq and Illumina Hiseq were used to reveal the defensive responses of *H. ammodendron* and *H. persicum* to drought stress.

SMRT-seq was able to obtain long reading or full-length transcripts, and more Illumina Hiseq single genes were obtained by mapping to SMRT-seq. The transcriptomes of *H. ammodendron* and *H. persicum* were sequenced using the Pacific Biosciences SMRT-seq platform; 35,096 and 20,621 unigenes were successfully collected, with 9,404 and 8,426 unigenes of 2,000–3,000 bp, and 4,281 and 6,603 unigenes of more than 3,000 bp. Therefore, a large number of candidate genes were detected by combining Illumina Hiseq and SMRT-seq. LncRNAs can be used as competitive endogenous RNA (ceRNA) to participate in the plant response to drought stress, representing a new gene regulatory layer (Pang et al., 2019; Ramirez et al., 2021). In this study, 838 and 71 LncRNAs were predicted in *H. ammodendron* and *H. persicum* samples, respectively. However, their functions need further study. Therefore, future study of the functions of these LncRNAs will

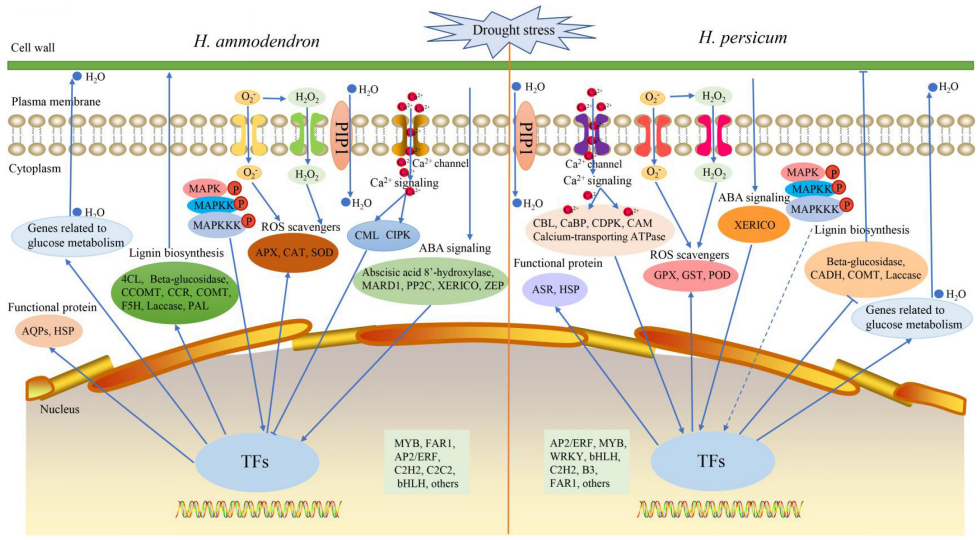


FIGURE 9
A hypothetical model of drought tolerance mechanism for *H. ammodendron* and *H. persicum*. Arrows indicate positive regulation, lines ending in bars indicate negative regulation, dashed arrows indicate neither up regulation nor down regulation.

help to better understand the response of *H. ammodendron* and *H. persicum* to drought stress at the molecular level.

Protein kinases related to Ca^{2+}, mitogen-activated protein kinase, and abscisic acid signaling pathways under drought stress

The regulation of drought tolerance in plants is a complex trait involving multiple genes. Under drought stress, the induction of signal transduction pathway-related genes is a common phenomenon, for example, the induction of the Ca^{2+} signal pathway, the MAPK signal pathway, the ABA signal pathway, and downstream regulatory pathways related to physiological adaptation (Mahmood et al., 2019; Lamers et al., 2020). Among the signal pathways of drought stress, the ABA signal pathway is important in signal transduction (Li et al., 2021). ZEP is an enzyme for zeaxanthin epoxidation in the ABA biosynthesis pathway. Overexpression of *AtZEP* enhances the tolerance of plants to drought stress (Park et al., 2008). NCED is a rate-limiting enzyme in the ABA biosynthesis pathway, and the *AtNCED3* gene is highly induced under drought stress (Sato et al., 2018). Under drought stress, *H. ammodendron* had three ZEP genes, and *H. persicum* had one *NCED3* homologous gene up-regulated. This result is consistent with the up-regulation of the NCED homologous genes of *Gossypium* spp. and *Vitis riparia* under drought stress, indicating that the ABA signaling pathway plays an important role in the response of plants to drought stress (Khadka et al., 2019; Mahmood et al., 2019). When the intracellular ABA level increases, the ABA receptor PYR/PYL/RCA protein binds to PP2C and releases SnRK2s (Kalapos et al., 2016). After that, SnRK2s can phosphorylate downstream substrates to actively activate the ABA response (Mahmood et al., 2019). SnRK2s protein is the main protein kinase that can transmit ABA signals throughout the entire plant (Zhang et al., 2022). In this study, one *PYL9* and one *PYL8*, 29 and 41 PP2C, and one and four SnRK2 genes of *H. ammodendron* and *H. persicum* were up-regulated, indicating that they are active in the ABA signal regulation system and play an important role in the process of drought tolerance.

As a secondary messenger, Ca^{2+} plays an important role in plant drought stress. Plant Ca^{2+} sensor proteins include calmodulin (CaMs), CBL, and Ca^{2+}-dependent protein kinases (CDPKs) (Aldon et al., 2018). CaM can target a variety of enzymes and structural proteins, while CBL only specifically targets a group of CDPKs designated as CIPK (Luan, 2002; Cui et al., 2018). Under drought stress, 70 and 98 CaM genes and 10 and 9 CIPK genes were significantly changed in *H. ammodendron* and *H. persicum*, respectively. These results support the view that the Ca^{2+} signaling pathway plays an important role in *H. ammodendron* and *H. persicum* under drought stress.

The MAPK signal is considered as a secondary signal regulation mechanism in response to drought stress (Zhu, 2016). The MAPK cascade signal pathway is composed of three types of protein kinases, MAP kinase kinase kinase (MAPKKK), MAP kinase kinase (MAPKK), and MAPK. MAPK amplifies and transmits external stimulus signals through MAPKKK-MAPKK-MAPK stepwise phosphorylation and activates stress response gene expression (Bigeard and Hirt, 2018). It was found

that overexpression of the maize *ZmMAPK1* gene could enhance the drought resistance of transgenic *Arabidopsis* plants (Wu et al., 2015). Weng et al. (2014) also found that overexpression of *BnMAPK1* in rape could enhance its drought resistance by increasing the water retention of cells and the activity of roots. In this study, the transcriptional levels of DEG encoding MAPK (12 and 9 genes), MAPKK (4 and 4 genes), and MAPKKK (2 and 6 genes) were up-regulated in *H. ammodendron* and *H. persicum*. KEGG pathway enrichment analysis showed that DEGs of *H. ammodendron* and *H. persicum* enriched the MAPK signal pathway. The data indicated that the MAPK signaling pathway is an important part of the drought stress response mechanism.

Transcription factor-related genes are key components of the drought response mechanism of *Haloxylon ammodendron* and *Haloxylon persicum*

Drought stress response is controlled by complex regulatory networks in plants. TFs are important regulators in this network, and they play key roles by activating or repressing the expression of downstream stress-related target genes (Xuan et al., 2022). For example, *AtFAR1* can strongly respond to drought stress, while *FAR1* can positively regulate the ABA signaling pathway and integrate light and ABA signaling to better adapt plants to environmental stress (Tang et al., 2013). Persak and Pitzschke (2014) found that *MYB44-REP* overexpression reduced drought stress tolerance in *Arabidopsis*. According to previous studies, the *AtMYB2* protein is involved in ABA-induced gene expression under drought stress (Yao et al., 2022). In *Arabidopsis*, drought, salinity, salicylic acid (SA), and H_2O_2 treatments up-regulated *AtWRKY46* expression (Ding et al., 2014). In *Gossypium hirsutum*, the *GhWRKY41* (Chu et al., 2016) gene regulates the production of ROS in the organism in an ABA-dependent manner (Ong et al., 2020), and in transgenic *Nicotiana benthamiana*, the homologous gene positively responds to drought and salt stress. Most studies have shown that multiple WRKYs respond to different abiotic stresses (especially drought and salt stress), for example, *TaWRKY1*, *TaWRKY33* (He et al., 2016), and *TaWRKY46* (Li X. R. et al., 2020). In addition, genes of the NAC, bZIP, and bHLH families are also involved in many drought stress responses (Li et al., 2021; Xuan et al., 2022). In this study, *H. ammodendron* identified 217 DEGs belonging to 41 TF families, including one WRKY DEG (Cluster-6558.4158), one Maf DEG (Cluster-1716.0), three ERF DEGs (Cluster-6558.23345, Cluster-6558.8862, and Cluster-6558.1467), three MYB DEGs (Cluster-7507.0, Cluster-13816.0, and Cluster-6558.8062), and four FAR1 DEGs (Cluster-6558.3436, Cluster-6558.3407, Cluster-6558.1612, and Cluster-363.0) that were markedly increased. *H. persicum* had four WRKY DEGs, one WRKY (Cluster-3181.31636) DEG, three bZIP DEGs, and six MYB DEGs, including two MYB (Cluster-11703.0, Cluster-3181.1164) DEGs, six FAR1 (Cluster-3181.261, Cluster-2360.1, Cluster-3181.2239, Cluster-3181.38499, Cluster-3181.43700, Cluster-629.0) DEGs that were highly expressed under drought stress. Given that TFs belonging to different families are expressed under drought induction, it can be inferred that TFs play a central role in the complex drought resistance regulatory network of *H. ammodendron* and *H. persicum*.

Antioxidative mechanisms against drought stress

Drought stress can lead to excessive accumulation of ROS in plants, inevitably causing oxidative damage (Tang et al., 2022). As the first enzyme in antioxidant action, SOD removes O^{2-} and produces H_2O_2 (Aleem et al., 2022). POD is an important regulator of H_2O_2 balance in plants, as it scavenges H_2O_2 to produce H_2O (Wang et al., 2009). GST and CAT protect plants from ROS damage (Sarker and Oba, 2018; Wahibah et al., 2018). Therefore, SOD, CAT, and GST are important antioxidant enzymes in plants. Under drought stress, SOD, POD, and GST genes were significantly differentially expressed in *H. ammodendron* and *H. persicum* (**Supplementary Table 5**). *H. persicum* accumulated more H_2O_2 than *H. ammodendron*, but H_2O_2 increased more than in *H. persicum*. The POD activity of *H. ammodendron* showed a significant upward trend, while the CAT activity showed a significant downward trend. There were no significant changes in the POD or CAT activities of *H. persicum* (**Figures 2E–H**).

The roles of functional proteins, lignin biosynthesis, and sugar metabolism in the responses of *Haloxylon ammodendron* and *Haloxylon persicum* to drought stress

During drought stress, the expression levels of many genes were significantly up-regulated in *H. ammodendron* and *H. persicum*, for example, AQPs, HSP, and ASR (**Supplementary Table 5**). AQPs are a class of channel proteins responsible for the transport of water molecules. They are primarily involved in passive transport processes, and they participate in regulating the water balance of the entire plant under drought conditions (Song et al., 2022). The resistance of tomato PIP2;7 and PIP2;5 overexpression lines to drought or osmotic stress was significantly enhanced (Wang et al., 2014). There were 14 (12 up-regulated and 2 down-regulated) and 20 (6 up-regulated and 14 down-regulated) DEGs involved in AQPs regulation in *H. ammodendron* and *H. persicum*, including 1

PIP1-3 (FC = 1.52), 2 PIP1-4 (FC = 2.41; FC = 2.01), 2 PIP1 (FC = 2.31; FC = 1.96), and 1 PIP2-7 (FC = 1.73) genes; PIP1 (FC = Infinity), PIP1-4 (FC = 271.92), and PIP2-1 (FC = 7.23) genes in *H. persicum*. Both were significantly up-regulated. The ASR family is part of the LEA protein family, and it can improve plant drought tolerance through an ABA-mediated pathway (Liang et al., 2019). The regulation of ASR in the two species was opposite; most of the genes encoding ASR in *H. ammodendron* were down-regulated, while in *H. persicum* these were mostly up-regulated. As molecular chaperones, HSP proteins play a role in the cellular stability of living plants from environmental stressors such as drought, high temperature, and salinity (Park and Seo, 2015). HSP90, one of the most abundant proteins in eukaryotes, typically targets small but critical signaling proteins, folds them when denatured under stress, and releases them after other signaling molecules bind to these proteins (Yamada and Nishimura, 2008). Overexpression of *AtHSP90* may alter the normal homeostasis of calbindin and disrupt the normal Ca^{2+} signaling pathway, thereby making transgenic plants overexpressing HSP90 more tolerant to high calcium concentrations and leading to increased tolerance to salt and drought stress (Song et al., 2009). The genes encoding HSP90 (FC = Infinity) and HSP90-5 (FC = Infinity) in *H. ammodendron*, and two HSP90-2 (FC = 18.06; FC = Infinity), HSP90-5 (FC = 41.88) and HSP90-6 (FC = 16.52) genes in *H. persicum* were highly expressed under drought stress. Therefore, functional proteins play an important role in the mechanism of plant drought resistance.

As a major component of secondary cell walls, lignin plays an important role in plant resistance to drought stress (Cao et al., 2020; Gu et al., 2020). Recently, it has been shown that the increase of lignin enhances the tolerance of *P. ussuriensis* to drought stress (Li et al., 2022). Monomer lignin proceeds through the styrene-acrylic biosynthetic pathway (Liu et al., 2020). In this study, the expression levels of genes involved in lignin biosynthesis of *H. ammodendron* (such as 4CL, Beta-glucosidase, CCR, and COMT) and those involved in lignin biosynthesis of *H. persicum* (such as Beta-glucosidase, CADH, COMT, and Laccase) were increased. Similar results were obtained in *Paeonia ostii* (Zhao et al., 2021) and *L. kaempferi* (Li et al., 2021), suggesting that plants may enhance tolerance to drought stress by promoting lignin biosynthesis acceptability.

Under drought stress, sugar allocation, metabolism, and transport in plants are significantly altered (Du et al., 2020). Studies have shown that under drought conditions, non-structural carbohydrates such as sucrose and sugar alcohols accumulate in cells and increase osmotic stress tolerance (Tomasella et al., 2019). Zanella et al. (2016) showed that β-amylase catalyzes the breakdown of starch into soluble sugars, and overexpression of *AtADH1* in *Arabidopsis* improved total soluble sugar accumulation and enhanced resistance to abiotic stress (Shi et al., 2017). In this study, eight β-amylase DEGs of *H. ammodendron* and seven ADH1 DEGs of *H. persicum* were up-regulated, possibly indicating that *H. ammodendron* and *H. persicum* increase soluble sugars to adapt to drought stress.

Schematic model of *Haloxylon ammodendron* and *Haloxylon persicum* response to drought stress

Based on the main contents of drought-responsive DEGs and their associated pathways/networks, we proposed a schematic model (**Figure 9**). Under drought stress, the expression of a large number of genes in *H. ammodendron* and *H. persicum* changed, including stress signal sensing genes, anti-oxidative stress genes, functional protein genes, lignin biosynthesis genes and sugar metabolism genes. When threatened by drought stress: (1) plant cells can sense stress signals and transmit them from extracellular to intracellular through the regulation of ABA (abscisic acid 8′-hydroxylase, PYL, NCED, PP2C, ZEP, SnRK2, XERICO), Ca^{2+} (CaMBP, CBL, calcium-transporting ATPase, CaM, CML, CIPK, CDPK, CaBP), and MAPK (MAPK, MAPKK, MAPKKK) signaling cascade-related protein kinase genes that are then transcribed by related TFs (MYB, FAR1, AP2/ERF) in the nucleus that regulate the expression of related genes. (2) A large amount of ROS is produced in cells under drought stress, and this may cause oxidative damage to cells (Zhang et al., 2022). The ROS scavenging system can neutralize excess ROS (Wan et al., 2022). TFs promote the up-regulation of ROS scavenging system-related genes (APX, CAT, SOD; GPX, GST, POD) and reduce the ROS content in cells to reduce their damage to cells. (3) To reduce the damage of drought stress, the osmotic regulation-related genes in *H. ammodendron* and *H. persicum* were regulated by TFs in the nucleus. The up-regulation of β-amylase and ADH1 increases the synthesis of soluble sugars, and macromolecular proteins such as (AQP and HSP; ASR and HSP) begin to accumulate in large quantities, which can balance the intracellular and extracellular water potential to a certain extent. In addition, PIP proteins located on the cell membrane and PIP proteins located on the vacuolar membrane can also regulate the water balance in cells and vacuoles. (4) Drought stress can lead to ROS accumulation and other changes in the cell wall (Zhu, 2016). Lignin is the main component of secondary cell walls, and drought stress promotes the increased expression of lignin biosynthesis genes (4CL, Beta-glucosidase, CCOMT, CCR, COMT, F5H, Laccase; Beta-glucosidase, CADH, COMT, Laccase), thereby enhancing plant drought tolerance.

Conclusion

The responses of *H. ammodendron* and *H. persicum* to drought stress were studied through the synergy of physiological and molecular responses. Compared with *H. ammodendron*,

the growth environment of *H. persicum* is harsher (lower soil water content), resulting in greater growth and physiological changes of *H. ammodendron* in response to drought, and the response was faster and more intense. The Illumina RNA-seq and SMRT long-read sequences were integrated to obtain the full-length transcripts of *H. ammodendron* and *H. persicum*. In addition, LncRNAs and SSRs were obtained, and DEGs involved in drought regulation were analyzed. We found that the Ca^{2+} signaling pathway, the MAPK cascade, and the ABA signaling pathway play important roles under drought conditions, but the genes involved in their regulation vary greatly in number and expression patterns. The study also found that TFs such as FAR1, AP2/ERF, MYB, and WRKY were involved in the response to drought stress, but most of the genes involved in regulating of *H. ammodendron* were up-regulated, on the contrary, *H. persicum*. Physiological index measurements and bioinformatic observations showed that the expression patterns of genes related to ROS balance, glucose metabolism, functional proteins, and lignin biosynthesis were different between the two species under drought stress, indicating that *H. ammodendron* and *H. persicum* have different regulatory mechanisms and drought tolerance in response to drought stress. This study is the first step to establishing the full-length unparameterized transcriptome of *H. ammodendron* and *H. persicum*, and the results provide a foundation for further research on their regulatory mechanisms.

Data availability statement

The original contributions presented in this study are publicly available. This data can be found here: NCBI, PRJNA855227 available at: https://submit.ncbi.nlm.nih.gov/subs/.

Author contributions

FY and GL conceived the study. FY collected the data, analyzed the data, and drafted the text. Both authors edited the manuscript.

Funding

This work was supported by the Xinjiang Uygur Autonomous Region Innovation Environment Construction Special Project and Science and Technology Innovation Base construction project (PT2107) and Xinjiang Uygur Autonomous Region Graduate Innovation Project (Physiological Metabolism and Molecular Mechanism of Dioecious *Populus euphratica* in Dry and Wet Environment) (XJ2021G040).

Acknowledgments

We thank LetPub (www.letpub.com) for its linguistic assistance during the preparation of this manuscript.

Conflict of interest

The authors declare that the research was conducted in the absence of any commercial or financial relationships that could be construed as a potential conflict of interest.

Publisher's note

All claims expressed in this article are solely those of the authors and do not necessarily represent those of their affiliated organizations, or those of the publisher, the editors and the reviewers. Any product that may be evaluated in this article, or claim that may be made by its manufacturer, is not guaranteed or endorsed by the publisher.

Supplementary material

The Supplementary Material for this article can be found online at: https://www.frontiersin.org/articles/10.3389/fpls.2022.981029/full#supplementary-material

References

Aldon, D., Mbengue, M., Mazars, C., and Galaud, J. P. (2018). Calcium signaling in plant biotic interactions. *Int. J. Mol. Sci.* 9:665. doi: 10.3390/ijms19030665

Aleem, M., Aleem, S., Sharif, I., Wu, Z. Y., Aleem, M., Tahir, A., et al. (2022). Characterization of SOD and GPX gene families in the soybeans in response to drought and salinity stresses. *Antioxidants* 11:460. doi: 10.3390/antiox11030460

Ardui, S., Ameur, A., Vermeesch, J. R., and Hestand, M. S. (2018). Single molecule real-time (SMRT) sequencing comes of age: applications and utilities for medical diagnostics. *Nucleic Acids Res.* 46, 2159–2168. doi: 10.1093/nar/gky066

Bigeard, J., and Hirt, H. (2018). Nuclear signaling of plant MAPKs. *Front. Plant Sci.* 9:469. doi: 10.3389/fpls.2018.00469

Cao, S. M., Huang, C., Luo, L. F., Zheng, S., Zhong, Y., Sun, J. Y., et al. (2020). Cell-specific suppression of 4-coumarate-CoA ligase gene reveals differential effect of lignin on cell physiological function in *Populus*. *Front. Plant Sci.* 11:589729. doi: 10.3389/fpls.2020.589729

Chu, X. Q., Wang, C., Chen, X. B., Lu, W. J., Li, H., Wang, X. L., et al. (2016). Correction: the cotton WRKY gene GhWRKY41 positively regulates salt

and drought stress tolerance in transgenic *Nicotiana benthamiana*. *PLoS One* 11:e0157026. doi: 10.1371/journal.pone.0157026

Cui, X. Y., Du, Y. T., Fu, J. D., Yu, T. F., Wang, C. T., Chen, M., et al. (2018). Wheat CBL-interacting protein kinase 23 positively regulates drought stress and ABA responses. *BMC Plant Biol.* 18:93. doi: 10.1186/s12870-018-1306-5

Deng, Y., Zheng, H., Yan, Z. C., Liao, D. Y., Li, C. L., Zhou, J. Y., et al. (2018). Full-length transcriptome survey and expression analysis of Cassia obtusifolia to discover putative genes related to aurantio-obtusin biosynthesis, seed formation and development, and stress response. *Int. J. Mol. Sci.* 19:2476. doi: 10.3390/ijms19092476

Ding, Z. J., Yan, J. Y., Xu, X. Y., Yu, D. Q., Li, G. X., Zhang, S. Q., et al. (2014). Transcription factor WRKY 46 regulates osmotic stress responses and stomatal movement independently in Arabidopsis. *Plant J.* 79, 13–27. doi: 10.1111/tpj.12538

Doerge, D. R., Divi, R. L., and Churchwell, M. I. (1997). Identification of the colored guaiacol oxidation product produced by peroxidases. *Anal. Biochem.* 250, 10–17. doi: 10.1006/abio.1997.2191

Du, Y. L., Zhao, Q., Chen, L. R., Yao, X. D., Zhang, W., Zhang, B., et al. (2020). Effect of drought stress on sugar metabolism in leaves and roots of soybean seedlings. *Plant Physiol. Biochem.* 146, 1–12. doi: 10.1016/j.plaphy.2019.11.003

Fan, L. G., Wang, G. N., Hu, W., Pantha, P., Tran, K. N., Zhang, H., et al. (2018). Transcriptomic view of survival during early seedling growth of the extremophyte *Haloxylon ammodendron*. *Plant Physiol. Biochem.* 132, 475–489. doi: 10.1016/j.plaphy.2018.09.024

Finn, R. D., Coggill, P., Eberhardt, R. Y., Eddy, S. R., Mistry, J., Mitchell, A. L., et al. (2016). The Pfam protein families database: towards a more sustainable future. *Nucleic Acids Res.* 44, D279–D285. doi: 10.1093/nar/gkv1344

Fu, L. M., Niu, B. F., Zhu, Z. W., Wu, S. T., and Li, W. Z. (2012). CD-HIT: accelerated for clustering the next-generation sequencing data. *Bioinformatics* 28, 3150–3152. doi: 10.1093/bioinformatics/bts565

Golldack, D., Li, C., Mohan, H., and Probst, N. (2014). Tolerance to drought and salt stress in plants: unravelling the signaling networks. *Front. Plant Sci.* 5:151. doi: 10.3389/fpls.2014.00151

Gong, X. W., and Lü, G. H. (2017). Species diversity and dominant species' niches of eremophyte communities of the Tugai forest in the Ebinur basin of Xinjiang, China. *Biodivers. Sci.* 25, 34–45. doi: 10.17520/biods.2016166

Gu, H. G., Wang, Y., Xie, H., Qiu, C., Zhang, S. N., Xiao, J., et al. (2020). Drought stress triggers proteomic changes involving lignin, flavonoids and fatty acids in tea plants. *Sci. Rep.* 10:15504. doi: 10.1038/s41598-020-72596-1

Gupta, A., Rico-Medina, A., and Cano-Delgado, A. I. (2020). The physiology of plant responses to drought. *Science* 368, 266–269. doi: 10.1126/science.aaz7614

He, G. H., Xu, J. Y., Wang, Y. X., Liu, J. M., Li, P. S., Chen, M., et al. (2016). Drought-responsive WRKY transcription factor genes TaWRKY1 and TaWRKY33 from wheat confer drought and/or heat resistance in Arabidopsis. *BMC Plant Biol.* 16:116. doi: 10.1186/s12870-016-0806-4

Jaakola, L., Pirttila, A. M., Halonen, M., and Hohtola, A. (2001). Isolation of high quality RNA from bilberry (*Vaccinium myrtillus* L.) fruit. *Mol. Biotechnol.* 19, 201–203. doi: 10.1385/MB:19:2:201

Johansson, L. H., and Borg, L. A. H. (1988). A spectrophotometric method for determination of catalase activity in small tissue samples. *Anal. Biochem.* 174, 331–336. doi: 10.1016/0003-2697(88)90554-4

Kalapos, B., Dobrev, P., Nagy, T., Vítámvás, P., Györgyey, J., Kocsy, G., et al. (2016). Transcript and hormone analyses reveal the involvement of ABA-signaling, hormone crosstalk and genotype-specific biological processes in cold-shock response in wheat. *Plant Sci.* 253, 86–97. doi: 10.1016/j.plantsci.2016.09.017

Kang, Y. J., Yang, D. C., Kong, L., Hou, M., Meng, Y. Q., Wei, L. P., et al. (2017). CPC2: a fast and accurate coding potential calculator based on sequence intrinsic features. *Nucleic Acids Res.* 45, W12–W16. doi: 10.1093/nar/gkx428

Khadka, V. S., Vaughn, K., Xie, J., Swaminathan, P., Ma, Q., Cramer, G. R., et al. (2019). Transcriptomic response is more sensitive to water deficit in shoots than roots of *Vitis riparia* (Michx.). *BMC Plant Biol.* 19:72. doi: 10.1186/s12870-019-1664-7

Kumar, M., Kim, I., Kim, Y. K., Heo, J. B., Suh, M. C., and Kim, H. U. (2019). Strigolactone signaling genes showing differential expression patterns in Arabidopsis max Mutants. *Plants* 8:352. doi: 10.3390/plants8090352

Lai, M., Sun, X. M., Chen, D. S., Xie, Y. H., and Zhang, S. G. (2014). Age-related trends in genetic parameters for *Larix kaempferi* and their implications for early selection. *BMC Genet.* 15(Suppl. 1):S10. doi: 10.1186/1471-2156-15-S1-S10

Lamers, J., van der Meer, T., and Testerink, C. (2020). How plants sense and respond to stressful environments. *Plant Physiol.* 182, 1624–1635. doi: 10.1104/pp.19.01464

Li, A. M., Zhang, J. Y., and Zhou, Z. Y. (2014). PLEK: a tool for predicting long non-coding RNAs and messenger RNAs based on an improved K-mer scheme. *BMC Bioinformatics* 15:311. doi: 10.1186/1471-2105-15-311

Li, D. D., Yang, J. L., Pak, S., Zeng, M. Z., Sun, J. L., Yu, S., et al. (2022). PuC3H35 confers drought tolerance by enhancing lignin and proanthocyanidin biosynthesis in the roots of *Populus ussuriensis*. *New Phytol.* 233, 390–408. doi: 10.1111/nph.17799

Li, H. Y., Zhang, X., Tong, B. T., Wang, Y. C., and Yang, C. P. (2020). Expression analysis of the BpARF genes in *Betula platyphylla* under drought stress. *Plant Physiol. Biochem.* 148, 273–281. doi: 10.1016/j.plaphy.2020.01.028

Li, W. L., Lee, J., Yu, S., Wang, F. D., Lv, W. Q., Zhang, X., et al. (2021). Characterization and analysis of the transcriptome response to drought in *Larix kaempferi* using PacBio full-length cDNA sequencing integrated with de novo RNA-seq reads. *Planta* 253:28. doi: 10.1007/s00425-020-03555-3

Li, X. R., Tang, Y., Zhou, C. J., Zhang, L. X., and Lv, J. Y. (2020). A wheat WRKY transcription factor TaWRKY46 enhances tolerance to osmotic stress in transgenic Arabidopsis plants. *Int. J. Mol. Sci.* 21:1321. doi: 10.3390/ijms21041321

Liang, Y. N., Jiang, Y. L., Du, M., Li, B. Y., Chen, L., Chen, M. C., et al. (2019). *ZmASR3* from the maize *ASR* gene family positively regulates drought tolerance in transgenic Arabidopsis. *Int. J. Mol. Sci.* 20:2278. doi: 10.3390/ijms20092278

Liu, W., Jiang, Y., Wang, C., Zhao, L. L., Jin, Y. Z., Xing, Q. J., et al. (2020). Lignin synthesized by *CmCAD2* and *CmCAD3* in oriental melon (*Cucumis melo* L.) seedlings contributes to drought tolerance. *Plant Mol. Biol.* 103, 689–704. doi: 10.1007/s11103-020-01018-7

Long, Y., Zhang, J. W., Tian, X. J., Wu, S. S., Zhang, Q., Zhang, J. P., et al. (2014). De novo assembly of the desert tree *Haloxylon ammodendron* (C. A. Mey.) based on RNA-Seq data provides insight into drought response, gene discovery and marker identification. *BMC Genomics* 15:1111. doi: 10.1186/1471-2164-15-1111

Luan, S. (2002). Signaling drought in guard cells. *Plant Cell Environ.* 25, 229–237. doi: 10.1046/j.1365-3040.2002.00758.x

Mahmood, T., Khalid, S., Abdullah, M., Ahmed, Z., Shah, M. K. N., Ghafoor, A., et al. (2019). Insights into drought stress signaling in plants and the molecular genetic basis of cotton drought tolerance. *Cells* 9:105. doi: 10.3390/cells9010105

Ong, A. L., Teh, C. K., Mayes, S., Massawe, F., Appleton, D. R., and Kulaveerasingam, H. (2020). An improved oil palm genome assembly as a valuable resource for crop improvement and comparative genomics in the arecoideae subfamily. *Plants* 9:1476. doi: 10.3390/plants9111476

Pang, J. L., Zhang, X., Ma, X. H., and Jun, Z. (2019). Spatio-temporal transcriptional dynamics of maize long non-coding RNAs responsive to drought stress. *Genes* 10:138. doi: 10.3390/genes10020138

Park, C. J., and Seo, Y. S. (2015). Heat shock proteins: a review of the molecular chaperones for plant immunity. *Plant Pathol. J.* 31, 323–333. doi: 10.5423/PPJ.RW.08.2015.0150

Park, H. Y., Seok, H. Y., Park, B. K., Kim, S. H., Goh, C. H., Lee, B., et al. (2008). Overexpression of *Arabidopsis* ZEP enhances tolerance to osmotic stress. *Biochem. Biophys. Res. Commun.* 375, 80–85. doi: 10.1016/j.bbrc.2008.07.128

Persak, H., and Pitzschke, A. (2014). Dominant repression by Arabidopsis transcription factor MYB44 causes oxidative damage and hypersensitivity to abiotic stress. *Int. J. Mol. Sci.* 15, 2517–2537. doi: 10.3390/ijms15022517

Qian, X. D., Sun, Y. P., Zhou, G. F., Yuan, Y. M., Li, J., Huang, H. L., et al. (2019). Single-molecule real-time transcript sequencing identified flowering regulatory genes in *Crocus sativus*. *BMC Genomics* 20:857. doi: 10.1186/s12864-019-6200-5

Ramirez, G. L., Shi, L., Bergonzi, S. B., Oortwijn, M., FrancoZorrilla, J. M., SolanoTavira, R., et al. (2021). Potato CYCLING DOF FACTOR 1 and its lncRNA counterpart StFLORE link tuber development and drought response. *Plant J.* 105, 855–869. doi: 10.1111/tpj.15093

Rhoads, A., and Au, K. F. (2015). PacBio sequencing and its applications. *Genom. Proteom. Bioinform.* 13, 278–289. doi: 10.1016/j.gpb.2015.08.002

Sah, S. K., Reddy, K. R., and Li, J. (2016). Abscisic acid and abiotic stress tolerance in crop plants. *Front. Plant Sci.* 7:571. doi: 10.3389/fpls.2016.00571

Salmela, L., and Rivals, E. (2014). LoRDEC: accurate and efficient long read error correction. *Bioinformatics* 30, 3506–3514. doi: 10.1093/bioinformatics/btu538

Sarker, U., and Oba, S. (2018). Catalase, superoxide dismutase and ascorbate-glutathione cycle enzymes confer drought tolerance of *Amaranthus tricolor*. *Sci. Rep.* 8:16496. doi: 10.1038/s41598-018-34944-0

Sato, H., Takasaki, H., Takahashi, F., Suzuki, T., Iuchi, S., Mitsuda, N., et al. (2018). *Arabidopsis thaliana* NGATHA1 transcription factor induces ABA biosynthesis by activating *NCED3* gene during dehydration stress. *Proc. Natl. Acad. Sci. U. S. A.* 115, E11178–E11187. doi: 10.1073/pnas.1811491115

Satterfield, C. N., and Bonnell, A. H. (1955). Interferences in titanium sulfate method for hydrogen peroxide. *Anal. Chem.* 27, 1174–1175. doi: 10.1021/ac60103a042

Shi, H. T., Liu, W., Yao, Y., Wei, Y. X., and Chan, Z. L. (2017). *Alcohol dehydrogenase 1* (*ADH1*) confers both abiotic and biotic stress resistance in Arabidopsis. *Plant Sci.* 262, 24–31. doi: 10.1016/j.plantsci.2017.05.013

Shimizu, K., Adachi, J., and Muraoka, Y. (2006). ANGLE: a sequencing errors resistant program for predicting protein coding regions in unfinished cDNA. *J. Bioinform. Comput. Biol.* 4, 649–664. doi: 10.1142/s0219720006002260

Song, H. M., Zhao, R. M., Fan, P. X., Wang, X. C., Chen, X. Y., and Li, Y. X. (2009). Overexpression of *AtHsp90.2*, *AtHsp90.5* and *AtHsp90.7* in *Arabidopsis thaliana* enhances plant sensitivity to salt and drought stresses. *Planta* 229, 955–964. doi: 10.1007/s00425-008-0886-y

Song, S., Zhang, D. H., Ma, F. N., Xing, W. T., Huang, D. M., Wu, B., et al. (2022). Genome-wide identification and expression analyses of the aquaporin gene family in passion fruit (*Passiflora edulis*), revealing *PeTIP3-2* to be involved in drought stress. *Int. J. Mol. Sci.* 23:5720. doi: 10.3390/ijms23105720

Sun, H. M., Zhao, W. R., Liu, H., Su, C., Qian, Y. H., and Jiao, F. (2020). *MaCDSP32* from mulberry enhances resilience post-drought by regulating antioxidant activity and the osmotic content in transgenic tobacco. *Front. Plant Sci.* 11:419. doi: 10.3389/fpls.2020.00419

Sun, L., Luo, H. T., Bu, D. C., Zhao, G. G., Yu, K. T., Zhang, C. H., et al. (2013). Utilizing sequence intrinsic composition to classify protein-coding and long non-coding transcripts. *Nucleic Acids Res.* 41:e166. doi: 10.1093/nar/gkt646

Tang, D. F., Quan, C. Q., Lin, Y., Wei, K. H., Qin, S. S., Liang, Y., et al. (2022). Physio-morphological, biochemical and transcriptomic analyses provide insights into drought stress responses in *Mesona chinensis* Benth. *Front. Plant Sci.* 13:809723. doi: 10.3389/fpls.2022.809723

Tang, W. J., Ji, Q., Huang, Y. P., Jiang, Z. M., Bao, M. Z., Wang, H. Y., et al. (2013). Far-red elongated hypocotyl3 and far-red impaired response1 transcription factors integrate light and abscisic acid signaling in Arabidopsis. *Plant Physiol.* 163, 857–866. doi: 10.1104/pp.113.224386

Thayale Purayil, F., Rajashekar, B., Kurup, S., Cheruth, A. J., Subramaniam, S., Hassan Tawfik, N., et al. (2020). Transcriptome profiling of *Haloxylon persicum* (Bunge ex Boiss and Buhse) an endangered plant species under PEG-induced drought stress. *Genes* 11:640. doi: 10.3390/genes11060640

Thudi, M., Li, Y. P., Jackson, S. A., May, G. D., and Varshney, R. K. (2012). Current state-of-art of sequencing technologies for plant genomics research. *Brief Funct. Genom.* 11, 3–11. doi: 10.1093/bfgp/elr045

Tomasella, M., Petrussa, E., Petruzzellis, F., Nardini, A., and Casolo, V. (2019). The possible role of non-structural carbohydrates in the regulation of tree hydraulics. *Int. J. Mol. Sci.* 21:114. doi: 10.3390/ijms21010144

Van Dijk, E. L., Jaszczyszyn, Y., Naquin, D., and Thermes, C. (2018). The third revolution in sequencing technology. *Trends Genet.* 34, 666–681. doi: 10.1016/j.tig.2018.05.008

Wahibah, N. N., Tsutsui, T., Tamaoki, D., Sato, K., and Nishiuchi, T. (2018). Expression of barley Glutathione S-Transferase13 gene reduces accumulation of reactive oxygen species by trichothecenes and paraquat in Arabidopsis plants. *Plant Biotechnol.* 35, 71–79. doi: 10.5511/plantbiotechnology.18.0205a

Wan, H. P., Qian, J. L., Zhang, H., Lu, H. C., Li, O. Q., Li, R. H., et al. (2022). Combined transcriptomics and metabolomics analysis reveals the molecular mechanism of salt tolerance of Huayouza 62, an elite cultivar in rapeseed (*Brassica napus* L.). *Int. J. Mol. Sci.* 23:1279. doi: 10.3390/ijms23031279

Wang, L. L., Chen, A. P., Zhong, N. Q., Liu, N., Wu, X. M., Wang, F., et al. (2014). The thellungiella salsuginea tonoplast aquaporin TsTIP1;2 functions in protection against multiple abiotic stresses. *Plant Cell Physiol.* 55, 148–161. doi: 10.1093/pcp/pct166

Wang, W. B., Kim, Y. H., Lee, H. S., Kim, K. Y., Deng, X. P., and Kwak, S. S. (2009). Analysis of antioxidant enzyme activity during germination of alfalfa under salt and drought stresses. *Plant Physiol. Biochem.* 47, 570–577. doi: 10.1016/j.plaphy.2009.02.009

Weng, C. M., Lu, J. X., Wan, H. F., Wang, S. W., Zhen, K., and Liang, Y. (2014). Over-expression of *BnMAPK1* in *Brassica napus* enhances tolerance to drought stress. *J. Integr. Agric.* 13, 2407–2415.doi: 10.1016/S2095-3119(13)60696-6

Wu, J. M., Mao, X. Z., Cai, T., Luo, J. C., and Wei, L. P. (2006). KOBAS server: a web-based platform for automated annotation and pathway identification. *Nucleic Acids Res.* 34(Suppl._2), W720–W724. doi: 10.1093/nar/gkl167

Wu, L. J., Zu, X. F., Zhang, H. M., Wu, L. C., Xi, G. Y., and Chen, Y. H. (2015). Overexpression of *ZmMAPKl* enhances drought and heat stress in transgenic *Arabidopsis thaliana*. *Plant Mol. Biol.* 88, 429–443.doi: 10.1007/s11103-015-0333-y

Xuan, H. D., Huang, Y. Z., Zhou, L., Deng, S. S., Wang, C. C., Xu, J. Y., et al. (2022). Key soybean seedlings drought-responsive genes and pathways revealed by comparative transcriptome analyses of two cultivars. *Int. J. Mol. Sci.* 23:2893. doi: 10.3390/ijms23052893

Yamada, K., and Nishimura, M. (2008). Cytosolic heat shock protein 90 regulates heat shock transcription factor in *Arabidopsis thaliana*. *Plant Signal. Behav.* 3, 660–662. doi: 10.4161/psb.3.9.5775

Yao, C. Y., Li, W. H., Liang, X. Q., Ren, C. K., Liu, W. D., Yang, G. H., et al. (2022). Molecular cloning and characterization of *MbMYB108*, a *Malus baccata* MYB transcription factor gene, with functions in tolerance to cold and drought stress in transgenic *Arabidopsis thaliana*. *Int. J. Mol. Sci.* 23:4846. doi: 10.3390/ijms23094846

Yildirim, K., and Kaya, Z. (2017). Gene regulation network behind drought escape, avoidance and tolerance strategies in black poplar (*Populus nigra* L.). *Plant Physiol. Biochem.* 115, 183–199. doi: 10.1016/j.plaphy.2017.03.020

Young, M. D., Wakefield, M. J., Smyth, G. K., and Oshlack, A. (2010). Gene ontology analysis for RNA-seq: accounting for selection bias. *Genome Biol.* 11:R14. doi: 10.1186/gb-2010-11-2-r14

Yu, W. Q., Zhao, R. R., Wang, L., Zhang, S. J., Li, R., Sheng, J. P., et al. (2019). ABA signaling rather than ABA metabolism is involved in trehalose-induced drought tolerance in tomato plants. *Planta* 250, 643–655. doi: 10.1007/s00425-019-03195-2

Zanella, M., Borghi, G. L., Pirone, C., Thalmann, M., Pazmino, D., Costa, A., et al. (2016). β-amylase 1 (BAM1) degrades transitory starch to sustain proline biosynthesis during drought stress. *J. Exp. Bot.* 67, 1819–1826. doi: 10.1093/jxb/erv572

Zhang, G. Q., Sun, M., Wang, J. F., Lei, M., Li, C. J., Zhao, D. J., et al. (2019). PacBio full-length cDNA sequencing integrated with RNA-seq reads drastically improves the discovery of splicing transcripts in rice. *Plant J.* 97, 296–305. doi: 10.1111/tpj.14120

Zhang, H. M., Zhu, J. H., Gong, Z. Z., and Zhu, J. K. (2022). Abiotic stress responses in plants. *Nat. Rev. Genet.* 23, 104–119. doi: 10.1038/s41576-021-00413-0

Zhao, D. Q., Luan, Y. T., Shi, W. B., Zhang, X. Y., Meng, J. S., and Tao, J. (2021). A *Paeonia ostii* caffeoyl-CoA O-methyltransferase confers drought stress tolerance by promoting lignin synthesis and ROS scavenging. *Plant Sci.* 303:110765. doi: 10.1016/j.plantsci.2020.110765

Zhao, Q., He, L., Wang, B., Liu, Q. L., Pan, Y. Z., Zhang, F., et al. (2018). Transcriptome comparative analysis of salt stress responsiveness in chrysanthemum (*Dendranthema grandiflorum*) roots by Illumina- and single-molecule real-time-based RNA sequencing. *DNA Cell Biol.* 37, 1016–1030. doi: 10.1089/dna.2018.4352

Zhu, J. K. (2016). Abiotic stress signaling and responses in plants. *Cell* 167, 313–324. doi: 10.1016/j.cell.2016.08.029

frontiers | Frontiers in Plant Science

TYPE Original Research
PUBLISHED 29 August 2022
DOI 10.3389/fpls.2022.991171

Check for updates

OPEN ACCESS

EDITED BY
Caroline Müller,
Universidade Federal da Fronteira Sul, Brazil

REVIEWED BY
Weijun Zheng,
Northwest A&F University, China
Xinlei Guo,
Henan Institute of Science and Technology, China
Zongyun Feng,
Sichuan Agricultural University, China

*CORRESPONDENCE
Yueming Yan
yanym@cnu.edu.cn

†These authors have contributed equally to this work

SPECIALTY SECTION
This article was submitted to Plant Abiotic Stress, a section of the journal Frontiers in Plant Science

RECEIVED 11 July 2022
ACCEPTED 09 August 2022
PUBLISHED 29 August 2022

CITATION
Gao X, Zou R, Sun H, Liu J, Duan W, Hu Y and Yan Y (2022) Genome-wide identification of wheat ABC1K gene family and functional dissection of *TaABC1K3* and *TaABC1K6* involved in drought tolerance. *Front. Plant Sci.* 13:991171. doi: 10.3389/fpls.2022.991171

COPYRIGHT
© 2022 Gao, Zou, Sun, Liu, Duan, Hu and Yan. This is an open-access article distributed under the terms of the Creative Commons Attribution License (CC BY). The use, distribution or reproduction in other forums is permitted, provided the original author(s) and the copyright owner(s) are credited and that the original publication in this journal is cited, in accordance with accepted academic practice. No use, distribution or reproduction is permitted which does not comply with these terms.

Genome-wide identification of wheat ABC1K gene family and functional dissection of *TaABC1K3* and *TaABC1K6* involved in drought tolerance

Xiaoran Gao†, Rong Zou†, Haocheng Sun†, Junxian Liu, Wenjing Duan, Yingkao Hu and Yueming Yan*

College of Life Science, Capital Normal University, Beijing, China

Activity of BC1 complex kinase (ABC1K) serves as an atypical kinase family involved in plant stress resistance. This study identified 44 *ABC1K* genes in the wheat genome, which contained three clades (I–III). *TaABC1K* genes generally had similar structural features, but differences were present in motif and exon compositions from different clade members. More type II functional divergence sites were detected between clade I and clade III and no positive selection site were found in *TaABC1K* family. The three-dimensional structure prediction by Alphafold2 showed that TaABC1K proteins had more α-helixes with a relatively even distribution, and different clade members had differences in the content of secondary structures. The *cis*-acting element analysis showed that *TaABC1K* genes contained abundant *cis*-acting elements related to plant hormones and environmental stress response in the promoter region, and generally displayed a significantly upregulated expression under drought stress. In particular, both *TaABC1K3* and *TaABC1K6* genes from clade I was highly induced by drought stress, and their overexpression in yeast and *Arabidopsis* enhanced drought tolerance by suppressing active oxygen burst and reducing photosynthesis impairment. Meanwhile, *TaABC1K3* and *TaABC1K6* could, respectively, complement the function of *Arabidopsis abc1k3* and *abc1k6* mutants and reduce photosynthesis damage caused by drought stress.

KEYWORDS

wheat, *ABC1K* genes, phylogenetics, *cis*-acting elements, drought stress, reactive oxygen species

Introduction

As an evolved primitive atypical kinase family, activity of BC1 complex kinase (ABC1K) is widely distributed in prokaryotes and eukaryotes. The atypical protein kinases (aPKs) have little or no homology with eukaryotic protein kinases (ePKs), although their crystal structures have similar protein kinase folds (Bayer et al., 2012). ABC1Ks do not have many of the ePKs features as the functional domain HMM (Scheeff and Bourne, 2005), and

generally possess the most conservative kinase motif, including VAIK catalytic motif, VAVK motif, and DFG motif (Jasinski et al., 2008). An ABC1K functional domain contains about 350 amino acid residues and 12 conserved motifs through analyzing the amino acid sequences of 100 ABC1K proteins from seven angiosperms (Lundquist et al., 2012a). Studies indicated that *ABC1K* proteins are localized in nucleoid, mitochondria, chloroplast, and plastoglobule of *Arabidopsis* (Gao et al., 2014), rice (Gao et al., 2011; Yang et al., 2012c), and maize (Gao et al., 2010). In *Arabidopsis*, 17 *ABC1K* family members were found, of which six were located in chloroplasts, mainly in plastids (Wang et al., 2011).

The first member of *ABC1K* family was found in *Saccharomyces cerevisiae*, which has the function of ensuring the correct formation of the cytochrome b6f complex by inhibiting the defects in cytochrome b mRNA translation produced by mutations in the *cbs2* gene of the nuclear translation activator (Bousquet et al., 1991; Bonnefoy et al., 1996). Since then, *ABC1Ks* have been found in rice (Yang et al., 2012c), maize (Gao et al., 2011), tomatoes (Li et al., 2015), and *Arabidopsis* (Jasinski et al., 2008). *AtABC1K8* (*AtOSA1*) was firstly identified in the chloroplast, which is essential for reactive oxygen species (ROS) scavenging under oxidative stress. The *AtABC1K8* mutant plants were more susceptible to cadmium toxicity, high light, and H_2O_2. In chloroplast, ABC1K could phosphorylate tocopherol cyclase VTE1 *in vitro* (Martinis et al., 2013, 2014), regulating vitamin E synthesis and recycling and promoting the production of α-tocopherol that function in the detoxification of $^1O_2$ (Kruk and Trebst, 2008; Martinis et al., 2013, 2014). In various signaling pathways, protein phosphorylation catalyzed by protein kinase is an important mechanism in which plants respond to abiotic stress, as well as a major post-translational modification in the signaling pathway (Ichimura et al., 2000). The products of *ABC1K1* and its homolog *ABC1K3* play an important regulatory role in the metabolism of chlorophyll and photooxidative damage of plants (Yang et al., 2012a). *ABC1K1* and *ABC1K3* deletions in *Arabidopsis* caused significant decrease in chlorophyll content and the degradation of chlorophyll-binding proteins, and the structural components of quinones on the membrane system were also affected (Yang et al., 2012b; Lundquist et al., 2013).

Wheat (*Triticum aestivum* L., $2n = 6x = 42$, AABBDD) is one of the three most important food crops with 17% of the world's crop area as well as the main food source for 30% of the global population (Gill et al., 2004; Mayer et al., 2014). In natural conditions, extreme environmental stress such as salt, drought, and high temperature stress seriously affects wheat growth and development and causes a significant decline in grain yield and quality (Xiong et al., 2002). As the increasing world's population as well as the great challenges for global food security, it is highly important to discover new stress-resistant genes and to improve the adaptability of wheat and other food crops.

TaABC1K proteins have more than 59.6% identities with the putative ABC1K proteins from *R. communis*, *P. tichocarpa*, and *Arabidopsis thaliana*. An aminoglycoside phosphotransferase choline kinase (APH_ChoK) domain is also present in the putative protein sequence of TaABC1K (Wang et al., 2011). The overexpressed wheat *TaABC1K* in *Arabidopsis* enhanced plant tolerance to drought, salt, cold stress, and stripe rust (Wang et al., 2013; Wu et al., 2020). Drought and rewatering experiments showed that 49–80% of the *TaABC1K* overexpressed plants survived whereas the corresponding survival rate in the wild type (WT) was only 25%. In addition, the maximum photochemistry efficiencies of PSII in the *TaABC1K* overexpressed plants under drought stress were significantly increased compared with WT. *TaABC1K* overexpressed plants had higher water retention and osmotic adjustment abilities, as well as decreased levels of damage to photosynthetic proteins and pigments, which were beneficial for enhancing tolerance to abiotic stresses. *TaABC1K* also serves as a regulatory factor participating in multiple stress-responsive genes such as DREB2A, RD29A, and ABF3 to decrease the damage of abiotic stresses (Wang et al., 2011). However, comprehensive studies on the structural and evolutionary characteristics and functional properties of the wheat *ABC1K* gene family still lack so far.

In this study, we used the newly released wheat genome database (IWGSC RefSeq v2.1) to perform a comprehensive genome-wide analysis of the wheat *ABC1K* gene family, and the function properties of *TaABC1K3* and *TaABC1K6* genes involved in drought response were further dissected through *S. cerevisiae* and *Arabidopsis* genetic transformation. We aim to further dissect the structure and molecular evolutionary characteristics of the wheat *ABC1K* gene family and its expression profiling and functional properties in response to abiotic stress.

Materials and methods

Retrieval and identification of wheat *ABC1K* genes

The amino acid sequences of 17 *AtABC1K* gene family members from *A. thaliana* were firstly downloaded from the Phytozome plant data website.[1] The obtained AtABC1K protein sequences were used for BLASTP operation to retrieve the newly released wheat genome database (IWGSC RefSeq v2.1) in Ensembl Plants.[2] The candidate TaABC1K sequences were analyzed

Abbreviations: ABRE, Abscisic acid response element; ARE, Cis-acting regulatory element; ASC, Ascorbate; CAT, Catalase; DAB, 3,3′-Diaminobenzidine; DCFH-DA, 2,7-Dichlorodihydrofluorescein diacetate; DPA, Day post-anthesis; GFP, Green fluorescent protein; GSH, Glutathione; LTR, Long terminal repeat; NBT, Nitrotetrazolium blue chloride; ROS, Reactive oxygen species; RT-qPCR, Quantitative real-time polymerase chain reaction; SOD, Superoxide dismutase; ZEP, Zeaxanthin cycleoxidase.

1 https://phytozome-next.jgi.doe.gov/

2 http://plants.ensembl.Org/

through SMART (Letunic and Bork, 2018) and Pfam[3] (Finn et al., 2014; Mistry et al., 2021) to verify if the obtained sequences contained conserved *ABC1* functional domain. HHMER was used to check the *TaABC1K* gene family based on the *ABC1* domain (Finn et al., 2011). The isoelectric point and molecular mass of wheat ABC1K proteins were identified using the ExPASy database[4] and the results were analyzed by SPSS software.

Chromosomal assignment and collinearity analysis of *TaABC1K* genes

The *TaABC1K* gene positions were determined by using *Ensembl Plant*s and MCScanX was used to analyze the amino acid sequences of *ABC1K* gene family members (Wang et al., 2012). The chromosomal localization and collinearity analysis of *ABC1K* gene family members were performed by TBtools (Chen et al., 2020).

Phylogenetic and exon-intron structure analysis

Multiple sequence alignment for the identified ABC1K protein sequences was carried out by using MUSCLE software (Han et al., 2019).[5] A Bayesian evolutionary tree was constructed by MrBayes 3.2.5 software according to the alignment files (Ronquist et al., 2012), and the reliability of the internal branches of the phylogenetic tree was evaluated through setting 1,000 cycles of self-priding resampling (Saitou and Nei, 1987; Tamura et al., 2013). The exon-intron structure characteristics of *ABC1K* gene family members were detected by gene structure display server (GSDS; Hu et al., 2014).[6] The conserved motifs of ABC1K proteins were analyzed by the online MEME (Bailey and Elkan, 1994; Bailey et al., 2009).[7] The maximum number of motifs was set to 15 and other parameters remained as default.

Three-dimensional structure simulation by AlphaFold2 and molecular evolution analysis of ABC1K gene family

The three-dimensional (3D) structures of TaABC1K proteins from different clades were predicted using the online Alphafold2 website according to Duan et al. (2022). As the latest developed protein predicting tool, Alphafold has high accuracy and easy-to-use (Jumper et al., 2021). The type I and type II functional divergence sites in different subfamilies were detected using DIVERGE 3.0, and the critical value of posterior probability (Qk) was set to 0.8 (Gu et al., 2013). The site model in the PAML 4.4 software package (Yang, 2007) was used for positive selection analysis, using the site-specific model. When the non-synonymous substitution rate (dN) is higher than the synonymous rate (dS), in which the ratio ω (dN/dS) is higher than 1, it represents a positive selection. In this study, two pairs of models were selected using the BEB estimation method. The model comparison was according to Wu et al. (2014). Finally, the likelihood ratio test was used to detect the positive selections. Coevolution sites between amino acids were detected by using Protein Sequences (CAPS) in PERL software (Fares and McNally, 2006).

The *cis*-acting element identification and RNA-seq expression analysis of *TaABC1K* genes

According to Li et al. (2021), 1,500 bp promoter region from the *TaABC1K* gene initiation codon was downloaded from the Ensembl Plant database, and the number and type of the *cis*-acting elements were analyzed by PlantCARE online website[8] based on Rombauts et al. (1999). The publicly Chinese Spring (CS) wheat RNA-seq database was used to analyze RNA-seq data of TaABC1K encoding genes from the expVIP website.[9] The transcriptional expression profiling at different grain developmental stages and in response to various stress treatments was detected. TPM was used for RNA-seq data and the data was normalized. TBtools was used for heatmap construction and cluster analysis according to Li et al. (2021).

Plant materials, cultivation, and treatments

The seeds of wheat variety CS were sterilized and cultured based on the reported method by Han et al. (2019). The samples from seedling roots, stems, and leaves at the three-leaf stage and developing grains at 15 days post anthesis (DPA) were collected from three biological replicates. At the same time, seedlings at the three-leaf stage were treated with the following abiotic stress conditions: simulated drought [20% (W/V) PEG 6000] and oxidation stress (15 mM H_2O_2). Seedlings with normal culture condition were used as control (CK). The leave samples were collected after 12 h of treatment, and then all samples were quickly frozen with liquid nitrogen and stored in −80°C for later use. *Arabidopsis abc1k3* and *abc1k6* mutants were purchased from SALK website and *A. thaliana* Col-0 was used as WT. The

3 http://pfam.xfam.org
4 https://web.expasy.org/compute_pi/
5 http://www.ebi.ac.uk/Tools/msa/muscle/
6 http://gsds.cbi.pku.edu.cn/
7 http://meme-suite.org/tools/meme
8 http://bioinformatics.psb.ugent.be/-webtools/plantcare/html/
9 http://www.wheat-expression.com/

Arabidopsis seeds were sterilized and cultured referred to Li et al. (2017).

RT-qPCR

Total RNA extractions of wheat seedling leaves from different treatments and RT-qPCR were conducted according to Zhu et al. (2021). The internal reference gene was 18S, and CFX96 real-time PCR detection system (Bio-RAD, Hercules, CA, United States) was used to perform RT-qPCR. The relative gene expression levels were calculated by $2^{-\Delta\Delta Ct}$ method (Livak and Schmittgen, 2001; Yu et al., 2016). Three biological replicates were carried out on each sample and the significance of the experimental results was detected by one-way ANOVA.

Subcellular localization

The subcellular localization of TaABC1K proteins was performed referring to the methods of Yoo et al. (2007) and Liu et al. (2018). GFP signal and chlorophyll red auto-fluorescence were observed and photographed by confocal laser scanning microscope (Zeiss LSM 780, Germany). The excitation light for GFP was 503–518 nm while the chloroplast spontaneous fluoresces were 590–608 nm.

Overexpression of *TaABC1K* genes in *Saccharomyces cerevisiae*

The full CDS of *TaABC1K* genes were cloned into vector pYES2.0. Empty vector and recombinant vectors were transformed into yeast strain BY4741 referred to the standard procedures (Invirogen), and then cultured in SD-Ura (2% glucose) solid medium for 3 days. Single colonies were selected and cultured in liquid SD-Ura (2% glucose) medium until OD = 2.0, and then diluted to six stepped concentration and dropped onto a solid SD-Ura (2% glucose) medium with or without 5 mm H_2O_2 and 600 mM mannitol (simulated drought treatment).

Overexpression and complementation of *TaABC1K* genes in *Arabidopsis*

The wild-type Col-0 and *abc1k3* and *abc1k6* mutants of *A. thaliana* were used as materials for overexpression and complementation experiments of *TaABC1K* genes, respectively. The recombinant plasmid pCAMBIA1302-*TaABC1K* was transferred into *Agrobacterium* GV3101 strain according to Weigel and Glazebrook (2006). Transgenic plants were generated using the stigma infiltration method (Bechtold and Bouchez, 1995) and consecutive identification and screening, in which the positive seedlings were selected on a ½ MS medium containing 50 mg/l kanamycin. Transgenic lines were generated after at least two generations of positive screening (Li et al., 2017).

Determination of hydrogen peroxide and superoxide in *Arabidopsis* under drought stress

H_2O_2 and O_2^- levels in *TaABC1K* overexpressed and complementary *A. thaliana* leaves were detected. The 5-day-old *Arabidopsis* seedlings were transferred into ½ MS petri dish and treated with 400 mM mannitol for 12 h. Seedlings in normal conditions were set as control group. H_2O_2 content was detected by DAB staining according to Wang et al. (2016) with minor modifications. The seedlings were soaked in 0.5% DAB with 10 mm Tris–HCl (pH 4) staining solution and vacuumed at 60 kPa for 10 min in dark, then chlorophyll was removed with bleaching solution (ethanol: acetic acid: glycerol = 3:1:1) in boiling bath. The O_2^- level was measured by NBT staining, where the samples were soaked in 1 mM NBT with 200 mM K_2HPHO_3 (pH 6.2) and vacuumed at 60 kPa for 10 min in dark. The samples were immersed in fixative solution (10 ml methanol, 2 ml HCl, 38 ml H_2O) for 15 min and decolorized with 7% NaOH and 60% ethanol in boiling bath. Seedlings were soaked in 50 mm DCFH-DA dye with 20 mM K_2HPO_3 and cultured in dark for 10 min. The roots of the treated seedlings were observed by confocal fluorescence microscope Zeiss LSM 780, and the excitation wavelength was set to 488.

Measurement of chlorophyll content and chlorophyll fluorescence

Chlorophyll fluorescence was tested using an IMAGING PAM chlorophyll fluorescence meter (Walz, Effeltrich, Germany). *A. thaliana* plants were treated with or without drought stress for 1 week and preconditioned to complete darkness for more than 30 min before measurement (Schreiber et al., 2007). The experiment was conducted according to Zhu et al. (2021). The related photosynthetic parameters were obtained and calculated during the measurement, including the maximum photosynthetic efficiency by $F_v/F_m = (F_m\text{-}F_o)/F_m$, and the photochemical efficiency of PSII in the light by $\Phi(\text{PSII}) = F_v'/F_m' = (F_m'\text{-}F_s)/F_m'$ according to Genty and Baker (1989).

Results

Genome-wide identification of wheat *ABC1K* gene family

Firstly, 17 ABC1K protein sequences from *Arabidopsis* were used to perform BlastP in the Phytozome and Ensembl Plant websites that cover the latest genomic data of wheat. In total, 180

ABC1K gene family members from eight plant species were identified (Supplementary Table 1). In wheat, 44 *TaABC1K* genes were identified. The physicochemical properties of 44 TaABC1K proteins are shown in Supplementary Table 2, including gene ID, sequence length, molecular weight, isoelectric point, and the locations on chromosome. The results showed that the length of the coding sequence (CDS) of wheat *ABC1K* genes ranged from 1,425 to 3,373 bp encoding 373–954 amino acid residues. The molecular weight of ABC1K members ranged from 42 to 105 kDa, with an average of 72.31 kDa. The pI fluctuated between 5.01 and 9.97 (average value 7.67) with weak alkalinity. These results indicated that the members of the wheat ABC1K family had great differences in protein size, isoelectric point, and other physicochemical properties, suggesting their functional differentiation during the evolutionary process.

Phylogenetic and structural analysis of *TaABC1K* genes

According to the Bayesian topology constructed by protein sequences from eight plant species (Figure 1), *ABC1K* gene family members were classified into three branches: Clade I (endoplast symbiotic branch), Clade II (mitochondrial endoplast symbiotic branch), and Clade III (ancestral branch). Most ABC1K genes belonged to clade I (101 genes), then clade II (56 genes), and clade III (23 genes). In particular, the *ABC1K* genes from each plant species were also classified into three same clades, indicating the close evolutionary relationships of plant *TaABC1K* gene family. Among 44 *TaABC1K* genes in wheat, 24, 14 and 6 members belonged to Clade I, Clade II, and Clade III, respectively (Supplementary Figure 1). An *ABC1* functional domain with about 120 amino acid residues was found in each *ABC1K* family member *via* SMART website. Additionally, *ABC1* functional domain had a VAVK-like motif (e.g., VAVK, VVIK, VAMK, or VVVK) and a DFG-like motif (e.g., DFG, DHG, or DVG; Supplementary Figure 2). All members included a VAVK-like motif except TraesCS4A03G0990700 and TraesCS2D03G 1171700 in Clade I and a DFG-like motif except TraesCS6B03 G0453400 in Clade III.

The sequence motifs of each member of *TaABC1K* genes were analyzed by the online website MEME (Figure 2A). A total of 10 motifs were found, of which motifs 1–7 were present in 33 *TaABC1K* genes. In clade I, the number of motifs ranged from 7 to 11, and 19 in 24 genes had motif 1–7, in which 11 genes had 10 motifs. In clade II and clade III, the number of motifs ranged from 6–10 to 5–8, 9 in 14 members of clade II contained motif 1–7, and 5 in 6 members in clade III contained motif 1–8. According to the detection, the numbers and positions of motifs were relatively conserved among the internal members of each clade, but differences in the number of motifs were present in different clades.

The intron-exon structure characteristics of wheat *ABC1K* genes were analyzed by using the GSDS. The results demonstrated that the intron-exon compositions of *TaABC1K* genes from the same branch had similar structural characteristics but differed greatly among different branches (Figure 2B). In clade I, the number of exons ranged from 5 to 20, which fluctuated greatly compared to the other clades. Members of clade II had 8–18 exons with similar distributions while those in clade III only had 2–4 exons and 1–5 introns.

Alphafold2 was used to predict the 3D structures of nine TaABC1K proteins from different clades. Alphafold has shown highly successful predicting protein 3D structure from their amino acid sequences (Jumper et al., 2021), and has clear advantages such as its remarkable success in independent assessments of prediction accuracy, which can predict 98.5% of the human proteome (Ruff and Pappu, 2021) as well as multimer interactions (Mirdita et al., 2021). As shown in Figure 3, TaABC1K proteins were constructed mainly by α-helix and random coil, and generally had 11–18 α-helixes with a relatively even distribution. In particular, based on the results of three proteins selected from each clade, the calculation of the percentage of α-helix, random coil, and β-sheet showed that three TaABC1K proteins from clade II had significantly higher α-helix and β-sheet, which was 29 and 57% higher than those from clade III. The three proteins from clade III had significantly higher random coil while the content of α-helix, random coil, and β-sheet of three TaABC1K proteins from clade I were between clade II and clade III (Supplementary Table 3).

Functional divergence, positive selection, and coevolution analysis of *TaABC1K* genes

The posterior probability (Qk) of divergence was set as $Qk < 0.8$ to screen important amino acid sites between every two clades according to Yang et al. (2005). As shown in Supplementary Table 4, the type I function divergence sites were found between clade I and clade III, and clade II and clade III with function divergence coefficient (θI) 0.28 to 0.5 and −0.048 to 0.188, respectively. Four type I function divergence sites (331 V, 365Y, 336Q 331G) were identified between clade I and clade III, and one site (331 V) was identified between clade II and clade III. At the same time, 31 type II function divergence sites between clade I and clade III with θII 0.69 to 0.71 were found. In particular, the amino acid sites 331 V and 365Y belonged to both type I and type II functional divergence sites, suggesting that both sites underwent divergences concurrently. Two pairs of site models (M0/M3 and M7/M8) were used for positive selection analysis, and no positive selection sites were detected (Supplementary Table 5). Coevolution analysis identified 18 groups of coevolution sites (Supplementary Table 6), of which 9 groups were adjacent in the primary structure, and most of them showed different distributions from functional divergence sites. These coevolutionary sites might be beneficial for *TaABC1K*s to maintain the spatial structure and to adapt to environmental changes.

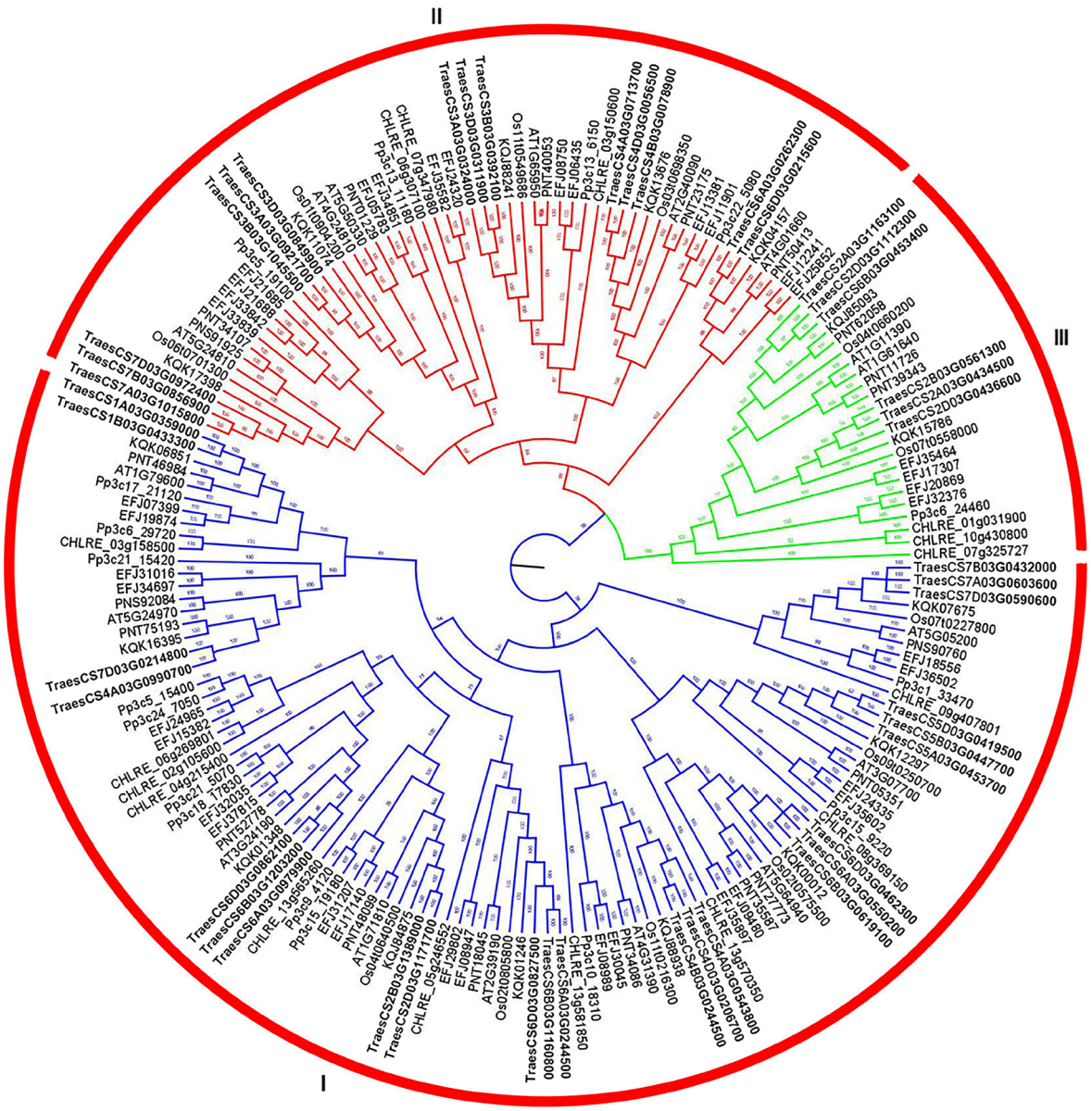


FIGURE 1
Bayesian phylogenetic tree of *ABC1K* gene family from *Triticum aestivum*, *Arabidopsis thaliana*, *Selaginella moellendorffii*, *Physcomitrella patens*, *Populus trichocarpa*, *Brachypodium distachyon*, *Chlamydomonas reinhardtii*, and *Oryza sativa*.

Chromosomal assignment and collinearity analysis of *TaABC1K* genes

The distribution of 44 *TaABC1K* family members on chromosomes was analyzed referred to the latest CS wheat genome data. As shown in Figure 4, 44 *TaABC1K* genes were unevenly distributed on the 20 chromosomes of wheat with an even distribution on three subgenomes: 15 on the chromosome A, 14 on the chromosome B, and 15 on chromosome D. Collinearity analysis showed that most of the *TaABC1K* genes had orthologous genes on A/B/D chromosomes such as TraesCS3A03G0324000, TraesCS3B03G0392100, and TraesCS3D03G0311900 while most of the orthologous genes were clustered on the chromosome 6 and 7. However, the 1D chromosome had no *TaABC1K* genes that might lost during species evolution. In addition, TraesCS4A03G0990700 on chromosome 4A and TraesCS7D03G0214800 on chromosome 7D were paralogous genes, possibly caused by fragment repetition.

Analysis of *cis*-acting elements in *TaABC1K* genes

The online tool PlantCARE was used to identify *cis*-acting elements in the 1,500 bp upstream promoter sequences of wheat

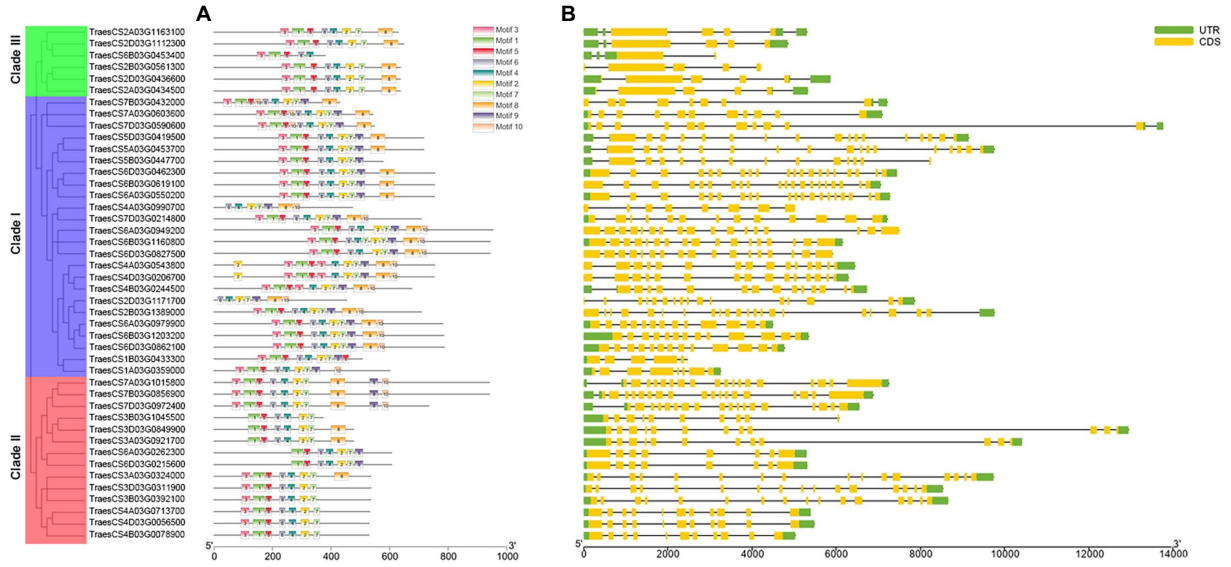


FIGURE 2
The motif and exon-intron structure of wheat ABC1K gene family members. **(A)** Conservative motifs of TaABC1K proteins. **(B)** Exon-intron structures of *TaABC1K* gene family.

ABC1K genes and the results are showed in Supplementary Figure 3. In general, *TaABC1K* genes from three branches had a similar composition of *cis*-acting elements (Supplementary Figure 3A), also reflecting the evolutionary conservation of the *TaABC1K* gene family.

Light response elements were widely present in wheat *ABC1K* genes and 27 *cis*-acting elements related to light reaction were identified, including G-box, SP1, and Box4 (Supplementary Figure 3B). Among them, G-box (CACGAC/CACGTG) was the most abundant light response element, and each subfamily member contained more than two copies of G-box elements on average. G-Box can combine with G-Box binding factors (GBFs) to regulate the expression of multiple genes (Gao et al., 2012). A total of 10 development-related elements were detected, of which CAT-box and CCGTCC-box were the most widely distributed. Each member contained one copy of each on average, suggesting that both elements in wheat *ABC1K* gene family play an important role in the regulation of plant growth and development.

The hormone response elements were also abundant in wheat *ABC1K* genes, 10 of which were detected. The most abundant elements were TGACG-motif and CGTCA-motif involved in the regulation of jasmonic acid synthesis as well as ABRE involved in response to abscisic acid. These three elements were present in almost every member of *TaABC1K* genes with an average copy number of 3.6, 3.1, and 4.2, respectively. Additionally, five environmental stress-related elements were detected in *TaABC1K* genes, including LTR, WUN-Motif, GC-motif, ARE, and TC-rich repeats. These elements were mainly involved in abiotic stress such as low temperature, hypoxia, drought, and cold stresses. Among them, LTR, GC-Motif, and ARE were the most widely distributed (Supplementary Figure 3B), which responded to low temperature, hypoxia, and anaerobic stress, respectively.

Two *TaABC1K* genes TraesCS1B03G0433300 from chromosome 1B (named as *TaABC1K3*) and TraesCS6A03G0979900 from chromosome 6A (named as *TaABC1K6*) were selected for further analysis, which were from clade I and had a similarity of 74 and 77% to *Arabidopsis ABC1K3* and *ABC1K6*, respectively. *TaABC1K3* had TCT-motif and G-box involved in light responsiveness, MBS (MYB binding site) involved in drought-inducibility, TC-rich repeats involved in defense and stress response as well as ABRE involved in abscisic acid response. *TaABC1K6* contained GATT-motif and GC-motif involved in light and anoxic response as well as ABRE, MBS, and G-box. Thus, the *cis*-elements of *TaABC1K3* and *TaABC1K6* mainly participated in light and stress responses.

Transcription expression profiling of *TaABC1K* genes in different organs and in response to abiotic stresses by RNA-seq

The publicly available RNA-seq data of 44 *TaABC1K* genes were obtained, and heat maps were constructed (Supplementary Figure 4). The expression profiling in different organs (Supplementary Figure 4A) showed that most *TaABC1K* genes had a high expression level in leaves and shoots, and some genes had medium expression level in roots, but the expression level in the developing grains was relatively low. In particular, *TaABC1K* genes from clade I generally had a high expression in leaves and shoots such as *TaABC1K3* and *TaABC1K6* whereas

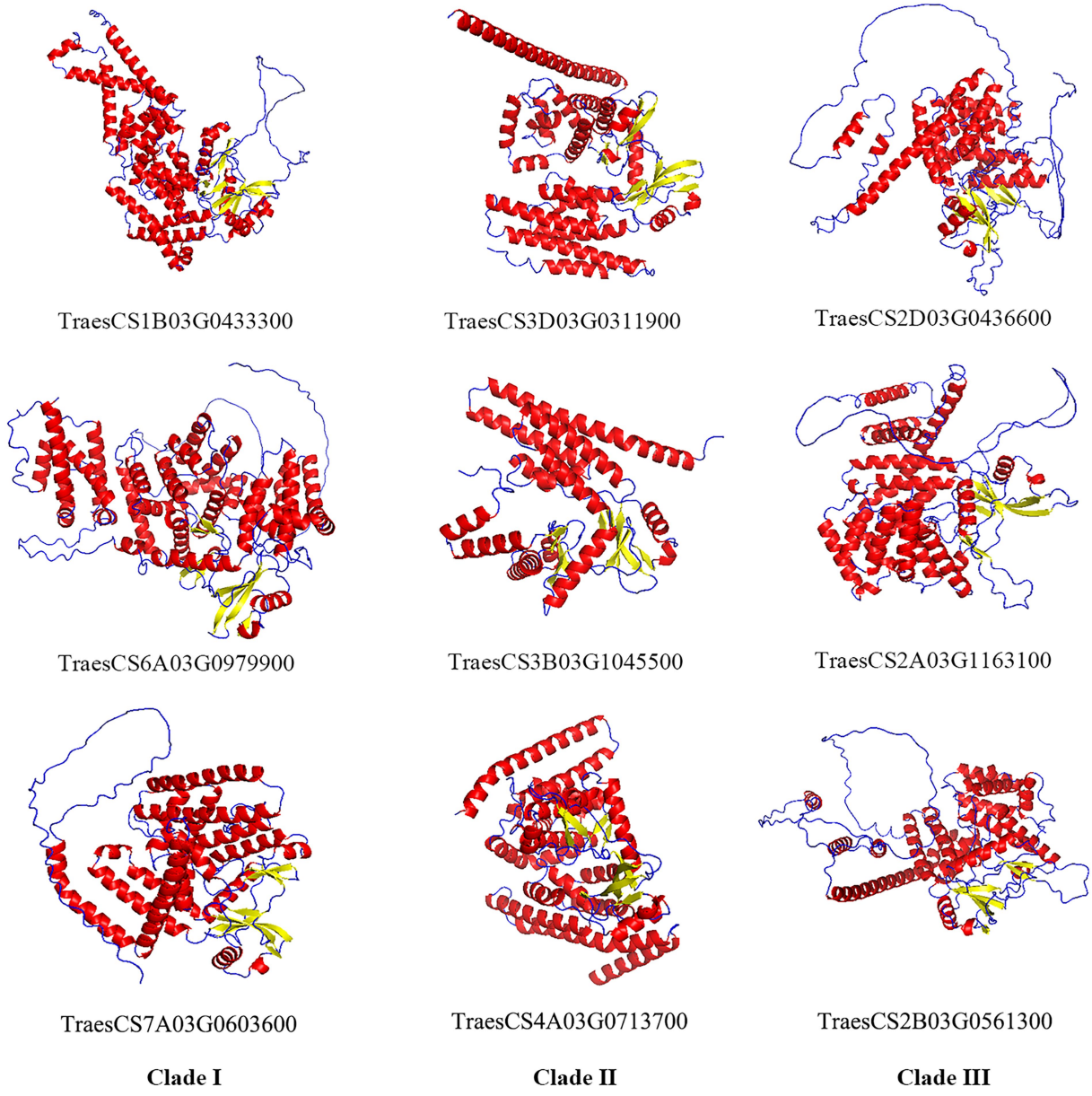


FIGURE 3
Three-dimensional structures of nine TaABC1K proteins from three different clades predicted by AlphaFold2. Red, α-helix; Blue, random coil; Yellow, β-sheet.

most of the genes from clades II and III showed a relatively low expression level in different organs.

TaABC1K genes generally displayed an upregulated expression under different abiotic stresses (Supplementary Figure 4B). Most of the genes from clade I were upregulated under multiple abiotic stresses, especially under drought and 2-week cold stresses, suggesting the potential roles of *TaABC1K* genes in clade I in response to abiotic stresses. 11 in 13 genes in clade I were upregulated under drought or PEG stress with a maximum increase of 74%. In particular, *TaABC1K3* had a significantly upregulated expression under heat (+38%), drought or PEG (+32%), and cold stresses (+49%). In contrast, the expression levels of the genes in clade II and clade III were relatively low in wheat. Although some of the data were missing, about half of the genes were still upregulated under PEG and cold stresses. Notably, the genes in clade I upregulated by up to 20 and 74% under drought and PEG stress, respectively, significantly higher than those from clade II (−3 and 35%, respectively), but lower than those of clade III (93 and 102%, respectively), possibly caused by their functional differentiation during the evolutionary process.

10.3389/fpls.2022.991171

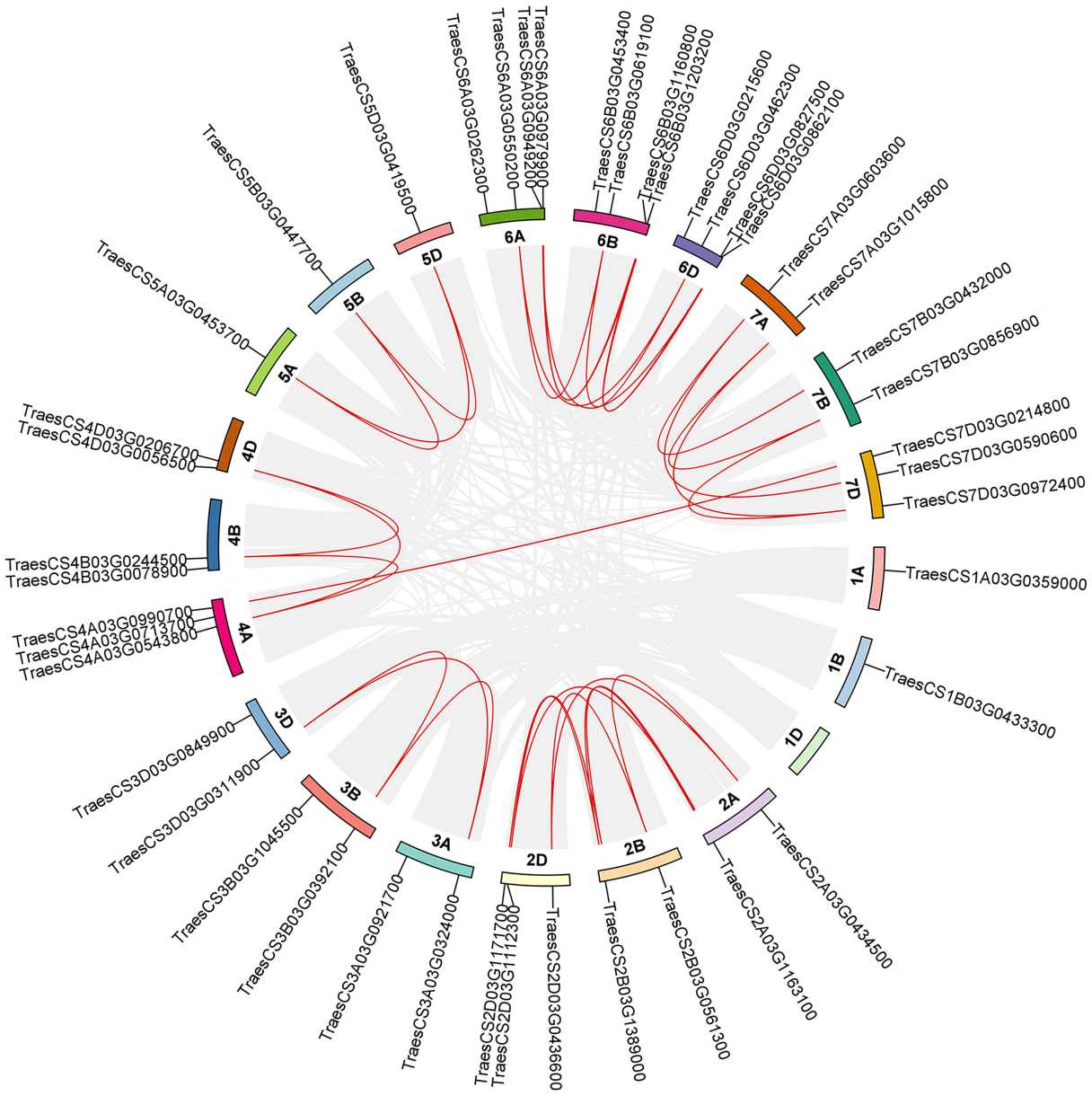


FIGURE 4
Distribution and collinearity of *ABC1K* gene family members in wheat chromosomes. The red lines represent the orthologous genes or tandem duplicated genes of *TaABC1K* and the gray lines represent the segmental duplication pairs in the whole wheat genome.

Subcellular localization of *TaABC1K3* and *TaABC1K6* and their expression patterns in different organs and abiotic stresses by RT-qPCR

The subcellular localization results of TaABC1K3 and TaABC1K6 observed by confocal scanning laser microscopy indicated that the GFP fluorescence of both TaABC1K3 and TaABC1K6 proteins was present in chloroplasts (Figure 5A). This confirmed that both proteins were localized in the chloroplast.

The transcription expression patterns of *TaABC1K3* and *TaABC1K6* genes in roots, stems, leaves, and developing grains of CS were further detected by RT-qPCR. The specific primers were designed and the primer sequences are shown in Supplementary Table 7. The results showed that the highest expression level of both *TaABC1K3* and *TaABC1K6* genes occurred in leaves. Meanwhile, *TaABC1K3* also had a high expression in the developing grains while *TaABC1K6* displayed a lower expression in roots, stems, and developing grains (Figure 5B). When subjected to PEG, NaCl and H_2O_2 stresses, both *TaABC1K3* and *TaABC1K6* genes were significantly

upregulated (Figure 5C). Particularly, the expression levels of *TaABC1K3* and *TaABC1K6* under PEG drought stress was dramatically increased by 6 and 27 times compared to the control, respectively. In addition, *TaABC1K3* also showed a sharp upregulation of 33 times under H_2O_2 stress, which all showed statistically significant compared with the control group.

Overexpression of *TaABC1K3* and *TaABC1K6* in yeast and *Arabidopsis* enhanced drought tolerance

Yeast transformation experiment showed that the growth rate of wild-type and *TaABC1K3 and TaABC1K6* overexpressed yeast strains under drought and H_2O_2 stresses were inhibited to different degrees along with the dilution of yeast culture medium concentration. However, the inhibition of *TaABC1K3* and *TaABC1K6* overexpressed yeast strains was significantly lower than that of the no-load strain (Figure 6). These results indicated that *TaABC1K3* and *TaABC1K6* genes could enhance the tolerance of yeast to drought and H_2O_2 stresses.

Further genetic transformation experiments of *TaABC1K3* and *TaABC1K6* genes to *Arabidopsis* wild-type Col-0, *abc1k3*, and *abc1k6* mutants were conducted. Six homozygous single-copy transgenic lines were produced through consecutive identification and screening, named OE3-1, OE3-2, and OE3-3 for *TaABC1K3* and OE6-1, OE6-2, and OE6-3 for *TaABC1K6*. Two complementary lines were generated, named *abc1k3/6* 35S: *TaABC1K3/6*. Inflorescence staining showed that *TaABC1K3* and *TaABC1K6* genes were integrated into the chromosomes of *Arabidopsis*. PCR identification confirmed that *TaABC1K3* and *TaABC1K6* genes were successfully transferred into overexpressed and complementary *Arabidopsis* plants (Supplementary Figure 5).

Phenotypic changes of *TaABC1K3* and *TaABC1K6* overexpressed plants and WT under drought stress are shown in Figures 7A,B. Under 400 mM mannitol simulated drought stress, the inhibition degree of root length in the *TaABC1K3* and *TaABC1K6* overexpressed plants was significantly lower than that of wild-type plants (Figures 7C,D), implying that both *TaABC1K3* and *TaABC1K6* genes could improve the resistance of *Arabidopsis* to drought stress. Further soil culture of transgenic lines under drought stress indicated that the wild-type plants had obvious chlorosis in leaves (Figure 8A) and the fresh weight was significantly reduced (Figure 8B). On the contrary, leaf chlorosis of *TaABC1K3* and *TaABC1K6* overexpressed plants was significantly mitigated, and the fresh weight was not declined significantly compared with the WT, demonstrating that the overexpressed *TaABC1K3* and *TaABC1K6* plants had better resistance to drought stress.

TaABC1K3 and *TaABC1K6* suppressed active oxygen burst and reduced photosynthesis impairment triggered by drought stress

The O_2^- and H_2O_2 levels in the transgenic *Arabidopsis* seedlings under drought stress were detected by DAB and NBT staining (Figures 9A,B). The results indicated that both DAB and NBT staining of transgenic and WT seedlings under normal conditions were light, indicating a lower content of O_2^- and H_2O_2. Under 400 mM mannitol treatment, however, the seedlings *abc1k3* and *abc1k6* mutants displayed the deepest staining, followed by WT seedlings, and *TaABC1K3 and TaABC1K6* overexpressed seedlings had the lightest staining. These results indicated that simulated drought stress caused a large accumulation of ROS in the seedlings of *abc1k3/6* mutants and WT. The overexpression of *TaABC1K3* and *TaABC1K6* could significantly reduce O_2^- and H_2O_2 content and ROS accumulation. DCFH-DA fluorescence staining was further used to measure the changes of ROS content in plants under drought stress (Figure 9C). The results showed that *abc1k3* and *abc1k6* mutants had the highest fluorescence intensity under 400 mM mannitol treatment, followed by WT. *TaABC1K3/6* overexpressed plants showed the lowest fluorescence intensity, indicating that *TaABC1K3* and *TaABC1K6* genes could reduce ROS accumulation and alleviate oxidative stress in plants.

Chlorophyll content measurement demonstrated that all materials had no significant differences under normal growth conditions (Figures 10A,B). The chloroplast content in all plants was significantly decreased under drought treatment (Figure 10C). In particular, the chloroplast content in *abc1k3* and *abc1k6* was dramatically decreased, respectively, by 80.19 and 79.28% compared to WT. However, *TaABC1K3* and *TaABC1K6* complementation lines showed similar chlorophyll content with WT, indicating that *TaABC1K3/6* genes could enhance chlorophyll synthesis under drought stress. Chlorophyll fluorescence imaging tests also showed similar results, and no significant phenotypic differences were found in the mutant plants, WT plants and the complementation plants under normal conditions. Under drought stress, the maximum photochemical mass yield (F_v/F_m) of PSII in *abc1k3* and *abc1k6* mutant plants under dark adaptation was significantly reduced by 69.01 and 73.84%, respectively (Figure 10D). The photochemical efficiency of PSII (ΦPSII) of *abc1k3* and *abc1k6* was decreased, respectively, by 75.9 and 68.05% while that in the complementary *TaABC1K3* and *TaABC1K6* plants was reduced, respectively, by 56.91 and 53.42% (Figure 10E). These results indicated that *TaABC1K3* and *TaABC1K6* could complement the loss of *Arabidopsis* mutants and enhance chlorophyll synthesis and photochemical efficiency under drought stress.

Discussion

At present, *ABC1K* genes have been detected in 42 species, including archaea, bacteria, and eukaryotes, which contain three

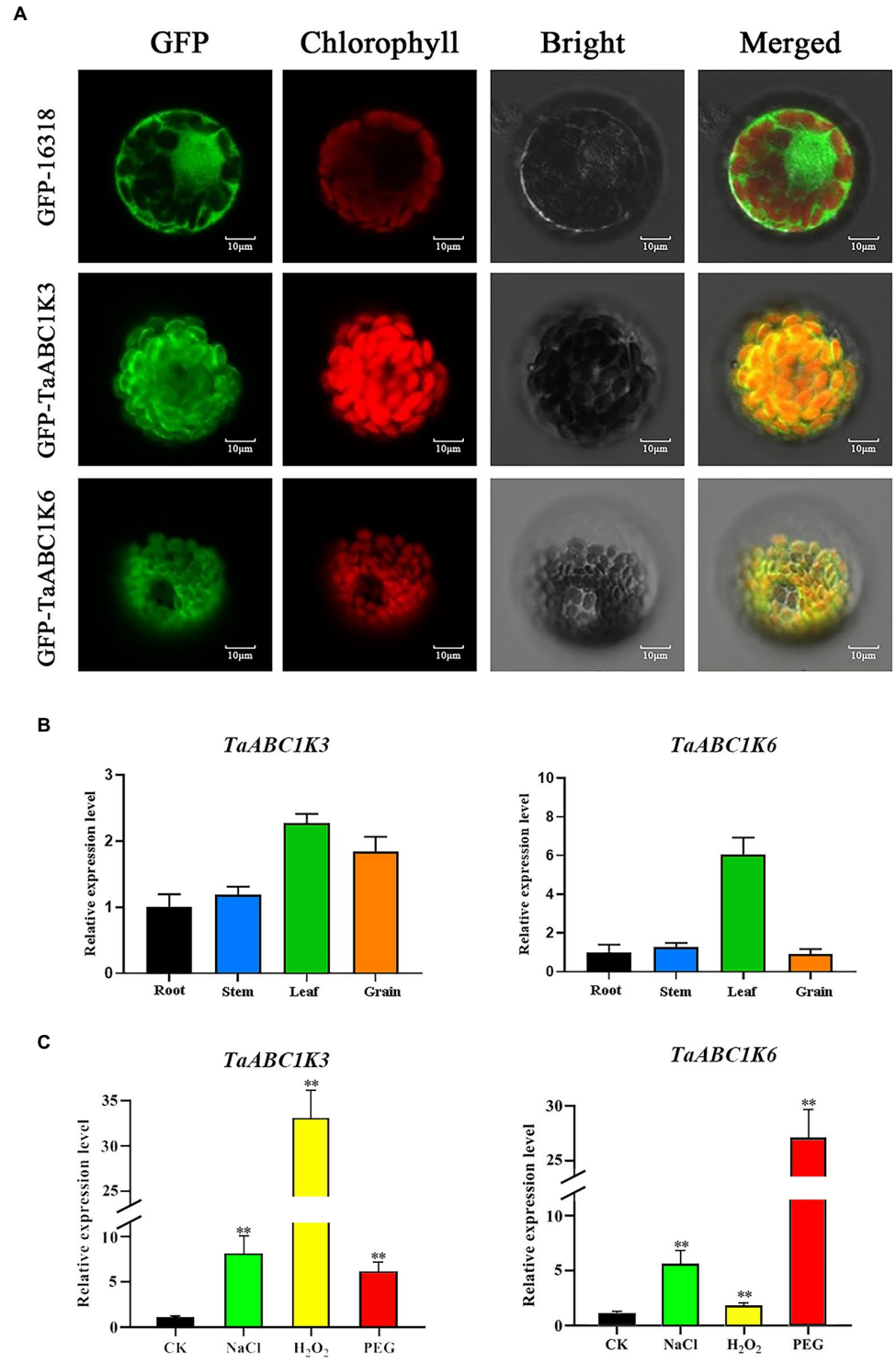


FIGURE 5
Subcellular localization and RT-qPCR analysis of *TaABC1K3* and *TaABC1K6*. **(A)** Subcellular localization of TaABC1K3 and TaABC1K6. GFP was induced fluorescence, chlorophyll is chloroplast autofluorescence. **(B)** RT-qPCR analysis of *TaABC1K3* and *TaABC1K6* genes in wheat different tissues. **(C)** RT-qPCR analysis of *TaABC1K3* and *TaABC1K6* genes under abiotic stresses. Statistically significant differences between control group and treatment group were calculated by an independent Student's *t*-tests: $^{**}p<0.01$.

branches in different species (Lundquist et al., 2012a). In allohexaploid wheat, 44 *TaABC1K* genes were also classified into three branches (Figure 1) and evenly distributed on A, B, and D subgenomes (Figure 4). *ABC1K* was considered to be a highly conserved gene family, two functional domains (VAVK-motif and DFG-motif) were found in every *ABC1K* genes in both wheat

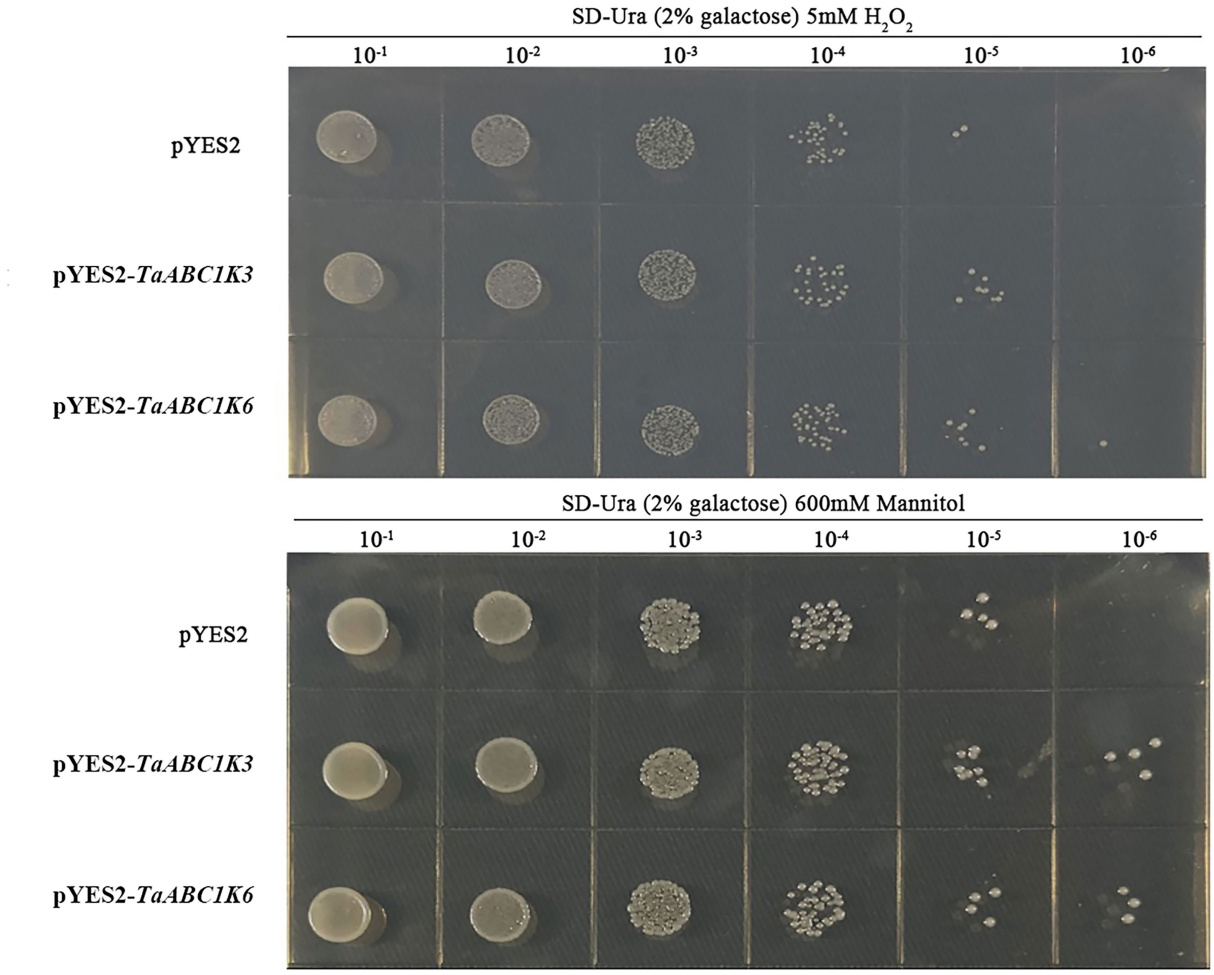


FIGURE 6
Overexpression of *TaABC1K3* and *TaABC1K6* genes enhanced the tolerance of yeast to abiotic stress.

(Supplementary Figure 2) and rice (Yang et al., 2012c). Positive selection sites were not found among *ABC1K* genes (Supplementary Table 5), indicating that wheat *ABC1K* gene family did not suffer from significant positive selection pressure during the evolution process. It is possible that genes that did not undergo positive selection might have undergone negative or purified selection (Yang, 2007). *ABC1K* genes in rice and *Arabidopsis* mainly experienced purifying selection, and the functions of most *ABC1K* genes tended to be conserved (Gao et al., 2014). However, wheat *ABC1K* genes from different clades showed some structural differences in motif and exon compositions, especially those from clade I (Figure 2), consistent with the previous reports in rice (Yang et al., 2012c) and maize (Gao et al., 2010). Additionally, the 3D structures of TaABC1K proteins predicted by AlphaFold2 also displayed differences in α-helix, β-sheet, and random coil compositions (Figure 3; Supplementary Table 3). These results imply that wheat the functional differentiation of *ABC1K* genes might happen during the evolutionary process. We also found that much more type II function divergence sites were present between clade I and clade II, implying that the differentiation in physicochemical properties played a leading role during the evolutionary process (Zhu et al., 2014). Only type I function divergence sites were found between clade II and clade III (Supplementary Table 4), and the changes in the evolutionary rate might be the main factor for the evolution of the two clades (Han et al., 2019; Liu et al., 2020).

Wheat *ABC1K* genes such as *TaABC1K3* and *TaABC1K6* have abundant *cis*-elements related to environmental stress, including ABRE, MBS, and G-box, etc. (Supplementary Figure 3), which could play important roles in defending various abiotic stresses. Drought stress causes ROS accumulation in plants, and as signal molecules, ROS also participates in various biotic and abiotic stress responses and played an important role in plant growth and development (Suzuki et al., 2011; Marino et al., 2012). Thus, increased ROS accumulation under drought stress could induce the upregulation of *TaABC1K* genes in the leaves and shoots (Supplementary Figure 4; Figures 5B,C), consistent with the previous reports (Wang et al., 2011; Wu et al., 2020). At the same time, the overexpression of *TaABC1K3* and *TaABC1K6* in yeast and *Arabidopsis* significantly promoted drought tolerance

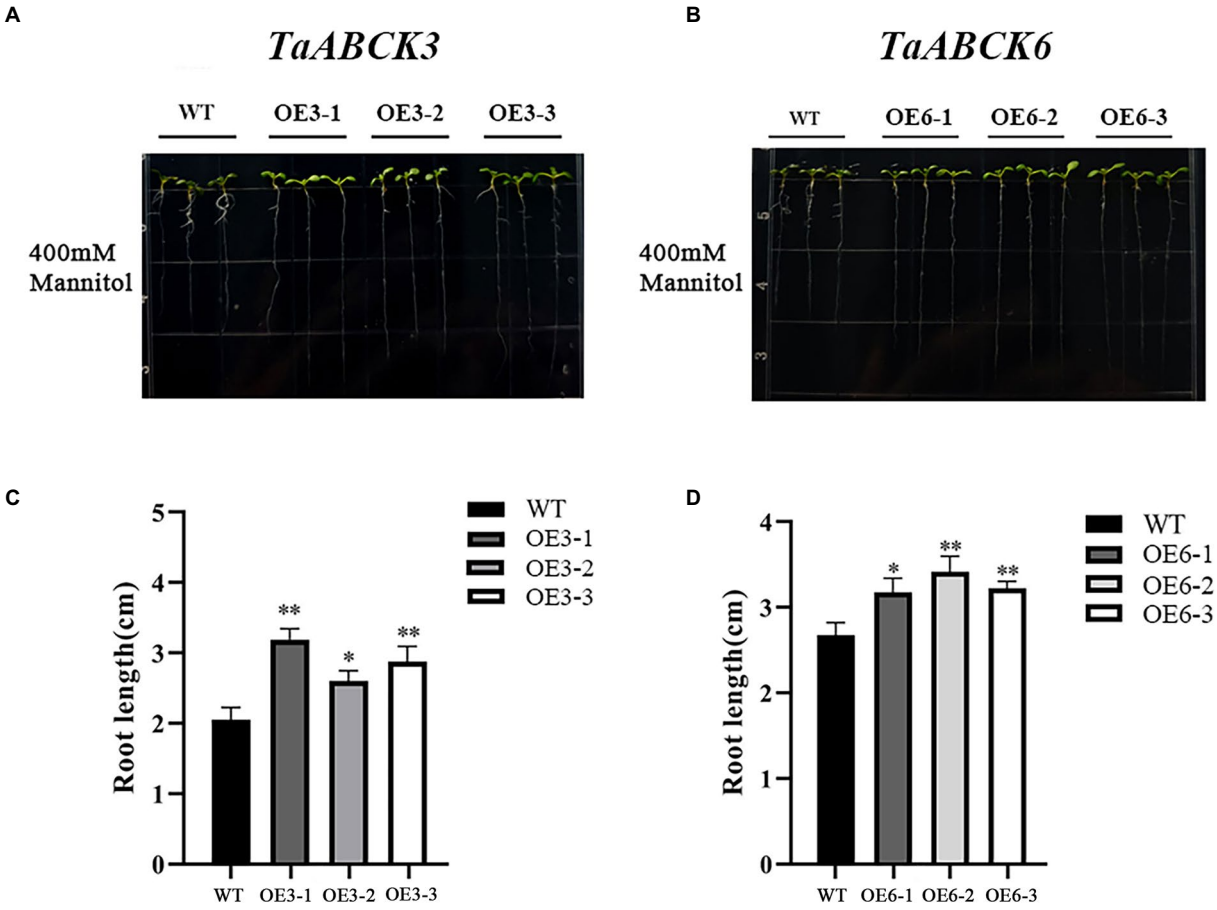


FIGURE 7
Overexpressed of *TaABC1K3* and *TaABC1K6* enhanced the drought tolerance of *Arabidopsis* seedlings. Phenotypic changes in wild-type **(A)** and *TaABC1K3* and *TaABC1K6* overexpressed seedlings **(B)**, relative fresh weight of overexpressed *Arabidopsis* **(C)**, and wild type **(D)** are indicated. Mean±SD of data from three independent biological replicates. Statistically significant differences between wild type and overexpressed plants were calculated by an independent Student's *t*-tests: *p<0.05; **p<0.01.

(Figures 6, 7). On the other hand, the absence of *Arabidopsis TaABC1K3* and *TaABC1K6* genes led to susceptible to drought while the complementation experiment of *TaABC1K3* and *TaABC1K6* could recover the drought resistance of *Arabidopsis* plants by reducing ROS accumulation caused by drought (Figure 10). *ABC1K10a* mutant in *Arabidopsis* also caused more susceptible to salt stress (Qin et al., 2020), and the double mutations of *Arabidopsis ABC1K AtSIA1* and *AtOSA1* were influenced by oxidative stress even in a normal condition and the SOD level in plants was significantly upregulated (Manara et al., 2014). Abiotic stresses could also produce oxidative damage to photosynthetic proteins and pigments. PSII (F_v/F_m) and Chl content are important indicators of photochemical efficiency, which can reflect physiological aging (Franke and Schreiber, 2007; Lim et al., 2007; Osakabe et al., 2010). The maximal quantum yield of PSII photochemistry (F_v/F_m) of wheat under 3 days osmotic stress was significantly lower than normal conditions. Compared to other stresses, wheat plants under 3 days osmotic stress had the most obvious decline in gas-exchange parameter (Wu et al., 2020). *TaABC1K* overexpressed plants under drought stress showed higher water retention ability and higher F_v/F_m than WT (Wang et al., 2011). In this study, *Arabidopsis abc1k3* and *abc1k6* mutations under drought stress significantly influenced chlorophyll content and photosynthetic efficiency in PSII, while *TaABC1K3* and *TaABC1K6* could complement for the loss of *ABC1Ks* in *Arabidopsis* and maintain the function of chlorophyll synthesis in plants (Figure 10). These results confirmed that *TaABC1K3* and *TaABC1K6* genes could maintain the stability of plant photosynthesis.

Abiotic stresses generally produce excessive production of ROS in plants, leading to damages to proteins, lipids, carbohydrates, and DNA, eventually leading to oxidative stress (Meijer et al., 2019). Non-enzymatic antioxidants such as ascorbic acid (ASC), glutathione (GSH), α-tocopherol, plastoquinone, and carotenoids could detoxify ROS and protect plants from abiotic stress (Bisby et al., 1999; Kruk et al., 2005; Kruk and Trebst, 2008). Studies found that ABC1K could phosphorylate tocopherol cyclase VTE1 *in vitro*, which might

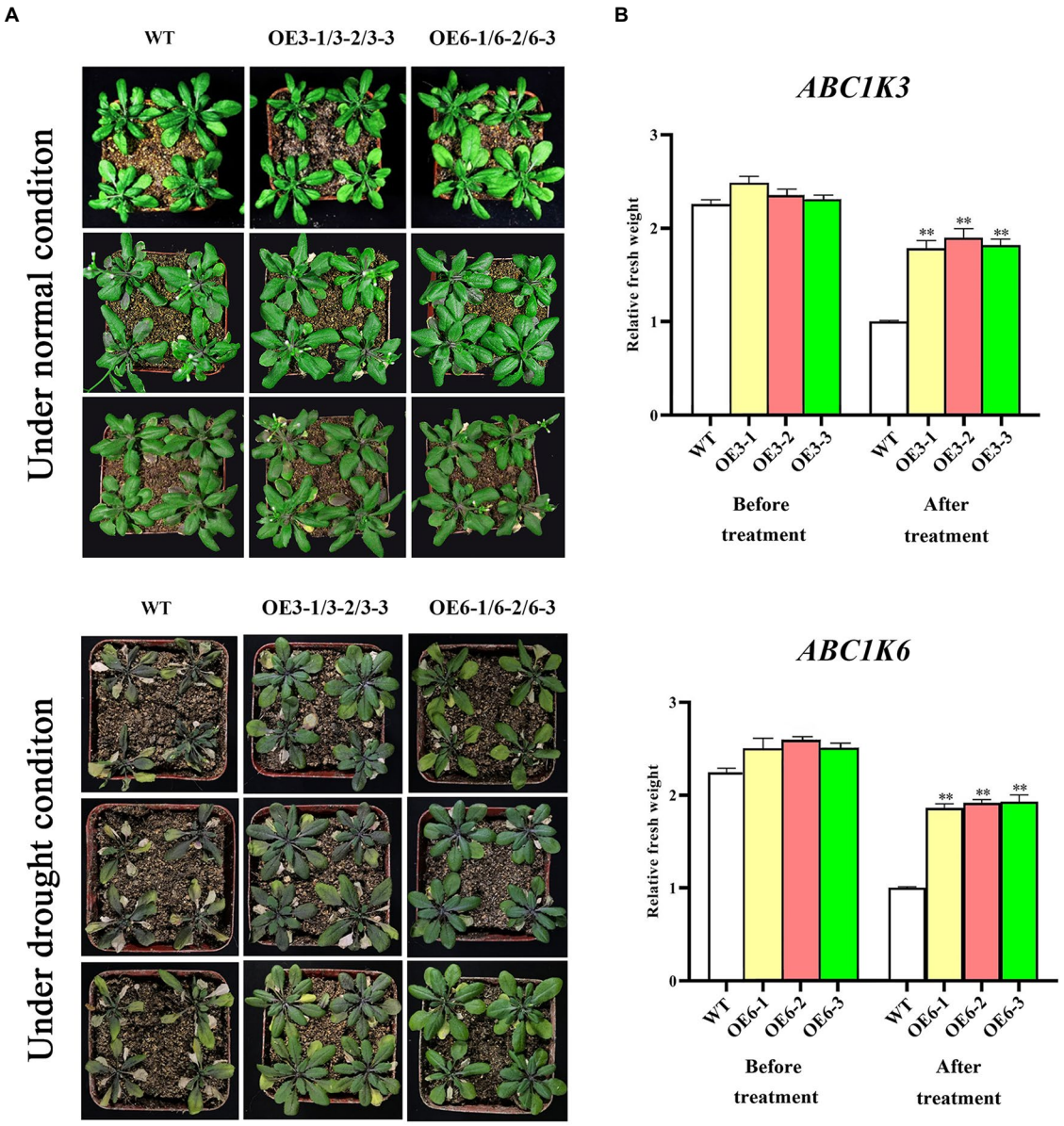


FIGURE 8
Phenotype changes of *TaABC1K3* and *TaABC1K6* overexpressed *Arabidopsis* plants under soil culture in response to drought stress. **(A)** Soil drought stress treatment was performed on wild-type, *TaABC1K3* and *TaABC1K6* overexpressed plants. **(B)** Comparison of fresh weight of wild-type, *TaABC1K3*, and *TaABC1K6* overexpressed plants under drought treatment and normal conditions. Statistically significant differences between control group and treatment group were calculated by an independent Student's *t*-tests: $^{**}p<0.01$.

protect VTE1 from degradation (Martinis et al., 2013, 2014), and VTE1 was a key enzyme in vitamin E synthesis and recycling (Kobayashi and Della Penna, 2008). As the hydrolysis product of vitamin E, a single α-tocopherol molecule could neutralize up to 220 $^1O_2$ molecules *in vitro* before being degraded (Gill and Tuteja, 2010). Therefore, ROS in chloroplast could be effectively decreased.

Drought can cause disequilibrium between light capture and its utilization, which reduces the rate of photosynthesis in leaves. This imbalance would induce excess light energy dissipated in the plant photosynthetic system (Mansur and Luiz, 2015). The excess energy absorbed by chlorophyll in the PSII antennae complex would further cause the conversion of singlet chlorophyll to deleterious triplet chlorophyll (^{3}Chl*; Pospíšil, 2016). The reaction of ^{3}Chl* and O_2 could produce highly oxidizing $^1O_2$ (Edreva, 2005). Carotenoids and lutein can scavenge $^1O_2$ to inhibit oxidative damage and quench ^{3}Chl* to prevent the formation of $^1O_2$, thus protecting the photosynthetic apparatus (Mozzo et al., 2008; Mansur and Luiz, 2015). Zeaxanthin cycleoxidase (ZEP) serves as an important enzyme to synthesize carotenoids in carotenoid metabolism and is involved in the reversible conversion of

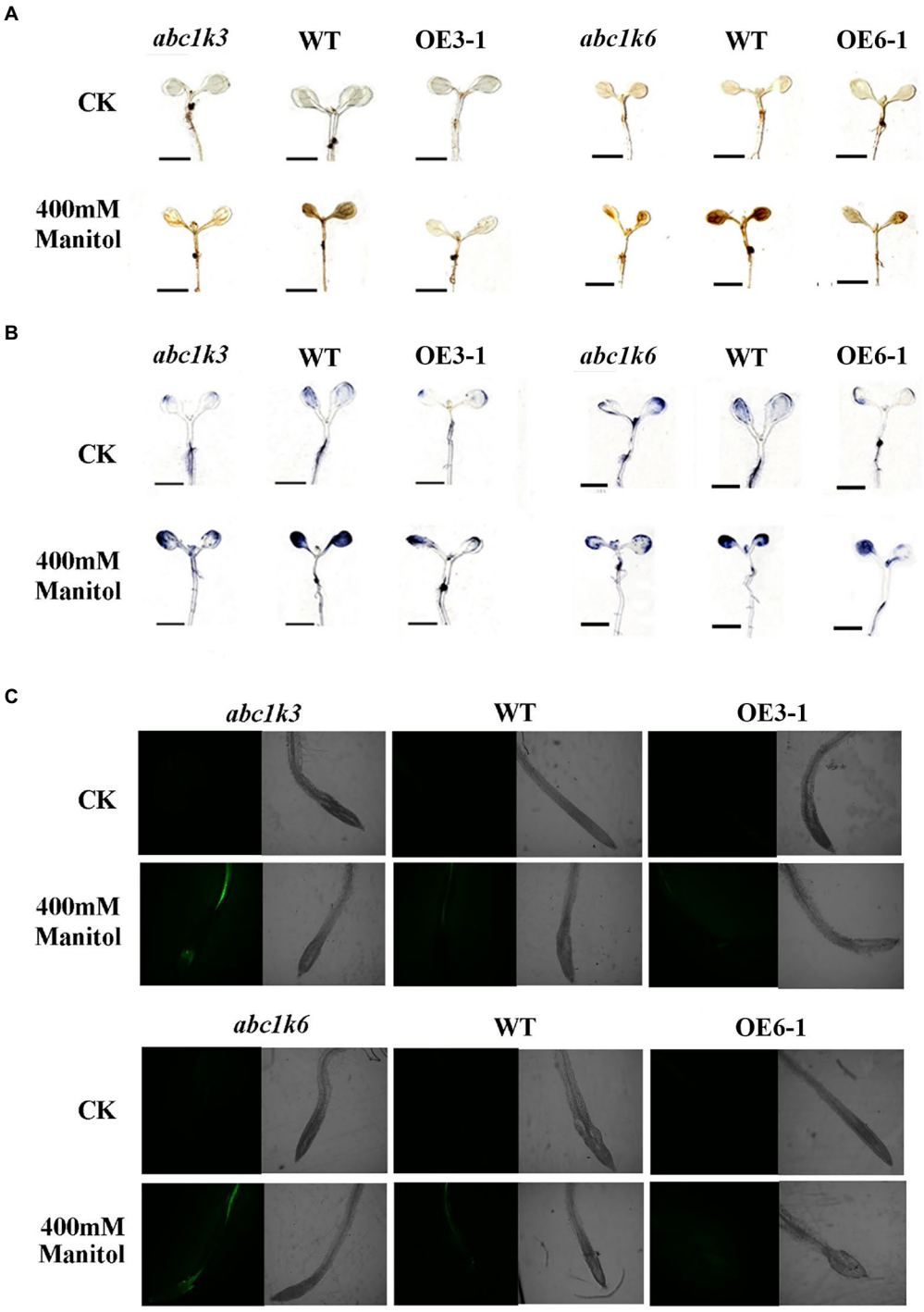


FIGURE 9
Overexpression of *TaABC1K3* and *TaABC1K6* suppressed the active oxygen burst triggered by drought stress in *Arabidopsis* mutant *abc1k3* and *abc1k 6*. **(A,B)** Differences of ROS content in *abc1k3/6* mutant, wild-type and *TaABC1K3/6* overexpressed plants under 400mM mannitol stress. The seedlings were stained by diaminobenzidine (DAB; **A**) to form brown precipitates in the presence of hydrogen peroxide, or by nitroblue tetrazolium staining (NBT; **B**) to produce blue precipitate in the presence of superoxide (Scale bar =5mm). **(C)** Seedlings of *abc1k3/6* mutant, wild-type and *TaABC1K3/6* overexpressed plants were subjected to DCFH-DA staining under 400mM Mannitol stress.

zeaxanthin to violaxanthin within the xanthophyll cycle (Yuan et al., 2015). The study also found that ZEP was centrally located in the gene expression network closely related to ABC1K, and ABC1K proteins might regulate ZEP activity (Lundquist et al., 2012b). Thus, TaABC1K might coexpressed with ZEP to participate in the regulation of the xanthophyll

10.3389/fpls.2022.991171

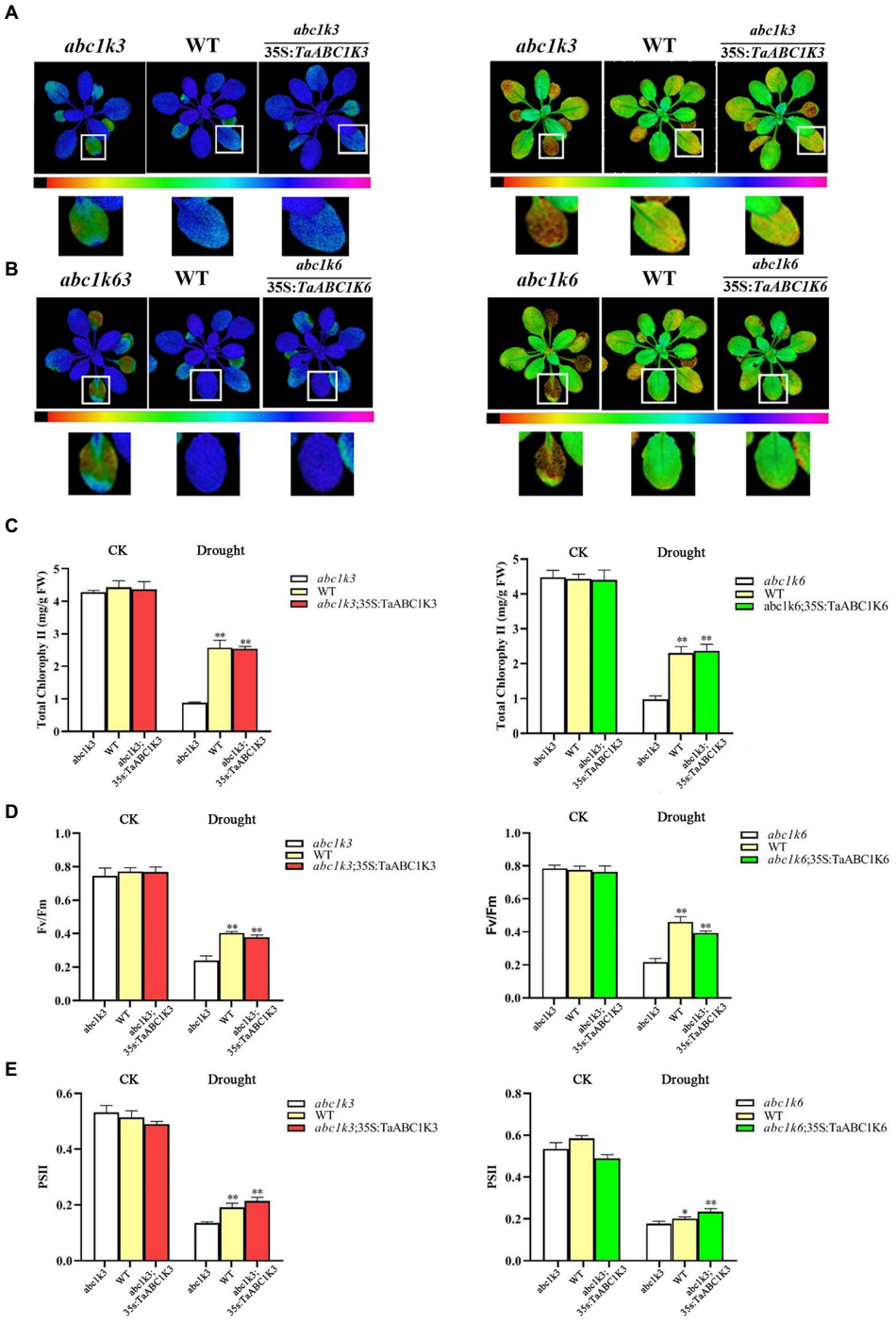


FIGURE 10
Overexpression of *TaABC1K3* and *TaABC1K6* alleviated the photosynthesis impairment induced by drought stress in *Arabidopsis* mutant *abc1k3* and *abc1k6*. **(A,B)** Chlorophyll fluorescence images showed the efficiency of PSII (FPSII), and the inhibition of PSII quantum yield (lnh) by *abc1k3/6 mutant*, wild type, and completed complementing experimental plants. **(C)** Changes in chlorophyll content of mutant, wild-type, and complemented experimental plants after drought stress treatment. **(D)** Maximum seed yield of each plant (F_v/F_m) of each plant. **(E)** PSII efficiency value of the plant in chlorophyll fluorescence image. Statistically significant differences between control group and treatment group were calculated by an independent Student's *t*-tests: **p*<0.05; ***p*<0.01.

cycle, and the increasement of carotenoids could scavenge $^1O_2$ and quench ^{3}Chl* to stabilize plant photosynthesis (Lundquist et al., 2012b).

Based on the results of this work as well as the previous studies, we proposed a putative responsive network of *TaABC1Ks* in wheat chloroplast under drought stress

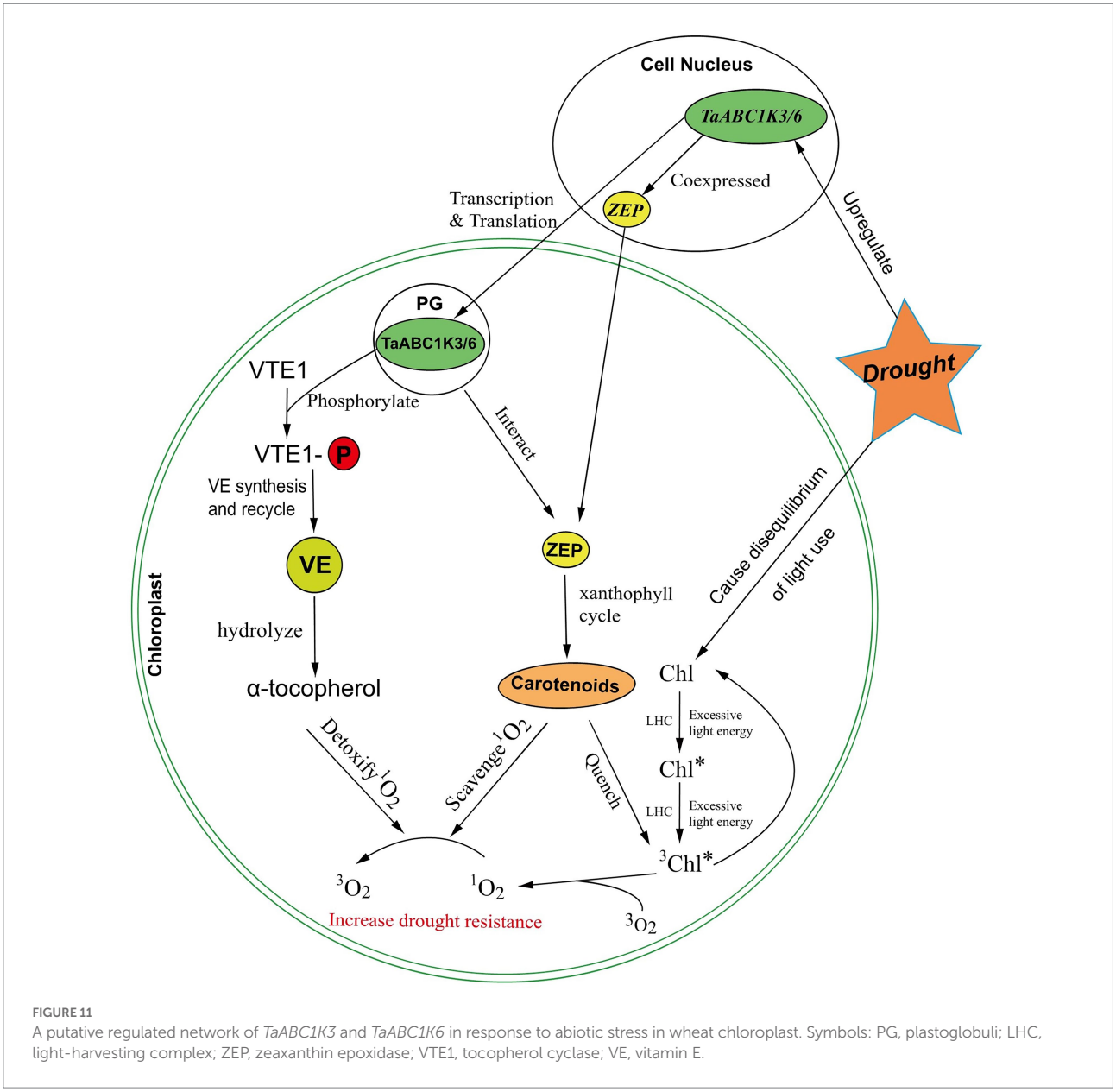


FIGURE 11
A putative regulated network of *TaABC1K3* and *TaABC1K6* in response to abiotic stress in wheat chloroplast. Symbols: PG, plastoglobuli; LHC, light-harvesting complex; ZEP, zeaxanthin epoxidase; VTE1, tocopherol cyclase; VE, vitamin E.

(Figure 11). When subjected to drought stress, the disequilibrium of light use produced excessive light energy to induce the production of ^{3}Chl*. The reaction of ^{3}Chl* and O_2 could produce ROS $^1O_2$. The increased ROS accumulation triggered the upregulated expression of *TaABC1K3* and *TaABC1K6* in the leaves. Carotenoid synthesis was enhanced by TaABC1K3 and TaABC1K6 coexpressing and interacting with ZEP in the chloroplast, which could quench ^{3}Chl to normal Chl and scavenge $^1O_2$. Meanwhile, TaABC1K3 and TaABC1K6 could phosphorylate VTE1 and activate the production of α-tocopherol to detoxify $^1O_2$. This could significantly decrease ROS accumulation under drought stress. Therefore, *TaABC1K3* and *TaABC1K6* could maintain the normal function of chloroplast by regulating the endogenous oxidation balance of chloroplasts to respond drought stress.

Conclusion

Genome-wide analysis identified 44 wheat *ABC1K* family genes that contained typical ABC1K kinase domain and three (I–III) clades. Each clade generally had similar structural features, but differences in the number of motifs and exons in *TaABC1K* genes as well as the content of α-helix, random coil and β-sheet in TaABC1K proteins from different clades were present. More II type functional divergence sites were found between clade I and clade III and no positive selection sites were found. *TaABC1K* genes possessed abundant *cis*-acting elements in the upstream promoter regions, including light responsive elements, development-related elements, hormone-responsive elements, and environmental stress-related elements. *TaABC1Ks* generally displayed a high expression in plant leaves and response to

drought stress. Overexpression of *TaABC1K3* and *TaABC1K6* in yeast and *Arabidopsis* significantly improved drought tolerance. Furthermore, *TaABC1K3* and *TaABC1K6* could, respectively, complement the function of *Arabidopsis abc1k3* and *abc1k6* mutants and alleviate photosynthesis damage caused by drought stress. Our results provided new insights into the structure, evolution, and function characteristics of wheat *ABC1K* genes.

Data availability statement

The datasets presented in this study can be found in online repositories. The names of the repository/repositories and accession number(s) can be found in the article/Supplementary material.

Author contributions

XG, RZ, and HS performed most of the experiments and data analysis. JL and WD performed confocal microscope observation and gene expression analysis. YH and YY designed the experiments and edited the manuscript. All authors contributed to the article and approved the submitted version.

Funding

This research was financially supported by the grant from the National Natural Science Foundation of China (31971931).

Conflict of interest

The authors declare that the research was conducted in the absence of any commercial or financial relationships that could be construed as a potential conflict of interest.

Publisher's note

All claims expressed in this article are solely those of the authors and do not necessarily represent those of their affiliated organizations, or those of the publisher, the editors and the reviewers. Any product that may be evaluated in this article, or claim that may be made by its manufacturer, is not guaranteed or endorsed by the publisher.

Supplementary material

The Supplementary material for this article can be found online at: https://www.frontiersin.org/articles/10.3389/fpls.2022.991171/full#supplementary-material

SUPPLEMENTARY FIGURE 1
The Bayesian phylogenetic tree of wheat ABC1K gene family.

SUPPLEMENTARY FIGURE 2
Conserved amino acid conservation sequences in the ABC1 domain of the *ABC1K* gene family in wheat. VAVK and DFG motifs are marked.

SUPPLEMENTARY FIGURE 3
The *cis*-acting element analysis in the *TaABC1K* gene promoters. **(A)** Distribution of cis-acting elements in each member of wheat *ABC1K* gene family. **(B)** Average number of *cis*-acting elements contained in subfamily members.

SUPPLEMENTARY FIGURE 4
Expression profile of *TaABC1K* genes in wheat different tissues and developmental stages **(A)** and abiotic stresses **(B)**.

SUPPLEMENTARY FIGURE 5
Identification of *abc1k3/6* mutant, *TaABC1K3/6* overexpressed plants and complement plants. **(A)** Using *Arabidopsis* genomic DNA as modle, chimeric primers were designed for PCR identification of T3 generation *TaABC1K3/6* overexpressed plants and complement plants, Lines 1–15 are overexpressed plant samples (complement plants), Line 16 is wild type negative control, and Line17 is plasmid positive controls. **(B)** The *Arabidopsis* mutant purchased from the Salk site was T-DNA insertion mutation, the *abc1k3* mutant was SALK_128696, and the *abc1k6* mutant was SALK_057147.

References

Bailey, T. L., Boden, M., Buske, F. A., Frith, M. C., Grant, C. E., Clementi, L., et al. (2009). MEME suite: tools for motif discovery and searching. *Nucleic Acids Res.* 37, W202–W208. doi: 10.1093/nar/gkp335

Bailey, T. L., and Elkan, C. (1994). Fitting a mixture model by expectation maximization to discover motifs in biopolymers. *Proc. Int. Conf. Intell. Syst. Mol. Biol.* 2, 28–36.

Bayer, R. G., Stael, S., Rocha, A. G., Mair, A., Vothknecht, U. C., and Teige, M. (2012). Chloroplast-localized protein kinases: a step forward towards a complete inventory. *J. Exp. Bot.* 63, 1713–1723. doi: 10.1093/jxb/err377

Bechtold, N., and Bouchez, D. (1995). In planta agrobacterium-mediated transformation of adult Arabidopsis thaliana plants by vacuum infiltration. *Plant Physiol.* 19:3. doi: 10.1007/978-3-642-79247-2_3

Bisby, R. H., Morgan, C. G., Hamblett, I., and Gorman, A. A. (1999). Quenching of singlet oxygen by Trolox C, ascorbate, and amino acids: effects of pH and temperature. *J. Physical Chem. A.* 103, 7454–7459. doi: 10.1021/jp990838c

Bonnefoy, N., Kermorgant, M., Brivet-Chevillotte, P., and Dujardin, G. (1996). Cloning by functional complementation and inactivation of the Schizosaccharomyces pombe homologue of the Saccharomyces cerevisiae gene ABC1. *Mol. Gen. Genomics.* 251, 204–210. doi: 10.1016/0378-1119(96)00095-9

Bousquet, I., Dujardin, G., and Slonimski, P. P. (1991). ABC1, a novel yeast nuclear gene has a dual function in mitochondria: it suppresses a cytochrome b mRNA translation defect and is essential for the electron transfer in the bc 1 complex. *EMBO J.* 10, 2023–2031. doi: 10.1002/j.1460-2075.1991.tb07732.x

Chen, C. J., Chen, H., Zhang, Y., Thomas, H. R., Frank, M. H., He, Y. H., et al. (2020). TBtools: An integrative toolkit developed for interactive analyses of big biological data. *Mol. Plant* 13, 1194–1202. doi: 10.1016/j.molp.2020.06.009

Duan, W., Lu, F., Cui, Y., Zhang, J., Du, X., Hu, Y., et al. (2022). Genome-wide identification and characterisation of wheat MATE genes reveals their roles in aluminium tolerance. *Int. J. Mol. Sci.* 23:4418. doi: 10.3390/ijms23084418

Edreva, A. (2005). Generation and scavenging of reactive oxygen species in chloroplasts: a submolecular approach. *Agric. Ecosyst. Environ.* 106, 119–133. doi: 10.1016/j.agee.2004.10.022

Fares, M. A., and Mcnally, D. (2006). CAPS: coevolution analysis using protein sequences. *Bioinformatics* 22, 2821–2822. doi: 10.1093/bioinformatics/btl493

Finn, R. D., Bateman, A., Clements, J., Coggill, P., Eberhardt, R. Y., Eddy, S. R., et al. (2014). Pfam: the protein families database. *Nucleic Acids Res.* 42, D222–D230. doi: 10.1093/nar/gkt1223

Finn, R. D., Clements, J., and Eddy, S. R. (2011). HMMER web server: interactive sequence similarity searching. *Nucleic Acids Res.* 39, W29–W37. doi: 10.1093/nar/gkr367

Franke, R., and Schreiber, L. (2007). Suberina biopolyester forming apoplastic plant interfaces. *Curr. Opin. Plant Biol.* 10, 252–259. doi: 10.1016/j.pbi.2007.04.004

Gao, Q. S., Yang, Z. F., Zhou, Y., Yin, Z., Qiu, J., and Liang, G. H. (2012). Characterization of an Abc 1 kinase family gene OsABC1-2 conferring enhanced tolerance to dark-induced stress in rice. *Gene* 498, 155–163. doi: 10.1016/j.gene.2012.02.017

Gao, Q., Yang, Z., Zhou, Y., Zhang, D., Yan, C., Liang, G., et al. (2010). Cloning of an ABC1-like gene ZmABC1-10 and its responses to cadmium and other abiotic stresses in maize (Zea mays L.). *Acta Agron. Sin.* 36, 2073–2083. doi: 10.1016/S1875-2780(09)60089-4

Gao, Q., Zang, H., Gao, Y., Yang, Z., Zhou, Y., Luo, Y., et al. (2014). Comprehensive molecular evolution and gene expression analyses of the ABC1 atypical kinase family in rice and Arabidopsis. *J. Plant Biochem. Biotechnol.* 24, 210–217. doi: 10.1007/s13562-014-0259-5

Gao, Q., Zhang, D., Xu, L., and Xu, C. W. (2011). Systematic identification of Rice ABC1 gene family and its response to abiotic stress. *Rice Sci.* 18, 167–177. doi: 10.1016/s1672-6308(11)60024-3

Genty, B., and Baker, N. R. (1989). Relationship between the quantum efficiencies of photosystems I and II in pea leaves. *Plant Physiol.* 90, 1029–1034. doi: 10.1104/pp.90.3.1029

Gill, B. S., Appels, R., Botha-Oberholster, A. M., Buell, C. R., Bennetzen, J. L., Chalhoub, B., et al. (2004). A workshop report on wheat genome sequencing: International genome research on wheat consortium. *Genetics* 168, 1087–1096. doi: 10.1534/genetics.104.034769

Gill, S. S., and Tuteja, N. (2010). Reactive oxygen species and antioxidant machinery in abiotic stress tolerance in crop plants. *Plant Physiol. Biochem.* 48, 909–930. doi: 10.1016/j.plaphy.2010.08.016

Gu, X., Zou, Y., Su, Z., Huang, W., Zhou, Z., Arendsee, Z., et al. (2013). An update of DIVERGE software for functional divergence analysis of protein family. *Mol. Biol. Evol.* 30, 1713–1719. doi: 10.1093/molbev/mst069

Han, Z., Liu, Y., Deng, X., Liu, D., Liu, Y., Hu, Y., et al. (2019). Genome-wide identification and expression analysis of expansin gene family in common wheat (*Triticum aestivum* L.). *BMC Genomics* 20:101. doi: 10.1186/s12864-019-5455-1

Hu, B., Jin, J., Guo, A. Y., Zhang, H., Luo, J., and Gao, G. (2014). GSDS 2.0: an upgraded gene feature visualization server. *Bioinformatics* 31, 1296–1297. doi: 10.1093/bioinformatics/btu817

Ichimura, K., Mizoguchi, T., Yoshida, R., Yuasa, T., and Shinozaki, K. (2000). Various abiotic stresses rapidly activate Arabidopsis MAP kinases ATMPK4 and ATMPK6. *Plant J.* 24, 655–665. doi: 10.1046/j.1365-313x.2000.00913.x

Jasinski, M., Sudre, D., Schansker, G., Schellenberg, M., Constant, S., Martinoia, E., et al. (2008). AtOSA1, a member of the ABC1-like family, as a new factor in cadmium and oxidative stress response. *Plant Physiol.* 147, 719–731. doi: 10.1104/pp.107.110247

Jumper, J., Evans, R., Pritzel, A., Green, T., Figurnov, M., Ronneberger, O., et al. (2021). Highly accurate protein structure prediction with alpha fold. *Nature* 596, 583–589. doi: 10.1038/s41586-021-03819-2

Kobayashi, N., and Della Penna, D. (2008). Tocopherol metabolism, oxidation and recycling under high light stress in Arabidopsis. *Plant J.* 55, 607–618. doi: 10.1111/j.1365-313X.2008.03539.x

Kruk, J., Hollander-Czytko, H., Oettmeier, W., and Trebst, A. (2005). Tocopherol as singlet oxygen scavenger in photosystem II. *J. Plant Physiol.* 162, 749–757. doi: 10.1016/j.jplph.2005.04.020

Kruk, J., and Trebst, A. (2008). Plastoquinol as a singlet oxygen scavenger in photosystem II. *Biochim. Biophys. Acta-Bioenergetics* 1777, 154–162. doi: 10.1007/978-1-4020-6709-9_323

Letunic, I., and Bork, P. (2018). 20 years of the SMART protein domain annotation resource. *Nucleic Acids Res.* 46, D493–D496. doi: 10.1093/nar/gkx922

Li, T., Shao, X. X., Li, Z. L., Xu, X. W., Ying, L., and Li, Z. X. (2015). Genome-wide identification, phylogenetic and expression analysis of ABC1K gene family in tomato (*Solanum lycopersicum* L.). *Int. J. Bioautom.* 19:287.

Li, Q., Zhang, X., Lv, Q., Zhu, D., Qiu, T., Xu, Y., et al. (2017). Physcomitrella patens dehydrins (PpDHNA and PpDHNC) confer salinity and drought tolerance to transgenic Arabidopsis plants. *Front. Plant Sci.* 8:1316. doi: 10.3389/fpls.2017.01316

Li, T., Zhu, D., Han, Z., Zhang, J., Zhang, M., and Yan, Y. (2021). Label-free quantitative proteome analysis reveals the underlying mechanisms of grain nuclear proteins involved in wheat water-deficit response. *Front. Plant Sci.* 12:748487. doi: 10.3389/fpls.2021.748487.

Lim, P. O., Kim, Y., and Breeze, E. (2007). Overexpression of a chromatin architecture-controlling AT-hook protein extends leaf longevity and increases the post-harvest storage life of plants. *Plant J.* 52, 1140–1153. doi: 10.1111/j.1365-313X.2007.03317.x

Liu, N., Dong, L., Deng, X., Liu, Y., Liu, D., Li, M., et al. (2018). Genome-wide identification, molecular evolution, and expression analysis of auxin response factor (ARF) gene family in *Brachypodium distachyon* L. *BMC Plant Biol.* 18:336. doi: 10.1186/s12870-018-1559-z

Liu, Y., Liu, N., Deng, X., Liu, D., Li, M., Cui, D., et al. (2020). Genome-wide analysis of wheat DNA-binding with one finger (Dof) transcription factor genes: evolutionary characteristics and diverse abiotic stress responses. *BMC Genomics* 21:276. doi: 10.1186/s12864-020-6691-0

Livak, K. J., and Schmittgen, T. D. (2001). Analysis of relative gene expression data using real-time quantitative PCR and the $2^{-\Delta\Delta CT}$ method. *Methods* 25, 402–408. doi: 10.1006/meth.2001.1262

Lundquist, P. K., Davis, J. I., and Van, W. K. J. (2012a). ABC1K atypical kinases in plants: filling the organellar kinase void. *Trends Plant Sci.* 17, 546–555. doi: 10.1016/j.tplants.2012.05.010

Lundquist, P. K., Poliakov, A., Bhuiyan, N. H., Zybailov, B., Sun, Q., and van Wijk, K. J. (2012b). The functional network of the Arabidopsis plastoglobule proteome based on quantitative proteomics and genome-wide coexpression analysis. *Plant Physiol.* 158, 1172–1192. doi: 10.1104/pp.111.193144

Lundquist, P. K., Poliakov, A., Giacomelli, L., Friso, G., Appel, M., Mcquinn, R. P., et al. (2013). Loss of plastoglobule kinases ABC1K1 and ABC1K3 causes conditional degreening, modified prenyl-lipids, and recruitment of the jasmonic acid pathway. *Plant Cell* 25, 1818–1839. doi: 10.1105/tpc.113.111120

Manara, A., Dalcorso, G., Leister, D., Jahns, P., Baldan, B., and Furini, A. (2014). AtSIA1 AND AtOSA1: two Abc 1 proteins involved in oxidative stress responses and iron distribution within chloroplasts. *New Phytol.* 201, 452–465. doi: 10.1111/nph.12533

Mansur, L., and Luiz, C. (2015). Oxidative stress in plants under drought conditions and the role of different enzymes. *Enzyme Engineering* 5, 1–6. doi: 10.4172/2329-6674.1000136

Marino, D., Dunand, C., Puppo, A., and Pauly, N. (2012). A burst of plant NADPH oxidases. *Trends Plant Sci.* 17, 9–15. doi: 10.1016/j.tplants.2011.10.001

Martinis, J., Glauser, G., Valimareanu, S., and Kessler, F. (2013). A chloroplast ABC1-like kinase regulates vitamin E metabolism in Arabidopsis. *Plant Physiol.* 162, 652–662. doi: 10.1104/pp.113.218644

Martinis, J., Glauser, G., Valimareanu, S., Stettler, M., Zeeman, S. C., Yamamoto, H., et al. (2014). ABC1K1/PGR6 kinase: A regulatory link between photosynthetic activity and chloroplast metabolism. *Plant J.* 77, 269–283. doi: 10.1111/tpj.12385

Mayer, K. F. X., Rogers, J., Dolezel, J., Pozniak, C., Eversole, K., Feuillet, C., et al. (2014). A chromosome-based draft sequence of the hexaploid bread wheat (*Triticum aestivum*) genome. *Science* 345:1251788. doi: 10.1126/science.1251788

Meijer, M. S., Talens, V. S., Hilbers, M. F., Kieltyka, R. E., Brouwer, A. M., Natile, M. M., et al. (2019). NIR-light-driven generation of reactive oxygen species using Ru (II)-decorated lipid-encapsulated upconverting nanoparticles. *Langmuir* 35, 12079–12090. doi: 10.1021/acs.langmuir.9b01318

Mirdita, M., Schütze, K., Moriwaki, Y., Heo, L., Ovchinnikov, S., and Steinegger, M. (2021). Colab fold-making protein folding accessible to all. *Nature Method.* 19, 679–682. doi: 10.21203/rs.3.rs-1032816/v1

Mistry, J., Chuguransky, S., Williams, L., Qureshi, M., Salazar, G. A., Sonnhammer, E. L., et al. (2021). Pfam: The protein families database in 2021. *Nucleic Acids Res.* 49, D412–D419. doi: 10.1093/nar/gkaa913

Mozzo, M., Dall'Osto, L., Hienerwadel, R., Bassi, R., and Croce, R. (2008). Photoprotection in the antenna complexes of photosystem II: role of individual xanthophylls in chlorophyll triplet quenching. *J. Biol. Chem.* 283, 6184–6192. doi: 10.1074/jbc.M708961200

Osakabe, Y., Mizuno, S., Tanaka, H., Maruyama, K., Osakabe, K., Todaka, D., et al. (2010). Overproduction of the membrane bound receptor-like protein kinase 1, RPK1, enhances abiotic stress tolerance in Arabidopsis. *J. Biol. Chem.* 285, 9190–9201. doi: 10.1074/jbc.M109.051938

Pospíšil, P. (2016). Production of reactive oxygen species by photosystem II as a response to light and temperature stress. *Front. Plant Sci.* 7:1950. doi: 10.3389/fpls.2016.01950

Qin, X. H., Duan, Z. K., Zheng, Y., Liu, W. C., Guo, S. Y., Botella, J. R., et al. (2020). ABC1K10a, an atypical kinase, functions in plant salt stress tolerance. *BMC Plant Biol.* 20:270. doi: 10.1186/s12870-020-02467-4

Rombauts, S., Déhais, P., Van, M. M., and Rouzé, P. (1999). Plant CARE, a plant cis-acting regulatory element database. *Nucleic Acids Res.* 27, 295–296. doi: 10.1093/nar/27.1.295

Ronquist, F., Teslenko, M., Van, D. M. P., Ayres, D. L., Darling, A., Hohna, S., et al. (2012). Mrbayes 3.2: efficient bayesian phylogenetic inference and model choice across a large model space. *Syst. Biol.* 61, 539–542. doi: 10.1093/sysbio/sys029

Ruff, K. M., and Pappu, R. V. (2021). Alpha fold and implications for intrinsically disordered proteins. *J. Mol. Biol.* 433:167208. doi: 10.1016/j.jmb.2021.167208

Saitou, N., and Nei, M. (1987). The neighbor-joining method: A new method for reconstructing phylogenetic trees. *Mol. Biol. Evol.* 4, 406–425. doi: 10.1093/oxfordjournals.molbev.a040454

Scheeff, E. D., and Bourne, P. E. (2005). Structural evolution of the protein kinase–like superfamily. *PLoS Comput. Biol.* 1:e49. doi: 10.1371/journal.pcbi.0010049

Schreiber, U., Quayle, P., Schmidt, S., Escher, B. I., and Mueller, J. F. (2007). Methodology and evaluation of a highly sensitive algae toxicity test based on multiwell chlorophyll fluorescence imaging. *Biosens. Bioelectron.* 22, 2554–2563. doi: 10.1016/j.bios.2006.10.018

Suzuki, N., Miller, G., Morales, J., Shulaev, V., Torres, M. A., and Mittler, R. (2011). Respiratory burst oxidases: the engines of ROS signaling. *Curr. Opin. Plant Biol.* 14, 691–699. doi: 10.1016/j.pbi.2011.07.014

Tamura, K., Stecher, G., Peterson, D., Filipski, A., and Kumar, S. (2013). MEGA6: Molecular evolutionary genetics analysis version 6.0. *Mol. Biol. Evol.* 30, 2725–2729. doi: 10.1093/molbev/mst197

Wang, C., Jing, R., Mao, X., Chang, X., and Li, A. (2011). TaABC1, a member of the activity of bc 1 complex protein kinase family from common wheat, confers enhanced tolerance to abiotic stresses in Arabidopsis. *J. Exp. Bot.* 62, 1299–1311. doi: 10.1093/jxb/erq377

Wang, Y., Tang, H., Debarry, J. D., Tan, X., Li, J., Wang, X., et al. (2012). MCScanX: a toolkit for detection and evolutionary analysis of gene synteny and collinearity. *Nucleic Acids Res.* 40:e49. doi: 10.1093/nar/gkr1293

Wang, X., Wang, X., Duan, Y., Yin, S., Zhang, H., and Huang, L. (2013). TaAbc1, a member of Abc 1-like family involved in hypersensitive response against the stripe rust fungal pathogen in wheat. *PLoS One* 8:e58969. doi: 10.1371/journal.pone.0058969

Wang, M., Zhao, X., Xiao, Z., Yin, X., Xing, T., and Xia, G. (2016). A wheat superoxide dismutase gene TaSOD2 enhances salt resistance through modulating redox homeostasis by promoting NADPH oxidase activity. *Plant Mol. Biol.* 91, 115–130. doi: 10.1007/s11103-016-0446-y

Weigel, D., and Glazebrook, J. (2006). Transformation of agrobacterium using the freeze-thaw method. *Cold Spring Harb Protoc* 2006:4666. doi: 10.1101/pdb.prot4666

Wu, N., Mao, H. T., Chen, M. Y., Dong, J., Yuan, M., Zhang, Z. W., et al. (2020). Different responses of photosystem and antioxidant defense system to three environmental stresses in wheat seedlings. *Photosynthetica* 58, 87–99. doi: 10.32615/ps.2019.156

Wu, N., Zhu, Y., Song, W., Li, Y., Yan, Y., and Hu, Y. (2014). Unusual tandem expansion and positive selection in subgroups of the plant GRAS transcription factor superfamily. *BMC Plant Biol.* 14, 373–321. doi: 10.1186/s12870-014-0373-5

Xiong, L., Schumaker, K. S., and Zhu, J. K. (2002). Cell signaling during cold, drought, and salt stress. *Plant Cell* 14, S165–S183. doi: 10.1105/tpc.000596

Yang, Z. (2007). PAML 4: phylogenetic analysis by maximum likelihood. *Mol. Biol. Evol.* 24, 1586–1591. doi: 10.1093/molbev/msm088

Yang, S., Li, T., Liu, M., Gao, S., Yang, S., Li, L., et al. (2012c). Phylogenetic, structure and expression analysis of ABC1Ps gene family in rice. *Biol. Plant.* 56, 667–674. doi: 10.1007/s10535-012-0247-3

Yang, Z., Wong, W. S., and Nielsen, R. (2005). Bayes empirical Bayes inference of amino acid sites under positive selection. *Mol. Biol. Evol.* 22, 1107–1118. doi: 10.1093/molbev/msi097

Yang, S., Zeng, X., Li, T., Liu, M., Zhang, S., Gao, S., et al. (2012a). AtACDO1, an ABC1-like kinase gene, is involved in chlorophyll degradation and the response to photooxidative stress in Arabidopsis. *J. Exp. Bot.* 63, 3959–3973. doi: 10.1093/jxb/ers072

Yang, S., Zhang, Q., Li, T., Du, D., Yang, S., and Yang, C. (2012b). AtSIA1, an ABC1-like kinase, regulates salt response in Arabidopsis. *Biologia* 67, 1107–1111. doi: 10.2478/s11756-012-0115-9

Yoo, S. D., Cho, Y. H., and Sheen, J. (2007). Arabidopsis mesophyll protoplasts: a versatile cell system for transient gene expression analysis. *Nat. Protoc.* 2, 1565–1572. doi: 10.1038/nprot.2007.199

Yu, Y., Zhu, D., Ma, C., Cao, H., Wang, Y., Xu, Y., et al. (2016). Transcriptome analysis reveals key differentially expressed genes involved in wheat grain development. *Crop J.* 4, 92–106. doi: 10.1016/j.cj.2016.01.006

Yuan, H., Zhang, J., Nageswaran, D., and Li, L. (2015). Carotenoid metabolism and regulation in horticultural crops. *Horticul. Res.* 2:15036. doi: 10.1038/hortres.2015.36

Zhu, D., Luo, F., Zou, R., Liu, J., and Yan, Y. (2021). Integrated physiological and chloroplast proteome analysis of wheat seedling leaves under salt and osmotic stresses. *J. Proteome* 234:104097. doi: 10.1016/j.jprot.2020.104097

Zhu, Y., Wu, N., Song, W., Yin, G., Qin, Y., Yan, Y., et al. (2014). Soybean (*Glycine max*) expansin gene superfamily origins: segmental and tandem duplication events followed by divergent selection among subfamilies. *BMC Plant Biol.* 14, 1–19. doi: 10.1186/1471-2229-14-93

frontiers | Frontiers in Plant Science

TYPE Original Research
PUBLISHED 12 September 2022
DOI 10.3389/fpls.2022.950796

Check for updates

OPEN ACCESS

EDITED BY
Caroline Müller,
Universidade Federal da Fronteira Sul, Brazil

REVIEWED BY
Ke Teng,
Beijing Academy of Agricultural and Forestry Sciences, China
Shah Fahad,
The University of Haripur, Pakistan

*CORRESPONDENCE
Zofia Szweykowska-Kulinska
zofszwey@amu.edu.pl
Artur Jarmolowski
artjarmo@amu.edu.pl

SPECIALTY SECTION
This article was submitted to Plant Abiotic Stress, a section of the journal Frontiers in Plant Science

RECEIVED 23 May 2022
ACCEPTED 15 July 2022
PUBLISHED 12 September 2022

CITATION
Smoczynska A, Pacak A, Grabowska A, Bielewicz D, Zadworny M, Singh K, Dolata J, Bajczyk M, Nuc P, Kesy J, Wozniak M, Ratajczak I, Harwood W, Karlowski WM, Jarmolowski A and Szweykowska-Kulinska Z (2022) Excess nitrogen responsive HvMADS27 transcription factor controls barley root architecture by regulating abscisic acid level.
Front. Plant Sci. 13:950796.
doi: 10.3389/fpls.2022.950796

COPYRIGHT
© 2022 Smoczynska, Pacak, Grabowska, Bielewicz, Zadworny, Singh, Dolata, Bajczyk, Nuc, Kesy, Wozniak, Ratajczak, Harwood, Karlowski, Jarmolowski and Szweykowska-Kulinska. This is an open-access article distributed under the terms of the Creative Commons Attribution License (CC BY). The use, distribution or reproduction in other forums is permitted, provided the original author(s) and the copyright owner(s) are credited and that the original publication in this journal is cited, in accordance with accepted academic practice. No use, distribution or reproduction is permitted which does not comply with these terms.

Excess nitrogen responsive HvMADS27 transcription factor controls barley root architecture by regulating abscisic acid level

Aleksandra Smoczynska[1], Andrzej Pacak[1], Aleksandra Grabowska[1], Dawid Bielewicz[1,2], Marcin Zadworny[3], Kashmir Singh[4], Jakub Dolata[1], Mateusz Bajczyk[1], Przemyslaw Nuc[1], Jacek Kesy[5], Magdalena Wozniak[6], Izabela Ratajczak[6], Wendy Harwood[7], Wojciech M. Karlowski[8], Artur Jarmolowski[1]* and Zofia Szweykowska-Kulinska[1]*

[1]Department of Gene Expression, Institute of Molecular Biology and Biotechnology, Faculty of Biology, Adam Mickiewicz University, Poznań, Poland, [2]Center for Advanced Technology, Adam Mickiewicz University, Poznań, Poland, [3]Institute of Dendrology, Polish Academy of Sciences, Kórnik, Poland, [4]Department of Biotechnology, Panjab University, Chandigarh, India, [5]Institute of Biology, Faculty of Biological and Veterinary Sciences, Nicolaus Copernicus University, Toruń, Poland, [6]Department of Chemistry, Faculty of Forestry and Wood Technology, Poznan University of Life Sciences, Poznań, Poland, [7]Department of Crop Genetics, John Innes Centre, Norwich Research Park, Norfolk, United Kingdom, [8]Department of Computational Biology, Institute of Molecular Biology and Biotechnology, Adam Mickiewicz University, Poznań, Poland

Nitrogen (N) is an important element for plant growth and development. Although several studies have examined plants' response to N deficiency, studies on plants' response to excess N, which is common in fertilizer-based agrosystems, are limited. Therefore, the aim of this study was to examine the response of barley to excess N conditions, specifically the root response. Additionally, genomic mechanism of excess N response in barley was elucidated using transcriptomic technologies. The results of the study showed that barley MADS27 transcription factor was mainly expressed in the roots and its gene contained N-responsive *cis*-regulatory elements in the promoter region. Additionally, there was a significant decrease in *HvMADS27* expression under excess N condition; however, its expression was not significantly affected under low N condition. Phenotypic analysis of the root system of *HvMADS27* knockdown and overexpressing barley plants revealed that HvMADS27 regulates barley root architecture under excess N stress. Further analysis of wild-type (WT) and transgenic barley plants (*hvmads27 kd* and *hvmads27 c-Myc OE*) revealed that HvMADS27 regulates the expression of HvBG1 β-glucosidase, which in turn regulates abscisic acid (ABA) level in roots. Overall, the findings of this study showed that *HvMADS27* expression is downregulated in barley roots under excess N stress, which induces *HvBG1* expression, leading to the release of ABA from ABA-glucose conjugate, and consequent shortening of the roots.

KEYWORDS

miRNA, nitrogen, barley, root architecture, abscisic acid, HvMADS27

Introduction

Nitrogen (N) availability is a primary factor affecting the size and quality of crop yield (Anas et al., 2020). Over the years, intensive crop production has led to increased fertilizer use, resulting environmental problems (Goulding et al., 2008; Jiao et al., 2016; Al-Tawaha et al., 2021). Studies have extensively examined plant response to N deficiency (Vos et al., 2005; Uribelarrea et al., 2009; Kant et al., 2011; Chen et al., 2015; Mu et al., 2016; Xiong et al., 2018); however, studies on plants response to high N supply are limited. Under excess N conditions, it is known that plants exhibit severe phenotypes, including reduced inflorescence, short roots, yellowing of leaves, reduced grain yield, and high susceptibility to pathogens (Lehmeier et al., 2013; Kong et al., 2017; Grabowska et al., 2020). Thus, illuminating the mechanisms of excess N response in barley (*Hordeum vulgare*), an economically important crop ranking fourth in global production, could improve fertilizer use efficiency in agroecosystems (Newton et al., 2011; Chaudhry et al., 2021).

Nitrate (NO_3^-) and ammonium (NH_4^+) ions are absorbed by the root system using specific transporters. Two nitrate uptake systems formed by LOW and HIGH-AFFINITY TRANSPORTERS (LATS and HATS, respectively) were identified. LATS is encoded by the *NITRATE TRANSPORTER 1/PEPTIDE TRANSPORTER* (*NRT1/PTR*) family genes (*NPF*), which includes 53 members in *Arabidopsis,* 93 in rice, and only three members have been identified in barley based on their similarity to rice proteins (*HvNRT1.1*, *HvNRT1.2*, and *HvNRT1.5*; Leran et al., 2014; Wittgenstein et al., 2014; Liu et al., 2020). HATS are encoded by the *NITRATE TRANSPORTER 2* (*NRT2*) gene family, and only seven members have been identified in Arabidopsis, five in rice, and four in barley (Chopin et al., 2007; Feng et al., 2011). NITRATE TRANSPORTER 1 (NRT1.1), which acts as a N sensor, is the most studied member of the LATS, and is exclusively expressed in roots (Ho et al., 2009). *NITRATE TRANSPORTER 2* (*NRT2*) genes encode HATS that act under low soil N conditions, and interacts with NITRATE ASSIMILATION RELATED PROTEIN (NAR2) family members, for proper functioning (Orsel et al., 2006). AMMONIUM TRANSPORTERS (AMTS) are involved in the absorption of ammonium ions (Ho et al., 2009). Presently, six AMTS genes have been identified in Arabidopsis, 10 in rice, and 16 in soybean (Gazzarrini et al., 1999; Sonoda et al., 2003; Kobae et al., 2010). Nitrate and ammonium ions absorbed by plants are further incorporated into amino acids. Ammonium is the most preferable source of nitrogen for plants, because nitrate needs to be reduced to ammonium, which requires more energy (Bloom et al., 1992; Filiz and Akbudak, 2020). First, nitrate is reduced to nitrite in the cytosol by nitrate reductase (Meyer and Stitt, 2001), and then translocated to the chloroplasts where it is reduced to ammonium by nitrite reductase (Meyer and Stitt, 2001). Ammonium is then assimilated in the GS/GOGAT cycle, where glutamine synthetase (GS) fixes ammonium on glutamate to form glutamine. Subsequently, glutamine 2-oxoglutarate amino transferase (GOGAT) catalyzes the reaction of glutamine with 2-oxoglutarate to form two molecules of glutamate (Lea and Miflin, 1974; Lea and Forde, 1994; Unno et al., 2006). Other amino acids are the result of transamination reactions in which glutamine is the substrate (Tcherkes and Hodges, 2008).

Several studies have examined the relationship between nitrogen metabolism in plants and the production of phytohormones, particularly abscisic acid (ABA; Finkelstein et al., 2002; Cutler et al., 2010; Yan et al., 2014; Sah et al., 2016; Harris and Ondzighi-Assoume, 2017; Jiao et al., 2020). ABA regulates several processes in plants, including seed germination, abiotic and biotic stress responses, and primary root growth (Finkelstein et al., 2002; Cutler et al., 2010; Yan et al., 2014; Sah et al., 2016; Jiao et al., 2020). In Arabidopsis, an increase in environmental N in the rhizosphere causes gradual accumulation of ABA in roots, and N induces ABA-responsive genes (Harris and Ondzighi-Assoume, 2017). In Arabidopsis, SCARECROW (SCR) transcription factor (TF) controls root elongation by repressing the expression of *ABA INSENSITIVE 4* (*ABI4*) and *ABA INSENSITIVE 5* (*ABI5*) transcription factor genes. Interestingly, it has been shown that *SCR* expression is controlled by both N and ABA (Harris and Ondzighi-Assoume, 2017). Although root development and growth are potentially beneficial for N uptake from soil (Wiren et al., 1997), an in-depth understanding of different traits and their drivers is essential to determine the process affecting N acquisition (Frescher et al., 2020; Rehman et al., 2021).

Recently, Wang et al. (2020) reported that the TaANR1-MADS-box transcription factor regulates ABA level in wheat roots by activating *TaBG1* β-glucosidase and regulating the expression level of *TaWabi5* transcription factor gene that controls the expression of wheat nitrogen transporter genes from the *TaNRT2* family. MADS-box transcription factors have been shown to play an important role in plant root responses to N and are conserved in nearly all eukaryotes (Yan et al., 2014; Yu et al., 2015; Zhang et al., 2018; Wang et al., 2020). MADS-box name is derived from the yeast MINICHROMOSOME MAINTENANCE 1 (MCM1; Passmore et al., 1988), the Arabidopsis AGAMOUS (AG; Yanofsky et al., 1990), the Antirrhinum DEFICIENS (DEFA; Schwarz-Sommer et al., 1990), and the mammalian SERUM RESPONSE FACTOR (SRF) proteins (Norman et al., 1988).

MADS-box domain consists of 58 amino acid residues at the N-terminus that binds to a consensus CC $[A/T]_6GG$ sequence, termed as the "CArG-box" motif (Hayes et al., 1988; Riechmann et al., 1996; Guo et al., 2013). Structure of MADS-box transcription factors consists of four protein domains: DNA binding MADS-box (M) domain, the less-conserved intervening domain (I) that ensures interaction specificity between different MADS-box transcription factors and/or other proteins, the keratin-like coiled-coil (K) domain for conferring protein–protein interactions, and a highly variable C-terminal (C) domain for regulating gene transcription or protein complexes formations (Hill et al., 2008).

Yan et al., 2014 reported that rice *OsMADS23,25,27,57,* and *61* regulate lateral root elongation in response to N and are regulated by miRNA444a. Overexpression of this miRNA results in reduced lateral root elongation, but promotes primary and adventitious

root growth in an N-dependent manner. Moreover, studies have shown that *OsMADS25*, which is specifically expressed in rice roots, regulates root development and affects plant N accumulation (Yu et al., 2015; Zhang et al., 2018). Although we have already knowledge on the role of rice MADS TFs and miRNAs from miR444 family in root response to N, nothing is known about the mechanisms of root response to N in barley plants.

Thus, the aim of this study was to reveal the role of selected MADS TF and miR444 family members in shaping barley root architecture in response to N. In this paper, we reveal a novel molecular mechanism of barley root shortening in response to N excess stress. We present the findings that *HvMADS27* expression is downregulated in barley roots under excess N stress, which induces *HvBG1* expression, leading to the release of ABA from ABA-glucose conjugate, and consequent shortening of the roots. It seems that miR444 family members do not exert the major role in the downregulation of *HvMADS27* expression under N excess stress.

The results of our studies may be relevant for plant scientist working on plant response to various environmental conditions and for breeding companies working on developing new strategies to engineer crop plants resistant to various environmental cues (Imran et al., 2021).

Materials and methods

Plant material and growth conditions

Seeds of spring barley (*H. vulgare* cultivar Golden Promise) were germinated on wet sterile Whatman filter paper for 3 days in a growth chamber (MLR35−1H, Sanyo, Panasonic) under a 16/8 h light/dark photoperiod at 20°C until white hypocotyls were visible. Two seedlings were then transferred to a single pot containing perlite supplemented with medium containing 28 mM NH_4NO_3, 20 mM KH_2PO_4, 4 mM K_2SO_4, 16 mM $MgSO_4$:$7H_2O$, 53 µM H_3BO_3, 8 µM $CuSO_4$, 4 µM $MnSO_4$:H_2O, and 120 µM $FeCl_3$:$6H_2O$ (Pacak et al., 2016a). To create high N stress condition, the concentration of NH_4NO_3 in the medium above was increased by 10 times, which falls within the range of concentrations recommended in agriculture (Lips et al., 1990; Yao et al., 2011; Heuermann et al., 2021). The expression of the *HvNRT1.1* transporter gene was used as a marker of N stress (Supplementary Figure S3). The plants were subsequently grown under controlled conditions (20°C day temperature and 15°C night temperature) under a 16/8 h light/dark photoperiod.

RNA isolation and quantitative PCR

Total RNA was extracted from the roots using the Direct-zol RNA Mini Prep Kit (Zymo Research), according to the manufacturer's instructions. RNA quality and quantity were assessed using NanoDrop ND-1000 spectrophotometer, and RNA integrity was estimated on a 1.2% agarose gels. Thereafter, 3 µg of DNA-free RNA was reverse-transcribed to generate cDNA using SuperScript III Reverse Transcriptase (Invitrogen, Carlsbad, CA, United States) and oligo$(dT)_{18}$ (Novazym, Poland) primers. cDNA samples were diluted 4-times and 1 µl was used as template. Quantitative real-time PCR was performed using Power SYBR® Green PCR Master MIX (Applied Biosystems, Warrington, United Kingdom) and two primers specific for the gene of interest (for example AS104 and AS105, respectively, when expression of *HvMADS27* was analyzed; see Supplementary Table S2). Final concentration 500 nM each on a 7900HT Fast Real-Time PCR System (Applied Biosystems) in 10 µl reaction volumes in 384-well plate. The PCR conditions were as follows: 10 min at 95°C, 40 cycles for 15 s at 95°C, and 1 min at 60°C. Each real-time PCR reaction was performed independently for the three biological replicates. The barley *ARF 1* (*ADP-RIBOSYLATION FACTOR 1-like*; GenBank: AJ508228.2) gene fragment of 61 nt was simultaneously amplified and detected as an internal reference (Grabowska et al., 2020).

RACE analysis

To analyze *HvMADS27* and *HvMIR444c* gene structure, 5′ RACE experiments were conducted using SMARTer® RACE cDNA Amplification Kit (Takara Bio, United States, Cat# 634860) and Advantage Polymerase as described by Kruszka et al. (2014). PCR products were cloned into the pGEM T-Easy vector (Promega) and sequenced (Faculty's Laboratory of Molecular Biology Techniques, Adam Mickiewicz University in Poznan, Poland).

Small RNA and transcriptomic library preparation

sRNA data of barley roots in the control and high N stress treatment groups used in this study were previously published by Grabowska et al. (2020) and deposited in the GO database under accession number GSE145799.

For transcriptomic analysis, total RNA was extracted from the root of WT and *HvMADS27* knockdown plants as described above and analyzed with RNA Nano Chips and Agilent Bioanalyzer System (Agilent Technologies, USA, No. 5067-1511). Samples with RIN numbers above 8 were further subjected to rRNA depletion using the RiboMinus Plant Kit for RNA-Seq (Invitrogen, United States, No. 2157461), and RNA concentration was further assessed using Qubit 3.0 Fluorometer (Invitrogen, United States). Approximately, 100 ng of RNA was used per library. Sequence libraries were prepared using NEB Ultra II Directional RNA Library Prep kit for Illumina (New England BioLabs, United States, No. E7760S), according to the manufacturer's instructions and the quality of the prepared libraries was assessed using an Agilent Bioanalyzer DNA Chip

(Agilent Technologies, No. 6067-1504, United States). Thereafter, samples were sequenced on Illumina platform. Sequence quality was assessed using the FASTQC program, and adaptor trimming was performed using Trimmomatic software. All obtained reads were mapped to the barley genome and transcriptome using HISAT2 and SALMON programs, respectively, and statistical analysis was performed in R studio environment using DESeq2 software (Love et al., 2014).

Obtained data are available under accession number: PRJNA746688.

PARE library construction

Barley Parallel Analysis of RNA Ends (PARE) library was constructed using protocol described by German and colleagues (German et al., 2009). For barley PARE library construction instead of MmeI restriction enzyme, we used EcoP15I restriction enzyme for generation of 26–27 bp fragments as described previously (Kruszka et al., 2014; Alaba et al., 2015). RNA and DNA adapters were modified for compatibility to the TruSeq sequencing system of Illumina. Poly(A)-enriched RNA was isolated from barley line Rolap harvested at 68-day-old stage (kernel formation), described by as previously (Pacak et al., 2016b). PARE library was sequenced using Illumina technology in Fasteris SA (Switzerland) as it was described previously (Alaba et al., 2015). NGS sequences were trimmed and analyzed using CLC Genomics Workbench (QIAGEN Aarhus A/S). T-plots showing microRNA directed cleavage sites were constructed using PAREsnip2 software (Thody et al., 2018).

Generation of transgenic lines

The WMD3-Web MicroRNA Designer[1] was used to construct transgenic lines overexpressing artificial miRNA amiRMADS27 that targets *HvMADS27* mRNA. From the ranking list, we chose miRNAs with the best qualities and ordered the GeneArt gateway-compatible vector containing artificial miRNA/miRNA* embedded in barley pre-miRNA167h body where miRNA167h and its cognate miRNA* were replaced accordingly (Kruszka et al., 2013; Zielezinski et al., 2015; see Supplementary Figure S4). Finally, we performed LR cloning using LR clonase according to the manufacturer's instructions, and cloned pre-miRNA167h with amiRMADS27 cassette into the designated vector, pBRACT214.[2]

To construct transgenic lines overexpressing *HvMADS27* with c-Myc tag, mRNA of *HvMADS27* was amplified on cDNA template from 2-week-old barley roots with primers containing restriction sites for EcoRI and BamHI, respectively. After restriction digestion at 37°C for 1 h, insert was cloned into the pGBKT7 plasmid containing the c-Myc tag. Then, we amplified *HvMADS27* cDNA with a c-Myc tag DNA insert with a forward primer containing CACC and a Kozak sequence at the 5′ end, reverse primer from the previous step, and cloned the insert into the pENTR plasmid. Finally, we performed cloning with LR clonase to the destination vector-pBRACT214.

To produce transgenic barley plants, we transformed *Agrobacterium tumefaciens* AGL1 strain with prepared constructs and performed barley immature embryo transformation at the John Innes Centre in Norwich according to the protocol of Hinchliffe and Harwood (2019).

Plants from a T0 generation were genotyped and the presence of a transgene was confirmed using PCR. In the next step, from four independent transgenic lines 100 plants of T1 generation were sown and further genotyped for the presence of the transgene as well as Northern blot experiments were performed for lines expressing artificial miRNA and western blot for lines expressing *HvMADS27* with c-Myc tag. Expression level of *HvMADS27* was analyzed and plants that exhibited the lowest and highest *HvMADS27* mRNA levels, respectively, were further bred. T2 generation plants were used for subsequent experiments.

Root structure analysis

To analyze the root structure of WT plants, *hvmads27* knockdown lines, and *hvmads27 c-Myc* overexpressing lines plants were grown for 2 weeks and collected. Plants representing four transgenic lines were used for the measurements. From each transgenic line 20 plants were used. Roots were cut off, placed in a tray with water, and scanned using an Epson scanner at 300 dpi resolution and WinRHIZO software (Regent Instruments, Inc., Quebec, Canada). The total root length was further examined. Data obtained were normalized using Shapiro–Wilk test, and analyzed using Statistica software 13.1 (Kraków, Poland). Mean comparison was performed using Kruskal–Wallis test, $*p < 0.05$, $**p < 0.01$, and $***p < 0.0001$.

Measurement of N and ABA levels

Plants for the N and ABA determination were grown under the conditions described above. However, for treatment with ABA synthesis inhibitor, we supplemented the medium with 100 µM norflurazon (Sigma cat num: 34364; Dong et al., 2013; Wang et al., 2020). Approximately, 200 mg of pulverized root was incubated overnight in a cold room (11°C) in a mixture of 80% acetonitrile with 5% formic acid and 1 mM BHT and an internal standard, deuterated ABA (10 ng/sample). Then, magnesium sulfate and sodium chloride (1:3) were added, and samples were vortexed for 1 min and then centrifuged for 8 min at maximum speed (14,000 × *g*). Sodium sulfate was added to the obtained supernatants, and the samples were vortexed and centrifuged as described above. The obtained supernatant was dried under a

1 https://www.wmd3.weigelworld.org

2 https://www.jic.ac.uk/technologies/genomic-services/bract

stream of nitrogen at 45°C and the remaining residue was suspended in 1 M formic acid. The samples were then extracted using solid-phase C18 octadecyl columns (J.T. Baker C18 columns #7020–01), dried under a stream of nitrogen at 45°C, and the remaining residue was suspended in 100 µl of 80% methanol, followed by suspension in 35% methanol.

The ABA concentration of the roots was determined using ultra-pressure liquid chromatography tandem mass spectrometry (UHPLC–MS/MS; Shimadzu Nexera XR UHPLC/LCMS-8045 system; Kyoto, Japan) equipped with an Ascentis Express C-18 column (2.7 µm, 100 × 2.1 mm, Supelco, United States). Then, the obtained peak surfaces of standard and endogenous ABA were exported to an Excel file and analyzed using the formula: (endogenous ABA peak surface/internal standard surface) × 10/weight of used tissue in grams. The obtained results were divided by a coefficiency factor of 0.98 and subjected to statistical analysis using Student's *t*-test $*p < 0.05$, $**p < 0.01$, and $***p < 0.0001$.

The N content of the samples was determined using a Flash 2000 elemental analyzer (Thermo Fisher Scientific, USA). Instrument calibration was performed using standard BBOT [2,5-bis- (tert-butyl-benzoxazol-2-yl) thiophene; Thermo Fisher Scientific, United States] and Alfalfa certified reference material (Elemental Microanalysis Ltd., United Kingdom). Six-point calibration curves were plotted for each element (C, H, N, S) using the K factor as the calibration method (Rybak et al., 2020).

ABA sensitivity assay

Germinated seedlings of WT plants, plants overexpressing *HvMADS27* with c-Myc tag and *HvMADS27* knockdown plants were grown on ½ MS plates (four seeds per plate, and three plates for variant) in a growth chamber (MLR35−1H, Sanyo, Panasonic) under long-day conditions at 20°C with supplementation with either 0.1 M NaOH in the control condition or 50 µM ABA dissolved in 0.1 M NaOH for ABA treatment. After a week, measurements of plant roots were taken and analyzed statistically using Excel software, and a standard *t*-test.

Western blot analysis

Protein extracts for western blot analysis were prepared using buffer containing 50 mM Tris–HCl pH 7.5, 100 mM NaCl, 0.25% Triton X-100, 1 mM EDTA, 10 mM NaF, 1 mM Na_3VO_4, 0.25% NP-40, 1 mM PMSF, 1x protease inhibitor complete EDTA-free (Roche), and 10 µM MG132. Protein extracts were separated by 13% SDS-PAGE, transferred to a polyvinylidene difluoride membrane (PVDF; Millipore), and analyzed by western blotting using antibodies at dilutions recommended by the manufacturer: anti-c-Myc HRP (9E10 cat num# MA1-980-HRP) anti-BG1 (Agrisera, AS20 4419), anti-H3 (Abcam, ab18521), and anti-rabbit (Agrisera, AS09 602).

Northern blot analysis

RNA electrophoresis, blotting, and hybridization were performed as previously described by Kruszka et al. (2013).

ChIP-qPCR

ChIP was performed as previously described by Dolata et al. (2015) using 2 g per biological replicate of pulverized root sample from WT plants and plants overexpressing *HvMADS27 c-Myc*. Approximately 2 µg of anti-c-Myc (Agrisera, AS15 3035) antibody per IP was used. For control, root samples from mutants without the addition of antibody and WT plants with the addition of anti-c-Myc antibody was used. Thereafter, IP samples were washed, eluted, and incubated with proteinase K for 6 h at 65°C and used as a template for RT-qPCR, and primers flanking used are listed Supplementary material.

Bioinformatic tools

Genomic sequences for *HvMADS27* and *HvMIR444c* were obtained from the Ensembl Plants database[3] and aligned with the cDNA sequence using MAFFT version 7.[4] Results from transcriptome sequencing were quality checked using the FASTQC program, and adaptor trimming was performed using Trimmomatic software. All obtained reads were mapped to the barley genome and transcriptome using HISAT2 and SALMON programs, respectively, and statistical analysis was performed in R studio environment using DESeq2 software (Love et al., 2014). Thereafter, the online tool WMD3-Web MicroRNA Designer[5] was used to prepare construct overexpressing artificial miRNA (amiRMADS27) that targets *HvMADS27* mRNA. Root systems were analyzed using an Epson scanner and WinRHIZO software (Regent Instruments, Inc., Quebec, Canada). Total root length was further analyzed statistically using Statistica software 13.1 (Kraków, Poland). Densitometric analysis of western blots was performed using Image Studio Lite program version 5.2.5, and the amount of BG1 protein was normalized using WT control to normalize all bands (treated as 1.0, LI-COR, United States).

Arabidopsis and barley protoplasts transfection and HvMADS27 localization

Berley leave protoplasts were isolated as described in (Frank et al., 2019) with minor modifications: Leaves of 1-week-old barley seedlings were cut and epiderma was removed. Leaves were

3 https://plants.ensembl.org/Hordeum_vulgare/
4 https://mafft.cbrc.jp/alignment/
5 www.wmd3.weigelworld.org

incubated in enzyme solution containing cellulase "Onozuka R-10" (#16419.05, Serva, Germany) and macerozyme R-10 (#M8002.0010 Duchefa Biochemie, Netherlands) in darkness in 28°C for 80 min. After that time buffer containing protoplasts was filtered using nylon filter (#NY8004700, Millipor) and centrifuged. Next, the gradient was prepared with creating a sublayer of floating buffer pH 5.8 (1 mM $CaCl_2x2H_20$, 40 mM sucrose, 100 nM sorbitol, and 5 mM MES) and upper layer of W5 buffer pH 5.8 (154 mM NaCl, 125 mM $CaCl_2x2H_20$, 5 mM KCl, and 5 mM glucose). Further, the middle layer containing live protoplasts was collected and then suspended in Wash Solution (500 mM sorbitol, 20 nM KCl, and 4 mM MES). Transformation was performed using 100 µl of protoplasts and two plasmids: one containing *GFP-HvMADS27* and one *RFP-SERRATE* using 40 %PEG in 1x MaMg solution. Samples were incubated overnight and observed under the microscope. SERRATE was used as a nuclear marker (Yang et al., 2006).

The isolation of protoplasts from Arabidopsis was done exactly as described previously (Bajczyk et al., 2020). Localization of MADS27-GFP and RFP-SERRATE in both Arabidopsis and barley protoplasts was done using a Nikon A1RSi Inverted Confocal Microscope using 40×/1.25 water-immersion objectives. Excitation was achieved with an Ion argon laser at 488 nm (GFP) and with a diode laser at 561 nm (RFP). Fluorescence was observed using the emission spectrum range of 525/50 nm (GFP) and 595/50 (RFP).

Results

HvMADS27 is expressed mainly in roots and is responsive to high N stress

The gene structure and genome position of *HvMADS27* was analyzed to determine its function. The 5′ and 3′ RACE experiments revealed that the *HvMADS27* gene contains seven exons and six introns, and is located on the second chromosome (HORVU2Hr1G080490) on the DNA strand opposite to the *MIR444c* gene. After transcription and transcript maturation, there was approximately 60 nucleotides overlap between them, including perfect complementarity between miR444c and target *HvMADS27* mRNA (Figure 1A). Furthermore, degradome analysis of 68-day old samples of barley grown under control growth conditions showed that *HvMADS27* mRNA is likely targeted by miR444c (Supplementary Figure S1). Deep sequencing of small RNAs from selected barley developmental stages revealed that miRNA444c was highly expressed in the 6th week of development (Figure 1B). RT-qPCR analysis showed that the highest expression of *HvMADS27* was during the second week of barley growth (Figure 1C). Furthermore, *HvMADS27* was mainly expressed in the roots of two-week-old barley plants, necessitating further focus on this organ (Figure 1F; Supplementary Figure S2). Analysis of GFP-HvMADS27 localization in barley and Arabidopsis protoplasts revealed nuclear localization of the protein (Supplementary Figure S3). To elucidate the biological function of *HvMADS27* gene, regulatory motifs on the promoters of both *MIR444c* and *HvMADS27* were examined, and the results showed several common elements connected to the N response (Supplementary Table S1). Additionally, analysis of the expression of *HvMADS27* in the roots under N deprivation and excess conditions showed that there was a considerable downregulation in the expression of *HvMADS27* mRNA under excess N stress and not under N deprivation conditions (Figure 1D). However, the correlation of *HvMADS27* mRNA level in roots under N excess with expression of mature miRNA444c revealed no significant changes in the expression of mature miRNA444c, suggesting that this miRNA was not involved in *HvMADS27* regulation, at least under excess N stress (Figure 1E). Physiological analysis showed that plants grown under N deprivation conditions were characterized by yellowing leaves and longer roots in comparison with those grown under normal condition. In contrast, plants grown under excess N condition exhibited shorter roots compared with those of plants grown under normal condition (Supplementary Figure S4).

HvMADS27 controls the root architecture of barley: Mutants with knockdown of *HvMADS27* display shorter roots while mutants overexpressing *HvMADS27* show similar phenotype to WT plants

To elucidate the function of *HvMADS27* gene, we generated *HvMADS27* knockdown (*mads27 kd*) and overexpressing (*mads27 c-Myc OE*) transgenic barley plants by *Agrobacterium*-mediated immature embryo transformation. Knockdown plants were obtained using artificial microRNA targeting *HvMADS27* mRNA (amiRMADS27), and plants overexpressing *HvMADS27* contained c-Myc tag (Figures 2A–D; Supplementary Figures S5A–C, S6A,B). Four independent transgenic lines showing similar expression of *amiRMADS27* for *mads27 kd* lines and *HvMADS27* with c-Myc for *mads27 c-Myc OE* lines were selected for further experiments. RT-qPCR showed that there was a significant downregulation in the expression of *HvMADS27* mRNA in transgenic barley plants expressing amiRMADS27 (Figures 2A,B). In contrast, *HvMADS27* expression was significantly upregulated at the mRNA level in transgenic plants overexpressing *HvMADS27c-Myc*; moreover, HvMADS27 c-Myc protein was detected in all transgenic plants (Figures 2C,D). Phenotypic analysis of the plants showed that *hvmads27 kd* plants had shorter roots compared with WT plants, whereas the total root length of *mads27 c-Myc OE* plants was not significantly different from that of WT plants (Figure 2E). Hence, we incorporated different root categories into analysis and we measured separately seminal and lateral roots. It turned out that in the case of all *mads27 c-Myc OE* mutant lines, seminal roots were longer while lateral roots were shorter in comparison with WT plants (Supplementary Figure S7). However, upon N excess stress seminal roots in WT and *mads27 c-Myc OE* mutant plants are shorter and similar in length as in WT plants.

10.3389/fpls.2022.950796

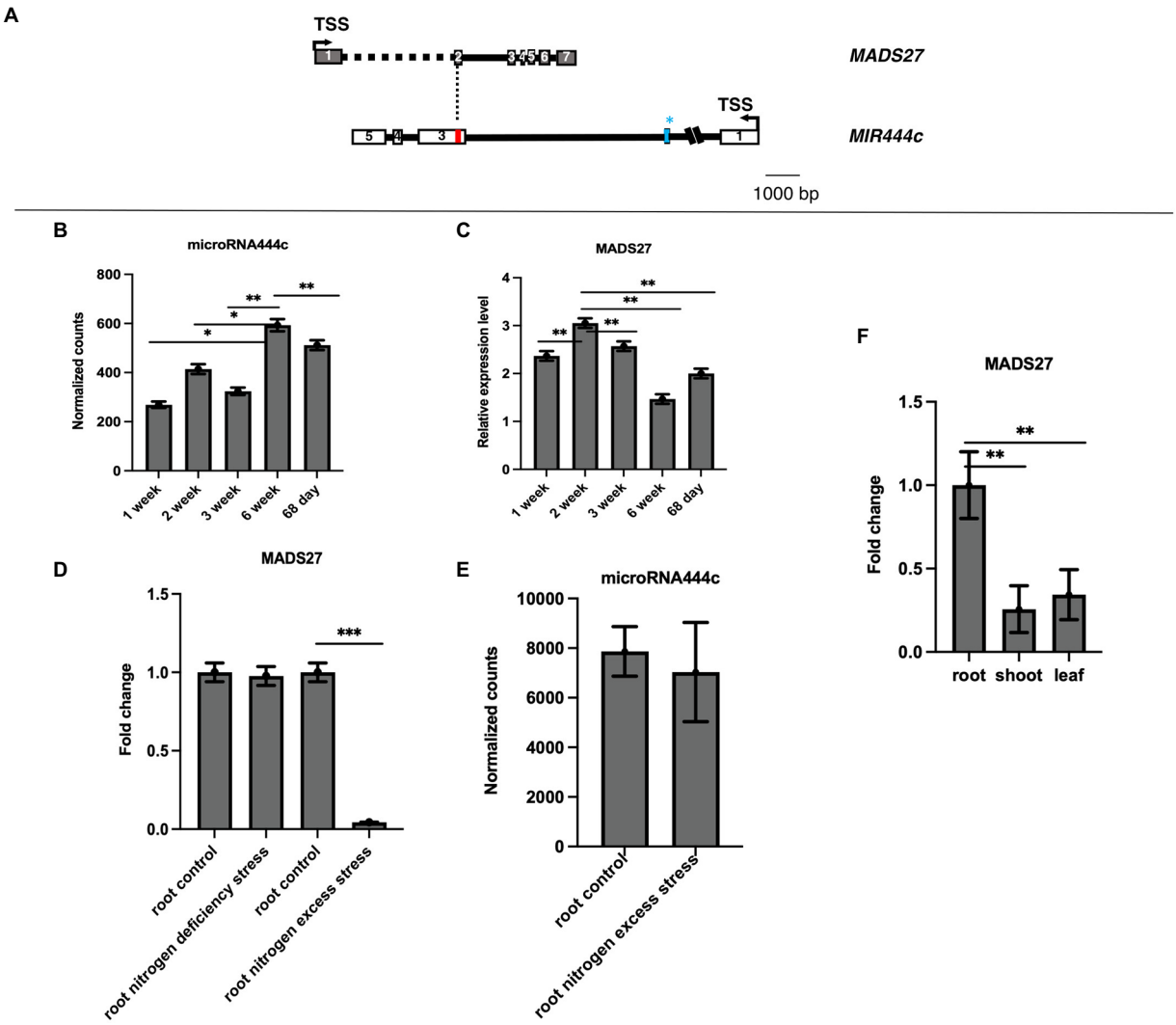


FIGURE 1
Gene structure and expression pattern of *HvMADS27* and *HvmiRNA444c*. **(A)** *HvMADS27* and *MIR444c* gene structures based on the 5′ and 3′ RACE analysis. White and gray blocks represent exons and black lines introns, blue bar in the secondexon of *MIR444c* gene represents miRNA444c* and red bar in the third exon represents miRNA444c, while dotted line marks overlap between two genes. **(B)** Results of deep sequencing of sRNA libraries, where the *x*-axis represents barley developmental stages and *y*-axis normalized counts. Mature miRNA444c occurred at the highest expression in sixth week of development. **(C)** *HvMADS27* mRNA relative to *ARF 1* mRNA level (Gene Bank: AJ508228.2) expression in barley at different developmental stages, with the *x*-axis representing developmental stages and y-axis expression of *HvMADS27*. The highest expression was observed at the second week of barley development. **(D)** RT-qPCR data showing *HvMADS27* expression in the roots of 2-week-old barley under N scarcity and excess N stress. There was a significant downregulation in *HvMADS27* expression under excess N stress, but no change was observed under N scarcity. **(E)** Level of mature miRNA444c based on deep sequencing of sRNA analysis in roots of plants grown under control and excess N conditions. No change was observed in the expression level of mature miRNA444c under excess N stress conditions compared with the control. *p* value based on Bonferroni correction was used. **(F)** RT-qPCR results showing that *HvMADS27* is mainly expressed in the roots of 2-week-old barley plants. **(D)** Student's *t*-test was applied; *$p<0.05$, **$p<0.01$, ***$p<0.0001$.

High N stress induces root shortening in WT and *hvmads27oe* mutant plants while the root system of plants with knockdown of *HvMADS27* is not responsive to N excess

Furthermore, the effect of excess N stress on the roots of WT, *hvmads27 kd*, and *mads27 c-Myc OE* plants were examined. The results showed that the root length of WT and *mads27 c-Myc OE* plants were significantly shorter under excess N stress than under normal condition. Additionally, *hvmads27 kd* mutants displayed significantly shorter roots under control conditions and did not respond to high N treatment (Figures 3A,B). Since it has been confirmed that the decrease in the root length under high N stress is associated with downregulation of *HvMADS27* mRNA, the response of *mads27 c-Myc OE* plants to high soil N and

10.3389/fpls.2022.950796

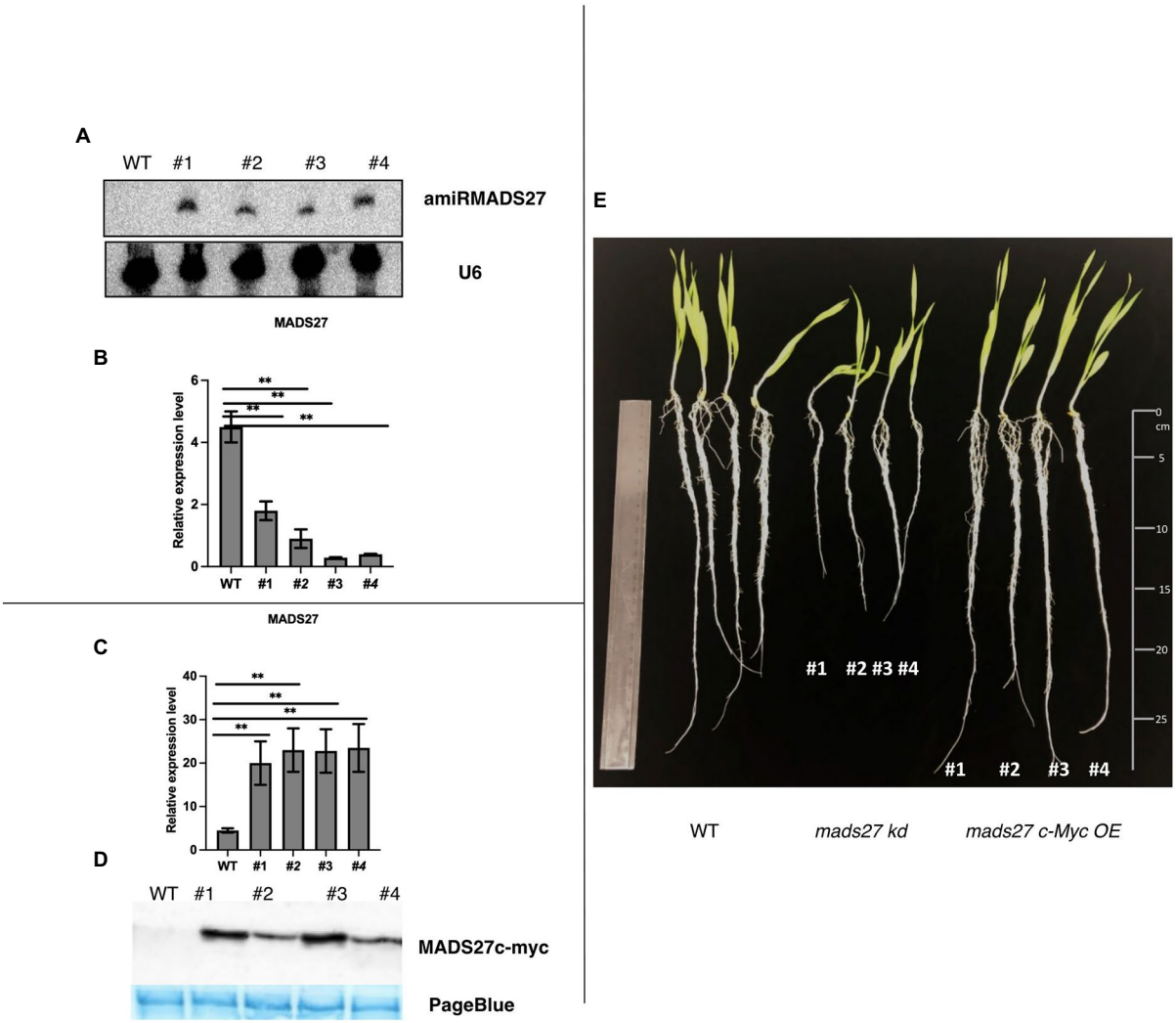


FIGURE 2
Characterization of *hvmads27* knockdown and overexpressing transgenic plants. **(A)** Northern blot analysis depicting the presence of amiRNAMADS27 in *mads27 kd* mutant lines using material from WT roots as control and U6 snRNA as loading control. **(B)** RT-qPCR analysis showing *HvMADS27* mRNA expression in *mads27 kd* mutant lines compared with WT plants relative to *ARF 1* mRNA level (Gene Bank: AJ508228.2), *x*-axis represents the transgenic lines and *y*-axis represents relative expression of mRNA. **(C)** RT-qPCR analysis showing *HvMADS27* mRNA expression in transgenic lines overexpressing *HvMADS27* with c-Myc tag relative to *ARF 1* mRNA level (Gene Bank: AJ508228.2); *x*-axis represents the transgenic lines and *y*-axis represents relative expression of *HvMADS27* mRNA. **(D)** Western blot experiment showing expression of HvMADS27 protein with c-Myc tag; lower panel showing loading control—PageBlue staining **(E)** 2-week old barley plants: WT plant, *mads27 kd*, and *mads27 c-Myc OE* mutants, respectively; *mads27 kd* plants exhibited short roots compared with the other transgenic lines. **(A–E)** #1, #2, #3, and #4 represent *mads27 kd*, *mads27 c-Myc OE* plants from four independent transgenic lines, respectively. *p* value was based on standard Student's *t*-test $^{**}p<0.01$.

normal conditions was examined at both the transcript and protein levels (Figures 3C,D). Although excess N stress did not significantly affect the expression of *HvMADS27* in *mads27 c-Myc OE* lines at the mRNA level (Figure 3C), there was decrease in HvMADS27 protein level under excess N condition compared with normal condition (Figure 3D). This is in agreement with the observed downregulation in *HvMADS27* expression in WT plants at the mRNA level and most probably at the protein level as well. Downregulation of the HvMADS27 c-Myc protein in transgenic plants explains the similar behavior of their roots systems in excess N stress to WT plants.

HvMADS27 TF regulates ABA level in barley roots by repressing *HvBG1* β-glucosidase transcription

In the present study, the molecular basis of the observed root phenotypes was investigated. First, the relationship between high N concentration in the rhizosphere and the root N content was examined. Overall, high rhizosphere N content caused accumulation of N in WT and *mads27 c-Myc OE* roots; however, higher amount of N was observed in *hvmads27 kd* plants under control condition, and the concentration was not significantly

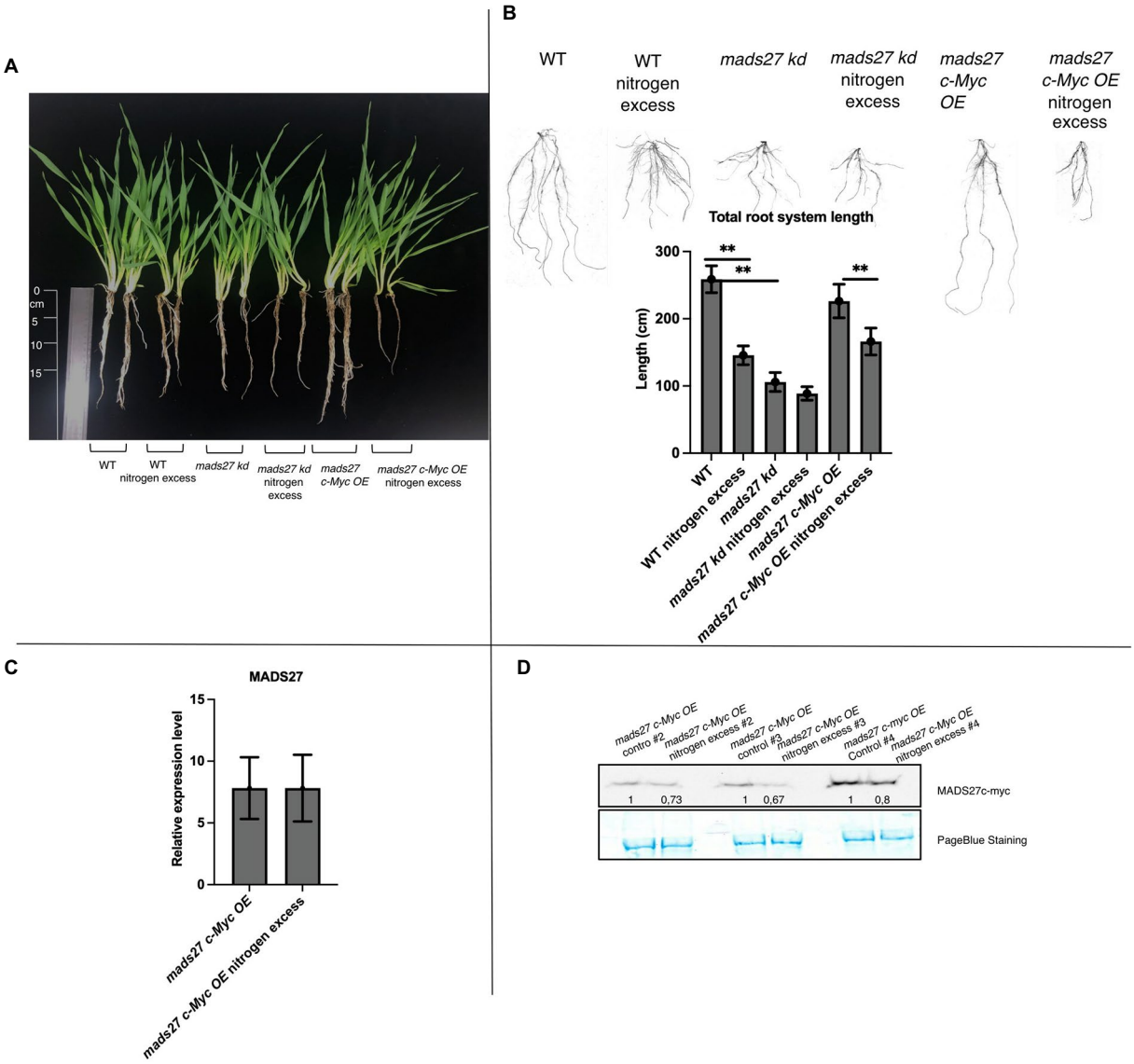


FIGURE 3
HvMADS27 regulates barley root architecture and excess N response. **(A)** WT and transgenic barley plants under control and excess N stress conditions. WT and *mads27 c-Myc OE* plants exhibited shorter roots under excess N condition compared with normal condition, whereas *mads27 kd* mutants exhibited shorter roots under control conditions, with no significant change under excess N stress. **(B)** Root length analysis using WinRHIZO software, with *x*-axis representing analyzed variants and *y*-axis representing total root length in cm. Scans of the root systems are provided. **(C)** RT-qPCR results depicting *HvMADS27* mRNA relative to *ARF 1* mRNA level (GenBank: AJ508228.2) expression in *mads27 c-Myc OE* mutant lines under control and excess N stress conditions. **(D)** Western blot analysis showed downregulation in HvMADS27 c-Myc protein level in *mads27 c-Myc OE* mutants under excess N treatment. PageBlue staining was used as loading control and numbers under MADS c-Myc signal depict results of densitometric analysis. Kruskal–Wallis test was performed to determine differences in root length; $^{**}p<0.01$.

affected under high N stress (Figure 4A). The results correlate with the expression pattern of nitrogen sensor and transporter *NRT1.1* mRNA, which is upregulated upon excess N stress in roots of WT and *mads27 c-Myc OE* plants and exhibits high expression in roots of *hvmads27 kd* both in control conditions and N excess treatment (Supplementary Figure S4). Roots of *mads27 kd* plants in control conditions display similar characteristics to those of WT plants under excess N stress, but lower N concentration compared with that of WT roots subjected to high N stress. A plausible explanation for this could be that HvMADS27 TF may also regulate other nitrogen transporters active in barley roots. Moreover, we observed slightly reduced expression of *NRT1.1* in *mads27 kd* mutants; however, this change was not statistically significant (Supplementary Figure S4).

To investigate the mechanism of high N-dependent root shortening, we examined the possibility of ABA and N crosstalk in root system architecture, which has been previously reported in Arabidopsis and wheat (Finkelstein et al., 2002; Cutler

et al., 2010; Yan et al., 2014; Sah et al., 2016; Harris and Ondzighi-Assoume, 2017; Jiao et al., 2020). First, the sensitivity to ABA in the roots of the barley mutants and WT plants was examined. The ABA sensitivity assay showed that there was a decrease in the root length of WT and *mads27 c-Myc OE* plants when exogenous ABA was supplied; however, the roots of *hvmads27 kd* mutants were short and not responsive to ABA treatment (Figures 4B,C). This result suggests that the HvMADS27 TF-mediated regulation of root growth is ABA-dependent. Therefore, the ABA content of the roots of WT plants and mutants was evaluated. Overall, there was an increase in the ABA content of the root of WT plants under excess N condition. However, the high ABA content of *hvmads27 kd* plants under control condition was not significantly affected by high soil N level. Plants overexpressing *HvMADS27* exhibited behavior similar to that of the WT (Figures 4C,D). Since the same observations concerning root shortening were made in WT and *hvmads27 kd, mads27 c-Myc OE* mutant plants subjected to N

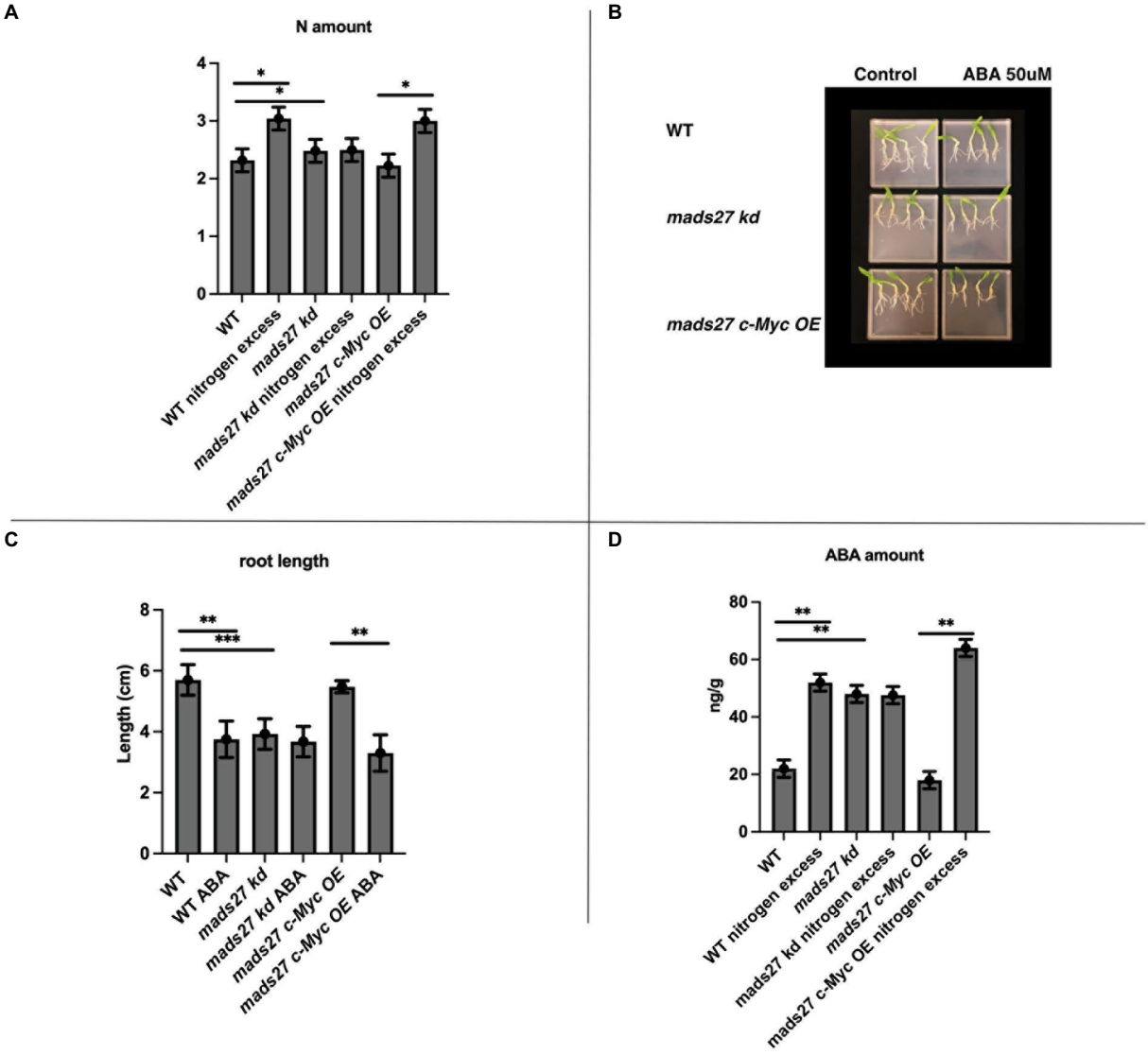
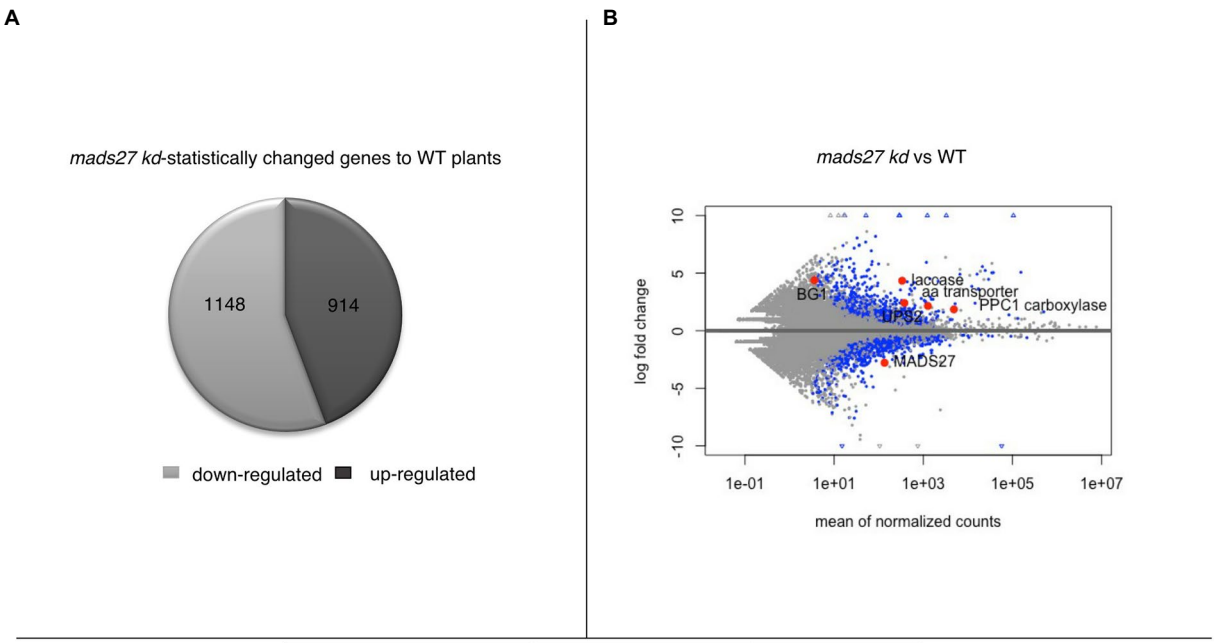


FIGURE 4
HvMADS27 controls N excess-dependent abscisic acid (ABA) accumulation in barley roots. **(A)** Determination of N content of the roots of WT, *mads27 kd*, and *mads27 c-Myc OE* plants using elemental analyzer. **(B)** ABA-sensitivity assay of the roots of WT and transgenic plants grown on ½ MS plates under control conditions or with 50μM ABA supplementation. **(C)** Calculation of root length, with *x*-axis representing the variants and *y*-axis representing root length in cm. Roots of *mads27 kd* plants were shorter than those of plants from the other lines under control conditions and did not respond to ABA supplementation, whereas the roots of *mads27 c-Myc OE* mutants responded to ABA in WT-like manner. **(D)** ABA concentration of the roots was determined using ultra-high-pressure liquid chromatography, with the *x*-axis representing the variants and the *y*-axis representing ABA concentration in ng/g. There was an accumulation in ABA and N concentration in the roots of WT and *mads27 c-Myc OE* plants under excess N stress, whereas the accumulation of N and ABA in the roots of *mads27 kd* mutants was high both under control and excess N stress conditions. Mean comparison was performed using Student's *t*-test; *p<0.05, **p<0.01, ***p<0.0001.

excess stress, this result confirmed the dominant role of HvMADS27 TF in controlling the ABA content in plant roots.

To better understand the mechanism of the observed behavior of *HvMADS27* mutants under high N stress, candidate genes regulated by HvMADS27 TF were identified by analysis of root transcriptome in WT and *hvmads27 kd* plants. We analyzed RNA-seq data for WT plants in control and N excess stress and identified 1,188 upregulated and 1817 downregulated genes (Supplementary Figure S8; Supplementary Table S3). Moreover, we identified 1,148 genes that were downregulated and 914 that were upregulated in *hvmads27 kd* plants when compared to WT plants in control conditions (Figure 5A). MADS-box transcription factors typically display inhibitory effects on regulated gene transcription; therefore, we mainly focused on the pool of upregulated genes and looked for the candidates that harbored in their promoters, the recognition motif for MADS-box TFs (CArG) binding (Guo et al., 2013; Muino et al., 2014; Aerts et al., 2018). Five potential candidate genes were selected (Figures 5B,C). *HvANT1* (HORVU6Hr1G034900) encoding a transmembrane protein involved in the transport of neutral and aromatic amino acids (Chen et al., 2001), *HvPPC1 CARBOXYLASE* (HORVU5Hr1G055350) encoding a protein involved in maintaining homeostasis in carbon/nitrogen metabolism (Li et al., 2020), *HvUPS2* (*UREIDE PERMEASE-2*; HORVU7Hr1G108790)



C

NAME	FUNCTION	MOTIF
HvANT1	Transmembrane protein capable of transport of neutral and aromatic amino acids	CATTAAATTTAG CATTAAATG
PPC1 CARBOXYLASE	Takes part in mantaining homeostasis in carbon/nitrogen metabolism nitrate and ammonium transport is impared in mutants	CATTAAAAAG
UREIDE PERMEASE-2 UPS2	transports a wide spectrum of derivatives of heterocyclic nitrogen compounds, including allantoin, uric acid and xanthine	CATTAAATTTAG
B-GLUCOSIDASE BG1	releases ABA from biologically inactive ester with glucose	2XCATTAAATTG
LACCASE	catalyzes polymerization and lignin deposition	CTTTAAAAAG

FIGURE 5
Transcriptomic analysis of roots of *mads27 kd* plants. **(A)** Pie chart depicting differentially expressed genes in the roots of *mads27 kd* mutants compared with that of WT roots. A total of 1,148 downregulated genes and 914 upregulated genes were identified. From upregulated group, genes harboring CArG motif in their promoter regions were selected for further analysis. **(B)** Volcano plot representing the expression level of candidate genes in the roots of *mads27 kd* mutant depicted in red dots. *X*-axis shows normalized counts and *y*-axis represents gene expression fold change. Blue dots in volcano plot represent significantly affected genes based on *p* value of Bonferroni correction. **(C)** List of the genes, function, and sequence of motif embedded in their promoters are shown in Table.

encoding a transporter of nitrogen compounds (Rentsch et al., 2007), *HvLACCASE* (HORVU3Hr1G097860) encoding an enzyme that catalyzes the polymerization of lignins (Rittstieg et al., 2002), and *HvBG1* (*B-GLUCOSIDASE*; HORVU2Hr1G023590) encoding an enzyme that releases ABA from ABA-glucose conjugate (Harris and Ondzighi-Assoume, 2017; Figure 5C; Supplementary Figure S9). Additionally, we considered the *NRT1.1* gene that was used as a nitrogen sensor because of the CArG motifs identified on its promoter (Supplementary Figure S9).

To prove that HvMADS27 TF binds to the promoter regions of selected genes, we performed a ChIP-qPCR experiment using *mads27 c-Myc OE* lines and primers flanking CArG motifs in the promoters of all six genes, including the *NRT1.1* gene (Figure 6A; Supplementary Figure S9). Root material from WT plants treated with anti-c-Myc antibody and mutant root material to which we did not add antibody against the c-Myc tag were used as the control group during immunoprecipitation. Only in the case of the *HvBG1 B-GLUCOSIDASE* gene, we observed enrichment of the PCR products representing fragments of the *HvBG1* promoter region containing the CArG motif. Moreover, HvMADS27 c-Myc occupancy on the *HvBG1* promoter decreased after high N treatment (Figure 6A). RT-qPCR analysis showed that there was an increase in *HvBG1* mRNA expression in the roots of WT and *hvmads27 c-Myc OE* mutant plants under nitrogen stress, while its level in *mads27 kd* plants was high under control conditions and remained unaffected under nitrogen stress (Figure 6B). Accordingly, western blot analysis of the HvBG1 protein level in roots of WT, *mads27 kd*, and *mads27 c-Myc OE* mutant plants under control conditions and excess N condition showed that HvBG1 was upregulated in the roots of WT and *mads27 c-Myc OE* plants under excess N condition. Regarding *hvmads27 kd* plants, the expression level of *HvBG1* was high both under control condition or under high N condition, with only slight upregulation after stress application (Figure 6B). These results indicated that HvMADS27 TF acts as a transcriptional repressor, at least in the case of *HvBG1*.

Finally, to determine the relationship between the ABA content of WT, *mads27 c-Myc OE*, and *hvmads27 kd* plants and HvBG1 activity and ABA release from ABA-glucose conjugate, the ABA content of the roots of plants growing in the presence of the ABA biosynthesis inhibitor norflurazon were measured (Figures 6C,D; Dong et al., 2013). Plants treated with norflurazon displayed typical hypocotyl bleaching (Figure 6C; Salome, 2019). Additionally, there was an increase in the ABA content of WT and *mads27 c-Myc OE* mutant plants under high N content. Moreover, we observed high amounts of ABA in Norflurazon-treated roots of *mads27 kd* mutants under both control conditions and high N stress (Figure 6D). These results indicated that the increased amount of ABA in WT and *mads27 c-Myc OE* plants resulted from the mobilization of the ABA-glucose conjugate. Furthermore, the expression levels of *HvSCR*, *HvABI4*, and *HvABI5* transcription factor mRNAs, which are involved in root shortening in Arabidopsis, were examined (Harris, 2015; Ondzighi-Assoume et al., 2016; Figures 6E,F; Supplementary Figure S10). There was a decrease in the expression of *HvABI5* mRNA under high nitrogen stress in WT and *hvmads27 c-Myc OE* plants compared with *HvABI5* mRNA level in plants grown in control conditions. Regarding *hvmads27 kd* mutants *HvABI5* mRNA level was lower than in WT and unaffected under high N stress. *HvSCR* and *HvABI4* expression were unaffected in all analyzed plants and conditions (Supplementary Figures S10A,B). Taking all results together we propose the mechanism of HvMADS27-mediated regulation of *HvBG1* β-glucosidase that is N excess-dependent, where the presence of high amounts of N in the barley rhizosphere causes severe downregulation of *HvMADS27* expression and upregulation of *NRT1.1* expression. The decreased occupancy of HvMADS27 on the *HvBG1* promoter causes activation of this enzyme and release of ABA from its ester with glucose. The high levels of ABA in turn cause shortening of the plant roots (Figure 7).

Discussion

In this study, we present a new mechanism of barley roots response to N excess stress: in control conditions barley HvMADS27 repressed the expression of *HvBG1* glucosidase and decreased the accumulation of active ABA in the roots. High N level caused a significant downregulation of HvMADS27, resulting in an increase in the expression of *HvBG1*, and consequently in an increased accumulation of ABA derived from the ABA-glucose conjugate.

In the presented study, there was a strong decrease in *HvMADS27* expression at the mRNA level in the root of barley under high N conditions. Phenotypic analyses of *HvMADS27* mutants showed that *HvMADS27* regulates barley root length in response to excess N stress. Plants with the knockdown of *HvMADS27* revealed shorter roots and did not shorten additionally in response to excess N stress. However, it was intriguing to observe similar effects on root length in the case of WT plant and plants overexpressing *HvMADS27 c-Myc*. In WT plants the level of HvMADS27 protein was controlled at the mRNA level, while it was not the case in *mads27 c-Myc OE* mutants where *HvMADS27* c-Myc cDNA was under control of 35S promoter. However, *HvMADS27 c-Myc* expression was indeed downregulated at the protein level in those plants in response to excess N stress. We were not able to measure directly the amount of HvMADS27 protein in WT plants regardless to control or stress conditions because antibodies specific to HvMADS27 are not available. Thus, we cannot compare the level of HvMADS27 protein in WT and *mads27 c-Myc OE* mutant plants. Similar effects of excess N on WT and *mads27 c-Myc OE* plants could be attributed to several plausible reasons. First, the interaction of HvMADS27 c-Myc and its partner was altered, which could affect the expression level of the partner, moreover a partner of HvMADS27 was affected by excess nitrogen, which could lead to degradation of HvMADS27 c-Myc. The effect of partner interaction on MADS-box TFs activity was previously reported in rice. It was evidenced by the EMSA assay that OsTB1 protein

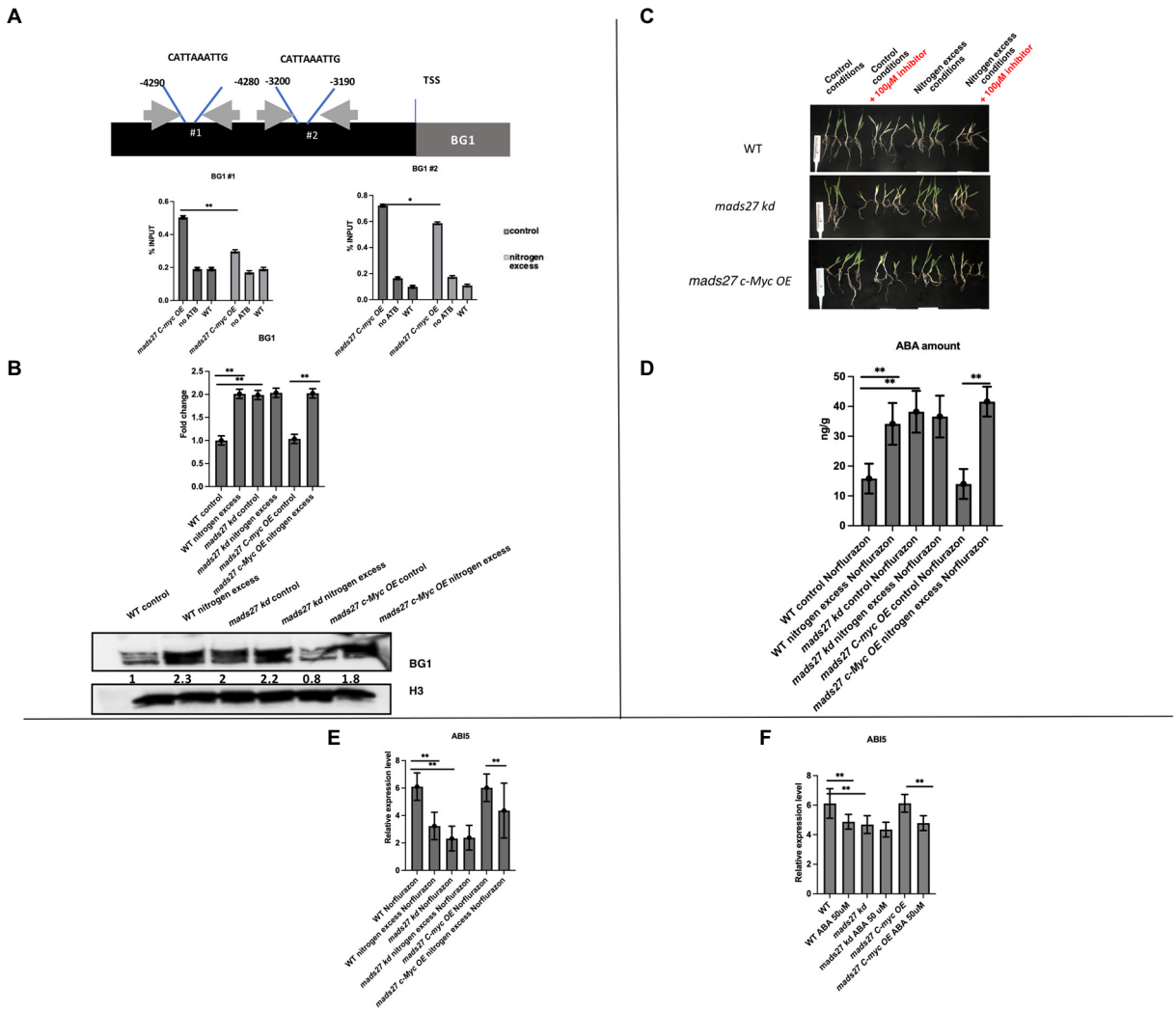


FIGURE 6
HvMADS27 transcription factor regulates expression of *BG1 β-GLUCOSIDASE* in barley roots. **(A)** Upper panel shows position of CArG motifs in *HvBG1* promoter, gray box indicates gene body, while black box indicates promoter sequence, blue lines flank the position of CArG motifs. Exact position of motif was identified by counting the number of nucleotides downstream of transcription start site. Gray arrows indicate the location of primers flanking CArG motifs. Lower panel presents the results of ChIP RT-qPCR of the roots of *mads27 c-Myc OE* plants under control and excess N stress conditions is presented using a graph. Accumulation of HvMADS27 on *HvBG1* promoter both in control and excess N conditions with lower occupation observed in stress. **(B)** Upper panel shows RT-qPCR results. There was an increase in the expression of *HvBG1* mRNA in the roots of WT and *mads27 c-Myc OE* lines under excess N stress, whereas *HvBG1* mRNA expression was high in the roots of *mads27 kd* mutant under control conditions and was not significantly affected by excess N stress. Lower panel shows western blot analysis of HvBG1 protein level in WT and mutant lines under control and excess N conditions. There was an increase in HvBG1 protein expression in the roots of *mads27 kd* mutant under both control and excess N conditions, whereas HvBG1 protein expression was increased in the roots of *mads27 c-Myc OE* mutant only under excess N stress. Below HvBG1 signal densitometric analysis is provided. HvBG1 level was validated using HvBG1 signal from roots of WT plants grown under control conditions. Signal from histon HvH3 was used as a loading control. **(C)** WT, *mads27 kd*, and *mads27 c-Myc OE* mutants plants grown under control and excess N stress conditions (supplemented with Norflurazon). Plants from *mads27 kd #3* line and *mads27 c-Myc OE #4* were used for the experiment. **(D)** The ABA content of the roots of WT and *mads27 kd, mads27 c-Myc OE* lines grown under control and excess N conditions (supplemented with Norflurazon) was determined by high-pressure liquid chromatography technique. There was an increase in the ABA concentration of Norflurazon-treated roots of WT, *mads27 kd*, and *mads27 c-Myc OE* plants under excess N stress, while in the case of *mads27 kd* ABA was high both under control and excess N stress conditions. **(E)** RT-qPCR results showing expression profiles of *HvABI5* mRNA in WT, *mads27 kd*, and *mads27 c-Myc OE* lines under control and excess N stress conditions supplemented with Norflurazon. *HvABI5* mRNA expression was significantly downregulated in the roots of WT and *mads27 c-Myc OE* lines under excess N, whereas the *HvAB15* mRNA was significantly lower in the root of *mads27 kd* mutants under both control and excess N stress conditions. **(F)** RT-qPCR results showing *HvABI5* mRNA level in WT and analyzed mutants in control and N excess conditions. Expression of *HvABI5* is downregulated upon ABA stress when compared to control conditions in WT plants, *mads27 c-Myc OE* plants. In *mads27 kd* plants the level of *HvABI5* is not changed upon the stress. **(E,F)** *x*-axis presents analyzed variants and *y*-axis expression level relative to *ARF 1* mRNA. **(A,B,D–F)** Statistical significance based on Student's *t*-test, *$p<0.05$, **$p<0.01$.

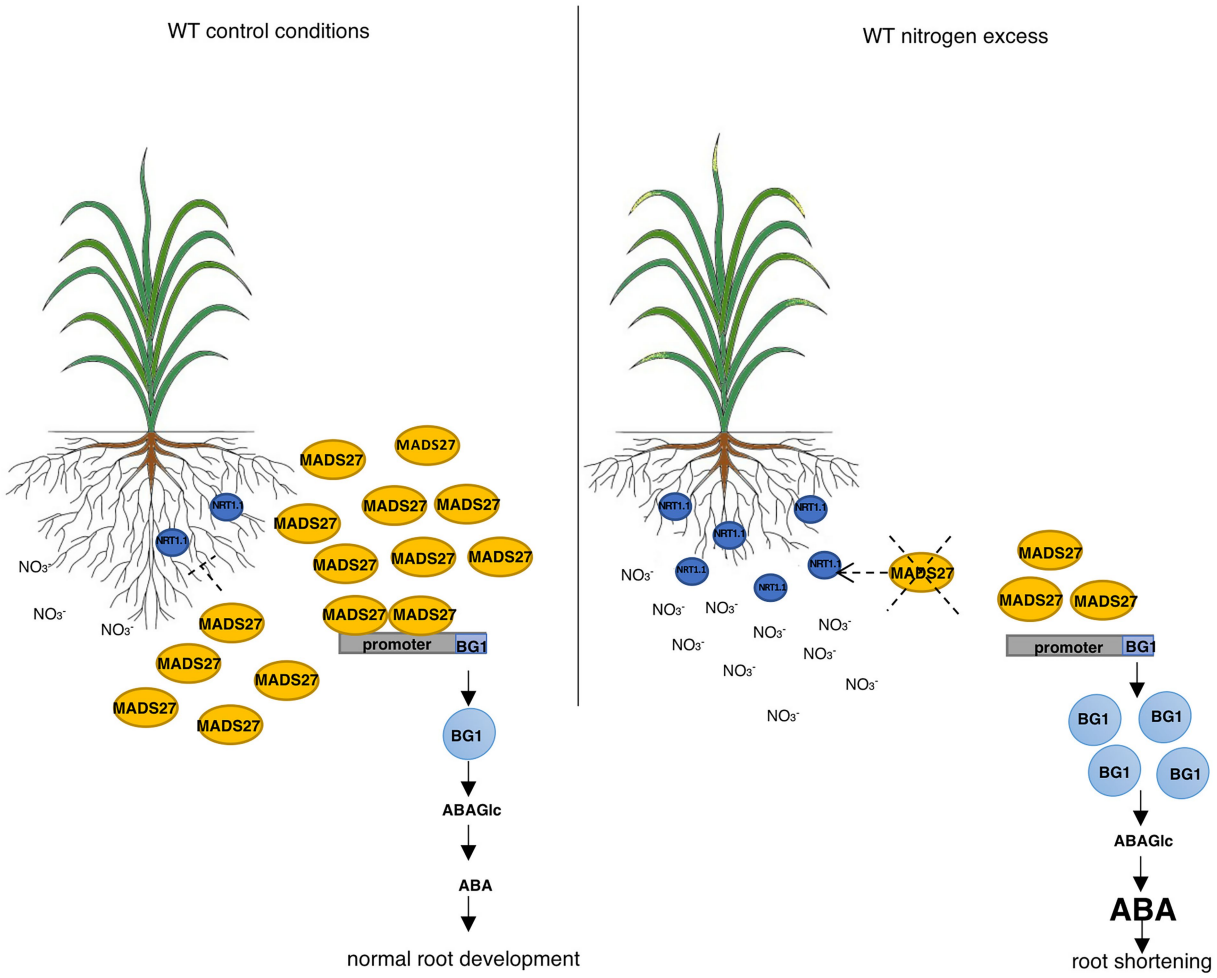


FIGURE 7
HvMADS27 regulates barley roots response to excess N stress. HvMADS27 regulated barley root response under excess N stress. Increased N concentration in the rhizosphere activates N sensor and transporter NRT1.1, which provides N influx to the root cells. High N concentration downregulates the expression of *HvMADS27*, which relieves the inhibition of *HvBG1* glucosidase expression. HvBG1 is activated and catalyzes the release of ABA from the ABA-glucose conjugate, which causes an increase in ABA levels and shortening of the barley roots.

binds to OsMADS57 regulating its activity (Chen et al., 2018). Additionally, we cannot rule out the possibility that *HvMADS27 c-Myc* mRNA as well as HvMADS27 protein activities were lower than that of WT *HvMADS27* mRNA and protein. It has been shown that other MADS-box TFs may act as homo-or heterodimers or in larger complexes; therefore, a lack of stoichiometric balance between subunits of the complex in overexpressing lines could lead to the observed HvMADS27 c-Myc degradation (Hugouvieux and Zubieta, 2018).

Transcriptomic analysis of *hvmads27 kd* mutants showed that nitrate transporter *NRT1.1* gene expression was upregulated. The *NRT1.1* gene promoter contains MADS TF CArG-binding motifs. However, ChIP-qPCR experiments showed that HvMADS27 was not bound to the *NRT1.1* gene promoter. Moreover, *NRT1.1* mRNA expression was inversely correlated with *HvMADS27* expression level. Low *HvMADS27* expression under excess N stress was correlated with high levels of *NRT1.1* mRNA, indicating that HvMADS27 indirectly regulated *NRT1.1* expression.

Transcriptomic analysis of *hvmads27 kd* mutants also showed significant downregulation of HvMADS27 TF and a significant increase in *HvBG1* expression. Furthermore, ChIP-qPCR confirmed that the HvMADS27 transcription factor binds to the *HvBG1* gene promoter, which contained CArG motifs. Therefore, we conclude that the *HvBG1* glucosidase gene expression is repressed by HvMADS27 under control conditions, whereas downregulation of HvMADS27 under excess N stress induces *HvBG1* expression.

Wang et al. showed that wheat MADS-box TF, a homolog of Arabidopsis ANR1, activates expression of both TaBG1 and TaWabi5 - transcription factor that regulate the expression of N transporters from the TaNRT2 family (Wang et al., 2020). The nucleotide and amino acid sequences of TaANR1 and HvMADS27 in 97% similar to each other. However, in contrast to its wheat homolog, HvMADS27 is a repressor of *HvBG1* expression, as demonstrated by the upregulation of *HvBG1* expression in *hvmads27 kd* mutants. Additionally, there was an

increase in *HvBGI* expression in WT plants under excess N condition at both mRNA and protein levels, which correlated with the downregulation of *HvMADS27* expression. The discrepancy between the modes of action of TaANR1 and HvMADS27 may be attributed to functional differentiation during the evolution of wheat and barley. Moreover, there are two *AtANR1* homologs in the wheat genome (AM502900.1 and XM_037629991.1), which is not the case in barley plants. This gene duplication may cause wheat AtANR1 MADS-box to create different complexes or dimerize with different partners than its barley counterpart, resulting in one being an activator and the other a repressor. Further experiments are needed to describe HvMADS27 and TaANR1 complexes. We also cannot exclude out the possibility that differences we observed in MADS27 behavior between wheat and barley result from different experimental approaches (N excess stress in barley vs. N starvation and supplementation to control conditions in wheat).

HvBG1 controls abscisic acid (ABA) levels in barley roots, with similar observations in wheat. ABA inhibits root growth through several mechanisms (Ondzighi-Assoume et al., 2016; Harris and Ondzighi-Assoume, 2017). In Arabidopsis, the *SCR* transcription factor gene expression is downregulated under higher N provision, with increase in ABA content, resulting in *ABI5* and *ABI4* expression upregulation, which could lead to root shortening. *ABI5* takes part in barley response to multiple abiotic stresses, especially drought which affects the movement and uptake of nutrients (Fahan et al., 2017; Collin et al., 2021). In this study, we observed a downregulation in *HvABI5* expression, which corresponds to root shortening in WT and *mads27 c-Myc OE* lines under excess N stress, and root shortening in *mads27kd* mutant plants under both control and excess N conditions. We performed analysis of *ABI5* mRNA level in control conditions and upon ABA treatment in WT and in all mutant plants. Indeed, the level of *ABI5* mRNA is downregulated in barley roots upon ABA treatment in WT plants and *hvMADS27 OE* mutant, while there is no significant change in *ABI5* mRNA level in *hvmads27 kd* mutant (Figure 6F). This confirms the difference between barley and Arabidopsis plants in response to ABA signaling. What is more, barley *ABI4* expression was not significantly downregulated (Supplementary Figure S10). Arabidopsis plants contain the *SCR* gene that is responsive to nitrogen; however, the expression of *SCR* in the roots of WT, *mads27 c-Myc OE*, and *mads27 kd* lines was not significantly affected by high N stress (Supplementary Figure S10). Thus, it seems that the mechanisms regulating *ABI5* expression in barley and Arabidopsis were different in response to N concentration. We also analyzed RNAseq data for the level of other core genes known to be involved in *de novo* biosynthesis of ABA and ABA signaling. The analysis was performed using RNAseq data from roots of *mads27 kd* plants compared to wild-type plants. Following genes were taken into consideration: *NCED1*, *NCED2*, *ABAOH8*, *ZEP, PP2C*, *PYR1*, *PYL2*, *PYL5*, *PYL8*, *ABI1*, *ABI2*, and *ABI3*. Generally, we observed no changes in their expression levels, which confirms that HvMADS27 is not involved in the control of ABA *de novo* biosynthesis but may be involved in ABA signaling (see Supplementary Table S3).

To identify important processes affecting N acquisition, root traits essential for N uptake and the expression of N uptake-related genes in the roots of barley were assessed. The root system of barley is a fibrous type consisting of seminal and nodal roots (crown roots) and lateral roots of diverse acquisitive capacity (Jia et al., 2019). Previous studies have shown that barley produces more lateral roots in response to N provision (Blaser et al., 2020). Similarly, there was an increase in lateral root formation in response to excess N stress in WT, *hvmads27 kd*, and *hvmads27 c-Myc OE* lines in the present study. Moreover, there was no significant difference in lateral root number of the WT and mutant lines under control conditions, indicating that *HvMADS27* regulates total root length but not lateral root number (Figure 3B; Supplementary Figure S11). Deeper rooting increases N uptake by increasing total soil exploration. Therefore, plants optimize roots to respond to changing mobile nutrients, such as nitrate, that tend to be more abundant in deeper soil layers (Giehl and von Wiren, 2014; Liu et al., 2020). Similar studies have been performed with *A. thaliana*: Excess N has been reported to shorten the root length and enhances the formation of lateral roots in Arabidopsis (Walch-Liu et al., 2006). Thus, this feature seems to be conserved across plant kingdom, although detail mechanisms underlying root shortening in N excess stress may differ between plant species.

Finally, *HvMADS27* mRNA, similar to several other MADS-box TF mRNAs, is specifically targeted by miRNA from the MIR444 family (Sunkar et al., 2005, 2008; Lu et al., 2008). Degradome analysis showed that miRNA444c cleaved *HvMADS27* mRNA under control conditions (Supplementary Figure S1). However, the expression of mature miRNA444c did not correlate with *HvMADS27* mRNA downregulation under high N condition. These findings suggest that miRNA444c did not significantly affect the expression of *HvMADS27* under these conditions. However, based on our analysis of expression patterns in barley developmental stages, miRNA444c-mediated regulation of *HvMADS27* expression may occur during other stages of plant development and/or in response to other stresses. Moreover, there were significant variations in miR444c level during week 1, 2, 3, and 6, and 68th day of barley growth, suggesting the role of miR444c and MADS27 TF during barley development (see Figure 1B).

The findings of the present study provide novel insights into barley root response to excess N stress and constitute a basis for further research on the mechanism of cereal response to over-fertilization. Moreover, the findings of the study provide candidate genes for the breeding and development of excess N-resistant crop varieties better adapted to leached agroecosystem soils. Moreover, this research creates new areas for future studies which can entail analyzing miRNA444c and *HvMADS27* roles in developmental stages that were not taken under consideration so far, exploring the structure and differences in partners that build

complexes with HvMADS27 and its homologs in other crop species or exploring the role of ABI5 in barley root response to N excess stress.

Data availability statement

The original contributions presented in the study are publicly available. This data can be found at: NCBI, PRJNA746688.

Author contributions

AS performed the majority of experiments included in this work and wrote the manuscript draft. AP performed degradome analysis and participated in barley protoplast preparation and discussion. AG took part in the transgenic line construction. DB and WMK carried out bioinformatic analyses. MZ helped in the root architecture analysis and participated in the discussion. KS participated in the phenotypic analysis of root behavior. JD participated in CHIP experiments and discussion. MB performed nuclear localization experiments in plant protoplasts. PN participated in degradome library construction. JK participated in ABA measurements and discussion. MW and IR performed N amount analysis and participated in the discussion. WH participated in amiRNAMADS27 transgenic line construction. AJ contributed to the discussion and writing of the results. ZS-K designed experiments and wrote the manuscript. All authors contributed to the article and approved the submitted version.

Funding

This study was funded by the OPUS project (2016/23/B/NZ9/00862) and PRELUDIUM project (2019/35/N/NZ9/01971) from the National Science Centre, Poland. Production of transgenic barley plants was possible thanks to Short Term Scientific Mission (STSM) founded by iPlanta Organization COST Action CA15223. Authors also received financial support from the Initiative of Excellence—Research University (05/IDUB/2019/94) at Adam Mickiewicz University, Poznan.

Conflict of interest

Since 16/11/2021, the co-author AS has been employed by Frontiers Media SA. AS declared his/her affiliation with Frontiers, and the handling Editor states that the process nevertheless met the standards of a fair and objective review.

The remaining authors declare that the research was conducted in the absence of any commercial or financial relationships that could be construed as a potential conflict of interest.

Publisher's note

All claims expressed in this article are solely those of the authors and do not necessarily represent those of their affiliated organizations, or those of the publisher, the editors and the reviewers. Any product that may be evaluated in this article, or claim that may be made by its manufacturer, is not guaranteed or endorsed by the publisher.

Supplementary material

The Supplementary material for this article can be found online at: https://www.frontiersin.org/articles/10.3389/fpls.2022.950796/full#supplementary-material

SUPPLEMENTARY FIGURE S1
HvMiRNA444c targets *HvMADS27* transcription factor mRNA. Degradome analysis of 68-day old barley plant grown under control conditions. Perfect complementarity between *HvMADS27* mRNA (accession number: HORVU2Hr1G080490.4) and miR444c is shown. The x-axis of the graph represents the length of the *HvMADS27* transcript (722 nt), and the y-axis depicts the abundance of identified cleavage and degradation fragments in read numbers. The red line indicates the miRNA444c- mediated cleavage site at position 287.

SUPPLEMENTARY FIGURE S2
HvMADS27 is mainly expressed in roots of two-week old barley plants. Results of RT-PCR of organ samples of two-week old barley plants; expression of *ARF1* mRNA was used as a loading control.

SUPPLEMENTARY FIGURE S3
MADS27-GFP localizes in the nucleus. Transient co-expression of fluorescent proteins in **(A)** Arabidopsis protoplasts and **(B)** Barley protoplast. RFP-SERRATE was used as a nuclear marker.

SUPPLEMENTARY FIGURE S4
Plants growing under N scarcity and excess N conditions. **(A)** WT plants grown under high N stress condition. **(B)** Expression level of *NRT1.1* mRNA transporter using RT-qPCR technique. *NRT1.1* mRNA was upregulated in response to high N stress. X-axis presents analyzed variants and y-axis shows expression level relative to *ARF 1* mRNA. **(C)** WT plants growing in N deprivation conditions. **(D)** RT-qPCR results depicting expression level of *NRT1.1* mRNA under N scarcity conditions. *NRT1.1* mRNA was downregulated under N scarcity. **(E)** Expression of *NRT1.1* mRNA in WT, *mads27 kd*, and *mads27 c-Myc OE* mutants under control and high N conditions. *NRT1.1* mRNA was upregulated in *mads27 kd* mutant and its expression was not affected under high N stress. Excess N stress caused an upregulation in *NRT1.1* mRNA expression in *mads27 c-Myc OE* mutant lines. Above the graphs statistical significance is provided based on standard Student *t*-test, $^{**}p < 0.01$.

SUPPLEMENTARY FIGURE S5
amiRMADS27 in miRNA167h precursor. **(A)** Structure of barley *MIR167h* gene with red bar marking mature miRNA167h position and blue bar marking miRNA*. TSS-transcription start site. **(B)** Structure and sequence of pre-miRNA167h, with red color indicating mature miRNA167h sequence and blue color miRNA*. Nucleotides marked in green were changed in amiRMADS27 precursor to improve hairpin structure. **(C)** Pre-miRNA167h with amiRMADS27 and its cognate miRNA*. ΔG = Gibbs free energy value of particular pre-miRNA.

SUPPLEMENTARY FIGURE S6
Phenotypes of plants from four independent transgenic lines. **(A)** Plants from four independent transgenic barley lines with knock-down of (*mads27 kd* #1, *mads27 kd* #2, *mads27 kd* #3, and *mads27 kd* #4, respectively). **(B)** Plants from four independent transgenic barley lines overexpressing *HvMADS27* with c-Myc tag (*mads27 c-Myc OE* #1, *mads27 c-Myc OE* #2, *mads27 c-Myc OE* #3, and *mads27 c-Myc OE* #4, respectively).

SUPPLEMENTARY FIGURE S7
Analysis of length of seminal and lateral roots in WT, *mads27 kd* and *mads27 c-Myc OE* plants in control and N excess stress conditions. In the case of all *mads27 c-Myc OE* mutant lines, seminal roots are longer while lateral roots are shorter in comparison to WT plants in control conditions. Upon N excess stress seminal roots in WT and *mads27 c-Myc OE* mutant plants are shorter and similar in length as in WT plants. Different capital letters indicate significant difference between root length means among WT, *mads27 c-Myc OE*, and *mads27 kd* within a given nitrogen condition and the same letters indicate lack of statistical significance according to Dunn test. Error bars represent the standard error. value of p <0.05.

SUPPLEMENTARY FIGURE S8
RNA-seq data from roots of WT barley plants grown in control conditions and N excess stress. Volcano plot representing comparison between RNA-seq data from roots of WT plants grown in control and N excess stress. Red dots depict genes changed with statistical significance based on p-value of Bonferroni correction. X-axis shows normalized counts and y-axis represents gene expression fold change.

SUPPLEMENTARY FIGURE S9
ChIP-qPCR results of candidate genes for regulation by HvMADS27. **(A–E)** Depict the results of ChIP-qPCR for *HvANT1*, *PPC1*, *UPS1*, *LACCASE*, and *NRT1.1* promoter genes, respectively. Black boxes represent promoter sequences, grey boxes depict gene bodies, and blue lines flank the position of CArG motifs. The exact positions of motifs were provided by the numbers of nucleotides upstream of the transcription start site. Grey arrows show the location of primers flanking the CArG motifs. Graphs depict ChIP-qPCR results from roots of *mads27 c-Myc OE* plants in control and excess N stress, using primers flanking CArG motifs. We observe no accumulation of HvMADS27 on analyzed promoters. No Atb-ChIP qPCR with no added anti-myc antibody or WT wild-type plants

SUPPLEMENTARY FIGURE S10
Expression pattern of *HvSCR, HvABI4* genes. **(A)** RT-qPCR result showing *HvSCR* mRNA level in WT and mutants under control and high soil N conditions, where x-axis represents analyzed variants and y-axis represents expression level relative to *ARF1* mRNA. There was no significant change in *HvSCR* expression in the mutants compared with WT plant. **(B)** RT-qPCR results showing *HvABI4* mRNA level in WT and analyzed mutants in control and excess N conditions where x-axis presents analyzed variants and y-axis expression level relative to *ARF 1* mRNA. Expression of *HvABI4* is not changed in excess N stress in WT and mutants when compared to control conditions.

SUPPLEMENTARY FIGURE S11
Number of lateral roots in WT and *hvmads27* mutant plants. Number of lateral roots calculated based on scans of root systems of WT, *mads27 kd* and *mads27 c-Myc OE* mutants, where x-axis shows analyzed variants and y-axis number of observed lateral roots. In each case (WT, *mads27 kd*, *mads27 c-Myc OE*) number of lateral roots was higher under high N stress. Statistical significance based on standard Student t-test is provided, $^{**}p < 0{,}01$.

References

Aerts, N., de Bruijn, S., van Mourik, H., Angenent, G. C., and van Dijk, A. D. J. (2018). Comparative analysis of binding patterns of MADS-domain proteins in *Arabidopsis thaliana*. *BMC Plant Biol.* 18:131. doi: 10.1186/s12870-018-1348-8

Alaba, S., Piszczalka, P., Pietrykowska, H., Pacak, A. M., Sierocka, I., Nuc, P. W., et al. (2015). The liverwort Pellia endivifolia shares microtranscriptomic traits that are common to green algae and land plants. *New Phytologist* 206, 352–367. doi: 10.1111/nph.13220

Al-Tawaha, A. R. M., Sheoran, S., Sharma, P., Singroh, G., Abu-Zaitoon, Y. M., Trioui, L., et al. (2021). "Biological nitrogen fixation in a changing climate," in *Susatinable soil and land Management and Climate change. Footprints of Climate Variablility on plant Diversity*. eds. F. S. Raton, O. Sonmez, V. Turan, M. Adnan, S. Saud and C. Wu et al. (Boca: CRC Press).

Anas, M., Liao, F., Verma, K. K., Sarwar Aqeel, M., Mahmood, A., Chen, Z. L., et al. (2020). Fate of nitrogen in agriculture and environment: agronomic, eco-physiological and molecular approaches to improve nitrogen use efficiency. *Biol. Res.* 53:47. doi: 10.1186/s40659-020-00312-4

Bajczyk, M., Lange, H., Bielewicz, D., Szewc, L., Bhat, S. S., Dolata, J., et al. (2020). SERRATE interacts with the nuclear exosome targeting (NEXT) complex to degrade primary miRNA precursors in Arabidopsis. *Nucleic Acids Res.* 48, 6839–6854. doi: 10.1093/nar/gkaa373

Blaser, S. R. G., Koebernick, N., Spott, O., Thiel, E., and Vetterlein, D. (2020). Dynamic of localized nitrogen supply and relevance for root growth of *Vicia faba* ('Fuego') and *Hordeum vulgare* ('Marthe') in soil. *Sci. Rep.* 10:15776. doi: 10.1038/s41598-020-72140-1

Bloom, A. J., Sukrapanna, S. S., and Warner, R. L. (1992). Root respiration associated with ammonium and nitrate absorption and assimilation by barley. *Plant Physiol.* 99, 1294–1301. doi: 10.1104/pp.99.4.1294

Chaudhry, U. K., Junaid, M. D., and Gokce, A. F. (2021). "Influence of environmental adversities on physiological changes in plants" in *Developing Climate Resilient crops: Improving Global Food Security and Safety. Footprints of Climate Varaiblility on plant Diversity*. eds. S. Fahad, O. Sonmez, S. Saud, D. Wang, C. Wu and M. Adnanet al. (Boca Raton: CRC Press).

Chen, K., Kumudini, S. V., Tollenaar, M., and Vyn, T. J. (2015). Plant biomass and nitrogen partitioning changes between silking and maturity in newer versus older maize hybrids. *Field Crop Res.* 183, 315–328. doi: 10.1016/j.fcr.2015.08.013

Chen, L., Ortiz-Lopez, A., Jung, A., and Bush, D. R. (2001). ANT1, an aromatic and neutral amino acid transporter in Arabidopsis. *Plant Physiol.* 125, 1813–1820. doi: 10.1104/pp.125.4.1813

Chen, L., Zhao, Y., Xu, S., Zhang, Z., Xu, Y., Zhang, J., et al. (2018). OsMADS57 together with OsTB1 coordinated transcription of its target OsWRKY94 and D14 to switch its organogenesis to defense for cold adaptation in rice. *New Phytol.* 218, 219–231. doi: 10.1111/nph.14977

Chopin, F., Orsel, M., Dorbe, M. F., Chardon, F., Truong, H.-N., Miller, A. J., et al. (2007). The Arabidopsis ATNRT2.7 nitrate transporter controls nitrate content in seeds. *Plant Cell* 19, 1590–1602. doi: 10.1105/tpc.107.050542

Collin, A., Daszkowska-Golec, A., and Szarejko, I. (2021). Updates on the of ABSCISIC ACID INTENSITIVE 5 (ABI5) and ABSCISIC ACID-RESPONSIVE ELEMENT BINDING FACTORs (ABFs) in ABA signaling in different developmental stages in plants. *Cell* 10:1996. doi: 10.3390/cells10081996

Cutler, S. R., Rodriguez, P. L., Finkelstein, R. R., and Abrams, S. R. (2010). Abscisic acid: emergence of a core signaling network. *Annu. Rev. Plant Biol.* 61, 651–679. doi: 10.1146/annurev-arplant-042809-112122

Dolata, J., Guo, Y., Kołowerzo, A., Smoliński, D., Brzyżek, G., Jarmołowski, A., et al. (2015). NTR1 is required for transcription elongation checkpoints at alternative exons in *Arabidopsis*. *EMBO* 34, 544–558. doi: 10.15252/embj.201489478

Dong, W., Wang, M., Xu, F., Quan, T., Peng, K., Xiao, L., et al. (2013). Wheat oxophytodienoate reductase gene TaOPR1 confers salinity tolerance via enhancement of abscisic acid signaling and reactive oxygen species scavenging. *Plant Physiol.* 161, 1217–1228. doi: 10.1104/pp.112.211854

Fahan, S., Bajwa, A., Nazir, U., Anjum, S., Farooq, A., Zohaib, A., et al. (2017). Crop production under drought and heat stress: plant responses and management options. *Front. Plant Sci.* 8:1147. doi: 10.3389/fpls.2017.01147

Feng, H., Yan, M., Fan, X., Li, B., Shen, Q., Miller, A. J., et al. (2011). Spatial expression and regulation of rice high-affinity nitrate transporters by nitrogen and carbon status. *J. Exp. Bot.* 7, 2319–2332. doi: 10.1093/jxb/erq403

Filiz, E., and Akbudak, M. A. (2020). Ammonium transporter 1 (AMT1) gene family in tomato (*Solanum lycopersicum* L.): bioinformatics, physiological and expression analyses under drought and salt stresses. *Genomics* 112, 3773–3782. doi: 10.1016/j.ygeno.2020.04.009

Finkelstein, R. R., Gampala, S. S. L., and Rock, C. D. (2002). Abscisic acid signaling in seeds and seedlings. *Plant Cell* 14, 15–45. doi: 10.1105/tpc.010441

Frank, S., Hollmann, J., Mulisch, M., Matros, A., Carrion, C. C., Mock, H.-P., et al. (2019). Barley cysteine protease PAP14 plays a role in degradation of chloroplast proteins. *J. Exp. Bot.* 21, 6057–6069. doi: 10.1093/jxb/erz356

Frescher, G. T., Roumet, C., Comasd, L. H., Weemstra, M., Bengough, A. G., Rewald, B., et al. (2020). Root traits as drivers of plant and ecosystem functioning: current understanding, pitfalls and future research needs. *New Phytol.* 232, 1123–1158. doi: 10.1111/nph.17072

Gazzarrini, S., Lejay, G. A., Ninnemann, O., Frommer, W. B., and Wiren, V. (1999). Three functional transporters for constitutive, diurnally regulated, and starvation-induced uptake of ammonium into Arabidopsis roots. *Plant Cell* 5, 937–948. doi: 10.1105/tpc.11.5.937

German, M. A., Luo, S., Schroth, G., Meyers, B. C., and Green, P. J. (2009). Construction of Parallel Analysis of RNA Ends (PARE) libraries for the study

cleaved miRNA targets and the RNA degradome. *Nat. Protoc.* 3, 356–362. doi: 10.1038/nprot.2009.8

Giehl, R. F. H., and von Wiren, N. (2014). Root nutrient foraging. *Plant Physiol.* 2, 509–517. doi: 10.1104/pp.114.245225

Goulding, K., Jarvis, S., and Whitmore, A. (2008). Optimizing nutrient management for farm systems. *Philos. Trans. R. Soc. Lond. Ser. B Biol. Sci.* 363, 667–680. doi: 10.1098/rstb.2007.2177

Grabowska, A., Smoczynska, A., Bielewicz, D., Pacak, A., Jarmolowski, A., and Szweykowska-Kulinska, Z. (2020). Barley microRNAs as metabolic sensors for soil nitrogen availability. *Plant Sci.* 299:110608. doi: 10.1016/j.plantsci.2020.110608

Guo, S., Xu, Y., Liu, H., Mao, Z., Zhang, C., Ma, Y., et al. (2013). The interaction between OsMADS57 and OsTB1 modulates rice tillering via DWARF14. *Nat. Commun.* 4:1566. doi: 10.1038/ncomms2542

Harris, J. M. (2015). Abscisic acid: hidden architect of root system structure. *Plan. Theory* 4, 548–572. doi: 10.3390/plants4030548

Harris, J. M., and Ondzighi-Assoume, C. A. (2017). Environmental nitrate signals through abscisic acid in the root tip. *Plant Signal. Behav.* 12:e1273303. doi: 10.1080/15592324.2016.1273303

Hayes, T. E., Sengupta, P., and Cochran, B. H. (1988). The human c-fos serum response factor and the yeast factors GRM/PRTF have related DNA-binding specificities. *Genes Dev.* 2, 1713–1722. doi: 10.1101/gad.2.12b.1713

Heuermann, D., Hahn, H., and Von Wiren, N. (2021). Seed yield and nitrogen efficiency in oilseed rape after ammonium nitrate or urea fertilization. *Front. Plant Sci.* 11, 2197. doi: 10.3389/fpls.2020.608785

Hill, K., Wang, H., and Perry, S. E. (2008). A transcriptional repression motif in the MADS factor AGL15 is involved in recruitment of histone deacetylase complex components. *Plant J.* 53, 172–185. doi: 10.1111/j.1365-313X.2007.03336.x

Hinchliffe, A., and Harwood, W. A. (2019). Agrobacterium-mediated transformation of barley immature embryos. *Methods Mol. Biol.* 1900, 115–126. doi: 10.1007/978-1-4939-8944-7_8

Ho, C.-H., Lin, S.-H., Hu, H.-C., and Tsay, Y.-F. (2009). CHL1 functions as a nitrate sensor in plants. *Cell* 138, 1184–1194. doi: 10.1016/j.cell.2009.07.004

Hugouvieux, V., and Zubieta, C. (2018). MADS transcription factors cooperate: complexities of complex formation. *J. Exp. Bot.* 68, 1821–1823. doi: 10.1093/jxb/ery099

Imran, F. S., Amanullah, K. S., Arif, M., and Al-Tawaha, A. R. (2021). "Climate change and climate smart plants production technology," in *Climate change and Plants: Biodiversity, Growth and Interactions. Footprints of Climate Variablility on plant Diversity*. eds. S. Fahad, O. Sonmez, S. Saud, D. Wang, C. Wu and M. Adnanet al. (Boca Raton: CRC Press).

Jia, Z., Liu, Y., Gruber, B. D., Neumann, K., Kilian, B., Graner, A., et al. (2019). Genetic dissection of root system architecture traits in spring barley. *Front. Plant Sci.* 10:400. doi: 10.3389/fpls.2019.00400

Jiao, X., Lyu, Y., Wu, X., Li, H., Cheng, L., Zhang, C., et al. (2016). Grain production versus resource and environmental costs: towards increasing sustainability of nutrient use in China. *J. Exp. Bot.* 67, 4935–4949. doi: 10.1093/jxb/erw282

Jiao, X., Wang, H., Yan, J., Kong, X., Lie, Y., Chu, J., et al. (2020). Promotion of BR biosynthesis by miR444 is required for ammonium-triggered inhibition of root growth. *Plant Physiol.* 182, 1454–1466. doi: 10.1104/pp.19.00190

Kant, S., Bi, Y. M., and Rothstein, S. J. (2011). Understanding plant response to nitrogen limitation for the improvement of crop nitrogen use efficiency. *J. Exp. Bot.* 62, 1499–1509. doi: 10.1093/jxb/erq297

Kobae, Y., Tamura, Y., Takai, S., Banba, M., and Hata, S. (2010). Localized expression of arbuscular mycorrhiza-inducible ammonium transporters in soybean. *Plant Cell Physiol.* 51, 1411–1415. doi: 10.1093/pcp/pcq099

Kong, L., Xie, Y., Hu, L., Si, J., and Wang, Z. (2017). Excessive nitrogen application dampens antioxidant capasity and grain filling in wheat as revealed by metabolic and physiological analyses. *Sci. Rep.* 7:43363. doi: 10.1038/srep43363

Kruszka, K., Pacak, A., Swida-Barteczka, A., Nuc, P., Alaba, S., Wroclewska, Z., et al. (2014). Transcriptionally and post-transcriptionaly regulated microRNAs in heat stress response in barley. *J. Exp. Bot.* 65, 6123–6135. doi: 10.1093/jxb/eru353

Kruszka, K., Pacak, A., Swida-Barteczka, A., Stefaniak, A. K., Kaja, E., Sierocka, I., et al. (2013). Developmentally regulated expression and complex processing of barley pri-microRNAs. *BMC Genomics* 14:34. doi: 10.1186/1471-2164-14-34

Lea, P. J., and Forde, B. G. (1994). The use of mutants and transgenic plants to study amino acid metabolism. *Plant Cell Environ.* 17, 541–556. doi: 10.1111/j.1365-3040.1994.tb00148.x

Lea, P. J., and Miflin, B. J. (1974). Alternative route for nitrogen assimilation in higher plants. *Nature* 251, 614–616. doi: 10.1038/251614a0

Lehmeier, C. A., Wild, M., and Schnyder, H. (2013). Nitrogen stress affects the turnover and size of nitrogen pools supplying leaf growth in a grass. *Plant Physiol.* 162, 2095–2105. doi: 10.1104/pp.113.219311

Leran, S., Varala, K., Boyer, J. C., Chiurazzi, M., Crawford, N., Daniel-Vedele, F., et al. (2014). A unified nomenclature of NITRATE TRANSPORTER1/PEPTIDE TRANSPORTER family members in plants. *Trends Plant Sci.* 19, 5–9. doi: 10.1016/j.tplants.2013.08.008

Li, X., Sanagi, M., Lu, Y., Nomura, Y., Stolze, S. C., Yasuda, S., et al. (2020). Protein phosphorylation dynamics under carbon/nitrogen-nutrient stress and identification of a cell death-related receptor-like kinase in Arabidopsis. *Front. Plant Sci.* 11, 377. doi: 10.3389/fpls.2020.00377

Lips, S. H., Leidi, E. O., Silberbush, M., Soares, M. I. M., and Lewis, O. E. M. (1990). Physiological aspects of ammonium and nitrate fertalization. *J. Plant Nutr.* 13, 1271–1289. doi: 10.1080/01904169009364151

Liu, Z., Giehl, R. F. H., Hartmann, A., Hajireazaei, R., Carpentier, S., and Von Wiren, N. (2020). Seminal and nodal roots of barley differ in anatomy proteome and nitrate uptake capacity. *Plant Cell Physiol.* 61, 1297–1308. doi: 10.1093/pcp/pcaa059

Love, M. I., Huber, W., and Anders, S. (2014). Moderate estimation of fold change and dispersion for RNA-seq data with DESeq2. *Genome Biol.* 15, 1–21. doi: 10.1186/s13059-014-0550-8

Lu, C., Jeong, D. H., Kulkarni, K., Pillay, M., Nobuta, K., German, R., et al. (2008). Genome-wide analysis for discovery of rice microRNAs reveals natural antisense microRNAs (nat-miRNAs). *Proc. Natl. Acad. Sci. U. S. A.* 105, 4951–4956. doi: 10.1073/pnas.0708743105

Meyer, C., and Stitt, M. (2001). "Nitrate reduction and signalling," in *Plant Nitrogen*. eds. P. J. Lea and J. F. Morot-Gaudry (Berlin: Springer), 37–59.

Mu, X., Chen, Q., Chen, F., Yuan, L., and Mi, G. (2016). Within-leaf nitrogen allocation in adaptation to low nitrogen supply in maize during grain-filling stage. *Front. Plant Sci.* 7:699. doi: 10.3389/fpls.2016.00699

Muino, J. M., Smaczniak, C., Angenent, G. C., Kaufmann, K., and Van Gijk, A. D. J. (2014). Structural determinants of DNA recognition by plant MADS-domain transcription factors. *Nucleic Acids Res.* 42, 2138–2146. doi: 10.1093/nar/gkt1172

Newton, A. C., Flavell, A. J., George, T. S., Leat, P., Mullgolland, B., Ramsay, L., et al. (2011). Crops that feed the world 4. Barley: a resilient crop? Strengths and weaknesses in the context of food security. *Food Secur.* 3, 141–178. doi: 10.1007/s12571-011-0126-3

Norman, C., Runswick, M., Pollock, R., and Treisman, R. (1988). Isolation and properties of cDNA clones encoding SRF, a transcription factor that binds to the c-fos serum response element. *Cell* 55, 989–1003. doi: 10.1016/0092-8674(88)90244-9

Ondzighi-Assoume, C. A., Chakraborty, A., and Harris, J. M. (2016). Environmental nitrate stimulates abscisic acid accumulation in Arabidopsis root tips by releasing it from inactive stores. *Plant Cell* 28, 729–745. doi: 10.1105/tpc.15.00946

Orsel, M., Chopin, F., Leleu, O., Smith, S. J., Krapp, A., Daniel-Vedele, F., et al. (2006). Characterization of a two-component high-affinity nitrate uptake system in Arabidopsis. *Plant Physiol.* 142, 1304–1317. doi: 10.1104/pp.106.085209

Pacak, A. M., Barciszewska-Pacak, M., Swida-Barteczka, A., Krusza, K., Sega, P., Milanowska, K., et al. (2016a). Heat stress affects Pi-related genes expression and inorganic phosphate deposition/accumulation in barley. *Fron. Plant Sci.* 7:926. doi: 10.3389/fpls.2016.00926

Pacak, A. M., Kruszka, K., Swida-Barteczka, A., Nuc, P., Karlowski, W., Jarmolowski, A., et al. (2016b). Developmental changes in barley microRNA expression profiles coupled with miRNA targets analysis. *Acta Biochim. Pol.* 63, 799–809. doi: 10.18388/abp.2016_1347

Passmore, S., Maine, G. T., Elble, R., Christ, C., and Tye, B.-K. (1988). *Saccharomyces cerevisiae* protein involved in plasmid maintenance is necessary for mating of MATα cells. *J. Mol. Biol.* 204, 593–606. doi: 10.1016/0022-2836(88)90358-0

Rehman, A., Almas, H. I., Qayyum, A., Li, H., Peng, Z., Qin, G., et al. (2021). "Abscisic acid and abiotic stress tolerance in crops," in *Plant Growth Regulators for Climate-Smart Agriculture Footprints of Climate Variablility on Plant Diversity*. eds. S. Fahad, O. Sonmez, S. Saud, D. Wang, C. Wu and M. Adnan et al. (Boca Raton: CRC Press)

Rentsch, D., Schmidt, S., and Tegeder, M. (2007). Transporters for uptake and allocation of organic nitrogen compounds in plants. *FEBS Lett.* 581, 2281–2289. doi: 10.1016/j.febslet.2007.04.013

Riechmann, J. L., Wang, M., and Meyerowitz, E. M. (1996). DNA-binding properties of Arabidopsis MADS domain homeotic proteins APETALA1, APETALA3, PISTILLATA and AGAMOUS. *Nucleic Acids Res.* 24, 3134–3141. doi: 10.1093/nar/24.16.3134

Rittstieg, K., Suurnakki, A., Suortti, T., Kruus, K., Guebitz, G., and Buchert, J. (2002). Investigations on the laccase-catalyzed polymerization of lignin model

compounds using size-exclusion HPLC. *Enzym. Microb. Technol.* 31, 403–410. doi: 10.1016/S0141-0229(02)00102-3

Rybak, M., Gąbka, M., Ratajczak, I., Woźniak, M., Sobczyński, T., and Joniak, T. (2020). In-situ behavioral response and ecological stoichiometry adjustment of macroalgae (Characeae, Charophyceae) to iron overload: implications for lake restoration. *Water Res.* 173:115602. doi: 10.1016/j.watres.2020.115602

Sah, S. K., Reddy, K. R., and Li, J. (2016). Abscisic acid and abiotic stress tolerance in crop plants. *Front. Plant Sci.* 7, 571. doi: 10.3389/fpls.2016.00571

Salome, P. A. (2019). The shade of things to come: plastid retrograde signaling and shade avoidance. *Plant Cell* 31:275. doi: 10.1105/tpc.19.00049

Schwarz-Sommer, Z., Huijser, P., Nacken, W., Saedler, H., and Sommer, H. (1990). Genetic control of flower development by homeotic genes in *Antirrhinum majus*. *Science* 250, 931–936. doi: 10.1126/science.250.4983.931

Sonoda, Y., Ikeda, A., Saiki, S., Yamaya, T., and Yamaguchi, J. (2003). Feedback regulation of the ammonium transporter gene family AMT1 by glutamine in rice. *Plant Cell Physiol.* 44, 1396–1402. doi: 10.1093/pcp/pcg169

Sunkar, R., Girke, T., Jain, P. K., and Zhu, J. K. (2005). Cloning and characterization of microRNAs from rice. *Plant Cell* 17, 1397–1411. doi: 10.1105/tpc.105.031682

Sunkar, R., Zhou, X., Zheng, Y., Zhang, W., and Zhu, J. K. (2008). Identification of novel and candidate miRNAs in rice by high throughput sequencing. *BMC Plant Biol.* 8:25. doi: 10.1186/1471-2229-8-25

Tcherkes, G., and Hodges, M. (2008). How stable isotopes may help to elucidate primary nitrogen metabolism and its interaction with (photo) respiration in C3 leaves. *J. Exp. Bot.* 59, 1685–1693. doi: 10.1093/jxb/erm115

Thody, J., Folkes, L., Medina-Calzada, Z., Xu, P., Dalmay, T., and Moulton, V. (2018). PAREsnip2: a tool for high-throughput prediction of small RNA targets from degradome sequencing data using configurable targeting rules. *Nucleic Acids Res.* 46, 8730–8739. doi: 10.1093/nar/gky609

Unno, H., Uchida, T., Sugawara, H., Kurisu, G., Sugiyama, T., Yamaya, T., et al. (2006). Atomic structure of plant glutamine synthetase: a key enzyme for plant productivity. *J. Biol. Chem.* 281, 29287–29296. doi: 10.1074/jbc.M601497200

Uribelarrea, M., Crafts-Brandner, S. J., and Below, F. E. (2009). Physiological N response of field-grown maize hybrids (*Zea mays* L.) with divergent yield potential and grain protein concentration. *Plant Soil* 316, 151–160. doi: 10.1007/s11104-008-9767-1

Vos, J., Van Der Putten, P., and Birch, C. J. (2005). Effect of nitrogen supply on leaf appearance, leaf growth, leaf nitrogen economy and photosynthetic capacity in maize (*Zea mays* L.). *Field Crop Res.* 93, 64–73. doi: 10.1016/j.fcr.2004.09.013

Walch-Liu, P., Ivanov, I. I., Filleur, S., Gan, Y., Remans, T., and Forde, B. G. (2006). Nitrogen regulation of root branching. *Ann. Bot.* 95, 875–881. doi: 10.1093/aob/mcj601

Wang, M., Zhang, P., Liu, Q., Li, G., Di, D., Xia, G., et al. (2020). TaANR1-TaBG1 and TaWabi5-TaNRT2s/NAR. Link ABA metabolism and nitrate acquisition in wheat roots. *Plant Physiol.* 182, 1440–1453. doi: 10.1104/pp.19.01482

Wiren, N., Gazzarrini, S., and Frommer, W. B. (1997). Regulation of mineral nitrogen uptake in plants. *Plant Soil* 196, 191–199. doi: 10.1023/A:1004241722172

Wittgenstein, N. J. J. B., Le, C. H., Hawkins, B. J., and Ehlting, J. (2014). Evolutionary classification of ammonium, nitrate, and peptide transporters in land plants. *BMC Evol. Biol.* 14:11. doi: 10.1186/1471-2148-14-11

Xiong, Q., Tang, G., Zhong, L., He, H., and Chen, X. (2018). Response to nitrogen deficiency and compensation on physiological characteristics, yield formation, and nitrogen utilization in rice. *Front. Plant Sci.* 9:1075. doi: 10.3389/fpls.2018.01075

Yan, Y., Wang, H., Hamera, S., Chen, X., and Fang, R. (2014). miR444a has multiple functions in the rice nitrate-signaling pathway. *Plant J.* 78, 44–55. doi: 10.1111/tpj.12446

Yang, L., Liu, Z., Lu, F., Dong, A., and Huang, H. (2006). SERRAYE is a novel nuclear regulator in primary microRNA processing in Arabisopsis. *Plant J.* 6, 841–850. doi: 10.1111/j.1365-313X.2006.02835.x

Yanofsky, M. F., Ma, H., Bowman, J. L., Drews, G. N., Feldmann, K. A., and Meyerowitz, E. M. (1990). The protein encoded by the Arabidopsis homeotic gene agamousresembles transcription factors. *Nature* 346, 35–39. doi: 10.1038/346035a0

Yao, B., Cao, J., Zhao, C., and Rengel, Z. (2011). Influence of ammonium and nitrate supply on growth, nitrate reductase activity and N-use efficiency in a natural hybrid pine and its parents. *Plant Ecol.* 4, 275–282. doi: 10.1093/jpe/rtq033

Yu, C., Li, Y., Zhang, A., Su, S., Yan, A., Huang, L., et al. (2015). MADS-box transcription factor OsMADS27 regulated root development through affection of nitrate accumulation in rice. *PLoS One* 10:e0135196. doi: 10.1371/journal.pone.0145585

Zhang, G., Xu, N., Chen, H., Wang, G., and Huang, J. (2018). OsMADS27 regulates root system development via auxin signaling in rice. *Plant J.* 95, 1004–1022. doi: 10.1111/tpj.14007

Zielezinski, A., Dolata, J., Alaba, S., Kruszka, K., Pacak, A., Swida-Barteczka, A., et al. (2015). mirEX 2.0-an integrated environment for expression profiling of plant microRNAs. *BMC Plant Biol.* 15:144. doi: 10.1186/s12870-015-0533-2

frontiers | Frontiers in Plant Science

TYPE Review
PUBLISHED 14 September 2022
DOI 10.3389/fpls.2022.949541

Check for updates

OPEN ACCESS

EDITED BY
Andrea Miyasaka Almeida,
Universidad Mayor, Chile

REVIEWED BY
Mirza Hasanuzzaman,
Sher-e-Bangla Agricultural University, Bangladesh
José M. Alvarez,
Andrés Bello University, Chile

*CORRESPONDENCE
Meng Guo
mguo@nxu.edu.cn
Jian-She Li
13709587801@163.com

SPECIALTY SECTION
This article was submitted to Plant Abiotic Stress, a section of the journal Frontiers in Plant Science

RECEIVED 21 May 2022
ACCEPTED 17 August 2022
PUBLISHED 14 September 2022

CITATION
Guo M, Wang X-S, Guo H-D, Bai S-Y, Khan A, Wang X-M, Gao Y-M and Li J-S (2022) Tomato salt tolerance mechanisms and their potential applications for fighting salinity: A review.
Front. Plant Sci. 13:949541.
doi: 10.3389/fpls.2022.949541

COPYRIGHT
© 2022 Guo, Wang, Guo, Bai, Khan, Wang, Gao and Li. This is an open-access article distributed under the terms of the Creative Commons Attribution License (CC BY). The use, distribution or reproduction in other forums is permitted, provided the original author(s) and the copyright owner(s) are credited and that the original publication in this journal is cited, in accordance with accepted academic practice. No use, distribution or reproduction is permitted which does not comply with these terms.

Tomato salt tolerance mechanisms and their potential applications for fighting salinity: A review

Meng Guo[1,2,3,4]*, Xin-Sheng Wang[1], Hui-Dan Guo[5], Sheng-Yi Bai[1], Abid Khan[6], Xiao-Min Wang[1,2,3,4], Yan-Ming Gao[1,2,3,4] and Jian-She Li[1,2,3,4]*

[1]School of Agriculture, Ningxia University, Yinchuan, China, [2]Key Laboratory of Modern Molecular Breeding for Dominant and Special Crops in Ningxia, Yinchuan, China, [3]Ningxia Modern Facility Horticulture Engineering Technology Research Center, Yinchuan, China, [4]Ningxia Facility Horticulture Technology Innovation Center, Ningxia University, Yinchuan, China, [5]College of Horticulture and Landscape, Henan Institute of Science and Technology, Xinxiang, China, [6]Department of Horticulture, The University of Haripur, Haripur, Pakistan

One of the most significant environmental factors affecting plant growth, development and productivity is salt stress. The damage caused by salt to plants mainly includes ionic, osmotic and secondary stresses, while the plants adapt to salt stress through multiple biochemical and molecular pathways. Tomato (*Solanum lycopersicum* L.) is one of the most widely cultivated vegetable crops and a model dicot plant. It is moderately sensitive to salinity throughout the period of growth and development. Biotechnological efforts to improve tomato salt tolerance hinge on a synthesized understanding of the mechanisms underlying salinity tolerance. This review provides a comprehensive review of major advances on the mechanisms controlling salt tolerance of tomato in terms of sensing and signaling, adaptive responses, and epigenetic regulation. Additionally, we discussed the potential application of these mechanisms in improving salt tolerance of tomato, including genetic engineering, marker-assisted selection, and eco-sustainable approaches.

KEYWORDS

tomato, salinity tolerance, mechanism, abiotic stress, genetic breeding

Introduction

Salinity has already affected more than one-third of irrigated areas, and it is expected that by 2050, more than half of the world's cultivated land would be salinized (FAO, 2011; Zhao et al., 2020). Soil salinization severely limits the land use and affects crop yields significantly (van Zelm et al., 2020). Therefore, salt stress has become one of the

major abiotic factors threatening food security worldwide. Although the saline-alkali land improvement technology helps in the expansion of arable land, the cost factor severely restricts its application. Cultivating salt-tolerant crops is a worth exploring direction to remediate this thorny problem. A clear understanding of the mechanisms mediating salt tolerance will accelerate the development of new varieties with enhanced salt tolerance.

Salt stress is commonly caused by high concentrations of sodium ion (Na^+) and chloride ion (Cl^-) in the soil solution, and its adverse effects on plants include primary stresses like osmotic stress and ion imbalance, as well as secondary stresses like oxidative stress and metabolic abnormalities (Yang and Guo, 2018a). The excessive accumulation of Na^+ causes the soil's osmotic pressure to rise, water potential to drop, and root water uptake to decrease, thereby reducing water availability (Julkowska and Testerink, 2015; van Zelm et al., 2020). Furthermore, the Na^+/potassium ion (K^+) ratio is disrupted, inhibiting the activities of numerous K^+-dependent enzymes in the cells (Wu et al., 2018). Chloride harms the plants primarily by causing an ion imbalance via interfering with the uptake or metabolism of other necessary ions (Bazihizina et al., 2019; Zhao et al., 2020). Salt-induced osmotic stress and ion imbalance may not only impair the photosynthesis, thus affecting plant energy metabolism, but also trigger the production of reactive oxygen species (ROS), resulting in oxidative damage.

Tomato (*Solanum lycopersicum* L.), one of the most important vegetable crops, is grown all over the world. Its fruits are widely used as food in the fresh market, and it's also a model plant for genetics, fruit development, and stress tolerance research (Rothan et al., 2019). Tomatoes are native to western South America, and their wild relatives have been adapted to severely saline coastal regions, however, cultivars have lost their salt resistance during domestication (Gálvez et al., 2012; Pailles et al., 2020). Salt tolerance is a complex trait, thus developing salt-tolerant cultivars necessitates a thorough study of physiological responses, metabolic changes, and gene expression patterns under salinity. To date, the vast majority of salt-tolerance research has been performed using model plants such as *Arabidopsis*, whose contributions to application-oriented research into salt-tolerance are limited by its inherently low levels of salt tolerance and lack of agronomically relevant yield-related traits (Morton et al., 2019). Tomato is a moderately salt-sensitive and yield-targeted crop that can overcome this limitation of *Arabidopsis*. In this review, we provide a critical review of the effects of salt stress, mechanisms of salt tolerance, and biotechniques to improve salt tolerance in tomato. Finally, we highlight research directions for accelerating the genetic improvement of salt tolerance in tomato. Understanding the response and tolerance of tomato to salt stress will enable translational applications to other yield-targeted crops, thus will contribute to the expansion of arable land, agricultural sustainability and global food security.

Impact of salinity on tomato

Morphological changes

Generally, the seed germination and early seedling growth stages are most susceptible to salinity, and roots are more vulnerable than other organs (Foolad, 2004). Salt stress delays germination and reduces the germination rate of tomato seeds through changing the activities of key enzymes and the levels of gibberellin (GA), respectively (Singh et al., 2012; Tanveer et al., 2020). Salinity induces the roots to absorb Na^+, resulting a decrease in the osmotic potential and water intake, which in turn inhibits root growth (Siddiqui et al., 2017; Tanveer et al., 2020). Nevertheless, the root:shoot ratio increased in response to increasing salinity indicating that shoot growth is restricted while root growth is less hindered (Singh et al., 2012). In addition, salinity also represses the development of leaf, flower and fruit by inhibiting cell division or elongation, hindering sugar metabolism and decreasing water import, respectively (Ghanem et al., 2009; Siddiqui et al., 2017; Pinedo-Guerrero et al., 2020).

Physiological and biochemical changes

Under high salinity stress, tomato plants collect more Na^+ and Cl^-, while the levels of K^+ and calcium ion (Ca^{2+}) decrease, disrupting ion homeostasis, which can be restored by rescuing seedlings from salinity (Rahman et al., 2016; Parvin et al., 2019b). Sodium preferentially accumulate in old leaves, protecting young leaves from the toxic effects of saline stress (Khelil et al., 2007). The detrimental effects of Cl^- result from interference in the uptake or metabolism of other essential ions, such as nitrate ion (NO_3^-) (Zhao et al., 2020).

Excessive ROS induced by high salinity can damage the structure of macromolecules (Waszczak et al., 2018). In roots, oxidative stress caused by salinity was earlier and more sensitive than that in leaves (Gapiñska et al., 2008). The increased anti-oxidase activity in salt-tolerant genotypes helps to protect against oxidative damage (Gharsallah et al., 2016b). Furthermore, the antioxidant defense system and the glyoxalase system work together to detoxify salt-induced ROS and improve salt tolerance in tomato (Parvin et al., 2019b).

Salinity also regulates the compatible solutes, such as proline (Pro) and glycine betaine (GB). Salinity significantly increases Pro, and its level in tomato leaves was higher than that in roots, which attributes in maintaining the chlorophyll content and cell turgidity to protect the photosynthetic activity (Gharsallah et al., 2016b; De la Torre-González et al., 2018). The GB content decreased both in two salt-stressed commercial genotypes, while the levels in the salt-tolerant genotype was lower than that in the sensitive genotype (De la Torre-González et al., 2018). However, exogenous application of GB or its accumulation by genetic

engineering alleviated salt-induced K^+ efflux, enhancing salt tolerance in tomato (Wei et al., 2017).

Short-term salt treatment reduces stomatal conductance, pore area and index, that strongly suppress the dynamic photosynthesis in leaves (Zhang et al., 2018). Under salt conditions, the phytohormones such as abscisic acid (ABA), ethylene (ET), and salicylic acid (SA) are also involved in tomato photosynthesis. ABA causes stomatal closure, reducing leaf gas exchange in salinized plants (Lovelli et al., 2012). ET controls net carbon dioxide (CO_2) fixation through stomatal or non-stomatal factors, and regulates the activity of photosystems and efficiency of photoprotective processes (Borbély et al., 2020). SA increases photosynthetic activity by inducing higher maximal CO_2 fixation rate, carboxylation efficiency of Rubisco, and photosynthetic quantum efficiency (Poór et al., 2011).

Unlike the severe damage caused by high salinity, moderate salt stress improves fruit quality by increasing soluble solid content, carotenoid levels, and the accumulation of glutamic acid (Glu), gamma-aminobutyric acid (GABA), glutamine, and α-tocopherol (Massaretto et al., 2018; Meza et al., 2020). The range of salinity to improve fruit quality without affecting tomato yield deserves special attention, which may depend on varieties and duration of stress.

Mechanisms for salt tolerance in tomato

Salt signaling pathways and ion transport

How salt enters the plants and salt perception remain unknown (Yang and Guo, 2018b; van Zelm et al., 2020). Ion uptake occurs mainly through the apoplastic and symplastic pathways, and water moves radially through the root via the apoplastic, symplastic and transcellular pathways (the latter two pathways are collectively referred to as cell-to-cell pathway) (Sánchez-Aguayo et al., 2004; Isayenkov and Maathuis, 2019). High salinity in the apoplast alters aqueous and ionic thermodynamic equilibria, which results in ionic and/or osmotic stresses. The percentage of water movement through the symplastic pathway in tomato plants treated with 75 mM NaCl was lower than that in untreated plants. The bulk flow of water and solutes along the apoplastic pathway under saline conditions would impart smaller selectivity and reduced ion uptake (Fernández-García et al., 2002; Sánchez-Aguayo et al., 2004). The contribution of the apoplastic pathway in tomato species that differ in salt tolerance needs to be further explored.

Various transporters are involved in Na^+ uptake and movement across the plasma membrane (PM), of which non-selective cation channels (NSCCs) are a main route of Na^+ influx into glycogenic plant roots (Isayenkov and Maathuis, 2019; **Figure 1**). NSCCs are regulated by different salt-induced early signals, such as Ca^{2+}, 3′,5′-cyclic guanosine monophosphate (cGMP), and ROS (van Zelm et al., 2020). K^+ transporters and transporters from the HKT family are also involved in primary sodium influx into roots (Kronzucker and Britto, 2011). When Na^+ enters the cell through NSCCs, the membrane depolarizes. This change in membrane voltage prevents the hyperpolarization and tomato *high-affinity K^+ transporter 5* (*HAK5*) expression induced by K^+ starvation (Nieves-Cordones et al., 2008). High Ca^{2+} reduces the Na^+-induced depolarization in tomato root cells and mitigates the repression of HAK5 mediated high-affinity K^+ uptake (Bacha et al., 2015).

Plants sense and respond to salt stress within a short period of time. But so far, no specific salt sensor has been identified in cells. The glucuronosyltransferase encoded by *monocation-induced $[Ca^{2+}]_i$ increases 1* (*MOCA1*) is involved in the biosynthesis of glycosyl-inositol phosphorylceramide (GIPC) sphingolipids at the PM. GIPCs directly bind to Na^+ and regulate the entry of Ca^{2+} into the cytosol, but the detailed signal transduction process remains unclear (Jiang et al., 2019; Zhao et al., 2020). The decreased pectin crosslinking caused by salt is sensed by a receptor-like kinase (RLK) FERONIA (FER), while the downstream signaling of this receptor is not part of the early signaling response (Feng et al., 2018). The response of plants to salt stress may be the result of sensing and integration of multiple signaling pathways (van Zelm et al., 2020; **Figure 2**).

High salinity rapidly induces the accumulation of cytosolic Ca^{2+}, which can form early signal components of salt sensing relays (Isayenkov and Maathuis, 2019). A series of Ca^{2+}-dependent proteins, such as calcineurin B-like proteins (CBLs), calcium-dependent protein kinases (CDPKs) and CBL-interacting protein kinases (CIPKs) are involved in the signal decoding of Ca^{2+} influx into the cytoplasm (Zhao et al., 2020). As the best-characterized CBL- CIPK route, Ca^{2+}-dependent salt overly sensitive (SOS) pathway governs ionic homeostasis and salt tolerance, and has been postulated as a molecular switch for salt stress responses (Huertas et al., 2012; Zhu, 2016). SOS3, a functional Ca^{2+}-binding protein, senses Ca^{2+} and physically interacts with SOS2 at the PM. SOS2 is a serine/threonine protein kinase functioning as a key regulator of ion transporters (Belver et al., 2012). SOS3–SOS2 complex phosphorylates and activates SOS1, a PM Na^+/H^+ antiporter that extrudes Na^+ out of the cell (Yang and Guo, 2018b). Tomato SOS3 is mainly expressed in roots (Cho et al., 2021), and SOS3–SOS2 complex can activate Na^+/H^+ antiport activity of *Arabidopsis* AtSOS1 (Huertas et al., 2012), indicating that the SOS pathway is conservative.

In tomato, decreased levels of *SOS1* lead to a salt-sensitive phenotype (Olías et al., 2009a; Wang Z. et al., 2021). Unlike only the overexpression of activated forms of *Arabidopsis AtSOS2* increases salinity tolerance in transgenic plants (Guo et al., 2004), overexpression of the both native and activated forms of

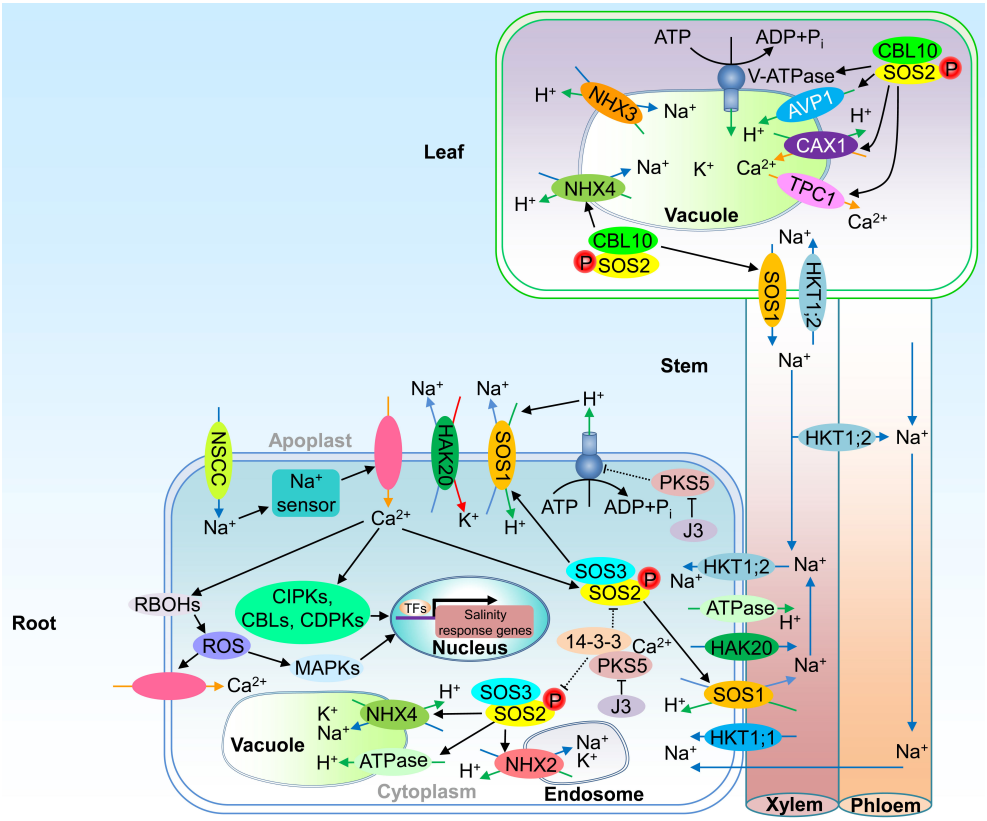


FIGURE 1
Schematic overview of sodium uptake into tomato roots and transport into leaves. Na^+ ions enter tomato root cells primarily through NSCC pathway. Na^+ entering the cell is sensed by a yet undetermined sensory mechanism. Subsequently, Ca^{2+}, ROS, and hormone (not shown) signaling pathways are activated. Ca^{2+} induces ROS production by RBOHs and ROS induces Ca^{2+} import. As one part of the Ca^{2+}-signaling pathway, CIPKs, CBLs, and CDPKs become active and alter the global transcriptional profile in the nucleus. MAPKs activated by Ca^{2+}-ROS-signaling pathway also transduce downstream gene transcription in the nucleus. These early signaling pathways result in activation of detoxification mechanisms. Cytosolic Ca^{2+} ions activate SOS3. SOS2 regulates ATPase, NHX2 and NHX4, increasing Na^+/H^+ and K^+/H^+ anti-transport activity in root vacuole and endosome. The kinase activity of SOS2 is negatively regulated by 14-3-3 proteins, and the inhibition on SOS2 is released by the Ca^{2+}-mediated binding of PKS5 with 14-3-3. SOS1 activated by SOS2-SOS3 heterologous kinase complex is responsible for extruding Na^+ out the root and partitioning Na^+ in organs. J3 inhibits PKS5 kinase activity, activating the activity of PM H^+-ATPases and generating a proton gradient required for Na^+ transport of SOS1. CBL10-SOS2 complex triggers the separation of Na^+ into leaf vacuole and the transport of Na^+ ions from leaves to xylem, activates the tonoplast targets TPC1 and AVP1, maintaining an appropriate Na^+/Ca^{2+} ratio and V-ATPase, and promotes the proton gradient necessary to energize the Ca^{2+} transport toward the vacuole through CAX1. HKT1;2 is involved in xylem Na^+ unloading and Na^+ uploading into the phloem, thus promoting Na^+ recirculation from shoots to roots, which can be additionally regulated by HKT1;1 in roots. HAK20 transports and regulates the homeostasis of Na^+ and K^+. ADP, adenosine diphosphate; ATP, adenosine triphosphate; AVP1, H^+-pyrophosphatase; CAX1, CATION EXCHANGER 1; CBL, calcineurin B-like protein; CDPKs, calcium-dependent protein kinases; CIPKs, CBL-interacting protein kinases; RBOHs, respiratory burst oxidase homologs; HAK, high-affinity K^+ transporter; HKT, high K^+ affinity transporter; J3, DNAJ HOMOLOG3; MAPK, mitogen-activated protein kinase; NHX, Na^+/H^+ exchanger; NSCCs, non-selective cation channels; PKS5, PROTEIN KINASE5; ROS, reactive oxygen species; SOS, salt overly sensitive; TFs, transcription factors; TPC1, TWO-PORE CHANNEL 1. The dashed lines indicate that the negative regulatory roles are released under salt stress.

tomato *SOS2* increase salt tolerance (Huertas et al., 2012; Cho et al., 2021). Activation of SOS1 in tomato plants overexpressing *SOS2* may contribute to the efflux of Na^+ out the root epidermal cells as well as the active loading of Na^+ into shoots (Olías et al., 2009a; Belver et al., 2012; Huertas et al., 2012). Overexpression of tomato *enhancer of SOS3-1* (*ENH1*) excludes more Na^+ from cytosol and transports into vacuoles, and maintains more K^+ in cytosol to reestablish ion homeostasis (Li D. et al., 2013).

Tomato SOS2 regulates the activity of V-ATPase, energizing the Na^+/H^+ antiport at the endosomal-prevacuolar as well as vacuolar compartments. Additionally, SOS2 activates the Na^+/H^+ and K^+/H^+ antiport activity in root intracellular membranes and the Na^+/H^+ antiport activity in root tonoplast vesicles, which are regulated by the endosomal-vacuolar K^+, Na^+/H^+ (NHX2 and NHX4) antiporters (Huertas et al., 2012). The K^+/H^+ antiporter NHX2 increases salt tolerance by improving K^+ uptake and compartmentalization (Rodríguez-Rosales et al., 2008; Huertas et al., 2013). Tomato plants overexpressing both *NHX2* and *SOS2* grow better under salinity conditions than plants overexpressing only one of them

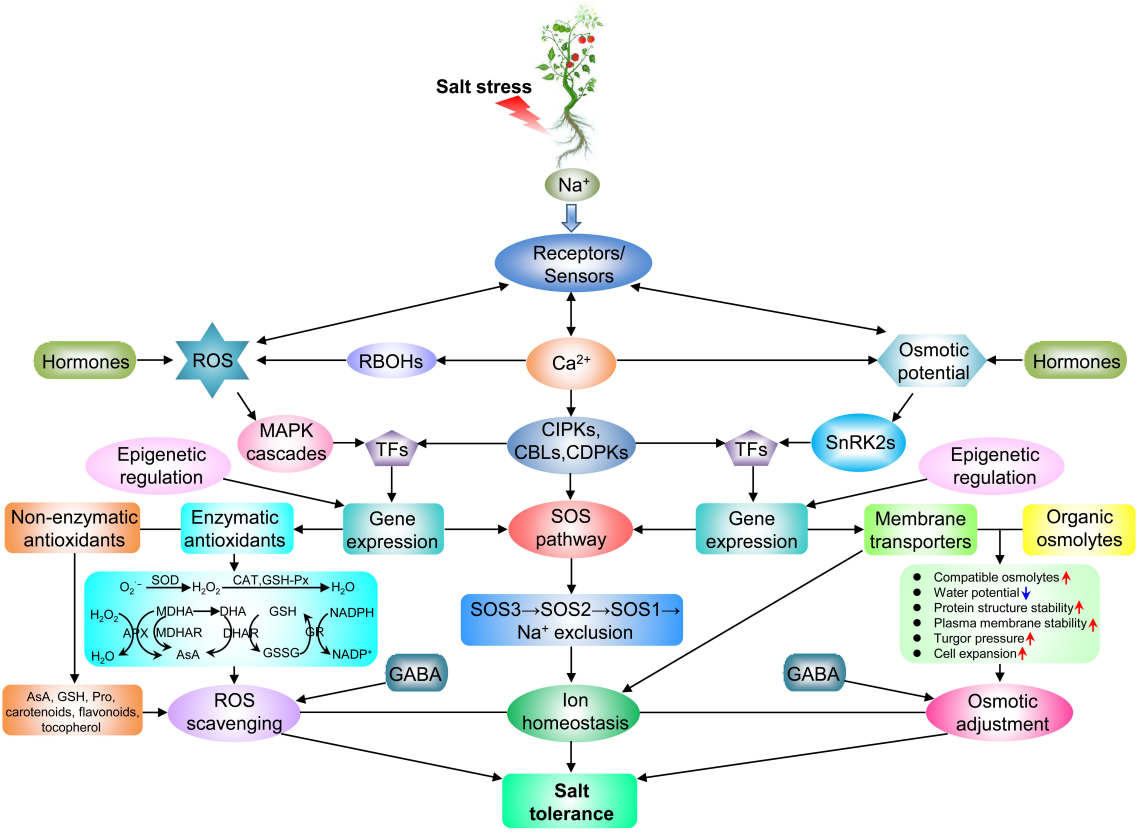


FIGURE 2
The potential mechanisms underlying salt tolerance in tomato. Salt stress is sensed by unknown receptors or sensors that act synergistically with Ca^{2+} waves, ROS production and osmotic potential. These changes activate antioxidant, ion transporter and osmoregulation pathways, leading to salt tolerance through ROS scavenging, ionic homeostasis and osmotic adaptation. Endogenous GABA participates in ROS scavenging and osmotic adaptation under salt conditions. The red and blue arrows in the box indicate the increase and decrease of the indicators, respectively. APX, ascorbate peroxidase; AsA, ascorbic acid; CAT, catalase; DHA, dehydroascorbate; DHAR, dehydroascorbate reductase; GABA, gamma-aminobutyric acid; GR, glutathione reductase; GSH, glutathione; GSH-Px, glutathione peroxidase; GSSG, oxidized glutathione; H_2O_2, hydrogen peroxide; MDHAR, monodehydroascorbate reductase; $NADP^+$, oxidized form of NADPH; NADPH, nicotinamide adenine dinucleotide phosphate; $O_2^{\cdot-}$, superoxide radical; Pro, proline; SnRK2s, sucrose non-fermenting-1-related protein kinase 2s; SOD, superoxide dismutase. The remaining abbreviations mentioned in this figure exist in **Figure 1**.

(Baghour et al., 2019). How SOS2 activates NHX transporters in tomato roots remains to be clarified.

Under salt conditions, tomato CBL10 can form a complex with SOS2. SOS2–CBL10 complex maintains a proper Na^+/Ca^{2+} ratio in the vacuole of leaf cells through the activation of tonoplast targets, therefore protecting young developing tissues from the damage caused by salt (**Figure 1**). The tonoplast targets include the cation channel TWO-PORE CHANNEL 1 (TPC1, mediating Ca^{2+} release from vacuoles) and two vacuolar H^+-pumps, H^+-pyrophosphatase AVP1 (AVP1) and V-ATPase (V-ATPase). The expression of tomato *SOS2* is associated with *CBL10*. Loss function of *CBL10* strongly inhibits the expression of *CATION EXCHANGER 1* (*CAX1*) and impairs the proton gradient necessary to energize the Ca^{2+} transport toward the vacuole through CAX1 antiporter (Egea et al., 2018). The role of tomato SOS2-CBL10 complex in regulating vacuolar Na^+ sequestration is not well characterized.

Plant 14-3-3 proteins are phosphoserine-binding proteins that regulate the activities of a wide array of targets, playing an important role in response to salt stress (Xu and Shi, 2006). 14-3-3 proteins inhibit the kinase activity of SOS2 under normal conditions. PROTEIN KINASE5 (PKS5) inhibits SOS2 activity by promoting the interaction between SOS2 and 14-3-3 proteins. Under salt conditions, chaperone DNAJ HOMOLOG3 (J3) interacts with PKS5 kinase and inhibits its activity, thereby releasing the inhibition of SOS2 activity by 14-3-3 protein, which is associated with salt-induced Ca^{2+} signal (Yang and Guo, 2018b; Yang et al., 2019; Zhao et al., 2020). At least 12 genes named *TOMATO 14-3-3 PROTEIN1 (TFT1)-TFT12* are predicted to encode tomato 14-3-3 proteins, and the levels of *TFT1*, *TFT4*, *TFT7*, and *TFT10* are significant up-regulated by salt (Xu and Shi, 2006). Enhanced salt tolerance in *TFT7*-overexpressing transgenic plants due to the reduction of oxidative stress injury rather than the maintenance and

reestablishment of cellular ion homeostasis (Xu and Shi, 2007). In addition to salt stress, tomato *TFT4* is also involved in response to alkali stress, but the functions of tomato *TFT4* in the integration of H^+ efflux, the basipetal indole-3-acetic acid (IAA) transport, and the PKS5-J3 pathway need to be further defined (Xu et al., 2013).

Salt stress induces the accumulation of ROS, including superoxide radical ($O_2^{\cdot -}$), hydroxyl radical ($OH^{\cdot}$), singlet oxygen ($^1O_2$), and hydrogen peroxide (H_2O_2) (Yang and Guo, 2018a). ROS have toxic effects at high concentrations, while function as signal transduction molecules at low concentrations (Miller et al., 2010). Under salt conditions, increased cytosolic Ca^{2+} induces respiratory burst oxidase homologs (RBOHs) to generate ROS, and ROS induces Ca^{2+} entry into stomata (van Zelm et al., 2020). In tomato, most of eight *RBOH* genes were significantly upregulated by persistent salt stress, showing that RBOHs are essential regulators response to long-term salinity stress (Raziq et al., 2022). Tomato *RBOH1*-dependent apoplastic H_2O_2 mediates epigallocatechin-3-gallate-induced abiotic stress tolerance (Li et al., 2019b), high atmospheric CO_2-dependent salt stress tolerance (Yi et al., 2015) and spermine-induced salinity-alkalinity stress tolerance (Xu et al., 2021). Furthermore, salt-induced ROS can activate downstream mitogen-activated protein kinase (MAPK) cascades. Activated MPKs transduce signals to downstream transcription factors (TFs) in the nucleus to induce the expression of stress-responsive genes (Isayenkov and Maathuis, 2019). MAPK cascade consists of three consecutively acting and phosphorylating protein kinases, MAP kinase kinase kinase (MAPKKK/MEKK), MAP kinase kinase (MAPKK/MKK), and MAP kinase (MAPK/MPK) (Mishra et al., 2006). In tomato genome, 16 *MAPK*, 5 *MAPKK* and 89 *MAPKKK* genes are identified (Kong et al., 2012; Wu et al., 2014). Tomato *MAPKK2* and *MAPKK5* were significantly upregulated by salt stress, and the transcript levels of 13 *MAPKKK* genes shown a more than 10-fold change under salt stress (Wu et al., 2014). Although there is no evidence that salt stress affects the expression levels of tomato MAPK family genes, *MAPK3* improves salt tolerance by increasing the expression levels of ET synthesis genes and SOS pathway genes (Shu et al., 2022).

Membrane transporters play critical roles in maintaining Na^+/K^+ homeostasis (**Figure 1**). The Na^+ transporter *HKT1;2* gene is responsible for the major quantitative trait loci (QTL) involved in Na^+ and K^+ homeostasis in tomato. Silencing of *HKT1;2* alters the Na^+/K^+ ratio, suppresses the response of *SOS1* to salt, and increases salt hypersensitivity (Asins et al., 2013; Jaime-Pérez et al., 2017; Romero-Aranda et al., 2020). HKT1;2 of *S. cheesmaniae* is not only involved in xylem Na^+ unloading but also involved in Na^+ uploading into the phloem, thus promoting Na^+ recirculation from aerial parts to the roots, which can be additionally favored by *HKT1;1* silencing at the roots (Romero-Aranda et al., 2021). Decreasing Na^+ content in young leaves is probably linked to the up-regulation of *SOS1* contributing to Na^+ exclusion from the cytosol toward the leaf apoplast. Nevertheless, preventing Na^+ accumulation in the cytosol of mature/old leaves may be mainly attributed to the combined action of HKT1-like transporters (mediating Na^+ unloading from the xylem) and NHX-type transporters (promoting Na^+ and K^+ accumulation in vacuoles and endosomes) (Olías et al., 2009b; Belver et al., 2012). CBL10 regulates the expression of *HKT1;2* and *SOS1*. The lack of *CBL10* severely inhibits Na^+ compartmentalization into vacuoles as well as Na^+ upload from xylem into cells, while promotes Na^+ extrusion from leaf cells to xylem, dilapidating its functional role in regulating Na^+ homeostasis and protecting shoot apex and developing tissues from salt damage (Egea et al., 2018). The HAK/KUP/KT (high-affinity K^+/K^+ uptake/K^+ transporter) family transporters primarily mediate K^+ fluxes. Tomato HAK20 is identified as the major player controlling root Na^+/K^+ ratio with genome-wide association studies (GWAS) (Wang et al., 2020). It functions in the loading of K^+ and Na^+ into the xylem in roots. The wild allele of *HAK20* loads more Na^+ into root xylem and enhances Na^+ efflux, therefore lowering the Na^+/K^+ ratio in roots and leading to higher salt tolerance, but its function in shoot is still elusive (Wang et al., 2020; Xiang and Jiménez-Gómez, 2020).

Osmotic adjustment

High salinity causes ionic imbalance and water deficit in plant cells, leading to osmotic stress (Zhao et al., 2021). A hyperosmolality-gated calcium-permeable channel encoded by *reduced hyperosmolality-induced* $[Ca^{2+}]_i$ *increase1 (OSCA1)* was identified as an osmotic stress sensor (Yuan et al., 2014), but the role of OSCA1 in the sense of high salinity-triggered osmotic stress is questioned (Zhao et al., 2020). Plants perform osmotic adjustment by increasing the concentration of solutes and decreasing water potential, which is vital for the alleviation of the osmotic imbalances and for maintaining cell turgor (Lv et al., 2019). Under osmotic stress, solutes can act as osmolytes or play a protective role by stabilizing the structure of biological macromolecules (**Figure 2**). Osmotic regulators mainly include inorganic ions and organic substances (Hao et al., 2021). The organic osmolytes includes sugar, complex sugars, Pro, GB, polyamines (PAs), polyols and late embryogenesis abundant (LEA) proteins (Yang and Guo, 2018b; Liu et al., 2022). Halophytes and salt-tolerant non-halophyte species synthesize organic solutes for osmotic adjustment in the cytoplasm only, while absorb Na^+ and Cl^- from the soil for the bulk of osmotic adjustment in the vacuole, a more energy-efficient strategy (Munns et al., 2016). Due to low tissue tolerance, a large portion of osmotic adjustment in salt-sensitive species occurs with organic solutes, but the high synthetic cost decreases the growth rate (Munns and Gilliham, 2015).

K^+ is one of the macronutrients required by plants for growth, and plays an important role in preventing cell damage caused by salt. Exogenous K^+ activates carbohydrate metabolism and Pro accumulation through endogenous hydrogen sulfide (H_2S) signaling, thereby increasing osmotic tolerance and enhancing the hydration levels of the salt stressed tomato seedlings (Khan et al., 2021). Under salt conditions, K^+, Na^+, Cl^-, and organic acids are the main osmolytes in tomato plants (Wang et al., 2011). The hydration ability of Pro helps the attached proteins bind more water, and prevents protein dehydration and denaturation under salt stress (Hao et al., 2021). The Pro increase in the tolerant tomato varieties supports the opinion that Pro counteracts the osmotic stress caused by salinity (De la Torre-González et al., 2018). On the other hand, the increased Pro in plants with salt treatment is generally not enough for beneficial effects, and the accumulation of Pro increases as the more stress effects. Thus, Pro concentration can be used as a negative indicator of tolerance. Foliar application of a mixture of Pro and Glu mitigated the negative effects of salt on tomato growth by accumulating total soluble sugars, but the concentration of Pro was significantly decreased (Alfosea-Simón et al., 2020). The beneficial effects of GB on reducing osmotic imbalance induced by salt stress have been demonstrated in various plants (Gupta and Huang, 2014; Lv et al., 2019). However, in some tomato genotypes, GB concentration is negatively correlated with salt tolerance, which may be due to the oxidative stress caused by H_2O_2 generated from the synthesis of GB via the choline pathway (De la Torre-González et al., 2018). The roles of Pro and GB in salt tolerance may depend on the species and cultivars. Foliar application of L-methionine (Met) and L-phenylalanine (Phe) induces salt tolerance of tomato by enhancing the PM stability, the contents of osmolytes, and the activity of antioxidative enzymes (Almas et al., 2021). Under salt stress, exogenous GABA inducing amino acid content increases osmotic adjustment capacity to resist water loss and neutralizes excessive Na^+ in the vacuoles in tomato leaves (Wu et al., 2020). Trehalose alleviates the salt damage of tomato plants by promoting the accumulation of osmotic substances Pro, GB, and soluble proteins (Yang Y. et al., 2022).

Cell wall-associated protein kinases (WAKs) localized in PM induce the changes of solutes contents. Mutation of tomato *WAK1* is tolerant to Na^+ homeostasis but not to osmotic homeostasis, and it increases sucrose content in roots. The salt sensitivity of *wak1* mutant is due to the altered osmotic and metabolic homeostasis (Meco et al., 2020). Under osmotic stress, the tomato cryptochrome 1a (cry1a) enhances the growth by reducing the MDA content and Pro accumulation, and specific blue light fluence rates are required for cry1a-mediated osmotic responses (D'Amico-Damião et al., 2021). The dehydrin *tas14* gene, a member of the tomato LEA family, improves osmotic tolerance by reducing osmotic potential and accumulating solutes (such as sugars and K^+). Plants overexpressed *tas14* transfer Na^+ into adult leaves while K^+ and sugars in young leaves, achieving osmotic balance in older leaves at a minimal energy cost (Muñoz-Mayor et al., 2012). Overexpression of tomato *ICE1a*, a MYC-type ICE1-like TF, increases the levels of Pro, soluble sugars and LEA proteins, enhancing osmotic and salt tolerance (Feng et al., 2013). In tomato plants, the accumulation of several osmotic protectants (Pro, sucrose, glucose, and GB) under salt conditions, depends on the regulation of key enzymes in their synthetic pathway at both transcriptional and post-transcriptional levels (Rivero et al., 2014).

Endogenous ABA improves short-term osmotic stress resistance in tomato via osmotic and hydraulic adjustments (Li et al., 2022). Tomato ABSCISIC ACID STRESS RIPENING1 (ASR1) protects yeast from osmotic stress by inducing downstream components of the high-osmolarity glycerol pathway (Moretti et al., 2006). ASR1 also binds directly to a tomato cellulose synthase-like (CSL) protein gene that may play key roles in osmotic stress (Ricardi et al., 2014). All the tomato *sucrose non-fermenting 1-related protein kinase 2* (*SnRK2*) genes are salt stress responsive and most of them are also induced by ABA (Yang et al., 2015; Chen et al., 2016). Overexpression of tomato *SnRK2.1* and *SnRK2.2* regulates the expression of stress-related genes and decreases osmotic tolerance, but the regulatory relationship between the activated SnRK2s and stress-related gene expression remains to be identified (Yang et al., 2015). In addition to ABA, ET and auxin also play important roles in osmotic stress response. Under osmotic stress, the ET-induced H_2S is required for ET-induced tomato stomatal closure (Jia et al., 2018). Overexpression of tomato *ET responsive factor 1* (*TERF1*) in tobacco induces not only the typical ET triple response but also salt tolerance by stimulating the expression of downstream genes. *TERF1* may be a linker in ET and osmotic signaling pathways (Huang et al., 2004). Down-regulation of tomato *Auxin Response Factor 4* (*ARF4*) improves salt and osmotic tolerance by reducing stomatal conductance along with increased leaf relative water content and ABA content (Bouzroud et al., 2020).

Reactive oxygen species generation and antioxidant defense

Reactive oxygen species accumulation

Salt stress rapidly induces the production of ROS in plant apoplast, chloroplasts, mitochondria, and peroxisomes (Chen et al., 2021). The apoplastic ROS are produced by the activation of PM-localized nicotinamide adenine dinucleotide phosphate (NADPH) oxidases (RBOHs), apoplastic peroxidases (PODs), diamine oxidases (DAOs), and PA oxidases (PAOs) (Qi et al., 2017). Salt induces the transcript of tomato *RBOH1* and enhances the activity of NADPH oxidase, deriving H_2O_2 accumulation in the apoplast. Inhibition of *RBOH1* expression

impairs the ROS scavenging induced by *RBOH1*-dependent H_2O_2 signal, while the downstream molecular players that transduce ROS signaling to the transcriptional level remain elusive (Li et al., 2019b). Tomato MAPK3 may increase salt tolerance and decrease heat tolerance through the RBOH1-dependent antioxidant system, respectively (Yu et al., 2019; Shu et al., 2022). How tomato MAPK3 and RBOH1 function in the combined response to salt and heat stress remains to be elucidated. Salt stress improves the activities of DAO and PAO. The terminal oxidation of PAs by DAO and PAO contributes to the production of H_2O_2. PAO inhibitor reduced the activity of PAOs and inhibited H_2O_2 production, but did not increase salt tolerance due to the significantly increased electrolytic leakage (Takács et al., 2017). PAO induced by spermidine (Spd) mediates the elevation of H_2O_2 level, thereby activating the antioxidant system to eliminate excess ROS accumulation and relieve membrane lipid peroxidative damage and growth inhibition under saline-alkali stress (Yang J. et al., 2022). These reports suggest that ROS are primarily used for stress-sensing and signaling (Mittler et al., 2022).

Both salt stress-induced stomatal closure and accumulation of high levels of Na^+ in the cytoplasm impair the photosynthetic machinery. As a result, the absorbed light exceeds the demand for photosynthesis, leading to the formation of ROS in chloroplasts, including $O_2^{\cdot-}$, $^1O_2$, and H_2O_2. $O_2^{\cdot-}$ is generated by the Mehler reaction in the photosystem I (PSI), $^1O_2$ is produced by photosystem II (PSII) in the thylakoid membrane because of limitation of the electron transport between photosystems, and H_2O_2 is produced at the electron-donor side of PSII via the incomplete oxidation of water (Zhao et al., 2020). In tomato, salt stress induced the increased ROS levels and the decreased PSII activity by reducing the oxygen-evolving complex (OEC) activity on the donor side of PSII, damaging the donor and acceptor sides of the photosystem, and blocking the electron transfer on receptor side of PSII. Melatonin (MT) reduces the production of ROS by balancing the distribution of photosynthetic electron flux and enhances the scavenging ability of ROS by promoting the activities of enzymes involved in the ascorbate glutathione (AsA-GSH) cycle, increasing salt tolerance in tomato (Yin et al., 2019).

Another pathway of ROS production is mitochondrial respiration. Electrons leak from complexes I and III of the mitochondrial electron transport chain to molecular oxygen, resulting in $O_2^{\cdot-}$ generation and then be rapidly catalyzed into H_2O_2 (Liu et al., 2020). Peroxisomes are one of the major sites where plants produce intracellular H_2O_2 (Liu et al., 2021). SA induces mitochondrial ROS production by reducing mitochondrial hexokinase (mtHXK) activity in tomato leaves (Poór et al., 2019). Salt induces the increase of mitochondrial H_2O_2 in the cultivated tomato roots, attributing to the non-enzymatic reduction of superoxide by AsA and GSH, while the decreased H_2O_2 of wild salt-tolerant related species is due to the higher rate of H_2O_2 detoxification. The decreased H_2O_2 in peroxisomes is in part the result of the activities of ascorbate peroxidase (APX) and catalase (CAT) over that of superoxide dismutase (SOD) (Mittova et al., 2004). The gene encoding peroxisome-localized PAO4 is regulated by salt and oxidative stress, suggesting that tomato PAOs may also be involved in ROS metabolism in peroxisomes under salt conditions (Hao et al., 2018).

Enzymatic scavenging system

Salt-induced overaccumulation of ROS imposes oxidative stress on plants, causing ionic imbalance, DNA mutation, peroxidation of lipids and carbohydrates, protein denaturation, pigment breakdown and impaired enzymatic activity (Liu et al., 2020). Tomato plants have formed the antioxidant defense system to mitigate ROS stress caused by salt (**Figure 2**). The antioxidant defense system consists of enzymatic and non-enzymatic antioxidants (Hao et al., 2021). Enzymatic antioxidants include RBOHs, SOD, APX, CAT, glutathione reductase (GR), glutathione S-transferase (GST), glutathione peroxidase (GSH-Px), monodehydroascorbate reductase (MDHAR), dehydroascorbate reductase (DHAR), and guaiacol peroxidase (GPOX). Non-enzymatic antioxidants include AsA, GSH, Pro, carotenoids, flavonoids, and tocopherol (Yang and Guo, 2018b; Liu et al., 2022).

Superoxide dismutase is the most effective ROS scavenger and converts $O_2^{\cdot-}$ to H_2O_2, which is further detoxified to H_2O by APX, CAT, and GSH-Px (Yang and Guo, 2018a). Based on the difference of metal cofactors and subcellular distribution, SODs are mainly categorized as copper/zinc SODs (Cu/Zn-SODs), iron SODs (Fe-SODs), and manganese SOD (Mn-SODs). Fe-SODs are mainly distributed in the chloroplast and cytoplasm, Mn-SODs in mitochondria, and Cu/Zn-SODs in chloroplasts, cytosol and peroxisomes (Czarnocka and Karpiński, 2018). There are at least nine *SOD* genes in tomato, including four *Cu/Zn-SODs*, three *Fe-SODs* and one *Mn-SOD*, and most of them are regulated by salt stress (Feng et al., 2016). CAT rapidly catalyzes H_2O_2, producing H_2O and O_2. The expression of tomato *CAT* gene is fine-tuned under salt stress (Hernández-Hernández et al., 2018). Recently tomato microRNA398b (miR398b) is found to regulate antioxidant system under salt conditions. The inhibition of *Cu/Zn-SOD 1* (*CSD1*) expression and SOD activity caused by miR398b promotes the accumulation of $O_2^{\cdot-}$. Meanwhile, miR398b also decreases the activity of APX and CAT, and the contents of GSH as well, leading to H_2O_2 accumulation (He et al., 2021).

The AsA-GSH recycling pathway, also known as Asada-Halliwell pathway comprises of AsA, GSH, and four enzymes (including APX, MDHAR, DHAR, and GR) (**Figure 2**). AsA-GSH pathway is the heart of antioxidant defense, which mainly detoxify the H_2O_2 (Hasanuzzaman et al., 2019). The first step of this pathway is catalyzed by APX, which converts H_2O_2 to water and monodehydroascorbate radical (MDHA) using AsA as the electron donor. The combination of salinity (100 mM NaCl) and

heat (42°C; 4 h/day) stress greatly enhanced the activity of APX to detoxify H_2O_2 and prevent oxidative damage in tomato plants (Sousa et al., 2022). MDHAR catalyzes the reduction of primary oxidation MDHA to AsA, thus maintaining the AsA pool. Overexpression of tomato chloroplast *MDHAR* elevates the AsA levels, sustains APX activity and accelerates the reductive detoxification of H_2O_2, therefore enhancing the tolerance to osmotic stress induced by salt and polyethylene glycol (PEG) (Li et al., 2012). The PA mediator transglutaminase (TGase) increases the PAs accumulation, that further promotes the activity of antioxidant enzymes (SOD, APX, MDHAR, and CAT), which reduces salt-induced oxidative damage in tomato (Zhong et al., 2020). The powerful antioxidant system of wild tomato mitigates salt-induced oxidative damage by the high expression of defense genes with the enhanced activities of antioxidant enzymes (Kashyap et al., 2020a). Through DHAR, GSH converts the oxidized form dehydroascorbate (DHA) to the reduced form AsA, yielding oxidized glutathione (GSSG). Finally, GSSG is reduced to GSH by GR using NADPH as the electron donor (Hao et al., 2021). Both GSH-Px and GST use GSH pool to detoxify H_2O_2 by catalyzing its conjugation with GSH. In tomato chloroplasts, exogenous GSH alleviates salt stress by improving the content of endogenous GSH, GSH/GSSH ratio and activities of H_2O_2-scavenging enzymes, but the detailed mechanism of GSH-induced salt stress amelioration and detoxification awaits further study (Zhou et al., 2018).

Non-enzymatic scavenging system

The already mentioned AsA and GSH, as well as Pro, carotenoids, flavonoids, and tocopherol, are non-enzymatic antioxidants that play a role in ROS detoxification and retrograde signaling (Czarnocka and Karpiński, 2018). AsA provides electrons for various antioxidant defense reactions, and participates in redox signal transduction and enzymatic activity regulation. The AsA accumulation enhances oxidative stress tolerance in tomato (Li et al., 2019c), and the inhibition of AsA oxidase increases AsA content and salt tolerance in cherry tomato (Abdelgawad et al., 2019). Seed priming with AsA enhances salt tolerance by modulation of antioxidant mechanisms (Alves et al., 2021). GSH plays an important antioxidant role as the reductant of ROS and the substrate for some peroxidase. Exogenous GSH increases tomato resistance to salt-induced oxidative stress by maintaining the homeostasis of cellular redox, cellular ion, and PAs (Zhou et al., 2017, 2019). Tocopherol can effectively scavenge ROS and lipid free radicals, and is a protector of biological membranes. Tocopherol in chloroplasts of tomato functions as an antioxidant under the moderate stress (50 mM NaCl) similarly as in the early phase of severe stress (150 mM NaCl for 2 days). While in the late phase of severe stress (150 mM NaCl for 5 days), it may be involved in senescence signaling pathway (Skłodowska et al., 2009). Carotenoids are essential components of the photosynthetic antenna and reaction center complex, and exhibit antioxidant activity by protecting the photosynthetic machinery. The key carotenoid-related genes and carotenoid biosynthesis in mature-green fruits of tomato are enhanced by salinity (Leiva-Ampuero et al., 2020). Flavonoids are thought to be antioxidants in photoprotection. Chloroplast-located flavonoids scavenge $^1O_2$ under stress and inhibit cellular lipid peroxidation (Czarnocka and Karpiński, 2018). The total flavonoid content is positively correlated with the salt tolerance of tomato, denoting the underlying role of flavonoids for enhancing salt tolerance (Alam et al., 2021). The osmotic regulator Pro is also an antioxidant with the ability of scavenging free radicals and inhibiting lipid peroxidation. The foliar spray of low concentration of Pro significantly increases Pro and total soluble protein contents and the glutamine synthetase activity, and enhances the salinity tolerance of tomato under field conditions (Kahlaoui et al., 2018). The Pro and AsA pathways synergistically maintain cellular redox homeostasis in tomato plants under the combination of salinity and heat (Lopez-Delacalle et al., 2021).

Phytohormones play important roles in salt stress-induced ROS signaling and scavenging pathways. Exogenous ABA promotes the accumulation of Pro and soluble sugar, reduces the content of ROS, and improves the ability of the antioxidant enzyme system in tomato plants under saline-alkaline stress (Xu et al., 2022). SA decreases the tomato mitochondrial hexokinases (*HXKs*) transcription and activity, which contributes to mitochondrial ROS production (Poór et al., 2019). The ROS accumulation is directly controlled by ET signaling triggered by salt stress. However, ET cannot influence the ROS generated by SA in tomato cell suspension (Poór et al., 2013). Brassinolide (BR)-induced H_2O_2 generation can stimulate ET biosynthesis, and ET can also promote H_2O_2 generation. While ET signaling pathway participates in BR-induced salt tolerance in tomato by reducing oxidative damage and enhancing antioxidant enzyme capacity (Zhu et al., 2016). Defective jasmonic acid (JA) synthesis in tomato plants under salt stress is associated with the reduced activity of enzymatic and non-enzymatic antioxidants (Abouelsaad and Renault, 2018). The roles of cross-talk among phytohormones in salt stress-induced ROS signaling and scavenging pathways in tomato need to be further investigated.

Gamma-aminobutyric acid metabolic pathway, also known as GABA shunt, is probably involved in salt tolerance of tomato by modulating amino acid synthesis and ROS metabolism. Exogenous GABA has positive effects on alleviating salt stress, which is mainly due to induced osmotic regulation and antioxidant metabolism by the salt- and exogenous GABA-induced endogenous GABA (Wu et al., 2020; **Figure 2**). In GABA shunt, glutamate decarboxylase (GAD) catalyzes the decarboxylation of glutamate to GABA, GABA transaminase (GABA-T) converts GABA to succinic semialdehyde (SSA), and SSA dehydrogenase (SSADH) catalyzes the oxidation of SSA to succinate. The enhanced ROS accumulation and increased salt

sensitivity in *GADs*- and *GABA-Ts*-silenced tomato plants are possibly attributed to the impaired function of mitochondrial electron transport chain caused by the decreased succinate. However, *SSADH*-silenced plants exhibited less sensitiveness to salt stress, that may possibly due to the similar levels of ROS between silenced and control plants under salt stress (Bao et al., 2015).

Epigenetic regulation

Epigenetic modifications, also known as chromatin modifications, contain DNA methylation, RNA-directed DNA methylation (RdDM), and histone modifications (Chinnusamy and Zhu, 2009; Deinlein et al., 2014). Epigenetic modifications regulate stress-responsive gene expression and plant development, conferring stress adaptation (Chinnusamy and Zhu, 2009; **Figure 2**).

DNA methylation is primarily catalyzed by the DNA methyltransferases (MTases) family. A total of 9 tomato MTases genes are identified, including 1 methyltransferase (MET) member (*MET1*), 3 chromomethylase (CMT) members (*CMT2*, *CMT3*, and *CMT4*), 4 domains rearranged methyltransferase (DRM) members (*DRM5*, *DRM6*, *DRM7*, and *DRM8*), and 1 DNA methyltransferase homolog 2 (DNMT2) member (*METL*). Except for *MET1* and *DRM8*, all other MTase genes are significantly regulated by salt stress, suggesting that tomato MTase genes may be involved in salt stress response (Guo et al., 2020). *PKE1* is a Pro-, lysine-, and glutamic-rich protein gene, and the lower expression level in tomato leaves is consistent with the hypermethylation of its coding sequence. Tomato PKE1 confers the salt tolerance involved in post-transcriptional regulation through binding to F-box proteins (Li et al., 2019a). The functions of heavy methylation in the promoter of *PKE1* in tomato fruit and leaf salt responses remain unclear (Li et al., 2019a; Liu and He, 2020).

Small RNAs play the pivotal role in environmental stress responses of crop plants by regulating gene expression, and their generation mainly depends on proteins encoded by respective Dicer-like (DCL), Argonaute (AGO), and RNA-dependent RNA polymerases (RDR) gene families (Huang et al., 2016). *Arabidopsis* AtAGO4 is required for RdDM of the *SUPERMAN* (*SUP*) locus (Zilberman et al., 2003). In tomato, a total of 15 AGO proteins are identified, and 4 members are orthologs of AtAGO4, namely AGO4A-AGO4D (Xian et al., 2013). Tomato *AGO4A* is significantly induced by salt and drought stress (Bai et al., 2012). Down-regulation of *AGO4A* conferred enhanced salt and drought tolerance in transgenic tomato by reducing the transcript levels of DNA MTase genes (*DRMs*) and RNA silencing pathway genes, suggesting that tomato *AGO4A* as a core factor of RdDM pathway plays a negative role under salt and drought stress probably through regulating methylation process-associated genes (Huang et al., 2016).

In general, histone modifications are associated with changes in stress-induced gene regulation (Chinnusamy and Zhu, 2009). Histone post-translational modifications (HPTMs) include acetylation and methylation, acetylation is dynamically regulated by histone acetylases (HATs) and histone deacetylases (HDACs), and methylation is balanced by the activities of histone methylases (HMTs) and histone demethylases (HDMs). Plant HDACs are divided into three subfamilies: RDP3/HDA1 (Reduced Potassium Dependence 3/Histone Deacetylase 1, hereinafter named HDAs), plant-specific HD2s (Histone Deacetylase 2), and SIR2 (Silent Information Regulator 2) (Guo et al., 2017), and the members of HDA subfamily share sequence homology in the HDAC domain and require the Zn^{2+} cofactor for deacetylase activity (Yang and Seto, 2007; Zhao et al., 2015). There are 124 histone modifiers (HMs) in tomato, including 32 HATs, 14 HDACs (9 HDAs, 3 HD2s, and 2 SIR2s), 52 HMTs, and 26 HDMs (Aiese Cigliano et al., 2013). Among nine tomato *HDA* genes (named as *HDA1-HDA9*), the expression levels of *HDA1*, *HDA4*, and *HDA9* in root and that of *HDA3* in leaf were significantly stimulated by slat treatment, and the levels of *HDA2*, *HDA5*, and *HDA6* were induced both in roots and leaves (Guo et al., 2017). The *HDA5*-silenced tomato plants exhibited reduced tolerance to salt stress (Yu et al., 2018), while the stress-related genes modified by HDA5 through histone deacetylation under salt conditions remains to be identified.

Not only HDACs but also HATs are implicated in regulation of salt tolerance. In *Arabidopsis*, HAT general control non-repressed protein 5 (GCN5)-mediated acetylation of lysine 9 (H3K9) and lysine 14 of histone H3 (H3K14) is associated with activation of cellulose synthesis genes *CTL1* (chitinase-like gene), *PGX3* (*polygalacturonase involved in expansion-3*) and *MYB54* (*MYB domain protein-54*) under salinity. The severe growth inhibition and defects in cell wall integrity phenotypes of *Arabidopsis gcn5* mutant under salt stress can be partially rescued by overexpression of chitinase-like protein *CTL1* and can be almost fully recaptured by constitutive wheat *TaGCN5* expression. GCN5 enhances salt tolerance through activating cellulose synthesis genes and GCN5-mediated salt tolerance may be conserved between monocot and dicot plants (Zheng et al., 2019). Tomato GCN5 can catalyze acetylation on histone H3 at H3K9 and H3K14 residues and constitutive *GCN5* expression almost fully rescues growth defect phenotype of *Arabidopsis* null-mutant *gcn5-7*, indicating that tomato GCN5 functions similarly as AtGCN5 in developmental processes (Hawar et al., 2022). Nonetheless, the function of *GCN5* in tomato salt tolerance requires further elucidation.

Gene expression changes

Plants generate salt tolerance mechanisms to minimize the adverse effects of salt stress by regulating the expression of salt response genes. Comprehensive analysis of gene expression

profiles under salt stress by transcriptome technology can provide key clues for elucidating the molecular mechanism of salt stress in tomato. However, genes involved in salt tolerance may occur in wild tomato species but not in cultivated species (Foolad, 2007).

The wild tomato genotype *S. pimpinellifolium* 'PI365967' is more salt tolerant than the cultivar *S. lycopersicum* 'Moneymaker' (Sun et al., 2010). After treatment with 200 mM NaCl for 5 h, the number of differentially expressed genes (DEGs) in Moneymaker (1386) was higher than that in PI365967 (948). Eighty-six genes were specifically up-regulated in PI365966, including the genes encoding salicylic acid-binding protein 2 (SABP2), CIPKs, plasma membrane ATPase 1, peroxidase, lactoylglutathione lyase/glyoxalase I, and TINY-like protein and AP2/ERF domain protein (both belonging to DREB TF superfamily). Additionally, several genes encoding glutathione S-transferase showed significantly higher basal expression in PI365967 than in Moneymaker. This suggests that multiple strategies, such as SA signaling, SOS pathway, transcriptional regulation, ROS scavenging and detoxification synergistically confer salt tolerance in wild tomato. Among the 82 genes specifically down-regulated in PI365967, the gene encoding putative high-affinity nitrate transporter (a repressor of lateral root initiation) was most down-regulated (8-fold), which may promote root growth in PI365967 under salt stress conditions (Sun et al., 2010).

Similarly, another report using transcriptome analysis to reveal salt tolerance mechanisms found that most of the upregulated DEGs were involved in catalysis, transcriptional regulation and molecular transduction in wild tomato *S. chilense* under 500 mM NaCl conditions. However, the down-regulated DEGs were mainly involved in binding, molecular function regulator and catalysis (Kashyap et al., 2020b). Specifically, genes actively involved in Pro and arginine metabolism, oxidoreductase activity, hormone metabolism, ROS scavenging systems, signaling regulation, transporters, osmotic regulation, defense and stress responses, homeostasis and TFs are significantly up-regulated, and play an important role in salt tolerance of *S. chilense*. Genes encoding pentatricopeptide repeat-containing protein in *S. chilense* are significantly down-regulated, possibly defending against salt stress. Interestingly, although the existence of *Wnt* signaling (Wingless-related integration site) in plant systems is unknown, it plays a crucial role in conferring salt tolerance in *S. chilense* (Kashyap et al., 2020b). Transcriptome analysis of *S. lycopersicum* cv. MicroTom under salt (150 mM NaCl for 6 h) and oxidative stress (20 mM H_2O_2 for 6 h) revealed 6,643 significantly DEGs, including 3,950 DEGs identified under oxidative stress and 4,617 DEGs found under salt stress (Keshishian et al., 2018). Whereas up to 67.6% (2557) of induced and 75.6% (2162) of repressed DEGs show unique stress (salt or oxidative stress) regulation. Of the 33 cytokinin-related DEGs that were significantly regulated by stress, only 10 were regulated by both oxidative and salt stress, suggesting that although there is crosstalk between salt and oxidative stress, the transcriptional patterns of their gene regulation are not identical (Keshishian et al., 2018). Overall, the comparative transcriptomic analysis of tomato cultivars with different salt tolerance can help to improve our understanding on possible molecular mechanisms underlying salt tolerance in tomato.

Approaches for improving salt tolerance of tomato

Genetic engineering

Salt-tolerant transgenic lines have been developed for different metabolic properties, such as ion transport, osmoregulation, antioxidants, stress proteins, and universal stress proteins (TFs and signal transduction) (Ashraf and Munns, 2022). A series of tomato TFs are used to regulate salt tolerance via genetic engineering (**Table 1**). Overexpression of C2H2 zinc-finger protein *ZFs* improves salt tolerance by maintaining photosynthesis, increasing PA biosynthesis, and improving the ability of antioxidant AsA-mediated removal of ROS (Hichri et al., 2014; Li Y. et al., 2018). *bZIP1*, a member of the basic region/leucine zipper (bZIP) family, positively regulates salt tolerance by modulating ABA-mediated signaling pathways (Zhu et al., 2018). Overexpression of basic helix-loop-helix (bHLH) transcription factor *bHLH22* enhances the resistance to salinity and drought by increasing osmotic potential, augmenting the accumulation of flavonoids and ABA, and improving the active oxygen scavenging system (Waseem et al., 2019). Tomato plants overexpressing *WRKY8* improves salinity tolerance through enhancing the transcriptional levels of stress-responsive genes, Pro accumulating and activities of ROS-scavenging enzymes (Gao et al., 2020). Overexpressing *MYB102* confers salt tolerance by regulating Na^+/K^+ homeostasis, ROS scavenging ability, and expression of salt stress-related genes (Zhang et al., 2020b). NAC transcription factor *TAF1* increases the accumulation of Pro and Na^+ ions in shoots, upregulates salt stress-responsive and ABA biosynthesis genes, and reduces stomatal conductance and stomatal pore area, thereby conferring salt tolerance (Devkar et al., 2020).

By genetic transformation, other genes involved in tomato oxidative stress and ion homeostasis have been shown to improve salt tolerance. RING finger E3 ligase *Ring* functions as a positive regulator of salt stress signaling through regulating the ion homeostasis of Na^+ and K^+, levels of H_2O_2 and lipid peroxidation, and expression of stress-related genes (Qi et al., 2016). Overexpression of the melatonin synthesis-related gene *Caffeic Acid O-Methyltransferase 1* (*COMT1*) increases salt tolerance via maintaining the balance of Na^+/K^+, decreasing ion damage by activating SOS pathway, enhancing the antioxidant capability, and upregulating stress-related genes

TABLE 1 Summary of genes involved in salt stress in tomato.

Gene name	Description	Function	References
Salt Overly Sensitive 1 (SOS1)	PM Na^+/H^+ antiporter	Maintained ion homeostasis, prevented Na^+ from reaching photosynthetic tissues; natural variations in cultivated tomato increased salt sensitivity	Olías et al., 2009a; Wang Z. et al., 2021
Salt Overly Sensitive 2 (SOS2)	Calcineurin-interacting protein kinase	Increased salinity tolerance via regulating Na^+/H^+ and (Na^+, K^+)/H^+ transporters responsible for cell ion homeostasis	Huertas et al., 2012
Na^+/H^+ antiporter 2 (NHX2)	K^+/H^+ antiporter	Conferred salt tolerance by improving K^+ homeostasis and compartmentalization, and through joint overexpressing with *SOS2*	Rodríguez-Rosales et al., 2008; Huertas et al., 2013; Baghour et al., 2019
DNA-binding with one finger 22 (Dof22)	TF with C2-C2 zinc finger	Suppressing *Dof22* increased the levels of AsA to 1.33- and 1.64-fold in leaves and ripe fruits, respectively; decreased chlorophyll content by 77∼80% under salt stress; significantly reduced the fresh weight after salt treatment; slightly induced the expression levels of antioxidant related genes (from 1.5- to 2-fold); significantly down-regulated *SOS1*, obviously induced *NHX1* and *NHX2*; Dof22 could bind to the promoter of *SOS1* in yeast	Cai et al., 2016
Basic region/leucine zipper 1 (bZIP1)	TF with basic leucine zipper	*bZIP1*-RNAi transgenic plants exhibited reduced salt tolerance, decreased ABA and chlorophyll content and CAT activity, increased MDA content, and downregulated transcription levels of multiple genes encoding defense proteins related to abiotic stress and biotic stress	Zhu et al., 2018
Basic region/leucine zipper 38 (bZIP38)	Basic leucine zipper TF	Overexpression of *bZIP38* significantly decreased salt tolerance in tomato, reduced the chlorophyll by 50% and free Pro content by 25% in leaves, but increased the MDA content (from 1.5- to 2-fold); bZIP38 is a negative regulator of salt resistance that acts by modulating ABA signaling	Pan et al., 2017
S-adenosylmethionine synthetase 1 (SAMS1)	S-adenosylmethionine synthetase	Overexpression of *SAMS1* improved salt tolerance, significantly enhanced water-retention capacity and photosynthetic capacity, reduced the accumulation of superoxide, H_2O_2 and MDA, and enhanced ABA content and ROS scavenging enzymes activities; modulated the generation of PAs and H_2O_2 to maintain a better water homeostasis; reduced water loss under ABA treatment	Zhang et al., 2020a
microRNA398b (miR398b)	Conserved miRNA regulated CSD transcription	Overexpression of *miR398b* increased the sensitivity to salinity, enhanced the oxidative stress via the accumulation of $O_2^{\cdot -}$, induced photoinhibition and inhibited the photosynthesis under salinity; miR398b regulated the expressions of antioxidant genes, activity of antioxidant enzymes and contents of antioxidants	He et al., 2021
High-affinity K^+ 20 (HAK20)	Na^+/K^+ transporter	HAK20 transported Na^+ and K^+ and regulated Na^+ and K^+ homeostasis under salt conditions; a variation in the coding sequence of *HAK20* was associated with Na^+/K^+ ratio and conferred salt tolerance in tomato; knockout mutations in *HAK20* resulted in hypersensitivity to salt stress	Wang et al., 2020
Basic helix-loop-helix 22 (bHLH22)	TF with a basic helix-loop-helix domain	Plants overexpressing *bHLH22* showed short height with small leaves and enhanced flavonoid accumulation; overexpressing *bHLH22* displayed an enhanced tolerant to salinity, significantly peaked the activities of CAT, SOD, and POD to minimize the impacts of ROS such as H_2O_2	Waseem et al., 2019
SALT TOLERANCE ENHANCER1 (STE1)	Protein without any known conserved domains	Overexpression of *STE1* enhanced the tolerance to multiple chloride salts and oxidative stress, along with elevated antioxidant enzyme activities, increased ABA and chlorophyll contents, reduced MDA and ROS accumulations, decreased K^+ efflux and increased H^+ efflux; *STE1*-RNAi plants displayed the decreased salt tolerance; *STE1*-overexpression plants showed the increased sensitivity to ABA; STE1 promoted ABA-dependent salt stress-responsive pathways by interacting with PYLs and SnRK2s	Meng et al., 2020
WRKY 3 (WRKY3)	TF with conserved WRKYGQK domain	Overexpression of *WRKY3* reduced oxidative stress and Pro content under salt conditions, decreased Na^+ content in leaves, induced accumulation of K^+ and Ca^{2+}, and up-regulated genes coding for antioxidant enzymes, ion and water transporters, or plant defense proteins	Hichri et al., 2017

(Continued)

TABLE 1 (Continued)

Gene name	Description	Function	References
WRKY 8 (WRKY8)	TF with conserved WRKYGQK domain	Overexpression of *WRKY8* in tomato displayed the alleviated wilting or chlorosis phenotype under salt stresses, with higher levels of stress-induced osmotic substances like Pro and higher transcript levels of the stress-responsive genes *AREB*, *DREB2A* and *RD29*	Gao et al., 2020
WRKY 39 (WRKY39)	TF with conserved WRKYGQK domain	Enhanced salt tolerance in tomato via accumulating Pro, reducing MDA, and up-regulating the expression of *RD22* and *DREB2A*	Sun et al., 2015
HD-Zip homeobox 2 (HB2)	TF with conserved HD and leucine zipper domains	*HB2*-RNAi transgenic plants increased the levels of chlorophyll and water content, reduced water loss rate and MDA content in the leaves, enhanced tolerance to salt stress; HB2 acted as a negative regulator in the high-salinity stress signaling pathways	Hu et al., 2017
Caffeic Acid O-Methyltransferase 1 (COMT1)	Critical enzyme for melatonin synthesis	Increased melatonin level and salt tolerance, maintained balance of Na^+/K^+, decreased ion damage, enhanced antioxidant capability, and up-regulated stress-related genes	Liu et al., 2019; Sun et al., 2020
DEFENSELESS1 (DEF1)	Protein involved in JA synthesis	Mutation of *DEF1* decreased nitrogen content in both leaves and roots, repressed the activity of both enzymatic antioxidants and non-enzymatic antioxidants; *def-1* plants exhibited oxidative stress symptoms and ionic imbalance	Abouelsaad and Renault, 2018
Glyoxalase I (GlyI) and Glyoxalase II (GlyII)	Two enzymes catalyzed conversion of methylglyoxal to D-lactic acid	The transgenic lines overexpressing *GlyI* and *GlyII* under a high NaCl concentration (800 mM) showed reduced lipid peroxidation and the production of H_2O_2 in leaves, and a lower decrease in the content of chlorophyll a + b	Viveros et al., 2013
MADS-box protein 8 (MBP8)	TF with typical MADS domain region in N-terminus	The *MBP8*-RNAi transgenic plants were less inhibited by salt at post-germination stage, improved tolerance to stress, displayed the higher levels of chlorophyll and water content, lower water loss rate and MDA content, and significantly up-regulated the expression of multiple stresses related genes; MBP8 functioned as a negative stress-responsive TF in the high salinity stress signaling pathways	Yin et al., 2017
MADS-box protein 11 (MBP11)	TF with typical MADS domain region in N-terminus	*MBP11*-RNAi plants were less tolerance to salt stress, decreased relative water and chlorophyll content, and increased relative electrolyte leakage and MDA content; overexpression of *MBP11* enhanced salt tolerance; MBP11 acted as a stress-responsive TF in the positive modulation of salt tolerance	Guo et al., 2016
Argonaute 4A (AGO4A)	Core factor of RdDM pathway	*AGO4A*-down-regulating transgenic plants showed enhanced tolerance to salt and drought stress; the expression levels of some DNA methyltransferase genes and RNAi pathway genes were significantly lower in *AGO4A*-down-regulating plants than in WT plants; *AGO4A* plays a negative role under salt stress probably through the modulation of DNA methylation as well as the classical RNAi pathway	Huang et al., 2016
Transcription Activation Factor 1 (TAF1)	TF with highly conserved NAM domain	Overexpression of *TAF1* improved salinity tolerance, lowering *TAF1* expression caused stronger salinity-induced damage; shoots of *TAF1* knockdown plants accumulated more toxic Na^+ ions; in *TAF1* knockdown plants during salinity stress, stomatal conductance and pore area were increased, salinity-induced changes in tricarboxylic acid cycle intermediates and amino acids are more pronounced, and Pro accumulation was decreased; TAF1 controls the tomato's response to salinity stress by combating both osmotic stress and ion toxicity	Devkar et al., 2020
Zinc Finger 2 (ZF2)	C2H2 zinc finger TF with ERF-associated amphiphilic repression domain	Tomato ZF2 enhanced salt sensitivity in *Arabidopsis*, whereas delayed senescence and improved salt tolerance in tomato, particularly by maintaining photosynthesis and increasing PA biosynthesis; *ZF2* is rapidly induced by ABA treatment, and tomato overexpressing *ZF2* accumulated more ABA than WT plants	Hichri et al., 2014
Zinc-finger protein 3 (ZF3)	TF with EAR motif	Overexpression of *ZF3* significantly increased the levels of AsA in tomato and *Arabidopsis* and the AsA-mediated ROS-scavenging capacity, enhanced the salt tolerance; ZF3 directly bound CSN5B and this interaction inhibited the binding of CSN5B to VTC1, a GDP-mannose pyrophosphorylase; the EAR domain promoted the stability of ZF3; ZF3 simultaneously promoted the accumulation of AsA and enhanced salt tolerance	Li Y. et al., 2018

(Continued)

TABLE 1 (Continued)

Gene name	Description	Function	References
RING (Ring)	E3 ubiquitin ligase with RING finger conserved region	Ring localized at the endoplasmic reticulum; Silencing of *Ring* increased the sensitivity to salt stress in wild tomato; Overexpression of *Ring* in *Arabidopsis* resulted in enhanced salt tolerance during seed germination and early seedling development; Ring functioned as a positive regulator of salt tolerance	Qi et al., 2016
NAM, ATAF and CUC transcription factor 35 (NAC35)	TF with conserved NAC domain and diversified C-terminal region	Overexpression of *NAC35* promoted root growth and development under salt stress, induced higher expressions of *ARF1*, *ARF2*, and *ARF8* in transgenic lines	Wang et al., 2016
Hybrid proline-rich protein 1 (HyPRP1)	Putative plant cell wall glycoprotein with repetitive Pro-rich N-terminal domain and conserved eight-cysteine motif C-terminal domain	*HyPRP1*-RNAi transgenic plants enhanced tolerance to various abiotic stresses (oxidative stress, dehydration, and salinity); SO_2 detoxification-related enzymes, including sulfite oxidase, Fds, and Msr A, interacted with HyPRP1; more sulfates and transcripts of *Msr A* and *Fds* were accumulated in *HyPRP1* knockdown lines exposed to SO_2 gas; HyPRP1 was a negative regulator of salt and oxidative stresses and was probably involved in sulfite metabolism	Li et al., 2016
Altered response to salt stress 1 (ARS1)	R1-type MYB TF with conserved MYB-like and adjacent P-rich domains	The *ars1* mutant reduced fruit yield under salt acclimation; the stomatal behavior of *ars1* mutant leaves induced higher Na^+ accumulation via the transpiration stream; the mutation affected stomatal closure in a response mediated by ABA; *ARS1* contributed to reduce transpirational water loss under salt stress	Campos et al., 2016
v-myb avian myeloblastosis viral oncogene homolog 49 (MYB49)	TF with two highly conserved HTH DNA-binding domains	Overexpression of *MYB49* decreased the accumulation of ROS, MDA content, and relative electrolyte leakage, and increased POD activity, SOD activity, chlorophyll content, and photosynthetic rate under salt stress, improving salt tolerance	Cui et al., 2018
v-myb avian myeloblastosis viral oncogene homolog 102 (MYB102)	TF with two highly conserved HTH DNA-binding domains	Overexpression of *MYB102* maintained a better K^+/Na^+ ratio, lower ROS and lower electrolytic leakage rates, increased accumulation of antioxidants and Pro, and upregulated transcripts of salt stress-related genes	Zhang et al., 2020b
BRASSINAZOLE RESISTANT 1 (BZR1)	TF with nuclear localization sequence, PEST domain, and BIN2 phosphorylation domain	Overexpression of *BZR1D* enhanced the BR response and improved salt tolerance in *Arabidopsis*; *BZR1D*-overexpressing tomato lines showed a short plant height, smaller and curly leaves, and delayed flowering; BZR1D positively regulated salt tolerance in tomato and upregulated the expression of multiple stress-related genes	Jia et al., 2021
Histone deacetylase A5 (HDA5)	Histone deacetylase protein with deacetylase catalytic domain	Seedlings growth of *HDA5*-RNAi plants were more inhibited on the medium containing salt compared with WT; under salt stress, chlorophyll in mature leaves degraded earlier in transgenic leaves, and transgenic plants displayed wilting earlier and more severe than WT; silencing of *HDA5* resulted in decreasing tolerance to salt	Yu et al., 2018
Heat stress transcription factor 3 (HsfA3)	TF with highly conserved DBD, OD, and putative NLS	HsfA3 played a negative role in controlling seed germination under salt stress; in the presence of 120 mM NaCl, half of the WT seeds were successfully germinated on the second day after stratification, whereas the germination percentages of *HsfA3*-overexpressing seeds were less than 10%	Li Z. et al., 2013
CALCINEURIN B-LIKE PROTEIN 10 (CBL10)	EF (helix-loop-helix structural motif)-hand Ca^{2+} protein sensor	Lack function of CBL10 leaded to the severe damage in the shoot apex and reproductive organs under salinity conditions; CBL10 mediated salt tolerance by regulating Na^+ and Ca^{2+} fluxes in the vacuole, cooperating with the vacuolar cation channel TPC1 and the two vacuolar H^+-pumps, AVP1 and VHA-A1, which in turn were potential targets of CBL10	Egea et al., 2018
Tomato 14-3-3 Protein 7 (TFT7)	Phosphoserine-binding protein with conserved target binding domain	Transgenic plants overexpressing *TFT7* improved germination rate, dry mass, total chlorophyll concentration and root length under salt stress; the degree of H_2O_2 and MDA accumulation were inhibited in transgenic plants; TFT7 upregulated the activity of APX that played the indispensable role in salt-induced oxidative stress	Xu and Shi, 2007

ABA, abscisic acid; APX, ascorbate peroxidase; AsA, ascorbic acid; BR, brassinolide; CAT, catalase; Fds, ferredoxins; MDA, malondialdehyde; Msr A, methionine sulfoxide reductase A; PAs, polyamines; PM, plasma membrane; POD, peroxidase; Pro, proline; RNAi, RNA interference; ROS, reactive oxygen species; SnRK2s, sucrose non-fermenting-1-related protein kinase 2s; SOD, superoxide dismutase; TF, transcription factor; TPC1, TWO-PORE CHANNEL 1; WT, wild type.

(Liu et al., 2019; Sun et al., 2020). Small SALT TOLERANCE ENHANCER1 (STE1) protein promotes ABA-dependent salt stress-responsive pathways by interacting with the ABA receptor PYLs and the positive ABA signaling regulator SnRK2s and by improving Na^+ and K^+ homeostasis and ROS scavenging (Meng et al., 2020).

Heterologous overexpression of salt stress-related genes can also improve salt tolerance in tomato. For example, overexpressing yeast *trehalose-6-phosphate synthase* (*TPS1*) in tomato increases salt tolerance, which is partly due to the promotion of trehalose biosynthesis (Cortina and Culiáñez-Macià, 2005), and the enhanced salt tolerance in tomato overexpressing *Arthrobacter globiformis* choline oxidase *codA* is partly attributed to the accumulating GB (Wei et al., 2017).

Although transgenic technology can improve the salt tolerance of plants through a single strategy, the degree of improvement is limited due to the polygenic trait of salt tolerance (Hao et al., 2021). Promising achievements in improving salt tolerance may be achieved by stacking/aggregating multiple genes (Ashraf and Munns, 2022). Precise editing of multi-target genes using clustered regularly interspaced short palindromic repeats (CRISPR)/CRISPR-associated (Cas) technology has emerged as an alternative to traditional plant breeding and transgenic methods (Hanin et al., 2016). As an ideal candidate for CRISPR/Cas9 based gene modulations, tomato has already achieved salt tolerance regulation through genome editing (Chandrasekaran et al., 2021). For instance, both mutant alleles *slsos1-1* and *slsos1-2* generated by the CRISPR/Cas9 system increase the Na^+/K^+ ratio in tomato roots and the sensitivity to salt stress (Wang Z. et al., 2021). As a negative regulator of ABA, *hybrid proline-rich protein 1* (*HyPRP1*) plays a negative role in salt tolerance of tomato (Li et al., 2016). The precise elimination of HyPRP1 negative-response domain(s) by CRISPR/Cas protein-based targeted mutagenesis improves salinity tolerance in both germination and vegetative phases (Tran et al., 2021). The application of CRISPR/Cas in tomato also includes enhancing cultivation, promoting growth, alleviating biotic stress, and improving tolerance to abiotic stresses such as drought and temperature. This technology has a good prospect in the breeding and genetic research of tomato (Chandrasekaran et al., 2021). The in-depth understanding of the molecular mechanism of salt stress and the advancement of efficient and precise CRISPR/Cas technology are expected to accelerate the breeding of salt-tolerant tomato varieties with high yields.

Marker-assisted selection

Since salt tolerance is a polygenic trait, traditional breeding methods to improve salt tolerance of crops are time-consuming and labor-intensive, and may introduce undesirable traits while selecting traits. The combination of QTL analysis and marker-assisted selection (MAS) is predicted to be an effective method for simplifying this process (Hanin et al., 2016). MAS can be used in the selection of lines following a crossing program and without the need to evaluate performance of plants under stress (Munns et al., 2002; Flowers and Flowers, 2005). Through association analysis of molecular markers and salt stress phenotypes can not only assess the molecular basis of tomato salt tolerance, but it also provides guidance for the introgression of salt tolerance traits in the target varieties (Gharsallah et al., 2016a; Ezin et al., 2018).

Many QTLs associated with tomato salt response (including plant height, stem diameter, leaf number, leaf and root fresh and dry mass, ion concentration, antioxidant response, and survival rate) have been identified (Foolad, 2007; Villalta et al., 2008; Frary et al., 2010, 2011; Asins et al., 2013). These QTLs may be useful in breeding of the salt tolerant cultivars. Nevertheless, the accuracy and precision of QTL identification, the complexity of genetic and environmental interactions and the lack of evaluation reports under field conditions greatly limit progress in marker-assisted breeding of salt tolerance (Ashraf and Foolad, 2013). Molecular linkage map and identification of salt tolerance related QTLs are the primary requisite for improving the salt tolerance in tomato through MAS and pyramiding, while the next generation sequencing (NGS) helps to obtain high density genetic maps, which promotes MAS to play a substantial role in the molecular breeding of salt-tolerant tomato varieties (Hanin et al., 2016; Kashyap et al., 2021).

Genome-wide association studies can overcome the limitations of traditional QTL mapping, provide higher mapping resolution, and detect multiple alleles at the same locus (Ashraf and Munns, 2022). GWAS has become a more efficient technique for studying genetics underlying trait variation (Morton et al., 2019). Valid phenotypic data is a prerequisite for gene/QTL discovery, association mapping and GWAS (Qin et al., 2020). A GWAS of the root Na^+/K^+ ratio trait in a tomato population comprising materials from different genetic backgrounds reveals that *HAK20* gene is effectively involved in the transport and maintenance of Na^+ and K^+ homeostasis under salt stress, thereby imparting salt tolerance to tomatoes (Wang et al., 2020). The model of high-throughput phenotype-genotype interaction will greatly facilitate the genetic dissection of salt tolerance-related traits in tomato, paving the way for the development of salt-tolerant lines/genotypes.

Grafting

Grafting is an economically justified and sustainable strategy to overcome saline stress, and offers an alternative to breeding of salt-tolerant tomato (Singh et al., 2020; **Table 2**). The effect of grafting depends on the characteristics of the scion and rootstock, their interaction and stress intensity

(Giordano et al., 2021). Grafting salt-susceptible tomato cultivars onto salt-tolerant rootstock can effectively reduce the adverse effects of salt stress on growth, yield, and fruit quality. The root system of grafted plants is stronger and more efficient in uptake of water and nutrients. In addition, grafted tomato plants improve salt tolerance by reducing ionic stress, increasing the transfer of K^+, Ca^{2+} and Mg^{2+} to shoots and leaves, and reducing ROS-induced oxidative damage (Koleška et al., 2018; Singh et al., 2020). The salt resistant tomato rootstock greatly reduces the yield loss of the sensitive genotypes and increases fruit quality under saline conditions. Salt-tolerant rootstock also controls the stomatal openness and closure of sensitive scions, improves the osmotic adjustment of leaves, and reduces the transport of accumulation of Na^+ ions accumulation to young leaves (Coban et al., 2020).

Intergeneric grafting is a promising approach for enhancing the salinity tolerance of tomato. Grafting on salt tolerant eggplant (*Solanum melongena*) rootstock increases the average fruit yield and improves salt tolerance of tomato scion. Grafted plants maintain higher relative water content and antioxidant enzyme activities, and balance the salt damage through accumulating Pro. Meanwhile, the eggplant rootstock confers Na^+ exclusion and K^+ retention properties to the tomato scion (Sanwal et al., 2022). Grafting tomato on potato (*Solanum tuberosum*) rootstock increases water productivity by 56.8% under saline water-irrigations, significantly alters dry matter allocation, and induces mineral compartmentalization processes (Parthasarathi et al., 2021). Although grafting tomato on halophyte wolfberry (*Lycium chinense*) can enhance salt tolerance, it reduces the growth and fruit yield of the grafted plants due to the limitation of thinner woody stem (Feng et al., 2019). In conclusion, the selection of suitable rootstocks is a prerequisite for getting the maximum benefit from grafting under salt stress.

Pretreatments

Pretreatments increase the ability of tomato plants to adapt to salinity (**Table 2**). Seed priming and drought pretreatment have been reviewed elsewhere and will be not covered in this review (Cuartero et al., 2006).

Heat induces salinity tolerance of tomato through improving Na^+ and K^+ homeostasis, improving water balance, reducing oxidative stress, and increasing efficient photosynthetic performance (Rivero et al., 2014). Heat stress-induced salt tolerance belongs to a phenomenon known as cross-tolerance in plants. Thus, salinity can have a beneficial regulatory role in enhancing tomato tolerance to other stresses, such as protecting it against excessive sulfur toxicity (Jiang et al., 2017), significantly reducing the infection of biotrophic fungus *Oidium neolycopersici* (Achuo et al., 2006), and synergistically increasing the effect of DL-β-aminobutyric acid (BABA) on triggering systemic resistance in tomato plants against *Pseudomonas syringae* pv. *tomato* infection (Baysal et al., 2007). Salinity acclimation reduces the negative effects of salt stress (Kamanga et al., 2020), and moderate salt stress improves tomato fruit quality without decreasing yield (Meza et al., 2020). Elevated CO_2 confers tomato tolerance to progressively higher soil salinity and secondary soil salinization by improving antioxidant capacity, ion homeostasis, and PA metabolism, decreasing ABA and ET levels, and suppressing transpiration (Yi et al., 2015; Brito et al., 2020; Zhang et al., 2020c). Furthermore, low red light (R) to far-red light (FR) ratio (R:FR) enhances salinity tolerance in tomato by regulating photosynthesis and ROS scavenging systems (Wang Y. et al., 2021).

Exogenous vanillic acid and quercetin improve salt tolerance by enhancing the action of glyoxalase system (Parvin et al., 2019a, 2020). Spermidine and 24-epibrassinolide (EBR) enhance tomato tolerance to salinity and alkalinity stress by regulating PA metabolism (Hu et al., 2012; Zheng et al., 2016). Application of exogenous GSH reduces the level of PAs and promotes the transformation of PAs between different morphologies in tomato seedlings under salinity conditions, contributing to the improvement of salt tolerance (Zhou et al., 2019). Application of omeprazole (benzimidazole proton pump inhibitor) increases nutrient uptake and allocation, enhances photosynthesis and plant performance, thus improving resource use efficiency and salinity tolerance in tomato (Rouphael et al., 2018). Vermicompost leachate reduces the impact of salinity on leaf senescence and enhances salinity tolerance, which is related to the decreased ET synthesis, increased anthocyanin contents, and increased Pro and jasmonate accumulation (Benazzouk et al., 2020). The combined microalgae-cyanobacteria extract formulations (MEF) stimulates tomato plant growth and salt tolerance response through the enhanced antioxidant enzyme activities and the improved root growth and nutrient uptake (Mutale-joan et al., 2021).

Pretreatments may be simpler and more economical than other strategies to improve salt tolerance in tomato. The adaptive mechanism of tomato to salt stress can provide a theoretical basis for pretreatments to improve salt tolerance. The integration of metabolomics and other omics approaches will provide comprehensive insight into the response of tomato to salt stress.

Modulation of the rhizosphere

Interaction with beneficial soil microorganisms improves salt tolerance (Hanin et al., 2016). As a product of the co-evolution between plants and microorganisms, plant growth promoting bacteria (PGPB) represent a new biological pathway for sustainable agriculture to alleviate salt stress (Singh et al., 2018). Inoculating tomato seedlings with endophytic *Pseudomonas* spp. strain OFT5 decreases salt-induced ET

TABLE 2 Summary of eco-sustainable approaches to improve salt tolerance in tomato.

Approach	Effect	References
Grafting		
Tomato grafted tomato	Grafting the sensitive genotype onto tolerant genotype reduced the yield loss from 44 to 3%, increased fruit size, total dry matter content, and vitamin C, while decreased pH under saline conditions; the tolerant rootstock controlled sensitive scions' stomatal openness and closure; the tolerant genotype ameliorated leaf osmotic adjustment of the sensitive genotype in grafting under salt stress, and decreased the transport of Na^+ ions to young leaves in the grafting combination	Coban et al., 2020
Tomato grafted eggplant	Grafting improved tomato plant performance under salt stress, and eggplant rootstock IC-111056 outperformed IC-354557; compared with non-grafted control at EC 6 and 9 dS m^{-1}, the increase in the average fruit yield of grafted plants with rootstock IC-111056 was 24.41 and 55.84%, respectively, and that with IC-354557 was 20.25 and 49.08%, respectively; grafted plants maintained a superior water status under saline irrigation along with higher Pro and antioxidant enzyme activities; rootstocks regulated the partitioning of toxic saline ions in the scions by promoting higher Na^+ accumulation in the old leaves and lower in the young leaves of grafted plants	Sanwal et al., 2022
Tomato grafted potato	The grafted plants balanced mineral partitioning across plant parts; grafted plants were superior in water productivity by 56.8 and 70.5% over the control plants under saline and non-saline water-irrigations, respectively; potato rootstock improved the tolerance of tomato scion to saline water irrigation through distinct changes in dry mass allocation, and the induction of mineral-compartmentalization processes	Parthasarathi et al., 2021
Tomato grafted wolfberry	Grafting onto wolfberry increased the SPAD in tomato leaves under salt stress, remained the light use ability of the leaf chlorophyll in saline soil; tomato grafted onto wolfberry had significantly increased fruit fiber and soluble sugar concentration and reduced vitamin C concentration; the growth and fruit yield of the tomato grafted on wolfberry were reduced, but the union was not sensitive to salt stress	Feng et al., 2019
Pretreatments		
Heat treatment	Increased the accumulation of GB and trehalose, maintained a higher K^+ level, with a better performance of cell water status and photosynthesis	Rivero et al., 2014
Salinity acclimation	Improved fruit quality, reduced the concentration of Na^+ in leaves, accumulated Pro, and activated antioxidant enzymes	Kamanga et al., 2020; Meza et al., 2020
Elevated CO_2	Enhanced growth, stimulated photosynthesis, reduced ABA and ET precursor, improved the antioxidant capacity, ion homeostasis and PA metabolism	Brito et al., 2020; Zhang et al., 2020c
Low red to far-red light ratio (R:FR)	Low R:FR significantly alleviated the damage of tomato seedlings from salt stress; On day 4, 8, and 12 at low R:FR, the Fv/Fm of PSII were increased by 4.53, 3.89, and 16.49%, respectively; the Pn of leaves were increased by 16.21, 90.81, and 118.00%, respectively; low R:FR enhanced the integrity and stability of the chloroplast structure through maintaining the high activities of antioxidant enzymes, mitigated the degradation rate of photosynthetic pigments caused by ROS, and upregulated the transcripts of antioxidative enzyme related genes, and enhanced salinity tolerance from the regulation of photosynthesis and ROS scavenging systems	Wang Z. et al., 2021
Vanillic acid and quercetin	Reduced Na^+ content, increased LRWC and Pro, and reduced H_2O_2 and MDA content, and LOX activity; increased glutathione *S*-transferase activity in salt-invaded seedlings; caused the reduction of toxic methylglyoxal accumulation through the enhancement of glyoxalase system; promoted plant growth and photosynthetic pigments synthesis under salt conditions	Parvin et al., 2019a, 2020
Spd and EBL	Exogenous Spd applied as a pre-soaking treatment to seeds promoted PA synthesis under salinity-alkalinity stress, and enhanced the salinity-alkalinity tolerance of tomato; EBL inhibited Na^+ upward transport in flowers and apiculus of salt-stressed tomato, induced an obvious increase of PAs in young leaves, increased fruit-PAs concentration in mid-anaphase, and promoted the (Spd + spermine)/putrescine ratio in premetaphase of fruit period, improving salt resistance	Hu et al., 2012; Zheng et al., 2016
GSH	Improved photosystem II efficiency, balanced uneven distribution of light energy, enhanced antioxidant defense system, regulated synthesis and metabolism of GSH and PA, alleviated ion imbalance and poisoning	Zhou et al., 2019
Omeprazole	Improved growth, protected photosynthetic system, increased quantum yield of PSII, ABA, and Ca^{2+}, decreased auxins, cytokinin, Na^+, and Cl^-	Rouphael et al., 2018
Vermicompost leachate	Improved growth, reduced Na^+, decreased ET synthesis, increased Pro and anthocyanin, increased jasmonate, modified cytokinin profile	Benazzouk et al., 2020
Melatonin	Improved photosynthetic activities, enhanced antioxidant system, Pro and carbohydrates metabolism, improved osmoregulation	Yin et al., 2019
GABA	Reducing Na^+ flux from root to leaves, increased amino acid content and strengthened antioxidant metabolism	Wu et al., 2020
Combined MEF	MEF-treatment significantly enhanced Pro accumulation in plants grown under 120 mM and 150 mM NaCl conditions, significantly improved nitrogen, phosphorus, and K^+ absorption in plants grown at 80 mM and 120 mM NaCl levels, and significantly decreased leaf lipid peroxidation through ROS oxidative stress with enhanced CAT and SOD activities; MEF triggered a significant decline in fatty acid content, enhanced K^+ uptake and reduced Na^+/K^+ ratio in the leaves of treated plants	Mutale-joan et al., 2021

(Continued)

TABLE 2 (Continued)

Approach	Effect	References
PGPB		
Endophytic *Pseudomonas* spp. strain OFT5	Plants inoculated with the OFT5 strain inhibited the reductions in total biomass caused by salt stress, reduced salt-induced ET production, and promoted shoot uptake of macronutrients and micronutrients, which might activate processes that alleviate the effects of salt	Win et al., 2018
Pseudomonas 16S	Plants inoculated with *Pseudomonas* 16S showed higher biomass than both uninoculated and *Enterobacter* 15S inoculated plants under saline conditions, *Pseudomonas* 16S was efficient in alleviating the saline stress; *Pseudomonas* 16S induced an increase in the content of ROS-scavenging and antioxidant compounds in addition to the facilitation of Fe acquisition	Zuluaga et al., 2021
Endophytic halotolerant *Bacillus velezensis* FMH2	FMH2 treatment promoted plant growth in presence of salt stress, decreased endogenous Na^+ accumulation and increased K^+ and Ca^{2+} uptake; FMH2-treatment improved chlorophyll contents, membrane integrity and phenol peroxidase concentrations, and reduced MDA and H_2O_2 levels under saline conditions	Masmoudi et al., 2021
Azotobacter chroococcum 76A	The *A. chroococcum* 76A strain enhanced salinity tolerance in tomato; stress priming in plants inoculated with *A. chroococcum* 76A increased the expression of key stress-related genes; the application of optimal nutritional levels appeared to be inhibitory to the growth promoting and stress protective effects of *A. chroococcum* 76A	Van Oosten et al., 2018
Pseudomonas oryzihabitans AXSa06	Inoculations with *Pseudomonas oryzihabitans* AXSa06 repressed stress-inducing signals through a dampened ET and ABA metabolism and a reduced activation of downstream TFs when stress was applied; inoculations with AXSa06 alleviated the negative impact of salinity on photosynthetic machinery and carbon assimilation, through a more active ruBisCO and NR, involving an efficient mechanism of Na^+ detoxification	Mellidou et al., 2021
AMF		
A mixture of *Glomus geosporum* and *Glomus intraradices*	Colonization of tomato roots with AMF significantly enhanced the reducing effect of salt stress on the transcription levels of tonoplast and PM aquaporin genes, and resulted in a dramatic increase in the mRNAs of three aquaporin genes in leaves under salt stress; AMF controlled the expression of aquaporins and thus might regulate water flow in tomato under salt stress	Ouziad et al., 2006
Glomus mosseae	AMF mitigated the adverse effects of salt stress, including reductions in root colonization, growth, leaf area, chlorophyll content, fruit fresh weight, and fruit yield; AM plants promoted P and K accumulation and reduced Na concentration; AMF colonization enhanced the activities of SOD, CAT, POD and APX in leaves, and reduced oxidative damage	Latef and Chaoxing, 2011
Nanoparticles		
Cu-NPs	The content of Cu increased in tomato plants under salinity with the application of Cu-NPs, which increased the phenols (16%) in the leaves and the content of vitamin C (80%), GSH (81%), and phenols (7.8%) in the fruit compared with the control; the enzyme activities of PAL, APX, GPX, SOD, and CAT increased in leaves by 104, 140, 26, 8, and 93%, respectively; foliar spraying of Cu-NPs on tomato plants under salinity appeared to induce stress tolerance to salinity by stimulating the antioxidant mechanisms	Pérez-Labrada et al., 2019
Cu-NPs + Cs-PVA	The application of Cs-PVA + Cu-NPs increased the stem diameter of tomato plants cultivated under non-stressed conditions; Cs-PVA + Cu-NPs increased plant height and stem diameter under salt conditions and induced the expression of the *SOD* and *JA* genes; the application of Cs-PVA and the Cu-NPs activated the antioxidant defense mechanisms and were mediated by the octadecanoid pathway of the jasmonates	Hernández-Hernández et al., 2018
ZnO-NPs	Foliar spray of ZnO-NPs significantly increased SL and RL, biomass, leaf area, chlorophyll content and photosynthetic attributes; ZnO-NPs mitigated the impacts of salt stress on tomato growth, and enhanced protein content and antioxidative enzyme activity such as POX, SOD and CAT; ZnO-NPs played an important role in the alleviation of salt toxicity in tomato plants	Faizan et al., 2021
Si-NPs + grafting	Foliar application of Si-NPs combined with grafting improved salt tolerance and reduced salt damage in tomato plants; plant growth, fruit yield, fruit quality, especially vitamin C content and TSS percentage, mineral content, and GA3, ABA, and Pro levels of grafted tomato combined with foliar application of Si-NPs were significantly higher than the self-grafted tomato under saline conditions	Sayed et al., 2022

AMF, arbuscular mycorrhizal fungi; Cs-PVA, chitosan-polyvinyl alcohol hydrogels; Cu-NPs, copper nanoparticles; DAS, days after sowing; EBL, 24-epibrassinolide; EC, electrical conductivity; ET, ethylene; Fv/Fm, maximum photochemical quantum yields; GA3, gibberellic acid; GABA, gamma-aminobutyric acid; JA, jasmonic acid; LOX, lipoxygenase; LRWC, leaf relative water content; MEF, microalgae-cyanobacteria extract formulations; NR, nitrate reductase; PAL, phenylalanine ammonia lyase; PGPB, plant growth promoting bacteria; Pn, net photosynthetic rates; POX, peroxidase; PSII, photosystem II; RL, root length; Si-NPs, silicon nanoparticles; SL, shoot length; SPAD, leaf chlorophyll index; Spd, spermidine; TSS, total soluble solids; ZnO-NPs, zinc oxide nanoparticles. The remaining abbreviations mentioned in this table exist in **Table 1**.

levels, but promotes shoot uptake of the macronutrients and micronutrients, improving plant growth under moderate salt conditions (Win et al., 2018). Tomato plants inoculated with *Pseudomonas* 16S showed higher biomass accumulation than uninoculated plants. It is the result of the facilitation of Fe acquisition and an increase in the content of ROS-scavenging and antioxidant compounds (Zuluaga et al., 2021). Endophytic halotolerant *Bacillus velezensis* FMH2 alleviates salt stress on tomato plants by regulating ion accumulation (decreased endogenous Na^+ accumulation,

increased K^+ and Ca^{2+} uptake) and enhancing antioxidant responses (Masmoudi et al., 2021). Root inoculation with *Azotobacter chroococcum* 76A not only enhances tomato adaptation to salt stress under low nitrogen conditions, but also promotes nutrient assimilation efficiency under moderate and severe salinity, showing its potential in improved nutrition and salt stress protection (Van Oosten et al., 2018). Comparative transcriptomics and metabolomics reveal that *Pseudomonas oryzihabitans* AXSa06 mediates salt tolerance in tomato by efficiently activating antioxidant metabolism, by dampening stress signals, by detoxifying Na^+, as well as by effectively assimilating carbon and nitrogen (Mellidou et al., 2021).

Arbuscular mycorrhizal fungi (AMF) can alleviate salt stress by enhancing assimilation and uptake of key elements, activating antioxidant systems and photosynthesis, regulating key hormone accumulation, and activating nutrient transporters and enzymes (Giordano et al., 2021). For instance, AMF colonization reduces the expression of aquaporins genes in roots of salt-treated tomato plants, whereas significantly increases their transcript levels in leaves, and thereby presumably regulates water flow in tomato under salt stress (Ouziad et al., 2006). Moreover, AMF colonization increases P and K concentration, decreases Na content, enhances the activities of SOD, CAT, POD and APX, and increases tomato fruit yield by 33.3 and 106% at 50- and 100-mM salinity levels, respectively (Latef and Chaoxing, 2011; **Table 2**).

Plant growth promoting bacteria and AMF not only act as biofertilizers to improve plant growth in saline soils, but also promote bioremediation of contaminated soils (Mokrani et al., 2020). Co-inoculation of different beneficial microorganisms may further improve salt tolerance (Hanin et al., 2016), which requires more attempts.

Nanobiotechnology

Enhanced ROS scavenging improves salt tolerance in plants. Using nanoparticles (NPs) with ROS scavenging ability is an emerging approach for modulating ROS homeostasis in plants under stress conditions (Liu et al., 2021). Environmentally friendly metal-based nanomaterials can improve salt tolerance in tomato plants (**Table 2**). Under salinity conditions, foliar application of copper NPs (Cu-NPs) increases the content of phenolic substances in leaves and vitamin C, glutathione and phenolics in fruits, also improves the activities of phenylalanine ammonia lyase (PAL), APX, GSH-Px, SOD, and CAT. Cu-NPs induce salt tolerance of tomato by stimulating the antioxidant mechanism (Pérez-Labrada et al., 2019). Another study confirmed that the application of chitosan-polyvinyl alcohol hydrogels (Cs-PVA) and Cu-NPs activates the antioxidant defense mechanisms of tomato plants and are mediated by the octadecanoid pathway of the jasmonates (Hernández-Hernández et al., 2018). In addition to antioxidant enzyme activities, zinc oxide nanoparticles (ZnO-NPs) also enhance protein content and photosynthetic properties under salt stress, improving growth performance and alleviating the adverse effects of salinity on tomato (Faizan et al., 2021). Notably, combining NPs with other strategies may be more effective in improving salt tolerance in tomato. For example, nano-silicon application combined with grafting enhances shoot and root growth, fruit yield and quality of tomato under salt stress, and increases the contents of mineral, GA3, ABA, and Pro, indicating that this method holds promise as alternative techniques for alleviating salt stress in commercial tomato cultivars (Sayed et al., 2022). Overall, nanobiotechnology has a strong potential to modulate ROS homeostasis in plants and improve salt tolerance, contributing to sustainable agriculture (Liu et al., 2021).

The above-mentioned methods for improving salt tolerance in tomato should be combined with the cultivation approaches adopted by farmers, including crop rotation, selection of sowing and planting dates and harvest times, appropriate irrigation techniques, planting density and mulching films (Giordano et al., 2021). The evaluation of the effect of improving salt tolerance needs to comprehensively consider the yield and quality of tomato under field conditions and the cost-benefit ratio (Hanin et al., 2016; Ashraf and Munns, 2022).

Conclusion and future perspectives

A clear salt tolerance mechanism and the identification of key genes in tomato plants that respond to salt stress will contribute to the fast-track breeding of salt tolerant varieties. In this review, we described the effect of salt stress on tomato growth and development, the mechanisms of tomato response to salinity, and the methods to improve tomato salt tolerance. High salt induces osmotic stress and ionic imbalance, thus inhibiting the growth and photosynthesis of tomato plants. Coping these adverse effects tomato plants have adopted strategies including maintaining ion homeostasis, improving osmotic regulation ability and antioxidant enzyme activities. At present, several problems in the regulation mechanism of salt tolerance in plants need to be resolved, including perception of Na^+, transport and detoxification mechanisms of Cl^-, mapping of toxicity at cell and tissue levels, new QTLs that improve salt tolerance, and cross-effect of different hormones under salt stress (Ismail and Horie, 2017; Isayenkov and Maathuis, 2019; Zhao et al., 2020).

Tomato has a more stable genetic transformation system, that is conducive to improve its salt tolerance with the introduction of foreign genes via transformation

(Cuartero et al., 2006). Although, overexpression of some genes in tomato has improved its salt tolerance, but the development of salt-tolerant varieties through genetic transformation has not been fully understood yet. The evaluation of salt tolerance in transgenic plants under laboratory or greenhouse conditions has little correlation with salt tolerance under field conditions, because the field environment is a compound stress, not just salt stress (Yamaguchi and Blumwald, 2005). Genetic transformation of the tomato transcription factors involved in salt stress may partially solve the problem as in field conditions the transgenic plants do not exhibits outstanding salt tolerance, because transcription factors are generally involved in a various stresses and initiate expression of multiple target genes (Cui et al., 2018; Waseem et al., 2019; Gao et al., 2020). Salt tolerance of tomatoes in the field can be evaluated through unmanned aerial vehicle-based phenotyping using morphometric and spectral analysis (Johansen et al., 2019).

Many genes involved in salt stress response are inducible expression type, while most transgenic plants are obtained by using constitutive promoters to drive the continuous expression of target genes, which may cause unexpected side effects. This could be alleviated by replacing constitutive promoters with stress-induced or tissue-specific promoters (Yamaguchi and Blumwald, 2005). For genetic transformation, special attention should be paid to the genetic background of the transformed plants, which may determine the effectiveness of salt-tolerant genes. For instance, tomato *ZF2* enhances salt sensitivity in transgenic *Arabidopsis*, whereas improves tomato salt tolerance (Hichri et al., 2014), whether this effect is also present in tomatoes with different genetic backgrounds remains to be further studied. Moreover, the safety of transgenic crops is widely questioned worldwide, and traditional breeding costs considerable resources and is a lengthy process (Ismail and Horie, 2017). As the genome editing complex is degraded in the recipient cells, genome editing is defined as non-genetically modified (GM), which is more acceptable to the public, and it can offer products that will be difficult to produce using traditional breeding methods (Kanchiswamy et al., 2015). Although major breakthroughs have been made in tomato genome editing, that mainly focuses on development, metabolism, biotic stresses, and abiotic stresses such as drought, chilling and herbicides (Xu et al., 2019), while studies on tomato salt stress are few and far between. Genome editing can simultaneously edit multiple salt stress-related genes in the same tomato variety, helping to improve salt tolerance.

Many wild tomato species harboring salt-tolerant alleles are excellent natural resources for improving salt tolerance of cultivated tomatoes (Pailles et al., 2020; Wang et al., 2020). Genome editing enables *de novo* domestication of wild tomato species without causing an associated drag on salt tolerance, accelerating the genetic improvement of wild tomato species (Li T. et al., 2018). Crossing of salt-tolerant wild tomato with salt-sensitive varieties produces segregating populations for studying the genetic structure of salt tolerance (Bai et al., 2018). In addition, salt-tolerant wild tomato species can be used as rootstocks for grafting susceptible but high yielding commercial cultivars (Singh et al., 2020). Overall, in future, we can use GWAS, genome, transcriptome and proteomic analysis to identify the new QTLs and improve the regulatory network of tomato salt stress, optimize the combination of cultivation techniques to improve salt tolerance. We can develop the identification methods of high-throughput phenotyping for tomato salt tolerance, strengthen the utilization of wild salt-tolerant species, adopt efficient gene editing and genetic transformation techniques to carry out precise breeding, and use MAS breeding to improve breeding efficiency, ultimately achieving the goal of producing high-yield and high-quality tomatoes under salinity conditions.

Author contributions

MG, X-MW, Y-MG, and J-SL conceived and designed the manuscript. MG, X-SW, H-DG, and S-YB collected and analyzed the literatures. MG wrote the manuscript. AK, Y-MG, and J-SL reviewed the manuscript. All authors contributed to the article and approved the submitted version.

Funding

This work was supported by the Natural Science Foundation of Ningxia (Grant No. 2021AAC03099), the Horticulture Western First-class Discipline Construction Project of Ningxia University (Grant No. NXYLXK2017B03), and the Science and Technology Major Project of Ningxia (Grant Nos. NXNYYZ20200101 and 2021BBF02024).

Conflict of interest

The authors declare that the research was conducted in the absence of any commercial or financial relationships that could be construed as a potential conflict of interest.

Publisher's note

All claims expressed in this article are solely those of the authors and do not necessarily represent those of their affiliated organizations, or those of the publisher, the editors and the reviewers. Any product that may be evaluated in this article, or claim that may be made by its manufacturer, is not guaranteed or endorsed by the publisher.

References

Abdelgawad, K. F., El-Mogy, M. M., Mohamed, M. I. A., Garchery, C., and Stevens, R. G. (2019). Increasing ascorbic acid content and salinity tolerance of cherry tomato plants by suppressed expression of the ascorbate oxidase gene. *Agronomy* 9:51. doi: 10.3390/agronomy9020051

Abouelsaad, I., and Renault, S. (2018). Enhanced oxidative stress in the jasmonic acid-deficient tomato mutant *def-1* exposed to NaCl stress. *J. Plant Physiol.* 226, 136–144. doi: 10.1016/j.jplph.2018.04.009

Achuo, E. A., Prinsen, E., and Höfte, M. (2006). Influence of drought, salt stress and abscisic acid on the resistance of tomato to *Botrytis cinerea* and *Oidium neolycopersici*. *Plant Pathol.* 55, 178–186. doi: 10.1111/j.1365-3059.2005.01340.x

Aiese Cigliano, R., Sanseverino, W., Cremona, G., Ercolano, M. R., Conicella, C., and Consiglio, F. M. (2013). Genome-wide analysis of histone modifiers in tomato: Gaining an insight into their developmental roles. *BMC Genomics* 14:57. doi: 10.1186/1471-2164-14-57

Alam, M. S., Tester, M., Fiene, G., and Mousa, M. A. A. (2021). Early growth stage characterization and the biochemical responses for salinity stress in tomato. *Plants* 10:712. doi: 10.3390/plants10040712

Alfosea-Simón, M., Zavala-Gonzalez, E. A., Camara-Zapata, J. M., Martínez-Nicolás, J. J., Simón, I., Simón-Grao, S., et al. (2020). Effect of foliar application of amino acids on the salinity tolerance of tomato plants cultivated under hydroponic system. *Sci. Hortic.* 272:109509. doi: 10.1016/j.scienta.2020.109509

Almas, H. I., Anwar, S., Kausar, A., Farhat, F., Munawar, M., and Khalizadieh, R. (2021). Exogenous application of methionine and phenylalanine confers salinity tolerance in tomato by concerted regulation of metabolites and antioxidants. *J. Soil Sci. Plant Nutr.* 21, 3051–3064. doi: 10.1007/s42729-021-00588-9

Alves, R. D. C., Rossatto, D. R., da Silva, J. D. S., Checchio, M. V., de Oliveira, K. R., Oliveira, F. D. A., et al. (2021). Seed priming with ascorbic acid enhances salt tolerance in micro-tom tomato plants by modifying the antioxidant defense system components. *Biocatal. Agric. Biotechnol.* 31:101927. doi: 10.1016/j.bcab.2021.101927

Ashraf, M., and Foolad, M. R. (2013). Crop breeding for salt tolerance in the era of molecular markers and marker-assisted selection. *Plant Breed.* 132, 10–20. doi: 10.1111/pbr.12000

Ashraf, M., and Munns, R. (2022). Evolution of approaches to increase the salt tolerance of crops. *Crit. Rev. Plant Sci.* 41, 128–160. doi: 10.1080/07352689.2022.2065136

Asins, M. J., Villalta, I., Aly, M. M., Olias, R., Álvarez De Morales, P. A. Z., Huertas, R., et al. (2013). Two closely linked tomato HKT coding genes are positional candidates for the major tomato QTL involved in Na^+/K^+ homeostasis. *Plant Cell Environ.* 36, 1171–1191. doi: 10.1111/pce.12051

Bacha, H., Ródenas, R., López-Gómez, E., García-Legaz, M. F., Nieves-Cordones, M., Rivero, R. M., et al. (2015). High Ca^{2+} reverts the repression of high-affinity K^+ uptake produced by Na^+ in *Solanum lycopersycum* L. (var. microtom) plants. *J. Plant Physiol.* 180, 72–79. doi: 10.1016/j.jplph.2015.03.014

Baghour, M., Gálvez, F. J., Sánchez, M. E., Aranda, M. N., Venema, K., and Rodríguez-Rosales, M. P. (2019). Overexpression of LeNHX2 and SlSOS2 increases salt tolerance and fruit production in double transgenic tomato plants. *Plant Physiol. Biochem.* 135, 77–86. doi: 10.1016/j.plaphy.2018.11.028

Bai, M., Yang, G. S., Chen, W. T., Mao, Z. C., Kang, H. X., Chen, G. H., et al. (2012). Genome-wide identification of Dicer-like, Argonaute and RNA-dependent RNA polymerase gene families and their expression analyses in response to viral infection and abiotic stresses in *Solanum lycopersicum*. *Gene* 501, 52–62. doi: 10.1016/j.gene.2012.02.009

Bai, Y., Kissoudis, C., Yan, Z., Visser, R. G., and van der Linden, G. (2018). Plant behaviour under combined stress: Tomato responses to combined salinity and pathogen stress. *Plant J.* 93, 781–793. doi: 10.1111/tpj.13800

Bao, H., Chen, X., Lv, S., Jiang, P., Feng, J., Fan, P., et al. (2015). Virus-induced gene silencing reveals control of reactive oxygen species accumulation and salt tolerance in tomato by γ-aminobutyric acid metabolic pathway. *Plant Cell Environ.* 38, 600–613. doi: 10.1111/pce.12419

Baysal, Ö., Gürsoy, Y. Z., Örnek, H., Cetinel, B., and Teixeira da Silva, J. A. (2007). Enhanced systemic resistance to bacterial speck disease caused by *Pseudomonas syringae* pv. *tomato* by DL-β-aminobutyric acid under salt stress. *Physiol. Plant.* 129, 493–506. doi: 10.1111/j.1399-3054.2006.00818.x

Bazihizina, N., Colmer, T. D., Cuin, T. A., Mancuso, S., and Shabala, S. (2019). Friend or foe? Chloride patterning in halophytes. *Trends Plant Sci.* 24, 142–151. doi: 10.1016/j.tplants.2018.11.003

Belver, A., Olías, R., Huertas, R., and Rodríguez-Rosales, M. P. (2012). Involvement of SlSOS2 in tomato salt tolerance. *Bioengineered* 3, 298–302. doi: 10.4161/bioe.20796

Benazzouk, S., Dobrev, P. I., Djazouli, Z. E., Motyka, V., and Lutts, S. (2020). Positive impact of vermicompost leachate on salt stress resistance in tomato (*Solanum lycopersicum* L.) at the seedling stage: A phytohormonal approach. *Plant Soil* 446, 145–162. doi: 10.1007/s11104-019-04361-x

Borbély, P., Poór, P., and Tari, I. (2020). Changes in physiological and photosynthetic parameters in tomato of different ethylene status under salt stress: Effects of exogenous 1-aminocyclopropane-1-carboxylic acid treatment and the inhibition of ethylene signalling. *Plant Physiol. Biochem.* 156, 345–356. doi: 10.1016/j.plaphy.2020.09.019

Bouzroud, S., Gasparini, K., Hu, G., Barbosa, M. A. M., Rosa, B. L., Fahr, M., et al. (2020). Down regulation and loss of *auxin response factor 4* function using CRISPR/Cas9 alters plant growth, stomatal function and improves tomato tolerance to salinity and osmotic stress. *Genes* 11:272. doi: 10.3390/genes11030272

Brito, F. A., Pimenta, T. M., Henschel, J. M., Martins, S. C., Zsögön, A., and Ribeiro, D. M. (2020). Elevated CO_2 improves assimilation rate and growth of tomato plants under progressively higher soil salinity by decreasing abscisic acid and ethylene levels. *Environ. Exp. Bot.* 176:104050. doi: 10.1016/j.envexpbot.2020.104050

Cai, X., Zhang, C., Shu, W., Ye, Z., Li, H., and Zhang, Y. (2016). The transcription factor SlDof22 involved in ascorbate accumulation and salinity stress in tomato. *Biochem. Biophys. Res. Commun.* 474, 736–741. doi: 10.1016/j.bbrc.2016.04.148

Campos, J. F., Cara, B., Pérez-Martín, F., Pineda, B., Egea, I., Flores, F. B., et al. (2016). The tomato mutant *ars1* (*altered response to salt stress 1*) identifies an R1-type MYB transcription factor involved in stomatal closure under salt acclimation. *Plant Biotechnol. J.* 14, 1345–1356. doi: 10.1111/pbi.12498

Chandrasekaran, M., Boopathi, T., and Paramasivan, M. (2021). A status-quo review on CRISPR-Cas9 gene editing applications in tomato. *Int. J. Biol. Macromol.* 190, 120–129. doi: 10.1016/j.ijbiomac.2021.08.169

Chen, P., Sun, Y. F., Kai, W. B., Liang, B., Zhang, Y. S., Zhai, X. W., et al. (2016). Interactions of ABA signaling core components (SlPYLs, SlPP2Cs, and SlSnRK2s) in tomato (*Solanum lycopersicon*). *J. Plant Physiol.* 205, 67–74. doi: 10.1016/j.jplph.2016.07.016

Chen, T., Shabala, S., Niu, Y., Chen, Z. H., Shabala, L., Meinke, H., et al. (2021). Molecular mechanisms of salinity tolerance in rice. *Crop J.* 9, 506–520. doi: 10.1016/j.cj.2021.03.005

Chinnusamy, V., and Zhu, J. K. (2009). Epigenetic regulation of stress responses in plants. *Curr. Opin. Plant Biol.* 12, 133–139. doi: 10.1016/j.pbi.2008.12.006

Cho, J. H., Sim, S. C., and Kim, K. N. (2021). Calcium sensor SlCBL4 associates with SlCIPK24 protein kinase and mediates salt tolerance in *Solanum lycopersicum*. *Plants* 10:2173. doi: 10.3390/plants10102173

Coban, A., Akhoundnejad, Y., Dere, S., and Dasgan, H. Y. (2020). Impact of salt-tolerant rootstock on the enhancement of sensitive tomato plant responses to salinity. *HortScience* 55, 35–39. doi: 10.21273/HORTSCI14476-19

Cortina, C., and Culiáñez-Macià, F. A. (2005). Tomato abiotic stress enhanced tolerance by trehalose biosynthesis. *Plant Sci.* 169, 75–82. doi: 10.1016/j.plantsci.2005.02.026

Cuartero, J., Bolarin, M. C., Asins, M. J., and Moreno, V. (2006). Increasing salt tolerance in the tomato. *J. Exp. Bot.* 57, 1045–1058. doi: 10.1093/jxb/erj102

Cui, J., Jiang, N., Zhou, X., Hou, X., Yang, G., Meng, J., et al. (2018). Tomato MYB49 enhances resistance to *Phytophthora infestans* and tolerance to water deficit and salt stress. *Planta* 248, 1487–1503. doi: 10.1007/s00425-018-2987-6

Czarnocka, W., and Karpiński, S. (2018). Friend or foe? Reactive oxygen species production, scavenging and signaling in plant response to environmental stresses. *Free Radic. Biol. Med.* 122, 4–20. doi: 10.1016/j.freeradbiomed.2018.01.011

D'Amico-Damião, V., Lúcio, J. C. B., Oliveira, R., Gaion, L. A., Barreto, R. F., and Carvalho, R. F. (2021). Cryptochrome 1a depends on blue light fluence rate to mediate osmotic stress responses in tomato. *J. Plant Physiol.* 258:153374. doi: 10.1016/j.jplph.2021.153374

De la Torre-González, A., Montesinos-Pereira, D., Blasco, B., and Ruiz, J. M. (2018). Influence of the proline metabolism and glycine betaine on tolerance to salt stress in tomato (*Solanum lycopersicum* L.) commercial genotypes. *J. Plant Physiol.* 231, 329–336. doi: 10.1016/j.jplph.2018.10.013

Deinlein, U., Stephan, A. B., Horie, T., Luo, W., Xu, G., and Schroeder, J. I. (2014). Plant salt-tolerance mechanisms. *Trends Plant Sci.* 19, 371–379. doi: 10.1016/j.tplants.2014.02.001

Devkar, V., Thirumalaikumar, V. P., Xue, G. P., Vallarino, J. G., Tureèková, V., Strnad, M., et al. (2020). Multifaceted regulatory function of tomato SlTAF1 in the response to salinity stress. *New Phytol.* 225, 1681–1698. doi: 10.1111/nph.16247

Egea, I., Pineda, B., Ortíz-Atienza, A., Plasencia, F. A., Drevensek, S., García-Sogo, B., et al. (2018). The SlCBL10 calcineurin B-like protein ensures plant growth under salt stress by regulating Na^+ and Ca^{2+} homeostasis. *Plant Physiol.* 176, 1676–1693. doi: 10.1104/pp.17.01605

Ezin, V., Dasenka, T., Agbobatinkpo, P. B., Ahanchede, A., and Handa, A. K. (2018). Molecular genetics of salt tolerance in tomato F_2 segregating population with the aid of RAPD markers. *Agric. Sci.* 9, 1553–1568. doi: 10.4236/as.2018.912109

Faizan, M., Bhat, J. A., Chen, C., Alyemeni, M. N., Wijaya, L., Ahmad, P., et al. (2021). Zinc oxide nanoparticles (ZnO-NPs) induce salt tolerance by improving the antioxidant system and photosynthetic machinery in tomato. *Plant Physiol. Biochem.* 161, 122–130. doi: 10.1016/j.plaphy.2021.02.002

FAO (2011). *The state of the world's land and water resources for Food and Agriculture (SOLAW)—managing systems at risk*. Abingdon: Food and Agriculture Organization of the United Nations and Earthscan.

Feng, H. L., Ma, N. N., Meng, X., Zhang, S., Wang, J. R., Chai, S., et al. (2013). A novel tomato MYC-type ICE1-like transcription factor, *SlICE1a*, confers cold, osmotic and salt tolerance in transgenic tobacco. *Plant Physiol. Biochem.* 73, 309–320. doi: 10.1016/j.plaphy.2013.09.014

Feng, K., Yu, J., Cheng, Y., Ruan, M., Wang, R., Ye, Q., et al. (2016). The *SOD* gene family in tomato: Identification, phylogenetic relationships, and expression patterns. *Front. Plant Sci.* 7:1279. doi: 10.3389/fpls.2016.01279

Feng, W., Kita, D., Peaucelle, A., Cartwright, H. N., Doan, V., Duan, Q., et al. (2018). The FERONIA receptor kinase maintains cell-wall integrity during salt stress through Ca^{2+} signaling. *Curr. Biol.* 28, 666–675. doi: 10.1016/j.cub.2018.01.023

Feng, X., Guo, K., Yang, C., Li, J., Chen, H., and Liu, X. (2019). Growth and fruit production of tomato grafted onto wolfberry (*Lycium chinense*) rootstock in saline soil. *Sci. Hortic.* 255, 298–305. doi: 10.1016/j.scienta.2019.05.028

Fernández-García, N., Martínez, V., Cerdá, A., and Carvajal, M. (2002). Water and nutrient uptake of grafted tomato plants grown under saline conditions. *J. Plant Physiol.* 159, 899–905. doi: 10.1078/0176-1617-00652

Flowers, T. J., and Flowers, S. A. (2005). Why does salinity pose such a difficult problem for plant breeders? *Agric. Water Manage.* 78, 15–24. doi: 10.1016/j.agwat.2005.04.015

Foolad, M. R. (2004). Recent advances in genetics of salt tolerance in tomato. *Plant Cell Tiss. Organ Cult.* 76, 101–119. doi: 10.1023/B:TICU.0000007308.47608.88

Foolad, M. R. (2007). Genome mapping and molecular breeding of tomato. *Int. J. Plant Genomics* 2007:64358. doi: 10.1155/2007/64358

Frary, A., Göl, D., Keleş, D., Okmen, B., Pinar, H., Siðva, H. O., et al. (2010). Salt tolerance in *Solanum pennellii*: Antioxidant response and related QTL. *BMC Plant Biol.* 10:58. doi: 10.1186/1471-2229-10-58

Frary, A., Keleş, D., Pinar, H., Göl, D., and Doðanlar, S. (2011). NaCl tolerance in *Lycopersicon pennellii* introgression lines: QTL related to physiological responses. *Biol. Plant.* 55, 461–468. doi: 10.1007/s10535-011-0111-x

Gálvez, F. J., Baghour, M., Hao, G., Cagnac, O., Rodríguez-Rosales, M. P., and Venema, K. (2012). Expression of LeNHX isoforms in response to salt stress in salt sensitive and salt tolerant tomato species. *Plant Physiol. Biochem.* 51, 109–115. doi: 10.1016/j.plaphy.2011.10.012

Gao, Y. F., Liu, J. K., Yang, F. M., Zhang, G. Y., Wang, D., Zhang, L., et al. (2020). The WRKY transcription factor WRKY8 promotes resistance to pathogen infection and mediates drought and salt stress tolerance in *Solanum lycopersicum*. *Physiol. Plant.* 168, 98–117. doi: 10.1111/ppl.12978

Gapińska, M., Skłodowska, M., and Gabara, B. (2008). Effect of short-and long-term salinity on the activities of antioxidative enzymes and lipid peroxidation in tomato roots. *Acta Physiol. Plant.* 30, 11–18. doi: 10.1007/s11738-007-0072-z

Ghanem, M. E., van Elteren, J., Albacete, A., Quinet, M., Martínez-Andújar, C., Kinet, J. M., et al. (2009). Impact of salinity on early reproductive physiology of tomato (*Solanum lycopersicum*) in relation to a heterogeneous distribution of toxic ions in flower organs. *Funct. Plant Biol.* 36, 125–136. doi: 10.1071/FP08256

Gharsallah, C., Fakhfakh, H., Grubb, D., and Gorsane, F. (2016b). Effect of salt stress on ion concentration, proline content, antioxidant enzyme activities and gene expression in tomato cultivars. *AoB Plants* 8:plw055. doi: 10.1093/aobpla/plw055

Gharsallah, C., Abdelkrim, A. B., Fakhfakh, H., Salhi-Hannachi, A., and Gorsane, F. (2016a). SSR marker-assisted screening of commercial tomato genotypes under salt stress. *Breed. Sci.* 66, 823–830. doi: 10.1270/jsbbs.16112

Giordano, M., Petropoulos, S. A., and Rouphael, Y. (2021). Response and defence mechanisms of vegetable crops against drought, heat and salinity stress. *Agriculture* 11:463. doi: 10.3390/agriculture11050463

Guo, J. E., Hu, Z., Guo, X., Zhang, L., Yu, X., Zhou, S., et al. (2017). Molecular characterization of nine tissue-specific or stress-responsive genes of histone deacetylase in tomato (*Solanum lycopersicum*). *J. Plant Growth Regul.* 36, 566–577. doi: 10.1007/s00344-016-9660-8

Guo, X., Chen, G., Cui, B., Gao, Q., Guo, J. E., Li, A., et al. (2016). *Solanum lycopersicum* agamous-like MADS-box protein AGL15-like gene, *SlMBP11*, confers salt stress tolerance. *Mol. Breed.* 36:125. doi: 10.1007/s11032-016-0544-1

Guo, X., Xie, Q., Li, B., and Su, H. (2020). Molecular characterization and transcription analysis of DNA methyltransferase genes in tomato (*Solanum lycopersicum*). *Genet. Mol. Biol.* 43:e20180295. doi: 10.1590/1678-4685-GMB-2018-0295

Guo, Y., Qiu, Q. S., Quintero, F. J., Pardo, J. M., Ohta, M., Zhang, C., et al. (2004). Transgenic evaluation of activated mutant alleles of *sos2* reveals a critical requirement for its kinase activity and C-terminal regulatory domain for salt tolerance in *Arabidopsis thaliana*. *Plant Cell* 16, 435–449. doi: 10.1105/tpc.019174

Gupta, B., and Huang, B. (2014). Mechanism of salinity tolerance in plants: Physiological, biochemical, and molecular characterization. *Int. J. Genomics* 2014:701596. doi: 10.1155/2014/701596

Hanin, M., Ebel, C., Ngom, M., Laplaze, L., and Masmoudi, K. (2016). New insights on plant salt tolerance mechanisms and their potential use for breeding. *Front. Plant Sci.* 7:1787. doi: 10.3389/fpls.2016.01787

Hao, S., Wang, Y., Yan, Y., Liu, Y., Wang, J., and Chen, S. (2021). A review on plant responses to salt stress and their mechanisms of salt resistance. *Horticulturae* 7:132. doi: 10.3390/horticulturae7060132

Hao, Y., Huang, B., Jia, D., Mann, T., Jiang, X., Qiu, Y., et al. (2018). Identification of seven polyamine oxidase genes in tomato (*Solanum lycopersicum* L.) and their expression profiles under physiological and various stress conditions. *J. Plant Physiol.* 228, 1–11. doi: 10.1016/j.jplph.2018.05.004

Hasanuzzaman, M., Bhuyan, M. B., Anee, T. I., Parvin, K., Nahar, K., Mahmud, J. A., et al. (2019). Regulation of ascorbate-glutathione pathway in mitigating oxidative damage in plants under abiotic stress. *Antioxidants* 8:384. doi: 10.3390/antiox8090384

Hawar, A., Xiong, S., Yang, Z., and Sun, B. (2022). Histone acetyltransferase SlGCN5 regulates shoot meristem and flower development in *Solanum lycopersicum*. *Front. Plant Sci.* 12:805879. doi: 10.3389/fpls.2021.805879

He, Y., Zhou, J., Hu, Y., Fang, C., Yu, Y., Yang, J., et al. (2021). Overexpression of sly-miR398b increased salt sensitivity likely via regulating antioxidant system and photosynthesis in tomato. *Environ. Exp. Bot.* 181:104273. doi: 10.1016/j.envexpbot.2020.104273

Hernández-Hernández, H., Juárez-Maldonado, A., Benavides-Mendoza, A., Ortega-Ortiz, H., Cadenas-Pliego, G., Sánchez-Aspeytia, D., et al. (2018). Chitosan-PVA and copper nanoparticles improve growth and overexpress the SOD and JA genes in tomato plants under salt stress. *Agronomy* 8:175. doi: 10.3390/agronomy8090175

Hichri, I., Muhovski, Y., Žižková, E., Dobrev, P. I., Franco-Zorrilla, J. M., Solano, R., et al. (2014). The *Solanum lycopersicum* zinc Finger2 cysteine-2/histidine-2 repressor-like transcription factor regulates development and tolerance to salinity in tomato and *Arabidopsis*. *Plant Physiol.* 164, 1967–1990. doi: 10.1104/pp.113.225920

Hichri, I., Muhovski, Y., Žižková, E., Dobrev, P. I., Gharbi, E., Franco-Zorrilla, J. M., et al. (2017). The *Solanum lycopersicum* WRKY3 transcription factor SlWRKY3 is involved in salt stress tolerance in tomato. *Front. Plant Sci.* 8:1343. doi: 10.3389/fpls.2017.01343

Hu, J., Chen, G., Yin, W., Cui, B., Yu, X., Lu, Y., et al. (2017). Silencing of *SlHB2* improves drought, salt stress tolerance, and induces stress-related gene expression in tomato. *J. Plant Growth Regul.* 36, 578–589. doi: 10.1007/s00344-017-9664-z

Hu, X., Zhang, Y., Shi, Y., Zhang, Z., Zou, Z., Zhang, H., et al. (2012). Effect of exogenous spermidine on polyamine content and metabolism in tomato exposed to salinity–alkalinity mixed stress. *Plant Physiol. Biochem.* 57, 200–209. doi: 10.1016/j.plaphy.2012.05.015

Huang, W., Xian, Z., Hu, G., and Li, Z. (2016). SlAGO4A, a core factor of RNA-directed DNA methylation (RdDM) pathway, plays an important role under salt and drought stress in tomato. *Mol. Breed.* 36:28. doi: 10.1007/s11032-016-0439-1

Huang, Z., Zhang, Z., Zhang, X., Zhang, H., Huang, D., and Huang, R. (2004). Tomato TERF1 modulates ethylene response and enhances osmotic stress tolerance by activating expression of downstream genes. *FEBS Lett.* 573, 110–116. doi: 10.1016/j.febslet.2004.07.064

Huertas, R., Olias, R., Eljakaoui, Z., Gálvez, F. J., Li, J. U. N., De Morales, P. A., et al. (2012). Overexpression of *SlSOS2* (*SlCIPK24*) confers salt tolerance to

transgenic tomato. *Plant Cell Environ.* 35, 1467–1482. doi: 10.1111/j.1365-3040.2012.02504.x

Huertas, R., Rubio, L., Cagnac, O., García-Sánchez, M. J., Alché, J. D. D., Venema, K., et al. (2013). The K^+/H^+ antiporter LeNHX2 increases salt tolerance by improving K^+ homeostasis in transgenic tomato. *Plant Cell Environ.* 36, 2135–2149. doi: 10.1111/pce.12109

Isayenkov, S. V., and Maathuis, F. J. (2019). Plant salinity stress: Many unanswered questions remain. *Front. Plant Sci.* 10:80. doi: 10.3389/fpls.2019.00080

Ismail, A. M., and Horie, T. (2017). Genomics, physiology, and molecular breeding approaches for improving salt tolerance. *Annu. Rev. Plant Biol.* 68, 405–434. doi: 10.1146/annurev-arplant-042916-040936

Jaime-Pérez, N., Pineda, B., García-Sogo, B., Atares, A., Athman, A., Byrt, C. S., et al. (2017). The sodium transporter encoded by the *HKT1;2* gene modulates sodium/potassium homeostasis in tomato shoots under salinity. *Plant Cell Environ.* 40, 658–671. doi: 10.1111/pce.12883

Jia, C., Zhao, S., Bao, T., Zhao, P., Peng, K., Guo, Q., et al. (2021). Tomato BZR/BES transcription factor SlBZR1 positively regulates BR signaling and salt stress tolerance in tomato and *Arabidopsis*. *Plant Sci.* 302:110719. doi: 10.1016/j.plantsci.2020.110719

Jia, H., Chen, S., Liu, D., Liesche, J., Shi, C., Wang, J., et al. (2018). Ethylene-induced hydrogen sulfide negatively regulates ethylene biosynthesis by persulfidation of ACO in tomato under osmotic stress. *Front. Plant Sci.* 9:1517. doi: 10.3389/fpls.2018.01517

Jiang, Y., Ding, X., Zhang, D., Deng, Q., Yu, C. L., Zhou, S., et al. (2017). Soil salinity increases the tolerance of excessive sulfur fumigation stress in tomato plants. *Environ. Exp. Bot.* 133, 70–77. doi: 10.1016/j.envexpbot.2016.10.002

Jiang, Z., Zhou, X., Tao, M., Yuan, F., Liu, L., Wu, F., et al. (2019). Plant cell-surface GIPC sphingolipids sense salt to trigger Ca^{2+} influx. *Nature* 572, 341–346. doi: 10.1038/s41586-019-1449-z

Johansen, K., Morton, M. J., Malbeteau, Y. M., Aragon, B., Al-Mashharawi, S. K., Ziliani, M. G., et al. (2019). Unmanned aerial vehicle-based phenotyping using morphometric and spectral analysis can quantify responses of wild tomato plants to salinity stress. *Front. Plant Sci.* 10:370. doi: 10.3389/fpls.2019.00370

Julkowska, M. M., and Testerink, C. (2015). Tuning plant signaling and growth to survive salt. *Trends Plant Sci.* 20, 586–594. doi: 10.1016/j.tplants.2015.06.008

Kahlaoui, B., Hachicha, M., Misle, E., Fidalgo, F., and Teixeira, J. (2018). Physiological and biochemical responses to the exogenous application of proline of tomato plants irrigated with saline water. *J. Saudi Soc. Agric. Sci.* 17, 17–23. doi: 10.1016/j.jssas.2015.12.002

Kamanga, R. M., Echigo, K., Yodoya, K., Mekawy, A. M. M., and Ueda, A. (2020). Salinity acclimation ameliorates salt stress in tomato (*Solanum lycopersicum* L.) seedlings by triggering a cascade of physiological processes in the leaves. *Sci. Hortic.* 270:109434. doi: 10.1016/j.scienta.2020.109434

Kanchiswamy, C. N., Sargent, D. J., Velasco, R., Maffei, M. E., and Malnoy, M. (2015). Looking forward to genetically edited fruit crops. *Trends Biotechnol.* 33, 62–64. doi: 10.1016/j.tibtech.2014.07.003

Kashyap, S. P., Kumari, N., Mishra, P., Moharana, D. P., and Aamir, M. (2021). Tapping the potential of *Solanum lycopersicum* L. pertaining to salinity tolerance: Perspectives and challenges. *Genet. Resour. Crop Evol.* 68, 2207–2233. doi: 10.1007/s10722-021-01174-9

Kashyap, S. P., Kumari, N., Mishra, P., Moharana, D. P., Aamir, M., Singh, B., et al. (2020a). Transcriptional regulation-mediating ROS homeostasis and physio-biochemical changes in wild tomato (*Solanum chilense*) and cultivated tomato (*Solanum lycopersicum*) under high salinity. *Saudi J. Biol. Sci.* 27, 1999–2009. doi: 10.1016/j.sjbs.2020.06.032

Kashyap, S. P., Prasanna, H. C., Kumari, N., Mishra, P., and Singh, B. (2020b). Understanding salt tolerance mechanism using transcriptome profiling and de novo assembly of wild tomato *Solanum chilense*. *Sci. Rep.* 10:15835. doi: 10.1038/s41598-020-72474-w

Keshishian, E. A., Hallmark, H. T., Ramaraj, T., Plaèková, L., Sundararajan, A., Schilkey, F., et al. (2018). Salt and oxidative stresses uniquely regulate tomato cytokinin levels and transcriptomic response. *Plant Direct* 2:e00071. doi: 10.1002/pld3.71

Khan, M. N., Mukherjee, S., Al-Huqail, A. A., Basahi, R. A., Ali, H. M., Al-Munqedhi, B. M., et al. (2021). Exogenous potassium (K^+) positively regulates Na^+/H^+ antiport system, carbohydrate metabolism, and ascorbate–glutathione cycle in H_2S-dependent manner in NaCl-stressed tomato seedling roots. *Plants* 10:948. doi: 10.3390/plants10050948

Khelil, A., Menu, T., and Ricard, B. (2007). Adaptive response to salt involving carbohydrate metabolism in leaves of a salt-sensitive tomato cultivar. *Plant Physiol. Biochem.* 45, 551–559. doi: 10.1016/j.plaphy.2007.05.003

Koleška, I., Hasanagiæ, D., Todoroviæ, V., Murtiæ, S., and Maksimoviæ, I. (2018). Grafting influence on the weight and quality of tomato fruit under salt stress. *Ann. Appl. Biol.* 172, 187–196. doi: 10.1111/aab.12411

Kong, F., Wang, J., Cheng, L., Liu, S., Wu, J., Peng, Z., et al. (2012). Genome-wide analysis of the mitogen-activated protein kinase gene family in *Solanum lycopersicum*. *Gene* 499, 108–120. doi: 10.1016/j.gene.2012.01.048

Kronzucker, H. J., and Britto, D. T. (2011). Sodium transport in plants: A critical review. *New Phytol.* 189, 54–81. doi: 10.1111/j.1469-8137.2010.03540.x

Latef, A., and Chaoxing, H. (2011). Effect of arbuscular mycorrhizal fungi on growth, mineral nutrition, antioxidant enzymes activity and fruit yield of tomato grown under salinity stress. *Sci. Hortic.* 127, 228–233. doi: 10.1016/j.scienta.2010.09.020

Leiva-Ampuero, A., Agurto, M., Matus, J. T., Hoppe, G., Huidobro, C., Inostroza-Blancheteau, C., et al. (2020). Salinity impairs photosynthetic capacity and enhances carotenoid-related gene expression and biosynthesis in tomato (*Solanum lycopersicum* L. cv. Micro-Tom). *PeerJ* 8:e9742. doi: 10.7717/peerj.9742

Li, D., Ma, N. N., Wang, J. R., Yang, D. Y., Zhao, S. J., and Meng, Q. W. (2013). Overexpression of tomato enhancer of SOS3-1 (LeENH1) in tobacco enhanced salinity tolerance by excluding Na^+ from the cytosol. *Plant Physiol. Biochem.* 70, 150–158. doi: 10.1016/j.plaphy.2013.05.014

Li, F., Wu, Q. Y., Duan, M., Dong, X. C., Li, B., and Meng, Q. W. (2012). Transgenic tomato plants overexpressing chloroplastic monodehydroascorbate reductase are resistant to salt-and PEG-induced osmotic stress. *Photosynthetica* 50, 120–128. doi: 10.1007/s11099-012-0021-y

Li, J., Ouyang, B., Wang, T., Luo, Z., Yang, C., Li, H., et al. (2016). HyPRP1 gene suppressed by multiple stresses plays a negative role in abiotic stress tolerance in tomato. *Front. Plant Sci.* 7:967. doi: 10.3389/fpls.2016.00967

Li, S., Wang, X., Liu, X., Thompson, A. J., and Liu, F. (2022). Elevated CO_2 and high endogenous ABA level alleviate PEG-induced short-term osmotic stress in tomato plants. *Environ. Exp. Bot.* 194:104763. doi: 10.1016/j.envexpbot.2021.104763

Li, T., Yang, X., Yu, Y., Si, X., Zhai, X., Zhang, H., et al. (2018). Domestication of wild tomato is accelerated by genome editing. *Nat. Biotechnol.* 36, 1160–1163. doi: 10.1038/nbt.4273

Li, X., Li, Y., Ahammed, G. J., Zhang, X. N., Ying, L., Zhang, L., et al. (2019b). *RBOH1*-dependent apoplastic H_2O_2 mediates epigallocatechin-3-gallate-induced abiotic stress tolerance in *Solanum lycopersicum* L. *Environ. Exp. Bot.* 161, 357–366. doi: 10.1016/j.envexpbot.2018.11.013

Li, X., Ye, J., Munir, S., Yang, T., Chen, W., Liu, G., et al. (2019c). Biosynthetic gene pyramiding leads to ascorbate accumulation with enhanced oxidative stress tolerance in tomato. *Int. J. Mol. Sci.* 20:1558. doi: 10.3390/ijms20071558

Li, J., Chen, C., Wei, J., Pan, Y., Su, C., and Zhang, X. (2019a). *SpPKE1*, a multiple stress-responsive gene confers salt tolerance in tomato and tobacco. *Int. J. Mol. Sci.* 20:2478. doi: 10.3390/ijms20102478

Li, Y., Chu, Z., Luo, J., Zhou, Y., Cai, Y., Lu, Y., et al. (2018). The C2H2 zinc-finger protein SlZF3 regulates AsA synthesis and salt tolerance by interacting with CSN5B. *Plant Biotechnol. J.* 16, 1201–1213. doi: 10.1111/pbi.12863

Li, Z., Zhang, L., Wang, A., Xu, X., and Li, J. (2013). Ectopic overexpression of *SlHsfA3*, a heat stress transcription factor from tomato, confers increased thermotolerance and salt hypersensitivity in germination in transgenic *Arabidopsis*. *PLoS One* 8:e54880. doi: 10.1371/journal.pone.0054880

Liu, C., Mao, B., Yuan, D., Chu, C., and Duan, M. (2022). Salt tolerance in rice: Physiological responses and molecular mechanisms. *Crop J.* 10, 13–25. doi: 10.1016/j.cj.2021.02.010

Liu, D. D., Sun, X. S., Liu, L., Shi, H. D., Chen, S. Y., and Zhao, D. K. (2019). Overexpression of the melatonin synthesis-related gene *SlCOMT1* improves the resistance of tomato to salt stress. *Molecules* 24:1514. doi: 10.3390/molecules24081514

Liu, J., Fu, C., Li, G., Khan, M. N., and Wu, H. (2021). ROS homeostasis and plant salt tolerance: Plant nanobiotechnology updates. *Sustainability* 13:3552. doi: 10.3390/su13063552

Liu, J., and He, Z. (2020). Small DNA methylation, big player in plant abiotic stress responses and memory. *Front. Plant Sci.* 11:595603. doi: 10.3389/fpls.2020.595603

Liu, M., Yu, H., Ouyang, B., Shi, C., Demidchik, V., Hao, Z., et al. (2020). NADPH oxidases and the evolution of plant salinity tolerance. *Plant Cell Environ.* 43, 2957–2968. doi: 10.1111/pce.13907

Lopez-Delacalle, M., Silva, C. J., Mestre, T. C., Martinez, V., Blanco-Ulate, B., and Rivero, R. M. (2021). Synchronization of proline, ascorbate and oxidative stress pathways under the combination of salinity and heat in tomato plants. *Environ. Exp. Bot.* 183:104351. doi: 10.1016/j.envexpbot.2020.104351

Lovelli, S., Scopa, A., Perniola, M., Di Tommaso, T., and Sofo, A. (2012). Abscisic acid root and leaf concentration in relation to biomass partitioning in salinized tomato plants. *J. Plant Physiol.* 169, 226–233. doi: 10.1016/j.jplph.2011.09.009

Lv, X., Chen, S., and Wang, Y. (2019). Advances in understanding the physiological and molecular responses of sugar beet to salt stress. *Front. Plant Sci.* 10:1431. doi: 10.3389/fpls.2019.01431

Masmoudi, F., Tounsi, S., Dunlap, C. A., and Trigui, M. (2021). Endophytic halotolerant *Bacillus velezensis* FMH2 alleviates salt stress on tomato plants by improving plant growth and altering physiological and antioxidant responses. *Plant Physiol. Biochem.* 165, 217–227. doi: 10.1016/j.plaphy.2021.05.025

Massaretto, I. L., Albaladejo, I., Purgatto, E., Flores, F. B., Plasencia, F., Egea-Fernández, J. M., et al. (2018). Recovering tomato landraces to simultaneously improve fruit yield and nutritional quality against salt stress. *Front. Plant Sci.* 9:1778. doi: 10.3389/fpls.2018.01778

Meco, V., Egea, I., Ortíz-Atienza, A., Drevensek, S., Esch, E., Yuste-Lisbona, F. J., et al. (2020). The salt sensitivity induced by disruption of cell wall-associated kinase 1 (*SlWAK1*) tomato gene is linked to altered osmotic and metabolic homeostasis. *Int. J. Mol. Sci.* 21:6308. doi: 10.3390/ijms21176308

Mellidou, I., Ainalidou, A., Papadopoulou, A., Leontidou, K., Genitsaris, S., Karagiannis, E., et al. (2021). Comparative transcriptomics and metabolomics reveal an intricate priming mechanism involved in PGPR-mediated salt tolerance in tomato. *Front. Plant Sci.* 12:713984. doi: 10.3389/fpls.2021.713984

Meng, X., Cai, J., Deng, L., Li, G., Sun, J., Han, Y., et al. (2020). *SlSTE1* promotes abscisic acid-dependent salt stress-responsive pathways via improving ion homeostasis and reactive oxygen species scavenging in tomato. *J. Integr. Plant Biol.* 62, 1942–1966. doi: 10.1111/jipb.12987

Meza, S. L., Egea, I., Massaretto, I. L., Morales, B., Purgatto, E., Egea-Fernández, J. M., et al. (2020). Traditional tomato varieties improve fruit quality without affecting fruit yield under moderate salt stress. *Front. Plant Sci.* 11:1717. doi: 10.3389/fpls.2020.587754

Miller, G., Suzuki, N., Ciftci-Yilmaz, S., and Mittler, R. (2010). Reactive oxygen species homeostasis and signalling during drought and salinity stresses. *Plant Cell Environ.* 33, 453–467. doi: 10.1111/j.1365-3040.2009.02041.x

Mishra, N. S., Tuteja, R., and Tuteja, N. (2006). Signaling through MAP kinase networks in plants. *Arch. Biochem. Biophys.* 452, 55–68. doi: 10.1016/j.abb.2006.05.001

Mittler, R., Zandalinas, S. I., Fichman, Y., and Van Breusegem, F. (2022). Reactive oxygen species signalling in plant stress responses. *Nat. Rev. Mol. Cell Biol.* 1–17. doi: 10.1038/s41580-022-00499-2 [Epub ahead of print].

Mittova, V., Guy, M., Tal, M., and Volokita, M. (2004). Salinity up-regulates the antioxidative system in root mitochondria and peroxisomes of the wild salt-tolerant tomato species *Lycopersicon pennellii*. *J. Exp. Bot.* 55, 1105–1113. doi: 10.1093/jxb/erh113

Mokrani, S., Nabti, E. H., and Cruz, C. (2020). Current advances in plant growth promoting bacteria alleviating salt stress for sustainable agriculture. *Appl. Sci.* 10:7025. doi: 10.3390/app10207025

Moretti, M. B., Maskin, L., Gudesblat, G., García, S. C., and Iusem, N. D. (2006). ASR1, a stress-induced tomato protein, protects yeast from osmotic stress. *Physiol. Plant.* 127, 111–118. doi: 10.1111/j.1399-3054.2006.00664.x

Morton, M. J., Awlia, M., Al-Tamimi, N., Saade, S., Pailles, Y., Negrão, S., et al. (2019). Salt stress under the scalpel–dissecting the genetics of salt tolerance. *Plant J.* 97, 148–163. doi: 10.1111/tpj.14189

Munns, R., and Gilliham, M. (2015). Salinity tolerance of crops–what is the cost? *New Phytol.* 208, 668–673. doi: 10.1111/nph.13519

Munns, R., Husain, S., Rivelli, A. R., James, R. A., Condon, A. G., Lindsay, M. P., et al. (2002). Avenues for increasing salt tolerance of crops, and the role of physiologically based selection traits. *Plant Soil* 247, 93–105. doi: 10.1007/978-94-017-2789-1_7

Munns, R., James, R. A., Gilliham, M., Flowers, T. J., and Colmer, T. D. (2016). Tissue tolerance: An essential but elusive trait for salt-tolerant crops. *Funct. Plant Biol.* 43, 1103–1113. doi: 10.1071/FP16187

Muñoz-Mayor, A., Pineda, B., Garcia-Abellán, J. O., Antón, T., Garcia-Sogo, B., Sanchez-Bel, P., et al. (2012). Overexpression of dehydrin *tas14* gene improves the osmotic stress imposed by drought and salinity in tomato. *J. Plant Physiol.* 169, 459–468. doi: 10.1016/j.jplph.2011.11.018

Mutale-joan, C., Rachidi, F., Mohamed, H. A., Mernissi, N. E., Aasfar, A., Barakate, M., et al. (2021). Microalgae-cyanobacteria–based biostimulant effect on salinity tolerance mechanisms, nutrient uptake, and tomato plant growth under salt stress. *J. Appl. Phycol.* 33, 3779–3795. doi: 10.1007/s10811-021-02559-0

Nieves-Cordones, M., Miller, A. J., Alemán, F., Martínez, V., and Rubio, F. (2008). A putative role for the plasma membrane potential in the control of the expression of the gene encoding the tomato high-affinity potassium transporter HAK5. *Plant Mol. Biol.* 68, 521–532. doi: 10.1007/s11103-008-9388-3

Olías, R., Eljakaoui, Z., Li, J., De Morales, P. A., Marin-Manzano, M. C., Pardo, J. M., et al. (2009a). The plasma membrane Na^+/H^+ antiporter SOS1 is essential for salt tolerance in tomato and affects the partitioning of Na^+ between plant organs. *Plant Cell Environ.* 32, 904–916. doi: 10.1111/j.1365-3040.2009.01971.x

Olías, R., Eljakaoui, Z., Pardo, J. M., and Belver, A. (2009b). The Na^+/H^+ exchanger SOS1 controls extrusion and distribution of Na^+ in tomato plants under salinity conditions. *Plant Signal. Behav.* 4, 973–976. doi: 10.4161/psb.4.10.9679

Ouziad, F., Wilde, P., Schmelzer, E., Hildebrandt, U., and Bothe, H. (2006). Analysis of expression of aquaporins and Na^+/H^+ transporters in tomato colonized by arbuscular mycorrhizal fungi and affected by salt stress. *Environ. Exp. Bot.* 57, 177–186. doi: 10.1016/j.envexpbot.2005.05.011

Pailles, Y., Awlia, M., Julkowska, M., Passone, L., Zemmouri, K., Negrão, S., et al. (2020). Diverse traits contribute to salinity tolerance of wild tomato seedlings from the Galapagos Islands. *Plant Physiol.* 182, 534–546. doi: 10.1104/pp.19.00700

Pan, Y., Hu, X., Li, C., Xu, X., Su, C., Li, J., et al. (2017). *SlbZIP38*, a tomato bZIP family gene downregulated by abscisic acid, is a negative regulator of drought and salt stress tolerance. *Genes* 8:402. doi: 10.3390/genes8120402

Parthasarathi, T., Ephrath, J. E., and Lazarovitch, N. (2021). Grafting of tomato (*Solanum lycopersicum* L.) onto potato (*Solanum tuberosum* L.) to improve salinity tolerance. *Sci. Hortic.* 282:110050. doi: 10.1016/j.scienta.2021.110050

Parvin, K., Hasanuzzaman, M., Bhuyan, M., Nahar, K., Mohsin, S. M., and Fujita, M. (2019b). Comparative physiological and biochemical changes in tomato (*Solanum lycopersicum* L.) under salt stress and recovery: Role of antioxidant defense and glyoxalase systems. *Antioxidants* 8:350. doi: 10.3390/antiox8090350

Parvin, K., Hasanuzzaman, M., Bhuyan, M., Mohsin, S. M., and Fujita, M. (2019a). Quercetin mediated salt tolerance in tomato through the enhancement of plant antioxidant defense and glyoxalase systems. *Plants* 8:247. doi: 10.3390/plants8080247

Parvin, K., Nahar, K., Hasanuzzaman, M., Bhuyan, M. B., Mohsin, S. M., and Fujita, M. (2020). Exogenous vanillic acid enhances salt tolerance of tomato: Insight into plant antioxidant defense and glyoxalase systems. *Plant Physiol. Biochem.* 150, 109–120. doi: 10.1016/j.plaphy.2020.02.030

Pérez-Labrada, F., López-Vargas, E. R., Ortega-Ortiz, H., Cadenas-Pliego, G., Benavides-Mendoza, A., and Juárez-Maldonado, A. (2019). Responses of tomato plants under saline stress to foliar application of copper nanoparticles. *Plants* 8:151. doi: 10.3390/plants8060151

Pinedo-Guerrero, Z. H., Cadenas-Pliego, G., Ortega-Ortiz, H., González-Morales, S., Benavides-Mendoza, A., Valdés-Reyna, J., et al. (2020). Form of silica improves yield, fruit quality and antioxidant defense system of tomato plants under salt stress. *Agriculture* 10:367. doi: 10.3390/agriculture10090367

Poór, P., Gémes, K., Horváth, F., Szepesi, A., Simon, M. L., and Tari, I. (2011). Salicylic acid treatment via the rooting medium interferes with stomatal response, CO_2 fixation rate and carbohydrate metabolism in tomato, and decreases harmful effects of subsequent salt stress. *Plant Biol.* 13, 105–114. doi: 10.1111/j.1438-8677.2010.00344.x

Poór, P., Kovács, J., Szopkó, D., and Tari, I. (2013). Ethylene signaling in salt stress-and salicylic acid-induced programmed cell death in tomato suspension cells. *Protoplasma* 250, 273–284. doi: 10.1007/s00709-012-0408-4

Poór, P., Patyi, G., Takács, Z., Szekeres, A., Bódi, N., Bagyánszki, M., et al. (2019). Salicylic acid-induced ROS production by mitochondrial electron transport chain depends on the activity of mitochondrial hexokinases in tomato (*Solanum lycopersicum* L.). *J. Plant Res.* 132, 273–283. doi: 10.1007/s10265-019-01085-y

Qi, J., Wang, J., Gong, Z., and Zhou, J. M. (2017). Apoplastic ROS signaling in plant immunity. *Curr. Opin. Plant Biol.* 38, 92–100. doi: 10.1016/j.pbi.2017.04.022

Qi, S., Lin, Q., Zhu, H., Gao, F., Zhang, W., and Hua, X. (2016). The RING finger E3 ligase SpRing is a positive regulator of salt stress signaling in salt-tolerant wild tomato species. *Plant Cell Physiol.* 57, 528–539. doi: 10.1093/pcp/pcw006

Qin, H., Li, Y., and Huang, R. (2020). Advances and challenges in the breeding of salt-tolerant rice. *Int. J. Mol. Sci.* 21:8385. doi: 10.3390/ijms21218385

Rahman, A., Nahar, K., Hasanuzzaman, M., and Fujita, M. (2016). Calcium supplementation improves Na^+/K^+ ratio, antioxidant defense and glyoxalase systems in salt-stressed rice seedlings. *Front. Plant Sci.* 7:609. doi: 10.3389/fpls.2016.00609

Raziq, A., Wang, Y., Mohi Ud Din, A., Sun, J., Shu, S., and Guo, S. (2022). A comprehensive evaluation of salt tolerance in tomato (Var. Ailsa Craig): Responses of physiological and transcriptional changes in RBOH's and ABA biosynthesis and signalling genes. *Int. J. Mol. Sci.* 23:1603. doi: 10.3390/ijms23031603

Ricardi, M. M., González, R. M., Zhong, S., Domínguez, P. G., Duffy, T., Turjanski, P. G., et al. (2014). Genome-wide data (ChIP-seq) enabled identification

of cell wall-related and aquaporin genes as targets of tomato ASR1, a drought stress-responsive transcription factor. *BMC Plant Biol.* 14:29. doi: 10.1186/1471-2229-14-29

Rivero, R. M., Mestre, T. C., Mittler, R., Rubio, F., Garcia-Sanchez, F., and Martinez, V. (2014). The combined effect of salinity and heat reveals a specific physiological, biochemical and molecular response in tomato plants. *Plant Cell Environ.* 37, 1059–1073. doi: 10.1111/pce.12199

Rodríguez-Rosales, M. P., Jiang, X., Gálvez, F. J., Aranda, M. N., Cubero, B., and Venema, K. (2008). Overexpression of the tomato K^+/H^+ antiporter LeNHX2 confers salt tolerance by improving potassium compartmentalization. *New Phytol.* 179, 366–377. doi: 10.1111/j.1469-8137.2008.02461.x

Romero-Aranda, M. R., Espinosa, J., González-Fernández, P., Jaime-Fernández, E., Traverso, J. Á., Asins, M. J., et al. (2021). Role of Na^+ transporters HKT1;1 and HKT1;2 in tomato salt tolerance. I. Function loss of cheesmaniae alleles in roots and aerial parts. *Plant Physiol. Biochem.* 168, 282–293. doi: 10.1016/j.plaphy.2021.10.018

Romero-Aranda, M. R., González-Fernández, P., Pérez-Tienda, J. R., López-Diaz, M. R., Espinosa, J., Granum, E., et al. (2020). Na^+ transporter HKT1;2 reduces flower Na^+ content and considerably mitigates the decline in tomato fruit yields under saline conditions. *Plant Physiol. Biochem.* 154, 341–352. doi: 10.1016/j.plaphy.2020.05.012

Rothan, C., Diouf, I., and Causse, M. (2019). Trait discovery and editing in tomato. *Plant J.* 97, 73–90. doi: 10.1111/tpj.14152

Rouphael, Y., Raimondi, G., Lucini, L., Carillo, P., Kyriacou, M. C., Colla, G., et al. (2018). Physiological and metabolic responses triggered by omeprazole improve tomato plant tolerance to NaCl stress. *Front. Plant Sci.* 9:249. doi: 10.3389/fpls.2018.00249

Sánchez-Aguayo, I., Rodríguez-Galán, J. M., García, R., Torreblanca, J., and Pardo, J. M. (2004). Salt stress enhances xylem development and expression of *S*-adenosyl-L-methionine synthase in lignifying tissues of tomato plants. *Planta* 220, 278–285. doi: 10.1007/s00425-004-1350-2

Sanwal, S. K., Mann, A., Kumar, A., Kesh, H., Kaur, G., Rai, A. K., et al. (2022). Salt tolerant eggplant rootstocks modulate sodium partitioning in tomato scion and improve performance under saline conditions. *Agriculture* 12:183. doi: 10.3390/agriculture12020183

Sayed, E. G., Mahmoud, A. W. M., El-Mogy, M. M., Ali, M. A., Fahmy, M. A., and Tawfic, G. A. (2022). The effective role of nano-silicon application in improving the productivity and quality of grafted tomato grown under salinity stress. *Horticulturae* 8:293. doi: 10.3390/horticulturae8040293

Shu, P., Li, Y., Li, Z., Sheng, J., and Shen, L. (2022). *SlMAPK3* enhances tolerance to salt stress in tomato plants by scavenging ROS accumulation and up-regulating the expression of ethylene signaling related genes. *Environ. Exp. Bot.* 193:104698. doi: 10.1016/j.envexpbot.2021.104698

Siddiqui, M. H., Alamri, S. A., Al-Khaishany, M. Y., Al-Qutami, M. A., Ali, H. M., Hala, A. R., et al. (2017). Exogenous application of nitric oxide and spermidine reduces the negative effects of salt stress on tomato. *Hortic. Environ. Biotechnol.* 58, 537–547. doi: 10.1007/s13580-017-0353-4

Singh, H., Kumar, P., Kumar, A., Kyriacou, M. C., Colla, G., and Rouphael, Y. (2020). Grafting tomato as a tool to improve salt tolerance. *Agronomy* 10:263. doi: 10.3390/agronomy10020263

Singh, J., Sastry, E. D., and Singh, V. (2012). Effect of salinity on tomato (*Lycopersicon esculentum* Mill.) during seed germination stage. *Physiol. Mol. Biol. Plants* 18, 45–50. doi: 10.1007/s12298-011-0097-z

Singh, V. K., Singh, A. K., Singh, P. P., and Kumar, A. (2018). Interaction of plant growth promoting bacteria with tomato under abiotic stress: A review. *Agric. Ecosyst. Environ.* 267, 129–140. doi: 10.1016/j.agee.2018.08.020

Skłodowska, M., Gapińska, M., Gajewska, E., and Gabara, B. (2009). Tocopherol content and enzymatic antioxidant activities in chloroplasts from NaCl-stressed tomato plants. *Acta Physiol. Plant.* 31, 393–400. doi: 10.1007/s11738-008-0248-1

Sousa, B., Rodrigues, F., Soares, C., Martins, M., Azenha, M., Lino-Neto, T., et al. (2022). Impact of combined heat and salt stresses on tomato plants-insights into nutrient uptake and redox homeostasis. *Antioxidants* 11:478. doi: 10.3390/antiox11030478

Sun, S., Wen, D., Yang, W., Meng, Q., Shi, Q., and Gong, B. (2020). Overexpression of caffeic acid O-methyltransferase 1 (*COMT1*) increases melatonin level and salt stress tolerance in tomato plant. *J. Plant Growth Regul.* 39, 1221–1235. doi: 10.1007/s00344-019-10058-3

Sun, W., Xu, X., Zhu, H., Liu, A., Liu, L., Li, J., et al. (2010). Comparative transcriptomic profiling of a salt-tolerant wild tomato species and a salt-sensitive tomato cultivar. *Plant Cell Physiol.* 51, 997–1006. doi: 10.1093/pcp/pcq056

Sun, X. C., Gao, Y. F., Li, H. R., Yang, S. Z., and Liu, Y. S. (2015). Over-expression of *SlWRKY39* leads to enhanced resistance to multiple stress factors in tomato. *J. Plant Biol.* 58, 52–60. doi: 10.1007/s12374-014-0407-4

Takács, Z., Poór, P., Szepesi, Á., and Tari, I. (2017). *In vivo* inhibition of polyamine oxidase by a spermine analogue, MDL-72527, in tomato exposed to sublethal and lethal salt stress. *Funct. Plant Biol.* 44, 480–492. doi: 10.1071/FP16280

Tanveer, K., Gilani, S., Hussain, Z., Ishaq, R., Adeel, M., and Ilyas, N. (2020). Effect of salt stress on tomato plant and the role of calcium. *J. Plant Nutr.* 43, 28–35. doi: 10.1080/01904167.2019.1659324

Tran, M. T., Doan, D. T. H., Kim, J., Song, Y. J., Sung, Y. W., Das, S., et al. (2021). CRISPR/Cas9-based precise excision of SlHyPRP1 domain(s) to obtain salt stress-tolerant tomato. *Plant Cell Rep.* 40, 999–1011. doi: 10.1007/s00299-020-02622-z

Van Oosten, M. J., Di Stasio, E., Cirillo, V., Silletti, S., Ventorino, V., Pepe, O., et al. (2018). Root inoculation with *Azotobacter chroococcum* 76A enhances tomato plants adaptation to salt stress under low N conditions. *BMC Plant Biol.* 18:205. doi: 10.1186/s12870-018-1411-5

van Zelm, E., Zhang, Y., and Testerink, C. (2020). Salt tolerance mechanisms of plants. *Annu. Rev. Plant Biol.* 71, 403–433. doi: 10.1146/annurev-arplant-050718-100005

Villalta, I., Reina-Sánchez, A., Bolarín, M. C., Cuartero, J., Belver, A., Venema, K., et al. (2008). Genetic analysis of Na^+ and K^+ concentrations in leaf and stem as physiological components of salt tolerance in tomato. *Theor. Appl. Genet.* 116, 869–880. doi: 10.1007/s00122-008-0720-8

Viveros, M. F. Á., Inostroza-Blancheteau, C., Timmermann, T., González, M., and Arce-Johnson, P. (2013). Overexpression of *GlyI* and *GlyII* genes in transgenic tomato (*Solanum lycopersicum* Mill.) plants confers salt tolerance by decreasing oxidative stress. *Mol. Biol. Rep.* 40, 3281–3290. doi: 10.1007/s11033-012-2403-4

Wang, G., Zhang, S., Ma, X., Wang, Y., Kong, F., and Meng, Q. (2016). A stress-associated NAC transcription factor (SlNAC35) from tomato plays a positive role in biotic and abiotic stresses. *Physiol. Plant.* 158, 45–64. doi: 10.1111/ppl.12444

Wang, X., Geng, S., Ri, Y. J., Cao, D., Liu, J., Shi, D., et al. (2011). Physiological responses and adaptive strategies of tomato plants to salt and alkali stresses. *Sci. Hortic.* 130, 248–255. doi: 10.1016/j.scienta.2011.07.006

Wang, Y., Bian, Z., Pan, T., Cao, K., and Zou, Z. (2021). Improvement of tomato salt tolerance by the regulation of photosynthetic performance and antioxidant enzyme capacity under a low red to far-red light ratio. *Plant Physiol. Biochem.* 167, 806–815. doi: 10.1016/j.plaphy.2021.09.008

Wang, Z., Hong, Y., Li, Y., Shi, H., Yao, J., Liu, X., et al. (2021). Natural variations in *SlSOS1* contribute to the loss of salt tolerance during tomato domestication. *Plant Biotechnol. J.* 19, 20–22. doi: 10.1111/pbi.13443

Wang, Z., Hong, Y., Zhu, G., Li, Y., Niu, Q., Yao, J., et al. (2020). Loss of salt tolerance during tomato domestication conferred by variation in a Na^+/K^+ transporter. *EMBO J.* 39, e103256. doi: 10.15252/embj.2019103256

Waseem, M., Rong, X., and Li, Z. (2019). Dissecting the role of a basic helix-loop-helix transcription factor, *SlbHLH22*, under salt and drought stresses in transgenic *Solanum lycopersicum* L. *Front. Plant Sci.* 10:734. doi: 10.3389/fpls.2019.00734

Waszczak, C., Carmody, M., and Kangasjärvi, J. (2018). Reactive oxygen species in plant signaling. *Annu. Rev. Plant Biol.* 69, 209–236. doi: 10.1146/annurev-arplant-042817-040322

Wei, D., Zhang, W., Wang, C., Meng, Q., Li, G., Chen, T. H., et al. (2017). Genetic engineering of the biosynthesis of glycinebetaine leads to alleviate salt-induced potassium efflux and enhances salt tolerance in tomato plants. *Plant Sci.* 257, 74–83. doi: 10.1016/j.plantsci.2017.01.012

Win, K. T., Tanaka, F., Okazaki, K., and Ohwaki, Y. (2018). The ACC deaminase expressing endophyte *Pseudomonas* spp. Enhances NaCl stress tolerance by reducing stress-related ethylene production, resulting in improved growth, photosynthetic performance, and ionic balance in tomato plants. *Plant Physiol. Biochem.* 127, 599–607. doi: 10.1016/j.plaphy.2018.04.038

Wu, H., Zhang, X., Giraldo, J. P., and Shabala, S. (2018). It is not all about sodium: Revealing tissue specificity and signalling roles of potassium in plant responses to salt stress. *Plant Soil* 431, 1–17. doi: 10.1007/s11104-018-3770-y

Wu, J., Wang, J., Pan, C., Guan, X., Wang, Y., Liu, S., et al. (2014). Genome-wide identification of MAPKK and MAPKKK gene families in tomato and transcriptional profiling analysis during development and stress response. *PLoS One* 9:e103032. doi: 10.1371/journal.pone.0103032

Wu, X., Jia, Q., Ji, S., Gong, B., Li, J., Lü, G., et al. (2020). Gamma-aminobutyric acid (GABA) alleviates salt damage in tomato by modulating Na^+ uptake, the *GAD* gene, amino acid synthesis and reactive oxygen species metabolism. *BMC Plant Biol.* 20:465. doi: 10.1186/s12870-020-02669-w

Xian, Z., Yang, Y., Huang, W., Tang, N., Wang, X., and Li, Z. (2013). Molecular cloning and characterisation of *SlAGO* family in tomato. *BMC Plant Biol.* 13:126. doi: 10.1186/1471-2229-13-126

Xiang, Y., and Jiménez-Gómez, J. M. (2020). SlHAK20: A new player in plant salt tolerance. *EMBO J.* 39:e104997. doi: 10.15252/embj.2020104997

Xu, J., Hua, K., and Lang, Z. (2019). Genome editing for horticultural crop improvement. *Hortic. Res.* 6:113. doi: 10.1038/s41438-019-0196-5

Xu, J., Kang, Z., Zhu, K., Zhao, D., Yuan, Y., Yang, S., et al. (2021). *RBOH1*-dependent H_2O_2 mediates spermine-induced antioxidant enzyme system to enhance tomato seedling tolerance to salinity-alkalinity stress. *Plant Physiol. Biochem.* 164, 237–246. doi: 10.1016/j.plaphy.2021.04.017

Xu, W., Jia, L., Shi, W., Baluıka, F., Kronzucker, H. J., Liang, J., et al. (2013). The tomato 14-3-3 protein TFT4 modulates H^+ efflux, basipetal auxin transport, and the PKS5-J3 pathway in the root growth response to alkaline stress. *Plant Physiol.* 163, 1817–1828. doi: 10.1104/pp.113.224758

Xu, W. F., and Shi, W. M. (2006). Expression profiling of the 14-3-3 gene family in response to salt stress and potassium and iron deficiencies in young tomato (*Solanum lycopersicum*) roots: Analysis by real-time RT–PCR. *Ann. Bot.* 98, 965–974. doi: 10.1093/aob/mcl189

Xu, W. F., and Shi, W. M. (2007). Mechanisms of salt tolerance in transgenic *Arabidopsis thaliana* constitutively overexpressing the tomato 14-3-3 protein *TFT7*. *Plant Soil* 301, 17–28. doi: 10.1007/s11104-007-9403-5

Xu, Z., Wang, J., Zhen, W., Sun, T., and Hu, X. (2022). Abscisic acid alleviates harmful effect of saline–alkaline stress on tomato seedlings. *Plant Physiol. Biochem.* 175, 58–67. doi: 10.1016/j.plaphy.2022.01.018

Yamaguchi, T., and Blumwald, E. (2005). Developing salt-tolerant crop plants: Challenges and opportunities. *Trends Plant Sci.* 10, 615–620. doi: 10.1016/j.tplants.2005.10.002

Yang, J., Wang, P., Li, S., Liu, T., and Hu, X. (2022). Polyamine oxidase triggers H_2O_2-mediated spermidine improved oxidative stress tolerance of tomato seedlings subjected to saline-alkaline stress. *Int. J. Mol. Sci.* 23:1625.

Yang, X. J., and Seto, E. (2007). HATs and HDACs: From structure, function and regulation to novel strategies for therapy and prevention. *Oncogene* 26, 5310–5318. doi: 10.1038/sj.onc.1210599

Yang, Y., and Guo, Y. (2018a). Elucidating the molecular mechanisms mediating plant salt-stress responses. *New Phytol.* 217, 523–539. doi: 10.1111/nph.14920

Yang, Y., and Guo, Y. (2018b). Unraveling salt stress signaling in plants. *J. Integr. Plant Biol.* 60, 796–804. doi: 10.1111/jipb.12689

Yang, Y., Tang, N., Xian, Z., and Li, Z. (2015). Two *SnRK2* protein kinases genes play a negative regulatory role in the osmotic stress response in tomato. *Plant Cell Tiss. Organ Cult.* 122, 421–434. doi: 10.1007/s11240-015-0779-2

Yang, Y., Yao, Y., Li, J., Zhang, J., Zhang, X., Hu, L., et al. (2022). Trehalose alleviated salt stress in tomato by regulating ROS metabolism, photosynthesis, osmolyte synthesis, and trehalose metabolic pathways. *Front. Plant Sci.* 13:772948. doi: 10.3389/fpls.2022.772948

Yang, Z., Wang, C., Xue, Y., Liu, X., Chen, S., Song, C., et al. (2019). Calcium-activated 14-3-3 proteins as a molecular switch in salt stress tolerance. *Nat. Commun.* 10, 1–12. doi: 10.1038/s41467-019-09181-2

Yi, C., Yao, K., Cai, S., Li, H., Zhou, J., Xia, X., et al. (2015). High atmospheric carbon dioxide-dependent alleviation of salt stress is linked to RESPIRATORY BURST OXIDASE 1 (*RBOH1*)-dependent H_2O_2 production in tomato (*Solanum lycopersicum*). *J. Exp. Bot.* 66, 7391–7404. doi: 10.1093/jxb/erv435

Yin, W., Hu, Z., Hu, J., Zhu, Z., Yu, X., Cui, B., et al. (2017). Tomato (*Solanum lycopersicum*) MADS-box transcription factor *SlMBP8* regulates drought, salt tolerance and stress-related genes. *Plant Growth Regul.* 83, 55–68. doi: 10.1007/s10725-017-0283-2

Yin, Z., Lu, J., Meng, S., Liu, Y., Mostafa, I., Qi, M., et al. (2019). Exogenous melatonin improves salt tolerance in tomato by regulating photosynthetic electron flux and the ascorbate–glutathione cycle. *J. Plant Interact.* 14, 453–463. doi: 10.1080/17429145.2019.1645895

Yu, W., Wang, L., Zhao, R., Sheng, J., Zhang, S., Li, R., et al. (2019). Knockout of *SlMAPK3* enhances tolerance to heat stress involving ROS homeostasis in tomato plants. *BMC Plant Biol.* 19:354. doi: 10.1186/s12870-019-1939-z

Yu, X., Gao, Q., Chen, G., Guo, J. E., Guo, X., Tang, B., et al. (2018). *SlHDA5*, a tomato histone deacetylase gene, is involved in responding to salt, drought, and ABA. *Plant Mol. Biol. Rep.* 36, 36–44. doi: 10.1007/s11105-017-1057-8

Yuan, F., Yang, H., Xue, Y., Kong, D., Ye, R., Li, C., et al. (2014). OSCA1 mediates osmotic-stress-evoked Ca^{2+} increases vital for osmosensing in *Arabidopsis*. *Nature* 514, 367–371. doi: 10.1038/nature13593

Zhang, Y., Kaiser, E., Zhang, Y., Yang, Q., and Li, T. (2018). Short-term salt stress strongly affects dynamic photosynthesis, but not steady-state photosynthesis, in tomato (*Solanum lycopersicum*). *Environ. Exp. Bot.* 149, 109–119. doi: 10.1016/j.envexpbot.2018.02.014

Zhang, X., Chen, L., Shi, Q., and Ren, Z. (2020b). *SlMYB102*, an R2R3-type MYB gene, confers salt tolerance in transgenic tomato. *Plant Sci.* 291:110356. doi: 10.1016/j.plantsci.2019.110356

Zhang, Y., Yao, Q., Shi, Y., Li, X., Hou, L., Xing, G., et al. (2020c). Elevated CO_2 improves antioxidant capacity, ion homeostasis, and polyamine metabolism in tomato seedlings under $Ca(NO_3)_2$-induced salt stress. *Sci. Hortic.* 273:109644. doi: 10.1016/j.scienta.2020.109644

Zhang, X., Bao, Z., Gong, B., and Shi, Q. (2020a). *S-adenosylmethionine synthetase 1* confers drought and salt tolerance in transgenic tomato. *Environ. Exp. Bot.* 179:104226. doi: 10.1016/j.envexpbot.2020.104226

Zhao, C., Zhang, H., Song, C., Zhu, J. K., and Shabala, S. (2020). Mechanisms of plant responses and adaptation to soil salinity. *Innovation* 1:100017. doi: 10.1016/j.xinn.2020.100017

Zhao, L., Lu, J., Zhang, J., Wu, P. Y., Yang, S., and Wu, K. (2015). Identification and characterization of histone deacetylases in tomato (*Solanum lycopersicum*). *Front. Plant Sci.* 5:760. doi: 10.3389/fpls.2014.00760

Zhao, S., Zhang, Q., Liu, M., Zhou, H., Ma, C., and Wang, P. (2021). Regulation of plant responses to salt stress. *Int. J. Mol. Sci.* 22:4609. doi: 10.3390/ijms22094609

Zheng, M., Liu, X., Lin, J., Liu, X., Wang, Z., Xin, M., et al. (2019). Histone acetyltransferase GCN5 contributes to cell wall integrity and salt stress tolerance by altering the expression of cellulose synthesis genes. *Plant J.* 97, 587–602. doi: 10.1111/tpj.14144

Zheng, Q., Liu, J., Liu, R., Wu, H., Jiang, C., Wang, C., et al. (2016). Temporal and spatial distributions of sodium and polyamines regulated by brassinosteroids in enhancing tomato salt resistance. *Plant Soil* 400, 147–164. doi: 10.1007/s11104-015-2712-1

Zhong, M., Song, R., Wang, Y., Shu, S., Sun, J., and Guo, S. (2020). TGase regulates salt stress tolerance through enhancing bound polyamines-mediated antioxidant enzymes activity in tomato. *Environ. Exp. Bot.* 179:104191. doi: 10.1016/j.envexpbot.2020.104191

Zhou, Y., Diao, M., Chen, X., Cui, J., Pang, S., Li, Y., et al. (2019). Application of exogenous glutathione confers salinity stress tolerance in tomato seedlings by modulating ions homeostasis and polyamine metabolism. *Sci. Hortic.* 250, 45–58. doi: 10.1016/j.scienta.2019.02.026

Zhou, Y., Ding, M., Cui, J. X., Chen, X. J., Wen, Z. L., Zhang, J. W., et al. (2018). Exogenous GSH protects tomatoes against salt stress by modulating photosystem II efficiency, absorbed light allocation and H_2O_2-scavenging system in chloroplasts. *J. Integr. Agric.* 17, 2257–2272. doi: 10.1016/S2095-3119(18)62068-4

Zhou, Y., Wen, Z., Zhang, J., Chen, X., Cui, J., Xu, W., et al. (2017). Exogenous glutathione alleviates salt-induced oxidative stress in tomato seedlings by regulating glutathione metabolism, redox status, and the antioxidant system. *Sci. Hortic.* 220, 90–101. doi: 10.1016/j.scienta.2017.02.021

Zhu, J. K. (2016). Abiotic stress signaling and responses in plants. *Cell* 167, 313–324. doi: 10.1016/j.cell.2016.08.029

Zhu, M., Meng, X., Cai, J., Li, G., Dong, T., and Li, Z. (2018). Basic leucine zipper transcription factor SlbZIP1 mediates salt and drought stress tolerance in tomato. *BMC Plant Biol.* 18:83. doi: 10.1186/s12870-018-1299-0

Zhu, T., Deng, X., Zhou, X., Zhu, L., Zou, L., Li, P., et al. (2016). Ethylene and hydrogen peroxide are involved in brassinosteroid-induced salt tolerance in tomato. *Sci. Rep.* 6:35392. doi: 10.1038/srep35392

Zilberman, D., Cao, X., and Jacobsen, S. E. (2003). *ARGONAUTE4* control of locus-specific siRNA accumulation and DNA and histone methylation. *Science* 299, 716–719. doi: 10.1126/science.1079695

Zuluaga, M. Y. A., Milani, K. M. L., Miras-Moreno, M. B., Lucini, L., Valentinuzzi, F., Mimmo, T., et al. (2021). The adaptive metabolomic profile and functional activity of tomato rhizosphere are revealed upon PGPB inoculation under saline stress. *Environ. Exp. Bot.* 189:104552. doi: 10.1016/j.envexpbot.2021.104552

frontiers | Frontiers in Plant Science

TYPE Review
PUBLISHED 20 September 2022
DOI 10.3389/fpls.2022.993194

Check for updates

OPEN ACCESS

EDITED BY
Caroline Müller,
Universidade Federal da Fronteira Sul, Brazil

REVIEWED BY
Ting Zheng,
Sichuan Normal University, China
Babar Usman,
Kyung Hee University, South Korea

*CORRESPONDENCE
Dinesh Kumar Yadav
dky@allduniv.ac.in

SPECIALTY SECTION
This article was submitted to Plant Abiotic Stress, a section of the journal Frontiers in Plant Science

RECEIVED 13 July 2022
ACCEPTED 16 August 2022
PUBLISHED 20 September 2022

CITATION
Singh M, Singh A, Yadav N and Yadav DK (2022) Current perspectives of ubiquitination and SUMOylation in abiotic stress tolerance in plants. *Front. Plant Sci.* 13:993194. doi: 10.3389/fpls.2022.993194

COPYRIGHT
© 2022 Singh, Singh, Yadav and Yadav. This is an open-access article distributed under the terms of the Creative Commons Attribution License (CC BY). The use, distribution or reproduction in other forums is permitted, provided the original author(s) and the copyright owner(s) are credited and that the original publication in this journal is cited, in accordance with accepted academic practice. No use, distribution or reproduction is permitted which does not comply with these terms.

Current perspectives of ubiquitination and SUMOylation in abiotic stress tolerance in plants

Madhavi Singh[1], Ananya Singh[1], Neelam Yadav[2] and Dinesh Kumar Yadav[1]*

[1]Plant Molecular Biology and Genetic Engineering Laboratory, Department of Botany, University of Allahabad, Prayagraj, India, [2]Department of Botany, University of Allahabad, Prayagraj, India

Post-translational modification (PTM) is a critical and rapid mechanism to regulate all the major cellular processes through the modification of diverse protein substrates. Substrate-specific covalent attachment of ubiquitin and Small Ubiquitin-Like Modifier (SUMO) with the target proteins, known as ubiquitination and SUMOylation, respectively, are crucial PTMs that regulate almost every process in the cell by modulating the stability and fidelity of the proteins. Ubiquitination and SUMOylation play a very significant role to provide tolerance to the plants in adverse environmental conditions by activating/deactivating the pre-existing proteins to a great extent. We reviewed the importance of ubiquitination and SUMOylation in plants, implicating its prospects in various abiotic stress regulations. An exhaustive study of molecular mechanisms of ubiquitination and SUMOylation of plant proteins and their role will contribute to the understanding of physiology underlying mitigation of the abiotic stresses and survival in plants. It will be helpful to strategize the improvement of crops for abiotic stress tolerance.

KEYWORDS

26S proteasome, abiotic stress, deubiquitination, E3 ligases, post-translational modification, SUMOylation, transcription factor, ubiquitination

Introduction

Plants are constantly exposed to a variety of unfavorable conditions which limit their growth. They maintain their homeostasis under stressful environments by modifying several metabolic cascades using complex multi-targeted molecular approaches that eventually alter the proteome to sense and alleviate the effects of stresses (Kosová et al., 2011; dos Reis et al., 2012). Plant proteome is remarkably transformed by post-translational modifications (PTMs) under stressful conditions and plays a key role to alter the structure, function, and abundance of cellular proteins by reversible/irreversible covalent attachment of reactive groups, complex molecules or peptides, and cleavage of oligopeptides (Figure 1; Table 1). PTMs regulate diverse cellular processes, including intracellular and extracellular signal transduction, protein-protein interaction, gene expression, and cell-cell interaction. Thus, PTMs greatly expand the dynamic regulation

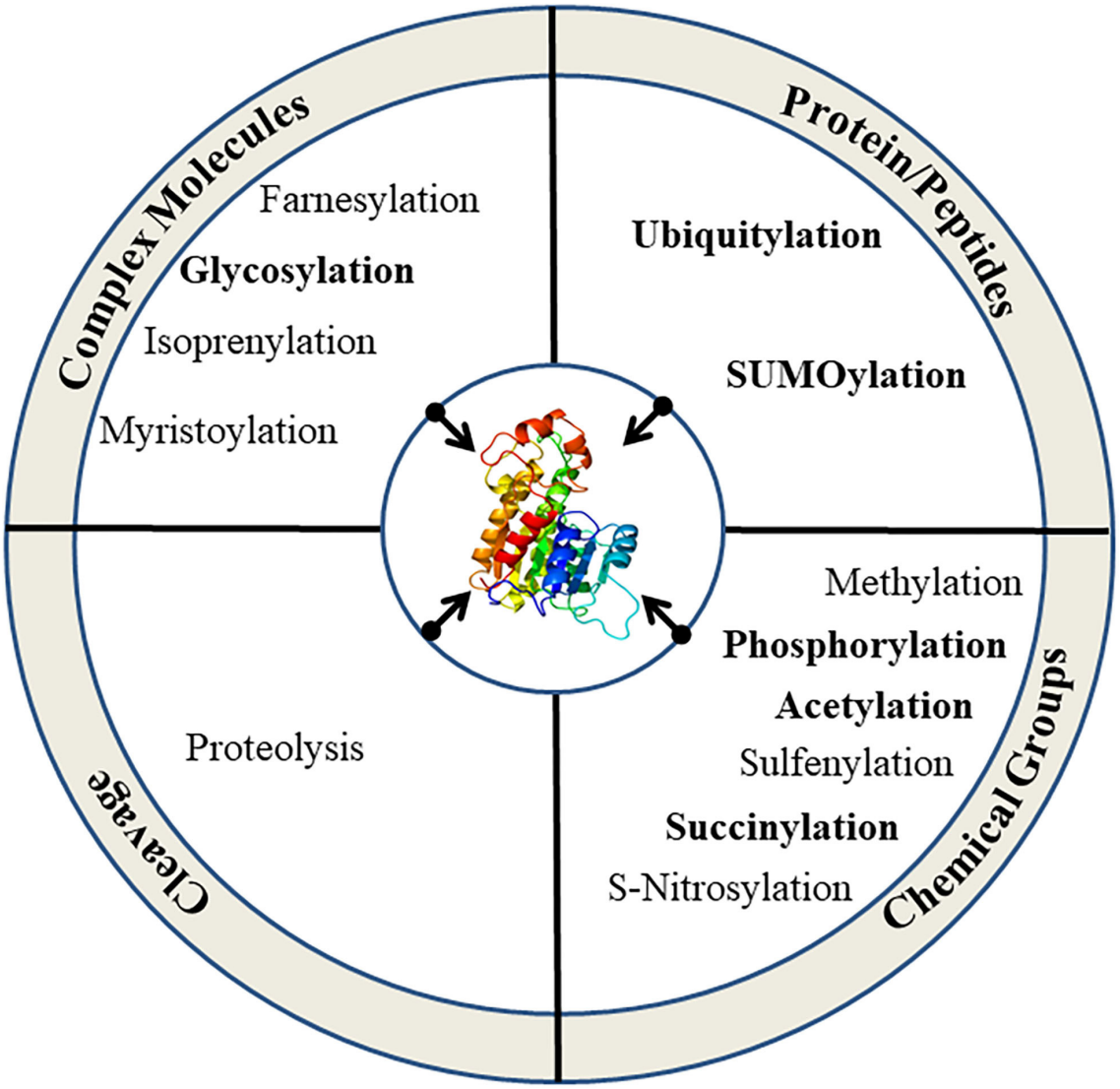


FIGURE 1
Types of PTMs in eukaryotic cells. More frequent types of PTMs are highlighted.

of cell physiology (Deribe et al., 2010; Shumyantseva et al., 2014). Advancement in proteomic technologies and bioinformatics has immensely facilitated the development of integrative databases of quantitative PTMs in plants (Table 2). Xue et al. (2022), presented >1 million experimentally identified PTM events under 583 conditions for 23 PTM types in 43 plants (http://qptmplants.omicsbio.info; Figure 2). The significance of PTMs in plants can be understood by the fact that 10% of the Arabidopsis genome is dedicated to the two most frequent PTMs viz. phosphorylation and ubiquitination (Lehti-shiu and Shiu, 2012). Furthermore, plants have a larger protein kinase superfamily than other eukaryotes (Mazzucotelli et al., 2006), possibly due to their increased need to be resilient (Hanada et al., 2008). The frequency of PTM types, sites, and chemical moieties covalently attached to proteins in various PTM events are shown in Table 1. Phosphorylation is the most frequent and important PTM-type and plays a crucial role in plant signaling and activation/deactivation of important enzymes/substrates (García-Mauriño et al., 2003), transcription factors (TFs) (Agarwal et al., 2007), and other effector proteins. Histone acetylation regulates gene expression, allowing transcription activation through DNA-binding proteins, and plays a key role under abiotic stresses (Weng et al., 2014; Hu et al., 2015; Li et al., 2021). Recently identified PTM types, such as butyrylation, crotonylation, glutarylation, malonylation, propionylation, succinylation, and 2-hydroxyisobutyrylation,

TABLE 1 Frequency of post-translational modification (PTM) types, sites, and chemical moieties covalently attached to proteins in various PTM events.

PTM-type	Frequency of PTM types (%)	PTM site on protein	Chemical moiety attached
Phosphorylation	55.67	R-R/K-x-S-ϕ	Phosphoryl- group
Lysine Acetylation	12.93	ε-NH_2 group of Lysine	Acetyl- group
Lysine Ubiquitination	8.63	ε-NH_2 group of Lysine	76- residues long Ubiquitin
Lysine 2-hydroxyisobutyrylation	6.66	KxxxxK$_{hib}$; K$_{hib}$xxxxK; KxxxxxxK$_{hib}$; K$_{hib}$xxxxxxK; KTxxxxK$_{hib}$; DxxK $_{hib}$	Hydroxyisobutryl group
Lysine Succinylation	3.41	-NH_2 group of Lysine	Succinyl- group
Lysine Crotonylation	3.10	ε-NH_2 group of Lysine	Crotonyl group
N-glycosylation	2.34	-NH_2 group of Asn in N-X-S/T site	Complex glycans
S-nitrosylation	1.77	-SH group of Cys; Phenyl group of Tyr-	Nitric oxide
N-terminal Acetylation	1.70	α-NH_2 of N-terminus of protein	Acetyl- group
S-sulfenylation	1.61	-SH group of Cys (R-SH)	Sulfenic acid (R-SOH)
Oxidation	0.54	Cys/Met/His/Arg/Lys/Pro/Trp	Oxo group,
Lysine Malonylation	0.41	-NH_2 group of Lysine	Malonyl- group
Methylation	0.31	Lys/Arg/Ala/Asn/His/Asp/Cys/Gly,	Methyl group
Glycation	0.23	ε-NH_2 group of Lysine/Arginine	Hexoses
Carbonylation	0.21	Lys/Arg/Pro/Thr	Carbonyl group
O-Glycosylation	0.20	-OH group of S/T in -P-(V/T)-g(S)-(S/T)-A	Complex glycans
Persulfidation	0.09	-SH group of Cys, Glutathione disulfide, Protein Sulfenic acid, Cys persulfide	Persulfide (R-S-SH) Polysulfides
Lysine SUMOylation	0.07	ψKXE/D	Small Ub-related protein modifiers
N-terminal Myristoylation	0.05	N-terminal Glycine	Myristoyl- lipid group
S-cyanylation	0.03	-SH group of Cys	Cyano group (R-S-CN)
S-glutathionylation	0.03	-SH group of Cys	Glutathione group (R-S-SG)
Lysine Butyrylation	0.01	ε-NH_2 group of Lysine	Butyryl group/Isobutyryl group

greatly influence the growth, differentiation, and metabolism of plants (Huang et al., 2017; Feng et al., 2021; Xu et al., 2021). Glycosylation has a vital role in protein folding, signaling, intermolecular interactions, cell-cell adhesion, ER signaling, etc. that leads to abiotic stress tolerance. Ubiquitination also plays a critical role in various abiotic stress responses (Ning et al., 2011; Yanagawa and Komatsu, 2012; Peng et al., 2019; Lim et al., 2020; Zhang et al., 2021). SUMOylation is another significant PTM that alters the function, location, and turnover of target proteins and plays a critical role in the development and abiotic stress tolerance (Kurepa et al., 2003; Conti et al., 2008; Castro et al., 2012; Augustine and Vierstra, 2018; Liu et al., 2019; Hu et al., 2022). We reviewed the prospects of molecular mechanism and cross-talk between ubiquitination and SUMOylation of plant proteome under abiotic stress conditions and their role in stress mitigation.

Ubiquitination

Protein ubiquitination is the third most frequent, reversible, and extremely diverse PTM type in plants. The ubiquitination processing machinery, Ubiquitin 26S Proteasome System (UPS), plays a crucial role in the precise regulation of gene transcription, DNA replication and repair, quality and abundance of short-lived regulatory proteins, misfolded proteins, and protein trafficking processes in eukaryotes (Vierstra, 2009). The UPS involves covalent attachment of 76 amino acids' long, highly conserved ubiquitin-protein modifier to lysine residues on target proteins in various configurations to accomplish diverse fates (Weissman, 2001). The UPS targets ∼80% of the proteins of a eukaryotic cell for degradation (Herrmann et al., 2007). Genome-wide studies showed that ∼6% of *Arabidopsis thaliana* genome is committed to UPS,

TABLE 2 Prediction and analysis tools for ubiquitination sites.

Tool	Algorithm	OS	Web address
UBPred	Random Forest	Linux, Windows	http://www.ubpred.org
CKSAAP_UbSite	SVM	Linux	http://protein.cau.edu.cn/cksaap_ubsite/
UbSite	SVM	–	No server
mRMR_Ub Site	Nearest Neighbor	–	No server
UbiNet	Densely connected neural networks	Windows	http://140.138.144.145/~ubinet/index.php
UbiComb	Deep learning	Windows	http://nsclbio.jbnu.ac.kr/tools/UbiComb/
plantsUPS	–	Windows	http://bioinformatics.cau.edu.cn/plantsUPS/

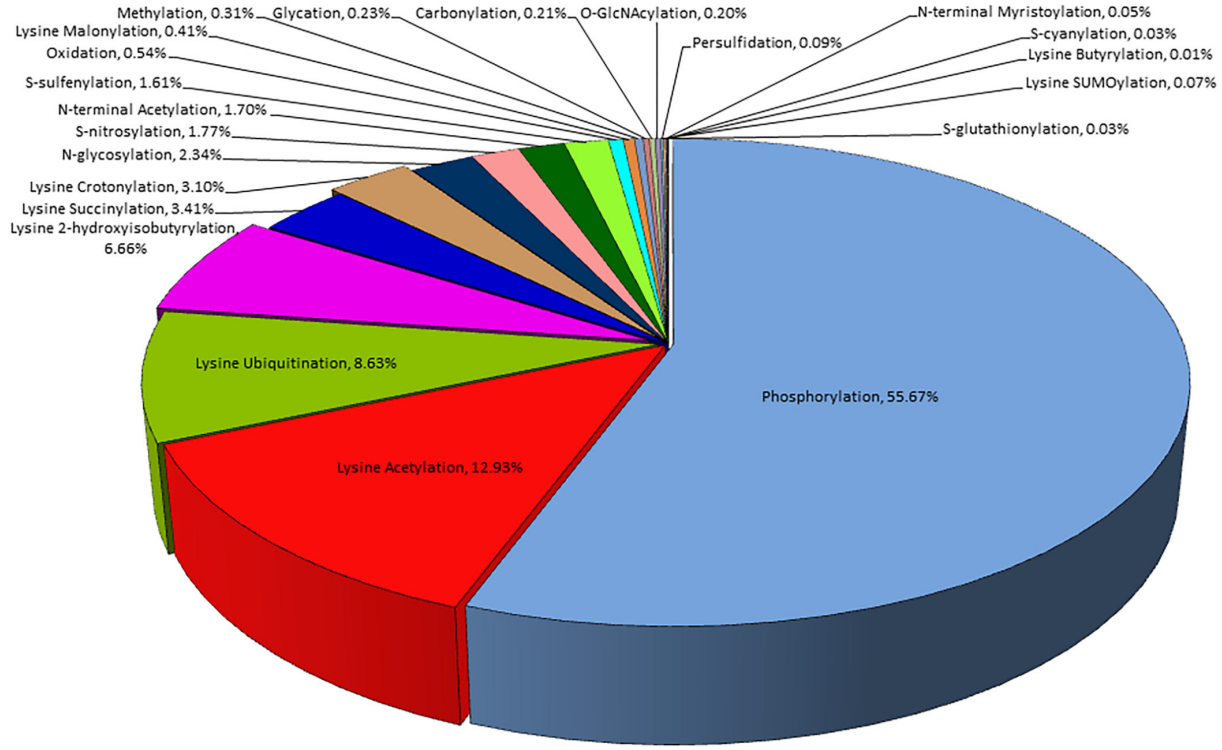


FIGURE 2
Frequency of common PTM types in plants.

the majority of which code for ubiquitin ligases (E3s) (Yu et al., 2016). The 3-D structure of ubiquitin characteristically has a signature β-grasp domain at the center, enclosing a conserved hydrophobic core. This compact globular structure and extensive H-bonding make ubiquitin unusually stable. Ubiquitin structure displays equipoise between rigidity and flexibility where flexible regions are centered on rigid hotspots to provide high binding affinity and specificity. Ubiquitin protein contains seven highly conserved lysine residues (Lys_6, Lys_{11}, Lys_{27}, Lys_{29}, Lys_{33}, Lys_{48}, and Lys_{63}), which can be selectively ubiquitinated to produce structurally diverse ubiquitination patterns in the target protein (Kirkpatrick et al., 2006; Kim et al., 2007). The NH_2- of methionine 1 at the N-terminus also serves as a receptor site for homotypic polyubiquitination (Rittinger and Ikeda, 2017). Diversity in ubiquitination patterns arises from the distinct length and topology of ubiquitin chain(s) attached to specific lysine residues. This interactive ability of ubiquitin might be the reason for the asymmetric complexity of the UPS that reinforces an extended interactome relying on a single molecule. Polyubiquitination of Lys48 of ubiquitin majorly leads to the degradation of misfolded proteins and obsolete proteins, through the ATP-dependent multimeric 26S proteasome system (Mazzucotelli et al., 2008). However, Lys63-linked polyubiquitination of target protein serves as a signal for endocytosis, protein activation, and intracellular trafficking (Pickart and Fushman, 2004). Several ubiquitin

moieties attached to the target protein, i.e., monoubiquitination of single or multiple lysine residues, are the additional criteria for ubiquitination and regulate the distribution and function of proteins, thereby regulating various metabolic pathways from transcriptional regulation to membrane transport (Hicke, 2001). Yeast and oat ubiquitin sequences differ by three residues from human ubiquitin but by only two residues from each other. These differences might have led to a functional variation of ubiquitin in plants and animals. However, their major H-bonding patterns and secondary structural features are uniformly conserved. Target proteins are ubiquitinated through sequential reactions carried out by three enzymes: ubiquitin-activating (UBA; E1), ubiquitin conjugation (UBC; E2), and ubiquitin ligase (E3) enzymes. Ubiquitination of protein initiates with the activation of ubiquitin by E1 in an ATP-dependent manner, forming a thioester bond between the C-terminus of activated ubiquitin and the thiol group of a catalytic cysteine residue, forming the E1-Ub intermediate. Thereafter, E2 accepts the activated ubiquitin from the E1-Ub complex and conjugates it onto the cysteine, forming a thioester-linked E2-Ub intermediate (Figure 3). A canonical E1 enzyme has three conserved domains: an adenylation domain for the formation of Ub-adenylate; a catalytic domain with a conserved cysteine residue that links with the di-glycine motif of Ub; and a ubiquitin fold domain (UFD) to associate with E2. In processes where other ubiquitin-like proteins (UBLs) are also part of the conjugation cascade, E1 enzymes confer specificity by matching a particular UBL with only cognate E2s. E2s have 140 amino acid UBC domains, possessing a highly conserved Cys-residue that accepts activated ubiquitin transferred from E1-Ub and facilitates interaction between E3 and E2-Ub intermediate (Wu et al., 2003; Kraft et al., 2005). Although there is an overlap between regions of the UBC domain interacting E1-Ub and E3, the binding of E2 to E1 and E3 is mutually exclusive. Certain members of the E2 family feature variable N- and/or C-terminal extensions that result in functional diversity of E2 to subcellular localization and pathway-specific E1/E2/E3 interactions. E2 enzymes mainly determine the length, specificity of chain assembly, and topology of ubiquitin networks (Kim et al., 2007; Ye and Rape, 2009; Rodrigo-Brenni et al., 2010). E2-E3 combination also determines the topology of the ubiquitin chain (Deshaies and Joazeiro, 2009). E3 ligases are critical regulators that dictate the efficiency and specificity of ubiquitination by recruiting the appropriate target proteins. Simultaneous but asymmetric loading of two ubiquitin molecules on E1, the non-covalent binding of Ub-adenylate, and cysteine-esterification of Ub are remarkable features of the E1-E2 cycle. Studies suggest that coupling of the second adenylation reaction to E2-Ub transfer stabilizes catalytically competent E1 into an energetically favorable conformation, which complements the rate of E2 transthiolation. The E2-Ub complex then concomitantly interacts with group-specific E3 ligases, which, in turn, associate with the target protein to form an isopeptide bond between the C-terminal glycine of activated ubiquitin and Lys of the target protein. This process of ubiquitination is repeated under the strict regulation of E2 and E3 (Komander and Rape, 2012) and can be reversed by deubiquitinating enzymes (DUBs) (Komander et al., 2009). Deubiquitination is the hydrolysis of peptide bonds at highly conserved Gly_{76} residue of ubiquitin, which has constitutive and regulated activities in the cell. DUBs are mainly involved in the following: (i) post-translational processing of ubiquitin precursors that are typically encoded as fusions to itself or other proteins to generate Ub monomers; (ii) protection of activated ubiquitin against various intracellular nucleophiles such as glutathione and polyamines; (iii) regeneration of ubiquitin and/or polyubiquitin chains from Ub-conjugates committed for proteasomal degradation; and (iv) disassembly of unanchored poly-Ub chains to restore and maintain an adequate pool of free ubiquitin in the cell. DUBs can also rescue committed substrates from proteasomal degradation by altering their half-life in response to specific signaling events, thereby serving as the negative regulators of protein degradation. Moreover, DUBs have been proposed to perform final proof-reading activity for the degradation to rescue proteins targeted inappropriately to the proteasome (Lam et al., 1997). DUBs have two signature motifs: the 18 amino acid long Cys-box and a His-box of varying length with conserved catalytic cysteine and histidine residues, respectively. DUBs are crucial in cellular ubiquitin homeostasis and comprise the ubiquitin C-terminal hydrolase (UCH) family and the ubiquitin-specific processing protease (UBP) family. The UCHs preferentially deubiquitinate small peptides and amino acids, while UBPs seem to remove ubiquitin specifically from the proteins targeted for ubiquitination. The Arabidopsis genome expresses 64 DUBs that are classified into five sub-families based on domain organization and catalytic residues: Ubiquitin-specific Protease/Ubiquitin-binding Protease (USP/UBP), Ubiquitin C-Terminal Hydrolase (UCH), Ovarian Tumor (OTU) protease, Machado-Joseph Domain Protease (MJD), and JAB1/MPN/MOV34 (JAMM) protease. The first four are cysteine proteases, while JAMM family members are metalloisopeptidases and require zinc as a cofactor. Often, polyubiquitination and deubiquitination reactions take place in unison, thereby ensuring the abundance of essential enzymes and the regulatory proteins required in the regulatory networks.

The extensive repertoire of E3s differentially modifies diverse target proteins. Plant genomes contain one or two E1s, tens of E2s, and >1,000 of E3s encoding genes (Chen and Hellmann, 2013). The Arabidopsis genome has two E1, 37 E2, 8 E2-like, and >1,300 E3 encoding genes or components of E3 complexes (Stone, 2014). Based on the domain architecture and mechanism of action, the E3 ubiquitin ligases are classified into four classes: Homology to E6-Associated Carboxyl-Terminus (HECT)-type, Really Interesting

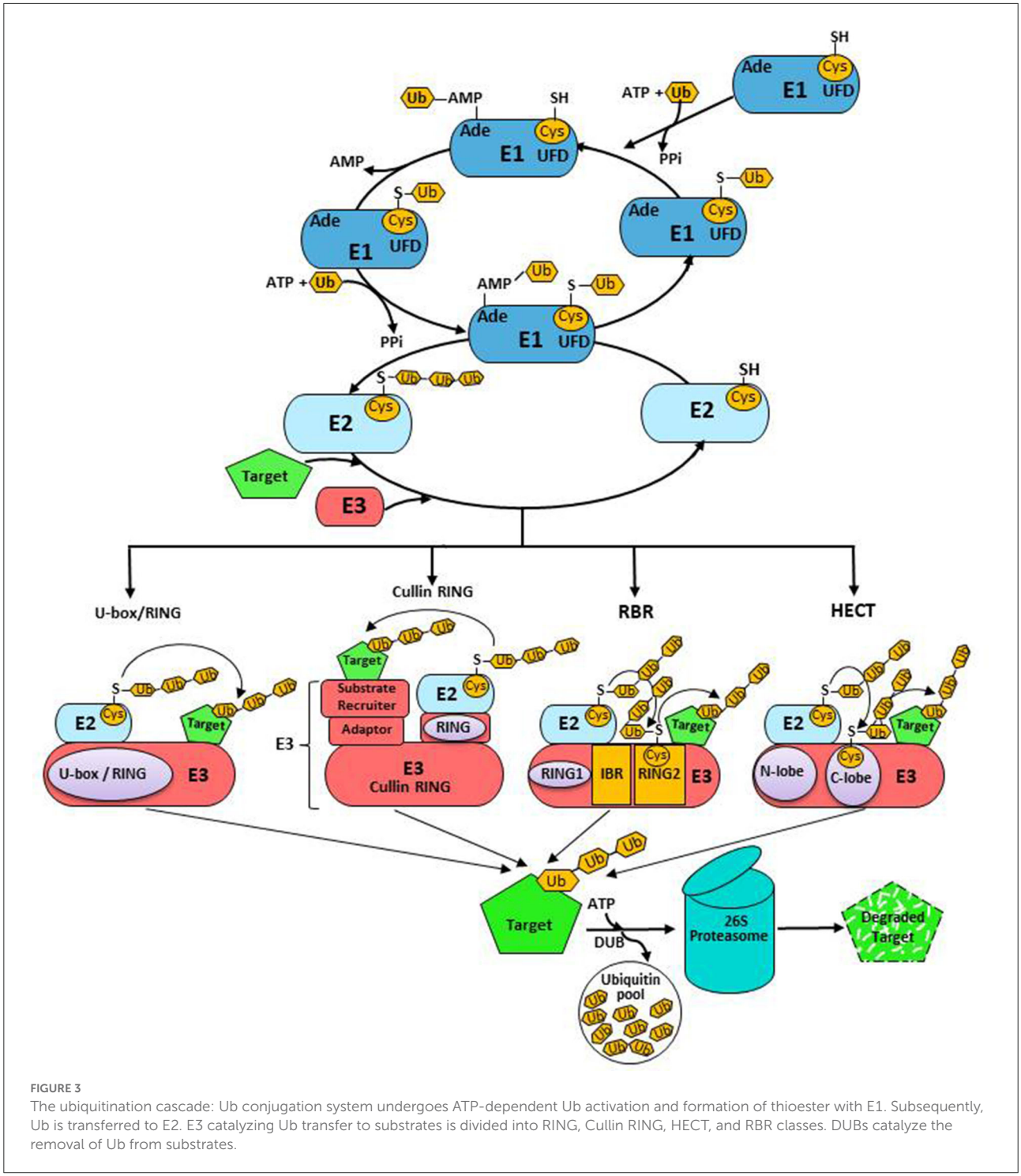


FIGURE 3
The ubiquitination cascade: Ub conjugation system undergoes ATP-dependent Ub activation and formation of thioester with E1. Subsequently, Ub is transferred to E2. E3 catalyzing Ub transfer to substrates is divided into RING, Cullin RING, HECT, and RBR classes. DUBs catalyze the removal of Ub from substrates.

New Gene (RING)-type/ U-box-type, Cullin RING ubiquitin Ligases (CRLs), and RING-IBR-RING (RBR) (Zheng and Shabek, 2017). Most of the plant E3s belong to the RING-type group and the Arabidopsis genome has >470 genes coding for RING-type E3s (Kraft et al., 2005). The majority of RING-type E3s are monomers containing RING-domain and substrate-recruiting modules in a single polypeptide. However, RING-type domains tend to form homo- or hetero-dimers. Unlike RING E3s that function as allosteric activators, HECT E3s are catalytically active and uniquely form E3-Ub thioester intermediate (Huibregtse et al., 1995) and catalyze polyubiquitination independent of their cognate E2s (Lorenz,

2018). Plant genomes contain significantly higher numbers of U-box protein-related genes as compared to other eukaryotes (Li et al., 2008; Yee and Goring, 2009; Lyzenga and Stone, 2012). The Arabidopsis and rice genomes have 64 and 77 U-box-related genes, respectively. U-box, ~70 amino acid long, is a modification of the RING-finger domain and folds into a scaffold structure like the RING domain. It lacks the classical zinc-chelating cysteine and histidine residues and forms multiple hydrogen bonds using cysteine, serine, and glutamate side chains. Hydrophobic interactions and salt bridges stabilize the corresponding hydrophobic core at the tertiary level (Callis, 2014).

Mechanistically, RBR-type E3s harbor a unique RING1-IN BETWEEN RING (IBR)-RING2 supra-domain that displays defined features of both RING- and HECT-type E3s. The N-terminal RING1, arranged in a cross-brace configuration, represents the typical RING domain, whereas RING2 and IBR domains adopt a common IBR-fold, coordinating two zinc ions that differ from the canonical cross-brace fold of RING1. The C-terminal RING2 is the catalytic subunit of RBR containing a conserved cysteine residue that accepts the donor ubiquitin from E2-Ub conjugate to generate a covalent E3-Ub intermediate, a feature typical of HECT-type E3s. With no catalytic cysteine, the IBR domain possesses two adjacent flexible linkers that enable three RBR sub-domains to adopt multiple conformations relative to each other, which, together with intramolecular interaction with regions outside the RBR domain, allow dynamic autoregulatory transitions between active and inhibited states. As aforementioned, RBR-type E3s function through a concerted RING/HECT-like molecular mechanism, wherein RING1 domains recruit and stabilize the cognate E2-Ub pair, facilitating the transfer of ubiquitin directly onto the RING2 cysteine to form a covalent HECT-like thioester intermediate. Subsequently, this charged Ub couples with its corresponding substrate. Unlike the RING and HECT-type E3s that are involved in the synthesis of diverse homohetrotypic chains, LUBAC, a multi-protein RBR, specifically catalyzes peptide-bond formation between Gly_{76} of existing and Met_1 of the incoming ubiquitin, yielding linear ubiquitin chains. Most of these ligases further strictly regulate their enzymatic activity by auto-inhibition and activation through specific protein-protein interactions and PTMs (Marín, 2010; Berndsen and Wolberger, 2014; Smit and Sixma, 2014; Dove and Klevit, 2017; Zheng and Shabek, 2017). Forty-two Arabidopsis RBR E3s are categorized into 4 sub-groups: Plant II (22 members), Plant I/helicase (3 members), ARA54 (1 member), and ARIADNE (16 members) (Fernandez et al., 2020). The RBR ligases are reported to regulate the turnover of core components of ABA signaling to modulate plant ABA responses. The ABA receptors, PYR/PYL/RCAR, are ubiquitinated in a spatial- and enzyme-dependent manner for the degradation *via* proteasomal or vacuolar pathways. For example, nuclear ubiquitination of PYR/PYL/RCAR ABA receptors is catalyzed by RFA4 and its cognate E2 UBC26, in addition to known CULLIN-RING E3 ligase (CRL4)-DDB1-ASSOCIATED1 (DDA1) complex, and is degraded in a proteasomal-dependent manner. By contrast, RSL1-mediated ubiquitination of PYL4 and PYR1 at plasma membrane destines modified proteins to endosome-mediated vacuolar degradation pathway through endosomal sorting complex required for transport (ESCRT) (Fernandez et al., 2020).

RING-type E3s exist in different structural contexts, one being multi-protein complexes, where a scaffold protein facilitates the assembly of different components. Plant CRLs are typical examples of multimeric RING E3 ligases and are further classified into four subfamilies: S phase kinase-associated protein 1-Cullin 1-F-box (SCF), Bric-a-brac-Tramtrack-Broad complex (BTB), DNA Damage-Binding domain-containing (DDB), and Anaphase-promoting complex (APC) (Hua and Vierstra, 2011). CRL family of E3 ligases is composed of four or five different protein subunits tethered together through a common adaptor protein. CRL uses Cullin proteins (CUL1, CUL3a/3b, or CUL4) as a platform to interact with E2-Ub binding RING proteins (RBX1/ROC1/ HRT1) at its C-terminal and substrate-recruiting protein at the N-terminal regions (Schwechheimer and Calderon Villalobos, 2004; Hotton and Callis, 2008). The substrate-recruiting subunit can either bind directly to the CUL protein or along with an adaptor protein. Degeneracy between catalytic and adaptor modules allows the association of diverse adaptors to the same catalytic subunit and forms distinct E3 complexes with a broad spectrum of substrate specificity exhibiting enormous plasticity in substrate specificity.

Ubiquitin code

Attachment of ubiquitin molecules to the substrate proteins in monomeric or polymeric forms linked through specific isopeptide bonds is known as ubiquitin code. Depending upon the linkage type, different ubiquitination patterns attain distinct conformations and lead to unique consequences in cells. Interestingly, ubiquitination has emerged as a cellular language to precisely communicate between and within cells. Monoubiquitination is the most basic form of ubiquitination and may occur on multiple Lys residues in the same protein to yield a multi-monoubiquitination. Owing to the type of linkage involved, ubiquitin chains can either be homotypic or heterotypic. In homotypic chains, all building blocks of the chain are linked through the same Lys or Met residues. However, heterotypic chains contain mixed and branched-type polyUb chains with different linkages in a single polymer. Thus, ubiquitin with its eight potential attachment sites, present all over the surface, enables the conjugates to adopt distinct but dynamic conformations. Moreover, ubiquitin is subject to additional PTMs like phosphorylation, acetylation, and ribosylation, which further expand the functional repertoire of Ub code. Extensive crosstalk among these PTMs directs

ubiquitin signal regulation and/or diversification. Various ubiquitin modifications are recognized by effector proteins with linkage-specific ubiquitin-binding domains (UBDs), which couple the modified substrate with the downstream events.

Proteomic analysis of the Arabidopsis ubiquitylome demonstrated that six of seven homogeneous substrate-bound Lys chains were in an order of abundance of Lys_{48} >Lys_{63} >Lys_{11}, followed by lower levels of Lys_{33} >Lys_{6} >Lys_{29} (Kim et al., 2013). Lys_{48} predominantly signals for proteasome-mediated degradation and is implicated in almost all aspects of plant signaling (Sadanandom et al., 2012; Walsh and Sadanandom, 2014). Lys_{63}-linked ubiquitin chains can also generate proteasomal degrons (Saeki et al., 2009) but mostly targets modified proteins to lysosome and vacuole for degradation (Welchman et al., 2005; Kirkin et al., 2009). Plants display similar abundance and patterns of the abovementioned ubiquitin modifications responsible for many cellular processes, including endocytic sorting, DNA repair, plant immunity, and plant nutritional deficiency responses (Miricescu et al., 2018). Additionally, a Ub linkage type, Lys_{29}, reportedly regulate the gibberellic acid (GA) pathway that signals for proteasomal degradation of DELLA proteins (Wang et al., 2009a). Other chains linked through Lys_{6}, Lys_{11}, and Lys_{33} are atypical to plants and have not been well-characterized. In addition to the polyubiquitin chain types, monoubiquitination is also responsive to various proteolytic (UPS or autophagy), as well as non-proteolytic signals, such as protein-protein interaction, localization, and activity modulation. Studies suggest that monoubiquitination of the histone H2B catalyzed by the E3 ligases, HISTONE MONOUBIQUITINYLATION 1 and 2 (HUB1 and HUB2), mediate plant immunity. Remarkably, to interpret and integrate the myriad of signals generated by the ubiquitin system, cells have evolved a range of specific UBDs that recognize multifaceted ubiquitin codes for different functions, primarily on the basis of a defined geometric assembly of different ubiquitin surfaces to trigger specific biological responses.

The ubiquitin 26S proteasome system (UPS)

The UPS is a large (∼2.5 MDa), multimeric ATP-dependent protease complex in all eukaryotic cells and serves as an elegant junk protein disposal system. It coordinates the abundance of various regulatory proteins involved in a myriad of signaling and metabolic pathways. Chaperon-assisted recognition and UPS-mediated degradation of aberrant proteins produced after translational errors or stresses emphasize the significance of UPS in protein quality control (Marshall and Vierstra, 2019). Since the proteasome is a negative regulator of the proteome, its regulation is critical for preserving homeostasis. Regulation of proteasome activity occurs at different levels, starting from its abundance and subcellular localization to proteolytic activity and post-function destruction, either through degradation of individual subunits or by removal of the proteasome as a whole (Livneh et al., 2016).

Substrate processing is a prerequisite for efficient protein degradation. The UPS combines strict substrate selectivity with extreme promiscuity for substrate processing to enable the degradation of thousands of proteins with high specificity. Importantly, tagging of proteins with Ubs is insufficient to label them for degradation. Apart from the protein sequence that determines ubiquitination, a loosely folded region near the end of the polypeptide is also required to determine the susceptibility of the target protein to proteasome for degradation. Thus, selective recognition of the Ub chain along with the poorly folded region is a fundamental basis for proteasomes to discriminate the target proteins for degradation from no-target proteins. Moreover, substrates' commitment to degradation is a critical and irreversible association between substrate and proteasome through its ATPase subunits, which, upon activation, drive the co-translational unfolding of substrates. The unstructured, unfolding-prone regions also serve as a starting point for translocation. Before the commitment, substrates undergo a reversible association with proteasome through intrinsic Ub receptors of 19S regulatory particle (RP) and facilitate their deubiquitination *via* DUBs. The majority of the substrates accomplish this binding to get deubiquitinated, but only those that undergo irreversible binding are designated as degron. Therefore, a kinetic competition between deubiquitination, release of the substrate, and allosteric activation of RP determine the fate of target proteins (Lee et al., 2001; Prakash et al., 2004; Peth et al., 2010; Yu et al., 2016; Collins and Goldberg, 2017).

UPS-dependent regulation of abiotic stresses in plants

Plants utilize the activity of UPS to combat various abiotic stresses by regulating the turnover of short-lived post-functional regulatory proteins or stress-induced damaged proteins to mitigate the effects of dynamic environmental stresses. Transcriptome and proteome studies in different abiotic stress-exposed plants showed altered levels of TFs, modulating the expression profile of stress-responsive genes (Ellis et al., 2002; Dooki et al., 2006; Zhang and Xie, 2007; Zhu et al., 2007; Guo et al., 2008; Pandey et al., 2008; Sharma and Pandey, 2019). Over-expression of mono/polyubiquitin genes was reported to independently modulate stress tolerance in different organs of Arabidopsis (Sun and Callis, 1997), maize (Christensen et al., 1992), tobacco (Genschik et al., 1992; Lyzenga and Stone, 2012), and potato (Garbarino et al., 1992).

The considerable number and functional diversity of E3 ligases indicate their significance in the modulation of multiple abiotic stress-induced responses. Various enzymes involved in hormone biosynthesis, the abundance of related TFs, and other effector proteins are potential substrates of E3 ligases. The Arabidopsis DELLA proteins, known to suppress GA signaling, are the typical example of ubiquitination-dependent regulation of hormone effect as degradation of DELLA proteins in presence of GA involves $SCF^{SLY/GID2}$ E3 ligase complex (Dill et al., 2004). The most common way employed by E3 ligases to regulate stress-related factors is to either act as a negative regulator that suppresses stress response pathways by targeting positive regulators for degradation or promotes stress signaling as positive response regulators that target negative regulators for degradation following stress perception or attenuate stress signaling by targeting positive regulators for degradation. In addition to E3, many E2 encoding genes are also stress-inducible. Transcript abundance of UBC2 in soybean (*GmUBC2*), groundnut (*AhUBC2*), and Arabidopsis (*AtUBC32*) was upregulated under water and/or salt stress (Zhou et al., 2010; Wan et al., 2011; Cui et al., 2012). Surprisingly, overexpression of *AtUBC32* rendered the plants sensitive to salt stress (Cui et al., 2012), while *atubc32* mutant plants were more tolerant to salt stress. Overexpression of mung bean UBC1 (*VrUBC1*), peanut (*AhUBC2*), or soybean (*GmUBC2*) genes in Arabidopsis plants showed improved tolerance to drought stress (Zhou et al., 2010; Wan et al., 2011; Chung et al., 2013). Overexpression of non-canonical cucumber Lys_{63}-linked polyubiquitinating conjugase (CsUBC13) in Arabidopsis regulates the Fe-responsive gene(s) and promotes root development under iron-deficient conditions (Li and Schmidt, 2010). Transgenic tobacco overexpressing wheat monoubiquitin gene, *Ta-Ub2*, ameliorates the salt, cold, and drought stress (Kang et al., 2016), and improves photosynthesis under high light stress (Tian et al., 2014). Wheat F-box protein gene *TaFBA1*, a core component of the SCF E3 ligase complex, provides heat tolerance (Li et al., 2018).

Altered UPS activity can also affect the plants' tolerance to various environmental stresses. Mutations in UPS, especially, in the RP subunits, decrease complex accumulation, reduce the rate of ubiquitin-dependent proteolysis, and amend plant response to abiotic stresses (Smalle et al., 2003; Smalle and Vierstra, 2004; Ueda et al., 2004; Kurepa et al., 2008). Arabidopsis mutants of *rpn10-1, rpn1a-4,* and *rpn1a-5* were less tolerant to salt stress (Smalle et al., 2003; Wang et al., 2009b). Also, *rpn10-1* plants were hypersensitive to UV-radiation and DNA-damaging agents (Smalle et al., 2003). *Rpn1a-4*, *rpn1a-5*, *rpn10-1*, *rpn12a-1*, and *rpt2a-2* exhibited reduced heat-shock tolerance (Kurepa et al., 2008; Wang et al., 2009b). Hypersensitivity to various stress conditions shown by RP mutants suggests the crucial role of the proteasome in modulating plant responses to adverse growth conditions. Expression analysis of 67 *Triticum aestivum* α- and β-type subunits of 20S proteasome core protease at the seedling stage showed that 10 genes were involved in heat stress responses, 4 genes were involved in drought tolerance, and 9 genes were expressed under both heat and drought stress conditions, suggesting their active role in multiple abiotic stresses (Sharma et al., 2022). A significant reduction in the number of ubiquitinated proteins in soybean roots by flood stress suggests a relationship between proteasome-mediated proteolysis and waterlogging (Yanagawa and Komatsu, 2012). Direct or indirect disruption of UPS and its after-effects establishes its importance in plant responses to various stress conditions.

E3 ligase function during drought stress

A well-described example of RING-type E3s is Dehydration Responsive Binding Element 2A (DREB2A) Interacting Protein1 (DRIP1) and DRIP2, which are involved in the regulation of stress-responsive ERF/AP2 transcription factor DREB2A that functions upstream of many drought- and salt-stress inducible genes (Figure 4A) (Qin et al., 2008). Accumulation of DREB2A only under drought conditions, *in vitro* ubiquitination of DREB2A by DRIP1, and increased stabilization of DREB2A in *drip1/drip2* double mutants indicate that the abundance of DREB2A is negatively regulated by DRIP1/2 (Sakuma et al., 2006a,b; Qin et al., 2008; Al-Saharin et al., 2022). Moreover, the increased abundance of DREB2A upon UPS inhibition and enhanced drought tolerance in *drip1/drip2* double mutants was concomitant with a significant increase in expression of several drought-inducible genes specifically regulated by DREB2A (Qin et al., 2008). It showed that DREB2A is unstable under non-stress conditions, and RING ligases DRIP1/2 function redundantly to suppress drought signaling *via* ubiquitin-mediated proteolysis of DREB2A. The presence of 30 residues' long serine and threonine-rich negative regulatory domain, the degron, makes DREB2A unstable and acts as a signal for ubiquitin-mediated degradation. In absence of stress, DRIP1/2 localizes in the nucleus, interacts with DREB2A, and directs the destruction of DREB2A (Qin et al., 2008). Under stress conditions, perhaps the DREB2A degron is made unavailable to degradation machinery, which leads to accumulation and stabilization of DREB2A. Since stress conditions do not affect the transcript levels of DRIP1/2, there is a possibility that drought-induced re-localization of DRIP1/2 to cytosol may lead to DREB2A stabilization. Stress Associated Protein5 (SAP5) is another E3 that functions upstream of DRIP1/2 ligases and promotes their degradation, thereby modulating drought-stress responses positively in Arabidopsis and wheat. Moreover, Arabidopsis SAP5 has been reported as a positive regulator of salt and osmotic stress tolerance (Al-Saharin et al., 2022; Table 3).

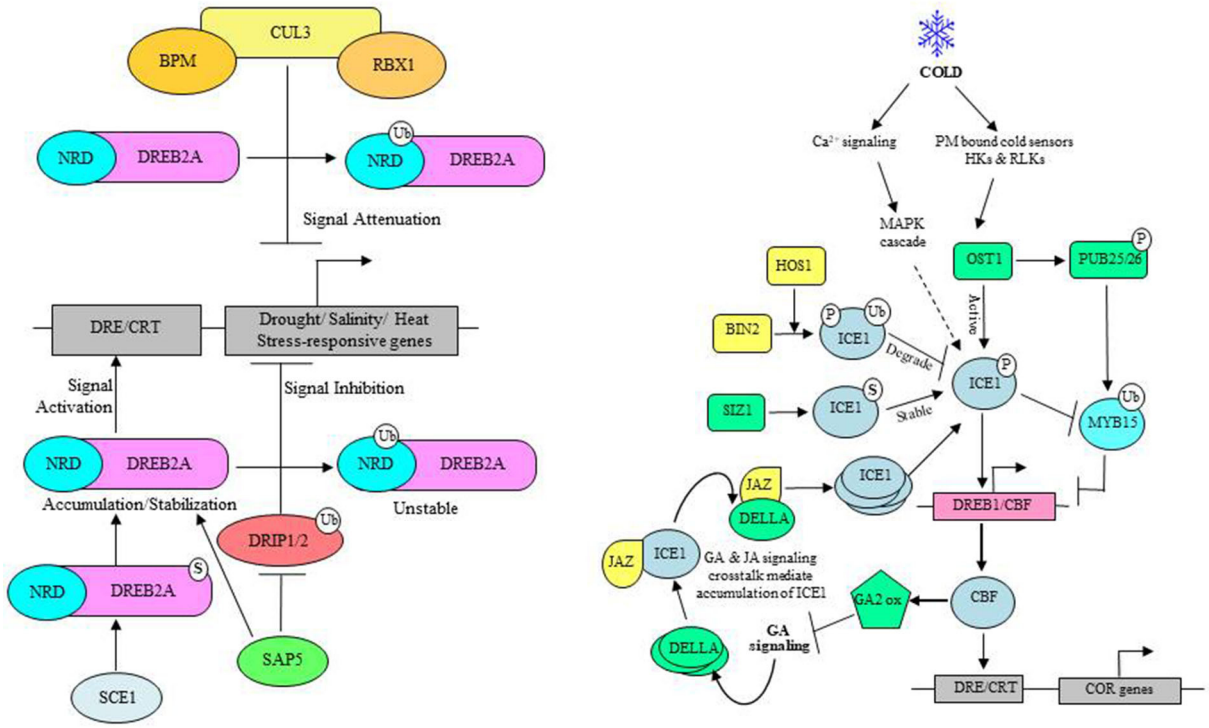


FIGURE 4
ABA-independent stress response. **(A)** Under drought and salt stress: DREB2A transcription factor functions upstream of various drought, salt, and heat-responsive genes. DRIP1/2 E3 ligase negatively regulates stress tolerance as a signaling inhibitor and targets DREB2A for UPS-mediated degradation. SAP5 E3 ligase reinforces stress signaling by regulating DRIP1/2 turnover. SCE1-mediated SUMOylation of DREB2A also enhances its stability. CUL3-based BPM ligases mark DREB2A for degradation as a signal attenuator. **(B)** Under cold stress: Cold stimulus is sensed by plasma membrane (PM) bound receptors, mostly histidine kinases (HKs) and receptor-like kinases (RLKs). Subsequent activation of Snf-related kinase (SnRKs), OST1, phosphorylates (P) ICE1, which enhances the expression of CBF and CBF-regulated cold stress-related (COR) genes. SIZ1 mediated SUMOylation (S) of ICE1 impedes the turnover rate and stabilizes ICE1. Cold stress-induced expression of MYB15 (a negative regulator of CBF) is ubiquitinated (Ub) and degraded *via* OST1 phosphorylated PUB25/26. BIN2 phosphorylated ICE1 levels are reduced by HOS1 E3 ligase in absence of stress. Cold stress-induced altered intracellular Ca^{2+} levels initiate MAPK signaling, which is also involved in ICE1 regulation, as shown by the dashed arrow. Crosstalk between GA and JA signaling also helps stabilize ICE1 wherein CBF stimulated GA2 oxidase inhibits bioactive GAs. This allows the accumulation of DELLA, which interacts and binds JAZ to release JAZ-bound ICE1, thereby promoting the accumulation of ICE1.

Plant U-box type E3s are also known to participate in the regulation of drought stress tolerance. For example, PUB11, by targeting Leucine-rich Repeat Protein1 (LRR1) and Kinase7 (KIN7), impedes stomatal closure and reduces drought tolerance. Other members of the U-box family that are known to downregulate drought tolerance are PUB19, PUB22, and PUB23 (Table 3). On contrary, PUB46 and PUB48 are reported as positive regulators of drought stress since their mutations lead to drought hypersensitivity, though their potential targets remain elusive (Al-Saharin et al., 2022). Rice PUB41 (OsPUB41) is known to have a negative influence on drought-responsive signaling as it mediates the degradation of Chloride Channel6 (OsCLC6), which is critical for modulating chloride homeostasis under water deficit conditions.

In *Capsicum annum*, the RING membrane-anchor 1 homolog 1 (Rma1H1) was originally identified as a dehydration-regulated gene (Park et al., 2003), which, when overexpressed in Arabidopsis, resulted in increased drought tolerance (Lee et al., 2009). The plasma membrane aquaporin PIP2/1 is known to serve as a potential target for Rma1H1 and was shown to interfere with a UPS inhibitor, MG132, suggesting the role of Rma1H1 in proteasome-mediated stress tolerance by regulating the aquaporin levels in plants. It has been suggested that aquaporins can negatively impact plants during water stress because they facilitate symplastic water transport (Jang et al., 2004; Alexandersson et al., 2005). Rma1-3 are the Arabidopsis homologs of Rma1H1 (Lee et al., 2009). Together, Rma1H1 and Rma1 promote drought tolerance by mediating the degradation of aquaporins. This contradicts

CaPUB1 and its Arabidopsis homolog AtPUB22/23 since their over-expression renders the transgenic plants more sensitive to drought and salt conditions. The RP subunits, which are Rpn6 and Rpn12a, are the potential substrate for CaPUB1 and PUB22/23, respectively. The significance of these interactions is still unknown, but ubiquitin-dependent regulation of Rpn subunits may regulate the activity of the UPS during the drought stress response.

Ubiquitination and salinity stress response

E3 ligases are also well-explored for their function in the regulation of salt-induced adaptive responses. Myriads of E3 ligases are reported that confer tolerance to more than one stress, such as drought and salt stresses, by regulating common factors functioning under both stresses. One shared factor is ABA, which is mainly a stress-induced hormone, that signals reprograming of cellular osmotic and ionic steady states to mitigate common physiological responses, such as stomatal movement regulation. In wheat, a U-box protein TaPUB15 has been implicated in positive salt stress tolerance (Table 3) by stabilizing the expression of stress-tolerant genes and maintaining low Na^+/K^+ ratios (Li et al., 2021). Conversely, PUB26 affects salt stress response negatively (Table 3) by interacting with one of the ATPase subunits of 26S proteasome, *T. aestivum* Regulatory Particle Triple-ATPase2A (TaRPT2a). Its gene expression is salt inducible, but the molecular mechanism underlying this interaction requires further studies (Al-Saharin et al., 2022). SALT TOLERANCE RING FINGER 1 (STRF1) is a membrane-associated RING-H2 type E3 ligase annotated as a positive modulator of salt stress in Arabidopsis (Table 3). It localizes to intracellular endosomes and confers salt stress by regulating membrane trafficking and ROS production (Tian et al., 2015). In rice, four members of the SALT-INDUCED RING PROTEIN (SIRP) family of RING-type E3 ligase have been identified. Overexpression of SIRP1/3/4 increased the sensitivity of transgenic plants toward salt stress, which indicated their roles as negative modulators of salt stress tolerance, whereas SIRP2 overexpressed plants with enhanced salt resistance suggested a positive role for SIRP2. While substrates of SIRP1 are not known, SIRP3 and SIRP4 are known to impose their inhibitory effects by facilitating the degradation of stress-induced positive regulators. While OsSIRP3 targets MADS-BOX GENE 70 (OsMADS70) and an ABC DOMAIN CONTAINING PROTEIN (OsABC1P11), SIRP4 triggers proteasomal degradation of PEROXISOMAL BIOGENESIS FACTOR11-1 (OsPEX11-1). The *O. sativa* Transketolase 1 (OsTKL1) has been identified as a potential target of OsSIRP2; however, the significance of ubiquitination-mediated degradation of OsTKL1 under salt stress is unclear (Al-Saharin et al., 2022).

Ubiquitination and temperature stress response

UPS also functions to attenuate cold stress signaling as exemplified by High expression of osmotically responsive gene1 (HOS1) RING-type E3 engaged in degradation of ICE1 (Inducer of CBF expression 1), a MYC transcription factor that controls the expression of cold-responsive transcription factor DREB1A/C-REPEAT BINDING FACTOR3 (CBF3) involved in the regulation of numerous cold-responsive genes (Figure 4B). Consistent with the role in mediating ICE1 protein turnover, overexpression of HOS1 suppresses the expression of ICE target genes while increasing the sensitivity to freezing conditions. Although HOS1 possesses a variant RING domain, it catalyzes *in vitro* and *in vivo* ubiquitination of cold-responsive ICE1 (Lee et al., 2001; Stone et al., 2005; Dong et al., 2006). Interestingly, both the upregulation and downregulation of ICE1 TF is a cold-induced phenomenon. However, cold-inducible genes are only transiently expressed (Chinnusamy et al., 2003) and facilitated by cold-induced relocalization of HOS1 from the cytoplasm to the nucleus, enabling proteasomal degradation of nucleus-localized ICE1 (Lee et al., 2001; Dong et al., 2006). Critical regulation of ICE1 activity by phosphorylation indirectly modulates its stability through UPS. High temperature also engages E3s to monitor the abundance and the activity of several TFs that promote or suppress transcription of stress-related genes to activate appropriate mitigation responses. Heat stimulus-based physiological responses involve increased production of ROS, alteration in protein structure, and perturbed membrane integrity due to lipid peroxidation. Mitigation of heat stress essentially requires transcriptional activation of thermotolerance-related genes and stabilization of upstream transcriptional activators. For example, A RING-finger E3 ligase in Arabidopsis known as PROTEIN WITH RING DOMAIN AND TMEMB1 (AtPPRT1) induces the expression of the following heat-responsive genes: HEAT SHOCK PROTEIN 21 (AtHSP21), HEAT SHOCK TRANSCRIPTION FACTOR A7A (AtHSFA7a), and ZINC-FINGER PROTEIN 12 (AtZAT12) by targeting transcriptional repressors of these genes. Related studies elucidated the role of AtPPRT1 in the negative regulation of drought and salt stress tolerance (Table 3). Similarly, overexpression of AtPUB48, a U-box type E3, acts as a positive regulator of heat stress-responsive genes and increases their expression. Following the fundamental theme of imparting stress tolerance by promoting turnover of negative elements and stabilization of positive elements, rice RING E3 ligase, HEAT-INDUCED RING FINGER PROTEIN1 (OsHIRP1), show heat stress

TABLE 3 List of abiotic stresses responsive E3 Ub ligases in plants.

Stress type	RING			U box	CRLs
Drought	AtRGLG1/5[a]	AtPPRT3[a]	OsZNF	AtPUB12/13	TaFBA1
	At/OsSAP5	AtRHA2B/2A[a]	CaASRF1	AtPUB46/48	AtDRS1
	AtAIRP1/2	AtRZP34/CHYR1	CaAIRE1	OsPUB67	AtWDR55
	AtAIRP3[a]	AtXBAT35.2[a]	CaDTR1	TaPUB1	
	AtNERF	AtXERICO[a]	CaRma1H1	GmPUB6/8[a]	
	AtRDUF1/2	AtRma1/2/3	CaATIR1[a]		
	AtSDIR1[a]	OsRF1[a]	CaAIRF1		
	AtDUF1/2[a]	OsRDCPS	ZmAIRP4		
	AtATL61/78[a]	OsRHP1	ZmRFP1		
	AtJUL1	OsSDIR1			
	AtRGLG2[a]	OsDHSRP1		AtPUB11	AtDOR[a]
	AtMIEL[a]	TaDIS1		AtPUB18/19[a]	AtAFA1[a]
	AtRZF1	CaAIR1[a]		AtPUB22/23[a]	AtSDR
	OsDSG1	CaREL1[a]		OsPUB41	AtPP2-B1
	OsDIS1	CaDIR1[a]		CaPUB1	AtHOS15
	OsSADR1	GmRFP1		GmPUB21	AtRAE1[a]
	OsDIRP1				OsCBE1
Salinity	AtSAP5	OsRHP1	TaZNF	AtPUB10	AtSDR
	AtAIRP1/2[a]	OsSIRF1	ZmRFP1	AtPUB15	AtPP2-B11
	AtAIRP3[a]	OsSIRP2	MfSTMIR	TaPUB1	TaFBA1
	AtRDUF1/2	OsSIRH2-14	SpRING	TaPUB15	
	AtSDIR1[a]	OsRMT1	GmRFP1		
	AtSTRF1	OsRF1[a]			
	AtXBAT35.2	OsSIRP1/3/4	OsDHSRP1	AtPUB10[a]	OsCBE1[a]
	AtPPRT1	OsSRFP1	GhSARP1	AtPUB30	
	OsDSG1	OsSADR1	MdMIEL	TaPUB26	
	OsMAR1	OsDIRP1		GmPUB21	
Cold	OsDIRP1			OsPUB2/3	-
	OsCOIN			CaPUB1	
	AtHOS1	AtATL80	OsSRF	–	OsCBE1
	AtATL61	OsSRFP1	GmRFP1		
	AtATL78	OsHOS1			
Heat	AtPPRT1			AtPUB48	TaFBA1
	OsHIRP1				
	OsDHSRP1				
Oxidative	–			AtPUB46	TaFBA1
				OsPUB15	
	OsSRFP1			AtPQT3	–
	OsSRF				
	MdMIEL				
Heavy metals	OsHIR1			TaPUB1	–
	OsAIR4.1/4.2				
	SlRING1				
	AtATRF1				
	OsHRZ				

Positive regulators and negative regulators have been shown with unshaded and shaded backgrounds, respectively.
"*a*" denotes ABA-dependence.

tolerance through proteasomal degradation of ALDO/KETO REDUCTASE4 (OsARK4) and HIRP1-REGULATED KINASE1 (OsHRK1) that likely affects heat-stress tolerance negatively (Al-Saharin et al., 2022).

Ubiquitination and UV radiation stress response

A significant amount of UV-B (280–320 nm) reaching the earth's surface is another source of abiotic stress. High levels of UV-B exposure generate reactive oxygen species (ROS) that lead to DNA damage. Conversely, low levels of UV-B act as a signal that triggers regulatory responses involved in repairing UV damage. Two basic mechanisms of DNA-damage repair are photoreactivation and nucleotide excision repair (NER) (Tuteja et al., 2009). The NER pathway involves a CUL4-DNA Damage Binding protein1 (DDB1)-based CRL that targets a nucleus-localized DDB2 protein, which binds to UV-induced bulky DNA lesions (Molinier et al., 2008). Nuclear translocation of DDB1, following UV irradiation, facilitates the degradation of DDB2. CUL4-DDB1-mediated removal of DDB2 from DNA lesions recruits and permits NER machinery to access the lesions. Ataxia Telangiectasia-mutated and Rad3-related (ATR) protein kinase, as well as De-etiolated1 (DET1) factors, assist in UV-induced CUL4-DDB1-mediated degradation of DDB2. ATR identifies the damaged DNA and ensures the presence of DDB1 in the nucleus through DET1 for the degradation of DDB2. DET1 degradation also occurs along with DDB2 in a CUL-DDB1-dependent manner. Overexpression of DDB1A and DDB2 in Arabidopsis was reported to enhance the UV-C tolerance (Molinier et al., 2008).

Ubiquitination and nutrient deprivation stress response

The role of UPS in mitigating stress-stimulated adverse effects extends beyond the proteolysis of TFs. Availability of nutrients after germination is crucial in determining whether the seedling can transit through the post-germinative developmental checkpoint or not (Lopez-Molina et al., 2001). The RING-type E3, Arabidopsis Toxicos EN Levadura6 (ATL6 and ATL31), are involved in the regulation of 14-3-3 proteins. The 14-3-3, are conserved regulatory proteins in eukaryotes involved in a multitude of signaling processes. Overexpression of 14-3-3χ protein, a target of ATL31 ubiquitin ligase, results in hypersensitivity to C/N stress (Sato et al., 2011; Maekawa et al., 2012). On this account, loss of ATL6 and ATL31 produce hypersensitivity to C/N stress, while over-expression of ATL6 and ATL31 rendered plants insensitive to C/N stress such that these transgenic plants were able to bypass early checkpoints despite the stress conditions (Sato et al., 2009). Importantly, C/N stress-induced accumulation of 14-3-3χ is observed in wild-type seedlings but not in *atl6atl31* seedlings, suggesting that ATL6/31 mediates the turnover of 14-3-3χ under non-stress conditions and degradation is prohibited during exposure to C/N stress.

Plants adapt to nitrogen-limiting conditions by redistributing nitrogen content from older to younger, actively growing organs and increasing the accumulation of anthocyanins (Kant et al., 2011). The adaptive response of plants to low nitrogen is facilitated by the presence of Nitrogen Limitation Adaptation (NLA), a RING-type ligase (Peng et al., 2007).

Ubiquitination in ABA-mediated stress response

Drought, cold, and salinity stress-activated signal transduction pathways share several related components that are linked with the ABA-mediated stress response and are regulated in a UPS-dependent manner. ABA is an important plant hormone that controls vital cellular and physiological responses in development and abiotic stresses. As a negative regulator of growth and development, ABA promotes dormancy, regulates seed maturation to ensure germination only under growth-promoting conditions, and suspends growth in seedlings exposed to stresses. ABA also mediates protective responses that mitigate the stress-induced damage in mature plants (Finkelstein et al., 2002; Himmelbach et al., 2003). ABA-dependent regulation of stomatal closure in response to water deficiency is a typical example of protective responses of ABA in plants to prevent excessive water loss.

Stresses stimulate ABA biosynthesis, which signals the expression of hundreds of ABA-responsive genes. ABA-responsive TFs, like basic leucine zipper (bZIP), alter gene expression by interacting with ABA-regulatory elements (ABRE) in the promoter region of stress-responsive genes (Hattori et al., 2002; Narusaka et al., 2003). UPS-mediated regulation of ABA signaling is achieved by modulating the stability of ABRE-binding TFs (Figure 5). ABA promotes the accumulation of short-lived bZIP TF Abscisic Acid Insensitive 5 (ABI5), which serves as an early developmental checkpoint for the growth of young seedlings under adverse conditions (Uno et al., 2000; Lopez-Molina et al., 2003). The abundance of ABI5 is regulated by Keep on Going (KEG), a trans-Golgi network/cytosol localized RING E3, which directs ubiquitination and degradation of ABI5 (Stone et al., 2007). Under non-stress conditions, KEG maintains low levels of ABI5 in the cytosol, which prevents the accumulation of ABI5 in the nucleus and attenuates ABA signaling to ensure seedling

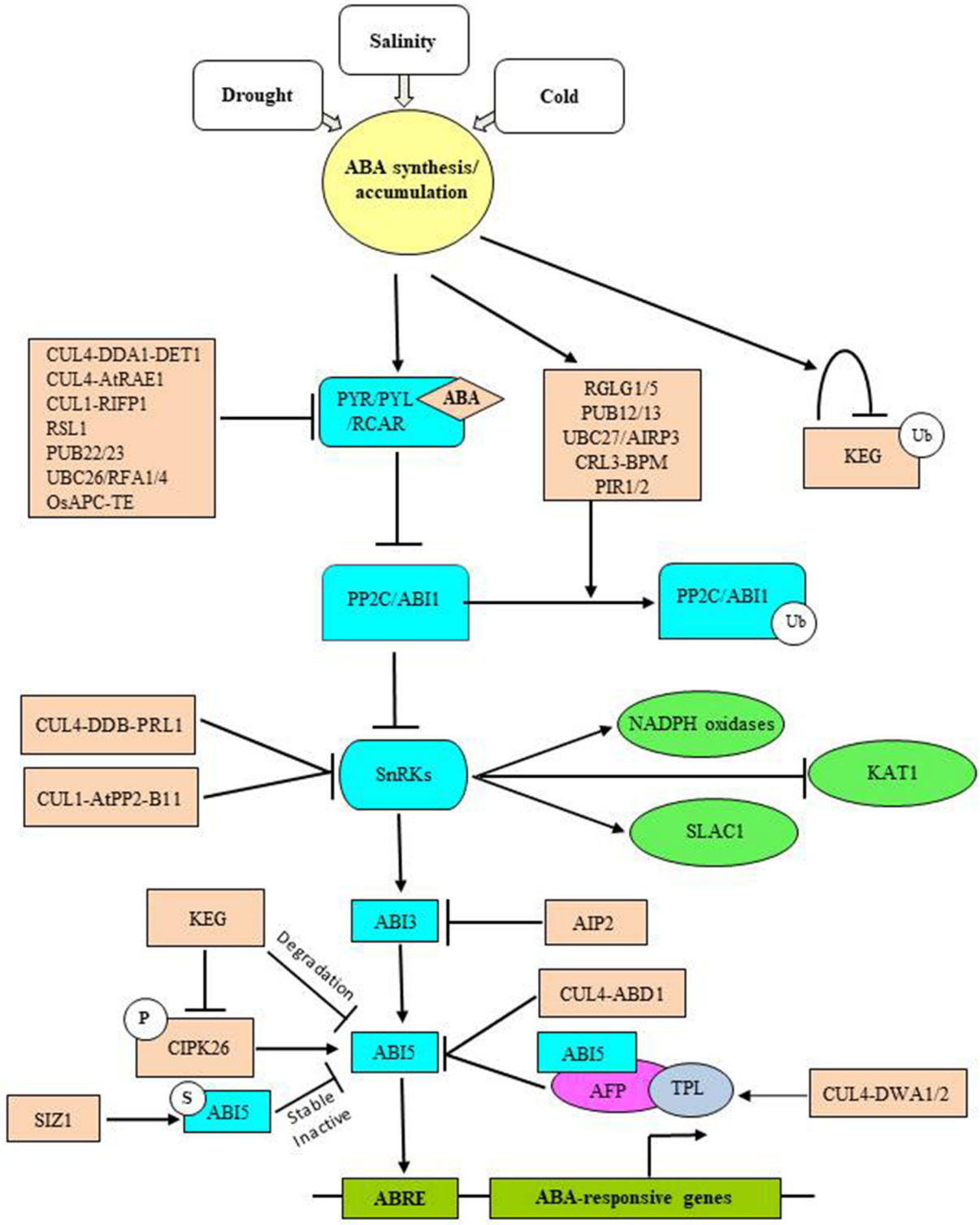


FIGURE 5
UPS-mediated ABA-dependent stress signaling/tolerance in plants. Abiotic stress triggers ABA biosynthesis and accumulation. In the absence of stress conditions, the positive regulators of ABA signaling like ABA receptors and TFs are maintained in a repressed state to inhibit ABA signaling and thus the expression of ABA-responsive genes. This is largely achieved through numerous E3 ligases that differentially modulate the turnover of ABA receptors and SnRKs, as these are major effectors of ABA responses. SIZ1-mediated SUMOylation opposes KEG-mediated degradation of ABI5 to maintain moderate ABI5 levels under no stress conditions. Auto-ubiquitination and degradation of KEG under-enhanced ABA levels stabilize ABI5. Upon ABA accumulation, ABA binds its receptors, which together capture PP2C in a ternary complex to release PP2C imposed
(Continued)

FIGURE 5 (Continued)
inhibition of SnRKs. PP2Cs also serve as targets for E3 ligases. Fully activated SnRKs then induce ABI3 activity, which turns on ABI5 functions. Other TFs like ABFs are also activated in the same manner. SnRKs also activate ROS scavenging enzymes (NADPH oxidases) and anion efflux channels (SLAC1), as well as inhibit K^+ influx channels (KAT1), to mitigate ROS and osmotic effects. Attenuation of ABA signaling requires UPS-mediated turnover of ABA TFs. As mentioned above, ABI3 functions upstream of ABI5 and is degraded by AIP2, whereas degradation of ABI5 employs CUL4-based ABD1 and DWA1/2 E3 ligases. DWA1/2-mediated breakdown of ABI5 occurs *via* ABI5-binding protein (AFP), which recruits the co-repressor of JA signaling, TOPLESS (TPL) to ABI5, to generate a transcriptional complex that represses the expression of ABA-responsive genes.

establishment. Conversely, elevated levels of ABA accelerate self-ubiquitination and degradation of KEG, which leads to the ABI5 stabilization and promotion of ABA responses. This suggests a feedback loop-like mechanism for ABI5 and KEG-mediated ABA signaling. Other bZIP TFs, like ABRE-binding factor 1 (ABF1) and ABF3, also serve as potential substrates for KEG.

E3 ligases, DWD-hypersensitive to ABA 1 (DWA1) and DWA2, have also been implicated in the regulation of ABI5 turnover. These are substrate-recruiting components of CUL4-based CRL and function as negative regulators of ABA signaling by targeting ABI5 for UPS-mediated degradation. Interestingly, ABI5 accumulation is observed only in ABA-treated *dwa1/2* mutants, which contradicts with *keg* mutants that show extremely high levels of ABI5 even in the absence of ABA. Thus, it suggests that KEG may function to maintain low levels of ABI5 in the absence of ABA and abiotic stress, while DWA1/2 may function to attenuate ABA signaling so that plants can readily re-establish growth once environmental conditions improve. DWA1/2-mediated breakdown of ABI5 has been proposed to occur *via* ABI5 binding protein (AFP), which adds further complexity to the UPS-mediated regulation of ABI5.

UPS-regulated ABI3, an ABA-responsive B3 type TF, functions upstream of ABI5 to mediate ABA-dependent responses (Finkelstein and Lynch, 2000; Lopez-Molina et al., 2002). RING-type E3 ABI3-interacting protein (AIP2) is a negative regulator of ABA signaling and targets ABI3 for proteasomal degradation to inhibit the ABA responses. The ABA-induced abundance of AIP2 suggests that ABA promotes the turnover of ABI3 *via* AIP2. Studies also suggested a proteolytic regulation for ABI4, ABF2, and ABF3 TFs. ABA-dependent stabilization of ABF3 involves phosphorylation of ABF3 *via* SnRK2 kinase, the Open Stomata 1 (OST1). Stabilization of ABF3 in response to phosphorylation demonstrates that ABA-activated kinases are not limited to the activation of TFs, but they may also be required for stability.

Moreover, RING-type E3 ligases, such as SDIR1, AtAIRP1, ATL61, RHA2a, and RHA2b, are shown to be the positive regulators (Table 3) of ABA signaling (Al-Saharin et al., 2022). Transgenic lines over-expressing these E3 ligases are hypersensitive to ABA-induced effects and were more tolerant to drought, while mutant plants were insensitive (Zhang et al., 2007; Bu et al., 2009; Ryu et al., 2010; Li et al., 2011; Yang et al., 2020). Overexpression of SDIR1, AtAIRP1, or RHA2b enhances drought tolerance *via* an increase in ABA-induced stomatal closure (Zhang et al., 2007; Ryu et al., 2010; Li et al., 2011). Expression of SDIR1 is induced in response to salt and drought conditions and functions upstream of ABA-responsive TFs ABI3 and ABI5 by degrading the SDIR INTERACTING PROTEIN 1 (SDIRIP1) (Shu and Yang, 2017). Unlike the aforementioned ligases, RHA2a and RHA2b are redundant in nature and function parallel to ABA-responsive TFs ABI3 and ABI5 (Bu et al., 2009; Li et al., 2011). Drought Tolerance Repressor 1 (DOR1), an F-box component of SCF E3 ligase complex in Arabidopsis, is reported as a negative regulator of ABA-mediated stomatal closure since *dor1* is hypersensitive to ABA with enhanced stomatal closure, hence improving stress tolerance. Nine *cis*-epoxycarotenoid dioxygenase 3 (NCED3), a key enzyme in ABA biosynthesis, is significantly upregulated in *dor* plants (Zhang et al., 2008). Another RING-type E3 linked to ABA biosynthesis is XERICO, whose overexpression produced ABA hypersensitive drought-resistant plants. A stronger and more sustained expression of NCED3 in XERICO, over-expressing plants upon ABA treatment, indicates that XERICO acts post-translationally to regulate ABA biosynthesis (Ko et al., 2006). Recently, novel RING-H2 types E3 in rice OsRF1, a homolog of Arabidopsis AtXerico, have been reported to elicit ABA biosynthesis and accumulation against drought. OsRF1 is also a positive player in salinity stress. A member of clade A PP2C protein family, OsPP2C09, which is a core suppressor of ABA signaling, has been identified as a potential target of OsRF1. Thus, OsRF1 confers stress tolerance in an ABA-dependent manner (Kim et al., 2022). Arabidopsis Ring Domain Ligase1 (RGLG1) and its homologs, RGLG2 and RGLG5, synchronize ABA-mediated plant responses during drought stress due to their dual but opposing behavior (Wu et al., 2016). RGLG2 signals UPS-mediated degradation of the positive regulators of drought signaling, Ethylene Response Factor53 (AtERF53) and MAPKKK18, to downregulate stress responses, whereas RGLG1 targets the repressor of drought-induced ABA signaling, PP2CA, to promote ABA-dependent drought tolerance. Upregulation of ABA signaling *via* RGLG1 involves ABA-mediated nuclear localization of RGLG1 by inhibiting N-myristoyltransferase 1 (NMT1), which, otherwise, myristoylate and target RGLG1 to the plasma membrane (Al-Saharin et al., 2022).

Ubiquitination in submergence stress response

Submergence gives rise to multiple stress conditions that occur simultaneously like hypoxia, decreased gaseous exchange, altered osmoticum, low transpiration, nutrient deficiency, oxidative, and salt stress (Tamang and Fukao, 2015; Fukao et al., 2019). Similarly, post-submergence plants are suddenly exposed to normoxia, photoinhibition, oxidative stress, and dehydration (Tamang and Fukao, 2015). Plants respond to transient deep flash floods through quiescence response while following escape response by rapid internodal elongation under slow progressive floods. Quiescence response involves economization of energy sources by suppressing GA signaling in brassinosteroids (BR)-dependent manner. This also involves the *SUBMERGENCE1A* (*SUB1A*) which is a member of ETHYLENE RESPONSIVE FACTOR (ERF- VII) family. The ethylene-dependent abundance of SUB1A promotes BR biosynthesis, which leads to the degradation of bioactive GAs and subsequent accumulation of DELLAs. However, *SNORKEL* (*SKs*), the antagonist of *SUB1A* although accumulates in an ethylene-dependent manner, downregulates BR production, which reverses the action of BR resulting in enhanced GA signaling and acquisition of escape response. There are five *ERF-VII* genes in Arabidopsis, two *HYPOXIA RESPONSIVE ERF* (*HRE*) genes, *HRE1* (*ERF73*) and *HRE2* (*ERF71*), and three *RELATED TO AP2* (*RAP2*) genes, *RAP2.2* (*ERF75*), *RAP2.3* (*ERF72*/*EBP*), and *RAP2.12* (*ERF74*), and all have been shown to promote submergence tolerance and oxygen deprivation. The UPS is implicated in the modulation of ERF-VII protein abundance *via* the N-end rule pathway. In this pathway, the constitutive cleavage of methionine from ERF-VII proteins conserved N-terminus, Met-Cys, by methionine aminopeptidases exposes cysteine, which in the presence of oxygen and NO, is oxidized by plant cysteine oxidases (PCOs), thereby producing cysteine sulfinic or cysteine sulfonic acid. Subsequent conjugation of oxidized cysteine with an arginine residue of arginyl tRNA transferases (ATEs) serves as a recognition and ubiquitination site for E3 Ub ligase, PROTEOLYSIS6 (PRT6), which signals proteasome-mediated degradation of ERF-VII proteins. While the *SUB1A* gene is associated with submergence tolerance in rice (Fukao et al., 2011), another APETELLA2/ETHYLENE RESPONSIVE FACTOR (AP2/ERF) type TF EREBP1 confers adaption to submergence, as well as drought in rice (Jisha et al., 2015). Another E3 Ub ligase SUMERGENCE RESISTANCE1 (*SR1*) in Arabidopsis has been identified as a modulator of submergence tolerance, wherein it synchronizes plant growth with stress acclimation through a switch module, including SR1-WRKY33-RAP2.2. The stress-induced phosphorylation of WRKY33 facilitates downstream activation of RAP2.2, which, in turn, induces the expression of hypoxia-related genes. Upon reoxygenation, SR1 catalyzes the ubiquitination and degradation of WRKY33, while RAP2.2 is degraded through the N-end rule pathway (Liu et al., 2021). Similarly, phosphorylation and ubiquitination negatively regulate the function and stability of nitrate reductase (NR) in normoxia (Kim et al., 2018; Fukao et al., 2019). The ubiquitin ligase, CONSTITUTIVE PHOTOMORPHOGENIC 1 (COP1), reportedly destabilizes the NR structure (Park et al., 2011). However, SUMOylation positively affects the stability of NR protein in normoxia by partitioning its subcellular location to the nucleus (Park et al., 2011; Kim et al., 2018). In the comparison of submergence-sensitive *Rumex acetosa* with submergence-tolerant *Rhodopseudomonas palustris*, plants of tolerant species showed higher expression of COP1 and nonsymbiotic hemoglobin concomitant with lower ammonia, higher nitrate, and protein concentrations even in normoxia due to post-translational suppression of NR through ubiquitination (van Veen et al., 2013).

Ubiquitination in epigenetic regulation of abiotic stresses

Although the intricate relationship between the chromatin remodeling dynamics and ubiquitin code is arduous, the epigenetic regulatory networks of histone modification play a vital role in genome stability, thereby regulating abiotic stress responses in plants. Lysine-rich histones are often ubiquitinated and play a critical role in DNA damage responses triggered in response to double-strand breaks (DSBs) due to genotoxic stresses (Mattiroli and Penengo, 2021). The H2A and H2B are the most abundant monoubiquitinated histone types and evoke an immediate response to DNA damages. Recruitment of Ub ligase RNF-8 and RNF168 at sites neighboring DSBs catalyzes K-63, K-27, and monoubiquitination of K13/15 in H2A type histones. Ubiquitinated histones then serve as docking sites for downstream repair machinery. RNF168-mediated ubiquitination of H2A is signaled by ataxia-telangiectasia mutated (ATM)-mediated phosphorylation of H2AX (H2A variant), followed by recruitment of RNF8, which catalyzes ubiquitination of H1 linker histones (Aquila and Atanassov, 2020). Studies report the implication of H2B monoubiquitination in abiotic stress tolerance in Arabidopsis and rice. For H2B ubiquitination, the Arabidopsis genome encodes two RING E3 ligases, HISTONE MONOUBIQUITINATION1 (HUB1) and HUB2, and three E2 conjugases, UBIQUITIN CARRIER PROTEIN1 (UBC1), UBC2, and UBC3 (Cao et al., 2008). The *hub1* and *hub2* mutants showed decreased H2B ubiquitination and increased sensitivity to salt stress. It demonstrates that H2Bub is involved in salt stress-induced microtubule depolymerization. Further, mutants showed downregulation of genes encoding for cutin and wax biosynthesis, revealing

their potential function as positive regulators of drought tolerance. Consistently, the ectopic expression of AtHUB2 in transgenic cotton conferred improved tolerance to drought stress. Similarly, OsHUB2 overexpression enhanced the ABA sensitivity and drought resistance in rice, suggesting that OsHUB2 monoubiquitination positively modulates drought tolerance in an ABA-dependent manner (Ueda and Seki, 2020).

SUMOylation

Eukaryotic cells employ a variety of small polypeptides as post-translational regulators of protein function. SUMOylation is another crucial PTM in eukaryotes that redefines the fate of various proteins by altering their intra- and inter-molecular interactions. Small Ub-related protein Modifiers (SUMOs) are small polypeptides of 10 kDa, which, like ubiquitin, attach to accessible lysine(s) of target proteins through an isopeptide bond. Lysine within ψKXE/D (ψ denotes bulky hydrophobic group and X represents any amino acid) motif is the minimal consensus required for the attachment of SUMO to a lysine residue in the substrate. Nascent SUMO polypeptides have a variable C-terminal extension cleaved by SUMO-specific proteases, a prerequisite for conjugation, to generate mature SUMO proteins with a signature glycine di-peptide at C-terminus implied in isopeptide bond formation. Although SUMO peptide folds into the ubiquitin-like β-grasp fold, they share only 20% sequence identity with ubiquitin and exhibit a completely different surface charge distribution. This might be because SUMOs evolved to have functional specialization while conserving the fundamentals of covalent PTMs. SUMO is unique to have 10–30 residue N-terminal extensions associated with polySUMOylation (Geiss-Friedlander and Melchior, 2007; Srivastava and Sadanandom, 2020). This intrinsically disordered structure seems to provide enough flexibility and solvent exposure, facilitating its modification *via* other PTMs or its attachment to host proteins. Apart from canonical SUMOs, plants express certain atypical SUMO forms that are tissue and/or condition-specific or lack signature Gly-Gly motif at C-terminus with an unusually long N-terminus (SUMO-variant/SUMO-v). Another variant with two β-grasp folds in tandem, known as diSUMO-like (DSUL), is exclusive to cereals. The highly conserved paralogs and DSULs have been identified as the only conjugating forms, the former being the widely expressed forms directing most of the functions (Augustine and Vierstra, 2018). There are a few other ubiquitin-like proteins, such as Ubiquitin fold modifier (UFM), Related to ubiquitin 1(RUB1), and homology to ubiquitin (HUB), that primarily regulate the protein activity, subcellular localization, and protein-protein interactions. The ubiquitous presence and conservation of SUMOylation across the eukaryotes signify its crucial role in sustaining proteome functions. Yeast, *C. elegans*, and *D. melanogaster* contain only one SUMO coding gene, while higher organisms have expanded gene families with several genes. For example, the human genome has four SUMO genes while Arabidopsis has eight isoforms, of which only the expressions of SUMO1, 2, 3, and 5 have been verified (Srivastava and Sadanandom, 2020). Non-complementation of *sumo1/sumo2* double mutants by SUMO3/5 suggests its non-redundant functions. However, SUMO1 and SUMO2 with 83% identity are known to complement each other. Less conserved SUMO3 and 5 share only 42 and 30% similarity with SUMO1, respectively. Constitutive expression studies of SUMO3/5, showing delayed growth and senescence-like symptoms, suggest a strict control over their expression for optimal growth in plants. No such growth defects were observed for SUMO1/2 constitutive expression. The rice genome has a repertoire of six SUMO genes (*SUMO1-6*). All isoforms were shown to rescue SUMO-deficient UV-sensitive *pmt3*Δ mutants of fission yeast. Of these, *SUMO3-6* contains SUMO-acceptor site ψKXE/D, indicating their involvement in the formation of SUMO chains (Teramura et al., 2021). *AtSUMO1/2* and *OsSUMO1/2* are plant homologs of human *SUMO2/3* (Miura et al., 2007).

Arabidopsis proteome has thousands of SUMO-target proteins suggesting SUMOylation as a major PTM like phosphorylation and ubiquitination (Augustine and Vierstra, 2018). Enhanced SUMOylation of nuclear proteins is among the most rapid response to various stresses but the precise mechanism of stress resilience through this PTM remains ambiguous. A major portion of identified SUMO substrates is nuclear proteins, such as TFs, coactivator/repressors, and chromatin modifiers, which indicate the imperative role of SUMOylation in regulating nuclear processes. For instance, SUMOylation controls nucleo-cytoplasmic trafficking of RanGAP1, its unmodified form is cytosolic, whereas modified RanGAP1 interacts with nucleoporin NUP358 (RanBP2) for its nuclear localization (Geiss-Friedlander and Melchior, 2007). The reversibility of SUMOylation is crucial for its regulatory role and is mediated by deSUMOylating proteases (DSPs). The higher number of DSPs than E3s in plants suggests that selectivity is important for SUMOylation but is critical to deSUMOylation as latter is required for the maintenance of a dynamic pool of SUMOylated and non-SUMOylated proteins to manifest the diverse responses (Augustine and Vierstra, 2018). The eukaryotic proteome is ∼15–20% SUMOylated. Three major functions of SUMOylome include regulating activity and localization of individual proteins; macromolecule biosynthesis; and SUMO-mediated proteasomal degradation (Drabikowski et al., 2018; Morrell and Sadanandom, 2019). SUMOylation-directed degradation of proteins involves SUMO-targeted Ub-ligases (STUBLs) comprising a novel class of Ub ligases that recognize and ubiquitinates SUMO-tagged proteins for proteasome degradation. The STUBLs essentially interact non-covalently with polySUMOylated proteins through SUMO-interacting motifs (SIM). Notably,

polySUMO chain formation is a function of SUMO E4 ligases that specifically adds multiple SUMOs to the target lysine of the desired substrate. In Arabidopsis, E4 ligases are represented by two members of PROTEIN INHIBITOR OF ACTIVATED STAT-like 1/2 (PIAL1 and 2). The STUBLs present a remarkable pathway for the regulation of protein turnover and demonstrate an important link between SUMOylation and ubiquitination.

Like ubiquitination, the SUMO-modification pathway is a three-step process catalyzed by an enzymatic cascade: E1 or SUMO-activating enzymes (SAE), E2 or SUMO-conjugating enzyme (SCE), and SUMO E3; which, respectively, activate, transfer, and conjugate SUMO to desired targets. The activation of SUMO is an ATP-dependent process and forms SUMO adenylate, releasing pyrophosphate. Further, SUMO is transferred to catalytic cysteine of E1 forming the E1-SUMO complex. Thio-esterification of SUMO to E1 is accompanied by a transesterification reaction, during which E2 is recruited to E1 UFD, which facilitates the subsequent transfer of SUMO to the internal cysteine of E2 enzymes. SUMO-conjugating enzymes are at the core of the SUMOylation pathway because they accomplish an essential link, directly or indirectly, between activated SUMO and its substrate *via* SUMO E3 ligases. In the former case, substrate selectivity is solely conferred by E2 enzymes, while the latter projects E3 ligases as a common interface which binds the charged SUMO∼E2 complex and substrate, orienting them in a way that facilitates the discharge of SUMO from E2 to a relevant substrate. The ability of E3 ligases to hold SUMO in a closed conformation through SIM motifs helps the efficient transfer of activated SUMO to the substrate protein.

E1 is a heterodimer of SAE1/2, where SAE1 is a small subunit with two equipotent isoforms, SAE1a and SAE1b, in plants. SAE2 is a large subunit with three functional domains: the adenylation domain, an active site with conserved Cys residue, and the UFD domain. Its C-terminal contains nuclear localization signal (NLS). Although the presence of SAE1a/1b in plants has not been related to any functional significance but contains a conserved Arg_{16}, which is the only residue that interacts with ATP in the adenylation domain (Lois, 2010). In plants, E1 enzymes offer selectivity to a certain extent by determining the specific SUMO isoforms that facilitate the entry to a particular SUMO pathway and regulate conjugation rates. A second non-canonical NLS at the C-terminus of SAE2 was also reported, which drives complete nuclear localization of SAE2, along with canonical NLS (Más et al., 2020). Proteolytic cleavage of second NLS restricts SAE2 within the cytosol. This novel PTM enables cytosolic SUMOylation and plays a definite role during seed development. The nuclear-cytosolic shuttling of E1 in plants suggests response mechanisms to various signals by modulating subcellular SUMOylation (Más et al., 2020). Arabidopsis has a single *AtSCE1a* gene while rice contains two E2s, *OsSCE1*, and *OsSCE3* with contrasting roles in drought stress.

Plants have three types of SUMO E3 ligases: the SAP AND MIZ1 DOMAIN-CONTAINING LIGASE (SIZs); the METHYL METHANESULFONATE-SENSITIVITY PROTEIN 21 (MMS21s); and the PROTEIN INHIBITOR OF ACTIVATED STAT-LIKE (PIALs). The most conserved domain of SUMO E3 ligases is SIZ/PIAL-RING (SP-RING), flanked by the SP C-terminal domain (SP-CTD). It activates the E2∼SUMO thioester bond for subsequent transfer reaction. SP-RING selectively establishes interaction with E2, while SP-CTD interacts with SUMO in a SIM-like manner to hold SUMO in a closed conformation. SP-RING domain displays similarities with α/β fold of RING and U-box domain of Ub-E3 ligases. In addition, SIZ1 and PIAL1/2 harbor domains and sequence motifs that mediate protein-protein interactions (PPI). The Plant HomeoDomain (PHD) is unique to plant SUMO ligases. It is required for SUMO-modification of global transcription factors E3 (GTE3) and helps in SUMOylation activity of SIZ1. SUMO E3 ligases, particularly SIZ1 and PIAL1/2, also contain SUMO-binding motifs and NLS. SIM motif of PIAL1/2 is associated with polySUMO chain assembly. Plant SIZ1 also possesses a valine-proline CONSTITUTIVE PHOTOMORPHOGENESIS PROTEIN 1 (VP COP1) binding motif, through which it physically interacts with the substrate binding pocket of Ub E3 ligase COP1, which is a point of integration of SUMOylation and ubiquitination (Jmii and Cappadocia, 2021). SIZ1 ligases are highly pleiotropic regulating multitudes of plant processes related to growth, development, reproduction, phytohormone signaling, and stress responses. MMS21 has been majorly associated with DNA damage responses, cell cycle regulation, and regulation of 26S proteasome activity. PIAL1 and 2 regulate transcriptional silencing and salt stress responses. Interestingly, knockout mutants of *pial1* and *pial2* showed improved salt tolerance with better PSII activity and higher biomass and displayed a greener phenotype (Jmii and Cappadocia, 2021).

Although reversible SUMOylation machinery in plants is conserved, it has a variable number of enzyme proteoforms with plant-specific functions. The expansion of the SUMO system in plants suggests the acquisition of novel functions by the SUMO-modification system during evolution. Factors instrumental to the specificity of SUMOylation remain enigmatic because of limited information about the components. Our current understanding regarding the mechanism of SUMOylation relies largely on a single universally conserved E2 and countable E3 ligases. This contrasts with Ub-system, in which substrate selectivity and specificity are majorly conferred by diverse E2-E3 combinations. Unlike Ub E2 enzymes that strictly rely on E3 ligases for exquisite substrate selectivity, SUMO E2s are less reliant on E3 ligases. Rather, they can directly engage substrates with canonical SUMOylation motifs to direct the transfer of SUMO to a lysine residue in substrates. Nevertheless,

SUMO ligases are essential for attaching SUMO to non-canonical motifs, thereby, expanding the substrate repertoire of SUMOylation (Gareau and Lima, 2010; Jmii and Cappadocia, 2021).

The cellular balance of SUMOylation and deSUMOylation is fine tuned by the action of E1-E2-E3 cascades and SUMO proteases, respectively. The downstream effect of SUMO-modification is, in part, mediated by effectors containing hydrophobic core possessing SUMO-interacting/binding motifs (SIM/SBM) surrounded by acidic and/or Ser residues. SIM/SBM harboring substrates through intramolecular interactions induce post-modification conformational changes. A non-covalent interaction between the modifier and its substrate adds specificity to the overall system since this interaction allows the substrate to select its cognate SUMO paralog. Functional consequences of SUMOylation imply critical PPIs that alter the conformation of modified target or change protein surface by exposing and/or masking interaction interfaces thereby facilitating or inhibiting trans-proteome interactions.

Signals that induce alterations in SUMOylome to regulate the structure, location, activity, solubility, stability, interaction profile, and PTM crosstalk of individual SUMO substrates allow reprogramming of cellular metabolism, signaling, gene expression, and chromatin remodeling to synchronize the physiological responses. It suggests the significance of SUMOylation in life-sustaining processes, such as cell division and proliferation, chromatin and epigenetic regulation, maintenance of nuclear integrity and transcription, differentiation and stemness, senescence, and stress responses.

SUMOylation and abiotic stress responses

SUMO proteases have a vital role in regulating plant stress responses by balancing the cellular levels of SUMOylated and non-SUMOylated proteins. Mutational studies presented a paradigm that SUMOylation regulates multiple facets of plant biology predominantly through transcriptional regulation of gene expression. Arabidopsis mutants defective in SUMO1/2, SAE, and SCE showed embryonic lethality, while ligase- and protease-deficient mutants had physiological and developmental defects. For example, the mutated AtSIZ1, a SUMO Ligase, resulted in compromised tolerance to cold and drought, early flowering, and phosphate starvation symptoms (Ghimire et al., 2021). Hyper-SUMOylation under acute heat, cold, high salinity, drought, oxidative stress, and nutrient deficiency marks the conserved SUMO stress response (SSR) in plants (Miura et al., 2005; Catala et al., 2007; Chen et al., 2011; Ghimire et al., 2020; Roy and Sadanandom, 2021; Han et al., 2022). SIZ1-mediated SUMOylation positively responds to salt and drought-induced osmotic stress; enhances metal stress tolerance and light signaling; and regulates N, P, and ROS homeostasis in plants (Fang et al., 2022). SUMOylation regulates heat stress positively at transcriptional, post-transcriptional, and translational levels. Heat shock triggers SSR, which promotes mass movement of SUMO1/2 from the cytoplasm to the nucleus. Elevated temperature results in the accumulation of unfolded proteins, which requires activation of unfolded protein response (UPR). In Arabidopsis, under normal conditions, a co-chaperon in UPR, BAG7, and a TF, bZIP28, remains associated with AtBiP2 in the ER membrane. Heat-shock-induced accumulation of unfolded protein signals SUMOylation, BiP2 dissociation, and nuclear translocation of BAG7, where it associates with nuclear TF, WRKY29, to activate transcription of stress-responsive chaperons. At the same time, dissociated bZIP28 moves to the nucleus and causes induction of BiP3 gene expression by UPR. SCE1-mediated SUMOylation of DREB2A enhances its stability, which then binds to DRE-elements for inducing transcription of stress-responsive genes (Han et al., 2021, 2022) (Figure 4A). SUMO1 conjugation represses expression of heat-shock TF, AtHSFA2, during the recovery phase, and on second exposure to heat-shock, it gets deSUMOylated, inducing expression of heat-shock proteins. AtHSF2 SUMOylation and deSUMOylation provide a primary response to heat shock until the plant stabilizes its response and acquires thermotolerance (Cohen-Peer et al., 2010). Another aspect of plants' response to heat is thermomorphogenesis, during which plant undergoes elongation growth to enhance cooling effects. AtSIZ1-dependent SUMOylation of Ub-E3 ligase COP1 stimulates SIZ1 and HY5 degradation and PIF4 stabilization. While COP1 activity is essential for transducing high-temperature signals, SIZ1 amplifies stress signals through this feedback loop. Elevated PIF4 levels enhance thermomorphogenesis and inhibit SNC1-dependent autoimmunity. Thus, SIZ1 has mutually dependent roles in modulating growth and defense at elevated temperatures (Hammoudi et al., 2018).

Cold, salinity, and drought-related genes are mainly under transcriptional control of DREB TFs. DREB binds to DRE/CRT *cis*-elements to activate their target gene expression. Low temperature induces SUMOylation of ICE1 at K_{393}. SUMO-ICE1 induced overexpression of DREB1/CBF3 leads to activation of CBF regulon and provides cold acclimatization. Also, SUMO-ICE1 counteracts the action of HOS1, which catalyzes polyubiquitination and proteasomal degradation of ICE1 (Figure 4B). Moreover, SUMO-conjugated ICE1 represses MYB15 (R_2R_3 MYB TF) expression, which, although induced by cold stress, is a negative regulator of CBF genes (Roy and Sadanandom, 2021). ICE1 is a pioneer of the cold signaling pathway in plants. ICE1-dependent induction of CBF expression involves interplay between GA and JA signaling. At optimal temperatures, JAZ, a repressor of JA signaling, remains associated with ICE1 to suppress CBF expression activation. However, low temperatures increase the ICE1 levels and activity through the accumulation of DELLA, the negative regulator of GA signaling, which binds JAZ to release ICE1. Consequently, the elevation in CBF gene expression reinforces

DELLA accumulation, which, in turn, releases more JAZ-bound ICE1. Therefore, CBF3 and DELLA show mutual regulation to modulate plant growth under stress. CBF is an upstream transcriptional activator of cold-responsive (COR) genes. Studies report that MeJA also contributes to the upregulation of CBF signaling by degrading JAZ. Also, DELLA interacts with JAZ to uplift JAZ-mediated inhibition of MYC2 TF, which is a positive regulator of JA signaling and enhances CBF gene transcription by binding ICE1 (Zhou et al., 2017; Ritonga and Chen, 2020). Brassinosteroids also impart basal freezing tolerance, as well as cold acclimatization, without retarding the plant growth. BR-deficient mutants showed repression of 6% of COR genes majority, which all were CBF controlled. BIN2 phosphorylates CESTA (CES) to prevent its SUMOylation. CES, a close homolog of BRASSINOSTEROIDS ENHANCED EXPRESSION1 (BEE1) and BEE3, is a bHLH TF, whose abundance, activity, and subnuclear localization are BR-regulated. BR, upon binding with its receptor BRI1, activates BR signaling to repress BIN2 activity, promotes SUMOylation (K_{72}), and translocates CES to the nucleus to induce COR gene expressions in CBF-dependent, as well as in CBF-independent, ways. In CBF-dependent expression of COR genes, CES has been shown to bind G-box motifs in CBF promoters (Eremina et al., 2016).

Srivastava et al. (2017) demonstrated the role of rice SUMO proteases (OsOTS1) in the mitigation of drought. OsOTS1 regulates the activity of OsbZIP23 and confers drought tolerance in an ABA-dependent manner. When sufficient hydration prevails, OsOTS1 interacts and maintains the deSUMOylated state of OsbZIP23. Drought-induced ABA accumulation promotes OsOTS1 degradation and OsbZIP23 SUMOylation, which positively regulates the expression of drought tolerant genes. OsOTS1 is also known to deSUMOylate and facilitate the degradation of DELLA proteins. Hyper-SUMOylation, followed by water-stress-mediated turnover of OTS1 proteases, results in the accumulation of rice DELLA proteins, SLR1, which impedes plant growth (Srivastava et al., 2017). OsSCE1 and SCE2 also contribute to drought tolerance but have opposing effects. Over-expression of OsSCE1 leads to hypersensitive phenotype, while OsSCE2 overexpression led to improved drought tolerance. In Arabidopsis, genome-wide expression analysis revealed that 1,700 genes are induced under desiccated conditions, and SIZ1 regulates the expression of ∼300 drought-induced genes through DREB2A and ABA-independent pathways. Such genes encode enzymes of anthocyanin biosynthesis and jasmonate signaling. This is consistent with the role of anthocyanin in the ROS detoxification pathway (Catala et al., 2007). Epistatic relations between AtSIZ1 and AtOTS1/2 have been shown to modulate stomatal closure and osmotic stress responses in Arabidopsis (Castro et al., 2016). Mutants, defective in AtSIZ1, exhibit reduced stomatal aperture, improved drought tolerance, and ABA hypersensitivity. Stomatal closure-dependent drought resistance is an effect of SA-induced ROS production, while ABA hypersensitivity is due to inhibition of SIZ1-mediated ABI5 SUMOylation. In the former case, the phenotype was complemented by exogenous treatment with salicylhydroxamic acid (SHAM) and azide but the application of NADPH oxidase inhibitor had no effect. It was inferred that SA accumulation and peroxidase-catalyzed ROS production are responsible for the *siz1* phenotype. Thus, it can be concluded that SUMO E3 ligase, SIZ1, modulates endogenous SA levels to regulate stomatal closure and drought tolerance. Notably, these effects are independent of ABA. Also, SIZ1-mediated SUMOylation of ABI5 has negative effects on ABA signaling (Miura et al., 2013). Similar to SIZ1, MMS21 is a negative regulator of ABA-dependent drought responses. Recent studies on *Malus domestica* evidenced the implication of SUMOylation in regulating DREB2A stability as a critical determinant of drought tolerance. Interestingly, it was reported that drought tolerance in apples involves a complex network of increased and reduced levels of SUMOylation and ubiquitination, respectively, where SUMOylated MdDREB2A serves as a target for RNF4-mediated ubiquitination and degradation (Li et al., 2022). Pepper dehydration-responsive homeobox1 domain (CaDRHB1) TF serves as a positive regulator of the desiccation stress response. The stability of CaDRHB1 is enhanced by CaDRHB1-interacting SIZ1 (CaDSIZ1) mediated SUMOylation under drought conditions by positively regulating ABA signaling and drought tolerance (Joo et al., 2022). AUXIN RESPONSE FACTOR7 (ARF7) plays a central role in hydropatterning, regulated by SUMOylation and deSUMOylation to modulate lateral root development. On the airside of the root, lateral root growth is suppressed due to ARF7 SUMOylation that facilitates its interaction with indole-3-acetic acid repressor *via* SIM motifs. Consequently, it inhibits ARF7 transcriptional activity and, hence, leads to activation of downstream-acting auxin-responsive genes. Root exposed to water has denser lateral roots to aid the water uptake. This happens when ARF7 is maintained in a non-SUMOylated state, likely, by the action of OTS1 proteases that promotes transcriptional activation of ARF7 target genes to stimulate lateral root formation (Roy and Sadanandom, 2021).

Likewise, SUMOylation affects the plants' responses to salinity. This is mediated by modifying transcriptional activity of an R2R3-MY-type TF, MYB30, which is known to regulate several other developmental, hormonal, and stress signaling and is subject to multiple PTMs. For example, S-nitrosylation of MYB30 consequently hampers its DNA binding ability; its activity is switched off following an initial stress response. Here, AtSIZ1-mediated SUMOylation of MYB30 at K283 leads to the expression of Alternative oxidase 1a (AOX1a), which subsequently activates cyanide-resistant respiration to restore cellular redox homeostasis to provide salt tolerance (Gong et al., 2020). AtOTS1/2 proteases govern plant growth under salinity stress. Increased levels of SUMO1/2 conjugated certain target proteins are also critical for retarding growth to tolerate

stress. Therefore, OTS1/2 not only enhances salt tolerance but also balances plant growth and survival under stressful conditions (Conti et al., 2009). Salt tolerance in rice involves homologs of Arabidopsis AtOTS1, but unlike AtOTS1, salt stress signals OsOTS1 degradation, which leads to accumulation of SUMO conjugates and eventually restraints growth through a common mechanism of SUMOylation-dependent abundance and stabilization of DELLA repressors. Salt resistance conferred by OsOTS1 is attributed to two interrelated mechanisms: regulation of gene-encoding components of the antioxidant system; and their activation by deSUMOylating enzymes, such as peroxidases and dismutases (Srivastava et al., 2016). SUMOylation also plays a significant role in nutrient acquisition and deficiency responses. Phosphorus, a macroelement, is available as inorganic phosphorous (Pi) in soil. Its low diffusion rates and fixation as organic complexes pose nutritional stress and affect the normal physiology of the plant. SUMOylation is instrumental in regulating the Pi homeostasis in plants. The SIZ1 is reported to control phosphate deficiency-induced responses in Arabidopsis and rice. The primary root tip in Arabidopsis can inherently sense local Pi concentrations irrespective of the internal Pi levels in the plant. Under Pi deficit condition, root tip cells experience progressive loss of meristematic activity, causing determinate root growth. This response was even aggravated in T-DNA insertional mutants of *siz1*, which also displayed lateral root development during Pi deprivation. SIZ1 was assumed to exert its regulatory influence on root system architecture in an auxin-dependent manner. Augmented growth of root hair number and length is also a well-characterized Pi-deficient adaptive response in Arabidopsis. The further analysis illustrated the negative impact of SIZ1 on auxin distribution patterns. Rice homolog of AtSIZ1, OsSIZ1, partially rescued the *siz1* mutant phenotype, while stimulated uptake of Pi observed in creeping bentgrass (*Agrostis stolonifera*) overexpressing OsSIZ1 suggests the possible implications of OsSIZ1 in the regulation of various root traits during Pi deficiency. Interestingly, Pi-deprived rice plants, having a more complex root system, showed significant stimulation in primary root growth and length of adventitious roots. Although auxin-signaling components, OsARF12 and OsARF16, are known to modulate Pi-deficiency-induced auxin-dependent root development responses, their dependence on SIZ1 is unexplored. These adaptive morphophysiological responses are the result of differential regulation of phosphate starvation responsive (PSR) gene expression by SIZ1. Some PSR genes like *Atpht1/4*, *AtRNS1*, and *AtIPS1* identified in Arabidopsis are shown to be involved in Pi acquisition, mobilization, and target mimicry, respectively. *AtG3Pp1* encodes for a putative organic P transporter whose expression is regulated by Pi availability in soil. SIZ1 induces the expression of *AtRNS1* and *AtIPS1* under Pi deficiency, while downregulating *Atpht1* and *AtG3Pp1* under optimal Pi concentrations, suggesting that SIZ1-dependent SUMOylation has stimulatory, as well as inhibitory, effects on the expression of PSR genes (Datta et al., 2018). Transcriptional activation of PSR genes is controlled by PHR1 (MYB TF), which binds to the PHR1-specific binding sequence (P1BS) found in the promoter region of PSR genes. SIZ1-mediated PHR1 SUMOylation at K_{261} and K_{372} residues stabilize the TF, resulting in increased abundance and DNA-binding activity of PHR1, thereby inducing target genes to exert adaptive changes in response to Pi starvation (Roy and Sadanandom, 2021). Rice PHR1-related TF, OsPHR2, is the major regulator of PSR genes and maintains cellular Pi homeostasis. OsSIZ1-modulated SUMOylation state of OsPHR1 drives the differential regulation of PSR genes under variable Pi regime (Datta et al., 2018). SUMOylation also facilitates coping with Fe deficiency. Differential regulation of stress-responsive genes through SUMOylation is mediated by the stabilization of upstream TFs. In apple, MdSIZ1 is known to directly SUMOylate and stabilize MdbHLP104 TF, which promotes Fe-responsive gene transcription. Resistance toward Al toxicity is acquired through activation of Al-resistance genes that are under transcriptional control of C_2H_2-type TF, STOP1. SUMOylation of STOP1 confers stability and stimulates the expression of target genes (Han et al., 2021). Excessive Cu^{2+} accumulation disrupts ROS homeostasis, which leads to toxicity. High Cu^{2+} level tolerance involves SUMOylation and deSUMOylation. To achieve optimal Cu^{2+} levels, plants precisely regulate the Cu^{2+} uptake, translocation, efflux, and sequestration. Related studies suggest that plant response to Cu^{2+} toxicity is a fine balance of SIZ1-mediated SUMOylation and OTS1-mediation deSUMOylation, which help plants to acquire Cu^{2+} homeostasis and tolerance (Zhan et al., 2018). SIZ1-mediated SUMOylation of NR NIA1 and NIA2 facilitate nitrogen assimilation, thereby, affecting overall growth and development in Arabidopsis (Datta et al., 2018).

Conclusion and future perspectives

Every organism undergoes differential reprogramming in response to various stresses and generates appropriate responses at the biochemical/cellular/organ/organism level. Being the workhorses of the cell, proteome organization is the foremost system to get amended upon the perception of stress stimuli. Changes in membrane integrity, ion fluxes, and osmotic potential are the primary physiological disruptions observed under various stresses. To realize the stress type and generate the respective response, the cell implements exclusive and extensive rearrangements at omic (proteome, genome, transcriptome, proteome, ionome, interactome, etc.) levels. Early responses are pivotal to confer immediate-early protection and largely manifest rapid, transient, and dynamic changes in proteome architecture. This eventually stabilizes the otherwise repressed stress-responsive factors through active inhibition/activation/elimination of upstream regulators, which

subsequently modulates gene expression profile to initiate long-term acclimation responses. The tolerance of plants to abiotic stress(es) is a complex phenomenon composite of manifold adaptive responses and synchronized operation of multiple signaling pathways simultaneously. A certain degree of overlap in the context of common elements that serve as PTM hotspots and function as switch boxes is crucial for such coordination and mediates the functional crosstalk in a stimulus-specific manner. Cross-modifications of catalytic machinery by distinct PTMs in the dialog are the alternative methods to mediate their crosstalk to respond to stress stimuli. Moreover, feedback mechanisms are also a part of the stress signaling network that regulates the intensity and duration of stress responses, thereby enabling plants to restore homeostasis.

We reviewed the role of ubiquitination and SUMOylation as covalent protein modifications in plants' immunity against abiotic stresses. Molecular mechanisms and enzymatic machineries underlying these modifications have been well-elucidated in eukaryotes, although prokaryotes have a UPS-like degradation system but lack SUMO proteins. The evolution of SUMOylation in eukaryotes suggests the expansion of ubiquitin-like modifications from a mere protein degradation unit to the regulators of virtually all aspects of protein functions. It is in agreement with the increasing complexity of eukaryotes. Although there is a striking similarity between ubiquitination and SUMOylation mechanism, as both are lysine residue modifiers and utilize concerted action of three enzyme systems, these PTMs often modify the same or different lysine residue(s) on single and/or multiple substrates and mutually regulate each other. It is quite likely that the dynamic addition of Ub and SUMO on the same protein might have opposing consequences, where the former usually accelerates the protein turnover, while the latter leads to stabilization, thus promoting the function of the target protein(s). This is not always the case; evidence supporting the complementary, as well as independent functions, has also been reported. For instance, (de)ubiquitination, apart from proteolysis, also codes for non-proteolytic functions during various developmental and stress signaling.

UPS has mainly evolved as a major protein degradation pathway in eukaryotes but underwent a massive gain-of-function and positive selection, committing ubiquitin-dependent processes to novel cellular functions. The conservation status of the ubiquitin modification system and its considerable expansion in higher organisms is consistent with its widespread role in regulating critical biological processes in the plant. SUMOylation evolved as a critical transcriptional modulator in plants due to its role in the regulation of a large complement of TFs and primarily controls their subcellular localization, stability, and interaction affecting chromatin association ability. Thus, group SUMOylation of multiple substrates facilitates their association to form functional protein complexes due to the enhanced SUMO-SIM interactions. Largely acting as a synergist or antagonist partner of ubiquitination, SUMOylation often cooperates or competes with the latter for similar targets to either support or defy each other's effect. STUBLs have emerged as exclusive crosstalk agents between SUMOylation and ubiquitination and specifically define substrates for the latter through SIM-mediated interpretation of SUMOylation on common substrates. Interestingly, STUBLs catalyzed SUMO-Ub hybrid chain formation is also reported to mark proteins as degrons. Ubiquitination and SUMOylation-mediated regulation of COP1 Ub ligase activity represent a classic example of their interdependent behavior. COP1 is a negative regulator of photomorphogenesis that ubiquitinates and signals positive regulators of photomorphogenesis for degradation in dark conditions. SIZ1 catalyzes SUMOylation of COP1 at K_{193} to enhance its trans-ubiquitination activity but has no effect on its abundance, dimerization, and translocation state, indicating that COP1 activity is only partly regulated by SIZ1. SUMOylation also facilitates the COP1 mediated degradation of ubiquitinated SIZ1, which suggests a positive regulation integrated negative feedback mechanism for mutually dependent functions of COP1 and SIZ1 ligases. Light-induced SUMOprotease-mediated deSUMOylation of COP1 and photoreceptor-mediated nuclear exclusion of COP1 lead to the stabilization of photomorphogenic factors, which activate light-responsive genes involved in photomorphogenic development in plants. Moreover, ubiquitination and SUMOylation cooperate with phosphorylation to form a tripartite regulatory network. This can be understood by their co-regulation of BR signaling where the transcription activator of BR responsive genes, BZR1, is targeted by all three PTMs to switch on and off BR responses under growth and stress conditions. BZR1 is phosphorylated by BIN2 for subsequent proteasomal degradation. SUMOylation counteracts the effect of phosphorylation and stabilizes BZR1 for activation of BR-responsive genes. However, salt stress-induced downregulation of BR responses is triggered by destabilization and accelerated degradation of phosphorylated BZR1. It is a consequence of the cytosolic accumulation of ULP1a/ELS1 SUMO protease, which deSUMOylates BZR1 and enhances its affinity for BIN2 phosphorylation and ubiquitin-dependent degradation (Han et al., 2021).

Ubiquitin and SUMOs, as well as their catalytic modules, have been considerably characterized, yet their potential substrates and downstream interacting partners are still enigmatic and need further investigations to decipher the molecular mechanisms. This will help to individually and/or holistically understand the operative signaling networks during various abiotic stresses to manifest abiotic stress tolerance in plants. This review will help to comprehend the importance of protein modifying enzymes as potential targets for bioengineering to accelerate the development of stress-tolerant plants in the future.

Author contributions

DKY conceived and designed the study, supervised the study, and revised the final version of the manuscript. MS, AS, and NY performed the literature search and wrote the manuscript. AS and NY designed the graphics. All authors have approved the final manuscript for submission.

Funding

This work was supported by the Department of Science and Technology, Science and Engineering Research Board, Government of India, under Start-up Research Grant (SB/YS/LS-185/2013) to DKY.

Conflict of interest

The authors declare that the research was conducted in the absence of any commercial or financial relationships that could be construed as a potential conflict of interest.

Publisher's note

All claims expressed in this article are solely those of the authors and do not necessarily represent those of their affiliated organizations, or those of the publisher, the editors and the reviewers. Any product that may be evaluated in this article, or claim that may be made by its manufacturer, is not guaranteed or endorsed by the publisher.

References

Agarwal, P., Agarwal, P. K., Nair, S., Sopory, S. K., and Reddy, M. K. (2007). Stress-inducible DREB2A transcription factor from *Pennisetum glaucum* is a phosphoprotein and its phosphorylation negatively regulates its DNA-binding activity. *Mol. Genet. Genomics* 277, 189–198. doi: 10.1007/s00438-006-0183-z

Alexandersson, E., Fraysse, L., Sjövall-Larsen, S., Gustavsson, S., Fellert, M., Karlsson, M., et al. (2005). Whole gene family expression and drought stress regulation of aquaporins. *Plant Mol. Biol.* 59, 469–484. doi: 10.1007/s11103-005-0352-1

Al-Saharin, R., Hellmann, H., and Mooney, S. (2022). Plant E3 ligases and their role in abiotic stress response. *Cells* 11, 890. doi: 10.3390/cells11050890

Aquila, L., and Atanassov, B. S. (2020). Regulation of histone ubiquitination in response to DNA double strand breaks. *Cells* 9, 1699. doi: 10.3390/cells9071699

Augustine, R. C., and Vierstra, R. D. (2018). SUMOylation: re-wiring the plant nucleus during stress and development. *Curr. Opin. Plant Biol.* 45, 143–154. doi: 10.1016/j.pbi.2018.06.006

Berndsen, C. E., and Wolberger, C. (2014). New insights into ubiquitin E3 ligase mechanism. *Nat. Struct. Mol. Biol.* 21, 301–307. doi: 10.1038/nsmb.2780

Bu, Q., Li, H., Zhao, Q., Jiang, H., Zhai, Q., Zhang, J., et al. (2009). The arabidopsis RING finger E3 ligase RHA2a is a novel positive regulator of abscisic acid signaling during seed germination and early seedling development. *Plant Physiol.* 150, 463–481. doi: 10.1104/pp.109.135269

Callis, J. (2014). The ubiquitination machinery of the ubiquitin system. *The Arabidopsis Book* 12, e0174. doi: 10.1199/tab.0174

Cao, Y., Dai, Y., Cui, S., and Ma, L. (2008). Histone H2B monoubiquitination in the chromatin of FLOWERING LOCUS C regulates flowering time in Arabidopsis. *Plant Cell* 20, 2586–2602. doi: 10.1105/tpc.108.062760

Castro, P. H., Couto, D., Freitas, S., Verde, N., Macho, A. P., Huguet, S., et al. (2016). SUMO proteases ULP1c and ULP1d are required for development and osmotic stress responses in *Arabidopsis thaliana*. *Plant Mol. Biol.* 92, 143–159. doi: 10.1007/s11103-016-0500-9

Castro, P. H., Tavares, R. M., Bejarano, E. R., and Azevedo, H. (2012). SUMO, a heavyweight player in plant abiotic stress responses. *Cell. Mol. Life Sci.* 69, 3269–3283. doi: 10.1007/s00018-012-1094-2

Catala, R., Ouyang, J., Abreu, I. A., Hu, Y., Seo, H., Zhang, X., et al. (2007). The Arabidopsis E3 SUMO ligase SIZ1 regulates plant growth and drought responses. *Plant Cell* 19, 2952–2966. doi: 10.1105/tpc.106.049981

Chen, C. C., Chen, Y. Y., Tang, I. C., Liang, H. M., Lai, C. C., Chiou, J. M., et al. (2011). Arabidopsis SUMO E3 Ligase SIZ1 is involved in excess copper tolerance. *Plant Physiol.* 156, 2225–2234. doi: 10.1104/pp.111.178996

Chen, L., and Hellmann, H. (2013). Plant E3 ligases: flexible enzymes in a sessile world. *Mol. Plant* 6, 1388–1404. doi: 10.1093/mp/sst005

Chinnusamy, V., Ohta, M., Kanrar, S., Lee, B., Hong, X., Agarwal, M., et al. (2003). ICE1: a regulator of cold-induced transcriptome and freezing tolerance in Arabidopsis. *Genes Dev.* 17, 1043–1054. doi: 10.1101/gad.1077503

Christensen, A. H., Sharrock, R. A., and Quail, P. H. (1992). Maize polyubiquitin genes: structure, thermal perturbation of expression and transcript splicing, and promoter activity following transfer to protoplasts by electroporation. *Plant Mol. Biol.* 18, 675–689. doi: 10.1007/BF00020010

Chung, E., Cho, C.-W., So, H.-A., Kang, J.-S., Chung, Y. S., and Lee, J.-H. (2013). Overexpression of VrUBC1, a mung bean E2 ubiquitin-conjugating enzyme, enhances osmotic stress tolerance in Arabidopsis. *PLoS One* 8, e66056. doi: 10.1371/journal.pone.0066056

Cohen-Peer, R., Schuster, S., Meiri, D., Breiman, A., and Avni, A. (2010). Sumoylation of Arabidopsis heat shock factor A2 (HsfA2) modifies its activity during acquired thermotolerance. *Plant Mol. Biol.* 74, 33–45. doi: 10.1007/s11103-010-9652-1

Collins, G. A., and Goldberg, A. L. (2017). The logic of the 26S proteasome. *Cell* 169, 792–806. doi: 10.1016/j.cell.2017.04.023

Conti, L., Kioumourtzoglou, D., O.', Donnell, E., Dominy, P., and Sadanandom, A. (2009). OTS1 and OTS2 SUMO proteases link plant development and survival under salt stress. *Plant Signal. Behav.* 4, 225–227. doi: 10.4161/psb.4.3.7867

Conti, L., Price, G., O'Donnell, E., Schwessinger, B., Dominy, P., and Sadanandom, A. (2008). Small ubiquitin-like modifier proteases OVERLY TOLERANT TO SALT1 and−2 regulate salt stress responses in Arabidopsis. *Plant Cell* 20, 2894–2908. doi: 10.1105/tpc.108.058669

Cui, F., Liu, L., Li, Q., Yang, C., and Xie, Q. (2012). UBC32 Mediated oxidative tolerance in Arabidopsis. *J. Genet. Genomics* 39, 415–417. doi: 10.1016/j.jgg.2012.05.005

Datta, M., Kaushik, S., Jyoti, A., Mathur, N., Kothari, S. L., and Jain, A., et al. (2018). SIZ1-mediated SUMOylation during phosphate homeostasis in plants: looking beyond the tip of the iceberg. *Semin. Cell Dev. Biol.* 74, 123–132. doi: 10.1016/j.semcdb.2017.09.016

Deribe, Y. L., Pawson, T., and Dikic, I. (2010). Post-translational modifications in signal integration. *Nat. Struct. Mol. Biol.* 17, 666–672. doi: 10.1038/nsmb.1842

Deshaies, R. J., and Joazeiro, C. A. P. (2009). RING domain E3 ubiquitin ligases. *Annu. Rev. Biochem.* 78, 399–434. doi: 10.1146/annurev.biochem.78.101807.093809

Dill, A., Thomas, S. G., Hu, J., Steber, C. M., and Sun, T. (2004). The Arabidopsis F-box protein SLEEPY1 targets gibberellin signaling repressors for gibberellin-induced degradation. *The Plant Cell* 16, 1392–1405. doi: 10.1105/tpc.020958

Dong, C.-H., Agarwal, M., Zhang, Y., Xie, Q., and Zhu, J.-K. (2006). The negative regulator of plant cold responses, HOS1, is a RING E3 ligase that mediates the ubiquitination and degradation of ICE1. *Proc. Natl. Acad. Sci. U. S. A.* 103, 8281–8286. doi: 10.1073/pnas.0602874103

Dooki, A. D., Mayer-Posner, F. J., Askari, H., Zaiee, A., and Salekdeh, G. H. (2006). Proteomic responses of rice young panicles to salinity. *Proteomics* 6, 6498–6507. doi: 10.1002/pmic.200600367

dos Reis, S. P., Tavares Lde, S., Costa Cde, N., Brígida, A. B., and de Souza, C. R. (2012). Molecular cloning and characterization of a novel RING zinc-finger protein gene upregulated under *in vitro* salt stress in cassava. *Mol. Biol. Rep*. 39, 6513–6519. doi: 10.1007/s11033-012-1479-1

Dove, K. K., and Klevit, R. E. (2017). RING-between-RING E3 ligases: emerging themes amid the variations. *J Mol. Biol*. 429, 3363–3375. doi: 10.1016/j.jmb.2017.08.008

Drabikowski, K., Ferralli, J., Kistowski, M., Oledzki, J., Dadlez, M., and Chiquet-Ehrismann, R. (2018). Comprehensive list of SUMO targets in Caenorhabditis elegans and its implication for evolutionary conservation of SUMO signaling. *Sci. Rep*. 8, 1139. doi: 10.1038/s41598-018-19424-9

Ellis, C., Turner, J. G., and Devoto, A. (2002). Protein complexes mediate signalling in plant responses to hormones, light, sucrose and pathogens. *Plant Mol. Biol*. 50, 971–980. doi: 10.1023/A:1021291522243

Eremina, M., Unterholzner, S. J., Rathnayake, A. I., Castellanos, M., Khan, M., Kugler, K. G., et al. (2016). Brassinosteroids participate in the control of basal and acquired freezing tolerance of plants. *Proc. Natl. Acad. Sci*. 113, E5982–E5991. doi: 10.1073/pnas.1611477113

Fang, S., Hou, X., and Liang, X. (2022). SIZ1-mediated SUMOylation responds to multiple abiotic stresses in plants. *Environ. Exp. Bot*. 201, 104977. doi: 10.1016/j.envexpbot.2022.104977

Feng, B., Li, S., Wang, Z., Cao, F., Wang, Z., Li, G., et al. (2021). Systematic analysis of lysine 2- hydroxyisobutyrylation posttranslational modification in wheat leaves. *PLoS ONE* 16, e0253325. doi: 10.1371/journal.pone.0253325

Fernandez, M. A., Belda-Palazon, B., Julian, J., Coego, A., Lozano-Juste, J., Iñigo, S., et al. (2020). RBR-Type E3 Ligases and the ubiquitin-conjugating enzyme UBC26 regulate abscisic acid receptor levels and signaling. *Plant Physiol*. 182, 1723–1742. doi: 10.1104/pp.19.00898

Finkelstein, R. R., Gampala, S. S. L., and Rock, C. D. (2002). Abscisic acid signaling in seeds and seedlings. *The Plant Cell* 14, S15–S45. doi: 10.1105/tpc.010441

Finkelstein, R. R., and Lynch, T. J. (2000). The Arabidopsis abscisic acid response gene ABI5 encodes a basic leucine zipper transcription factor. *Plant Cell* 12, 599–609. doi: 10.1105/tpc.12.4.599

Fukao, T., Barrera-Figueroa, B. E., Juntawong, P., and Peña-Castro, J. M. (2019). Submergence and waterlogging stress in plants: aq review highlighting research opportunities and understudied aspects. *Front. Plant Sci*. 10, 340. doi: 10.3389/fpls.2019.00340

Fukao, T., Yeung, E., and Bailey-Serres, J. (2011). The submergence tolerance regulator SUB1A mediates crosstalk between submergence and drought tolerance in rice. *Plant Cell* 23, 412–427. doi: 10.1105/tpc.110.080325

Garbarino, J. E., Rockhold, D. R., and Belknap, W. R. (1992). Expression of stress-responsive ubiquitin genes in potato tubers. *Plant Mol. Biol*. 20, 235–244. doi: 10.1007/BF00014491

García-Mauriño, S., Monreal, J., Alvarez, R., Vidal, J., and Echevarría, C. (2003). Characterization of salt stress-enhanced phosphoenolpyruvate carboxylase kinase activity in leaves of *Sorghum vulgare*: independence from osmotic stress, involvement of ion toxicity and significance of dark phosphorylation. *Planta* 216, 648–655. doi: 10.1007/s00425-002-0893-3

Gareau, J. R., and Lima, C. D. (2010). The SUMO pathway: emerging mechanisms that shape specificity, conjugation and recognition. *Nat. Rev. Mol. Cell Biol*. 11, 861–871. doi: 10.1038/nrm3011

Geiss-Friedlander, R., and Melchior, F. (2007). Concepts in sumoylation: a decade on. *Nat. Rev. Mol. Cell Biol*. 8, 947–956. doi: 10.1038/nrm2293

Genschik, P., Parmentier, Y., Durr, A., Marbach, J., Criqui, M.-C., Jamet, E., et al. (1992). Ubiquitin genes are differentially regulated in protoplast-derived cultures of *Nicotiana sylvestris* and in response to various stresses. *Plant Mol. Biol*. 20, 897–910. doi: 10.1007/BF00027161

Ghimire, S., Tang, X., Liu, W., Fu, X., Zhang, H., Zhang, N., et al. (2021). SUMO conjugating enzyme: a vital player of SUMO pathway in plants. *Physiol. Mol. Biol. Plants* 27, 2421–2431. doi: 10.1007/s12298-021-01075-2

Ghimire, S., Tang, X., Zhang, N., Liu, W., and Si, H. (2020). SUMO and SUMOylation in plant abiotic stress. *Plant Growth Regul*. 91, 317–325. doi: 10.1007/s10725-020-00624-1

Gong, Q., Li, S., Zheng, Y., Duan, H., Xiao, F., Zhuang, Y., et al. (2020). SUMOylation of MYB30 enhances salt tolerance by elevating alternative respiration via transcriptionally upregulating AOX1a in Arabidopsis. *Plant J*. 102, 1157–1171. doi: 10.1111/tpj.14689

Guo, Q., Zhang, J., Gao, Q., Xing, S., Li, F., and Wang, W. (2008). Drought tolerance through overexpression of monoubiquitin in transgenic tobacco. *J. Plant Physiol*. 165, 1745–1755. doi: 10.1016/j.jplph.2007.10.002

Hammoudi, V., Fokkens, L., Beerens, B., Vlachakis, G., Chatterjee, S., Arroyo-Mateos, M., et al. (2018). The Arabidopsis SUMO E3 ligase SIZ1 mediates the temperature dependent trade-off between plant immunity and growth. *PLOS Genet*. 14, e1007157. doi: 10.1371/journal.pgen.1007157

Han, D., Lai, J., and Yang, C. (2021). SUMOylation: a critical transcription modulator in plant cells. *Plant Sci*. 310, 110987. doi: 10.1016/j.plantsci.2021.110987

Han, D., Yu, Z., Lai, J., and Yang, C. (2022). Post-translational modification: a strategic response to high temperature in plants. *aBIOTECH* 3, 49–64. doi: 10.1007/s42994-021-00067-w

Hanada, K., Zou, C., Lehti-Shiu, M. D., Shinozaki, K., and Shiu, S.-H. (2008). Importance of lineage-specific expansion of plant tandem duplicates in the adaptive response to environmental stimuli. *Plant Physiol*. 148, 993–1003. doi: 10.1104/pp.108.122457

Hattori, T., Totsuka, M., Hobo, T., Kagaya, Y., and Yamamoto-Toyoda, A. (2002). Experimentally determined sequence requirement of ACGT-containing abscisic acid response element. *Plant Cell Physiol*. 43, 136–140. doi: 10.1093/pcp/pcf014

Herrmann, J., Lerman, L. O., and Lerman, A. (2007). Ubiquitin and ubiquitin-like proteins in protein regulation. *Circ. Res*. 100, 1276–1291. doi: 10.1161/01.RES.0000264500.11888.f0

Hicke, L. (2001). Protein regulation by monoubiquitin. *Nat. Rev. Mol. Cell Biol*. 2, 195–201. doi: 10.1038/35056583

Himmelbach, A., Yang, Y., and Grill, E. (2003). Relay and control of abscisic acid signaling. *Curr. Opin. Plant Biol*. 6, 470–479. doi: 10.1016/S1369-5266(03)00090-6

Hotton, S. K., and Callis, J. (2008). Regulation of cullin RING ligases. *Annu. Rev. Plant Biol*. 59, 467–489. doi: 10.1146/annurev.arplant.58.032806.104011

Hu, X., Xiao, X., Zhang, C. L., Wang, G. L., Zhang, Y. L., Li, Y. Y., et al. (2022). Organization and regulation of the apple SUMOylation system under salt and ABA. *Plant Physiol. Biochem*. 182, 22–35. doi: 10.1016/j.plaphy.2022.03.034

Hu, Z., Song, N., Zheng, M., Liu, X., Liu, Z., Xing, J., et al. (2015). Histone acetyltransferase GCN5 is essential for heat stress-responsive gene activation and thermotolerance in Arabidopsis. *Plant J*. 84, 1178–1191. doi: 10.1111/tpj.13076

Hua, Z., and Vierstra, R. D. (2011). The cullin-RING ubiquitin-protein ligases. *Ann. Rev. Plant Biol*. 62, 299–334. doi: 10.1146/annurev-arplant-042809-112256

Huang, J., Luo, Z., Ying, W., Cao, Q., Huang, H., Dong, J., et al. (2017). 2-Hydroxyisobutyrylation on histone H4K8 is regulated by glucose homeostasis in *Saccharomyces cerevisiae*. *Proc. Natl. Acad. Sci. U. S. A*. 114, 8782–8787. doi: 10.1073/pnas.1700796114

Huibregtse, J. M., Scheffner, M., Beaudenon, S., and Howley, P. M. (1995). A family of proteins structurally and functionally related to the E6-AP ubiquitin-protein ligase. *Proc. Natl. Acad. Sci. U. S. A*. 92, 2563–2567. doi: 10.1073/pnas.92.7.2563

Jang, J. Y., Kim, D. G., Kim, Y. O., Kim, J. S., and Kang, H. (2004). An expression analysis of a gene family encoding plasma membrane aquaporins in response to abiotic stresses in *Arabidopsis thaliana*. *Plant Mol. Biol*. 54, 713–725. doi: 10.1023/B:PLAN.0000040900.61345.a6

Jisha, V., Dampanaboina, L., Vadassery, J., Mithöfer, A., Kappara, S., and Ramanan, R. (2015). Overexpression of an AP2/ERF type transcription factor OsEREBP1 confers biotic and abiotic stress tolerance in rice. *PLoS ONE* 10, e0127831. doi: 10.1371/journal.pone.0127831

Jmii, S., and Cappadocia, L. (2021). Plant SUMO E3 ligases: function, structural organization, and connection with DNA. *Front. Plant Sci*. 12, 652170. doi: 10.3389/fpls.2021.652170

Joo, H., Lim, C. W., and Lee, S. C. (2022). Pepper SUMO E3 ligase CaDSIZ1 enhances drought tolerance by stabilizing the transcription factor CaDRHB1. *New Phytol*. 235, 2313–30. doi: 10.1111/nph.18300

Kang, H., Zhang, M., Zhou, S., Guo, Q., Chen, F., Wu, J., et al. (2016). Overexpression of wheat ubiquitin gene, Ta-Ub2, improves abiotic stress tolerance of *Brachypodium distachyon*. *Plant Sci. Int. J. Exp. Plant Biol*. 248, 102–115. doi: 10.1016/j.plantsci.2016.04.015

Kant, S., Bi, Y. M., and Rothstein, S. J. (2011). Understanding plant response to nitrogen limitation for the improvement of crop nitrogen use efficiency. *J. Exp. Bot*. 62, 1499–509. doi: 10.1093/jxb/erq297

Kim, D. Y., Scalf, M., Smith, L. M., and Vierstra, R. D. (2013). Advanced proteomic analyses yield a deep catalog of ubiquitylation targets in Arabidopsis. *Plant Cell* 25, 1523–1540. doi: 10.1105/tpc.112.108613

Kim, H. T., Pyo, K., Lledias, F., Kisselev, A. F., Scaglione, K. M., Skowyra, D., et al. (2007). Certain pairs of ubiquitin-conjugating enzymes (E2s) and ubiquitin-protein ligases (E3s) synthesize nondegradable forked ubiquitin chains containing all possible isopeptide linkages. *J. Biol. Chem*. 282, 17375–17386. doi: 10.1074/jbc.M609659200

Kim, J. Y., Park, B. S., Park, S. W., Lee, H. Y., Song, J. T., and Seo, H. S. (2018). Nitrate reductases are relocalized to the nucleus by atsiz1 and their levels are negatively regulated by COP1 and ammonium. *Int. J. Mol. Sci*. 19, 1202. doi: 10.3390/ijms19041202

Kim, S., Park, S., Kwon, H., Cho, M. H., Kim, B.-G., Chung, J. H., et al. (2022). The rice abscisic acid-responsive RING finger E3 ligase OsRF1 targets OsPP2C09 for degradation and confers drought and salinity tolerance in rice. *Front. Plant Sci*. 12, 797940. doi: 10.3389/fpls.2021.797940

Kirkin, V., McEwan, D. G., Novak, I., and Dikic, I. (2009). A role for ubiquitin in selective autophagy. *Mol. Cell* 34, 259–269. doi: 10.1016/j.molcel.2009.04.026

Kirkpatrick, D. S., Hathaway, N. A., Hanna, J., Elsasser, S., Rush, J., Finley, D., et al. (2006). Quantitative analysis of *in vitro* ubiquitinated cyclin B1 reveals complex chain topology. *Nat. Cell Biol*. 8, 700–710. doi: 10.1038/ncb1436

Ko, J.-H., Yang, S. H., and Han, K.-H. (2006). Upregulation of an Arabidopsis RING-H2 gene, XERICO, confers drought tolerance through increased abscisic acid biosynthesis. *Plant J*. 47, 343–355. doi: 10.1111/j.1365-313X.2006.02782.x

Komander, D., Clague, M. J., and Urbé, S. (2009). Breaking the chains: structure and function of the deubiquitinases. *Nat. Rev. Mol. Cell Biol*. 10, 550–563. doi: 10.1038/nrm2731

Komander, D., and Rape, M. (2012). The ubiquitin code. *Annu. Rev. Biochem*. 81, 203–229. doi: 10.1146/annurev-biochem-060310-170328

Kosová, K., Vítámvás, P., Prášil, I. T., and Renaut, J. (2011). Plant proteome changes under abiotic stress - contribution of proteomics studies to understanding plant stress response. *J. Proteomics* 74, 1301–1322. doi: 10.1016/j.jprot.2011.02.006

Kraft, E., Stone, S. L., Ma, L., Su, N., Gao, Y., Lau, O.-S., et al. (2005). Genome analysis and functional characterization of the E2 and RING-Type E3 ligase ubiquitination enzymes of Arabidopsis. *Plant Physiol*. 139, 1597–1611. doi: 10.1104/pp.105.067983

Kurepa, J., Toh,-E., A., and Smalle, J. (2008). 26S proteasome regulatory particle mutants have increased oxidative stress tolerance. *Plant J*. 53, 102–114. doi: 10.1111/j.1365-313X.2007.03322.x

Kurepa, J., Walker, J. M., Smalle, J., Gosink, M. M., Davis, S. J., Durham, T. L., et al. (2003). The small ubiquitin-like modifier (SUMO) protein modification system in Arabidopsis. Accumulation of SUMO1 and−2 conjugates is increased by stress. *J. Biol. Chem*. 278, 6862–6872. doi: 10.1074/jbc.M209694200

Lam, Y. A., Xu, W., De Martino, G. N., and Cohen, R. E. (1997). Editing of ubiquitin conjugates by an isopeptidase in the 26S proteasome. *Nature* 385, 737–740. doi: 10.1038/385737a0

Lee, H. K., Cho, S. K., Son, O., Xu, Z., Hwang, I., and Kim, W. T. (2009). Drought stress-induced Rma1H1, a RING membrane-anchor E3 ubiquitin ligase homolog, regulates aquaporin levels via ubiquitination in transgenic Arabidopsis plants. *Plant Cell* 21, 622–641. doi: 10.1105/tpc.108.061994

Lee, S.-J., Choi, J.-Y., Sung, Y.-M., Park, H., Rhim, H., and Kang, S. (2001). E3 ligase activity of RING finger proteins that interact with Hip-2, a human ubiquitin-conjugating enzyme. *FEBS Lett*. 503, 61–64. doi: 10.1016/S0014-5793(01)02689-8

Lehti-shiu, M. D., and Shiu, S. (2012). Diversity, classification and function of the plant protein kinase superfamily. *Philos. Trans. R. Soc. Lond., B Biol. Sci*. 367, 2619–2639. doi: 10.1098/rstb.2012.0003

Li, H., Jiang, H., Bu, Q., Zhao, Q., Sun, J., Xie, Q., et al. (2011). The Arabidopsis RING finger E3 ligase RHA2b acts additively with RHA2a in regulating abscisic acid signaling and drought response. *Plant Physiol*. 156, 550–563. doi: 10.1104/pp.111.176214

Li, Q., Wang, W., Wang, W., Zhang, G., Liu, Y., Wang, Y., et al. (2018). Wheat F-box protein gene TaFBA1 is involved in plant tolerance to heat stress. *Front. Plant Sci*. 9, 521. doi: 10.3389/fpls.2018.00521

Li, S., He, X., Gao, Y., Zhou, C., Chiang, V. L., and Li, W. (2021). Histone acetylation changes in plant response to drought stress. *Genes* 12, 1409. doi: 10.3390/genes12091409

Li, W., Bengtson, M. H., Ulbrich, A., Matsuda, A., Reddy, V. A., Orth, A., et al. (2008). Genome-wide and functional annotation of human E3 ubiquitin ligases identifies MULAN, a mitochondrial E3 that regulates the organelle's dynamics and signaling. *PLoS ONE* 3, e1487. doi: 10.1371/journal.pone.0001487

Li, W., and Schmidt, W. (2010). A lysine-63-linked ubiquitin chain-forming conjugase, UBC13, promotes the developmental responses to iron deficiency in Arabidopsis roots. *Plant J*. 62, 330–343. doi: 10.1111/j.1365-313X.2010.04150.x

Li, X., Zhou, S., Liu, Z., Lu, L., Dang, H., Li, H., et al. (2022). Fine-tuning of SUMOylation modulates drought tolerance of apple. *Plant Biotechnol. J*. 20, 903–919. doi: 10.1111/pbi.13772

Lim, S. D., Oh, D. G., Park, Y. C., and Jang, C. S. (2020). Molecular characterization of a RING E3 ligase SbHCI1 in sorghum under heat and abscisic acid stress. *Planta* 252, 89. doi: 10.1007/s00425-020-03469-0

Liu, B., Jiang, Y., Tang, H., Tong, S., Lou, S., Shao, C., et al. (2021). The ubiquitin E3 ligase SR1 modulates the submergence response by degrading phosphorylated WRKY33 in Arabidopsis. *Plant Cell* 33, 1771–1789. doi: 10.1093/plcell/koab062

Liu, Y., Zhu, J., Sun, S., Cui, F., Han, Y., Peng, Z., et al. (2019). Defining the function of SUMO system in pod development and abiotic stresses in Peanut. *BMC Plant Biol.* 19, 593. doi: 10.1186/s12870-019-2136-9

Livneh, I., Cohen-Kaplan, V., Cohen-Rosenzweig, C., Avni, N., and Ciechanover, A. (2016). The life cycle of the 26S proteasome: from birth, through regulation and function, and onto its death. *Cell Res*.26, 869–885. doi: 10.1038/cr.2016.86

Lois, L. M. (2010). Diversity of the SUMOylation machinery in plants. *Biochem. Soc. Trans*. 38, 60–64. doi: 10.1042/BST0380060

Lopez-Molina, L., Mongrand, S., and Chua, N.-H. (2001). A postgermination developmental arrest checkpoint is mediated by abscisic acid and requires the ABI5 transcription factor in Arabidopsis. *Proc. Natl. Acad. Sci. U. S. A*. 98, 4782–4787. doi: 10.1073/pnas.081594298

Lopez-Molina, L., Mongrand, S., Kinoshita, N., and Chua, N.-H. (2003). AFP is a novel negative regulator of ABA signaling that promotes ABI5 protein degradation. *Genes Dev*. 17, 410–418. doi: 10.1101/gad.1055803

Lopez-Molina, L., Mongrand, S., McLachlin, D. T., Chait, B. T., and Chua, N.-H. (2002). ABI5 acts downstream of ABI3 to execute an ABA-dependent growth arrest during germination. *Plant J*. 32, 317–328. doi: 10.1046/j.1365-313X.2002.01430.x

Lorenz, S. (2018). Structural mechanisms of HECT-type ubiquitin ligases. *Biol. Chem*. 399, 127–145. doi: 10.1515/hsz-2017-0184

Lyzenga, W. J., and Stone, S. L. (2012). Abiotic stress tolerance mediated by protein ubiquitination. *J. Exp. Bot*. 63, 599–616. doi: 10.1093/jxb/err310

Maekawa, S., Sato, T., Asada, Y., Yasuda, S., Yoshida, M., Chiba, Y., et al. (2012). The Arabidopsis ubiquitin ligases ATL31 and ATL6 control the defense response as well as the carbon/nitrogen response. *Plant Mol. Biol*. 79, 217–227. doi: 10.1007/s11103-012-9907-0

Marín, I. (2010). Diversification and specialization of plant RBR ubiquitin ligases. *PLoS ONE* 5, e11579. doi: 10.1371/journal.pone.0011579

Marshall, R. S., and Vierstra, R. D. (2019). Dynamic regulation of the 26S proteasome: from synthesis to degradation. *Front. Mol. Biosci*. 6, 40. doi: 10.3389/fmolb.2019.00040

Más, A., Castaño-Miquel, L., Carretero-Paulet, L., Colomé, N., Canals, F., and Lois, L. M. (2020). Evolution of molecular determinants for SUMO-activating enzyme subcellular localization in plants. *bioRxiv*. doi: 10.1101/2020.10.05.326249

Mattiroli, F., and Penengo, L. (2021). Histone ubiquitination: an integrative signaling platform in genome stability. *Trends Genet*. 37, 566–581. doi: 10.1016/j.tig.2020.12.005

Mazzucotelli, E., Belloni, S., Marone, D., De Leonardis, A., Guerra, D., Di Fonzo, N., et al. (2006). The E3 ubiquitin ligase gene family in plants: regulation by degradation. *Curr. Genomics* 7, 509–522. doi: 10.2174/138920206779315728

Mazzucotelli, E., Mastrangelo, A. M., Crosatti, C., Guerra, D., Stanca, A. M., and Cattivelli, L. (2008). Abiotic stress response in plants: when post-transcriptional and post-translational regulations control transcription. *Plant Sci*. 174, 420–431. doi: 10.1016/j.plantsci.2008.02.005

Miricescu, A., Goslin, K., and Graciet, E. (2018). Ubiquitylation in plants: signaling hub for the integration of environmental signals. *J. Exp. Bot*. 69, 4511–4527. doi: 10.1093/jxb/ery165

Miura, K., Jin, J. B., and Haegawa, P. M. (2007). Sumoylation, a post-translational regulatory process in plants. *Curr. Opin. Plant Biol.* 10, 495–502. doi: 10.1016/j.pbi.2007.07.002

Miura, K., Okamoto, H., Okuma, E., Shiba, H., Kamada, H., Hasegawa, P. M., et al. (2013). SIZ1 deficiency causes reduced stomatal aperture and enhanced drought tolerance via controlling salicylic acid-induced accumulation of reactive oxygen species in Arabidopsis. *Plant J*. 73, 91–104. doi: 10.1111/tpj.12014

Miura, K., Rus, A., Sharkhuu, A., Yokoi, S., Karthikeyan, A. S., Raghothama, K. G., et al. (2005). The Arabidopsis SUMO E3 ligase SIZ1 controls phosphate deficiency responses. *Proc. Natl. Acad. Sci. U. S. A*. 102, 7760–7765. doi: 10.1073/pnas.0500778102

Molinier, J., Lechner, E., Dumbliauskas, E., and Genschik, P. (2008). Regulation and role of Arabidopsis CUL4-DDB1A-DDB2 in maintaining genome integrity upon UV stress. *PLoS Genet.* 4, e1000093. doi: 10.1371/journal.pgen.1000093

Morrell, R., and Sadanandom, A. (2019). Dealing with stress: a review of plant SUMO proteases. *Front. Plant Sci*. 10:1122. doi: 10.3389/fpls.2019.01122

Narusaka, Y., Nakashima, K., Shinwari, Z. K., Sakuma, Y., Furihata, T., Abe, H., et al. (2003). Interaction between two cis-acting elements, ABRE and DRE, in ABA-dependent expression of Arabidopsis rd29A gene in response to dehydration and high-salinity stresses. *Plant J*. 34, 137–148. doi: 10.1046/j.1365-313X.2003.01708.x

Ning, Y., Jantasuriyarat, C., Zhao, Q., Zhang, H., Chen, S., Liu, J., et al. (2011). The SINA E3 ligase OsDIS1 negatively regulates drought response in rice. *Plant Physiol.* 157, 242–255. doi: 10.1104/pp.111.180893

Pandey, A., Chakraborty, S., Datta, A., and Chakraborty, N. (2008). Proteomics approach to identify dehydration responsive nuclear proteins from chickpea (*Cicer arietinum* L.). *Mol. Cell. Proteomics* 7, 88–107. doi: 10.1074/mcp.M700314-MCP200

Park, B. S., Song, J. T., and Seo, H. S. (2011). Arabidopsis nitrate reductase activity is stimulated by the E3 SUMO ligase AtSIZ1. *Nat. Commun.* 2, 400. doi: 10.1038/ncomms1408

Park, J.-A., Cho, S. K., Kim, J. E., Chung, H. S., Hong, J.-P., Hwang, B., et al. (2003). Isolation of cDNAs differentially expressed in response to drought stress and characterization of the Ca-LEAL1 gene encoding a new family of atypical LEA-like protein homologue in hot pepper (*Capsicum annuum* L. cv. Pukang). *Plant Sci.* 165, 471–481. doi: 10.1016/S0168-9452(03)00165-1

Peng, L., Wan, X., Huang, K., Pei, L., Xiong, J., Li, X., et al. (2019). AtPUB48 E3 ligase plays a crucial role in the thermotolerance of Arabidopsis. *Biochem. Biophys. Res. Commun.* 509, 281–286. doi: 10.1016/j.bbrc.2018.12.123

Peng, M., Hannam, C., Gu, H., Bi, Y.-M., and Rothstein, S. J. (2007). A mutation in NLA, which encodes a RING-type ubiquitin ligase, disrupts the adaptability of Arabidopsis to nitrogen limitation. *Plant J.* 50, 320–337. doi: 10.1111/j.1365-313X.2007.03050.x

Peth, A., Uchiki, T., and Goldberg, A. L. (2010). ATP-dependent steps in the binding of ubiquitin conjugates to the 26S proteasome that commit to degradation. *Mol. Cell.* 40, 671–681. doi: 10.1016/j.molcel.2010.11.002

Pickart, C. M., and Fushman, D. (2004). Polyubiquitin chains: polymeric protein signals. *Curr. Opin. Chem. Biol.* 8, 610–616. doi: 10.1016/j.cbpa.2004.09.009

Prakash, S., Tian, L., Ratliff, K. S., Lehotzky, R. E., and Matouschek, A. (2004). An unstructured initiation site is required for efficient proteasome-mediated degradation. *Nat. Struct. Mol. Biol.* 11, 830–837. doi: 10.1038/nsmb814

Qin, F., Sakuma, Y., Tran, L.-S. P., Maruyama, K., Kidokoro, S., Fujita, Y., et al. (2008). Arabidopsis DREB2A-interacting proteins function as RING E3 ligases and negatively regulate plant drought stress–responsive gene expression. *Plant Cell* 20, 1693–1707. doi: 10.1105/tpc.107.057380

Ritonga, F. N., and Chen, S. (2020). Physiological and molecular mechanism involved in cold stress tolerance in plants. *Plants* 9, 560. doi: 10.3390/plants9050560

Rittinger, K., and Ikeda, F. (2017). Linear ubiquitin chains: enzymes, mechanisms and biology. *Open Biol.* 7, 170026. doi: 10.1098/rsob.170026

Rodrigo-Brenni, M. C., Foster, S. A., and Morgan, D. O. (2010). Catalysis of lysine 48-specific ubiquitin chain assembly by residues in E2 and ubiquitin. *Mol. Cell* 39, 548–559. doi: 10.1016/j.molcel.2010.07.027

Roy, D., and Sadanandom, A. (2021). SUMO mediated regulation of transcription factors as a mechanism for transducing environmental cues into cellular signaling in plants. *Cell. Mol. Life Sci.* 78, 2641–2664. doi: 10.1007/s00018-020-03723-4

Ryu, M. Y., Cho, S. K., and Kim, W. T. (2010). The Arabidopsis C3H2C3-Type RING E3 ubiquitin ligase AtAIRP1 is a positive regulator of an abscisic acid-dependent response to drought Stress. *Plant Physiol.* 154, 1983–1997. doi: 10.1104/pp.110.164749

Sadanandom, A., Bailey, M., Ewan, R., Lee, J., and Nelis, S. (2012). The ubiquitin–proteasome system: central modifier of plant signalling. *New Phytol.* 196, 13–28. doi: 10.1111/j.1469-8137.2012.04266.x

Saeki, Y., Kudo, T., Sone, T., Kikuchi, Y., Yokosawa, H., Toh-e, A., et al. (2009). Lysine 63-linked polyubiquitin chain may serve as a targeting signal for the 26S proteasome. *EMBO J.* 28, 359–371. doi: 10.1038/emboj.2008.305

Sakuma, Y., Maruyama, K., Osakabe, Y., Qin, F., Seki, M., Shinozaki, K., et al. (2006a). Functional analysis of an Arabidopsis transcription factor, DREB2A, involved in drought-responsive gene expression. *Plant Cell* 18, 1292–1309. doi: 10.1105/tpc.105.035881

Sakuma, Y., Maruyama, K., Qin, F., Osakabe, Y., Shinozaki, K., and Yamaguchi-Shinozaki, K. (2006b). Dual function of an Arabidopsis transcription factor DREB2A in water-stress-responsive and heat-stress-responsive gene expression. *Proc. Natl. Acad. Sci. U. S. A.* 103, 18822–18827. doi: 10.1073/pnas.0605639103

Sato, T., Maekawa, S., Yasuda, S., Domeki, Y., Sueyoshi, K., Fujiwara, M., et al. (2011). Identification of 14-3-3 proteins as a target of ATL31 ubiquitin ligase, a regulator of the C/N response in Arabidopsis. *Plant J.* 68, 137–146. doi: 10.1111/j.1365-313X.2011.04673.x

Sato, T., Maekawa, S., Yasuda, S., Sonoda, Y., Katoh, E., Ichikawa, T., et al. (2009). CNI1/ATL31, a RING-type ubiquitin ligase that functions in the carbon/nitrogen response for growth phase transition in Arabidopsis seedlings. *Plant J.* 60, 852–864. doi: 10.1111/j.1365-313X.2009.04006.x

Schwechheimer, C., and Calderon Villalobos, L. I. (2004). Cullin-containing E3 ubiquitin ligases in plant development. *Curr. Opin. Plant Biol.* 7, 677–686. doi: 10.1016/j.pbi.2004.09.009

Sharma, H., Batra, R., Kumar, S., Kumar, M., Kumar, S., Balyan, H. S., et al. (2022). Identification and characterization of 20S proteasome genes and their relevance to heat/drought tolerance in bread wheat. *Gene Rep.* 27, 101552. doi: 10.1016/j.genrep.2022.101552

Sharma, M., and Pandey, G. K. (2019). OsPUB75, an Armadillo/U-box protein interacts with GSK3 kinase and functions as negative regulator of abiotic stress responses. *Environ. Exp. Bot.* 161, 388–398. doi: 10.1016/j.envexpbot.2018.10.022

Shu, K., and Yang, W. (2017). E3 ubiquitin ligases: ubiquitous actors in plant development and abiotic stress responses. *Plant Cell Physiol.* 58, 1461–1476. doi: 10.1093/pcp/pcx071

Shumyantseva, V. V., Suprun, E. V., Bulko, T. V., and Archakov, A. I. (2014). Electrochemical methods for detection of post-translational modifications of proteins. *Biosens. Bioelectron.* 61, 131–139. doi: 10.1016/j.bios.2014.05.001

Smalle, J., Kurepa, J., Yang, P., Emborg, T. J., Babiychuk, E., Kushnir, S., et al. (2003). The pleiotropic role of the 26S proteasome subunit RPN10 in Arabidopsis growth and development supports a substrate-specific function in abscisic acid signaling. *Plant Cell* 15:965–80. doi: 10.1105/tpc.009217

Smalle, J., and Vierstra, R. D. (2004). The ubiquitin 26s proteasome proteolytic pathway. *Annu. Rev. Plant Biol.* 55, 555–590. doi: 10.1146/annurev.arplant.55.031903.141801

Smit, J. J., and Sixma, T. K. (2014). 'RBR E3-ligases at work. *EMBO Rep.* 15, 142–154. doi: 10.1002/embr.201338166

Srivastava, A. K., Zhang, C., Caine, R. S., Gray, J., and Sadanandom, A. (2017). Rice SUMO protease overly tolerant to salt 1 targets the transcription factor, OsbZIP23 to promote drought tolerance in rice. *Plant J.* 92, 1031–1043. doi: 10.1111/tpj.13739

Srivastava, A. K., Zhang, C., Yates, G., Bailey, M., Brown, A., and Sadanandom, A. (2016). SUMO is a critical regulator of salt stress responses in rice. *Plant Physiol.* 170, 2378–2391. doi: 10.1104/pp.15.01530

Srivastava, M., and Sadanandom, A. (2020). An insight into the factors influencing specificity of the SUMO system in plants. *Plants* 9, 1788. doi: 10.3390/plants9121788

Stone, S. L. (2014). The role of ubiquitin and the 26S proteasome in plant abiotic stress signaling. *Front. Plant Sci.* 5, 135. doi: 10.3389/fpls.2014.00135

Stone, S. L., Hauksdóttir, H., Troy, A., Herschleb, J., Kraft, E., and Callis, J. (2005). Functional analysis of the RING-type ubiquitin ligase family of Arabidopsis. *Plant Physiol.* 137, 13–30. doi: 10.1104/pp.104.052423

Stone, S. L., Williams, L. A., Farmer, L. M., Vierstra, R. D., and Callis, J. (2007). KEEP ON GOING, a RING E3 ligase essential for Arabidopsis growth and development, is involved in abscisic acid signaling. *Plant Cell* 18, 3415–3428. doi: 10.1105/tpc.106.046532

Sun, C.-W., and Callis, J. (1997). Independent modulation of Arabidopsis thaliana polyubiquitin mRNAs in different organs and in response to environmental changes. *Plant J.* 11, 1017–1027. doi: 10.1046/j.1365-313X.1997.11051017.x

Tamang, B. G., and Fukao, T. (2015). Plant adaptation to multiple stresses during submergence and following desubmergence. *Int. J. Mol. Sci.* 16, 30164–30180. doi: 10.3390/ijms161226226

Teramura, H., Yamada, K., Ito, K., Kasahara, K., Kikuchi, T., Kioka, N., et al. (2021). Characterization of novel SUMO family genes in the rice genome. *Genes Genet. Syst.* 96, 25–32. doi: 10.1266/ggs.20-00034

Tian, F., Gong, J., Zhang, J., Feng, Y., Wang, G., Guo, Q., et al. (2014). Overexpression of monoubiquitin improves photosynthesis in transgenic tobacco plants following high temperature stress. *Plant Sci. Int. J. Exp. Plant Biol.* 226, 92–100. doi: 10.1016/j.plantsci.2014.03.006

Tian, M., Lou, L., Liu, L., Yu, F., Zhao, Q., Zhang, H., et al. (2015). The RING finger E3 ligase STRF1 is involved in membrane trafficking and modulates salt-stress response in Arabidopsis thaliana. *Plant J.* 82, 81–92. doi: 10.1111/tpj.12797

Tuteja, N., Ahmad, P., Panda, B. B., and Tuteja, R. (2009). Genotoxic stress in plants: shedding light on DNA damage, repair and DNA repair helicases. *Mutat. Res.* 681, 134–149. doi: 10.1016/j.mrrev.2008.06.004

Ueda, M., Matsui, K., Ishiguro, S., Sano, R., Wada, T., Paponov, I., et al. (2004). The HALTED ROOT gene encoding the 26S proteasome subunit RPT2a is essential for the maintenance of Arabidopsis meristems. *Development* 131, 2101–2111. doi: 10.1242/dev.01096

Ueda, M., and Seki, M. (2020). Histone modifications form epigenetic regulatory networks to regulate abiotic stress response. *Plant Physiol.* 182, 15–26. doi: 10.1104/pp.19.00988

Uno, Y., Furihata, T., Abe, H., Yoshida, R., Shinozaki, K., and Yamaguchi-Shinozaki, K. (2000). Arabidopsis basic leucine zipper transcription factors involved in an abscisic acid-dependent signal transduction pathway under drought and high-salinity conditions. *Proc. Natl. Acad. Sci. U. S. A.* 97, 11632–11637. doi: 10.1073/pnas.190309197

van Veen, H., Mustroph, A., Barding, G. A., Vergeer-van Eijk, M., Welschen-Evertman, R. A., Pedersen, O., et al. (2013). Two Rumex species from contrasting hydrological niches regulate flooding tolerance through distinct mechanisms. *Plant Cell* 25, 4691–707. doi: 10.1105/tpc.113.119016

Vierstra, R. D. (2009). The ubiquitin−26S proteasome system at the nexus of plant biology. *Nat. Rev. Mol. Cell Biol.* 10, 385–397. doi: 10.1038/nrm2688

Walsh, C. K., and Sadanandom, A. (2014). Ubiquitin chain topology in plant cell signaling: a new facet to an evergreen story. *Front. Plant Sci.* 5, 122. doi: 10.3389/fpls.2014.00122

Wan, X., Mo, A., Liu, S., Yang, L., and Li, L. (2011). Constitutive expression of a peanut ubiquitin-conjugating enzyme gene in Arabidopsis confers improved water-stress tolerance through regulation of stress-responsive gene expression. *J. Biosci. Bioeng.* 111, 478–484. doi: 10.1016/j.jbiosc.2010.11.021

Wang, F., Zhu, D., Huang, X., Li, S., Gong, Y., Yao, Q., et al. (2009a). Biochemical insights on degradation of Arabidopsis DELLA proteins gained from a cell-free assay system. *The Plant Cell* 21, 2378–2390. doi: 10.1105/tpc.108.065433

Wang, S., Kurepa, J., and Smalle, J. A. (2009b). The Arabidopsis 26S proteasome subunit RPN1a is required for optimal plant growth and stress responses. *Plant Cell Physiol.* 50, 1721–1725. doi: 10.1093/pcp/pcp105

Weissman, A. M. (2001). Themes and variations on ubiquitylation. *Nat. Rev. Mol. Cell Biol.* 2, 169–178. doi: 10.1038/35056563

Welchman, R. L., Gordon, C., and Mayer, R. J. (2005). Ubiquitin and ubiquitin-like proteins as multifunctional signals. *Nat. Rev. Mol. Cell Biol.* 6, 599–609. doi: 10.1038/nrm1700

Weng, M., Yang, Y., Feng, H., Pan, Z., Shen, W. H., Zhu, Y., et al. (2014). Histone chaperone ASF1 is involved in gene transcription activation in response to heat stress in Arabidopsis thaliana. *Plant Cell Environ.* 37, 2128–2138. doi: 10.1111/pce.12299

Wu, G., Xu, G., Schulman, B. A., Jeffrey, P. D., Harper, J. W., and Pavletich, N. P. (2003). Structure of a β-TrCP1-Skp1-β-catenin complex. *Mol. Cell* 11, 1445–1456. doi: 10.1016/S1097-2765(03)00234-X

Wu, Q., Zhang, X., Peirats-Llobet, M., Belda-Palazon, B., Wang, X., Cui, S., et al. (2016). Ubiquitin ligases RGLG1 and RGLG5 regulate abscisic acid signaling by controlling the turnover of phosphatase PP2CA. *Plant Cell* 28, 2178–2196. doi: 10.1105/tpc.16.00364

Xu, M., Zhang, X., Yu, J., Guo, Z., Li, Y., Song, X., et al. (2021). Proteome-wide analysis of lysine 2-hydroxyisobutyrylation in *Aspergillus niger* in peanuts. *Front. Microbiol.* 12, 719337. doi: 10.3389/fmicb.2021.719337

Xue, H., Zhang, Q., Wang, P., Cao, B., Jia, C., Cheng, B., et al. (2022). qPTMplants: an integrative database of quantitative post-translational modifications in plants. *Nucleic Acids Res.* 50, D1491–D1499. doi: 10.1093/nar/gkab945

Yanagawa, Y., and Komatsu, S. (2012). Ubiquitin/proteasome-mediated proteolysis is involved in the response to flooding stress in soybean roots, independent of oxygen limitation. *Plant Sci.* 185–186, 250–258. doi: 10.1016/j.plantsci.2011.11.014

Yang, R., Wang, T., Shi, W., Li, S., Liu, Z., Wang, J., et al. (2020). E3 ubiquitin ligase ATL61 acts as a positive regulator in abscisic acid mediated drought response in Arabidopsis. *Biochem. Biophys. Res. Commun.* 528, 292–298. doi: 10.1016/j.bbrc.2020.05.067

Ye, Y., and Rape, M. (2009). Building ubiquitin chains: E2 enzymes at work. *Nat. Rev. Mol. Cell Biol.* 10, 755–764. doi: 10.1038/nrm2780

Yee, D., and Goring, D. R. (2009). The diversity of plant U-box E3 ubiquitin ligases: from upstream activators to downstream target substrates. *J. Exp. Bot.* 60, 1109–1121. doi: 10.1093/jxb/ern369

Yu, F., Wu, Y., and Xie, Q. (2016). Ubiquitin-proteasome system in ABA signaling: from perception to action. *Mol. Plant* 9, 21–33. doi: 10.1016/j.molp.2015.09.015

Zhan, E., Zhou, H., Li, S., Liu, L., Tan, T., and Lin, H. (2018). OTS1-dependent deSUMOylation increases tolerance to high copper levels in Arabidopsis. *J. Integr. Plant Biol.* 60, 310–322. doi: 10.1111/jipb.12618

Zhang, Y., Lai, X., Yang, S., Ren, H., Yuan, J., Jin, H., et al. (2021). Functional analysis of tomato CHIP ubiquitin E3 ligase in heat tolerance. *Sci. Rep.* 11, 1713. doi: 10.1038/s41598-021-81372-8

Zhang, Y., Xu, W., Li, Z., Deng, X. W., Wu, W., and Xue, Y. (2008). F-box protein DOR functions as a novel inhibitory factor for abscisic acid-induced stomatal closure under drought stress in Arabidopsis. *Plant Physiol.* 148, 2121–2133. doi: 10.1104/pp.108.126912

Zhang, Y., Yang, C., Li, Y., Zheng, N., Chen, H., Zhao, Q., et al. (2007). SDIR1 is a RING finger E3 ligase that positively regulates stress-responsive abscisic acid signaling in Arabidopsis. *Plant Cell* 19, 1912–29. doi: 10.1105/tpc.106.048488

Zhang, Y.-Y., and Xie, Q. (2007). Ubiquitination in abscisic acid-related pathway. *J. Integr. Plant Biol.* 49, 87–93. doi: 10.1111/j.1744-7909.2006.00417.x

Zheng, N., and Shabek, N. (2017). Ubiquitin ligases: structure, function, and regulation. *Annu. Rev. Biochem.* 86, 129–157. doi: 10.1146/annurev-biochem-060815-014922

Zhou, G.-A., Chang, R.-Z., and Qiu, L.-J. (2010). Overexpression of soybean ubiquitin-conjugating enzyme gene GmUBC2 confers enhanced drought and salt tolerance through modulating abiotic stress-responsive gene expression in Arabidopsis. *Plant Mol. Biol.* 72, 357–367. doi: 10.1007/s11103-009-9575-x

Zhou, M., Chen, H., Wei, D., Ma, H., and Lin, J. (2017). Arabidopsis CBF3 and DELLAs positively regulate each other in response to low temperature. *Sci. Rep.* 7, 39819. doi: 10.1038/srep39819

Zhu, J., Dong, C.-H., and Zhu, J.-K. (2007). Interplay between cold-responsive gene regulation, metabolism and RNA processing during plant cold acclimation. *Curr. Opin. Plant Biol.* 10, 290–295. doi: 10.1016/j.pbi.2007.04.010

frontiers | Frontiers in Plant Science

TYPE Mini Review
PUBLISHED 23 September 2022
DOI 10.3389/fpls.2022.926214

Check for updates

OPEN ACCESS

EDITED BY
Andrea Miyasaka Almeida,
Universidad Mayor, Chile

REVIEWED BY
Allah Wasaya,
Bahauddin Zakariya University, Pakistan
Luis Duque,
The Pennsylvania State University (PSU), United States

*CORRESPONDENCE
Jagesh Kumar Tiwari
jageshtiwari@gmail.com

†PRESENT ADDRESSES
Jagesh Kumar Tiwari,
Indian Council of Agricultural Research (ICAR)-Indian Institute of Vegetable Research, Varanasi, Uttar Pradesh, India

Rajesh K. Singh,
Indian Council of Agricultural Research (ICAR)-Indian Institute of Vegetable Research, Varanasi, Uttar Pradesh, India

Anuj K. Poonia,
Institute of Biotechnology, Chandigarh University, Mohali, Punjab, India

SPECIALTY SECTION
This article was submitted to Plant Abiotic Stress, a section of the journal Frontiers in Plant Science

RECEIVED 22 April 2022
ACCEPTED 25 August 2022
PUBLISHED 23 September 2022

CITATION
Zinta R, Tiwari JK, Buckseth T, Thakur K, Goutam U, Kumar D, Challam C, Bhatia N, Poonia AK, Naik S, Singh RK, Thakur AK, Dalamu D, Luthra SK, Kumar V and Kumar M (2022) Root system architecture for abiotic stress tolerance in potato: Lessons from plants. *Front. Plant Sci.* 13:926214. doi: 10.3389/fpls.2022.926214

COPYRIGHT
© 2022 Zinta, Tiwari, Buckseth, Thakur, Goutam, Kumar, Challam, Bhatia, Poonia, Naik, Singh, Thakur, Dalamu, Luthra, Kumar and Kumar. This is an open-access article distributed under the terms of the Creative Commons Attribution License (CC BY). The use, distribution or reproduction in other forums is permitted, provided the original author(s) and the copyright owner(s) are credited and that the original publication in this journal is cited, in accordance with accepted academic practice. No use, distribution or reproduction is permitted which does not comply with these terms.

Root system architecture for abiotic stress tolerance in potato: Lessons from plants

Rasna Zinta[1,2], Jagesh Kumar Tiwari[1*†], Tanuja Buckseth[1], Kanika Thakur[1], Umesh Goutam[2], Devendra Kumar[3], Clarissa Challam[4], Nisha Bhatia[1,5], Anuj K. Poonia[5†], Sharmistha Naik[1,6], Rajesh K. Singh[1†], Ajay K. Thakur[1], Dalamu Dalamu[1], Satish K. Luthra[3], Vinod Kumar[1] and Manoj Kumar[3]

[1]Indian Council of Agricultural Research (ICAR)-Central Potato Research Institute, Shimla, Himachal Pradesh, India, [2]Lovely Professional University, Phagwada, Punjab, India, [3]Indian Council of Agricultural Research (ICAR)-Central Potato Research Institute, Regional Station, Meerut, India, [4]Indian Council of Agricultural Research (ICAR)-Central Potato Research Institute, Regional Station, Shillong, India, [5]School of Biotechnology, Shoolini University, Solan, Himachal Pradesh, India, [6]Indian Council of Agricultural Research (ICAR)-National Research Centre for Grapes, Pune, Maharashtra, India

The root is an important plant organ, which uptakes nutrients and water from the soil, and provides anchorage for the plant. Abiotic stresses like heat, drought, nutrients, salinity, and cold are the major problems of potato cultivation. Substantial research advances have been achieved in cereals and model plants on root system architecture (RSA), and so root ideotype (e.g., maize) have been developed for efficient nutrient capture to enhance nutrient use efficiency along with genes regulating root architecture in plants. However, limited work is available on potatoes, with a few illustrations on root morphology in drought and nitrogen stress. The role of root architecture in potatoes has been investigated to some extent under heat, drought, and nitrogen stresses. Hence, this mini-review aims to update knowledge and prospects of strengthening RSA research by applying multi-disciplinary physiological, biochemical, and molecular approaches to abiotic stress tolerance to potatoes with lessons learned from model plants, cereals, and other plants.

KEYWORDS

abiotic stress, root system architecture, potato, plant, nitrogen, heat, drought

Introduction

The root is an integral plant part that provides anchorage, water, and nutrients to the plant. The aboveground plant parts (e.g., stems and leaves) have been widely investigated by several groups worldwide in crops for abiotic stresses like heat and drought tolerance (Tracy et al., 2020; van der Bom et al., 2020), but limited reports are available on underground roots. The root system architecture (RSA) is the 3-dimensional structure of the root system of a plant in soil, and it is highly essential for efficient water and nutrient acquisition and plant growth and development (Lynch, 2019). Although, substantial information has been generated and deployed in cereals for enhancing nutrient use efficiency (Lynch, 2019, 2021) and

some RSA reports are also available on potatoes on heat, drought, and nitrogen use efficiency (Villordon et al., 2014; Tiwari et al., 2018, 2020). Hence, there is an urgent need to enhance knowledge of root architecture in the potato by applying multi-disciplinary physiological, biochemical, and molecular approaches. Thus, RSA profiling is now a promising breeding strategy for developing resource-efficient potato cultivars.

The availability of information on RSA is crucial for abiotic stress tolerance in potatoes, particularly heat and drought stress. In potatoes, the tuber is the most economically important plant part and the root is a vital organ, that supplies nutrients and water for stolon formation, and then tuber growth and development (Iwama, 2008). Considerable research on RSA has been evidenced in cereals (Lynch, 2021) but very little on potatoes (Wishart et al., 2013). For example, maize root ideotype *Steep, Cheap, and Deep* has been designed to increase the efficient uptake of water and nutrients through roots from deep and shallow soils (Lynch, 2019). Likewise, a large number of studies have been illustrated on heat and drought stress tolerance but limited research on the exploitation of RSA for crop improvement, except a few demonstrated toward improving nitrogen use efficiency of plants (van Bueren and Struik, 2017). Genetic variability has been explored in potatoes, including root traits of *N* stress in potatoes (Zebarth et al., 2008; Trehan and Singh, 2013; Ospina et al., 2014; van Bueren and Struik, 2017). Aeroponics technology has also been proven in potatoes for precision phenotyping of root traits for improving *N* use efficiency (Tiwari et al., 2018, 2020). Moreover, exploration of root traits is essential to meet sustainable potato production by improving nutrient and water use efficiency (Garnett et al., 2009; Duque and Villordon, 2019; White, 2019; Tracy et al., 2020). Overall, the focus has been driven to harness the potential of root traits toward increasing nutrient acquisition along with water for abiotic stress tolerance in plants.

Abiotic stresses in potato

Heat and drought stress

Potato is considered a crop of cool and temperate climate, and high temperatures inhibit tuber growth and yield due to heat stress. In general, tuberization is reduced at high night temperatures above 20°C with complete inhibition of tuberization above 25°C. Exposure of potato plants to high temperatures alters the hormonal balance in the plants. The heat stress tolerance breeding program considers tuberization under high night temperatures (>22°C). Potato is mostly an irrigated crop in plains, and rain-fed crops in hilly regions. Drought is an emerging problem in potato production due to erratic rainfall and the unavailability of irrigation water (Monneveux et al., 2013). The potato plant is highly sensitive to moisture availability and the decline in photosynthesis is fast and substantial even at relatively low water potentials of −3 to −5 bars. Tuber traits such as shape, cracking, dry matter content, and reducing sugars are highly influenced by the availability of soil moisture during the vegetative period.

Nutrient, salinity, and cold stress

Macro- and micro-nutrients are essential for good vegetative growth, yield, and quality of potatoes. Potato is a shallow-rooted crop and irrigated cultivation is followed on sandy-loam soils in India. Out of the total *N* fertilizer applied, nearly 40–50% is only used by plants (Garnett et al., 2015). The excessive application of *N* fertilizers in potatoes increases production cost and also causes nitrate leaching, and groundwater contamination, and thereby causes environmental pollution (Tiwari et al., 2018, 2020). Salinity is also another problem that could be due to soil salinity or irrigation water. It causes nutritional imbalances, restricts plant growth, and early senescence, and reduces tuber yield, particularly in semi-arid/arid regions. Besides, cold is one of the problems in temperate regions. Temperatures below −2°C can result in partial or complete loss of crops. In temperate zones, freezing injury can occur during the spring season when the crop is at the initial stage of vegetative growth or during autumn when it is near maturity.

Root system architecture research in plants

Determining root ideotypes for efficient nutrient uptake/utilization

Harnessing the potential of RSA is now a priority research to develop varieties for abiotic stress tolerance particularly, heat and drought stress. A root ideotype with narrow and deep root systems is ideal for *N* acquisition. The crops having deeper roots are more efficient in *N* acquisition facilitated by steeper root growth angles, fewer axial roots, lesser lateral branching, and anatomical structures (Lynch, 2021). The *Steep, Cheap, and Deep* root ideotype of maize is beneficial for subsoil foraging or capture of *N* and water from deeper soils, which consists of special architectural, anatomical, and physiological features (Lynch, 2013, 2019). Dechorgnat et al. (2018) witnessed a dense maize root ideotype of brace, seminal, and crown roots with mainly increased crown root profile (root length, surface area, and volume). More aerial nodal roots and fewer crown roots increase the uptake of *N* and deep water under dense planting in maize (Zhang et al., 2018). Lynch (2021) pointed out that crop genotypes with reduced metabolic costs of soil exploration

TABLE 1 Root system architecture studies on different abiotic stresses in potato.

Sr. No.	Trait/stress	Potato genotype	Technology used	Key findings	References
1.	High-throughput root-trait phenotyping	Root and tuber crops	High-throughput root-trait phenotyping techniques	Discussed new phenotyping methods based on root branching and nutrient capture, and examined root morphology, anatomy, and germplasm screening with enhanced root architecture. Non-invasive *in situ* imaging in the field were advocated such as X-ray computed tomography, laser, nuclear magnetic resonance (NMR), ground penetrating radar (GPR), infrared (IR) imaging, and near-infrared (NIR) imaging alongside a robust database and data analysis pipeline	Villordon et al. (2014), Khan et al. (2016), Duque and Villordon (2019)
2.	Root morphology	IWA1/2/3/4 Norin 1 Konafubuki	Win-RHIZO software	Root mass showed a negative correlation with early tuber bulking, but a positive correlation with shoot mass and final tuber yield	Iwama (2008)
3.	Potato root architecture	Desirée	ImageJ program (http://imagej.nih.gov/ij/)	Described adventitious root (AR) growth and lateral root (LR) branching. Elucidated understanding of origin and nature of AR systems in potato. Results indicate that LR formation in potatoes follows a similar pattern as in model plants, and facilitates its manipulation to improve soil exploitation and yield.	Joshi et al. (2016), Joshi and Ginzberg (2021)
4.	Canopy development and nitrogen use efficiency	189 cultivars	Field phenotyping	Assessed phenotypic variation for NUE traits in potatoes and determined association between NUE and canopy development under high and low *N* input.	Ospina et al. (2014)
5.	Root traits under *N* stress	Kufri Jyoti, Kufri Gaurav	Aeroponics and WinRhizo software	Demonstrated precision phenotyping of potato roots and determined NUE variables in aeroponics under low and high *N* supply.	Tiwari et al. (2020), Tiwari et al. (2022)
6.	Root traits	28 genotypes (Tuberosum and Phureja groups)	Root excavation from field and glass house screening	Root traits variation indicated that final yield was correlated negatively with basal root length, and weakly but positively with total root weight. Phureja genotypes had more numerous basal roots than stolon roots compared to Tuberosum group.	Wishart et al. (2013)
7.	Drought stress	12 genotypes	Destructive field phenotyping and general linear model (GLM)	Applied field phenotyping to identify the useful traits to an environmental stress. Study showed that stolon root traits were associated with drought tolerance in potato and could be used to select genotypes with resilience to drought.	Wishart et al. (2014)
8.	Root traits under drought stress	Tolerant: Gwiazda and Tajfun Sensitive: Oberon and Cekin	Field phenotyping	Established relationship between root system architecture and drought tolerance. Root dry mass decreased under drought stress, and drought-tolerant cultivars developed elongated roots, unlike drought-sensitive cultivars.	Boguszewska-Mańkowska et al. (2020)

(Continued)

10.3389/fpls.2022.926214

TABLE 1 (Continued)

Sr. No.	Trait/stress	Potato genotype	Technology used	Key findings	References
9.	Potato morphology under drought stress	Bintje, Dérirée and many lines	WinRhizo and other softwares	Concluded that small canopies increase harvest index and decrease evapotranspiration, whereas open stem-type canopies increase light penetration and shallow but densely rooted cultivars increase water uptake.	Hill et al. (2021)
10.	Root phenotyping model	Fujin, Zaodabai, and Helanshiwu	3D model for potato roots	Developed 3D models of the tuber-root systems based on topological and geometric structures.	Zhao et al. (2020)
11.	Plant architecture	*Solanum tuberosum* subsp. *andigena* 7540	Grafting	A potential graft-transmissible microRNA *miR156*, a phloem mobile signal, plays vital role in plant architecture and tuberization in potato.	Bhogale et al. (2014)
12.	Root architecture	Desiree, Longshu3	Nikon D3000 digital camera imaging	Potato *miR160a/b* plays key roles in root architecture and auxin signaling-related gene expression. Knockdown *miR160* led to a reduction in root length and fresh weight, and an increase in lateral root number.	Yang et al. (2021)

See examples of other crops in Supplementary File S1.

can improve water and nutrient acquisition efficiency. Table 1 summarizes some recent work on root architecture studies in potatoes.

The role of the roots-based approach has been described in breeding for nutrient uptake in cereals and other crops (Garnett et al., 2009). It is now clearly evident that root branching plays a very crucial function in nutrient acquisition, which determines plant growth and tuber yield in potatoes (Duque and Villordon, 2019; White, 2019; Tracy et al., 2020). The potato is a model tuber crop species for analyzing underground plant parts like roots, stolons, and tubers (Iwama, 2008). Potato is a shallow-rooted crop that includes basal and stolon roots. The basal roots are involved in plant anchorage and water uptake, whereas the stolon roots capture nutrients and promote tuber growth in potatoes (Villordon et al., 2014). The deeper basal roots and numerous short roots are more advantageous for high tuber yield (White, 2019). It has been determined that basal root length and total root weight are associated with total tuber yield in potatoes (Wishart et al., 2013), and root length and surface area are correlated with higher *N* uptake (Sattelmacher et al., 1990). Khan et al. (2016) suggest that root traits such as root length, spread, number, and length of lateral roots show greater plasticity in response to environmental changes and have better nutrient use efficiency in potatoes. It is evident that the concentration of abscisic acid (ABA) increases in roots under drought stress and shows a linear relationship with stomatal conductance in potatoes (Liu et al., 2005). Drought stress has been witnessed to increase root depth with a high root-to-shoot ratio and allow for uptake of water from deeper strata, whereas, decreased total rot length, increased or decreased root dry mass and stolon number were recorded in different reports (Hill et al., 2021). High-temperature stress reduces plant growth, including reduced root and stolon, delayed tuberization, and thereby lowers tuber yield but increases starch degrading enzymes, heat-sock proteins, and transpiration rate in potatoes (Dahal et al., 2019). Salinity causes reduced root length, root volume, and tuber yield, while it causes stomatal closure and increased ABA, proline, and Na^+ transport in potato roots (Dahal et al., 2019). Despite these studies, root branching, adventitious roots, and lateral roots, and their mechanism as well as functions in plant growth and development are poorly understood in potatoes. Hence, research on root architecture needs a priority in potato breeding for developing nutrient-use efficient cultivars. In our study, Figure 1A depicts root morphology in potatoes under the field and aeroponics (a soil-less culture of liquid nutrient supply in the mist form) conditions: (a) plant canopy and root biomass at 45 days after planting (DAP) in aeroponics, (b) hanging root growth and tuber initiation in aeroponics system at 45 DAP, (c) harvesting of minitubers at 50 DAP in aeroponics, (d–e) pattern of root branching and laterals development of 10 days-old seedlings in aeroponics, and (f) root biomass of plants at harvesting stage (90 DAP) grown in the field with limited *N* (50 kg/ha)

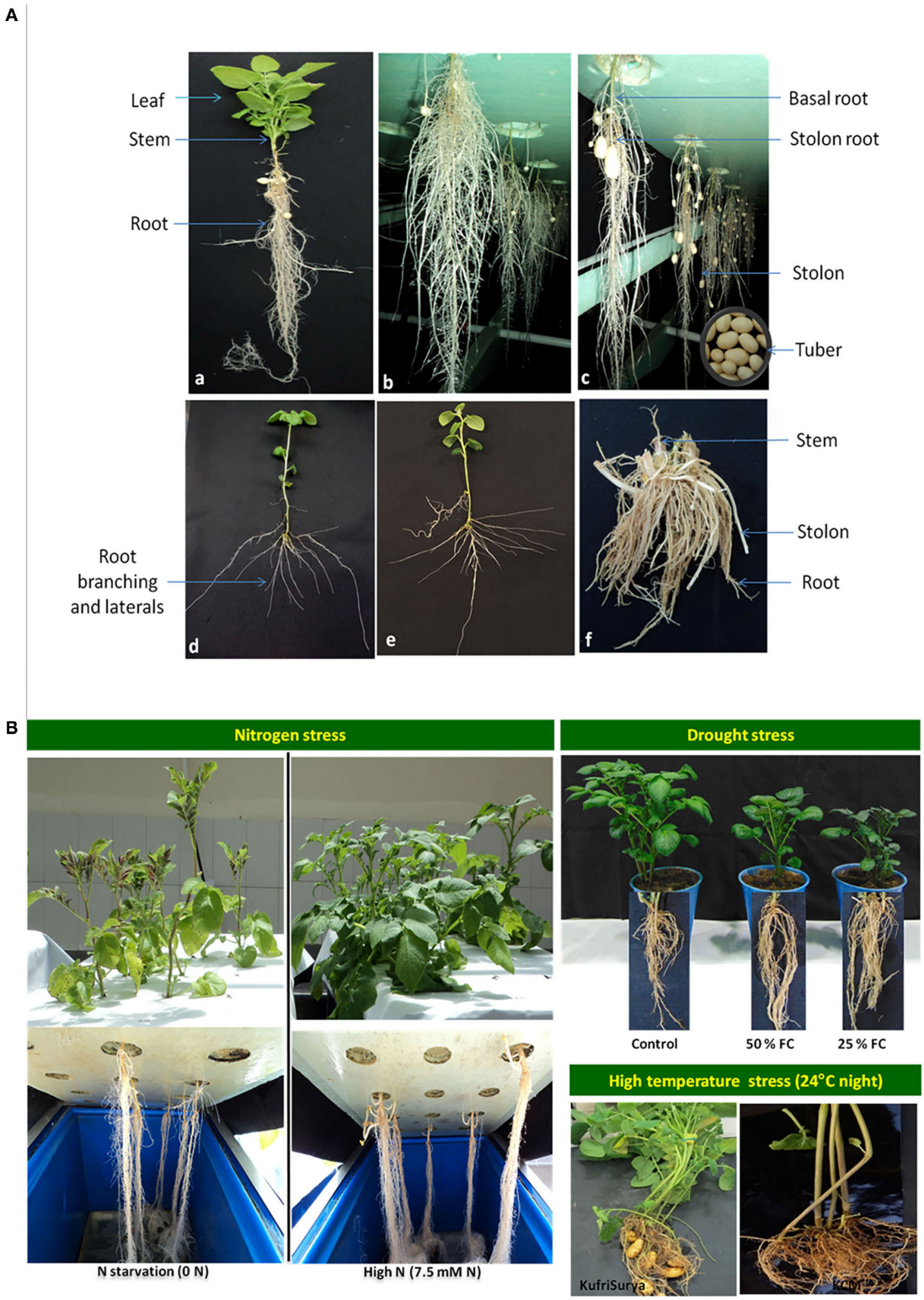


FIGURE 1
(A) Illustrates the root biomass and tuber growth in potato plants grown under aeroponics: a) complete plant growth including root biomass at 45 days after planting (DAP), b) root architecture showing root volume and tuber initiation under hanging roots in aeroponics system at 45 DAP, c) fully grown tubers and harvesting of minitubers at 50 DAP (<5 g each), d, e) pattern of root branching and laterals development at a very early stage (10 days-old seedlings), and f) root biomass of plants at harvesting stage (90 DAP) grown in the field with limited *N* (50 kg/ha) supply. **(B)** depicts plant phenotype (foliage and roots) under different stresses like nitrogen (left) (*N* starvation vs. high *N*), drought (right top) (control, 50% field capacity and 25% field capacity) and high temperature stress (right bottom) (>24°C night temperatures).

supply. In our other studies, Figure 1B illustrates plant foliage and roots under different stresses like nitrogen (*N* starvation vs. high *N*), drought (control, 50% field capacity soil moisture, and 25% field capacity soil moisture), and high temperatures stress (>24°C night). In aeroponics, we observed variable responses for root traits in 56 potato varieties under optimal *N* supply (Tiwari et al., 2022), and in two contrasting varieties under *N* stress and *N* sufficient conditions (Tiwari et al., 2018, 2020). Under heat stress, lesser root growth and little or no tuber formation were observed at above 24°C night temperatures in potatoes compared to the counterpart, and similar was the case under drought stress. Taken together, the effects of these stresses are detrimental to plant growth particularly root and stolon development, and thus reduces tuber yield in potatoes.

Multi-disciplinary approaches to investigate root traits

A large number of agronomic, physiological, breeding, and molecular works substantiate root traits studies in many plants such as *Arabidopsis thaliana* (De Pessemier et al., 2013) and tomato (Abenavoli et al., 2016) targeting different traits (Table 1). The significance of RSA to improve nutrient acquisition, translocation, remobilization, and nutrient utilization efficiency has been remarkably known in plants (Chen and Liao, 2017). Recently, Lecarpentier et al. (2021) measured the plasticity of RSA, where lateral root density played a key role under limited *N* in *Brassica napus*. Sinha et al. (2020) documented genetic variation in wheat RSA traits and association with high- and low-affinity nitrate transport systems under optimum and limited *N*. The roles of nitrate and amino acid regulation of shoot branching, flowering, and panicle development, as well as cell division and expansion in shaping of plant architecture have been demonstrated in cereals (Luo et al., 2020). In plants, *N* regulation of root branching (Walch-Liu et al., 2006) and the process of nitrate- and auxin-mediated regulation of root structure have been unveiled recently (Hu et al., 2021).

In potatoes, very high genetic variability has been observed in varieties/germplasm for yield, *N* use efficiency (NUE), and root traits under field conditions (Errebhi et al., 1999; Zebarth et al., 2008; Vos, 2009; Ospina et al., 2014), and aeroponics (Tiwari et al., 2020). Studies confirmed that genetic variation in root traits and root dry weight was positively correlated with final tuber yield (Sattelmacher et al., 1990; Stalham and Allen, 2001; Wishart et al., 2013). Recently, our aeroponics study demonstrated a highly significant and positive correlation between root traits and tuber yield along with *N* use efficiency in potatoes (Tiwari et al., 2022). In RSA studies on drought stress in potatoes, Wishart et al. (2014) evidence that stolon roots are associated with drought tolerance in fields, whereas elongated roots are noticed in drought-tolerant cultivars (Boguszewska-Mańkowska et al., 2020). Recently, Hill et al. (2021) concluded that an open stem-type plant canopy increases light penetration and shallow but densely rooted cultivars increase water uptake under drought stress in potatoes. The adventitious roots of potatoes are formed post-embryonically from consecutive nodes on shoots and also include lateral root formation through auxin-dependent cell cycle activation, whereas the tap/primary root is formed in the embryo (Joshi et al., 2016). Thus, the root elongation, growth angles, lateral branching, and longevity are governed by genetic, physiological, and environmental factors in potatoes (Joshi and Ginzberg, 2021).

The knowledge about genes involved in *N* metabolism is an essential requirement for providing abiotic stress tolerance by applying modern genomics tools. The understanding of the genes/quantitative trait loci (QTLs) regulation of the symbiotic associations between host plants and arbuscular mycorrhiza fungi or rhizobial bacteria is an important strategy to enhance nutrient acquisition (Li et al., 2016). In rice, the QTL *DEEPER ROOTING 1* was evidenced to increase root growth angle to increase *N* uptake under limited *N* availability (Arai-Sanoh et al., 2014). Kiba and Krapp (2016) highlighted increasing nitrogen acquisition efficiency through high-affinity nitrogen transporters, and root architecture modifications through low-nitrogen-availability-specific regulators of primary and lateral root growth under low *N*. Another study illustrated genomic regions for marker-assisted selection on root morphology in *Brassica napus* (Wang et al., 2017). MicroRNAs play key roles in abiotic stress tolerance like plant adaptation under limited *N* (Khan et al., 2011; Fischer et al., 2013). Recently, Shi and Tong (2021) demonstrated that the *TaLAMP1* gene expression determines wheat plant architecture by regulating spike number/plant and grain number/spike in response to *N* (Table 1). Many genes have been proven in various plants such as Arabidopsis for root architecture (e.g., *NRT1.1*, *TAR2*, *AHA2*, and *miR393*) and lateral root development (e.g., *NRT2.1*, *CLE-CLV1*, and *miR167*); and root architecture modification in rice (*OsMADS25*, *EL5*, and *OsNAR2.1*) and wheat (*TaNAC2-5A*; review by Li et al., 2016). The root-specific *N* transporters such as nitrate transporter (NRT), ammonium transporter (AMT), and signaling molecules or regulatory elements (transcription factors and miRNAs) could be targeted for engineering new genotypes with better nutrient use efficiency, heat and drought stress tolerance. The *miR156* is a potential graft-transmissible and a phloem mobile signal that plays a key role in plant architecture and tuberization (Bhogale et al., 2014). Recently, a study illustrated that *miR160a/b* participates in root architecture and auxin signaling-related gene expression in potatoes. The knockdown *miR160* led to a reduction in root length and fresh weight but an increase in lateral root number (Yang et al., 2021). Overall, integrated agronomic, physiological, breeding,

and molecular research strengthens our understanding of root architecture.

High-throughput phenotyping to dissect root architecture

The available approaches for root phenotyping in laboratory, greenhouse, and field include simple agar plates to labor-intensive root digging ("shovelomics") and soil boring methods, the construction of underground root observation stations, and now sophisticated computer-assisted root imaging techniques. A wide range of high-throughput phenotyping (HTP) systems has been demonstrated in crop species to measure RSA and multiple plant phenotypic traits (Nguyen and Kant, 2018; Tracy et al., 2020). Table 1 outlines the RSA studies on potatoes. Paez-Garcia et al. (2015) summarized root architectural traits relevant to crop productivity and developed root phenotyping strategies for crop and forage breeding programs. A scanner system has been developed for high-resolution quantification of root growth dynamics in *Brassica rapa* (Adu et al., 2014). Araya et al. (2016) applied a statistical modeling approach to investigate modulations of root architecture in *Arabidopsis thaliana* in response to varied *N* availability. The RhizoTubes system has been deployed for high throughput imaging of plant roots architecture in the model plant *Medicago truncatula,* crops like *Pisum sativum, Brassica napus, Vitis vinifera, Triticum aestivum*, and weed species *Vulpia myuros* (Jeudy et al., 2016). The selection criteria have been developed for spinach roots under low *N* using machine learning tools based on root architecture traits such as the number of root tips, root length, crossings, and root average diameter (Awika et al., 2021). Thus, HTP methods and simulation models will necessarily speed up the trait improvement by non-destructive simultaneous phenotyping of both roots and shoots.

A non-invasive and non-destructive phenotyping technique warrants special attention for a more accurate assessment of root traits in response to various stresses, for instance, limited *N* availability. In recent years, different platforms have been developed for root HTP under environment-controlled as well as natural field conditions, such as the in situ root imaging technique (Richner et al., 2000). Han et al. (2009) successfully applied the X-ray computed tomography (CT) technique to extract the architecture of first-order roots in potatoes. The magnetic resonance imaging (MRI) technique can be deployed to assess RSA in the early stage of potato growth (Monneveux et al., 2013). Root phenotyping techniques comprise some degree of automation with imaging, image analysis, and processing. Various imaging and its analysis techniques/software have been found effective as reliable tools for root phenotyping, such as WinRhizo, Smart Root, EZ-Rhizo, Image J, Root System Analyzer, Root Nav, IJ_Rhizo, and Root Trace (Wasaya et al., 2018). Duque and Villordon (2019) discussed the role of investigation on root morphology and anatomy under *N* stress in potatoes. Recently, 3D models have been developed for tuber-root systems based on topological and geometric structures (Zhao et al., 2020). The advancement in sensor technology allows for measuring root architecture and tuber growth in potatoes. The use of HTP at the harvesting stage will help to assess tuber characteristics such as shape, size, skin color, texture, and number, and to predict yield. Moreover, hyperspectral and multispectral imaging could be used to assess the tuber quality parameters like carbohydrates, starch, protein, reducing sugar, and water content. Thus, there is an immense opportunity to harness the potential of HTP in potato improvement via dissection of root traits.

Concluding remarks and future perspectives

Nutrients, heat, drought, salinity, and cold are the important abiotic stresses of potatoes. Excessive application of chemical fertilizers, mainly nitrogen, increases production costs and causes a negative impact on the environment. Knowledge of root architecture, anatomy, and function is important for nutrient-efficient crop breeding (Lobet et al., 2019). Root architecture plays a very essential role in plant anchorage, nutrient and water acquisition, and environmental benefits such as carbon sequestration and reducing soil erosion. Unlike advanced research on rice, wheat, and maize, limited information is available on RSA in potatoes. Given that *N* compounds are mobile and prone to leaching underground, a shallow-rooted potato root ideotype can capture nutrients and water from top soils, whereas a deep root ideotype would be advantageous for deeper soils. In addition, the molecular and genetic basis and physiological or developmental regulation of basal and stolon root architecture variation will greatly benefit breeding for abiotic stress tolerance (Kochian, 2016). Information about the association between basal and stolon roots architecture vis-a-vis carbon partitioning and tuber yield remains unclear in potatoes. The advancement in modern technologies such as sensors, robotics, cameras, and HTP platforms allow dissection of root architecture and phenomics-based crop breeding. Concomitantly, it is a challenging task due to massive data and computation analysis. In the 21st century, crop breeding will shift from single root traits to rhizosphere selection and phenotype-based crop improvement. Profiling RSA and its application is a promising and underexploited avenue to address climate-resilient and resource-efficient crops that are urgently needed in global agriculture. Thus, a renewed emphasis is needed on root architecture to develop abiotic stress-tolerant varieties by applying modern genomics tools.

Author contributions

JT conceived the idea and wrote the manuscript. All authors contributed to the research work and literature, editing, and approving the manuscript for publication.

Funding

This work is funded under the institute Biotechnology program by ICAR-CPRI, Shimla, CABin Scheme, and ICAR-LBS Outstanding Young Scientist Award project to JT.

Acknowledgments

The authors thank the competent authorities of the ICAR-CPRI, CABin Scheme (ICAR-IASRI, New Delhi) and the ICAR-LBS Outstanding Young Scientist Award project to JT for necessary support. Thanks to the editor and reviewers for their valuable comments to improve the article.

Conflict of interest

The authors declare that the research was conducted in the absence of any commercial or financial relationships that could be construed as a potential conflict of interest.

Publisher's note

All claims expressed in this article are solely those of the authors and do not necessarily represent those of their affiliated organizations, or those of the publisher, the editors and the reviewers. Any product that may be evaluated in this article, or claim that may be made by its manufacturer, is not guaranteed or endorsed by the publisher.

Supplementary material

The Supplementary Material for this article can be found online at: https://www.frontiersin.org/articles/10.3389/fpls.2022.926214/full#supplementary-material

References

Abenavoli, M. R., Longo, C., Lupini, A., Miller, A. J., Araniti, F., Mercati, F., et al. (2016). Phenotyping two tomato genotypes with different nitrogen use efficiency. *Plant Physiol. Biochem.* 107, 21–32. doi: 10.1016/j.plaphy.2016.04.021

Adu, M. O., Chatot, A., Wiesel, L., Bennett, M. J., Broadley, M. R., White, P. J., et al. (2014). A scanner system for high-resolution quantification of variation in root growth dynamics of *Brassica rapa* genotypes. *J. Exp. Bot.* 65, 2039–2048. doi: 10.1093/jxb/eru048

Arai-Sanoh, Y., Takai, T., Yoshinaga, S., Nakano, H., Kojima, M., Sakakibara, H., et al. (2014). Deep rooting conferred by DEEPER ROOTING 1 enhances rice yield in paddy fields. *Sci. Rep.* 4, 5563. doi: 10.1038/srep05563

Araya, T., Kubo, T., von Wirén, N., and Takahashi, H. (2016). Statistical modeling of nitrogen-dependent modulation of root system architecture in *Arabidopsis thaliana*. *J. Integ. Plant Biol.* 58, 254–265. doi: 10.1111/jipb.12433

Awika, H. O., Mishra, A. K., Gill, H., DiPiazza, J., Avila, C. A., and Joshi, V. (2021). Selection of nitrogen responsive root architectural traits in spinach using machine learning and genetic correlations. *Sci. Rep.* 11, 9536. doi: 10.1038/s41598-021-87870-z

Bhogale, S., Mahajan, A. S., Natarajan, B., Rajabhoj, M., Thulasiram, H. V., and Banerjee, A. K. (2014). MicroRNA156: a potential graft-transmissible microRNA that modulates plant architecture and tuberization in *Solanum tuberosum* ssp. andigena. *Plant Physiol.* 164, 1011–1027. doi: 10.1104/pp.113.230714

Boguszewska-Mańkowska, D., Zarzyńska, K., and Nosalewicz, A. (2020). Drought differentially affects root system size and architecture of potato cultivars with differing drought tolerance. *Am. J. Potato Res.* 97, 54–62. doi: 10.1007/s12230-019-09755-2

Chen, L., and Liao, H. (2017). Engineering crop nutrient efficiency for sustainable agriculture. *J. Integr. Plant Biol.* 59, 710–735. doi: 10.1111/jipb.12559

Dahal, K., Li, X.-Q., Tai, H., Creelman, A., and Bizimungu, B. (2019). Improving potato stress tolerance and tuber yield under a climate change scenario: a current overview. *Front. Plant Sci.* 10, 563. doi: 10.3389/fpls.2019.00563

De Pessemier, J., Chardon, F., Juraniec, M., Delaplace, P., and Hermans, C. (2013). Natural variation of the root morphological response to nitrate supply in *Arabidopsis thaliana*. *Mech. Develop.* 130, 45–53. doi: 10.1016/j.mod.2012.05.010

Dechorgnat, J., Francis, K. L., Dhugga, K. S., Rafalski, J. A., Tyerman, S. D., and Kaiser, B. N. (2018). Root ideotype influences nitrogen transport and assimilation in maize. *Front. Plant Sci.* 9, 531. doi: 10.3389/fpls.2018.00531

Duque, L. O., and Villordon, A. (2019). Root branching and nutrient efficiency: status and way forward in root and tuber crops. *Front. Plant Sci.* 10, 237. doi: 10.3389/fpls.2019.00237

Errebhi, M., Rosen, C. J., Lauer, F. I., Martin, M. W., and Bamberg, J. B. (1999). Evaluation of tuber-bearing *Solanum* species for nitrogen use efficiency and biomass partitioning. *Am. J. Potato Res.* 76, 143–151.

Fischer, J. J., Beatty, P. H., Good, A. G., and Muench, D. G. (2013). Manipulation of microRNA expression to improve nitrogen use efficiency. *Plant Sci.* 210, 70–81. doi: 10.1016/j.plantsci.2013.05.009

Garnett, T., Conn, V., and Kaiser, B. N. (2009). Root based approaches to improving nitrogen use efficiency in plants. *Plant Cell Environ.* 32, 1272–1283. doi: 10.1111/j.1365-3040.2009.02011.x

Garnett, T., Plett, D., Heuer, S., and Okamoto, M. (2015). Genetic approaches to enhancing nitrogen-use efficiency (NUE) in cereals: challenges and future directions. *Funct. Plant Biol.* 42, 921–941. doi: 10.1071/FP15025

Han, L., Dutilleul, P., Prasher, S. O., Beaulieu, C., and Smith, D. L. (2009). Assessment of density effects of the common scab-inducing pathogen on the seed and peripheral organs of potato during growth using computed tomography scanning data. *Trans. ASABE* 52, 305–311. doi: 10.13031/2013.25924

Hill, D., Nelson, D., Hammond, J., and Bell, L. (2021). Morphophysiology of potato (*Solanum tuberosum*) in response to drought stress: paving the way forward. *Front. Plant Sci.* 11:597554. doi: 10.3389/fpls.2020.597554

Hu, Q. Q., Shu, J. Q., Li, W. M., and Wang, G. Z. (2021). Role of auxin and nitrate signaling in the development of root system architecture. *Front. Plant Sci.* 12, 690363. doi: 10.3389/fpls.2021.690363

Iwama, K. (2008). Physiology of the potato: new insights into root system and repercussions for crop management. *Potato Res.* 51, 333–353. doi: 10.1007/s11540-008-9120-3

Jeudy, C., Adrian, M., Baussard, C., Bernard, C., Bernaud, E., Bourion, V., et al. (2016). RhizoTubes as a new tool for high throughput imaging of plant

root development and architecture: test, comparison with pot grown plants and validation. *Plant Methods* 12, 31. doi: 10.1186/s13007-016-0131-9

Joshi, M., Fogelman, E., Belausov, E., and Ginzberg, I. (2016). Potato root system development and factors that determine its architecture. *J. Plant Physiol.* 205, 113–123. doi: 10.1016/j.jplph.2016.08.014

Joshi, M., and Ginzberg, I. (2021). Adventitious root formation in crops-potato as an example. *Physiol. Plant.* 172, 124–133. doi: 10.1111/ppl.13305

Khan, G. A., Declerck, M., Sorin, C., Hartmann, C., Crespi, M., and Lelandais-Brière, C. (2011). MicroRNAs as regulators of root development and architecture. *Plant Mol. Biol.* 77, 47–58. doi: 10.1007/s11103-011-9793-x

Khan, M. A., Gemenet, D. C., and Villordon, A. (2016). Root system architecture and abiotic stress tolerance: current knowledge in root and tuber crops. *Front. Plant Sci.* 7, 1584. doi: 10.3389/fpls.2016.01584

Kiba, T., and Krapp, A. (2016). Plant nitrogen acquisition under low availability: regulation of uptake and root architecture. *Plant Cell Physiol.* 57, 707–714. doi: 10.1093/pcp/pcw052

Kochian, L. V. (2016). Root architecture. *J. Integr. Plant Biol.* 58, 190–192. doi: 10.1111/jipb.12471

Lecarpentier, C., Pagès, L., and Richard-Molard, C. (2021). Genotypic diversity and plasticity of root system architecture to nitrogen availability in oilseed rape. *PLoS ONE* 16, e0250966. doi: 10.1371/journal.pone.0250966

Li, X., Zeng, R., and Liao, H. (2016). Improving crop nutrient efficiency through root architecture modifications. *J. Integ. Plant Biol.* 58, 193–202. doi: 10.1111/jipb.12434

Liu, F., Jensen, C. R., Shahanzari, A., Andersen, M. N., and Jacobsen, S. E. (2005). ABA regulated stomatal control and photosynthetic water use efficiency of potato (*Solanum tuberosum* L.) during progressive soil drying. *Plant Sci.* 168, 831–836. doi: 10.1016/j.plantsci.2004.10.016

Lobet, G., Paez-Garcia, A., Schneider, H., Junker, A., Atkinson, J. A., and Tracy, S. (2019). Demystifying roots: a need for clarification and extended concepts in root phenotyping. *Plant Sci.* 282, 11–13. doi: 10.1016/j.plantsci.2018.09.015

Luo, L., Zhang, Y., and Xu, G. (2020). How does nitrogen shape plant architecture? *J. Exp. Bot.* 71, 4415–4427. doi: 10.1093/jxb/eraa187

Lynch, J. P. (2013). Steep, cheap and deep: an ideotype to optimize water and N acquisition by maize root systems. *Ann. Bot.* 112, 347–357. doi: 10.1093/aob/mcs293

Lynch, J. P. (2019). Root phenotypes for improved nutrient capture: an underexploited opportunity for global agriculture. *New Phytol.* 223, 548–564. doi: 10.1111/nph.15738

Lynch, J. P. (2021). Harnessing root architecture to address global challenges. *Plant J.* 109, 415–431. doi: 10.1111/tpj.15560

Monneveux, P., Ramírez, D. A., and Pino, M. T. (2013). Drought tolerance in potato (*S. tuberosum* L.): can we learn from drought tolerance research in cereals? *Plant Sci.* 205, 76–86. doi: 10.1016/j.plantsci.2013.01.011

Nguyen, G. N., and Kant, S. (2018). Improving nitrogen use efficiency in plants: effective phenotyping in conjunction with agronomic and genetic approaches. *Funct. Plant Biol.* 45, 606–619. doi: 10.1071/FP17266

Ospina, C. A., van Bueren, E. T. L., Allefs, J. J. H. M., Engel, B., van der Putten, P. E. L., van der Linden, C. G., et al. (2014). Diversity of crop development traits and nitrogen use efficiency among potato cultivars grown under contrasting nitrogen regimes. *Euphytica* 199, 13–29. doi: 10.1007/s10681-014-1203-4

Paez-Garcia, A., Motes, C. M., Scheible, W. -R., Chen, R., Blancaflor, E. B., and Monteros, M. J. (2015). Root traits and phenotyping strategies for plant improvement. *Plants* 4, 334–355. doi: 10.3390/plants4020334

Richner, W., Liedgens, M., Bürgi, H., Soldati, A., and Stamp, P. (2000). "Root image analysis and interpretation," in *Root Methods*, eds A. L. Smit, et al. (Berlin, Heidelberg: Springer).

Sattelmacher, B., Klotz, F., and Marschner, H. (1990). Influence of the nitrogen level on root growth and morphology of two potato varieties differing in nitrogen acquisition. *Plant Soil* 132, 131–137.

Shi, J., and Tong, Y. (2021). *TaLAMP*1 plays key roles in plant architecture and yield response to nitrogen fertilizer in wheat. *Front. Plant Sci.* 11, 598015. doi: 10.3389/fpls.2020.598015

Sinha, S. K., Kumar, A., Tyagi, A., Venkatesh, K., Paul, D., Singh, N. K., et al. (2020). Root architecture traits variation and nitrate-influx responses in diverse wheat genotypes under different external nitrogen concentrations. *Plant Physiol. Biochem.* 148, 246–259. doi: 10.1016/j.plaphy.2020.01.018

Stalham, M. A., and Allen, E. J. (2001). Effect of variety, irrigation regime and planting date on depth, rate, duration and density of root growth in the potato (*Solanum tuberosum*) crop. *J. Agric. Sci.* 137, 251–270. doi: 10.1017/S0021859601001332

Tiwari, J. K., Buckseth, T., Singh, R. K., Zinta, R., Thakur, K., Bhardwaj, V., et al. (2022). Aeroponic evaluation identifies variation in Indian potato varieties for root morphology, nitrogen use efficiency parameters and yield traits. *J. Plant Nutr.* 45, 2696–2709. doi: 10.1080/01904167.2022.2046080

Tiwari, J. K., Devi, S., Buckesth, T., Ali, N., Singh, R. K., Zinta, R., et al. (2020). Precision phenotyping of contrasting potato (*Solanum tuberosum* L.) varieties in a novel aeroponics system for improving nitrogen use efficiency: in search of key traits and genes. *J. Integr. Agric.* 19, 51–61. doi: 10.1016/S2095-3119(19)62625-0

Tiwari, J. K., Plett, D., Garnett, T., Chakrabarti, S. K., and Singh, R. K. (2018). Integrated genomics, physiology and breeding approaches for improving nitrogen use efficiency in potato: translating knowledge from other crops. *Funct. Plant Biol.* 45, 587–605. doi: 10.1071/FP17303

Tracy, S. R., Nagel, K. A., Postma, J. A., Fassbender, H., Wasson, A., and Watt, M. (2020). Crop improvement from phenotyping roots: highlights reveal expanding opportunities. *Trends Plant Sci.* 25, 105–118. doi: 10.1016/j.tplants.2019.10.015

Trehan, S. P., and Singh, B. P. (2013). Nutrient efficiency of different crop species and potato varieties - in retrospect and prospect. *Potato J.* 40, 1–21.

van Bueren, E. T. L., and Struik, P. C. (2017). Diverse concepts of breeding for nitrogen use efficiency?A review. *Agron. Sustain. Dev.* 37:50. doi: 10.1007/s13593-017-0457-3

van der Bom, F., Williams, A., and Bell, M. J. (2020). Root architecture for improved resource capture: trade-offs in complex environments. *J. Exp. Bot.* 71, 5752–5763. doi: 10.1093/jxb/eraa324

Villordon, A. Q., Ginzberg, I., and Firon, N. (2014). Root architecture and root and tuber crop productivity. *Trends Plant Sci.* 19, 419–425. doi: 10.1016/j.tplants.2014.02.002

Vos, J. (2009). Nitrogen responses and nitrogen management in potato. *Potato Res.* 52, 305–317. doi: 10.1007/s11540-009-9145-2

Walch-Liu, P., Ivanov, I. I., Filleur, S., Gan, Y., Remans, T., and Forde, B. G. (2006). Nitrogen regulation of root branching. *Ann. Bot.*, 97, 875–881. doi: 10.1093/aob/mcj601

Wang, J., Dun, X., Shi, J., Wang, X., Liu, G., and Wang, H. (2017). Genetic dissection of root morphological traits related to nitrogen use efficiency in *Brassica napus* L. under two contrasting nitrogen conditions. *Front. Plant Sci.* 8, 1709. doi: 10.3389/fpls.2017.01709

Wasaya, A., Zhang, X., Fang, Q., and Yan, Z. (2018). Root phenotyping for drought tolerance: a review. *Agronomy* 8, 241. doi: 10.3390/agronomy8110241

White, P. J. (2019). Root traits benefitting crop production in environments with limited water and nutrient availability. *Ann. Bot.* 124, 883–890. doi: 10.1093/aob/mcz162

Wishart, J., George, T. S., Brown, L. K., Ramsay, G., Bradshaw, J. E., White, P. J., et al. (2013). Measuring variation in potato roots in both field and glasshouse: the search for useful yield predictors and a simple screen for root traits. *Plant Soil* 368, 231–249. doi: 10.1007/s11104-012-1483-1

Wishart, J., George, T. S., Brown, L. K., White, P. J., Ramsay, G., Jones, H., et al. (2014). Field phenotyping of potato to assess root and shoot characteristics associated with drought tolerance. *Plant Soil* 378, 351–363. doi: 10.1007/s11104-014-2029-5

Yang, J., Zhang, N., Zhang, J., Jin, X., Zhu, X., Ma, R., et al. (2021). Knockdown of microRNA160a/b by STTM leads to root architecture changes via auxin signaling in *Solanum tuberosum*. *Plant Physiol. Biochem.* 166, 939–949. doi: 10.1016/j.plaphy.2021.06.051

Zebarth, B. J., Tarn, T. R., de Jong, H., and Murphy, A. (2008). Nitrogen use efficiency characteristics of andigena and diploid potato selections. *Am. J. Potato Res.* 85, 210–218. doi: 10.1007/s12230-008-9014-6

Zhang, Z., Zhang, X., Lin, Z., Wang, J., Xu, M., Lai, J., et al. (2018). The genetic architecture of nodal root number in maize. *Plant J.* 93, 1032–1044. doi: 10.1111/tpj.13828

Zhao, P., Tian, Y., Li, Y., Xu, G., Tian, S., and Huang, Z. (2020). Potato (*Solanum tuberosum* L.) tuber-root modeling method based on physical properties. *PLoS ONE* 15, e0239093. doi: 10.1371/journal.pone.0239093

frontiers | Frontiers in Plant Science

TYPE Original Research
PUBLISHED 28 September 2022
DOI 10.3389/fpls.2022.998293

Check for updates

OPEN ACCESS

EDITED BY
Giselle Camargo Mendes,
Instituto Federal de Santa Catarina (IFSC), Brazil

REVIEWED BY
Jen-Tsung Chen,
National University of Kaohsiung, Taiwan
Mohammad Sohidul Islam,
Hajee Mohammad Danesh Science & Technology University, Bangladesh

*CORRESPONDENCE
Jianming Xie
xiejianminggs@126.com

SPECIALTY SECTION
This article was submitted to Plant Abiotic Stress, a section of the journal Frontiers in Plant Science

RECEIVED 19 July 2022
ACCEPTED 12 September 2022
PUBLISHED 28 September 2022

CITATION
Li J, Xie J, Yu J, Lyv J, Zhang J, Ding D, Li N, Zhang J, Bakpa EP, Yang Y, Niu T and Gao F (2022) Melatonin enhanced low-temperature combined with low-light tolerance of pepper (*Capsicum annuum* L.) seedlings by regulating root growth, antioxidant defense system, and osmotic adjustment.
Front. Plant Sci. 13:998293.
doi: 10.3389/fpls.2022.998293

COPYRIGHT
© 2022 Li, Xie, Yu, Lyv, Zhang, Ding, Li, Zhang, Bakpa, Yang, Niu and Gao. This is an open-access article distributed under the terms of the Creative Commons Attribution License (CC BY). The use, distribution or reproduction in other forums is permitted, provided the original author(s) and the copyright owner(s) are credited and that the original publication in this journal is cited, in accordance with accepted academic practice. No use, distribution or reproduction is permitted which does not comply with these terms.

Melatonin enhanced low-temperature combined with low-light tolerance of pepper (*Capsicum annuum* L.) seedlings by regulating root growth, antioxidant defense system, and osmotic adjustment

Jing Li[1], Jianming Xie[1]*, Jihua Yu[1], Jian Lyv[1], Junfeng Zhang[2], Dongxia Ding[1], Nenghui Li[1], Jing Zhang[1], Emily Patience Bakpa[1], Yan Yang[1], Tianhang Niu[1] and Feng Gao[1]

[1]College of Horticulture, Gansu Agricultural University, Lanzhou, China, [2]Institution of Vegetable, Gansu Academy of Agricultural Science, Lanzhou, China

Melatonin (MT) is an important biologically active hormone that plays a vital role in plant growth and development. In particular, it has been investigated for its roles in abiotic stress management. In this study, pepper seedlings were subjected to low-temperature combined with low-light stress (LL) (15/5°C, 100 μmol $m^{-2}s^{-1}$) prior to a foliar spray of 200mM MT for 168h to investigate the protective role of MT in pepper seedlings. Our results demonstrated that LL stress negatively affected root growth, and accelerated the accumulation of reactive oxygen species (ROS), including H_2O_2 and O_2^-, changed the osmolytes contents, and antioxidative system. However, these were reversed by exogenous MT application. MT effectively promoted the root growth as indicated by significant increase in root length, surface area, root volume, tips, forks, and crossings. In addition, MT reduced the burst of ROS and MDA contents induced by LL, enhanced the activities of SOD, CAT, POD, APX, DHAR, and MDHAR resulted by upregulated expressions of *CaSOD*, *CaPOD*, *CaCAT*, *CaAPX*, *CaDHAR*, and *CaMDHAR*, and elevated the contents of AsA and GSH, declined DHA and GSSH contents, which prevented membrane lipid peroxidation and protected plants from oxidative damages under LL stress. Furthermore, seedlings treated with MT released high contents of soluble sugar and soluble protein in leave, which might enhance LL tolerance by maintaining substance biosynthesis and maintaining cellular homeostasis resulted by high levels of osmolytes and carbohydrate in the cytosol. Our current findings confirmed the mitigating potential of MT application for LL stress by promoting pepper root growth, improving antioxidative defense system, ascorbate-glutathione cycle, and osmotic adjustment.

KEYWORDS

pepper, melatonin, root morphology, reactive oxygen species, antioxidant defense system, ascorbate-glutathione cycle, osmotic adjustment

1 Introduction

The growth of pepper (*Capsicum annuum* L.) is closely related to suitable external conditions including light, temperature, water, gas, fertilizer and other factors (Eom et al., 2010). Pepper is a typically thermophilous and heliophilic vegetable that originated from South Africa. It is mainly cultivated in protected facilities out of season during the winter-spring season, especially in northwest China. Due to the limited heat preservation performance and poor controllability of solar greenhouses, temperature and light are often difficult to reach the level needed for growth and development of pepper (Ou et al., 2015; Li et al., 2021; Tang et al., 2021). Low-temperature combined with low-light stress (LL) not only seriously affects the yield and quality of pepper, but also decreases the production and management costs.

Chilling stress decrease the plant root growth by decreasing the biomass of the roots, and this root growth inhibition is contributed to the constrain of cell elongation and differentiation shape of root cells (Nagasuga et al., 2011; Zhu et al., 2015; Yamori et al., 2022). In contrast, light regime affects the root distribution, and low light leads to longer but less branched roots in plants (Page et al., 2012). Besides, the cell membrane is the first place where plants are damaged by low-temperature stress. Low-temperature stress leads to changes of the membrane phase, decreased fluidity, and increased cell membrane permeability, eventually causing ion metabolism disorders as a result of cytoplasmic exudation (Barrero-Sicilia et al., 2017). In addition, under low-temperature stress, reactive oxygen species (ROS) react with unsaturated fatty acids in the cell membrane to produce malondialdehyde (MDA) (Dey et al., 2021). The decreased of ROS scavenging ability of plants under low-temperature stress leads to the production of a large number of MDA, and finally changes the structure and function of membrane proteins (Lado et al., 2016; Chen et al., 2018). Under stress, plants will activate the enzymatic defense system, which can significantly increase the activities of defense enzymes such as superoxide dismutase (SOD), peroxidase (POD), catalase (CAT), ascorbate peroxidase (APX), glutathione reductase (GR), dehydroascorbate reductase (DHAR), monodehydroascorbate reductase (MDHAR), and ascorbate-glutathione (AsA-GSH) cycle and key genes expressions, and eliminate excess free radicals to protect from the injury caused by stress (Zhao et al., 2016). In addition, light intensity directly affects plant growth characteristics and plant metabolism. Weak light causes a significant increase in ROS, which in turn leads to an increase in MDA, resulting in changes in the antioxidant activity of a series of enzymes, and osmotic regulation (Meng et al., 2017; Mclay et al., 2018). However, studies on the effects of low-temperature combined with low-light stress on the root and antioxidant defense system of pepper plants are not available.

Melatonin (N-acetyl-5-methoxytryptamine, MT) is an indole hormone with multiple functions and is ubiquitously present in animals, plants, and algae (Hattori et al., 1995). Endogenous MT plays a vital role in plants, such as regulating seed germination, plant growth, root system architecture (root elongation, adventitious root formation, and lateral development), and circadian rhythm (Park and Back, 2012; Zhang et al., 2013; Balabusta et al., 2016). Additionally, MT acts as an endogenous oxygen free radical scavenger that can eliminate excessive ROS caused by stress, improve the activity of antioxidant enzyme and the regulation ability of the ASA-GSH system, and inhibit the content of H_2O_2 and O_2^- in plants protecting plants from oxidative damage (Zhang N. et al., 2015; Xu et al., 2016; Chen et al., 2017; Li et al., 2019a; Moustafa-Farag et al., 2020; Zeng et al., 2022). Numerous studies have proved the antioxidative effect of MT on rice, cucumber, tomato, maize, *Coffea arabica* L., and *Camellia sinensis* L. (Debnath et al., 2018; Li et al., 2018; Wei et al., 2018; Ahammed et al., 2019; Ahmad et al., 2019; Campos et al., 2019; Ahammed et al., 2020; Wang et al., 2020; Zhang T. et al., 2020; Yan et al., 2021). Therefore, MT regulates the metabolic process of plants to improve plant resistance, and effectively alleviate many stresses such as low temperature, high temperature, drought, and salinity (Li et al., 2017; Zhang et al., 2017a; Sharma and Zheng, 2019; Ren et al., 2020; Wang et al., 2020; Imran et al., 2021).

Although much distinct progress has been made in exploring the role of MT in response to abiotic stress, little is known about the mechanism of MT on LL tolerance in pepper. In this study, the

Abbreviations: APX, ascorbate peroxidase; AsA, reduced ascorbic acid; AsA-GSH, reduced ascorbic acid- reduced glutathione; CAT, catalase; DHA, dehydroascorbate; DHAR, dehydroascorbate reductase; GR, glutathione reductase; GSH, reduced glutathione; GSSG, oxidized glutathione; H_2O_2, hydrogen peroxide; low-temperature combined with low-light (LL); MDA, malondialdehyde; MDHAR, monodehydroascorbate reductase; MT, melatonin; NBT, nitroblue tetrazolium; O_2^-, superoxide anion radical; POD, peroxidase; qRT-PCR, quantitative real-time polymerase chain reaction; ROS, reactive oxygen species; SOD, superoxide dismutase.

impacts of exogenous MT pre-application on the root structure, H_2O_2, O_2^-, and MDA contents; soluble sugar and soluble protein contents; as well as activities of SOD, POD, CAT, APX, DHAR, MDHAR, and contents of AsA, DHA, GSH, GSSH of pepper seedlings under LL stress were investigated to elucidate the possible mechanism of MT involved in response to LL.

2 Materials and methods

2.1 Plant materials, and growth conditions

Two geminated pepper seeds (*Capsicum annuum* L.) cv. 'Hangjiao 4' (purchased from Tianshui Academy of Agricultural Sciences) were sown in substrate (vermiculite: grass carbon: cow dung = 3:1:1). The growth conditions were maintained at 28°C/18°C (day/night) temperature with relative humidity of 70%-80% under 12h photoperiod (300μmol m^{-2} s^{-1}) in the greenhouse of Gansu Agricultural University (N36°05'39.86", E103°42'31.09''). The plants were watered every day, and fertilized with 1/2 Hoagland nutrient solution once a week.

2.2 Treatments

Pepper seedlings at the five-leaf stage were selected for stress treatments. Four treatments were conducted in this study including (1) CK, 28 °C/18 °C, 300 μmol m^{-2} s^{-1}, distilled water; (2) CK+MT 28 °C/18 °C, 300 μmol m^{-2} s^{-1}, 200 μM MT; (3) LL, 15°C/5°C, 100 μmol m^{-2} s^{-1}, distilled water; and (4) LL+MT, 15 °C/5 °C, 100 μmol m^{-2} s^{-1}, 200 μM MT. The melatonin (Sigma-Aldrich, USA) was dissolved in little ethanol followed by dilution with distilled water [ethanol/water (v/v) = 1/10,000]. All solutions contained 1% Tween 80 and each spray was carried out at 8:00 pm for four continuous days, while control seedlings were instead of equal amounts of distilled water. After that, the seedlings were transferred to an artificial climate incubator (RDN-400E-4, Zhejiang, China) for different temperature and light stresses. The third expanded pepper leaves were collected randomly, then frozen in liquid nitrogen, and kept at -80 °C for physiological and biochemical analysis after 0, 6, 12, 24, 48, and 168h of the treatment. Each treatment was repeated three times with 30 plants per replicate.

2.3 Root structure

The root structure was scanned by using a root scanner (Epson). The root length, root surface area, root volume, tips, forks, and crossing of pepper seedlings treated for 168h were determined using WinRHIZO software (LC4800-II LA2400, Sainte Foy, Canada) (Zhang et al., 2013).

2.4 Histochemical staining and analyses of ROS and MDA content

Superoxide anion (O_2^-) was detected visually by treating leaves with nitro blue tetrazolium (NBT) after 168h as described by Tang et al. (2021). Pepper leaves during five-leaf stage of 0.1g grounded into powders with liquid nitrogen was used to measure O_2^- and H_2O_2 content in accordance with the instructions of reagent kits after 0, 6, 12, 24, 48, and 168 h (Suzhou Keming Biotechnology Co., Ltd, China). Finally, the absorbances of samples were measured at 530nm and 415nm, respectively. The MDA content was determined using the thiobarbituric acid method *via* detecting the absorbance at 450, 532, and 600nm according to the method of Kong et al. (2014).

2.5 Analyses of osmotic adjustment substances

Soluble sugar was determined using the anthrone method based on a precious study (Shi et al., 2015). In brief, 0.1g of fresh pepper leaves was added to 2mL of 80% ethanol, and boiled for 30 min. Then 100μL of the extracts was added to 2mL anthrone, followed by boiling water bath for 10min. The absorbance of the above mixture was measured at 620 nm wavelength with a spectrophotometer. Total soluble proteins were determined with the Bradford reagent. The absorbance at 595 nm was recorded, and the soluble protein level was calculated according to the standard curve (Bradford, 1976).

2.6 Extractions and assays of antioxidant enzymes

2.6.1 Activity of SOD, POD, and CAT

About 0.5g of fresh leaves and 0.1 g of quartz sands were homogenized in 5.0 mL of 50mM phosphate buffer (pH 7.5) containing 0.1mM ethylene diamine tetraacetic acid and 5.0% (w/v) polyvinylpyrrolidone with a cold mortar. Then they were transferred into centrifugal tubes, and centrifuged at 15,000g for 15 min under 4°C. The supernatants were used for measurements of SOD, POD, CAT. All of these antioxidant enzymes were assayed according to the instruction of the reagent kits (Suzhou Keming Biotechnology Co., Ltd, China). The activities of enzymes were determined by observing at 470, 560, and 240 nm, respectively.

2.6.2 Determination of ASA-GSH cycle contents and key enzymes

The contents of antioxidant, including reduced ascorbic acid (AsA), dehydroascorbate (DHA), reduced glutathione (GSH) (Kong et al., 2014), and oxidized glutathione (GSSG), and the activities of key enzymes in AsA-GSH, including APX, MDHAR,

DHAR were determined by using reagent kits purchased from Suzhou Keming Biotechnology Company (China).

2.7 Data validation and gene expression analysis by quantitative real-time polymerase chain reaction (qRT-PCR)

The transcript levels of genes, including *CaSOD*, *CaPOD*, *CaCAT*, *CaAPX*, *CaDHAR*, and *CaMDHAR*, in pepper leaves were determined by qRT-PCR. Total RNA from fresh pepper leaves was extracted by using an RNAprep Pure Plant kit (Tiangen Biotech Co., Ltd., Shanghai, China). The RNA quality and concentration were detected by Nanodrop 2000 (Thermo, MA, USA). RNA of 0.5 micrograms was reverse-transcribed into cDNA using the cDNA Synthesis Kit (Takara Biotech Co., Ltd., Dalian, China). Oligo7 software was used to design primers, and the primer sequence of target genes is provided in Table S1. Finally, qRT-PCR was performed using the TransStart Green qPCR SuperMix reagent Kit (TransGen Biotech, Beijing, China) on a LightCycler 480 II system (Roche, Switzerland). The reaction conditions include 30 s preincubation at 94°C, followed by 40 cycles at 95°C for 5 s, 60°C for 30 s, and 72°C for 15 s. Each sample was measured with three technical replicates. Actin was used as an internal reference gene and the relative expressions of the relative expressions of target genes were analyzed using the $2^{-\Delta\Delta Ct}$ method (Livak and Schmittgen, 2001).

3 Statistical analysis

All experiments were conducted using three biological repeats. Duncan's multiple comparison test at a significance level of $P < 0.05$ was carried out using SPSS19.0 software (IBM SPSS 22.0, IBM Corporation, New York, USA) for statistical analysis. The figures were generated in Origin ver. 8.5 and Adobe Photoshop CS 6.

4 Results

4.1 Effect of exogenous MT on root morphology and growth in pepper under LL stress

After 168 h, no significant changes in root growth of pepper seedlings were observed under CK and CK+MT; however, LL stress conditions severely hampered the root growth, which was reversed by MT pre-spraying (Table 1 and Figure 1). The root length, surface area, root volume, tips, forks, and crossing of pepper seedlings pre-sprayed with MT showed no significant changes under normal conditions compared with those under CK. However, LL stress remarkably reduced the root length, surface area, root volume, tips, forks, and crossing of pepper seedlings by 58.14, 69.08, 76.67, 42.14, 76.45, and 74.85%, respectively, compared with CK. Compared with LL, the root volume, root length, surface area, tips, forks, and crossing were increased by 69.55, 105.25, 142.86, 67.60, 142.92, and 164.75%, respectively, after pre-application of MT. Except the root volume, all parameters reached significant levels ($P < 0.05$).

4.2 Effect of exogenous MT on ROS accumulation in pepper under LL stress

Histochemical detection of O_2^- contents in pepper leaves was performed by using NBT staining. As shown in Figure 2A, the blue areas and depth of pepper leaves were the highest under LL treatment for 168h. However, this was reversed by MT pretreatment. The blue area was obviously reduced and only spread over half of the leaf. This finding was consistent with that shown in Figures 2B, C wherein the O_2^- and H_2O_2 contents significantly accumulated under LL stress, gradually increased over time, and reached highest contents after 168h with 1.24-fold and 2.49-fold of CK, respectively. Both O_2^- and H_2O_2 contents in leaves of seedlings treated under LL were still the highest among four treatments after 6, 12, 24, 48, and 168 h. However, MT pre-spraying reduced the ROS contents of pepper leaves under LL. The contents of O_2^- and H_2O_2 significantly decreased by 18.33, 18.39, 19.24, 14.49 and 21.41%, and 29.95, 24.41, 22.91, 13.60 and 15.72% after 6, 12, 24, 48 and 168h, respectively.

4.3 Effect of exogenous MT on soluble sugar, soluble protein, and MDA in pepper leaves under LL stress

The effect of MT on soluble sugar, soluble protein, and MDA is displayed in Figure 3. Under LL stress, the soluble sugar content significantly decreased ($P < 0.05$) at the first 6 h and then

TABLE 1 Effect of exogenous MT on the root growth in pepper under LL stress.

Treatment	Length (cm)	Surface Area (cm^2)	Root Volume (cm^3)	Tips	Forks	Crossings
CK	539.87 ± 42.05a	77.64 ± 11.45a	0.90 ± 0.20a	480 ± 35.51a	2760 ± 476.30a	586.5 ± 83.12a
CK+MT	558.57 ± 37.00a	80.48 ± 6.29a	0.93 ± 0.09a	563.25 ± 48.32a	2711 ± 328.59a	568.5 ± 98.29a
LL	226.01 ± 28.94c	24.00 ± 3.07c	0.21 ± 0.04b	277.75 ± 32.22b	650 ± 91.11c	147.5 ± 29.88b
LL+MT	383.21 ± 19.47b	49.26 ± 2.34b	0.51 ± 0.03b	465.5 ± 78.66a	1579 ± 68.15b	390.5 ± 22.82a

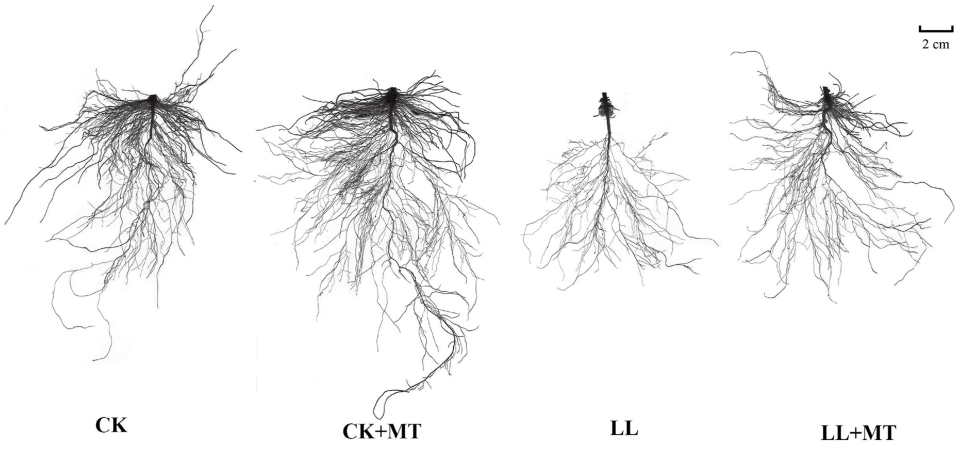


FIGURE 1
Effect of exogenous MT on the root morphology in pepper under LL stress. CK (normal temperature and light, 28°C/18°C and 300 µmol photons m^{-2} s^{-1}), CK+MT (normal temperature and light, 28°C/18°C and 300 µmol photons m^{-2} s^{-1}, 200 µmol L^{-1} melatonin), LL (low-temperature combined with low-light, 15°C/5°C and 100 µmol m^{-2} s^{-1}), and LL+MT (low–temperature combined with low-light, 15°C/5°C and 100 µmol m^{-2} s^{-1}, 200 µmol L^{-1} melatonin). Vertical bars represent the standard errors of the means (three replicates. Different letters denote statistically significant differences among treatments within same time at a level of $P < 0.05$ by Duncan's multiple comparison tests.

increased from 12 h to 168 h with contents ranging from 0.262 mg g^{-1} FW to 0.845 mg g^{-1} FW. Meanwhile, exogenous MT significantly enhanced the content of soluble sugar at 6, 48, and 168 h compared with LL, and the highest contents were observed at 168 h (0.948 mg g^{-1} FW, an increase of 12.22%). In terms of soluble protein, LL greatly decreased the soluble protein content at the first 24 h. Then, the content significantly increased after 168 h. The highest soluble protein content was 29.14 mg g^{-1} FW (an increase of 7.57%) at 168 h compared with CK. After the application of MT under LL, the contents of soluble protein significantly increased by 139.97, 125.82, 120.99, 82.71, and 59.47% at 6, 12, 24, 48, and 168 h, respectively However, the MDA contents significantly increased gradually with time under LL stress. Exogenous MT significantly decreased the LL-induced increases in MDA content by 25, 20.50, 28.66, and 24.36% at 12, 24, 48, and 168 h, respectively.

4.4 Effect of exogenous MT on antioxidant enzyme activity and the relative expression of related genes in pepper leaves under LL stress

The activities of SOD, POD, and CAT enzymes and the relative expression of *CaSOD*, *CaPOD*, and *CaCAT* under different treatments were investigated (Figure 4) in pepper leaves to estimate the effects of MT pre-application. Obviously, when exposed to LL stress, the SOD activity (Figure 4A) of pepper leaves with and without MT significantly increased by 57.12, 72.34, 40.17, and 21.81% at 6, 12, 24, and 48 h, respectively, and then significantly decreased by 54.38% at 168 h in contrast to CK. The SOD activity with MT pretreatment showed the same tendency under LL. Notably, the SOD activity increased significantly by 6.27 and 74.26% at 48 and 168h, respectively ($P < 0.05$) compared with LL. LL stress significantly enhanced the POD activity (Figure 4B) from 24 h to 48 h and finally decreased by 21.27% at 168 h compared with no stress. Meanwhile, the POD of MT-pretreated seedlings was significantly higher than those of other treatments (CK, CK+MT, and LL) at 12, 24, 48, and 168 h, displaying an increase of 176.09, 43.22, 36.08, and 121.05%, respectively compared with LL. After LL stress, the CAT activity (Figure 4C) of seedlings increased during the first 24 h, and then gradually decreased, which was still higher than that of CK with an increase of 53.06-97.22% within 168 h. The pre-application of MT increased CAT activity of pepper seedlings under LL, and showed a significant increase by 21.80, 16.94, and 31.70% at 12, 24, and 168 h, respectively, compared with LL.

Figures 4D–Fshow that compared with CK, LL downregulated the relative expression of *CaSOD*, *CaPOD*, and *CaCAT* during the first 12h. Then, LL upregulated *CaSOD* and *CaPOD* from 24 h to 48 h, finally, downregulated by 50.84 and 35.78% at 168 h. *CaCAT* gradually increased from 24 h to 168 h, which was 127.17-fold higher than that of CK at 168 h. MT spraying showed significant effects on the relative expression of *CaSOD*, *CaPOD*, and *CaCAT* at 168 h under LL stress (increased by 54.00, 193.02, and 147.73%, respectively).

10.3389/fpls.2022.998293

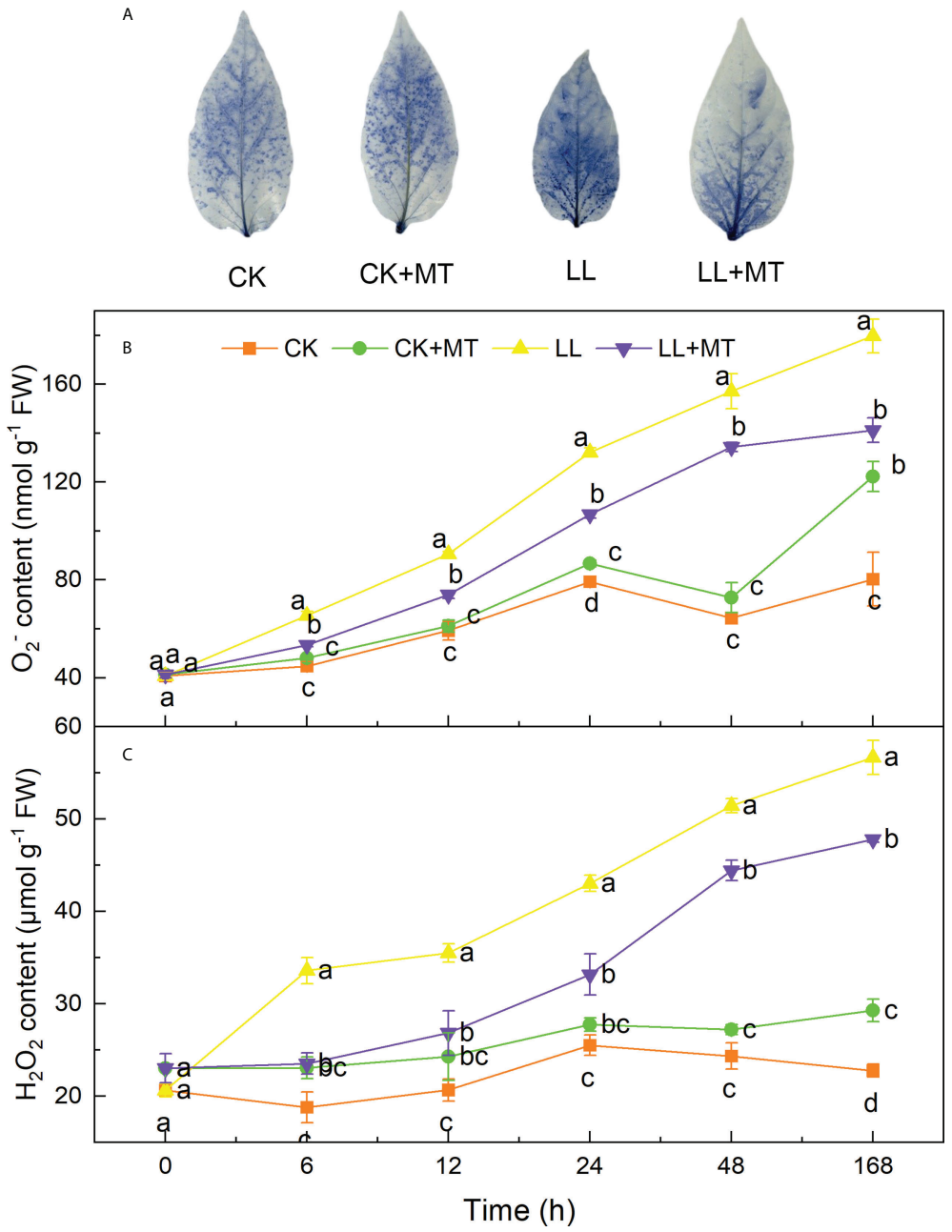


FIGURE 2
Effect of exogenous MT on the accumulation of ROS in pepper under LL stress. **(A)** Image of NBT staining after treated for 168h, **(B)** superoxide anion (O_2^{-1}) content, **(C)** Hydrogen peroxide (H_2O_2) content. CK (normal temperature and light, 28°C/18°C and 300 μmol photons m^{-2} s^{-1}), CK+MT (normal temperature and light, 28°C/18°C and 300 μmol photons m^{-2} s^{-1}, 200 μmol L^{-1} melatonin), LL (low−temperature combined with low−light, 15°C/5°C and 100 μmol m^{-2} s^{-1}), and LL+MT (low−temperature combined with low−light, 15°C/5°C and 100 μmol m^{-2} s^{-1}, 200 μmol L^{-1} melatonin). Vertical bars represent the standard errors of the means (three replicates. Different letters denote statistically significant differences among treatments within same time at a level of $P < 0.05$ by Duncan's multiple comparison tests.

10.3389/fpls.2022.998293

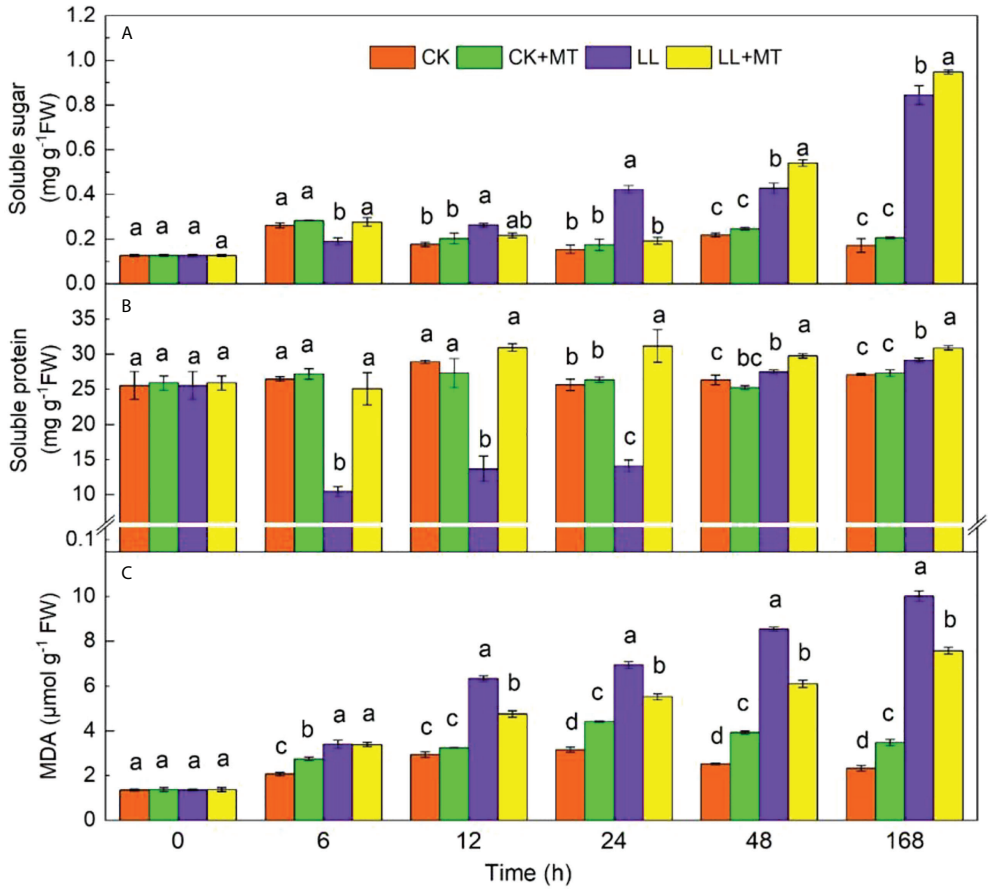


FIGURE 3
Effect of exogenous MT on **(A)** Soluble sugar content, **(B)** Soluble protein content, **(C)** Malondialdehyde (MDA) content of pepper leaves under LL stress. CK (normal temperature and light, 28°C/18°C and 300 μmol photons m^{-2} s^{-1}), CK+MT (normal temperature and light, 28°C/18°C and 300 μmol photons m^{-2} s^{-1}, 200 μmol L^{-1} melatonin), LL (low–temperature combined with low–light, 15°C/5°C and 100 μmol m^{-2} s^{-1}), and LL +MT (low–temperature combined with low–light, 15°C/5°C and 100 μmol m^{-2} s^{-1}, 200 μmol L^{-1} melatonin). Vertical bars represent the standard errors of the means (three replicates). Different letters denote statistically significant differences among treatments within same time at a level of $P < 0.05$ by Duncan's multiple comparison tests.

4.5 Effect of exogenous MT on AsA-GSH enzyme activity and genes in pepper leaves under LL stress

Figure 5 shows the changes in the activity levels of enzymes involved in the AsA–GSH cycle of pepper leaves pretreated with MT under LL. Relative to CK, LL stress influenced the activities of enzymes in the AsA–GSH cycle. The activities of APX showed a significant increase at 12 h but decreased at 168 h (declining by 24.10%). The APX activities were significantly enhanced by pretreated with MT, and reached a peak value of 23.24 U g^{-1} FW (increased by 77.89%) at 24 h. Then, the value decreased from 24 h to 168 h, which was still significantly higher than that of LL, and increased by 87.95% after 168 h. LL remarkably suppressed the DHAR activity (Figure 5B) in pepper leaves at 6 h but enhanced the activity at 24, 48, and 168 h. The peak value of DHAR activity was 1.16 times higher than that in CK at 24 h. The DHAR activities of seedlings pretreated with MT after LL stress were significantly higher than those with LL at any time except at 6 h. The highest value was observed at 24 h, which was 19.65% higher than that of LL. Figure 5C demonstrates that the MDHAR activity significantly increased by 74.43, 41.70, 65.70, and 32.81% at 6, 24, 48, and 168 h under LL stress, respectively. MT application remarkably increased the activity of MDHAR by 14.83, 65.70, and 50.38% at 6, 12, and 168 h, respectively.

Similarly, the relative expression level of *CaAPX* (Figure 5D) notably increased at 24 h and decreased at 6, 48 h, and 168 h under LL. However, the relative expression of *CaAPX* in pepper leaves treated with MT increased at 6–168 h compared with LL, and 43.69 times of LL after treated for 168h under LL. The expression of *CaDHAR* (Figure 5E) was obviously inhibited by LL treatment at 6 and 12 h; however, it was enhanced at 24 to

10.3389/fpls.2022.998293

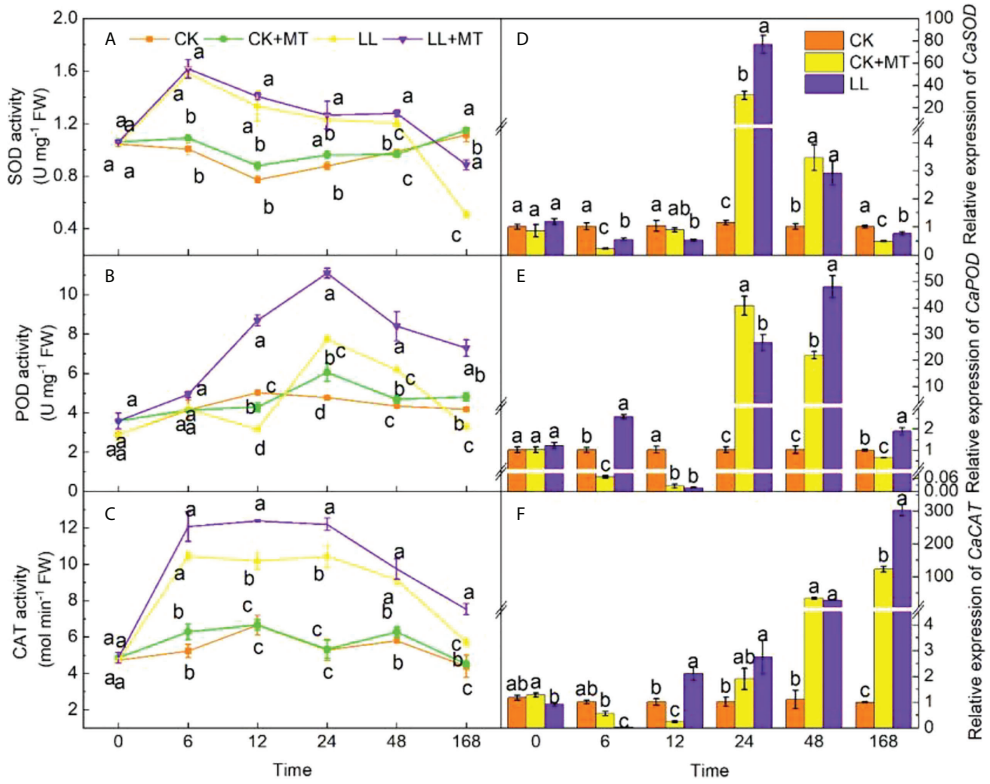


FIGURE 4
Effect of exogenous MT on antioxidant enzyme activity of pepper leaves under LL stress. **(A)** Superoxide dismutase (SOD) activity, **(B)** Peroxidase (POD) activity, **(C)** Catalase (CAT) activity. **(D)** Relative expression of *CaSOD*, **(E)** Relative expression of *CaPOD*, **(F)** Relative expression of *CaCAT*. CK (normal temperature and light, 28°C/18°C and 300 μmol photons m^{-2} s^{-1}), CK+MT (normal temperature and light, 28°C/18°C and 300 μmol photons m^{-2} s^{-1}, 200 μmol L^{-1} melatonin), LL (low−temperature combined with low−light, 15°C/5°C and 100 μmol m^{-2} s^{-1}), and LL+MT (low−temperature combined with low−light, 15°C/5°C and 100 μmol m^{-2} s^{-1}, 200 μmol L^{-1} melatonin). Vertical bars represent the standard errors of the means (three replicates). Different letters denote statistically significant differences among treatments within same time at a level of $P < 0.05$ by Duncan's multiple comparison tests.

168 h and showed significant differences at 6 (decreased by 49.97%) and 48 and 168 h ((increased by 165.08 and 193.60%, respectively). MT application remarkably increased the expression of *CaDHAR* after 12, 24, 48, and168 h, and were 350.38, 1.18, 4.02, and 0.90 times higher than that of LL. The relative expression of *CaMDHAR* (Figure 5F) in pepper seedlings was significantly enhanced at 6, 24, and 168 h and was 6.78, 8.77, and 6.87 times higher than that of CK, respectively. After pretreatment with MT under LL, the expression of *CaMDHAR* was dramatically increased by 56.96, 60.89, 12.33, and 41.69% at 6, 12, 48, and 168 h, respectively.

4.6 Effect of exogenous MT on AsA-GSH cycle contents in pepper leaves under LL stress

Figure 6 demonstrated the changes in the contents of AsA, DHA, AsA+DHA, GSH, GSSG, and GSH+GSSG after MT pre-application under LL in pepper leaves. ASA contents (Figure 6A) significantly decreased by 86.71, 48.56, 44.91, 77.10, and 41.53 at 6, 12, 24, 48 and 168 h under LL compared with CK. However, the AsA contents in seedlings treated with MT under LL were significantly enhanced, which were 6.99, 4.17, 0.59, 3.44, and 0.34 times higher at 6, 12, 24, 48 and 168 h than those of LL, respectively. The DHA contents (Figure 6B) displayed no significant differences under LL at 6 and 12 h, compared to CK, but significant increases of 75.37, 37.20, and 91.40% were observed at 24, 48, and 168 h. Whereas, MT pre-application significantly declined DHA contents by 42.48, 39.93, 24.13, and 41.57% at 12, 24, 48 and 168 h under LL. The varies of AsA+DHA contents were similar to ASA contents, which significantly declined by 31.57% after LL stress for 168h compared to CK, while were reversed by pre-adding MT and increased by 18.11% in comparison with LL (Figure 6C).

As shown in Figure 6D, compared to CK, GSH contents of seedlings under LL stress showed no changes at 6 and 48 h, but significantly decreased by 61.21% at 24h, and slightly increased

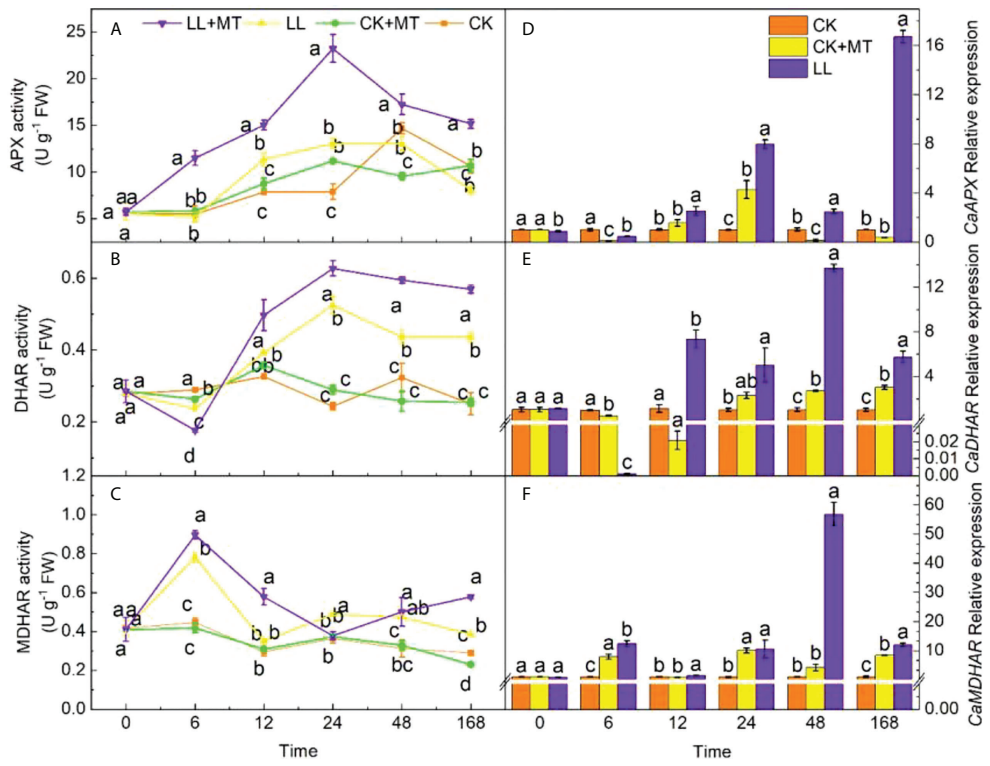


FIGURE 5
Effect of exogenous MT on ASA-GSH enzyme activity and genes in pepper leaves under LL stress. **(A)** Ascorbate peroxidase (APX) activity, **(B)** Dehydroascorbate reductase (DHAR), **(C)** Monodehydroascorbate reductase (MDHAR) activity. **(D)** Relative expression of *CaAPX*, **(E)** Relative expression of *CaDHAR*, **(F)** Relative expression of *CaMDHAR*. CK (normal temperature and light, 28°C/18°C and 300 μmol photons m^{-2} s^{-1}), CK +MT (normal temperature and light, 28°C/18°C and 300 μmol photons m^{-2} s^{-1}, 200 μmol L^{-1} melatonin), LL (low−temperature combined with low−light, 15°C/5°C and 100 μmol m^{-2} s^{-1}), and LL+MT (low−temperature combined with low−light, 15°C/5°C and 100 μmol m^{-2} s^{-1}, 200 μmol L^{-1} melatonin). Vertical bars represent the standard errors of the means (three replicates). Different letters denote statistically significant differences among treatments within same time at a level of $P < 0.05$ by Duncan's multiple comparison tests.

by 40.23 and 38.66% at 12 and 168h. In contrast, MT dramatically increased GSH contents in pepper under LL after 6, 12, 24, 48, and 168 h, which increased by 162.55, 31.62, 91.06, 53.96, and 77.78%, respectively, compared with LL. Differently, GSSG contents (Figure 6D) significantly increased by 64.93, 77.36, 36.55, 66.55, and 42.16% at 6, 12, 24, 48, and 168 h under LL, whereas, these were reversed by MT pre-application, which declined by 11.20, 22.36, 14.62, 22.11, and 14.35%. The changes of GSH + GSSG contents (Figure 6F) were similar to GSH contents, compared with CK, declined by 56.67% at 24 h, but enhanced by 36.34% at 168h under LL. While, GSH + GSSG contents in seedlings pre-treated with MT were 1.24, 0.31, 0.79, 0.51, 0.70 times higher than those of LL at 6, 12, 24, 48, and 168 h, respectively.

5 Discussion

Low temperature combined with low-light stress is one of the most devastating stresses limiting the growth and development of plants by causing a series of physiological, biochemical, and molecular disorders (Cui et al., 2016; Shu et al., 2016; Bi et al., 2017; Anwar et al., 2020; Bawa et al., 2020; Liu et al., 2020b; Zhang J.F. et al., 2020). As reported previous, LL has adverse effects on plant seedlings and results in significant reduction in growth (Li et al., 2021; Ding et al., 2022; Li et al., 2022). Our results demonstrated that the LL-induced inhibition was associated with significant increases in ROS and changes in antioxidant enzymes in pepper seedlings. MT is a naturally pleiotropic molecule in plants, and is considered to be a plant growth regulator involved in improving plant resistance against environmental stresses (Zhang et al., 2015; Li et al., 2019a; Chen et al., 2020; Yan et al., 2021). The present findings revealed that MT-pre-application treatment significantly influenced the pepper seedling root and antioxidant systems under LL stress.

The root system plays a dominant role in absorbing water and nutrients from the soil or substrate, and reflects whether the plants are stressed. Hussain et al. (2020) indicated that the root surface area and root volume of XD889, XD319, Yu13, and Yu37

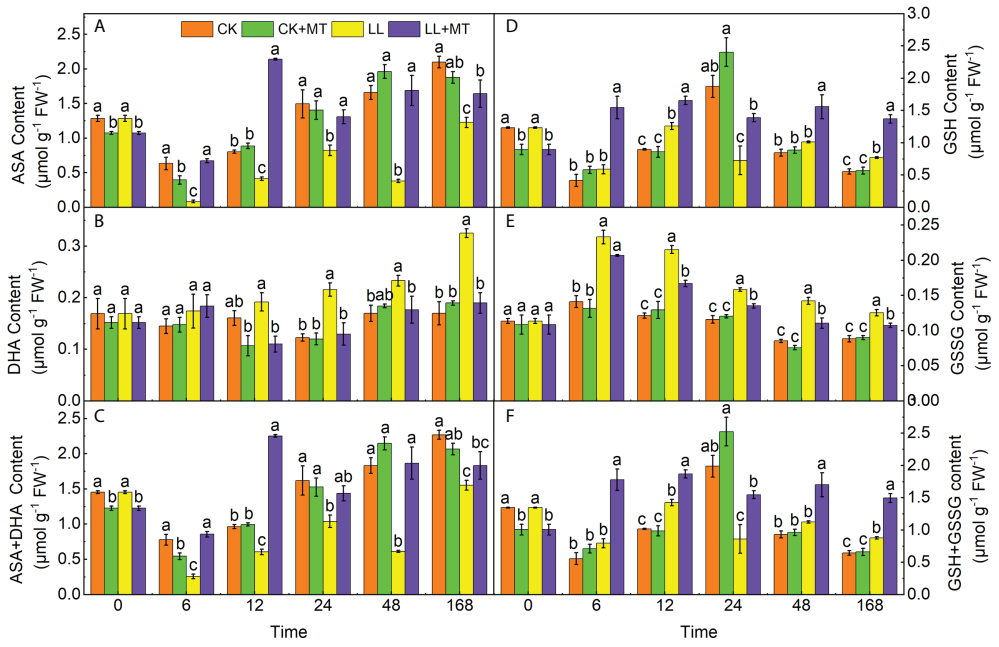


FIGURE 6
Effect of exogenous MT on ASA-GSH contents in pepper leaves under LL stress. **(A)** Ascorbic acid (AsA) content, **(B)** Dehydroascorbate (DHA) content, ((**C**)AsA + DHA content, **(D)** Glutathione content, **(E)** Oxidized glutathione (GSSG) content, **(F)** GSH + GSSG content. CK (normal temperature and light, 28°C/18°C and 300 μmol photons m^{-2} s^{-1}), CK+MT (normal temperature and light, 28°C/18°C and 300 μmol photons m^{-2} s^{-1}, 200 μmol L^{-1} melatonin), LL (low−temperature combined with low−light, 15°C/5°C and 100 μmol m^{-2} s^{-1}), and LL+MT (low−temperature combined with low−light, 15°C/5°C and 100 μmol m^{-2} s^{-1}, 200 μmol L^{-1} melatonin). Vertical bars represent the standard errors of the means (three replicates). Different letters denote statistically significant differences among treatments within same time at a level of $P < 0.05$ by Duncan's multiple comparison tests.

maize cultivars were significantly reduced under a low temperature of 15°C. In the present study, the root surface area, root volume, total root length, forks, tips, and crossing of pepper seedlings were all decreased after 168h under LL stress. Recent evidence showed that MT treatment stimulated adventitious and lateral root formation and root elongation (Arnao and Hernandez-Ruiz, 2007; Park and Back, 2012; Sarropoulou et al., 2012; Zhang et al., 2013; Wang et al., 2016). Zhang et al. (2019) found that aluminum-induced inhibition of *Arabidopsis* root length may be associated with the reduced MT caused by *AtSNAT* downregulation, which was reversed by exogenous MT application and endogenous MT synthesis (Zhang et al., 2019). Similarity, a study found that the soybean root growth was increased after supplementation with low concentration of MT (0.1-1.0 μM) under aluminium toxicity, which might be contributed to the enhanced expression of *NSI-X1* and *NSI-X2* involved in MT biosynthesis (Zhang et al., 2017b). Dai et al. (2020) stated that the taproot and lateral root length of rapeseed (*Brassica napus* L.) *cv* Qinyou 8 seedlings irrigated with 100 μM MT for 7 days were promoted under drought, enabling normal water uptake, compared with seedlings without MT. While, no pronounced effects on total root length, root surface area, root diameter, and root volume were found, indicating that MT enhance drought tolerance by improving lateral and taproot growth (Dai et al., 2020). This is inconsistent with the results of our study, wherein the root length, root surface area, tips, forks, and crossing were increased compared with seedlings without MT-spraying by 105.25, 142.86, 67.60, 142.92, and 164.75% ($P < 0.05$), respectively (Table 1). The reason for these inconsistent results may be due to different stresses or species. Our findings suggested that MT improved the LL-tolerance of pepper seedlings by alleviating LL-induced root growth limitation, which might be upregulate the key genes in MT biosynthesis in roots.

The plasma membrane is the first site that senses the temperature, and low temperature induced substantially alterations in lipid composition (Lado et al., 2016). Plants are expose to adverse environment throughout their life which generally cause excessive ROS generation causing lipids damage (Hassan et al., 2021). ROS are widely considered to be signaling molecules that are involved in oxidative stress. Although plants possess well-developed antioxidant system and other defense systems, stresses are likely to induce surfeit accumulation of ROS, resulting in membrane lipid peroxidation and reduction of enzyme activity (Heidarvand and Amiri, 2010). In the present study, short time (0-48h) and long time (168h) LL stress

significantly increased the O_2^- and H_2O_2 contents (Figure 2), causing oxidative stress to seedlings as a result of continuously increased MDA concentration (Figure 3), and suggesting critically irreparable lipid peroxidation and severe damage to the plasma membrane. Exogenous substances have been widely used to enhance plant tolerance to LL. However, the role of MT in ROS and antioxidant system in pepper seedlings is still limited. In the present study, pretreated with MT, although the O_2^- and H_2O_2 contents in pepper leaves under LL stress were obviously higher than those under CK, but significantly decreased after 6, 12, 24, 48, and 168h compared with LL, which indicated that exogenous MT effectively alleviated the LL-induced damage in pepper plants. Our results are consistent with those of a previous study that in "Zhongnong 37" cucumber (*Cucumis sativus* L.) sprayed 200μM MT for 5 days during 2-leaf stage, a significant decrease of 246.1% in MDA contents were observed on 6th day under 15/10°C and 95% humidity, in addition, the H_2O_2 contents were greatly reduced on the second and fourth day, and the production of O_2^- was dramatically suppressed, compared to the seedlings without MT treatment (Amin et al., 2022). Membrane stability damage is considered to be a dominant stress caused by low temperature combined with low light as indicated by the accumulations of H_2O_2 and O_2^-. While, MT functions as an antioxidant and a free radical scavenger, its supplementation protects the membrane and maintains membrane stability by scavenging ROS. Zhang et al. (2021) reported that the H_2O_2 content displayed a 65.5% increase when cucumber seedlings were exposed to 8°C or 5°C, however, this effect was reversed by application of MT, in which less H_2O_2 content increase (37.8%) was detected compared with the seedlings treated with H_2O (Zhang et al., 2021). Whereas, more evidence proved that the favorable function of MT is not merely participated in ROS scavenging, MT also could strongly induce ROS signaling and desensitize plant ion channels to ROS (Liu et al., 2020a). Generally, plants use increasing ROS generated by stresses to stimulate multiple Ca^{2+} signaling pathways acting upstream or post-translational adaptive mechanisms (Huang et al., 2022). Studies have demonstrated that transcript levels of many calcium signals and stress-related kinases were upregulated in Arabidopsis treated with MT (Weeda et al., 2014). These results affirmed that exogenous MT substantially reduced MDA and ROS accumulation, and the possible role of MT in triggering more efficient ROS signaling, preventing membrane lipid peroxidation and oxidative injury, maintaining membrane stability, (Tan et al., 2007), eventually improving the tolerance to LL.

The accumulation of osmolytes, especially carbohydrate, is an imperative mechanisms in response to stresses in plants (Hassan et al., 2021). The contents of carbohydrate, including soluble sugar and soluble protein, are necessary for plants as a source of energy, and play a crucial role in plant tolerance against stress. Stresses have been shown to change the soluble sugar and soluble protein concentrations to adapt to environmental alternation (Kobylinska et al., 2018). In a previous report, plants accumulated higher osmolyte in the cytosol to prevent the adverse effects of osmotic stress (Latef and He, 2011), and tolerant plant species with good growth performance release high concentrations of osmolytes under stress, which enhance protein function and tissue water contents (Ahanger et al., 2018). Consistently, in our study, LL stress significantly reduced the soluble protein content after stressed for short time (6, 12, and 24h), but increased after 48 and 168h compared with CK. Differently, the soluble sugar content decreased at 6h, but increased at 12, 24, 48, and 168 h, which implied that the soluble protein and soluble sugar contents were changed in response to LL stress. However, the response of soluble sugar response was faster than that of soluble protein in pepper seedlings. The foliar spray of MT maintained higher soluble sugar after 48 and 168h stress, but soluble protein contents for any time under LL stress that kept cell water contents, maintain membrane stability, and improved the plant LL tolerance. Irshad et al. (2021) also found the osmolyte agents (proline, glycine betaine, soluble sugars, and protein) in *Medicago truncatula* were increased by pre-application of 75 μM MT under cold stress (Irshad et al., 2021). Similar results of MT-enhanced osmolytes were found to be induced in alfalfa under low temperature (Liu et al., 2019), grafted *Carya cathayensis* plants under drought (Sharma et al., 2020), and sorghum seedlings exposed to waterlogging (Zhang et al., 2022). Except the regulation of osmotic adjustment, soluble sugar and soluble protein function as energy reservoirs, providing carbon and nitrogen storage for plant growth and key components for cell survival (Singh et al., 1987). Therefore, MT pretreatment was inferred to enhance LL tolerance by effectively maintaining substance biosynthesis and membrane stability caused by improved osmolyte and carbohydrate levels.

ROS induced by LL are closely related to the antioxidant defense system, and are considered as the direct pathway to alleviate the negative impact of ROS. SOD, POD, and CAT are vital enzymes responsible for scavenging ROS in the plant defense system, SOD first catalyzes O_2^- to H_2O_2, and then POD and CAT decompose H_2O_2 to H_2O and O_2, which present oxidative injury induced by stresses (Anwar et al., 2018). Numerous researches have proved that exogenous MT application enhances the antioxidant defense mechanism against adverse conditions (Ding et al., 2018; Wei et al., 2018; Wang et al., 2020). The SOD, POD, and CAT activities of cucumber seedlings treated with MT were increased by 201.30, 213.92, and 477.63%, respectively under low temperature and high humidity for 4 days. The key enzyme-encoding genes (*CsSOD*, *CsPOD*) were dramatically upregulated at day 2, 4, and 6, and the highest expression level was obtained at day 4, increasing by 69.25 and 95.33% in comparison with those of seedlings without MT. However, *CsCAT* increased from day 0 to day 6 (Amin et al., 2022). In our experiment, MT pretreatment exerted slight effects on the SOD, POD, and CAT activities under control condition. Pepper seedlings exposed to LL stress significantly enhanced the activities of SOD after 6-48h, CAT after 6-168h, POD after 24-48h, but all activities in seedlings pretreated with MT increased from 0h to 168h except SOD at 168h (Figures 3A–C). At the

same time, the maximum relative expression levels of *CaSOD*, *CaPOD*, and *CaCAT* were obtained in MT groups under LL at 24, 48, and 168h, respectively. The reduction in ROS accumulation triggered by MT improved plant performance under stress, which was positively correlated with the strengthened activities of antioxidant enzymes. Sun et al. (2018) also proposed that the upregulated expression of Cu/Zn and Fe-SOD genes caused by MT caused the increase of SOD activity, mitigating oxidative stress and enhancing tolerance against cold (Sun et al., 2018). These results implied that MT plays a synergistic role in LL resistance.

ROS in plants exhibit homeostasis under suitable conditions, whereas excess ROS content generated by abiotic stress causes the oxidative injury (Xu et al., 2019). Consequently, to cope with the oxidative injury triggered by stresses, plants initiate enzymatic antioxidant defense mechanisms and nonenzymatic mechanisms. Most importantly, it has to mention that AsA and GSH are indispensable nonenzymatic antioxidants located in plant cell organelles and cytoplasm. In the current study, H_2O_2 and MDA accumulated in pepper seedling leaves under LL stress and the NBT staining result showed a dark blue color (Figure 2), which suggested that cell membrane lipid peroxidation already occurred. The dominant pathway to clear H_2O_2 in plants is through the AsA-GSH cycle, and APX, DHAR, MDHAR, AsA, and GSH levels are enhanced in LL-stressed seedlings to conquer reduced oxidative stress (MDA, H_2O_2, O_2^-). However, the capacity of ROS scavenging was limited, especially in severe stress. The pretreatment of MT significantly boosts the antioxidant system by improving antioxidant enzyme activities and expression of related genes (Sun et al., 2019). Rice plants with over-expressed dehydroascorbate reductase gene (*OsDHAR1*) exhibited enhanced ascorbate levels, photosynthetic ability, and membrane stability (Kim et al., 2022). Similar trends were reported in tomato seedlings, wherein the GR and APX activities as well as AsA contents were significantly increased after exposure to 0.1mM MT for 3 days under drought (Liu et al., 2015). Li et al. (2017) also revealed that under salinity conditions, the activities of main enzymes including APX, DHAR, and MDHAR were significantly decreased, but the decrease was mitigated when *Citrullus lanatus* L. was treated with 150 μM MT. Moreover, AsA and GSH were dramatically higher in plants treated with MT than those treated with H_2O, resulting highest ratios of GSH/GSSH and AsA/DHA (Li et al., 2017). Additionally, in MT-deficient tomato seedlings, increasing ROS accumulation and server lipid peroxidation were observed which was associated with significantly declined endogenous MT under chilling, however, MT-supplementation improved this, meanwhile, reduced ratios of AsA/DHA in MT deficient seedlings displayed low antioxidant enzymes capacity were reversed by exogenous MT (Wang et al., 2020). These results were well agreed with our findings, wherein MT promoted APX, DHAR, and MDHAR activities, as well as AsA and GSH contents, and inhibited the increased contents of DHA and GSSH caused by LL. Furthermore, a experiment conducted by Li et al. (2019b) demonstrated that MT positively upregulated the expression of *CsAPX* in tea plant under stresses of cold, salt, and drought stresses, leading to increased ROS elimination (Li et al., 2019b). The

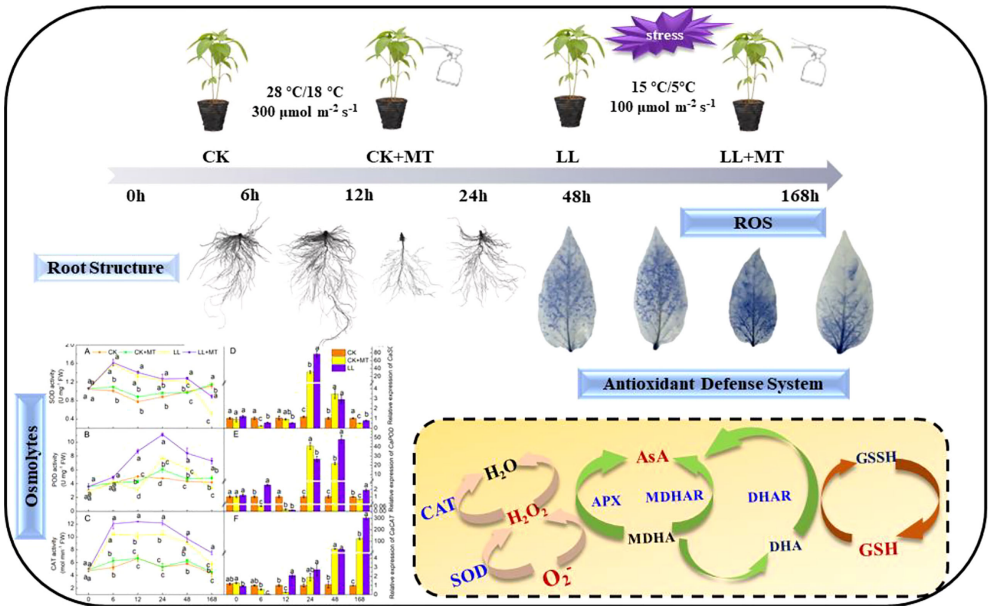


FIGURE 7
Schematic overview of melatonin enhanced low-temperature combined with low-light tolerance of pepper (*Capsicum annuum* l.) seedlings by regulating root growth, antioxidant defense system, and osmotic adjustment.

expressions of *CsAPX*, *CsMDHAR*, *CsDHAR*, and *CsGR* in cucumber were all upregulated by MT under low-temperature and high-humidity stress (Amin et al., 2022). This result was consistent with our findings in which *CaAPX*, *CaDHAR*, and *CaMDHAR* were upregulated by pre-application of MT after 12, 24, 48, and 168h LL stress (Figure 6). These findings indicated that MT could improve cell redox homeostasis and cell membrane stability by inducing the activities of enzymatic and non-enzymatic antioxidant defense system, regulating AsA-GSH cycle, and upregulating the expression of antioxidant enzymes genes.

6 Conclusions

LL stress inhibited pepper root growth and caused oxidative stress by increasing accumulations of ROS levels and lipid peroxidation degrees in pepper seedlings. However, MT reversed the phenomena and enhanced LL tolerance in pepper seedlings. MT Preapplication improved the root morphology structure and cell structure. Additionally, MT application rescued the LL-induced oxidative stress by exerting a synergistic effect that regulated of osmotic adjustment (soluble sugar and soluble protein) and a series of antioxidant enzymes (SOD, POD, CAT, APX, DHAR, MDHAR) and substances (AsA, DHA, GSH, and GSSH), as well as upregulating the expression of *CaSOD*, *CaPOD*, *CaCAT*, *CaAPX*, *CaDHAR*, *CaMDHAR*. Therefore, MT pretreatment was inferred to enhance LL tolerance by effectively maintaining substance biosynthesis, membrane stability, and ROS scavenging (Figure 7).

Data availability statement

The original contributions presented in the study are included in the article/Supplementary Material. Further inquiries can be directed to the corresponding author.

Author contributions

JL, JX, JY, JLy, and JFZ: conceptualization. JL, DD, and NL: methodology. JL, DD, NL, FG: software. JL, JFZ, DD, NL, JZ, YY, and TN: formal analysis, investigation. JL: writing—original draft preparation. JL and JX: writing—review and editing. JX: resources, supervision, project administration, and funding acquisition. All authors contributed to the article and approved the submitted version.

Funding

The work was financially supported by the Natural Science Foundation of Gansu Province (20JR10RA515), Scientific Research Start-up Funds for Openly-Recruited Doctors (GAU-KYQD-2018-35), National Natural Science Foundation of China (32072657), and the Special Fund for Technical System of Melon and Vegetable Industry of Gansu Province (GARS-GC-1), Special Fund for Sci. & Tech. Innovation and Development Guided by Gansu Province (2018ZX-02), National Key Research and Development Program of China (2016YFD0201005), and The writers extremely acknowledge all the authors, the editors and the reviewers for the precious and valuable comments and suggestions, which have greatly improved the article.

Conflict of interest

The authors declare that the research was conducted in the absence of any commercial or financial relationships that could be construed as a potential conflict of interest.

Publisher's note

All claims expressed in this article are solely those of the authors and do not necessarily represent those of their affiliated organizations, or those of the publisher, the editors and the reviewers. Any product that may be evaluated in this article, or claim that may be made by its manufacturer, is not guaranteed or endorsed by the publisher.

Supplementary material

The Supplementary Material for this article can be found online at: https://www.frontiersin.org/articles/10.3389/fpls.2022.998293/full#supplementary-material

References

Ahammed, G. J., Wu, M., Wang, Y., Yan, Y., Mao, Q., Ren, J., et al. (2020). Melatonin alleviates iron stress by improving iron homeostasis, antioxidant defense and secondary metabolism in cucumber. *Sci. Hortic.* 265, 109205. doi: 10.1016/j.scienta.2020.109205

Ahammed, G. J., Xu, W., Liu, A., and Chen, S. (2019). Endogenous melatonin deficiency aggravates high temperature-induced oxidative stress in solanum lycopersicum l. *Environ. Exp. Bot.* 161, 303–311. doi: 10.1016/j.envexpbot.2018.06.006

Ahanger, M. A., Alyemen, i., Wijaya, L., Alamri, S. A., Alam, P., Ashraf, M., et al. (2018). Potential of exogenously sourced kinetin in protecting solanum lycopersicum from NaCl-induced oxidative stress through up-regulation of the antioxidant system, ascorbate-glutathione cycle and glyoxalase system. *PloS One* 13 (9), e0202175. doi: 10.1371/journal.pone.0202175

Ahmad, S., Kamran, M., Ding, R., Meng, X., Wang, H., Ahmad, I., et al. (2019). Exogenous melatonin confers drought stress by promoting plant growth, photosynthetic capacity and antioxidant defense system of maize seedlings. *Peerj* 7, e7793. doi: 10.7717/peerj.7793

Amin, B., Atif., M. J., Meng, H., Ali, M., Li, S., Alharby, H. F., et al. (2022). Melatonin rescues photosynthesis and triggers antioxidant defense response in *Cucumis sativus* plants challenged by low temperature and high humidity. *Front. Plant Sci.* 13. doi: 10.3389/fpls.2022.855900

Anwar, A., Wang, J., Yu, X. C., He, C. X., and Li, Y. S. (2020). Substrate application of 5-aminolevulinic acid enhanced low-temperature and weak-light stress tolerance in cucumber (*Cucumis sativus* l.). *Agronomy-Basel* 10 (4), 472. doi: 10.3390/agronomy10040472

Anwar, A., Yan, Y., Liu, Y., Li, Y., and Yu, X. (2018). 5-aminolevulinic acid improves nutrient uptake and endogenous hormone accumulation, enhancing low-temperature stress tolerance in cucumbers. *Int. J. Mol. Sci.* 19 (11), 3379. doi: 10.3390/ijms19113379

Arnao, M. B., and Hernandez-Ruiz, J. (2007). Melatonin promotes adventitious- and lateral root regeneration in etiolated hypocotyls of *Lupinus albus* l. *J. Pineal Res.* 42 (2), 147–152. doi: 10.1111/j.1600-079X.2006.00396.x

Balabusta, M., Szafranska, K., and Posmyk, M. M. (2016). Exogenous melatonin improves antioxidant defensein cucumber seeds (*Cucumis sativus* l.) germinated under chilling stress. *Front. Plant Sci.* 7. doi: 10.3389/fpls.2016.00575

Barrero-Sicilia, C., Silvestre, S., Haslam, R. P., and Michaelson, L. V. (2017). Lipid remodelling: unravelling the response to cold stress in arabidopsis and its extremophile relative *Eutrema salsugineum*. *Plant Sci.* 263, 194–200. doi: 10.1016/j.plantsci.2017.07.017

Bawa, G., Feng, L. Y., Chen, G. P., Chen, H., Hu, Y., Pu, T., et al. (2020). Gibberellins and auxin regulate soybean hypocotyl elongation under low light and high-temperature interaction. *Physiol. Plantarum* 170 (3), 345–356. doi: 10.1111/ppl.13158

Bi, H. G., Liu, P. P., Jiang, Z. S., and Ai, X. Z. (2017). Overexpression of the rubisco activase gene improves growth and low temperature and weak light tolerance in cucumis sativus. *Physiol. Plantarum* 161 (2), 224–234. doi: 10.1111/ppl.12587

Bradford, M. M. (1976). A rapid and sensitive method for the quantitation of microgram quantities of protein utilizing the principle of protein-dye binding. *Anal. Biochem.* 72, 248–254. doi: 10.1006/abio.1976.9999

Campos, C. N., Avila, R. G., Dazio De Souza, K. R., Azevedo, L. M., and Aalves, J. D. (2019). Melatonin reduces oxidative stress and promotes drought tolerance in young *Coffea arabica* l. *plants. Agr. Water Manage* 211, 37–47. doi: 10.1016/j.agwat.2018.09.025

Chen, L., Fan, J., Hu, Z., Huang, X., Amombo, E., Liu, A., et al. (2017). Melatonin is involved in regulation of bermudagrass growth and development and response to low k^+ stress. *Front. Plant Sci.* 8, 2038. doi: 10.3389/fpls.2017.02038

Chen, L., Liu, L. T., Lu, B., Ma, T. T., Jiang, D., Li, J., et al. (2020). Exogenous melatonin promotes seed germination and osmotic regulation under salt stress in cotton (*Gossypium hirsutum* l.). *PloS One* 15 (1), e0228241. doi: 10.1371/journal.pone.0228241

Chen, L., Zhao, Y., Xu, S., Zhang, Z., Xu, Y., Zhang, J., et al. (2018). *OsMADS57* together with *OsTB1* coordinates transcription of its target *OsWRKY94* and *D14* to switch its organogenesis to defense for cold adaptation in rice. *New Phytol.* 218 (1), 219–231. doi: 10.1111/nph.14977

Cui, L. R., Zou, Z. R., Zhang, J., Zhao, Y. Y., and Yan., F. (2016). 24-epibrassinoslide enhances plant tolerance to stress from low temperatures and poor light intensities in tomato (*Lycopersicon esculentum* mill.). *Funct. Integr. Genomic.* 16 (1), 29–35. doi: 10.1007/s10142-015-0464-x

Dai, L., Li, J., Harmens, H., Zheng, X., and Zhang, C. (2020). Melatonin enhances drought resistance by regulating leaf stomatal behaviour, root growth and catalase activity in two contrasting rapeseed (*Brassica napus* l.) genotypes. *Plant Physiol. Bioch.* 149, 86–95. doi: 10.1016/j.plaphy.2020.01.039

Debnath, B., Hussain, M., Irshad, M., Mitra, S., Li, M., Liu, S., et al. (2018). Exogenous melatonin mitigates acid rain stress to tomato plants through modulation of leaf ultrastructure, photosynthesis and antioxidant potential. *Molecules* 23 (2), 388. doi: 10.3390/molecules23020388

Dey, S., Biswas, A., Huang, S., Li, D., Liu, L., Deng, Y., et al. (2021). Low temperature effect on different varieties of corchorus capsularis and corchorus olitorius at seedling stage. *Agronomy-Basel* 11 (12), 2547. doi: 10.3390/agronomy11122547

Ding, D., Li, J., Xie, J., Li, N., Bakpa, E. P., Han, K., et al. (2022). Exogenous zeaxanthin alleviates low temperature combined with low light induced photosynthesis inhibition and oxidative stress in pepper (*Capsicum annuum* l.) plants. *Curr. Issues Mol. Biol.* 44 (6), 2453–2471. doi: 10.3390/cimb44060168

Ding, F., Wang, G., and Zhang, S. (2018). Exogenous melatonin mitigates methyl viologen-triggered oxidative stress in poplar leaf. *Molecules* 23 (11), 2852. doi: 10.3390/molecules23112852

Eom, K. C., Jung, P. ,. K., Choi, S. H., Kim, T. W., Yoo, S. Y., Park, S. H., et al. (2010). Water requirement of red pepper in different growth stages. *Korean J. Soil Sci. Fertilizer* 43 (6), 844–847.

Hassan, M. U., Chattha, M. U., Khan, I., Chattha, M. B., Barbanti, L., Aamer, M., et al. (2021). Heat stress in cultivated plants: nature, impact, mechanisms, and mitigation strategies-a review. *Plant Biosyst.* 155 (2), 211–234. doi: 10.1080/11263504.2020.1727987

Hattori, A., Migitaka, H., Iigo, M., Itoh, M., Yamamoto, K., Ohtani-Kaneko, R., et al. (1995). Identification of melatonin in plants and its effects on plasma melatonin levels and binding to melatonin receptors in vertebrates. *Biochem. Mol. Biol. Int.* 35 (3), 627–634.

Heidarvand, L., and Amiri, R. M. (2010). What happens in plant molecular responses to cold stress? *Acta Physiol. Plant* 32 (3), 419–431. doi: 10.1007/s11738-009-0451-8

Huang, X., Tanveer, M., Min, Y., and Shabala, S. (2022). Melatonin as a regulator of plant ionic homeostasis: implications for abiotic stress tolerance. *J. Exp. Bot.* erac224 doi: 10.1093/jxb/erac224

Hussain, H. A., Men, S., Hussain, S., Zhang, Q., Ashraf, U., Anjum, S. A., et al. (2020). Maize tolerance against drought and chilling stresses varied with root morphology and antioxidative defense system. *Plants-Basel* 9 (6), 720. doi: 10.3390/plants9060720

Imran, M., Khan, M. A., Shahzad, R., Bilal, S., Khan, M., Yun, B. W., et al. (2021). Melatonin ameliorates thermotolerance in soybean seedling through balancing redox homeostasis and modulating antioxidant defense, phytohormones and polyamines biosynthesis. *Molecules* 26 (17), 5116. doi: 10.3390/molecules26175116

Irshad, A., Ur Rehman, R. N., Kareem, H. A., Yang, P., and Hu, T. (2021). Addressing the challenge of cold stress resilience with the synergistic effect of rhizobium inoculation and exogenous melatonin application in medicago truncatula. *Ecotox. Environ. Safe* 226, 112816. doi: 10.1016/j.ecoenv.2021.112816

Kim, Y. S., Park, S. I., Kim, J. J., Shin, S. Y., Kwak, S. S., Lee, C. H., et al. (2022). Over-expression of dehydroascorbate reductase improves salt tolerance, environmental adaptability and productivity in *Oryza sativa*. *Antioxidants* 11 (6), 1077. doi: 10.3390/antiox11061077

Kobylinska, A., Borek, S., and Posmyk, M. M. (2018). Melatonin redirects carbohydrates metabolism during sugar starvation in plant cells. *J. Pineal Res.* 64 (4), e12466. doi: 10.1111/jpi.12466

Kong, F., Deng, Y., Zhou, B., Wang, G., Wang, Y., and Meng, Q. (2014). A chloroplast-targeted DnaJ protein contributes to maintenance of photosystem II under chilling stress. *J. Exp. Bot.* 65 (1), 143–158. doi: 10.1093/jxb/ert357

Lado, J., Rodrigo, M. J., Lopez-Climent, M., Gomez-Cadenas, A., and Zacarias, L. (2016). Implication of the antioxidant system in chilling injury tolerance in the red peel of grapefruit. *Postharvest Biol. Tec.* 111, 214–223. doi: 10.1016/j.postharvbio.2015.09.013

Latef, A., and He, C. X. (2011). Arbuscular mycorrhizal influence on growth, photosynthetic pigments, osmotic adjustment and oxidative stress in tomato plants subjected to low temperature stress. *Acta Physiol. Plant* 33 (4), 1217–1225. doi: 10.1007/s11738-010-0650-3

Li, H., Chang, J., Chen, H., Wang, Z., Gu, X., Wei, C., et al. (2017). Exogenous melatonin confers salt stress tolerance to watermelon by improving photosynthesis and redox homeostasis. *Front. Plant Sci.* 8. doi: 10.3389/fpls.2017.00295

Li, J., Ding, D., Li, N., Xie, J., Yu, J., Lyv, J., et al. (2022). Melatonin enhances the low-temperature combined low-light tolerance of pepper (*Capsicum annuum* l.) seedlings by regulating photosynthesis, carotenoid, and hormone metabolism. *Environ. Exp. Bot.* 199, 104868. doi: 10.1016/j.envexpbot.2022.104868

Li, J., Liu, J., Zhu, T., Zhao, C., Li, L., and Chen, M. (2019a). The role of melatonin in salt stress responses. *Int. J. Mol. Sci.* 20 (7), 1735. doi: 10.3390/ijms20071735

Liu, Y.-S., Geng, J.-C., Sha, X.-Y., Zhao, Y.-X., Hu, T.-M., and Yang, P.-Z. (2019). Effect of rhizobium symbiosis on low-temperature tolerance and antioxidant response in alfalfa (*Medicago sativa* l.). *Front. Plant Sci.* 10. doi: 10.3389/fpls.2019.00538

Liu, J., Shabala, S., Zhang, J., Ma, G., Chen, D., Shabala, L., et al. (2020a). Melatonin improves rice salinity stress tolerance by NADPH oxidase-dependent control of the plasma membrane k^+ transporters and k^+ homeostasis. *Plant Cell Environ.* 43 (11), 2591–2605. doi: 10.1111/pce.13759

Liu, J., Wang, B., Li, Y., Huang, L., Zhang, Q., Zhu, H., et al. (2020b). RNA Sequencing analysis of low temperature and low light intensity-responsive transcriptomes of zucchini (*Cucurbita pepo* l.). *Sci. Hortic.* 265. doi: 10.1016/j.scienta.2020.109263

Liu, J., Wang, W., Wang, L., and Sun, Y. (2015). Exogenous melatonin improves seedling health index and drought tolerance in tomato. *Plant Growth Regul.* 77 (3), 317–326. doi: 10.1007/s10725-015-0066-6

Livak, K. J., and Schmittgen, T. D. (2001). Analysis of relative gene expression data using real-time quantitative PCR and the 2(-delta delta C(T)) method. *Methods* 25 (4), 402–408. doi: 10.1006/meth.2001.1262

Li, X., Wei, J., Scott, E. R., Liu, J., Guo, S., Li, Y., et al. (2018). Exogenous melatonin alleviates cold stress by promoting antioxidant defense and redox homeostasis in *Camellia sinensis* l. *Molecules* 23 (1), 165. doi: 10.3390/molecules23010165

Li, J., Xie, J., Yu, J., Lyv, J., Bakpa, E. P., Zhang, X., et al. (2021). Transcriptome sequence and physiological analysis revealed the roles of carotenoids and photosynthesis under low temperature combined with low-light stress on pepper (*Capsicum annuum* l.). *Photosynthetica* 59 (1), 24–36. doi: 10.32615/ps.2020.083

Li, J., Yang, Y., Sun, K., Chen, Y., Chen, X., and Li, X. (2019b). Exogenous melatonin enhances cold, salt and drought stress tolerance by improving antioxidant defense in tea plant (*Camellia sinensis* (L.) o. kuntze). *Molecules* 24 (9), 1826. doi: 10.3390/molecules24091826

Mclay, L. K., Nagarajan-Radha, V., Green, M. P., and Jones, T. M. (2018). Dim artificial light at night affects mating, reproductive output, and reactive oxygen species in drosophila melanogaster. *J. Exp. Zool. Part. A.* 329 (8-9), 419–428. doi: 10.1002/jez.2164

Meng, Z., Lu, T., Zhang, G., Qi, M., Tang, W., Li, L., et al. (2017). Photosystem inhibition and protection in tomato leaves under low light. *Sci. Hortic.* 217, 145–155. doi: 10.1016/j.scienta.2017.01.039

Moustafa-Farag, M., Mahmoud, A., Arnao, M. B., Sheteiwy, M. S., Dafea, M., Soltan, M., et al. (2020). Melatonin-induced water stress tolerance in plants: Recent advances. *Antioxidants* 9 (9), 809. doi: 10.3390/antiox9090809

Nagasuga, K., Murai-Hatano, M., and Kuwagata, T. (2011). Effects of low root temperature on dry matter production and root water uptake in rice plants. *Plant Prod. Sci.* 14 (1), 22–29. doi: 10.1626/pps.14.22

Ou, L. J., Wei, G., Zhang, Z. Q., Dai, X. Z., and Zou, X. X. (2015). Effects of low temperature and low irradiance on the physiological characteristics and related gene expression of different pepper species. *Photosynthetica* 53 (1), 85–94. doi: 10.1007/s11099-015-0084-7

Page, V., Bloesch, R. M., and Feller, U. (2012). Regulation of shoot growth, root development and manganese allocation in wheat (*Triticum aestivum*) genotypes by light intensity. *Plant Growth Regul.* 67 (3), 209–215. doi: 10.1007/s10725-012-9679-1

Park, S., and Back, K. (2012). Melatonin promotes seminal root elongation and root growth in transgenic rice after germination. *J. Pineal Res.* 53 (4), 385–389. doi: 10.1111/j.1600-079X.2012.01008.x

Ren, J., Ye, J., Yin, L., Li, G., Deng, X., and Wang, S. (2020). Exogenous melatonin improves salt tolerance by mitigating osmotic, ion, and oxidative stresses in maize seedlings. *Agronomy-Basel* 10 (5), 663. doi: 10.3390/agronomy10050663

Sarropoulou, V., Dimassi-Theriou, K., Therios, I., and Koukourikou-Petridou, M. (2012). Melatonin enhances root regeneration, photosynthetic pigments, biomass, total carbohydrates and proline content in the cherry rootstock PHL-c (*Prunus avium x prunus cerasus*). *Plant Physiol. Bioch.* 61, 162–168. doi: 10.1016/j.plaphy.2012.10.001

Sharma, A., Wang, J., Xu, D., Tao, S., Chong, S., Yan, D., et al. (2020). Melatonin regulates the functional components of photosynthesis, antioxidant system, gene expression, and metabolic pathways to induce drought resistance in grafted carya cathayensis plants. *Sci. Total Environ.* 713, 136675. doi: 10.1016/j.scitotenv.2020.136675

Sharma, A., and Zheng, B. (2019). Melatonin mediated regulation of drought stress: Physiological and molecular aspects. *Plants-Basel* 8 (7), 190. doi: 10.3390/plants8070190

Shi, H., Qian, Y., Tan, D. X., Reiter, R. J., and He, C. (2015). Melatonin induces the transcripts of CBF/DREB1s and their involvement in both abiotic and biotic stresses in arabidopsis. *J. Pineal Res.* 59 (3), 334–342. doi: 10.1111/jpi.12262

Shu, S., Tang, Y. Y., Yuan, Y. H., Sun, J., Zhong, M., and Guo, S. R. (2016). The role of 24-epibrassinolide in the regulation of photosynthetic characteristics and nitrogen metabolism of tomato seedlings under a combined low temperature and weak light stress. *Plant Physiol. Bioch.* 107, 344–353. doi: 10.1016/j.plaphy.2016.06.021

Singh, N. K., Bracker, C. A., Hasegawa, P. M., Handa, A. K., Buckel, S., Hermodson, M. A., et al. (1987). Characterization of osmotin: a thaumatin-like protein associated with osmotic adaptation in plant cells. *Plant Physiol.* 85 (2), 529–536. doi: 10.1104/pp.85.2.529

Sun, Y., Liu, Z., Lan, G., Jiao, C., and Sun, Y. (2019). Effect of exogenous melatonin on resistance of cucumber to downy mildew. *Sci. Hortic.* 255, 231–241. doi: 10.1016/j.scienta.2019.04.057

Sun, L., Li, X., Wang, Z., Sun, Z., Zhu, X., Liu, S., et al. (2018). Cold priming induced tolerance to subsequent low temperature stress is enhanced by melatonin application during recovery in wheat. *Molecules* 23 (5), 1091. doi: 10.3390/molecules23051091

Tang, C., Xie, J., Lv, J., Jing, L., Zhang, J., Wang, C., et al. (2021). Alleviating damage of photosystem and oxidative stress from chilling stress with exogenous zeaxanthin in pepper (*Capsicum annuum* l.) seedlings. *Plant Physiol. Bioch.* 162, 395–409. doi: 10.1016/j.plaphy.2021.03.010

Tan, D.-X., Mancheste, r., Helton, P., and Reiter, R. J. (2007). Phytoremediative capacity of plants enriched with melatonin. *Plant Signal. Behav.* 2 (6), 514–516. doi: 10.4161/psb.2.6.4639

Wang, Q., An, B., Wei, Y., Reiter, R. J., Shi, H., Luo, H., et al. (2016). Melatonin regulates root meristem by repressing auxin synthesis and polar auxin transport in arabidopsis. *Front. Plant Sci.* 7, 1882. doi: 10.3389/fpls.2016.01882

Wang, M., Zhang, S., and Ding, F. (2020). Melatonin mitigates chilling-induced oxidative stress and photosynthesis inhibition in tomato plants. *Antioxidants* 9 (3), 218. doi: 10.3390/antiox9030218

Weeda, S., Zhang, N., Zhao, X., Ndip, G., Guo, Y., Buck, G. A., et al. (2014). Arabidopsis transcriptome analysis reveals key roles of melatonin in plant defense systems. *PloS One* 9 (3), e93462. doi: 10.1371/journal.pone.0093462

Wei, Z., Gao, T., Liang, B., Zhao, Q., Ma, F., and Li, C. (2018). Effects of exogenous melatonin on methyl viologen-mediated oxidative stress in apple leaf. *Int. J. Mol. Sci.* 19 (1), 316. doi: 10.3390/ijms19010316

Xu, W., Cai, S.-Y., Zhang, Y., Wang, Y., Ahammed, G. J., Xia, X.-J., et al. (2016). Melatonin enhances thermotolerance by promoting cellular protein protection in tomato plants. *J. Pineal Res.* 61 (4), 457–469. doi: 10.1111/jpi.12359

Xu, Y., Charles, M. T., Luo, Z., Mimee, B., Tong, Z., Veronneau, P.-Y., et al. (2019). Ultraviolet-c priming of strawberry leaves against subsequent mycosphaerella fragariae infection involves the action of reactive oxygen species, plant hormones, and terpenes. *Plant Cell Environ.* 42 (3), 815–831. doi: 10.1111/pce.13491

Yamori, N., Levine, C. P., Mattson, N. S., and Yamori, W. (2022). Optimum root zone temperature of photosynthesis and plant growth depends on air temperature in lettuce plants. *Plant Mol. Biol.* 2022, 1–11. doi: 10.1007/s11103-022-01249-w

Yan, F. Y., Wei, H. M., Ding, Y. F., Li, W. W., Liu, Z. H., Chen, L., et al. (2021). Melatonin regulates antioxidant strategy in response to continuous salt stress in rice seedlings. *Plant Physiol. Bioch.* 165, 239–250. doi: 10.1016/j.plaphy.2021.05.003

Zeng, W., Mostafa, S., Lu, Z., and Jin, B. (2022). Melatonin-mediated abiotic stress tolerance in plants. *Front. Plant Sci.* 13. doi: 10.3389/fpls.2022.847175

Zhang, X., Feng, Y., Jing, T., Liu, X., Ai, X., and Bi, H. (2021). Melatonin promotes the chilling tolerance of cucumber seedlings by regulating antioxidant system and relieving photoinhibition. *Front. Plant Sci.* 12. doi: 10.3389/fpls.2021.789617

Zhang, J., Li, D., Wei, J., Ma, W., Kong, X., Rengel, Z., et al. (2019). Melatonin alleviates aluminum-induced root growth inhibition by interfering with nitric oxide production in arabidopsis. *Environ. Exp. Bot.* 161, 157–165. doi: 10.1016/j.envexpbot.2018.08.014

Zhang, J. F., Li, J., Xie, J. M., Yu, J. H., Dawuda, M. M., Lyv, J., et al. (2020). Changes in photosynthesis and carotenoid composition of pepper (Capsicum annuum l.) in response to low-light stress and low temperature combined with low-light stress. *Photosynthetica* 58 (1), 125–136. doi: 10.32615/ps.2019.175

Zhang, J., Shi, Y., Zhang, X., Du, H., Xu, B., and Huang, B. (2017a). Melatonin suppression of heat-induced leaf senescence involves changes in abscisic acid and cytokinin biosynthesis and signaling pathways in perennial ryegrass (*Lolium perenne* l.). *Environ. Exp. Bot.* 138, 36–45. doi: 10.1016/j.envexpbot.2017.02.012

Zhang, T., Shi, Z., Zhang, X., Zheng, S., Wang, J., and Mo, J. (2020). Alleviating effects of exogenous melatonin on salt stress in cucumber. *Sci. Hortic.* 262. doi: 10.1016/j.scienta.2019.109070

Zhang, N., Sun, Q., Zhang, H., Cao, Y., Weeda, S., Ren, S., et al. (2015). Roles of melatonin in abiotic stress resistance in plants. *J. Exp. Bot.* 66 (3), 647–656. doi: 10.1093/jxb/eru336

Zhang, R., Yue, Z., Chen, X., Wang, Y., Zhou, Y., Xu, W., et al. (2022). Foliar applications of urea and melatonin to alleviate waterlogging stress on photosynthesis and antioxidant metabolism in sorghum seedlings. *Plant Growth Regul.* 97 (2), 429–438. doi: 10.1007/s10725-021-00705-9

Zhang, J., Zeng, B., Mao, Y., Kong, X., Wang, X., Yang, Y., et al. (2017b). Melatonin alleviates aluminium toxicity through modulating antioxidative enzymes and enhancing organic acid anion exudation in soybean. *Funct. Plant Biol.* 44 (10), 961–968. doi: 10.1071/fp17003

Zhang, N., Zhao, B., Zhang, H.-J., Weeda, S., Yang, C., Yang, Z.-C., et al. (2013). Melatonin promotes water-stress tolerance, lateral root formation, and seed germination in cucumber (Cucumis sativus l.). *J. Pineal Res.* 54 (1), 15–23. doi: 10.1111/j.1600-079X.2012.01015.x

Zhao, H., Ye, L., Wang, Y., Zhou, X., Yang, J., Wang, J., et al. (2016). Melatonin increases the chilling tolerance of chloroplast in cucumber seedlings by regulating photosynthetic electron flux and the ascorbate-glutathione cycle. *Front. Plant Sci.* 7. doi: 10.3389/fpls.2016.01874

Zhu, J., Zhang, K.-X., Wang, W.-S., Gong, W., Liu, W.-C., Chen, H.-G., et al. (2015). Low temperature inhibits root growth by reducing auxin accumulation *via* ARR1/12. *Plant Cell Physiol.* 56 (4), 727–736. doi: 10.1093/pcp/pcu217

frontiers | Frontiers in Plant Science

TYPE Original Research
PUBLISHED 28 September 2022
DOI 10.3389/fpls.2022.998841

Check for updates

OPEN ACCESS

EDITED BY
Caroline Müller,
Universidade Federal da Fronteira Sul, Brazil

REVIEWED BY
Yunpeng Cao,
Chinese Academy of Sciences (CAS), China
Maria Helena S. Goldman,
University of São Paulo, Brazil
Xinyang Wu,
China Jiliang University, China

*CORRESPONDENCE
Ruyan Xu
xy_xury@jszygs.com
Minmin Xie
xieminmin@caas.cn

†These authors have contributed equally to this work

SPECIALTY SECTION
This article was submitted to Plant Abiotic Stress, a section of the journal Frontiers in Plant Science

RECEIVED 20 July 2022
ACCEPTED 05 September 2022
PUBLISHED 28 September 2022

CITATION
Sun J, Tian Z, Li X, Li S, Li Z, Wang J, Hu Z, Chen H, Guo C, Xie M and Xu R (2022) Systematic analysis of the pectin methylesterase gene family in *Nicotiana tabacum* and reveal their multiple roles in plant development and abiotic stresses. *Front. Plant Sci.* 13:998841. doi: 10.3389/fpls.2022.998841

COPYRIGHT
© 2022 Sun, Tian, Li, Li, Li, Wang, Hu, Chen, Guo, Xie and Xu. This is an open-access article distributed under the terms of the Creative Commons Attribution License (CC BY). The use, distribution or reproduction in other forums is permitted, provided the original author(s) and the copyright owner(s) are credited and that the original publication in this journal is cited, in accordance with accepted academic practice. No use, distribution or reproduction is permitted which does not comply with these terms.

Systematic analysis of the pectin methylesterase gene family in *Nicotiana tabacum* and reveal their multiple roles in plant development and abiotic stresses

Jinhao Sun[1,2†], Zhen Tian[1†], Xiaoxu Li[2†], Shaopeng Li[1], Zhiyuan Li[2], Jinling Wang[1], Zongyu Hu[1], Haiqing Chen[1], Cun Guo[2,3], Minmin Xie[2*] and Ruyan Xu[1*]

[1]Technology Center, China Tobacco Jiangsu Industrial Co., Ltd., Nanjing, China, [2]Key Laboratory for Tobacco Gene Resources, Tobacco Research Institute, Chinese Academy of Agricultural Sciences, Qingdao, China, [3]Kunming Branch of Yunnan Provincial Tobacco Company, Kunming, China

The pectin methylesterases (PMEs) play multiple roles in regulating plant development and responses to various stresses. In our study, a total of 121 *PME* genes were identified in the tobacco genome, which were clustered into two groups based on phylogenetic analysis together with *Arabidopsis* members. The investigations of gene structure and conserved motif indicated that exon/intron and motif organizations were relatively conserved in each group. Additionally, several stress-related elements were identified in the promoter region of these genes. The survey of duplication events revealed that segmental duplications were critical to the expansion of the *PME* gene family in tobacco. The expression profiles analysis revealed that these genes were expressed in various tissues and could be induced by diverse abiotic stresses. Notably, *NtPME029* and *NtPME043*, were identified as homologues with *AtPME3* and *AtPME31*, respectively. Furthermore, *NtPME029* was highly expressed in roots and the over-expression of the *NtPME029* gene could promote the development of roots. While *NtPME043* could be induced by salt and ABA treatments, and the over-expression of the *NtPME043* gene could significantly enhance the salt-stress tolerance in tobacco. Overall, these findings may shed light on the biological and functional characterization of *NtPME* genes in tobacco.

KEYWORDS

tobacco, PME genes, genome-wide analysis, abiotic stresses, root development

Introduction

The plant cell walls mainly contain structural proteins and three types of polysaccharides, including cellulose, hemicellulose, and pectins (Zhao et al., 2019). Pectins as highly heterogeneous polymers exist between the intercellular layer and the primary wall and it accounts for 30-40% of the cell wall of dicots and non-graminaceous monocots. The pectin modification leads to crucial changes in plant cell walls' structure and function, affecting plant development, including fruit ripening and softening, organ abscission and senescence, pollen dehiscence, pollen tube growth, and stress resistance (Al-Qsous et al., 2004; Bosch et al., 2005; An et al., 2008; Zhang et al., 2010; Verma et al., 2014; Wallace and Williams, 2017). Pectins are synthesized with a highly methylesterified form and then are catalyzed to decrease methyl esterification by a large enzyme family of pectin methylesterases (PMEs) (EC. 3.1.1.11) that reside in the cell wall (Yapo et al., 2007; Wolf et al., 2009).

In plants, PMEs can be divided into two groups (Type I and Type II) according to whether it contains the PMEI (pectin methylesterase inhibitor domain) domain. Type I (PME type) contain the PME domain and the pro-region of its N-terminal, which is very short or missing. However, type II (ProPME type) contains simultaneously PME and PMEI domain and a long N-end pro-region (Udall et al., 2006). The pro-region was reported to fold the protein correctly and inhibit the PME activity (Micheli, 2001; Pelloux et al., 2007). Previous research has reported that there are five conserved structure regions, including Region I (GxYxE), Region II (QAVAxR), Region III (QDTL), Region IV (DFIFG), and Region V (YLGRxWx) in the secondary structure of PME proteins (Markovic and Janecek, 2004). The Region I is conserved in all PME proteins, while the remaining regions have diverse conservation in different plants.

A total of 66 PMEs have been identified in the *Arabidopsis*, 22 members falling into type I and 44 into type II, and the contributions of some PMEs to various developmental processes have been characterized (Tian et al., 2006; Levesque-Tremblay et al., 2015). For example, *AtPME6* and *AtPME58* express highly during mucilage secretion, which is involved in embryo development and mucilage extrusion, respectively (Levesque-Tremblay et al., 2015; Turbant et al., 2016). In addition, the knockout mutants of *AtPME1* specifically exhibit curved, irregular morphology and are significantly stunted in the pollen tube compared that with wild type (Tian et al., 2006). *AtPME48* specifically expressed in the male gametophyte and functioned to influence pollen grain germination (Leroux et al., 2015). Furthermore, *AtPME5*-overexpressing transgenic plants were reported to increase the cell walls elasticity in shoot apical meristem (Peaucelle et al., 2011). *AtPME35* influences the mechanical strength of the stem by regulating the PME demethylesterifification (Hongo et al., 2012). *AtPME17* is significantly expressed in vegetative tissues and could be processed by SBT3.5 (subtilisin-type serine protease 3.5) to modify PME activity which is involved in root growth (Sénéchal et al., 2014). Moreover, *AtPME3*-overexpressing plants showed longer roots compared to wild-type, whereas the RNAi plants showed the opposite phenotype (Hewezi et al., 2008).

Besides, many PMEs facilitate responses to multiple biotic and abiotic stresses in *Arabidopsis*. Over-expressed *AtPME31* provides broad-spectrum insect resistance in transgenic tobacco plants (Dixit et al., 2013). Moreover, *AtPME31* could be significantly induced under salt stress and positively modulate the expression levels of salt stress-induced genes to enhance the salt stress tolerance of plants (Yan et al., 2018). *AtPME34* is proposed that responds to heat and salt stress through ABA (abscisic acid) pathway (Huang et al., 2017). It was verified that *AtPME41* contributes to freezing tolerance by modulating the mechanical properties of cell walls through the BR (brassinosteroid) signaling (Qu et al., 2011).

Tobacco is one of the most significant economic crops and widely cultivated all over the world, while various abiotic stresses can severely threaten tobacco quality and yield. The *PME* genes have been reported to be involved in response to abiotic stresses and affect development in a variety of species. Although the PME family proteins have been characterized in several plants (Duan et al., 2016; Zega and D'Ovidio, 2016; Zhang et al., 2019; Li et al., 2020), limited information is available about PME family proteins in tobacco. In this study, a comprehensive analysis was performed, including phylogenetic analyses, gene structure, motif organization, *cis*-elements, chromosomal distributions, duplication events, and expression profiles. The results of the current study imply that the tobacco NtPME family proteins play multiple roles in various biological processes.

Materials and methods

The identification and phylogenetic analysis of NtPME proteins

The full-length protein sequences for each AtPME in *Arabidopsis* were downloaded from TAIR (The *Arabidopsis* Information Resource) database (http://www.arabidopsis.org/), while the genomic data for tobacco (*N. tabacum*V1.0) were obtained from the SGN (Sol Genomics Network) database (https://solgenomics.net/). Then, the protein sequences of AtPME were used as queries to detect the potential NtPME proteins in tobacco by the BLASTp searches (E-value < 0.01) (Li et al., 2021). Subsequently, the potential sequences were examined using the SMART (Letunic et al., 2015) and PFAM (Finn et al., 2016) databases to determine the PME domains. The remaining NtPME numbers were renamed according to their

physical locations on the chromosome or scaffold. The Mw (molecular weight) and theoretical pI (isoelectric points) of these finally identified NtPME numbers were predicted by ProtParam toolkits (Garg et al., 2016). The sequences of NtPME and AtPME proteins were aligned using Clustal X (Larkin et al., 2007), and the alignments were used to construct the neighbor-joining (NJ) tree by MEGA 6 with the default parameters method (Kumar et al., 2018). The subcellular localization of NtPME proteins was also predicted by Cell-PLoc 2.0 and WOLF POSRT II (https://www.genscript.com/psort.html) (Ren et al., 2019).

Chromosomal localization and duplication event analysis of *NtPME* genes

The chromosomal location image of *NtPME* genes was visualized by MG2C, according to the data obtained from the SGN database (Chao et al., 2015). The segmental duplication events were identified and visualized by the MCScanX program and Circos, respectively (Cao et al., 2016). The syntenic analysis of the orthologous genes obtained from tobacco and other four plant species was investigated by Synteny Plotter (Xie et al., 2018). Then, the synonymous substitution (Ks) and non-synonymous substitution (Ka) rates were calculated by DnaSP 5.0 software (Librado and Rozas, 2009).

Gene structure, conserved motifs, and *cis*-elements analyses of NtPME proteins

The gene structure of *NtPME* genes was analyzed and visualized using GSDS (http://gsds.cbi.pku.edu.cn) according to their genomic and coding sequence (Hu et al., 2015). The Multiple Em for Motif Elicitation (MEME) online tool was adopted to identify and visualize conserved motifs of the NtPME full-length protein sequences (Bailey et al., 2015). The promoter regions, 2000-bp sequences upstream of tobacco *NtPME* genes, were obtained by TBtools software (Chen et al., 2020), and then the *cis*-regulatory elements of these promoters were analyzed by the PlantCARE tool (Lescot et al., 2002).

Expression analysis of NtPME genes in tobacco

The RNA-seq data for each tissue of *NtPME* genes in tobacco K326 were obtained from the GEO database (accession number: GSE95717) (Edwards et al., 2017). The absolute transcript abundance values of three tissues (root, shoot, and apex) of the *NtPME* genes were normalized and illustrated using R.

Tobacco plant growth and stress treatments

The Cultivated tobacco K326 (*Nicotiana tabacum* L. Cv. K326) was used in the current study. The tobacco plants were cultivated in the growth conditions described in the previous report (Li et al., 2021). Different tissues, including the shoots, roots, leaves, and flowers were harvested to explore tissue-specific expression patterns and visualized in a heat map by TBtools (Wu et al., 2020). For abiotic stress (salt and ABA) treatments, the seedlings were treated with 50 μM Abscisic Acid (ABA) or 150 mM NaCl, and then harvested at 0, 1, 3, or 6 h after treatment (Sun et al., 2021). All the collected samples were frozen by the liquid nitrogen and then stored at -80 °C for RNA extraction.

RNA extraction and RT-qPCR analysis

Total RNA was extracted and 1 μg RNA was synthesized to the first-strand complementary DNA (cDNA) by the method previously reported (Li et al., 2019a; Ren et al., 2019). The qRT-PCR was carried out on an ABI7500 Real-Time PCR System (Applied Biosystems, Foster City, CA, United States) with 2.5 μL template cDNA. The ribosomal protein gene *L25* (GenBank No. L18908) of tobacco was adopted as the internal control. All reactions were performed with three biological replications and the resulting data were evaluated by the $2^{-\Delta\Delta CT}$ method (Livak et al., 2001). The specific relative primer sequences were designed by Primer Premier 5.0 and the details were shown in Supplementary Table S1.

Subcellular localization

The coding regions of *NtPME029* and *NtPME043* were amplified by PCR with specific cloning primers and then generated into the *p*CHF3-GFP vector. The *NtPME029-GFP* and *NtPME043-GFP* fragments were driven by the *CaMV-35S* promoter, and the control was the GFP fragment driven by the *CaMV-35S* promoter. Subsequently, these constructs were injected into *Nicotiana benthamiana* leaves separately for transient expression as previously reported (Li et al., 2019b). After 3 days of growth in a light condition, the GFP fluorescence signals in these leaves were monitored by using the confocal microscope (TCS-SP8 Leica, Wetzlar, Germany) (Li et al., 2018).

Overexpression analysis

The coding sequences of *NtPME029* and *NtPME043* were amplified and then generated into the expression vector

(*p*CAMBIA1300). The *NtPME029* and *NtPME043* over-expression vectors were transformed into K326 tobacco plants by an *Agrobacterium*-mediated method and the empty vector as the control (Buschmann, 2016). The T0-generation seeds were screened in half-strength MS medium with 20 mg/L of hygromycin to obtain T1 seeds as the previous report (Li et al., 2021). The one-week-old T1 plants and wild-type tobacco plants were transferred to MS medium with or without 150 mM NaCl to grow for two weeks. Subsequently, the changes in root length were statistically analyzed.

Statistical analysis

Student's *t*-tests in GraphPad Prism 8 revealed significant differences from the control. *P* values less than 0.01 were considered significant. All data were analyzed in three replicates.

Results

Identification of *PME* genes in tobacco

To identify *PME* family genes in tobacco, we used the PME numbers of *Arabidopsis* as references to the BLASTP search. A total of 121 *PME* genes were identified in tobacco and named *NtPME001* to *NtPME121* based on their physical locations on chromosomes or scaffolds (Supplementary Table S2). Subsequently, the biochemical characteristics of *PME* genes were analyzed. As shown in Supplementary Table S2, the ORF (open reading frame) lengths ranged from 348 bp (*NtPME037*) to 3348 bp (*NtPME84*) and their protein weights (MWs) ranged from 12.63 (NtPME037) to 124.45 kDa (NtPME84). The isoelectric points (PIs) values of different NtPME proteins ranged from 4.30 (NtPME087) to 10.47 (NtPME034). The prediction of subcellular localization indicated that all NtPME proteins were located on the cell wall.

Phylogenetic analysis of the NtPME members

To better elucidate the evolutionary relationship of PME family members in tobacco, the MEGA7.0 software was employed to construct a neighbor-joining (NJ) tree consisting of tobacco (121 members) and *Arabidopsis* (66 members). The 121 NtPME proteins could be clustered into two groups(Group I and Group II) according to the PME or PMEI domain contained in these proteins with previous support (Li et al., 2020). Group II was further subdivided into three subclasses Group II-a, Group II-b, and Group II-c in this neighbor-joining (NJ) tree (Figure 1). Group I included 30 NtPME members with only PME domains, accounting for 24.8% of the total numbers. Seven of the members contained two PME domains, including NtPME20, NtPME23, NtPME27, NtPME60, NtPME63, NtPME99. However, the remaining others contained only one PME domain. Group II included 91 NtPME members with simultaneously PME and PMEI domains, accounting for

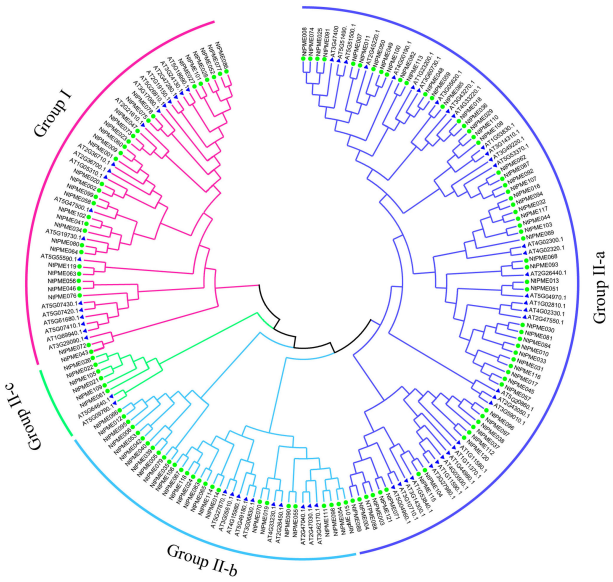


FIGURE 1
Phylogenetic relationship dendrogram of NtPME members in tobacco. The phylogenetic tree was generated by NtPME proteins of tobacco and *Arabidopsis* using the Neighbor-Joining method.

75.2% of the total numbers. To further understand the number and proportion of *NtPME* gene family members in plant genomes, six representative plant species were counted the members and the proportion of PME and PMEI, such as tobacco, *Arabidopsis*, rice, potato, Asian cotton, and *physcomitrella patens* (Table 1). As shown in Table 1, the number of PME proteins in Group I was generally less than that in Group II in plant species except for rice. The number of genes in Group I is approximately the same in different plant species. Notably, the 13 PME numbers in *physcomitrella patens* all belong to Group I. This result indicated that the PME genes of Group II may appear after the evolutionary differentiation of bryophytes plants. However, the number of PME proteins of Group II in tobacco far exceeded other species, which may be since tobacco is allopolytraploid.

Chromosomal distribution and duplication events

In this study, a total of 121 *NtPMEs* were identified in tobacco and the information on chromosomal distribution was shown in Figure 2. The results showed that only 60 *NtPMEs* were mapped on 22 chromosomes, and the remaining genes were located on scaffolds. Chromosome 17 contained the largest number of *NtPMEs* (11 *NtPMEs*), while the other remaining chromosomes harbored less than four *NtPMEs*, for instance, chromosome 2 and chromosome 12. In this study, tandem events were carefully screened in the tobacco genome and indicated that no many tandem events were found between these *NtPME* genes.

In addition, the segmental duplication analysis of *NtPMEs* was visualized using the MCScanX program (Cao et al., 2016). Notably, nine segmental duplication pairs in 17 *NtPMEs* were identified (Figure 3) and the details of these genes were listed in Supplementary Table S3. Four pairs of segmental duplication occurred in Group I (*NtPME001*/*NtPME060*, *NtPME002*/*NtPME020*, *NtPME023*/*NtPME047* and *NtPME028*/*NtPME052*) and Group II-a (*NtPME007*/*NtPME048*, *NtPME10*/*NtPME30*, *NtPME10*/*NtPME33* and *NtPME031*/*NtPME045*), respectively. However, only one pair of duplications (*NtPME005*/*NtPME039*) occurred in Group II-b. These results suggested that about 14% of the *NtPMEs* may be generated by segmental duplication events, which played a major role in the expansion of the *NtPMEs* family in tobacco. In addition, the ratio between non-synonymous and synonymous substitutions (Ka/Ks) can be used to estimate the purifying selection, neutral mutations, and beneficial mutations. In the present study, the Ka/Ks ratios of 9 segmental duplication gene pairs were calculated and the results showed that all the Ka/Ks ratios were less than 1, revealing that these *NtPMEs* may have undergone purifying selective pressure in the process of evolution.

Syntenic analysis of *NtPME* genes

To further understand the genetic relationship of *NtPMEs*, the synthetic analysis of *PMEs* from dicotyledonous plants (*Arabidopsis*, tomato, and grape) and monocotyledonous plants (rice) were performed with *NtPMEs* (Figure 4A). The results showed that the numbers of predicted collinear pairs between tobacco and tomato were 46, followed by grape (28), *Arabidopsis* (16), and rice (7), respectively. The collinearity of tobacco with the other four plants indicated that a close genetic relationship existed between *NtPMEs* and tomato *PME* genes. Meanwhile, only four *NtPMEs* (*NtPME32*, *NtPME44*, *NtPME45*, *NtPME58*) formed collinear pairs with *PME* genes from all the other four plants, suggesting that these *NtPMEs* may have existed before the divergence of these plant species. (Figure 4B and Supplementary Table S4)

Gene structure, multiple sequence alignment, and conserved motif analysis

To further analyze the structural diversity of *NtPMEs* in tobacco, the neighbor-joining phylogenetic tree had been

TABLE 1 Statistics on the number of *PME* genes in six plant species.

Plant species	Group I (PME domain)		Group II (PME and PMEI domain)		Total number
	Number of genes	The proportion of total number (%)	Number of genes	The proportion of total number (%)	
Arabidopsis	23	34.8	43	65.2	66
Rice	23	56.1	18	43.9	41
Potato	26	48.1	28	51.9	54
Asian cotton	33	41.3	47	58.7	80
physcomitrella patens	13	100.0	0	0	13
Tobacco	30	24.8	91	75.2	121

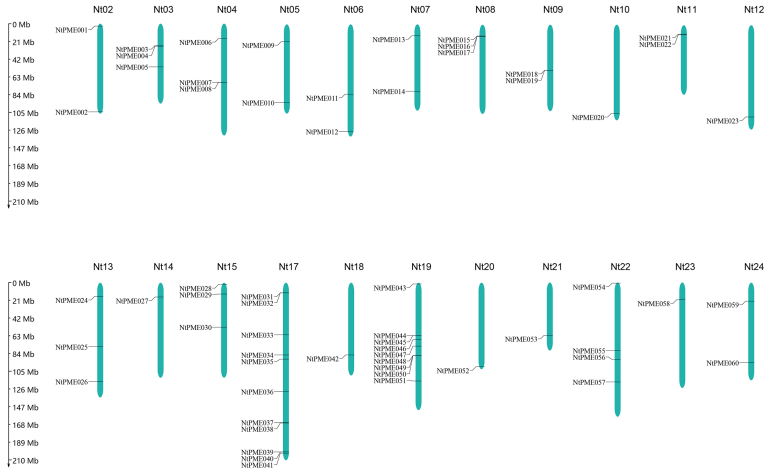


FIGURE 2
Distribution of 121 *NtPME* genes on the 24 chromosomes in tobacco.

constructed with only NtPME members (Figure 5A). Each NtPME was clustered into different groups, consistent with its distribution in the evolutionary tree of *Arabidopsis* and tobacco, suggesting that the construction of the neighbor-joining phylogenetic tree is reasonable. In addition, the number and arrangement of exon-intron in *NtPMEs* were also identified to provide insights into the evolution of these genes in tobacco (Figure 5B). The results showed that these *NtPMEs* clustered into the same group generally have almost identical exon-intron structures. The coding sequences of the *NtPMEs* were interrupted by introns, and the number of exons varied from one to 11. Notably, *NtPMEs* in Group I generally have more introns than that *NtPMEs* in Group II. In Group I, only one *NtPME* gene (*NtPME060*) has two introns, and the remaining *NtPMEs* contained more than three introns, of which *PME063* contained 10 introns. In Group II, there are 50 *NtPMEs* with only one intron (*NtPME017*, *NtPME030*, *NtPME045*, *NtPME068*, *NtPME093*, etc) and most of the remaining genes contain 2-3 introns (*NtPME010*, *NtPME031*, *NtPME033*, *NtPME071*, etc). These results indicate that the structure of *NtPMEs* in Group II is relatively simple compared to Group I. The effect of different intron numbers in *NtPMEs* on the function of these genes is a question worthy of further research.

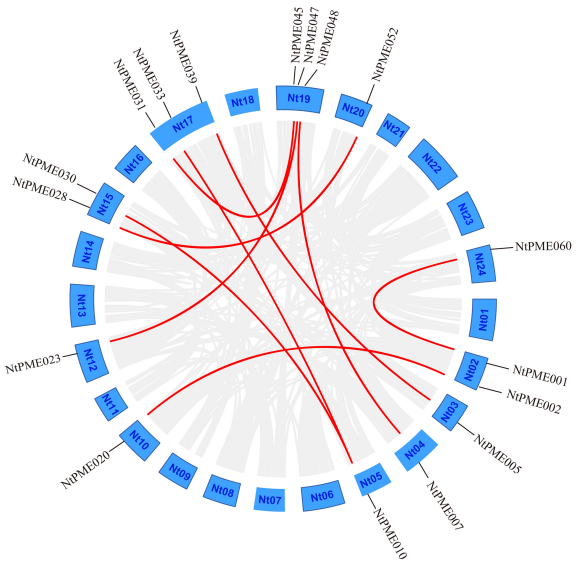


FIGURE 3
Segmental duplication analysis of the *NtPME* genes. The putative segmental duplication pairs are displayed by the gray line, whereas the *NtPME* segmental duplication pairs are revealed by the red line.

The PME proteins generally have five conserved domains, including Region I (GxYxE), Region II (QAVAxR), Region III (QDTL), Region IV (DFIFG), and Region V (YLGRxWx). To further investigate the conserved domains of NtPME proteins in tobacco, 121 NtPME proteins were subjected to multiple sequence alignments of amino acid sequences, and the basic region was counted in Supplementary Table S5. As the results show that not all NtPME proteins contained all the conserved structural regions. There were 28 NtPME proteins contained less than five conserved structural regions, such as the NtPME006 protein sequence only contained four conserved structural regions. Moreover, there are ten conserved motifs (motif 1-motif 10) were analyzed by using MEME. The NtPME numbers in the same branch of the evolutionary tree usually have similar motif types and orders (Figure 5C). In addition, the motif 7, motif 4, and motif 2 correspond to Region I (GxYxE), Region II (QAVAxR), and V (YLGRxWx) conserved domains,

10.3389/fpls.2022.998841

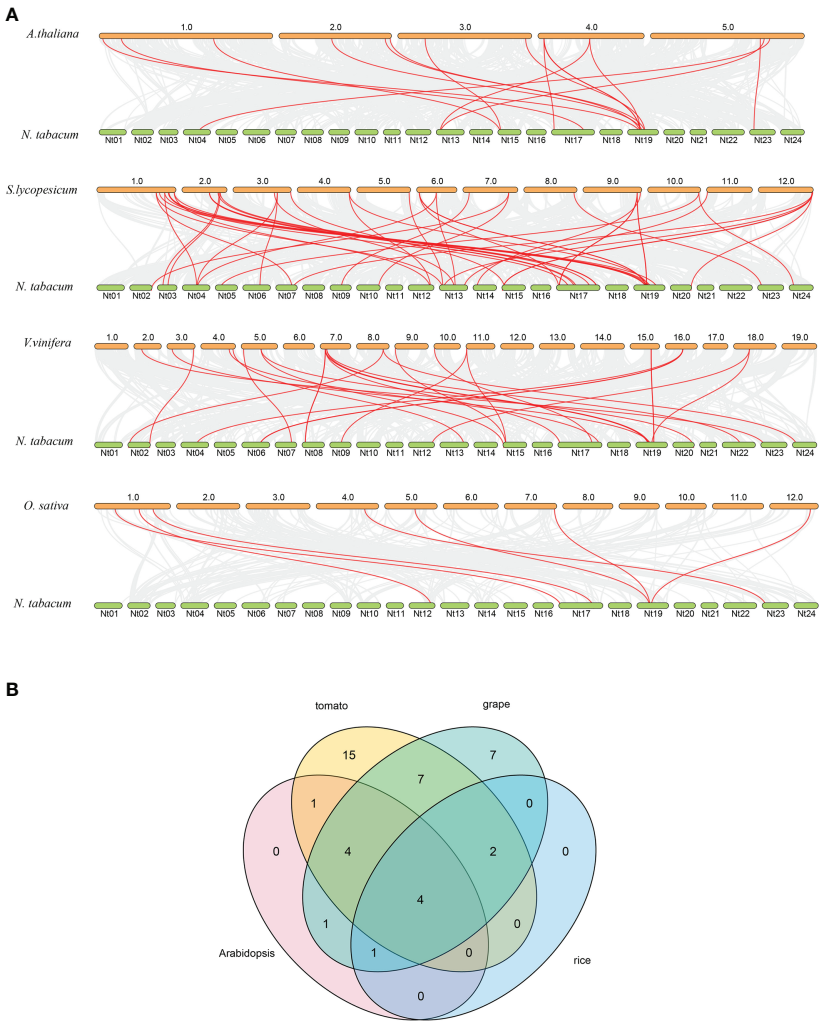


FIGURE 4
Syntenic relationship analysis dendrogram of *PME* genes among tobacco and four other plant species. **(A)** The collinear pairs between tobacco and four other plant species are displayed by the gray line, whereas the collinear *PME* gene pairs are revealed by the red color; **(B)** The *PME* genes formed the syntenic pairs between tobacco and all the other four plant species.

respectively. Motif 1 contains Region III (QDTL) and Region IV (DFIFG) conserved domains.

Promoter analysis of *NtPME* genes

In general, it was found that various *cis*-elements were identified in the tobacco *NtPMEs* promoters (Supplementary Table S6). Furthermore, 11 *cis*-elements involved in different hormone responses, developmental processes, and stress responses were selected for further analysis (Figure S1). The result showed that there were many *cis*-acting elements related to stress response in promoter regions of *NtPME* genes, for instance, ARE (anaerobic induction element), LTR (low-temperature-responsive element), MBS (MYB binding site), TC-rich repeats (stress-responsive element) and WUN-motif (wound-responsive element). The genes containing these *cis*-acting elements accounted for 88%, 49%, 50%, 45%, and 52% of all *NtPMEs*, respectively. In addition, the hormone-response elements were also identified in promoter regions, including ABRE, AuxRR-core, TCA-element, and CGTCA-motif. These *cis*-elements are potential responses to abscisic acid, auxin, ethylene, and methyl jasmonate, respectively.

Gene expression patterns of *NtPME* genes

To preliminarily investigate the significant roles of *NtPMEs* in tobacco growth and development, the transcript data of

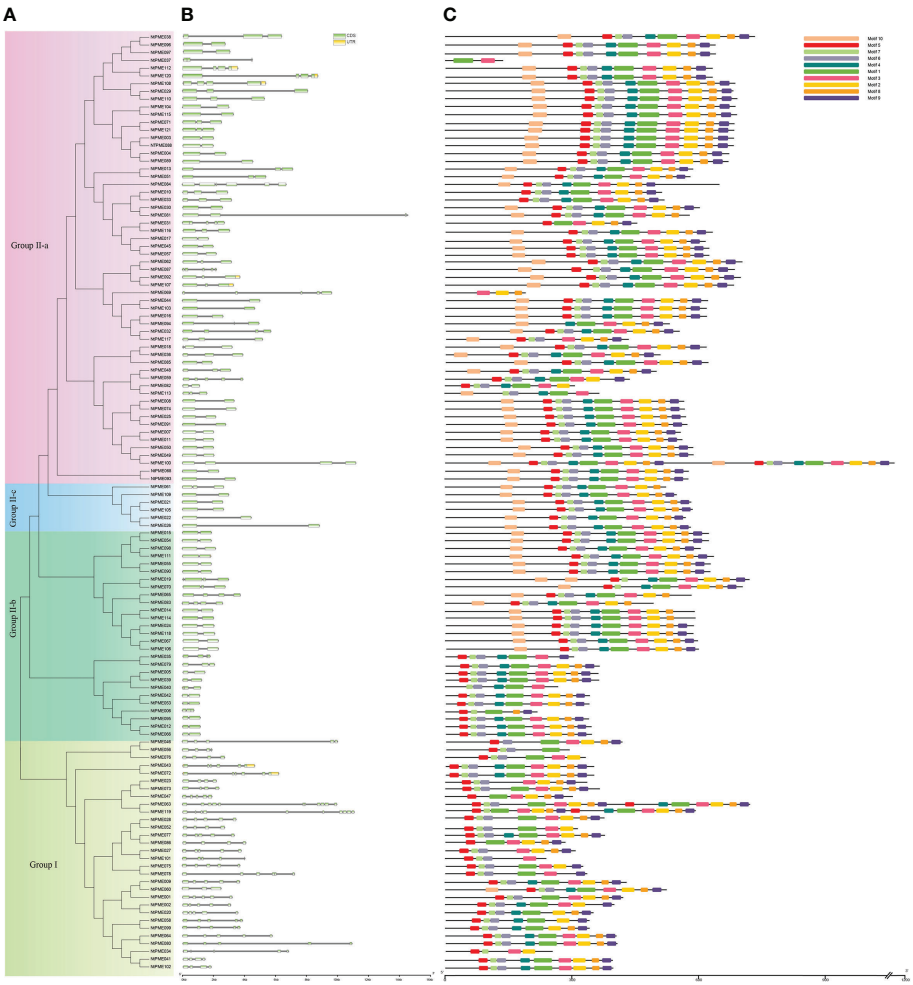


FIGURE 5
Gene structure and motif organizations analysis of NtPME members in tobacco. **(A)** The phylogenetic analysis tree of *NtPME* genes; **(B)** Gene structure of *NtPME* genes. Introns and exons are revealed by grey lines and light green boxes, respectively; **(C)** Distribution of conserved motifs in NtPME proteins. Different color boxes highlight different motifs.

NtPMEs in three tissues (root, shoot, and shoot apex) were downloaded from the GEO database and analyzed (Figure S2). The results showed that 2/3 of 121 *NtPME* genes were detected to be expressed in at least one tested tissue, and seven *NtPMEs* (*NtPME029*, *NtPME032*, *NtPME038*, *NtPME092*, *NtPME096*, *NtPME108* and *NtPME116*) were highly expressed in all three tested tissues. Furthermore, many *NtPMEs* were exclusively expressed in a tissue-specific manner. For instance, *NtPME038*, *NtPME073*, and *NtPME096* genes were the most exclusively expressed in the roots. *NtPME046* and *NtPME103* were detected highly expressed in the shoot apex. In addition, high-level expressions of *NtPME062*, and *NtPME093* were detected in the shoot and shoot apex.

To verify the reliability of *NtPMEs* RNA sequencing data analysis, we selected representative *NtPME* genes in different groups to carry out qRT-PCR analysis (Figure S3). *NtPME058*, *NtPME062*, and *NtPME093* were detected highly expressed in the shoot apex and shoot, respectively, which were consistent with the RNA sequencing data. In Group I, *NtPME072* was observed to be highly expressed in both leaves and flowers, while *NtPME47* was highly expressed in both roots and flowers. In Group II-a, *NtPME108* was detected highly expressed in the shoot, shoot apex, and flowers, whereas *NtPME029* was found to be highly expressed in root and shoot apex. Furthermore, *NtPME024* and *NtPME106*, classified into Group II-b, were found to exhibit similar expression patterns to *NtPME082* (Group II-a) and *NtPME056* (Group II-c), which were highly expressed in flowers. The results showed slight differences between qRT-PCR results and RNA sequencing data analysis, which might be due to the harvest of different sample methods and tissue development status.

In addition, to further investigate the expression patterns of *NtPMEs* under abiotic stress, the expression levels of 12 *NtPME*

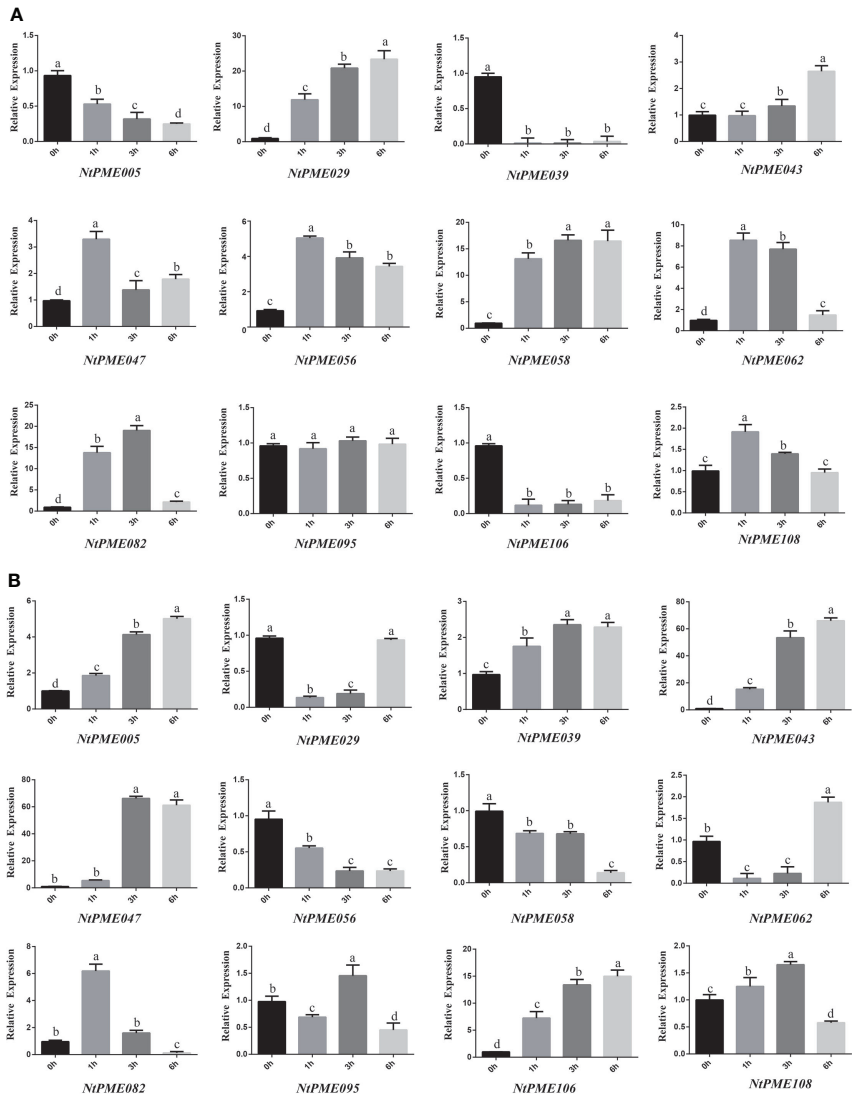


FIGURE 6
The expression patterns of *NtPME* genes under **(A)** Abscisic Acid (ABA) and **(B)** NaCl. For abiotic stress (salt and ABA) treatments, the seedlings were treated with 50 μM Abscisic Acid (ABA) or 150 mM NaCl, and then harvested at 0, 1, 3, or 6 h after treatment. Three biological replicates were performed. Values with superscript letters a, b, c, and d are significantly different across columns ($P < 0.005$).

genes were determined under ABA (Figure 6A) and salt (Figure 6B) treatments. In Group I, *NtPME043*, *NtPME047*, *NtPME056*, and *NtPME058* were induced and up-regulated by ABA treatments, whereas these four genes were detected to exhibit different expression patterns under salt stress, *NtPME043* and *NtPME047* were induced and up-regulated, and *NtPME056* and *NtPME058* were down-regulated. Interestingly, the expression patterns of *NtPMEs* in Group II-a were different under ABA and salt treatments. It was found that ABA-induced and continually up-regulated *NtPME029* with the prolongation of treatment time, while the expression levels of *NtPME062*, *NtPME082*, and *NtPME108* first increased and then decreased with the increase of treatment time. Furthermore, with increasing treatment time, *NtPME029* and *NtPME062* were down-regulated by salt, while *NtPME082* and *NtPME108* behaved oppositely. In Group II-b, *NtPME005*, *NtPME039*, and *NtPME106* were found to induce by NaCl stress and down-regulated under ABA treatments. The expression of selected *NtPME* genes in NaCl and ABA treatment seemed to have opposite trend, suggesting that these genes may be involved in ABA pathway to response to NaCl abiotic stresses. How NtPME members including NtPME005 and NtPME039 involved in ABA and NaCl pathway will be the next questions to be addressed in this field.

Subcellular localization analysis

To further investigate the potential functions of the *NtPMEs*, the NtPME029 and *NtPME043* were selected for subcellular localization analysis (Figure 7). The *p35S::NtPME029-GFP* and *p35S::NtPME043-GFP* constructs were introduced into the leaves of *Nicotiana benthamiana* and the *p35S:: GFP* as a contrast. The fluorescence signals showed that NtPME029 and NtPME043 may be the cell wall localization proteins.

NtPME genes involvement in root development and salt tolerance of tobacco

In *Arabidopsis*, *AtPME3*-overexpressing plants showed longer root development compared to wild-type. In addition, *AtPME31* could be significantly induced under salt stress and enhance the salt stress tolerance of plants. *NtPME029* and *NtPME043*, were identified as homologues with *AtPME3* and *AtPME31*, respectively. Furthermore, *NtPME029* was highly expressed in roots, while *NtPME043* could be induced by salt treatments.

To further explore the function of the *NtPME029* gene in root development, the root elongation assay of wild-type (WT) and the *NtPME029*-overexpressed transgenic tobacco plants were assessed (Figures 8A–C). As result, the over-expressing *NtPME029* displayed longer root lengths than WT after three weeks of growth under normal conditions, suggesting that the *NtPME029* gene positively regulates the root development in tobacco.

To further analyze the function of the *NtPME043* gene in salt tolerance of tobacco, the root elongation assay of WT and the over-expressing *NtPME043* transgenic tobacco plants were also assessed (Figures 8D–F). The *NtPME043*-overexpressed plants displayed no significant differences in root length grown normal nutrient medium. However, the transgenic tobacco plants produced longer root lengths than WT after three weeks of growing under 150 mM NaCl plates. It indicated that the *NtPME043* gene could enhance salt tolerance when overexpressed in tobacco.

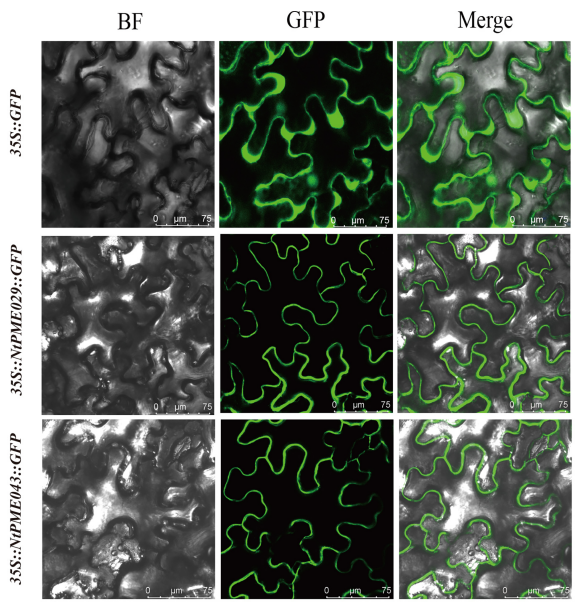


FIGURE 7
Subcellular localization of NtPME029 and NtPME043 proteins. The *NtPME029-GFP*, *NtPME043-GFP* fusion construct, and *GFP* gene all driven by the CaMV-35S promoter were transiently expressed in *N.benthamiana* leaves individually. BF, the signal of bright filed; GFP, the signal of GFP protein; Merge, the merge signal of GFP and BF signals. Scale bar = 75 μm.

Discussion

Previous studies reported that *PMEs* play critical roles in response to diverse abiotic stresses and plant development processes (Jeong et al., 2015; Duan et al., 2016; Zhang et al., 2019). In the present study, a total of 121 members of the *NtPME* genes were identified in the tobacco genome using BLASTP searches. Furthermore, the *NtPMEs* were analyzed using phylogeny, gene structure, motif organization, chromosomal distributions, duplication events, *cis*-elements, expression profiles, and potential functions.

The 121 NtPME members were divided into two groups according to the phylogeny analysis of *Arabidopsis* NtPME members. (Louvet et al., 2006). The NtPME members in the same group contained similar gene structure and motif organization consistent with the previous reports (Li et al., 2020), suggesting the evolutionary relationship and classification analysis of *NtPME* genes were reliable. Additionally, some *NtPME* genes of the same group contained similar *cis*-elements types, implying that they may reflect similar functions in plant development and abiotic stress responses. Interestingly, statistics on the number of *PME* genes in six plant species found the *PME* genes in tobacco significantly larger than in other plants (Table 1), probably due to tobacco being an allopolytraploid. Meanwhile, five higher plants all have Group I and Group II PME genes, while hyscomitrella patens only have Group I *PME* genes, implying that the *PME* genes of Group II appeared after the differentiation of moss and vascular plants, which is consistent with the study of Pelloux and Markovic et al., (Markovic and Janecek, 2004; Pelloux et al., 2007). The synthetic analysis of *NtPMEs* found four genes may have existed before the divergence of dicotyledonous and monocotyledonous plant species (Figure 4), suggesting that these genes were relatively conserved during evolution.

Previous studies suggested that the whole genome duplication events contribute to the expansion of gene families

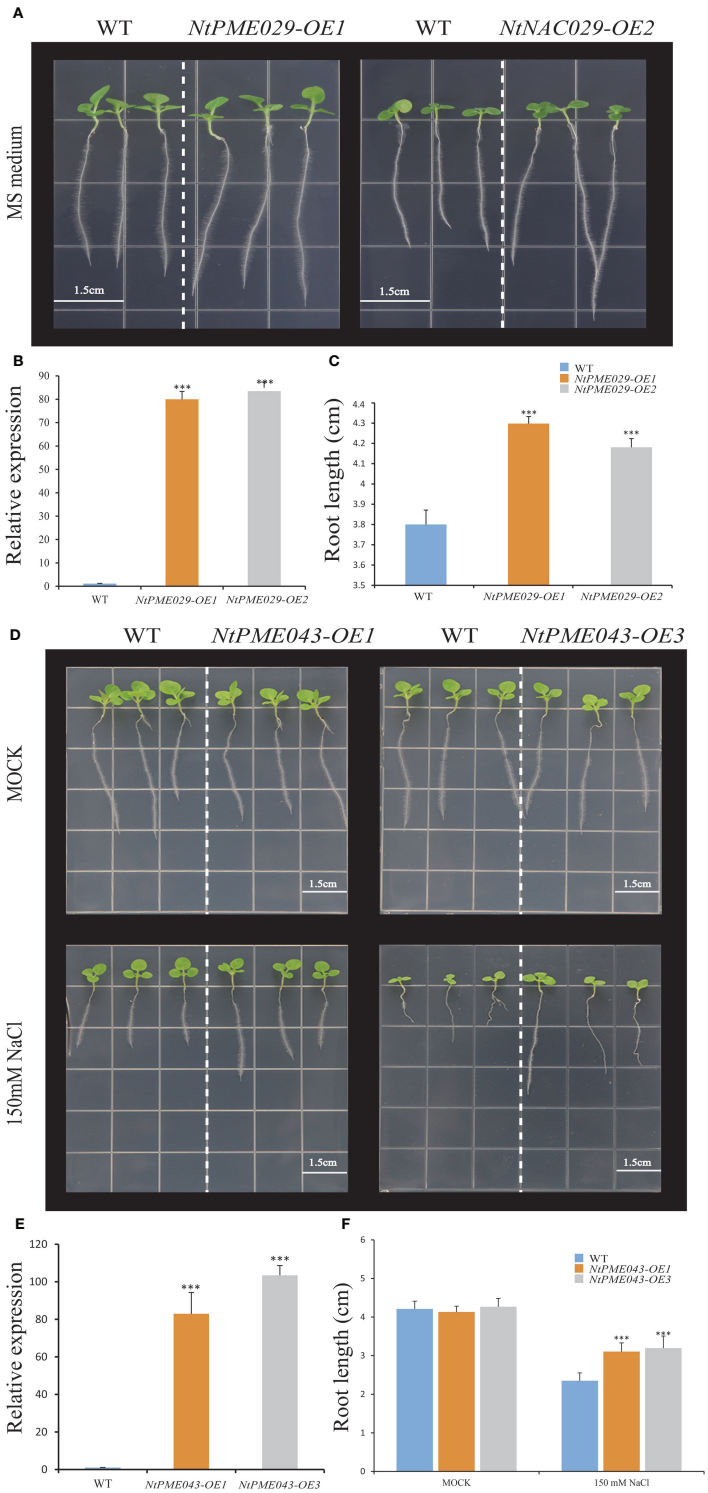


FIGURE 8
The over-expressing *NtPME029* and over-expressing *NtPME043* transgenic plants promote root growth and enhance salt stress, respectively. **(A, D)** Root growth of WT (wild type) and over-expressing *NtPME029* and over-expressing *NtPME043* lines under MS medium or MS contained 150 mM NaCl; **(B, E)** The expression level analysis of over-expressing *NtPME029* and over-expressing *NtPME043* tobacco plants, respectively; **(C, F)** Quantification and analysis of primary root length on media were retrieved from 27 plants of each genotype with three biological replicates. *** means $P < 0.01$ (Student's *t*-test).

(Duan et al., 2016; Khan et al., 2019). In this study, the expansion of the tobacco *NtPME* gene family may be mainly attributable to segmental duplications, not tandem duplication. A total of nine segmental duplication pairs were identified in *NtPMEs*, with the Ka/Ks ratios of these duplication pairs being less than 1 (Figure 3 and Supplementary Table S3), suggesting that these *NtPME*s might have undergone purifying selective pressure. Especially, *NtPME005* and *NtPME039* as duplicated gene pair was found to exhibit similar gene structure, conserved motif organization, and expression patterns (Figures 5, 6), which indicates the similarity of their functions.

According to previous reports, several PME members affect the plant development in *Arabidopsis*. Specifically, *AtPME5* (*AT5G47500*) facilitates shoot development (Peaucelle et al., 2011), while *NtPME058* (Group II-a) as its syntenic pair gene in tobacco was detected to be highly expressed in the shoots and shoot apex, indicating that *NtPME058* may regulate the shoot development (Figure S3). In plants, floral development could affect seed formation, with implications for seed embryo development. In Group II-b, *AtPME58* reportedly played a significant role in seed maturation (Turbant et al., 2016). As tobacco homologs, *NtPME024* and *NtPME106*, are highly expressed in flowers. In Group I, *AtPME48* (*AT5G07410*) is highly expressed in the flower and functions to influence pollen development (Leroux et al., 2015). *NtPME043*, *NtPME056*, and *NtPME072* classified in the same group as *AtPME48* were both highly expressed in flowers, implying that these genes may also modulate floral development. The evidence indicates that *AtPME3* and *AtPME17* specifically regulate the root growth and development of *Arabidopsis* (Hewezi et al., 2008; Sénéchal et al., 2014). Notably, the *NtPME029* was highly expressed in the root and identified as homologues with *AtPME3*, suggesting that they might have similar biological functions in the root growth and development. The experiment of *NtPME029*-overexpressing also validated this idea (Figures 6, 8A, C). Additionally, the promoter regions analysis of *NtPME029* was found to harbor ABRE and AuxRR-core elements, implying that this gene might participate in ABA and auxin pathways to mediate the root development. Whereas, in the same group, *NtPME082* was highly expressed in the flowers, indicating possible functional divergence between these *NtPME* genes.

Previous studies have indicated that *AtPME* genes mediate responses to various abiotic stresses. In Group II-b, *AtPME28* (*AT5G27870*) is induced by NaCl treatment to regulate salt stress (Qu et al., 2011). Consistent with *AtPME28*, the expression of *NtPME005*, *NtPME039* and *NtPME106* could also be induced under salt treatments, suggesting that these genes clustered in the same group may display similar functions in response to abiotic stress. *NtPME047* embedded low-temperature-responsive element (LTR) was closely related to *AtPME41* (*AT4G02330*), enhancing freezing tolerance (Qu et al., 2011), indicating that *NtPME047* may have a similar function under chilling stress. In-plant tissues, *PME* genes with the ABA response element (ABRE) can be induced by ABA treatment. In Group II-a, *AtPME34* (*AT3G49220*) is verified to respond to heat and salt stress through the signaling of the ABA (abscisic acid) pathway (Huang et al., 2017). *NtPM0E62* and *NtPME092*, containing ABRE elements, were detected to induce by both ABA and NaCl treatment, implying that they may be involved in the ABA synthesis pathway in response to salt stress. In Group I, *AtPME31* (*AT3G29090*) could be significantly induced under salt stress and positively modulate the expression levels of salt stress-induced genes to enhance the salt stress tolerance of plants (Yan et al., 2018). Its tobacco homolog, *NtPME043*, was also induced under salt stress and contained the stress-responsive element (TC-rich repeats) and MYB binding site (MBS) associated with stress response, implying that *NtPME043* may contribute to the salt stress response of tobacco. Furthermore, *NtPME043*-overexpressing analyses demonstrated that the *NtPME043* gene could enhance the salt tolerance of tobacco (Figures 8D, F). Additionally, the *NtPME029-GFP* and *NtPME043-GFP* fusion proteins located on the cell wall are consistent with previous evidence of PME proteins' location (Yapo et al., 2007; Wolf et al., 2009).

Conclusions

In this study, 121 *NtPME* genes were identified in the tobacco genome. The comprehensive analysis indicated that the *NtPME* gene family may play multiple roles in various biological processes of tobacco. The PME homologous members between *Arabidopsis* and tobacco displayed the conserved function in plant development and stress responses. Notably, the *NtPME029* was highly expressed in the root and *NtPME029*-overexpressing transgenic plants could promote root development. Furthermore, *NtPME043* could be induced by salt and ABA treatments, and the *NtPME043*-overexpressing transgenic plants significantly enhanced the salt-stress tolerance. This study could provide insight into the further biological functional characterization of *NtPME* genes in tobacco.

Data availability statement

The original contributions presented in the study are included in the article/Supplementary Material. Further inquiries can be directed to the corresponding authors.

Author contributions

JS, ZT, and XL conducted the research and participated in drafting the manuscript. The other authors assisted in data collection and analysis. MX and RX conceived this research,

designed the experiments and drafted the manuscript. All authors contributed to the article and approved the submitted version.

Funding

This work was supported by the Optimization of Quality Assurance Technology for China Tobacco special aroma 301 Variety and Its Application in Middle and High-end Cigarettes (Y02J202102); the Agricultural Science and Technology Innovation Program (ASTIP-TRIC02); the China Tobacco Genome Project [110202001029(JY-12)] and the China Tobacco Hunan Industrial Co., Ltd. Technology Project (KY2022YC0010).

Conflict of interest

JS, ZT, SL, JW, ZH, HC, and RX were employed by China Tobacco Jiangsu Industrial Co., Ltd.

The remaining authors declare that the research was conducted in the absence of any commercial or financial relationships that could be construed as a potential conflict of interest.

Publisher's note

All claims expressed in this article are solely those of the authors and do not necessarily represent those of their affiliated organizations, or those of the publisher, the editors and the reviewers. Any product that may be evaluated in this article, or claim that may be made by its manufacturer, is not guaranteed or endorsed by the publisher.

Supplementary material

The Supplementary Material for this article can be found online at: https://www.frontiersin.org/articles/10.3389/fpls.2022.998841/full#supplementary-material

References

Al-Qsous, S., Carpentier, E., Klein-Eude, D., Burel, C., Mareck, A., Dauchel, H., et al. (2004). Identification and isolation of a pectin methylesterase isoform that could be involved in flax cell wall stiffening. *Planta.* 219, 369–378. doi: 10.1007/s00425-004-1246-1

An, S. H., Sohn, K. H., Choi, H. W., Hwang, I. S., Lee, S. C., and Hwang, B. K. (2008). Pepper pectin methylesterase inhibitor protein CaPMEI1 is required for antifungal activity, basal disease resistance, and abiotic stress tolerance. *Planta.* 228, 61–78. doi: 10.1007/s00425-008-0719-z

Bailey, T. L., Johnson, J., Grant, C. E., and Noble, W. S. (2015). The MEME suite. *Nucleic Acids Res.* 43, W39–W49. doi: 10.1093/nar/gkv416

Bosch, M., Cheung, A. Y., and Hepler, P. K. (2005). Pectin methylesterase, a regulator of pollen tube growth. *Plant Physiol.* 138, 1334–1346. doi: 10.1104/pp.105.059865

Buschmann, H. (2016). Plant cell division analyzed by transient agrobacterium-mediated transformation of tobacco BY-2 cells. *Methods Mol. Biol.* 1370, 17–25. doi: 10.1007/978-1-4939-3142-2_2

Cao, Y., Han, Y., Li, D., Lin, Y., and Cai, Y. (2016). MYB transcription factors in Chinese pear (*Pyrus bretschneideri rehd.*): Genome-wide identification, classification, and expression profiling during fruit development. *Front. Plant Sci.* 7. doi: 10.3389/fpls.2016.00577

Chen, C. J., Chen, H., Zhang, Y., Thomas, H. R., Frank, M. H., He, Y. H., et al. (2020). TBtools: An integrative toolkit developed for interactive analyses of big biological data. *Mol. Plant* 13, 1194–1202. doi: 10.1016/j.molp.2020.06.009

Chao, J., Kong, Y., Wang, Q., Sun, Y., and Liu, G. (2015). MapGene2Chrom, a tool to draw gene physical map based on Perl and SVG languages. *Hereditas* 37, 91–97. doi: 10.16288/j.yczz.2015.01.013

Dixit, S., Upadhyay, S. K., Singh, H., Sidhu, O. P., Verma, P. C., and Chandrashekar, C. (2013). Enhanced methanol production in plants provides broad spectrum insect resistance. *PloS One* 8, e79664. doi: 10.1371/journal.pone.0079664

Duan, W., Huang, Z., Song, X., Liu, T., Liu, H., Hou, X., et al. (2016). Comprehensive analysis of the polygalacturonase and pectin methylesterase genes in *Brassica rapa* shed light on their different evolutionary patterns. *Sci. Rep.* 6, 25107. doi: 10.1038/srep25107

Edwards, K. D., Fernandez-Pozo, N., Drake-Stowe, K., Humphry, M., Evans, A. D., Bombarely, A., et al. (2017). A reference genome for *Nicotiana tabacum* enables map-based cloning of homeologous loci implicated in nitrogen efficiency. *BMC Genom.* 18, 448. doi: 10.1186/s12864-017-3791-6

Finn, R. D., Coggill, P., Eberhardt, R. Y., Eddy, S. R., Mistry, J., Mitchell, A. L., et al. (2016). The pfam protein families database: Towards a more sustainable future. *Nucleic Acids Res.* 44, D279–D285. doi: 10.1093/nar/gkv1344

Garg, V. K., Avashthi, H., and Tiwari, A. (2016). MFPPI–multi FASTA protparam interface. *Bioinformation.* 12, 74–77. doi: 10.6026/97320630012074

Hewezi, T., Howe, P., Maier, T. ,. R., Hussey, R. S., Mitchum, M. G., Davis, E. L., et al. (2008). Cellulose binding protein from the parasitic nematode heterodera schachtii interacts with *Arabidopsis* pectin methylesterase: cooperative cell wall modification during parasitism. *Plant Cell.* 20, 3080–3093. doi: 10.1105/tpc.108.063065

Hongo, S., Sato, K., Yokoyama, R., and Nishitani, K. (2012). Demethylesterification of the primary wall by PECTIN METHYLESTERASE35 provides mechanical support to the *Arabidopsis* stem. *Plant Cell.* 24, 2624–2634. doi: 10.1105/tpc.112.099325

Huang, Y. C., Wu, H. C., Wang, Y. D., Liu, C. H., Lin, C. C., Luo, D. L., et al. (2017). PECTIN METHYLESTERASE34 contributes to heat tolerance through its role in promoting stomatal movement. *Plant Physiol.* 174, 748–763. doi: 10.1104/pp.17.00335

Hu, B., Jin, J. P., Guo, A. Y., Zhang, H., Luo, J. C., and Gao, G. (2015). GSDS 2.0: An upgraded gene feature visualization server. *Bioinf.* 31(8), 1296–1297. doi: 10.1093/bioinformatics/btu817

Jenkins, J., Mayans, O., Smith, D., Worboys, K., and Pickersgill, R. W. (2001). The third-dimensional structure of erwinia chrysanthemi pectin methylesterase reveals a novel esterase active site. *J. Mol. Biol.* 305, 951–960. doi: 10.1006/jmbi.2000.4324

Jeong, H. Y., Nguyen, H. P., and Lee, C. (2015). Genome-wide identification and expression analysis of rice pectin methylesterases: Implication of functional roles of pectin modification in rice physiology. *J. Plant Physiol.* 183, 23. doi: 10.1016/j.jplph.2015.05.001

Jiangtao, C., Yingzhen, K., Qian, W., Yuhe, S., and Guanshan, L. (2015). MapGene2Chrom, a tool to draw gene physical map based on Perl and SVG languages. *Hereditas.* 37, 91. doi: 10.16288/j.yczz.2015.01.013

Khan, N., Fatima, F., Haider, M. S., Shazadee, H., Liu, Z., Zheng, T., et al. (2019). Genome-wide identification and expression profiling of the polygalacturonase (PG) and pectin methylesterase (PME) genes in grapevine (*Vitisvinifera* l.). *Int. J. Mol. Sci.* 20 (13), 3180. doi: 10.3390/ijms20133180

Kumar, S., Stecher, G., Li, M., Knyaz, C., and Tamura, K. (2018). MEGA X: Molecular evolutionary genetics analysis across computing platforms. *Mol. Biol. Evol.* 35, 1547–1549. doi: 10.1093/molbev/msy096

Larkin, M. A., Blackshields, G., Brown, N. P., Chenna, R., McGettigan, P. A., McWilliam, H., et al. (2007). Clustal W and clustal X version 2.0. *Bioinformatics.* 23, 2947–2948. doi: 10.1093/bioinformatics/btm404

Leroux, C., Bouton, S., Kiefer-Meyer, M. C., Fabrice, T. N., Mareck, A., Guénin, S., et al. (2015). PECTIN METHYLESTERASE48 is involved in *Arabidopsis* pollen grain germination. *Plant Physiol.* 167, 367–380. doi: 10.1104/pp.114.250928

Lescot, M., Dehais, P., Thijs, G., Marchal, K., Moreau, Y., Van de Peer, Y., et al. (2002). PlantCARE, a database of plant cis-acting regulatory elements and a portal to tools for *in silico* analysis of promoter sequences. *Nucleic Acids Res.* 30, 325–327. doi: 10.1093/nar/30.1.325

Letunic, I., Doerks, T., and Bork, P. (2015). SMART: Recent updates, new developments and status in 2015. *Nucleic Acids Res.* 43, D257–D260. doi: 10.1093/nar/gku949

Levesque-Tremblay, G., Müller, K., Mansfield, S. D., and Haughn, G. W. (2015). Highly methyl esterified seeds is a pectin methyl esterase involved in embryo development. *Plant Physiol.* 167, 725–737. doi: 10.1104/pp.114.255604

Li, X., Hamyat, M., Liu, C., Ahmad, S., Gao, X., Guo, C., et al. (2018). Identification and characterization of the WOX family genes in five solanaceae species reveal their conserved roles in peptide signaling. *Genes.* 9, 260. doi: 10.3390/genes9050260

Li, X., Ahmad, S., Ali, A., Guo, C., Li, H., Yu, J., et al. (2019a). Characterization of somatic embryogenesis receptor-like kinase 4 as a negative regulator of leaf senescence in *Arabidopsis*. *Cells.* 8, 50. doi: 10.3390/cells8010050

Li, X., Guo, C., Ahmad, S., Wang, Q., Yu, J., Liu, C., et al. (2019b). Systematic analysis of MYB family genes in potato and their multiple roles in development and stress responses. *Biomolecules.* 9 (8), 317. doi: 10.3390/biom9080317

Li, Y., He, H., and He, L. ,. F. (2020). Genome-wide analysis of the pectin methylesterase gene family in potato. *Potato Res.* 64, 1–19. doi: 10.1007/s11540-020-09453-1

Li, Z., Chao, J., Li, X., Li, G., Song, D., Guo, Y., et al. (2021). Systematic analysis of the bZIP family in tobacco and functional characterization of NtbZIP62 involvement in salt stress. *Agronomy.* 11, 148. doi: 10.3390/agronomy11010148

Librado, P., and Rozas, J. (2009). DnaSP v5: A software for comprehensive analysis of DNA polymorphism data. *Bioinformatics.* 25, 1451–1452. doi: 10.1093/bioinformatics/btp187

Livak, K. J., and Schmittgen, T. D. (2001). Analysis of relative gene expression data using real-time quantitative PCR and the 2 (-delta delta c (T)) method. *Methods.* 25, 402–408. doi: 10.1006/meth.2001.1262

Louvet, R., Cavel, E., Gutierrez, L., Guénin, S., Roger, D., Gillet, F., et al. (2006). Comprehensive expression profiling of the pectin methylesterase gene family during silique development in *Arabidopsis thaliana*. *Planta.* 224 (4), 782–791. doi: 10.1007/s00425-006-0261-9

Markovic, O., and Janecek, S. (2004). Pectin methylesterases: sequence-structural features and phylogenetic relationships. *Carbohydr Res.* 339 (13), 2281–2295. doi: 10.1016/j.carres.2004.06.023

Micheli, F. (2001). Pectin methylesterases: cell wall enzymes with important roles in plant physiology. *Trends Plant Science.* 6, 414–419. doi: 10.1016/s1360-1385(01)02045-3

Peaucelle, A., Braybrook, S. A., Le Guillou, L., Bron, E., Kuhlemeier, C., and Höfte, H. (2011). Pectin-induced changes in cell wall mechanics underlie organ initiation in *Arabidopsis*. *Curr. Biol.* 21, 1720–1726. doi: 10.1016/j.cub.2011.08.057

Pelloux, J., Rustérucci, C., and Mellerowicz, E. J. (2007). New insights into pectin methylesterase structure and function. *Trends Plant Sci.* 12 (6), 267–277. doi: 10.1016/j.tplants.2007.04.001

Qu, T., Liu, R., Wang, W., An, L., Chen, T., Liu, G., et al. (2011). Brassinosteroids regulate pectin methylesterase activity and AtPME41 expression in *Arabidopsis* under chilling stress. *Cryobiology.* 63, 111–117. doi: 10.1016/j.cryobiol.2011.07.003

Ren, A., Ahmed, R. I., Chen, H., Han, L., Sun, J., Ding, A., et al. (2019). Genome-wide identification, characterization and expression patterns of the pectin methylesterase inhibitor genes in sorghum bicolor. *Genes.* 10 (10), 755. doi: 10.3390/genes10100755

Sénéchal, F., Graff, L., Surcouf, O., Marcelo, P., Rayon, C., Bouton, S., et al. (2014). *Arabidopsis* PECTIN METHYLESTERASE17 is co-expressed with and processed by SBT3.5, a subtilisin-like serine protease. *Ann. Bot.* 114, 1161–1175. doi: 10.1093/aob/mcu035

Sun, J., Xie, M., Li, X., Li, Z., and Sun, Y. (2021). Systematic investigations of the ZF-HD gene family in tobacco reveal their multiple roles in abiotic stresses. *Agronomy.* 11, 406. doi: 10.3390/agronomy11030406

Tian, G. W., Chen, M. H., Zaltsman, A., and Citovsky, V. (2006). Pollen-specific pectin methylesterase involved in pollen tube growth. *Dev. Biol.* 294, 83–91. doi: 10.1016/j.ydbio.2006.02.026

Turbant, A., Fournet, F., Lequart, M., Zabijak, L., Pageau, K., Bouton, S., et al. (2016). PME58 plays a role in pectin distribution during seed coat mucilage extrusion through homogalacturonan modification. *J. Exp. Bot.* 67, 2177–2190. doi: 10.1093/jxb/erw025

Udall, J. A., Swanson, J. M., Haller, K., Rapp, R. A., Sparks, M. E., Hatfield, J., et al. (2006). A global assembly of cotton ESTs. *Genome Res.* 16, 441–450. doi: 10.1101/gr.4602906

Verma, C., Singh, R. K., and Mishra, S. (2014). Biochemical characterization of pectin methylesterase from musa acuminata referring to delayed ripening. *IOSR-JPBS.* 9, 42–47. doi: 10.9790/3008-49709134247

Wallace, S., and Williams, J. H. (2017). Evolutionary origins of pectin methylesterase genes associated with novel aspects of angiosperm pollen tube walls. *Biochem. Biophys. Res. Commun.* 487, 509–516. doi: 10.1016/j.bbrc.2017.04.027

Wolf, S., Mouille, G., and Pelloux, J. (2009). Homogalacturonan methyl-esterification and plant development. *Mol. Plant* 2, 851–860. doi: 10.1093/mp/ssp066

Wu, X., Lai, Y., Lv, L., Ji, M., Han, K., Yan, D., et al. (2020). Fasciclin-like arabinogalactan gene family in *Nicotiana benthamiana*: genome-wide identification, classification and expression in response to pathogens. *BMC Plant Biol.* 20, 305. doi: 10.1186/s12870-020-02501-5

Xie, T., Chen, C., Li, C., Liu, J., Liu, C., and He, Y. (2018). Genome-wide investigation of WRKY gene family in pineapple: Evolution and expression profiles during development and stress. *BMC Genom.* 19, 490. doi: 10.1186/s12864-018-4880-x

Yan, J., He, H., Fang, L., and Zhang, A. (2018). Pectin methylesterase31 positively regulates salt stress tolerance in. *Arabidopsis. Biochem. Biophys. Res. Commun.* 496, 497–501. doi: 10.1016/j.bbrc.2018.01.025

Yapo, B. M., Lerouge, P., Thibault, J. F., and Ralet, M. C. (2007). Pectins from citrus peel cell walls contain homogalacturonans homogenous with respect to molar mass, rhamnogalacturonan I and rhamnogalacturonan II. *Carbohydr. Polym.* 69, 426–435. doi: 10.1016/j.carbpol.2006.12.024

Zega, A., and D'Ovidio, R. (2016). Genome-wide characterization of pectin methyl esterase genes reveals members differentially expressed in tolerant and susceptible wheats in response to *Fusarium graminearum*. *Plant Physiol. Biochem.* 108, 1–11. doi: 10.1016/j.plaphy.2016.06.033

Zhang, G. Y., Feng, J., Wu, J., and Wang, X. W. (2010). BoPMEI1, a pollen-specific pectin methylesterase inhibitor, has an essential role in pollen tube growth. *Planta* 231, 1323–1334. doi: 10.1007/s00425-010-1136-7

Zhang, P., Wang, H., Qin, X., Chen, K., Zhao, J., Zhao, Y., et al. (2019). Genome-wide identification, phylogeny and expression analysis of the PME and PMEI gene families in maize. *Sci. Rep.* 9, 19918. doi: 10.1038/s41598-019-56254-9

Zhao, Y., Man, Y., Wen, J., Guo, Y., and Lin, J. (2019). Advances in imaging plant cell walls. *Trends Plant Sci.* 482, 867–878. doi: 10.1016/j.tplants.2019.05.009

frontiers | Frontiers in Plant Science

TYPE Original Research
PUBLISHED 29 September 2022
DOI 10.3389/fpls.2022.986628

Check for updates

OPEN ACCESS

EDITED BY
Giselle Camargo Mendes,
Instituto Federal de Santa Catarina (IFSC), Brazil

REVIEWED BY
Abid Khan,
University of Haripur, Pakistan
Md Mahmudul Hassan,
Patuakhali Science and Technology University, Bangladesh

*CORRESPONDENCE
Yexiong Qian,
qyx2011@ahnu.edu.cn

SPECIALTY SECTION
This article was submitted to Plant Abiotic Stress, a section of the journal Frontiers in Plant Science

RECEIVED 05 July 2022
ACCEPTED 12 September 2022
PUBLISHED 29 September 2022

CITATION
Xi Y, Ling Q, Zhou Y, Liu X and Qian Y (2022) ZmNAC074, a maize stress-responsive NAC transcription factor, confers heat stress tolerance in transgenic *Arabidopsis*. *Front. Plant Sci.* 13:986628. doi: 10.3389/fpls.2022.986628

COPYRIGHT
© 2022 Xi, Ling, Zhou, Liu and Qian. This is an open-access article distributed under the terms of the Creative Commons Attribution License (CC BY). The use, distribution or reproduction in other forums is permitted, provided the original author(s) and the copyright owner(s) are credited and that the original publication in this journal is cited, in accordance with accepted academic practice. No use, distribution or reproduction is permitted which does not comply with these terms.

ZmNAC074, a maize stress-responsive NAC transcription factor, confers heat stress tolerance in transgenic *Arabidopsis*

Yan Xi, Qiqi Ling, Yue Zhou, Xiang Liu and Yexiong Qian*

Anhui Provincial Key Laboratory of Conservation and Exploitation of Important Biological Resources, College of Life Sciences, Anhui Normal University, Wuhu, China

The harsh environment such as high temperature greatly limits the growth, development and production of crops worldwide. NAC (NAM, ATAF1/2, and CUC2) transcription factors (TFs) play key regulatory roles in abiotic stress responses of plants. However, the functional roles of NAC TFs in heat stress response of maize remain elusive. In our present study, we identified and isolated a stress-responsive NAC transcription factor gene in maize, designated as *ZmNAC074* and orthologous with rice *OsNTL3*. Further studies revealed that *ZmNAC074* may encode a membrane-bound transcription factor (MTF) of NAC family in maize, which is comprised of 517 amino acid residues with a transmembrane domain at the C-terminus. Moreover, *ZmNAC074* was highly expressed and induced by various abiotic stresses in maize seedlings, especially in leaf tissues under heat stress. Through generating *ZmNAC074* transgenic plants, phenotypic and physiological analyses further displayed that overexpression of *ZmNAC074* in transgenic *Arabidopsis* confers enhanced heat stress tolerance significantly through modulating the accumulation of a variety of stress metabolites, including reactive oxygen species (ROS), antioxidants, malondialdehyde (MDA), proline, soluble protein, chlorophyll and carotenoid. Further, quantitative real-time PCR analysis showed that the expression levels of most ROS scavenging and HSR- and UPR-associated genes in transgenic *Arabidopsis* were significantly up-regulated under heat stress treatments, suggesting that *ZmNAC074* may encode a positive regulator that activates the expression of ROS-scavenging genes and HSR- and UPR-associated genes to enhance plant thermotolerance under heat stress conditions. Overall, our present study suggests that *ZmNAC074* may play a crucial role in conferring heat stress tolerance in plants, providing a key candidate regulatory gene for heat stress tolerance regulation and genetic improvement in maize as well as in other crops.

KEYWORDS

maize, heat stress, *ZmNAC074*, transcription factor, ROS homeostasis, stress tolerance

Introduction

According to previous studies, maize, rice, and wheat account for 89% of the global cereal production (Botticella et al., 2021). Maize, a crucial economic grain crop, contributes significantly to health and nutrition worldwide (Poole et al., 2020). The sixth assessment report from the IPCC points out that the surface temperature on the earth has increased by around 1.1°C compared with the average temperature from 1850 to 1900 and forecasts that the global average temperature will continue to rise (Tollefson, 2021). Global warming poses a major threat to human health and nutrition, seriously damaging crop growth, yield and food security (Guihur et al., 2022). Without adapting to the environment and human intervention, for every 1°C increase in global average temperature, maize yield will decrease by an average of 7.4% (Zhao et al., 2017). Previous studies have shown that the growth and development of maize has been affected by heat stress, such as inhibiting grain weight and starch deposition, reducing the pollen viability and the production of photosynthetic components, and the decline of nutrient absorption and yield traits (Lesk et al., 2016; Yang et al., 2018; Hussain et al., 2019; Wang et al., 2020; Li and Howell, 2021). Therefore, understanding the molecular regulatory mechanism underlying heat stress response in maize will enhance our ability to achieve agricultural productivity to the growing world population.

The survival of plants is seriously negatively affected by heat stress (Driedonks et al., 2016). Considering that plants are sessile organisms, the processes of plant growth and development largely depend on the effective activation of heat-tolerant regulatory networks to alleviate the damage resulted from heat stress response (Nievola et al., 2017). The mechanisms of plant heat stress response mainly involve heat shock response (HSR), unfolded protein response (UPR), ROS homeostasis, epigenetic controls and hormone-mediated regulation in plants (Liu et al., 2015; Ohama et al., 2017; Li et al., 2020a; Li et al., 2020b; Zhao et al., 2020). Studies have shown that numerous stress-associated defense genes and transcription factors (TFs) are involved in the regulation of heat stress response of plants, such as MAPK, CDPK, bZIP, and NAC TFs (Wu et al., 2015; Li et al., 2018; Li et al., 2020b; Liu et al., 2020; Zhao et al., 2021). Especially, TFs play a crucial role in regulating heat stress responses of plants. Numerous studies have shown that NAC TFs play different roles under heat stress in rice, *Arabidopsis* and other plants, such as OsNTL3, SNAC3, ANAC042, NAC019, and CaNAC035 (Shahnejat-Bushehri et al., 2012; Guan et al., 2014; Fang et al., 2015; Liu et al., 2020; Zhang et al., 2020). However, little is known regarding the roles of heat stress tolerance of NAC TFs in maize.

NAC (NAM, ATAF1/2, and CUC2) protein has been identified in Petunia for the first time (Souer et al., 1996). NAC family proteins share a highly conserved NAC-bound domain at the N-terminus and a variable and diverse transcriptional regulatory region at the C-terminus (Ooka et al., 2003; Olsen et al., 2005; Christianson et al., 2010). As one of the largest families of TFs in plants, NAC TFs play crucial roles in the regulation of plant growth, development and responses to biotic and abiotic stresses (Shao et al., 2015; Ohbayashi and Sugiyama, 2017; Mathew and Agarwal, 2018; Diao et al., 2020; Singh et al., 2021). For instance, rice *SNAC3* can enhance heat and drought resistance by regulating the dynamic balance of reactive oxygen species (ROS) (Fang et al., 2015). Overexpression of *ANAC087* gene in *Arabidopsis* can induce the increase of branching in inflorescence stems and involve in rosette development (Vargas-Hernández et al., 2022). Moreover, silencing *GhJUB1L1* gene can reduce drought tolerance and inhibit the development of secondary cell walls in cotton, suggesting that *GhJUB1L1* plays a positive regulatory role in the occurrence of drought stress tolerance and the development of secondary cell walls in cotton (Chen et al., 2021). Furthermore, ectopic overexpression of *ZmNAC126* in transgenic *Arabidopsis* and maize can enhance chlorophyll degradation and promote leaf senescence, suggesting that *ZmNAC126* plays a key role in regulating chlorophyll degradation during maize leaf senescence. Further, based on EMSA and CHIP-seq analyses, ZmNAC126 was revealed to directly bind to the promoters of major chlorophyll catabolic genes including *ZmNYE1*, *ZmNYC1*, *ZmPAO* and *ZmRCCR*, indicating that ZmNAC126 can positively regulate these chlorophyll catabolic genes in maize. Moreover, the expression of *ZmNAC126* can be induced by ethylene, and ZmEIN3, a major TF of ethylene signaling, can bind to its promoter to transactivate its expression during leaf senescence (Yang et al., 2020). In addition, the overexpression of *ZmNAC55* in *Arabidopsis* led to the sensitivity of transgenic *Arabidopsis* lines to ABA at germination stage, but improved the drought resistance compared with wild-type seedlings (Mao et al., 2016).

Recently, a considerable attention has been paid to the functional roles of NAC TFs in response to heat stress. For example, it has been revealed that OsNTL3 can interact with OsbZIP74 to activate the regulatory circuits of the nucleus, endoplasmic reticulum and plasma membrane under heat stress to enhance heat resistance of rice (Liu et al., 2020). *ONAC127* and *ONAC129* in rice have been displayed to respond to heat stress and regulate grain filling by modulating sugar transport and abiotic stress responses (Ren et al., 2021). Moreover, overexpression of *JUNGBRUNNEN1* (*JUB1*; *ANAC042*) could increase the longevity of *Arabidopsis* and enhance the tolerance to heat stress (Shahnejat-Bushehri et al., 2012). Overexpression of *TaNAC2L* can regulate the expression of heat stress-associated genes, thereby promoting heat resistance in transgenic *Arabidopsis* (Guo et al., 2015). Taken together, these studies have revealed that NAC TFs may play vital regulatory roles in dealing with heat stress responses of plants. At present, a total of 148 *NAC* genes (*ZmNAC1*-*ZmNAC148*) have been identified in maize (Peng et al., 2015).

However, up to now, knowledge regarding the regulatory roles of NAC TFs in response to heat stress in maize remains scarce. In our previous studies, one transcript (*ZmNAC074*) has been identified through high- throughput sequencing analysis of maize B73 inbred line and exhibited significantly up-regulated expression level in leaves of maize seedling after heat stress treatment (Qian et al., 2019).

Previously, *ZmNAC074* (also known as *ZmNTL1* or *ZmNAC45*) was reported to encode a membrane-bound transcription factor of NAC family in maize and respond to oxidative stress (Shiriga et al., 2014; Lu et al., 2015; Wang et al., 2016). Generally, some TFs are immobilized on plasma membrane as MTFs and remain dormant under normal conditions, but these MTFs are likely to be released from the plasma membrane by proteolytic cleavage to become active TFs under stress conditions (Seo et al, 2008) , such as TaNTL1 (Sun et al., 2022), OsNTL3 (Liu et al., 2020), and ANAC062(NTL6) (Yang et al., 2014a). Previous studies have revealed that some NAC MTFs, such as OsNTL3, AtNAC062, AtNAC089 and AtNAC103, are associated with UPR, especially through interaction with the members of bZIP protein family (Sun et al., 2013; Yang et al., 2014a; Yang et al., 2014b; Liu et al., 2020). Therefore, we strive to reveal potential regulatory roles of ZmNAC074 as a MTF under heat stress treatments in this study.

Taken together, the goals of the present study were to validate the biological function of *ZmNAC074* in response to heat stress and to provide a molecular basis for using *ZmNAC074* to improve maize thermotolerance *via* transgenic and genome editing approaches. By characterizing the *ZmNAC074* overexpression transgenic *Arabidopsis* lines under heat stress treatments, we demonstrate that *ZmNAC074* may play a positive regulatory role in regulating heat resistance by modulating the accumulation of multiple stress metabolites and participating in the processes of HSR, UPR and ROS homeostasis. Overall, our study will provide an important theoretical basis for further improvement of heat resistance of maize or other crops through genetic engineering.

Materials and methods

Plant materials and growth conditions

In this study, the seeds of maize B73 Inbred Line were obtained from Anhui Agricultural University, China. The seeds germinated on the wet cotton cloth at 28°C for 3 days, and then the germinated seeds were transplanted to nutritious soil and grew at 28°C with long-day conditions of 15 h (550 μmol $m^{-2}s^{-1}$) and 9 h of dark and the relative humidity of 60% for the whole growth and developmental period. At the V4 developmental period (there is a visible ring in the leaf base of the fourth leaf), the maize seedlings were transferred to a dark incubator with 42°C treatment for 0, 4, and 8 h. Moreover, according to the previous methods (Hu et al., 2021), the seedlings were subjected to drought and salt treatments (200 mM NaCl) for 0, 4, and 8 h, respectively. The treated seedling roots, stems and leaves were collected after the three stress treatments, respectively. All these collected tissues were stored in liquid nitrogen to further extract RNA. In addition, *Arabidopsis* ecotype Columbia (Col) was used as original materials for genetic transformation to obtain transgenic plants and perform further functional analysis. All *Arabidopsis* plants were grown in the controlled chamber (22°C,16h light (120 μmol $m^{-2}s^{-1}$)/8 h darkness, and 60% relative humidity).

Bioinformatic analysis of *ZmNAC074*

The full-length CDS sequence of *ZmNAC074* was extracted from the NCBI database (http://www.ncbi.nlm.nih.gov). The orthologous protein sequences in rice and *Arabidopsis* were retrieved from Phytozome (https://phytozome-next.jgi.doe.gov/) and NCBI (http://www.ncbi.nlm.nih.gov) (Zhang et al., 2022). Furthermore, the molecular weight and theoretical isoelectric point (PI) of ZmNAC074 protein were calculated in Expasy (http://web.expasy.org/compute_pi/) (Khan et al., 2018). The multiple amino acid sequences were calibrated and compared using ClustalW program. The phylogenetic tree was constructed using MEGA 7.0 software with the neighbor-joining method and 1000 bootstrap replicates in this study. The conserved motifs were predicted using online MEME website (http://alternate.meme-suite.org/tools/meme). In addition, the structure of these genes was analyzed by GSDS website (http://gsds.cbi.pku.edu.cn/) referring to our previous methods (Hu et al., 2021). The amino acid sequences of ZmNAC074 and OsNTL3 proteins were further compared using DNAMAN software. The transmembrane domain of ZmNAC074 was predicted using TMHHM 2.0 (https://services.healthtech.dtu.dk/service.php?TMHMM-2.0). The three dimensional (3D) structural model of ZmNAC074 protein was predicted using the I-TASSER server (https://seq2fun.dcmb.med.umich.edu//I-TASSER/) (Yang and Zhang, 2015; Zhang et al., 2017; Zheng et al., 2021). The predicted model was edited and annotated using the PyMOL software. Moreover, the functional associations of several NAC MTFs and stress response-associated proteins in *Arabidopsis* and rice were predicted to construct their protein protein interaction networks by the STRING website (https://cn.string-db.org/), respectively.

Quantitative real-time PCR analysis

The total RNA was isolated with Trizol reagent (TIANGEN, China) (Gai et al., 2020). The first strand of cDNA was synthesized from 2μg of total RNA using the FastKing RT Kit (TIANGEN, China). Quantitative real time-PCR (qRT-PCR) was performed using Light-CykerR96 real-time PCR system (BioRad, USA). The reaction conditions are as follows:

preincubation at 95°C for 600 s, and then performing 40 cycles of 95°C for 10s, 55°C for 30s and 72°C for 30s. In maize and *Arabidopsis*, the relative gene expression data were calculated using the $2^{-\triangle\triangle Ct}$ method with the expression of *ZmActin* and *AtActin* as internal controls, respectively. All qRT-PCR analyses were performed by three biological replicates. The primer sequences used were listed in Supplementary Table S1.

Vector construction and *Arabidopsis* transformation

The full-length CDS sequence of *ZmNAC074* was amplified by PCR and inserted into the PHB vector driven by the cauliflower mosaic virus (CaMV) 35S promoter to generate a recombinant vector, which was confirmed *via* double digestion validation with Hind III and Xba I enzymes and sequencing. The constructed vector was further transformed into *Arabidopsis* ecotype Col-0 using the floral dipping method mediated by *Agrobacterium tumefaciens* strain GV3101. The seeds of T_0 and T_1 generations were screened with 1/2 MS media containing 30 mg/L hygromycin and identified by RT-PCR. Three T_3 homozygotes of *ZmNAC074* transgenic overexpression lines (line 1, line 2, and line 9) were ultimately selected for further functional analysis (Gai et al., 2020).

Heat stress treatment

The three-week-old transgenic *Arabidopsis* and WT *Arabidopsis* seedlings were treated at 42°C for 24h and 48h, respectively (Huang et al., 2019). Then, these two kinds of *Arabidopsis* plants with different treatment time were restored to normal environmental conditions growing for one week. The determination of physiological characteristics and related gene expression was performed just at the end of heat stress treatments.

Physiological and enzymatic analyses of transgenic *Arabidopsis* plants

Hydrogen peroxide (H_2O_2) in leaves was determined with 3, 3'-diaminobenzidine (DAB) solution. According to the previously described methods (Daudi and O'brien, 2012), the leaves were immersed in 1.0 mg/mL DAB-HCl solution (add the mixed solution of 0.05% (v/v) Tween 20 and 8 times the volume of 200 mM Na_2HPO_4 to adjust the PH of DAB-HCl solution to 7.0) for 8 h at 25 °C and dark. Then place the stained leaves in a beaker containing 95% (v/v) alcohol and carefully place them in a boiling water bath (95°C) for 15 ± 5 minutes until the brown spots appear on the leaves and there are no green areas (Ali et al., 2020). Further, the histochemical staining of superoxide radical (O_2^-) was mentioned as previously described (Xia et al., 2009; Liu et al., 2012), but with slight modifications. The leaves were incubated in 0.1% nitro blue tetrazolium (NBT) with 50 mM potassium phosphate buffer (pH 7.8) at 25°C for 12 h. Then, the same decolorization method mentioned above was used for bleaching and photography.

The sample pretreatment methods for some physiological indexs (MDA, soluble protein and proline) in this experiment are as follows: weigh 0.1g of leaves, add 900 mL of physiological saline, mechanically homogenize in an ice-water bath, centrifuge at 10,000 rpm for 10 min and take the sample supernatant for subsequent experiments. The activities of superoxide dismutase (SOD) and catalase (CAT) were determined using xanthine-xanthine oxidase method and ammonium molybdate spectrophotometric method, respectively (Hadwan and Abed, 2016). SOD and CAT activities were calculated by the absorbance value obtained at the wavelength of 550 nm and 405 nm, respectively. Moreover, the total antioxidant capacity (T-AOC) was determined by colorimetry at 520nm as directed by the manufacturer. In addition, the H_2O_2 content was determined with molybdenic acid colorimetry. H_2O_2 bound with molybdenic acid to form a complex (Zhou et al., 2021), which was measured by using spectrophotometer at the wavelength of 405nm. Then, the content of H_2O_2 was calculated from the measured absorbance. Malondialdehyde (MDA) content was determined using the thiobarbituric acid (TBA) assay (Aguilar Diaz De Leon and Borges, 2020). For this, 0.1mL of the sample supernatant was mixed with 4.1mL of the mixed solution containing TBA configured according to the manufacturer's instructions and heated at 95°C for 40min. The reaction mixture was taken to determine the absorbance at 532nm and calculate the content of MDA. The content of soluble protein was determined by Coomassie Brilliant Blue method (Goldring, 2019) through adding 50μL the sample supernatant to 3mL Coomassie Brilliant Blue dye reagent, which was mixed and incubated at 25°C for 10 minutes. The graph of absorbance readings and soluble protein content at 595nm was plotted. The content of soluble protein was calculated by using the absorbance value of the reaction mixture and the graph. Furthermore, the proline content in leaves was determined by acid ninhydrin method (Shabnam et al., 2016). 0.5mL of sample supernatant mixed with 2mL of 1.25% (v/v) ninhydrin in 2mL glacial acetic acid at 100°C for 30 min. After cooling, the reaction mixture was taken to determine the absorbance at 520 nm. Moreover, to identify the content of photosynthetic pigments, 1g leaf tissue (ground with liquid nitrogen) was treated with 80% (v/v) acetone. The absorbance was measured at 470nm, 645nm, and 633nm, respectively (Zengin, 2013). Using the absorbance value, the contents of chlorophyll and carotenoid were calculated, respectively. All analyses were performed for three biological replicates. All the above kits or reagents were purchased from Nanjing Jiancheng Bioengineering Institute. Spectrophotometer

(Shanghai Youke instrument Co., Ltd., UV752N) was used for all measurements.

Statistical analysis

Statistical analysis was carried out using the SPSS 20 software. The data were analyzed by one-way ANOVA and the means were compared by Duncan's multiple range test. Compared with the control group, $P < 0.05$ is considered to be statistically significant and $P < 0.01$ extremely significant.

Results

Sequence characterization of ZmNAC074 as a typical NAC membrane-bound TF

The open reading frame (ORF) of *ZmNAC074* is consisted of 1556 bp, which encodes 517 amino acids (AA) with a molecular weight of 57.5 kDa and a theoretical isoelectric point (PI) of 5.49. It is suggested that ZmNAC074 protein is a kind of acidic protein and under the condition of isoelectric point (PI=5.49), this protein shows its minimum solubility, viscosity, osmotic pressure and swelling property. The phylogenetic tree of NAC proteins in maize, rice, and *Arabidopsis* revealed that ZmNAC074 protein shares a close evolutionary relationship with rice OsNTL3 protein (Figure 1A). In addition, AtNAC089, AtNAC60 and AtNTL8 also belong to the same branch with ZmNAC074, indicating that the evolutionary relationships among them are relatively conserved. Information of corresponding genes encoding these NAC proteins in plants was listed in Supplementary Table S2. According to sequence characteristics of these NAC proteins, 10 conserved motifs (motif 1-10) were predicted using the MEME program (Figure 1B). All NAC proteins contain motifs 1-4. Except for AtNAC089, AtNAC60, and AtNTL8, all other proteins contain motif 5. It is worth noting that ZmNAC074 and OsNTL3 contain the same motif distribution (motif 1-5). Annotations of the motifs are listed in Supplementary Table S3. In addition, the corresponding genes encoding these NAC proteins (including ZmNAC074, OsNTL3, AtNAC089, AtNAC60 and AtNTL8) in the same branch share a common feature in gene structure, namely only containing three introns (Figure 1C). Moreover, the N-terminus and C-terminus of ZmNAC074 protein contain a NAC domain (10-136 AA) and a transmembrane domain (488-510 AA), respectively (Figure 1D). Moreover, the amino acid sequence alignment between ZmNAC074 and OsNTL3 showed that their NAC domains share high similarity, indicating that ZmNAC074 may have a similar function to OsNTL3 (Figure 1E). In addition, according to the TMHMM prediction, ZmNAC074 protein only contains one transmembrane domain, which is distributed at the C-terminus of ZmNAC074 protein (Figure 1F). The positions of the N- terminus (represented by the white letter N) and the C- terminus (represented by the white letter C) of ZmNAC074 protein are marked in the picture of the 3D model (Figure 1G). In addition, the middle region of the two labeled amino acids (ALA-488 and TYR-510) represents the transmembrane domain of this protein. Moreover, the α-helix and β-strand are depicted as red and yellow ribbon diagrams, respectively, and loops as green lines.

ZmNAC074 is responsive to various abiotic stresses in maize

To examine whether *ZmNAC074* responds to heat stress and other abiotic stresses, the expression pattern of *ZmNAC074* was evaluated under heat (42°C), salt (200mM NaCl), and drought stress treatments for 0, 4, and 8 h in maize B73 inbred line, respectively. The results showed that *ZmNAC074* was expressed in roots, stems, and leaves under normal conditions, but its expression level was the highest in leaves in comparison to other tissues (Figure 2). The expression level of *ZmNAC074* was significantly upregulated following heat, drought and salt stress treatments, especially under heat stress treatment, respectively (Figures 2A–C). After heat stress, the expression level of *ZmNAC074* in three different tissues increased gradually with the prolongation of stress time (Figure 2A). After drought stress, the expression levels of *ZmNAC074* in stem and root tissues gradually increased, peaked at 4h, and then decreased (Figure 2B). After salt stress, the expression levels of *ZmNAC074* in stem and root tissues decreased at 4h and then increased at 8h (Figure 2A). Overall, these results demonstrate that *ZmNAC074* can respond to heat, drought, and salt stress, but the response to heat stress is particularly strong. Therefore, the regulatory role of *ZmNAC074* in heat stress tolerance was focused on in the subsequent study.

Generation of *ZmNAC074*-overexpressed transgenic *Arabidopsis*

To investigate the potential functions of *ZmNAC074* under heat stress, *ZmNAC074* was successfully introduced into *Arabidopsis* driven by *CaMV 35S* promoter (Figures 3A–B) (Zuo et al., 2022). The schematic diagram of constructed vector containing *ZmNAC074* under the control of *CaMV 35S* promoter was displayed (Figure 3C). The recombinant vector was further transformed into *Arabidopsis* and 16 *ZmNAC074*-overexpressed transgenic *Arabidopsis* lines were obtained in this study. The amplification map showed that the exogenous *ZmNAC074* has been integrated into the genome of 15 transgenic *Arabidopsis* lines (Figure 3D). Quantitative RT-PCR analysis showed that there was no significant difference in the

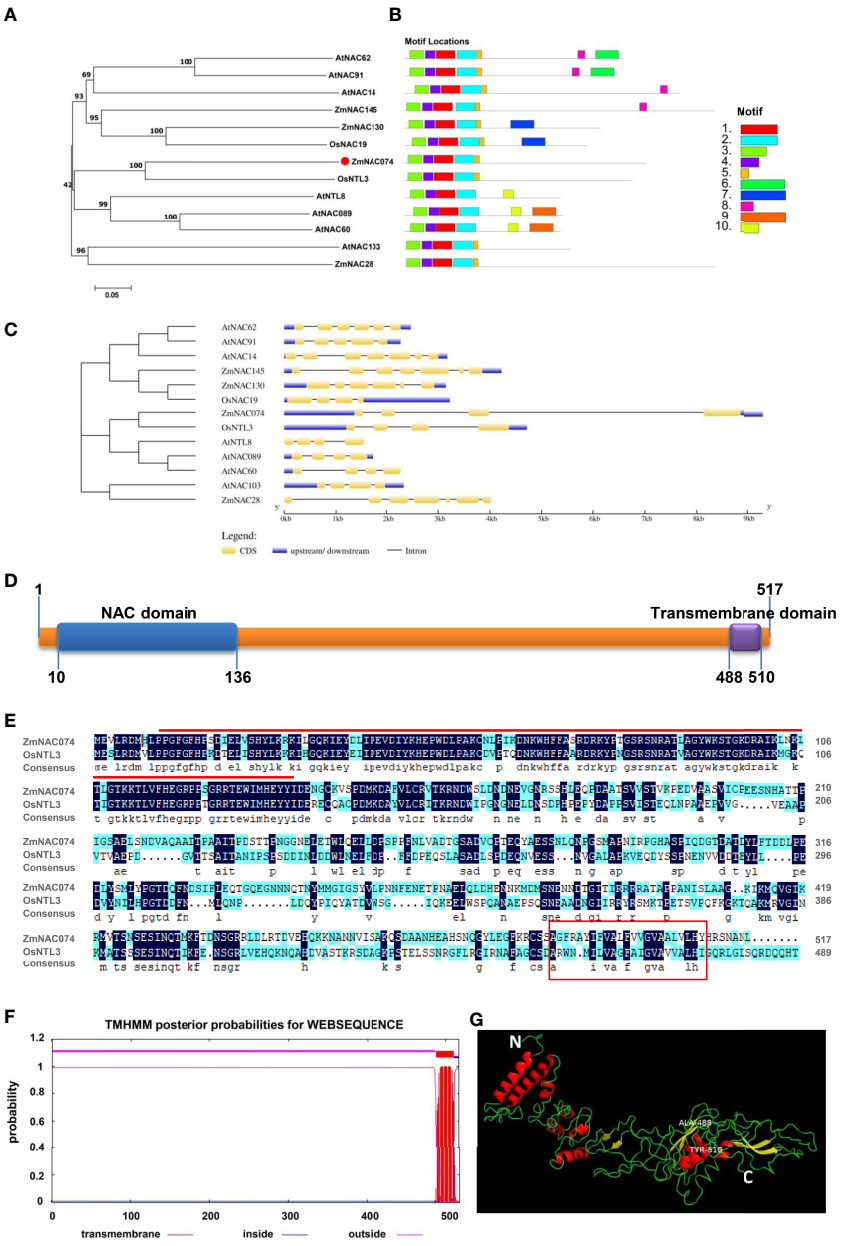


FIGURE 1
Bioinformatics analysis of the ZmNAC074 protein. **(A)** The phylogenetic tree of ZmNAC074 and other different NAC proteins. Bootstrap support values are indicated on each node. **(B)** The conserved motifs of these NAC proteins. **(C)** The gene structures of these NAC genes. **(D)** The domain distribution in ZmNAC074 protein. **(E)** Alignment of protein sequences of ZmNAC074 and OsNTL3. Red line represents NAC domain and red box represents transmembrane region. **(F)** The prediction of secondary transmembrane domain. **(G)** The 3D structural model of ZmNAC074 protein. N and C represent the N-terminus and C-terminus of ZmNAC074 protein, respectively.

expression of *ZmNAC074* among line 1, line 2, and line 9 when they were three weeks old (Figure 3E). Moreover, when growing under normal conditions, there was no visible phenotypic difference between the three lines and WT *Arabidopsis* (Figure 3F). Therefore, line 1, line 2 and line 9 can be selected as three biological repeats for further exploration.

Overexpression of *ZmNAC074* affects the accumulation of stress-related metabolites during heat stress response

To further verify whether *ZmNAC074* is associated with heat resistance, three-week-old WT *Arabidopsis* and selected

10.3389/fpls.2022.986628

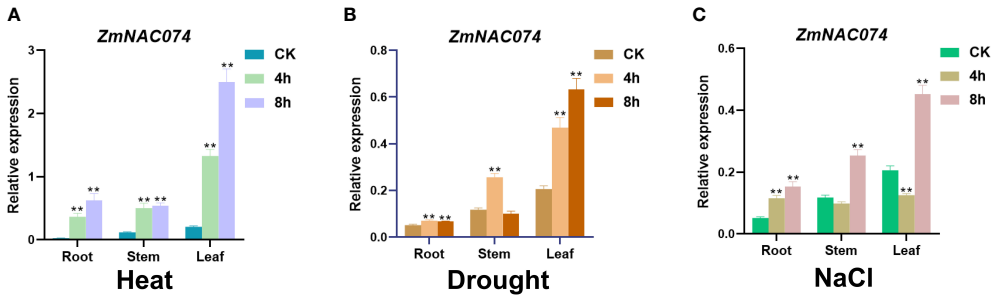


FIGURE 2
Expression pattern analyses of *ZmNAC074* in maize seedlings under various abiotic stress treatments. Expression levels of *ZmNAC074* in maize root, stem and leaf tissues after treatment with 42°CC **(A)**, drought **(B)**, and 200 Mm NaCl **(C)**, respectively. *ZmActin* was used as an internal control. The error bar is calculated through three biological replications. Asterisks above the error bar indicate significant differences (**, $P < 0.01$) using one-way ANOVA and a Fisher's least significant difference (LSD).

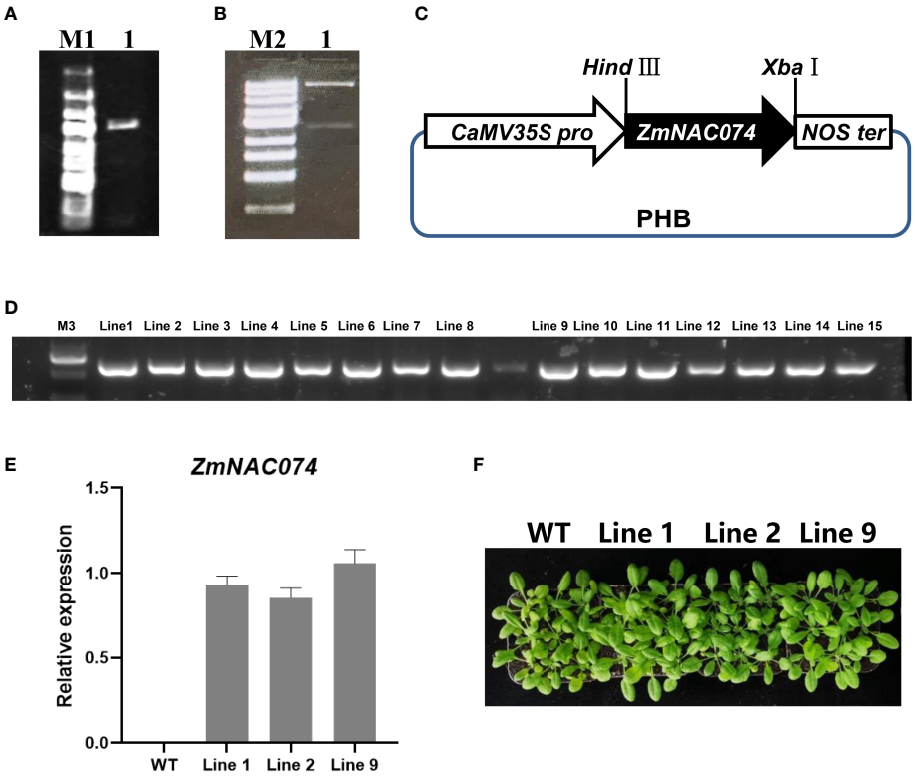


FIGURE 3
Generation and characterization of transgenic *Arabidopsis* plants overexpressing *ZmNAC074*. **(A)** Amplification of full-length CDS of *ZmNAC074*. Marker 1: 5k, 3k, 2k, 1500, 1000, 750, 500, 250, 100 (bp). **(B)** Enzyme validation of recombinant vector with *ZmNAC074* successfully inserted into the PHB vector. Marker 2: 10k, 5k, 3k, 2k, 1500, 1000, 750, 500, 250bp. **(C)** Schematic diagram of recombinant vector construction. **(D)** Detection of hygromycin resistance gene by PCR. Marker 3: 2k, 1000, 750, 500, 250, 100 (bp). **(E)** The qRT-PCR analysis of transgenic *Arabidopsis* plants overexpressing *ZmNAC074*. **(F)** The phenotype analysis of three transgenic *Arabidopsis* lines and WT *Arabidopsis* plants. The error bar is calculated through three biological replications. Asterisks above the error bar indicate significant differences using one-way ANOVA and a Fisher's least significant difference (LSD).

transgenic *Arabidopsis* lines were subjected to heat stress treatments for 24h and 48h, respectively. No visible difference was observed between WT *Arabidopsis* and transgenic *Arabidopsis* lines under normal conditions (Figure 4A). However, under heat stress conditions, after all treated plants were transferred to normal growth environmental conditions and recovered for one week, the WT *Arabidopsis* leaves showed serious wilting symptoms, whereas numerous transgenic *Arabidopsis* leaves remained green (Figure 4A). Notably, the phenotypic difference between WT *Arabidopsis* and transgenic *Arabidopsis* plants under heat stress treatment for 48h was more significant than that for 24h (Figure 4A). According to statistics, after heat treatment for 24h, the survival ratio of transgenic *Arabidopsis* lines were 1.16-1.32 times higher than that of WT *Arabidopsis* plants, respectively. In contrast, after heat treatment for 48h, the survival ratio of all transgenic *Arabidopsis* lines was more than 70%, whereas that of WT *Arabidopsis* was less than 50% (Figure 4B). The results indicated that transgenic *Arabidopsis* exhibited more obvious thermotolerance than WT *Arabidopsis*.

Furthermore, to investigate whether the heat tolerance phenotype of transgenic *Arabidopsis* lines was resulted from alteration of ROS homeostasis, the accumulation of ROS in transgenic *Arabidopsis* lines and WT *Arabidopsis* plants under normal and heat stress conditions was compared, respectively. Qualitative staining by DAB and NBT and quantitative measurement showed that the staining of H_2O_2 and superoxide anion (O_2^-) and the accumulation of H_2O_2 in leaf tissues of transgenic *Arabidopsis* lines were indistinguishable from those in WT *Arabidopsis* plants grown under normal conditions (Figures 4C–E). However, after heat stress treatment, the staining of H_2O_2 and superoxide anion (O_2^-) was more evident and the accumulation of H_2O_2 was revealed to significantly increase in leaf tissues of transgenic *Arabidopsis* lines and WT *Arabidopsis* plants than that of corresponding control plants growing under normal conditions (Figures 4C–E). Although the accumulation of ROS in all plants increased with the prolongation of heat stress treatment time, the staining of H_2O_2 and superoxide anion (O_2^-) in leaf tissues of transgenic *Arabidopsis* lines was less evident than that of WT *Arabidopsis* plants when treated with heat stress treatment for 24h and 48h, respectively. Accordingly, the transgenic *Arabidopsis* lines showed lower H_2O_2 accumulation levels than WT *Arabidopsis* plants. Thus, these results suggest that the cellular oxidative damage of transgenic *Arabidopsis* lines is lesser than that of WT *Arabidopsis* plants. Further, to detect the ability of plants to scavenge ROS, the activities of related SOD and CAT antioxidant enzymes and total antioxidant capacity (T-AOC) were evaluated in this study. Under normal conditions, there were no obvious differences in the SOD and CAT activities and T-AOC between the WT *Arabidopsis* and transgenic *Arabidopsis* lines. However, with the extension of heat stress time, the SOD and CAT activities and T-AOC of all plants were exhibited to increase, but the SOD and CAT activities and T-AOC of transgenic *Arabidopsis* lines were much higher than those of WT *Arabidopsis* plants (Figures 4F–H). Thus, these results suggest that heat stress resistance of *ZmNAC074*-overexpressed transgenic *Arabidopsis* lines may be resulted from their enhanced ROS-scavenging capability.

Moreover, MDA (Malondialdehyde) can severely damage plant cell membranes, and thereby the degree of MDA accumulation is usually regarded as an important indicator of membrane-lipid peroxidation (Davey et al., 2005). In this study, no differences were observed in accumulation of MDA contents between all plants under normal conditions. However, after heat stress treatment, MDA contents of transgenic *Arabidopsis* lines were significantly lower than in WT *Arabidopsis* plants (Figure 4I). Therefore, these results suggest that overexpression of *ZmNAC074* in transgenic *Arabidopsis* may weaken the membrane lipid peroxidation and enhance the stability of cell membrane under heat stress, thereby contributing to slow down the oxidative damage caused by heat stress. In addition, compared with WT *Arabidopsis* plants, heat stress increased the accumulation of osmotic adjustment substances, including soluble proteins and proline in transgenic *Arabidopsis* lines (Figures 4J, K). Moreover, without heat stress treatment, the leaf chlorophyll and carotenoid contents of transgenic *Arabidopsis* lines were comparable to those of WT *Arabidopsis* plants (Figures 4L, M). Interestingly, after 24h of heat stress treatment, there was no significant difference in chlorophyll content between transgenic *Arabidopsis* lines and WT *Arabidopsis* plants, but the carotenoid content of transgenic *Arabidopsis* lines was 1.05-1.08 times higher than that of WT *Arabidopsis* plants. Moreover, after 48h of heat stress treatment, the leaf chlorophyll and carotenoid contents of transgenic *Arabidopsis* lines were 1.14-1.17 and 1.11-1.13 times higher than those of WT *Arabidopsis* plants, respectively. Therefore, these results demonstrate that transgenic *Arabidopsis* lines can enhance heat stress tolerance by retaining more chlorophyll and carotenoids to protect photosystem II under heat stress.

Overexpression of *ZmNAC074* alters expression patterns of heat stress responsive genes

To elucidate the possible regulatory roles of *ZmNAC074* in heat stress tolerance, the expression levels of *ZmNAC074* and heat stress responsive genes have been characterized by qRT-PCR (Figure 5A). There was no significant difference in the expression level of *ZmNAC074* among three transgenic *Arabidopsis* lines under normal conditions and after heat stress treatment for 24h. However, after 48h of heat stress treatment, the expression level of *ZmNAC074* in line 9 was higher than those in line 1 and line 2. It was worth noting that with the prolongation of heat stress treatment

10.3389/fpls.2022.986628

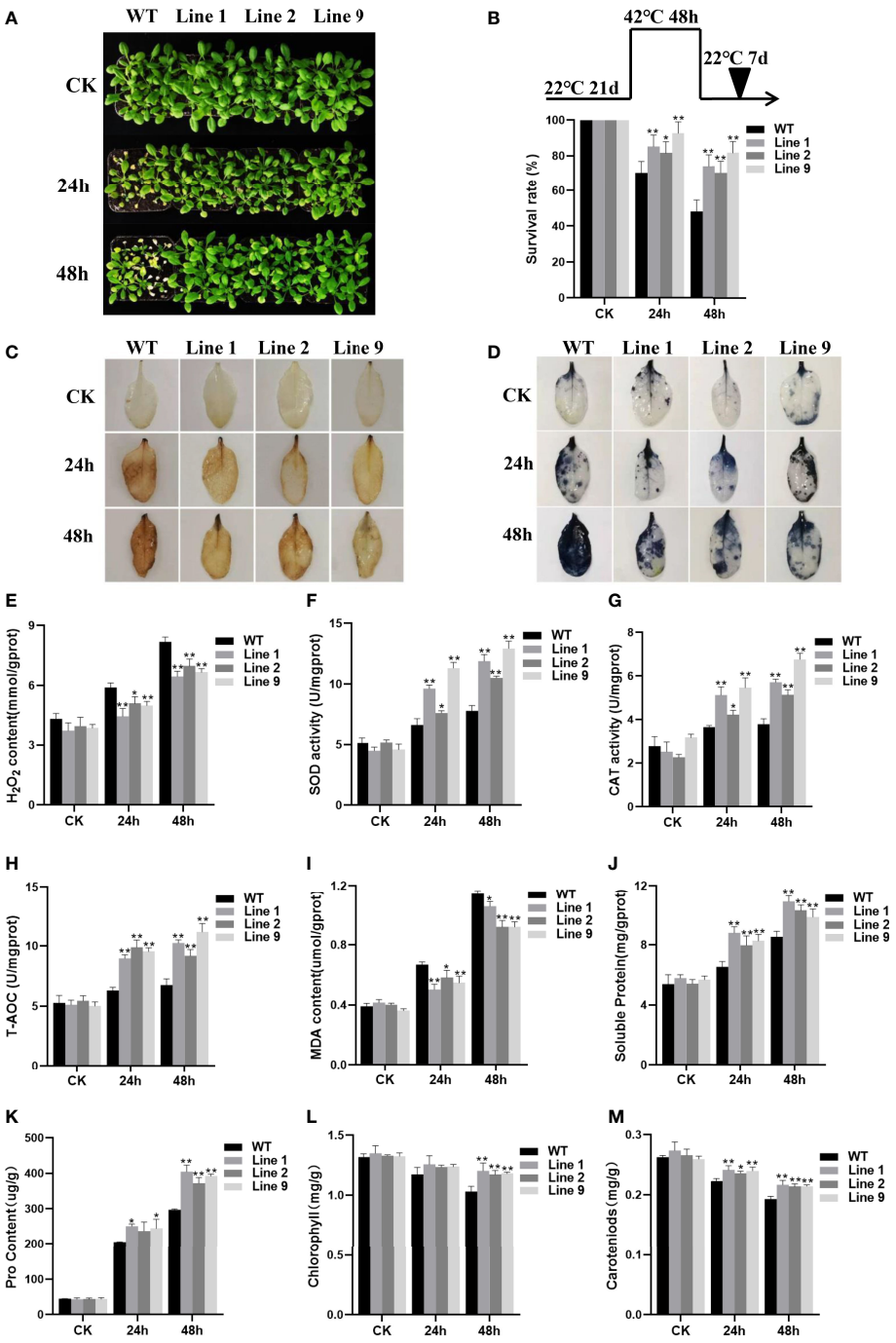


FIGURE 4
Analysis of heat resistance of transgenic plants overexpressing *ZmNAC074*. **(A)** Transgenic and WT *Arabidopsis* following heat stress treatment at 42°C for 24 h and 48h, respectively, and recovery for one week under 22°C normal conditions. Plants continually grown at 22°C were used as controls. **(B)** Survival rates of transgenic *Arabidopsis* lines and WT *Arabidopsis* plants after heat stress treatments. **(C, D)** H_2O_2 and O^{2-} accumulation was detected by using histochemical staining with DAB and NBT, respectively. **(E)** H_2O_2 contents in leaves of transgenic *Arabidopsis* lines and WT *Arabidopsis* plants before and after heat stress treatments. **(F–H)** Changes in activities of antioxidant enzymes SOD and CAT and the total antioxidant capacity in leaves of transgenic *Arabidopsis* lines and WT *Arabidopsis* plants before and after heat stress treatments. **(I–K)** Analyses of MDA, soluble protein and proline contents in leaves of transgenic *Arabidopsis* lines and WT *Arabidopsis* plants before and after heat stress treatments. **(L, M)** The leaf chlorophyll and carotenoid contents of transgenic *Arabidopsis* lines and WT *Arabidopsis* plants before and after heat stress treatments. *AtActin* was used as an internal control. The error bar is calculated through three biological replications. Asterisks above the error bar indicate significant differences ($P < 0.05$, $P < 0.01$) using one-way ANOVA and a Fisher's least significant difference (LSD).

time, the expression level of *ZmNAC074* gradually increased. In addition, the expression levels of 11 heat stress responsive genes (*AtHsp70-4*, *AtHsp101*, *AtHsp18.2*, *AtHsfA1a-e*, *AtHsfA2*, *AtHsfA3*, *AtHsfA7a*, and *AtbZIP60*) were detected (Figures 5B–L). Under normal conditions, except that the expression levels of *AtHsfA1b* and *AtHsfA2* genes in transgenic *Arabidopsis* lines were significantly higher than those in WT *Arabidopsis* plants, there was no significant difference in the expression levels of other genes between transgenic *Arabidopsis* lines and WT *Arabidopsis* plants under normal conditions. In contrast, under heat stress treatment, except that the expression level of *AtHsfA3* gene in transgenic *Arabidopsis* lines was lower than that in WT *Arabidopsis* plants, the

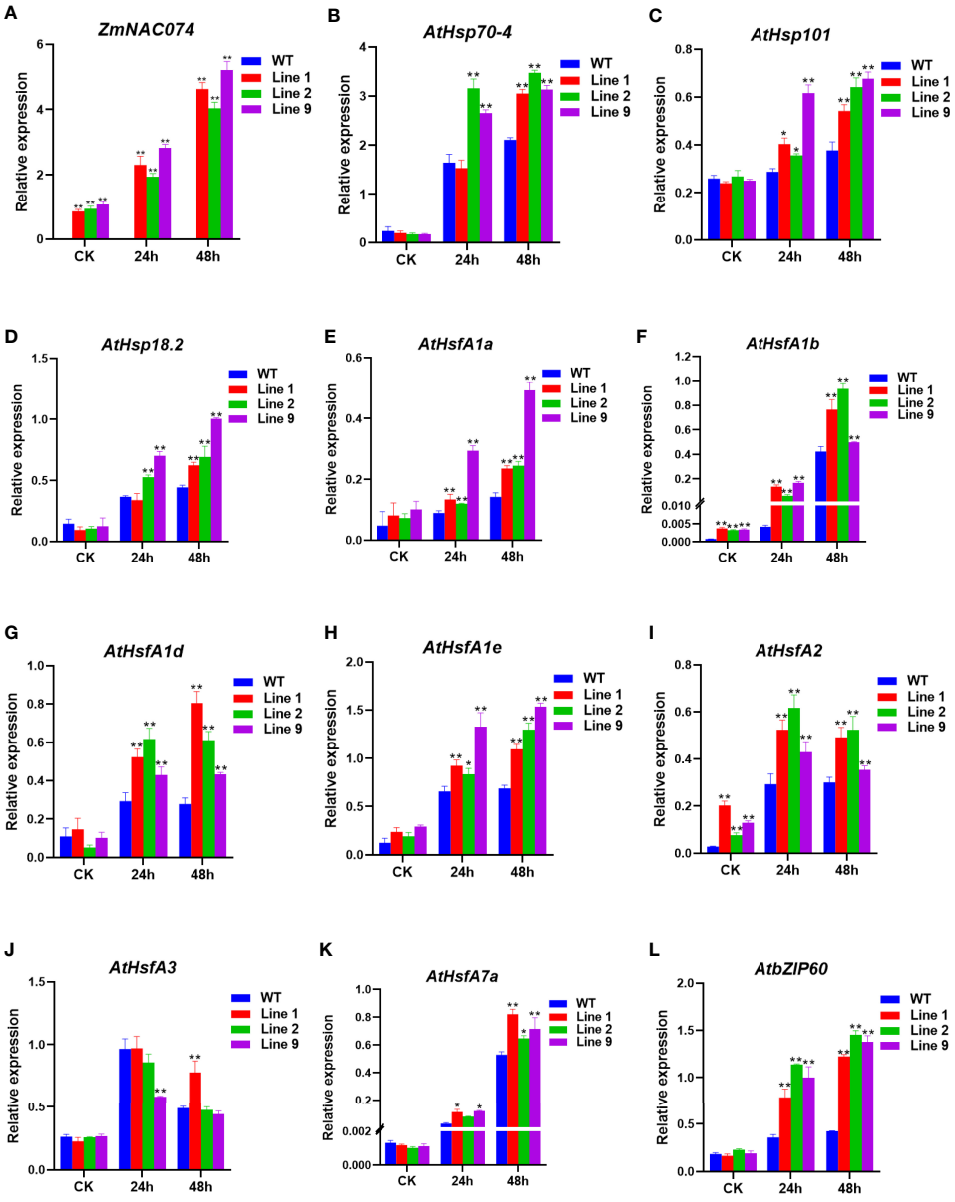


FIGURE 5
Expression levels of *ZmNAC074* and stress-responsive genes by qRT-PCR in transgenic *Arabidopsis* lines and WT *Arabidopsis* plants before and after heat stress treatments. Three-week-old transgenic *Arabidopsis* lines and WT *Arabidopsis* plants were exposed to heat stress (42°C) for 24 h and 48 h, and leaves were sampled for RNA extraction, cDNA synthesis and qPCR analysis. Gene-specific primers were used for detection of relative expression levels of stress-responsive genes, the raw date were normalized using *AtActin* as an internal control. For each experiment, three technical replicates were conducted. **(A–L)** The expression levels of *ZmNAC074*, *AtHsp70-4*, *AtHsp101*, *AtHsp18.2*, *AtHsfA1a-e*, *AtHsfA2*, *AtHsfA3*, *AtHsfA7a* and *AtbZIP60* were determined by qRT-PCR. *AtActin* was used as an internal control. The error bar is calculated through three biological replications. Asterisks above the error bar indicate significant differences (*P < 0.05, **P < 0.01) using one-way ANOVA and a Fisher's least significant difference (LSD).

expression levels of other genes in transgenic *Arabidopsis* lines were higher than those in WT *Arabidopsis* plants. Thus, these results suggest that *ZmNAC074* may enhance heat stress tolerance by regulating heat stress responsive genes.

Overexpression of *ZmNAC074* affects the expression levels of genes associated with ROS scavenging

To further detect the ability of the *ZmNAC074*-overexpressed transgenic *Arabidopsis* to scavenge ROS, the expression levels of some antioxidant-related genes (*AtAPX1-8* and *AtGPX1-8*) between transgenic *Arabidopsis* lines and WT *Arabidopsis* plants under normal conditions and heat stress treatments were determined, respectively (Figures 6A–P). Under normal conditions, there were no significant differences in the expression levels of most antioxidant-related genes between transgenic *Arabidopsis* lines and WT *Arabidopsis* plants, except for *AtAPX3*, *AtAPX7*, *AtAPX8*, *AtGPX1*, and *AtGPX2*. However, under heat stress treatments, the expression levels of most antioxidant-related genes in transgenic *Arabidopsis* lines were significantly higher than those in WT *Arabidopsis* plants. Noticeably, the expression levels of *AtGPX2* in three transgenic *Arabidopsis* lines was lower than that in WT *Arabidopsis* plants after heat stress treatment for 24h, and only transgenic line 9 exhibited higher *AtGPX2* expression level than WT *Arabidopsis* plants after heat stress treatment for 48h. Interestingly, the expression levels of most antioxidant-related genes were the highest in transgenic

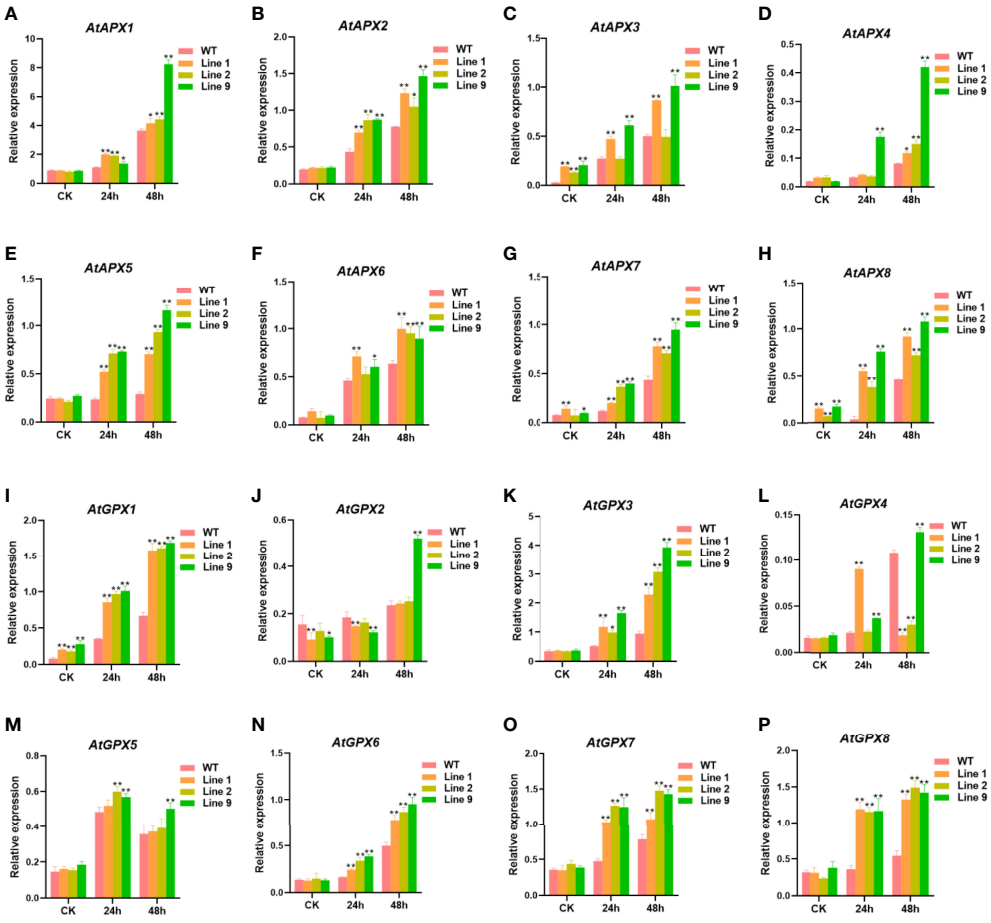


FIGURE 6
Expression levels of antioxidant-associated genes in transgenic *Arabidopsis* lines and WT *Arabidopsis* plants before and after heat stress treatments. Three-week-old transgenic *Arabidopsis* lines and WT *Arabidopsis* plants were exposed to heat stress (42°C) for 24 h and 48 h, and leaves were sampled for RNA extraction, cDNA synthesis and qPCR analysis. Gene-specific primers were used for detection of relative expression levels of stress-responsive genes, the raw date were normalized using *AtActin* as an internal control. For each experiment, three technical replicates were conducted. **(A–P)** The expression levels of *AtAPX1-8* and *AtGPX1-8* were determined by qRT-PCR. *AtActin* was used as an internal control. The error bar is calculated through three biological replications. Asterisks above the error bar indicate significant differences (*P < 0.05, **WFI 2P < 0.01) using one-way ANOVA and a Fisher's least significant difference (LSD).

line 9 and the lowest in transgenic line 2. Taken together, these results suggest that overexpression of *ZmNAC074* in transgenic *Arabidopsis* can upregulate the expression levels of antioxidant-related genes under heat stress treatments.

Protein protein interaction networks between several NAC MTFs and stress response- associated proteins in *Arabidopsis* and rice

To reveal the potential interaction effects of ZmNAC074 in response to heat stress, the possible interactions between some NAC MTFs and stress response-associated proteins in *Arabidopsis* and rice were integrated, especially OsNTL3 and AtNAC089, which are closely related to ZmNAC074 protein. The analysis of protein protein interaction network in *Arabidopsis* showed that bZIP family members, especially bZIP60, may be the central regulators of functional association network, which can interact with three NAC MTFs (including AtNAC089, AtNAC62, and AtNAC103) (Figure 7A). Further, the analysis of protein protein interaction network in rice displayed that BIP2 and BIP4 can interact with OsNTL3 (Figure 7B). Moreover, BIP2 and BIP4 are also closely related to bZIP family members, indicating the interaction between HSR-associated proteins and bZIP proteins. These networks are extremely complex, and there may be a variety of hierarchical regulation of NAC proteins in plants under heat or ER stress, such as the possibility of the interaction between OsNTL3 and BIP2, BIP2 and BZIP50 (a transcription factor involved in ER stress response), and BZIP50 and HSFA3 (a transcriptional regulator that specifically binds DNA of heat shock promoter elements). Moreover, the protein information involved in the figures was described as shown in Supplementary Table S4. Overall, these results suggest that NAC MTFs, including ZmNAC074 protein, may interact with UPR- and HSR-associated proteins to enhance stress tolerance.

Discussion

Plants have developed sophisticated signaling pathways to deal with heat stress (Guihur et al., 2022). Numerous NAC TF genes from various plants, such as *ANAC042* and *NAC019* from *Arabidopsis* (Shahnejat-Bushehri et al., 2012; Guan et al., 2014), *OsNTL3* and *SNAC3* from rice (Fang et al., 2015; Liu et al., 2020), *TaNAC2L* from wheat (Guo et al., 2015), *CaNAC035*, *CaNAC46* and *CaNAC2c* from pepper (Zhang et al., 2020; Cai et al., 2021; Ma et al., 2021), have been verified to respond to heat stress, suggesting their potential functions in heat stress tolerance. However, there are few reports on functional identification of heat resistance of NAC TFs in maize. Thus, in this study, *ZmNAC074* was selected from our previous transcriptome data (Qian et al., 2019) and qRT-PCR analysis in maize response to heat stress to perform further functional verification. Further, physiological and molecular responses of transgenic *Arabidopsis* overexpressing *ZmNAC074* under heat stress treatments were revealed in this study.

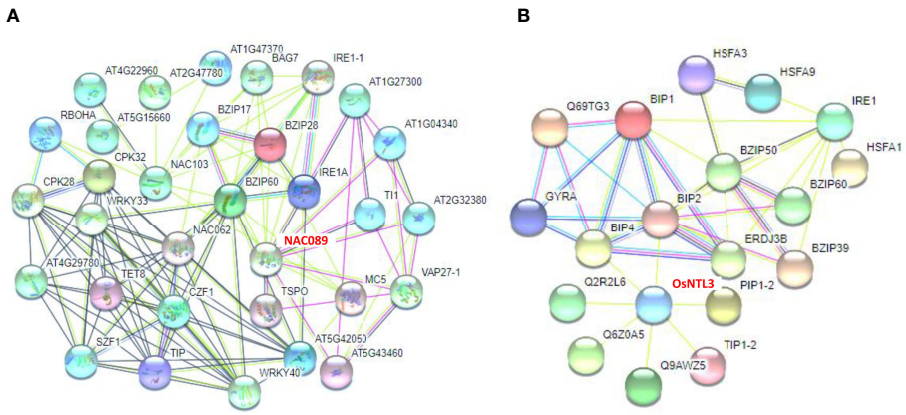


FIGURE 7
Protein Protein Interaction networks of NAC MTFs and stress response-associated proteins. **(A)** Functional association networks of NAC MTFs and stress response-associated proteins in *Arabidopsis*. AtNAC089 (shown in red font as NAC089) was highlighted to interact with the endoplasmic reticulum (ER) associated protein IRE1A. **(B)** Functional association networks of OsNTL3 (shown in red font) and heat or ER stress response-associated proteins in rice. OsNTL3 was highlighted to interact with BIP2 (a heat shock 70 kDa protein that functions as chaperone during ER stress response). Thick lines indicate high interaction.

ZmNAC074 is responsive to various abiotic stresses in maize

Studies have shown that under abiotic stresses, membrane-bound transcription factor (MTF) can be transferred into the nucleus and become an active TF (Seo and Kim, 2008), such as TaNTL1 and OsNTL3 (Liu et al., 2020; Sun et al., 2022). A previous study has shown that ZmNAC074 (also known as ZmNTL1) can be localized to plasma membrane and that the GFP-ZmNTL1-△TM (lacking the transmembrane motif) fusion construct product can be co-localized with nuclear marker (Wang et al., 2016). Moreover, ZmNAC074 protein shares high similarity of amino acid sequence with the reported orthologous OsNTL3 protein in rice, suggesting a similar functional role can exist in between ZmNAC074 and OsNTL3. Therefore, we speculate that ZmNAC074, like OsNTL3, can be localized to the plasma membrane under normal conditions and translocate to the nucleus in response to heat stress or other stresses (Liu et al., 2020). For another, *ZmNAC074* may play a crucial role in response to heat, drought, and salt stress, especially heat stress. In addition, under these three kinds of various stresses, the expression of *ZmNAC074* in leaves was changed highly and significantly compared with other tissues, indicating that *ZmNAC074* may play a vital role through the tissue-specific expression in leaves.

Overexpression of *ZmNAC074* confers thermotolerance in transgenic *Arabidopsis* by regulating the accumulation of multiple stress-related metabolites

Plants have evolved a variety of morphological, physiological and biochemical mechanisms to cope with heat stress, and the corresponding indicators have been used to evaluate heat resistance (Guihur et al., 2022). Phenotypically, the thermotolerance of transgenic *Arabidopsis* was significantly enhanced after heat stress. The enhancement of the adaptability of these transgenic *Arabidopsis* plants to heat stress was inseparable from the synchronous adaptation changes of external morphology and biochemical levels (Lephatsi et al., 2021). For example, levels of lipid oxidation markers such as MDA are typically reduced in plants designed as heat-resistant (Davey et al., 2005; Alché, 2019), while soluble proteins and proline, a penetrant or a free radical scavenger, increase (Alvarez et al., 2022; Ghosh et al., 2022). Therefore, the overexpression of exogenous *ZmNAC074* may enhance tolerance to heat stress through decreasing lipid peroxidation, maintaining the stability of plant membrane structure and inducing proline and soluble protein biosynthesis to enhance osmotic potential in transgenic *Arabidopsis*.

Furthermore, the photosynthetic organelles of plants are highly sensitive to heat stress treatment and plants with higher chlorophyll content can be considered to exhibit greater heat tolerance (Hu et al., 2020; Muhammad et al., 2020). Carotenoids can be used as a stress-protective metabolite and mitigate harmful stress-induced ROS (Kang et al., 2018; Felemban et al., 2019; Guihur et al., 2022). After heat stress treatment, the content of carotenoids in transgenic *Arabidopsis* was higher than that in WT *Arabidopsis*, probably because the overexpression of *ZmNAC074* in *Arabidopsis* may promote the synthesis of carotenoid production related enzymes under heat stress. However, there was no significant difference in chlorophyll content between WT *Arabidopsis* and transgenic *Arabidopsis* plants under heat stress after 24 h, but the chlorophyll content of transgenic *Arabidopsis* was significantly higher than that of WT *Arabidopsis* after 48 h, which may be due to the slight damage caused by heat stress in a short time was not enough for ZmNAC074 to activate numerous related chlorophyll degradation genes. In any case, further study is deserved to excavate the exact mechanisms underlying the positive role of *ZmNAC074* in regulating heat stress response.

Overexpression of *ZmNAC074* plays a pivotal role in regulating ROS homeostasis

ROS is similar to a double-edged sword and ROS homeostasis is vital for plant growth, development and acclimatization against stresses (Sachdev et al., 2021). Excessive ROS generated by heat stress are toxic molecules capable of causing oxidative damage to proteins, nucleic acids, carbohydrates, cell membranes, lipids, and other sites of cells (Huchzermeyer et al., 2022). However, plants have evolved an antioxidant defense system including diverse antioxidants like SOD and CAT, which can protect them against oxidative damage (Baxter et al., 2014). Consistently, in this study, H_2O_2 levels and O_2^- contents were lower while SOD and CAT activities were higher in transgenic *Arabidopsis* than WT *Arabidopsis* under heat stress treatments, indicating that increased SOD and CAT activities resulted from *ZmNAC074* overexpression in transgenic *Arabidopsis* is associated with heat stress tolerance through ROS-mediated stress responsive signaling pathway.

Further, APXs and GPXs can protect cells from stress-induced oxidative damage and play a key role in plant development and growth (Bela et al., 2015; Li et al., 2019; Singh et al., 2022). In this study, the significantly up-regulated expression of *AtAPX1-8* and *AtGPX1-8* in transgenic *Arabidopsis* suggested that *ZmNAC074* may enhance the ability of antioxidants to scavenge excessive ROS by up-regulating these antioxidant enzyme genes, thus enhancing the ability to resist heat stress. Notably, several genes (*AtAPX3*,

AtAPX7, *AtAPX8*, and *AtGPX1*) in transgenic *Arabidopsis* were expressed at higher levels than in WT *Arabidopsis* under normal conditions. We speculate that *ZmNAC074* may trigger antioxidant defense system through signaling before heat stress. Under heat stress treatments, the antioxidant response was elevated, further increasing the activity of antioxidant enzymes. This protective mechanism may appear to cause more limited damage to cellular components in transgenic *Arabidopsis* lines in comparison to WT *Arabidopsis* plants. In conclusion, these results have evidenced that overexpression of *ZmNAC074* can trigger the expression levels of numerous stress-associated genes in transgenic *Arabidopsis*. These genes can be considered as direct or indirect downstream genes of *ZmNAC074*, and further works are required to reveal the signal transduction pathways associated with *ZmNAC074* during heat stress.

Overexpression of *ZmNAC074* regulates the expression of HSR-associated genes in transgenic *Arabidopsis*

Previous studies have demonstrated that heat shock response (HSR) in cytoplasm and unfolded protein response (UPR) in ER act as two evolutionarily conserved systems that protect plants from heat stress (Li et al., 2020b). Heat stress induces HSR, in which heat shock transcription factors (HSFs) are a class of conservative transcription factors and can bind to heat shock cis-regulatory elements in promoter regions of *HSP* genes and promote the expression of *HSP* genes (Hayes et al., 2021; Li and Howell, 2021). HSPs, as molecular chaperones, promote the correct folding and aggregation of proteins (Hayes et al., 2021). In this study, the expression levels of most *HSP* and *HSF* genes in transgenic *Arabidopsis* were more highly expressed in the transgenic *Arabidopsis* lines, indicating that overexpression of *ZmNAC074* confers enhanced heat stress tolerance of transgenic *Arabidopsis* by up-regulating the expression levels of these heat stress responsive genes. Therefore, *ZmNAC074* may be a candidate gene for genetic engineering in generating crops to enhance heat tolerance.

Overexpression of *ZmNAC074* regulates the expression of *AtbZIP60* (UPR-associated gene) in transgenic *Arabidopsis*

Previous studies have revealed that *AtbZIP60* can encode an UPR-associated transcription factor, and respond to NaCl and tunicamycin (TM) and thereby induce endoplasmic reticulum (ER) stress and enhance the abiotic stress tolerance in *Arabidopsis* (Li et al., 2017). Moreover, the close relationship between plant NAC proteins and ER stress has been revealed (Yu et al., 2022). For instance, three *Arabidopsis* NAC TFs (including AtNAC062, AtNAC089, and AtNAC103) can be activated to respond to ER stress and regulate different UPR-associated gene clusters (Sun et al., 2013; Yang et al., 2014a; Yang et al., 2014b). Notably, it has been reported that OsNTL3 (orthologous with ZmNAC074) directly binds to the promoter of *OsbZIP74* (orthologous with *AtbZIP60*) and regulates its expression in response to heat stress (Liu et al., 2020). Thus, in this study, the expression level of *AtbZIP60* in transgenic *Arabidopsis* was significantly higher than that in WT *Arabidopsis* under heat stress, indicating that *ZmNAC074* may act on *AtbZIP60* to alleviate UPR caused by heat stress to enhance heat stress tolerance. Moreover, the protein protein interaction networks further revealed that AtNAC089 (orthologous with ZmNAC074) interacted with AtbZIP60 in *Arabidopsis* and OsNTL3 may also affect OsbZIP50 (orthologous to AtbZIP60) by interacting with BiP2 or BiP4 in rice, implying that ZmNAC074 may function in heat stress-induced UPR-associated regulatory pathways. However, further investigations are needed to clarify the detailed mechanisms of the interactions between ZmNAC074 and these bZIP proteins in regulating stress responses in maize.

Taken together, we successfully constructed transgenic *Arabidopsis* plants overexpressing *ZmNAC074* under the control of *CaMV 35S* promoter in this study. As expected, the transgenic *Arabidopsis* plants exhibited enhanced tolerance to heat stress, which might be associated with modulating HSR, UPR and ROS homeostasis as shown in the proposed model in this study (Figure 8). Therefore, overexpression of *ZmNAC074* may confer thermotolerance in transgenic *Arabidopsis* through the involvement in multiple diverse regulatory pathways. However, the molecular mechanisms underlying heat stress response still remain to be further elucidated.

Conclusion

In conclusion, our results in this study demonstrate that *ZmNAC074* encodes a maize stress- responsive NAC transcription factor, which may be involved in response to various abiotic stresses such as heat, drought and salt. Moreover, functional analysis displays that overexpression of *ZmNAC074* can confer enhanced tolerance to heat stress through modulating the alterations of various stress-related metabolites including reactive oxygen species (ROS), antioxidant, malondialdehyde (MDA), proline, soluble protein, chlorophyll and carotenoid contents in transgenic *Arabidopsis*, indicating that *ZmNAC074* may play a crucial role in enhancing heat tolerance of transgenic *Arabidopsis* through the

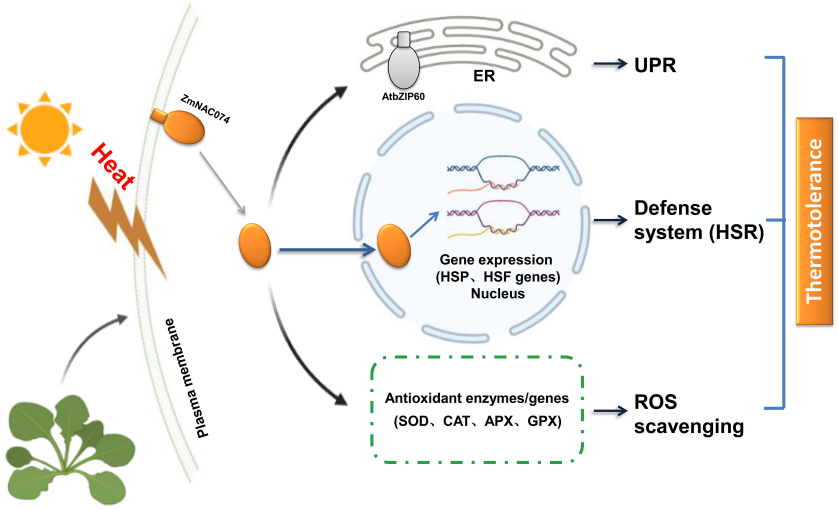


FIGURE 8
A proposed model for the potential roles of *ZmNAC074* in response to heat stress in transgenic *Arabidopsis*. Under normal conditions, the putative protein, ZmNAC074, is located on the plasma membrane. However, under heat stress treatments, ZmNAC074 protein may be treated by an unknown mechanism to relocate the activated ZmNAC074 protein from the plasma membrane to the nucleus and up-regulate the expression of *AtbZIP60* that associated with UPR and other downstream genes that associated with HSR and ROS. Therefore, ZmNAC074 protein may transfer heat stress signals from the plasma membrane to the nucleus and regulate heat stress-related genes to confer enhanced thermotolerance in transgenic *Arabidopsis*..

involvement in several different metabolic pathways. Further, the expression analyses of some ROS scavenging genes, HSR- and UPR-associated genes demonstrate that *ZmNAC074* can enhance heat resistance in transgenic *Arabidopsis* through modulating HSR, UPR and ROS homeostasis. Taken together, our results demonstrate that *ZmNAC074* may encode a functional TF in maize and act as a key candidate regulatory gene for heat stress tolerance regulation and genetic improvement in maize as well as in other crops.

Data availability statement

The datasets presented in this study can be found in online repositories. The names of the repository/repositories and accession number(s) can be found in the article/ Supplementary Material.

Ethics statement

This article does not contain any studies with human participants or animals performed by the authors. These methods were carried out in accordance with relevant guidelines and regulations including the IUCN Policy Statement on Research Involving Species at Risk of Extinction and the Convention on the Trade in Endangered Species of Wild Fauna and Flora. We confirm that all experimental protocols were approved by Anhui Agriculture University and Anhui Normal University.

Author contributions

These studies were designed by YQ. YX, QL, YZ and XL carried out all the experimental analyses and prepared all figures and tables. The manuscript was drafted by YX. YQ assisted in explaining the results and revised the final manuscript. All authors have reviewed and approved the final manuscript.

Funding

This study was supported by grants from the National Natural Science Foundation of China (NSFC) (Grant NO.31571673) and the open fundings of National Engineering Laboratory of Crop Stress Resistance Breeding (Grant NO.KNZJ1023) and Anhui Provincial Key Laboratory of the Conservation and Exploitation of Biological Resources (Grant NO.Swzy202003) and Anhui Provincial Academic Funding Project for Top Talents in Disciplines (Majors) (Grant NO.gxbjZD 2021044). The funders had no role in the study design, collection, analysis and interpretation of data, or in the

writing of the report or decision to submit the article for publication.

Acknowledgments

The authors are grateful to the editor and reviewers for critically evaluating the manuscript and providing constructive comments for its improvement.

Conflict of interest

The authors declare that the research was conducted in the absence of any commercial or financial relationships that could be construed as a potential conflict of interest.

Publisher's note

All claims expressed in this article are solely those of the authors and do not necessarily represent those of their affiliated organizations, or those of the publisher, the editors and the reviewers. Any product that may be evaluated in this article, or claim that may be made by its manufacturer, is not guaranteed or endorsed by the publisher.

Supplementary material

The Supplementary Material for this article can be found online at: https://www.frontiersin.org/articles/10.3389/fpls.2022.986628/full#supplementary-material

References

Aguilar Diaz De Leon, J., and Borges, C. R. (2020). Evaluation of oxidative stress in biological samples using the thiobarbituric acid reactive substances assay. *J. Vis. Exp.* 159, e61122. doi: 10.3791/61122

Alché, J. D. (2019). A concise appraisal of lipid oxidation and lipoxidation in higher plants. *Redox Biol.* 23, 101136. doi: 10.1016/j.redox.2019.101136

Ali, M., Muhammad, I., Ul Haq, S., Alam, M., Khattak, A. M., Akhtar, K., et al. (2020). The *CaChiVI2* gene of *Capsicum annuum* l. confers resistance against heat stress and infection of phytophthora capsici. *Front. Plant Sci.* 11. doi: 10.3389/fpls.2020.00219

Alvarez, M. E., Savouré, A., and Szabados, L. (2022). Proline metabolism as regulatory hub. *Trends Plant Sci.* 27, 39–55. doi: 10.1016/j.tplants.2021.07.009

Baxter, A., Mittler, R., and Suzuki, N. (2014). ROS as key players in plant stress signalling. *J. Exp. Bot.* 65, 1229–1240. doi: 10.1093/jxb/ert375

Bela, K., Horváth, E., Gallé, Á., Szabados, L., Tari, I., and Csiszár, J. (2015). Plant glutathione peroxidases: emerging role of the antioxidant enzymes in plant development and stress responses. *J. Plant Physiol.* 176, 192–201. doi: 10.1016/j.jplph.2014.12.014

Botticella, E., Savatin, D. V., and Sestili, F. (2021). The triple jags of dietary fibers in cereals: How biotechnology is longing for high fiber grains. *Front. Plant Sci.* 12. doi: 10.3389/fpls.2021.745579

Cai, W., Yang, S., Wu, R., Cao, J., Shen, L., Guan, D., et al. (2021). Pepper NAC-type transcription factor NAC2c balances the trade-off between growth and defense responses. *Plant Physiol.* 186, 2169–2189. doi: 10.1093/plphys/kiab190

Chen, Q., Bao, C., Xu, F., Ma, C., Huang, L., Guo, Q., et al. (2021). Silencing *GhJUB1L1* (*JUB1-like 1*) reduces cotton (*Gossypium hirsutum*) drought tolerance. *PloS One* 16, e0259382. doi: 10.1371/journal.pone.0259382

Christianson, J. A., Dennis, E. S., Llewellyn, D. J., and Wilson, I. W. (2010). ATAF NAC transcription factors: regulators of plant stress signaling. *Plant Signal Behav.* 5, 428–432. doi: 10.4161/psb.5.4.10847

Daudi, A., and O'brien, J. A. (2012). Detection of hydrogen peroxide by DAB staining in *Arabidopsis* leaves. *Bio Protoc.* 2 (18), e263.

Davey, M. W., Stals, E., Panis, B., Keulemans, J., and Swennen, R. L. (2005). High-throughput determination of malondialdehyde in plant tissues. *Anal. Biochem.* 347, 201–207. doi: 10.1016/j.ab.2005.09.041

Diao, P., Chen, C., Zhang, Y., Meng, Q., Lv, W., and Ma, N. (2020). The role of NAC transcription factor in plant cold response. *Plant Signal Behav.* 15, 1785668. doi: 10.1080/15592324.2020.1785668

Driedonks, N., Rieu, I., and Vriezen, W. H. (2016). Breeding for plant heat tolerance at vegetative and reproductive stages. *Plant Reprod.* 29, 67–79. doi: 10.1007/s00497-016-0275-9

Fang, Y., Liao, K., Du, H., Xu, Y., Song, H., Li, X., et al. (2015). A stress-responsive NAC transcription factor SNAC3 confers heat and drought tolerance through modulation of reactive oxygen species in rice. *J. Exp. Bot.* 66, 6803–6817. doi: 10.1093/jxb/erv386

Felemban, A., Braguy, J., Zurbriggen, M. D., and Al-Babili, S. (2019). Apocarotenoids involved in plant development and stress response. *Front. Plant Sci.* 10, 1168. doi: 10.3389/fpls.2019.01168

Gai, W. X., Ma, X., Li, Y., Xiao, J. J., Khan, A., Li, Q. H., et al. (2020). *CaHsfA1d* improves plant thermotolerance *via* regulating the expression of stress- and antioxidant-related genes. *Int. J. Mol. Sci.* 21, 8374. doi: 10.3390/ijms21218374

Ghosh, U. K., Islam, M. N., Siddiqui, M. N., Cao, X., and Khan, M. (2022). Proline, a multifaceted signalling molecule in plant responses to abiotic stress: understanding the physiological mechanisms. *Plant Biol. (Stuttg).* 24, 227–239. doi: 10.1111/plb.13363

Goldring, J. P. D. (2019). Measuring protein concentration with absorbance, lowry, Bradford coomassie blue, or the smith bicinchoninic acid assay before electrophoresis. *Methods Mol. Biol.* 1855, 31–39. doi: 10.1007/978-1-4939-8793-1_3

Guan, Q., Yue, X., Zeng, H., and Zhu, J. (2014). The protein phosphatase RCF2 and its interacting partner NAC019 are critical for heat stress-responsive gene regulation and thermotolerance in *Arabidopsis*. *Plant Cell* 26, 438–453. doi: 10.1105/tpc.113.118927

Guihur, A., Rebeaud, M. E., and Goloubinoff, P. (2022). How do plants feel the heat and survive? *Trends Biochem. Sci.* 47, 824–838. doi: 10.1016/j.tibs.2022.05.004

Guo, W., Zhang, J., Zhang, N., Xin, M., Peng, H., Hu, Z., et al. (2015). The wheat NAC transcription factor TaNAC2L is regulated at the transcriptional and post-translational levels and promotes heat stress tolerance in transgenic *Arabidopsis*. *PloS One* 10, e0135667. doi: 10.1371/journal.pone.0135667

Hadwan, M. H., and Abed, H. N. (2016). Data supporting the spectrophotometric method for the estimation of catalase activity. *Data Brief* 6, 194–199. doi: 10.1016/j.dib.2015.12.012

Hayes, S., Schachtschabel, J., Mishkind, M., Munnik, T., and Arisz, S. A. (2021). Hot topic: Thermosensing in plants. *Plant Cell Environ.* 44, 2018–2033. doi: 10.1111/pce.13979

Huang, L. J., Cheng, G. X., Khan, A., Wei, A. M., Yu, Q. H., Yang, S. B., et al. (2019). *CaHSP16.4*, a small heat shock protein gene in pepper, is involved in heat and drought tolerance. *Protoplasma* 256, 39–51. doi: 10.1007/s00709-018-1280-7

Huchzermeyer, B., Menghani, E., Khardia, P., and Shilu, A. (2022). Metabolic pathway of natural antioxidants, antioxidant enzymes and ROS providence. *Antioxidants. (Basel).* 11, 761. doi: 10.3390/antiox11040761

Hu, S., Ding, Y., and Zhu, C. (2020). Sensitivity and responses of chloroplasts to heat stress in plants. *Front. Plant Sci.* 11. doi: 10.3389/fpls.2020.00375

Hu, W., Ren, Q., Chen, Y., Xu, G., and Qian, Y. (2021). Genome-wide identification and analysis of *WRKY* gene family in maize provide insights into regulatory network in response to abiotic stresses. *BMC Plant Biol.* 21, 427. doi: 10.1186/s12870-021-03206-z

Hussain, H. A., Men, S., Hussain, S., Chen, Y., Ali, S., Zhang, S., et al. (2019). Interactive effects of drought and heat stresses on morpho-physiological attributes,

yield, nutrient uptake and oxidative status in maize hybrids. *Sci. Rep.* 9, 3890. doi: 10.1038/s41598-019-40362-7

Kang, C., He, S., Zhai, H., Li, R., Zhao, N., and Liu, Q. (2018). A sweetpotato auxin response factor gene (*IbARF5*) is involved in carotenoid biosynthesis and salt and drought tolerance in transgenic *Arabidopsis*. *Front. Plant Sci.* 9, 1307. doi: 10.3389/fpls.2018.01307

Khan, A., Li, R. J., Sun, J. T., Ma, F., Zhang, H. X., Jin, J. H., et al. (2018). Genome-wide analysis of dirigent gene family in pepper (*Capsicum annuum* l.) and characterization of *CaDIR7* in biotic and abiotic stresses. *Sci. Rep.* 8, 5500. doi: 10.1038/s41598-018-23761-0

Lephatsi, M. M., Meyer, V., Piater, L. A., Dubery, I. A., and Tugizimana, F. (2021). Plant responses to abiotic stresses and rhizobacterial biostimulants: Metabolomics and epigenetics perspectives. *Metabolites* 11, 457. doi: 10.3390/metabo11070457

Lesk, C., Rowhani, P., and Ramankutty, N. (2016). Influence of extreme weather disasters on global crop production. *Nature* 529, 84–87. doi: 10.1038/nature16467

Li, N., Euring, D., Cha, J. Y., Lin, Z., Lu, M., Huang, L. J., et al. (2020a). Plant hormone-mediated regulation of heat tolerance in response to global climate change. *Front. Plant Sci.* 11. doi: 10.3389/fpls.2020.627969

Li, Z., and Howell, S. H. (2021). Heat stress responses and thermotolerance in maize. *Int. J. Mol. Sci.* 22, 948. doi: 10.3390/ijms22020948

Li, Z. Q., Li, J. T., Bing, J., and Zhang, G. F. (2019). [The role analysis of *APX* gene family in the growth and developmental processes and in response to abiotic stresses in *Arabidopsis thaliana*]. *Yi. Chuan* 41, 534–547. doi: 10.16288/j.yczz.19-026

Li, Z., Srivastava, R., Tang, J., Zheng, Z., and Howell, S. H. (2018). *Cis*-effects condition the induction of a major unfolded protein response factor, *ZmbZIP60*, in response to heat stress in maize. *Front. Plant Sci.* 9. doi: 10.3389/fpls.2018.00833

Li, Z., Tang, J., Srivastava, R., Bassham, D. C., and Howell, S. H. (2020b). The transcription factor bZIP60 links the unfolded protein response to the heat stress response in maize. *Plant Cell* 32, 3559–3575. doi: 10.1105/tpc.20.00260

Liu, J., Feng, L., Li, J., and He, Z. (2015). Genetic and epigenetic control of plant heat responses. *Front. Plant Sci.* 6. doi: 10.3389/fpls.2015.00267

Liu, X. H., Lyu, Y. S., Yang, W., Yang, Z. T., Lu, S. J., and Liu, J. X. (2020). A membrane-associated NAC transcription factor OsNTL3 is involved in thermotolerance in rice. *Plant Biotechnol. J.* 18, 1317–1329. doi: 10.1111/pbi.13297

Liu, H., Ouyang, B., Zhang, J., Wang, T., Li, H., Zhang, Y., et al. (2012). Differential modulation of photosynthesis, signaling, and transcriptional regulation between tolerant and sensitive tomato genotypes under cold stress. *PloS One* 7, e50785. doi: 10.1371/journal.pone.0050785

Li, Q., Wei, H., Liu, L., Yang, X., Zhang, X., and Xie, Q. (2017). Unfolded protein response activation compensates endoplasmic reticulum-associated degradation deficiency in *Arabidopsis*. *J. Integr. Plant Biol.* 59, 506–521. doi: 10.1111/jipb.12544

Lu, M., Sun, Q. P., Zhang, D. F., Wang, T. Y., and Pan, J. B. (2015). Identification of 7 stress-related NAC transcription factor members in maize (*Zea mays* l.) and characterization of the expression pattern of these genes. *Biochem. Biophys. Res. Commun.* 462, 144–150. doi: 10.1016/j.bbrc.2015.04.113

Mao, H., Yu, L., Han, R., Li, Z., and Liu, H. (2016). ZmNAC55, a maize stress-responsive NAC transcription factor, confers drought resistance in transgenic *Arabidopsis*. *Plant Physiol. Biochem.* 105, 55–66. doi: 10.1016/j.plaphy.2016.04.018

Mathew, I. E., and Agarwal, P. (2018). May the fittest protein evolve: Favoring the plant-specific origin and expansion of NAC transcription factors. *Bioessays* 40, e1800018. doi: 10.1002/bies.201800018

Ma, J., Wang, L. Y., Dai, J. X., Wang, Y., and Lin, D. (2021). The NAC-type transcription factor CaNAC46 regulates the salt and drought tolerance of transgenic *Arabidopsis thaliana*. *BMC Plant Biol.* 21, 11. doi: 10.1186/s12870-020-02764-y

Muhammad, I., Shalmani, A., Ali, M., Yang, Q. H., Ahmad, H., and Li, F. B. (2020). Mechanisms regulating the dynamics of photosynthesis under abiotic stresses. *Front. Plant Sci.* 11. doi: 10.3389/fpls.2020.615942

Nievola, C. C., Carvalho, C. P., Carvalho, V., and Rodrigues, E. (2017). Rapid responses of plants to temperature changes. *Temperature. (Austin).* 4, 371–405. doi: 10.1080/23328940.2017.1377812

Ohama, N., Sato, H., Shinozaki, K., and Yamaguchi-Shinozaki, K. (2017). Transcriptional regulatory network of plant heat stress response. *Trends Plant Sci.* 22, 53–65. doi: 10.1016/j.tplants.2016.08.015

Ohbayashi, I. , and Sugiyama, M. (2017). Plant nucleolar stress response, a new face in the NAC-dependent cellular stress responses. *Front. Plant Sci.* 8, 2247. doi: 10.3389/fpls.2017.02247

Olsen, A. N., Ernst, H. A., Leggio, L. L., and Skriver, K. (2005). NAC transcription factors: structurally distinct, functionally diverse. *Trends Plant Sci.* 10, 79–87. doi: 10.1016/j.tplants.2004.12.010

Ooka, H., Satoh, K., Doi, K., Nagata, T., Otomo, Y., Murakami, K., et al. (2003). Comprehensive analysis of NAC family genes in *Oryza sativa* and *Arabidopsis thaliana*. *DNA Res.* 10, 239–247. doi: 10.1093/dnares/10.6.239

Peng, X., Zhao, Y., Li, X., Wu, M., Chai, W., Sheng, L., et al. (2015). Genomewide identification, classification and analysis of NAC type gene family in maize. *J. Genet.* 94, 377–390. doi: 10.1007/s12041-015-0526-9

Poole, N., Donovan, J., and Erenstein, O. (2020). Agri-nutrition research: Revisiting the contribution of maize and wheat to human nutrition and health. *Food Policy*. 100, 101976. doi: 10.1016/j.foodpol.2020.101976

Qian, Y., Ren, Q., Zhang, J., and Chen, L. (2019). Transcriptomic analysis of the maize (Zea mays l.) inbred line B73 response to heat stress at the seedling stage. *Gene* 692, 68–78. doi: 10.1016/j.gene.2018.12.062

Ren, Y., Huang, Z., Jiang, H., Wang, Z., Wu, F., Xiong, Y., et al. (2021). A heat stress responsive NAC transcription factor heterodimer plays key roles in rice grain filling. *J. Exp. Bot.* 72, 2947–2964. doi: 10.1093/jxb/erab027

Sachdev, S., Ansari, S. A., Ansari, M. I., Fujita, M., and Hasanuzzaman, M. (2021). Abiotic stress and reactive oxygen species: Generation, signaling, and defense mechanisms. *Antioxidants. (Basel).* 10, 277. doi: 10.3390/antiox10020277

Seo, P. J., Kim, S. G., and Park, C. M. (2008). Membrane-bound transcription factors in plants. *M. Trends Plant Sci.* 13, 550–556. doi: 10.1016/j.tplants.2008.06.008

Shabnam, N., Tripathi, I., Sharmila, P., and Pardha-Saradhi, P. (2016). A rapid, ideal, and eco-friendlier protocol for quantifying proline. *Protoplasma* 253, 1577–1582. doi: 10.1007/s00709-015-0910-6

Shahnejat-Bushehri, S., Mueller-Roeber, B., and Balazadeh, S. (2012). *Arabidopsis* NAC transcription factor JUNGBRUNNEN1 affects thermomemory-associated genes and enhances heat stress tolerance in primed and unprimed conditions. *Plant Signal Behav.* 7, 1518–1521. doi: 10.4161/psb.22092

Shao, H., Wang, H., and Tang, X. (2015). NAC transcription factors in plant multiple abiotic stress responses: progress and prospects. *Front. Plant Sci.* 6. doi: 10.3389/fpls.2015.00902

Shiriga, K., Sharma, R., Kumar, K., Yadav, S. K., Hossain, F., and Thirunavukkarasu, N. (2014). Genome-wide identification and expression pattern of drought-responsive members of the NAC family in maize. *Meta. Gene* 2, 407–417. doi: 10.1016/j.mgene.2014.05.001

Singh, S., Koyama, H., Bhati, K. K., and Alok, A. (2021). The biotechnological importance of the plant-specific NAC transcription factor family in crop improvement. *J. Plant Res.* 134, 475–495. doi: 10.1007/s10265-021-01270-y

Singh, A., Mehta, S., Yadav, S., Nagar, G., Ghosh, R., Roy, A., et al. (2022). How to cope with the challenges of environmental stresses in the era of global climate change: An update on ROS stave off in plants. *Int. J. Mol. Sci.* 23, 1995. doi: 10.3390/ijms23041995

Souer, E., Van Houwelingen, A., Kloos, D., Mol, J., and Koes, R. (1996). *The no apical meristem* gene of petunia is required for pattern formation in embryos and flowers and is expressed at meristem and primordia boundaries. *Cell* 85, 159–170. doi: 10.1016/s0092-8674(00)81093-4

Sun, H., Xie, Y., Yang, W., Lv, Q., Chen, L., Li, J., et al. (2022). Membrane-bound transcription factor TaNTL1 positively regulates drought stress tolerance in transgenic *Arabidopsis*. *Plant Physiol. Biochem.* 182, 182–193. doi: 10.1016/j.plaphy.2022.04.023

Sun, L., Yang, Z. T., Song, Z. T., Wang, M. J., Sun, L., Lu, S. J., et al. (2013). The plant-specific transcription factor gene *NAC103* is induced by bZIP60 through a new *cis*-regulatory element to modulate the unfolded protein response in *Arabidopsis*. *Plant J.* 76, 274–286. doi: 10.1111/tpj.12287

Tollefson, J. (2021). IPCC climate report: Earth is warmer than it's been in 125,000 years. *Nature* 596, 171–172. doi: 10.1038/d41586-021-02179-1

Vargas-Hernández, B. Y., Núñez-Muñoz, L., Calderón-Pérez, B., Xoconostle-Cázares, B., and Ruiz-Medrano, R. (2022). The NAC transcription factor *ANAC087* induces aerial rosette development and leaf senescence in *Arabidopsis*. *Front. Plant Sci.* 13. doi: 10.3389/fpls.2022.818107

Wang, Y., Tao, H., Zhang, P., Hou, X., Sheng, D., Tian, B., et al. (2020). Reduction in seed set upon exposure to high night temperature during flowering in maize. *Physiol. Plant* 169, 73–82. doi: 10.1111/ppl.13049

Wang, D., Yu, Y., Liu, Z., Li, S., Wang, Z., and Xiang, F. (2016). Membrane-bound NAC transcription factors in maize and their contribution to the oxidative stress response. *Plant Sci.* 250, 30–39. doi: 10.1016/j.plantsci.2016.05.019

Wu, L., Zu, X., Zhang, H., Wu, L., Xi, Z., and Chen, Y. (2015). Overexpression of *ZmMAPK1* enhances drought and heat stress in transgenic *Arabidopsis thaliana*. *Plant Mol. Biol.* 88, 429–443. doi: 10.1007/s11103-015-0333-y

Xia, X. J., Wang, Y. J., Zhou, Y. H., Tao, Y., Mao, W. H., Shi, K., et al. (2009). Reactive oxygen species are involved in brassinosteroid-induced stress tolerance in cucumber. *Plant Physiol.* 150, 801–814. doi: 10.1104/pp.109.138230

Yang, H., Gu, X., Ding, M., Lu, W., and Lu, D. (2018). Heat stress during grain filling affects activities of enzymes involved in grain protein and starch synthesis in waxy maize. *Sci. Rep.* 8, 15665. doi: 10.1038/s41598-018-33644-z

Yang, Z. T., Lu, S. J., Wang, M. J., Bi, D. L., Sun, L., Zhou, S. F., et al. (2014a). A plasma membrane-tethered transcription factor, NAC062/ANAC062/NTL6, mediates the unfolded protein response in *Arabidopsis*. *Plant J.* 79, 1033–1043. doi: 10.1111/tpj.12604

Yang, Z., Wang, C., Qiu, K., Chen, H., Li, Z., Li, X., et al. (2020). The transcription factor ZmNAC126 accelerates leaf senescence downstream of the ethylene signalling pathway in maize. *Plant Cell Environ.* 43, 2287–2300. doi: 10.1111/pce.13803

Yang, Z. T., Wang, M. J., Sun, L., Lu, S. J., Bi, D. L., Sun, L., et al. (2014b). The membrane-associated transcription factor NAC089 controls ER-stress-induced programmed cell death in plants. *PloS Genet.* 10, e1004243. doi: 10.1371/journal.pgen.1004243

Yang, J., and Zhang, Y. (2015). I-TASSER server: new development for protein structure and function predictions. *Nucleic Acids Res.* 43, W174–W181. doi: 10.1093/nar/gkv342

Yu, C. Y., Cho, Y., Sharma, O., and Kanehara, K. (2022). What's unique? the unfolded protein response in plants. *J. Exp. Bot.* 73, 1268–1276. doi: 10.1093/jxb/erab513

Zengin, F. (2013). Physiological behavior of bean (Phaseolus vulgaris l.) seedlings under metal stress. *Biol. Res.* 46, 79–85. doi: 10.4067/s0716-97602013000100012

Zhang, C., Freddolino, P. L., and Zhang, Y. (2017). COFACTOR: improved protein function prediction by combining structure, sequence and protein-protein interaction information. *Nucleic Acids Res.* 45, W291–w299. doi: 10.1093/nar/gkx366

Zhang, J., Liao, J., Ling, Q., Xi, Y., and Qian, Y. (2022). Genome-wide identification and expression profiling analysis of maize AP2/ERF superfamily genes reveal essential roles in abiotic stress tolerance. *BMC Genomics* 23, 125. doi: 10.1186/s12864-022-08345-7

Zhang, H., Ma, F., Wang, X., Liu, S., Saeed, U. H., Hou, X., et al. (2020). Molecular and functional characterization of *CaNAC035*, an NAC transcription factor from pepper (*Capsicum annuum* l.). *Front. Plant Sci.* 11. doi: 10.3389/fpls.2020.00014

Zhao, Y., Du, H., Wang, Y., Wang, H., Yang, S., Li, C., et al. (2021). The calcium-dependent protein kinase ZmCDPK7 functions in heat-stress tolerance in maize. *J. Integr. Plant Biol.* 63, 510–527. doi: 10.1111/jipb.13056

Zhao, C., Liu, B., Piao, S., Wang, X., Lobell, D. B., Huang, Y., et al. (2017). Temperature increase reduces global yields of major crops in four independent estimates. *Proc. Natl. Acad. Sci. U.S.A.* 114, 9326–9331. doi: 10.1073/pnas.1701762114

Zhao, J., Lu, Z., Wang, L., and Jin, B. (2020). Plant responses to heat stress: Physiology, transcription, noncoding RNAs, and epigenetics. *Int. J. Mol. Sci.* 22, 117. doi: 10.3390/ijms22010117

Zheng, W., Zhang, C., Li, Y., Pearce, R., Bell, E. W., and Zhang, Y. (2021). Folding non-homologous proteins by coupling deep-learning contact maps with I-TASSER assembly simulations. *Cell Rep. Methods* 1, 100014. doi: 10.1016/j.crmeth.2021.100014

Zhou, X., Li, X., Wei, W., Duan, X., Zhang, H., Ding, M., et al. (2021). Association between genetic polymorphisms of telomere pathway genes and hydrogen peroxide level in omethoate exposure workers. *Environ. Toxicol. Pharmacol.* 82, 103541. doi: 10.1016/j.etap.2020.103541

Zuo, X., Xiang, W., Li, K., Liu, Y., Zheng, S., Khan, A., et al. (2022). MdGRF11, a growth-regulating factor, participates in the regulation of flowering time and interacts with MdTFL1/MdFT1 in apple. *Plant Sci.* 321, 111339. doi: 10.1016/j.plantsci.2022.111339

frontiers | Frontiers in Plant Science

TYPE Original Research
PUBLISHED 17 October 2022
DOI 10.3389/fpls.2022.1020367

Check for updates

OPEN ACCESS

EDITED BY
Andrea Miyasaka Almeida,
Universidad Mayor, Chile

REVIEWED BY
Abid Khan,
University of Haripur, Pakistan
Xiao Ma,
Sichuan Agricultural University, China

*CORRESPONDENCE
Guanghui Lv
guanghui_xju@sina.com

SPECIALTY SECTION
This article was submitted to Plant Abiotic Stress, a section of the journal Frontiers in Plant Science

RECEIVED 16 August 2022
ACCEPTED 28 September 2022
PUBLISHED 17 October 2022

CITATION
Yang F and Lv G (2022) Combined analysis of transcriptome and metabolome reveals the molecular mechanism and candidate genes of *Haloxylon* drought tolerance. *Front. Plant Sci.* 13:1020367. doi: 10.3389/fpls.2022.1020367

COPYRIGHT
© 2022 Yang and Lv. This is an open-access article distributed under the terms of the Creative Commons Attribution License (CC BY). The use, distribution or reproduction in other forums is permitted, provided the original author(s) and the copyright owner(s) are credited and that the original publication in this journal is cited, in accordance with accepted academic practice. No use, distribution or reproduction is permitted which does not comply with these terms.

Combined analysis of transcriptome and metabolome reveals the molecular mechanism and candidate genes of *Haloxylon* drought tolerance

Fang Yang[1,2,3] and Guanghui Lv[1,2,3]*

[1]School of Ecology and Environment, Xinjiang University, Urumqi, China, [2]Key Laboratory of Oasis Ecology, Ministry of Education, Urumqi, China, [3]Xinjiang Jinghe Observation and Research Station of Temperate Desert Ecosystem, Ministry of Education, Jinghe, China

Haloxylon ammodendron and *Haloxylon persicum*, as typical desert plants, show strong drought tolerance and environmental adaptability. They are ideal model plants for studying the molecular mechanisms of drought tolerance. Transcriptomic and metabolomic analyses were performed to reveal the response mechanisms of *H. ammodendron* and *H. persicum* to a drought environment at the levels of transcription and physiological metabolism. The results showed that the morphological structures of *H. ammodendron* and *H. persicum* showed adaptability to drought stress. Under drought conditions, the peroxidase activity, abscisic acid content, auxin content, and gibberellin content of *H. ammodendron* increased, while the contents of proline and malondialdehyde decreased. The amino acid content of *H. persicum* was increased, while the contents of proline, malondialdehyde, auxin, and gibberellin were decreased. Under drought conditions, 12,233 and 17,953 differentially expressed genes (DEGs) were identified in *H. ammodendron* and *H. persicum*, respectively, including members of multiple transcription factor families such as FAR1, AP2/ERF, C2H2, bHLH, MYB, C2C2, and WRKY that were significantly up-regulated under drought stress. In the positive ion mode, 296 and 452 differential metabolites (DEMs) were identified in *H. ammodendron* and *H. persicum*, respectively; in the negative ion mode, 252 and 354 DEMs were identified, primarily in carbohydrate and lipid metabolism. A combined transcriptome and metabolome analysis showed that drought stress promoted the glycolysis/gluconeogenesis pathways of *H. ammodendron* and *H. persicum* and increased the expression of amino acid synthesis pathways, consistent with the physiological results. In addition, transcriptome and metabolome were jointly used to analyze the expression changes of the genes/metabolites of *H. ammodendron* and *H. persicum* that were associated with drought tolerance but were regulated differently in the

two plants. This study identified drought-tolerance genes and metabolites in *H. ammodendron* and *H. persicum* and has provided new ideas for studying the drought stress response of *Haloxylon*.

KEYWORDS

***Haloxylon ammodendron*, *Haloxylon persicum*, drought stress, transcriptomics, metabolomics**

Introduction

Plants are exposed to biotic and abiotic stress, such as pathogen infections, pest attacks, extreme temperatures, drought, and salinity (Huang et al., 2018). In dry regions, moisture is one of the major environmental factors limiting plant growth and productivity. During drought stress, plants undergo several changes that ultimately lead to reduced levels of gas exchange and photosynthesis as well as reduced cell division and cell expansion due to decreased enzymatic activity and lack of energy (Lawson et al., 2003 ; Kiani Poormohammad et al., 2007). In response, plants have evolved some sophisticated defense mechanisms, including oxidative burst, the regulation of signaling networks, physiological, molecular, and cellular modifications, to combat these stresses (Khan et al., 2018). Drought is the crucial and threatening abiotic factor that limits the productivity of many crops in the current changing climatic conditions. This stress, in combination with other abiotic stresses such as high light and temperature stress, negatively affects plant morphological, physiological and molecular characteristics, which leads to lowered photosynthesis, hormonal imbalance, mineral nutrient starvation and an ultimate oxidative stress (Haq et al., 2019). These complex drought tolerance mechanisms show differences between different plant species (Ramanjulu and Bartels, 2002). Plants have evolved complex mechanisms for efficient water uptake and respond to drought stress by reprogramming their metabolism and growth, resulting in various morphological, physiological, and biochemical changes at the whole plant level (Claeys and Inze, 2013). Ultimately, physiological responses to drought stress are underpinned by the reprogramming of metabolism and gene expression (Oono et al., 2003; Boominathan et al., 2004; Talame et al., 2007). Therefore, elucidation of these protective mechanisms is necessary to better understand how plants adapt to drought conditions. Transcriptomic analysis (RNA-Seq) has been applied to various plants such as *Populus trichocarpa* (Tang et al., 2015) and *Ammopiptanthus mongolicus* (Gao et al., 2015). The transcription levels of plant genes will change under stress conditions. There are two main types of genes involved in responding to stress: one type encodes proteins that control the formation of metabolites, thereby maintaining the balance of metabolism and osmosis; the other type encodes proteins related to signal receptors to ensure normal signal transduction in plants (Valliyodan and Nguyen, 2006). Previous studies have identified differences in the transcriptional profiles of *Hordeum spontaneum* (Hübner et al., 2015) and Trifolium pratense (Yates et al., 2014) in response to drought stress by comparing key genes for sexual differences. Hu et al. (2018) characterized the root transcriptional changes and physiological responses of different drought-resistant wheat varieties under water deficit conditions and identified 8,197 differentially expressed genes (DEGs) related to drought resistance. These genes were involved in carbon metabolism, flavonoid biosynthesis, and phytohormone signal transduction. Under water stress, the numbers and expression levels of genes involved in antioxidant and osmotic stress resistance were higher in JM-262 (a drought-resistant type). Such application of transcriptomic analysis in mining drought tolerance genes is a promising avenue for gene detection.

Metabolomics is the quantitative analysis of all metabolites in an organism and the relevant relationships between metabolites and physiological changes (Fiehn, 2002). Metabolomics can detect small molecular weight compounds and exogenous substances in tissues and organs where the molecular mass is < 1000 (Wishart, 2007). Metabolites are the end products of cellular regulatory processes, and their levels can be viewed as the ultimate responses of biological systems to genetic or environmental changes (Fernie and Schauer, 2009). Previous studies on the effects of drought stress on the metabolomics of plants have shown that significant increases in amino acids, organic acids, sugars, and polyols is the general metabolic law of plants in response to water deficit (Warren et al., 2012; Catola et al., 2016). These compounds can improve plant drought resistance through osmoregulation, scavenging of ROS, protecting cellular components, maintaining membrane lipid stability, and inducing phytohormone production (Krasensky and Jonak, 2012). Different types of metabolites accumulate in plants in response to various stress factors. The contents of amino acids in leaves of Pisum sativum L. under drought stress were significantly increased; which included proline, valine, threonine, homoserine, inositol, r-aminobutyric

acid (GABA), and trigonelline (Niacin betaine) (Charlton et al., 2008). The leaves of *Capsicum annuum* L. mainly accumulated fructose, sucrose, inositol galactoside, cadaverine, putrescine, and spermidine under drought stress (Sziderics et al., 2010). *Capsicum annuum* L. mainly accumulated rosinol, proline, and malic acid under drought stress (Yates et al., 2014). However, the metabolites in *H. ammodendron* and *H. persicum* that respond to drought stress have yet to be characterized.

H. ammodendron and *H. persicum* belongs to the genus Haloxylon Riccoides and are extremely important drought-tolerant tree species in northwest China. The plants of the genus have an extensive root system that makes the plants useful for stabilizing sandy soils, especially in desert ecosystems. The drought and heat resistance of the plants is useful in combating desertification and land degradation in arid regions (Fan et al., 2018; Thaylale Purayil et al., 2020). These trees are rapidly approaching extinction due to a number of factors (Long et al., 2014; Thaylale Purayil et al., 2020) and the molecular mechanisms underlying the long-term responses of *H. ammodendron* and *H. persicum* to drought stress in the natural environment remain unclear. To explore the changes in *H. ammodendron* and *H. persicum* under drought stress, the responses of *H. ammodendron* (humid (HS): soil water content 9.70–15.00%; drought (LS): soil water content 2.41–4.00%) and *H. persicum* (humid (HB): soil water content 3.38–5.12%; drought (LB): soil water content 1.05–3.11%) in humid and arid ecological environments were examined. First, the morphological and physiological changes under drought stress were studied, and then the assimilation branches were analyzed by transcriptomic and metabolomics to identify differentially expressed genes (DEGs) and differential metabolites (DEMs) involved in drought tolerance. Finally, key candidate genes and metabolites related to drought tolerance were identified. This study provides theoretical support for future research on physiological and molecular mechanisms of Haloxylon plants responding to drought stress.

Materials and methods

Sample plot setting

The test site was located north of the management station of the East Bridge of the Aibi Lake Wetland National Nature Reserve in Jinghe County, Xinjiang (44°30′–45°09′N, 82°36′–83°50′E). Starting from the East Bridge Management Station of Ebinur Lake Wetland Nature Reserve, transects (width 0.1 km × 2.0 km) were set up perpendicular to the Aqiksu River in the areas with *H. ammodendron* and *H. persicum* and labeled as transect 1 (in the distribution area of *H. ammodendron*) and transect 2 (in the distribution area of *H. persicum*). The two soil water environments, i.e., humid and arid, were selected according to the previous study (Gong and Lu, 2017). A quadrat size of 50 m × 50 m was used in each of the two soil moisture environments (*H. ammodendron*: A: humid and low salinity (HS), and B: drought and low salinity (LS); *H. persicum*: C: humid and low salinity (HB), and D: arid and low salinity (LB)) (Figure 1). We investigated the number and abundance of woody plant species in the plots and selected five individuals of *H. ammodendron* and *H. persicum* with similar individual sizes regarding plant height, crown width, and base diameter for sampling and determination.

Production of assimilation branch

The assimilated branches were fixed by FAA for more than 24 hours, dehydrated, transparent, waxed and embedded. The horizontal sections of assimilated branches were made by Leica microtome, stained with safranine solid green, and sealed with neutral gum. The target area of the tissue was selected with eclipse ci-l photographic microscope for 40, 200 and 400 times imaging, and representative paraffin sectioning photography was selected to record the cross-sectional characteristics of assimilated branches. Image Pro Plus 6.0 (media cybemetrics, U.S.A) measurement software was used to measure the assimilation branch diameter, cuticle thickness, palisade tissue thickness, vascular column thickness and catheter diameter. The microscopic data were the average of 5 visual fields of 3 repeated slices.

Determination of physiological indexes

The proline determination kit was used to determine the proline content (Bhaskara et al., 2015). Protein quantitative Kit (Bicinchoninic Acid Assay, i.e., BCA method) was used to determine the content of soluble protein (Campion et al., 2011). The amino acid (AA) content was measured using an AA assay kit. The superoxide dismutase (SOD) activity was measured using a total SOD assay kit (Li et al., 2022). The peroxidase (POD) activity was measured using a POD assay kit (Li et al., 2022). The malondialdehyde (MDA) content was measured using a MDA assay kit (Li et al., 2022). The endogenous hormones (abscisic acid, auxin and gibberellin) content was determined by high performance liquid chromatography (HPLC) (Yang et al., 2014).

RNA isolation, cDNA library construction, sequencing and data analysis

Total twelve plant libraries (*Haloxylon ammodendron*: HS1, HS2, HS3, LS1, LS2, LS3; *Haloxylon persicum*: HB1, HB2, HB3, LB1, LB2, LB3) were collected from two species under two soil moisture conditions for transcriptome sequencing. Total RNA

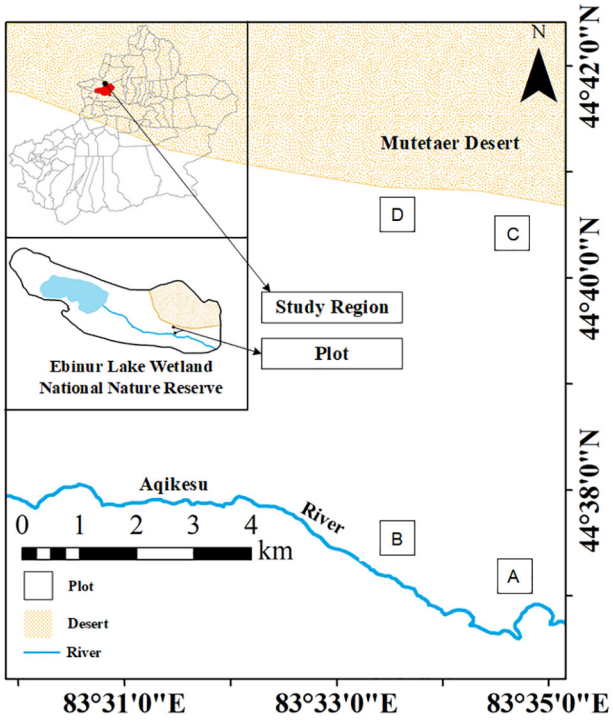


FIGURE 1
Study area and plot layout. The distribution area of *H. ammodendron*: **(A)**: humid and low salinity, and **(B)**: arid and low salt; the distribution area of *H. persicum*: **(C)**: humid and low salinity, and **(D)**: arid and low-salinity.

was extracted using a TIANGEN Polysaccharide Polyphenol Kit (Qiagen, Germany), and then using the kit NEBNext® Ultra™ Directional RNA Library ep Kit for Illumina®. RNA concentration was measured using Agilent 2100 Bioanalyzer (Agilent Technologies, Santa Clara, CA, USA) and the purity of RNA was evaluated using NanoDropTM (Thermo Scientific, Waltham, MA, USA). Sequencing was performed using an Illumina NovaSeq 6000 paired-end sequencing system (Illumina, USA). The basic principle of sequencing is to synthesize and sequence at the same time (Sequencing by Synthesis). Four fluorescent labeled dNTP, DNA polymerase and splice primers were added to the sequenced flowcell and amplified. When the sequence cluster extends the complementary chain, each dNTP labeled by fluorescence can release the corresponding fluorescence. The sequencer captures the fluorescence signal and converts the optical signal into the sequencing peak by computer software, so as to obtain the sequence information of the fragment to be tested. After cDNA library sequencing, clean data (clean reads) were obtained by removing reads containing adapter, reads containing N base and low quality reads (The alkali base of Qphred <= 20 accounts for more than 50% of the total read length) from raw data. At the same time, Q20, Q30 and GC content the clean data were calculated. All the downstream analyses were based on the clean data with high quality. After the clean reads was obtained, the Trinity software (version 2.6.6) was used to assemble the clean reads for the reference sequence obtained after the continued analysis. Corset cluster analysis could aggregate redundant transcripts and improved the detection rate of differentially expressed genes. On the basis of splicing, Corset (version 4.6) (Davidson and Oshlack, 2014) aggregateed transcripts into many cluster according to inter-transcriptional SharedReads. Then, combined with the expression level of transcripts among different samples and H-Cluster algorithm, transcripts with different expression differences between samples were separated from the original clusterto establish a new cluster. Finally, each cluster was defined as “Gene”. The unigenes were compared to public databases [Non-redundant Protein Database (NR), Gene Ontology (GO), Kyoto Encyclopedia of Genes and Genomes (KEGG), Kyoto Encyclopedia of Genes and Genomes (KOG), Clusters of Orthologous Groups (COG), Protein Family Database (Pfam), and Non-redundant Protein Sequence Database (Swiss-Prot)] using BLAST with an e-value threshold of 10-5 (Altschul et al., 1997). The library construction and sequencing were performed by Beijing Novogene Technology Co., LTD (China).

Identification and analysis of differentially expressed genes

In order to verify the transcriptional expression level of all samples, FPKM (fragments per kilobase of transcription per million mapped reads) was used to quantify the gene expression level (Trapnell et al., 2010). Differential expression analysis of two conditions (three biological replicates per condition) was performed using the DESeq2 R package (1.20.0). DESeq2 provide statistical routines for determining differential expression in digital gene expression data using a model based on the negative binomial distribution (Love et al., 2014). The resulting P-values were adjusted using the Benjamini and Hochberg's approach for controlling the false discovery rate. Padj < 0.05 and |log2(foldchange)| > 1 were set as the threshold for significantly differential expression.

GO and KEGG enrichment analysis of differentially expressed genes

GOseq (1.10.0) (Young et al., 2010) and KOBAS (v2.0.12) (Mao et al., 2005) software were used for GO (Gene Ontology) function enrichment analysis (Ali et al., 2018) and KEGG (Kyoto Encyclopedia of Genes and Genomes) pathway enrichment analysis of differential gene sets (Li et al., 2021). Enrichment analysis based on hypergeometric distribution principle. Differential gene sets are the gene set obtained by significant difference analysis and annotated to the GO or KEGG database. Background gene sets are all genes that are analyzed with significant differences and annotated to the GO or KEGG database. The result of enrichment analysis is the enrichment of all differential gene sets, up-regulated differential gene sets and down-regulated differential genes in each differential comparison combination.

Quantitative real-time polymerase chain reaction verification

The 10 DEGs were randomly selected for reverse transcription-quantitative PCR (qRT-PCR) assays to validate the reliability of RNA-seq analysis. Reverse-transcription was performed using the PrimeScript RT First Strand cDNA Synthesis Kit (Toyobo, Osaka, Japan). The first-strand cDNA synthesized from 1μg purified RNA was reverse-transcribed using a Reverse Transcriptase kit (EP0442, Thermos Fisher). The qRT-PCR was carried out using a AceQ Universal SYBR qPCR Master Mix (Vazyme, Nanjing, China) with PCR conditions following the manufacturer's instructions. Quantitative RT-PCR reactions were conducted in 96-well plates with a Real time PCR System (Stepone plus, ABI) using the AceQ Universal SYBR qPCR Master Mix (Vazyme, Nanjing, China). Ha18SrRNA was used as an internal control. The 2-ΔΔCT method was used to determine the relative abundance of transcripts (Xuan et al., 2022). For accuracy, the whole experiment was conducted thrice. All primers used in this study are listed in Supplementary Table S1.

LC-MS (gas chromatography-mass spectrometry) for metabolite determination

Tissues (100 mg) were individually grounded with liquid nitrogen and the homogenate wasresuspended with prechilled 80% methanol and 0.1% formic acid by well vortex. The sampleswere incubated on ice for 5 min and then were centrifuged at 15,000 g, 4°C for 20 min. Some of supernatant was diluted to final concentration containing 53% methanol by LC-MS grade water. Thesamples were subsequently transferred to a fresh Eppendorf tube and then were centrifuged at 15000 g, 4°C for 20 min. Finally, the supernatant was injected into the LC-MS/MS system analysis (Want et al., 2012).

LC-MS(gas chromatography-mass spectrometry) analysis

UHPLC-MS/MS analyses were performed using a Vanquish UHPLC system (ThermoFisher, Germany) coupled with an Orbitrap Q ExactiveTMHF-X mass spectrometer (Thermo Fisher, Germany) in Novogene Co., Ltd. (Beijing, China). Samples were injected onto a Hypesil Gold column (100×2.1 mm, 1.9μm) using a 17-min linear gradient at a flow rate of 0.2mL/min. The eluents for the positive polarity mode were eluent A (0.1% FA in Water) and eluent B (Methanol). The eluents for the negative polarity mode were eluent A (5 mMammonium acetate, pH 9.0) and eluent B (Methanol). The solvent gradient was set as follows: 2% B, 1.5 min; 2-100% B, 12.0 min; 100% B, 14.0 min;100-2% B, 14.1 min;2% B, 17 min. Q ExactiveTMHF-X mass spectrometer was operated in positive/negative polarity mode with spray voltage of 3.2 kV, capillary temperature of 320°C, sheath gas flow rate of 40 arb and aux gasflow rate of 10 arb. The raw data files generated by UHPLC-MS/MS were processed using the Compound Discoverer 3.1 (CD3.1, ThermoFisher) to perform peak alignment, peak picking, and quantitation for each metabolite. The main parameterswere set as follows: retention time tolerance, 0.2 minutes; actual mass tolerance, 5 ppm; signal intensity tolerance, 30%; signal/noise ratio, 3; and minimum intensity, 100,000. After that, peak intensitieswere normalized to the total spectral intensity. The normalized data was used to predict the molecular formula based on additive ions, molecular ion peaks and fragment ions. And then peaks were matched with the mzCloud (https://www.mzcloud.org/), mzVaultand

MassListdatabase to obtain the accuratequalitative and relative quantitative results. Statistical analyses were performed using the statistical software R (R version R-3.4.3), Python (Python 2.7.6 version) and CentOS (CentOS release 6.6). When data were not normally distributed, normal transformations were attempted using of area normalization method.

Metabolite data analysis to obtain differential metabolites

These metabolites were annotated using the KEGG database (https://www.genome.jp/kegg/pathway.html), HMDB database (https://hmdb.ca/metabolites) and LIPIDMaps database (http://www.lipidmaps.org/). Principal components analysis (PCA) and Partial least squares discriminant analysis (PLS-DA) were performed at metaX (a flexible and comprehensive software for processing metabolomics data). We applied univariate analysis (t-test) to calculate the statistical significance (P-value). The metabolites with VIP > 1 and P-value < 0.05 and fold change ≥ 2 or FC ≤ 0.5 were considered to be differential metabolites.

Statistical analysis of data

All statistical analyses were performed by using statistical package for the social sciences (SPSS) software version 20 (IBM, Chicago, IL, USA), and significant differences were evaluated by using T-test. Different letters indicate significant differences at $P < 0.05$.

Results

Comparison of the characteristics and parameters of the anatomical structure of the assimilatory branches of *H. ammodendron* and *H. persicum*

The anatomical structure of the middle part of the assimilatory branch of *H. persicum* is similar to that of *H. ammodendron* (Figure 2). The cross-sections are nearly circular. Crystal cells are scattered in the palisade tissue cell layer; these are large and often protrude into the lower cortex. Palisade cells are vascular bundle sheath cells that contain chloroplasts and starch. This is a water storage tissue containing crystal cells. Small vascular bundles are distributed between the water storage tissue and the vascular bundle sheath cells. Two large bundles of fibroblasts are present in the water storage tissue. There is a large vascular bundle in the center of the assimilation branch; the pith is underdeveloped, and the pith ray is wider. In the mesophyll cells, vascular sheaths and vascular bundles form a wreath structure.

Under a drought environment, the diameter and cuticle thickness of LS and LB were higher than those of HS and HB, but the increase in cuticle thickness of *H. persicum* was more significant, indicating that the assimilatory branch of LB was more drought tolerant (Table 1). The palisade tissue thicknesses of LS (35.8 μm) and LB (33.9 μm) were higher than those of HS (33.5 μm) and HB (32.5 μm). The widths of the vascular columns of *H. ammodendron* and *H. persicum* were between 322.9–323.2 μm and 220.0–312.4 μm, respectively, accounting for 68.04% and 64.41% of the radius. There was a significant difference in the duct pore size between LS and HS, but no significant difference between LB and HB. However, the duct pore size of both species was the largest in the drought environment, indicating that the duct pore size was correlated with drought tolerance, and that it showed greater plasticity.

Changes in physiological traits related to *H. ammodendron* and *H. persicum*

By measuring the physiological changes in the *H. ammodendron* and *H. persicum*, we found that the Pro content of both species was significantly decreased under drought conditions, but the soluble protein did not change significantly (Figures 3A, B). The AA contents of LS and HS were higher than those of HS and HB, but the increase in *H. ammodendron* was smaller, while the content in *H. persicum* was significantly increased (Figure 3C). The activity of SOD enzyme, which is related to ROS scavenging, was slightly decreased in both species under drought stress, but the POD activity was significantly enhanced in *H. ammodendron* while significantly decreased in *H. persicum* (Figures 3D, E). MDA content, an indicator characterizing the degree of membrane lipid peroxidation, showed a smaller decrease in both species under drought stress (Figure 3F). Under drought stress conditions, the ABA, IAA, and GA3 contents of the *H. ammodendron* were accumulated significantly, while that of *H. persicum* were significantly decreased (Figures 3G–I).

Transcriptome sequencing and gene expression analysis

RNA-seq was used to study transcriptome changes in *H. ammodendron* and *H. persicum* during drought. Totals of 140,111,843 raw reads were generated in *H. ammodendron*; after filtering, 138,256,912 high-quality clean reads were obtained. Totals of 136,979,246 raw reads and 135,939,253 clean reads were generated by *H. persicum*. The contents of G and C bases in *H. ammodendron* and *H. persicum* accounted for about 42% of the total number of bases, and the values of Q20 and Q30 were greater than 97% and 93%, respectively, indicating that the data quality was sufficient and could be used for subsequent analysis (Table 2).

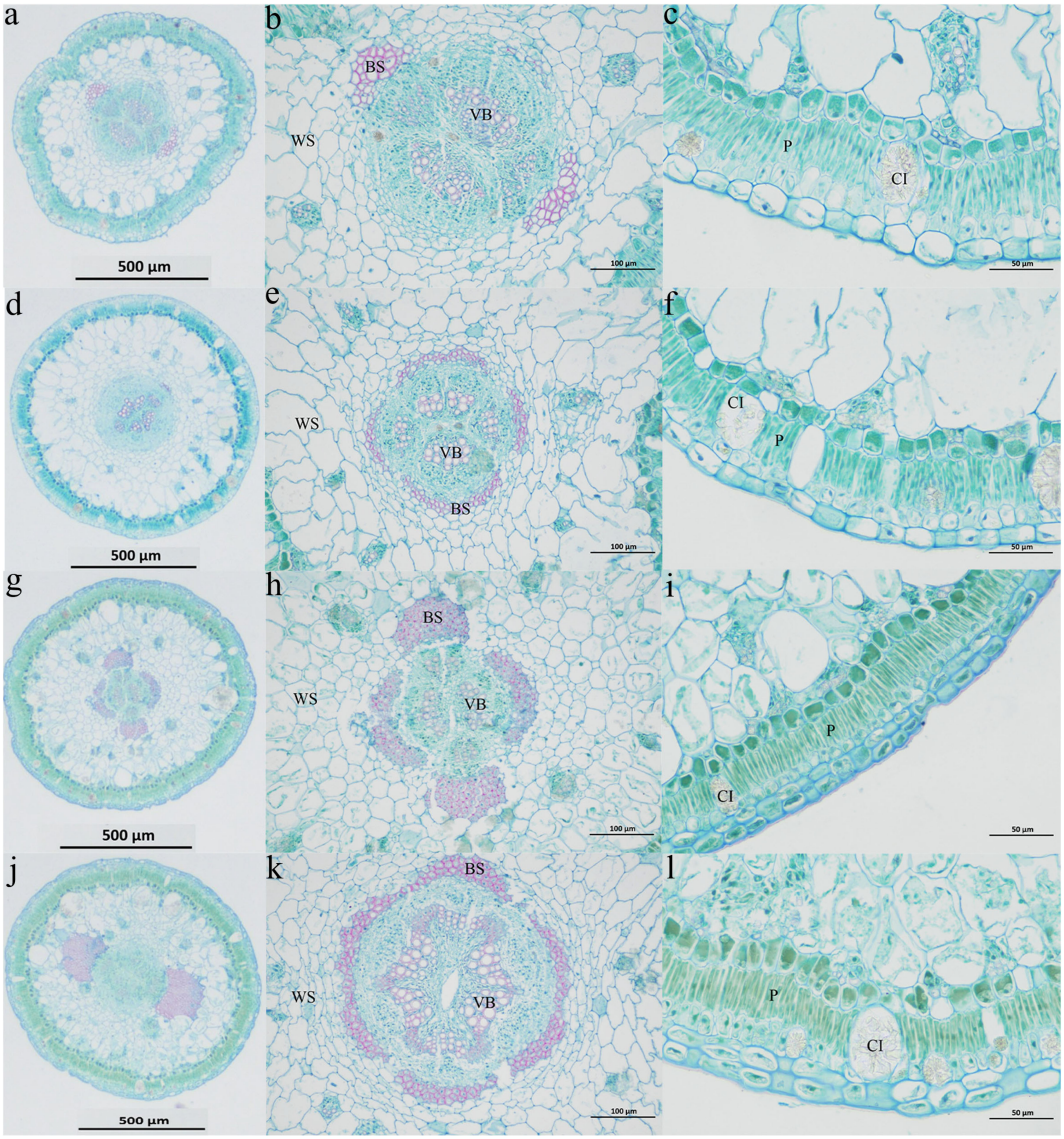


FIGURE 2
Cross-section anatomy of the assimilatory branches of *H. ammodendron* and *H. persicum*. **(A–C)** represent the cross sections (HS) of *H. ammodendron* in a moist soil environment. **(D–F)** represent the cross-sections (LS) of *H. ammodendron* in an arid soil environment. **(G–I)** represent the cross-sections (HB) of *H. persicum* in the moist soil environment. **(J–L)** represent the cross-sections (LB) of *H. persicum* in an arid soil environment. BS: Vascular bundle sheath cells; CI: Crystalline cells; P: Palisade tissue; VB: Vascular bundle; WS: Aqueous tissue.

In total, 159,006 and 173,803 transcripts were identified in *H. ammodendron* and *H. persicum*, and the expression level of each gene was normalized to FPKM (number of fragments per kilobase length per million fragments from a gene). Based on the gene expression levels in wet and dry environments, the correlations of gene expression levels between plants in the two environments were calculated. The results showed that the correlations between the three biological repeats of HS and HB were higher than those of LS and LB, suggesting differences in gene expression in LS vs. HS and LB vs. HB (Figures 4A, D). Unsupervised PCA analysis was performed (Figure 4B, E), and the results showed that LS vs. HS and LB vs. HB were clearly distinguishable on the score map, indicating significant differences in transcriptomes. Furthermore, both species displayed changes in the gene expression levels shown on axis 1 under drought stress. Using the violin plots of the FPKM values (Figure 4C, F), we analyzed the *H. ammodendron* (HS1, HS2, HS3, LS1, LS2, and LS3) and *H. persicum* (HB1, HB2, HB3, LB1, LB2, and LB3) gene expression levels and correlations in 12 samples and found similar gene expression levels between LS vs. HS and LB vs. HB.

TABLE 1 Comparison of anatomical characteristics of assimilating branches of *H. ammodendron* and *H. persicum* under different soil moisture conditions.

Species	Soil moisture condition	Diameter of assimilating branches	Cuticle		Palisade tissue		Aqueous tissue		Diameter of vascular cylinder		Pore of catheter	
		T/μm	T/μm	R/%	T/μm	R/%	T/μm	R/%	T/μm	R/%	T/μm	R/%
Haloxylon ammodendron	HS	950a	1.92a	0.40	33.5a	7.05	188.8b	39.75	323.2a	68.04	9.08b	1.91
	LS	1010a	1.97a	0.39	35.8a	7.09	241.6a	47.84	322.9a	63.94	12.04a	2.38
Haloxylon persicum	HB	900b	1.82b	0.40	32.5a	7.22	255.0a	56.67	220.0a	48.89	9.28a	2.06
	LB	970a	2.28a	0.47	33.9a	6.99	235.5a	48.56	312.4a	64.41	9.55a	1.97

T. thickness; R. percentage of radius. Different letters in the same column meant significant difference at 0.05 level.

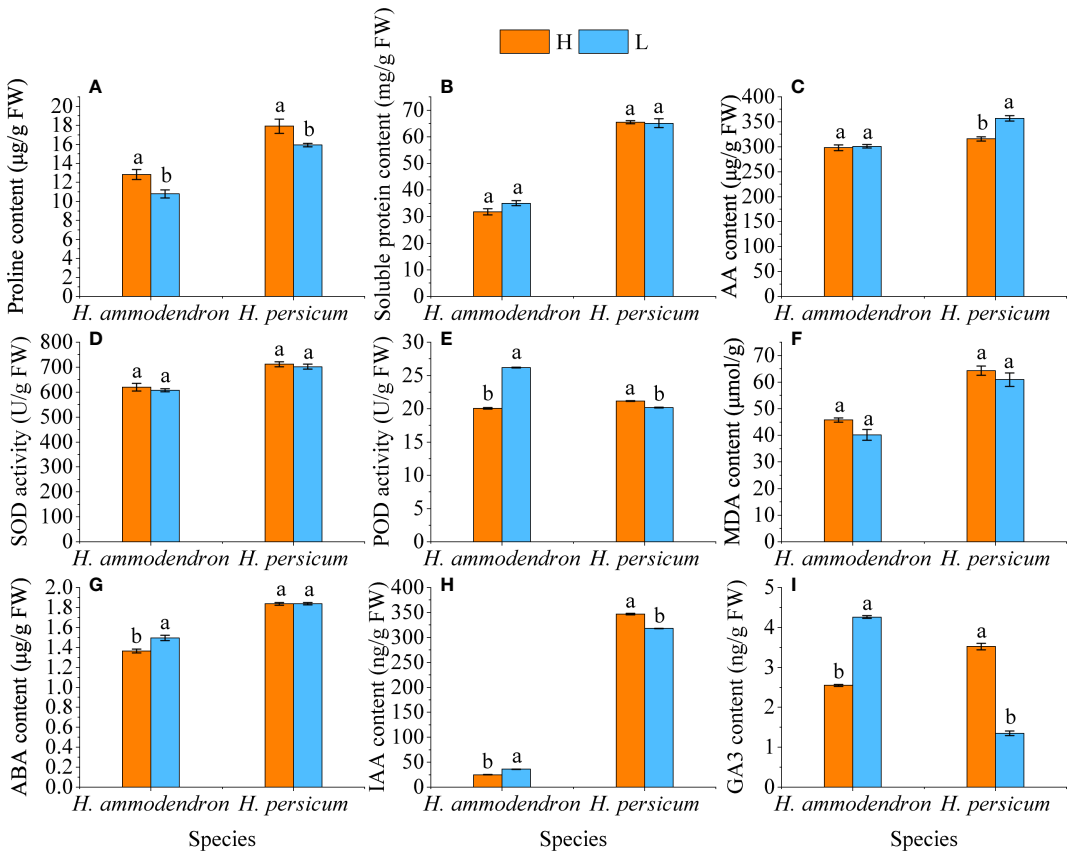


FIGURE 3
Effects of drought stress on the physiological changes in *H. ammodendron* and *H. persicum*. **(A)** Pro content; **(B)** Soluble protein content; **(C)** AA content; **(D)** SOD activity; **(E)** POD content; **(F)** MDA content; **(G)** ABA content; **(H)** IAA content; **(I)** GA3 content. Different letters indicate significant differences at $P < 0.05$. The values shown are the means of three biological replicates ± SE ($n = 3$). H: Wet environment; L: Dry environment.

TABLE 2 Transcriptome sequencing data of all samples.

Sample	Raw reads	Clean reads	Clean bases	Error rate	Q20	Q30	GCcontent
HS1	21539473	21183332	6.4G	0.03	97.72	93.29	42.37
HS2	24301276	24049096	7.2G	0.03	97.73	93.34	42.37
HS3	24481926	24160239	7.2G	0.03	97.63	93.1	42.28
LS1	23191184	22911690	6.9G	0.03	97.8	93.48	42.36
LS2	24028000	23683965	7.1G	0.03	97.81	93.52	42.33
LS3	22569984	22268590	6.7G	0.03	97.79	93.46	42.31
HB1	23550049	23227103	7G	0.03	97.83	93.54	42.28
HB2	23454270	23150331	6.9G	0.03	97.97	93.89	42.27
HB3	24025797	23718176	7.1G	0.03	97.64	93.07	42.31
LB1	21116006	20796664	6.2G	0.03	97.8	93.47	42.51
LB2	20892405	20596877	6.2G	0.03	97.63	93.06	42.46
LB3	23940719	23550102	7.1G	0.03	97.81	93.48	41.98

Identification and analysis of differentially expressed genes

Under drought stress, 12,233 (6829 up-regulated and 5404 down-regulated) and 17,953 (10,199 up-regulated and 7754 down-regulated) DEGs were differentially expressed in *H. ammodendron* and *H. persicum* respectively (Figures 5A, B). The differentially expressed genes of all the comparison groups were merged as the differential gene set, and the FPKM values of the genes were analyzed by hierarchical clustering. A

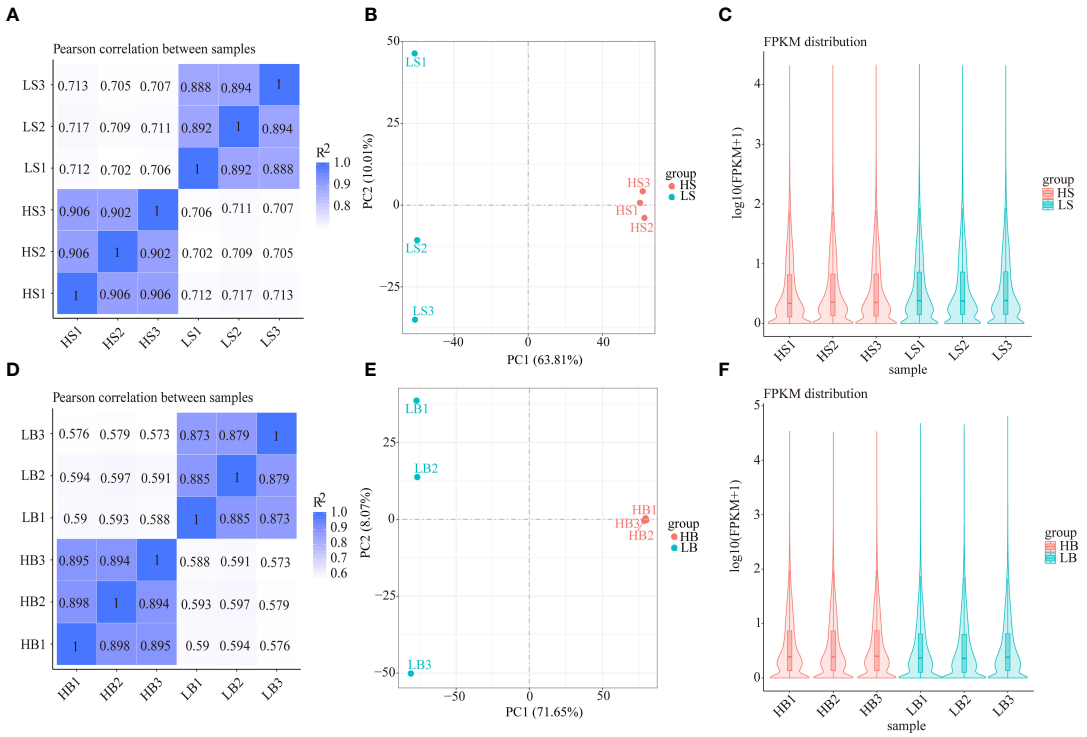


FIGURE 4
Gene expression analysis of *H. ammodendron* and *H. persicum* in an arid environment. **(A, D)** are heat maps of the correlation coefficients of the gene expression of *H. ammodendron* and *H. persicum* in humid and arid environments. The abscissa is the log10(FPKM+1) of sample 1; the ordinate is the log10(FPKM+1) of sample 2. R^2: The square of the Pearson correlation coefficient. **(B, E)** are the PCA score maps of the transcriptome data of the two species' samples. **(C, F)** are the comparison charts of the gene expression levels of the two species in humid and arid environments. The abscissa is the sample name, and the ordinate is log10(FPKM+1).

hierarchical clustering heat map was generated to illustrate the expression patterns of *H. ammodendron* and *H. persicum* in arid environments (Figures 5C, D). The gene expression patterns of *H. ammodendron* (LS and HS) and *H. ammodendron* (LB and HB) were significantly different between groups, with good repeatability (three replicates) within the group. In addition, expression levels of most genes were significantly altered in the process of hierarchical clustering, indicating that differentially expressed genes in the transcript levels of LS and HS, LB, and HB could determine the drought-tolerance specificity of *H. ammodendron* and *H. persicum*.

Functional annotation analysis of DEGs

GO (Gene Ontology) is widely used for gene function annotation and enrichment analysis (Ali et al., 2018). The main role of GO was to classify the functions of the predicted *H. ammodendron* and *H. persicum* genes. GO comprises three domains: biological process (BP), cellular component (CC), and molecular function (MF). In this study, there were 448 significant DEGs (275 up-regulated genes and 173 down-regulated genes) and 414 significant DEGs (220 up-regulated genes and 194 down-regulated genes) in *H. ammodendron* and *H. persicum*. For *H. ammodendron*, 45 genes were found to be involved in the transposition of the BP category (GO:0032196). In addition, 233 and 170 genes were involved in nuclease activity (GO:0004518) and structural constituent of ribosome (GO:0003735) in the MF category, respectively. For *H. persicum*, there were 56 DEGs involved in transposition under BP (GO:0032196). In the MF category, 358 DEGs were involved in nuclease activity (GO:0004518) (Figures 6A, C). In both species, the same GO terms associated with different functional classes were aggregated, suggesting that these GO terms are involved in drought stress response and tolerance.

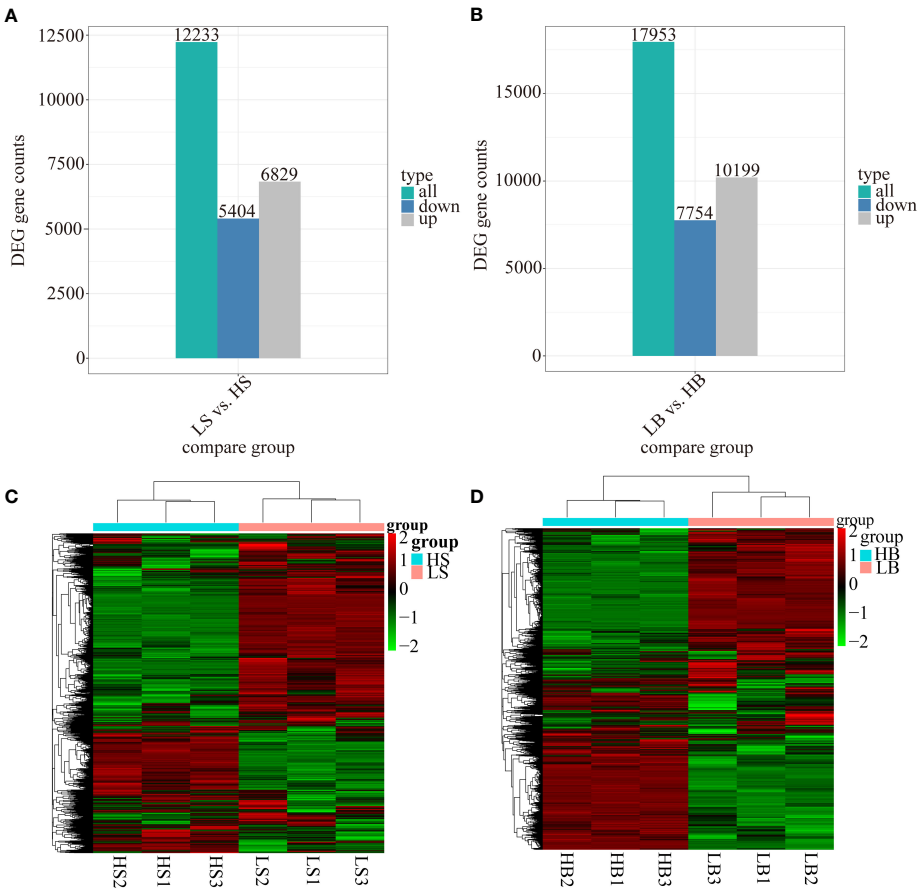


FIGURE 5
Identification and analysis of the differentially expressed genes of *H. ammodendron* and *H. persicum*. **(A, B)** are the numbers of *H. ammodendron* and *H. persicum* DEGs in humid and arid environments. **(C, D)** show the hierarchical clustering of DEGs of all samples of *H. ammodendron* and *H. persicum*.

The KEGG pathway-enriched DEGs were further analyzed as to their biological functions. A P-value ≤ 0.05 was defined as indicating DEGs with significant differences. In this study, there were two and ten significant pathways (P < 0.05) in the KEGG enrichment analysis of *H. ammodendron* and *H. persicum*, respectively (Table S2). As shown in Figures 6A, B, the top 20 significant pathway enrichments (with P values within the range [0, 1]) were screened for the analysis of both species. Both *H. ammodendron* and *H. persicum* significantly enriched the plant-pathogen interaction (ko04626) pathway. For *H. ammodendron*, there were two significantly enriched pathways with a large number of DEGs: ribosome (ko03010, 157 genes) and plant-pathogen interaction (ko04626, 93 genes) (P < 0.05) (Figure 6B). For *H. persicum*, flavonoid biosynthesis (ko00941, 24 genes), cutin, suberine, and wax biosynthesis (ko00073, 14 genes), stilbenoid, diarylheptanoid, and gingerol biosynthesis (ko00945, 8 genes), phenylpropanoid biosynthesis (ko00940, 73 genes), glycerophospholipid metabolism (ko00564, 50 genes), ether lipid metabolism (ko00565, 21 genes), metabolism of xenobiotics by cytochrome P450 (ko00980, 29 genes) and tyrosine metabolism (ko00350, 31 genes) were the main pathways (Figure 6D). The enrichment of the KEGG pathways suggested that the two species activated different molecular mechanisms of drought resistance (Figures 6B, D). We speculated that these pathways may play crucial roles in Haloxylon responses to drought stress.

Changes in transcription factor gene expression under drought stress

To analyze the regulatory mechanisms of drought-responsive genes, 217 (161 up-regulated and 56 down-regulated) and 397 (163 up-regulated and 235 down-regulated) DEGs encoding TFs were identified in *H. ammodendron* and *H. persicum* (Figures 7A, B; Table S3). A total of 41 transcription factor families were identified in *H. ammodendron*, including MYB, FAR1, AP2/ERF, C2H2, and bHLH (Figure 7A; Table S3). According to the gene expression of each transcription factor family, the top three transcription factor families were MYB (n = 19), FAR1 (n = 18), and AP2/ERF (n = 17). There were a total of 50 transcription factor families in *H. persicum*, and those with relatively high gene expression included AP2/ERF (n = 38), MYB (n = 35), WRKY (n = 27), bHLH (n = 26), C2H2 (n = 22)

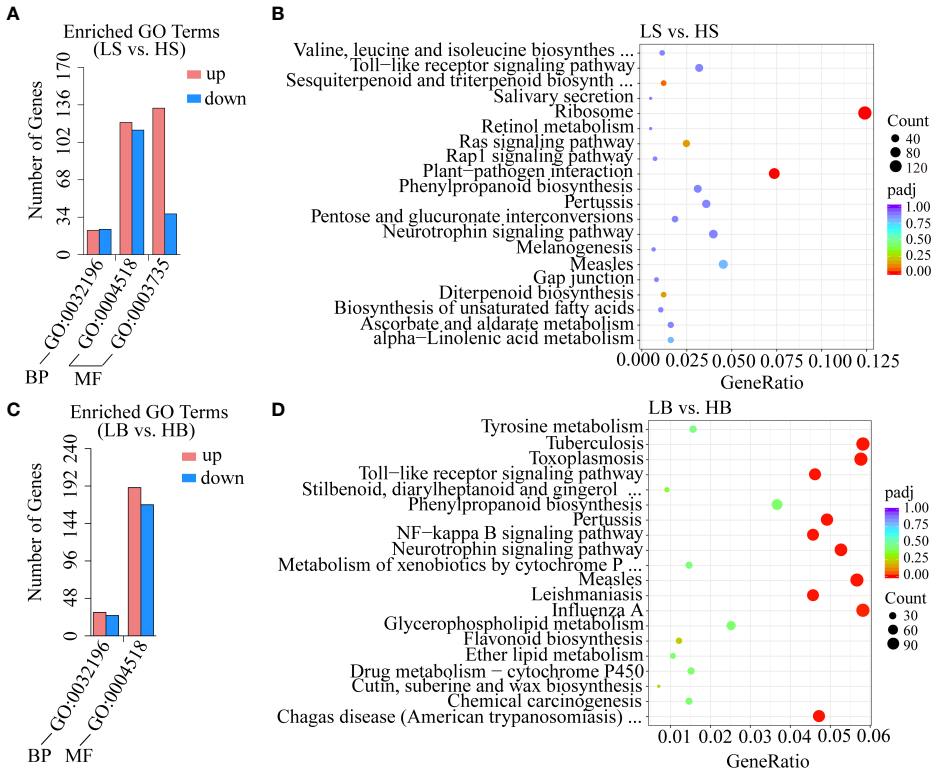


FIGURE 6
GO and KEGG enrichment analyses of DEGs. **(A, B)** are the enrichment analyses of GO and KEGG (the most significant 20 pathways enriched) of *H. ammodendron* DEGs. **(C, D)** are the enrichment analyses of GO and KEGG (the 20 pathways with the most significant enrichment) of *H. persicum* DEGs.

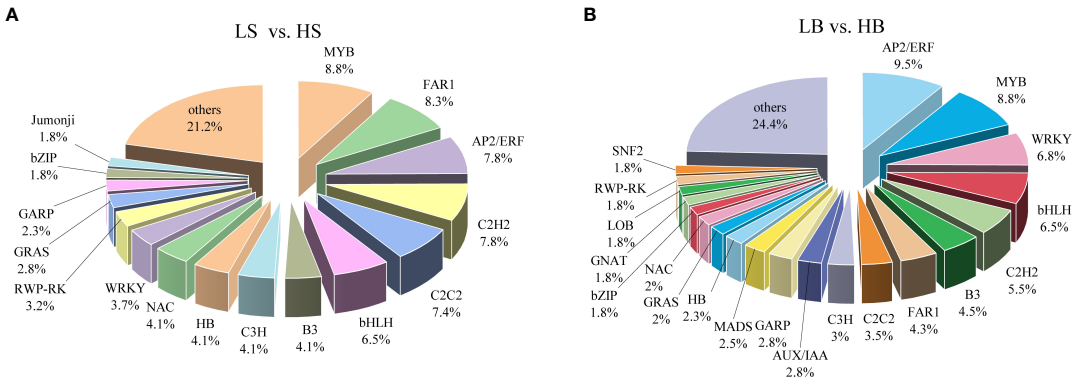


FIGURE 7
Distribution of drought-responsive transcription factor genes. **(A)** Classification of drought-tolerant TFs in *H ammodendron*. **(B)** Taxonomy of drought-tolerant TFs in *H persicum*.

(Figure 7B; Table S3). The proportions of major TFs genes in *H. ammodendron* and *H. persicum* were high (ranging from 5% to 9.5%); these included FAR1, AP2/ERF, C2H2, bHLH, MYB, C2C2, and WRKY (Figures 7A, B). Among these TFs genes, FAR1 (Cluster-6558.180) and FAR1 (Cluster-3181.261) were exclusively expressed in *H. ammodendron* and *H. persicum*, respectively, and both were significantly up-regulated (FC = 7.09, 128.5). ERF110 was expressed in both *H. ammodendron* (Cluster-6558.26745) and *H. persicum* (Cluster-3181.42435) and was significantly down-regulated (FC = 0.29) and up-regulated (FC = 127.89), respectively. The results suggest that these transcription factors may be the main drought-responsive genes and play important roles in Haloxylon drought tolerance.

Validation of RNA-Seq expression levels by qRT-PCR

To verify the reliability of the RNA-seq data, the mRNA abundances of 10 DEGs were identified using qRT-PCR. The 10 DEGs identified by qRT-PCR varied significantly between wet and dry environments, similar to those observed by RNA-seq analysis (Figure 8). Although the fold changes were not exactly as shown by the transcriptome analysis data, all the validated genes showed similar expression patterns.

Identification of differentially expressed metabolites under drought stress

UHPLC-MS/MS (Ultra-high performance liquid chromatography coupled with high-resolution mass spectrometry) was used to detect metabolites produced by *H. ammodendron* and *H. persicum* during drought tolerance. In the metabolic analysis, six replicates were carried out for both wet and dry soil environments to ensure the reliability of the experiment. The data were analyzed in positive and negative ion modes using PCA and PLS-DA analyses (Figures 9A, B; Figure S1). In the positive and negative ion modes for *H. ammodendron*, the two groups of samples were clearly separated. For positive ion samples, Axis 1 and Axis 2 of the PCA explained 72.49% of the total variance (Figure 9A). For *H. persicum*, the LB and HB samples were highly separated in negative ion mode, and the Axes 1 and 2 of the PCA explained 73.54% of the total variance (Figure 9B). The PCA analysis and the PLS-DA analysis could clearly distinguish the sample data points of the two species, indicating that the metabolites of each group of samples differed according to species, quantity, and concentration.

Differentially expressed metabolites (DEMs) screening conditions were (1) VIP > 1.0; (2) Fold change > 1.5 or Fold change < 0.667; (3) P value < 0.05. Under the positive ion mode, totals of 296 (183 up-regulated and 113 down-regulated) and 452 (254 up-regulated and 198 down-regulated) DEMs were detected respectively in *H. ammodendron* and *H. persicum*. For the negative ion mode, totals of 252 (119 up-regulated and 133 down-regulated) and 354 (173 up-regulated and 181 down-regulated) DEMs were detected respectively in *H. ammodendron* and *H. persicum* (Figures 9C, D). Table S4 lists DEMs highly expressed by the two species under drought stress. Sedum heptulose 7-phosphate (s7p) and N1-(4-bromophenyl)-2-[4-(tert-butyl) phenoxy] propanamid were significantly down-regulated (FC = 0.11; FC = 0.08) and up-regulated (FC = 37.72; FC = 119.72) in *H. ammodendron* and *H. persicum*, respectively.

KEGG enrichment analysis of differentially expressed metabolites

To better understand the functions of DEMs, all DEMs were mapped to the KEGG path database. Under the positive

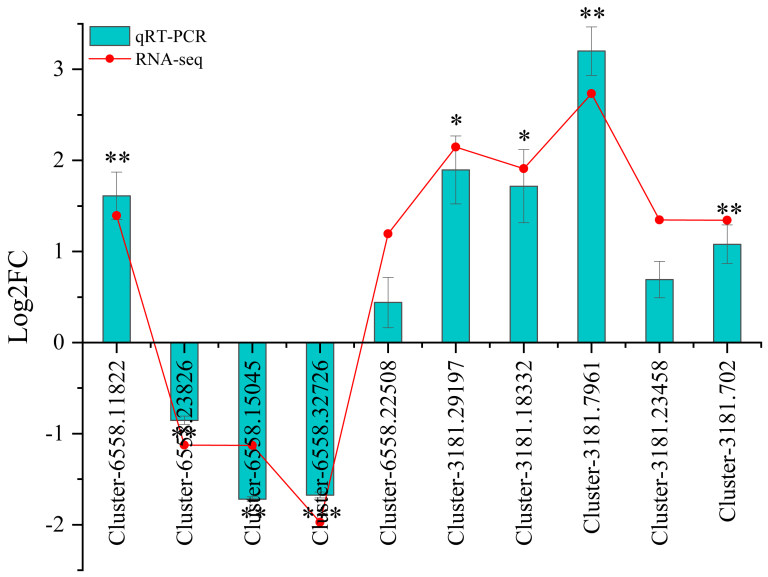


FIGURE 8
Relative expression *via* qRT-PCR and RNA-seq of 10 DEGs. Significance was defined as *(P < 0.05), **(P < 0.01), and ***(P < 0.001).

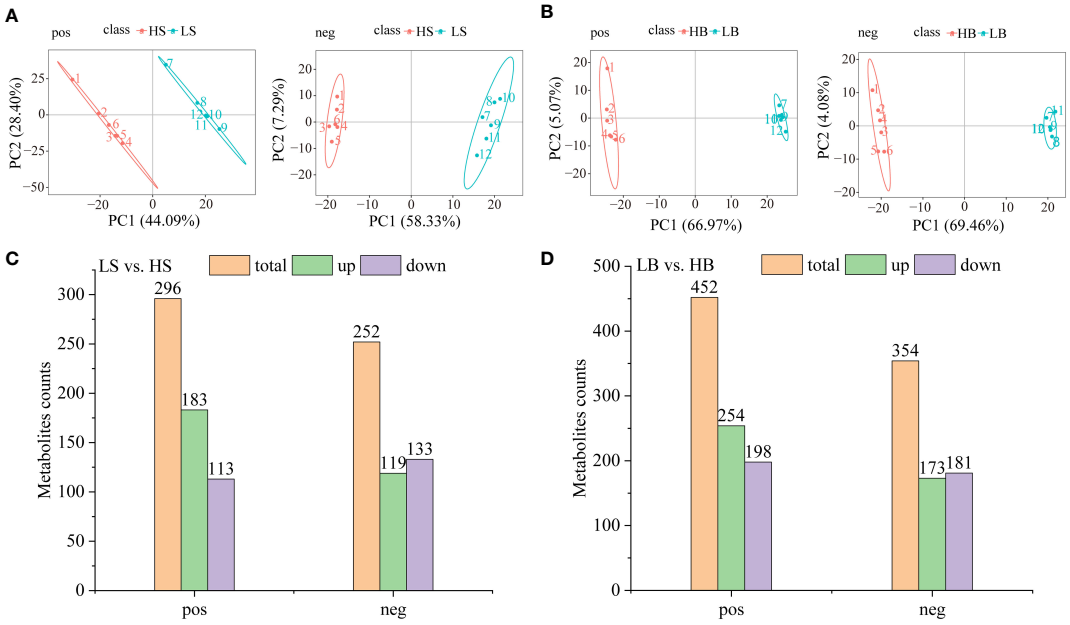


FIGURE 9
Differential metabolites of *H ammodendron* and *H persicum* under drought stress. **(A)** Principal component analysis scores of the two groups of samples of (*H ammodendron* in positive ion (pos) and negative ion mode (neg). **(B)** Principal component analysis score maps of the two groups of samples of *H persicum* in positive ion (pos) and negative ion mode (neg). **(C)** DEMs of *H ammodendron* in positive and negative ion mode. **(D)** DEMs of *H persicum* in positive and negative ion mode.

ion mode, 38 DEMs of *H. ammodendron* were enriched in "Metabolic pathway", "Biosynthesis of secondary metabolites" and "Amino acid metabolism pathway", including "Flavonoid biosynthesis", "Isoquinoline alkaloid biosynthesis", "Tyrosine metabolism" and "Phenylalanine metabolism" (Figure 10A; Table S5). In the negative ion mode, most of the DEMs were enriched in "Biosynthesis of secondary metabolites", "Biosynthesis of unsaturated fatty acids", "Isoquinoline alkaloid biosynthesis", "Sugar metabolism" and "Biosynthesis of amino acids synthesis". These included "Phenylalanine, tyrosine and tryptophan metabolism", "Alanine, aspartate and glutamate metabolism", "Glycine, serine and threonine metabolism", "Glycolysis/gluconeogenesis", "Fructose and mannose metabolism", and "Amino sugar and nucleotide sugar metabolism" (Figure 10B; Table S5). There were 147 and 162 DEMs enriched in the positive and negative ion modes, respectively. For the positive ion mode, the main enriched pathways were "Metabolic pathways", "Biosynthesis of secondary metabolites", "Isoquinoline alkaloid biosynthesis", "Tropane, piperidine and pyridine alkaloid biosynthesis", "Amino acid biosynthesis" and "ABC transporters" (Figure 10C; Table S6). For the negative ion mode, "Metabolic pathways", "Biosynthesis of secondary metabolites", "Ascorbate and aldarate metabolism", "Glutathione metabolism", "Purine metabolism", "Glyoxylate and dicarboxylate metabolism", "Phenylalanine metabolism", and "Phenylpropane biosynthesis" were the major enrichment pathways (Figure 10D; Table S6). Most of the intermediates involved in amino acid metabolism and synthesis under the positive and negative ion modes of *H. ammodendron* and *H. persicum* were up-regulated, indicating that drought stress could promote the normal metabolic processing of their amino acids. Salicylic acid involved in plant hormone signal transduction was up-regulated in the positive ion mode of *H. ammodendron*, and jasmonic acid and abscisic acid were down-regulated in the negative ion mode. Abscisic acid and indole-3-acetic acid were up-regulated in the positive ion mode of *H. persicum*, while jasmonic acid was down-regulated in the negative ion mode. Citric acid, an important metabolic intermediate involved in the TCA cycle of *H. ammodendron*, was down-regulated in negative ion mode. In contrast, several important metabolic intermediates involved in the TCA cycle in the positive and negative ion modes of *H. persicum* were all up-regulated, including α-ketoglutarate, succinic acid, and citric acid, indicating that enhanced its energy metabolism pathways under drought stress.

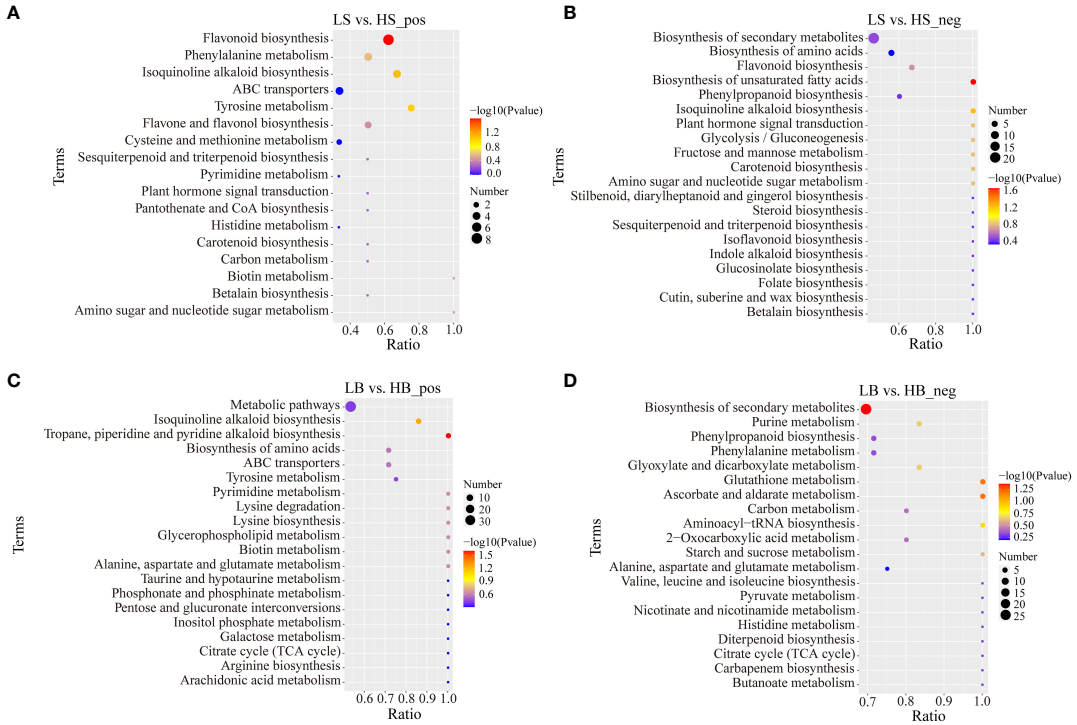


FIGURE 10
KEGG enrichment analysis of DEMs in positive and negative ion mode (only the top 20 results are shown). **(A)** Bubble plot of KEGG enrichment analysis of *H ammodendron* DEMs in positive ion mode. **(B)** Bubble plot of KEGG enrichment analysis of *H ammodendron* DEMs in negative ion mode. **(C)** Bubble plot of KEGG enrichment analysis of DEMs in positive ion mode of *H persicum*. **(D)** Bubble plot of KEGG enrichment analysis of DEMs in the positive ion mode of *H persicum*.

Association analysis of transcriptome and metabolome data

The DEGs obtained by transcriptome analysis and the DEMs obtained by metabolomics analysis were analyzed using the Pearson correlation. The correlations between the top 50 DEMs and the top 100 DEGs (in ascending order of P value) are shown in Figures S2–S5. Most of the DEGs in *H. ammodendron* and *H. persicum* were positively correlated with the DEMs (|Corr| > 0.9, P < 0.001). Mapping the obtained DEGs and DEMs to the KEGG pathway database was performed to obtain common pathway information and to determine the main biochemical and signal transduction pathways in which the DEGs and DEMs jointly participated. In the positive ion mode, the *H. ammodendron* and *H. persicum* DEGs and DEMs were mapped to 15 and 42 pathways, respectively, and in the negative ion mode they were mapped to 34 and 45 pathways (Figure 11). DEGs and DEMs were more enriched in flavonoid biosynthesis (Tran: 13; Meta: 8), phenylalanine metabolism (Tran: 10; Meta: 4), ABC transporter (Tran: 11; Meta: 4), and tyrosine metabolism (Tran: 13; Meta: 3) pathways in LS vs. HS_pos (Figure 11A). LS vs HS_ neg was enriched in phenylpropane biosynthesis (Tran: 39; Meta: 3), flavonoid biosynthesis (Tran: 13; Meta: 4), unsaturated fatty acid biosynthesis (Tran: 13; Meta: 4), plant hormone signal transduction (Tran: 30; Meta: 2), carbon metabolism (Tran: 65; Meta: 2), glycolysis/gluconeogenesis (Tran: 33; Meta: 2), amino sugar and nucleotide sugar metabolism (Tran: 32; Meta: 2), and amino acid biosynthesis (Tran: 52; Meta: 5) (Figure 11B). LB vs. HB_pos was enriched in Tropane, piperidine, and pyridine alkaloid biosynthesis (Tran: 22; Meta: 5), ABC transporter (Tran: 15; Meta: 5), Tyrosine metabolism (Tran: 31; Meta: 3), Isoquinoline alkaloid biosynthesis (Tran: 23; Meta: 6), and Biosynthesis of amino acids (Tran: 72; Meta: 5) (Figure 11C). LB vs. HB_neg was enriched in phenylpropanoid biosynthesis (Tran: 73; Meta: 5), starch and sucrose metabolism (Tran: 68; Meta: 3), 2-Oxocarboxylic acid metabolism (Tran: 24; Meta: 4), ascorbate and aldarate metabolism (Tran: 18; Meta: 5), purine metabolism (Tran: 65; Meta: 5), aminoacyl-tRNA

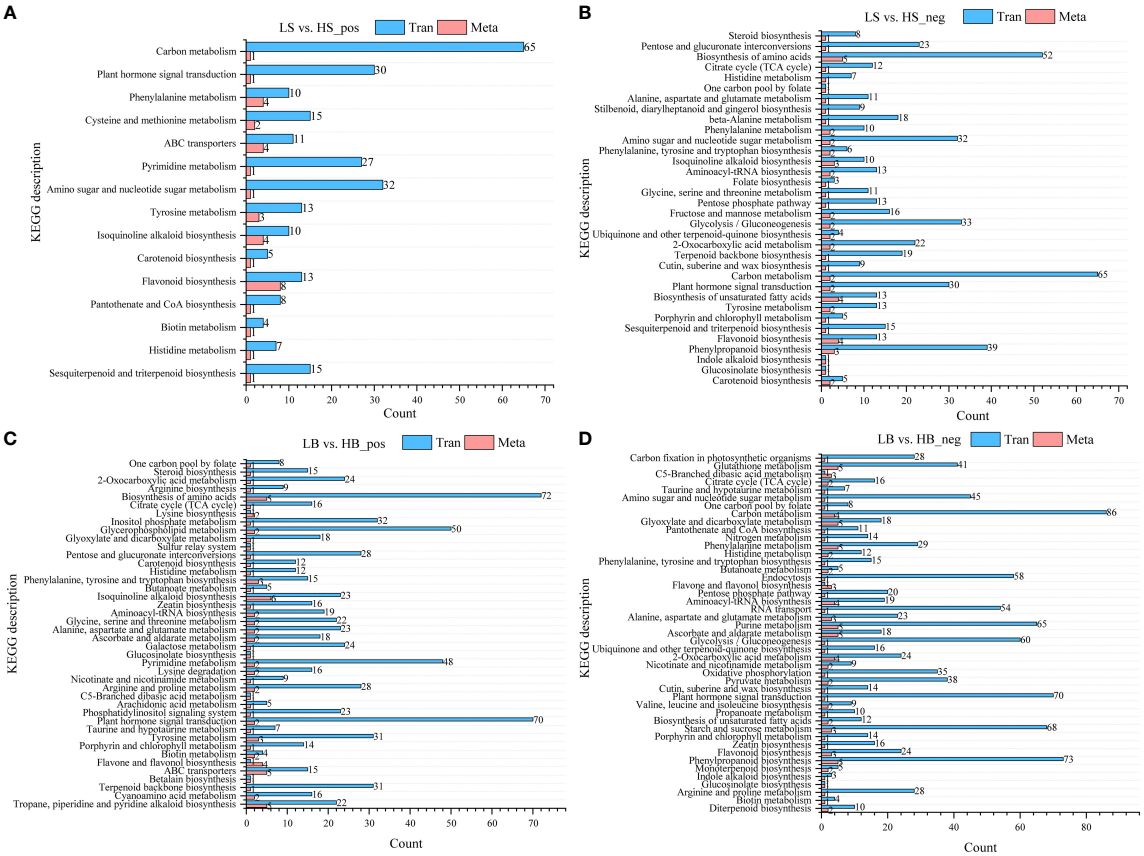


FIGURE 11
DEGs and DEMs KEGG enrichment pathways. **(A)** Pathway information of DEGs and DEMs of LS vs. HS in positive ion mode; **(B)** Pathway information of DEGs and DEMs of LS vs. HS in negative ion mode; **(C)** Pathway information of DEGs and DEMs of LB vs. HB in positive ion mode; **(D)** pathway information of DEGs and DEMs of LB vs. HB in negative ion mode. Tran: DEGs; Meta: DEMs.

biosynthesis (Tran: 19; Meta: 4), phenylalanine metabolism (Tran: 29; Meta: 5), glyoxylate and dicarboxylate metabolism (Tran: 18; Meta: 5), carbon metabolism (Tran: 86; Meta: 4), and glutathione metabolism (Tran: 41; Meta: 5) (Figure 11D).

Combined analysis of transcriptional, metabolic, and physiological levels

To screen metabolites and differential genes more accurately, transcriptome and metabolome data were further analyzed to understand the regulation of metabolic pathways under drought stress, and the relationships between gene expression and many metabolites were identified. Tables S7, S8 provide a list of *H. ammodendron* and *H. persicum* metabolites, related genes, major metabolic pathways, and genes regulating physiological indicators. Combined transcriptome and metabolome analysis showed that among the metabolites detected by the phytohormone signal transduction pathway, salicylic acid (FC = 2.58, up-regulated) and indole-3-acetic acid (FC = 1.56, up-regulated) were exclusively expressed in *H. ammodendron* and *H. persicum*, respectively. The content of jasmonic acid (FC = 0.52; FC = 0.56) was significantly decreased in both species, while the content of abscisic acid (FC = 0.53; FC = 1.65) was decreased in *H. ammodendron* and increased in *H. persicum*. Meanwhile, there were 30 (23 up-regulated and 7 down-regulated) and 70 (26 up-regulated and 44 down-regulated) genes involved in plant hormone signal transduction in *H. ammodendron* and *H. persicum*, respectively, generally encoding auxin-responsive factors and auxin-responsive proteins. There were two metabolites (β-D-Fructose 6-phosphate and arbutin) and one (arbutin) involved in the glycolysis/gluconeogenesis metabolic pathway in *H. ammodendron* and *H. persicum*, with 33 (24 up-regulated and 9 down regulated) and 60 (44 up regulated and 16 down regulated) related genes, respectively, including alcohol dehydrogenase, 6-phosphofructokinase, hexokinase, pyruvate kinase, pyruvate decarboxylase, and phosphoenolpyruvate carboxykinase. The metabolites involved in amino acid biosynthesis in *H. ammodendron* are β- D-fructose 6-phosphate (FC = 1.89), s-sulfo-l-cysteine (FC = 3.18), L-histidine (FC = 0.41), citric acid (FC = 0.41), and L-tryptophan (FC = 1.51), while the contents of five metabolites (l-saccharine, S-adenosylmethionine, shikimic acid, L-phenylalanine, and L-asparagine) in *H. persicum* were significantly increased, and most genes involved in amino acid biosynthesis were also up-regulated. The contents of four metabolites involved in flavonoid biosynthesis of *H. ammodendron* were decreased under drought stress, and eight were increased, while there were three metabolites in *H. persicum*, but only the content of pelargonidin chloride was increased significantly. Most genes involved in flavonoid biosynthesis were down-regulated in both species.

Starch and sucrose metabolism and glutathione metabolic pathways were the only metabolic pathways enriched in the association analysis of the transcriptome and metabolome of *H. persicum*. Isomaltose, sucrose, and α,α-trehalose were the main metabolites of starch and sucrose metabolic pathways, and the contents were increased significantly under drought stress, encoding UDP glucose 6-dehydrogenase (Cluster-3181.36869, FC = 29.48), sucrose synthase (Cluster-7552.1, FC = 8.37), 4-alpha-glucanotransferase (Cluster-3181.42590, FC = 181.02), fructokinase (Cluster-3181.18760; FC = 8.78), beta-glucosidase (Cluster-3181.19347, FC = 30.49; Cluster-3181.2748, FC = 90.51), and α,α-trehalase (Cluster-3181.4409; FC = 29.48) genes were highly up-regulated under drought stress. Under drought stress, in addition to the significant decrease in the content of the metabolite ascorbic acid, the contents of L-glutamic acid, dehydroascorbic acid, glutathione, and oxidized glutathione were significantly increased in the glutathione metabolic pathway, and the genes involved in this metabolic pathway encode glutathione S-transferase and glutathione reductase.

Under drought stress, 14 (up: 4, down: 10) genes encoding ABA, 30 (up: 27, down: 3) genes encoding IAA, 9 (up: 7, down: 2) genes encoding GA, 4 (up: 2, down: 2) genes encoding SOD, 15 (up: 15, down: 0) genes encoding POD, 9 (up: 2, down: 7) genes encoding lipoxygenase, 35 (up: 18, down: 17) genes encoding proline, 52 (up: 31, down: 21) genes encoding AA, 8 (up: 7, down: 1) genes encoding aquaporin and 4 (up: 1, down: 3) genes encoding LEA protein were identified in *H. ammodendron*. For *H. persicum*, 120 (up: 73, down: 47) genes encoding ABA, 55 (up: 16, down: 39) genes encoding IAA, 9 (up: 5, down: 4) genes encoding GA, 9 (up: 1, down: 8) genes encoding SOD, 33 (up: 19, down: 14) genes encoding POD, 20 (up: 9, down: 11) genes encoding lipoxygenase, 53 (up: 23, down: 30) genes encoding proline, 71 (up: 51, down: 20) genes encoding AA, 15 (up: 3, down: 12) genes encoding aquaporin and 5 (up: 3, down: 2) genes encoding LEA protein were identified under drought stress.

Discussion

Drought tolerance is a key characteristic of desert plants. In these regions, programmed selection is performed to improve crop drought tolerance through precise stress testing strategies (Michaletti et al., 2018). Drought tolerance is a complex process that is regulated by the interaction of multiple genes (Tardieu and Tuberosa, 2010); therefore, manipulating a group of genes or a single gene is not sufficient to study drought tolerance. In this study, two species of Haloxylon (*H. ammodendron* and *H. persicum*) growing under natural conditions in arid areas were used as the research objects to reveal the molecular mechanisms of drought response and to screen for candidate genes involved in drought tolerance in wet and arid soil environments. Furthermore, this study is the first to combine transcriptomics

and metabolomics to better understand the differences in drought tolerance between the two Haloxylon species. Drought stress had significant effects on anatomical structure and physiological and biochemical indicators, metabolite profiles, and gene expression.

The assimilating branches of *H. ammodendron* and *H. persicum* are formed by leaf degradation, and the formation of assimilating branches represents the peak of the evolution of *H. ammodendron* in response to drought conditions (Thayale Purayil et al., 2020). Succulent shoots enhance water retention (Fan et al., 2018); assimilating shoots are located between leaves and stems, and they have unique structural features (Yue et al., 2013). The cuticle reduces the evaporation of leaf water and is an important structure for plant water retention (Han et al., 2006). In the mesophyll, the palisade tissue is developed, and the spongy tissue is simplified (Kocsis et al., 2004), adaptations that allow the plant to increase the photosynthetic rate and enhance drought resistance (Kou et al., 2008). Vascular bundles play a role in nutrient transport and mechanical support in plants. Therefore, the more developed the vascular column, the more vigorous the plant, and the stronger the drought resistance (Wang et al., 2021). The results showed that the leaves of *H. ammodendron* and *H. persicum* degenerated into assimilating branches for photosynthesis, with the cuticle outside the epidermis, continuous and close palisade tissue, wreath structures, crystal containing cells, and water storage tissue, features that can effectively improve the photosynthetic efficiency, water retention, and water absorption capacity of the plants. Due to long-term existence in an arid environment, the morphological and structural characteristics of *H. ammodendron* and *H. persicum* have continuously evolved. Under drought stress, the water storage tissue and duct pore diameter of *H. ammodendron* increased significantly. Although there were no significant differences in the diameters of assimilating branches, the thickness of the cuticle and palisade tissue, or vascular bundle diameter, these increased with the decrease of the soil water content. Assimilatory branch diameter and cuticle thickness were significantly different in LB vs. HB, while palisade tissue, vascular bundle diameter, and duct pore diameter were increased in arid conditions.

Organic solutes such as proline, soluble proteins, and amino acids can protect plants from stress and contribute to osmoregulation, reduction of reactive oxygen species, stabilization of membrane structures, and structural characterization of proteins and enzymes (Farooq et al., 2009). Studies have shown that with the increase of drought stress intensity, both soluble protein and proline contents increase (Wei et al., 2019). Osmoregulation proteins (OSMs) are widely present in various tissues of plants (Wan et al., 2022). The OSM process involves proteins being synthesized to adapt to osmotic pressure (Wan et al., 2022). When plant cells are under osmotic stress, osmotic regulatory proteins in their cells can absorb water by changing the permeability of the membrane and reducing excessive water loss (Wan et al., 2022). Aquaporins (AQPs) are integral membrane proteins that efficiently and specifically transport water molecules (Tyerman et al., 2010). LEA protein (Late-embryogenesis-abundance protein) is widespread in higher plants and is accumulated in large amounts during the later stages of seed embryogenesis (Zheng et al., 2019). Under osmotic stress, the accumulation of a large amount of LEA protein in plants can alleviate cell damage caused by reduced water potential (Hu, 2008; Bies-Ethève et al., 2008). In this study, the proline contents of both *H. ammodendron* and *H. persicum* were significantly decreased under drought stress, while the amino acid contents were increased, and the soluble protein was increased in *H. ammodendron* and decreased in *H. persicum*. At the same time, most of the genes encoding Pro, AA, and AQPs in *H. ammodendron* were up-regulated, while most of the genes encoding Pro, AA, AQPs, and LEA in *H. persicum* were down-regulated. This indicates that different plants have different osmotic regulation mechanisms in response to drought stress (physiological performance precedes gene regulation). Soluble proteins and amino acids are positively regulated in the drought tolerance response of *H. ammodendron*, while *H. persicum* increases the amino acid content to protect against drought stress. ROS are by-products of aerobic metabolism in plants, and excessive accumulation of ROS can damage the structure and function of plant cells (Choudhury et al., 2017; Hussain et al., 2018). Studies have shown that the production of ROS is related to membrane lipid peroxidation catalyzed by lipoxygenase (LOX) (Xin et al., 2017). Under drought stress, the MDA contents of *H. ammodendron* and *H. persicum* were decreased, and the genes encoding LOX were differentially expressed in both species; most were down-regulated, providing evidence at the molecular level indicating that *H. ammodendron* and *H. persicum* may maintain the stability of the cytoplasmic membrane under drought stress by maintaining lower LOX activity to generate less ROS and to weaken membrane lipid peroxidation. Under abiotic stress, plants control the overproduction of ROS through enzymatic components and non-enzymatic antioxidants (Choudhury et al., 2017; Hussain et al., 2018). Under drought stress, higher POD activity was observed in *H. ammodendron*, and genes encoding POD were all significantly up-regulated, suggesting that *H. ammodendron* decomposes ROS through higher POD activity to protect cells from damage. Plant hormones play an important role in plant stress response. During drought induction, environmental stress factors induce the secretion of phytohormones that mediate immediate cellular responses by triggering phytohormone signal transduction pathways (Thayale Purayil et al., 2020). In this study, the contents of three hormones of *H. ammodendron* were significantly increased. With the exception of the genes encoding ABA that were down-regulated, most of the genes encoding IAA and GA were up-regulated, indicating that drought stress induced the secretion of *H. ammodendron* hormones and activated the

corresponding hormone signal transduction pathway to respond to the damage. The contents of IAA and GA3 in *H. persicum* were significantly decreased, and there was no significant change in ABA content, although most genes encoding ABA and GA were up-regulated.

TFs not only play a role in the drought responsive genes (Budak et al., 2015; Gu et al., 2019), but also play an important role in the regulation of gene expression networks (Zhang et al., 2019). In this study, most of the differentially expressed TFs were members of the FAR1, AP2/ERF, C2H2, bHLH, MYB, C2C2, and WRKY families (Figure 7). Numerous studies have shown that these TF subfamilies are involved in plant drought resistance (Baillo et al., 2019; Li et al., 2020; Yao et al., 2020; Li et al., 2021). Some TF family members play important roles in drought resistance through ABA-mediated pathways (Luo et al., 2013; Sun et al., 2015). AtFAR1 can strongly respond to drought stress, and FAR1 can positively regulate the ABA signaling pathway and integrate light and ABA signaling to better adapt plants to environmental stress (Tang et al., 2013). Most of the genes of the FAR1 family in *H. ammodendron* and *H. persicum* were positively regulated under drought stress. The response of the WRKY TF family to drought stress has been intensively studied in many species. For example, overexpression of GsWRKY20 in A. thaliana enhances drought tolerance by mediating ABA signaling, and overexpression of BdWRKY36 in tobacco enhances drought tolerance and ABA biosynthesis (Luo et al., 2013; Sun et al., 2015). In this study, 8 and 27 WRKY TFs homologous genes were differentially expressed in *H. ammodendron* and *H. persicum*, respectively, among which WRKY3 and WRKY76 were highly expressed, indicating that these WRKY TFs play specific roles in drought resistance. MYB, one of the largest TF families in plants, positively regulates drought stress response through an ABA-mediated pathway. Overexpression of SiMYB75 in A. thaliana increases its tolerance to drought stress (Dossa et al., 2020). Under drought stress, multiple genes of the MYB family in *H. ammodendron* and *H. persicum* were differentially expressed, and most genes were up-regulated in *H. ammodendron*, while *H. persicum* was the opposite. The results indicate that MYB has a regulatory role in the drought stress response in *H. ammodendron* and *H. persicum*. This may also be one of the reasons for the increase in ABA content in *H. ammodendron*.

In addition, in this study AP2/ERF family members whose expression levels were significantly altered by drought stress were also identified. Similar results have been obtained in other plants such as V. riparia, P. davidiana, and L. kaempferi (Mun et al., 2017; Khadka et al., 2019; Li et al., 2021). Under drought stress, the genes encoding ERF017, ERF014 and ERF021 in *H. ammodendron*, ABR1-like, ERF071-like, ERF113-like and ERF027-like were highly upregulated (Table S3). These TFs have been shown to positively regulate drought resistance in other plants (Pan et al., 2012; Guttikonda et al., 2014). In addition, down-regulated genes also help plants adapt to drought stress. For example, Dong and Liu (2010) observed that AtRAP2.1 was found in Arabidopsis thaliana plays a negative role in response to drought stress. The present study found that under drought stress, two homologous ERF genes, one ABR1 gene, and one WIN1 gene of *H. ammodendron* were specifically down-regulated; Eleven ERF homologous genes, two DREB homologous genes, two ANT homologous genes, one CRF5 gene, one WIN1 gene, and one TINY gene were specifically down-regulated under drought stress in *H. persicum* (Table S3). Our study is in contrast with the findings of Meng et al. (2021), who found that under drought stress the DREB2A was strongly induced in the CaDHN3 transgenic Arabidopsis. Further exploration of these TFs may contribute to a deeper understanding of the regulation of drought tolerance in the genus Haloxylon.

Metabolite profiling not only provides a deeper understanding of complex regulatory processes but also determines the phenotype of a specific compound and the chemical signature of a specific phenotype (Fiehn et al., 2000). The metabolomic responses of plants to drought stress have been reported in many studies (Raorane et al., 2015; Nam et al., 2016; Guo et al., 2018; Michaletti et al., 2018). For example, in rice GC-MS identified 47 and 69 DEMs in IAC1246 (a drought-tolerant genotype) and IRAT109 (a drought-intolerant genotype) (Ma et al., 2016). Several key metabolic compounds were also found in IAC1246 (a drought-tolerant genotype), including ferulic acid, 4-hydroxycinnamic acid, putrescine, 5-methoxytryptamine, malonic acid, and cumic acid (Ma et al., 2016). Under drought stress, GC-MS detected 19 and 32 DEMs in drought-intolerant and drought-tolerant wheat varieties, respectively (Guo et al., 2018). The results also showed that the key metabolites in wheat were primarily organic acids, sugars, and amino acids (Guo et al., 2018). Michaletti et al. (2018) identified 14 and 16 drought-tolerant metabolites in drought-tolerant and drought-intolerant wheat varieties by LC-MS, and the results showed that levels of organic acids, amino acids, and sugars were significantly altered in response to water scarcity. For *H. ammodendron* and *H. persicum*, 296 and 452 DEMs were identified in the positive ion mode, and 252 and 354 DEMs were identified in the negative ion mode respectively. In addition, major metabolites (i.e. Adenosine, Monocrotaline and L-Dopa, Table S4) related to the drought tolerance of *H. ammodendron* and *H. persicum* were also detected.

To explore the molecular mechanism of plant drought resistance, many studies have identified key candidate genes, metabolites, and pathways that may play important roles in the process of plant drought resistance. These include MDH, PDH, P5CS, heat shock protein genes, zinc finger proteins genes and cytochrome P450s genes, and metabolites including glucose, fructose, phenylpropanoids, the carotenoid zeaxanthin, monoterpenes, 4-hydroxycinnamic acid, and ferulic acid. These are likely to determine drought tolerance, and they are involved in a series of important metabolic pathways such as the

TCA cycle, glycolysis, glutamate mediated proline biosynthesis pathway, sucrose and starch metabolism, tyrosine metabolism, phenylalanine metabolism, and phenylalanine biosynthesis and secondary metabolism (Jia et al., 2016; Ma et al., 2016; Savoi et al., 2016; Meyer et al., 2014). In this study, key candidate genes (CER1, Z-ISO, NCED, CTR1, SAUR, HCBT3, ABCB21, ALDO; GH3, GLT1, PER12, CCOMT, DPE2, ALDH, IMPL2, and FAR3) and major metabolites (Farnesyl pyrophosphate, Salicylic acid, Vitexin, Naringenin, 1,2-Benzenedicarboxylic acid, β-D-Fructose 6-phosphate, S-Sulfo-L-cysteine, Stylopine, Salidroside; L-Dopa, Coniferyl alcohol, Isomaltose, Glutathione) were identified in *H. ammodendron* and *H. persicum*. These genes and metabolites are collectively involved in important carbohydrate metabolism (glycolysis/gluconeogenesis, carbon metabolism, starch and sucrose metabolism, pyruvate metabolism, ascorbate and aldarate metabolism, glyoxylate and dicarboxylate metabolism, and carotene metabolism), amino acid metabolism (phenylalanine metabolism, tyrosine metabolism, amino acid biosynthesis, and glutathione metabolism), lipid metabolism (unsaturated fatty acid biosynthesis, cutin, suberine and wax biosynthesis, and 2-Oxocarboxylic acid metabolism), secondary metabolism (flavonoid biosynthesis, isoquinoline alkaloid biosynthesis, phenylpropane biosynthesis, tropane, and piperidine and pyridine alkaloid biosynthesis), signal transduction (plant hormone signal transduction and phenylalanine metabolism), transport and catalysis (ABC transporters), and transcriptional and post-transcriptional regulation (aminoacyl-tRNA biosynthesis) pathways.

There are four main hormones that respond to drought stress in plants, namely abscisic acid (ABA), salicylic acid (SA), jasmonic acid (JA), and ethylene (ETH). In addition, auxin (IAA) and cytokinin (CTK) are involved in the regulation of many aspects of plant growth and development, and they play important roles in rehydration after drought stress (Shinozaki and Yamaguchi-Shinozaki, 2007). Numerous studies have emphasized the role of SA in regulating physiological processes such as photosynthesis, osmotic fluid production, and antioxidant enzyme activity, thereby improving the relationship of plants to water under stress (Hayat et al., 2008). In this study, the increase of SA content may have increased the activity of antioxidant enzymes to a certain extent, improved the water balance, and thus improved the drought tolerance of *H. ammodendron*. Drought stress affected the expression of related genes in auxin biosynthesis and signal transduction pathways. Studies have shown that AUX1 in A. thaliana encodes a high-affinity auxin influx carrier, while the Arabidopsis AUX/LAX gene encodes a series of auxin influx transporters that have different growth and development functions and regulatory mechanisms (Péret et al., 2012). The present study found that auxin response factor and most SAUR-like auxin-responsive family proteins were induced in *H. ammodendron* and inhibited in *H. persicum*. The above shows that under drought stress, *H. ammodendron* can avoid the reduction of IAA by inducing the expression of auxin-related genes, thereby maintaining a high physiological response to stress. *H. persicum* responds to drought stress by altering the expression of genes related to the auxin synthesis pathway and slowing down its growth. The results at the physiological level also provide evidence for this.

Carbohydrate metabolism involves a large number of biochemical processes and is important for the formation, breakdown, and interconversion of carbohydrates in organisms that can affect plant growth and its response to stress (Chen et al., 2013). β-D-Fructose 6-phosphate is one of the products generated during glycolysis. In the present study, the metabolite β-D-Fructose 6-phosphate content was increased under drought stress and was involved in the fusiform glycolysis/gluconeogenesis metabolic pathway. Under drought stress, most of the genes involved in the glycolysis/gluconeogenesis metabolic pathways of *H. ammodendron* and *H. persicum* were up-regulated, indicating that the energy production of the two species changed significantly, and the transition from photophosphorylation to oxidative phosphorylation was the main method of supplying ATP. The expression of the 6-phosphofructokinase gene of *H. ammodendron* was up-regulated or down-regulated. The hexokinase gene was only up-regulated in *H. persicum*, and the pyruvate kinase gene was up-regulated in both species, indicating that under drought stress the two species maintained ATP supply by constantly changing the transcription levels of key enzyme genes in the glycolysis/gluconeogenesis pathway. Phosphoenolpyruvate carboxykinase (PEPCK) is a bifunctional enzyme with both decarboxylase and carboxylase activities. It plays a key role in the physiological metabolism of plants (Penfield et al., 2012). This study found that three PEPCK [ATP] (cluster-6558.18891, cluster-6558.23431, cluster-6558.22745) genes in *H. ammodendron* were down-regulated, while one PEPCK [ATP] (cluster-3181.4222) gene in *H. persicum* was up-regulated. This indicated that the expression of PEPCK genes in *H. persicum* was less affected by drought stress compared with *H. ammodendron*, and this functioned to maintain its normal amino acid metabolism, citric acid cycle replenishment, and pH regulation.

Under drought stress, the carbon assimilation process is preferentially used to synthesize osmotic regulators, and starch is degraded to glucose that is involved in plant osmotic regulation and resistance or adaptation to drought stress (Liu et al., 2016). Starch and sucrose metabolism plays an important role in improving the tolerance of Verbena officinalis L. to drought stress (Wang et al., 2018). Sucrose is the main form of carbohydrate transport in plants (Pan et al., 2002), and drought stress affects the size of the sucrose pool. Although the total amount of carbon assimilation decreases under drought stress, the content of soluble carbohydrates increases, and this can increase the osmotic potential of cells (Quick et al., 1992). Trehalose, as an osmotic protector or stabilizing molecule, plays

an important role in plant growth and development and stress response (Kosar et al., 2019; Lin et al., 2020; Fichtner and Lunn, 2021). Sucrose and α, α-trehalose contents increased significantly under drought stress, suggesting that *H. persicum* may increase the contents of soluble sugars (mannose, trehalose, and sucrose) to adapt to drought stress. Trehalose-6-phosphate synthase (TPS) is a key enzyme in the trehalose synthesis pathway. Lyu et al. (2018) introduced a fusion gene encoding trehalose-6-phosphate synthase/phosphatase (TPSP) from Escherichia coli into tomato, and the results showed that plants overexpressing the TPSP gene increased levels of trehalose in seeds. Accumulated trehalose and related metabolites can act as signaling molecules to enhance the expression of heat stress-responsive genes and stress tolerance in seeds (Lyu et al., 2018). This study found that genes encoding TPSP were both up-regulated and down-regulated, and the genes encoding trehalose 6-phosphate phosphatase (TPP) and α, α-trehalose were up-regulated, indicating that these genes play an important role in the drought tolerance response of *H. persicum*. In addition, drought stress inhibited the expression of sucrose metabolic enzyme genes, and the two sucrose phosphate synthase genes were down-regulated. Similar results were also obtained in previous studies on the expression changes of key enzymes involved in the metabolism of non-soluble sugars (starch) and soluble sugars (mannitol, trehalose, and sucrose) in tea plants under drought stress (Liu et al., 2016).

Amino acid metabolism is very important for plant growth and development. Amino acids are also precursors for the synthesis of many signal molecules, and they are used in a variety of intermediate pathways. Under drought stress, DEGs identified in Populus simonii involved amino acid metabolism and transport, and amino acid transport is mediated by plasma membrane transporters (Mortazavi et al., 2008). In this study, the expression of metabolites and related genes involved in the amino acid biosynthetic metabolic pathways of the two species played positive regulatory roles under drought stress, indicating that the amino acid biosynthetic pathways play important roles in the drought tolerance of the two species.

Flavonoids are the main components of specific/secondary metabolism in plants, and these metabolites are considered the main defense substances against environmental stresses. Nakabayashi et al. (2014) reported that flavonoids are a specific class of metabolites, including flavonols and anthocyanins with strong free radical scavenging activities, that help alleviate oxidative and drought stress in Arabidopsis. Yobi et al. (2012) found that the abundance of amino acid-derived flavonoids (such as Apigenin, Luteolin and Naringenin) increased in drought-resistant S. lepidophylla under two water states. In this study, hesperetin, dihydrokaempferol, galangin, pinocembrin, taxifolin, vitexin, naringenin, and chrysin were involved in *H. ammodendron* flavonoid biosynthesis, and their abundance increased under drought stress. The abundance of luteolin and naringin decreased under drought stress, while pelargonidin chloride increased under drought stress. This indicated that drought stress had different effects on secondary metabolism in the two plant species. In this study, 13 and 24 genes were involved in flavonoid biosynthesis in *H. ammodendron* and *H. persicum*, respectively, and most genes in *H. ammodendron* were down-regulated, including naringenin, 2-oxoglutarate 3-dioxygenase-likevinorine synthase-like, caffeoyl-CoA O-methyltransferase, flavonoid 3',5'-methyltransferase-like, cytochrome P450 98A2-like, and chalcone synthase 2-like. In *H. persicum* there were 4 chalcone synthase, flavonol synthase, flavonoid 3'-monooxygenase, 2 naringenin 3-dioxygenase, 6 shikimate O-hydroxycinnamoyltransferase, and 2 coumaroylquinate (coumaroylshikimate) 3'-monooxygenase, indicating that drought stress significantly inhibited the flavonoid biosynthesis and metabolism pathways of the two species.

Under drought stress, the formation of cutin and wax can effectively prevent water loss caused by non-stomatal transpiration. Drought stress significantly altered the expression levels of genes related to cutin and wax metabolism (Ye et al., 2018). Under drought stress, the remodeling of the cuticle in plants may be a survival mechanism to adapt to the environment. In this study, there was only one metabolite involved in *H. ammodendron* and *H. persicum* berberine and wax biosynthesis, and the expression pattern in the two species was opposite, indicating that the effect of drought stress on lipid metabolism differed between the plants. Ksouri et al. (2016) analyzed the transcriptome of peach leaves and roots under drought stress and identified DEGs involved in cuticle formation, including genes involved in cuticle biosynthesis and deposition and wax transport. The up-regulated expression of these genes helped to strengthen the resistance of the plants to external environmental stresses. The CER1 protein plays an important role in plant cuticle formation and is thus important in water conservation. Transcripts of the gene encoding the CER1 protein in Populus simonii increased under drought stress (Chen et al., 2013). This study found that nine (nine up-regulated and none down-regulated) and 14 (five up regulated and nine down regulated) genes were involved in the biosynthesis of berberine and wax in *H. ammodendron* and *H. persicum*, respectively. Two genes (cluster-6558.3735 and cluster-6558.30032) encoding CER1 proteins were highly up-regulated in *H. ammodendron*, indicating that cutin, suberine, and wax biosynthesis may be an important feature for the two species to restrict water loss. These genes participated in the process of adapting to drought stress, and their regulation ability in *H. ammodendron* was stronger than in *H. persicum*.

Conclusions

To explore the changes of *H. ammodendron* and *H. persicum* under drought stress, their morphological structure,

physiological and biochemical characteristics, and key candidate genes and metabolites were determined. The morphological structure (assimilation branch diameter, cuticle thickness, and aqueous tissue), osmoregulation substances (Pro and AA), antioxidant enzymes (POD), and plant hormones (ABA, IAA and GA3) of the two species were affected by drought stress. The transcriptome and metabolome were combined to analyze the expression changes of genes/metabolites in the two species, identify the metabolic pathways that DEGs and DEMs jointly participated in, and screen for key candidate genes and metabolites. The results showed that these genes and metabolites were associated with drought tolerance, but regulated differently. In addition, the physiological changes and the expression levels of regulated genes in the two species were also analyzed, and the results showed that most of the physiological changes were strongly supported by transcriptomics. However, studies have shown that these transcripts do not always coincide with the final protein products. This difference may be due to the accumulation of metabolites affected by post-translational regulation, or other unknown genes involved in the regulation of the relevant pathway. Combined analysis of transcriptome and metabolome data provides a new avenue for studying the complex drought stress response mechanism of Haloxylon.

Data availability statement

The data presented in the study are deposited in the NCBI and MetaboLights repository, accession numbers PRJNA855227, MTBLS5721.

Authors' contributions

FY and GL conceived the study. FY collected data, analyzed data and drafted the text. Both authors contributed to the article and approved the submitted version

Funding

This work was supported by the Xinjiang Uyghur Autonomous Region Innovation Environment Construction special project, Science and Technology Innovation Base construction project (PT2107), and Xinjiang Uyghur Autonomous Region Graduate Innovation Project (Physiological Metabolism and Molecular Mechanism of Dioecious Populus euphratica in Dry and Wet Environments) (XJ2021G040).

Acknowledgments

We thank LetPub (www.letpub.com) for its linguistic assistance during the preparation of this manuscript.

Conflict of interest

The authors declare that the research was conducted in the absence of any commercial or financial relationships that could be construed as a potential conflict of interest.

Publisher's note

All claims expressed in this article are solely those of the authors and do not necessarily represent those of their affiliated organizations, or those of the publisher, the editors and the reviewers. Any product that may be evaluated in this article, or claim that may be made by its manufacturer, is not guaranteed or endorsed by the publisher.

Supplementary material

The Supplementary Material for this article can be found online at: https://www.frontiersin.org/articles/10.3389/fpls.2022.1020367/full#supplementary-material

References

Ali, M., Luo, D. X., Khan, A., Haq, S. U., Gai, W. X., Zhang, H. X., et al. (2018). Classification and genome-wide analysis of chitin-binding proteins gene family in pepper (Capsicum annuum l.) and transcriptional regulation to phytophthora capsici, abiotic stresses and hormonal applications. *Int. J. Mol. Sci.* 19, 2216. doi: 10.3390/ijms19082216

Altschul, S. F., Madden, T. L., Schäffer, A. A., Zhang, J., Zhang, Z., Miller, W., et al. (1997). Gapped BLAST and PSI-BLAST: a new generation of protein database search programs. *Nucleic Acids Res.* 25 (17), 3389–3402. doi: 10.1093/nar/25.17.3389

Baillo, E. H., Kimotho, R. N., Zhang, Z., and Xu, P. (2019). Transcription factors associated with abiotic and biotic stress tolerance and their potential for crops improvement. *Genes* 10, 771. doi: 10.3390/genes10100771

Bhaskara, G. B., Yang, T.-H., and Verslues, P. E. (2015). Dynamic proline metabolism: importance and regulation in water limited environments. *Front. Plant Sci.* 6. doi: 10.3389/fpls.2015.00484

Bies-Ethève, N., Gaubier-Comella, P., Debures, A., Lasserre, E., Jobet, E., Raynal, M., et al. (2008). Inventory, evolution and expression profiling diversity of the LEA (late embryogenesis abundant) protein gene family in *Arabidopsis thaliana*. *Plant Mol. Biol.* 67, 107–124. doi: 10.1007/s11103-008-9304-x

Boominathan, P., Shukla, R., Kumar, A., Manna, D., Negi, D., Verma, P. K., et al. (2004). Long term transcript accumulation during the development of dehydration adaptation in *Cicer arietinum*. *Plant Physiol.* 135, 1608–1620. doi: 10.1104/pp.104.043141

Budak, H., Hussain, B., Khan, Z., Ozturk, N. Z., and Ullah, N. (2015). From genetics to functional genomics: Improvement in drought signaling and tolerance in wheat. *Front. Plant Sci.* 6. doi: 10.3389/fpls.2015.01012

Campion, E. M., Loughran, S. T., and Walls, D. (2011). Protein quantitation and analysis of purity. *Methods Mol. Biol.* 681, 229–258. doi: 10.1007/978-1-60761-913-0_13

Catola, S., Marino, G., Emiliani, G., Huseynova, T., Musayev, M., Akparov, Z., et al. (2016). Physiological and metabolomic analysis of *Punica granatum* (L.) under drought stress. *Planta* 243 (2), 441–449. doi: 10.1007/s00425-015-2414-1

Charlton, A. J., Donarski, J. A., Harrison, M., Jones, S. A., Godward, J., Oehlschlager, S., et al. (2008). Responses of the pea (*Pisum sativum* l.) leaf metabolome to drought stress assessed by nuclear magnetic resonance spectroscopy. *Metabolomics* 4 (4), 312–327. doi: 10.1007/s11306-008-0128-0

Chen, J. H., Song, Y. P., Zhang, H., and Zhang, D. Q. (2013). Genome-wide analysis of gene expression in response to drought stress in *Populus simonii*. *Plant Mol. Biol. Rep.* 31 (4), 946–962. doi: 10.1007/s11105-013-0563-6

Choudhury, F. K., Rivero, R. M., Blumwald, E., and Mittler, R. (2017). Reactive oxygen species, abiotic stress and stress combination. *Plant J.* 90, 856–867. doi: 10.1111/tpj.13299

Claeys, H., and Inze, D. (2013). The agony of choice: how plants balance growth and survival under water-limiting conditions. *Plant Physiol.* 162, 1768–1779. doi: 10.1104/pp.113.220921

Davidson, N. M., and Oshlack, A. (2014). Corset: enabling differential gene expression analysis for *de novo* assembled transcriptomes. *Genome Biol.* 15 (7), 410. doi: 10.1186/s13059-014-0410-6

Dong, C. J., and Liu, J. Y. (2010). The arabidopsis EAR-motif-containing protein RAP2.1 functions as an active transcriptional repressor to keep stress responses under tight control. *BMC Plant Biol.* 10, 47. doi: 10.1186/1471-2229-10-47

Dossa, K., Mmadi, M. A., Zhou, R., Liu, A., Yang, Y., Diouf, D., et al. (2020). Ectopic expression of the sesame MYB transcription factor *SiMYB305* promotes root growth and modulates ABA-mediated tolerance to drought and salt stresses in arabidopsis. *AoB Plants* 12 (1), plz081. doi: 10.1093/aobpla/plz081

Fan, L. G., Wang, G. N., Hu, W., Pantha, P., Tran, K. N., Zhang, H., et al. (2018). Transcriptomic view of survival during early seedling growth of the extremophyte *Haloxylon ammodendron*. *Plant Physiol. Bioch* 132, 475–489. doi: 10.1016/j.plaphy.2018.09.024

Farooq, M., Wahid, A., Kobayashi, N., Fujita, D., and Basra, S. M. A. (2009). Plant drought stress: effects, mechanisms and management. *Agron. Sustain Dev.* 29, 185–212. doi: 10.1007/978-90-481-2666-8_12

Fernie, A. R., and Schauer, N. (2009). Metabolomics-assisted breeding: A viable option for crop improvement? *Trends Genet.* 25, 39–48. doi: 10.1016/j.tig.2008.10.010

Fichtner, F., and Lunn, J. E. (2021). The role of trehalose 6-phosphate (Tre6P) in plant metabolism and development. *Annu. Rev. Plant Biol.* 72, 737–760. doi: 10.1146/annurev-arplant-050718-095929

Fiehn, O. (2002). Metabolomics-the link between genotypes and phenotypes. *Plant Mol. Biol.* 48, 155–171.

Fiehn, O., Kopka, J., Dörmann, P., Altmann, T., Trethewey, R. N., and Willmitzer, L. (2000). Metabolite profiling for plant functional genomics. *Nat. Biotechnol.* 18, 1157–1161. doi: 10.1038/81137

Gao, F., Wang, J. Y., Wei, S. J., Li, Z. L., Wang, N., Li, H. Y., et al. (2015). Transcriptomic analysis of drought stress responses in *Ammopiptanthus mongolicus* leaves using the RNA-seq technique. *PLoS One* 10 (4), e0124382. doi: 10.1371/journal.pone.0124382

Gong, X. W., and Lü, G. H. (2017). Species diversity and dominant species' niches of eremophyte communities of the tugai forest in the ebinur basin of xinjiang, China. *Biodiversity Sci.* 25 (1), 34–45. doi: 10.17520/biods.2016166

Guo, R., Shi, L. X., Jiao, Y., Li, M., Zhong, X., Gu, F., et al. (2018). Metabolic responses to drought stress in the tissues of drought-tolerant and drought-sensitive wheat genotype seedlings. *AoB Plants* 10 (2), ply016. doi: 10.1093/aobpla/ply016

Guttikonda, S. K., Valliyodan, B., Neelakandan, A. K., Tran, L. S., Kumar, R., Quach, T. N., et al. (2014). Overexpression of *AtDREB1D* transcription factor improves drought tolerance in soybean. *Mol. Biol. Rep.* 41, 7995–8008. doi: 10.1007/s11033-014-3695-3

Gu, H., Yang, Y., Xing, M., Yue, C., Wei, F., Zhang, Y., et al. (2019). Physiological and transcriptome analyses of *Opisthopappus taihangensis* in response to drought stress. *Cell Biosc* 9, 56. doi: 10.1186/s13578-019-0318-7

Han, G., Li, S. X., Xu, P., and Han, E. X. (2006). Analysis of drought resistance on anatomical leaves of six species of shrubs. *J. Northwest Forestry Univ.* 21 (4), 43–46. doi: 10.3969/j.issn.1001-7461.2006.04.011

Haq, S., Khan, A., Ali, M., Khattak, A. M., Gai, W. X., Zhang, H. X., et al. (2019). Heat shock proteins: Dynamic biomolecules to counter plant biotic and abiotic stresses. *Int. J. Mol. Sci.* 20, 5321. doi: 10.3390/ijms20215321

Hayat, S., Hasan, S. A., Fariduddin, Q., and Ahmad, A. (2008). Growth of tomato (*Lycopersicon esculentum*) in response to salicylic acid under water stress. *J. Plant Interact.* 3, 297–304. doi: 10.1080/17429140802320797

Hu, T. Z. (2008). *OsLEA3*, a late embryogenesis abundant protein gene from rice, confers tolerance to water deficit and salt stress to transgenic rice. *Russ J. Plant Physiol.* 55, 530–537. doi: 10.1134/S1021443708040158

Huang, L. J., Cheng, G. X., Khan, A., Wei, A. M., Yu, Q. H., Yang, S. B., et al. (2018). CaHSP16.4, a small heat shock protein gene in pepper, is involved in heat and drought tolerance. *Protoplasma* 256, 39–51. doi: 10.1007/s00709-018-1280-7

Hübner, S., Korol, A. B., and Schmid, K. J. (2015). RNA-Seq analysis identifies genes associated with differential reproductive success under drought-stress in accessions of wild barley *Hordeum spontaneum*. *BMC Plant Biol.* 15, 134. doi: 10.1186/s12870-015-0528-z

Hussain, H. A., Hussain, S., Khaliq, A., Ashraf, U., Anjum, S. A., Men, S., et al. (2018). Chilling and drought stresses in crop plants: Implications, cross talk, and potential management opportunities. *Front. Plant Sci.* 9. doi: 10.3389/fpls.2018.00393

Hu, L., Xie, Y., Fan, S., Wang, Z., Wang, F., Zhang, B., et al. (2018). Comparative analysis of root transcriptome profiles between drought-resistant and susceptible wheat genotypes in response to water stress. *Plant Sci.* 272, 276–293. doi: 10.1016/j.plantsci.2018.03.036

Jia, X., Sun, C. S., Zuo, Y. C., Li, G. Y., Li, G. B., Ren, L. Y., et al. (2016). Integrating transcriptomics and metabolomics to characterise the response of *Astragalus membranaceus* bge. var. *mongolicus* (bge.) to progressive drought stress. *BMC Genomics* 17, 188. doi: 10.1186/s12864-016-2554-0

Khadka, V. S., Vaughn, K., Xie, J., Swaminathan, P., Ma, Q., Cramer, G. R., et al. (2019). Transcriptomic response is more sensitive to water deficit in shoots than roots of *Vitis riparia* (Michx.). *BMC Plant Biol.* 19, 72. doi: 10.1186/s12870-019-1664-7

Khan, A., Li, R. J., Sun, J. T., Ma, F., Zhang, H. X., Jin, J. H., et al. (2018). Genome-wide analysis of dirigent gene family in pepper (*Capsicum annuum* l.) and characterization of *CaDIR7* in biotic and abiotic stresses. *Sci. Rep.* 8, 5500. doi: 10.1038/s41598-018-23761-0

Kiani Poormohammad, S., Grieu, P., Maury, P., Hewezi, T., Gentzbittel, L., and Sarrafi, A. (2007). Genetic variability for physiological traits under drought conditions and differential expression of water stress-associated genes in sunflower (*Helianthus annuus* l.). *Theor. Appl. Genet.* 114, 193–207. doi: 10.1007/s00122-006-0419-7

Kocsis, M., Darók, J., and Borhidi, A. (2004). Comparative leaf anatomy and morphology of some neotropical *Rondeletia* (Rubiaceae) species. *Plant Syst. Evol.* 248 (1-4), 205–218. doi: 10.1007/s00606-002-0144-0

Kosar, F., Akram, N. A., Sadiq, M., Al-Qurainy, F., and Ashraf, M. (2019). Trehalose: a key organic osmolyte effectively involved in plant abiotic stress tolerance. *J. Plant Growth Regul.* 38, 606–618. doi: 10.1007/s00344-018-9876-x

Kou, J. C., Yang, W. Q., Jia, Z. K., Di, S. M., and Han, Q. F. (2008). Study on leaves anatomical structures relative to drought resistance of *Medicago sativa* varieties. *J. Northwest A F Univ. (Natural Sci. Edition)* 36 (8), 67–72. doi: 10.13207/j.cnki.jnwafu.2008.08.012

Krasensky, J., and Jonak, C. (2012). Drought, salt, and temperature stress-induced metabolic rearrangements and regulatory networks. *J. Exp. Bot.* 63 (4), 1593–1608. doi: 10.1093/jxb/err460

Ksouri, N., Jiménez, S., Wells, C. E., Contreras-Moreira, B., and Gogorcena, Y. (2016). Transcriptional responses in root and leaf of *Prunus persica* under drought stress using RNA sequencing. *Front. Plant Sci.* 7. doi: 10.3389/fpls.2016.01715

Lawson, T., Oxborough, K., Morison, J. I., and Baker, N. R. (2003). The responses of guard and mesophyll cell photosynthesis to CO_2, O_2, light and water stress in a range of species are similar. *J. Exp. Bot.* 54, 1743–1752. doi: 10.1093/jxb/erg186

Li, W., Lee, J., Yu, S., Wang, F., Lv, W., Zhang, X., et al. (2021). Characterization and analysis of the transcriptome response to drought in *Larix kaempferi* using PacBio full-length cDNA sequencing integrated with *de novo* RNA-seq reads. *Planta* 253, 28. doi: 10.1007/S00425-020-03555-3

Li, W. L., Liu, Z. W., Feng, H., Yang, J. L., and Li, C. H. (2022). Characterization of the gene expression profile response to drought stress in *Populus ussuriensis* using PacBio SMRT and illumina sequencing. *Int. J. Mol. Sci.* 23, 3840. doi: 10.3390/ijms23073840

Lin, Q. F., Wang, S., Dao, Y. H., Dao, Y. H., Wang, J. Y., and Wang, K. (2020). *Arabidopsis thaliana* trehalose-6-phosphate phosphatase gene *TPPI* enhances drought tolerance by regulating stomatal apertures. *J. Exp. Bot.* 71 (14), 4285–4297. doi: 10.1093/jxb/eraa173

Li, W., Pang, S., Lu, Z., and Jin, B. (2020). Function and mechanism of WRKY transcription factors in abiotic stress responses of plants. *Plants* 9, 1515. doi: 10.3390/plants9111515

Liu, S. C., Jin, J. Q., Ma, J. Q., Yao, M. Z., Ma, C. L., Li, C. F., et al. (2016). Transcriptomic analysis of tea plant responding to drought stress and recovery. *PloS One* 11 (1), e0147306. doi: 10.1371/journal.pone.0147306

Long, Y., Zhang, J. W., Tian, X. J., Wu, S. S., Zhang, Q., Zhang, J. P., et al. (2014). *De novo* assembly of the desert tree *Haloxylon ammodendron* (C. a. mey.) based on RNA-seq data provides insight into drought response, gene discovery and marker identification. *BMC Genomics* 15, 1111. doi: 10.1186/1471-2164-15-1111

Love, M. I., Huber, W., and Anders, S. (2014). Moderated estimation of fold change and dispersion for RNA-seq data with DESeq2. *Genome Biol.* 15 (12), 550. doi: 10.1186/s13059-014-0550-8

Luo, X., Bai, X., Sun, X., Zhu, D., Liu, B., Ji, W., et al. (2013). Expression of wild soybean WRKY20 in arabidopsis enhances drought tolerance and regulates ABA signaling. *J. Exp. Bot.* 64 (8), 2155–2169. doi: 10.1093/jxb/ert073

Lyu, J. I., Park, J. H., Kim, J. K., Bae, C. H., Jeong, W. J., Min, S. R., et al. (2018). Enhanced tolerance to heat stress in transgenic tomato seeds and seedlings overexpressing a trehalose-6-phosphate synthase/phosphatase fusion gene. *Plant Biotechnol. Rep.* 12 (6), 399–408. doi: 10.1007/s11816-018-0505-8

Mao, X., Cai, T., Olyarchuk, J. G., and Wei, L. (2005). Automated genome annotation and pathway identification using the KEGG orthology (KO) as a controlled vocabulary. *Bioinformatics* 21 (19), 3787–3793. doi: 10.1093/bioinformatics/bti430

Ma, X. S., Xia, H., Liu, Y. H., Wei, H., Zheng, X., Song, C., et al. (2016). Transcriptomic and metabolomic studies disclose key metabolism pathways contributing to well-maintained photosynthesis under the drought and the consequent drought-tolerance in rice. *Front. Plant Sci.* 7. doi: 10.3389/fpls.2016.01886

Meng, Y. C., Zhang, H. F., Pan, X. X., Chen, N., Hu, H. F., Haq, S. U., et al. (2021). *CaDHN3*, a pepper (*Capsicum annuum* l.) dehydrin gene enhances the tolerance against salt and drought stresses by reducing ROS accumulation. *Int. J. Mol. Sci.* 22 (6), 3205. doi: 10.3390/ijms22063205

Michaletti, A., Naghavi, M. R., Toorchi, M., Zolla, L., and Rinalducci, S. (2018). Metabolomics and proteomics reveal drought-stress responses of leaf tissues from spring-wheat. *Sci. Repuk* 8 (1), 5710. doi: 10.1038/s41598-018-24012-y

Mortazavi, A., Williams, B. A., Mccue, K., Schaeffer, L., and Wold, B. (2008). Mapping and quantifying mammalian transcriptomes by RNA-seq. *Nat. Methods* 5, 621–628. doi: 10.1038/nmeth.1226

Mun, B. G., Lee, S. U., Park, E. J., Kim, H. H., Hussain, A., Imran, Q. M., et al. (2017). Analysis of transcription factors among differentially expressed genes induced by drought stress in *Populus davidiana*. *3 Biotech.* 7, 209. doi: 10.1007/s13205-017-0858-7

Nakabayashi, R., Mori, T., and Saito, K. (2014). Alternation of flavonoid accumulation under drought stress in *Arabidopsis thaliana*. *Plant Signal Behav.* 9 (8), e29518. doi: 10.4161/psb.29518

Nam, K. H., Shin, H. J., Pack, I. S., Park, J. H., Kim, H. B., and Kim, C. G. (2016). Metabolomic changes in grains of well-watered and drought-stressed transgenic rice. *J. Sci. Food Agr* 96, 807–814. doi: 10.1002/jsfa.7152

Oono, Y., Seki, M., Nanjo, T., Narusaka, M., Fujita, M., Satoh, R., et al. (2003). Monitoring expression profiles of *Arabidopsis* gene expression during rehydration process after dehydration using ca. 7000 full-length cDNA microarray. *Plant J.* 34, 868–887. doi: 10.1046/j.1365-313x.2003.01774.x

Pan, Q. M., Han, X. G., Bai, Y. F., and Yang, J. C. (2002). Advances in physiology and ecology studies on stored non-structure carbohydrates in plants. *Chin. Bull. Bot.* 19 (1), 30–38. doi: 10.3969/j.issn.1674-3466.2002.01.004

Pan, Y., Seymour, G. B., Lu, C., Hu, Z., Chen, X., and Chen, G. (2012). An ethylene response factor (ERF5) promoting adaptation to drought and salt tolerance in tomato. *Plant Cell Rep.* 31, 349–360. doi: 10.1007/s00299-011-1170-3

Penfield, S., Clements, S., Bailey, K. J., Gilday, A. D., Leegood, R. C., Gray, J. E., et al. (2012). Expression and manipulation of phosphoenolpyruvate carboxy kinase 1 identifies a role for malate metabolism in stomatal closure. *Plant J.* 69 (4), 679–688. doi: 10.1111/j.1365-313X.2011.04822.x

Péret, B., Swarup, K., Ferguson, A., Seth, M., Yang, Y., Dhondt, S., et al. (2012). AUX/LAX genes encode a family of auxin influx transporters that perform distinct functions during arabidopsis development. *Plant Cell* 24 (7), 2874–2885. doi: 10.1105/tpc.112.097766

Quick, W. P., Chaves, M. M., and Wendler, R. (1992). The effect of water stress on photosynthetic carbon metabolism in four species grown under field conditions. *Plant Cell Environ.* 15 (1), 25–35. doi: 10.1111/j.1365-3040.1992.tb01455.x

Ramanjulu, S., and Bartels, D. (2002). Drought and desiccation induced modulation of gene expression in plants. *Plant Cell Environ.* 25, 141–151. doi: 10.1046/j.0016-8025.2001.00764.x

Raorane, M. L., Pabuayon, M. I., Miro, B., Kalladan, R., Reza-Hajirezai, M., Oane, R. H., et al. (2015). Variation in primary metabolites in parental and nearisogenic lines of the QTL *qDTY* $_{12.1}$: altered roots and flag leaves but similar spikelets of rice under drought. *Mol. Breed.* 35, 138. doi: 10.1007/s11032-015-0322-5

Shinozaki, K., and Yamaguchi-Shinozaki, K. (2007). Gene networks involved in drought stress response and tolerance. *J. Exp. Bot.* 58 (2), 221–227. doi: 10.1093/jxb/erl164

Sun, J., Hu, W., Zhou, R., Wang, L., Wang, X., Wang, Q., et al. (2015). The *Brachypodium distachyon BdWRKY36* gene confers tolerance to drought stress in transgenic tobacco plants. *Plant Cell Rep.* 34, 23–35. doi: 10.1007/s00299-014-1684-6

Sziderics, A. H., Oufir, M., Trognitz, F., Kopecky, D., Matusíková, I., Hausman, J. F., et al. (2010). Organ-specific defence strategies of pepper (*Capsicum annuum* l.) during early phase of water deficit. *Plant Cell Rep.* 29 (3), 295–305. doi: 10.1007/s00299-010-0822-z

Talamè, V., Ozturk, N. Z., Bohnert, H. J., and Tuberosa, R. (2007). Barley transcript profiles under dehydration shock and drought stress treatments: a comparative analysis. *J. Exp. Bot.* 58 (2), 229–240. doi: 10.1093/jxb/erl163

Tang, S., Dong, Y., Liang, D., Zhang, Z. J., Ye, C. Y., Shuai, P., et al. (2015). Analysis of the drought stress-responsive transcriptome of black cottonwood (*Populus trichocarpa*) using deep RNA sequencing. *Plant Mol. Bio Rep.* 33 (3), 424–438. doi: 10.1007/s11105-014-0759-4

Tang, W., Ji, Q., Huang, Y., Jiang, Z., Bao, M., Wang, H., et al. (2013). FAR-RED ELONGATED HYPOCOTYL3 and FAR-RED IMPAIRED RESPONSE1 transcription factors integrate light and abscisic acid signaling in arabidopsis. *Plant Physiol.* 163 (2), 857–866. doi: 10.1104/pp.113.224386

Tardieu, F., and Tuberosa, R. (2010). Dissection and modelling of abiotic stress tolerance in plants. *Curr. Opin. Plant Biol.* 13, 206–212. doi: 10.1016/j.pbi.2009.12.012

Thayale Purayil, F., Rajashekar B, S., Kurup, S., Cheruth, A. J., Subramaniam, S., Hassan Tawfik, N., et al. (2020). Transcriptome profiling of *Haloxylon persicum* (Bunge ex boiss and buhse) an endangered plant species under PEG-induced drought stress. *Gene* 11, 640. doi: 10.3390/genes11060640

Trapnell, C., Williams, B. A., Pertea, G., Mortazavi, A., Kwan, G., van Baren, M. J., et al. (2010). Transcript assembly and quantification by RNA-seq reveals unannotated transcripts and isoform switching during cell differentiation. *Nat. Biotechnol.* 28 (5), 511–515. doi: 10.1038/nbt.1621

Tyerman, S. D., Niemietz, C. M., and Bramley, H. H. (2010). Plant aquaporins: Multifunctional water and solute channels with expanding roles. *Plant Cell Environ.* 25, 173–194. doi: 10.1046/j.0016-8025.2001.00791.x

Valliyodan, B., and Nguyen, H. T. (2006). Understanding regulatory networks and engineering for enhanced drought tolerance in plants. *Curr. Opin. Plant Biol.* 9, 189–195. doi: 10.1016/j.pbi.2006.01.019

Wang, F., Guo, S. J., Zhang, W. X., Wang, F. L., Han, F. G., and Zhang, Y. N. (2021). Anatomic structure characteristics of assimilating shoots of *haloxylon ammodendron* in different ages and their response to soil conditions. *Acta Bot. Boreal-Occident Sin.* 41 (3), 0473–0479. doi: 10.7606/j.issn.1000-4025.2021.03.0473

Wang, B., Lv, X. Q., He, L., Zhao, Q., Xu, M. S., Zhang, L., et al. (2018). Whole-transcriptome sequence analysis of *Verbena bonariensis* in response to drought stress. *Int. J. Mol. Sci.* 19 (6), 1957. doi: 10.3390/ijms19061751

Wan, H. P., Qian, J. L., Zhang, H., Lu, H. C., Li, O. Q., Li, R. H., et al. (2022). Combined transcriptomics and metabolomics analysis reveals the molecular mechanism of salt tolerance of huayouza 62, an elite cultivar in rapeseed (*Brassica napus* l.). *Int. J. Mol. Sci.* 23, 1279. doi: 10.3390/ijms23031279

Want, E. J., Masson, P., Michopoulos, F., Wilson, I. D., Theodoridis, G., Plumb, R. S., et al. (2012). Global metabolic profiling of animal and human tissues *via* UPLC-MS. *Nat. Protoc.* 8 (1), 17–32. doi: 10.1038/nprot.2012.135

Warren, C. R., Aranda, I., and Cano, F. J. (2012). Metabolomics demonstrates divergent responses of two *Eucalyptus* species to water stress. *Metabolomics* 8 (2), 186–200. doi: 10.1007/s11306-011-0299-y

Wei, B., Yang, J. X., and Li, D. D. (2019). The physiological responses of safflower (*Carthamus tinctorius* l.) to osmotic stress. *Int. J. Agric. Biol.* 21 (5), 1106–1116. doi: 10.17957/IJAB/15.1000

Wishart, D. S. (2007). Current progress in computational metabolomics. *Brief Bioinform.* 5, 279–293. doi: 10.1093/bib/bbm030

Xin, Z. J., Zhang, J., Ge, L. G., Lei, S., Han, J., Zhang, X., et al. (2017). A putative 12-oxophytodienoate reductase gene *CsOPR3* from, *Camellia sinensis*, is involved in wound and herbivore infestation responses. *Gene* 615, 18–24. doi: 10.1016/j.gene.2017.03.013

Xuan, H. D., Huang, Y. Z., Zhou, L., Deng, S. S., Wang, C. C., Xu, J. Y., et al. (2022). Key soybean seedlings drought-responsive genes and pathways revealed by comparative transcriptome analyses of two cultivars. *Int. J. Mol. Sci.* 23, 2893. doi: 10.3390/ijms23052893

Yang, R., Yang, T., Zhang, H., Qi, Y., Xing, Y., Zhang, N., et al. (2014). Hormone profiling and transcription analysis reveal a major role of ABA in tomato salt tolerance. *Plant Physiol. Bioch* 77, 23–34. doi: 10.1016/j.plaphy.2014.01.015

Yao, T., Zhang, J., Xie, M., Yuan, G., Tschaplinski, T. J., Muchero, W., et al. (2020). Transcriptional regulation of drought response in arabidopsis and woody plants. *Front. Plant Sci.* 11. doi: 10.3389/fpls.2020.572137

Yates, S. A., Swain, M. T., Hegarty, M. J., Chernukin, I., Lowe, M., Allison, G. G., et al. (2014). *De novo* assembly of red clover transcriptome based on RNA-seq data provides insight into drought response, gene discovery and marker identification. *BMC Genomics* 15, 453. doi: 10.1186/1471-2164-15-453

Ye, G. S., Ma, Y. H., Feng, Z. P., and Zhang, X. F. (2018). Transcriptomic analysis of drought stress responses of sea buckthorn (*Hippophae rhamnoides* subsp. *sinensis) by RNA-Seq. PloS One* 13 (8), e0202213. doi: 10.1371/journal.pone.0202213

Yobi, A., Wone, B. W. M., Xu, W., Alexander, D. C., Guo, L., Ryals, J. A., et al. (2012). Comparative metabolic profiling between desiccation-sensitive and desiccation-tolerant species of *Selaginella* reveals insights into the resurrection trait. *Plant J.* 72 (6), 983–999. doi: 10.1111/tpj.12008

Young, M. D., Wakefield, M. J., Smyth, G. K., and Oshlack, A. (2010). Gene ontology analysis for RNA-seq: accounting for selection bias. *Genome Biol.* 11 (2), R14. doi: 10.1186/gb-2010-11-2-r14

Yue, L. J., Ma, Q., Zhou, X. R., Wang, P., and Wang, S. M. (2013). Sodium compound fertilizer in improving the growth and drought resistance of desert plants *Halaxylon ammodendron Nitraria tangutorum* and *Reaumuria soongorica. J. Lanzhou Univ. (Natural Sciences)* 49 (5), 666–674. doi: 10.13885/j.issn.0455-2059.2013.05.009

Zhang, H. X., Ali, M., Feng, X. H., Jin, J. H., Huang, L. J., Khan, A., et al. (2019). A novel transcription factor *CaSBP12* gene negatively regulates the defense response against phytophthora capsici in pepper (*Capsicum annuum* l. *). Int. J. Mol. Sci.* 20, 48. doi: 10.3390/ijms20010048

Zheng, J., Su, H., Lin, R., Zhang, H., Xia, K., Jian, S., et al. (2019). Isolation and characterization of an atypical *LEA* gene *(IpLEA*) from *Ipomoea pescaprae* conferring salt/drought and oxidative stress tolerance. *Sci. Rep.* 9, 14838. doi: 10.1038/s41598-019-50813-w

frontiers | Frontiers in Plant Science

TYPE Original Research
PUBLISHED 08 December 2022
DOI 10.3389/fpls.2022.1033915

Check for updates

OPEN ACCESS

EDITED BY
Caroline Müller,
Universidade Federal da Fronteira Sul, Brazil

REVIEWED BY
Milan Kumar Lal,
Central Potato Research Institute (ICAR), India
Hongbin Li,
Shihezi University, China

*CORRESPONDENCE
Xinhui Zhang
zhang2013512@163.com

SPECIALTY SECTION
This article was submitted to Plant Abiotic Stress, a section of the journal Frontiers in Plant Science

RECEIVED 01 September 2022
ACCEPTED 14 November 2022
PUBLISHED 08 December 2022

CITATION
Ma X, Xu Z, Lang D, Zhou L, Zhang W and Zhang X (2022) Comprehensive physiological, transcriptomic, and metabolomic analyses reveal the synergistic mechanism of *Bacillus pumilus* G5 combined with silicon alleviate oxidative stress in drought-stressed *Glycyrrhiza uralensis* Fisch. *Front. Plant Sci.* 13:1033915. doi: 10.3389/fpls.2022.1033915

COPYRIGHT
© 2022 Ma, Xu, Lang, Zhou, Zhang and Zhang. This is an open-access article distributed under the terms of the Creative Commons Attribution License (CC BY). The use, distribution or reproduction in other forums is permitted, provided the original author(s) and the copyright owner(s) are credited and that the original publication in this journal is cited, in accordance with accepted academic practice. No use, distribution or reproduction is permitted which does not comply with these terms.

Comprehensive physiological, transcriptomic, and metabolomic analyses reveal the synergistic mechanism of *Bacillus pumilus* G5 combined with silicon alleviate oxidative stress in drought-stressed *Glycyrrhiza uralensis* Fisch.

Xin Ma[1], Zhanchao Xu[1], Duoyong Lang[2], Li Zhou[1], Wenjin Zhang[1,3] and Xinhui Zhang[1,3]*

[1]College of Pharmacy, Ningxia Medical University, Yinchuan, China, [2]Laboratory Animal Center, Ningxia Medical University, Yinchuan, China, [3]Ningxia Engineering and Technology Research Center of Regional Characteristic Traditional Chinese Medicine, Ningxia Collaborative Innovation Center of Regional Characteristic Traditional Chinese Medicine, Key Laboratory of Ningxia Minority Medicine Modernization, Ministry of Education, Yinchuan, China

Glycyrrhiza uralensis Fisch. is often cultivated in arid, semi-arid, and salt-affected regions that suffer from drought stress, which leads to the accumulation of reactive oxygen species (ROS), thus causing oxidative stress. Plant growth-promoting bacteria (PGPB) and silicon (Si) have been widely reported to be beneficial in improving the tolerance of plants to drought stress by maintaining plant ROS homeostasis. Herein, combining physiological, transcriptomic, and metabolomic analyses, we investigated the response of the antioxidant system of *G. uralensis* seedlings under drought stress to *Bacillus pumilus* (G5) and/or Si treatment. The results showed that drought stress caused the overproduction of ROS, accompanied by the low efficiency of antioxidants [i.e., superoxide dismutase (SOD), catalase (CAT), peroxidase (POD), the ascorbate (AsA)–glutathione (GSH) pool, total carotenoids, and total flavonoids]. Inversely, supplementation with G5 and/or Si enhanced the antioxidant defense system in drought-stressed *G. uralensis* seedlings, and the complex regulation of the combination of G5 and Si differed from that of G5 or Si alone. The combination of G5 and Si enhanced the antioxidant enzyme system, accelerated the AsA–GSH cycle, and triggered the carotenoid and flavonoid metabolism, which acted in combination *via* different pathways to eliminate the excess ROS induced by drought stress, thereby alleviating oxidative stress. These findings provide new insights into the comparative

and synergistic roles of PGPB and Si in the antioxidant system of plants exposed to drought and a guide for the application of PGPB combined with Si to modulate the tolerance of plants to stress.

KEYWORDS

drought stress, *Glycyrrhiza uralensis*, *Bacillus pumilus* G5 combined with silicon, AsA–GSH cycle, carotenoid biosynthesis, flavonoid biosynthesis

Introduction

Drought stress is a major environmental constraint that limits plant growth and development, crop productivity, and geographic distribution, especially in arid and semi-arid regions of the world (Carter and Dickman, 2022; Wu et al., 2022a). Drought limited the water uptake in plants and the nutrient absorption and transportation from the roots (Khan et al., 2020a), reduced the utilization rate and metabolism of nutrients, and increased the production of reactive oxygen species (ROS) (Jan et al., 2019; Rane et al., 2022). Excessive levels of ROS impair the enzyme activities, degrade proteins, and eventually induce plant cell death (Qi et al., 2018). Correspondingly, drought-exposed plants have evolved several defense mechanisms to maintain ROS homeostasis and protect cells against oxidative damage, and the antioxidant system serves as the first line of defense in eradicating the stress-induced excess ROS, which plays a key role in the response of plants to environmental stresses (Kartik et al., 2021). Thus, improving plant antioxidant pathways appears a useful strategy to increasing the tolerance of plants to drought stress.

In the antioxidant defense system, superoxide dismutase (SOD), catalase (CAT), and peroxidase (POD) are the major contributors to stress tolerance that mediate the protection of important physiological and biochemical processes (Hasanuzzaman et al., 2017). Simultaneously, the ascorbate (AsA)–glutathione (GSH) cycle is considered to control the levels of ROS through its scavenging activity and to contribute to redox sensing and signaling (Mittler, 2017). AsA and GSH, as powerful antioxidants of plant cells, can detoxify H_2O_2 to H_2O, and the metabolic pools of AsA and GSH are tightly linked by the activity of the enzymes involved in the AsA–GSH cycle, i.e., ascorbate peroxidase (APX), glutathione peroxidase (GPX), monodehydroascorbate reductase (MDHAR), dehydroascorbate reductase (DHAR), and glutathione reductase (GR) (Mishra et al., 2022). Moreover, as the predominant antioxidants, carotenoids and flavonoids participate in the maintenance of redox buffering for the optimal performance of important pathways such as energy metabolism and photosynthetic electron transport (Ahanger and Agarwal, 2017; Das and Roychoudhury, 2014; Huchzermeyer et al., 2022). Thereby, each antioxidant plays a specific role in combating the specific type of ROS induced by stress.

Plant growth-promoting bacteria (PGPB), which alleviate drought stress, can produce exopolysaccharides and siderophores, facilitate the synthesis of 1-aminocyclopropane-1-carboxylate deaminase (ACCD), amplify nitrogen fixation and phosphate solubilization, improve the photosynthesis rate, regulate phytohormones and osmotic pressure, activate the antioxidant defense response system to scavenge ROS, modulate the transcription of the stress response genes, and induce the drought-tolerant change of host plants (Ilangumaran and Smith, 2017; Pathania et al., 2020; Kabiraj and Majhi, 2020; Zheng et al., 2022). Previous studies reported the bio-inoculation of PGPB to mitigate drought stress through the regulation of the antioxidant defense in a number of plants, including *Amaranthus tricolor*, *Glycyrrhiza uralensis* Fisch., *Zea mays*, and *Oryza sativa* L. (Gusain et al., 2015; Sarker and Oba, 2018a; Xie et al., 2019; Vishnupradeep et al., 2022). Similarly, Si is a widely recognized beneficial element in plants, and its mechanisms in strengthening drought tolerance, such as water balance, photosynthetic assimilation, gas exchange, nutrient absorption, secondary metabolite production, and antioxidant defense, have been reported (Zahedi et al., 2020; Sattar et al., 2020; Cui et al., 2021; Souri et al., 2021). Similar to PGPB, the protective effects of Si against oxidative damage have been documented in different plants, and the mechanism varies in different species (Khattab et al., 2014; Biju et al., 2017; Coskun et al., 2019; Cao et al., 2020). Recently, the synergistic effects of PGPB and Si for the amelioration of abiotic stress in plants have been examined. Fatemi et al. (2020) reported that the combined application of PGPB and Si produced better results in improving the growth traits of *Coriandrum sativum* under heavy metal stress compared to the single treatment. Furthermore, the combination of PGPB and Si conferred promising results in the mitigation of salinity stress in cucumber and mung bean (Mahmood et al., 2016; Mahmood et al., 2017; Kaloterakis et al., 2021). In wheat, the combined application of PGPB strains and Si improved drought tolerance by increasing the nutrient uptake and upregulating the antioxidant enzymes (SOD, POD, and CAT), and the effect of this combined treatment was better than that of the individual treatments (Akhtar et al., 2021).

G. uralensis, a perennial herb of the legume family, is commonly used as a food sweetener, tobacco flavoring agent, and Chinese medicine (Dang et al., 2021; Zhang et al., 2022; Bi et al., 2022). Due to its wide cultivation in arid and semi-arid desert steppes and edges, the yield of *G. uralensis* has been severely reduced (Li et al., 2022; Liu et al., 2022). Thus, it is of considerable economic and social importance to develop an effective method for improving the drought tolerance of cultivated *G. uralensis*. Although the specific role of PGPB or Si in the amelioration of drought stress has been well established in *G. uralensis* (Zhang et al., 2020; Zhang et al., 2021a), the comparative and synergistic application of PGPB and Si in alleviating drought stress in *G. uralensis* has not been thoroughly studied. Therefore, the objective of this study was to analyze the comparative and synergistic roles of PGPB and Si in the antioxidant system of *G. uralensis* under drought stress using physiological, transcriptomic, and metabolomic techniques, aiming to determine whether they trigger similar responses, use the same mechanisms, and whether they can be used together for synergistic benefits to improve drought tolerance in *G. uralensis*.

Materials and methods

Plant material, *B. pumilus* material, and preparation of *Bacillus* inoculate

G. uralensis seeds were collected from wild plants in Urad Front Banner, Inner Mongolia, China, in September 2019. Healthy seeds were selected and stored in a kraft paper bag at 4°C until use.

The G5 strain utilized in this study was obtained from *G. uralensis* roots and was identified as *B. pumilus* by Sangon Biotech Co., Ltd. (Shanghai, China). The strain was preserved at the China National Center for Total Culture of Microbes under preservation no. CGMCC 16879 and is listed in NCBI as MT 822869.

G5 was cultured at 28°C for 24 h in nutrient agar solid medium (3 g beef extract, 10 g tryptone, 5 g NaCl, 1,000 ml H_2O, and 16 g agar pH 7.0–7.2) and then inoculated in sterilized nutrient broth liquid medium (3 g beef extract, 10 g tryptone, 5 g NaCl, and 1,000 ml H_2O, pH 7.0–7.2) for 48 h with shaking at 180 rpm and 28°C. The optical density (OD_{600}) was adjusted to about 1 with diluted sterile water, and the concentration of G5 was 10^8 CFU/ml. As shown in Supplementary Figure S1, G5 and Si were used in combination according to the absence of a bacteriostatic band (Zheng et al., 2022).

Plant growth conditions and treatments

The seeds of *G. uralensis* were steeped with concentrated sulfuric acid for 45 min to break the seed coat, surface sterilized with 0.1% H_2O_2 for 10 min, cleaned three times using distilled water, and finally imbibed in distilled water for 8 h at 25°C. Each pot was filled with 1,500 g of autoclaved and fully dried sandy soil collected from native desert regions and then pre-irrigated with 300 ml of distilled water. Subsequently, 65 water-absorbing fully filled seeds were selected and sown uniformly, then covered with 380 g of sandy soil in each pot. The experiment was conducted in an indoor environment with natural light and an air temperature of 23–28°CC during the day and night.

The experiment had a randomized design and included the following groups: i) control (CK) group, where plants were watered to keep 65%–75% of the saturation moisture content; ii) drought stress (D) group, in which plants were watered to keep 35%–45% of the saturation moisture content; iii) drought stress with G5 (D+G5) group, where plants were watered to keep 35%–45% of the saturation moisture content and G5 was added (10^8 CFU/ml^{-1}); iv) drought stress with Si (D+Si) group, where plants were watered to keep 35%–45% of the saturation moisture content and Si was added (2 mM); and v) drought stress with combined G5 and Si application (D+G5 +Si) group, in which plants were watered to keep 35%–45% of the saturation moisture content and both G5 (10^8 CFU/ml) and Si (2 mM) were applied. Si was added as 2 mM K_2SiO_3. The concentration of G5 inoculation was 10^8 CFU/ml. A solution of the exogenous substance (G5, Si, or G5+Si) was prepared in 300 ml distilled water and irrigated the roots of *G. uralensis* seedlings after the appearance of the third true leaf. After 5 days, drought stress was simulated by controlling the saturated moisture content at 35%–45% (using the weighing method).

All treatments had three replications, and all pots were randomly arranged and periodically rotated to minimize the effect of environmental heterogeneity. The samples were collected 15 days after drought, immediately frozen in liquid nitrogen, and then stored at −80°CC until use.

Measurement of the oxidative stress marker contents

Measurement of the production rate of $O_2^{\cdot-}$ was performed according to Siddiqui et al. (2020), with slight modifications. Absorbance was measured at 530 nm, and the standard curve was constructed with $NaNO_2$. The H_2O_2 content was determined according to Siddiqui et al. (2020), with slight modifications. Absorbance was measured at 410 nm, and the standard curve was obtained using H_2O_2. The malondialdehyde (MDA) content was determined using the method of Zhou et al. (2004), with slight changes, and absorbance was measured at 532 and 600 nm.

Measurement of the activities of SOD, CAT, and POD

The activity of SOD as determined using reagent kits (Beijing Solarbio Science & Technology Co., Ltd., Beijing,

China) according to the manufacturer's instructions. Absorbance was measured at 560 nm. A unit of SOD activity was defined as the quantity of enzyme required to reduce the inhibition of nitroblue tetrazolium by 50%. The activity of CAT was assessed according to Hasanuzzaman et al. (2011), with minimal changes. A unit of CAT activity was defined as a 0.01-unit change in absorbance per minute. The activity of POD was assessed using the method of Pan et al. (2006), with slight modifications. A unit of POD activity was defined as a 0.01-unit change in absorbance per minute.

Measurement of the contents of key compounds related to the AsA–GSH cycle

The AsA content was determined according to the method of Hodges et al. (1997), with minor modifications. The standard curve was constructed with the AsA standard and the absorbance measured at 534 nm. The DHA content was estimated as the difference between the total AsA content and the AsA content, and absorbance was measured at 534 nm (Hodges et al., 1997).

The GSH and GSSG contents were determined using reagent kits (Beijing Solarbio Science & Technology Co., Ltd.) according to the manufacturer's instructions. Absorbance was measured at 412 nm.

Measurement of the activities of key enzymes related to the AsA–GSH cycle

The activity of APX as assayed according to the method of Lopez-Delacalle et al. (2021), with minor modifications. Absorbance was measured at 240 nm, and one unit of APX activity was defined as 0.01 unit of absorbance change per minute.

The activity of MDHAR was assayed as described previously (Hossain et al., 1984), with minor modifications. Absorbance was measured at 340 nm, and the activity was calculated based on the change in absorbance after 1 min (with an extinction coefficient of 6.2 mM^{-1} cm^{-1}).

The activity of DHAR was measured as previously described (Nakano and Asada, 1981), with minor modifications. Absorbance was measured at 265 nm, and the activity was calculated based on the change in absorbance after 1 min (the extinction coefficient was 14 mM^{-1} cm^{-1}).

The activity of GR was measured as previously described (Cakmak et al., 1993), with minor modifications. The change in absorbance was recorded at 340 nm within 1 min (with an extinction coefficient of 6.2 mM^{-1} cm^{-1}).

The activity of GPX was determined using reagent kits (Beijing Solarbio Science & Technology Co., Ltd.) according to the manufacturer's instructions. Absorbance was measured at 412 nm, and one unit of GPX activity was defined as the oxidation of 1 nmol GSH per minute.

Measurement of the contents of total carotenoids and total flavonoids

The total carotenoid content was estimated by extracting the leaves using 96% ethanol following the method described by Lichtenthaler et al. (1987). Absorbance was read at wavelengths of 646, 663, and 470 nm.

The total flavonoid content was calculated according to the method of Zhang et al. (2019), with minor modifications. Absorbance was recorded at 530 nm, and the content was quantified to the standard curve of rutin.

RNA extraction, cDNA library construction, and RNA-seq

Transcriptome sequencing was carried out by Beijing Baimeike Company. The experimental process followed the method provided by Oxford Nanopore Technologies, which included the following steps: 1) *G. uralensis* seedlings collected from the five treatment groups (CK, D, D+G5, D+Si, and D+G5+Si) were ground and biologically replicated for RNA preparation. Three biological replicates per sample were used for the RNA sequencing (RNA-seq) experiments; 2) RNA was extracted and its purity, concentration, and integrity were examined; 3) a library was constructed, which included primer annealing, reverse transcription into cDNA, and oligo switching, as well as synthesis of the complementary chains, DNA damage and terminal repair, and magnetic bead purification; and 4) finally, the sequencing connector was added for on-machine sequencing.

Transcriptome data assembly

For data assembly, low-quality (length< 500 bp, *Q* score< 7) sequences and ribosomal RNA sequences from the original landing sequence were filtered and the full-length sequence according to the presence of primers at both ends of the sequence was obtained. The full-length sequence obtained in the previous step was polished to obtain a consistent sequence. Contig comparisons with reference genomes or constructed contig sequences were performed to remove redundancy.

Transcription quantification

Transcriptome sequencing can be simulated as a random sampling process. To make the number of fragments truly reflect the expression levels of the transcripts, it is necessary to

normalize the number of mapped reads in the sample. Counts per million (CPM) (Zhou et al., 2014) was used as an indicator to measure the expression levels of transcripts or genes.

Quantification of the gene/transcript expression levels and differential expression analysis

Full-length reads were mapped to the reference transcriptome sequence. Reads with a match quality above 5 were further used for quantification. The expression levels were estimated as reads per gene/transcript per 10,000 mapped reads.

For samples with biological replicates, differential expression analysis of two conditions/groups was performed using the DESeq R package (1.18.0). DESeq provides statistical routines to determine the differential expression in digital gene expression data using a model based on the negative binomial distribution. The resulting *p*-values were adjusted using the Benjamini–Hochberg approach for controlling the false discovery rate. Genes with a $p< 0.05$ and fold change (FC) ≥ 1.5 found by DESeq were considered differentially expressed.

Metabolite extraction and UPLC-MS/MS analysis

The LC/MS system used for metabolomics analysis was composed of the Waters Acquity I-Class PLUS ultra-high performance liquid tandem Waters Xevo G2-XS QTof high-resolution mass spectrometer. The column used was a Waters Acquity UPLC HSS T3 column (1.8 μm, 2.1 mm × 100 mm). For the positive ion mode, mobile phase A consisted of 0.1% formic acid aqueous solution, while mobile phase B was 0.1% formic acid acetonitrile. For the negative ion mode, mobile phase A was 0.1% formic acid aqueous solution, while mobile phase B consisted of 0.1% formic acid acetonitrile. The Waters Xevo G2-XS QTof high-resolution mass spectrometer can collect primary and secondary mass spectrometry data in MSe mode under the control of the acquisition software (MassLynx v4.2; Waters Corporation, Milford, MA, USA).

Metabolite data preprocessing and annotation

The raw data collected using MassLynx v4.2 were processed with the Progenesis QI software for peak extraction, peak alignment, and other data processing operations based on the Progenesis QI software online METLIN database and the self-built library of Biomark for identification; at the same time, the theoretical fragment identification and mass deviation were all within 100 ppm.

Metabolite data analysis

After normalizing the original peak area information with the total peak area, follow-up analysis was performed. Principal component analysis (PCA) and Spearman's correlation analysis were used to examine the repeatability of the samples within the group and the quality control samples. The identified compounds were investigated for classification and pathway information in Kyoto Encyclopedia of Genes and Genomes (KEGG), Human Metabolome Database (HMDB), and the LIPID MAPS database. According to the grouping information, the difference multiples were calculated and compared, and Student's *t*-test was used to calculate the significant difference *p*-value of each compound. The R language package "ropls" was used to perform orthogonal partial least squares discriminant analysis (OPLS-DA) modeling, with 200 times permutation tests performed to verify the reliability of the model. The variable importance in projection (VIP) value of the model was calculated using multiple cross-validation. The method of combining the difference multiple, the *p*-value, and the VIP value of the OPLS-DA model were used to screen the differential metabolites. The screening criteria were: FC ≥ 1, $p< 0.05$, and VIP > 1. Significance of the differential metabolites of the KEGG pathway enrichment was calculated using a hypergeometric distribution test.

Statistical analyses

All treatments had three replications presented as the mean and the standard deviation of each experiment. One-way ANOVA was carried out and physiological data were examined for significant treatment differences using Duncan's multiple range tests, and a $p< 0.05$ was considered as statistically significant. Correlation analysis of the physiological parameters in *G. uralensis* under the five conditions was conducted. PCA was performed on the physiological parameters of the response variables to separate the plants in the different treatments. The first two principal components, which accounted for the highest variation, were then used to plot two-dimensional scatter plots. All statistical analyses were performed using SPSS Statistics 25, Origin 2018 Statistics.

Results

Effects of G5 and/or Si on the oxidative stress markers in drought-stressed *G. uralensis* seedlings

As shown in Figure 1A, the production rate of O_2^- and the contents of H_2O_2 and MDA were significantly increased in *G.*

10.3389/fpls.2022.1033915

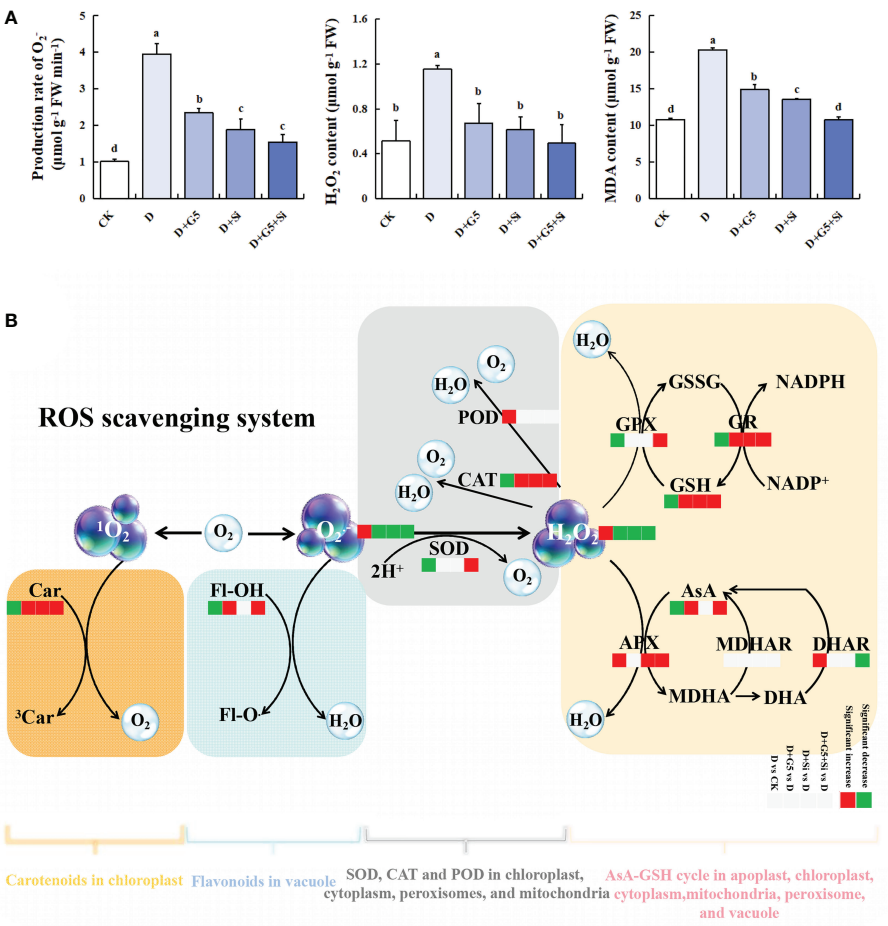


FIGURE 1
Effects of *Bacillus pumilus* (G5) and/or silicon (Si) on oxidative stress markers and the reactive oxygen species (ROS) scavenging system in drought-stressed *G lycyrrhiza uralensis* seedlings. **(A)** Oxidative stress markers. **(B)** ROS scavenging system. *CK*, control group; *D*, drought stress group; *D+G5*, drought stress with G5 group; *D+Si*, drought stress with Si group; *D+G5+Si*, drought stress with combined G5 and Si application group. *MDA*, malondialdehyde; *Car*, carotenoids; *Fl-OH*, *Fl-O*, flavonoids; *SOD*, superoxide dismutase; *POD*, peroxidase; *CAT*, catalase; *AsA*, ascorbate; *MDHA*, monodehydroascorbate; *DHA*, dehydroascorbate; *APX*, ascorbate peroxidase; *MDHAR*, monodehydroascorbate reductase; *DHAR*, dehydroascorbate reductase; *GSH*, glutathione; *GSSG*, glutathione disulfide; *GPX*, glutathione peroxidase; *GR*, glutathione reductase. *Different letters* within the different treatments indicate significant difference at $p < 0.05$. Values are the mean ± SE ($n = 3$).

uralensis seedlings under drought stress ($p < 0.01$). Interestingly, G5, Si, and the combination of G5 and Si significantly decreased the O_2^- production rate and the H_2O_2 and MDA contents in *G. uralensis* seedlings under drought stress ($p < 0.05$).

Effects of G5 and/or Si on the activities of SOD, POD, and CAT in drought-stressed *G. uralensis* seedlings

The activities of SOD and CAT were significantly decreased, while that of POD was significantly increased in *G. uralensis* seedlings under drought stress ($p < 0.05$). However, G5 or Si alone significantly increased only the activity of CAT, while their combination significantly increased the activities of both SOD and CAT in *G. uralensis* seedlings under drought stress ($p < 0.05$) (Figures 1B, 2A, B).

The transcriptomic analysis showed that the genes encoding SOD and POD were differentially expressed under different treatments ($p < 0.05$, FC ≥ 1.5) (Figures 2B, C, Table 1). Specifically, the expression levels of one gene encoding SOD and two genes encoding POD were upregulated, while nine genes encoding POD were downregulated in *G. uralensis* seedlings under drought stress. Interestingly, G5 downregulated the expression of three genes encoding SOD and six genes encoding POD, while Si upregulated the expression of 11 genes encoding POD, but downregulated the expression of three genes encoding POD. On the other hand, the

combination of G5 and Si upregulated the expression of one gene encoding SOD and three genes encoding POD, but downregulated the expression of one gene encoding SOD and six genes encoding POD in *G. uralensis* under drought stress.

Effects of G5 and/or Si on the AsA–GSH cycle in drought-stressed *G. uralensis* seedlings

The contents of AsA, GSH, and GSSG were significantly decreased, but the DHA content was significantly increased in *G. uralensis* seedlings under drought stress ($p< 0.05$). Interestingly, G5 alone and the combination of G5 and Si significantly increased the contents of AsA, GSH, and GSSG, but decreased the DHA content, while Si only significantly increased the GSH content in *G. uralensis* seedlings under drought stress ($p< 0.05$) (Figures 1B and 3). Moreover, according to the metabolomic analysis, drought stress increased the glucuronolactone content in *G. uralensis* seedlings (FC ≥ 1, $p< 0.05$, and VIP > 1). However, G5 decreased the glucuronolactone content, while the combination of G5 and Si increased the L-glutamate content in *G. uralensis* seedlings under drought stress (Table 2).

The transcriptomic analysis revealed that, for AsA metabolism, drought stress upregulated the expression of the genes encoding aldehyde dehydrogenase (ALDH) and GDP-mannose 3,5-epimerase (GME), but downregulated the expression of the genes encoding ALDH and inositol oxygenase (MIOX) in *G. uralensis* seedlings ($p< 0.05$, FC ≥ 1.5). However, G5 upregulated the expression of three genes encoding UDP-sugar pyrophosphorylase (UDPase), two genes encoding glucuronokinase (GlcAK), and one gene encoding MIOX, but downregulated the genes encoding UDP-glucose 6-dehydrogenase (UGDH) and GME in *G. uralensis* seedlings under drought stress. Si upregulated the expression of the genes encoding GlcAK and MIOX, but downregulated the expression of the genes encoding ALDH and GDP-L-galactose phosphorylase (GGP) in *G. uralensis* seedlings under drought stress. The combination of G5 and Si upregulated the expression of two genes encoding UGDH, the gene encoding UDPase, three genes encoding GlcAK, the gene encoding MIOX, and the gene encoding ALDH, but downregulated the expression of the genes encoding GME and GGP in *G. uralensis* seedlings under drought stress ($p< 0.05$, FC ≥ 1.5) (Figure 3 and Table 3).

In GSH metabolism, drought stress also downregulated the expression of six genes encoding glutathione S-transferase (GST) in *G. uralensis* seedlings. G5 upregulated the expression of four genes, but downregulated the expression of two genes encoding GST; on the other hand, Si upregulated the expression of six genes encoding GST, but downregulated the expression of the gene encoding GST. The combination of G5 and Si upregulated the expression of three genes encoding GST and the gene

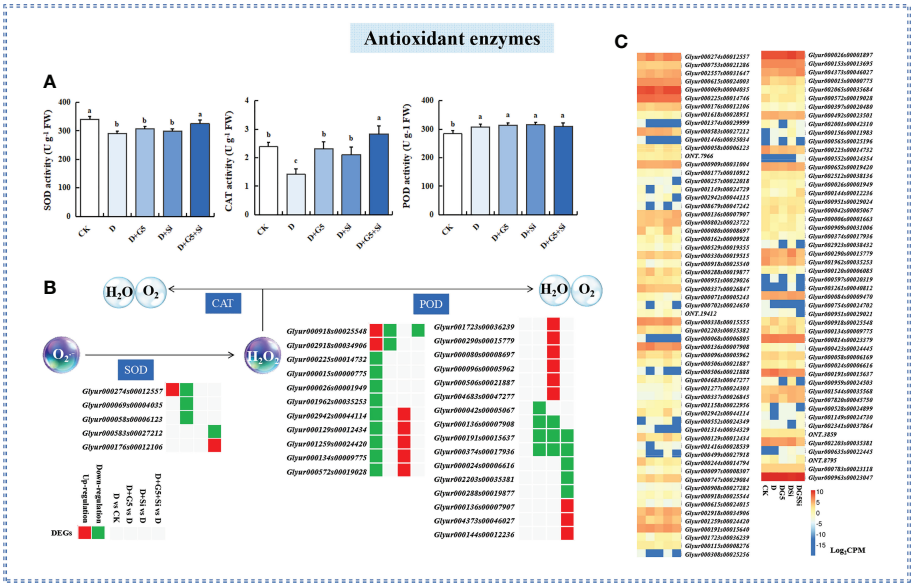


FIGURE 2
Effects of *Bacillus pumilus* (G5) and/or silicon (Si) on the antioxidant enzymes in drought-stressed *Glycyrrhiza uralensis* seedlings. **(A)** Activities of the antioxidant enzymes. **(B)** Expression patterns of the differentially expressed genes (DEGs) related to antioxidant enzymes. **(C)** Expression patterns of the genes related to antioxidant enzymes. *CK*, control group; *D*, drought stress group; *D+G5*, drought stress with G5 group; *D+Si*, drought stress with Si group; *D+G5+Si*, drought stress with combined G5 and Si application group. *SOD*, superoxide dismutase; *POD*, peroxidase; *CAT*, catalase. *Different letters* within the different treatments indicate significant difference at $p< 0.05$. Values are the mean ± SE ($n = 3$). Genes with $p< 0.05$ and fold change ≥ 1.5 were considered differentially expressed.

TABLE 1 Regulation of the antioxidant enzyme-related differentially expressed genes (DEGs) in *Glycyrrhiza uralensis* Fisch. by *Bacillus pumilus* (G5) and/or silicon under drought stress.

Enzyme name	Definition (EC)	Gene name	Gene ID	Regulated			
				D *vs.* CK	D+G5 *vs.* D	D+Si *vs.* D	D+G5+Si *vs.* D
SOD	Superoxide dismutase [EC:1.15.1.1]	*SODCP*	Glyur000274s00012557	Up	Down	–	–
		SOD1	Glyur000069s00004035	–	Down	–	–
		FSD3	Glyur000058s00006123	–	Down	–	–
		SODB	Glyur000583s00027212	–	–	–	Down
		At3g02290	Glyur000176s00012106	–	–	–	Up
POD	Peroxidase [EC:1.11.1.7]	*GSVIVT00023967001*	Glyur000918s00025548	Up	Down	–	Down
		PER64	Glyur002918s00034906	Up	Down	–	–
		PER52	Glyur000225s00014732	Down	–	–	–
		GSVIVT00037159001	Glyur000015s00000775	Down	–	–	–
		PER43	Glyur000026s00001949	Down	–		–
		PER12	Glyur001962s00035253	Down	–		–
		PER12	Glyur002942s00044114	Down	–	Up	–
		PER47	Glyur000129s00012434	Down	–	Up	–
		PER10	Glyur001259s00024420	Down	–	Up	–
		PER72	Glyur000134s00009775	Down	–	Up	–
		PER20	Glyur000572s00019028	Down	–	Up	–
		PNC1	Glyur001723s00036239	–	–	Up	–
		pod	Glyur000290s00015779	–	–	Up	–
		HRPN	Glyur000080s00008697	–	–	Up	–
		PER72	Glyur000096s00005962	–	–	Up	–
		PER16	Glyur000506s00021887	–	–	Up	–
		PER12	Glyur004683s00047277	–	–	Up	–
		PER50	Glyur000042s00005067	–	Down	–	–
		PNC2	Glyur000136s00007908	–	Down	Down	–
		PER12	Glyur000191s00015637	–	Down	Down	Down
		PER3	Glyur000374s00017936	–	Down	Down	Down
		PER53	Glyur000024s00006616	–	–	–	Down
		GSVIVT00023967001	Glyur002203s00035381	–	–	–	Down
		GSVIVT00023967001	Glyur000288s00019877	–	–	–	Down
		PNC2	Glyur000136s00007907	–	–	–	Up
		PER55	Glyur004373s00046027	–	–	–	Up
		GSVIVT00037159001	Glyur000144s00012236	–	–	–	Up

CK, control group; D, drought stress group; D+G5, drought stress with G5 group; D+Si, drought stress with Si group; D+G5+Si, drought stress with combined G5 and Si application group.

encoding gamma-glutamyl transpeptidase (GGT), but downregulated the expression of the genes encoding GST and APN in *G. uralensis* seedlings under drought stress ($p< 0.05$, FC ≥ 1.5) (Table 3).

Furthermore, the activities of the AsA–GSH cycle enzymes (APX, GPX, DHAR, MDHAR, and GR) varied under the different treatments. Specifically, the activities of APX and DHAR were significantly increased, but those of GPX and GR were significantly decreased in *G. uralensis* seedlings under drought stress ($p< 0.05$). However, G5 significantly increased the activity of GR, while Si significantly increased the activities of APX and GR; on the other hand, the combination of G5 and Si significantly increased the activities of APX, GPX, and GR, but decreased the activity of DHAR in *G. uralensis* seedlings under drought stress ($p< 0.05$) (Figures 1B and 3).

Moreover, transcriptomic analysis showed that drought stress upregulated the expression of the genes encoding APX and DHAR in *G. uralensis*. Si upregulated the expression of the genes encoding APX and L-ascorbate oxidase (AO), but downregulated the gene encoding GPX; however, the combination of G5 and Si upregulated the expression of the genes encoding AO and GPX, but downregulated the genes encoding MDHAR, DHAR, GPX, and glucose-6-phosphate 1-dehydrogenase (G6PD) in *G. uralensis* seedlings under drought stress ($p< 0.05$, FC ≥ 1.5) (Table 3).

10.3389/fpls.2022.1033915

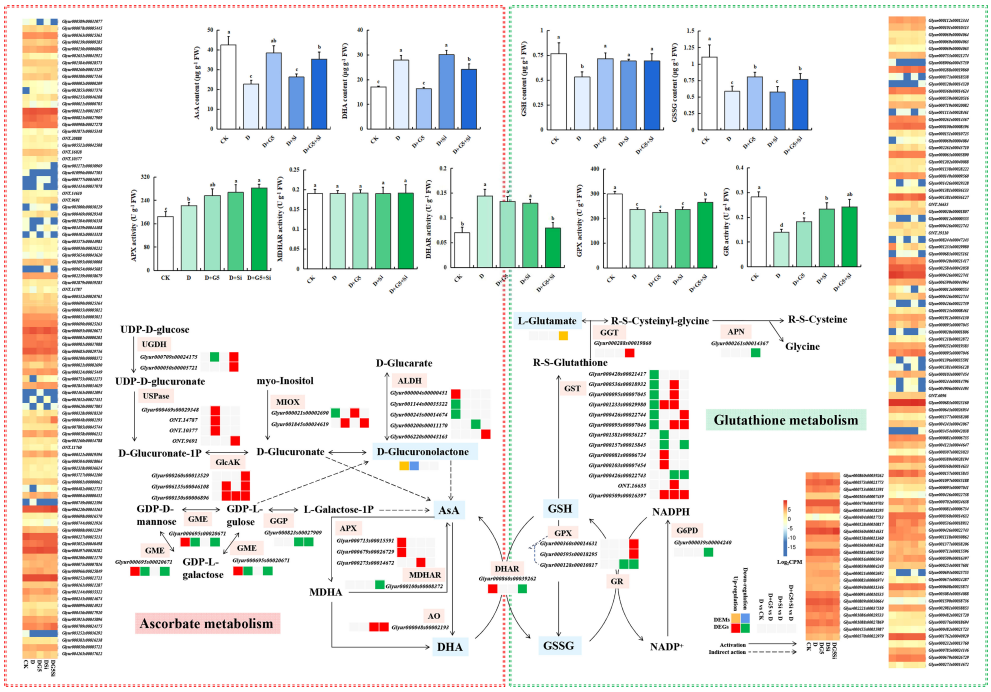


FIGURE 3
Effects of *Bacillus pumilus* (G5) and/or silicon (Si) on the ascorbate (AsA)–glutathione (GSH) cycle in drought-stressed *Glycyrrhiza uralensis* seedlings. *CK*, control group; *D*, drought stress group; *D+G5*, drought stress with G5 group; *D+Si*, drought stress with Si group; *D+G5+Si*, drought stress with combined G5 and Si application group. *AsA*, ascorbate; *MDHA*, monodehydroascorbate; *DHA*, dehydroascorbate; *GSH*, glutathione; *GSSG*, glutathione disulfide; *APX*, ascorbate peroxidase; *MDHAR*, monodehydroascorbate reductase; *DHAR*, dehydroascorbate reductase; *GPX*, glutathione peroxidase; *GR*, glutathione reductase; *UGDH*, UDP-glucose 6-dehydrogenase; *UDPase*, UDP-sugar pyrophosphorylase; *GlcAK*, glucuronokinase; *MIOX*, inositol oxygenase; *ALDH*, aldehyde dehydrogenase (NAD+); *GGP*, GDP-L-galactose phosphorylase; *GME*, GDP-mannose-3′,5′-epimerase; *AO*, L-ascorbate oxidase; *APX*, ascorbate peroxidase; *GPX*, glutathione peroxidase; *MDHAR*, monodehydroascorbate reductase; *DHAR*, dehydroascorbate reductase; *GST*, glutathione S-transferase; *G6PDH*, glucose-6-phosphate 1-dehydrogenase; *GGT*, gamma-glutamyl transpeptidase; *APN*, aminopeptidase N. *Different letters* within the different treatments indicate significant difference at $p < 0.05$. Values are the mean ± SE ($n = 3$). Genes with $p < 0.05$ and fold change ≥ 1.5 were considered differentially expressed; metabolites with $p < 0.05$, variable importance in projection (VIP) > 1, and fold change ≥ 1 were considered differentially expressed.

Effects of G5 and/or Si on carotenoid biosynthesis in drought-stressed *G. uralensis* seedlings

As shown in Figures 1B and 4A, the contents of total carotenoids were significantly decreased in *G. uralensis* seedlings under drought stress ($p < 0.05$). Interestingly, G5 and/or Si remarkably increased the total carotenoid content in *G. uralensis* under drought stress ($p < 0.05$).

The transcriptomic analysis revealed that G5 and Si individually downregulated the expression of the gene encoding β-carotene hydroxylase (CHXB), while Si alone and the combination of G5 and Si downregulated the expression of the genes encoding phytoene synthase (PSY), CHXB, and

TABLE 2 Regulation of the ascorbate and glutathione cycle-related differentially expressed metabolites (DEMs) in *Glycyrrhiza uralensis* Fisch. by *Bacillus pumilus* (G5) and/or silicon under drought stress.

Pathway	Metabolite name	Metabolite ID	Regulated			
			D *vs.* CK	D+G5 *vs.* D	D+Si *vs.* D	D+G5+Si *vs.* D
Ascorbate and aldarate metabolism (ko00053)	Glucuronolactone	neg_1365	Up	Down	–	–
Glutathione metabolism (ko00480)	L-Glutamate	neg_927	–	–	–	Up

CK, control group; D, drought stress group; D+G5, drought stress with G5 group; D+Si, drought stress with Si group; D+G5+Si, drought stress with combined G5 and Si application group.

TABLE 3 Regulation of the ascorbate and glutathione cycle-related differentially expressed genes (DEGs) in *Glycyrrhiza uralensis* Fisch. by *Bacillus pumilus* (G5) and/or silicon under drought stress.

Enzyme name	Definition (EC)	Gene name	Gene ID	Regulated			
				D *vs.* CK	D+G5 *vs.* D	D+Si *vs.* D	D+G5+Si *vs.* D
UGDH	UDP-glucose 6-dehydrogenase [EC:1.1.1.22]	*UGD1*	Glyur000709s00024175	–	Down	–	Up
		UGD1	Glyur000050s00005721	–	–	–	Up
UDPase	UDP-sugar pyrophosphorylase [EC:2.7.7.64]	*RE1*	Glyur000469s00029348	–	Up	–	–
		RE1	ONT.14787	–	Up	–	–
		RE1	ONT.10377	–	Up	–	–
		RE2	ONT.9691	–	–	–	Up
GlcAK	Glucuronokinase [EC:2.7.1.43]	*SCRM*	Glyur000260s00013529	–	–	–	Up
		BHLH35	Glyur006135s00046108	–	Up		Up
		GLCAK1	Glyur000130s00006896	–	Up	Up	Up
MIOX	Inositol oxygenase [EC:1.13.99.1]	*MIOX1*	Glyur000021s00002690	Down	–	Up	–
		MIOX2	Glyur001845s00034619		Up	–	Up
ALDH	Aldehyde dehydrogenase (NAD^+) [EC:1.2.1.3]	*ALDH3F1*	Glyur000004s00000451	Up	–	–	–
		ALDH3H1	Glyur001144s00035322	Down	–	–	–
		ALDH3I1	Glyur000200s00011170	–	–	Down	–
		ALDH3H1	Glyur000245s00014674	Down	–	–	–
		ALDH2B7	Glyur006220s00043163	–	–	–	Up
GME	GDP-D-mannose 3′, 5′-epimerase [EC:5.1.3.18]	*GME1*	Glyur000695s00020671	Up	Down	–	Down
GGP	GDP-L-galactose phosphorylase [EC:2.7.7.69]	*VTC2*	Glyur000823s00027909	–	–	Down	Down
APX	L-Ascorbate peroxidase [EC:1.11.1.11]	*PAP12*	Glyur000713s00015591	Up	–	–	–
		CLEB3J9	Glyur000679s00026729	Up	–	–	–
		APX1	Glyur000273s00014672	–	–	Up	–
AO	L-Ascorbate oxidase [EC:1.10.3.3]	–	Glyur000048s00002193	–	–	Up	Up
MDHAR	Monodehydroascorbate reductase (NADH) [EC:1.6.5.4]	*MDAR5*	Glyur000100s00008372	–	–	–	Down
DHAR	Glutathione dehydrogenase/transferase [EC:1.8.5.1 2.5.1.18]	*DHAR3*	Glyur000860s00039262	Up	–	–	Down
GPX	Glutathione peroxidase [EC:1.11.1.9]	*CSA*	Glyur000360s00014631	–	–	–	Up
		GPX6	Glyur000595s00018295	–	–	–	Up
		–	Glyur000128s00010817	–	–	Down	Down
G6PD	Glucose-6-phosphate 1-dehydrogenase [EC:1.1.1.49 1.1.1.363]	–	Glyur000039s00004240	–	–	–	Down
GST	Glutathione S-transferase [EC:2.5.1.18]	*HSP26-A*	Glyur000420s00021417	Down	–	–	–
		PARB	Glyur000536s00018932	Down	–	Up	–
		–	Glyur000095s00007045	Down	–	Up	–
		PARA	Glyur001233s00029980	Down	Up	Up	–
		GST3	Glyur000426s00022744	Down	–	–	Up
		–	Glyur000095s00007046	Down	–	Up	Up
		HSP26–A	Glyur001381s00036127	–	Down	–	–
		GSTU17	Glyur000157s00015845	–	Down	–	Down
		GSTL3	Glyur000081s00006734	–	Up	–	–
		–	Glyur000103s00007454	–	Up	–	–
		PARC	Glyur000426s00022743	–	–	Down	Down
		–	ONT.16635	–	–	Up	–
		–	Glyur000509s00016397	–	Up	Up	Up
GGT	Gamma-glutamyl transpeptidase/glutathione hydrolase [EC:2.3.2.2 3.4.19.13]	*GGT1*	Glyur000288s00019860	–	–	–	Up
APN	Aminopeptidase N [EC:3.4.11.2]	*At2g34460*	Glyur000261s00014367	–	–	–	Down

CK, control group; D, drought stress group; D+G5, drought stress with G5 group; D+Si, drought stress with Si group; D+G5+Si, drought stress with combined G5 and Si application group.

zeaxanthin epoxidase (ZEP) in *G. uralensis* seedlings under drought stress. Furthermore, the combination of G5 and Si upregulated the expression of the gene encoding ξ-carotene isomerase (Z-ISO) in *G. uralensis* under drought stress ($p< 0.05$, FC ≥ 1.5) (Figures 4B, C and Table 4).

Effects of G5 and/or Si on flavonoid biosynthesis in drought-stressed *G. uralensis* seedlings

Figures 1B and 5A display the contents of total flavonoids, which were significantly decreased in *G. uralensis* seedlings under drought stress ($p< 0.05$). However, G5 alone and the combination of G5 and Si remarkably increased the total flavonoid content in *G. uralensis* seedlings under drought stress ($p< 0.05$).

Moreover, the transcriptomic analysis revealed that drought stress induced the downregulation of the expression of the genes encoding phenylalanine ammonia lyase (PAL), shikimate *O*-hydroxycinnamoyltransferase (HCT), chalcone synthase (CHS), chalcone isomerase (CHI), isoflavone 7-*O*-glucoside 6"-*O*-malonyltransferase (MAT), flavonoid 3′,5′-hydroxylase (F3′,5′H), isoflavone/4′-methoxyisoflavone 2′-hydroxylase (CYP81E1/E8), and flavonoid 3′-monooxygenase (CYP75B), while it upregulated the expression of the gene encoding HCT in *G. uralensis* ($p< 0.05$, FC ≥ 1.5) (Figures 5B, C and Table 5).

However, with the application of G5, the genes encoding PAL, CHS, CHR, CHI, CYP81E1/E8, and MAT were upregulated, but the genes encoding 4-coumarate-CoA ligase (4CL), CHS, CYP81E1/E8, MAT, and HCT were downregulated in *G. uralensis* under drought stress. With the application of Si, the genes encoding PAL, HCT, CHS, CHR, CHI, MAT, isoflavone 7-*O*-glucosyltransferase (UGT), vestitone reductase (VR), F3′,5′H, and CYP75B were upregulated, while those encoding MAT and VR were downregulated in *G. uralensis* under drought stress. Moreover, the combination of G5 and Si upregulated the genes encoding PAL, 4CL, *trans*-cinnamate 4-monooxygenase (C4H), HCT, CHS, CHR, MAT, and UGT, but downregulated the genes encoding PAL, 4CL, HCT, 5-*O*-(4-coumaroyl)-D-quinate 3′-monooxygenase (CYP98A2), caffeic acid 3-*O*-methyltransferase/acetylserotonin *O*-methyltransferase (CCOMT), CHS, VR, MAT, UGT, flavonol synthase (FLS), and CYP75B in *G. uralensis* under drought stress ($P< 0.05$ and FC ≥ 1.5) (Figures 5B, C and Table 5).

Moreover, metabolomic analysis showed that drought stress decreased the contents of daidzein, glycitin, and (−)-medicarpin, but increased the coumestrol and glycitein contents in *G. uralensis*. However, G5 increased the contents of (−)-medicarpin, vitexin, and 3-*O*-methylquercetin; similarly, the combination of G5 and Si increased the contents of daidzein, (−)-medicarpin, glycitin, and astragalin, while G5 and/or Si decreased the content of glycitein in *G. uralensis* under drought stress ($p< 0.05$, FC ≥ 1, VIP > 1) (Figures 5B, C and Table 6).

Hierarchical clustering with heatmap and principal component analysis

The results of all the physiological–biochemical parameters (the oxidative stress markers, key substances, the enzymes related to the AsA–GSH cycle, and the contents of total

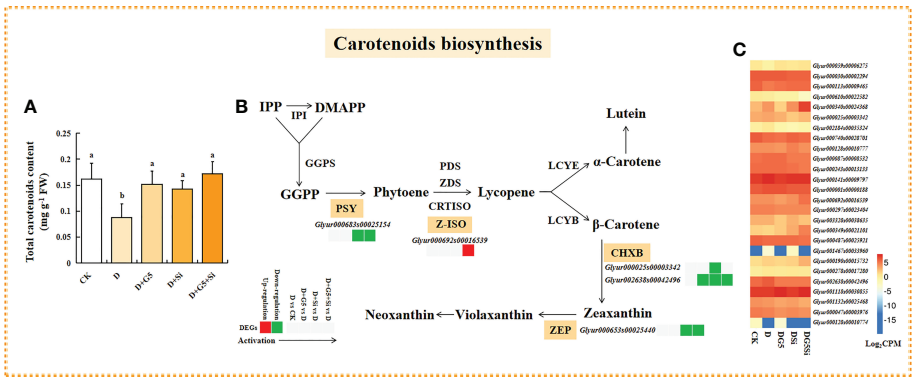


FIGURE 4
Effects of *Bacillus pumilus* (G5) and/or silicon (Si) on carotenoid biosynthesis in drought-stressed *Glycyrrhiza uralensis* seedlings. **(A)** Total carotenoid content. **(B)** Carotenoid biosynthesis process. **(C)** Expression patterns of the genes related to carotenoid biosynthesis. *CK*, control group; *D*, drought stress group; *D+G5*, drought stress with G5 group; *D+Si*, drought stress with Si group; *D+G5+Si*, drought stress with combined G5 and Si application group. *IPP*, isopentenyl diphosphate; *DMAPP*, dimethylallyl diphosphate; *GGPS*, geranylgeranyl diphosphate synthase; *PSY*, phytoene synthase; *PDS*, phytoene desaturase; *ZDS*, ξ-carotene desaturase; *CRTISO*, carotenoid isomerase; *Z-ISO*, ξ-carotene isomerase; *LCYE*, lycopene ϵ-cyclase; *LCYB*, lycopene β-cyclase; *CHXE*, ϵ-carotene hydroxylase; *CHXB*, β-carotene hydroxylase; *ZEP*, zeaxanthin epoxidase. *Different letters* within the different treatments indicate significant difference at $p< 0.05$. Values are the mean ± SE (n = 3). Genes with $p< 0.05$ and fold change ≥ 1.5 were considered differentially expressed.

TABLE 4 Regulation of the carotenoid biosynthesis-related differentially expressed genes (DEGs) in *Glycyrrhiza uralensis* Fisch. by *Bacillus pumilus* (G5) and/or silicon under drought stress.

Enzyme name	Definition (EC)	Gene name	Gene ID	Regulated			
				D *vs.* CK	D+G5 *vs.* D	D+Si *vs.* D	D+G5+Si *vs.* D
PSY	15-*cis*-Phytoene synthase [EC:2.5.1.32]	*PSY*	Glyur000683s00025154	–	–	Down	Down
Z-ISO	Zeta-carotene isomerase [EC:5.2.1.12]	*Z-ISO*	Glyur000692s00016539	–	–	–	Up
CHXB	β-carotene hydroxylase [EC:1.14.15.24]	*CA2*	Glyur000025s00003342	–	–	Down	–
		CA2	Glyur002638s00042496	–	Down	Down	Down
ZEP	Zeaxanthin epoxidase [EC:1.14.15.21]	–	Glyur000653s00025440	–	–	Down	Down

CK, control group; D, drought stress group; D+G5, drought stress with G5 group; D+Si, drought stress with Si group; D+G5+Si, drought stress with combined G5 and Si application group.

carotenoids and total flavonoids) were subjected to heatmap analysis with hierarchical clustering (Figure 6A). Hierarchical clustering revealed the categorization of all the studied variables into two clusters: cluster 1, which covered MDA, O_2^-, DHAR, H_2O_2, and the DHA variables, and cluster 2, which included total carotenoids, AsA, total flavonoids, GR, GSH, GPX, and the SOD variables. Compared with the D group, the variables of cluster 1 showed a decreasing pattern in most of the cases under the D+G5, D+Si, and D+G5+Si treatments, while these variables displayed an increasing trend in the D-treated compared to CK-

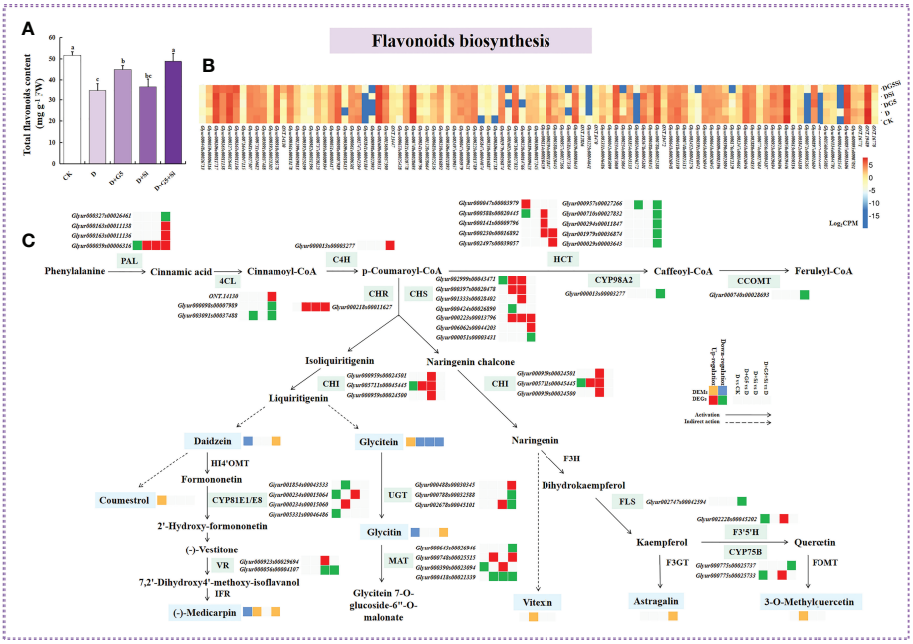


FIGURE 5
Effects of *Bacillus pumilus* (G5) and/or silicon (Si) on flavonoid biosynthesis in drought-stressed *Glycyrrhiza uralensis* seedlings. **(A)** Total flavonoid content. **(B)** Flavonoid biosynthesis pathway. **(C)** Expression patterns of the genes related to flavonoid biosynthesis. *CK*, control group; *D*, drought stress group; *D+G5*, drought stress with G5 group; *D+Si*, drought stress with Si group; *D+G5+Si*, drought stress with combined G5 and Si application group. *PAL*, phenylalanine ammonia-lyase; *4CL*, 4-coumarate-CoA ligase; *C4H*, *trans*-cinnamate 4-monooxygenase; *HCT*, shikimate *O*-hydroxycinnamoyltransferase; CYP98A2, 5-*O*-(4-coumaroyl)-D-quinate 3′-monooxygenase; *CCOMT*, caffeic acid 3-*O*-methyltransferase/acetylserotonin *O*-methyltransferase; *CHS*, chalcone synthase; *CHI*, chalcone isomerase; *CHR*, chalcone reductase; *HI4'OMT*, 2,7,4′-trihydroxyisoflavanone 4′-*O*-methyltransferase; *CYP81E1/E8*, isoflavone/4′-methoxyisoflavone 2′-hydroxylase; *VR*, vestitone reductase; *IFR*, 2′-hydroxyisoflavone reductase; *UGT*, isoflavone 7-*O*-glucosyltransferase; *MAT*, isoflavone 7-*O*-glucoside-6"-*O*-malonyltransferase; *F3H*, flavanone 3-hydroxylase; *FLS*, flavonol synthase; *F3′,5′H*, flavonoid 3′,5′-hydroxylase; *CYP75B*, flavonoid 3′-monooxygenase; *F3GT*, flavonol 3-*O*-glucosyltransferase. *Different letters* within the different treatments indicate significant difference at $p < 0.05$. Values are the mean ± SE ($n = 3$). Genes with $p < 0.05$ and fold change ≥ 1.5 were considered differentially expressed; metabolites with $p < 0.05$, and variable importance in projection (VIP) > 1, and fold change ≥ 1 were considered differentially expressed.

TABLE 5 Regulation of the flavonoid biosynthesis-related differentially expressed genes (DEGs) in *Glycyrrhiza uralensis* Fisch. by *Bacillus pumilus* (G5) and/or silicon under drought stress.

Enzyme name	Definition (EC)	Gene name	Gene ID	Regulated			
				D *vs.* CK	D+G5 *vs.* D	D+Si *vs.* D	D+G5+Si *vs.* D
PAL	Phenylalanine ammonia-lyase [EC:4.3.1.24]	*PAL1*	Glyur000327s00026461	–	–	–	Down
		PAL1	Glyur000163s00011138	–	–	–	Up
		PAL1	Glyur000163s00011136	–	–	–	Up
		–	Glyur000059s00006316	Down	Up	Up	Up
4CL	4-Coumarate-CoA ligase [EC:6.2.1.12]	*4CLL7*	ONT.14130	–	–	–	Up
		4CL1	Glyur000098s00007989	–	–	–	Down
		4CLL6	Glyur003091s00037488	–	Down	–	Down
C4H	*trans*-Cinnamate 4-monooxygenase [EC:1.14.14.91]	–	Glyur000002s00000296	–	–	–	Up
HCT	Shikimate *O*-hydroxycinnamoyltransferase [EC:2.3.1.133]	–	Glyur000047s00003979	Up	–	–	–
		AT1	Glyur000588s00020445	Down	–	Up	–
		–	Glyur000141s00009796	–	–	Up	–
		SHT	Glyur000230s00016892	–	–	Up	Up
		CER2	Glyur002497s00039057	–	–	–	Up
		SAT	Glyur000957s00027266	–	Down	–	Down
		HST	Glyur000710s00027832	–	–	–	Down
		CER26L	Glyur000294s00011847	–	–	–	Down
		PHT1	Glyur001979s00036874	–	–	–	Down
		SHT	Glyur000029s00003643	–	–	–	Down
CYP98A2	5-*O*-(4-coumaroyl)-D-quinate 3′-monooxygenase [EC:1.14.14.96]	*CYP98A2*	Glyur000013s00003277	–	–	–	Down
CCOMT	Caffeoyl-CoA *O*-methyltransferase [EC:2.1.1.104]	*CCOMT*	Glyur000740s00028693	–	–	–	Down
CHS	Chalcone synthase [EC:2.3.1.74]	*CHS2*	Glyur000424s00026890	–	Down	–	–
		CHS	Glyur002999s00043471	Down	Up	Up	–
		CHS6	Glyur000397s00020478	–	Up	Up	–
		CHS5	Glyur001333s00028402	–	–	Up	–
		CHS1	Glyur000223s00013796	–	Up	Up	Up
		CHS1	Glyur006062s00044203	–	–	–	Up
		CHS1	Glyur000051s00003431	–	–	–	Down
CHR	Chalcone reductase	–	Glyur000218s00011627	–	Up	Up	Up
CHI	Chalcone isomerase [EC:5.5.1.6]	*CHI1B1*	Glyur000959s00024501	–	–	Up	–
		CHI1	Glyur005711s00045445	Down	Up	Up	–
		CHI1B1	Glyur000959s00024500	–	–	Up	–
CYP81E1/E8	Isoflavone/4′-methoxyisoflavone 2'-hydroxylase [EC:1.14.14.90 1.14.14.89]	*CYP81E1*	Glyur000234s00015064	Down	–	Up	–
		CYP81E8	Glyur005331s00046486	Down	–	–	–
		CYP81E1	Glyur000234s00015060	–	Up	–	–
		CYP81E8	Glyur001854s00043533	–	Down	–	–
VR	Vestitone reductase [EC:1.1.1.348]	–	Glyur000923s00029694	–	–	Up	–
		–	Glyur000056s00004107	–	–	Down	Down
UGT	Isoflavone 7-*O*-glucosyltransferase [EC:2.4.1.170]	*UGT13*	Glyur000488s00030345	–	–	–	Up
		UGT1	Glyur000788s00032588	–	–	–	Down
		UGT2	Glyur002678s00045101	–	–	Up	Down
MAT	Isoflavone 7-*O*-glucoside-6′-*O*-malonyltransferase [EC:2.3.1.115]	*PMAT1*	Glyur000643s00026946	–	–	–	Down
		PMAT1	Glyur000748s00025515	–	Up	–	Up
		PMAT1	Glyur000390s00023094	Down	–	Up	–
		5MAT	Glyur000418s00021339	–	Down	Down	Down
FLS	Flavonol synthase [EC:1.14.20.6]	*FLS*	Glyur002747s00042594	–	–	–	Down

(Continued)

TABLE 5 Continued

Enzyme name	Definition (EC)	Gene name	Gene ID	Regulated			
				D *vs.* CK	D+G5 *vs.* D	D+Si *vs.* D	D+G5+Si *vs.* D
F3′,5′H	Flavonoid 3′,5′-hydroxylase [EC:1.14.14.81]	*CYP75A1*	Glyur002228s00045202	Down	–	Up	–
CYP75B	Flavonoid 3′-monooxygenase [EC:1.14.14.82]	*CYP75B2*	Glyur000775s00025737	–	–	–	Down
		CYP75B1	Glyur000775s00025733	Down	–	Up	–

CK, control group; D, drought stress group; D+G5, drought stress with G5 group; D+Si, drought stress with Si group; D+G5+Si, drought stress with combined G5 and Si application group.

treated *G. uralensis*. However, this effect was partially reversed in cluster 2; specifically, compared with the D group, the variables of cluster 2 showed an increasing pattern in some of the cases under the D+G5, D+Si, and D+G5+Si treatments, while these variables displayed a decreasing trend in most of the cases in the D-treated compared to CK-treated *G. uralensis*.

The results of the PCA related to all the physiological–biochemical parameters showed that PC1 explained 59.80% of the total variation, while PC2 accounted for 15.18% of the total variation (Figure 6B). PC1 formation covered the oxidative stress markers (O_2^- and MDA), non-enzymatic antioxidants (GSH, DHA, AsA, total flavonoids, and total carotenoids), and the enzymatic antioxidant (DHAR) and was separated by these parameters between plants in the CK and D treatment groups and between plants in the D+G5+Si and D+G5 treatment groups or the D+Si treatment. PC2 distinctly separated the plants given treatment D from those given the G5 and/or Si treatments because of the oxidative stress marker (H_2O_2), non-enzymatic antioxidant (GSSG), and the enzymatic antioxidants (APX, GPX, POD, CAT, GR, SOD, and MDHAR). Specifically, compared with the single treatment of G5 or Si, the combined G5 and Si treatment had a stronger correlation with the majority of the antioxidants (i.e., CAT, GSSG, ASA, GSH, total flavonoids, and total carotenoids) under drought stress, suggesting that the effects of the combination of G5 and Si on the antioxidants in *G. uralensis* under drought stress are greater than that of G5 or Si alone (Figure 6B).

The number and correlation network map of the DEGs and DEMs involved in the biosynthesis of the major antioxidants of drought-stressed *G. uralensis* seedlings

As shown in Figure 6C, comparison of the D and CK treatments showed 14 differentially expressed genes (DEGs) and one differentially expressed metabolite (DEM) related to the AsA–GSH cycle and 10 DEGs and five DEMs related to flavonoid biosynthesis. These results indicated that drought mainly affects the ability of *G. uralensis* to scavenge ROS mainly by affecting the AsA–GSH cycle and flavonoid biosynthesis.

Interestingly, comparison of the D+G5 and D treatments, revealed 14 DEGs and one DEM related to the AsA–GSH cycle, two DEGs related to carotenoid biosynthesis, and eight DEGs and four DEMs related to flavonoid biosynthesis. The comparison of D+Si and D treatments revealed 13 DEGs related to the AsA–GSH cycle, four DEGs related to carotenoid biosynthesis, and 11 DEGs and one DEM related to flavonoid biosynthesis. In the D+G5+Si *vs.* D treatment, there were 21 DEGs and one DEM related to the AsA–GSH cycle, four DEGs related to carotenoid biosynthesis, and 30 DEGs and five DEMs related to flavonoid biosynthesis, From these results, it was observed that the numbers of DEGs and DEMs regulated by

TABLE 6 Regulation of the flavonoid biosynthesis-related differentially expressed metabolites (DEMs) in *Glycyrrhiza uralensis* Fisch. by *Bacillus pumilus* (G5) and/or silicon under drought stress.

Metabolite name	Metabolite ID	Regulated			
		D *vs.* CK	D+G5 *vs.* D	D+Si *vs.* D	D+G5+Si *vs.* D
Glycitein	neg_10761	Up	Down	Down	Down
Vitexin	neg_5513	–	Up	–	–
Astragalin	neg_6043	–	–	–	Up
Coumestrol	neg_8315	Up	–	–	–
Daidzein	pos_13283	Down	–	–	Up
(–)-Medicarpin	pos_11757	Down	Up	–	Up
3-*O*-Methylquercetin	pos_8398	–	Up	–	–
Glycitin	neg_4482	Down	–	–	Up

CK, control group; D, drought stress group; D+G5, drought stress with G5 group; D+Si, drought stress with Si group; D+G5+Si, drought stress with combined G5 and Si application group.

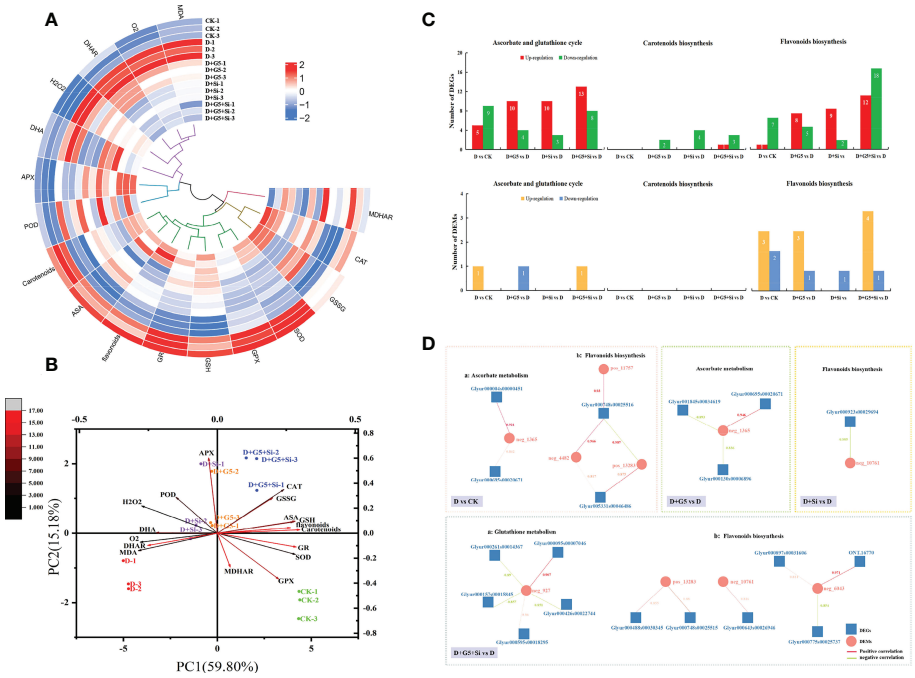


FIGURE 6
Hierarchical clustering with heatmap **(A)** and principal component analysis of the reactive oxygen species (ROS) scavenging system **(B)**, the number of differentially expressed genes (DEGs) and differentially expressed metabolites (DEMs) **(C)**, and correlation network map of the DEGs and DEMs involved in antioxidant biosynthesis **(D)** in drought-stressed *Glycyrrhiza uralensis* seedlings. *CK*, control group; *D*, drought stress group; *D+G5*, drought stress with G5 group; *D+Si*, drought stress with Si group; *D+G5+Si*, drought stress with combined G5 and Si application group. *MDA*, malondialdehyde; *AsA*, ascorbate; *MDHA*, monodehydroascorbic acid; *DHA*, dehydroascorbate; *GSH*, glutathione; *GSSG*, glutathione disulfide; *SOD*, superoxide dismutase; *POD*, peroxidase; *CAT*, catalase; *APX*, ascorbate peroxidase; *GPX*, glutathione peroxidase; *MDHAR*, monodehydroascorbate reductase; *DHAR*, dehydroascorbate reductase; *neg_1365*, glucuronolactone; *pos_11757*, (–)-medicarpin; *neg_4482*, glycitin; *pos_13283*, daidzein; *neg_10761*, glycitein; *neg_6043*, astragalin. **(A)** Values of the various parameters obtained in this study normalized and analyzed in the hierarchical clustering and heatmap. Two distinct clusters were identified at the variable level. In the heatmap, the *color scale* displays the intensity of the normalized values. **(B)** Principal component analysis. The *depth of the color of the arrow line* represents the degree of contribution, while the *angle of the arrow line* represents correlations. **(C)** In the number of differentially expressed genes (DEGs) and differentially expressed metabolites (DEMs), genes with $p < 0.05$ and fold change ≥ 1.5 were considered differentially expressed; metabolites with $p < 0.05$, variable importance in projection (VIP) > 1, and fold change ≥ 1 were considered differentially expressed. **(D)** Correlation network map showing the DEGs positively or negatively correlated with the DEMs, representing metabolite changes that may be positively or negatively regulated by the genes. Values on the DEG and DEM line represent the correlation coefficients.

the combination of G5 and Si were the highest and that their regulatory effects were more diverse (Figure 6C).

To examine the relationship between the DEGs and DEMs in the G5- and/or Si-treated *G. uralensis* plants during drought stress, a co-expression network analysis of the DEGs and DEMs was conducted (Figure 6D). The co-expression networks of the DEGs and DEMs in the comparison between the D and CK treatments were found to be related to AsA metabolism and flavonoid biosynthesis. Interestingly, the co-expression networks of the DEGs and DEMs in the D+G5 *vs.* D treatment were only enriched in AsA metabolism, those in D+Si *vs.* D were only enriched in flavonoid biosynthesis, and the networks in D+G5+Si *vs.* D were mainly enriched in GSH metabolism and flavonoid biosynthesis. The results indicate that G5 and/or Si could modulate the co-expression of the DEGs and DEMs related to the biosynthesis of the major antioxidants in *G. uralensis* during drought stress, and the expression patterns were different depending on the application of G5 and/or Si. Notably, G5 combined with Si uniquely regulated the co-expression of the DEGs and DEMs related to GSH metabolism in *G. uralensis* under drought stress.

Discussion

G5 and/or Si reduced the oxidative stress markers in drought-stressed *G. uralensis* seedlings

Drought stress induced oxidative stress in plants caused by excessive ROS such as O_2^-, $^1O_2$, and H_2O_2 (Choudhury et al., 2017; Laxa et al., 2019), which impaired the membrane lipids,

proteins, and nucleic acids of plant cells and then correspondingly increased the level of MDA. Researchers have found that drought stress increased the contents of O_2^- and H_2O_2 in *G. uralensis* (Zhang et al., 2017), *Z. mays* L. (Li et al., 2021b), and *Glycine max* (Chen et al., 2021) and increased the concentrations of MDA in *Triticum aestivum* L. (Nasirzadeh et al., 2021) and *Pimpinella anisum* L. (Esim et al., 2021). Similarly, in the present study, the O_2^- and H_2O_2 production and the MDA concentration were significantly increased under drought stress in *G. uralensis*, indicating an oxidative burst and prompting cellular damage in plants due to water deficit (Figure 1A). Inversely, the production of O_2^- and H_2O_2 was significantly reduced by G5 and/or Si, which could alleviate oxidative damage, and a decline in the MDA level was then correspondingly observed. These results are similar to the effects of Si on *Solanum lycopersicum* L. (Shi et al., 2016) and *T. aestivum* L. (Ma et al., 2016) and of PGPB on *Lolium perenne* L. (He et al., 2021). It is worth noting that, compared to single treatment with G5 or Si, alleviation of the effects of ROS accumulation in *G. uralensis* seedlings was greater when G5 and Si were combined; the levels of MDA were evenly comparable to those of the control treatment, indicating that both G5 and Si have synergistic effects on the mitigation of oxidative stress in *G. uralensis* seedlings.

G5 and/or Si regulated the antioxidant enzyme system in drought-stressed *G. uralensis* seedlings

SOD, POD, and CAT are the main enzymes that scavenge ROS, and these antioxidant enzymes are found in various locations throughout plant cells and collaborate to detoxify ROS (Laxa et al., 2019). Drought stress altered the contents and the activities of the enzymes involved in ROS scavenging in different species (Ritonga et al., 2021; Meng et al., 2021). The present study showed that drought stress significantly decreased the activities of SOD and CAT in *G. uralensis*, indicating that drought stress remarkably inhibited the activity of some antioxidant enzymes; thus, the ROS generated by oxidative stress was not eradicated in time and led to its accumulation, resulting in cell damage. However, the activity of POD significantly increased under drought stress in *G. uralensis*; the reason behind this could be that the reduction in CAT activity was compensated by the increase in PODs, which can be used to scavenge the H_2O_2 under drought stress (Sarker and Oba, 2018a). Moreover, the transcriptomic analysis showed that drought stress upregulated one gene encoding SOD, which was not consistent with the trend of the enzyme activity, indicating that the gene might not be a key gene for the regulation of SOD activity in *G. uralensis* under drought stress (Figure 2B).

PGPB and/or Si play an important role in regulating the activities of antioxidant enzymes to mitigate the oxidative damage caused by drought stress (Rahimzadeh and Pirzad, 2017; Bukhari et al., 2021; Akhtar et al., 2021). Our research found that Si or G5 alone significantly increased the activity of CAT and that G5 combined with Si significantly increased the activities of SOD and CAT in *G. uralensis* seedlings under drought stress (Figure 2A), suggesting that the combination of G5 and Si had a unique regulatory effect that is different from the simple superposition of the effects of G5 and Si separately. Specifically, the combination of G5 and Si accelerated the dismutation of O_2^- into H_2O_2 by improving the SOD activity in *G. uralensis* seedlings under the drought condition; subsequently, the excess H_2O_2 can be directly decomposed by boosting the activity of CAT, thus could be maintained as free radicals at a lower level and finally alleviate lipid peroxidation damage of the cell membrane in *G. uralensis* seedlings under drought stress. Complementarily, the transcriptomic analysis showed that the combination of G5 and Si upregulated the expression of one gene encoding SOD and three genes encoding POD, while it downregulated the expression of one gene encoding SOD and six genes encoding POD in *G. uralensis* under drought stress, implying that the effects of G5 and/or Si on the SOD and POD activities at physiological levels may be the result of the integrated action of all genes and related to the function of different genes encoding the same enzyme.

G5 and/or Si accelerated the AsA–GSH cycle in drought-stressed *G. uralensis* seedlings

In addition to the antioxidant enzymes, the non-enzymatic components may also directly scavenge ROS. The AsA–GSH cycle is composed of AsA, GSH, and NADPH, which are continuously oxidized and reduced under the catalysis of several enzymes and maintain the integrity of the photosynthetic membranes under oxidative stress (Sarker and Oba, 2018b). Increases in the levels of GSH and AsA and the enzyme activities related to their biosynthesis and metabolism are strongly connected to the responses of plants to drought stress (Asthir et al., 2020).

In AsA metabolism, AsA synthesis is mainly affected by D-glucuronate, D-glucuronolactone, and L-galactose-1P. D-Glucuronateon the other hand, is synthesized from UDP-glucose or myoinositol. UDP-glucose can produce D-glucuronate through UDPase, UGDH, and GlcAK (Xiao et al., 2017), in which UDPase and UGDH catalyze UDP-glucose to the glucoronate-1P that was transformed to D-glucuronate by GlcAK, while myoinositol can produce to D-glucuronate with MIOX (Nepal et al., 2019). D-Glucuronolactone is converted from D-glucuronate or GDP-L-glucose. Moreover, D-glucuronolactone is generated by D-glucoronate under the catalysis of ALDH (Watanabe et al., 2007). Our results showed that drought stress increased the D-glucuronolactone content in

G. uralensis, which might be due to the upregulation of the genes encoding GME and ALDH (Figure 3). Interestingly, the combination of G5 and Si upregulated the genes encoding UDPase, UGDH, and ALDH and three genes encoding GlcAK in *G. uralensis* under drought stress, exhibiting that this treatment combination might relieve the AsA deficiency by promoting D-glucuronate accumulation in *G. uralensis* under drought stress. For the synthesis of L-galactose-1P, GME catalyzed the conversion of GDP-D-mannose to GDP-L-galactose in the D-mannose/L-galactose pathway (Ma et al., 2014a). GGP is known to catalyze GDP-L-galactose to L-galactose-1-P (Dowdle et al., 2007). In this study, drought stress upregulated the gene encoding GME, while the combination of G5 and Si downregulated the genes encoding GME and GGP in *G. uralensis* under drought stress (Table 3), suggesting that their combination mainly promoted the accumulation of AsA by increasing the synthesis of D-glucuronate instead of L-galactose-1P. In addition, with G5 application, the content of D-glucuronolactone was decreased, as shown in the metabolomic analysis of *G. uralensis* under drought stress, which might be due to the downregulation of the gene encoding GME. However, G5 promoted the accumulation of AsA in *G. uralensis* under drought stress, which might be due to the improved production of D-glucuronate with the upregulation of three genes encoding UDPase, two genes encoding GlcAK, and the gene encoding MIOX. On the contrary, Si had no significant effect on AsA content in *G. uralensis* under drought stress, which could be ascribed to the combined effects of the expression of the genes encoding the key enzymes GlcAK, MIOX, ALDH, GGP, APX, and AO.

Regarding GSH metabolism, previous studies have demonstrated that the enzyme GST utilizes GSH and has great potential in plant defense metabolism. Its mechanism helps to reduce the secondary noxious products caused by exposure to stress-induced ROS (Anderson and Davis, 2004). Additionally, the overexpression of GST improved drought tolerance in transgenic *Arabidopsis thaliana* (Xu et al., 2015). In this study, drought stress affected the scavenging ability of ROS in *G. uralensis* through the downregulation of six genes encoding GST. Interestingly, the combination of G5 and Si upregulated three genes but downregulated two genes encoding GST in *G. uralensis* under drought stress, indicating that their combination might reduce the secondary injury products of ROS in *G. uralensis* under drought stress by activating the expression of the GST genes. Among the factors regulating GSH accumulation, GGT catalyzes the transfer of a γ-glutamyl moiety of GSH, GSSG, and other c-glutamyl compounds to amino acids, small peptides, or water (Li et al., 2012; Gu et al., 2020). The transfer of a γ-glutamyl moiety is an important first step in GSH metabolism and recycling and is an essential factor in maintaining redox homeostasis in the cellular environment (Balakrishna and Prabhune., 2014). In the present study, the combination of G5 and Si upregulated the gene encoding GGT and increased the L-glutamate content in *G. uralensis* under drought stress (Table 2), which might be due to the promotion of GSH regeneration or proline synthesis from the substrate level (Jones et al., 2021), finally mitigating the cell damage in *G. uralensis* under drought stress.

Furthermore, the AsA–GSH cycle enzymes APX, GPX, AO, DHAR, MDHAR, and GR work together for the detoxification of ROS (Hamid et al., 2010). Previous studies have reported that drought enhanced the enzymatic activities of APX, DHAR, and GR in *Cajanus cajan* (Sreeharsha et al., 2019), but decreased the contents of AsA and GSH and the activities of MDHAR, DHAR, and GR in *Brassica napus* L. (Hasanuzzaman et al., 2018). Herein, drought stress decreased the AsA and GSH levels in *G. uralensis*. This may be the result of the increased APX activity that accelerated the reduction of AsA to monodehydroascorbic acid and the DHAR activity that is related to GSH regeneration, which could be attributed to the upregulation of two genes encoding APX and one gene encoding DHAR. Moreover, the decreased GSH content was attributed to the decreased GPX and GR activities and the downregulated GST genes (Figure 3). These results indicate that drought stress reduced the detoxifying co-substrate levels of enzymes such as PODs and GST, thus repressing the ROS scavenging capacity in *G. uralensis*. PGPB and/or Si could, by regulating the AsA–GSH cycle, alleviate the oxidative damage caused by drought stress (Fialová et al., 2018). Under drought stress, PGPB significantly enhanced the activities of APX and GPX in *Ocimum basilicum* L. (Kaushal and Wani, 2016), while Si upregulated the GR activity and increased the AsA content in wheat plants (Gong et al., 2005; Ma et al., 2016). In this study, G5 increased the AsA level by promoting D-glucuronate synthesis and the GSH level by increasing the GR activity, while Si increased the GSH content mainly by increasing the GR activity but decreasing the DHAR activity in *G. uralensis* under drought stress. Thus, the role of G5 or Si in alleviating oxidative stress was related to the increased AsA and GSH contents regulated by the activities of the enzymes related to the AsA–GSH cycle in *G. uralensis* under drought stress, with the specific type of substance and enzyme being different depending on the application of G5 or Si. Notably, G5 combined with Si upregulated three genes encoding GPX, as well as downregulated one gene encoding DHAR, which is consistent with the trend of enzyme activity change at the physiological level. Firstly, G5 combined with Si promoted AsA accumulation by increasing the synthesis of D-glucuronate and accelerated AsA conversion by upregulating the AO gene, enhancing the APX activity, and reducing the DHAR activity, thus providing more substrates for GSH synthesis. The combination of G5 and Si also further boosted the generation of GSH by increasing the GR and GPX activities and upregulating the GST and GGT genes. These results reflect that the combination of G5 and Si enhanced the entire AsA–GSH cycle to maintain its redox balance, which further eliminated the excess ROS that was not removed in time by SOD and CAT, finally resulting in reduced oxidative stress in

G. uralensis exposed to drought stress; correspondingly, a reduction in plasma membrane permeability was observed.

G5 and/or Si triggered carotenoid biosynthesis in drought-stressed *G. uralensis* seedlings

As the second line of defense against ROS, carotenoids, comprising some of the important non-enzymatic antioxidants, (Gowayed et al., 2017), play a key role in maintaining cell homeostasis and the antioxidant response in plants (Cicevan et al., 2016). Generally, carotenoids can prevent oxidative damage by scavenging $^1O_2$, stimulating chlorophyll (Chl*), quenching the triplet sensitizer (3Chl*), dissipating excess energy, and shielding the photosynthetic apparatus (Uarrota et al., 2018). Previous studies reported that the carotenoid contents were reduced in *B. napus*, *Melissa officinalis*, and *Daucus carota* under a water deficit condition (Bukhari et al., 2021; Eshaghi et al., 2022; Zhang et al., 2021b). In the present study, the total carotenoid content was significantly decreased in *G. uralensis* under drought stress (Figure 4A), which implied that drought could damage the photosynthetic system and promote carotenoid degradation. Interestingly, PGPB or Si acts as a modulator activating the accumulation of carotenoids in plants, thereby limiting the oxidative injury in various plants caused by drought stress (Yasmin et al., 2017; Khan et al., 2020b; Özdemir, 2021). In this study, G5 and/or Si remarkably increased the total carotenoid content in *G. uralensis* under drought stress, and this increased effect was greater in the combination treatment with G5 and Si than that in G5 or Si treatment alone (Figure 4A). It was illustrated that G5 and/or Si might prevent photosystem II overexcitation and regulate the energy dissipation and ROS homeostasis by promoting the accumulation of carotenoids, thus alleviating the oxidative stress caused by drought in *G. uralensis* (Uarrota et al., 2018).

Carotenoids are classified into carotenes and xanthophylls, which mainly include lycopene, α-carotene, β-carotene, lutein, zeaxanthin, violaxanthin, and neoxanthin. Regarding their capacity to scavenge ROS, lycopene, β-carotene, and zeaxanthin can directly reduce oxidative damage in plants (MacDonald et al., 2009; Moise et al., 2014). In the present study, Si or the combination of G5 and Si downregulated the expression of the gene encoding PSY, while the combination of G5 and Si upregulated the expression of the gene encoding Z-ISO in *G. uralensis* under drought stress (Figures 4B, C and Table 4), indicating that Si alone or its combination with G5 might inhibit phytoene synthesis at the substrate level by inhibiting the PSY activity resulting from the downregulation of the gene; however, the combination of G5 and Si promoted lycopene synthesis through upregulating the expression of the gene encoding Z-ISO, thus preserving the level of lycopene in *G. uralensis* under drought stress (Maass et al., 2009; Efremov et al., 2021). Moreover, the accumulation of lycopene induced by the combination of G5 and Si might further promote the synthesis of β-carotene in *G. uralensis* under drought stress because, apart from the ability to directly scavenge $^1O_2$, lycopene is a mainly biochemical precursor for the synthesis of α-carotene and β-carotene (Klunklin and Savage, 2017). In addition, the components of the xanthophyll cycle pool play a function in photoprotection and excess energy dissipation, thereby protecting membranes from oxidative damage (Li et al., 2021a). Herein, Si or the combination of G5 and Si downregulated the expression of the gene encoding CHXB and ZEP that is closely related to β-carotene conversion to xanthophylls (Figures 4B, C and Table 4), illustrating that Si alone or its combined application with G5 might depress the transformation of β-carotene to zeaxanthin and violaxanthin in *G. uralensis*. As a result, the combination of G5 and Si might play a specific role in photosynthetic protection and energy dissipation in drought-stressed *G. uralensis* mainly by promoting the accumulation of lycopene and β-carotene instead of xanthophyll, which coordinated with SOD, CAT, and the AsA–GSH cycle to reduce the oxidative damage in *G. uralensis* induced by drought stress.

G5 and/or Si activated flavonoid biosynthesis in drought-stressed *G. uralensis* seedlings

Flavonoids, as important plant secondary metabolites that protect plants from drought conditions, are powerful ROS scavengers (Farooq et al., 2021). Generally, they can prevent the generation of ROS in plants through chelating metal ions and inhibiting ROS-producing enzymes such as xanthine oxidase and lipoxygenase (Ferdinando et al., 2012; Sarker and Oba, 2018b), thereby helping to maintain ROS homeostasis and membrane stability and reducing oxidative damage (Ozfidan-Konakci et al., 2020). The flavonoid content was increased by drought stress in wheat (Ma et al., 2014b), but was decreased in *Glycyrrhiza glabra* and *G. uralensis* (Xie et al., 2019; Khaitov et al., 2021). Similarly, drought stress also significantly decreased the total flavonoid content in *G. uralensis* seedlings in the present study, suggesting that the change in the trend of flavonoid content vary according to the plant species or the stress level. Moreover, PGPB inoculation or Si application could reduce the oxidative damage to plants caused by abiotic stresses by stimulating the accumulation of flavonoids (Ma et al., 2016; Chattha et al., 2017). In the present study, G5 or the combination of G5 and Si remarkably increased the total flavonoid content in *G. uralensis* seedlings under drought stress, and this increased effect was greater in the combined G5 and Si treatment than in the G5 treatment alone (Figure 5A). These findings suggest that G5 alone or its combination with Si can prevent ROS generation by improving flavonoid

accumulation, which could be attributed to the chelation of metal ions and the inhibition of ROS-producing enzymes. Further studies are needed to verify the reasons.

Flavonoid biosynthesis plays a key role in the development of plant tolerance to drought stress (Hahlbrock and Scheel, 1989; Giordano et al., 2016). In this study, the transcriptomic analysis (Figures 5B, C and Table 5) revealed that drought downregulated the expression of the PAL and HCT genes, but upregulated the expression of the HCT gene in *G. uralensis*, which might have inhibited the transformation of phenylalanine into the key intermediates of flavonoid synthesis in *G. uralensis*. Interestingly, the application of G5 in drought-stressed *G. uralensis* upregulated the gene encoding PAL, but downregulated the genes encoding 4CL and HCT; conversely, Si application upregulated the genes encoding PAL and HCT. These results suggest that G5 might help in the accumulation of cinnamic acid and *p*-coumaroyl-CoA, while Si might enhance the synthesis of caffeoyl-CoA, the downstream metabolite of *p*-coumaroyl-CoA, in drought-stressed *G. uralensis*.

Previous studies have revealed that the genes encoding PAL, HCT, and C4H play important roles in modulating flavonoid biosynthesis in the resistance to oxidative stress in plants (Khakdan et al., 2018). In the present study, the combination of G5 and Si upregulated the genes associated with the synthesis of *p*-coumaroyl-CoA, including PAL, 4CL, and C4H, but downregulated the genes involved in the conversion of *p*-coumaroyl-CoA, such as HCT, CYP98A2, and CCOMT, in drought-stressed *G. uralensis*, indicating that this combination treatment could affect the accumulation of *p*-coumaroyl-CoA by regulating the genes related to its synthesis and transformation, correspondingly affecting the carbon flux distribution and finally enhancing flavonoid biosynthesis in drought-stressed *G. uralensis* (Gallego-Giraldo et al., 2014; Yang et al., 2021).

p-Coumaroyl-CoA, a key intermediate in the flavonoid biosynthesis pathway, provides the C6–C3–C6 carbon skeleton to the flavonoid compounds (Yu et al., 2021). After the production of *p*-coumaroyl-CoA, the biosynthetic pathway of flavonoids begins to branch under the activity of CHS, CHR, and CHI (Wang et al., 2015). In the present study, under drought stress, the genes encoding CHS and CHI were downregulated in *G. uralensis*, which could inhibit the activities of CHS and CHI and further inhibit the conversion of *p*-coumaroyl-CoA to its downstream metabolites. Interestingly, in drought-stressed *G. uralensis*, the genes encoding CHS, CHR, and CHI were upregulated by G5 or Si alone, while those encoding CHS and CHR were upregulated by the combination of G5 and Si. These results indicate that G5 and/or Si might accelerate the synthesis of naringenin and liquiritigenin by upregulating the CHS and CHR genes, thus providing sufficient substrate for subsequent antioxidant derivatives (Kim et al., 2004).

As the downstream metabolite of naringenin, kaempferol and quercetin have a significant influence on the scavenging ROS and the detoxification of free radicals, which strengthen tolerance to environmental changes (Tattini et al., 2005; Belinha et al., 2007). In the present study, the expression of the genes encoding F3′,5′H and CYP75B were downregulated in *G. uralensis* by drought stress, which might affect the conversion of kaempferol into quercetin (Wu et al., 2022b). However, the content of 3-*O*-methylquercetin, a derivative of quercetin, was enhanced by G5 application. The expression of the genes encoding F3′,5′H and CYP75B were upregulated by Si, which might accelerate the synthesis of quercetin in *G. uralensis*. These results indicate that G5 or Si might alleviate oxidative stress by increasing the contents of 3-*O*-methylquercetin and quercetin in drought-stressed *G. uralensis*. Notably, in drought-stressed *G. uralensis*, the expression of the genes encoding FLS and CYP75B were downregulated by the combined application of G5 and Si, which could help in the accumulation of kaempferol by inhibiting its degradation, triggering the second stage of the antioxidant system, thus enhancing the tolerance of *G. uralensis* to oxidative stresses induced by drought stress (Ma et al., 2020).

In addition, according to the metabolomic analysis in this study, the downstream metabolites of daidzein, medicarpin, glycitin, and astragalin have different response patterns to drought stress and to G5 and/or Si application (Figure 5B and Table 6). These flavonoids may be the key to alleviating the oxidative stress caused by drought; however, at present, there are only a few reports on these flavonoids alleviating oxidative stress in plants, and most of the research has been focused on animals (Miriama et al., 2019; Tomar et al., 2020; Wang et al., 2022). Whether they participate in the alleviation of plant oxidative stress needs to be clarified in future research.

Conclusion

G5 and/or Si have beneficial effects on the antioxidant system of *G. uralensis* seedlings under drought stress, especially their combined application. Through transcriptional and physiological regulation, the combination of G5 and Si increased the activities of SOD and CAT, enhanced the entire AsA–GSH cycle, and triggered the accumulation of the major antioxidant carotenoids and flavonoids in *G. uralensis* exposed to drought stress. This might have contributed to maintaining redox balance by increasing the levels of AsA and GSH and the activities of the key enzymes, including SOD, CAT, APX, GPX, and GR, and upregulating the expression levels of the related genes such as GPX, AO, and GST, in addition to protecting the photosynthetic activity and dissipating excess energy through facilitating the accumulation of total carotenoids and total flavonoids by modulating the key genes related to their biosynthesis processes, thus protecting *G. uralensis* seedlings from membrane lipid peroxidation induced by drought stress. Our findings not only contribute to an in-depth understanding

of the role of the combined application of G5 and Si in *G. uralensis* under drought stress based on our previous studies but also provide new insights into the comparative and synergistic roles of PGPB and Si in the antioxidant system of plants exposed to drought conditions.

Data availability statement

The data presented in the study are deposited in Sequence Read Archive (SRA) database at NCBI (SRA BioProject PRJNA885037).

Author contributions

XZ designed the experiment, performed and supervised the project, and edited and reviewed the manuscript. XM wrote the manuscript, analyzed the data, and performed the experiments. ZX, DL, LZ, and WZ performed the experiments. All authors contributed to the article and approved the submitted version.

Funding

This work received financial support provided by the project of the National Natural Science Foundation of China (82160724) and the Ningxia Natural Science Foundation (2022AAC02037).

Conflict of interest

The authors declare that the research was conducted in the absence of any commercial or financial relationships that could be construed as a potential conflict of interest.

Publisher's note

All claims expressed in this article are solely those of the authors and do not necessarily represent those of their affiliated organizations, or those of the publisher, the editors and the reviewers. Any product that may be evaluated in this article, or claim that may be made by its manufacturer, is not guaranteed or endorsed by the publisher.

Supplementary material

The Supplementary Material for this article can be found online at: https://www.frontiersin.org/articles/10.3389/fpls.2022.1033915/full#supplementary-material

SUPPLEMENTARY FIGURE

Bio-compatibility interaction of G5 and Si. The G5 (200 µL) was uniformly coated on the plate, and a hole with a radius of 0.5 mm was punched using a sterile punch, and 200 µL of Si (2 mM K_2SiO_3) was injected into NA plates for bio-compatibility interaction testing at 28°C. Finally, based on the existence or absence of a bacteriostatic band during 24 to 48 hours, it is determined whether the two can be used in combination.

References

Ahanger, M. A., and Agarwal, R. M. (2017). Salinity stress induced alterations in antioxidant metabolism and nitrogen assimilation in wheat (*Triticum aestivum* l.) as influenced by potassium supplementation. *Plant Physiol. Bioch* 115, 449–460.

Akhtar, N., Ilyas, N., Mashwani, Z. U., Hayat, R., Yasmin, H., Noureldeen, A., et al. (2021). Synergistic effects of plant growth promoting rhizobacteria and silicon dioxide nano-particles for amelioration of drought stress in wheat. *Plant Physiol. Bioch* 166, 160–176.

Anderson, J. V., and Davis, D. G. (2004). Abiotic stress alters transcript profiles and activity of glutathione s-transferase, glutathione peroxidase, and glutathione reductase in *Euphorbia esula*. *Physiol. Plant* 120 (3), 421–433.

Asthir, B., Kaur, G., and Kaur, B. (2020). Convergence of pathways towards ascorbate-glutathione for stress mitigation. *J. Plant Biol.* 63 (4), 243–257.

Balakrishna, S., and Prabhune, A. A. (2014). Gamma-glutamyl transferases: a structural, mechanistic and physiological perspective. *Front. Biosci.* 9 (1), 51–65.

Belinha, I., Amorim, M. A., Rodrigues, P., de Freitas, V., Moradas-Ferreira, P., Mateus, N., et al. (2007). Quercetin increases oxidative stress resistance and longevity in *Saccharomyces cerevisiae*. *J. Agr Food Chem.* 55 (6), 2446–2451.

Biju, S., Fuentes, S., and Gupta, D. (2017). Silicon improves seed germination and alleviates drought stress in lentil crops by regulating osmolytes, hydrolytic enzymes and antioxidant defense system. *Plant Physiol. Bioch* 119, 250–264.

Bi, Q., Yao, H., Wang, F., He, D., Xu, W., Xie, S., et al. (2022). Integrative analysis of the pharmaceutical active ingredient and transcriptome of the aerial parts of glycyrrhiza uralensis under salt stress reveals liquiritin accumulation *via* ABA-mediated signaling. *Mol. Genet. Genomics* 297 (2), 333–343.

Bukhari, M. A., Sharif, M. S., Ahmad, Z., Barutcular, C., Afzal, M., Hossain, A., et al. (2021). Silicon mitigates the adverse effect of drought in canola (*Brassica napus* l.) through promoting the physiological and antioxidants activity. *Silicon* 13 (11), 3817–3826.

Cakmak, I., Strbac, D., and Marschner, H. (1993). Activities of hydrogen peroxide-scavenging enzymes in germinating wheat seeds. *J. Exp. Bot.* 44 (1), 127–132.

Cao, B. L., Ma, Q., and Xu, K. (2020). Silicon restrains drought-induced ROS accumulation by promoting energy dissipation in leaves of tomato. *Protoplasma* 257 (2), 537–547.

Carter, K. R., and Dickman, L. T. (2022). Recovery of seedling carbon balance despite hydraulic impairment following hot drought. *Tree Physiol.* 42 (8), 1527–1531.

Chattha, M. B., Iqbal, A., Chattha, M. U., Hassan, M. U., Khan, I., Ashraf, I., et al. (2017). PGPR inoculated-seed increases the productivity of forage sorghum under fertilized conditions. *Aust. J. Basic Appl. Sci.* 13, 150–153.

Chen, Z. F., Ru, J. N., Sun, G. Z., Du, Y., Chen, J., Zhou, Y. B., et al. (2021). Genomic-wide analysis of the PLC family and detection of GmPI-PLC7 responses to drought and salt stresses in soybean. *Front. Plant Sci.* 325.

Choudhury, F. K., Rivero, R. M., Blumwald, E., and Mittler, R. (2017). Reactive oxygen species, abiotic stress and stress combination. *Plant J.* 90 (5), 856–867.

Cicevan, R., Al Hassan, M., Sestras, A. F., Prohens, J., Vicente, O., Sestras, R. E., et al. (2016). Screening for drought tolerance in cultivars of the ornamental genus tagetes (Asteraceae). *PeerJ* 4, e2133.

Coskun, D., Deshmukh, R., Sonah, H., Menzies, J. G., Reynolds, O., Ma, J. F., et al. (2019). The controversies of silicon's role in plant biology. *New Phytol.* 221 (1), 67–85.

Cui, G., Xiao, X., Zhang, W., Lang, D., Li, Z., and Zhang, X. (2021). Exogenous silicon relieve drought stress and salt stress of glycyrrhiza uralensis seedlings by

regulating proline metabolism and nitrogen assimilation. *J. Hortic. Sci. Biotech.* 96 (6), 728–737.

Dang, H., Zhang, T., Li, Y., Li, G., Zhuang, L., and Pu, X. (2021). Population evolution, genetic diversity and structure of the medicinal legume, *Glycyrrhiza uralensis* and the effects of geographical distribution on leaves nutrient elements and photosynthesis. *Front. Plant Sci.* 12.

Das, K., and Roychoudhury, A. (2014). Reactive oxygen species (ROS) and response of antioxidants as ROS-scavengers during environmental stress in plants. *Front. Environ. Sci.* 2, e53.

Dowdle, J., Ishikawa, T., Gatzek, S., Rolinski, S., and Smirnoff, N. (2007). Two genes in arabidopsis thaliana encoding GDP-l-galactose phosphorylase are required for ascorbate biosynthesis and seedling viability. *Plant J.* 52 (4), 673–689.

Efremov, G. I., Shchennikova, A. V., and Kochieva, E. Z. (2021). Characterization of 15-cis-ζ-Carotene isomerase z-ISO in cultivated and wild tomato species differing in ripe fruit pigmentation. *Plants* 10 (11), 2365.

Eshaghi Gorgi, O., Fallah, H., Niknejad, Y., and Barari Tari, D. (2022). Effect of plant growth promoting rhizobacteria (PGPR) and mycorrhizal fungi inoculations on essential oil in Melissa officinalis l. under drought stress. *Biologia* 77 (1), 11–20.

Esim, N., and Günes, H.. (2021). Effects of Drought and Salinity on Antioxidant Mechanisms and Secondary Metabolites in Anise (Pimpinella anisum L.) Leaves. *Russ. J. Plant Physl.* 68 (4), 708–717.

Farooq, M., Ahmad, R., Shahzad, M., Sajjad, Y., Hassan, A., Shah, M. M., et al. (2021). Differential variations in total flavonoid content and antioxidant enzymes activities in pea under different salt and drought stresses. *Sci. Hortic.* 287, 110258.

Fatemi, H., Pour, B. E., and Rizwan, M. (2020). Isolation and characterization of lead (Pb) resistant microbes and their combined use with silicon nanoparticles improved the growth, photosynthesis and antioxidant capacity of coriander (*Coriandrum sativum* l.) under Pb stress. *Environ. pollut.* 266, 114982.

Ferdinando, M. D., Brunetti, C., Fini, A., and Tattini, M. (2012). Flavonoids as antioxidants in plants under abiotic stresses. *Abiotic Stress responses Plants*, 159–179.

Fialová, I., Šimková, L., Vaculíková, M., and Luxová, M. (2018). Effect of Si on the antioxidative defense of young maize roots under NaCl stress. *Silicon* 10 (6), 2911–2914.

Gallego-Giraldo, L., Bhattarai, K., Pislariu, C. I., Nakashima, J., Jikumaru, Y., Kamiya, Y., et al. (2014). Lignin modification leads to increased nodule numbers in alfalfa. *Plant Physiol.* 164 (3), 1139–1150.

Giordano, D., Provenzano, S., Ferrandino, A., Vitali, M., Pagliarani, C., Roman, F., et al. (2016). Characterization of a multifunctional caffeoyl-CoA O-methyltransferase activated in grape berries upon drought stress. *Plant Physiol. Bioch* 101, 23–32.

Gong, H., Zhu, X., Chen, K., Wang, S., and Zhang, C. (2005). Silicon alleviates oxidative damage of wheat plants in pots under drought. *Plant Sci.* 169 (2), 313–321.

Gowayed, M. H., Al-Zahrani, H. S., and Metwali, E. M. (2017). Improving the salinity tolerance in potato (*Solanum tuberosum*) by exogenous application of silicon dioxide nanoparticles. *Int. J. Agric. Biol.* 19 (1), 183–194.

Gusain, Y. S., Singh, U. S., and Sharma, A. K. (2015). Bacterial mediated amelioration of drought stress in drought tolerant and susceptible cultivars of rice (*Oryza sativa* l.). *Afr J. Biotechnol.* 14 (9), 764–773.

Gu, H., Wang, Y., Xie, H., Qiu, C., Zhang, S., Xiao, J., et al. (2020). Drought stress triggers proteomic changes involving lignin, flavonoids and fatty acids in tea plants. *Sci. Rep.* 10 (1), 1–11.

Hahlbrock, K., and Scheel, D. (1989). Physiology and molecular biology of phenylpropanoid metabolism. *Annu. Rev. Plant Physiol. Plant Mol. Biol.* 40 (1), 347–369.

Hamid, A. A., Aiyelaagbe, O. O., Usman, L. A., Ameen, O. M., and Lawal, A. (2010). Antioxidants: Its medicinal and pharmacological applications. *Afr J. Pure Appl. Chem.* 4 (8), 142–151.

Hasanuzzaman, M., Hossain, M. A., and Fujita, M. (2011). Nitric oxide modulates antioxidant defense and the methylglyoxal detoxification system and reduces salinity-induced damage of wheat seedlings. *Plant Biotechnol. Rep.* 5 (4), 353–365.

Hasanuzzaman, M., Nahar, K., Anee, T. I., and Fujita, M. (2017). Glutathione in plants: biosynthesis and physiological role in environmental stress tolerance. *Physiol. Mol. Biol. pla* 23, 249–268.

Hasanuzzaman, M., Nahar, K., Anee, T. I., Khan, M. I. R., and Fujita, M. (2018). Silicon-mediated regulation of antioxidant defense and glyoxalase systems confers drought stress tolerance in *Brassica napus* l. *S Afr J. Bot.* 115, 50–57.

He, A., Niu, S., Yang, D., Ren, W., Zhao, L., Sun, Y., et al. (2021). Two PGPR strains from the rhizosphere of haloxylon ammodendron promoted growth and enhanced drought tolerance of ryegrass. *Plant Physiol. Biochem.* 161, 74–85.

He, Y., Wu, Z., Wang, W., Ye, B. C., Zhang, F., and Liu, X. (2019). Different responses of *Capsicum annuum* l. root and shoot to salt stress with pseudomonas putida rs-198 inoculation. *J. Plant Growth Regul.* 38 (3), 799–811.

Hodges, D. M., Andrews, C. J., Johnson, D. A., and Hamilton, R. I. (1997). Antioxidant enzyme responses to chilling stress in differentially sensitive inbred maize lines. *J. Exp. Bot.* 48 (5), 1105–1113.

Hossain, M. A., Nakano, Y., and Asada, K. (1984). Monodehydroascorbate reductase in spinach chloroplasts and its participation in regeneration of ascorbate for scavenging hydrogen peroxide. *Plant Cell Physiol.* 25 (3), 385–395.

Huchzermeyer, B., Menghani, E., Khardia, P., and Shilu, A. (2022). Metabolic pathway of natural antioxidants, antioxidant enzymes and ROS providence. *Antioxidants* 11 (4), 761.

Ilangumaran, G., and Smith, D. L. (2017). Plant growth promoting rhizobacteria in amelioration of salinity stress: A systems biology perspective. *Front. Plant Sci.* 8.

Jan, S., Abbas, N., Ashraf, M., and Ahmad, P. (2019). Roles of potential plant hormones and transcription factors in controlling leaf senescence and drought tolerance. *Protoplasma* 256, 313–329.

Jones, B., Balasubramaniam, M., Lebowitz, J. J., Taylor, A., Villalta, F., Khoshbouei, H., et al. (2021). Activation of proline biosynthesis is critical to maintain glutamate homeostasis during acute methamphetamine exposure. *Sci. Rep.* 11 (1), 1–16.

Kabiraj, A., and Majhi, K. (2020). "Role of plant growth-promoting rhizobacteria (PGPR) for crop stress management," in *Sustainable agriculture in the era of climate change*. (Springer: Cham, Switzerland), 367–389.

Kaloterakis, N., van Delden, S. H., Hartley, S., and De Deyn, G. B. (2021). Silicon application and plant growth promoting rhizobacteria consisting of six pure bacillus species alleviate salinity stress in cucumber (*Cucumis sativus* l). *Sci. Hortic.* 288, 110383.

Kartik, V. P., Jinal, H. N., and Amaresan, N. (2021). Inoculation of cucumber (*Cucumis sativus* l.) seedlings with salt-tolerant plant growth promoting bacteria improves nutrient uptake, plant attributes and physiological profiles. *J. Plant Growth Regul.* 40 (4), 1728–1740.

Kaushal, M., and Wani, S. P. (2016). Plant-growth-promoting rhizobacteria: drought stress alleviators to ameliorate crop production in drylands. *Ann. Microbiol.* 66 (1), 35–42.

Khaitov, B., Urmonova, M., Karimov, A., Sulaymonov, B., Allanov, K., Israilov, I., et al. (2021). Licorice (*Glycyrrhiza glabra*)-growth and phytochemical compound secretion in degraded lands under drought stress. *Sustainability* 13 (5), 1–11.

Khakdan, F., Alizadeh, H., and Ranjbar, M. (2018). Molecular cloning, functional characterization and expression of a drought inducible phenylalanine ammonia-lyase gene (ObPAL) from *Ocimum basilicum* l. *Plant Physio. Biochem.* 130, 464–472.

Khan, M. N., Alsolami, M. A., Basahi, R. A., Siddiqui, M. H., and Khan, F. (2020a). Nitric oxide is involved in nano-titanium dioxide-induced activation of antioxidant defense system and accumulation of osmolytes under water-deficit stress in *Vicia faba* l. *Ecotoxicol. Environ. Saf.* 190, 110152.

Khan, N., Bano, A., and Curá, J. A. (2020b). Role of beneficial microorganisms and salicylic acid in improving rainfed agriculture and future food safety. *Microorganisms* 8 (7), 1018.

Khattab, H. I., Emam, M. A., Emam, M. M., Helal, N. M., and Mohamed, M. R. (2014). Effect of selenium and silicon on transcription factors NAC5 and DREB2A involved in drought-responsive gene expression in rice. *Biol. Plantarum* 58 (2), 265–273.

Kim, S., Jones, R., Yoo, K. S., and Pike, L. M. (2004). Gold color in onions (*Allium cepa*): a natural mutation of the chalcone isomerase gene resulting in a premature stop codon. *Mol. Genet. Genomics* 272 (4), 411–419.

Klunklin, W., and Savage, G. (2017). Effect on quality characteristics of tomatoes grown under well-watered and drought stress conditions. *Foods* 6 (8), 56.

Laxa, M., Liebthal, M., Telman, W., Chibani, K., and Dietz, K. J. (2019). The role of the plant antioxidant system in drought tolerance. *Antioxidants* 8 (4), 94.

Li, M., Liang, X., and Rollins, J. A. (2012). Sclerotinia sclerotiorum γ-glutamyl transpeptidase (Ss-Ggt1) is required for regulating glutathione accumulation and development of sclerotia and compound appressoria. *Mol. Plant Microbe Interact.* 25 (3), 412–420.

Li, T., Liu, J. X., Deng, Y. J., Xu, Z. S., and Xiong, A. S. (2021a). Overexpression of a carrot BCH gene, DcBCH1, improves tolerance to drought in arabidopsis thaliana. *BMC Plant Biol.* 21 (1), 1–13.

Li, Z., Su, X., Chen, Y., Fan, X., He, L., Guo, J., et al. (2021b). Melatonin improves drought resistance in maize seedlings by enhancing the antioxidant system and regulating abscisic acid metabolism to maintain stomatal opening under PEG-induced drought. *J. Plant Biol.* 64 (4), 299–312.

Liu, Y., Li, D., Gao, H., Li, Y., Chen, W., Jiao, S., et al. (2022). Regulation of soil micro-foodwebs to root secondary metabolites in cultivated and wild licorice plants. *Sci. Total Environ.* 828, 154302.

Li, G., Xu, D., Huang, G., Bi, Q., Yang, M., Shen, H., et al. (2022). Analysis of whole-transcriptome RNA-seq data reveals the involvement of alternative splicing in the drought response of glycyrrhiza uralensis. *Front. Genet.* 13.

Lichtenthaler, H. K. (1987). Chlorophylls and carotenoids: pigments of photosynthetic biomembranes. In *Methods in enzymology* 148, 350–382.

Lopez-Delacalle, M., Silva, C. J., Mestre, T. C., Martinez, V., Blanco-Ulate, B., and Rivero, R. M. (2021). Synchronization of proline, ascorbate and oxidative stress pathways under the combination of salinity and heat in tomato plants. *Environ. Exp. Bot.* 183, 104351.

Maass, D., Arango, J., Wust, F., Beyer, P., and Welsch, R. (2009). Carotenoid crystal formation in arabidopsis and carrot roots caused by increased phytoene synthase protein levels. *PloS One* 4 (7), e6373.

MacDonald, M. T., Lada, R. R., Robinson, A. R., and Hoyle, J. (2009). Seed preconditioning with natural and synthetic antioxidants induces drought tolerance in tomato seedlings. *Hort Sci.* 44 (5), 1323–1329.

Mahmood, S., Daur, I., Al-Solaimani, S. G., Ahmad, S., Madkour, M. H., Yasir, M., et al. (2016). Plant growth promoting rhizobacteria and silicon synergistically enhance salinity tolerance of mung bean. *Front. Plant Sci.* 7, 876.

Mahmood, S., Daur, I., Hussain, M. B., Nazir, Q., Al-Solaimani, S. G., Ahmad, S., et al. (2017). Silicon application and rhizobacterial inoculation regulate mung bean response to saline water irrigation. *Clean-Soil Air Water* 45 (8), 1600436.

Ma, D., Sun, D., Wang, C., Li, Y., and Guo, T. (2014b). Expression of flavonoid biosynthesis genes and accumulation of flavonoid in wheat leaves in response to drought stress. *Plant Physiol. Biochem.* 80, 60–66.

Ma, D., Sun, D., Wang, C., Qin, H., Ding, H., Li, Y., et al. (2016). Silicon application alleviates drought stress in wheat through transcriptional regulation of multiple antioxidant defense pathways. *J. Plant Growth Regul.* 35 (1), 1–10.

Ma, L., Wang, Y., Liu, W., and Liu, Z. (2014a). Overexpression of an alfalfa GDP-mannose 3, 5-epimerase gene enhances acid, drought and salt tolerance in transgenic arabidopsis by increasing ascorbate accumulation. *Biotechnol. Lett.* 36 (11), 2331–2341.

Ma, S., Lv, L., Meng, C., Zhang, C., and Li, Y. (2020). Integrative analysis of the metabolome and transcriptome of sorghum bicolor reveals dynamic changes in flavonoids accumulation under saline -alkali stress. *J Agr Food Chem* 68 (50), 14781–14789.

Meng, Y. C., Zhang, H. F., Pan, X. X., Chen, N., Hu, H. F., Haq, S. U., et al. (2021). CaDHN3, a pepper (*Capsicum annuum* l.) dehydrin gene enhances the tolerance against salt and drought stresses by reducing ROS accumulation. *Int. J. Mol. Sci.* 22 (6), 3205.

Miriama, S, Saleh, H., Alwasel, I, Alhazza, M., and Klaudia, J. (2019). Management of oxidative stress and other pathologies in alzheimer's disease. *Arch. Toxicol.* 93 (9), 2491–2513.

Mishra, R. K., Mishra, G., Singh, R., Parihar, P., Kumar, J., Srivastava, P. K., et al. (2022). Managing arsenic (V) toxicity by phosphate supplementation in rice seedlings: modulations in AsA-GSH cycle and other antioxidant enzymes. *Environ. Sci. pollut. R* 29 (10), 14418–14429.

Mittler, R. (2017). ROS are good. *Trends Plant Sci.* 22 (1), 11–19.

Moise, A. R., Al-Babili, S., and Wurtzel, E. T. (2014). Mechanistic aspects of carotenoid biosynthesis. *Chem. Rev.* 114 (1), 164–193.

Nakano, Y., and Asada, K. (1981). Hydrogen peroxide is scavenged by ascorbate-specific peroxidase in spinach chloroplasts. *Plant Cell Physiol.* 22 (5), 867–880.

Nasirzadeh, L., Sorkhilaleloo, B., Majidi Hervan, E., and Fatehi, F. (2021). Changes in antioxidant enzyme activities and gene expression profiles under drought stress in tolerant, intermediate, and susceptible wheat genotypes. *Cereal Res. Commu.* 49 (1), 83–89.

Nepal, N., Yactayo-Chang, J. P., Medina-Jiménez, K., Acosta-Gamboa, L. M., González-Romero, M. E., Arteaga-Vázquez, M. A., et al. (2019). Mechanisms underlying the enhanced biomass and abiotic stress tolerance phenotype of an arabidopsis MIOX over-expresser. *Plant direct* 3 (9), e00165.

Nguyen, Y. T. H., Hoang, H. T. T., Mai, A. T. H., Nguyen, L. T. N., Nguyen, Q. H., Pham, N. T. T., et al. (2021). The aconitum carmichaelii F3′5′H gene overexpression increases flavonoid accumulation in transgenic tobacco plants. *Hortic* 7 (10), 384.

Ozdemir, E. (2021). Silicon stimulated bioactive and physiological metabolisms of purple corn (*Zea mays indentata* l.) under deficit and well-watered conditions. *3 Biotech.* 11 (7), 1–13.

Ozfidan-Konakci, C., Yildiztugay, E., Alp, F. N., Kucukoduk, M., and Turkan, I. (2020). Naringenin induces tolerance to salt/osmotic stress through the regulation of nitrogen metabolism, cellular redox and ROS scavenging capacity in bean plants. *Plant Physiol. Biochem.* 157, 264–275.

Pan, Y., Wu, L. J., and Yu, Z. L. (2006). Effect of salt and drought stress on antioxidant enzymes activities and SOD isoenzymes of liquorice (*Glycyrrhiza uralensis* fisch). *Plant Growth Regul.* 49 (2), 157–165.

Pathania, P., Rajta, A., Singh, P. C., and Bhatia, R. (2020). Role of plant growth-promoting bacteria in sustainable agriculture. *Biocatal Agric. Biotechnol.* 30, 101842.

Qi, J., Song, C. P., Wang, B., Zhou, J., Kangasjärvi, J., Zhu, J. K., et al. (2018). Reactive oxygen species signaling and stomatal movement in plant responses to drought stress and pathogen attack. *J. Integr. Plant Biol.* 60 (9), 805–826.

Rahimzadeh, S., and Pirzad, A. (2017). Arbuscular mycorrhizal fungi and pseudomonas in reduce drought stress damage in flax (*Linum usitatissimum* l.): a field study. *Mycorrhiza* 27 (6), 537–552.

Rane, J., Singh, A. K., Tiwari, M., Prasad, P., and Jagadish, S. (2022). Effective use of water in crop plants in dryland agriculture: implications of reactive oxygen species and antioxidative system. *Front. Plant Sci.* 12, 778270.

Ritonga, F. N., Ngatia, J. N., Song, R. X., Farooq, U., Somadona, S., Lestari, A. T., et al. (2021). Abiotic stresses induced physiological, biochemical, and molecular changes in betula platyphylla: a review. *Silva Fenn.* 55, 24.

Sarker, U., and Oba, S. (2018a). Catalase, superoxide dismutase and ascorbate-glutathione cycle enzymes confer drought tolerance of amaranthus tricolor. *Sci. Rep.* 8 (1), 1–12.

Sarker, U., and Oba, S. (2018b). Drought stress effects on growth, ROS markers, compatible solutes, phenolics, flavonoids, and antioxidant activity in amaranthus tricolor. *Appl. Biochem. Biotechnol.* 186 (4), 999–1016.

Sattar, A., Sher, A., Ijaz, M., Ul-Allah, S., Butt, M., Irfan, M., et al. (2020). Interactive effect of biochar and silicon on improving morpho-physiological and biochemical attributes of maize by reducing drought hazards. *J. Soil Sci. Plant Nut* 20 (4), 1819–1826.

Shi, Y., Zhang, Y., Han, W., Feng, R., Hu, Y., Guo, J., et al. (2016). Silicon enhances water stress tolerance by improving root hydraulic conductance in solanum lycopersicum l. *Front. Plant Sci.* 7, 196.

Siddiqui, M. H., Alamri, S., Alsubaie, Q. D., and Ali, H. M. (2020). Melatonin and gibberellic acid promote growth and chlorophyll biosynthesis by regulating antioxidant and methylglyoxal detoxification system in tomato seedlings under salinity. *J. Plant Growth Regul.* 39 (4), 1488–1502.

Souri, Z., Khanna, K., Karimi, N., and Ahmad, P. (2021). Silicon and plants: current knowledge and future prospects. *J. Plant Growth Regul.* 40 (3), 906–925.

Sreeharsha, R. V., Mudalkar, S., Sengupta, D., Unnikrishnan, D. K., and Reddy, A. R. (2019). Mitigation of drought-induced oxidative damage by enhanced carbon assimilation and an efficient antioxidative metabolism under high CO_2 environment in pigeonpea (*Cajanus cajan* l.). *Photosynth. Res.* 139 (1), 425–439.

Tattini, M., Guidi, L., Morassi-Bonzi, L., Pinelli, P., Remorini, D., Degl'Innocenti, E., et al. (2005). On the role of flavonoids in the integrated mechanisms of response of ligustrum vulgare and phillyrea latifolia to high solar radiation. *New Phytol.* 167 (2), 457–470.

Tomar, A., Kaushik, S., Khan, S. I., Bisht, K., Nag, T. C., Arya, D. S., et al. (2020). The dietary isoflavone daidzein mitigates oxidative stress, apoptosis, and inflammation in CDDP-induced kidney injury in rats: Impact of the MAPK signaling pathway. *J. Biochem. Mol. Toxicol.* 34 (2), e22431.

Uarrota, V. G., Stefen, D. L. V., Leolato, L. S., Gindri, D. M., and Nerling, D. (2018). "Revisiting carotenoids and their role in plant stress responses: from biosynthesis to plant signaling mechanisms during stress," in *Antioxidants and antioxidant enzymes in higher plants* (Berlin/Heidelberg, Germany: Springer), 207–232.

Vishnupradeep, R., Bruno, L. B., Taj, Z., Karthik, C., Challabathula, D., Kumar, A., et al. (2022). Plant growth promoting bacteria improve growth and phytostabilization potential of zea mays under chromium and drought stress by altering photosynthetic and antioxidant responses. *Environ. Technol. Innov.* 25, 102154.

Wang, X., Li, S., Li, J., Li, C., and Zhang, Y. (2015). *De novo* transcriptome sequencing in pueraria lobata to identify putative genes involved in isoflavones biosynthesis. *Plant Cell Rep.* 34 (5), 733–743.

Wang, Y., Yang, R., Yan, F., Jin, Y., Liu, X., and Wang, T. (2022). Medicarpin protects cerebral microvascular endothelial cells against oxygen-glucose deprivation/reoxygenation-induced injury *via* the PI3K/Akt/FoxO pathway: a study of network pharmacology analysis and experimental validation. *Neurochem. Res.* 47 (2), 347–357.

Watanabe, S., Yamada, M., Ohtsu, I., and Makino, K. (2007). α-ketoglutaric semialdehyde dehydrogenase isozymes involved in metabolic pathways of d-glucarate, d-galactarate, and hydroxy-l-proline: molecular and metabolic convergent evolution. *J. Biol. Chem.* 282 (9), 6685–6695.

Wu, Q., Liu, Y., Xie, Z., Yu, B., Sun, Y., and Huang, J. (2022a). OsNAC016 regulates plant architecture and drought tolerance by interacting with the kinases GSK2 and SAPK8. *Plant Physiol.* 189 (3), 1296–1313.

Wu, Y., Zhang, C., Huang, Z., Lyu, L., Li, W., and Wu, W. (2022b). Integrative analysis of the metabolomic and transcriptome provides insights into the mechanisms of flavonoid biosynthesis in blackberry. *Food Res. Int.* 153, 110948.

Xiao, W., Hu, S., Zhou, X., Yao, R., Luo, J., Yuan, C., et al. (2017). A glucuronokinase gene in arabidopsis, AtGlcAK, is involved in drought tolerance by modulating sugar metabolism. *Plant Mol. Biol. Rep.* 35 (2), 298–311.

Xie, Z., Chu, Y., Zhang, W., Lang, D., and Zhang, X. (2019). *Bacillus pumilus* alleviates drought stress and increases metabolite accumulation in *Glycyrrhiza uralensis* fisch. *Environ. Exp. Bot.* 158, 99–106.

Xu, J., Xing, X. J., Tian, Y. S., Peng, R. H., Xue, Y., Zhao, W., et al. (2015). Transgenic arabidopsis plants expressing tomato glutathione s-transferase showed enhanced resistance to salt and drought stress. *PloS One* 10 (9), e0136960.

Yasmin, H., Nosheen, A., Naz, R., Bano, A., and Keyani, R. (2017). L -tryptophan-assisted PGPR-mediated induction of drought tolerance in maize (Zea mays l.). *J. Plant. Interact* 12 (1), 567–578.

Yang, Y. H., Yang, H., Li, R. F., Li, C. X., Zeng, L., Wang, C. J., et al. (2021). A rehmannia glutinosa cinnamate 4-hydroxylase promotes phenolic accumulation and enhances tolerance to oxidative stress. *Plant Cell Rep.* 40 (2), 375–391.

Yu, L., Huang, D., Gu, J., Pan, D., Tan, Y., Huang, R., et al. (2021). Identification of isoflavonoid biosynthesis-related R2R3-MYB transcription factors in *Callerya speciosa* (champ. ex *Benth.*) schot using transcriptome-based gene coexpression analysis. *Int. J. Genomics* 2021, 1–13.

Zahedi, S. M., Moharrami, F., Sarikhani, S., and Padervand, M. (2020). Selenium and silica nanostructure-based recovery of strawberry plants subjected to drought stress. *Sci. Rep.* 10 (1), 1–18.

Zhang, K., Cui, H., Cao, S., Yan, L., Li, M., and Sun, Y. (2019). Overexpression of CrCOMT from carex rigescens increases salt stress and modulates melatonin synthesis in arabidopsis thaliana. *Plant Cell Rep.* 38 (12), 1501–1514.

Zhang, X., Lin, S., Peng, D., Wu, Q., Liao, X., Xiang, K., et al. (2022). Integrated multi-omic data and analyses reveal the pathways underlying key ornamental traits in carnation flowers. *Plant Biotechnol. J.* 20 (6), 1182–1196.

Zhang, R. R., Wang, Y. H., Li, T., Tan, G. F., Tao, J. P., Su, X. J., et al. (2021b). Effects of simulated drought stress on carotenoid contents and expression of related genes in carrot taproots. *Protoplasma* 258 (2), 379–390.

Zhang, X., Xie, Z., Lang, D., Chu, Y., Cui, G., and Jia, X. (2021a). *Bacillus pumilus* improved drought tolerance in *Glycyrrhiza uralensis* G5 seedlings through enhancing primary and secondary metabolisms. *Physiol. Plant* 171 (3), 388–399.

Zhang, W., Xie, Z., Wang, L., Li, M., Lang, D., and Zhang, X. (2017). Silicon alleviates salt and drought stress of *Glycyrrhiza uralensis* seedling by altering antioxidant metabolism and osmotic adjustment. *J. Plant Res.* 130 (3), 611–624.

Zhang, W. J., Zhang, X. J., Lang, D. Y., Li, M., Liu, H., and Zhang, X. H. (2020). Silicon alleviates salt and drought stress of *Glycyrrhiza uralensis* plants by improving photosynthesis and water status. *Biol. Plant* 64, 302–313.

Zheng, J., Liang, L. X., Xuan, Q. G., Guo, H. Y., and Zhou, Z. G. (2022). Screening and identification of antagonistic endophytic bacteria against *phytophthora drechsleri* in cucumber. *Guangdong Agr Sci.* 4, 81–87.

Zhou, X., Lindsay, H., and Robinson, M. D. (2014). Robustly detecting differential expression in RNA sequencing data using observation weights. *Nucleic Acids Res.* 42 (11), e91.

Zhou, Y. H., Yu, J. Q., Huang, L. F., and Nogués, S. (2004). The relationship between CO_2 assimilation, photosynthetic electron transport and water-water cycle in chill-exposed cucumber leaves under low light and subsequent recovery. *Plant Cell Environ.* 27 (12), 1503–1514.

10.3389/fpls.2022.1033915

Glossary

ROS	reactive oxygen species
PGPB	plant growth-promoting bacteria
Si	silicon
G5	*Bacillus pumilus*
SOD	superoxide dismutase
CAT	catalase
POD	peroxidase
AsA	ascorbate
GSH	glutathione
G. uralensis	*Glycyrrhiza uralensis* Fisch.
APX	ascorbate peroxidase
GPX	glutathione peroxidase
MDHAR	monodehydroascorbate reductase
DHAR	dehydroascorbate reductase
GR	glutathione reductase
O_2^-	superoxide
H_2O_2	hydrogen peroxide
MDA	malondialdehyde
DHA	dehydroascorbate
GSSG	glutathione disulfide
UGDH	UDP-glucose 6-dehydrogenase
UDPase	UDP-sugar pyrophosphorylase
GlcAK	glucuronokinase
MIOX	inositol oxygenase
ALDH	aldehyde dehydrogenase (NAD^+)
GGP	GDP-L-galactose phosphorylase
GME	GDP-mannose-3′,5′-epimerase
AO	L-ascorbate oxidase
G6PDH	glucose-6-phosphate 1-dehydrogenase
GGT	gamma-glutamyl transpeptidase
APN	aminopeptidase N
CHXB	β-carotene hydroxylase
PSY	phytoene synthase
Z-ISO	ξ-carotene isomerase
ZEP	zeaxanthin epoxidase
PAL	phenylalanine ammonia lyase
4CL	4-coumarate-CoA ligase
C4H	*trans*-cinnamate 4-monooxygenase
HCT	shikimate *O*-hydroxycinnamoyltransferase
CYP98A2	5-*O*-(4-coumaroyl)-D-quinate 3′-monooxygenase
CCOMT	caffeic acid 3-*O*-methyltransferase/acetylserotonin *O*-methyltransferase
CHS	chalcone synthase
CHI	chalcone isomerase
CHR	chalcone reductase
CYP81E1/E8	isoflavone/4′-methoxyisoflavone 2′-hydroxylase
VR	vestitone reductase
UGT	isoflavone 7-*O*-glucosyltransferase
MAT	isoflavone 7-*O*-glucoside-6″-*O*-malonyltransferase
FLS	flavonol synthase
F3′,5′H	flavonoid 3′,5′-hydroxylase
CYP75B	flavonoid 3′-monooxygenase
CPM	counts per million
VIP	variable importance in projection

(Continued)

frontiers | Frontiers in Plant Science

TYPE Original Research
PUBLISHED 24 February 2023
DOI 10.3389/fpls.2023.1018874

Check for updates

OPEN ACCESS

EDITED BY
Giselle Camargo Mendes,
Instituto Federal de Santa Catarina (IFSC), Brazil

REVIEWED BY
Dong Fang Ma,
Yangtze University, China
Xiaoxu Li,
Chinese Academy of Agricultural Sciences (CAAS), China
Nan Wang,
Shandong Agricultural University, China

*CORRESPONDENCE
Yang Song
songyang@caas.cn

†These authors share first authorship

SPECIALTY SECTION
This article was submitted to Plant Abiotic Stress, a section of the journal Frontiers in Plant Science

RECEIVED 14 August 2022
ACCEPTED 10 February 2023
PUBLISHED 24 February 2023

CITATION
Wang X, Tang Q, Chi F, Liu H, Zhang H and Song Y (2023) Sucrose non-fermenting1-related protein kinase VcSnRK2.3 promotes anthocyanin biosynthesis in association with VcMYB1 in blueberry. *Front. Plant Sci.* 14:1018874. doi: 10.3389/fpls.2023.1018874

COPYRIGHT
© 2023 Wang, Tang, Chi, Liu, Zhang and Song. This is an open-access article distributed under the terms of the Creative Commons Attribution License (CC BY). The use, distribution or reproduction in other forums is permitted, provided the original author(s) and the copyright owner(s) are credited and that the original publication in this journal is cited, in accordance with accepted academic practice. No use, distribution or reproduction is permitted which does not comply with these terms.

Sucrose non-fermenting1-related protein kinase VcSnRK2.3 promotes anthocyanin biosynthesis in association with VcMYB1 in blueberry

Xuan Wang†, Qi Tang†, Fumei Chi, Hongdi Liu, Hongjun Zhang and Yang Song*

Key Laboratory of Biology and Genetic Improvement of Horticultural Crops (Germplasm Resources Utilization), Research Institute of Pomology, Chinese Academy of Agricultural Sciences, Ministry of Agriculture, Xingcheng, China

Sucrose non-fermenting1-related protein kinase-2 (SnRK2) is a plant-specific protein kinase family and an important component of the abscisic acid (ABA) signaling pathway. However, there is a lack of relevant studies in blueberry (*Vaccinium corymbosum*). In this study, we identified six SnRK2 family members (from *VcSnRK2.1* to *VcSnRK2.6*) in blueberries for the first time. In addition, we found that *VcSnRK2.3* expression was not only positively correlated with fruit ripening but was also induced by ABA signaling. Transient expression in blueberry fruits also proved that *VcSnRK2.3* promoted anthocyanin accumulation and the expression of anthocyanin synthesis-related genes such as *VcF3H*, *VcDFR*, *VcANS*, and *VcUFGT*. Transgenic *Arabidopsis thaliana* seeds and seedlings overexpressing *VcSnRK2.3* showed anthocyanin pigmentation. Yeast two-hybrid assays (Y2H) and Bimolecular fluorescence complementation assays (BiFC) demonstrated that *VcSnRK2.3* could interact with the anthocyanin positive regulator *VcMYB1*. Finally, *VcSnRK2.3* was able to enhance the binding of *VcMYB1* to the *VcDFR* promoter. *Via* regulation transcription of anthocyanin biosynthesis genes, *VcSnRK2.3* promoted anthocyanin accumulation in blueberry. The above results suggest that *VcSnRK2.3* plays an important role in blueberry anthocyanin synthesis, is induced by ABA, and can interact with *VcMYB1* to promote anthocyanin biosynthesis in blueberry.

KEYWORDS

SnRK2, ABA signaling pathway, fruit ripening, anthocyanin synthesis, *VcMYB1*, *Vaccinium corymbosum*

1 Introduction

Blueberries (*Vaccinium corymbosum*, Ericaceae) are one of the most nutritious foods cultivated worldwide. In general, highbush blueberry (*V. corymbosum* L.) is considered to be a commercially important blueberry. Highbush blueberries include three types: southern highbush blueberry (SHB), half highbush blueberry (HHB), and northern highbush

blueberry (NHB) (Yang et al., 2022). Blueberries are rich in flavonoids (mainly anthocyanins) and polyphenols (proanthocyanidins), which are recognized by the Food and Agriculture Organization of the United Nations (FAO) as one of the top five health foods for humans and have a promising commercial future. Anthocyanins have anti-cancer, anti-obesity, and anti-inflammatory effects, protect vision, prevent heart disease, improve immunity, and improve cognitive decline (Ma et al., 2018; Guan et al., 2021).

A change in fruit color is an important indicator of fruit maturity, which is mainly determined by anthocyanins, carotenoids and phenols (Ballester et al., 2010; Wang et al., 2020), and the anthocyanin concentration is a major factor that determines plant color. Anthocyanins are an important secondary metabolite of plants and are synthesized *via* the phenylalanine metabolic pathway (Allan et al., 2008; Jaakola, 2013; An et al., 2020a). Functionally, genes that affect anthocyanin biosynthesis are divided into two groups. The anthocyanin synthesis pathway's essential structural genes make up one group, such as chalcone synthase (CHS), chalcone isomerase (CHI), lavanone 3-hydroxylase (F3H), dihydroflavonol 4-reductase (DFR), anthocyanidin synthase (ANS), and UDP-glucose flavonoid 3-O-glucosyltransferase (UFGT) (Boss et al., 1996; Ma et al., 2014). The other group consists of transcription factors that are not directly involved in anthocyanin synthesis but are used to regulate the expression of structural genes, such as MYB, bHLH and WD40, which usually form the transcriptional complex MYB-bHLH-WD40 ("MBW" transcription factor) (Petroni and Tonelli, 2011; Zhao et al., 2019). Previous studies have found that *MYB75*, *MYB113* and *MYB114* in *Arabidopsis* contribute to the accumulation of anthocyanins (Teng et al., 2005; Gonzalez et al., 2008; Chen et al., 2022). In apple, *MdMYB1* and its alleles play important roles in anthocyanin biosynthesis (Ban et al., 2007; Espley et al., 2007). In recent studies, *VcMYB1* was shown to function as a regulator of anthocyanin biosynthesis, and *VcMYB1* positively regulates anthocyanin synthesis and accumulation by binding to the *VcDFR* and *VcUFGT* anthocyanin biosynthesis genes' promoters (Tang et al., 2021; Zhang et al., 2021). In addition, it has been demonstrated that the transcription factors *MYBA* and *MYBPA* co-regulate anthocyanin biosynthesis in blueberries (Karppinen et al., 2021; Lafferty et al., 2022). Although many species' anthocyanin synthesis pathways have been examined, and attempts have been made to identify their molecular mechanisms, few relevant studies have been carried out in blueberries.

Abscisic acid (ABA) is a sesquiterpenoid compound discovered in the 1960s (Bassaganya-Riera et al., 2010). In addition to being a crucial part in plant growth, development, and stress response, ABA is also a major regulator of ripening in non-climacteric fruits (Chen et al., 2020b; Zhang et al., 2021; Gupta et al., 2022). ABA has been shown to promote ripening and anthocyanin synthesis in many non-climacteric fruits, including strawberry, pear, sweet cherry, grape, cucumber, and blueberry, as well as climacteric fruits, such as tomato, peach, mango, and melon (Karppinen et al., 2018; Oh et al., 2018). Thus, fruit ripening is significantly influenced by ABA. In a recent study, silencing of *VmNCED1*, a key gene for ABA biosynthesis, resulted in down-regulation of the expression of key anthocyanin biosynthesis genes in blueberry (Karppinen et al., 2018). Inhibiting the expression of the essential ABA biosynthesis gene *FaNCED1* in strawberries prevented ABA biosynthesis, and some fruit that was not colored could be supplemented with exogenous ABA, suggesting a molecular mechanism for the role of ABA in fruit ripening (Jia et al., 2011). Many transcription factors associated with anthocyanin accumulation and fruit ripening that are regulated by ABA have been discovered in studies. These transcription factors include MYB, bZIP, and bHLH (Shen et al., 2014; An et al., 2018; An et al., 2021). In apple, by regulating the MYB1-bHLH3 complex, *ABI5* regulates the ABA-induced anthocyanin synthesis, and ABA treatment enhances the interaction between *MdbHLH3* and *MdMYB1* (An et al., 2021). ABA signaling plays an important regulatory role in fruit ripening, but the genes and key regulators involved in its downstream regulation of non-climacteric fruit ripening and anthocyanin accumulation are poorly understood.

Reversible phosphorylation of proteins catalyzed by protein phosphatases and protein kinases is the main mechanism of post-translational regulation of protein activity and intracellular signal transduction in eukaryotes (Halford and Hey, 2009). Sucrose non-fermenting1-related protein kinase-2 (SnRK2) is one of the protein kinases involved in signal transduction in adversity (Boudsocq and Laurière, 2005). In *Arabidopsis*, the SnRK2 family contains ten members named *SnRK2.1* to *SnRK2.10* (Hrabak et al., 2003). And there are ten SnRK2 members in *Oryza sativa* and *Triticum aestivum*. *Fragaria ananassa* contains nine, *Solanum tuberosum* contains eight and *Zea mays* contains eleven (Boudsocq et al., 2004; Kobayashi et al., 2004; Han et al., 2015; Zhang et al., 2016; Bai et al., 2017). Subsequently, in many species, members of the SnRK2 family have been discovered, including *Lycopersicon esculentum* (Sun et al., 2011), *Vitis vinifera* (Boneh et al., 2012), *Malus prunifolia* (Shao et al., 2014), *Prunus avium* (Shen et al., 2017), *Musa acuminata* (Hu et al., 2017), *Pyrus bretschneideri* (Chen et al., 2020a), *Fragaria vesca* (Zhang et al., 2020).

SnRK2 is involved in osmotic stress and the ABA response and plays an important role in stress signal transduction (Yoshida et al., 2006; Huai et al., 2008; Cutler et al., 2010; Fujii et al., 2011). Studies on *Arabidopsis* have demonstrated that ABA elicits cellular responses by binding to the ABA receptor pyrabactin resistance1/PYR1-like/regulatory components of the ABA receptor (PYR/PYL/RCAR). ABA binding to the receptor protein PYR1/PYL/RCAR disables the inhibition of SnRK2 kinase by PP2C phosphatase and thus activates *SnRK2* (Cutler et al., 2010; Moreno-Alvero et al., 2017; Islam et al., 2021). Activated *SnRK2* then phosphorylates and regulates its downstream targets such as bZIP-like transcription factor *ABF*, slow anion channel 1 (SLAC1) and the MAPK signaling cascade pathway (Fujita et al., 2009; Geiger et al., 2009; de Zelicourt et al., 2016). Furthermore, *SnRK2* plays key roles in plant growth and development and a range of stress reactions (Fujii et al., 2011; Fujita et al., 2013), including the modulation of fruit development and ripening and anthocyanin biosynthesis. For example, in strawberry, virus-induced gene silencing of the ABA receptor *FaPYR1* delayed ripening and significantly decreased critical ABA signaling molecules, such as *ABI1*, *ABI3*, *ABI4*, *ABI5*, and *SnRK2s* (Chai et al., 2011). By contrast, *FaABI1* interference resulted in the overexpression of most genes associated with fruit ripening, including *ABI3*, *SnRK2s*, and *AREB1* (Jia et al., 2013). Previous studies identified *FaSnRK2.6* as a

member of the SnRK2-III family, and *FaSnRK2.6* was a negative regulator of strawberry fruit ripening and anthocyanin accumulation (Han et al., 2015; Jia et al., 2022). Dehydration stress in sweet cherry resulted the expression of all *PacSnRK2* and *PacPP2C genes*, and it also promoted the accumulation of ABA and anthocyanin (Shen et al., 2017). In addition, *FvSnRK2.6* was found to mediate low-temperature-regulated anthocyanin accumulation in strawberry fruit (Mao et al., 2022).

Blueberries are rich in anthocyanins and have a high nutritional value. In this study, we selected blueberry (*V. corymbosum* "Duke") as experimental material and identified its SnRK2 gene family members. In addition, we explored the regulatory effect of exogenous ABA on *VcSnRK2.3*. We also sought to determine the regulatory effect of *VcSnRK2.3* on blueberry and to assess whether this protein participates in the control of ripening and anthocyanin synthesis in blueberry fruit, particularly to determine its interaction with *VcMYB1*. Our data provide a novel mechanism for blueberry anthocyanin biosynthesis and could potentially lead to improved ripening practices.

2 Materials and methods

2.1 Plant materials

Nine-year-old blueberry (*V. corymbosum* "Duke") plants collected from the small berry garden of the Fruit Tree Research Institute, Chinese Academy of Agricultural Sciences were used as experimental material. Experiments were conducted from March 2019 to February 2022 at the Ministry of Agriculture Key Laboratory of horticultural crop germplasm resources utilization, Institute of Fruit Tree Research, Chinese Academy of Agricultural Sciences (Xingcheng, Liaoning, China) and College of Horticulture Sciences, Shandong Agricultural University (Tai'an, Shandong, China). To ensure the consistency of the material, fruits were collected from the top of the inflorescence (first to mature). Samples were taken from plants under the same growth conditions for organ (root, stem, leaf, flower, and fruit)-specific expression. All samples were rapidly frozen in liquid nitrogen and stored at −80°C.

2.2 Gene isolation and nomenclature

Blueberry transcriptome data obtained from Illumina and SMRT sequencing were used to identify the gene family members of SnRK2 in blueberry (Tang et al., 2021). The excavated VcSnRK2 protein sequences were analyzed using the Basic Local Alignment Search Tool (BLAST) program (http://www.ncbi.nlm.nih.gov/BLAST/) in the National Center for Biotechnology Information (NCBI) database. The results showed that the six VcSnRK2 sequences had high homology with the SnRK2 protein sequences of *Solanum tuberosum*, *Arabidopsis thaliana* and *Zea mays*. The six genes were named according to the Phylogenetic Tree Construction. If VcSnRK2 clusters with *Solanum tuberosum*, it is named after the same number, including *VcSnRK2.1, 2.3, 2.4*, and *2.5*. For *VcSnRK2.2* and *2.6*, which do not cluster as closely with *Solanum tuberosum*, they are named sequentially according to their position on the chromosome in sequence.

2.3 Amino acid sequence analysis

The amino acid secondary structure of VcSnRK2 was predicted using the Simple Modular Architecture Research Tool (SMART) software program (http://smart.emb-lheidelberg.de/) through three rounds of PCR. The deduced amino acid sequences of VcSnRK2s were aligned using CLC Sequence Viewer 6.0 software with the default settings.

2.4 Quantitative real-time-PCR (qRT-PCR) analysis

RNA was extracted from different organs and different fruit stages of blueberry plants, and *Arabidopsis* leaves using TaKaRa MiniBEST Plant RNA Extration Kit (TaKaRa, Shiga, Japan). qRT-PCR was performed with *VcACTIN* as a reference gene. *Arabidopsis* polyubiquitin 10 (*AtUBQ10*) was used as a reference gene. Single-stranded cDNA was obtained using a reverse transcription kit (TaKaRa, Shiga, Japan). 4 μg RNA was used as a template for cDNA synthesis. The procedure for cDNA synthesis was to incubate the reaction solution at 65°C for five minutes, 42°C for 60 minutes, and 70°C for 5 minutes. qPCR assays were performed on a CFX Connect real-time PCR assay system (Bio-Rad, USA) using the SYBR Green I chimeric fluorescence assay. The amplification reaction procedure was as follows: Stage 1 pre-denaturation, the mixture was reacted at 95°C for 30 sec, one cycle; Stage 2 cyclic reaction, 95°C for 10 sec, 60°C for 30 sec, 40 cycles; Stage 3 melting curve, 95°C for 15 sec, 60°C for 60 sec, 95°C for 15 sec, one cycle. The qPCR results were all analyzed using the comparative CT method. Three biological replicates and three technical replicates were conducted. All primers used in this study are listed in Supplementary Table S1.

2.5 Analysis of the anthocyanin content by high-performance liquid chromatography

Extraction methods for anthocyanins were based on previous studies (Latti et al., 2010; Pertuzatti et al., 2021). Separation, identification, and quantification of anthocyanins by high-performance liquid chromatography (HPLC) was conducted on an Agilent 1100 Series system (Agilent, Germany), equipped with DAD (G1315B), and an LC/MSD Trap VL (G2445C VL) electrospray ionization mass spectrometry (ESIMSn) system that was coupled to an Agilent ChemStation (version B.01.03) data-processing station (Castillo-Munãoz et al., 2009). Mass spectra data were processed with Agilent LC/MS Trap software (version 5.3). ESI-MSn was used to determine the anthocyanin profiles and the following parameters were employed: positive ionization mode; dry gas, N2, 11 mL/min; drying temperature, 350°C; nebulizer, 65 psi; capillary, −2500 V; capillary exit offset, 70 V; skimmer1, 20 V; skimmer 2, 6 V; compound stability, 100%; scan range, 50–1,200 m/z (Pertuzatti et al., 2016). For the purposes of quantification, DAD chromatograms were extracted at 520 nm for anthocyanins.

2.6 Ectopic expression of VcSnRK2.3 in *Arabidopsis*

Agrobacterium tumefaciens GV3101 transformed the pRI101-AN vector with the open reading frame (ORF) after it had been cloned and inserted. Transformation of *Agrobacterium* into *Arabidopsis* by flower dip method. On MS media containing 50 mg L^{-1} kanamycin, T1 *VcSnRK2.3* transgenic plants were selected. Until seed set, kanamycin-resistant T1 seedlings were cultivated in a growth chamber at 22°C and a 16 h day length. Seeds of T1 plants were planted and germinated to obtain T2 seedlings. T2 seedlings were also selected on MS medium containing 50 mg L^{-1} kanamycin.

2.7 Blueberry injection assays

Blueberry fruit injection assays were performed with reference to previous studies (An et al., 2019; Tang et al., 2021). The open reading frame of the *SnRK2.3* gene was cloned into the pGreenII62-SK vector to obtain the *VcSnRK2.3*-pGreenII62-SK vector. Blueberry peels were injected with the mixed vector and *Agrobacterium* solutions.

2.8 Yeast two-hybrid assay (Y2H)

The Y2H experiment was performed according to Clontech's instructions. The ORF, N-terminus, and C-terminus of *VcSnRK2.3* and the ORF of *MdMYB1* were inserted into pGAD and pGBD vectors. The plasmids were co-transformed into yeast strain Y2H Gold (TaKaRa, Beijing, China) by using the lithium acetate method with reference to Veries et al. For transformation, 4-5 µl of plasmid and 50 µg of denatured salmon sperm vector DNA are mixed. Then 500 µl of polyethylene glycol (PEG) lithium acetate solution is added. After incubation 20 µl DMSO is added and incubated again. The transformed yeast strains were grown on medium lacking Leucine and Tryptophan (SD-L/-T), Leucine, Tryptophan, Histidine and Adenine (SD-L/-T/-H/-A) or Leucine, Tryptophan, Histidine, Adenine and X-gal (SD-T/-L/-H/-A+X-gal) at 28°C for 3 days.

2.9 BiFC assay

The ORF and C-terminus of *VcSnRK2.3* and the ORF of *MdMYB1* were inserted into YFP^C or YFP^N to generate the *VcSnRK2.3*-C-YFP^C, *VcSnRK2.3*-YFP^C and *VcMYB1*-YFP^N plasmids. The constructs were transformed into *Agrobacterium* GV3101. The specified plasmid-carrying *Agrobacterium* solution was incubated with prepared tobacco leaves for 30 minutes. After 2 days of darkness at 24°C, the transformed tobacco leaves were observed under a Confocal microscope (Zeiss LSM 780, Lena, Germany). The excitation wavelength of YFP is 510 nm, and the emission wavelength is 527 nm.

2.10 Firefly luciferase complementation assay

VcDFR promoter sequences were obtained from pre-lab data (Tang et al., 2021). Tobacco transient expression assays were carried out according to previous studies (Shang et al., 2010; An et al., 2017). The VcDFRpro : Luc reporter construct was created by amplifying the VcDFR promoter and cloning it into the pGreenII0800-LUC vector. The ORFs of *VcMYB1* and *VcSnRK2.3* were cloned into the pGreenII62-SK vector to generate 35Spro : *VcMYB1* and 35Spro : *VcSnRK2.3*, respectively. Transformed leaves were sprayed with 100 mM luciferin and placed in the dark for 5 minutes before being examined for luminescence. The LUC pictures were collected using a charge-coupled device-imaging apparatus (NightOWL LB983 in conjunction with Indigo software).

2.11 GUS staining and activity analysis

Effector constructs were generated from *Agrobacterium* GV3101 strains containing the pRI101-*VcSnRK2.3* and pRI101-*VcMYB1* genes. The reporter constructs were generated using the promoter sequences of *VcDFR* cloned upstream of the β-glucuronidase (GUS) reporter gene in the pCAMBIA1301 vector. *Agrobacterium* GV3101 strains carrying pRI101-*VcSnRK2.3* and pRI101-*VcMYB1* were co-injected into the abaxial surface of tobacco leaves. Infected leaves were grown in growth chambers for 3-4 days and then analyzed for GUS activity. Proteins were extracted from infected leaves and fluorescence was measured with a fluorometer (VersaFluor Fluorometer, Bio-Rad) (http://www.bio-rad.com) with reference to Jefferson et al., 1987 and Bowling et al., 1994.

3 Results

3.1 Genome-wide identification of VcSnRK2 subfamily members

Based on the blueberry transcriptome data, we obtained six blueberry SnRK2 gene family members, named *VcSnRK2.1* to *VcSnRK2.6*. We analyzed the physicochemical properties of the blueberry SnRK2 gene family members using the online software ProtParam. Table 1 shows that the amino acid lengths of the six blueberry SnRK2 proteins, ranging from 340 (VcSnRK2.1) AAs to 362 (VcSnRK2.3) AAs, and the molecular weights ranged from 38.56 kDa (VcSnRK2.1) to 41.04 (VcSnRK2.3) kDa. In addition, the pI was in the range of 4.75 (VcSnRK2.6) to 5.62 (VcSnRK2.4). To investigate the structural features of the SnRK2 protein sequences, we conducted a comparative analysis of the amino acid sequences of the blueberry SnRK2 proteins (Figure 1A). The results showed that all family members contain ATP binding domains and a protein kinase activation loop and were relatively conserved (Boudsocq et al., 2004; Han et al., 2015).

In addition, to investigate the evolutionary relationship between the blueberry SnRK2 gene and SnRK2 members in other plants, we downloaded the entire SnRK2 gene sequence from the NCBI website for *Arabidopsis*, *Solanum tuberosum*, and *Zea mays*. The Protein BLAST program was used to obtain homologs of *Arabidopsis*, *Solanum tuberosum* and *Zea mays* SnRK2. The evolutionary tree was constructed in MEGA-X software using neighbor- joining, which contained a total of 34 SnRK2 protein

10.3389/fpls.2023.1018874

TABLE 1 Characteristics of VcSnRK2 genes in blueberry (*V. corymbosum*).

Gene name	Group	Chromosome location	Size (Amino Acids)	MW (kDa)	PI	Genbank accession numbers
VcSnRK2.4	I	Chr9:12023838.12028814	357	40.92	5.62	OP626311
VcSnRK2.1	II	Chr5:7032403.7039108	340	38.56	5.59	OP626312
VcSnRK2.5	II	Chr8:1241970.1244296	341	38.69	5.06	OP626313
VcSnRK2.3	III	Chr9:21836159.21841564	362	41.04	4.79	OP626314
VcSnRK2.2	III	Chr5:23480352.23503781	356	40.72	4.84	OP626315
VcSnRK2.6	III	Chr8:14557973.14564911	357	40.68	4.75	OP626316

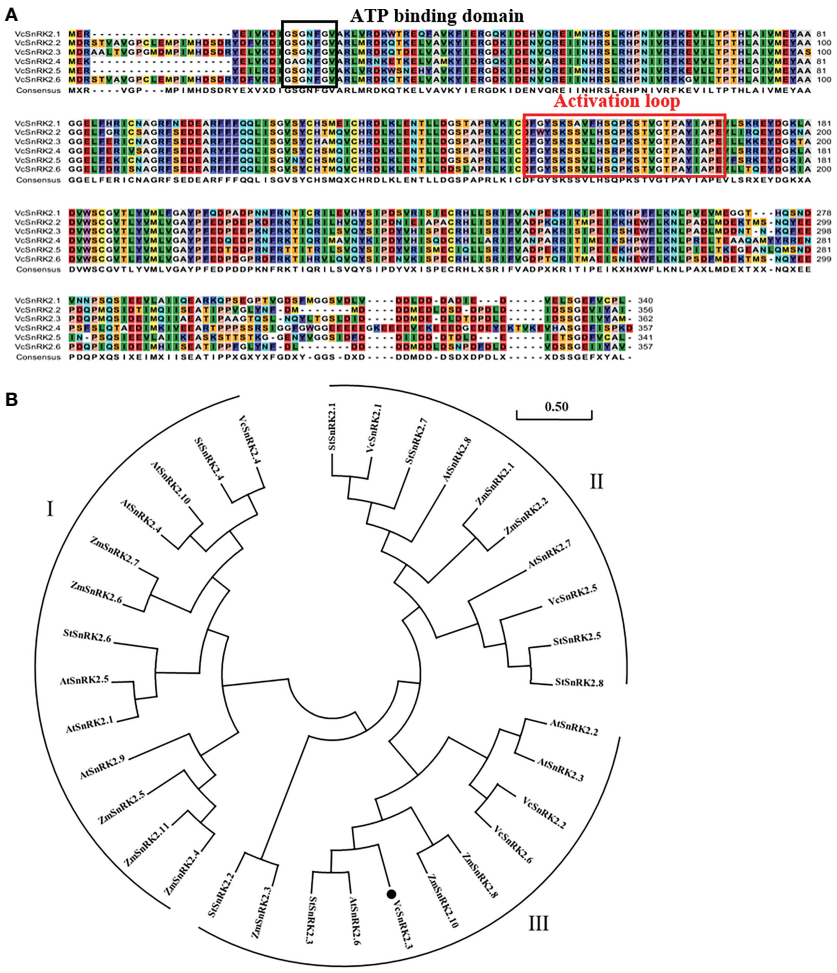


FIGURE 1
Sequence alignments and phylogenetic analysis of SnRK2.3. **(A)** Sequence alignments of the deduced amino acid sequences of *VcSnRK2.1* to *VcSnRK2.6*. The same color shading indicates the same amino acid residues. The deduced amino acid sequences of VcSnRK2s were aligned using CLC Sequence Viewer 6 software with the default settings. The predicted functional domains are boxed. **(B)** Phylogenic analysis of VcSnRK2 and its homologs in *Arabidopsis, Solanum tuberosum* and *Zea mays*. VcSnRK2.3 is denoted by the black spot. SnRK2 of *Arabidopsis, Solanum tuberosum* and *Zea mays* (AtSnRK2.1: AT5G08590.1; AtSnRK2.2: AT3G50500.2; AtSnRK2.3: AT5G66880.1; AtSnRK2.4: AT1G10940.2; AtSnRK2.5: AT5G63650.1; AtSnRK2.6: AT4G33950.1; AtSnRK2.7: AT4G40010.1; AtSnRK2.8: AtSnRK2.9: AT2G23030.1; AtSnRK2.10: AT1G60940.1; StSnRK2.1: JX280911; StSnRK2.1: JX280911; StSnRK2.2: JX280912; StSnRK2.3: JX280913; StSnRK2.4: JX280914; StSnRK2.5: JX280915; StSnRK2.6: JX280916; StSnRK2.7: JX280917; StSnRK2.8: JX280918; ZmSnRK2.1: EU676033.1; ZmSnRK2.2: EU676034.1; ZmSnRK2.3: EU676035.1; ZmSnRK2.4: EU676036.1; ZmSnRK2.5: EU676037.1; ZmSnRK2.6: EU676038.1; ZmSnRK2.7: EU676039.1; ZmSnRK2.8: EU676040.1; ZmSnRK2.10: EU676041.1; ZmSnRK2.11: EU676042.1).

10.3389/fpls.2023.1018874

sequences. Based on the evolutionary results, *VcSnRK2.3* had the highest similarity to *StSnRK2.3* and *AtSnRK2.6* (Figure 1B).

3.2 Temporospatial expression of *VcSnRK2.3*

To analyze the expression of each member of the blueberry VcSnRK2 subfamily at different fruiting stages, we examined the expression of VcSnRK2 during the green, pink, and blue fruit stages of blueberry using quantitative real-time PCR analysis (qRT-PCR). According to Figure 2A, the expression of *VcSnRK2.3* increased significantly when blueberry fruit ripened from the green fruit stage, indicating a possible positive regulatory relationship between *VcSnRK2.3* and blueberry fruit ripening. In contrast, the expression of *VcSnRK2.4* decreased significantly with fruit ripening, and the expression of *VcSnRK2.1* and *VcSnRK2.5* decreased slightly. For *VcSnRK2.2* and *VcSnRK2.6*, we did not observe any correlation with fruit ripening. Thus, we hypothesized that *VcSnRK2.3* could positively regulate the ripening of blueberry fruits. And further experiments were designed to verify its function.

Therefore, we investigated the distribution of *VcSnRK2.3* in different organs of blueberry, and qRT-PCR analysis was carried out on sample materials. The results showed that *VcSnRK2.3* genes were expressed in roots, stems, leaves, flowers and fruits. The expression

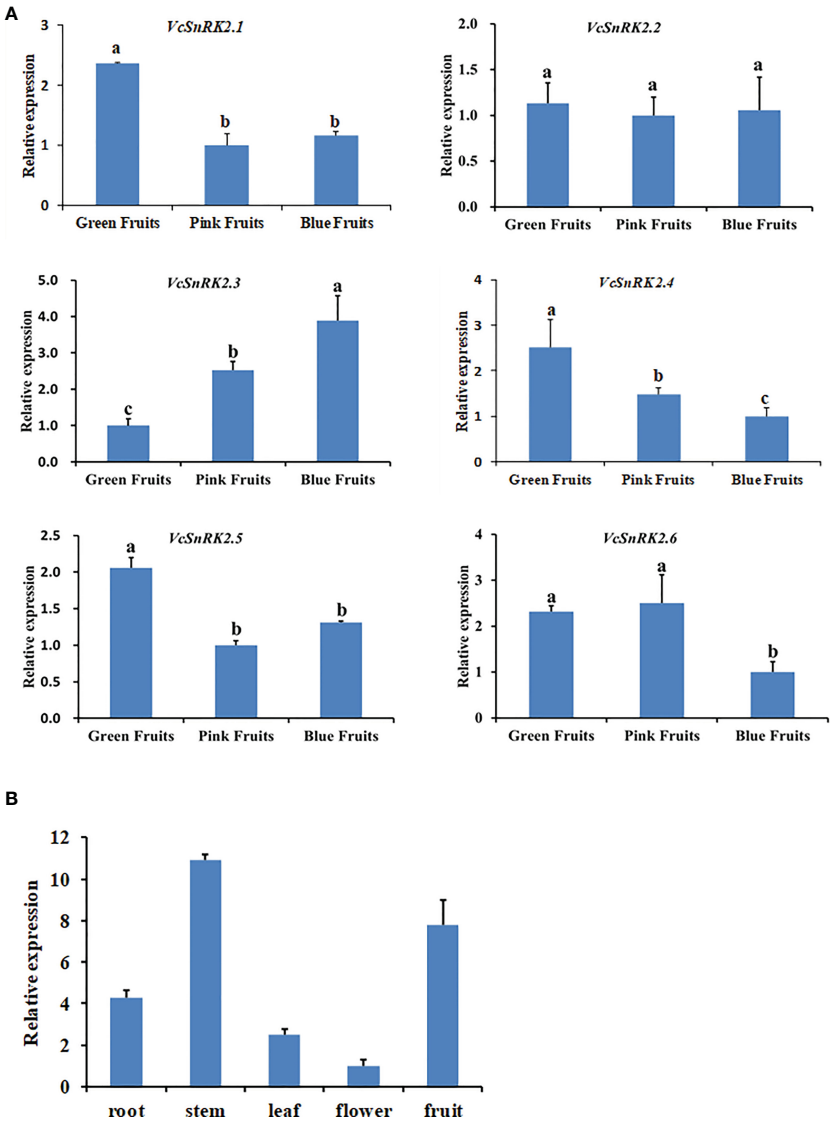


FIGURE 2
Temporospatial pattern of VcSnRK2 expression in blueberry fruits. **(A)** Quantitative real-time PCR (qRT-PCR) analysis of VcSnRK2.1 to VcSnRK2.6 expression in blueberry fruits at different developmental stages. Green fruits (40 days after flowering), pink fruits (65 days after flowering), and blue fruits (80 days after flowering). The qRT-PCR was performed with *VcGAPDH* as a reference gene. Different letters above the bars indicate a significant difference based on one-way ANOVA ($P < 0.05$). Values are the means + SD of three biological replicates. **(B)** qRT-PCR analysis of *VcSnRK2.3* expression in different organs of blueberry plants. Total RNA was isolated from organs (roots, stems, leaves, flowers and fruits). The qRT-PCR was performed with *VcGAPDH* as a reference gene. Values are the means + SD of three biological replicate.

of *VcSnRK2.3* was stem > fruit > root > leaf > flower (Figure 2B). Because the relative expression of VcSnRK2.3 was high in blueberry stems and fruits, we speculated that *SnRK2.3* may play a relatively important role in stems and fruits.

3.3 Expression of *VcSnRK2.3* in response to ABA

ABA has been shown to promote anthocyanin accumulation during blueberry fruit ripening. In our study, ABA treatment promoted the synthesis of blueberry anthocyanins. The color of blueberry fruits gradually changed from green to pink as the treatment continued within the 24 h period (Figure 3A). In addition, when compared to the control (CK) treatment, the anthocyanin content of ripen blueberry fruits was considerably higher following ABA treatment (Figure 3B). To investigate the response of blueberry *VcSnRK2.3* to ABA, we measured the expression of *VcSnRK2.3* after ABA treatment of blueberry fruits. As shown in Figure 3C, the control (CK) treatment had no significant effect on the expression of *VcSnRK2.3* in fruits. The expression of *VcSnRK2.3* increased gradually and then decreased slightly with the increase in the ABA treatment time, and the highest value at 12 h was 2.8 times that of the CK treatment (Figure 3C). The results indicated that *VcSnRK2.3* was strongly induced by ABA, which is in line with other discoveries (Boudsocq et al., 2004; Kulik et al., 2011).

3.4 Functional validation of VcSnRK2.3

In strawberry, fruit ripening and anthocyanin accumulation were shown to be negatively regulated by *FaSnRK2.6* (Han et al., 2015). To study the function of *VcSnRK2.3* and validate its effect on anthocyanin biosynthesis, we carried out heterologous expression in *Arabidopsis* (ecotype Columbia) under CaMV-35S control. Compared with the wild-type (WT), transgenic *Arabidopsis* had red pigmentation in seeds 8–10 days after flowering (Figure 4A). The cotyledons and hypocotyls of *Arabidopsis* seedlings grown from the above seeds were also pigmented (Figure 4B). The total anthocyanin content of WT *Arabidopsis* was 1.513 mg/kg, while the mean value for total anthocyanin contents of *VcSnRK2.3 Arabidopsis* (*VcSnRK2.3*-L1, L2) was 119.91 mg/kg (Figure 4C). In addition, RNA was extracted from the above plants and examined using qRT-PCR. The results demonstrated that overexpression of *VcSnRK2.3* up-regulated the expression of primary genes involved in the flavonoid biosynthetic pathway, including *AtPAP1, At4CL, AtCHS, AtCHI, AtDFR* and *AtANS* (Figure 4D). Among them, the transgenic *Arabidopsis* plants had the highest expression of structural genes *AtDFR* and *AtANS*.

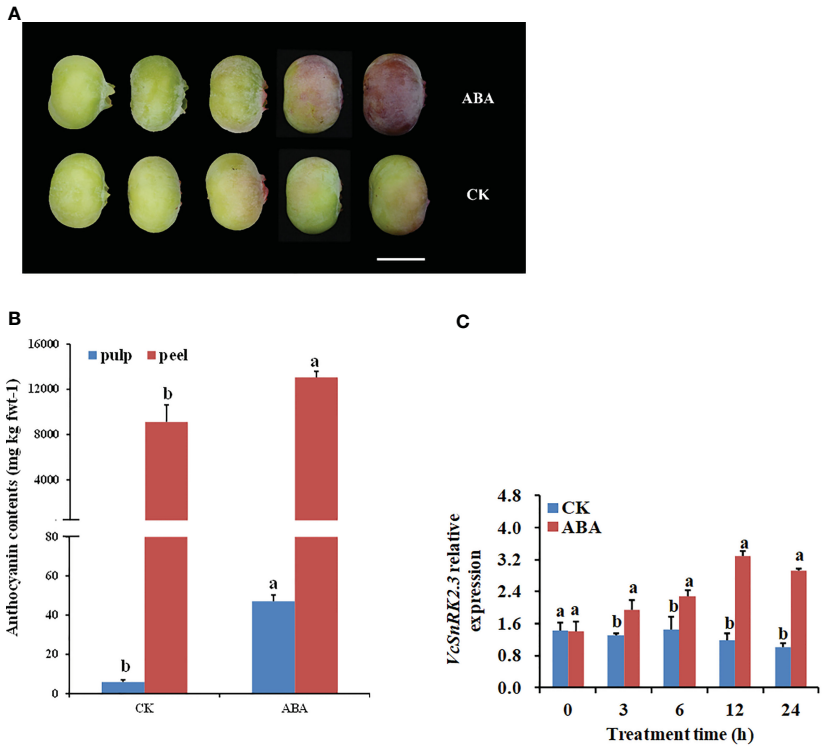


FIGURE 3
ABA and CK treatment in blueberry fruits. **(A)** Isolated blueberry fruits were treated with 100 μM ABA immersion at 0, 3, 6, 12, and 24 h. CK indicates the negative control (no treatment). Scale bar = 8 mm. **(B)** Anthocyanin contents of ripe blueberry fruits. Different letters above the bars indicate a significant difference based on a t-test ($P < 0.05$). Values are the means + SD of three biological replicates. **(C)** qRT-PCR analysis of *VcSnRK2.3* relative expression in blueberry fruits. Different letters above the bars indicate a significant difference based on a t-test ($P < 0.05$). Values are the means + SD of three biological replicates.

10.3389/fpls.2023.1018874

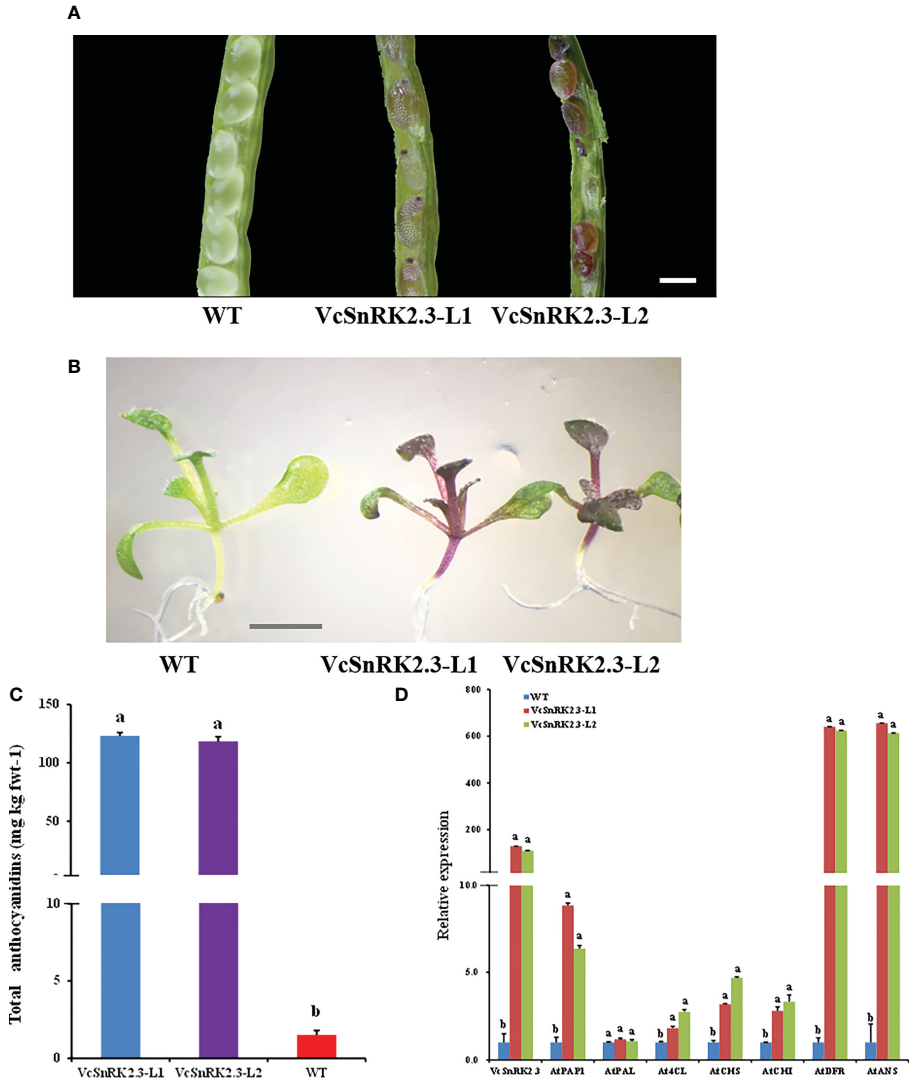


FIGURE 4
Functional analysis of *VcSnRK2.3* in a heterologous system. **(A)** Seeds of *Arabidopsis thaliana* (ecotype Columbia) plants wild-type (WT) and overexpressing 35S:*VcSnRK2.3* (*VcSnRK2.3*-L1, L2). Scale bar = 1 mm. **(B)** *Arabidopsis* plants wild-type and overexpressing 35S:*VcSnRK2.3* (*VcSnRK2.3*-L1, L2). Scale bar = 5 mm. **(C)** Anthocyanin contents of *Arabidopsis* plants overexpressing 35S:*VcSnRK2.3* (*VcSnRK2.3*-L1, L2) and the wild-type. Different asterisks above the bars indicate significant differences based on a t-test ($P < 0.01$). Values are the means + SD of three biological replicates. **(D)** Relative expression levels of *VcSnRK2.3*, *AtPAP1*, *AtPAL*, *At4CL*, *AtCHS*, *AtCHI*, *AtDFR* and *AtANS* in *Arabidopsis* plants overexpressing 35S:*VcSnRK2.3* (*VcSnRK2.3*-L1, L2) and the wild-type. All values were calculated based on the housekeeping gene *AtUBQ10*. Different asterisks above the bars indicate significant differences based on a t-test ($P < 0.01$). Values are the means + SD of three biological replicates.

To further demonstrate the function of *VcSnRK2.3*, we carried out *Agrobacterium*-mediated transient transformation assay in blueberry fruits 40 days after flowering. The control was the pGreenII62-SK empty vector, and the experimental group was the *VcSnRK2.3*-pGreenII62-SK vector (*VcSnRK2.3*-L1, L2 and L3). The results showed that overexpression of *VcSnRK2.3* facilitated anthocyanin accumulation in blueberry injection sites (Figure 5A). And the phenotype can be observed two days after gene overexpression and can last until fruit ripening. The total anthocyanin content, including the levels of delphinidin, cyanidin, petunidin, peonidin, and malvidin, was significantly increased (Figure 5B). In addition, compared with the pGreenII62-SK vector, the expression levels of *VcMYB1* and anthocyanin genes such as *VcF3H*, *VcDFR*, *VcANS*, and *VcUFGT* were considerably increased by the overexpression of *VcSnRK2.3* (Figure 5C). Therefore, based on the above two experiments, we might infer that *VcSnRK2.3* can promote not only anthocyanin biosynthesis but also the expression of *VcMYB1*.

3.5 Interaction analysis of *VcSnRK2.3* and *VcMYB1*

The above results demonstrated that *VcSnRK2.3* can promote *VcMYB1* expression and anthocyanin accumulation in blueberry fruits (Figure 5). Therefore, Y2H assays were carried out to confirm the interaction between VcSnRK2.3 and VcMYB1. After transforming *VcMYB1*-pGBD and *VcSnRK2.3*-pGAD into yeast

10.3389/fpls.2023.1018874

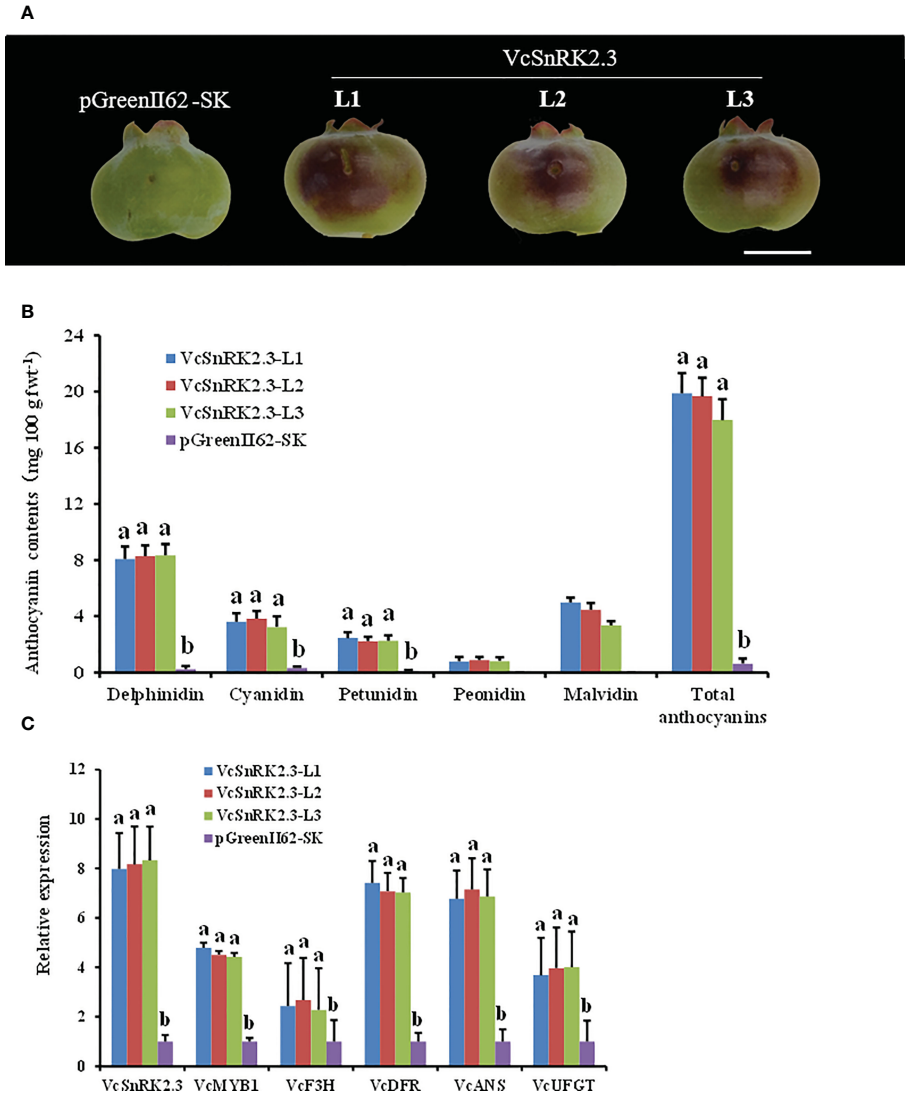


FIGURE 5
Functional analysis of Vc*SnRK2.3* in blueberry. **(A)** Blueberry fruits overexpressing pGreenII62-SK and *VcSnRK2.3*-pGreenII62-SK (*VcSnRK2.3*-L1, L2 and L3). Scale bar = 5 mm. **(B)** Anthocyanin contents of fruits overexpressing *VcSnRK2.3*-pGreenII62-SK (*VcSnRK2.3*-L1, L2 and L3) and pGreenII62-SK. Different English letters above the bars indicate a significant difference based on a t-test ($P < 0.05$). Values are the means + SD of three biological replicates. **(C)** Relative expression levels of *VcSnRK2.3, VcMYB1, VcF3H, VcDFR, VcANS* and *VcUFGT* in overexpressed *VcSnRK2.3*-pGreenII62-SK (*VcSnRK2.3*-L1, L2 and L3) and pGreenII62 -SK fruits. The qRT-PCR served as a reference gene with *VcGAPDH*. Different letters above the bars indicate a significant difference based on a t-test ($P < 0.05$). Values are the means + SD of three biological replicates.

cells, the results showed that *VcMYB1*-pGBD and *VcSnRK2.3*-pGAD as well as *VcMYB1*-pGBD and *VcSnRK2.3*-N-pGAD were able to grow on SD/-Leu-Trp -His-Ade medium (Figure 6A). This indicated that VcSnRK2.3 interacts with VcMYB1 in yeast cells, and the action site is located at the N-terminus of VcSnRK2.3. In addition, the interaction between VcSnRK2.3 and VcMYB1 was tested by BiFC assay. As shown in Figure 6B, when *VcSnRK2.3*-YFP^C and *VcMYB1*-YFP^N were co-expressed, the YFP fluorescent signals could be detected. In contrast, other combinations such as *VcSnRK2.3*-YFP^C + YFP^N, YFP^C + *VcMYB1*- YFP^N, *VcSnRK2.3*-C-YFP^C + *VcMYB1*-YFP^N, and *VcSnRK2.3*-C-YFP^C + YFP^N did not detect fluorescent signals (Figure 6B). Therefore, it was further demonstrated that VcSnRK2.3 and VcMYB1 interacted with each other.

3.6 *VcSnRK2.3* and *VcMYB1* activate *VcDFR* promoters

DFR plays a crucial role in the biosynthesis of anthocyanins. When the expression level of DFR increased, the anthocyanin content in plants increased (An et al., 2020b). A previous study showed that *MdMYB1* promotes the synthesis of anthocyanins by directly binding to the promoter sequences of *MdDFR* and *MdUF3GT* (An et al., 2018). To verify the action of the *VcDFR* promoter by *VcSnRK2.3* and *VcMYB1*, we carried out firefly luciferase complementation assay (Figure 7A). The results showed that the luciferase signal was highest when the *VcDFR* promoter was co-injected with *VcSnRK2.3* and *VcMYB1*, and the signal was second highest when the *VcDFR* promoter was co-injected with

10.3389/fpls.2023.1018874

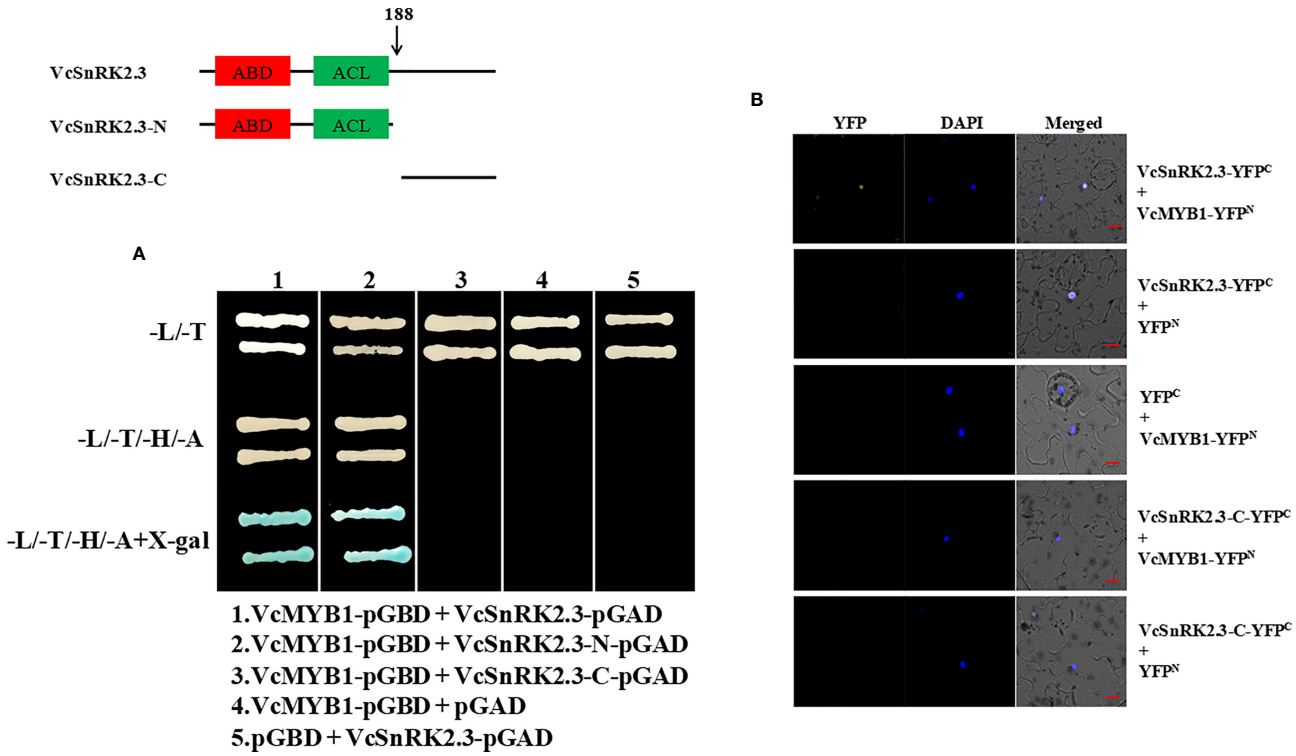


FIGURE 6
VcSnRK2.3 interacts with VcMYB1. **(A)** Yeast two-hybrid assays. The N-terminus of VcSnRK2.3 interacts specifically with VcMYB1. Yeast grown in SD-Leu/-Trp (-L/-T) medium, SD-Leu/-Trp/-His/-Ade (-L/-T/-H/-A) medium or SD-Trp/-Leu/-His/-Ade supplemented with X-gal (-T/-L/-H/-A+X-gal) medium. **(B)** Bimolecular fluorescence complementation assays. The open reading frames of *VcSnRK2.3* and *VcMYB1* were fused to the C-terminus part of YFP and the N-terminus part of YFP. Scale bar = 10 μm. A representative image was presented after this experiment was carried out three times with similar results.

VcMYB1. Both were significantly higher than the luciferase signal of the control group (Figure 7B).

In a different assay, as shown in Figure 7C, the *VcDFR* promoter region was fused to the GUS gene as a reporter marker. The GUS activity was highest when the *VcDFR* promoter was co-injected with *VcSnRK2.3* and *VcMYB1*. And the GUS activity was also significantly higher than control when the *VcDFR* promoter was injected with *VcSnRK2.3* or *VcMYB1* alone. These results suggested that the presence of *VcSnRK2.3* up-regulated the binding of *VcMYB1* to the target promoter and activated the transcription of the anthocyanin biosynthesis genes.

4 Discussion

Blueberry fruits contain a large amount of anthocyanins, which are not only beneficial to human health but also improve the tolerance of plants to oxidative and drought stresses, but the biosynthesis and metabolic mechanisms of blueberry anthocyanin biosynthesis are poorly studied (Chalker-Scott, 1999; Kalt et al., 2020). Moreover, in previous studies on genes related to anthocyanin synthesis in blueberries, most of them focused on the "MBW" transcription factor and paid less attention to other genes. In this study, we identified a novel signaling component *VcSnRK2.3* that is strongly induced by ABA signaling and acts as a positive regulator of anthocyanin synthesis.

SnRK2 is a family of plant-specific protein kinases, and its members are widely distributed in plants. In this study, we identified six SnRK2 members from blueberry, and the evolutionary results showed that blueberry SnRK2 family members are divided into three subfamilies as in *Arabidopsis*, *Solanum tuberosum*, and *Zea mays* (Figure 1B). *OST1* is closely associated with osmotic stress in plants such as *Arabidopsis* and *Zea mays* and enhances plant drought tolerance mainly by promoting stomatal closure and reducing the rate of plant water loss (Boudsocq et al., 2004; Huai et al., 2008). In this study, we found that *VcSnRK2.3* has high homology with *OST1*. Previous studies have shown that *FaSnRK2.6*, *PacSnRK2*, and *FvSnRK2.6* can be induced by drought and temperature signals to mediate anthocyanin synthesis in fruits (Han et al., 2015; Shen et al., 2017; Mao et al., 2022). Therefore, in this study, *VcSnRK2.3* was overexpressed in *Arabidopsis*, and the results showed that the total anthocyanin content as well as anthocyanin synthesis genes increased significantly (Figure 4). This suggested that *VcSnRK2.3* can regulate anthocyanin accumulation in *Arabidopsis*.

In plant like apple and blueberry, the MYB1 gene has been found to promote fruit ripening and anthocyanin accumulation. It also enhances the expression of genes involved in anthocyanin

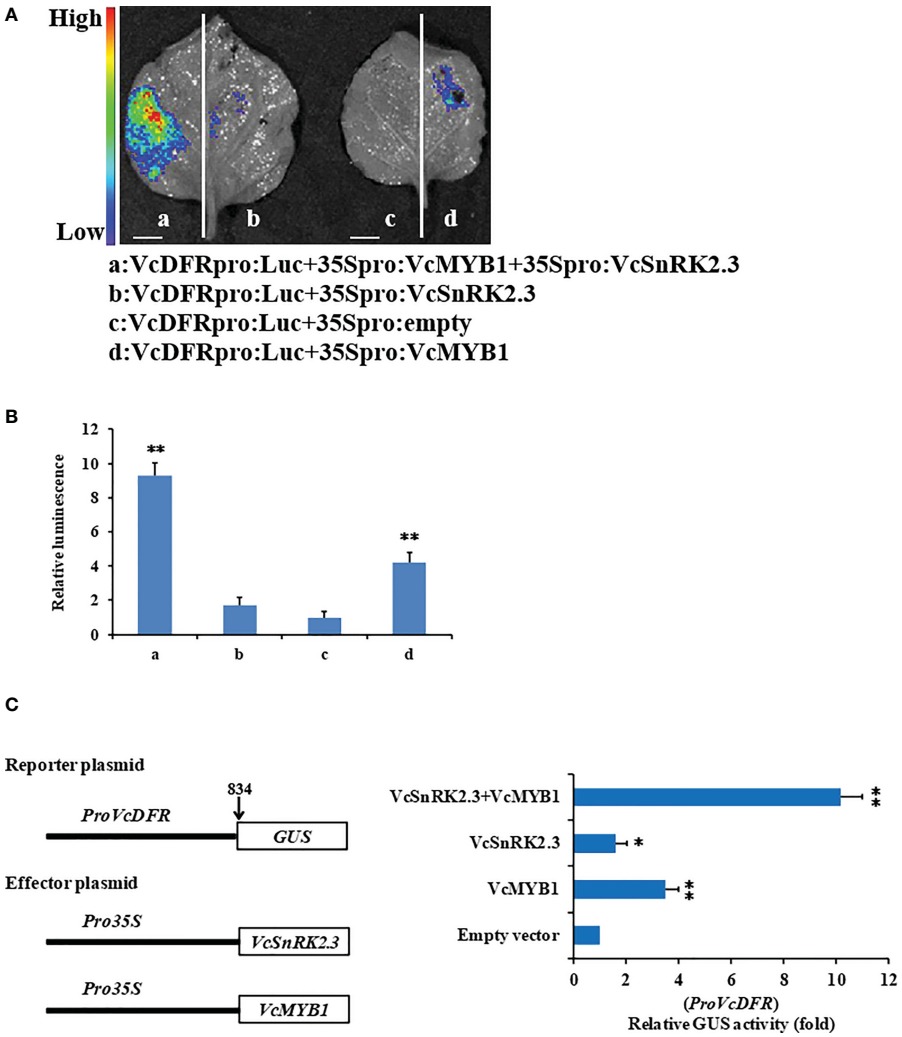


FIGURE 7
Regulation of *VcDFR*pro by *VcMYB1* and *VcSnRK2.3*. **(A)** Firefly luciferase complementation assay analysis showed that VcSnRK2.3 and VcMYB1 can activate *VcDFR* promoter activity in tobacco (*Nicotiana tabacum*) leaves. (a) *VcDFR*pro : Luc+35Spro : *VcMYB1*+ 35Spro : *VcSnRK2.3*, (b) *VcDFR*pro : Luc+35Spro : *VcSnRK2.3*, (c) *VcDFR*pro : Luc +35Spro:empty, (d) *VcDFR*pro : Luc+35Spro : *VcMYB1*. Scale bar = 10 mm. **(B)** Quantitative analysis of luminescence intensity. The value for column c (*VcDFR*pro : Luc+35Spro:empty) was set to 1. Different asterisks above the bars indicate significant differences based on a t-test (**$P < 0.01$). Values are the means + SD of three biological replicates. **(C)** Analysis of GUS activity. Effector vectors containing *VcSnRK2.3* and *VcMYB1* and a reporter vector containing the *VcDFR* promoter were co-injected into wild-type tobacco leaves. VcSnRK2.3 and VcMYB1 can activate *VcDFR* promoter activity. Co-injection of *VcSnRK2.3* and *VcMYB1* largely increased the activity of the *VcDFR* promoter. Empty vector used as the reference. Different asterisks above the bars indicate significant differences based on a t-test (**$P < 0.01$, *$P < 0.05$). Values are the means + SD of three biological replicates.

synthesis, such as DFR, ANS, and UFGT (An et al., 2018; Tang et al., 2021). In our study, transient injection of *VcSnRK2.3* in blueberry fruits was able to increase the anthocyanin content and expression of genes involved in the process of anthocyanin synthesis, including *VcF3H, VcDFR, VcANS*, and *VcUFGT* (Figure 5). Interestingly, transient injection also increased the expression of MYB1. Therefore, we hypothesized that the promotion effect of *VcSnRK2.3* on *VcMYB1* expression is a branch of the blueberry anthocyanin biosynthetic pathway, and there is an interaction between *VcSnRK2.3* and *VcMYB1*.

Most previous studies focused on the interaction of SnRK2 with upstream signals of the ABA signaling pathway, while there are few studies on downstream transcription factors and targets. In strawberry plants, *FvMAPK3* activated acted as a downstream target of *FvSnRK2.6*, phosphorylating *FvMYB10* and reducing its transcriptional activity (Mao et al., 2022). Therefore, in this study, we explored the interaction of *VcSnRK2.3* with MYB1, a positive regulator of anthocyanin biosynthesis, as a way to enrich the mechanism of blueberry anthocyanin synthesis. Yeast two-hybrid and bimolecular fluorescence complementation analyses showed that the ATP binding domain or protein kinase activation domain of the N-terminal, the VcSnRK2.3 protein could interact with the MYB1 gene (Figure 6). This provided us with a new idea of anthocyanin biosynthesis in blueberry and enriches the network of anthocyanin synthesis in blueberry. In our study, MYB1 transcription factor has been shown to interact with *VcSnRK2.3* to positively regulate blueberry anthocyanin synthesis. However, the mechanism by which both regulate downstream anthocyanin

synthesis-related structural genes is unclear. Therefore, we conducted further experiments to demonstrate this process.

Previous studies have shown that VcMYB1 can bind to the *VcDFR* promoter and directly control the expression of structural genes, thus, promoting anthocyanin biosynthesis (Tang et al., 2021). In blueberries overexpressing *VcSnRK2.3*, the *DFR* gene was the most differentially expressed of the anthocyanin synthesis-related genes compared to the wild type. (Figure 5C). Therefore, we hypothesized that DFR structural genes play a major role in regulating anthocyanin synthesis in blueberry fruits. The results showed that fluorescence and higher GUS activity were detected in the presence of *VcMYB1* alone, demonstrating that *VcMYB1* can promote anthocyanin synthesis by initiating the expression of *VcDFR*. More importantly, the fluorescence effect and GUS activity were more significant when *VcSnRK2.3* and *VcMYB1* were co-expressed (Figure 7). The reason is that the presence of *VcSnRK2.3* enhanced the binding of *VcMYB1* to the target promoter, thus increasing the transcriptional activity of the anthocyanin biosynthesis structural gene. In the study of *MdWRKY40* and *MdERF38, MdMYB1* not only bound to the *MdDFR* and *MdUF3GT* promoter regions, but the presence of MdWRKY40 and MdERF38 enhanced the binding of MdMYB1 to its target promoter (An et al., 2019; An et al., 2020a). This may be similar to the regulatory model of this study, where the presence of an exogenous gene regulates the transcriptional activity of MYB on the target genes, thus ultimately promoting anthocyanin accumulation in the plants.

The three key ABA receptor proteins PYR/PYL/PCAR, PP2C, and SnRK2, as well as the downstream transcription factors, make up the ABA signaling pathway. This is the more well-known signaling pathway ABA-PYR/PYL/RCARs-PP2Cs-SnRK2s (Li et al., 2016; Wu et al., 2016). In this study, we investigated the effect of *VcSnRK2.3* overexpression on blueberry anthocyanin biosynthesis and its interaction with *VcMYB1* in an attempt to find a novel pathway to regulate anthocyanin anabolism in blueberry. Previous studies on anthocyanin synthesis have focused on transcription factors such as MYB and bHLH and less on ABA signal transduction pathway genes. Therefore, through this study, we investigated the ABA signaling pathway gene *SnRK2*, thus broadening our understanding of genes related to anthocyanin synthesis. In addition, our study has enriched the knowledge of the ripening process of blueberry fruits and laid the foundation for elucidating the ripening mechanism of non-climacteric plants and other fruit trees. ABA signaling pathway genes have been identified in many plants, but there are few studies on the effects of SnRK2 downstream targets and transcription factors on anthocyanin metabolism, which may be further explored in the future.

In conclusion, we identified a new protein VcSnRK2.3 in blueberries that is involved in the regulation of blueberry anthocyanin biosynthesis. *VcSnRK2.3* expression not only positively correlated with fruit ripening but could also be induced by ABA signaling. In addition, VcSnRK2.3 can interact with *VcMYB1* to promote anthocyanin accumulation by enhancing the binding of VcMYB1 to the *VcDFR* promoter.

Data availability statement

The datasets presented in this study can be found in online repositories. The names of the repository/repositories and accession number(s) can be found below: https://www.ncbi.nlm.nih.gov/, OP626311 OP626312 OP626313 OP626314 OP626315 OP626316.

Author contributions

YS conceived and designed the experiments. XW, QT and YS performed the research. XW, QT, YS, FC, HL, and HZ analyzed the data. YS and XW wrote the paper. All authors contributed to the article and approved the submitted version.

Funding

This study was supported by the Central Public-interest Scientific Institution Basal Research Fund (No.Y2022PT15), the Chinese Academy of Agricultural Sciences-Agricultural Science and Technology Innovation Program (CAAS-ASTIP).

Acknowledgments

We appreciate the experimental assistance provided by Xiu-hong An (Hebei Agricultural University).

Conflict of interest

The authors declare that the research was conducted in the absence of any commercial or financial relationships that could be construed as a potential conflict of interest.

The reviewer XL declared a shared affiliation with the authors to the handling editor at the time of the review.

Publisher's note

All claims expressed in this article are solely those of the authors and do not necessarily represent those of their affiliated organizations, or those of the publisher, the editors and the reviewers. Any product that may be evaluated in this article, or claim that may be made by its manufacturer, is not guaranteed or endorsed by the publisher.

Supplementary material

The Supplementary Material for this article can be found online at: https://www.frontiersin.org/articles/10.3389/fpls.2023.1018874/full#supplementary-material

References

Allan, A. C., Hellens, R. P., and Laing, W. A. (2008). MYB transcription factors that colour our fruit. *Trends. Plant Sci.* 13, 99–102. doi: 10.1016/j.tplants.2007.11.012

An, J. P., Qu, F. J., Yao, J. F., Wang, X. N., You, C. X., Wang, X. F., et al. (2017). The bZIPtranscription factor *MdHY5* regulates anthocyanin accumulation and nitrate assimilation in apple. *Hortic. Res.* 4, 17023. doi: 10.1038/hortres.2017.23

An, J. P., Wang, X. F., Zhang, X. W., Xu, H. F., Bi, S. Q., You, C. X., et al. (2020b). An apple MYB transcription factor regulates cold tolerance and anthocyanin accumulation and undergoes MIEL1-mediated degradation. *Plant Biotechnol. J.* 18, 337–353. doi: 10.1111/pbi.13201

An, J. P., Yao, J. F., Xu, R. R., You, C. X., Wang, X. F., and Hao, Y. J. (2018). Apple bZIP transcription factor *MdbZIP44* regulates abscisic acid-promoted anthocyanin accumulation. *Plant Cell Environ.* 41, 2678–2692. doi: 10.1111/pce.13393

An, J. P., Zhang, X. W., Bi, S. Q., You, C. X., Wang, X. F., and Hao, Y. J. (2020a). The ERF transcription factor *MdERF38* promotes drought stress-induced anthocyanin biosynthesis in apple. *Plant J.* 101, 573–589. doi: 10.1111/tpj.14555

An, J. P., Zhang, X. W., Liu, Y. J., Wang, X. F., You, C. X., and Hao, Y. J. (2021). ABI5 regulates ABA-induced anthocyanin biosynthesis by modulating the MYB1-bHLH3 complex in apple. *J. Exp. Bot.* 72, 1460–1472. doi: 10.1093/jxb/eraa525

An, J. P., Zhang, X. W., You, C. X., Bi, S. Q., Wang, X. F., and Hao, Y. J. (2019). *MdWRKY40* promotes wounding-induced anthocyanin biosynthesis in association with *MdMYB1* and undergoes MdBT2-mediated degradation. *New Phytol.* 224, 380–395. doi: 10.1111/nph.16008

Bai, J., Mao, J., Yang, H., Khan, A., Fan, A., Liu, S., et al. (2017). Sucrose non-ferment 1 related protein kinase 2 (SnRK2) genes could mediate the stress responses in potato (Solanum tuberosum l.). *BMC Genet.* 18, 41. doi: 10.1186/s12863-017-0506-6

Ballester, A. R., Molthoff, J., de Vos, R., Hekkert, B., Orzaez, D., Fernández-Moreno, J. P., et al. (2010). Biochemical and molecular analysis of pink tomatoes: Deregulated expression of the gene encoding transcription factor *SlMYB12* leads to pink tomato fruit color. *Plant Physiol.* 152, 71–84. doi: 10.1104/pp.109.147322

Ban, Y., Honda, C., Hatsuyama, Y., Igarashi, M., Bessho, H., and Moriguchi, T. (2007). Isolation and functional analysis of a MYB transcription factor gene that is a key regulator for the development of red coloration in apple skin. *Plant Cell Physiol.* 48, 958–970. doi: 10.1093/pcp/pcm066

Bassaganya-Riera, J., Skoneczka, J., Kingston, D., Krishnan, A., Misyak, S., Guri, A., et al. (2010). Mechanisms of action and medicinal applications of abscisic acid. *Curr. Med. Chem.* 17, 467–478. doi: 10.2174/092986710790226110

Boneh, U., Biton, I., Schwartz, A., and Ben-Ari, G. (2012). Characterization of the ABA signal transduction pathway in vitis vinifera. *Plant Sci.* 187, 89–96. doi: 10.1016/j.plantsci.2012.01.015

Boss, P. K., Davies, C., and Robinson, S. P. (1996). Analysis of the expression of anthocyanin pathway genes in developing vitis vinifera l. cv Shiraz grape berries and the implications for pathway regulation. *Plant Physiol.* 111, 1059–1066. doi: 10.1104/pp.111.4.1059

Boudsocq, M., Barbier-Brygoo, H., and Laurière, C. (2004). Identification of nine sucrose nonfermenting 1-related protein kinases 2 activated by hyperosmotic and saline stresses in arabidopsis thaliana. *J. Biol. Chem.* 279, 41758–41766. doi: 10.1074/jbc.M405259200

Boudsocq, M., and Laurière, C. (2005). Osmotic signaling in plants: Multiple pathways mediated by emerging kinase families. *Plant Physiol.* 138, 1185–1194. doi: 10.1104/pp.105.061275

Bowling, S. A., Guo, A., Cao, H., Gordon, A. S., Klessig, D. F., and Dong, X. (1994). A mutation in arabidopsis that leads to constitutive expression of systemic acquired resistance. *Plant Cell.* 6, 1845–1857. doi: 10.1105/tpc.6.12.1845

Castillo-Munãoz, N., Goímez-Alonso, S., Garciía-Romero, E., Gómez, M. V., Velders, A. H., and Hermosiín-Gutieírrez, I. (2009). Flavonol 3-o-glycosides series of vitis vinifera cv. Petit verdot red wine grapes. *J. Agric. Food Chem.* 57, 209–219. doi: 10.1021/jf802863g

Chai, Y. M., Jia, H. F., Li, C. L., Dong, Q. H., and Shen, Y. Y. (2011). *FaPYR1* is involved in strawberry fruit ripening. *J. Exp. Bot.* 62, 5079–5089. doi: 10.1093/jxb/err207

Chalker-Scott, L. (1999). Environmental significance of anthocyanins in plant stress responses. *Photochem. Photobiol.* 70, 1–9. doi: 10.1111/j.1751-1097.1999.tb01944.x

Chen, K., Li, G. J., Bressan, R. A., Song, C. P., Zhu, J. K., and Zhao, Y. (2020b). Abscisic acid dynamics, signaling, and functions in plants. *J. Integr. Plant Biol.* 62, 25–54. doi: 10.1111/jipb.12899

Chen, R. C., Mao, L. C., Guan, W. L., Wei, X. B., Huang, Z. H., and Wu, Y. Y. (2022). ABA-mediated miR5290 promotes anthocyanin biosynthesis by inhibiting the expression of *FaMADS1* in postharvest strawberry fruit. *Postharvest Biol. Technol.* 189, 111934. doi: 10.1016/j.postharvbio.2022.111934

Chen, G., Wang, J., Qiao, X., Jin, C., Duan, W., Sun, X., et al. (2020a). Genome-wide survey of sucrose non-fermenting 1-related protein kinase 2 in rosaceae and expression analysis of *PbrSnRK2* in response to ABA stress. *BMC Genomics* 21, 781. doi: 10.1186/s12864-020-07201-w

Cutler, S. R., Rodriguez, P. L., Finkelstein, R. R., and Abrams, S. R. (2010). Abscisic acid: Emergence of a core signaling network. *Annu. Rev. Plant Biol.* 61, 651–679. doi: 10.1146/annurev-arplant-042809-112122

de Zelicourt, A., Colcombet, J., and Hirt, H. (2016). The role of MAPK modules and ABA during abiotic stress signaling. *Trends. Plant Sci.* 21, 677–685. doi: 10.1016/j.tplants.2016.04.004

Espley, R. V., Hellens, R. P., Putterill, J., Stevenson, D. E., Kutty-Amma, S., and Allan, A. C. (2007). Red colouration in apple fruit is due to the activity of the MYB transcription factor, *MdMYB10*. *Plant J.* 49, 414–427. doi: 10.1111/j.1365-313X.2006.02964.x

Fujii, H., Verslues, P. E., and Zhu, J. K. (2011). Arabidopsis decuple mutant reveals the importance of SnRK2 kinases in osmotic stress responses *in vivo*. *Proc. Natl. Acad. Sci. U. S. A.* 108, 1717–1722. doi: 10.1073/pnas.1018367108

Fujita, Y., Nakashima, K., Yoshida, T., Katagiri, T., Kidokoro, S., Kanamori, N., et al. (2009). Three SnRK2 protein kinases are the main positive regulators of abscisic acid signaling in response to water stress in arabidopsis. *Plant Cell Physiol.* 50, 2123–2132. doi: 10.1093/pcp/pcp147

Fujita, Y., Yoshida, T., and Yamaguchi-Shinozaki, K. (2013). Pivotal role of the AREB/ABF-SnRK2 pathway in ABRE-mediated transcription in response to osmotic stress in plants. *Physiol. Plant* 147, 15–27. doi: 10.1111/j.1399-3054.2012.01635.x

Geiger, D., Scherzer, S., Mumm, P., Stange, A., Marten, I., Bauer, H., et al. (2009). Activity of guard cell anion channel SLAC1 is controlled by drought-stress signaling kinase-phosphatase pair. *Proc. Natl. Acad. Sci. U. S. A.* 106, 21425–21430. doi: 10.1073/pnas.0912021106

Gonzalez, A., Zhao, M., Leavitt, J. M., and Lloyd, A. M. (2008). Regulation of the anthocyanin biosynthetic pathway by the TTG1/bHLH/Myb transcriptional complex in arabidopsis seedlings. *Plant J.* 53, 814–827. doi: 10.1111/j.1365-313X.2007.03373.x

Guan, R., Van Le, Q., Yang, H., Zhang, D., Gu, H., Yang, Y., et al. (2021). A review of dietary phytochemicals and their relation to oxidative stress and human diseases. *Chemosphere.* 271, 129499. doi: 10.1016/j.chemosphere.2020.129499

Gupta, K., Wani, S. ,. H., Razzaq, A., Skalicky, M., Samantara, K., Gupta, S., et al. (2022). Abscisic acid: Role in fruit development and ripening. *Front. Plant Sci.* 10. doi: 10.3389/fpls.2022.817500

Halford, N. G., and Hey, S. J. (2009). Snf1-related protein kinases (SnRKs) act within an intricate network that links metabolic and stress signalling in plants. *Biochem. J.* 419, 247–259. doi: 10.1042/bj20082408

Han, Y., Dang, R., Li, J., Jiang, J., Zhang, N., Jia, M., et al. (2015). SUCROSE NONFERMENTING1-RELATED PROTEIN KINASE2.6, an ortholog of OPEN STOMATA1, is a negative regulator of strawberry fruit development and ripening. *Plant Physiol.* 167, 915–930. doi: 10.1104/pp.114.251314

Hrabak, E. M., Chan, C. W., Gribskov, M., Harper, J. F., Choi, J. H., Halford, N., et al. (2003). The arabidopsis CDPK-SnRK superfamily of protein kinases. *Plant Physiol.* 132, 666–680. doi: 10.1104/pp.102.011999

Hu, W., Yan, Y., Shi, H., Liu, J., Miao, H., Tie, W., et al. (2017). The core regulatory network of the abscisic acid pathway in banana: Genome-wide identification and expression analyses during development, ripening, and abiotic stress. *BMC Plant Biol.* 17, 145. doi: 10.1186/s12870-017-1093-4

Huai, J., Wang, M., He, J., Zheng, J., Dong, Z., Lv, H., et al. (2008). Cloning and characterization of the SnRK2 gene family from zea mays. *Plant Cell Rep.* 27, 1861–1868. doi: 10.1007/s00299-008-0608-8

Islam, M., Inoue, T., Hiraide, M., Khatun, N., Jahan, A., Kuwata, K., et al. (2021). Activation of SnRK2 by raf-like kinase ARK represents a primary mechanism of ABA and abiotic stress responses. *Plant Physiol.* 185, 533–546. doi: 10.1093/plphys/kiaa046

Jaakola, L. (2013). New insights into the regulation of anthocyanin biosynthesis in fruits. *Trends. Plant Sci.* 18, 477–483. doi: 10.1016/j.tplants.2013.06.003

Jefferson, R. A., Kavanagh, T. A., and Bevan, M. W. (1987). GUS fusions: beta-glucuronidase as a sensitive and versatile gene fusion marker in higher plants. *EMBO. J.* 6, 3901–3907. doi: 10.1002/j.1460-2075.1987.tb02730.x

Jia, H. F., Chai, Y. M., Li, C. L., Lu, D., Luo, J. J., Qin, L., et al. (2011). Abscisic acid plays an important role in the regulation of strawberry fruit ripening. *Plant Physiol.* 157, 188–199. doi: 10.1104/pp.111.177311

Jia, M., Li, X., Wang, W., Li, T., Dai, Z., Chen, Y., et al. (2022). SnRK2 subfamily I protein kinases regulate ethylene biosynthesis by phosphorylating HB transcription factors to induce ACO1 expression in apple. *New Phytol.* 234, 1262–1277. doi: 10.1111/nph.18040

Jia, H. F., Lu, D., Sun, J. H., Li, C. L., Xing, Y., Qin, L., et al. (2013). Type 2C protein phosphatase ABI1 is a negative regulator of strawberry fruit ripening. *J. Exp. Bot.* 64, 1677–1687. doi: 10.1093/jxb/ert028

Kalt, W., Cassidy, A., Howard, L. R., Krikorian, R., Stull, A. J., Tremblay, F., et al. (2020). Recent research on the health benefits of blueberries and their anthocyanins. *Adv. Nutr.* 11, 224–236. doi: 10.1093/advances/nmz065

Karppinen, K., Lafferty, D. J., Albert, N. W., Mikkola, N., McGhie, T., Allan, A. C., et al. (2021). MYBA and MYBPA transcription factors co-regulate anthocyanin

biosynthesis in blue-coloured berries. *New Phytol.* 232, 1350–1367. doi: 10.1111/nph.17669

Karppinen, K., Tegelberg, P., Häggman, H., and Jaakola, L. (2018). Abscisic acid regulates anthocyanin biosynthesis and gene expression associated with cell wall modification in ripening bilberry (Vaccinium myrtillus l.) fruits. *Front. Plant Sci.* 9.1259 doi: 10.3389/fpls.2018.01259

Kobayashi, Y., Yamamoto, S., Minami, H., Kagaya, Y., and Hattori, T. (2004). Differential activation of the rice sucrose nonfermenting1-related protein kinase2 family by hyperosmotic stress and abscisic acid. *Plant Cell.* 16, 1163–1177. doi: 10.1105/tpc.019943

Kulik, A., Wawer, I., Krzywińska, E., Bucholc, M., and Dobrowolska, G. (2011). SnRK2 protein kinases–key regulators of plant response to abiotic stresses. *OMICS.* 15, 859–872. doi: 10.1089/omi.2011.0091

Lafferty, D. J., Espley, R. V., Deng, C. H., Günther, C. S., Plunkett, B., Turner, J. L., et al. (2022). Hierarchical regulation of MYBPA1 by anthocyanin- and proanthocyanidin-related MYB proteins is conserved in vaccinium species. *J. Exp. Bot.* 73, 1344–1356. doi: 10.1093/jxb/erab460

Latti, A. K., Jaakola, L., Riihinen, K. R., and Kainulainen, P. (2010). Anthocyanin and flavonol variation in bog bilberries (Vaccinium uliginosum l.) in Finland. *J. Agric. Food Chem.* 58, 427–433. doi: 10.1021/jf903033m

Li, D., Mou, W., Luo, Z., Li, L., Limwachiranon, J., Mao, L., et al. (2016). Developmental and stress regulation on expression of a novel miRNA, fan-miR73, and its target ABI5 in strawberry. *Sci. Rep.* 6, 28385. doi: 10.1038/srep28385

Ma, D., Sun, D., Wang, C., Li, Y., and Guo, T. (2014). Expression of flavonoid biosynthesis genes and accumulation of flavonoid in wheat leaves in response to drought stress. *Plant Physiol. Biochem.* 80, 60–66. doi: 10.1016/j.plaphy.2014.03.024

Ma, L., Sun, Z., Zeng, Y., Luo, M., and Yang, J. (2018). Molecular mechanism and health role of functional ingredients in blueberry for chronic disease in human beings. *Int. J. Mol. Sci.* 19 (9), 2785 doi: 10.3390/ijms19092785

Mao, W., Han, Y., Chen, Y., Sun, M., Feng, Q., Li, L., et al. (2022). Low temperature inhibits anthocyanin accumulation in strawberry fruit by activating *FvMAPK3*-induced phosphorylation of *FvMYB10* and degradation of chalcone synthase 1. *Plant Cell.* 34, 1226–1249. doi: 10.1093/plcell/koac006

Moreno-Alvero, M., Yunta, C., Gonzalez-Guzman, M., Lozano-Juste, J., Benavente, J. L., Arbona, V., et al. (2017). Structure of ligand-bound intermediates of crop ABA receptors highlights PP2C as necessary ABA Co-receptor. *Mol. Plant* 10, 1250–1253. doi: 10.1016/j.molp.2017.07.004

Oh, H. D., Yu, D. J., Chung, S. W., Chea, S., and Lee, H. J. (2018). Abscisic acid stimulates anthocyanin accumulation in 'Jersey' highbush blueberry fruits during ripening. *Food Chem.* 244, 403–407. doi: 10.1016/j.foodchem.2017.10.051

Pertuzatti, P. B., Barcia, M. T., Gómez-Alonso, S., Godoy, H. T., and Hermosin-Gutierrez, I. J. F. C. (2021). Phenolics profiling by HPLC-DAD-ESI-MSn aided by principal component analysis to classify rabbiteye and highbush blueberries. *Food Chem.* 340, 127958. doi: 10.1016/j.foodchem.2020.127958

Pertuzatti, P. B., Barcia, M. T., Rebello, L. P. G., Gómez-Alonso, S., Duarte, R. M. T., Duarte, M. C. T., et al. (2016). Antimicrobial activity and differentiation of anthocyanin profiles of rabbiteye and highbush blueberries using HPLC–DAD–ESI-MSn and multivariate analysis. *J. Funct. Foods.* 26, 506–516. doi: 10.1016/j.jff.2016.07.026

Petroni, K., and Tonelli, C. (2011). Recent advances on the regulation of anthocyanin synthesis in reproductive organs. *Plant Sci.* 181, 219–229. doi: 10.1016/j.plantsci.2011.05.009

Shang, Y., Yan, L., Liu, Z. Q., Cao, Z., Mei, C., Xin, Q., et al. (2010). The mg-chelatase h subunit of arabidopsis antagonizes a group of WRKY transcription repressors to relieve ABA-responsive genes of inhibition. *Plant Cell.* 22, 1909–1935. doi: 10.1105/tpc.110.073874

Shao, Y., Qin, Y., Zou, Y., and Ma, F. (2014). Genome-wide identification and expression profiling of the SnRK2 gene family in malus prunifolia. *Gene.* 552, 87–97. doi: 10.1016/j.gene.2014.09.017

Shen, X., Guo, X., Zhao, D., Zhang, Q., Jiang, Y., Wang, Y., et al. (2017). Cloning and expression profiling of the *PacSnRK2* and *PacPP2C* gene families during fruit development, ABA treatment, and dehydration stress in sweet cherry. *Plant Physiol. Biochem.* 119, 275–285. doi: 10.1016/j.plaphy.2017.08.025

Shen, X., Zhao, K., Liu, L., Zhang, K., Yuan, H., Liao, X., et al. (2014). A role for *PacMYBA* in ABA-regulated anthocyanin biosynthesis in red-colored sweet cherry cv. Hong deng (Prunus avium l.). *Plant Cell Physiol.* 55, 862–880. doi: 10.1093/pcp/pcu013

Sun, L., Wang, Y.P., Chen, P., Ren, J., Ji, K., Li, Q., and Leng, P. (2011). Transcriptional regulation of SlPYL, SlPP2C, and SlSnRK2 gene families encoding ABA signal core components during tomato fruit development and drought stress. *J Exp Bot.* 62(15), 5659–5669. doi: 10.1093/jxb/err252

Tang, Q., Chi, F. M., Liu, H. D., Zhang, H. J., and Song, Y. (2021). Single-molecule real-time and illumina sequencing to analyze transcriptional regulation of flavonoid synthesis in blueberry. *Front. Plant Sci.* 12. doi: 10.3389/fpls.2021.754325

Teng, S., Keurentjes, J., Bentsink, L., Koornneef, M., and Smeekens, S. (2005). Sucrose-specific induction of anthocyanin biosynthesis in arabidopsis requires the *MYB75/PAP1* gene. *Plant Physiol.* 139, 1840–1852. doi: 10.1104/pp.105.066688

Wang, Y., Li, W., Chang, H., Zhou, J., Luo, Y., Zhang, K., et al. (2020). SRNAome and transcriptome analysis provide insight into strawberry fruit ripening. *Genomics.* 112, 2369–2378. doi: 10.1016/j.ygeno.2020.01.008

Wu, Q., Zhang, X., Peirats-Llobet, M., Belda-Palazon, B., Wang, X., Cui, S., et al. (2016). Ubiquitin ligases RGLG1 and RGLG5 regulate abscisic acid signaling by controlling the turnover of phosphatase PP2CA. *Plant Cell.* 28, 2178–2196. doi: 10.1105/tpc.16.00364

Yang, W., Guo, Y., Liu, M., Chen, X., Xiao, X., Wang, S., et al. (2022). Structure and function of blueberry anthocyanins: A review of recent advances. *J. Funct. Foods.* 88, 104864. doi: 10.1016/j.jff.2021.104864

Yoshida, R., Umezawa, T., Mizoguchi, T., Takahashi, S., Takahashi, F., and Shinozaki, K. (2006). The regulatory domain of SRK2E/OST1/SnRK2.6 interacts with ABI1 and integrates abscisic acid (ABA) and osmotic stress signals controlling stomatal closure in arabidopsis. *J. Biol. Chem.* 281, 5310–5318. doi: 10.1074/jbc.M509820200

Zhang, H., Li, W., Mao, X., Jing, R., and Jia, H. (2016). Differential activation of the wheat SnRK2 family by abiotic stresses. *Front. Plant Sci.* 7. doi: 10.3389/fpls.2016.00420

Zhang, Y. L., Lin-Wang, K., Albert, N. W., Elborough, C., Espley, R. V., Andre, C. M., et al. (2021). Identification of a strong anthocyanin activator, VbMYBA, from berries of vaccinium bracteatum thunb. *Front. Plant Sci.* 12. doi: 10.3389/fpls.2021.697212

Zhang, Y., Ye, Y., Jiang, L., Lin, Y., Gu, X., Chen, Q., et al. (2020). Genome-wide characterization of Snf1-related protein kinases (SnRKs) and expression analysis of SnRK1.1 in strawberry. *Genes (Basel).* 11 (4), 427. doi: 10.3390/genes11040427

Zhao, M., Li, J., Zhu, L., Chang, P., Li, L., and Zhang, L. (2019). Identification and characterization of MYB-bHLH-WD40 regulatory complex members controlling anthocyanidin biosynthesis in blueberry fruits development. *Genes.* 10, 496. doi: 10.3390/genes10070496

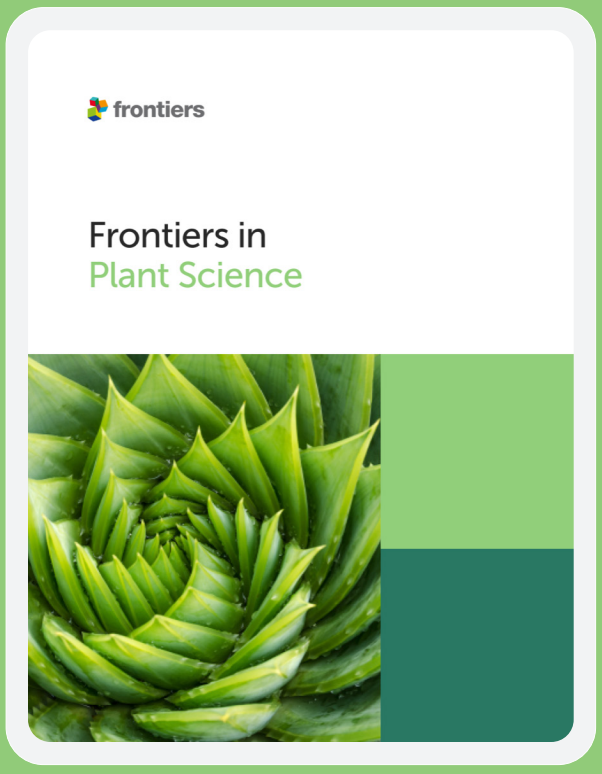
Frontiers in
Plant Science

Cultivates the science of plant biology and its applications

The most cited plant science journal, which advances our understanding of plant biology for sustainable food security, functional ecosystems and human health.

Discover the latest Research Topics

See more →



Frontiers

Avenue du Tribunal-Fédéral 34
1005 Lausanne, Switzerland
frontiersin.org

Contact us

+41 (0)21 510 17 00
frontiersin.org/about/contact